

ITAIPU HYDROELECTRIC PROJECT



Engineering Features

ITAIPU

HYDROELECTRIC PROJECT

Engineering Features

ITAIPU BINACIONAL
1994

Copyright ITAIPU BINACIONAL 1994
Editorial Coordination: *John Reginald Cotrim*
Managing Editor: *Gustavo Enrique Reyes Reverol*
Consultants and Technical Production: *Consortium IECO-elc*
Graphic Coordination: *Gustavo Enrique Reyes Reverol*
Graphic Design: *Regina Célia de Paula, Cristine Nogueira Nunes and Beatriz Araújo Campos*
Desktop Publishing: *Cristine Nogueira Nunes and Kátia Prado*
Final Artwork: *Cristine Nogueira Nunes, Sandra Baptista Ribeiro, Júlio Serrano Rodriguez, Jorge Noblat, Neiton dos Santos and Valdonier Ferreira Maciel*
Cover Design: *Oromar Pinho Duboc*
Printing/Binding Coordination: *Saulo Kozel Teixeira*
Films and Color Separation: *Grafcolor Reproduções Gráficas Ltda.*
Printing: *Gráfica Editora Pallotti*
Binding: *Henrique Berkovitz Encadernadores Ltda.*

Printed in Brazil
Published in 1994 by ITAIPU BINACIONAL

ISBN: 85-85263-02-4

Dados Internacionais de Catalogação na Publicação (CIP)
(Câmara Brasileira do Livro, SP, Brasil)

Itaipu : Hydroelectric Project. -- Curitiba, PR :
ITAIPU BINACIONAL, 1994.

"Engineering Features"

1. Itaipu Binacional

93-3666

CDD-627.8098

Indices para catálogo sistemático:

1. Itaipu : Represas : América do Sul 627.8098
2. Represa de Itaipu : América do Sul 627.8098

FOREWORD

On the occasion of the 20th anniversary of the creation of the Entity, ITAIPU BINACIONAL has the pleasure to present a book which describes how this magnificent undertaking, the ITAIPU Hydroelectric Project, was conceived, designed, constructed and commissioned.

This volume is the result of systematic work which was started in 1976 when construction was just beginning. All relevant aspects of the venture were recorded as the work progressed, in order that, when the Project was ready to commence operation, they could be compiled in a publication worthy of the importance of the enterprise.

As it took a long time to complete the Project, several ITAIPU BINACIONAL company administrations were involved in the preparation of this volume. Credit is due to them all, and especially to the Technical Directors and their staff for their constant diligence in the collection of data without which achieving the high professional standard of this book would have been impossible.

The general coordinator of the engineering aspects of the Project, the IECO/ELC Consortium, has from the start handled the editorial work while also being in charge of the publication of the book. Eng. G.S. Sarkaria, who served as chief editor and reviewer of this book, deserves special commendation in this respect.

The principal credit for the publication of this comprehensive technical treatise is due to Eng. John R. Cotrim who was Technical Director of ITAIPU BINACIONAL from 1974 to 1985. During his tenure as Director, he instituted the systematic compilation and analysis of the engineering data, and preparation of technical reports and bulletins which were later incorporated into this book. After 1985, as a special consultant to ITAIPU BINACIONAL, Eng. Cotrim continuously coordinated and guided the preparation of this book until its publication; an uninterrupted dedication to the task for over eighteen years.

Since this book is about a binational project of great international significance and interest, it was decided to have it published in the English language. It would thus receive wide international circulation and be of particular service and benefit to engineers and professionals throughout the world who are interested in the technical aspects of this unique hydroelectric enterprise.

Lastly, ITAIPU BINACIONAL gives special thanks to ELETROBRAS and ANDE for their constant support during the long years it took to compile and print this volume.

PRINCIPAL ITAIPU LANDMARKS

Preparatory Period

Iguaçu Agreement (Iguaçu Act)	June 22, 1966
Creation of Brazilian-Paraguayan Joint Technical Commission	February 12, 1967
Contracting of Consortium of International Consultants for Investigation of Site	November 18, 1970
Presentation by Consultants of Report on Alternative Project Sites and Layouts	December 31, 1972
Signing of the ITAIPU Treaty	April 26, 1973

Execution of the Project

Constitution of ITAIPU Binational	May 17, 1974
Commencement of Civil Works Construction	May 2, 1975
River Diversion	October 20, 1978
Closure of Diversion Gates and Start of Filling of Reservoir	October 13, 1982
First Unit on Line	May 5, 1984
Last Unit on Line	April 4, 1991

OFFICERS OF ITAIPU BINACIONAL

1974 – 1993

Administrative Council

Brasil

Amyr Borges Fortes	May 17, 1974 to January 7, 1986
Espedito de Freitas Resende	May 17, 1974 to January 7, 1986
Lucas Nogueira Garcez	May 17, 1974 to March 27, 1977 April 2, 1979 to May 11, 1982
Mario Penna Bhering	May 17, 1974 to March 9, 1977 May 14, 1985 to May 16, 1992
Helio Marcos Penna Beltrão	May 17, 1974 to July 30, 1979
Mauro Moreira	May 17, 1974 to May 9, 1985
João Hermes Pereira de Araujo	January 15, 1976 to August 9, 1981
Antonio Carlos Peixoto de Magalhães	January 15, 1976 to June 18, 1978
Arnaldo Rodrigues Barbalho	April 1 st , 1977 to March 29, 1979 December 11, 1979 to May 9, 1985
Luiz Marcello Moreira de Azevedo	April 1 st , 1977 to March 29, 1979
Ney Webster de Araujo	June 26, 1978 to March 29, 1979
Octaviano Massa	April 2, 1979 to December 9, 1979
Mauricio Schulman	April 2, 1979 to July 9, 1990
José Flávio Pécora	August 23, 1979 to May 9, 1985
Rubens Ricupero	August 11, 1981 to November 4, 1987
Miguel Reale	Since June 23, 1982
Paulo Richer	May 14, 1985 to November 4, 1987
Sebastião Marcos Vital	May 14, 1985 to October 7, 1985
João Batista de Abreu	October 14, 1985 to June 21, 1987
Mailson Ferreira da Nóbrega	July 6, 1987 to February 21, 1988
Guy Maria Villela Pascoal	November 17, 1987 to February 16, 1989
Gilberto Coutinho Paranhos Velloso	November 17, 1987 to August 17, 1988
Mario Jorge Gusmão Berard	March 15, 1988 to May 9, 1988
Paulo Cezar Ximenes Alves Pereira	May 17, 1988 to May 16, 1990
José Nogueira Filho	August 23, 1988 to April 23, 1990
Antonio Carlos Tatit Holtz	March 7, 1989 to May 17, 1990
Fernando Guimarães Reis	April 30, 1990 to November 24, 1993
Eduardo de Freitas Teixeira	October 7, 1990 to April 21, 1991
Rubens Vaz da Costa	July 10, 1990 to April 21, 1991
José Maria Siqueira de Barros	July 10, 1990 to December 15, 1992
João da Silva Maia	April 23, 1991 to May 17, 1991
Armando Ribeiro de Araújo	April 23, 1991 to August 31, 1992

Luiz Antônio Andrade Gonçalves
 Márcio Fortes de Almeida
 Jorge Nacli Neto
 Eliseu Resende
 José Luiz Alqueres
 Francisco Luiz Sibut Gomide
 Wando Pereira Borges
 Ney Aminthas de Barros Braga
 Clóvis de Barros Carvalho
 Luiz Filipe de Macedo Soares Guimarães

May 20, 1991 to May 7, 1993
 September 15, 1992 to May 7, 1993
 May 20, 1992 to March 27, 1993
 January 11, 1993 to March 10, 1993
 Since March 24, 1993
 Since April 6, 1993
 May 13, 1993 to July 9, 1993
 Since May 13, 1993
 Since July 20, 1993
 Since November 25, 1993

Paraguay

Ezequiel González Alsina
 Andres Gomez Opitz
 Alberto Nogués
 Mario Coscia Tavarozzi
 Milciades Ramos Giménez
 Rogelio Cadogan
 Luis Maria Argaña
 Salvador Rubén Paredes
 Luis Martínez Miltos
 Silvio Meza Brítez
 Luiz Peralta Baez
 Alejandro Blanco Centurion
 Nelson Chaves
 Edgar Jimenez Meza
 Leopoldo Ostertag
 Rubén Stanley
 Emilio Mateu
 Zoilo Rodas Rodas
 Miguel Angel Gonzales Casabianca
 Hans W. Krauch
 Ricardo Rodríguez Silvero
 Agustin González Insfran
 Leopoldo A. Seifart S.
 Angel Manuel Villalba
 Carlos Podestá
 Mario Mauricio Salinas Alcaráz
 Hector Ernesto Federico Richer Becker
 Joaquin Rodríguez Villalba
 Salvador Oscar Gulino
 Miguel Luciano Jimenéz

May 17, 1974 to June 25, 1989
 May 17, 1974 to September 1990
 May 17, 1974 to May 17, 1986
 May 17, 1974 to March 24, 1986
 May 17, 1974 to May 1986
 May 17, 1974 to May 1986
 May 9, 1974 to September 19, 1983
 October 11, 1983 to March 23, 1987
 May 17, 1986 to September 1990
 May 17, 1986 to September 1990
 May 17, 1986 to May 30, 1986
 April 20, 1987 to May 28, 1989
 March 10, 1989 to September 1990
 June 2, 1989 to September 1990
 December 27, 1989 to September 1990
 July 27, 1989 to September 1990
 December 27, 1989 to September 1990
 September 13, 1990 to February 1st, 1993
 September 13, 1990 to June 29, 1993
 September 13, 1990 to May 31, 1991
 September 13, 1990 to January 26, 1993
 September 13, 1990 to January 26, 1993
 June 3, 1991 to May 17, 1992
 January 6, 1992 to February 1st, 1993
 January 27, 1993 to August 1993
 Since January 27, 1993
 Since February 2, 1993
 Since February 2, 1993
 April 21, 1992 to January 5, 1993
 Since January 6, 1993

Representatives of the Ministries of Foreign Affairs

Participants as Observers in the Administrative Council Meetings

Brasil

João Hermes Pereira de Araujo	May 17, 1974 to January 7, 1976
José Nogueira Filho	January 15, 1976 to March 29, 1979
Orlando Soares Carbonar	April 2, 1979 to February 5, 1984
Sérgio Martins Thompson Flores	April 24, 1984 to April 29, 1985
Rubens Antonio Barbosa	May 6, 1985 to February 23, 1986
João Tabajara de Oliveira	February 25, 1986 to December 4, 1986
Renato Prado Guimarães	December 9, 1986 to August 17, 1988
Gilberto Coutinho Paranhos Velloso	August 23, 1988 to April 23, 1990
José Nogueira Filho	April 30, 1990 to March 19, 1993
Synésio Sampaio Goes Filho	Since March 20, 1993

Paraguay

Carlos Augusto Saldivar	May 17, 1974 to September 19, 1983
José Antonio Moreno Ruffinelli	October 11, 1983 to May 1989
Bernardino Hugo Saguier Caballero	June 2, 1989 to September 1990
Jorge Rafael Gross Brown	December 28, 1990 to January 26, 1993
Julio César Vasconcellos	Since January 27, 1993

Directors

Organizational Structure up to May 1992

General Director

Brasil

José Costa Cavalcanti	May 17, 1974 to May 17, 1985
Ney Aminthas de Barros Braga	May 17, 1985 to May 28, 1990
Fernando Xavier Ferreira	May 30, 1990 to December 31, 1991
Jorge Nacli Neto	January 2, 1992 to May 17, 1992

Paraguay

Enzo Debernardi	May 17, 1974 to February 9, 1989
Fidencio Juan Tardivo	February 15, 1989 to May 30, 1991
Oscar Salvador Gulino	June 3, 1991 to May 17, 1992

Technical Director

Brasil

John Reginald Cotrim
Roberto Leite Schulman
Rubens Vianna de Andrade
Márcio de Almeida Abreu

May 17, 1974 to May 17, 1985
May 17, 1985 to July 9, 1990
July 10, 1990 to May 14, 1991
May 20, 1991 to May 17, 1992

Paraguay

Hans W. Krauch
Leopoldo A. Seifart S.
José Szwako Demiańuk

May 17, 1974 to September 10, 1990
September 13, 1990 to May 30, 1991
June 3, 1991 to May 17, 1992

Financial Director

Brasil

Manuel Pinto de Aguiar
Moacyr Teixeira
Jorge Nacli Neto
Elio Edvino Winter

May 17, 1974 to May 16, 1975
May 17, 1975 to July 8, 1990
July 10, 1990 to December 31, 1991
January 2, 1992 to May 17, 1992

Paraguay

Fidencio Juan Tardivo
Miguel Luciano Jimenez

May 17, 1974 to February 10, 1989
February 15, 1989 to April 21, 1992

Administrative Director

Brasil

Aluisio Guimarães Mendes
Jucundino da Silva Furtado
Fabiano Braga Côrtes
Nivaldo Almeida Neto
Elio Edvino Winter
Tércio Alves de Albuquerque

May 17, 1974 to October 23, 1985
May 17, 1986 to August 13, 1988
September 19, 1988 to July 9, 1990
July 10, 1990 to October 21, 1991
October 21, 1991 to December 31, 1991
January 2, 1992 to May 17, 1992

Paraguay

Victorino Vega Gimenez
Edgar Mengual Haken R.
Hugo Henrique Gomez

May 17, 1974 to February 18, 1990
February 26, 1990 to May 30, 1991
June 3, 1991 to May 17, 1992

Legal Director

Brasil

Paulo José Nogueira da Cunha
Clóvis Ferro Costa
João Carlos de Almeida

May 17, 1974 to March 18, 1986
March 24, 1986 to July 9 1990
July 10, 1990 to December 31, 1991

Paraguay

Antonio Colmán Rodríguez
Anastacio Acosta Amarilla

May 17, 1974 to February 9, 1989
February 15, 1989 to December 31, 1991

Director of Coordination

Brasil

Cassio de Paula Freitas
Luiz Eduardo Veiga Lopes
Nelson Farhat
Tércio Alves de Albuquerque

May 17, 1974 to May 17, 1985
May 17, 1985 to July 9, 1990
July 10, 1990 to May 20, 1991
May 20, 1991 to December 31, 1991

Paraguay

Carlos Alberto Facetti
Oscar Salvador Gulino
Miguel Angel Villalba

May 17, 1974 to September 13, 1989
September 18, 1989 to May 31, 1991
June 3, 1991 to December 31, 1991

Directors

Organizational Structure Since May 1992

General Director

Brasil

Jorge Nacli Neto
Francisco Luiz Sibut Gomide

May 20, 1992 to March 27, 1993
Since April 6, 1993

Paraguay

Salvador Oscar Gulino
Miguel Luciano Jimenez

May 20, 1992 to January 6, 1993
Since January 6, 1993

Director of Engineering and Operation

Márcio de Almeida Abreu
Flávio Decat de Moura

May 20, 1992 to August 12, 1993
Since August 16, 1993

Director of Maintenance and Construction

José Szwako Demiańuk
Pedro Lozano Dietrich

May 20, 1992 to January 6, 1993
Since January 6, 1993

Financial Director

Elio Edvino Winter
Edson Neves Guimarães

May 20, 1992 to August 12, 1993
Since August 16, 1993

Director of Supplies

Hugo Henrique Gomez
Edgar Mengual Herken R.

May 20, 1992 to January 6, 1993
Since January 6, 1993

Administrative Director

Brasil

Tércio Alves de Albuquerque
Luiz Eduardo Veiga Lopes

May 20, 1992 to August 12, 1993
Since August 16, 1993

Paraguay

Miguel Luciano Jimenez
Hugo Henrique Gómez
Félix Hermann Kemper Gonzales

May 20, 1992 to October 1992
October 1992 to January 6, 1993
Since January 6, 1993

INTRODUCTION

The 12 600 MW Itaipu hydroelectric development, which was constructed in compliance with the treaty signed by Brazil and Paraguay on April 26, 1973, has just reached completion and it is the largest development of its kind ever built.

Started in 1975, a year after the creation of the binational entity called ITAIPU BINACIONAL, the project had its first 700 MW unit commissioned in 1984, and followed with the installation of two to three units a year until the last one, the 18th, went on line in April 1991.

Ever since it was announced, the Itaipu project has raised considerable interest amongst the engineering, construction and hydroelectric professionals in general.

On the other hand, it would be inconceivable that a project of this magnitude and international significance would be left, after its conclusion, without a permanent record accessible to the technical world, of its quite unique engineering and construction features.

Thus, with the dual purpose of providing the interested parties with information on the progress of the project and of preparing material for a future comprehensive record of its outstanding engineering and construction aspects, technical papers have been regularly prepared by the personnel of ITAIPU BINACIONAL and its consulting engineers since work at the site began. These papers have been published in international magazines or presented at engineering seminars and congresses.

These articles, which cover the principal aspects of the project from the viewpoints of planning and design, as well as from the viewpoint of construction, comprise a valuable pool of information regarding Itaipu. This information, however, can only be utilized through the review and study of a large variety of publications in various languages, some of which are not easily obtained. This publication will ensure the availability of such technical information to those interested in the engineering aspects of the Itaipu project.

This volume is not merely a reproduction of already published papers and articles, because its compilation required their extensive updating and editing in order to provide a comprehensive and cohesive perspective of the more important technical aspects of the project.

At the time of ICOLD's 1982 Congress on Large Dams held in Rio de Janeiro in April 1982, a visiting tour of the Itaipu construction site was planned for the participants. For the benefit of these visitors, a first edition of this book was prepared.

Note to the reader

The chief purpose of this book is to report the technical aspects of the Itaipu project. Therefore, the photographs are of the best quality available and for the most part they were taken by the construction personnel during the construction period with the sole objective of recording the progress of the works.

Except where indicated, the dimensions of the illustrations are in meters for civil structures and in millimeters for metal parts and structures.

All elevations are in meters.

The international system of units (SI) has been adopted for this book. However, units acceptable to the SI, as well as other units, are used when deemed necessary, to simplify the reading and comprehension of the reader.

CONTENTS

Introductory Chapters

v	FOREWORD
vii	PRINCIPAL ITAIPU LANDMARKS
viii	OFFICERS OF ITAIPU BINACIONAL 1974-1993
xv	INTRODUCTION
xvi	NOTE TO THE READER

Itaipu Hydroelectric Project

1	ITAIPU PROJECT AND ITS EXECUTION
2	PROJECT FEASIBILITY STUDIES
3	PROJECT BASIC DATA AND FEATURES
4	GEOLOGY, GEOTECHNICAL INVESTIGATIONS AND SUBSURFACE TREATMENT
5	CONSTRUCTION PLANNING, PLANT AND METHODS
6	RIVER DIVERSION
7	EARTHFILL AND ROCKFILL DAMS
8	SPILLWAY AND OPERATION OF RESERVOIR
9	HOLLOW GRAVITY AND BUTTRESS DAMS
10	POWER INTAKES, PENSTOCKS AND EQUIPMENT IN THE CONCRETE DAM
11	POWERHOUSE ARRANGEMENT, DESIGN AND CONSTRUCTION
12	POWERHOUSE GENERATION EQUIPMENT
13	POWERHOUSE AUXILIARY EQUIPMENT AND SYSTEMS
14	CONTROL, SUPERVISION AND PROTECTION
15	THE INTERCONNECTED ELECTRICAL SYSTEM
16	ENVIRONMENTAL AND ECOLOGICAL ASPECTS
17	PROJECT SITE INFRASTRUCTURE
18	REFERENCES AND FURTHER READINGS
19	APPENDIX

ITAIPU PROJECT

AND ITS EXECUTION

ORIGIN AND AIMS OF THE PROJECT	1.3
Introduction	1.3
The Paraná Basin	1.3
The Hydropower Potential at the Itaipu Site	1.5
Previous Studies	1.5
Origin and Aims	1.6
Joint Technical Commission	1.7
Inventory and Feasibility Studies	1.7
THE ITAIPU TREATY AND CREATION OF ITAIPU BINACIONAL	1.7
The Binational Spirit	1.7
The Treaty	1.7
The Ownership of Energy	1.9
The Price of Itaipu Energy	1.9
MANAGEMENT STRUCTURE OF ITAIPU FOR THE EXECUTION OF THE PROJECT	1.9
Itaipu Binacional and its Organization	1.10
General Engineering Coordination	1.10
Engineering Design	1.10
Construction Planning	1.11
Civil Works	1.11
Manúfacture of Permanent Electromechanical Equipment	1.12
Quality Control and Inspection	1.12
Erection and Installation of Electromechanical Equipment	1.12

ITAIPU PROJECT AND ITS EXECUTION

ORIGIN AND AIMS OF THE PROJECT

INTRODUCTION

Itaipu is the largest hydroelectric project in the world, and it represents the efforts and accomplishments of two neighboring countries, Brazil and Paraguay, in developing their common energy resources for mutual benefits. It is located on the Paraná river, where it forms the boundary between the two countries, 14 km upstream from the international bridge which joins the cities of Foz do Iguaçu in Brazil and Ciudad del Este (formerly known as Presidente Stroessner) in Paraguay, see Fig. 1.1

The project takes its name from a small rocky island originally at the damsite, called Itaipu, which means "the singing stone" in the local Indian language (Guarani).

THE PARANÁ BASIN

The Paraná river originates in Brazil at the confluence of the Paranaíba and Rio Grande rivers. It runs in a southwesterly direction as far as the Salto Grande das Sete Quedas or Salto del Guairá, at which point it turns south and forms the 190 km border between Brazil and Paraguay



*View of the Itaipu
island in 1974*

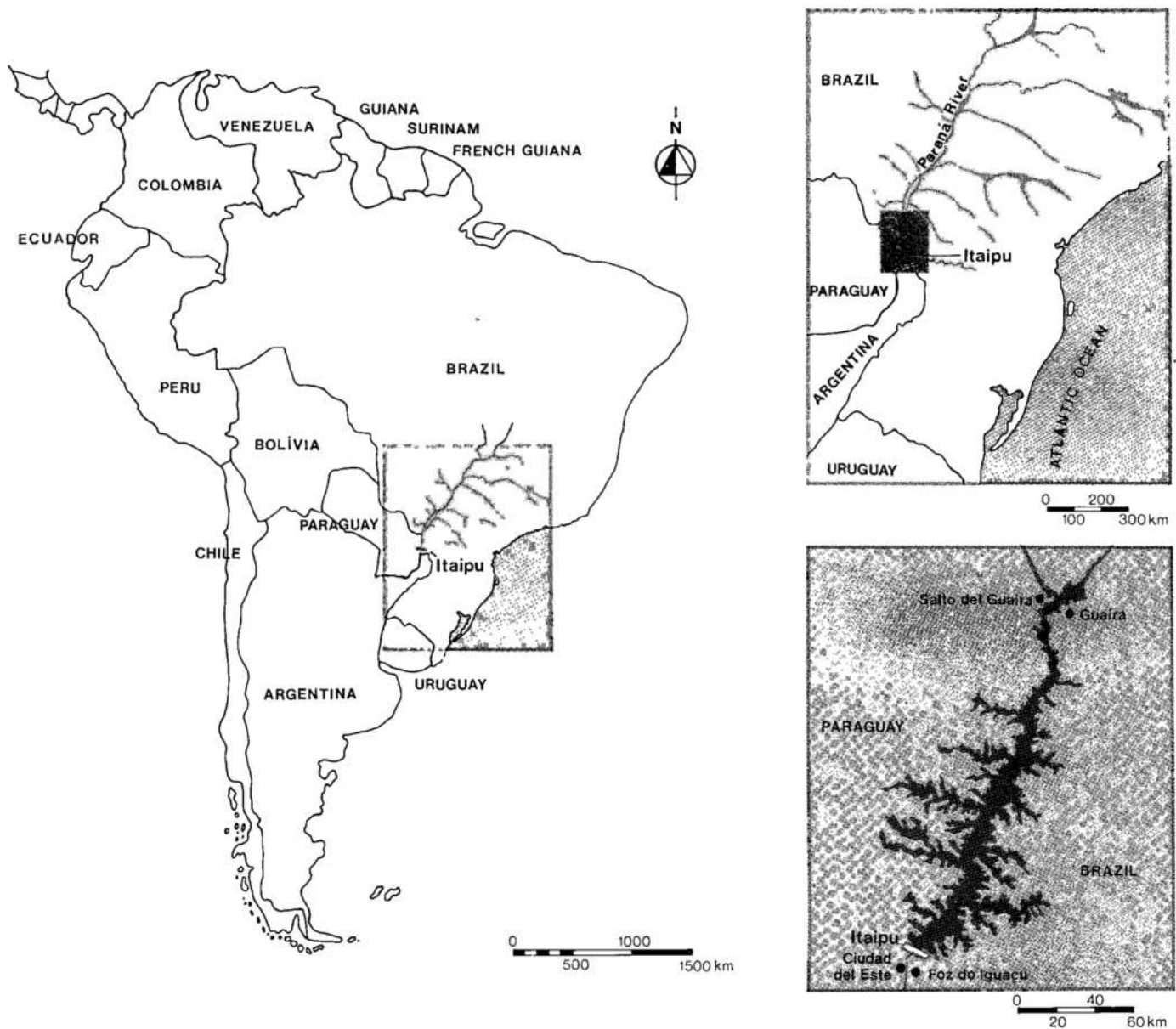


Fig. 1.1 Project location map

until it receives the waters of the Iguazú river from Brazil and the Acaray river from Paraguay, see Fig. 1.2. From that point, it flows between Paraguay and Argentina, joining the Paraguay river further on, and then turns west and flows southward through Argentina to join the Río de la Plata. From the origin of its principal tributaries in Brazil, the Paraná river flows over 3500 km before joining the Río de la Plata. The entire basin encompasses about 3 000 000 km². The estimated total hydropower potential of the Paraná river and its tributaries, upstream of and

including Itaipu, is about 40 000 MW.

The Paraná river basin is among the world's largest systems and for more than 50 years its enormous hydropower potential has been acknowledged. Because the river represents the common border first between Brazil and Paraguay and then between Paraguay and Argentina, affecting the interests of the three countries, diplomacy has played a pivotal role in harmonizing the various interests in the beneficial development of this potential.

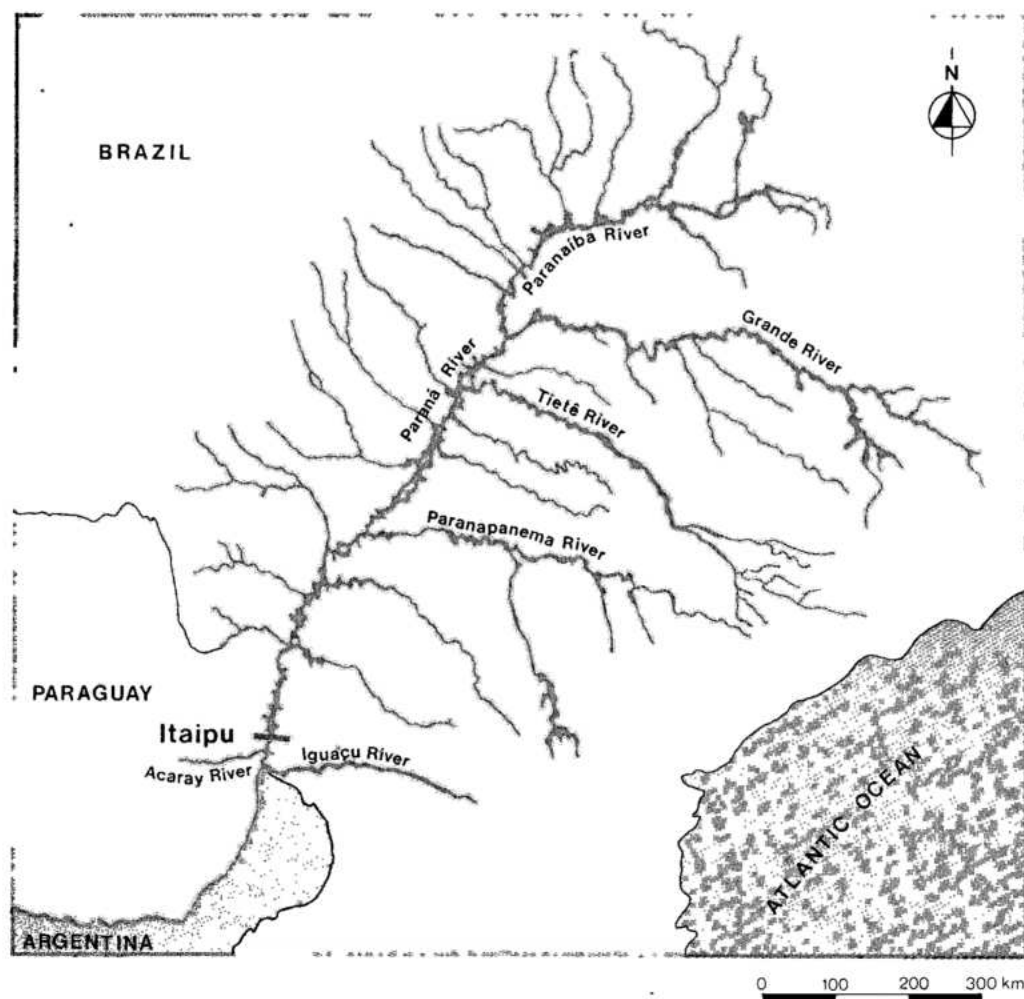


Fig. 1.2 Paraná river basin

THE HYDROPOWER POTENTIAL AT THE ITAIPU SITE

At the Salto Grande das Sete Quedas or Salto del Guairá, the Paraná river prior to the construction of Itaipu dam dropped into a deep canyon and followed a turbulent course for about 60 km, at which point there was a 100 m difference in levels. Throughout the remaining 130 km before reaching the Iguazu river, the Paraná river gradually widened; the level drop being about 20 m. Thus a total head of approximately 120 m could be developed in the bi-national reach. Over the years Brazil has developed several hydroprojects with storage reservoirs throughout the upper Paraná river basin, which have considerably improved the regulation of the river flow at the Itaipu site, thereby substantially increasing its dependable power capacity.

PREVIOUS STUDIES

Preliminary studies to develop the hydropower potential of the Salto Grande das Sete Quedas date back to 1955, when the Canadian electric company Light, which supplied power to the cities of Rio de Janeiro and São Paulo, requested authorization from the Brazilian government to undertake studies. Other studies were conducted in 1956 by the Paraná-Uruguay Basin Interstate Commission. In 1959, a 1200 kW powerplant on one of the reaches of the Salto Grande das Sete Quedas was constructed by the Navigation Service of the Prata Basin. This plant operated until 1982 when it was dismantled because of inundation by the Itaipu reservoir. Other preliminary studies of lesser significance were undertaken at the request of the Navigation Services of the Prata Basin, but with no practical results.

A C T A F I N A L

A los veintiuno y veintidós días del mes de junio de mil novecientos sesenta y seis, se reunieron, en Puerto Presidente Stroessner y Foz de Yguazú, el Ministro de Relaciones Exteriores de la República del Paraguay, Doctor Raúl Sapena Pastor, y el Ministro de Relaciones Exteriores de los Estados Unidos del Brasil, Embajador Juracy Magalhães, con el objeto de pasar revista a los varios aspectos de las relaciones entre los dos países, inclusive aquellos puntos alrededor de los cuales han surgido últimamente divergencias entre las dos Cancillerías.

Después de haber mantenido varias entrevistas de carácter personal y otras con la presencia de sus delegaciones, los Ministros de Relaciones Exteriores de la República del Paraguay y de los Estados Unidos del Brasil llegaron a las siguientes conclusiones, que hacen constar en la presente Acta.

- I. SE MANIFESTARON acordes los dos Cancilleres en reafirmar la tradicional amistad entre los dos pueblos hermanos, amistad fundada en el respeto mutuo y que constituye la base indestructible de las relaciones entre los dos países;
- II. EXPRESARON el vivo deseo de superar, dentro de un mismo espíritu de buena voluntad y de concordia, cualesquiera dificultades o problemas, encontrándoles soluciones compatibles con los intereses de ambas naciones;
- III. PROCLAMARON la disposición de sus respectivos Gobiernos de proceder, de común acuerdo, al estudio y evaluación de las posibilidades económicas, en particular de los recursos hidráulicos, pertenecientes en condominio a los dos países, del Salto del Guairá o Salto Grande de las Siete Caídas;

Doat JM

.....

Doat JM

.....

- 3 -

- VII. EN LO RELATIVO a los trabajos de la "Comisión Mixta de Límites y Caracterización de la Frontera Paraguay-Brasil", convinieron los dos Cancilleres en que dichos trabajos serán proseguídos en la fecha que ambos Gobiernos lo estimen conveniente;
- VIII. SE CONGRATULARON finalmente los dos Cancilleres, por el espíritu constructivo que prevaleció durante las conversaciones y formularon votos por la siempre creciente y fraternal unión entre el Paraguay y el Brasil comprometidos además a no escatimar esfuerzos para estrechar cada vez más los lazos de amistad que unen a los dos países.

La presente Acta, hecha en dos copias en los idiomas español y portugués, después de leída y aprobada, fué firmada en Foz de Yguazú por los Ministros de Relaciones Exteriores de la República del Paraguay y de los Estados Unidos del Brasil, a los veintidós días del mes de junio de mil novecientos sesenta y seis.

Juracy Magalhães
Juracy Magalhães
Ministro de Estado de
Relaciones Exteriores
de los Estados Unidos
del Brasil

Raúl Sapena Pastor
Raúl Sapena Pastor
Ministro de Relaciones
Exteriores de la Repu-
blica del Paraguay

Iguaçu
Act

ORIGIN AND AIMS

In the early 1960's, when the rapidly growing demand for power in south central Brazil started to concern national planners, the Brazilian government contracted the engineering firm OMF, headed by Engineer Octavio Marcondes Ferraz, to study the

feasibility of a hydroelectric scheme in the area of the Salto das Sete Quedas. The proposed scheme, known as the Sete Quedas project, consisted of a diversion dam to be located on the Paraná river upstream of the falls, in Brazilian territory. The river would be diverted into a 60 km long canal along the left bank of the river, also in Brazil, which would

by-pass the falls and return the flow to the main river channel below the canyon, where a powerhouse with a capacity of 10 000 MW would be located. This unilateral scheme was not acceptable because of the international nature of the site, which eventually led Brazil and Paraguay to an agreement for a joint development not only of the Sete Quedas site, but also of the entire stretch of the Paraná river that constitutes the border between the two countries. Thus, the Ministers of Foreign Affairs of both countries signed on June 22, 1966 an Act known as Ata de Iguaçu or Ata das Cataratas, declaring the intention of their respective governments to carry out, in joint agreement, the study and evaluation of the technical and economic feasibility of developing these hydraulic resources.

JOINT TECHNICAL COMMISSION

A Paraguayan-Brazilian Joint Technical Commission was created on February 12, 1967, to conduct the studies. In April 1970, the Joint Technical Commission signed a Cooperation Agreement with the Administración Nacional de Electricidad (ANDE) of Paraguay and the Centrais Elétricas Brasileiras S.A. (ELETROBRÁS) of Brazil, delegating to them the management of the studies and establishing the conditions which would regulate the execution of the studies and investigations.

Along with the technical and economic evaluation, it was decreed that the studies should also include a general appraisal of the multiple uses of the water, such as navigation, municipal and industrial water supply, irrigation and other related benefits.

INVENTORY AND FEASIBILITY STUDIES

Considering that the results of the studies would have extremely important consequences for both countries, it was decided that the execution of the studies would be entrusted to an international consortium of engineering firms.

After due evaluation of the proposals of several qualified groups, the international consortium IECO-ELC, formed by IECO International Engineering Company Inc. of San Francisco, U.S.A. and ELC Electroconsult Spa, of Milan, Italy, was selected. The contract was signed on November 18, 1970 and work actually started on February 1, 1971. The studies included field surveys, hydrological analyses, geotechnical investigations and a complete inventory of possible project alternatives,

which included ten possible dam sites and fifty different conceptual arrangements.

Layouts, comparative cost estimates and simulated operation studies of the alternative projects led to a preference for two alternative solutions as follows:

- A single dam at Itaipu island developing the entire potential at a single powerplant.
- Two dams, one at Itaipu island and the other at Santa Maria 150 km upstream, which would develop the potential by means of two powerplants, one at the foot of each dam.

Comparison between both alternatives clearly indicated the advantages of a single dam and powerplant at Itaipu island. This was duly acknowledged by the two governments, who finally selected it as the alternative to be adopted for construction, and instructed the engineering consortium to proceed with a complete feasibility study of the scheme with all the detail and thoroughness required for financing by international lending agencies.

The two governments decided also to proceed immediately with the implementation of the scheme.

THE ITAIPU TREATY AND CREATION OF ITAIPU BINACIONAL

THE BINATIONAL SPIRIT

For the Itaipu project to be successful, it was necessary that any conflicting issues associated with political and economic differences between the two countries be harmonized in a manner that would provide a well balanced participation of each country in the management and execution of the project. Each country would have equal weight in decision making and equal opportunity to supply labor, services, materials and equipment, limited only by its capability. These were the basic guiding principles of the Itaipu Treaty, and of the subsequent establishment of the administrative structure of ITAIPU BINACIONAL.

THE TREATY

As a culmination of the negotiations that started in 1966, the "Treaty between the Paraguayan Republic and the Federative Republic of Brazil for the

Acta
A los diez y siete días del mes de Mayo de mil novecientos setenta y cuatro, en ocasión de la entrevista del Excelentísimo Señor Presidente de la República del Paraguay, General de Ejército Alfredo Stroessner, con el Excelentísimo Señor Presidente de la República Federativa del Brasil, General de Ejército Ernesto Geisel, realizada en "Quinto Presidente Stroessner" y en "Foz de Iguazú" se procedió a la suscripción de la entidad binacional Itaipu creada por el Tratado del 26 de abril de 1973.
A dicho efecto, los señores Ministros de Relaciones Exteriores y de Obras Públicas y Comunicaciones del Paraguay, doctor Raúl Sapena Ovelar y General de División Juan S. Cáceres, juntamente con los señores Ministros de Estado de Relaciones Exteriores y de Minas y Energía, del Brasil, Embajador Antonio Francisco Sáenz de Silveira y doctor Shigehi Iku, pusieron en el ejercicio de sus respectivos cargos a los miembros del Consejo de Administración, señores doctores Alberto Vagstad, Enriquez González Alaina, General de División (S.A.) Mauro Corsia Baranetti, ingeniero Andrés Gómez, General de División (S.A.) Wilson dos Ramos Simoes, ingeniero Rogério Cardozo, Embajador Expedito de Freitas Almeida, ingeniero Mauro Penna Chiering, General de Brigada Carlos Fátis, ingeniero Lucas Nogueira Garcia, doctor Helio Marcos Penna Beltrão e ingeniero Marcos Moreira, a los Ministros del Ejecutivo Brasileño, Director General General José Costa Laroche, Director General Adjunto ingeniero Enzo Delbenardi, Director Técnico ingeniero John Kizinko Lotum, Director Técnico Adjunto ingeniero Thomás Keauch, Director Jurídico doctor Antonio Polman Rodriguez, Director Jurídico Adjunto doctor Paulo José Nogueira da Cunha, Director Administrativo doctor Victorino Silva Guimarães, Director Admona.

Brasilero Adjunto Economista Heitor Guimarães, Ministro, Director Financiero Professor Manoel Gut de Aguiar, Director Financiero Adjunto ingeniero Edmundo J. Cardoso, Director de Coordinación ingeniero Carlos H. Facetti y Director de Contabilidad Adjunto Coronel Carmo de Santa Feitos. En la misma oportunidad asistieron las funciones, a que se refiere la nota Personal sobre los asuntos de que tratan el Parágrafo Primero del Artículo VIII y el Artículo VIII del Tratado, para las cuales fueron designados los señores doctores Carlos Augusto Saldivar y Ministro José Hermes Pereira de Araújo. En testimonio de lo cual suscriben la presente Acta los Excelentísimos Señores Presidentes de la República del Paraguay y de la República Federativa del Brasil, así como también los Señores Ministros Representantes de las Altas Partes, basándose además los Consejeros y Directores mencionados.

Handwritten signatures and stamps:
- A large rectangular stamp with the text "Itaipu Binacional" and "Foz de Iguazú".
- Signature: "Gustavo Gaid"
- Signature: "Ricardo..."
- Signature: "Antonio..."

Handwritten signatures and stamps:
- A large rectangular stamp with the text "Itaipu Binacional" and "Foz de Iguazú".
- Signature: "Helio..."
- Signature: "Antonio..."
- Signature: "Ricardo..."
- Signature: "Antonio..."

Act of establishment
of ITAIPU
BINACIONAL

hydroelectric development of the hydraulic resources of the Paraná river belonging to both countries in condominium from and including the Salto del Guairá or Salto Grande das Sete Quedas to the mouth of the Iguaçu river", known as the Itaipu Treaty, was signed on April 26, 1973.

The Treaty has twenty-five articles and sets the regulations for the development of the hydraulic resources of the Paraná river and for the implementation of the project, essentially in accordance with the recommendations of the feasibility study.

The Treaty created a binational entity, named ITAIPU BINACIONAL (also called ITAIPU), with headquarters in Brasília and Asunción and the mandate to jointly and in condominium, build, own and operate the hydroelectric development at Itaipu island. The Treaty stipulates that the facilities for the production of electric power and the auxiliary works should not affect nor produce any modifications in the boundaries between Brazil and Paraguay.

- Annex A: defines the statutes of the binational entity known as ITAIPU, and establishes the administrative Board and the Executive Board of directors as its ultimate management bodies.

- Annex B: defines and describes the facilities for production of electric power and the auxiliary works, with eventual modifications, as may be necessary. The feasibility study served as the basis for this Annex.

- Annex C: defines the financial basis and arrangements for delivery of electric energy and services by ITAIPU.

THE OWNERSHIP OF ENERGY

In Annex C, the Treaty establishes the principle of equitable division of the energy to be produced, and it states that the electricity produced by Itaipu project will be divided equally between the two countries, with each having the right to purchase from ITAIPU the electric power not consumed by the other country for its own use.

Brazil and Paraguay purchase the power produced by Itaipu project through ELETROBRÁS and ANDE, or, at their discretion, through other Brazilian or Paraguayan entities on the basis of a ten year schedule of projected power, covering the total output of the project over that period.

THE PRICE OF ITAIPU ENERGY

The energy output of the project is sold at cost, as defined below. Each purchase is billed in US dollars on the basis of actual usage.

The Treaty defines the annual cost of production as the sum of:

1. Twelve % of the paid-in capital of ITAIPU.
2. Payments of principal and interest on the indebtedness of ITAIPU.
3. Monthly royalty payments for the use of hydroelectric resources, equal to US\$ 650 per gigawatt-hour generated, as measured at the power station. Such amount is to be not less than

US\$ 18 million annually and to be divided equally between Brazil and Paraguay.

4. Compensation for administrative and supervisory services provided by ELETROBRÁS and ANDE at the rate of US\$ 50 per gigawatt-hour generated, as measured at the power station. Such compensation is to be divided equally between ELETROBRÁS and ANDE.

5. Operating costs.

6. Monthly compensation by one country for energy ceded to the other country at the rate of US\$ 300 per gigawatt-hour assigned.

7. The prior year's operating deficit, or minus the prior year's surplus.

The values indicated in items 3, 4 and 6 above were established on the basis of 1973 prices, and are subject to readjustments in order to maintain their constant purchasing power.

Each purchasing agency contracts with ITAIPU for the purchase of fractions of the installed capacity and has the right to utilize all the energy that can be produced by such capacity, up to a limit to be established annually by ITAIPU, essentially on the basis of hydrological conditions.

MANAGEMENT STRUCTURE OF ITAIPU FOR THE EXECUTION OF THE PROJECT

ITAIPU BINACIONAL was established on May 17, 1974. Immediately thereafter, its Executive Board of Directors assumed responsibility for the continuation of the works previously initiated under the Joint Technical Commission. They also proceeded with the procurement of heavy construction equipment required for the excavation of the diversion channel, the design and construction of site infrastructure, the elaboration of engineering designs and specifications, and execution of construction.

As a result of a basic policy set by the two governments, contracts were awarded such that the material, equipment, goods and services necessary for the execution of the project were procured preferably in Brazil and Paraguay.

The overall management of all operations, including contracts for construction, procurement and supplies, planning and engineering, was the responsibility of the ITAIPU Executive Directorate. Field supervision of construction, surveys,

measurements, and laboratory testing were performed by ITAIPU personnel.

In view of the tight time schedule, ITAIPU decided initially to make use of the available experienced consulting engineering firms rather than setting up its own engineering structure. Several Paraguayan and Brazilian consulting engineering firms participated in the engineering design, jobsite planning and general construction.

ITAIPU BINACIONAL AND ITS ORGANIZATION

The management of ITAIPU is the responsibility of the Administration Council and the Executive Board of Directors, each composed of an equal number of members from Brazil and Paraguay.

The Administrative Council is composed of twelve members and is responsible for the performance and enforcement of the terms of the Treaty. It has authority over such matters as administrative procedures and policies, budgets, commitments and loans, and the basis for providing electric power and services.

The execution of the project and the day to day management of ITAIPU is carried out by the Executive Board and its Directors; each Director having specific functions established in the Statutes and Internal Regulations. The Executive Board is composed of twelve members who represent six Directorates, namely: General, Technical, Financial, Administrative, Legal and Coordination.

Each Directorate is headed by an Executive Director from one country and a Director from the other country, each having the same status on the Board and with equal authority and vote.

With this arrangement, representatives of each country have effective participation in decision making of their respective Directorates, as well as in the discussions that lead to decisions by the Board. This same principle prevails throughout the ITAIPU organization, assuring a balanced participation of both countries in decision making, management and effective execution of the project.

GENERAL ENGINEERING COORDINATION

ITAIPU decided to retain the consortium IECO-ELC as coordinator of engineering work for the following reasons:

- The binational nature of the project and the need to maintain an independent technical advice throughout its execution.

- To retain continuity between the basic project defined during the feasibility study and the elaboration of the detailed design to be done by the Brazilian-Paraguayan consortia.
- To implement a uniform set of criteria and quality standards throughout the project.
- To assure an integrated interfacing between the design work and the overall construction chronogram of the project.

ENGINEERING DESIGN

The following Paraguayan consulting engineering firms, formed a single group named Grupo Consultor Alto Paraná (GCAP) to assure participation in all features of engineering for the project: Bosio, Chase y Asociados S.R.L., Consultec S.R.L., Inconpar S.R.L., Paraconsult S.R.L. and Técnicar S.R.L.

For the engineering design, the following Brazilian firms formed four consortia with the Grupo Consultor Alto Paraná from Paraguay, and were contracted for the following tasks:

- Engevix Engenharia S.A. Final design and specifications for the spillway and the right wing buttress dam, including spillway gates and associated equipment.
- Promon Engenharia Ltda Final design and specifications for the main hollow gravity dam, including power intake equipment and penstocks.
- Themag Engenharia Ltda. Final design and specifications for the powerhouse and the equipment assembly areas, including powerhouse auxiliary equipment.
- Hidroservice Engenharia Ltda. Final design and specifications for the earthfill dams and the future navigation facilities.

All work by the above four consortia was performed under the general coordination of IECO-ELC, with the support of the Brazilian consortium formed by IESA - Internacional de Engenharia S.A. and Enerconsult Engenharia Ltda., and the Paraguayan consortium formed by ELC Electroconsult del Paraguay S.A., and CII Compañía Internacional de Ingeniería S.A.

In view of its experience, IECO-ELC was also assigned the following specific tasks: the designs and specifications for the diversion works and the rockfill dam, and the specifications and contract administration for the turbines, generators, main transformers and gas insulated switchgear (GIS). This work was also performed with the support of the two consortia mentioned above.

Many other consultants and specialists and institutions involved in model testing also participated when necessary, solving specific civil engineering problems, and aspects related to the design, manufacture and operation of the generating equipment; see Chapter 19.

CONSTRUCTION PLANNING

The consortium formed by the Brazilian group composed by Enge-Rio Engenharia e Consultoria S.A. and Logos Engenharia S.A. and the Grupo Consultor Alto Paraná from Paraguay, was responsible for the construction planning and assistance to ITAIPU's construction management.

CIVIL WORKS

Construction of the site accommodations and the infrastructure started in January 1975, and construction of the civil works commenced in May 1975.

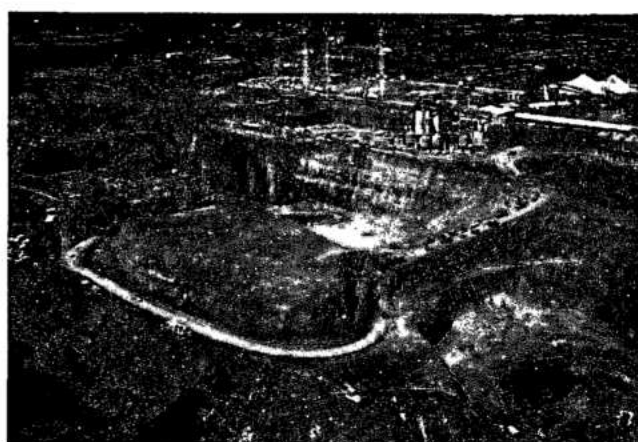
For construction of the civil works, ITAIPU pre-qualified and selected those Brazilian and Paraguayan firms which had extensive experience, qualified technical staff, specialized equipment and financial capacity. The civil works were contracted to the consortium UNICON-CONEMPA, which consisted of five large Brazilian contractors in joint-venture (UNICON): Cetenco Engenharia S.A., Companhia Brasileira de Projetos e Obras-CBPO, Camargo Correa S.A., Andrade Gutierrez S.A., and Mendes Junior S.A., and six Paraguayan contractors also in joint-venture (CONEMPA): Barrail Hermanos S.A. de Construcciones, Cia. General de Construcciones S.R.L., Compañia de Obras de Ingenieria de Obras S.R.L., Ing. Civil Hermann Baumann - Empresário de Obras Ing. Juan Carlos Wasmosy y Asociados, and Jimenez Gaona y Lima, Ingenieros Civiles - Empresa de Construcciones.

The contract for excavation of the diversion channel and for construction of the rockfill dam, the earthfill dams and the main cofferdams was awarded on October 6, 1975. The contract for the remaining civil works, comprising all the concrete structures, except for the four-unit powerhouse section in the diversion channel, was awarded on May 17, 1977. Work on the powerhouse in the diversion channel was done as an extension of the original contract and started in January 1986.

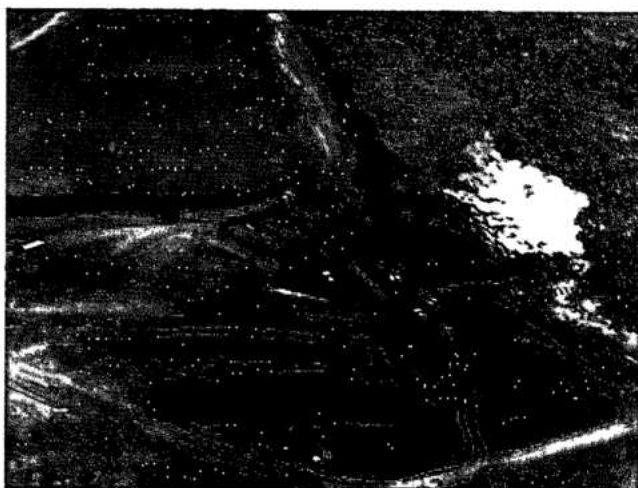
At the peak of the construction works, about 30 000 workers were employed at the site; they and their families were lodged in the several construction villages provided by ITAIPU on both sides of the river.



View of initial installations at site, showing access to the site



Beginning of civil works - excavation of diversion channel



Beginning of civil works - grading of spillway area



Initial construction villages

MANUFACTURE OF PERMANENT ELECTROMECHANICAL EQUIPMENT

Most of the equipment was manufactured in Brazil and Paraguay, with less than 20% imported from other countries. At one stage, almost every major manufacturer in Brazil and Paraguay was involved in the manufacture of heavy equipment for Itaipu.

The main permanent equipment was manufactured by the following companies:

- Generating units, including turbines and lower bend of penstocks, generators, isolated bus-bars, local control panels and motor control centers. Consortium CIEM, which consisted of six firms from Brazil: Bardella S.A. Indústrias Mecânicas, BSI - Indústrias Mecânicas S.A., Mecânica Pesada S.A. Siemens S.A., Voith S.A. Máquinas e Equipamentos; one firm from Paraguay: Consórcio de Ingeniería Electromecánica S.A. - CIE; formed by the following Paraguayan firms: Sague S.R.L., 14 de Julio S.R.L., Oti, Electromec S.A. Cotepa S.R.L. and Ing. Dorino da Re and seven firms from Europe: AG Brown Boveri & Cie. from Switzerland, Alsthom Atlantique, Creusot Loire and Neyrpic from France and Brown Boveri & Cie. AG, Siemens Aktiengesellschaft and J.M. Voith GmbH from Germany.
- Generator step-up transformers. Consortium CITRAM formed by Indústria Elétrica Brown Boveri & Cie AG S.A. and Transformadores União Ltda. - TUSA; and by Coemsa - Construções Eletromecânicas S.A.
- SF₆ gas-insulated 500 kV. switchgear and switching equipment. AG Brown Boveri & Cie.
- Centralized control system. Brown Boveri & Cie AG and Cie-Siemens AG.

- Diversion and water-intake gates. Mecânica Pesada S.A., Bardella S.A. - Indústrias Mecânicas, BSI - Indústrias Mecânicas S.A. and BVS - Bouchayer Viallet Schneider.
- Spillway gates. Badoni ATB Indústria Metal-Mecânica S.A., Coemsa - Construções Eletromecânicas S.A. and Ishibrás - Ishikawagima do Brasil Estaleiros S.A.
- Penstocks (excluding lower bend). Badoni ATP - Indústria Metal-Mecânica S.A.

Manufacturers of other important permanent equipment are listed in Chapter 19.

QUALITY CONTROL AND INSPECTION

Quality control of manufacturing was organized and executed by IECO-ELC. Factory inspections were made, under the auspices of IECO-ELC, by the following companies which comprised the ITAIPU inspection consortium: Themag Engenharia Ltda; Promon Engenharia Ltda; Barbosa & Mortara S/C Ltda; Engetest Serviços de Engenharia S/C Ltda; Hidroservice Engenharia Ltda; Engevix Engenharia S.A.; Berenhauer S.A. Engenharia, Consultoria e Projetos from Brazil and Electromon S.A. Consultoria from Paraguay.

ERECTION AND INSTALLATION OF ELECTROMECHANICAL EQUIPMENT

For erection and installation of the permanent equipment, the consortium ITAMON - Construções Industriais Ltda. was contracted. It was composed of eight Brazilian and one Paraguayan firms, as follows: A. Araújo S.A.-Engenharia e Montagens; EBE - Empresa Brasileira de Engenharia S.A.; Montreal Engenharia S.A.; SADE-Sul Americana de Engenharia S.A.; Sertep Serviços-S.A; Engenharia e Montagens; Technint-Companhia Técnica Internacional; Tenenge-Técnica Nacional de Engenharia S.A.; Ultratec Engenharia S.A., from Brazil, and Consórcio de Ingeniería Electromecánica S.A. - CIE of Paraguay.

The first Itaipu unit entered into commercial service in May 1984 and the eighteenth in April 1991.

PROJECT FEASIBILITY

STUDIES

STUDY OBJECTIVES AND PHASES OF THE STUDIES	2.3
PHASE 1	2.5
Hydrologic Studies	2.5
Alternative Sites	2.11
Geological Reconnaissance	2.12
Conclusions of Phase 1	2.15
PHASE 2	2.15
Final Comparison	2.15
PHASE 3	2.17
PHASE 4	2.17
Hydrology	2.17
Spillway Design Flood	2.20
Flood Frequency Studies	2.23
Powerplant Installed Capacity	2.25
Model Tests of River Regulation and Navigation Facilities	2.29
Main Generating Units	2.30
Dual Frequency	2.32
General Arrangement	2.35
Spillway	2.35
Dams	2.36
Powerhouse	2.40

PROJECT FEASIBILITY STUDIES

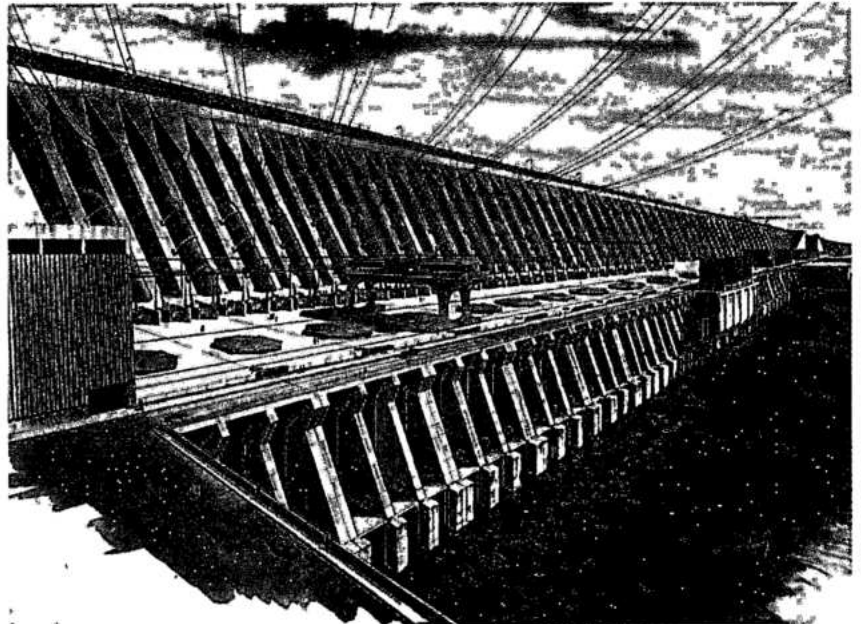
STUDY OBJECTIVES AND PHASES OF THE STUDIES

The comprehensive economic and technical feasibility studies for the optimum development of the power potential of the 190 km bi-national reach of the Paraná river were performed during 1971-74. The principal objectives of the studies were to:

- Determine the exploitable energy potential;
- Inventory the more favorable project sites, make preliminary layouts and evaluate their relative feasibility;
- Prepare a rational plan of development comprising projects which were economically and technically the most attractive;
- Determine the cost of the recommended plan, a tentative schedule for its implementation, and the cost of energy produced.

The feasibility studies were conducted in four phases:

Phase 1. Classification and analysis of existing information and the acquisition of additional pertinent data regarding: meteorology, rainfall, streamflow, sedimentation, topography, geological and geotechnical conditions, availability of construction materials and transportation. Identification of project sites suitable for partial or full utilization of the 120 m head in the bi-national reach of the river.



*Preliminary
conception of Itaipu
powerhouse*

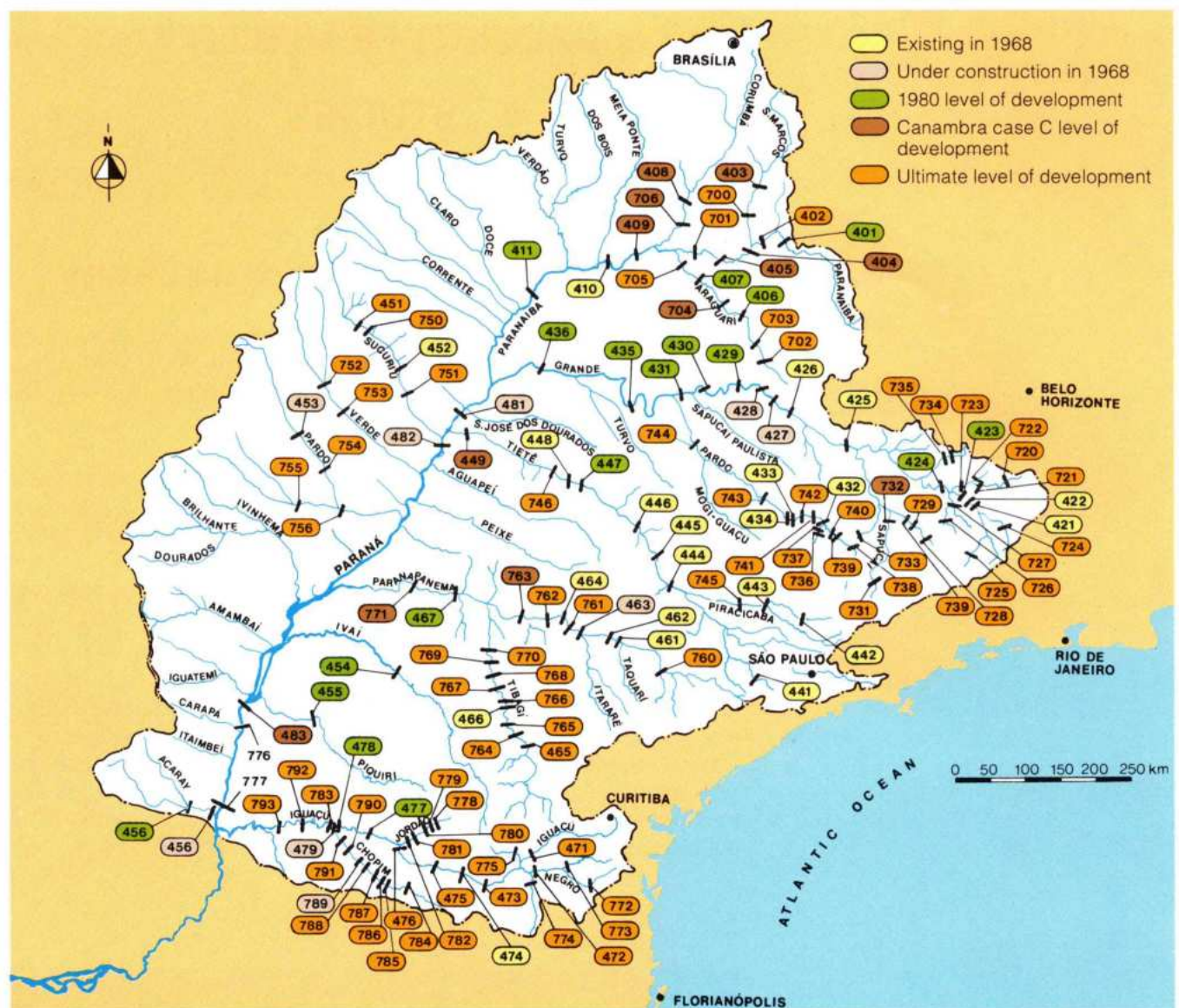


Fig. 2.1 Major reservoirs and powerplants in 1971 (in operation, under construction or planned) in the Paraná Basin

777 Itaipu	475 Areia	782 Fundão	768 Almoço
776 Santa Maria	474 Salto Grande	781 Jacú	767 Apucarantina
456 Acaray	473 Langa	780 Pinhão	766 Ximbuva
456 Yguazu	471 São Mateus	779 Curucaca	466 Presidente Vargas
483 Ilha Grande	775 Pontilhas	778 Taguá	765 Salto Aparado
793 Capanema	774 Jangada	455 Salto dos Apertados	764 Salto Conceição
792 Salto Caxias	472 Três Barras	454 Ivatuba	465 Santo Antônio
783 Cruzeiro	773 Barracas	771 Taguaruçu	482 Jupia
478 Salto Osório	772 Rio Negrinho	467 Capivara	449 Três Irmãos
477 Salto Santiago	479 Foz do Chopim	763 Porto Canoas	746 Rui Barbosa
476 Segredo	791 Erveira	762 Porto Leopoldina	448 Avanhandava
	790 Águas do Vere	464 Salto Grande	447 Promissão
	789 Salto Chopim	463 Xavantes	446 Ibitinga
	788 Salto Grande	462 Piraju	445 Bariri
	787 Salto Alemão	461 Jurumirim	444 Barra Bonita
	786 São João	760 Confluência	745 Piracicaba
	785 São Luís	770 Jataizinho	443 Americana
	784 Cel. Soares	769 Cebolão	442 Jaguari

Phase 2. Analyses of the technical and economic aspects of the identified possible sites using preliminary project layouts. Ranking the alternative sites and projects on the basis of their economic benefits and technical advantages. At a pre-feasibility level, formulation of the optimum development plan, complete with preliminary project layouts, designs and cost estimates.

Phase 3. Evaluation of the recommended development plan by the Brazilian-Paraguayan Joint Technical Commission, and selection of the project scheme for further detailed feasibility studies.

Phase 4. Comprehensive feasibility study of the chosen scheme to standards considered adequate by international financing institutions and the Joint Technical Commission. Preliminary project layouts were refined, types of major structures were confirmed and the installed capacity of the powerhouse was established on the basis of reservoir operation and power studies. A practical schedule for implementation of the project was prepared and included in the final feasibility report.

PHASE 1

HYDROLOGIC STUDIES

General

The Rio Paraná begins at the confluence of the Rio Paranaíba and the Rio Grande. The distance from the confluence to Guaíra, at the entrance to Itaipu reservoir, is about 600 km, and the river slope for this reach is very flat, falling only 30 m in 500 km from Jupiá to Guaíra. Thereafter, the river dropped about 80 m in a series of cascades over 15 km to Santa Maria. The river gradient from Santa Maria was more moderate, the drop being 75 m over 175 km to the mouth of the Iguaçu river.

In 1971 the upper Paraná basin was already well developed. Fig. 2.1 shows the major reservoirs and powerplants which were then either operating, or under construction or planned for the future in the Paraná basin upstream of Itaipu and in the Iguaçu river basin. The drainage areas of the major tributaries and along the Paraná river are shown in Table 2.1.

441 Itupararanga	427 Estreito	723 Inferno	410 Cachoeira Dourada
756 Indaiá	426 Peixoto	722 Palmital	409 Itumbiara
755 Inhanduí	425 Furnas	721 Cassiterita	701 Anhanguera
754 Piracanjuba	733 Poço Fundo	720 Carandaí	405 Emborcação
453 Mimoso	732 Sapucaí	744 São Bartolomeu	404 Cachoeira do Sertão
753 Água Clara	730 Boa Vista	743 Itaipava	402 Bacaina
752 São Domingos	729 Penedo	434 Limoeiro	401 Escada Grande
751 Porto Caleano	728 Lambari	433 Euclides da Cunha	706 Fecho da Onça
452 Inocência	735 Anil	742 São José	408 Corumbá
750 Porto das Pedras	734 Jacaré	741 Carrapatos	705 Tupaciguara
451 Alto Sucuriú	424 Funil	432 Graminha	407 Capim Branco
481 Ilha Solteira	423 São Miguel	737 Cascata	407 Capim Branco
436 Água Vermelha	422 Itutinga	736 Bauxita	704 Miranda
435 Marimbondo	421 Camargos	740 Carmo	406 Nova Ponte
431 Porto Colômbia	724 Garambu	739 Bandeira	703 Pai Joaquim
430 Volta Grande	727 Itumirim	738 Açude	702 Perdizes
429 Igarapova	726 Luminárias	731 Euclides	700 Anta Gorda
428 Jaguará	725 Aiuruoca	411 São Simão	403 Paulistas

Table 2.1 Drainage area for major tributaries in the Paraná Basin

River	Location	Drainage area (km ²)
Paranaíba	Mouth	221 800
Grande	Mouth	144 700
Tietê	Mouth	71 600
Paraná	Jupia	474 000
Paranapanema	Mouth	99 900
Paraná	Below Ivaí mouth	751 000
Paraná	Guaíra	800 000
Paraná	Itaipu site	820 000
Iguaçu	Mouth	68 700
Paraná	Below Iguaçu mouth	899 000
Paraná	Posadas	932 900

The hydrological studies considered three levels of development in the Paraná basin:

- Through 1980.
- Intermediate stage.
- Ultimate development.

The intermediate stage included storage and regulation by all future projects costing less than \$300/KW (1964 costs), representing about 80% development of the total basin potential. Basic data were obtained from the comprehensive studies of the hydroelectric resources of south-central Brazil made by Canambra Engineering Consultants, Ltd. during 1962-69. The ultimate development condition included all feasible projects and essentially complete regulation of the upper Paraná river and its tributaries. In 1972, there were forty dams and reservoirs upstream of Itaipu. With ultimate development, there will be over 130 projects in the Paraná and Rio Iguaçu basins.

Significant regulation of streamflow in the Rio Grande basin commenced in November 1956 with the completion of Peixoto dam, followed by Camargos dam in September 1960 and storage in the large Furnas reservoir in January 1964. On the Rio Tietê, regulation began in October 1962 with the completion of Barra Bonita dam, and on the Rio Paranapanema it commenced with Jumirim dam in February 1963.

The large Ilha Solteira and Jupia reservoirs on the Paraná were filled by January 1969.

Streamflow data

In addition to the comprehensive studies of the hydropower potential of south-central Brazil by Canambra Engineering Consultants, several other

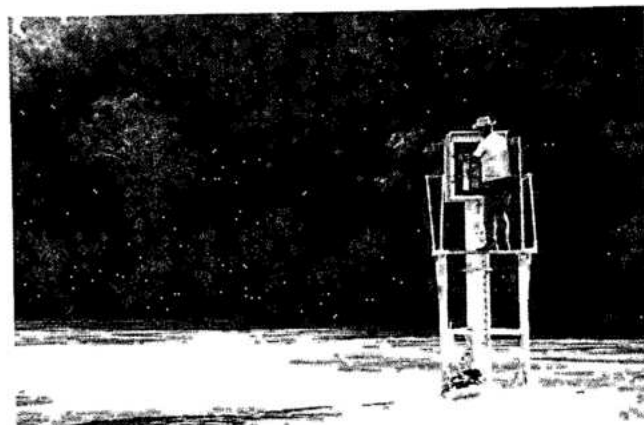
studies of the Paraná near Guaíra and the bi-national stretch were made by other engineering entities.

On the Paraguayan side, starting in 1959 considerable work was done on planning and feasibility studies for power development of the Rio Acaray, which culminated in 1968 with the construction of the Acaray reservoir and powerplant just above Ciudad del Este, where the plant discharges into the Paraná. The large amount of hydrologic and reservoir operation data from the previous studies and existing projects were analyzed and incorporated into the basic data for the Itaipu feasibility studies. Only the water level and discharge data from selected gaging stations which had the longest records and represented good areal coverage were used. Fig. 2.2 shows the location of the stream gaging stations and the bar chart of Fig. 2.3 indicates the length of the records and types of data available for each station.

Additional records were available starting 1965 from gages at Acaray power station and Puerto Embalse. As an independent check IECO-ELC in March 1971 established the additional gages shown in Fig. 2.2.

Establishment of an accurate rating curve for the Paraná river in the potential project area was essential, measurements taken at Guaíra thus being the most important of all available data.

Discharge measurements at Guaíra had been made by Hidroservice from 1963 to 1968 leading to the rating curve designated CORESP Curve A, see Fig. 2.4. Centrais Elétricas de São Paulo (CESP) measured discharge from 1969 and developed the CESP Curve B shown also in Fig. 2.4. Additional discharge measurements were made by the company Hidrologia for IECO-ELC during the period February-August 1972. These measurements were made with a propeller type current meter suspended on a weighted line from a boat. Measurements were taken at more than twenty stations across the river with at least six vertical points at each



Discharge measurements



五



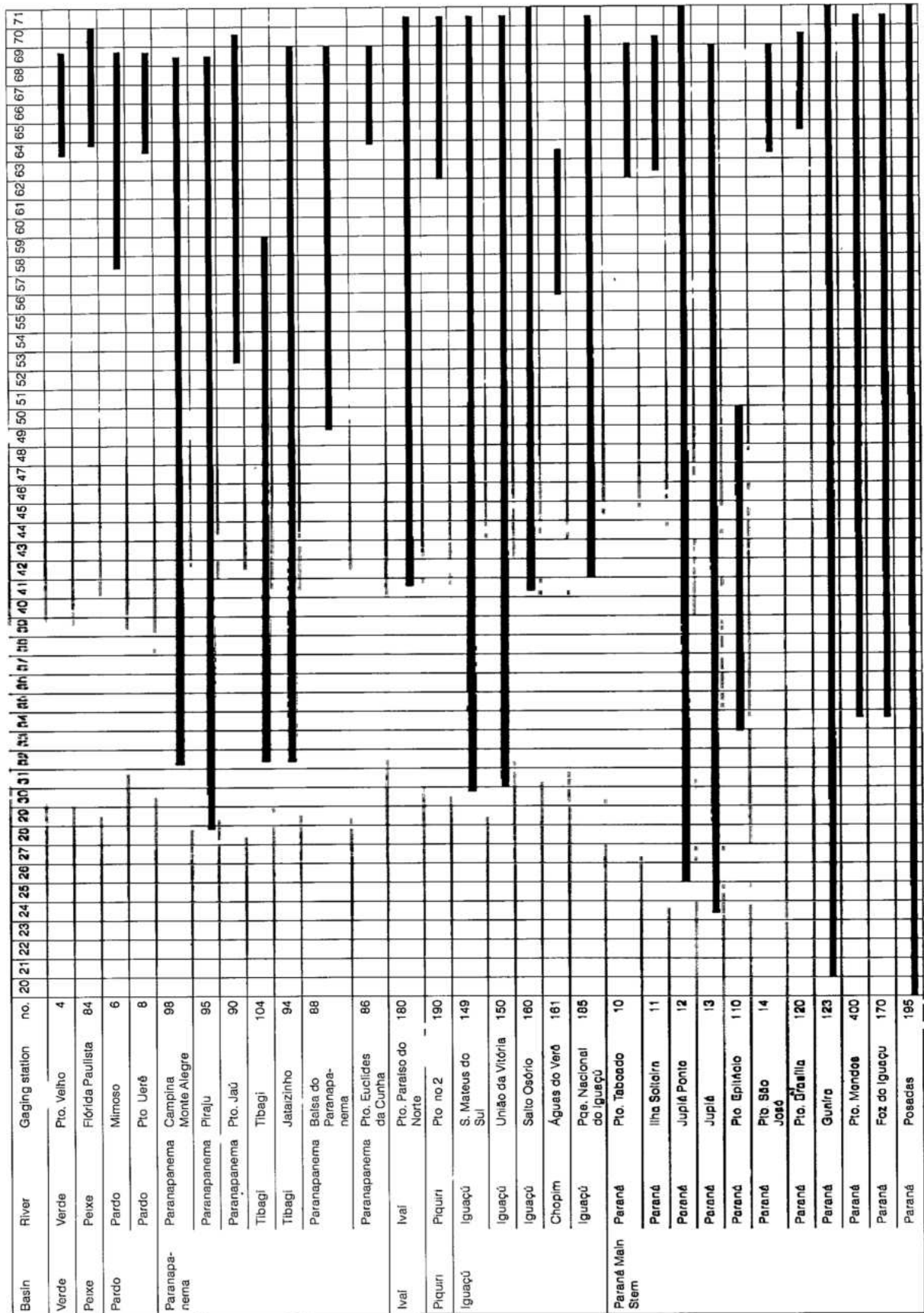


Fig. 2.4 Discharge at Guaira

Y Gage height at Guaira (m)
 X Discharge at Guaira ($10^3 \text{ m}^3/\text{s}$)
 1 Curve A (CORESP)
 2 Curve B (CESP)

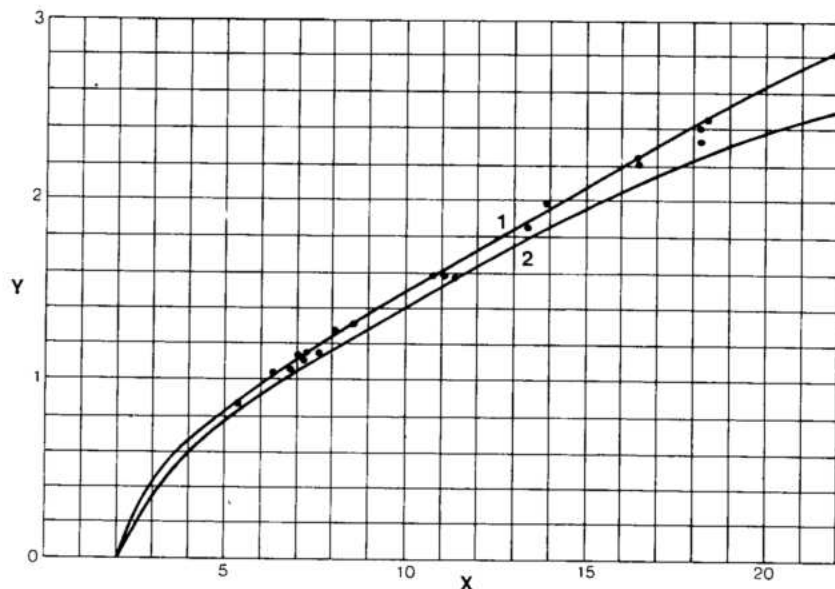


Table 2.2 Average annual natural flow in the upper Rio Paraná basin (water-years 1932-1969)

Site no.	River and location	Drainage area (km ²)	Flow	
			m ³ /s	l/s/km ²
441	Paranaíba at São Simão	171 000	2198	12.8
436	Grande at Água Vermelha	139 900	1901	13.6
449	Tietê at Três Irmãos	70 600	571	8.1
452	Sucuriú at Inocência	16 300	182	11.2
482	Paraná at Jupiá	474 000	5590	11.8
771	Paranapanema at Porto Taquaruçu	88 000	940	10.7
454	Ivaí at Ivatuba	23 300	307	13.2
483	Paraná at Guaíra	800 000	8740	10.9
777	Paraná at Itaipu	820 000	9070	11.0

The mean annual natural flows thus obtained for the key locations of the upper Rio Paraná basin are shown in Table 2.2.

Regulated flows

The monthly regulated flows at Guaíra were determined from a monthly operation study of each reservoir in the basin. Each of the three levels of development were studied. Monthly regulated flows of the Rio Iguaçu were determined in a similar manner. Each reservoir upstream of the project site

was operated independently to draw it down to the minimum allowable storage at least once during the 38-year study period 1932 to 1969. The operation studies of the upstream reservoirs were examined for incremental flow inconsistencies. Flow balance and minor adjustments were made, as necessary, to ensure that the total of the incremental area flows at the upstream sites equaled the Guaíra gage flows.

The operation studies ended on the Rio Paraná at Guaíra, resulting in regulated inflows to the proposed Ilha Grande reservoir. Regulated flows of Rio Iguaçu and Rio Acaray were combined with natural flows from

Table 2.3 Average inflow at Ilha Grande/Guaíra for water-years 1932-1969 (m^3/s)

Level of development	Averages for water-years 1932-1969	Maximum		Minimum	
		Water-year	Month	Water-year	Month
Natural	8740	12 090	23 520	5720	3040
1980	8680	11 950	23 830	5990	4180
Intermediate	8540	11 740	23 410	6160	4450
Ultimate	8560	11 880	23 540	6130	4470

the area below the project site to a point below the mouths of Rio Acaray and Rio Iguaçu. The regulated flows were then used in the operation studies, and also for obtaining tailwater levels at the project site.

Monthly and annual flows at Guaíra for the natural condition and for the three levels of development are summarized in Table 2.3.

Sedimentation and water quality

For the phase 1 and phase 2 studies sufficient sedimentation and water quality data were available from existing records. Sedimentation data were available from sampling in 1963 on the Rio Grande at Porto José Américo (Sta. 303), Rio Tietê at Lussanvira (Sta. 22), Rio Paraná at Porto Taboado (Sta. 10), and Rio Paraná at Guardia Cué (below Posadas), and water quality in the lower River Paraná was known from samples taken during 1958 to 1962 at Corrientes and Posadas.

Meteorological data

Data from all meteorological stations were gathered and screened for validity and a network of meteorological

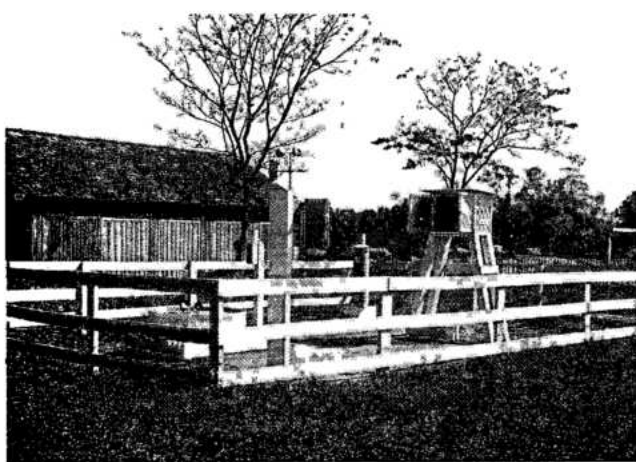
stations was selected for use in the feasibility study, see Fig. 2.5. The type of information available for each station included atmospheric pressure, temperature, relative humidity, cloud cover, precipitation, evaporation, and sunshine hours. In addition, detailed summary of meteorologic data at Guaíra and the two Acaray powerplants were collected.

A new meteorological station was established at Salto del Guairá in January 1973 with the following instruments: piche evaporimeter, evaporation pan, recording rain gage, psychrometer, maximum-minimum thermometer and recording anemometer. When the Santa Maria damsite was eliminated as a possibility these instruments were moved to the Itaipu site.

Wind data were available for the project site from measuring stations at Ciudad del Este, Puerto Presidente Franco and Foz do Iguaçu.

ALTERNATIVE SITES

Fig. 2.6 shows the profile and plan of the bi-national portion of the Rio Paraná and the location of the following ten sites at which power developments were studied at an inventory level: Guaíra, Santa Maria, Laguna Verá, Alex Gage, Arroio Guaçu, Porto Mendes, São Francisco Verdadeiro, Itaipu, Puerto Embalse and Ilha Acaray. Fifty project layouts were studied and combined into power development schemes which were compared at a uniform level of detail and accuracy. They consisted of a single installation, or a two or a three-site combination necessary to develop the full head between maximum normal upper site reservoir El.220 and average lower site tailwater El.105; during later definitive studies, average lower site tailwater level was determined to be El.100. Project comparison indices were determined for each of the schemes. Schematic profiles of eight of the more suitable alternative schemes are shown in Fig. 2.7.



Meteorological station

Table 2.3 Average inflow at Ilha Grande/Guaíra for water-years 1932-1969 (m^3/s)

Level of development	Averages for water-years 1932-1969	Maximum		Minimum	
		Water-year	Month	Water-year	Month
Natural	8740	12 090	23 520	5720	3040
1980	8680	11 950	23 830	5990	4180
Intermediate	8540	11 740	23 410	6160	4450
Ultimate	8560	11 880	23 540	6130	4470

the area below the project site to a point below the mouths of Rio Acaray and Rio Iguaçu. The regulated flows were then used in the operation studies, and also for obtaining tailwater levels at the project site.

Monthly and annual flows at Guaíra for the natural condition and for the three levels of development are summarized in Table 2.3.

Sedimentation and water quality

For the phase 1 and phase 2 studies sufficient sedimentation and water quality data were available from existing records. Sedimentation data were available from sampling in 1963 on the Rio Grande at Porto José Américo (Sta. 303), Rio Tietê at Lussanvira (Sta. 22), Rio Paraná at Porto Taboado (Sta. 10), and Rio Paraná at Guardia Cuê (below Posadas), and water quality in the lower River Paraná was known from samples taken during 1958 to 1962 at Corrientes and Posadas.

Meteorological data

Data from all meteorological stations were gathered and screened for validity and a network of meteorological

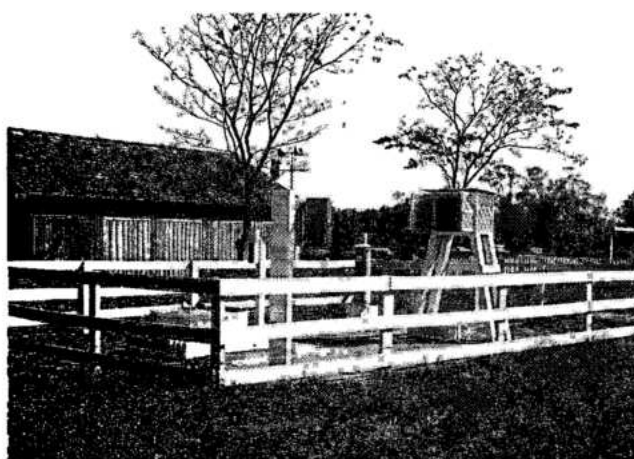
stations was selected for use in the feasibility study, see Fig. 2.5. The type of information available for each station included atmospheric pressure, temperature, relative humidity, cloud cover, precipitation, evaporation, and sunshine hours. In addition, detailed summary of meteorologic data at Guaíra and the two Acaray powerplants were collected.

A new meteorological station was established at Salto del Guairá in January 1973 with the following instruments: piche evaporimeter, evaporation pan, recording rain gage, psychrometer, maximum-minimum thermometer and recording anemometer. When the Santa Maria damsite was eliminated as a possibility these instruments were moved to the Itaipu site.

Wind data were available for the project site from measuring stations at Ciudad del Este, Puerto Presidente Franco and Foz do Iguaçu.

ALTERNATIVE SITES

Fig. 2.6 shows the profile and plan of the bi-national portion of the Rio Paraná and the location of the following ten sites at which power developments were studied at an inventory level: Guaíra, Santa Maria, Laguna Verá, Alex Gage, Arroio Guaçu, Porto Mendes, São Francisco Verdadeiro, Itaipu, Puerto Embalse and Ilha Acaray. Fifty project layouts were studied and combined into power development schemes which were compared at a uniform level of detail and accuracy. They consisted of a single installation, or a two or a three-site combination necessary to develop the full head between maximum normal upper site reservoir El.220 and average lower site tailwater El.105; during later definitive studies, average lower site tailwater level was determined to be El.100. Project comparison indices were determined for each of the schemes. Schematic profiles of eight of the more suitable alternative schemes are shown in Fig. 2.7.



Meteorological station



Fig. 2.5 Selected network of meteorological stations (numbers refer to the sites selected at feasibility stage)

GEOLOGICAL RECONNAISSANCE

Geologically, the lower Rio Paraná basin comprising eastern Paraguay and parts of southern Brazil, is remarkably uniform. In the bi-national reach of the river rock formations of mainly the Jurassic, Triassic and Cretaceous ages were encountered. Among these, the Serra Geral formation of volcanic rocks which lie in the relatively uniform and mainly subhorizontal layers were found at the various project sites investigated during the feasibility studies.

Field reconnaissance of the river banks and the potential sites, indicated that generally the massive basalts had excellent mechanical properties and would be suitable both as foundations and as construction material. However, the breccia and agglomerate, which were also present in continuous layers within the Serra Geral formation, were relatively weak and heterogeneous and would require thorough investigation regarding their suitability.

The abundance of impervious silty or clayey residual soils derived from weathered basalt, which

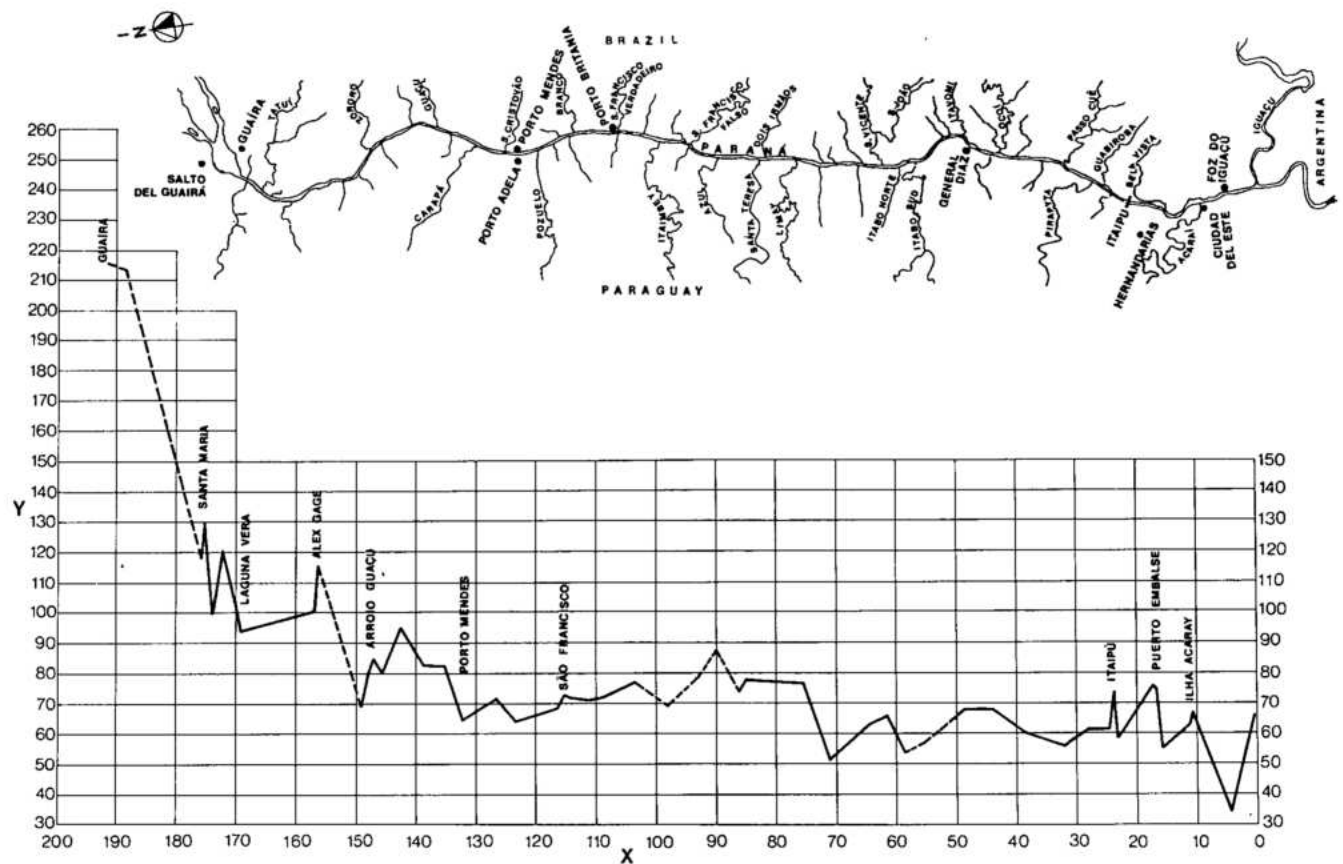


Fig. 2.6 Plan and profile of binational reach of Rio Paraná

Y Elevation (m)

X Distance (km)



Geological field reconnaissance

would be suitable for embankment dams, was also confirmed near all potential project sites by early reconnaissance. On the other hand, natural high quality gravels were not found in sufficient quantities along the river or in higher terraces on the banks. Natural sand deposits were found at several locations, but their suitability would need to be assessed for each project site taking into consideration the cost of transportation.

Investigations at study sites

During the first phase of the feasibility study, geological data were analyzed in equal detail for the ten potential project sites included in the inventory. The data were obtained from site reconnaissance, geophysical survey in the river channel, exploratory trenches, and rotary drilling. For each site, criteria for depth of excavation, stable slopes and foundation treatment were developed for use in project layouts and for estimating quantities of work and costs.

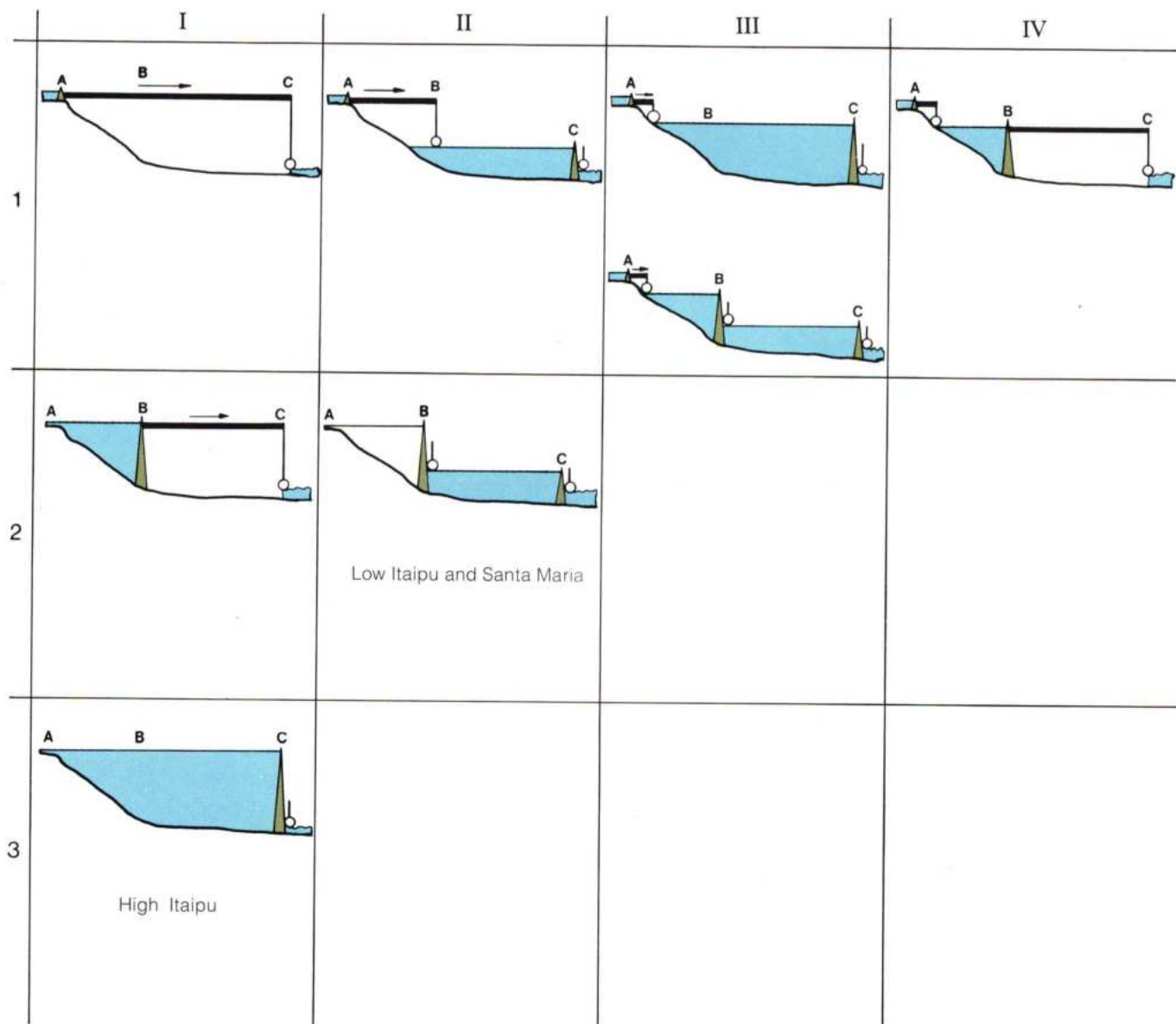


Fig. 2.7 Schematic profiles of the eight more suitable alternatives

I Site 1- Power development at Acaray

II Site 2 - Power development at Pto.Mendes and Acaray

III Site 3 - Power development at Guaira and Acaray

IV Site 4 - Power development at Guaira, Pto.Mendes and Acaray

A Guaira


B Pto.Mendes

C Acaray

1 Scheme 1- Upstream - most dam at Guaira (dam, either across the falls or extending to right side of Ilha Grande powerhouse)

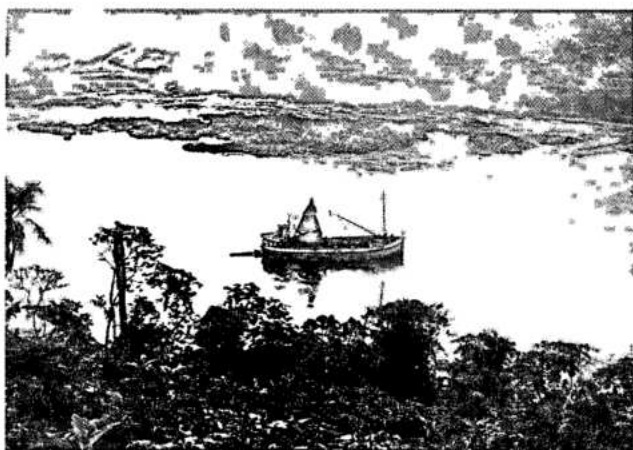
2 Scheme 2 - Upstream - most dam at Pto.Mendes

3 Scheme 3 - Upstream - most dam at Acaray

 Dams and reservoirs

 Powerhouses

 Power canals



Geophysical survey in river channel at Itaipu island

CONCLUSIONS OF PHASE 1

Phase 1 concluded that two alternatives, namely the single-dam scheme with the High Itaipu project and the two-dam scheme with the Low Itaipu and Santa Maria projects, were determined to be economically superior to all other alternatives and suitable for further detailed study of phase 2.

PHASE 2

Following the initial investigation of phase 1 the two chosen alternative sites were examined in detail. Hydrology, geology and economic considerations were studied as follows.

Reservoir operation and power studies were made for determining the reservoir storage, height of dam, size of spillway, the installed capacity and the energy output at the Santa Maria and Itaipu sites. The results of the operation studies were crucial to the comparison and selection of the most economic project alternatives.

For the two-dam scheme, normal maximum reservoir level was established at El.220 for Santa Maria and at El.180 for Itaipu. For the single-dam scheme at the Itaipu site, normal maximum reservoir elevation was established at El.220. All studies were based on values of prime power and dependable capacity corresponding to maximum upper reservoir drawdown to El.197. Operation studies for other intermediate drawdown cases, including no drawdown or run-of-river, were also made. For all cases studied, prime power was greater for the single-dam than the two-dam scheme. The operation studies, together with other economic and technical considerations, indicated that for the single-dam scheme, the total installed capacity was in the range of 10 700 MW to 15 300 MW. For the two-dam scheme with equivalent total output, the installed capacities at Santa Maria and Low Itaipu were about 2400 to 3700 MW and 7760 to 9900 MW, respectively.

FINAL COMPARISON

The summary of results of the preliminary comparative feasibility studies for the two schemes selected for detailed analyses are given in Table 2.4.

During the second phase, when the study was narrowed to the two most favorable sites, namely Santa Maria and Itaipu, extensive land and

Table 2.4 Summary of preliminary comparative results - 1972

Basic data	Unit	Selected schemes			
		Single dam	Two dams		
		High Itaipu	Low Itaipu	Santa Maria	Total
Dam height	m	171	131	92	
Normal water level					
Reservoir	m	220	180	220	
Tailwater	m	100	100	180	
Installed capacity	MW	10 710	7755	2385	10 140
Reservoir area	km ²	1350	140	42	182
Reservoir capacity	10 ⁶ m ³	29 000	4980	440	5420
Spillway capacity	m ³ /s	58 000	61 400	61 400	
Estimative capital cost (including 230-kV swyd.)	10 ⁶ US\$	2033	1663	826	2489
Cost of installed generation capacity	US\$/kW	190	214	346	245
Cost of 765-kV switchyard and other facilities *	US\$/kW	14.5			22.9

* Without transmission line cost

river-channel geophysical surveys, grouting tests, excavation of exploratory trenches and test pits were performed at the two sites over a reach of 6 km from and including Itaipu Island. Additional exploration included tunnels and in-situ rock mechanics tests.

With respect to engineering feasibility of projects proposed at the two sites, the geological investigations provided the following conclusions:

- All basalt and breccia flows at both sites were easily correlated on both banks of the river, indicating that no major faults were present in the river channel or in other project areas.
- Water loss tests indicated that the dense and vesicular basalts had very low permeability. However, the contact areas and breccia layers had low to very high permeability.
- The physical and mechanical properties of the sound basalt were adequate for the foundations of all proposed concrete structures.
- While the strength of sound breccia was not as high as that of basalt, with proper selection and treatment it would provide suitable foundations for most concrete structures.
- Special treatment, including drainage galleries, would be required to control seepage and uplift in certain contact zones.

- At higher elevations above the river, where the topography was of general relief, the basalt and breccia had weathered into reddish clayey and silty residual soil and saprolite up to 35 m deep.

- The residual soils above the water table were of low in-place density. Therefore, wing dams would have to be earthfill embankments with very flat slopes.

The studies also compared in greater detail the geological conditions at the Santa Maria and Itaipu sites with respect to foundation treatment, excavation, disposal of excavated material and the adequacy of the site materials for construction. The general conclusion was that while almost all concrete dams at Itaipu would be founded on sound basalt with 3 to 6 m of excavation, at Santa Maria deeper excavation and more extensive treatment would be required to obtain suitable rock foundation.

Since initial studies of river diversion compared open channels and tunnels at the Santa Maria and Itaipu sites, the geological studies also developed the criteria for tunnel supports, excavation sequences, blasting techniques, slopes, and height and width of benches. These criteria were used in the construction planning and scheduling studies, and in the comparative cost estimates.

The studies indicated the following advantages and disadvantages of the two chosen alternatives:

Single-dam scheme – High Itaipu project. In addition to favorable economic factors, the High Itaipu project had several other features and characteristics which indicated its superiority over the other alternative with two dams and powerhouses.

Foundation conditions for the main dam and powerhouse in the river channel at the Itaipu site were generally superior to the Santa Maria site and were physically adequate for any type of high dam.

Because of Itaipu Island and relatively shallow channels for about 1 km, river diversion at Itaipu would be easier and less risky than at Santa Maria site.

Access by road along both banks or by barge would be better and more economical at Itaipu than at Santa Maria site. Existing unpaved, but passable roads linked the Itaipu site with the main highway at the International Bridge between Ciudad del Este and Foz do Iguaçu. Access by barge to Santa Maria would be prevented by rapids above Porto Mendes.

The High Itaipu reservoir would capture and regulate up to 75% of the Rio Paraná basin runoff at the lower end of the study reach. The single large reservoir at Itaipu would have the capability for better and more flexible river regulation than the two smaller reservoirs.

With the High Itaipu project, the peak inflow of the probable maximum flood would be reduced from 72 000 m³/s to an outflow peak of about 62 600 m³/s after the flood is routed through the reservoir utilizing 3 m of storage above the normal maximum pool.

The two smaller reservoirs would have a much lower flood attenuation capability.

Installed powerplant capacity at High Itaipu would be about 5.5% greater, and prime power about 33% greater than for the Santa Maria–Low Itaipu combination.

The High Itaipu concrete dam layout would be able to accommodate the entire powerhouse at the toe of the dam. At the same time, the layout would permit further expansion of the powerplant in the distant future at minimum expense and without interruption of power operation.

Two-dam scheme – Low Itaipu and Santa Maria projects. The Low Itaipu dam would develop the site to a lower level than High Itaipu. Site characteristics would be identical. Power development costs would be higher because of the much lower head and the detrimental effect of tailwater fluctuations which would further reduce the head.

Although foundation and river diversion conditions were not as good as at the Itaipu site, the Santa Maria site was considered adequate for the type and size of

proposed project structures. Its location was more remote, and providing access would have been considerably more expensive than for the Itaipu site.

Singly or in combination, the unit costs of power development at these two sites were higher than for High Itaipu. This was partly because: costs of river diversion and spillways would be duplicated; net heads would be lower and power installation costs higher; and Santa Maria site costs would be higher than a similar development at Itaipu because of topography, geology and riverflow conditions.

PHASE 3

The report on the preliminary feasibility study was presented in early 1972 to the Joint Technical Commission. The Commission accepted the recommendation of the report and selected the High Itaipu project (thereinafter called Itaipu) for further detailed feasibility and confirmation studies in phase 4.

PHASE 4

The definitive analyses of the two best alternatives conclusively established that the single dam scheme would provide the highest installed capacity at the lowest cost per kW. Thereafter, the final phase of the studies was to evaluate and confirm the economic and technical feasibility of the Itaipu project.

A draft of the final feasibility report was presented to the Joint Technical Commission in early 1973, when the decision to proceed with the scheme was taken, leading to the signing of the Itaipu Treaty on April 26, 1973. The final report was presented by IECO-ELC in July 1974 and incorporated the following.

HYDROLOGY

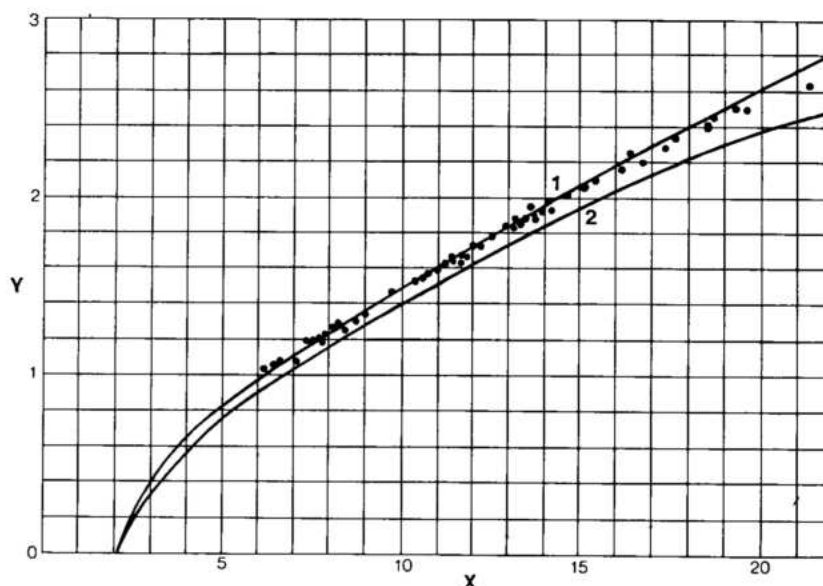
Hydrological studies started in phase 1 were continued with further refinement of the data for the chosen solution.

Guaíra rating curves

An essential component in computing streamflow conditions at the Itaipu site was the Guaíra rating

Fig. 2.8 Guaíra gaging station discharge measurement plot

Y Gage height at Guaíra (m)
 X Discharge at Guaíra ($10^3 \text{ m}^3/\text{s}$)
 1 Curve A (CORESP)
 2 Curve B (CESP)



curve, the accuracy of which was in doubt. Additional discharge measurements, similar to those taken by Hidroservice, were made by IECO-ELC starting in August 1972. In June 1973 and later in October 1973 combined discharge measurements to allow direct comparison of measurement techniques and accuracy of equipment were made by CESP and IECO-ELC on subsequent days. All current meters used were laboratory calibrated before the tests. The final results are shown in Fig. 2.8, based upon which, for final power studies curve A was used.

Itaipu tailwater rating curves

Water levels at Itaipu are a function of the flows in the Rio Paraná and the Rio Iguaçu, which enters the Rio Paraná immediately downstream of Foz do Iguaçu. The backwater effect of Rio Iguaçu flows extended upstream beyond Porto Mendes, leading to recorded variations at the Foz do Iguaçu gage of up to 38 m. Above Porto Mendes the river became steeper and the backwater effect gradually disappeared, the measurement at the Santa Maria site showing a direct relationship with discharge at Guaíra.

Thus an accurate knowledge of the expected range of discharge of the Iguaçu river was essential in determining the Itaipu tailwater rating curves. Discharge measurements were made at Poço Preto (Rio Iguaçu) by Hidrologia between April and August 1972, and additional measurements were made by IECO-ELC at the same location, beginning January 1973. Concurrent water level at Foz do Iguaçu and discharge for the Paraná at Guaíra were available for the period 1934 to 1973. Poço Preto discharge measurements were extended by

regression techniques using previous recorded discharges upstream at Aguas do Vere (Rio Chopim) and Salto Osório, to obtain a full daily flow record for the Iguaçu river for the period December 1940 to May 1973. Discharge in the Paraná at Foz do Iguaçu was estimated by combining the Guaíra discharge routed to Foz do Iguaçu with incremental flow from the area between Guaíra and Foz do Iguaçu (excluding Rio Iguaçu). The data thus obtained produced a set of rating curves for the Foz do Iguaçu station for various flows in the Iguaçu river. These curves were translated to the Itaipu site by means of the known relationship between the water level gages at Foz do Iguaçu and Itaipu. The final Itaipu tailwater rating curves are shown in Fig. 2.9. Using backwater studies these curves were extended to a flow of $40\,000 \text{ m}^3/\text{s}$ as shown in the same figure.

Sediment transport and water quality

From February to August 1972, a series of measurements were conducted in the Rio Paraná at Guaíra and at Ilha Acaray just above the mouth of the Iguaçu. The measurements included sampling of suspended sediment and bed material and discharge. Dry weight of each sample was determined; then a composite sample of all materials was used to obtain the grain size distribution curves of the sediments. These data were used with monthly mean river discharges for the 1921-71 period, giving an estimated average sediment transport rate at Itaipu of $4.5 \times 10^7 \text{ t/year}$. Assuming an in-place density of 1.3 t/m^3 , the annual transport rate by volume was $3.5 \times 10^7 \text{ m}^3/\text{year}$. At this rate Itaipu reservoir, with a volume of $30 \times 10^9 \text{ m}^3$ at El.220,

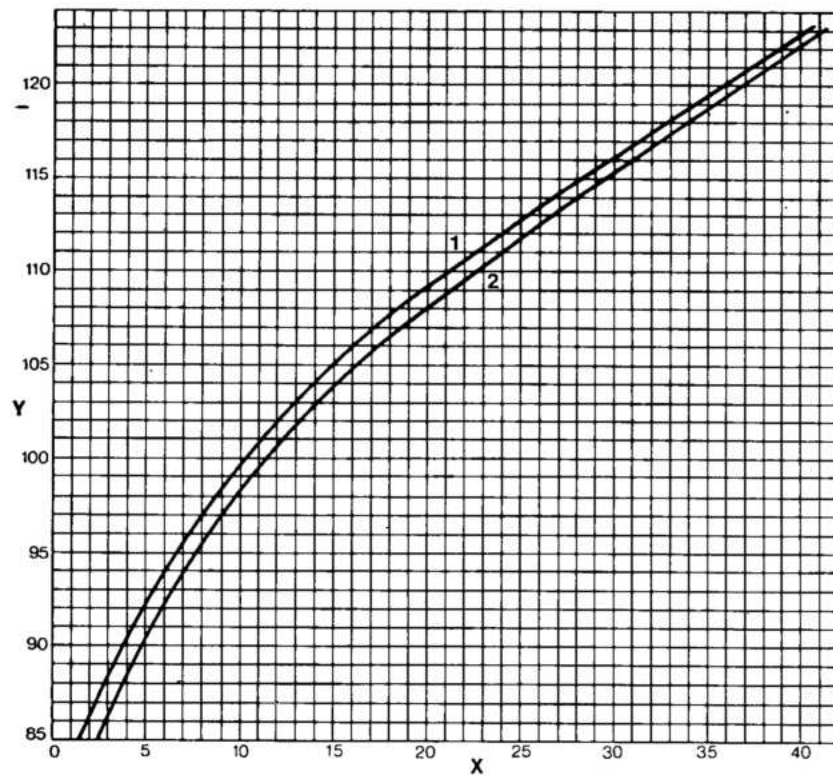
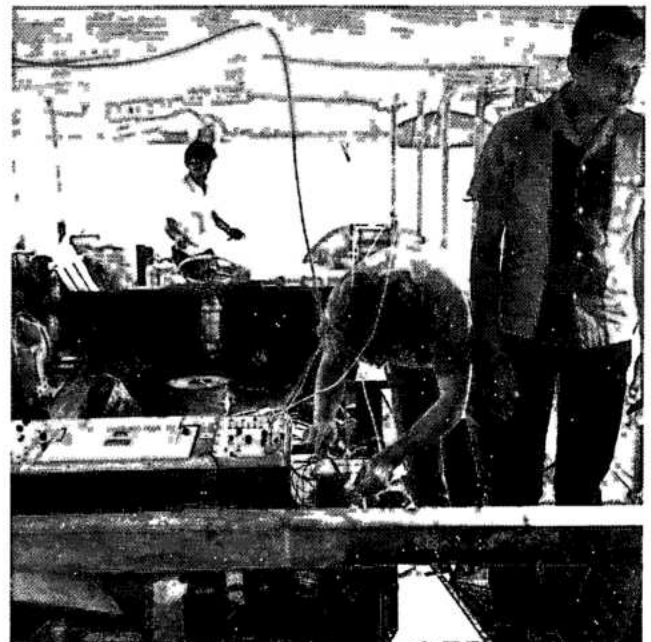
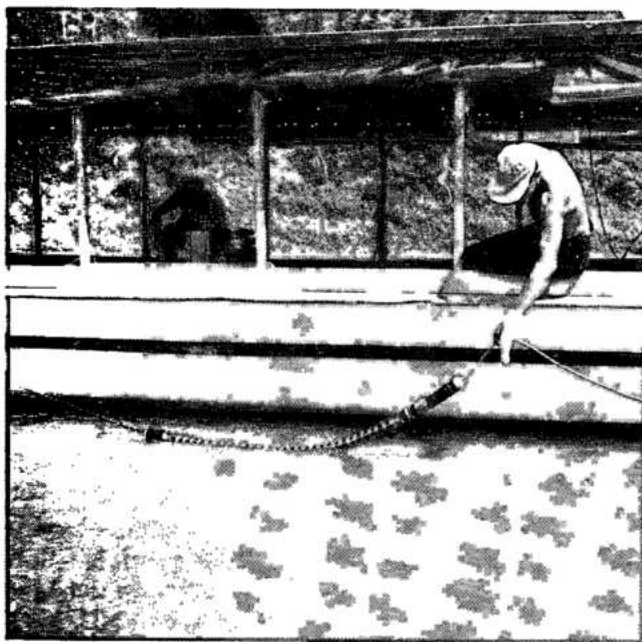


Fig. 2.9 Itaipu tailwater rating curve

Y Water level (m)
 X Total discharge ($10^3 \text{ m}^3/\text{s}$)
 1 Water level at Itaipu
 2 Water level at Foz do Iguaçu gaging station



Sediment transport and water quality measurements

would take theoretically over 800 years to fill, assuming that upstream conditions remained unchanged and all sediment was retained in the reservoir. With dead storage of $10 \times 10^9 \text{ m}^3$ at El. 197 and an assumed trap efficiency of 85%, the time to accumulate that volume of sediment would be over 300 years.

Water samples were taken during 1972 and 1973 at Guaíra, Ilha Acaray, Rio Bela Vista and Arroio Ita-Pytá. Results of these water quality analyses were combined and integrated with those on record to give the projected values for the reservoir. Twice-daily observations of water temperature of the Rio Paraná at Itaipu commenced mid 1973.

SPILLWAY DESIGN FLOOD

Historic floods

Published newspaper reports of a flood in May and June of 1905 called it the greatest known flood on the Rio Paraguay and the Rio Paraná below Posadas. During the 1905 flood, water levels in the Paraná near the mouth of Rio Iguaçu rose 43 m and a maximum daily discharge of $45\,000 \text{ m}^3/\text{s}$ at Posadas was recorded on May 25, 1905.

During the period of record, 1920-73, the historic maximum daily discharge at Guaíra was $28\,400 \text{ m}^3/\text{s}$ on March 3, 1929. This flood was produced by storms in the upper Rio Tietê and Rio Grande basins. In the upper Paraná basin, the floods of 1878 and 1891 exceeded the 1905 flood. However, data were insufficient to determine the magnitude of the 1878 and 1891 floods at Guaíra for comparison with the 1929 flood.

Computation of design flood

General methodology. Feasibility study criteria required the spillway at Itaipu to pass safely the probable maximum flood (PMF) as routed through the Itaipu reservoir. The approach used to develop the hydrograph for the PMF was to determine the probable maximum precipitation (PMP) on the basin, estimate the rainfall retention losses, and compute the flood flows and duration at points of interest using unit hydrographs and flood routing techniques, taking into consideration the various levels of development in the basin.

Because of the large watershed, an assumed series of storms over a period of several months was required to produce extreme floods at the project site. Simultaneous occurrence of probable maximum storms at all sub-basins over such a large area would be meteorologically impossible.

Therefore historic storms within a calendar month which had occurred were combined in a synthetic 7-month sequence which had not occurred but was meteorologically possible and had low occurrence probability. Values of actual recorded rainfall at the stations were used in the calculation; the daily values were not maximized. The PMP was thus synthesized by placing the months with the highest calculated average basin rainfall in sequence, forming a wet season.

Monthly basin rainfall and design rainfall sequence.

Monthly rainfall records were available for sixty stations in and near the project basin for the period 1926-1969, see Fig. 2.5. Some earlier records were available, but the area covered before 1926 was inadequate to determine average basin rainfall. Monthly rainfall over the entire project basin was computed for each month for the period October through April, for 1926-1969. For each month in the 7-month series, the three highest values of average entire basin rainfall were selected for detailed study. They are shown in the Table 2.5; the first line for each rank shows the rainfall and the second line the year.

Isohyetal maps for the highest ranking months were drawn, based on monthly rainfall for all the stations used in the network, to examine the storm patterns and for selecting a meteorologically reasonable sequence, supplemented by available weather synoptic charts. High precipitation in the lower part of the basin is more effective in producing peak discharge at Guaíra than the same average basin rainfall spread uniformly over the basin or concentrated in the upper end. The most critical condition for floods at Guaíra was with storms over the whole Paraná basin for the first few months, giving high base flows and peak discharges from the upper basin, followed by storms concentrated in the lower part of the basin. This combination would produce the greatest peak discharge at Guaíra. A separate study, therefore, was made of average rainfall in only the lower part of the basin, from the Paranapanema basin southward leading to the values given in Table 2.6.

The peak discharge was estimated to occur in about January-February on the upper basin, and in March or April on the lower basin; with high flows in February from the middle and upper basin combining with high flows from the lower basin in March or April. The highest average basin rainfall in February, 1964 was concentrated in the middle and upper basin. To fit the above conditions, selection of February, 1964 in the design storm was followed by the months March, 1928 and April, 1956, with the highest average rainfall in the lower basin. The selected March and April were the

Table 2.5 Maximum average entire basin rainfall (mm) and year of occurrence

Rank	Oct	Nov	Dec	Jan	Feb	Mar	Apr
1	258 1930	284 1939	379 1926	364 1951	293 1964	266 1926	201 1926
2	223 1937	256 1937	328 1936	355 1929	288 1929	247 1928	177 1956
3	222 1965	241 1925	326 1932	336 1926	285 1940	241 1952	161 1942

Table 2.6 Maximum average rainfall (mm) in the lower basin and year of occurrence

Rank	Oct	Nov	Dec	Jan	Feb	Mar	Apr
1	329 1930	340 1939	292 1934	350 1926	362 1946	241 1928	230 1956
2	276 1935	260 1963	262 1930	322 1929	279 1947	216 1946	211 1961
3	248 1928	232 1937	257 1926	315 1951	259 1964	204 1955	185 1965

Table 2.7 Selected 7-month sequence design storm and average entire basin rainfall (mm)

	Oct	Nov	Dec	Jan	Feb	Mar	Apr
Year	1930	1939	1926	1951	1964	1928	1956
Rainfall	258	284	379	364	293	247	177

second highest rank for average rainfall on the whole basin. Thus, the selected total 7-month sequence consisted of October 1930, November 1939, December 1926, January 1951, February 1964, March 1928 and April 1956, see Table 2.7.

Runoff from rainfall. Runoff from the basin depends not only on the amount of rainfall but also upon the vegetal cover, evapotranspiration, infiltration rate, soil-moisture storage capacity, the amount of moisture in storage, the surface storage, rate of groundwater outflow, losses due to deep percolation and other factors. Many of these parameters are interrelated.

A computer program was developed for moisture accounting in each sub-basin, patterned after the Stanford Watershed Model. The input to this program was daily rainfall. Output was net rainfall available for surface runoff and net moisture for groundwater flow. Net rainfall available for surface runoff was distributed into channel runoff, using the unit-hydrograph method, and the contributions to the baseflow from groundwater

and bank storages, and then the total runoff at the sub-basin outlet was computed.

The sub-basin characteristics of soil-moisture storage, infiltration index and other parameters were determined by trial and error in calibration studies against known runoff for sub-basins with flood data, and estimated for the remaining sub-basins from the calibrated results. Fig. 2.10 shows the total sub-basin configurations and indicates those used for calibration.

The flow from sub-basins was computed in a downstream order, using the Muskingum method of routing to downstream points culminating in the flow from each major basin of the Paraná (Paranaíba, Grande, Tietê, Paranapanema and Iguaçu).

Using the rainfall for the period October 1958 through April 1959, each major basin was calibrated. This period was selected because of good areal coverage of rainfall data and little regulation of streamflow, except by the Peixoto reservoir on the Rio Grande, the effects of which were considered negligible.

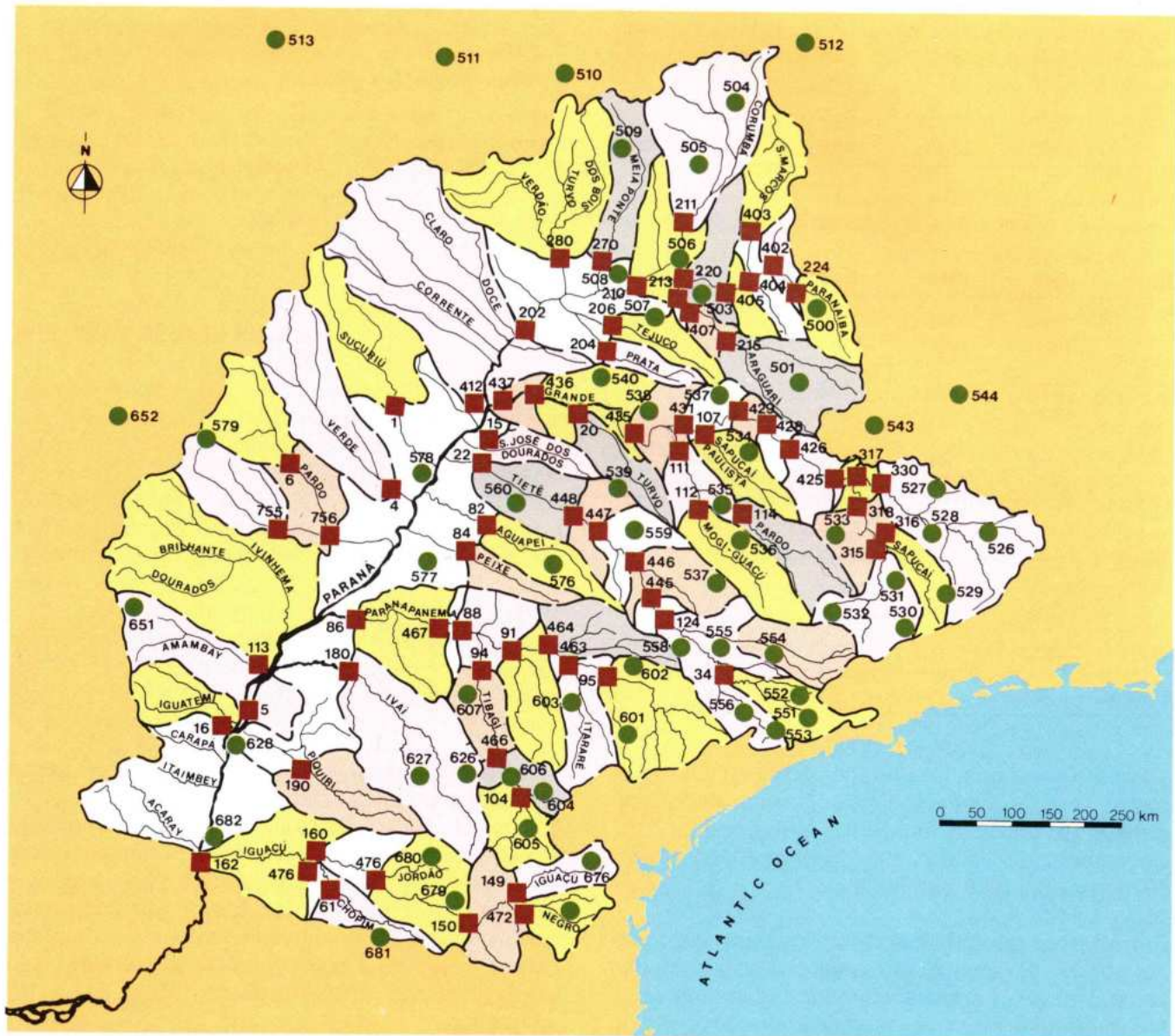


Fig. 2.10 Sub-basins configurations (numbers refer to the sites selected at feasibility stage)

● Location and number of the sub-basin selected in spillway design flood study

■ Precipitation station used in design flood study and assigned station number

▭ Sub-basins for which unit hydrographs were used in computing runoff

▭ Sub-basins for which runoffs were estimated by proportioning

The computed discharge was plotted along with the observed discharge at the stream gaging locations shown in Table 2.8 and in Fig. 2.2. Adjustments were made to channel routing coefficients and to sub-basin coefficients for basins where estimated values were used, until a satisfactory match of computed and observed discharge hydrographs was obtained.

Table 2.8 Discharge at the stream gaging stations used for watershed model calibration

Gage no.	River	Location
220	Paranaíba	Ponte Veloso
210	Paranaíba	Itumbiara
317	Grande	São José da Barra
303	Grande	Porto José Américo
124	Tietê	Barra Bonita
22	Tietê	Lussanvira
95	Paranapanema	Piraju
94	Tibagi	Jataizinho
88	Paranapanema	Balsa do Paranapanema
150	Iguaçu	União da Vitória
160	Iguaçu	Salto Osório
12	Paraná	Jupiá Ponte
6	Pardo	Mimoso
180	Ivaí	Porto Paraíso do Norte
123	Paraná	Guaíra
195	Paraná	Posadas

After computing runoff from all major basins, the runoff from the Paranaíba and the Grande basins was combined, runoff from other sub-basins tributary to the Paraná computed, and other major basin inflows added in downstream sequence. Flood computations were thus carried into the study area.

Reservoirs reduce the flood-travel time required to traverse the corresponding lengths of the natural river channel. Thus, if a reservoir is full, the flood peak will arrive sooner than under natural river conditions without the reservoir because of faster velocity of propagation through the reservoir. If reservoirs encroach on the stream channels within sub-basins, the runoff time in sub-basins is also reduced. On the other hand, flood-water storage in the backwater above the reservoir and that obtained by permitting surcharge in the reservoir level tends to reduce flood peak discharges.

Therefore, the design flood was computed for the natural river condition (without reservoirs) and the ultimate level of development, with all reservoirs constructed. Also for the ultimate level of development, the design flood hydrograph was computed with and without Ilha Grande reservoir to determine the effect of Ilha Grande reservoir only on the peak discharge downstream.

The computed peak discharges of the PMF inflow at the Itaipu site were:

- Natural condition, 53 800 m³/s;
- Ultimate development without Ilha Grande, 61 370 m³/s;
- Ultimate development with Ilha Grande, 72 020 m³/s.

The three PMF inflow hydrographs are shown on Fig. 2.11. The peak discharge for the ultimate condition with Ilha Grande exceeds that for the natural condition by 34%, which is due mainly to the reduced travel time for the flood from all parts of the basin above the Paranapanema river and a closer synchronization between the flood from above the Paranapanema and the high peak discharge from the Paranapanema itself.

Routing studies of the PMF of 72 020 m³/s through the Itaipu reservoir resulted in a spillway design capacity of 62 600 m³/s.

FLOOD FREQUENCY STUDIES

The flood peak discharges and maximum water levels at the project site for a range of return periods during different seasons of the year were determined to establish the crest levels of the cofferdams and the discharge capacity of the river diversion works. Basic data for developing the frequency curves were Guaíra daily discharges (1921-1971), Foz do Iguaçu daily water levels (1934-1971) and the developed relationships of discharge and water levels between Guaíra, Itaipu site, and Foz do Iguaçu.

Frequency curves of maximum average daily peak discharge for each month at Itaipu were prepared for two conditions:

- For the daily discharge at the site on the day of the maximum water level, which was assumed to be that at Guaíra one day before, adjusted to the 1980 level of development.
- For the highest daily discharge in any month, regardless of the height of water level at the site.

Corrections to recorded peak discharge at Guaíra during each month were made by subtracting the recorded average flow at Guaíra for that month from the 1980 level average monthly flow at Itaipu and adding the peak discharge at Guaíra to obtain the peak at Itaipu.

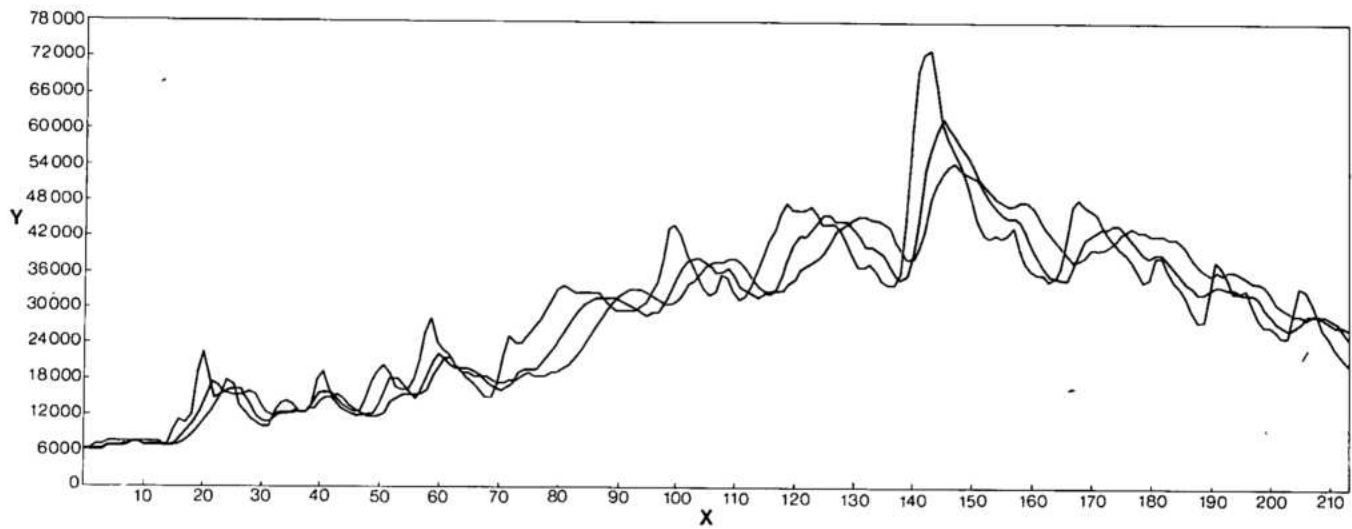


Fig. 2.11 PMF inflow hydrographs at Itaipu site

Y Discharge (m^3/s)
 X Days

— Natural condition — Ultimate development without Ilha Grande reservoir — Ultimate development with Ilha Grande reservoir

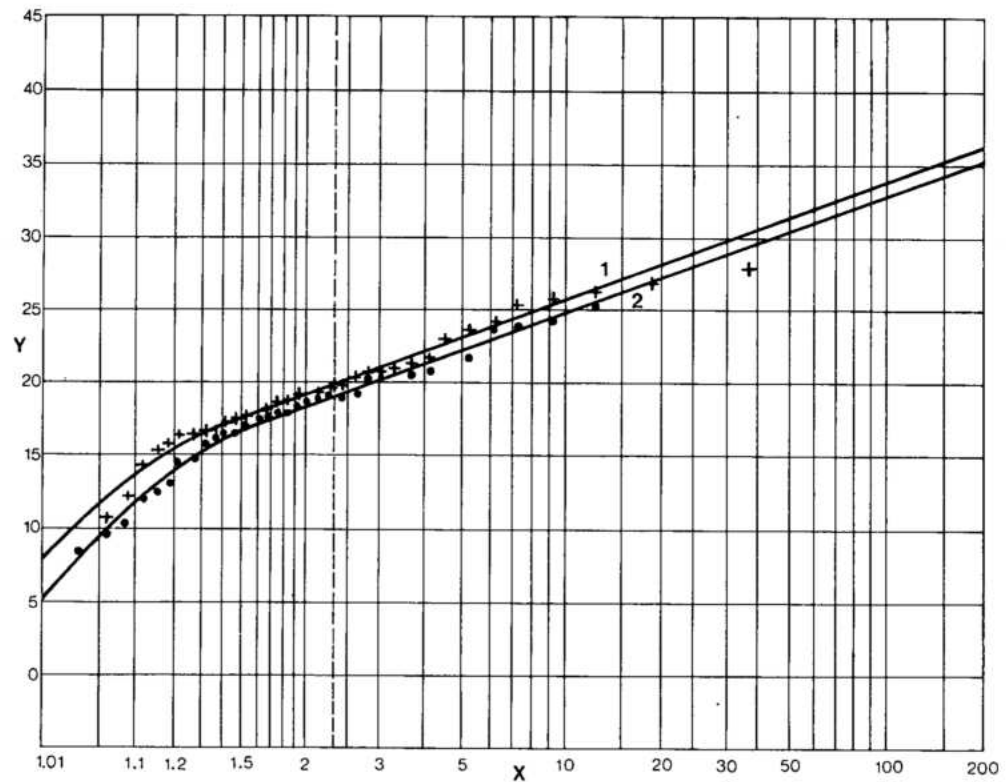


Fig. 2.12 Annual frequency curves of maximum average daily discharge

Y Discharge ($10^3 \text{ m}^3/\text{s}$)
 X Reference interval (years)

1 Maximum average daily discharge
 2 Discharge on day of maximum average daily water level

Fig. 2.12 shows the annual frequency curves of maximum average daily discharge for two conditions: discharge at time of maximum water level at Itaipu, and maximum discharge regardless of time of maximum water level. The

upper curve was for determining maximum discharge in river diversion studies, if water level was not critical.

The annual and monthly curves of maximum water level at Foz do Iguaçu are shown in Fig. 2.13.

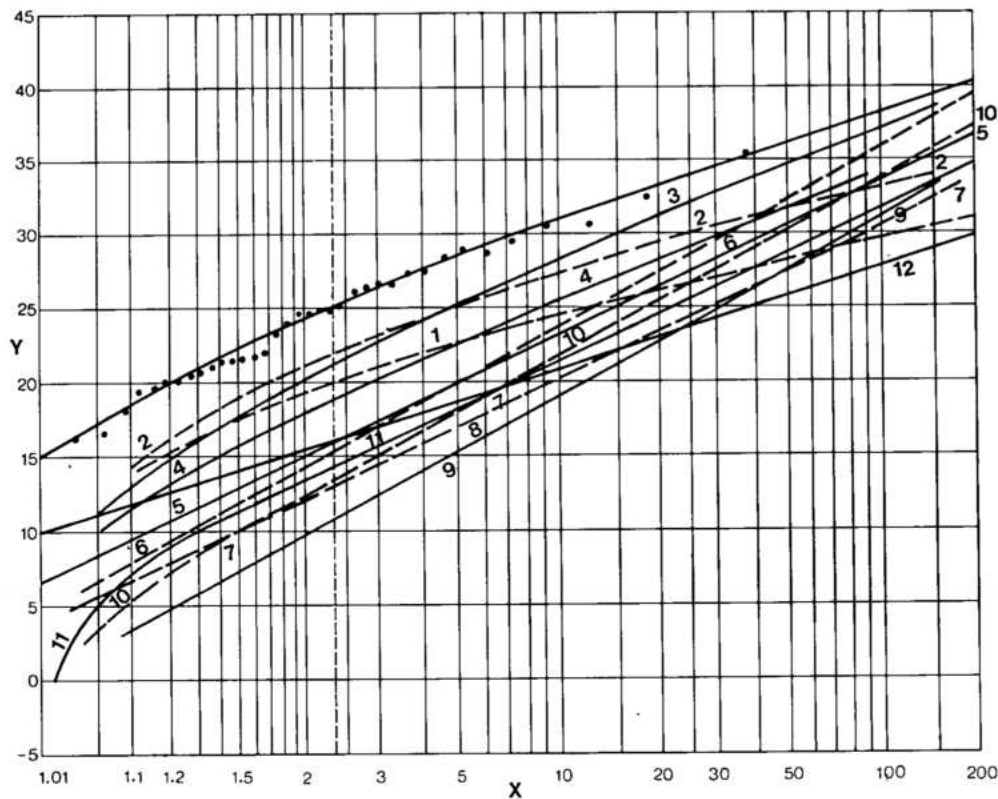


Fig. 2.13 Maximum recorded water levels at Foz do Iguaçu converted to the 1980 level of development

Y Gage heights (m)
 X Recurrence interval (years)
 1 January
 2 February
 . . .
 . . .
 12 December
 • Annual points

POWERPLANT INSTALLED CAPACITY

Further investigations were conducted on the optimum installed capacity of the Itaipu project, the best compromise between number of units and unit size, and Itaipu's primary power for the three stages of development.

Primary power is defined as the minimum average continuous Itaipu power available for transmission; being an average of Itaipu's monthly hypothetical generation over the historic lowest water flow period in the Paraná river (critical flow period) found in the study to be as follows:

- All without reservoir drawdown from May 1952 to November 1955.
- Ultimate development with reservoir drawdown from May 1952 to November 1956.

Secondary power is that over and above primary power and is only available some of the time.

Three generator sizes were considered in the studies: 700 MW, 750 MW and 800 MW. The number of units varied from a minimum of fourteen for base-load operation, to a maximum of twenty-four.

Power generation from nine alternatives is compared in Table 2.9.

Costs of the alternative plants were based on preliminary estimates of the basic project. Cost of

transmission lines to potential load centers were included. Table 2.10 summarizes the relative capital and annual operation, maintenance and replacement (O & M) costs for the alternatives.

Economic benefits considered both the value of capacity as capital cost of an alternative thermal plant and the value of energy as the cost of fuel for a thermal alternative.

All future costs and benefits were discounted to the date of initial operation of the complete plant, at a rate of 12% per annum. Table 2.11 gives the relative incremental costs, the incremental benefits, both excluding and including secondary power, and net benefits, as well as the benefit/cost ratios based on total costs and total benefits.

Results of the economic comparisons supported a proposed installation of 12 600 MW (18 x 700 MW units), because based on primary power it maximized net benefits and also had the highest benefit-cost ratio. The net benefit figures using total power (primary and secondary), would support a larger installation; but under the 1973 conditions and probably for several years after completion of the project, absorption of secondary power in the power system could not be economically justified.

Detailed operation studies for the Itaipu project were performed taking into account hydropower generation at upstream reservoirs, system load factor, thermal

Table 2.9 Power generation of plant alternatives (MW)

Plant alternative	Dependable capacity		Primary power		Total power	
	Site*	Load	Site	Load	Site	Load
14 x 700	7280	6843	6945	6667	7465	7166
14 x 750	7280	6843	7000	6720	7640	7334
14 x 800	7280	6843	7030	6749	7787	7476
18 x 700	9360	8798	7064	6781	8042	7720
18 x 750	9360	8798	7040	6758	8160	7834
18 x 800	9360	8798	7035	6754	8260	7930
24 x 700	12 480	11 731	7015	6734	8444	8106
24 x 750	12 480	11 731	6995	6715	8500	8160
24 x 800	12 480	11 731	6980	6701	8540	8198

* Tailwater effects not accounted for.

Table 2.10 Cost of plant alternatives (US\$ 10⁶) - November, 1973

Plant alternative	Dam and power plant			Transmission	
	Construction	Capital	O&M/yr	Capital	O&M/yr
14 x 700	2128	2884	27.29	613	5.73
14 x 750	2145	2907	27.66	657	6.14
14 x 800	2162	2930	28.04	701	6.55
18 x 700	2317	3076	32.17	788	7.36
18 x 750	2338	3104	32.64	845	7.89
18 x 800	2360	3133	33.11	901	8.42
24 x 700	2779	3689	41.07	1051	9.82
24 x 750	2808	3727	41.70	1126	10.52
24 x 800	2836	3765	42.33	1201	11.22

plants in the system, and system prime power requirements, and assuming some or no drawdown at Itaipu. A comprehensive mathematical model was developed to simulate the hydro-regulation and integrated power system of southeast Brazil. Each hydroplant in the system was modeled and its monthly power generation and peaking capability were simulated based on inflows, reservoir storage and drawdowns, and powerplant outflows. All reservoirs were operated in conjunction such that the peaking capacity and power generated by the power system satisfied the system peaking and base-load power requirements for the month. The main purpose of the

mathematical model was to determine the maximum primary power of the individual hydroplants and how to integrate the thermal plants into system operation during the critical dry streamflow period. This defined the optimum use of reservoir storage under drought conditions and provided planning insights to the power system expansion as load demand grew.

In the hydro-system regulation program, all plant and reservoir data, operating constraints, reservoir rule curves, load patterns and load factors, inflows and outflows, minimum generation, and outflow requirements were compiled and individually modeled. The three levels of development of the

Table 2.11 Present worth (12%) of incremental costs and benefits (US\$ 10⁶)

Alternative plant	Incremental cost PW	Incremental benefit						
		W/primary power				W/total power		
		Present worth		B/C ratio	Present worth		B/C ratio	
		Benefit	Net benefit		Benefit	Net benefit		
14 x 700	0	0	0	1.79	0	0	1.88	
14 x 750	73	37	−35	1.74	119	46	1.86	
14 x 800	147	58	−88	1.73	220	73	1.87	
18 x 700	421	648	227	1.76	962	540	1.92	
18 x 750	514	632	117	1.72	1042	528	1.90	
18 x 800	607	628	21	1.68	1111	503	1.87	
24 x 700	1391	1465	74	1.59	2087	696	1.78	
24 x 750	1515	1451	−63	1.55	2126	610	1.74	
24 x 800	1639	1441	−198	1.51	2153	513	1.71	

Paraná river basin were investigated with monthly simulation of the 40-year streamflow period, detailed simulation runs for the critical period, and varying the number of units (installed capacities) at Itaipu to account for the proposed two stage development, that is an initial 14 700 MW in the riverbed and four additional units in the diversion channel. Figure 2.14 shows typical operational curves obtained, the studies leading to the following conclusions:

1982 level of development. Primary power increased as the installed capacity increased from 9800 MW to 11 200 MW, and thereafter remained about the same for capacities up to 12 600 MW. The highest primary power produced was 7075 MW for 11 200 MW (16 x 700 MW units) installed, reducing to 7069 MW for 12 600 MW (18 x 700 MW units) with live storage in the reservoir.

Primary power increased as the amount of active storage or allowable drawdown was increased to a point at which it was reduced because of operation at lower head and higher tailwater elevations due to higher discharges required for the same output at a lower head.

When operated as a run of the river plant, that is with no drawdown of Itaipu reservoir, the primary power was 6907 MW and 6945 MW for the 9800 MW and 12 600 MW installation, respectively.

Intermediate and ultimate levels of development.

For the intermediate level of development (with 12 600 MW installed capacity), primary power at Itaipu with reservoir drawdown reduced to 6942 MW, because of the increase in evaporation and water loss from those new upstream reservoirs which did not contribute appreciable additional storage. However, under the ultimate level of development, Itaipu maximum primary power with reservoir drawdown increased to 7125 MW, because substantial net usable storage was contributed by some new large reservoirs.

Reservoir drawdown. The comprehensive system operation studies indicated that for the entire flow period of 40 years, the Itaipu hypothetical reservoir drawdown would occur only during the critical flow period from May 1952 through November 1955 (1982 and intermediate levels) and from May 1952 through November 1956 (ultimate level). Besides this period, there were only two other years where partial drawdown of the reservoir would occur. For the 1982 level of development, minimum peaking capability of Itaipu with $18.9 \times 10^9 \text{ m}^3$ active storage, would be controlled by the head at the lowest reservoir drawdown level. For an installation of 9800 MW the minimum peaking capability would be 7670 MW, and for 12 600 MW it would be 9270 MW.

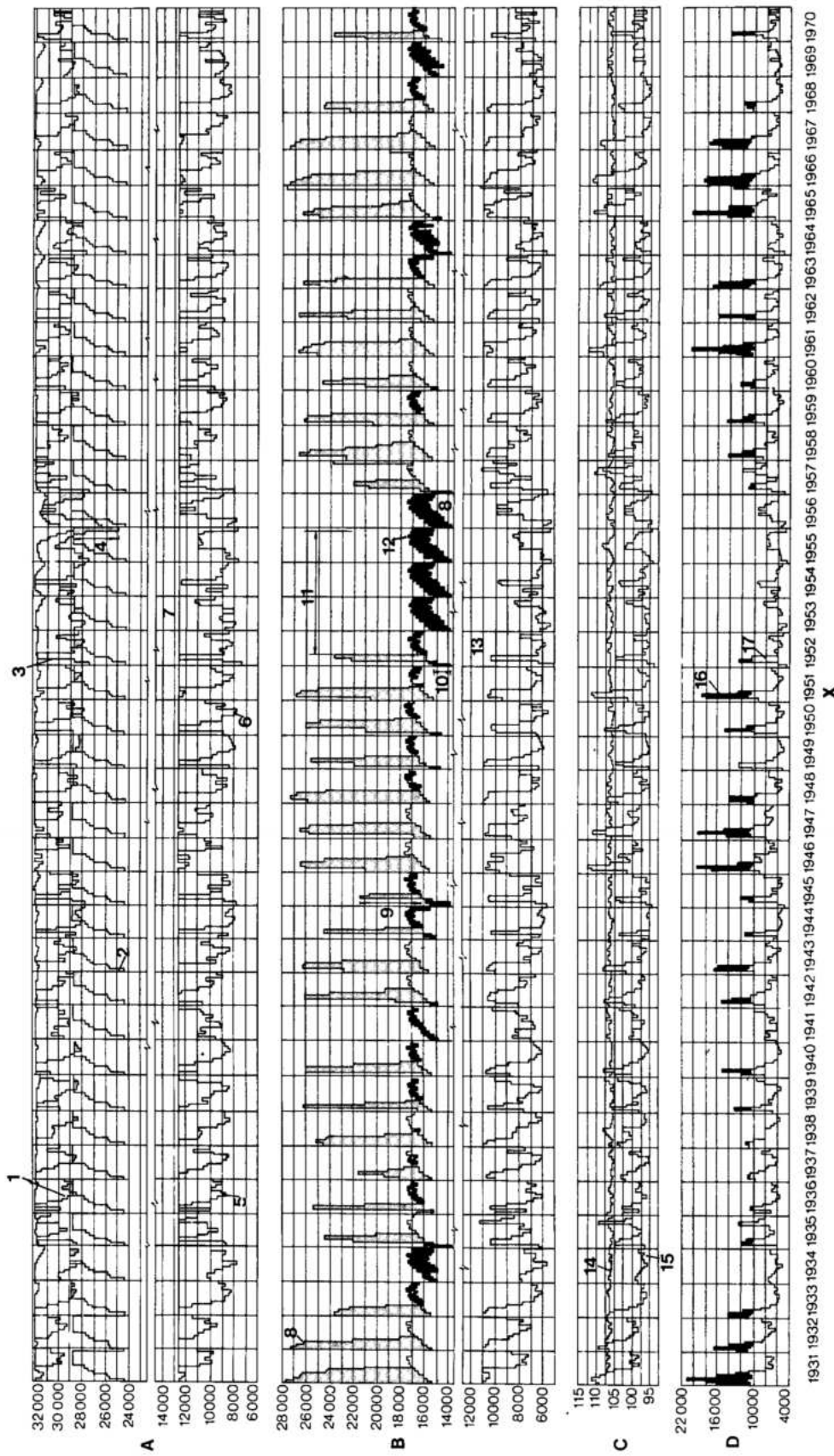


Fig. 2.14 Typical usage curves

X Years

A Peak capability (MW)

B Energy capability (MW average)

C Tailwater level (m)

D Inflow and spill (m^3/s)

1 System peaking capability for Itaipu minimum peaking capability

2 System peak load

3 System peak

4 Peak deficiency with 4 m tailwater difference limitation

5 Minimum peaking capability as controlled by high tailwater

6 Itaipu peak with 4 m maximum difference between average and peak tailwater

7 Itaipu peak

8 Hydro system generation

9 Surplus secondary energy

10 Thermal generation

11 Critical period

12 System energy load

13 Itaipu generation

14 Peak tailwater

15 Average monthly tailwater

16 Spill

17 Inflow to Itaipu

When operating Itaipu as a run of the river plant, minimum peaking capability benefited from constant high headwater level, but was slightly penalized by high tailwater during temporary peaking. However, the operation studies showed that when the entire system peaking capability was critical, Itaipu operating on a run of the river basis could produce the full installed outputs of 9800 MW (fourteen units) and 12 600 MW (eighteen units). Therefore, the best operational advantage of Itaipu to the integrated system would be to operate it as a run of the river plant, with reservoir level fluctuations only as required for temporary pondage. Although the primary power of 6907 MW and 6945 MW with 14 x 700 MW and 18 x 700 MW units installations respectively, were slightly less than those with reservoir drawdowns, the substantial gain in peaking capability far outweighed the minor loss in the prime power to the system.

For maximum peaking benefits the four diversion channel units should be installed as quickly as the construction program allowed, bringing the full capacity of the station to eighteen units.

MODEL TESTS OF RIVER REGULATION AND NAVIGATION FACILITIES

Comprehensive River Channel Model

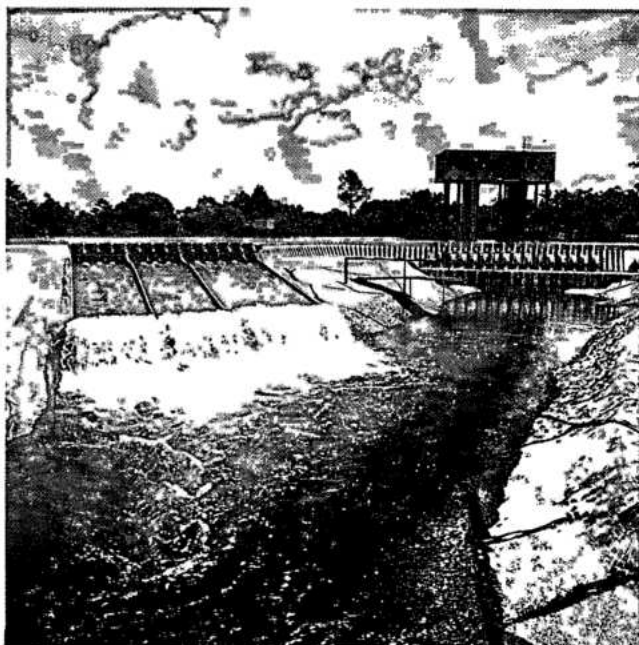
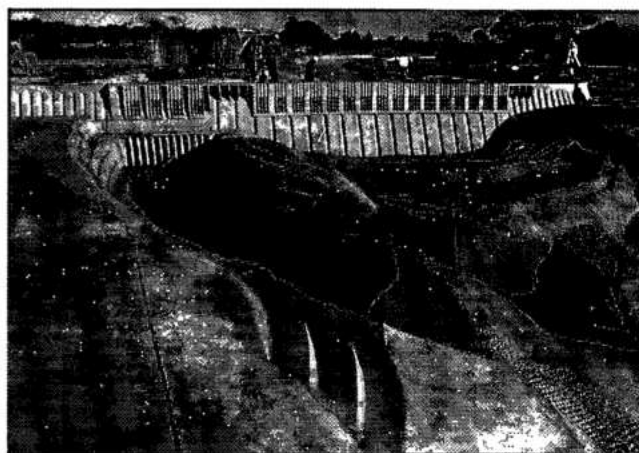
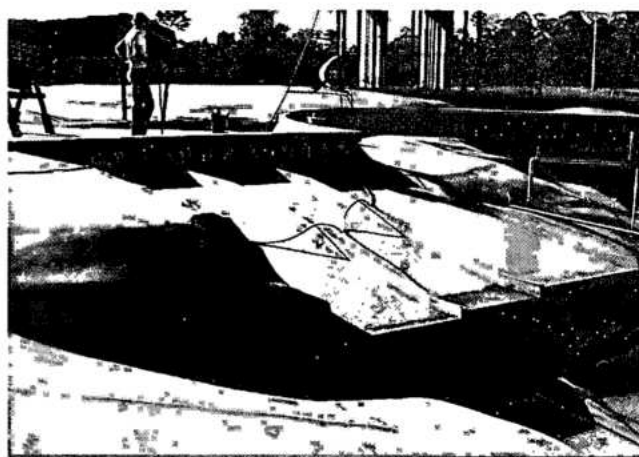
A large hydraulic model of Itaipu project facilities and Paraná river has been built at the ITAIPU Hydraulic Laboratory on the right bank. With horizontal and vertical scales of 1:100, the model reproduces a 27 km reach of the Paraná river commencing 2.6 km upstream of the axis of the dam and extending 2.3 km downstream of the confluence with Iguaçu river, and including such tributaries as Rio Acaray and Rio Monday. All already completed structures of Itaipu project are reproduced in the model.

To conform with Froude's law, the following scales were applicable in the tests:

Physical dimensions	1:100
Areas	1:10 000
Velocity and time	1:10
Discharge	1:100 000

The total length of the model is 280 m, including 10 m of the exit flume, and an area of 5500 m² modeled in concrete.

There are three separate weirs and spillways for controlling and measuring the flows from Paraná, Acaray and Iguaçu rivers.



Hydraulic laboratory on the right bank

River regulation for the following operational conditions was tested on the comprehensive model:

- Normal operation of Itaipu, various conditions of separate and joint operation of the powerplant and the spillway.
- Extreme flood conditions, study of various combinations of Itaipu spillway discharge and backwater caused by Iguaçu and Acaray inflows which would raise the tailwater at Itaipu to El. 142. Higher tailwater levels would inundate the powerhouse.
- Powerplant operation, study of powerplant operation to comply with the restriction that under normal conditions downstream water level fluctuations should not exceed 0.50 m/hour.
- Influence of corpus project, all the above tests were made with or without the proposed downstream Corpus dam.

An extensive series of tests was performed to verify the feasibility of the future navigation facilities on both banks. These tests included the following:

- Suitable locations for entry to the navigation channels downstream of the dam.
- Most suitable alignments of the channels and the minimum number of stages or flights of locks considered technically suitable.
- Size of the navigation locks.
- Study of routing convoys of barges through the navigation works.

Initial tests indicated that access or entry conditions for maneuvering barge convoys would be unfavorable because of the strong currents and high velocities in the entry areas. Subsequently, tests were made to study the size and location of spur dikes or groynes which would deflect the current and permit relatively calm water conditions at the entrances. After several tests, the following spur dikes were considered suitable for the purpose:

- for the right bank, 100 m long and volume of 8000 m³.
- for the left bank, 170 m long and volume of 112 000 m³.

Conditions at the upper or reservoir entrance to the navigation channel on the right bank were also studied in the model. The objective was to ensure that the operation of the spillway will not endanger safe passage of the traffic through the navigation works.

Model Tests of the Navigation Lock

A 1:25 scale indoor model was constructed to test the hydraulic design of a typical proposed navigation lock, with the following principal characteristics:

Max volume of chamber	156 795 m ³	
Maximum lift	43.92 m	
Rate of change of water level	3.5 m/min	
Flow velocity at intakes	1.5 m/s	
Flow velocity in supply tunnel	12.5 m/s	
Rate of filling	208 m ³ /s	
Time to empty chamber	12.5 min	
Gate opening time	4 min	
Chamber dimensions:		
	Prototype	Model
Length	210 m	8.40 m
Width	17 m	0.68 m
Height	48.92 m	1957 m

Further model testing will be carried out to refine the design of the navigation facilities.

MAIN GENERATING UNITS

Turbines

Economic and operation studies had indicated an installed capacity for Itaipu of 18 x 700 MW units, which also fitted well into the proposed project arrangement.

Turbine net heads were envisaged to be between 90 and 124 m with a possible rated head of 108 m, for the 715 MW rated turbine (corresponding to 700 MW generator rating). It was therefore indisputable that the turbine would be mixed flow, fixed blade (Francis) type and the arrangement would be vertical, that is, with the generator above the turbine. In respect of hydraulic characteristics Francis turbine technology was well established, however the proposed Itaipu units were to be among the largest in the world, raising particular concerns in respect of mechanical arrangement, manufacture and erection.

Preoccupation concerning potential manufacturing problems was exacerbated by the knowledge that a large percentage of the supply would be from the factories of Brazil and Paraguay which at the time had produced a Francis turbine of 440 MW only (Itumbiara). A questionnaire was sent to all leading turbine manufacturers and operators of large hydraulic turbines worldwide, which, together with visits to selected projects and manufacturers, formed the basis of a comprehensive report on the then current state of art and trends. Among the questions to be resolved were:

- Rotational speed.
- Turbine setting.

- Expected efficiency.
- Part load and low load running characteristics.
- Dimensions for project design.
- Runner manufacture.
- Number of bearings and location of thrust bearing support.
- Type of wicket gate servomotor system.

The main findings and recommendations of the study were:

Rotational speed. The basis for determining the rotational speed of a hydraulic turbine is the specific speed versus head experience curve, see Fig. 2.15. Turbines of the same specific speed operating at the same head have the same hydraulic characteristics and are subjected to the same forces and stresses. Hence, in this way a smaller unit can serve as a precedent for a large unit. However, the tendency with large units is for designers to specify higher specific speed for the same head to reduce the dimensions and hence cost of the turbine and to some extent the powerhouse. This increases velocities and dynamic forces and thus takes the turbine design beyond known precedents. Weighing

cost and prudence, the specific speed of the Itaipu units was tentatively set at about 242 rpm $\text{kW}^{1/2}/\text{m}^{5/4}$ which resulted in a rotational speed of 85.7 rpm.

If dual speed runner or separate runners were used for the two frequencies (see the subsequent section on dual frequency) then these turbines would rotate at 71.4 rpm for 50 Hz. The study recognized that these speeds were conservative and were to be re-evaluated as design progressed.

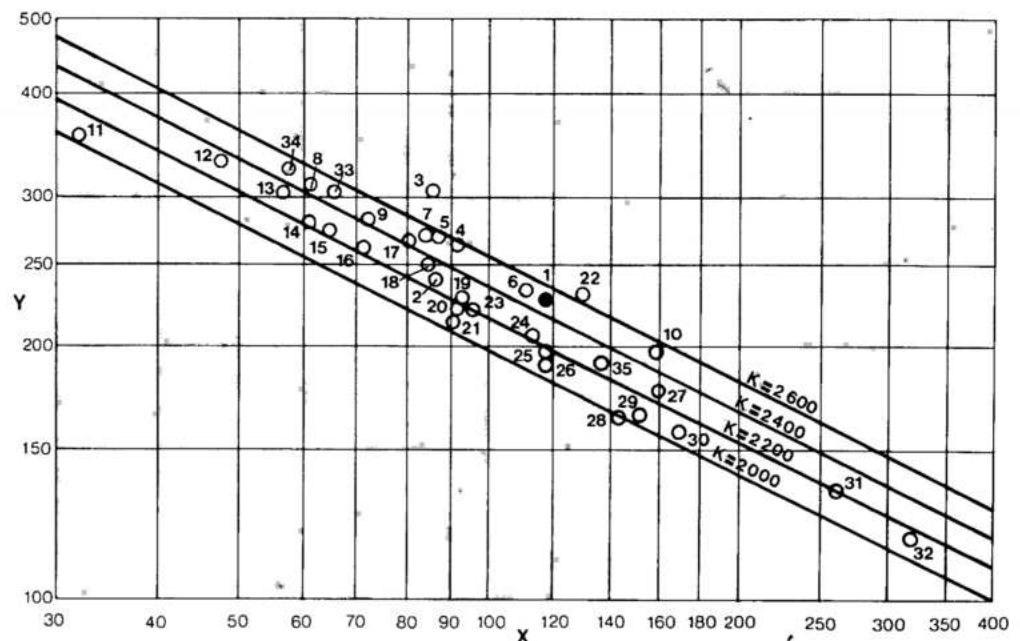
Turbine setting. Hydraulic turbines suffer from cavitation damage which can be minimized by lowering the turbine centerline relative to tailwater level. However, the lower the centerline setting the more expensive the excavation. Using Thoma cavitation coefficient versus specific speed curves as shown in Fig. 2.16, the turbine centerline was set at El. 87.5. With this setting a mild steel turbine runner could be used with stainless steel overlay of critical areas as a protection against cavitation damage.

Efficiency and performance. Turbine efficiency for this large unit was expected to be about 94% when new and with proper air admission no problems were

Fig. 2.15 Specific speed of hydraulic turbines

Y Specific speed n_s
X Design head H (m)
K = Specific speed constant
(K - factor metric)

- 1 Itaipu
- 2 Grand Coulee III
- 3 Grand Coulee III
- 4 Krasnoyarsk
- 5 Paulo Afonso III
- 6 Paulo Afonso IV
- 7 Ust Ilmsk
- 8 Estreito
- 9 Salto Osório
- 10 Tumut 3
- 11 Cachoeira Dourada
- 12 Ilha Solteira
- 13 Aswan
- 14 Marimbondo
- 15 Akosombo
- 16 São Simão
- 17 Itumbiara
- 18 Messaure
- 19 Furnas
- 20 Manicougan 3



- 21 Guri I
- 22 Guri III
- 23 Bratsk
- 24 Cabora Bassa
- 25 Keban

- 26 Big Bend
- 27 Reza Shah-Kabir
- 28 Outardes 3
- 29 Portage Mountain
- 30 Mica

- 31 Murray 2
- 32 Churchill Falls
- 33 Tucuruí
- 34 Água Vermelha
- 35 La Grande II

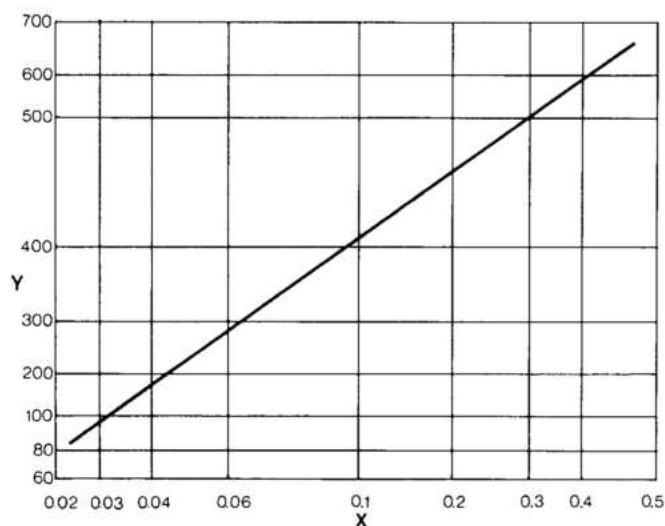


Fig. 2.16 Thomas cavitation coefficient

Y Specific speed n_s

X Cavitation coefficient σ

foreseen with operation in the load range required for some of the machines to serve the 50 Hz Paraguayan system. Normal operation was not envisaged in the 30% to 60% load range in which Francis units suffer from draft tube pressure fluctuations.

Initial design. The following basic turbine features were tentatively recommended at the feasibility stage:

- The spiral casing would be manufactured from welded, rolled mild steel plate.
- The width of each unit bay would be 37 m as governed by the spiral casing dimensions.
- With the speeds envisaged the turbine runner would be 9.8 m diameter weighing 4400 kN. This large size would make overland transportation very difficult and necessitate site manufacture.
- Thrust bearing would be mounted on the turbine head cover.
- Individual wicket gate servomotors would be used.

Generators

Based on the turbine characteristics described, the generators would have a nominal 700 MW output and operate at 85.7 rpm for the 60 Hz system and 71.4 rpm for the 50 Hz. The generators, although among the largest in the world, were considered to be within the industry experience range at the time.

A survey of manufacturers and users was carried out to ascertain design, installation, and operating experience of similar units. Of special interest were the unit characteristics, ratings, design features, and erection procedures.

Generator rating and arrangement. The generator output was selected as 635 MW, a continuous overload capability of 10% gave a nominal 700 MW, and a further short term rating gave a maximum of 730 MW. The thrust bearing was placed under the rotor, but mounted on the turbine head-cover, and an upper guide bearing was foreseen.

Efficiency and performance. The use of a water cooled stator winding improved the overall efficiency to an expected value of 98.5%, in the operating range of 635 to 700 MW.

Since only ac transmission was proposed at the time of the feasibility study no significant differences were required between the 50 and 60 Hz units and relatively standard values of inertia and reactance were assumed.

Initial design. The following basic generator features were tentatively recommended:

- 84 poles at 85.7 rpm for 60 Hz operation or for 50 Hz at 71.4 rpm.
- Water cooled stator and air cooled rotor.
- Stator stacked and wound at site, in the pit.
- Rotor assembled in the assembly area.
- Static excitation system.
- 23 kV terminal voltage.

It was proposed that one of the nine 50 Hz units would initially operate at 50 Hz while the other eight would operate at 60 Hz. Conversion of the eight units would be carried out as the 50 Hz load developed. To allow fine adjustment of generation to load requirements, and to back-up the 50 Hz unit, a 800 MW static frequency converter was to be supplied between the 50 Hz and 60 Hz systems. House units were envisaged to supply the station auxiliary services.

DUAL FREQUENCY

The difference in frequencies, 60 Hz in Brazil and 50 Hz in Paraguay, coupled with the low 50 Hz power demand in the early operating stages of the project, created a serious problem of how best to supply the two systems.

In early 1973 a report on frequency differences was prepared on the basis of the expected requirements of the Paraguayan system for 20 years from first power in 1982. The alternatives studied were:

1. Converting the Paraguayan system from 50 Hz to 60 Hz.
2. Six 100 MW 50 Hz generators, coaxial with six 700 MW 60 Hz generators.
3. Seven 100 MW 60/50 Hz dual frequency generators.

4. Seven 100 MW 60/50 Hz rotating frequency converters.
5. Five 125 MW 60/50 Hz static frequency converters for back-to-back operation.
6. Five 125 MW 60/50 Hz static frequency converters for back-to-back operation and two direct current transmission circuits.

Alternatives 3 to 6 included 700 MW 60 Hz generators.

Alternatives involving long distance direct current transmission on the Brazilian side were not included because worldwide experience with large thyristors and high voltage direct current transmission in general was still limited and, therefore, considered too risky.

The most economic solution was to convert the Paraguayan system and the second most economic was to install seven 100 MW 60/50 Hz generating units. It was recognized however that the study did not address the system problems in the later stages, that is after the year 2003, when the 50 Hz demand could be higher.

Conversion of Paraguay to 60 Hz was not politically acceptable because of potential future projects between Paraguay and other neighboring nations which also generate at 50 Hz. Also, because of the difficulty in accurately determining future growth in Paraguay, the provision of limited generating facilities at 50 Hz in Itaipu was not acceptable. Thus in November 1973 the criterion for a study was established that retained the 50 Hz system in Paraguay and would result in final general plant symmetry at Itaipu having half the installed generating capacity at each frequency. The criterion allowed for the gradual increase in 50 Hz system, with fine adjustment of power production to match demand on both systems, and for the further energy interchanges between Paraguay and Brazil.

The basic criterion led to the investigation of three main alternatives:

1. Back-to-back 50 Hz to 60 Hz static conversion of half the plant output.
2. Dual frequency constant speed units for half the plant which could be gradually changed from 60 Hz to 50 Hz generation.
3. Dual speed units to operate at either 50 Hz or 60 Hz for half the plant.

In alternatives 2 and 3 it was recognized that static conversion of one unit capacity (700 MW) would be required between the 50 Hz and 60 Hz systems to allow full utilization of the generating capacity.

At this stage, for alternative 1, dc transmission on the 60 Hz system to the load demand center was not considered (but was studied later and finally adopted).

Alternative 1. Static conversion of half the plant output from 50 Hz to 60 Hz was known to be technically feasible. It also had the advantages of being asynchronous and allowing the maximum freedom in turbine and generator selection for both frequencies. Although this maintained the efficiency of the generating units the conversion introduced an estimated 3 to 3.5% loss and lower power factor requirement for the 50 Hz generator.

The major disadvantage, based on a back-to-back conversion, was the relatively high cost, estimated at more than double the other alternatives.

Alternative 2. Dual frequency constant speed units (50 and 60 Hz) were concluded to be technically feasible but had rarely been used in the past and never at the size required. The main advantage was that the turbine could be selected for the speed used and was not subject to later change. This alternative considered both modifying the pole arrangement to effect the frequency change (slow pole changing) and providing two sets of switchable poles (quick pole changing).

The major disadvantage of the slow pole changing was that the generator stator and rotor would have to be extensively reworked if the machine characteristics and performance were to be maintained. This could include complete reconnection of the stator winding and replacement of the rotor rim. The quick pole changing alternative posed excessive risk with the state of art at that time.

Alternative 3. Dual speed units (50 Hz and 60 Hz) were considered technically feasible, and had been used in several cases in the past although never at the size required. The main advantage was that the generator could be designed to meet the two speed requirements with minor changes in machine characteristics and performance and was not subject to later change. The unit could also change frequency quickly. The major disadvantage was that the turbine runner would operate at a speed other than its design speed. This could result in increased cavitation and lower efficiency. Consideration was also given to using two different runners to overcome this problem.

As noted earlier, alternatives 2 and 3 required static conversion of one unit capacity between the 50 Hz and 60 Hz systems. Although technically this was considered feasible it did introduce virtually all the specialized engineering of alternative 1. Consideration was given to use of rotating converters instead but these would be difficult to utilize as the size of the 50 Hz system increased and the rotating converter became a smaller percentage of the total 50 Hz generation when,

because they are synchronous in operation, disturbances from the larger system would affect stability of their operation.

The above study results tended to favor alternative 3, but recognized that the requirements of the Brazilian and Paraguayan transmission systems could have a significant effect. It was also noted that the study had been restricted by the time available and that the alternatives should be further examined in the next stage.

In late 1973 the following criteria were established as a basis for the final project feasibility study (1974):

- 50 Hz system at 400 kV and 230 kV for Paraguay.
- 60 Hz system at 750 kV for Brazil.
- Half the installed capacity to be variable in its supply to the 50 and 60 Hz systems including precise adjustment to the demands.

This resulted in a proposed arrangement of generator transformer banks on the upstream side of the main powerhouse deck with the transmission lines strained from the downstream face of the dam. The limited space available precluded the use of conventional outdoor switchgear, so low voltage generator circuit breakers were to be used along with nine 400 kV lines for the 50 Hz and five 750 kV lines for the 60 Hz sector.

Separate switchyards, 400 kV and 230 kV for the 50 Hz and 750 kV and 400 kV for the 60 Hz, on the right and left banks respectively, were required for additional transformation and for the high voltage switchgear associated with the main transmission lines. In addition a 700 MW static frequency converter between the two switchyards was required. This arrangement was proposed in the 1974 final feasibility report and presented to the Joint Technical Commission. However it was recognized that further study was needed to optimize the power station arrangements to satisfy the needs of the two systems.

One problem with this arrangement was its complexity and that it lacked operational flexibility and reliability. Time, however, was available before the final decisions had to be reached, which made it possible to study the development of 500 kV gas insulated switchgear (GIS-SF₆) and the rapid advancements in the high voltage direct current transmission field, therefore warranting a new evaluation of possible alternatives.

Other alternatives considered in 1975 were:

- 50 Hz power supply obtained through back-to-back conversion made in 350 MW modules, scheduled to be installed as the 50 Hz load increased.
- Installation of a separate powerhouse on the right bank, accommodating several generating units of 350 MW operating at 50 Hz. The ratings of this installation would be more consistent with available 50 Hz load.

Both alternatives were judged politically unacceptable.

The use of 500 kV GIS and a common 500 kV voltage for both sectors would enable the elimination of the low voltage generator circuit breakers in the powerhouse and reduce the size of the outdoor switchyard and the number of transmission lines. The single line arrangement would also improve flexibility and reliability of operation. Also the economic benefits of long distance high voltage direct current (HVDC) transmission, as compared to back-to-back conversion, were recognized.

Based on these considerations the powerhouse and substation layouts and the transmission system were reviewed so that by 1978 a general agreement was reached on the following:

- 500 kV gas insulated switchgear (GIS-SF₆) would be installed in the powerhouse.
- 500 kV transmission, using four lines for each frequency sector, would take the power to the right and left bank areas.
- 750 kV ac and ± 600 kV dc would be used for transmission in Brazil.
- 230 kV ac and future 500 kV ac would be used for transmission in Paraguay.

The general arrangement selected with nine 50 Hz and nine 60 Hz units required no provisions for changing frequency. Power would be supplied to both bank areas at 500 kV ac. The 60 Hz power would be stepped-up to 750 kV for transmission to the load centers. The 50 Hz power needed in Paraguay would be stepped-down to 230 kV ac, initially, with provision for transmission at 500 kV ac in the future. The bulk of the 50 Hz power, initially, would be transmitted at 500 kV ac to the left bank for conversion to ± 600 kV dc for transmission to the São Paulo area.

This chosen arrangement had the following advantages:

- Politically acceptable to both countries.
- Greater flexibility in accommodating the future growth of energy use in Paraguay.
- No restrictions with respect to possible interconnections with other neighboring nations generating at 50 Hz.
- Greater flexibility in determining turbine and generator characteristics for the two frequencies.
- For Brazil, gaining experience with HVDC transmission and conversion which would be of great use in other areas, especially transmission from future hydrostations in the Amazon to the country's load centers.
- No major technical difficulties.

Although not the least cost solution, the savings in both initial cost and efficiency of the transmission

lines partly compensated the cost of conversion and conversion losses.

There were attendant complications in that much auxiliary equipment had to work with both frequencies, involving switching circuits and dual frequency motors etc. These were not considered major factors.

GENERAL ARRANGEMENT

For diversion of the river and continuous construction of the powerhouse and the main dam, the left bank of the river was determined to be the more suitable site for a diversion channel. The material excavated from the diversion channel would be used up entirely in the rockfill dam on the left bank and for crushing aggregate for concrete. Selection of the location of the main dam, the single powerhouse at the toe of the dam and the diversion facilities on the left bank determined that the plateau on the right bank would be the logical and economical site for the spillway. With the basic configuration of the project determined, further studies were conducted to elaborate this arrangement to form the basis for final design.

SPILLWAY

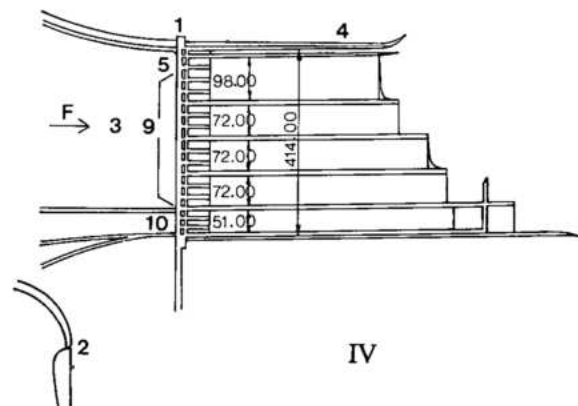
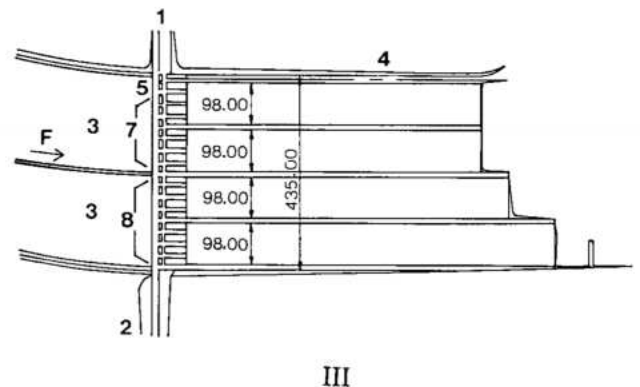
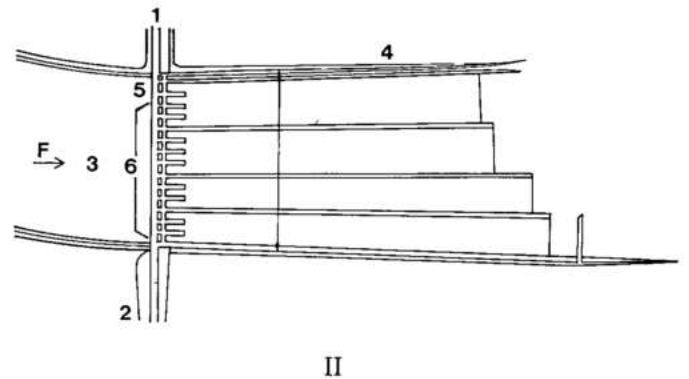
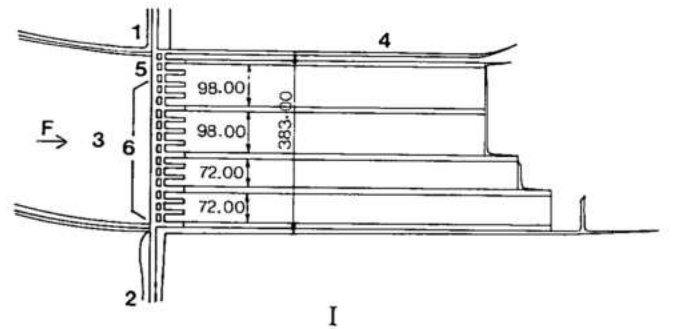
As well as fitting in with the overall project arrangement, the spillway on the right bank had the following additional advantages:

- Least interference with powerplant operation.
- The area between the spillway and the powerhouse could be used for a possible additional powerhouse in the future. During construction it could be used to house a concrete batch plant which would otherwise have been difficult to locate.
- Construction of the spillway could be independent of the main works.

Four right bank alternative spillway layouts were analyzed and compared, see Fig. 2.17.

Fig. 2.17 Spillway layout alternatives

- | | |
|--|-----------------------------------|
| I Alternative 1 (Parallel walls) | 4 Log chute (9 m) |
| II Alternative 2 (Gradual widening of channels) | 5 One 9 x 4 m gate |
| III Alternative 3 | 6 Fourteen 20 x 20 m gates |
| IV Alternative 4 (Displaced 220 m downstream) | 7 Eight 20 x 20 m gates |
| 1 Concrete dam | 8 Eight 20 x 16.5 m gates |
| 2 Rockfill dam | 9 Thirteen 20 x 20 m gates |
| 3 Spillway approach channel | 10 Three 13 x 13 m gates |
| | F Flow direction |



Alternative 1. Included fourteen 20 m x 20 m radial gates and split-elevation chute with four channels.

Alternative 2. Had the same general layout as the first alternative, but the four chute channels were flared in plan, with channel width gradually increasing downstream for potential improvement in energy dissipation due to wider jets.

Alternative 3. Was at the same location, but included eight 20 m x 20 m main radial gates and eight smaller service gates, 20 m wide and 16.5 m high. A longer spillway structure and a wider chute were required to accommodate the additional number of gates, but relative to alternative 1, the operation would be more flexible, and conditions for energy dissipation at the exit improved.

Alternative 4. Included thirteen 20 m x 20 m main gates and three smaller 13 m x 13 m auxiliary radial gates, affording sufficient flexibility of operation. Five separate parallel chute channels were provided. The gate structure was shifted downstream by about 220 m with respect to the other alternatives, with a corresponding reduction in length of the discharge chute; but the right wing dam, connecting the main dam to the spillway, was longer.

Final evaluation of the alternative spillway layouts was based on comparative cost indices, including both civil works and mechanical equipment, as well as assessment of technical adequacy. The comparative data were:

Item	Alternative			
	1	2	3	4
Cost index (civil construction)	100	104	109	100
Flexibility of operation	Fair	Fair	Average	Good

Alternative 1 had about the same cost as alternative 4, with the advantage of having gates of uniform size. But, as in the case of alternative 2, flexibility of operation was potentially curtailed since only the large gates would be available. Alternative 3 would be more flexible in operation than alternatives 1 and 2, but at a substantially higher cost.

Alternative 4 had a good flexibility of operation at no additional cost when compared to alternative 1. Cost estimates included the additional length of the right wing dam as compared with the other alternatives.

Based on the above considerations, alternative 4 was recommended as the most viable solution

(subject to further cost analysis and hydraulic model studies), because it satisfactorily fulfilled the basic design requirements of capacity, flexibility and economy. This arrangement was later changed resulting from further study, see Chapter 8.

DAMS

Dam axis

Eight alternative axes were investigated, covering a 6 km stretch of the river in the general vicinity of Itaipu Island. After preliminary screening, the following four axes were selected for final optimization analyses:

- Axis A1, crossing the Rio Paraná immediately downstream of Itaipu Island, corresponding to the general layout used in the early phases of the feasibility studies.
- Axis A2, about 300 m downstream from A1.
- Axis C1a, about 800 m downstream from A1.
- Axis E, about 3100 m downstream from A1.

Comparative analyses of the layouts along the four axes were conducted taking into account economic factors and other qualitative evaluations, to obtain a comprehensive appraisal of the relative worth of each alternative.

Cost estimates were prepared on a uniform basis and included allowances for factors of difficult itemization.

Comparative cost indices were:

Layout axis	A1	A2	C1a	E
Cost index	100	93.6	91.5	96.0

Additional discriminating factors were then considered in the final evaluation:

- Damsite morphology on the abutments was the least favorable at axis E for incorporating wing dams, future powerplant extensions and construction facilities; while best conditions were found at axis C1a.
- Damsite bathymetry was most favorable at axis E.
- Cofferdam construction and closure, a most critical item for project implementation, could be performed under good conditions at axis E due to shallow water at upstream sites. Axis A2 was best for cofferdam construction.
- Geologic conditions for dam foundation were best at axis E. At the upstream axes, conditions were also good, but some special treatment of some weaker rock zones might be required.
- Spillway discharge was not expected to have adverse effects at the three upstream axes. However, spillway at axis E close to an S shaped river bend could involve high risks of heavy erosion

and subsequent formation of river bars; in addition, operation of both the Acaray powerhouse and the future navigation facilities at a short distance downstream could be endangered. The adoption of a minimum distance of 800 m between the spillway and powerhouse would minimize the effects of turbulence on turbine operation.

- Embankment dam construction could develop some practical difficulties due to the high natural moisture content of local clays. Remedial measures to reduce the moisture content would increase the cost of embankment dams; this factor most adversely affected axis E, which would have the highest embankments.
- Future powerplant extensions would have greater flexibility in design at axes A1 and A2.
- Construction plant layout would be relatively more complex at axes A1 and E.

The above discriminating factors, as well as the cost indices, were ranged in order of relative attractiveness for final evaluation, according to the following classification criteria: 3-very good; 2-good; 1-fair. Table 2.12 summarizes the results of the final evaluation of alternative layout.

Table 2.12 Final evaluation of alternative dam axis layouts

Discriminating factors	A1	A2	C1a	E
Morphology	2	2	3	2
Bathymetry	1	2	1	3
Cofferdam construction	2	2	1	3
Concrete dam foundations	2	2	2	3
Spillway effects	2	3	3	1
Embankment dams	3	3	3	1
Future plant extensions	3	3	2	2
Construction plant	3	3	2	2
Navigation & other factors	3	3	3	1
Construction cost	1	3	3	2
Overall evaluation	22	26	23	20

Based on the above results, the layout at axis A2 was considered the most suitable and adopted for development of the final layout of the Itaipu project.

Type of main dam and right wing dam

Four types of main dams were investigated, as follows:

- Concrete buttress or hollow gravity.
- Concrete solid gravity.
- Concrete arch gravity.
- Rockfill.

The earthfill type dam was rejected during the preliminary studies, which also indicated that the concrete arch gravity and the rockfill type dams, although feasible, did not compare favorably with either the gravity or the buttress types of concrete dam.

Comprehensive studies were made of the solid gravity and buttress or hollow gravity types of concrete dam, covering section optimization, foundation conditions, stress and stability analyses, construction aspects and costs, in order to assess the relative technical and economic merits of both types.

Results of the stability analyses showed that both types of dams were adequately safe against shearing-sliding at and through the foundations. However, in order to obtain a shear-friction factor of safety higher than 2.5 at or through the anticipated weaker rock strata or discontinuities, beneficiation or replacement of 30% of the weaker zones would be sufficient for the hollow gravity, but not for the solid gravity dam. Also, for comparable conditions and loading criteria, shear-friction factors were about 25% higher for the hollow gravity than for the solid gravity dam.

Conventional and FEM analyses indicated that, for comparable loading conditions, the foundation stresses and associated displacements would be lower for the lighter and more flexible hollow gravity dam than for the solid gravity dam.

Foundation treatment for the solid gravity and the hollow gravity or buttress dams would have the same objectives, and would normally consist of:

- Area-wide shallow consolidation grouting.
- Removal of weaker material from certain strata or contact zones under the foundation and replacement by concrete.
- Deep cut-off grouting.
- Curtains of drilled drainage holes.
- Supplementary foundation grout and drainage curtains from tunnels extending into the abutments.

Since it would cover a larger foundation area, a solid gravity dam block would be subjected to greater hydraulic uplift than the buttress dam. In a buttress or hollow gravity dam, hydraulic uplift is effective mainly under its upstream head. Conversely, seepage flow under the buttress or hollow gravity dam can be greater than under the solid dam. Also, the factors that deserve special consideration in the design of the buttress dam are the tendency for seepage flow to emerge downstream of the buttress head and for high uplift pressure gradients to occur at that point. Foundation cutoff grouting and the drainage curtain would be similar for both dam types, but would be somewhat greater in magnitude for the buttress than for the solid gravity dam. However, it would be easier and more

economical to provide future supplementary grouting and foundation drainage in a buttress or hollow gravity dam than in a solid gravity dam.

Analyses of the construction aspects of the two types of dams considered such factors as total volume of concrete, height of lift, sizes of pours, number of monoliths, cement and fly ash content, formwork, construction joint treatment and temperature control.

Comparative quantity and cost estimates based on foundation excavation, concrete, steel reinforcement, grout curtain and drainage holes of the two alternative types for the main and the right wing dams, indicated that the buttress and hollow gravity alternative would require about 25% less concrete and cost about 12% less than the solid gravity dam.

Although these analyses conclusively favored the buttress and hollow gravity types of dam, the feasibility report recommended that the final selection should be made after the geotechnical investigations were concluded. The selection of the hollow gravity type for the main dam and the massive head buttress type for the right wing dam was confirmed in November 1974, see Chapter 9.

Type of rockfill dam for left bank

Due to its major importance within the project, and the impossibility of lowering at will the reservoir level, the design of the rockfill dam on the left bank was based on strict safety requirements for structural stability. Additionally, the design incorporated efficient and economical use of the large quantities of material to be excavated in the diversion channel.

The following four alternative solutions were investigated for the rockfill dam on the left bank:

Alternative 1. Section with upstream impervious facing would allow maximum flexibility for construction. Upstream transition and facing could be added at a later date, after rockfill placement. Handling and treatment of excessively wet clays would be avoided. However, as dewatering of Itaipu reservoir for maintenance and repair would not be practical, any cracking or other damage to the membrane facing due to unavoidable settlements or other causes, would jeopardize the safety of the project. Accordingly, this section was eliminated as an alternative.

Alternative 2. Section with upstream impervious zone including a first-stage rockfill built of material from channel excavation, later completed by a thick, compacted-clay wedge on the upstream side. While construction flexibility would be good, a large amount

of sandy clay would be required for a stable impervious zone. Also, stability problems during reservoir draw-down would require careful investigation and adequate design provisions.

Alternative 3. Section with sloping core similar to the second alternative, but including a thinner upstream clay zone, protected by a larger upstream rockfill shell for added stability. The whole of the main downstream shell would be built earlier with rock from diversion channel excavation and the clay core and the upstream rock shell would be added later. This solution was judged to have unsatisfactory safety features, since its imperviousness depended entirely on a relatively thin clay layer placed on thin filters.

Alternative 4. Section with a slightly inclined relatively thick central clay core backed by a thick transition zone and flanked by rockfill shells. It had the best stability conditions and intrinsic safety, but required that the rockfill from diversion channel excavation and the clay core and filters be placed concurrently, thus limiting somewhat the construction flexibility. However, as a certain difference in levels of core and shell zones could be allowed during construction, clay placement rate could be easily adjusted for weather conditions while rock placement continued at a more constant rate.

Relative quantities and costs determined for the three feasible sections were:

Item	Alternative		
	2	3	4
Rock volume (10^6 m^3)	12.65	12.65	11.95
Clay volume (10^6 m^3)	7.00	1.85	1.55
Cost index	124	109	100

Based on the above considerations and data, the section with a slightly inclined central clay core was selected for design.

Materials for embankment dams

During phase 4 of the feasibility study, as more detailed layouts and estimates of quantities of materials required for construction were developed for the alternative projects, the following basic rules were followed for selection of materials for the earth and rockfill embankment dams and cofferdams:

- Whenever practical, rock and earth materials obtained from excavation for the works should be used in the embankments.

- Borrow areas for soils should be within economic and practical haul distances on both sides of the river.
- Because of the heavy rainfall in the area throughout the year and the resulting high natural moisture content of the red clays, special procedures might have to be used for selecting suitable material and controlling the moisture content. These procedures would entail higher costs.

The red clays, which could be used for the impervious cores of the cofferdams, the rockfill and the earth dams, were of critical importance. In its natural state, this material is highly porous with medium to high plasticity and a high natural moisture content. The red clays are generally poor foundation material due to low strength and high compressibility, and consequently greatly influence the stability of the low earth dams which would have to be located on them. However, when compacted at optimum moisture content, they are excellent for embankments. To reduce the natural moisture content of the clays to acceptable values, the following methods were tested in the field:

- Gravity drainage in borrow areas prior to excavation.
- Natural drying by harrowing and reworking, either in borrow area, or on the fill, or both.
- Partial drying by one of the above methods, followed by blending with drier materials such as crushed breccia, or silty sands from distant borrow areas.

Decomposed rock or saprolite, which underlies the red clays at depths of 2 to 15 m, was also abundantly available in the area. This material was generally plastic with high moisture content and low shear strength. While not considered suitable for impervious cores of the embankment dams, it could be used in the random fill zones of the cofferdams.

The search for suitable borrow areas extended over 2 to 6 km from Itaipu. To estimate quantities of various types of soils available, geophysical surveys were combined with test pits and auger hole sampling on a grid pattern over four prospective areas on each bank. The field investigations were complemented by laboratory tests on both undisturbed and remolded representative samples.

Using estimated volumes of suitable soils at each prospective borrow area, economic comparisons were made considering the haul distance and the necessity of processing, stock-piling and rehandling before placing them in permanent embankments. From these analyses borrow areas were tentatively identified for inclusion in the feasibility studies of the project.

Sound rock was located near the project site at depths of 2 to 20 m below ground surface, the transition from overlying decomposed rock being

generally abrupt. The sound rocks would be competent materials for foundations of the embankment dams. Sound basalt would be excellent for rockfill construction and crushed sound breccia could be used for the transition zones of the embankment dams. In addition to the standard tests for physical properties, various grades of basalt and breccia were tested for durability when subjected to submergence in water and cyclical wetting and drying. Duration of the tests was nearly 3 years; they confirmed the suitability of sound basalt for embankment dam construction.

While reconnaissance surveys had not located any terrace deposits of sand at higher elevations, several small deposits were found along the river during moderate flows. Considering the large amount of sand required for filters in the embankment dams and for concrete, geophysical surveys of sand deposits on the river bed were conducted over a distance of 13 km between Itaipu and Acaray island. Reconnaissance surveys extended another 150 km downstream of Acaray. Representative samples of the natural sand were obtained from the larger deposits and tested for suitability for filters, as well as for concrete. The cost estimates assumed that the sand would be hauled by barges.

Materials for concrete structures

Concrete aggregates. Since no significant deposits of natural gravels were found within or near the bi-national reach of the Rio Paraná, it was decided during the early stages of the study that aggregates for concrete would have to be crushed from local sound rock. Weathered basalt or breccia had relatively poor physical properties and were not considered suitable; therefore, only sound dense basalt was to be used for aggregates.

Standard laboratory tests for physical properties, durability and susceptibility to alkali-aggregate reaction were performed to establish suitability of the basalt. Because vesicles in the amygdaloidal basalt were filled with calcite, zeolites and quartz, there was some concern about potential alkali reactivity. Therefore, it was decided that such material should be excluded from concrete aggregates.

Preliminary studies were made of the crushing characteristics of basalt and the type of crushing, screening and blending plant required for obtaining suitable concrete aggregate. Since the large amount of rock to be excavated for project structures and the diversion facilities was to be used for embankments, as well as for concrete aggregates, preliminary construction planning, interface scheduling and material balance studies were made to determine the cost of crushed rock aggregate for feasibility

analyses. Since only selected basalt was to be used, there was an additional cost for the aggregates.

The natural sand deposits in the river channel which were plentiful and economical to haul, were tested in the laboratory and used for preliminary concrete mix design. While these sands were physically satisfactory, they were too fine and uniform. Therefore, it was concluded that it would be necessary to improve the grading of the fine aggregate by blending natural sand with fine crushed basalt. However, the subject was not investigated further at that stage, because it did not influence the feasibility of the project alternative being studied.

Concrete dam foundations. The following general criteria were adopted for preliminary design of foundations of concrete dams for the various project alternatives:

- Concrete dams higher than 50 m should be founded on sound dense basalt.
- A minimum of 10 m of dense basalt should be maintained between the dam foundation and the underlying breccia.

- Where at foundation level breccia and basalt would be intermixed and it would not be practical to lower the foundation level, at least 65% of the breccia was to be removed and replaced by concrete to improve shearing resistance.

- Where structures would be founded on vesicular basalt, the foundation would be 2.5 m below the top of the vesicular zone where scoriaceous materials may be found.

- Drainage and grouting tunnels would be located in weak cavernous breccia or at the permeable contact zones under both abutments of the main concrete dams in the river channel.

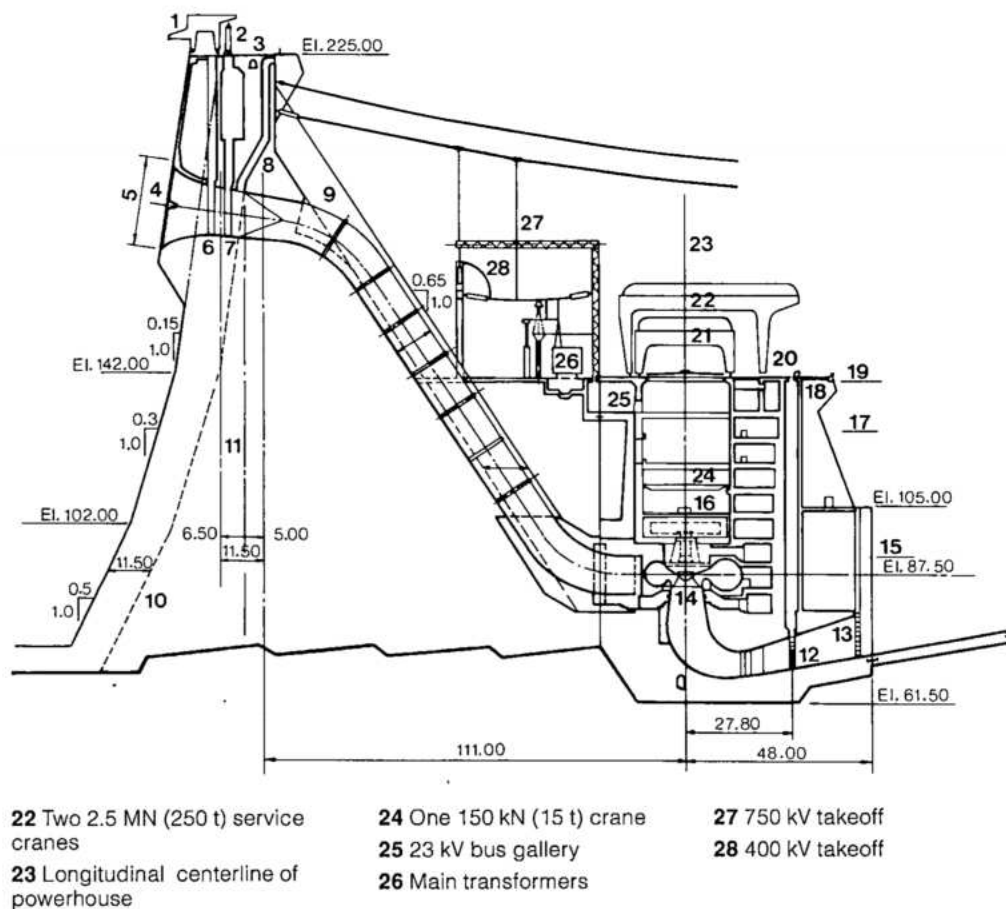
The above geotechnical criteria were uniformly applied to the layouts and the quantity and cost estimates developed at various stages of the preliminary studies and feasibility analyses.

POWERHOUSE

With the characteristics of the main units tentatively established the powerhouse was provisionally defined as follows, see Fig. 2.18:

Fig. 2.18 Preliminary powerhouse design

- 1 Intake crane and trashrack rakes
- 2 Gate hoist
- 3 Roadway
- 4 Trashracks
- 5 Two 11.50 x 23.00 openings
- 6 Stoplogs
- 7 Intake gates
- 8 Air vent (ϕ 2.00)
- 9 Penstock
- 10 Face of adjoining non-intake block
- 11 Axis of dam
- 12 Draft tube gates
- 13 Stoplogs
- 14 Eighteen Francis turbines, 650 MW
- 15 Assumed min TW El. 92
- 16 Eighteen - Generators, 635 MW rated capability, 700 MW continuous output
- 17 Max nor. TW El. 125
- 18 Air ducts
- 19 Max flood TW El. 138
- 20 Cable gallery
- 21 One 1.9 MN (190 t) main crane



- Eighteen units in total, fourteen in the river bed and four in the diversion channel. Unit spacing to be 37 m.
- Outdoor type power station with hatch covers over the units.
- Each set of two units contained in a single bay, watertight to the powerhouse roof at El.144. This design was to eliminate any possibility of flooding the complete station by accident.
- Two 2.5 MN and one 1.9 MN gantry cranes servicing the units.
- All service galleries located downstream of the units.
- Penstocks secured by prestressed cables strained to the dam.
- Transformers at El.144 and high voltage switching at the right and left bank switchyards.

This powerhouse design was considerably modified as a result of further investigations of layout, construction program and equipment characteristics, see Chapter 11.

PROJECT BASIC

DATA AND FEATURES

PROJECT LOCATION	3.3
BASIC PROJECT LAYOUT, DATA AND CONCISE LIST OF FEATURES	3.4
General	3.4
Civil Construction Works	3.6
Permanent Equipment	3.8
Powerhouse	3.11
Substations	3.14
Powerlines	3.18
MAGNITUDE OF ITAIPU	3.18
FINANCIAL ASPECTS	3.21
NAVIGATION	3.23

PROJECT BASIC

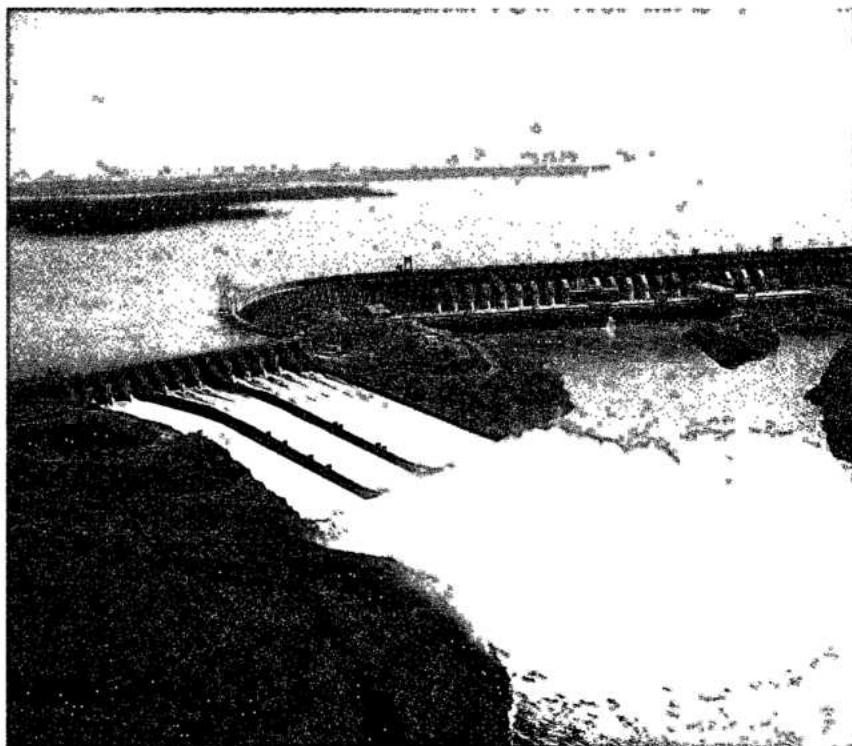
DATA AND FEATURES

PROJECT LOCATION

The Itaipu project has a pivotal geographic location in relation to the largest industrial and urban areas of Brazil and Paraguay, see Fig. 3.1; its distance from these areas is as follows:

Brazil	km	Paraguay	km
Rio de Janeiro	1500	Asunción	330
São Paulo	1060	Encarnación	290
Belo Horizonte	1670	Ciudad del Este	14
Curitiba	650		
Florianópolis	965		
Porto Alegre	1380		
Foz do Iguaçu	14		

Because of the relatively flat plateau in the vicinity of the project, it was possible to provide excellent access to the site by highways on both sides of the river. From the city of Foz do Iguaçu there is a 10 km long highway to the site and from Ciudad del Este there is a highway of 20 km.



*General view of Itaipu
hydroelectric scheme*



Fig. 3.1 Itaipu project area

BASIC PROJECT LAYOUT, DATA AND CONCISE LIST OF FEATURES

The general layout of the main permanent facilities of Itaipu project is shown in Fig. 3.2.

A summary of the more significant basic data of the various project features and facilities is given below. These differ from those determined at the feasibility stage. Detailed descriptions of the planning, design, construction and manufacturing aspects of the various structures and permanent equipment of Itaipu project, which led to these changes are presented in subsequent chapters.

GENERAL

Location

Country	Brazil and Paraguay
River	Paraná
Latitude	25° 30'S
Longitude	54° 30'W

Basic data

Project drainage basin	820 000 km ²
Average annual precipitation	1400 mm
Average annual temperature	22°C
Maximum temperature	40°C
Minimum temperature	- 4°C
Average annual relative humidity	75 %
Climate	Subtropical

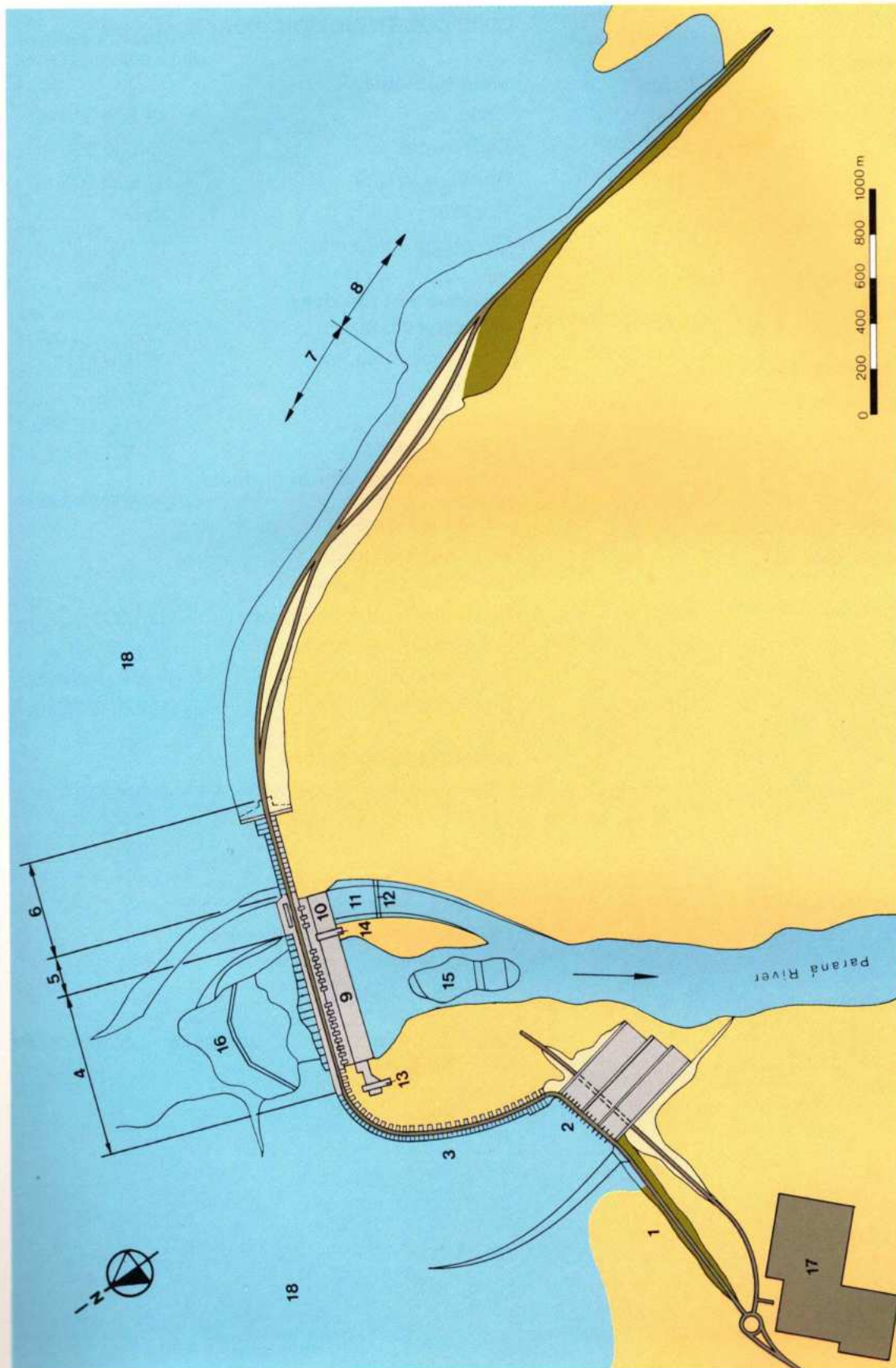


Fig. 3.2 Project general layout

- | | | | | |
|--|--|--|--|---------------------------------|
| 1 Right Earthfill Dam | 4 Main dam, blocks F (36) plus right buttress dam, blocks E (6) | 7 Rockfill dam | 10 Power house in diversion channel, blocks U16 to U18A | 14 Left assembly area |
| 2 Spillway, blocks A (15) | 5 Diversion structure, blocks H (14) | 8 Left Earthfill dam | 11 Diversion Channel | 15 Downstream cofferdam |
| 3 Right wing dam, blocks D (58) | 6 Left buttress dam, blocks I (27) | 9 Power house in riverbed, blocks U1 to U15 | 12 Service bridge | 16 Upstream cofferdam |
| | | | 13 Right assembly area | 17 Right bank substation |
| | | | | 18 Reservoir |

Reservoir

Surface area at maximum normal level	1350 km ²
Reach length	170 km
Total volume	29 x 10 ⁹ m ³
Active volume	19 x 10 ⁹ m ³
Maximum normal level	220 m
Maximum flood level	223 m
Minimum exceptional level	197 m
Average annual water temperature	22°C
Maximum water temperature	30°C
Minimum water temperature	10°C

Tailrace

Maximum normal level	106.10 m
Minimum normal level	96.6 m
Maximum exceptional level with downstream development	142.5 m
Maximum exceptional level without downstream development	138 m
Minimum exceptional level	92 m

Net head

Maximum	129.7 m
Average	118.4 m
Minimum	83.7 m

River flows and design floods**RECORDED AT GUAÍRA**

Average (1921-1971)	9070 m ³ /s
Minimum daily average	3075 m ³ /s
Maximum daily average	39 790 m ³ /s

DIVERSION DESIGN FLOW

Maximum design flow	35 000 m ³ /s
---------------------	--------------------------

SPILLWAY DESIGN FLOW

Probable maximum flood inflow	72 020 m ³ /s
Design maximum outflow	62 200 m ³ /s

Generating capacity

Total installed	12 600 MW
Average production	75 x 10 ⁹ kWh/year

CIVIL CONSTRUCTION WORKS**Main quantities**

Concrete	12 300 000 m ³
Earth excavation	23 600 000 m ³
Rock excavation	32 000 000 m ³
Rockfill	15 000 000 m ³
Clay, aggregate, etc.	16 700 000 m ³

Diversion of the river**DIVERSION CHANNEL**

Discharge capacity	35 000 m ³ /s
Length	2000 m
Bottom width	150 m
Maximum depth	90 m
Excavated volume – in diversion channel	22 500 000 m ³

Main cofferdam**UPSTREAM COFFERDAM**

Volume of earth excavation	327 000 m ³
Volume of rock excavation	390 000 m ³
Volume of fill	7 220 000 m ³
Crest elevation	140 m

DOWNSTREAM COFFERDAM

Volume of earth excavation	305 000 m ³
Volume of rock excavation	557 000 m ³
Volume of fill	4 100 000 m ³
Crest elevation	125 m

COFFERDAM IN DIVERSION CHANNEL

Volume of fill	1 130 000 m ³
Crest elevation	136 m

ARCH CONCRETE COFFERDAM

	UPSTREAM	DOWNSTREAM
Maximum height	35 m	31.5 m
Crest length	164 m	134 m
Top thickness	1.7 m	1.7 m
Bottom thickness	5.0 m	4.6 m
Concrete volume	22 000 m ³	13 000 m ³

Dikes

Hernandarias earthfill and clay core volume	50 800 m ³
Boa Vista e Pomba Quê earthfill and claycore volume	631 000 m ³

Project structures**RIGHT EARTHFILL DAM**

Type	Zoned
Crest elevation	225 m
Length of the crest	872 m
Maximum height	25 m
Total volume of fill	400 000 m ³

SPILLWAY

Number of blocks	15
Crest elevation	200 m
Maximum height	44 m
Total width	380 m
Total length (chute + crest)	483 m
Rock excavation	5 200 000 m ³
Earth excavation	7 100 000 m ³
Concrete	800 000 m ³

RIGHT-WING DAM (concrete)

Type	Massive head buttress
Crest elevation	225 m
Length of the crest	986 m
Maximum height	64.5 m
Rock excavation	523 000 m ³
Earth excavation	950 000 m ³
Concrete	775 000 m ³

MAIN DAM (concrete)

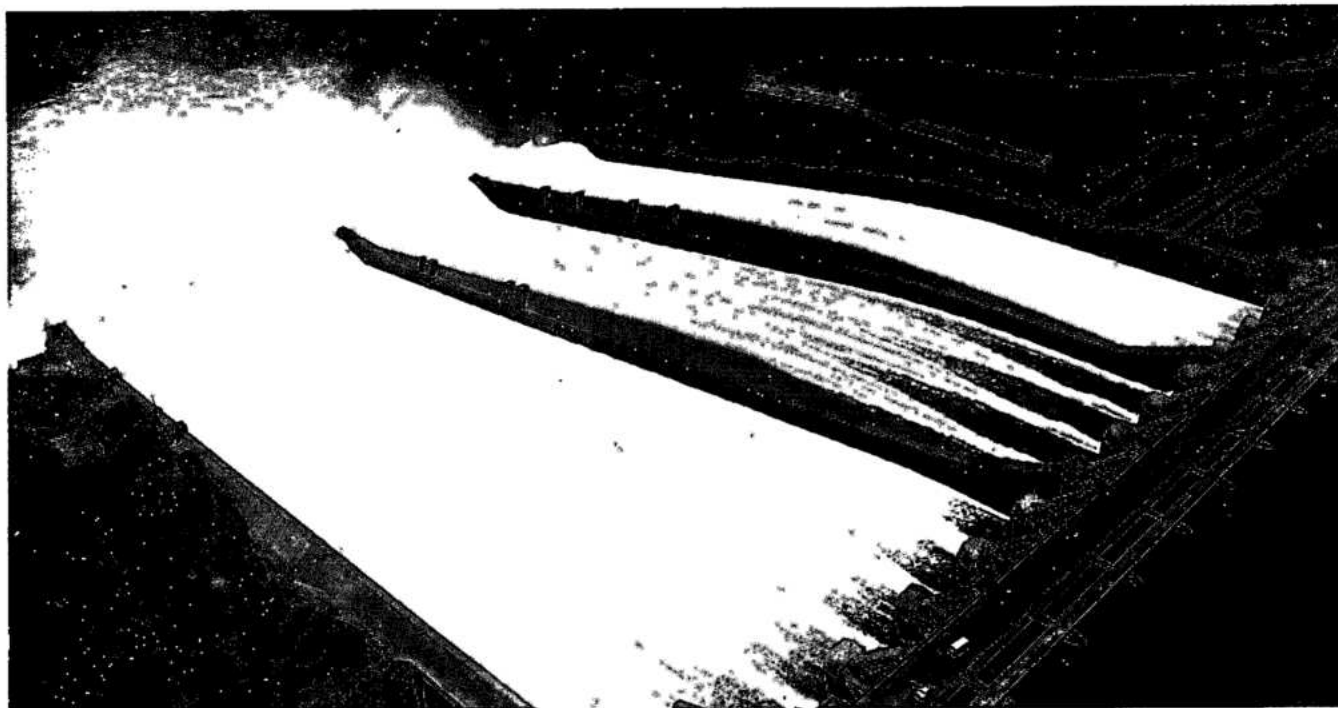
Type	Buttress and hollow gravity
Crest elevation	225 m
Length of the crest	1064 m
Maximum height	196 m
Rock excavation	2 200 000 m ³
Earth excavation	500 000 m ³
Concrete	5 300 000 m ³

DIVERSION CONTROL STRUCTURE (concrete)

Type	Gravity
Crest elevation	225 m
Length of the crest	170 m
Maximum height	162 m
Concrete	2 200 000 m ³

ROCKFILL DAM

Type	Zoned
Crest elevation	225 m
Length of the crest	1984 m
Maximum height	70 m
Excavation for the foundations	5 100 000 m ³
Total volume of fill	12 800 000 m ³

*Spillway*

LEFT EARTHFILL DAM

Type	Zoned
Crest elevation	225 m
Length of the crest	2294 m
Maximum height	30 m
Total volume of fill	4 400 000 m ³

POWERHOUSE (including erection areas)

Length	968 m
Width	99 m
Maximum height	100 m
Rock excavation	4 300 000 m ³
Earth excavation	1 200 000 m ³
Concrete	3 200 000 m ³

TAILRACE

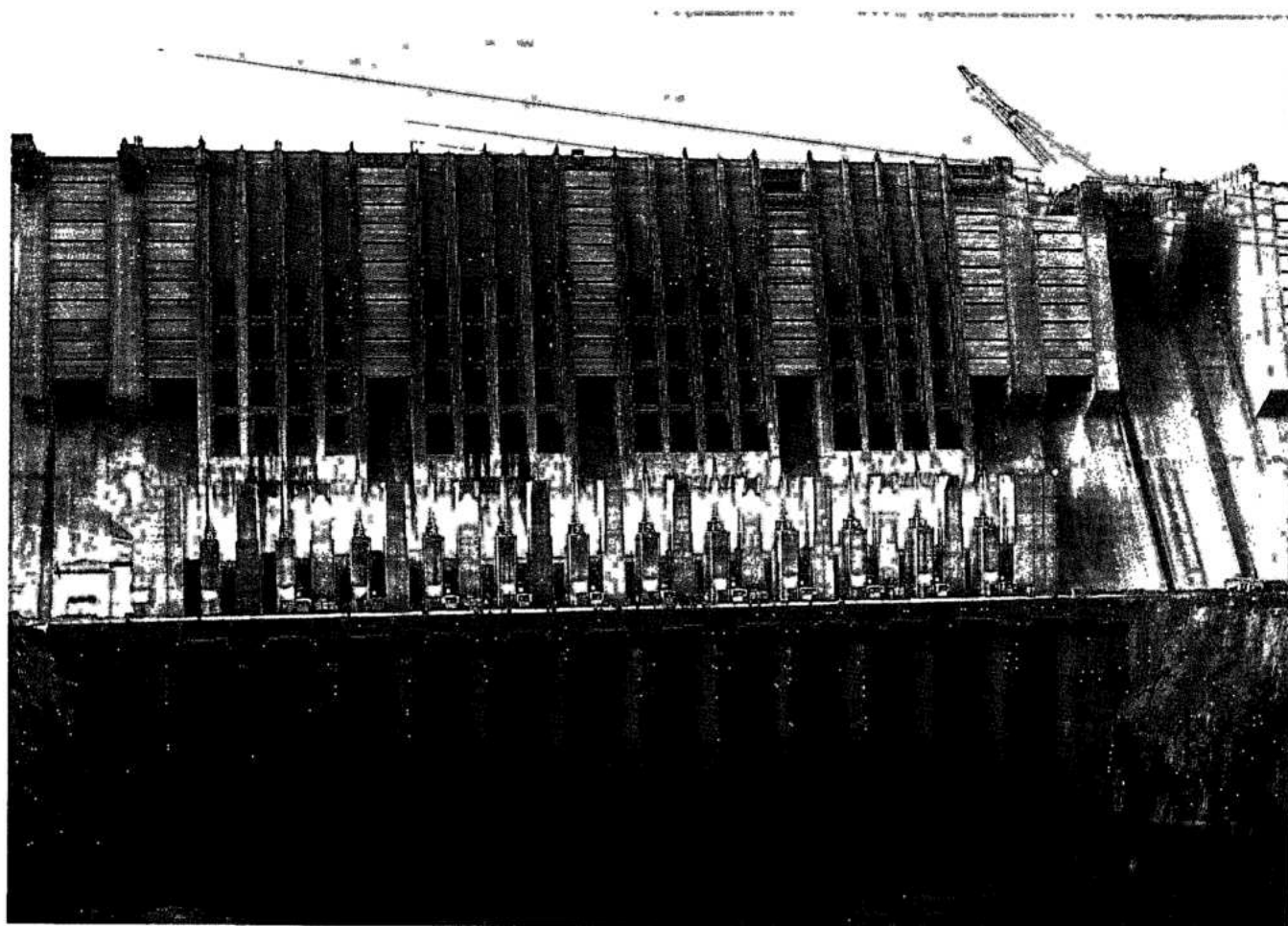
Excavation volume	2 248 000 m ³
-------------------	--------------------------

PERMANENT EQUIPMENT**Spillway****STOPLOGS**

Span	20.70 m
Height (set of six elements)	21.53 m
Number of elements per opening	6
Number of sets	2

SPILLWAY GATES

Quantity	14
Type	Tainter
Span	20 m
Height	21.34 m
External radius of skinplate	20.016 m
Sill beam elevation	199.16 m

*Diversion control structure*

GANTRY CRANE

Quantity	1
Capacity	785 kN (78.5 t)
Vertical lift of the hook	27 m
Maximum hoisting speed	2 m/min
Minimum hoisting speed	0.2 m/min
Maximum travelling speed	30 m/min
Minimum travelling speed	3 m/min

ROLLING TRACK OF GANTRY CRANE

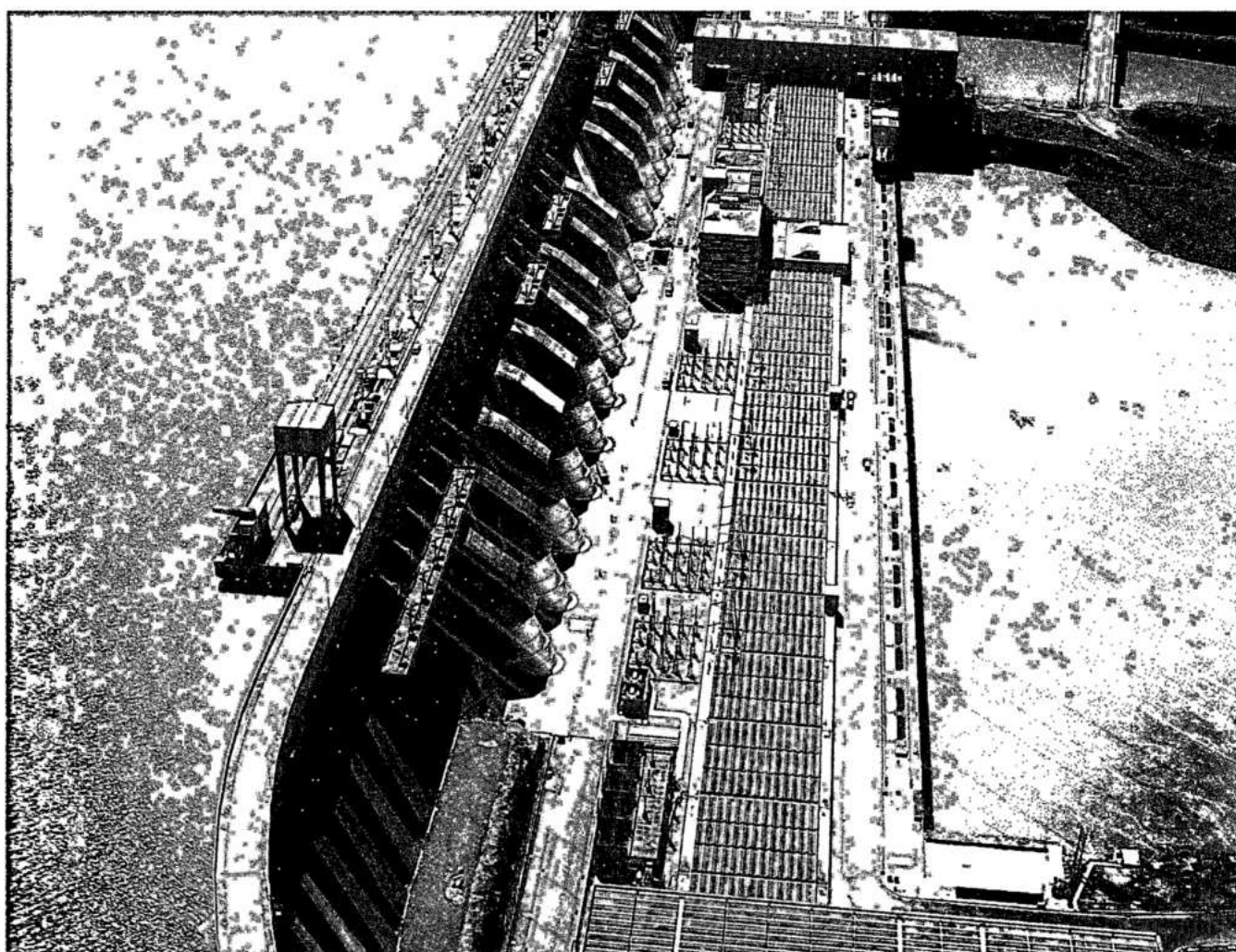
Span	5 m
Total length	355.7 m
Rail-top elevation	225.25 m

Main dam and diversion control structure**PASSENGER ELEVATORS**

Quantity	6
Unit capacity	9.8 to 14 kN (14 to 20 persons)

POWER-INTAKE**Service gates**

Quantity	18
Span	8.18 m
Total height	19.25 m
Type	Fixed wheel
Sill beam elevation	177.56 m
Maximum flow per intake	750 m ³ /s

*Main dam and powerhouse*

Stoplogs

Sill beam elevation	177.17 m
Span	7.46 m
Height (set of 7 elements)	17.51 m
Number of elements per opening	7

Gantry cranes

Quantity	2
Capacity	1.1 MN/400 kN (110/40 t)
Vertical lift of the hook	81.2 m
Hoisting speed (50/60 Hz) (with 400 kN)	4.58/5.5 m/min
Hoisting speed (50/60 Hz) (with 1100 kN)	1.67/2 m/min
Nominal travelling speed	25/30 m/min

Rolling track of gantry cranes

Span	10 m
Total length	857.55 m
Rail-top elevation	225 m

Penstocks (lower bend not included)

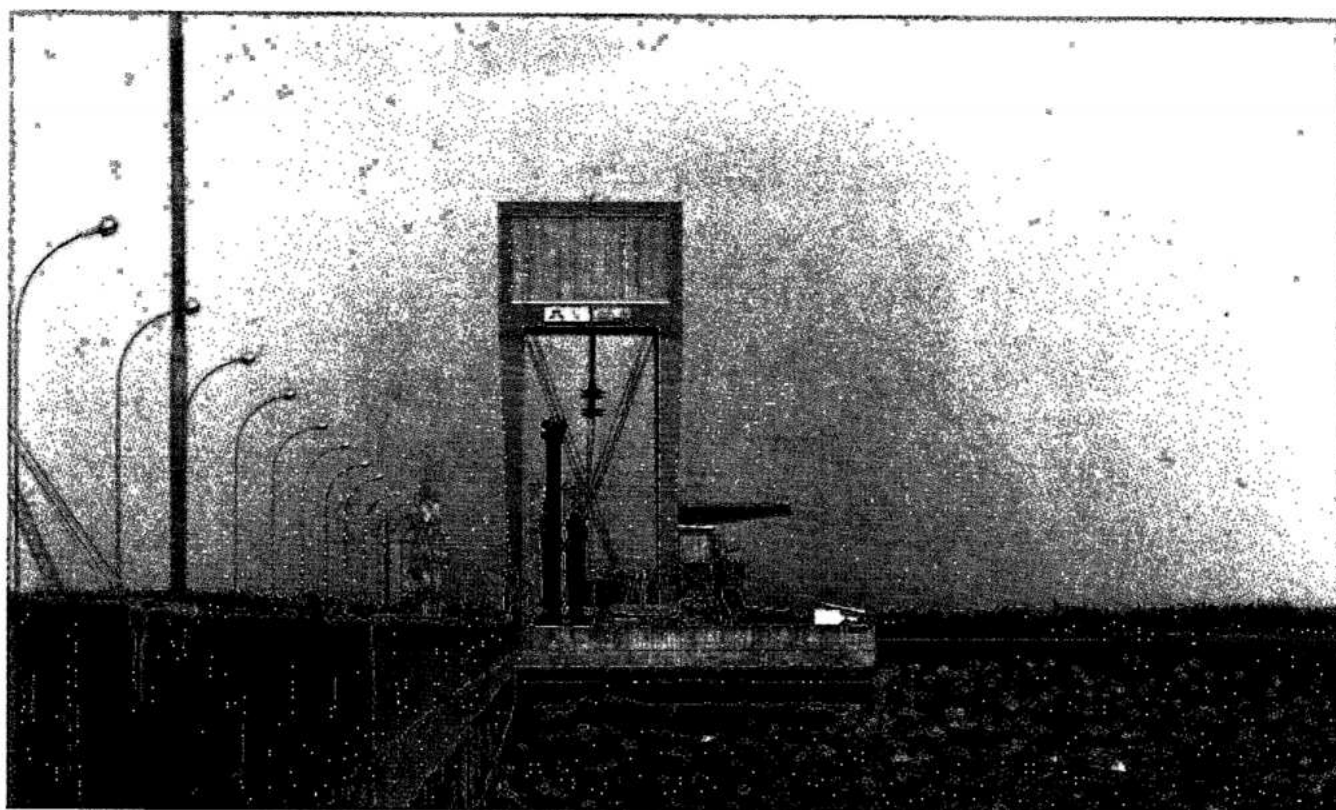
Quantity	18
Number of rings per penstock	44
Weight of each penstock	8.83 MN (883 t)
Inside diameter	10.5 m
Maximum length	94.1 m

Trashracks for power-intakes

Quantity (water intakes)	18
Trashrack panels per intake	24
Dimensions of standard panel	4.73 m x 5.5 m

Trashrack-cleaning machine

Quantity	2
Jib crane capacity	200 kN (20 t)
Vertical lift of the rake	61.5 m
Rake capacity	2 m ³ /2.5 kN



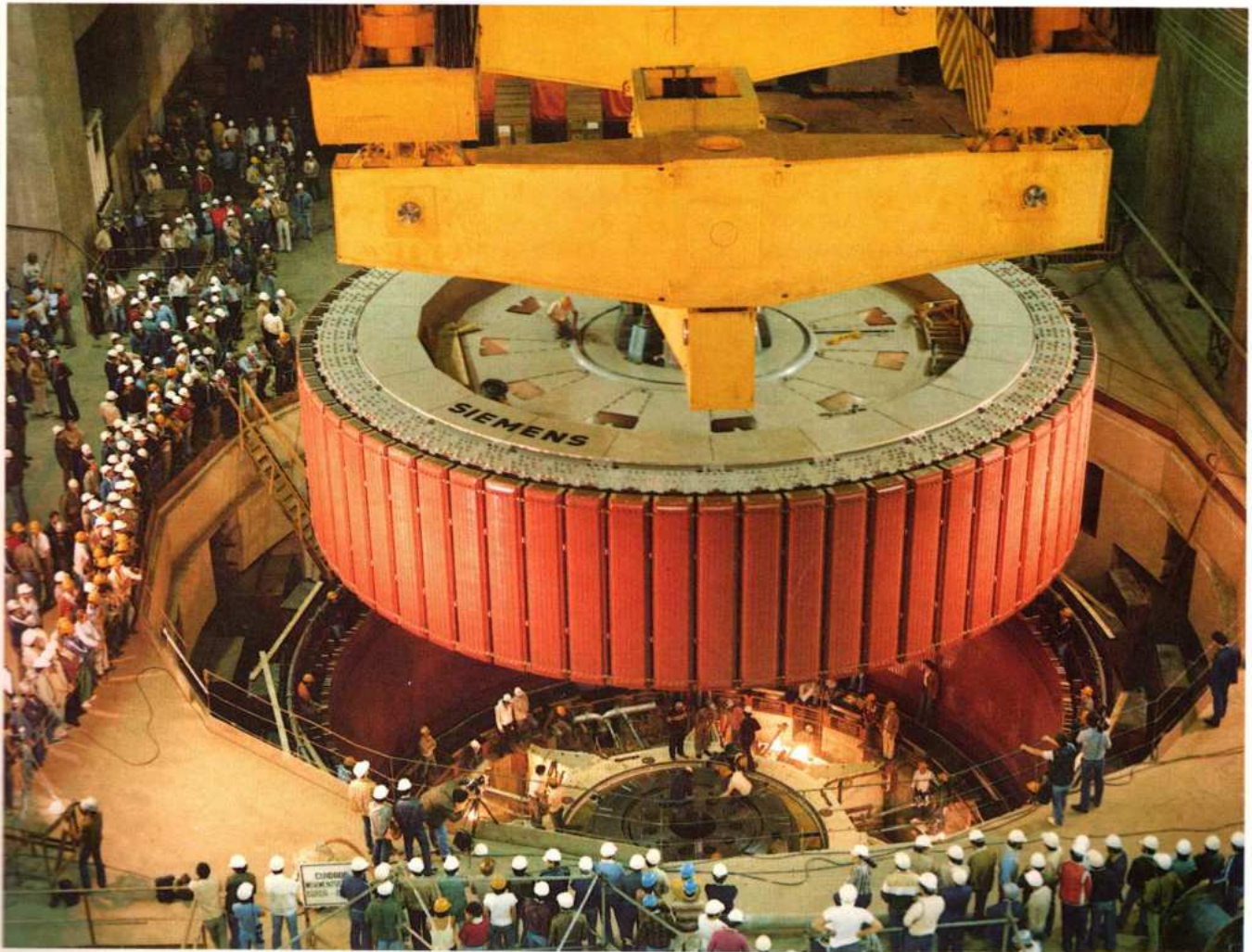
Gantry cranes in water intake area

POWERHOUSE**TURBINES**

Quantity	18
Type	Francis
Rated power	715 MW
Design speed (50/60 Hz)	90.9/92.3 rpm
Head for best efficiency	118.4 m
Rated head	112.9 m
Flow at rated output and rated head	690 m ³ /s
Weight of runner	2902 kN (290 t)
Weight of shaft	1255 kN (126 t)
Weight of stay ring	3826 kN (383 t)

GENERATORS

Quantity (9-50 Hz & 9-60 Hz)	18
Type	Synchronous
Rated power (50/60Hz)	823.6/737 MVA
Design speed (50/60Hz)	90.9/92.3 rpm
Rated voltage	18 ± 5% kV
Number of poles (50/60 Hz)	66/78
Inertia constant (H) (50/60 Hz)	4.4/5.3 kWs/kVA
Power factor (50/60 Hz)	0.85/0.95
Heaviest component (rotor)	17.6 MN (1760 t)
Weight of each unit (50/60 Hz)	33.43/32.42 MN (3343/3242 t)



Generator's rotor

MAIN STEP-UP TRANSFORMERS – 1 PHASE

Quantity (28-50 Hz & 28-60 Hz)	18 banks + one 50 Hz unit and one 60 Hz unit (spares)
Type (water cooled)	OFWF
Rated power (3 phase bank 50/60Hz)	825/768 MVA
Voltage	$525/\sqrt{3} \pm 2 \times 2.5\%$ –18 kV
Type of connection	wye grd. / delta
Impulse/Switching surge level	
HV winding (ph. to neutral)	1550/1300 kV
LV winding (Impulse-BIL)	125 kV
Weight of each single phase unit(50/60 Hz)	2500 /1790 kN

MAIN AUXILIARY SERVICE TRANSFORMERS – 1 PHASE

Quantity (4-50 Hz & 4-60 Hz)	2 banks + one 50 Hz and 60 Hz (spares)
Type (air cooled)	ONAN
Rated power (3 phase banks 50/60 Hz)	45 MVA
Voltage	$525/\sqrt{3} \pm 2 \times 2.5\%$ –13.8/ $\sqrt{3}$ –13.8 kV
Type of connection	wye grd. / wye grd. / delta

STANDBY AUXILIARY SERVICES TRANSFORMERS – 3 PHASE

Quantity (50/60 Hz)	1/1
Rated power (50/60 Hz)	45/30 MVA
Voltage (50 Hz)	$66 \pm 2 \times 2.5\%$ –13.8 – 13.8 kV
Voltage (60 Hz)	$66 + 11.73 - 15.08\%$ – 13.8 kV

EMERGENCY DIESEL GENERATORS

Quantity (50/60 Hz)	2/2
Rated power	5.25 MVA
Rated voltage	6.9 kV
Power factor	0.8

MAIN POWERHOUSE CRANES

Quantity	4
Capacity of each crane	10 MN (1000 t)
Vertical lift of main hook	38 m
Hoisting speed of main hook (unloaded)	2 m/min
Hoisting speed of main hook (loaded)	0.8 m/min
Span	29 m
Rail-top elevation	125 m

SECONDARY POWERHOUSE CRANES

Quantity	2
Capacity of each crane	2.5 MN/200 kN (250/20 t)
Vertical lift of main hook	51 m
Hoisting speed of main hook (unloaded)	15.8 m/min
Hoisting speed of main hook (loaded)	1.7 m/min

ROLLING TRACK OF MAIN AND SECONDARY CRANES

Span	29 m
Rail- top elevation	125 m

AUXILIARY POWERHOUSE CRANES

Quantity	2
Capacity	1 MN/200 kN (100/20 t)
Vertical lift of main hook	74 m
Hoisting speed of main hook (unloaded)	15 m/min
Hoisting speed of main hook (loaded)	3.0/0.6 m/min

ROLLING TRACK OF AUXILIARY CRANES

Span	29 m
Rail-top elevation	136.5 m

CRANES FOR MAIN TRANSFORMERS

Quantity	2
Capacity of each crane	2.5 MN/150 kN (250/15 t)
Vertical lift of main crane	47 m
Maximum hoisting speed of main hook(loaded) (50/60 Hz)	0.83/1 m/min
Minimum hoisting speed of main hook (loaded) (50/60 Hz)	0.17/0.2 m/min

ROLLING TRACK OF CRANES FOR MAIN TRANSFORMERS

Span	10 m
Rail-top elevation	120.3 m

CRANES FOR SF₆ GIS

Quantity	2
Capacity	100 kN (10 t)
Vertical lift of hook	14 m
Maximum hoisting speed (50/60Hz)	4.16/5 m/min
Minimum hoisting speed (50/60 Hz)	0.41/0.5 m/min

ROLLING TRACK OF CRANES FOR SF₆ GIS

Span	20.65 m
Rail-top elevation	139 m

CRANES IN ASSEMBLY AREAS

Quantity	4
Capacity	2.5 MN/200 kN (250/20 t)
Vertical lift of the main hook	51 m
Hoisting speed (unloaded)	15.8 m/min
Hoisting speed (loaded)	1.7 m/min

ROLLING TRACK OF CRANES IN ASSEMBLY AREAS

Span	28 m
Rail-top elevation	160 m

CARGO ELEVATORS IN ASSEMBLY AREAS

Quantity	2
Unit capacity	300 kN (30 t)

PASSENGER ELEVATORS

Quantity	12
Unit capacity	9.8 to 29.4 kN (14 to 42 persons)

GATES FOR DRAFT TUBE

Number of gates per unit	2
Total number of gates	10
Sill beam elevation	66.01 m
Span	10.84 m
Height	10.11 m

DRAFT TUBE GANTRY-CRANES

Quantity	3
Capacity	1.4 MN (140 t)
Vertical lift of the hook	82 m
Hoisting speed(unloaded) (50/60 Hz)	12.5/15 m/min
Hoisting speed (loaded) (50/60 Hz)	2/2.4 m/min
Nominal travelling speed of gantry (50/60 Hz)	30/36 m/min

ROLLING TRACK OF GANTRY CRANES

Span	7 m
Total length	730 m
Rail-top elevation	144.15 m

Powerhouse substation (GIS)**CIRCUIT BREAKERS – 3 PHASE**

(with 2 disconnect switches, 2 groundswitches , and 2 current transformers each)	
Quantity (50/60 Hz)	26/26
Rated current	4000 A rms
Voltage (maximum)	550 kV rms
Impulse level (BIL)	1550 kV crest
Switching surge level	1240 kV crest

DISCONNECT SWITCHES – TRANSFORMER 3 PHASE

Quantity (50/60 Hz)	9/9
---------------------	-----

DISCONNECT SWITCHES – 3 PHASE

Quantity (50/60 Hz)	1/1
---------------------	-----

GROUND SWITCHES – 3 PHASE

Quantity (50/60 Hz)	33/33
---------------------	-------

CURRENT TRANSFORMERS – 1 CORE

Quantity (50/60 Hz)	14/14
---------------------	-------

SURGE ARRESTERS – 1 PHASE

Quantity(50/60 Hz)	63/63
Type(50/60 Hz)	ZnO
Rating	444 kV

POTENTIAL TRANSFORMERS – 1 PHASE

Quantity (50/60 Hz)	12/12
---------------------	-------

BUSHINGS – SF₆ TO AIR – 1 PHASE

Quantity (50/60 Hz)	15/15
---------------------	-------

Powerhouse line terminals (conventional)**SURGE ARRESTERS – 1 PHASE**

Quantity (50/60 Hz)	27/27
Type (50/60 Hz)	ZnO
Rating (50/60 Hz)	420 kV

CAPACITIVE POTENTIAL DIVIDERS – 1 PHASE

Quantity (50/60 Hz)	12/12
---------------------	-------

WAVE TRAPS – 1 PHASE

Quantity (50/60 Hz)	9/9
---------------------	-----

SUBSTATIONS**Right-bank substation – 50 Hz – 500 kV****CIRCUIT BREAKERS – 3 PHASE**

(with 2 disconnect switches and 1 current transformer per phase) – main bus/line positions

Quantity	6
Type	Air blast
Rated current	4000 A rms
Voltage (maximum)	550 kV rms
Impulse level (BIL)	1800 kV crest
Interrupting capability	50 kA sym

CIRCUIT BREAKERS – 3 PHASE

(with 2 disconnect switches and 1 current transformer per phase)–

main bus/line positions

Transformer/ANDE lines

Quantity (initial/ultimate)	5/23
Type	SF ₆ puffer
Rated current	2000 A rms

DISCONNECT SWITCHES – 3 PHASE

Quantity (4000 A-line positions) (initial/ultimate)	4/8
---	-----

Quantity (3000 A-transformer/ANDE lines) (initial/ultimate)	3/10
---	------

GROUND SWITCHES – 3 PHASE

Quantity(initial/ultimate)	7/18
----------------------------	------

SURGE ARRESTERS – 1 PHASE

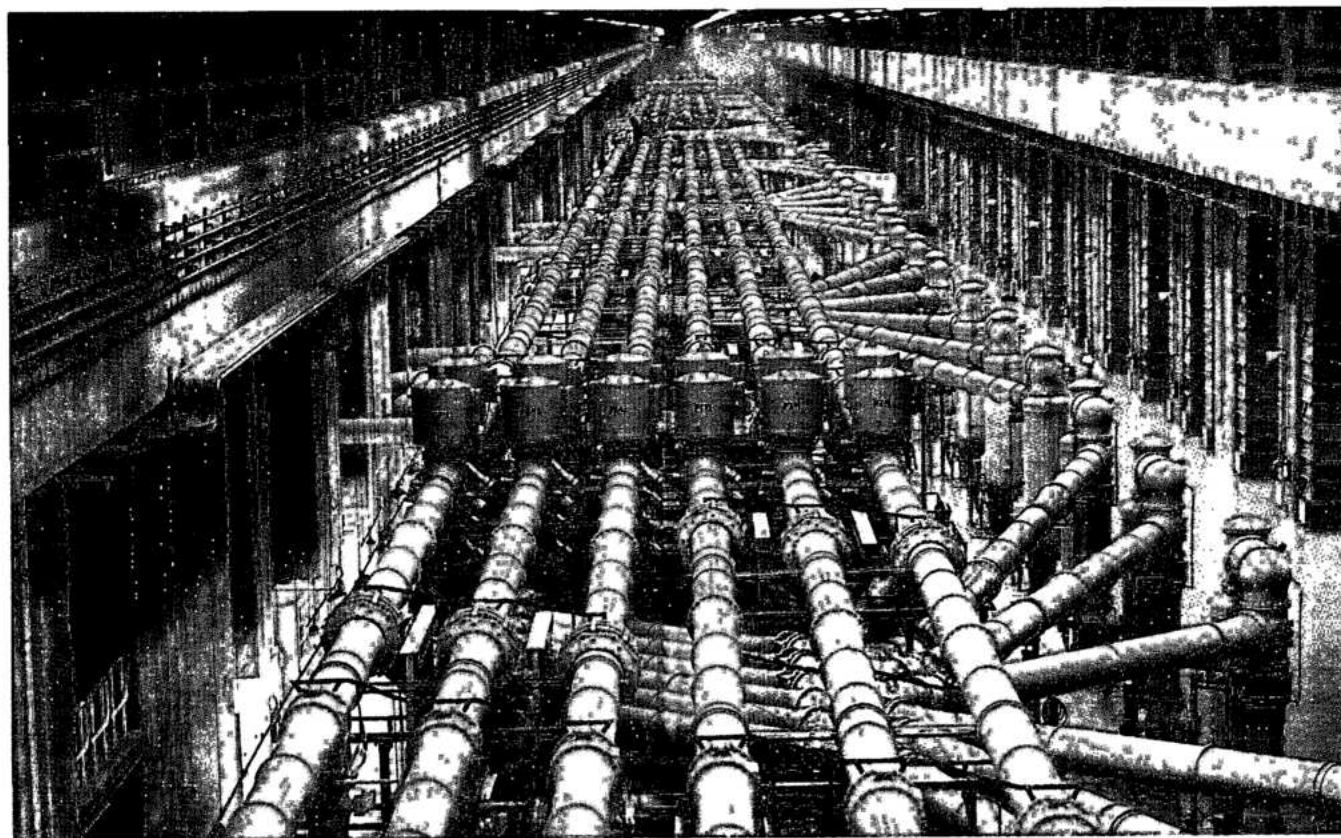
Quantity (initial/ultimate)	21/54
Type	ZnO
Rating	420 kV

CAPACITIVE POTENTIAL DIVIDERS – 1 PHASE

Quantity (initial/ultimate)	18/36
-----------------------------	-------

WAVE TRAPS – 1 PHASE

Quantity (initial/ultimate)	10/18
-----------------------------	-------

Substation SF₆

Right-bank substation – 50 Hz – 220 kV**AUTO TRANSFORMER – 3 PHASE**

Quantity (initial/ultimate)	3/5
Type (air cooled)	0A/F0A/F0A
Rated power	375 MVA
Voltage	525/241.5 –13.8 kV
Type of connection	wye grd. / wye grd. / delta

VOLTAGE REGULATOR – 3 PHASE

Quantity (initial/ultimate)	3/5
Type (air cooled)	0A/F0A/F0A
Rated power (through-put)	375 MVA
Voltage	241.5 ± 10% kV

CIRCUIT BREAKER – 3 PHASE(with 2 disconnect switches and
1 current transformer per phase)

Quantity (initial/ultimate)	12/23
Type	SF ₆ puffer
Rated current	2000 A
Voltage	220 kV
Impulse (BIL)	1050 kV
Interrupting capability	31.5 kA

SURGE ARRESTERS – 1 PHASE

Quantity (initial/ultimate)	33/57
Type	ZnO
Rating	240 kV

*Left bank substation*

CAPACITIVE POTENTIAL DIVIDERS – 1 PHASE

Quantity (initial/ultimate) 15/33

WAVE TRAPS – 1 PHASE

Quantity (initial/ultimate) 8/16

Right-bank substation – 50 Hz – 66 kV**TRANSFORMER – 3 PHASE**

Quantity 2
 Type (air cooled) ONAF
 Rated power 25 MVA
 Voltage 230–66–13.8 kV
 Type of connection wye grd. / wye
 grd. / delta

CIRCUIT BREAKERS – 3 PHASE

(with 2 disconnect switches each)

Quantity 5

CURRENT TRANSFORMERS

Quantity 6

POTENTIAL TRANSFORMERS

Quantity 6

SURGE ARRESTERS – 72 kV

Quantity 12

Left-bank substation – 60 Hz – 500kV**AUTO TRANSFORMERS – 1 PHASE**

Quantity (3 phase banks) 4 banks + one unit
 spare
 Type (air cooled) ONAN/ONAF/OFAF
 Rated power 1650 MVA
 Voltage 765-525-69 kV
 Type of connection wye grd. / wye grd.
 / delta
 Impulse level (BIL) 1950–1425–350 kV and
 1950–1550–350 kV

CIRCUIT BREAKER – 3 PHASE(with 2 disconnect switches and
1 current transformer per phase)

Quantity 4
 Type SF₆ and air
 blast
 Rated current 3150 A
 Voltage 550 kV
 Impulse level (BIL) 1550 kV
 Interrupting capability 40 kA

DISCONNECT SWITCHES – 3 PHASE

Quantity (breaker by-pass) 4
 Type Vertical reach

SURGE ARRESTERS – 1 PHASE

Quantity 24
 Type ZnO
 Rating 420 kV

CAPACITIVE POTENTIAL DIVIDERS – 1 PHASE

Quantity 12

WAVE FILTERS

Quantity 12

Left-bank substation – 60 Hz – 765 kV**CIRCUIT BREAKERS – 3 PHASE**(with 2 disconnect switches and
1 current transformer per phase)

Quantity 11
 Type SF₆ and air
 blast
 Rated current 3150 A
 Voltage (maximum) 800 kV
 Interrupting capability 40 kA
 Impulse level (BIL) 2100 kV

DISCONNECT SWITCHES – 3 PHASE

Quantity (without ground service
 – transformer/reactors) 7
 Quantity (with grid service-line) 3
 Type Vertical reach

SURGE ARRESTERS – 1 PHASE

Quantity 30
 Type ZnO
 Rating 588 kV

CAPACITIVE POTENTIAL DIVIDERS – 1 PHASE

Quantity 11

WAVE TRAPS – 1 PHASE

Quantity 9

REACTORS – 1 PHASE

Quantity (3 phase banks) 3
 Type Shunt
 Rating (3 phase bank) 360 MVar
 Voltage 800 / $\sqrt{3}$ kV
 Impulse level (BIL) 1800 kV and
 1950 kV

Left-bank substation – 50 Hz – 500kV**CONVERTER TRANSFORMERS – 1 PHASE**

Quantity (high voltage section)	12 (+ 4 spare)
Quantity (low voltage section)	12
Type (air cooled)	OFAF
Rated power (1 phase)	314 MVA
Voltage	$500/\sqrt{3} - 127.4/\sqrt{3}$ – 127.4 kV
Type of connection	wye grd. / wye grd. / delta
Tap changer positions (+ 20 – 6 at 1.25%)	26
Impulse levels (BIL)	
HV section	1425 – 1800 – 1300 kV
LV section	1425 – 1175 – 650 kV
Switching surge levels	
HV section	1175 – 1494 – 1079 kV
LV section	1175 – 975 – 540 kV

MAIN AUXILIARY SERVICE TRANSFORMERS – 3 PHASE

Quantity	2
Type (air cooled)	ONAN
Rated power	10 MVA
Voltage	$500 \pm 2 \times 2.5\%$ – 13.8 – 13.8kV
Type of connection	wye grd. / wye grd. / delta

CIRCUIT BREAKER – 3 PHASE

Quantity	30
Type	Air blast
Rated current	3150 A
Voltage	550 kV
Impulse level	1550 kV
Interrupting capability	50 kA

CURRENT TRANSFORMERS

Quantity (6 core for breaker and half)	78
(2 core for bus)	12

DISCONNECT SWITCHES – 3 PHASE

Quantity (with ground switch)	17
(without ground switch)	58
Type	Vertical break

SURGE ARRESTERS – 1 PHASE

Quantity	42
Type	ZnO
Rating	420 kV

CAPACITIVE POTENTIAL DIVIDERS – 1 PHASE

Quantity	48
----------	----

WAVE TRAPS – 1 PHASE

Quantity	12
----------	----

FILTER BANKS – 3 PHASE

Quantity (350 MVar)	2
Quantity (280.3 MVar)	3
Type (odd frequencies)	Capacitor

Left bank converter station and 600 kV substation**dc CONVERTER**

Quantity (bipoles)	2
Nominal rating (per bipole)	3150 MW
Voltage (bipole)	± 600 kV

SMOOTHING REACTORS – 1 POLE

Quantity	4 (+ 1 spare p/station)
Type (air cooled)	OFAF
Rated current	2610 A
Overload current (5/20 s)	3410/3130 A
Voltage	600 kV dc
Impulse level (BIL)	1675 kV
Switching surge level	1390 kV

dc CIRCUIT BREAKERS (BY-PASS) – 1 POLE

Quantity (HV/LV)	2/2
Type (separate interruptors/ isolators)	Minimum oil
Rated current	2930 A
Voltage (HV/LV)	600 – 300 / 300 – 7 kV dc
Impulse level (HV/LV)	1675 – 850 / 850 – 325 kV
Switching surge (HV/LV)	1448 – 724 / 724 – 150 kV

DISCONNECTING SWITCHES – 1 POLE

Quantity (600 kV dc)	28
(300 kV dc)	12
(7 kV dc)	24
Type (used for sectionalizing/ by-passing)	Varies

SURGE ARRESTERS – 1 PHASE

Quantity (600 kV)	8
(348 kV)	8
(300 kV)	4
(10 kV)	20

CAPACITIVE POTENTIAL DIVIDERS – 1 PHASE

Quantity	4
----------	---

FILTER BANKS – 1 POLE

Quantity	12
----------	----

POWERLINES**Overhead****500 kV**

Powerhouse - water-intake area (8 lines, 50/60Hz)	0.1 km/line
Power-intakes area – right bank substation (4 lines, 50Hz)	2.1 km/line
Power-intakes area – Foz do Iguaçu substation (4 lines, 60 Hz)	7.8 km/line
Right bank substation – Foz do Iguaçu substation – converter (4 lines, 50 Hz)	8.9 km/line
Number of towers per km	2.7
Phase conductor – 954 kcmil ACSR (RAIL)	4 per phase
Shield wire 266.8 kcmil ACSR (PARTRIDGE)	4 at first 3 spans 2 at other spans

220 kV – 50 Hz

Right bank substation – Acaray plant (2 lines)	5 km/line
Number of towers per km	3
Phase conductor – 954 kcmil ACSR (RAIL)	2 per phase
Shield wire – 266.8 kcmil ACSR (PARTRIDGE)	2 per line

66 kV – 50 Hz

Right bank substation – Foz do Iguaçu substation – converter	9.3 km
Number of structures per km	5.7
Phase conductor 266.8 kcmil ACSR (PARTRIDGE)	1 per phase
Shield wire galvanized-steel diameter 7.94 mm HS	1 per line

765 kV – 60 Hz

Foz do Iguaçu to Ivaiporã (3 lines)	320 km/line
Ivaiporã to Itaberá (3 lines)	265 km/line
Itaberá to Tijuco Preto (3 lines)	304 km/line
Number of towers per km	2.3
Phase conductor 1113 kcmil ACSR (BLUEJAY)	4 per phase
Shield wire ACSR 176.9 kcmil steel and 110.8 kcmil	2 per line

± 600 KV dc

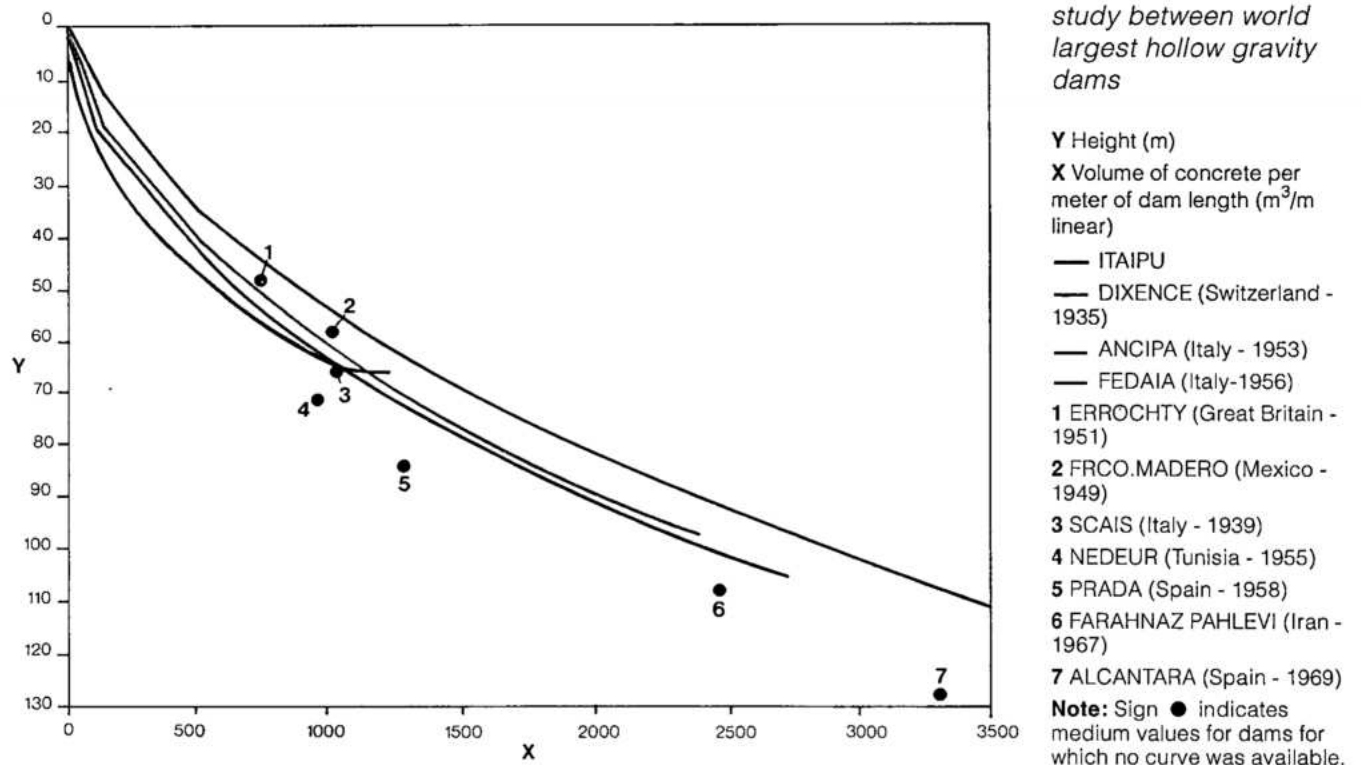
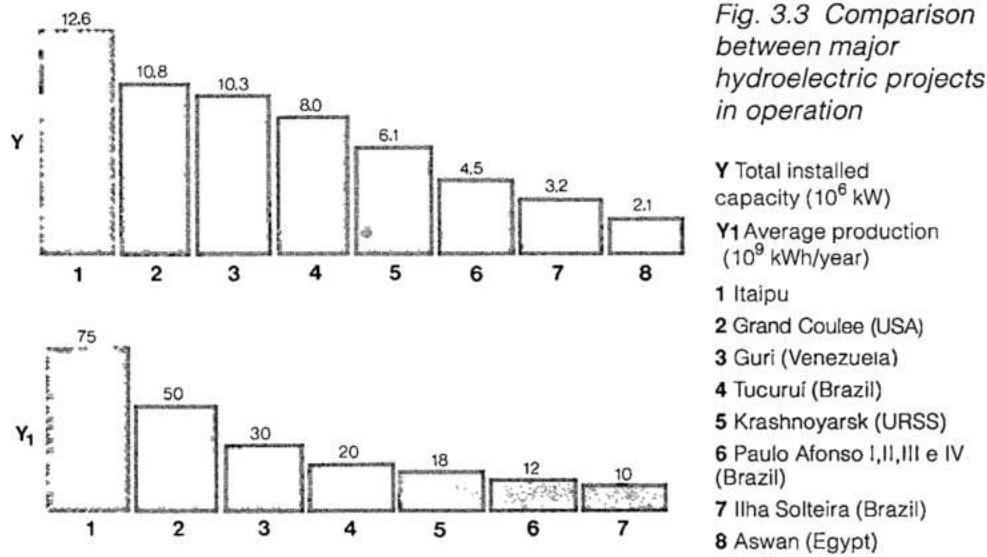
Foz do Iguaçu to Ibiúna (1 line)	792 km
Foz do Iguaçu to Ibiúna (1 line)	816 km
Number of towers per km	2.1
Pole conductor 1272 kcmil ACSR (BITTERN)	4 per pole
Shield wire galvanized-steel 9.525 mm diameter	2 per line

Underground**66 kV – 50 Hz**

Right-bank substation – powerhouse	3 km
Single conductor cable (oil-insulated)	12 km

MAGNITUDE OF ITAIPU

Itaipu is the world's largest single hydroelectric project and it has the single largest powerhouse of any kind. Its grandeur is better appreciated when compared with other major hydroelectric projects currently in operation, see Figs. 3.3. and 3.4.

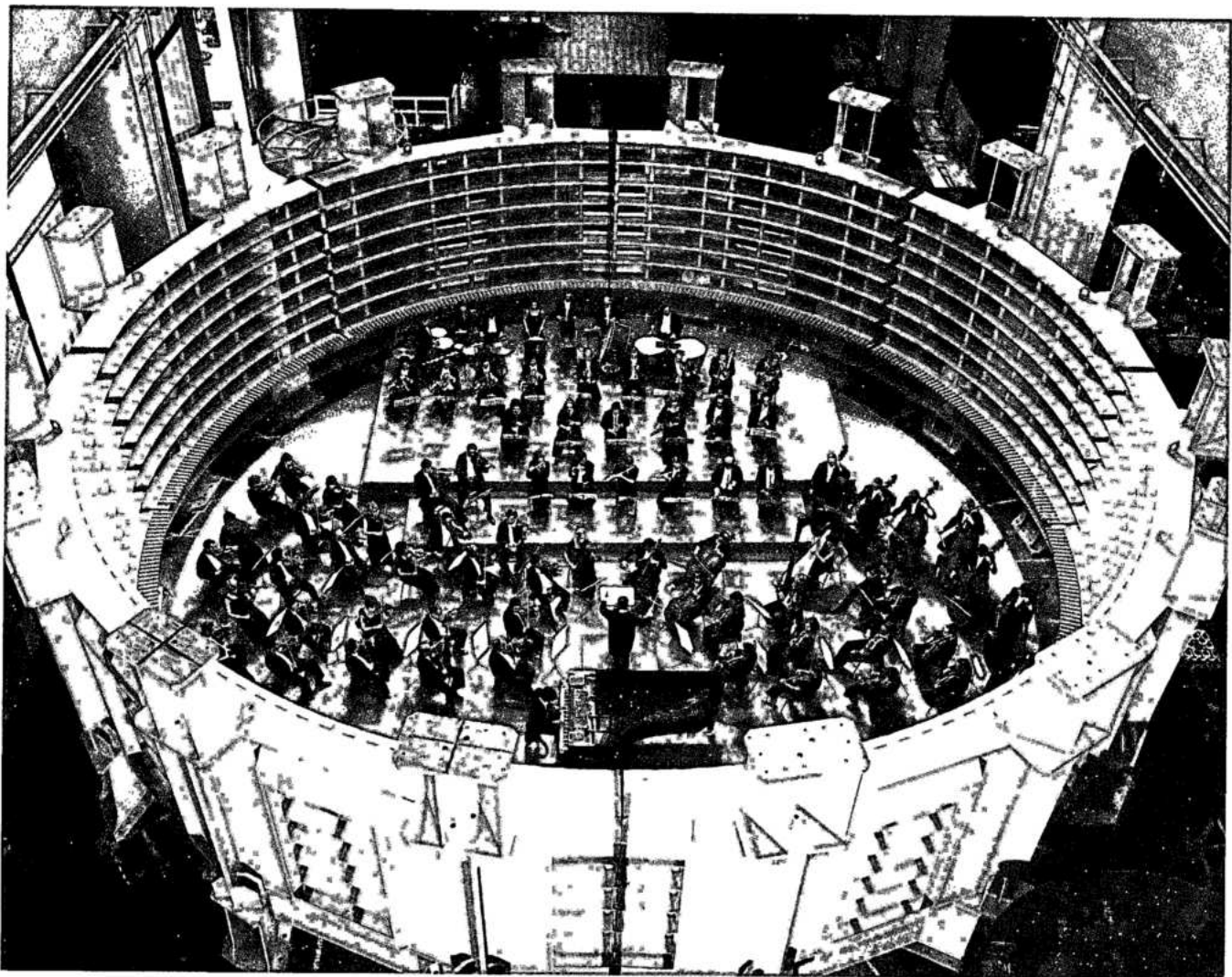


The rated capacity and energy generated for the world's largest hydroelectric facilities compares as follows:

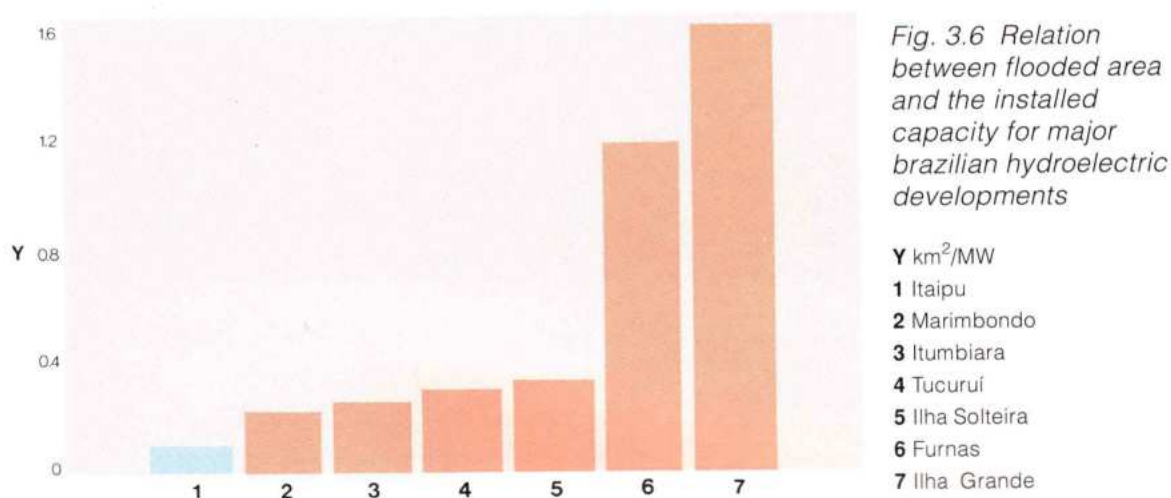
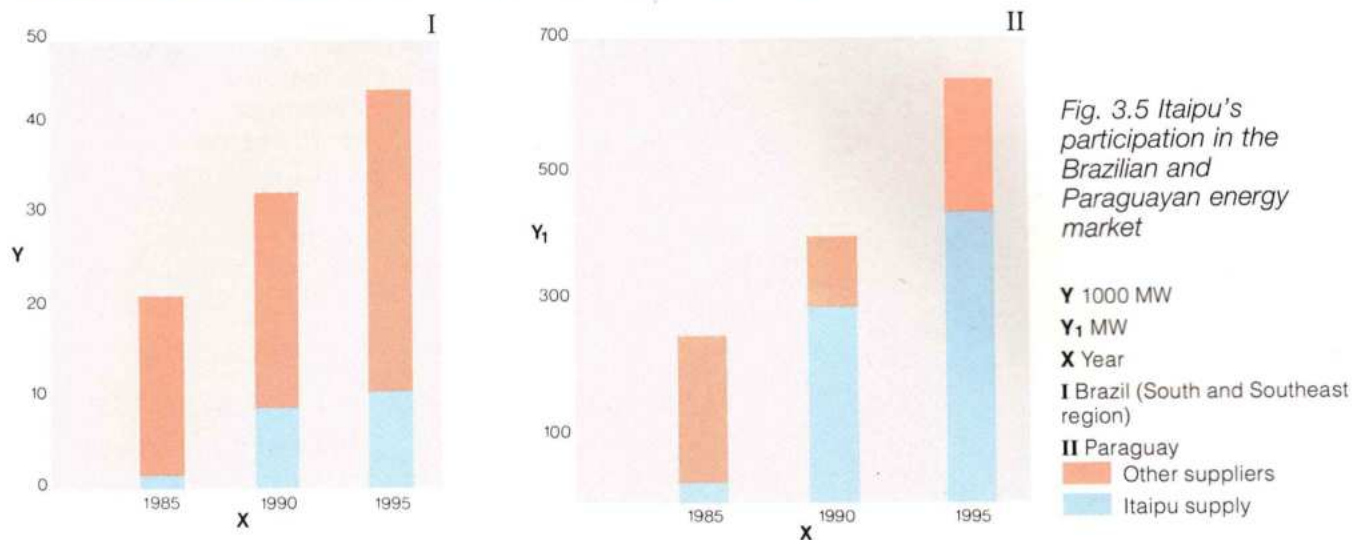
Project	Country	MW	kWh10 ⁹ /year
Itaipu	Brazil/ Paraguay	12 600	75
Grand Coulee	USA	10 830	20
Guri	Venezuela	10 300	50
Tucuruí	Brazil	8000	43
Krasnoyarsk	USSR	6100	30
Aswan	Egypt	2100	10

The capacity of hydroturbines has increased almost six-fold over the last 30 years. In 1957 the most powerful operating turbines were rated at about 110 MW. Today Itaipu's turbines are among the most powerful operating units:

Project	Maximum MW
Grand Coulee	820
Itaipu	800
Guri	730
Krasnoyarsk	505
Churchill Falls	475



An illustration of the magnitude of the Itaipu generator. The stator can accomodate a full orchestra



In terms of energy supply, Itaipu was planned with the objective of supplying energy to Paraguay and to the south and southeast regions of Brazil.

In 1988 Itaipu was responsible for supplying 20% of the energy consumed in the south and southeast regions of Brazil, and 58% of the energy consumed in Paraguay.

In 1990 Itaipu will provide about 30% of the energy consumption in the south and southeast region of Brazil and 70% of the total Paraguayan energy needs. In 1991 the Brazilian total nominal installed generating capacity will amount to about 58 000 MW, of which approximately 22% will correspond to Itaipu.

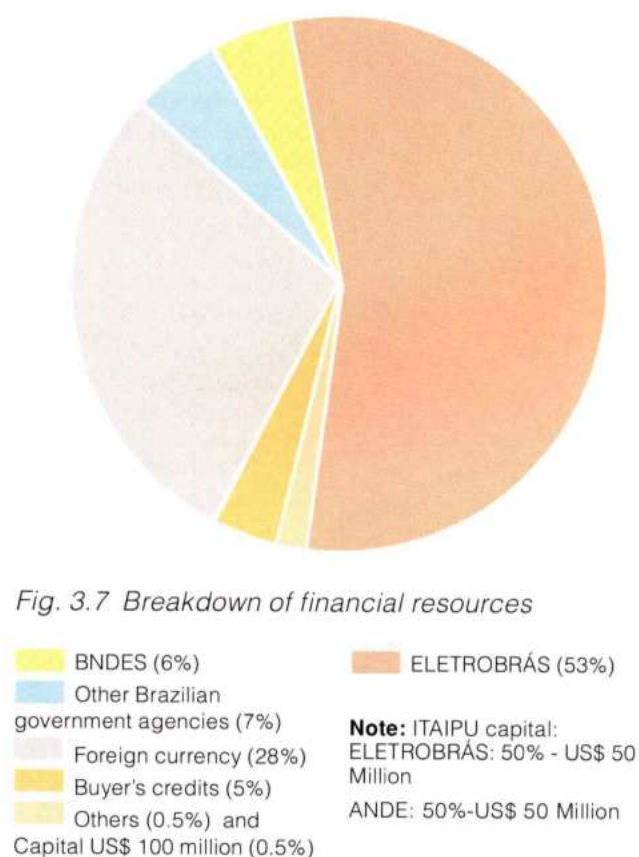
Fig. 3.5 shows the growth in time of Itaipu's participation in the Brazilian and Paraguayan energy market as compared with other sources of energy.

With respect to the use of natural resources, Fig. 3.6 shows the relation between the flooded area

and the installed capacity for the major Brazilian hydroelectric developments. In comparison Itaipu has the lowest ratio.

FINANCIAL ASPECTS

While the primary purpose of this book is to cover the engineering aspects of Itaipu project, it would be incomplete without some mention of the cost of the project and its financing. No doubt, because of their complexities, they will be dealt with in detail in other publications; here only the essential and salient factors will be mentioned.



One of the basic problems in establishing the actual costs of Itaipu project is the time lapse from its conception and initial estimates, to its completion and final costs. The initial cost estimates were made in 1973 before the first petroleum shock and the construction reached its peak at the end of the second petroleum shock, in 1979. The worldwide effects of these major financial instabilities were reflected in Brazil and Paraguay in terms of escalating material and labor costs and uncertain exchange rates. Because of its binational structure, costs for Itaipu were always converted and quoted in US\$. However, the dollar exchange corrections seldom reflected the true dollar inflation of the currencies in the two countries. Hence it is unrealistic and irrelevant to attempt a comparison between the original and the final estimates for the project. A far better and more meaningful analysis is to compare the unit cost of Itaipu power and energy with the current values for other hydroelectric schemes worldwide. Estimates made in 1987 foresaw the direct cost of Itaipu as US\$ 11.33×10^6 . This figure included all direct construction costs but did not include interest during construction, transmission costs and other

financial charges. Included however were the costs of civil construction, materials, permanent equipment, engineering, site supervision and total administration by ITAIPU during the construction period. This results in US\$ 900/kW, or based upon the expected output of the project, in US\$ 0.016/kWh. However, because of exchange rate distortions at the time of the estimate these values should be discounted about 15%, resulting in the following 1990 comparative values:

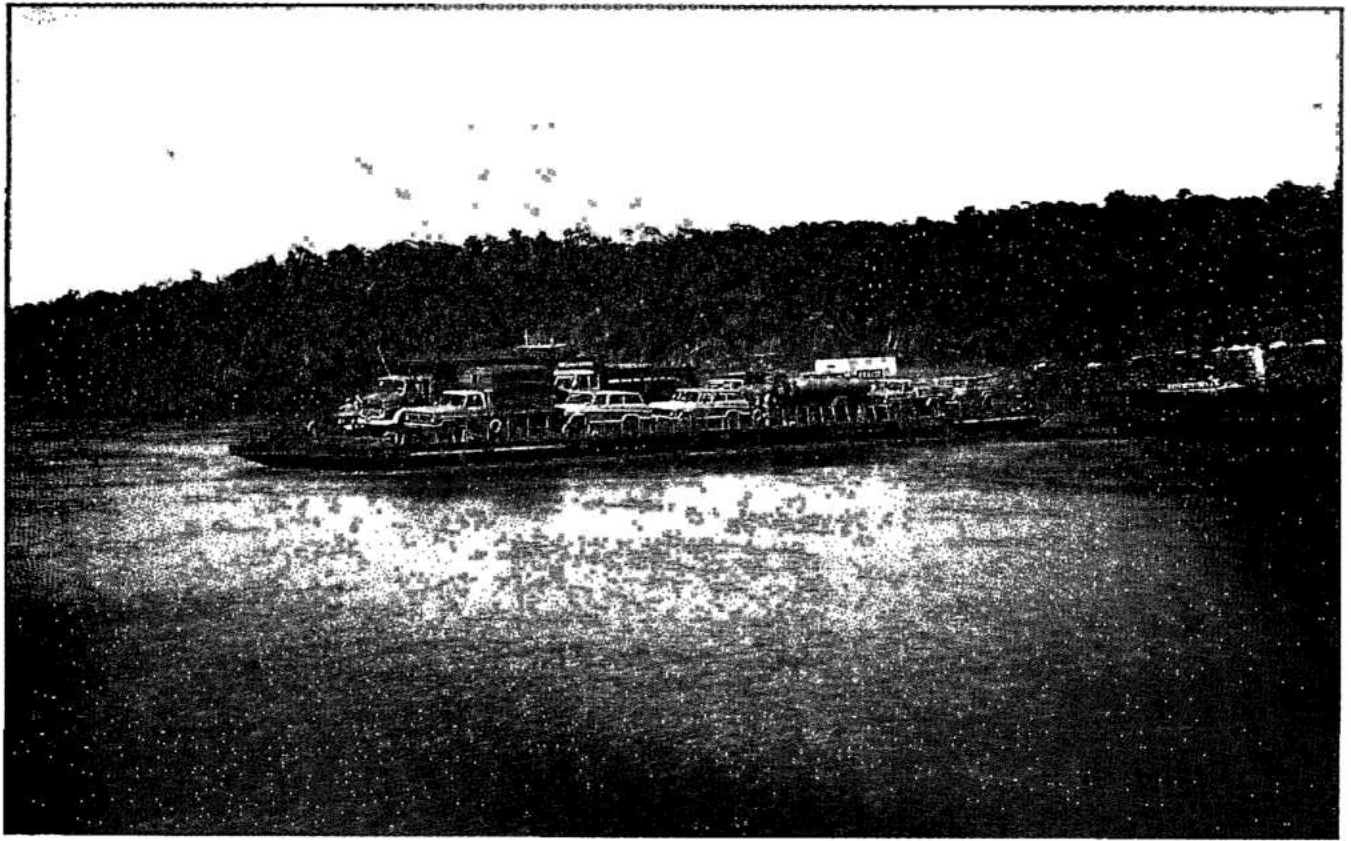
	Capital cost US\$/kW	Generation cost US\$/kWh
Itaipu	765	0.014
Average of planned hydroelectric project in Brazil (Plan 2010)		0.020
Coal fired thermal	1200	0.033
Nuclear	1400	0.039
Oil fired thermal	1000	0.065

The percentage breakdown of the costs of Itaipu is as follows:

	%
Civil works	50
Permanent equipment	25
Power plant subtotal	75
Access roads, land and reservoir works infra-structure for construction and operation	10
Engineering, construction supervision and general administration	15
Total	100

The equity for Itaipu was set at a nominal value of US\$ 100×10^6 to be held in equal and non transferable parts, by ELETROBRÁS on behalf of Brazil and by ANDE for Paraguay. Thus Itaipu project was entirely financed by debt financing with about two-thirds from Brazilian sources and the rest from foreign banks, see Fig 3.7.

The long maturity period of the project combined with the high interest rates of the late 1970s and early 1980s resulted in an abnormal burden of interest during construction on the cost of the project. It may reach approximately 50% of the total cost of the project when it is completed and fully operational. However, even with these, Itaipu energy is very competitive both nationally and internationally and the project is highly cost effective.



Navigation facilities after creation of reservoir

NAVIGATION

Prior to the construction of Itaipu project the Paraná river was navigable from the Rio de la Plata to the toe of the Salto Grande das Sete Quedas or Saltos del Guairá and also above the falls. Communication between the two navigable sections above and below the falls, was done by means of transshipment by land by-passing the falls.

With the creation of the Itaipu reservoir, which necessarily submerged the falls, continuous navigation is now possible between the reservoir and the upper reaches of the Paraná river.

Locks, canals and other facilities will be necessary to bypass Itaipu dam and overcome the 100 m difference of levels between the lake and the tailrace in order to again establish continuous navigation by water between the upper and lower reaches of the river.

Although the execution of these navigation facilities at Itaipu dam is not the direct responsibility of ITAIPU, the treaty and supplementary agreements established that the engineering studies of Itaipu project should include complete plans for these works, and that ITAIPU should provide facilities for transshipment by land, by-passing the dam until permanent water-ways are built.

Several schemes for future navigation facilities have been studied, which in due course will be presented to the Brazilian and Paraguayan governments for selection and implementation and also to decide which authority will develop them. Meanwhile transshipment facilities by land, during and after construction, have been provided comprising the following docks, with corresponding access roads, along the Paraná river: Guairá in Brazil and Puerto Franco and Saltos del Guairá in Paraguay.

GEOLOGY, GEOTECHNICAL
INVESTIGATIONS
AND SUBSURFACE TREATMENT

GEOLOGY OF THE PROJECT AREA	4.3
Main Characteristics	4.3
GEOLOGICAL AND GEOTECHNICAL INVESTIGATIONS	4.7
PRINCIPAL FOUNDATION DISCONTINUITIES	4.9
Discontinuities	4.9
Shear zones	4.9
Subsurface Treatment	4.11
INSTRUMENTATION IN THE SHEAR KEY GRID	4.15

GEOLOGY, GEOTECHNICAL INVESTIGATIONS AND SUBSURFACE TREATMENT

GEOLOGY OF THE PROJECT AREA

MAIN CHARACTERISTICS

The Itaipu project area and the reservoir are underlain by the large basalt flows of the upper Paraná basin, belonging to the Serra Geral formation of the lower Jurassic Period, see Fig. 4.1

The main geological characteristics of this area as shown in Fig. 4.2 are:

- Basalt flows, essentially horizontal, 20 to 60 m thick.
- Breccia layers between the basalt flows, 1 to 30 m thick; mostly heterogeneous, usually weaker and more deformable than the basalt.
- Discontinuities in planes parallel to the basalt flows, usually located at the contact between flows or at the base of the transition zone.
- Horizontal permeability several times higher than vertical permeability.

The basalt flows are relatively uniform, grading from a dark grey, fine to coarse-grained basalt in the central portion to vesicular, amygdaloidal and brecciated transition zones near the upper boundary.

The thickness, lithology and porosity of the breccia layers are highly variable. In the period between two lava flows, the scoriaceous and irregular surface of the flow was subjected to weathering with erosion and deposition of sand or silt by wind or water. The subsequent flow



*General view
of excavations*

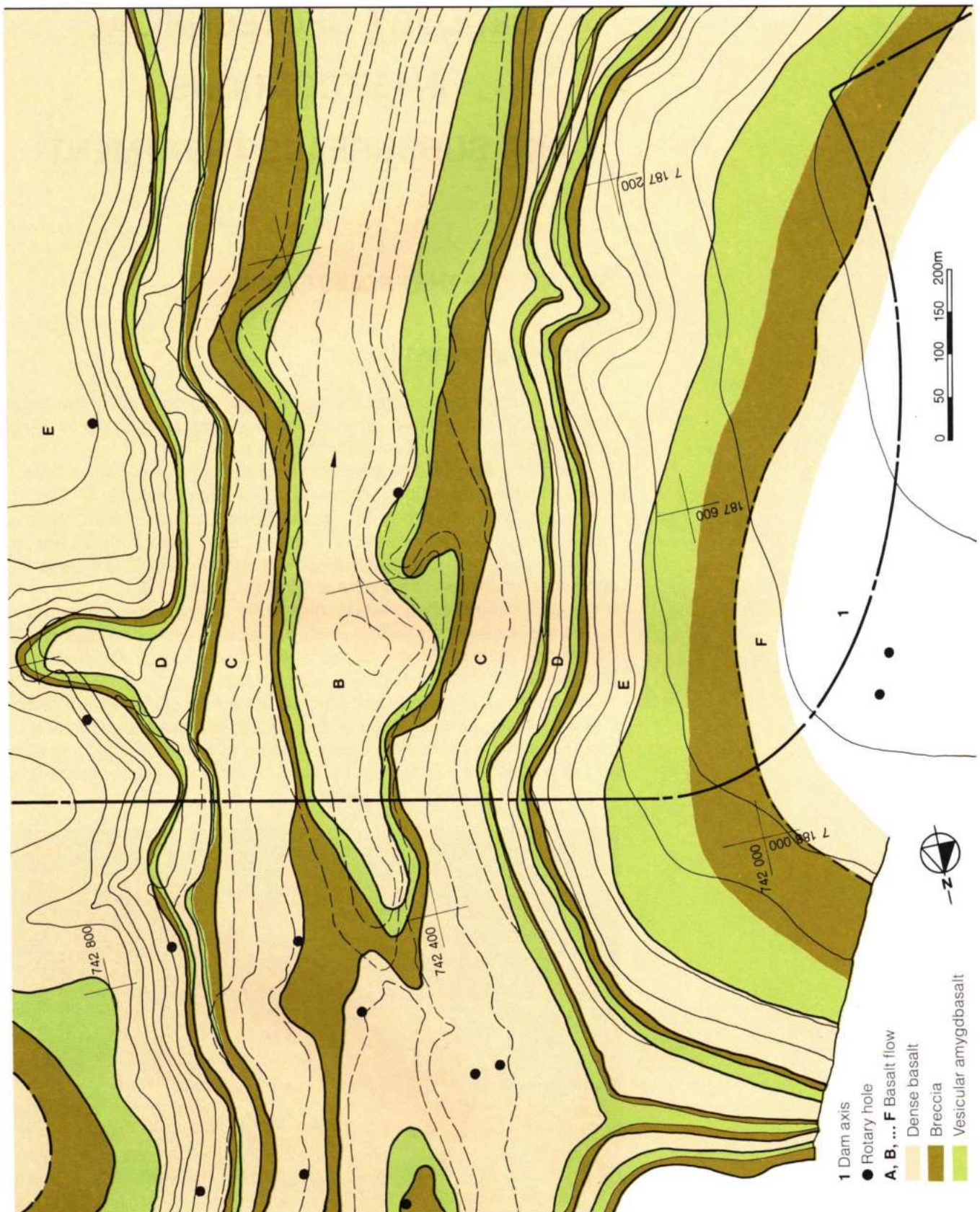


Fig. 4.1 General geologic map

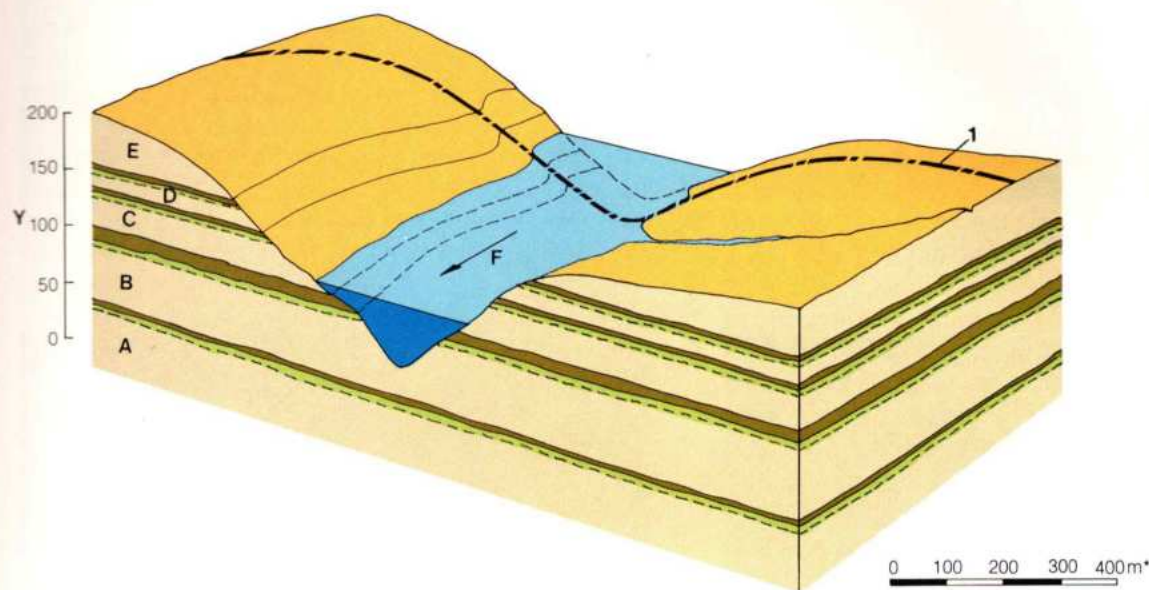


Fig. 4.2 Typical geologic section at Itaipu site

Y Elevation (m)
 1 Dam axis
 A, B ... E Basalt flows
 F Flow direction

Dense basalt
 Breccia
 Vesicular amygdalobasalt

then remolded and welded this material, thus forming the brecciated upper layers of each flow which are heterogeneous.

Another special feature of these basaltic flows is the syngenetic discontinuity which usually is found at the base of the vesicular-amygdaloidal zone of each flow. This was probably a result of the concentration of clayey minerals at this horizon, deposited when the flow was in a viscous state. An alternative reason for these discontinuities was the shear movement at this boundary, between the upper crust which was already solid and the still liquid and moving inner core of the flow.

At the project site, the basalt flows have a regional dip of 3° towards the northeast. The principal alignments in the area, observed in the aerial photographs, have directions between 30° N to 50° W (17%), 50° N to 70° W (15%) and 30° N to 50° E (13%). The latter corresponds to the general

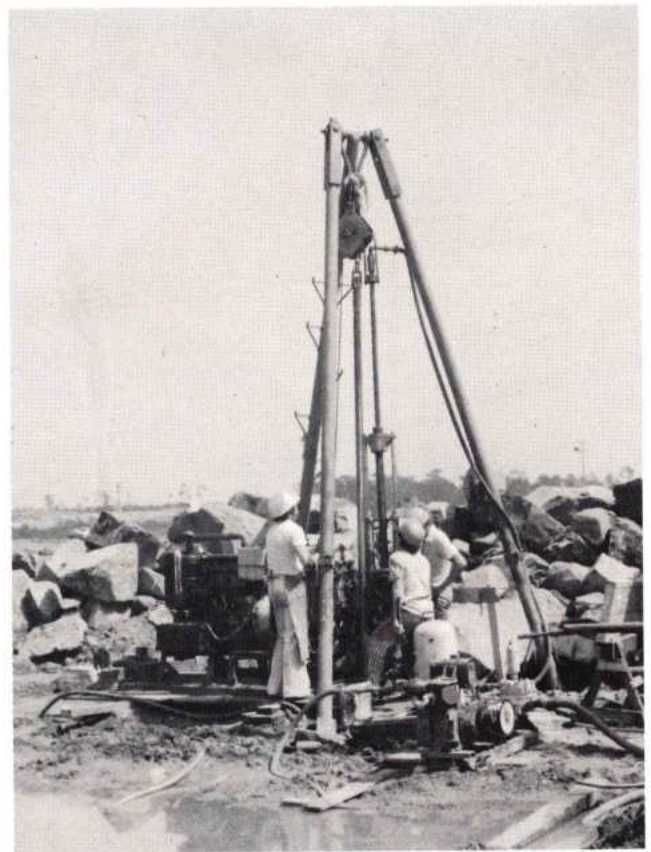
alignment of the Paraná river in the project area.

There are five basaltic flows in the area directly related to the project; they were denominated, in an ascending order, A, B, C, D and E, with variable thicknesses of 30 to 70 m; see Fig.4.3. Sub-horizontal discontinuities were also found, having been formed by the erosion of the Paraná River such that the unconfined rock mass had been slightly displaced toward the river channel due to horizontal forces. The massive rock of the river channel also has shear zones, in a general direction parallel to the river and dipping either east or west, which were most likely caused by the action of horizontal compressive forces in the east-west direction. The sub-horizontal discontinuities associated with basalt of different mineral composition are a peculiar characteristic of this area. Examples of these joints are the discontinuities called joint A at El.12 and joint B at El.62.

Each of the flows presents three distinct types of basaltic rock:

- Dense basalt, characterized by its micro-crystalline texture, high density (2.95) and high deformability modulus ($> 2000 \text{ kN/cm}^2$). This basalt, because of its intrinsic rigidity, is highly fractured.
- Amygdaloidal vesicular basalt, having a texture similar to the dense basalt but containing vesicles and being much less fractured than the dense basalt. Its density ranges from 2.6 to 2.7 and it has a deformability modulus between 1000 and 1500 kN/cm^2 . This lithology does not show pervious zones.
- Breccia and scoriaceous lava, comprising a highly vesicular lava surrounding angular blocks of other different types of basalt, sandstone and siltstone, and having irregular cavities partially filled with carbonate, zeolite and amorphous and crystalline quartz. Density values range from 2.1 to 2.4 and locally are lower than 2. The deformability modulus is about 700 kN/cm^2 . The high porosity and the interconnected cavities result in a permeability higher than 10^{-3} cm/s .

The discontinuities generally occurring at the region of contact of the upper part of the breccia and the lower part of the dense basalt were important features with respect to the stability of the dams and the other structures.



Geologic sounding investigations on the left bank

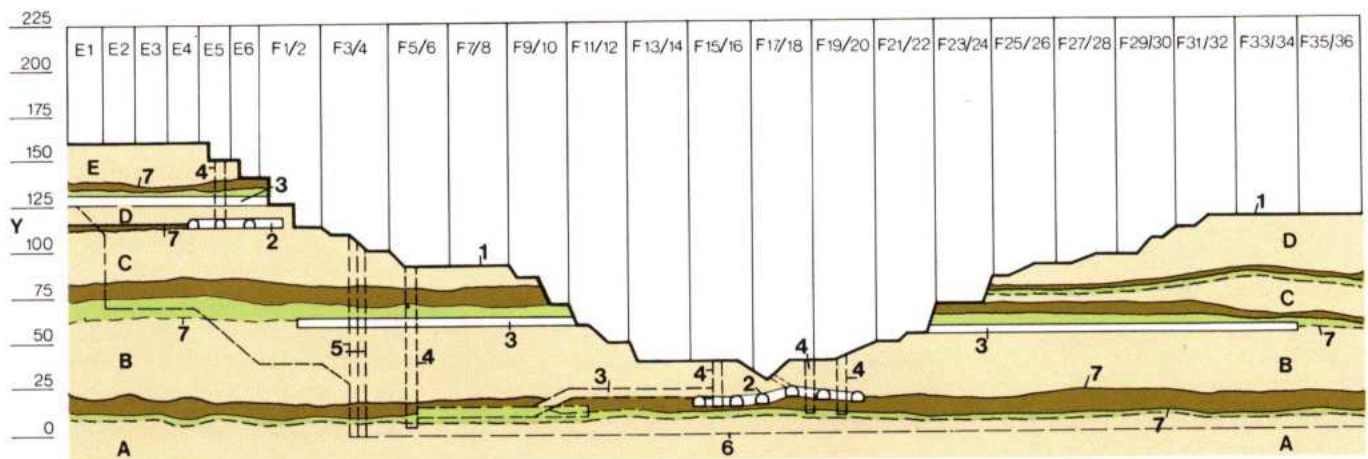


Fig. 4.3 Main dam geological foundation - longitudinal section

Y Elevation (m)
1 Profile of the excavation
2 Shear keys
3 Exploratory tunnels

4 Prospection shafts
5 Transversal grout curtain
6 Limit of the grout curtain
7 Discontinuities

E1 ... E6 Right wing dam
F 1/2 ... F35/36 Main dam blocks
A, B ... E Basalt flows

Dense basalt
Breccia
Vesicular amygdalobasalt

GEOLOGICAL AND GEOTECHNICAL INVESTIGATIONS

Explorations conducted at the beginning of the project studies were mainly done to establish the viability of the proposed layout. Rotary core holes were drilled to obtain an overall geological knowledge of the area, from which it was possible to define the characteristics of the basalt flows, their thickness, and most important, the nature of the breccias. At this early stage, trenches and exploratory tunnels were also excavated along the banks to visually examine the characteristics of the rock formations. The examination and in situ tests permitted the determination of the geotechnical characteristics of the breccia, which, because of their low modulus of deformability, were considered problematic strata. Eight in situ shearing tests of the breccia and flat jack tests to determine the modulus of deformability were performed in the tunnels. Laboratory tests on representative samples obtained from the drill holes were also conducted to obtain the lithological characteristics of the various rock strata.

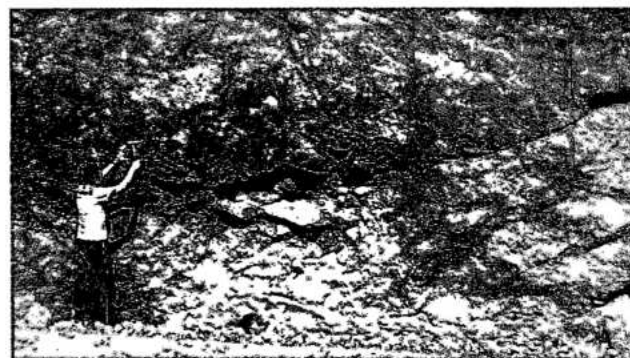
Subsequent investigations obtained the data necessary to define the foundation levels for the structures and the foundation treatment. These investigations also provided better understanding of the horizontal discontinuities which were initially estimated from the correlation of drill hole data and later confirmed by the outcroppings along the river banks. Integral sampling was performed, and shafts and tunnels were excavated at various locations so that the geotechnical features of the discontinuities could be established.

An exploratory shaft, 4 m in diameter, was excavated from El. 125 down to El. 7 on the right bank of the river, near the axis of the dam. This shaft crossed most of the discontinuities of significance for the foundations of the main dam. From this shaft, exploratory tunnels at El. 70, El. 59 and El. 12 were excavated and from the last tunnel, another sloping tunnel reached the region of contact between flows A and B at El. 20. The tunnel at El. 70 was excavated so that a thorough investigation of the geotechnical properties of breccia B could be carried out. The objective of the tunnels at El. 59 and El. 12 was to determine the characteristics of the following discontinuities:

- The layers and joints welded with calcitic cement at El. 62 (joint B).
- Fractured zones at the bottom of flow B.
- The region of contact of flows A and B at El. 20 and the joint A at El. 12.



Geologic investigation of breccia B at the road access



Geologic survey at the right bank

In the tunnels at El. 62 and El. 20, in situ direct shearing tests were performed on 1 m x 1 m blocks at the discontinuities.

After the diversion of the river in October 1978, joint B was investigated along two drainage tunnels; a 165 m long tunnel at El. 60 on the right bank and a 210 m long tunnel at El. 55 on the left bank. The subhorizontal joint in flow D was investigated from the tunnel excavated on the right bank at El. 125.

To obtain better and more reliable geotechnical data of the discontinuities at El. 20 and El. 12, shafts and exploratory tunnels were excavated in the riverbed after the diversion of the river. These tunnels disclosed other discontinuities associated with the discontinuity at contact A/B. These consisted of shearing joints with clayey material surrounding blocks of basalt, with thickness ranging from 0.3 to 0.05 m, some dipping to the right bank and others to the left bank and, at points, dipping upstream or downstream.

Results of the laboratory and in situ tests are shown in Table 4.1.

Table 4.1 Physical properties of foundation rock

Type of material	Flow	"In situ" tests				Laboratory tests			
		Deformability		Strength		Deformability		Strength	
		$E_d \times 10^3$	$E_s \times 10^3$	ν	k_t	$E_d \times 10^3$	$E_s \times 10^3$	ϕ	σ_c
Rocks									
Basaltic breccia									
Massive/Intermediate	B	1.6-1.9	1.0 (1)	0.22		1.7	2.0	35	
Intermediate	B	1.6-1.9	1.3 (1)	0.22		2.5	2.3	35	
Cavernous	B	0.9-1.2	0.5 (1)	0.23		1.0	0.7		
Massive	D							35	440
Cavernous	B		0.4 (3)						
Cavernous	B		0.3 (3)						
Intermediate	B		0.6 (3)						
Sound	(4)					2.4	2.1	0.14	2.8
Slightly weathered	(4)					2.3	1.4	0.11	2.6
Weathered	(4)					1.7	1.3	0.20	1.5
									0.1
Vesicular basalt	B	2.5-4.0		0.30					
Gray sound	A		0.7 (3)						
Gray	A		0.8 (3)						
Sound	(4)					4.9	4.4	0.12	5.2
Slightly weathered	(4)						2.2	0.31	3.0
Weathered						2.5	1.8	0.20	3.3
									0.5
Dense basalt	C		2.6 (2)				5.9	0.15	
Gray sound	B		1.7 (3)						
Gray over joint B	B		0.1 (3)						
Sound	(4)					5.1	6.4	0.19	9.3
									2.0
Joints									
Discontinuity D El.125								33-45	0-360
Discontinuity B El.61					14	35	0	15-45	0-180
Contact A/B El.20					8	26	0	30	0
Discontinuity A El. 12								30	70-360
Notes									
(1) Values obtained from flat jack tests									
(2) Dilatometer tests									
(3) Plate loading tests									
(4) These are average values of several tests made during the feasibility project									
		E_d (kN/cm ²) - dynamic modulus of deformability			ν Poisson ratio		c (N/cm ²) - cohesion		
		E_s (kN/cm ²) - static modulus of deformability			k_t (kN/cm ³) - unit shear stiffness		σ_c (kN/cm ²) - unconfined compressive strength		
					ϕ (Degree)- friction angle		σ_t (kN/cm ²) - tensile strength		

PRINCIPAL FOUNDATION DISCONTINUITIES

DISCONTINUITIES

Sub-horizontal joint of flow D

This is a discontinuity which affected blocks E1 to E6 of the buttress dam and block F1/2 of the main dam on the right bank, where it appeared at El.125. On the left bank it is located at El.116 under blocks F33/34 and F35/36. It has clay infilling, slightly undulated, 10 to 30 cm thick, with an estimated angle of internal friction $\phi = 30^\circ$ at the right bank and 25° in the area next to the diversion control structure.

Contact between basalt flows C and D

This is a discontinuity situated at El.112, under the E blocks and block F1/2 of the main dam on the right bank, where the joint is open, smooth and filled with plastic clay. The geotechnical characteristics improve gradually with increased distance from the ground surface. A ϕ of about 20° was estimated under block F1/2 and about 30° under block E4. This discontinuity also affected blocks F33/34 and F35/36 on the left bank where, at El.110, it appears with a thickness of a few centimeters, without outstanding irregularities and with an assumed ϕ of about 40° .

Fractured zone of the dense basalt flow C

This consists of a bundle of discontinuous fractures with oxidized surfaces, affecting principally blocks F33/34 and F35/36 on the right bank, where it appears at El.96. A $\phi = 40^\circ$ and cohesion $c = 40 \text{ N/cm}^2$ were estimated for this zone.

Joint B at El.55 - 62

This is a bundle of joints distributed 1 to 5 cm apart, welded with calcium carbonate, with portions partially open. Because of the way the crystals of calcium carbonate have developed, the joints have a low value of ϕ . The resistance of this joint was estimated at $\phi = 35^\circ$ and $c = 50 \text{ N/cm}^2$.

Breccia B at El.70 - 80

The thickest breccia encountered had a thickness of 10 to 15 m and within the area of the dam, the average thickness was 10 m. The breccia has heterogeneous geotechnical characteristics ranging from compact with little porosity, to cavernous, which was inadequate as Foundation for the structures. The average deformability modulus for compact breccia in the foundations was estimated at 700 kN/cm^2 and the parameters of resistance, were estimated at $\phi = 35^\circ$ and $c = 50 \text{ N/cm}^2$.



Left side of diversion structure between El. 105 and El. 125. Discontinuity D is visible on the left side of the photograph

Joint A

This joint is a slightly weathered horizon without a defined fracture in the areas where the contact between flows A and B is open. On the left bank, under blocks F19/20 to F35/36, the thickness of the clay infilling, in the joint was 3 to 5 cm and the estimated ϕ was 35° .

SHEAR ZONES

Shear zones at base of basalt flow B

For stability of the main dam and the powerhouse, the most important feature of the foundations was the shear zones of the river channel at the base of basalt flow B. These shear zones constitute at least four main planes, see Fig. 4.4.

Shear zone 1. On the right abutment, this zone virtually coincides with the contact between flows A and B at about El.20, rising in the direction of the left bank, until intercepted by zone 2. Offsets of up to 30 cm were recorded in this zone away from the contact areas. In some areas, the shear zone 1 is

filled with concentrations of highly plastic clay, and at other locations with mylonitized material. As this zone approaches, and finally joins the contact A/B, it has, in some places, a clay infilling, and in others an open discontinuity, where it is extremely pervious, as demonstrated by the infiltrations into the tunnels during construction. Possibly because of the high degree of weathering, the presence of slickensides or any other sign of movement along the discontinuity was not observed.

Shear zone 2. This was the first to be detected as it exits under the stem of block F17. Its geomechanical condition varies from the higher elevations where the clay concentration is high, to the lowest levels where rock-to-rock contact is predominant.

Where the clay concentration is high there is a considerable evidence of movement and off-sets of an average of 10 cm were observed. Where this zone intercepts zone 1, a thick pack of rock with multiple horizontal fractures occurs, which was responsible for some rock falls during tunnel excavation. The angle formed by these two zones measures 20° . In the foundation area this zone has a strike predominantly in the N-S direction, and a 15° dip to E.

Shear zone 3. This zone is smaller than zones 1 and 2 and is located on the downstream side of the dam. It has a downstream dip which is conducive to sliding.

Towards the upstream, this zone closes and disappears before daylighting, and thus was not detected during the preparation of the foundation surface. In the downstream direction it virtually reaches the contact A/B. Cataclastic infilling with crushed rock fragments predominate, sometimes

enveloped in a clayey matrix. There is clear evidence of movement in the E-W direction. An upper network of tunnels and shear keys at El.30 was constructed to treat this feature.

Shear zone 4. This zone, whose area is only about 40 m x 50 m, was detected between El.30 and El.35. In this zone, there were only small deformations resulting from the dam being under construction and hence it was left untreated. For the exploration and inspection of this zone, a shaft 9.5 m deep was driven.

The exploratory investigations showed the infilling of this zone to be irregular and confirmed its location and extent as originally established by drilling.

There were several different opinions as to the origin of the shear zones in the main river channel foundation. However, there was an agreement that these discontinuities were related to horizontal stresses associated with river erosion, producing a typical pattern of buckling and shearing rupture, see Fig. 4.4.

That these shear zones may have originated due to redistribution of an original natural stress field, resulting only from the rock weight and elastic rock properties due to the erosion of the river canyon was thought unlikely. Even considering 100 to 200 m of overburden on the top of the valley eroded during geological times, the resultant horizontal stresses would be low and able to buckle only a relatively thin (10 m) basalt stratum but not to shear it, since such stresses are much lower than the unconfined compressive strength of basalt. Therefore, there must have been a contribution of horizontal stress by either regional subsidence or lateral crustal compression or a combination of the two processes.

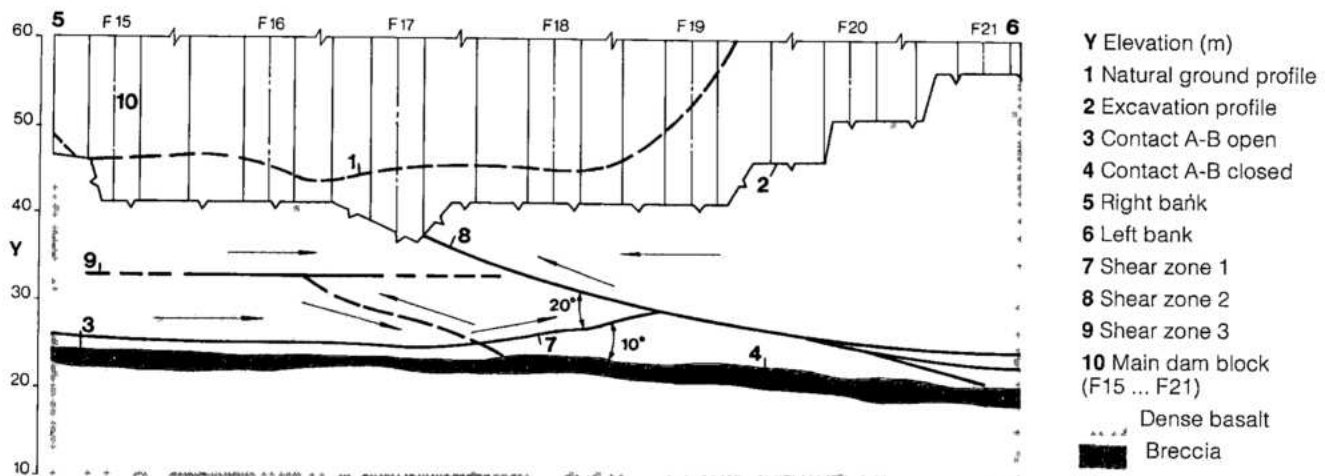


Fig. 4.4 Main dam foundation - probable mechanism of formation of river

SUBSURFACE TREATMENT

Subsurface treatment of right bank discontinuity

Treatment at contact between basalt flows C and D consisted of a grid of three longitudinal keys and a transverse key under blocks F1, E6, E5 and E4 of the dam, totalling about 600 m of tunnels and 6000 m³ of concrete backfill, see Fig. 4.5. The discontinuity is coincident with contact C/D at about El.112.

The underground treatment covered half of one hollow gravity block and five single buttress blocks. This was necessary because of the low shear strength of the clayey material in the discontinuity and because this portion of the foundation is unconfined on two sides; on the left due to stepped down foundation, and on the downstream side where there is a deep excavation for the right assembly area. The treatment improved the shear strength of the weak planes sufficiently to obtain adequate safety factors against shearing-sliding at the discontinuity.

Subsurface treatment of foundations of main dam in the river channel

The most extensive foundation treatment was under the highest blocks of the main dam in the river channel.

Of the several alternatives considered for this treatment, such as deepening of excavation, trench or cut-off excavation, washing of weak materials and grouting, shear keys, etc., two were selected for detailed analysis:

1. Partial lowering of the downstream third of the foundation.
2. Concrete shear keys at contact A / B.

A comparison of the two remedial treatment alternatives arrived at the following conclusions:

- Both would provide equivalent factors of safety.
- With respect to technical feasibility, both were essentially equal.
- If part of the foundation was lowered to El.20, the following additional quantities would be required: 190 000 m³ of excavation and 180 000 m³ of concrete.
- Even considering the higher unit prices for the shear keys, the subterranean treatment alternative would be 20% cheaper.
- For the first alternative, about 7 months would be required to excavate the rock and backfill with concrete from El.40 to El.20, which would impede the construction schedule for the high blocks of the main dam.
- Underground treatment (the second alternative) could be carried out simultaneously with the construction of the dam blocks with minimum interference.

Based on the above conclusions, it was decided to proceed with the second alternative that was underground treatment with shear keys. The final arrangement consisted of a grid of eight shear keys parallel and eight perpendicular to the axis of the dam, see Figs. 4.6 and 4.7. Individual shear keys comprise tunnels 3.5 m wide and 2.5 m high at El.20, some 15 to 20 m below the surface, backfilled with concrete and contact grouted.

Total length of the shear keys was 2600 m and the total volume of concrete used, 30 000 m³. The grid is circumscribed by a perimetral drainage tunnel,

Fig. 4.5 Main dam - foundation treatment on right bank

- 1 Access shaft
- 2 Shear keys
- 3 Discontinuity
- 4 Grout curtain
- 5 Drainage tunnels

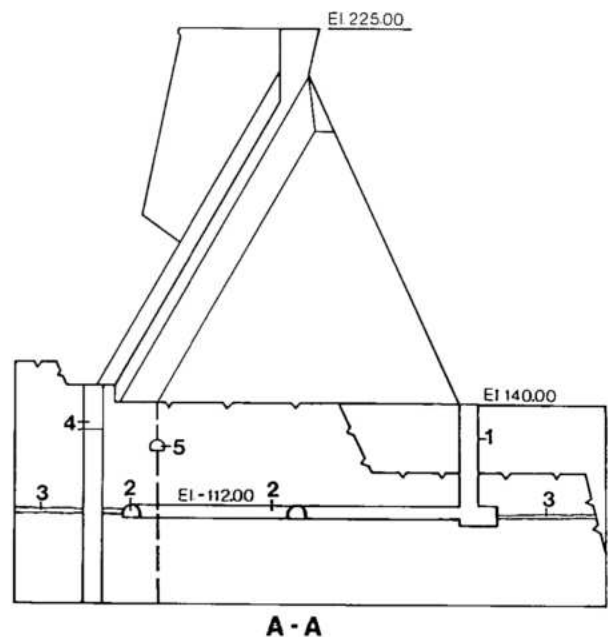
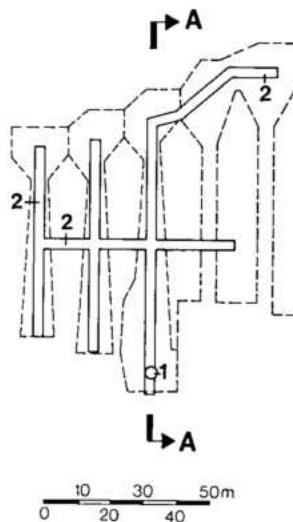
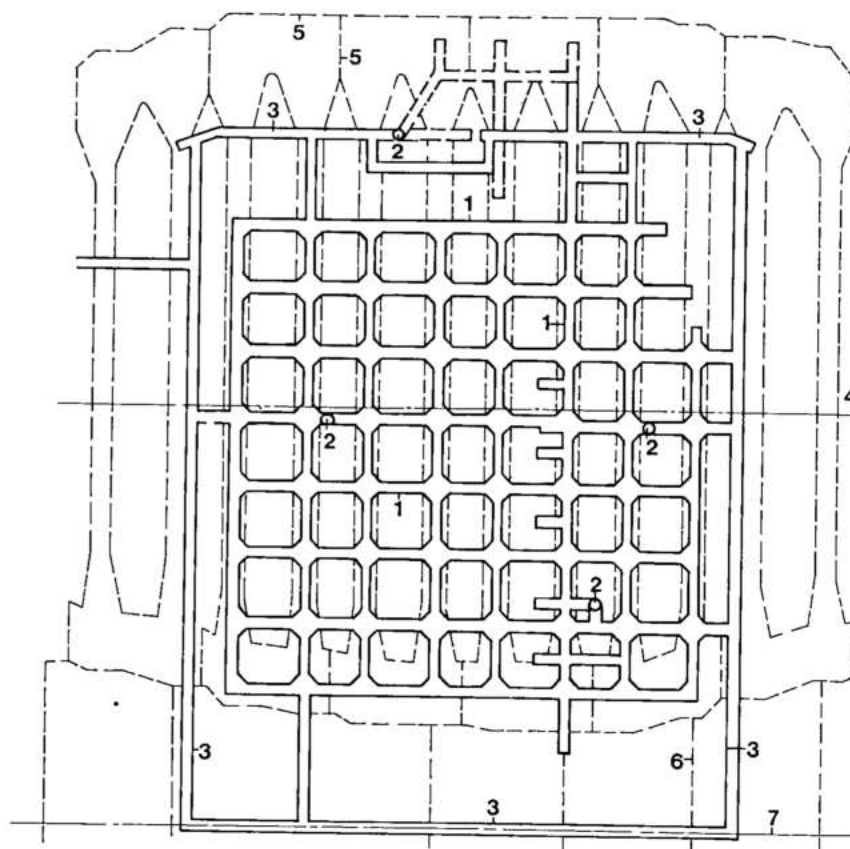


Fig. 4.6 Main dam and powerhouse in the river channel foundation treatment - plan at El. 20

- 1 Shear keys
- 2 Investigation and access shaft
- 3 Perimetral drainage tunnel
- 4 Axis of dam
- 5 Main dam - hollow gravity block
- 6 Powerhouse block
- 7 Axis of powerhouse



800 m long, excavated along contact A/B at about El.20, which isolates the treated region so that uplift in the inner area is reduced to a minimum.

Design of the shear key foundation treatment

Criteria. The grid of concrete keys along the discontinuities was designed to provide resistance against shearing-sliding along the planes of weakness. Furthermore, it replaced with concrete enough of the more deformable seams and layers to reduce differential settlement of the foundations.

The basic criteria for the treatment were as follows:

- The behavior of the dam and its foundation should stay well within the elastic range.
- A well distributed transmission of the forces through the plane of the discontinuities should be assured.
- The perimetral drainage gallery should be finished before filling of the reservoir.
- Weak and fractured layers should be located, examined and treated.

Conventional stability analyses. The area of the foundation under each hollow gravity block requiring treatment was determined by conventional stability analyses of equilibrium limits against shearing-sliding using the following assumptions:

- A horizontal sliding plane, because of the small dip (1° to 2°) of the discontinuity.
- Uplift diagram according to design criteria, considering the effect of the drainage tunnels.
- Vertical upstream and downstream cracks in the foundation reaching El.20 with full hydrostatic load.
- No consideration of lateral rock resistance (between foundation surface and discontinuity, El.40 to El.20) as the analysis was two-dimensional.
- No consideration of downstream wedge rock resistance because these forces would be mobilized only after the deformation of the foundation had reached the elastic limit.
- Only the first stage of the powerhouse was constructed.

- Shear strength contribution of the concrete shear keys equals 0.5 kN/cm^2 ; laboratory tests had confirmed this value.
- Contribution of the untreated area with $c = 0$ and $\phi = 15^\circ$. Although the estimated ϕ was 20° to 25° , because of the great difference in the deformability of concrete and the untreated discontinuity, the concrete reaches its shear strength limit at low strain levels while the stresses in the discontinuity are hardly mobilized. Thus a lower value of ϕ was assumed.
- No contribution of the vertical load of the dam on the concrete keys as the keys were built simultaneously with the dam blocks. It was estimated that only 28% of the dam weight would contribute to the mobilization of the frictional resistance in the keys.

Most of the assumptions gave conservative results in the calculation of dam stability.

The analyses indicated that to obtain an adequate factor of safety, the minimum area to be treated by concrete keys should be about 25% of the gross foundation area under the four blocks of the dam.

Stress studies by the finite element method. Finite element analysis was used to establish the arrangement of the keys and resulting stress distribution in the discontinuities.

Longitudinally oriented keys were first considered, because it was thought that a key normal to the direction of the hydraulic load would resist the shearing loads better. However, it was found that stresses tended to be concentrated in the upstream keys, which could lead to progressive failure. Alternatively transverse (upstream-downstream)

keys, being continuous under each stem of the blocks, would provide effective shearing resistance over the whole width, including the bridging-over of the heterogeneous areas of the foundation.

Thus, to obtain the best from both orientations and have the most uniformly distributed treatment, it was decided to adopt a grid of transverse and longitudinal tunnels filled with concrete to form the shear keys.

The following conclusions were drawn from studies of this solution:

- Longitudinal keys are subjected to higher shear stresses at lower values of shear stiffness of the discontinuity.
- The shear stresses are lower in the longitudinal keys and increase gradually to a peak in the transverse keys.
- The upstream and downstream end regions work at a higher shear stress level.
- In all cases the shear stresses are below the allowable limits over the entire treated foundation.

Rock blasting and subsurface foundation treatment

The sequence of excavation of the tunnels for the shear keys was planned to ensure safe working conditions, to avoid damage to the sound rock and to minimize interference with the construction of the dam. Tunnels had to be located along the more fractured regions and zones of weakness which often resulted in excavation in unstable and hazardous regions. Consequently, rock stabilization with a wide range of methods was adopted.

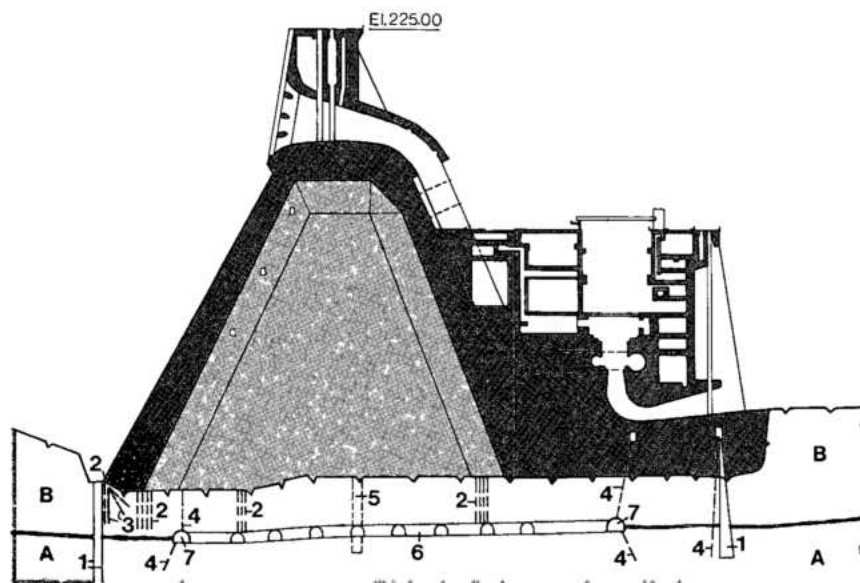


Fig. 4.7 Main dam and powerhouse foundation treatment cross section

- 1 Grout curtain
 - 2 Contact grouting
 - 3 Consolidation grouting
 - 4 Drain holes
 - 5 Investigation and access shaft
 - 6 Shear keys
 - 7 Drainage tunnel
- A, B Flow designation
 Dense basalt
 Breccia

The blasting for and excavation of tunnels was controlled, avoiding damage to the concrete in the dam blocks located 15-20 m above, in the nearby shear keys, or the surrounding rock itself. Accordingly, strict rules for monitoring the blasting vibrations were established, which determined the permissible quantity of charge per delay and, consequently, the rate of advance of the tunnels. Particle velocities given below were not to be exceeded at the concrete of indicated age.

Concrete age (hours)	Max. particle velocity (cm/s)
0 - 8	No restriction
8 - 24	0.25
24 - 36	0.5
36 - 48	1.0
48 - 60	1.75
60 - 72	3.0
>72	5.0

The maximum advance for each round of blasting was 1.6 m, with the excavated material removed by special compact loaders. Occasionally two or more discontinuities at the same location required tunnel excavation in benches, resulting in a final tunnel height of 8-10 m, compared with the design height of 2.5 m. This sometimes resulted in local instability corrected by quick placement of concrete. During planning of the excavations, these cases were foreseen, and the work directed to reach these sites during the last stage of opening of each tunnel, thus minimizing the time between the end of the excavation and the start of concrete placement. Some shear keys were also extended under the upstream head of the central blocks due to the presence of a deformable weak seam at a shallow depth of 10-15 m, see Fig. 4.6.

Systematic rock stabilization was applied at each tunnel heading immediately after mucking out. Typically, this consisted of rock bolts 2.4 to 3.2 m long, 16 to 25 mm in diameter, and a steel wire mesh tied by the same bolts or by clamps. When highly fractured rock was encountered, pre-stressed rock bolts were installed from the work face with a forward inclination and grouted, which resulted in improved performance and faster rate of advance. In stretches of rock where fracturing of single rock blocks of small volume ($< 0.5 \text{ m}^3$) occurred and where the installation of rock bolts was impractical,



Tunnels for transverse keys

flat steel bars were installed, tied by bolts at both ends and molded to fit the contour of the tunnel. More unstable rock conditions required application of shotcrete, either as a preliminary treatment before drilling holes to place rock bolts, or to supplement other stabilization measures.

Following excavation and rock stabilization and after removal of large loose material, the exposed rock surface was washed with water and compressed air jets to remove all fine material which could prevent a good bond between the concrete and the rock. Similarly, the sheared zone was washed, removing all superficial clay. Detailed geological mapping was then done and the area released for placement of concrete.

Concrete used for backfilling of tunnels had a compressive strength f_{ck} of 2.8 kN/cm^2 at one year of age and a maximum aggregate size 38 mm. It was placed from the surface, through 152 mm diameter holes, 4 to 8 m apart, made with a down-the-hole percussion drill. Concrete was initially vibrated in the tunnel up to a certain height, thereafter, consolidation was continued from the surface by lowering the vibrator down the placement hole. The final lift of concrete near the roof of the tunnel contained an expansive admixture. In places where the tunnels were of exceptional height, the placement of concrete was carried out in more than one lift. Vertical construction joints in the concrete keys were usually located midway between the intersection of the tunnel grid.

The roof contact areas of the shear keys were grouted from the surface through drill holes spaced 6 m apart. This was to fill any voids due to concrete shrinkage or inadequate filling of the irregularities in the rock surface, joints opened during blasting or

stress relief above and around the tunnel roof. The effective grout pressure was 0.6 times the height of the rock above the tunnel roof and was intended also to ensure penetration of small open fractures at the base of Flow B. On completion of grouting, rotary holes were drilled to obtain cores from the grouted area and to test for loss of water under pressure. Six months later, second stage grouting was performed through grout holes drilled between the first stage holes. A total of 20 000 m of holes was drilled for grouting the shear key area.

Grout curtains and drainage

Based upon comparative data from other similar projects, a foundation permeability of 20 Lugeons or approximately 100 l/min was taken as the upper limit above which a grout curtain and drilled drainage was considered mandatory. Between measured values of 0.2 Lugeons and 2 Lugeons the situation was monitored during construction with a view to treatment if considered necessary. Details of the grout curtain and drainage measures are given in the chapters dealing with the respective structures.

INSTRUMENTATION IN THE SHEAR KEY GRID

The following instruments were installed in the foundation rock in the area subjected to subsurface treatment and in the concrete shear keys themselves:

Piezometers	16
Multiple extensometers	9
Sets of pins for portable jointmeters	12
Strain meter rosettes	4
Seepage discharge weirs	5

Location of the instrumentation in the subsurface treatment grid under the four central blocks of the main dam is shown in Fig. 4.8.

During excavation of the tunnels, the multiple extensometers which were installed before the start of the underground work, were useful in detecting potentially risky areas of excessive overbreak and special rock stabilization. As the subsurface treatment progressed, from periodic extensometer measurements it was possible to analyze the

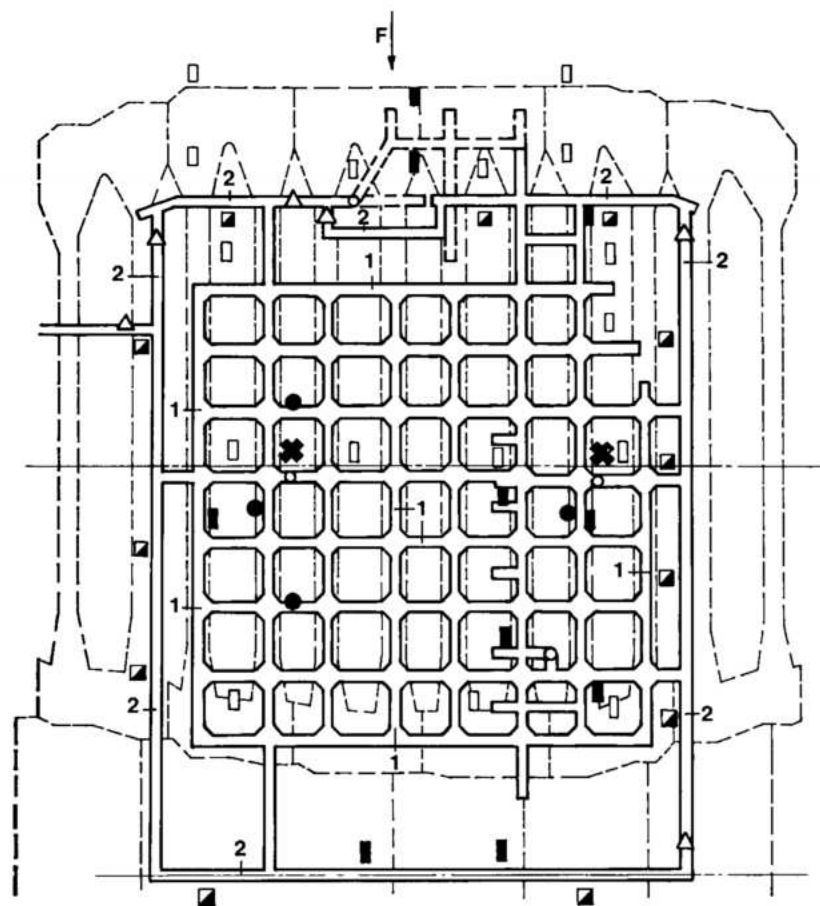


Fig. 4.8 Main dam foundation treatment instrumentation of the concrete keys-plan

- 1 Concrete shear keys and strips
- 2 Drainage tunnels
- Piezometer
- Multiple extensometer
- ▣ Group of pins for removable joint meter
- Rosette of strainmeter
- ✱ Pendulum
- △ Discharge weirs
- F Flow

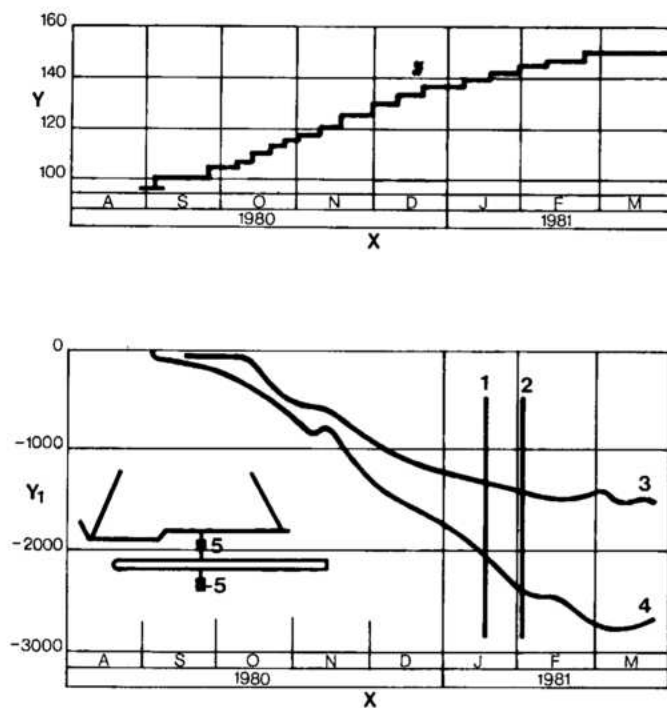


Fig. 4.9 Main dam - settlement during subsurface treatment

- | | |
|---|------------------------------------|
| Y Elevation of main dam block (m) | 3 Upper anchor of extensometer |
| X Time (months) | 4 Lower anchor of extensometer |
| Y ₁ Settlement in micron | 5 Location of extensometer anchors |
| 1 Start of excavation in the vicinity of the extensometer | |
| 2 End of excavation in the vicinity of the extensometer | |

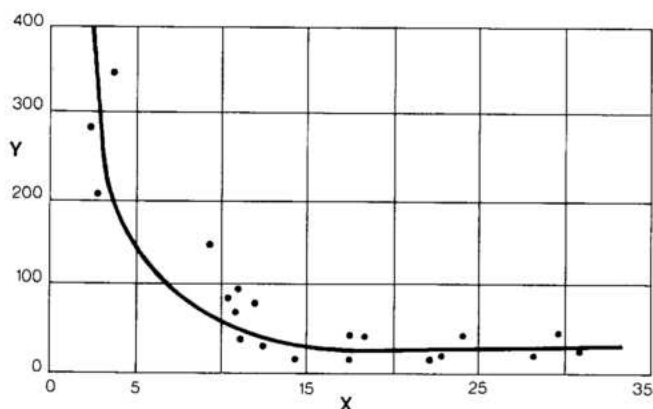


Fig. 4.10 Relation between blasting and settlement

- | | |
|---|---|
| Y Settlement in micron/per blast measured by extensometer | X Distance of extensometer from blasting location (m) |
|---|---|

settlements due to blasting, the progressively increasing weight of the dam, the concreting of the tunnels and the pressure grouting. Where high deformation rates were observed, the causes were identified and additional treatment carried out to control settlement. Extensometer measurements after completion of tunnel excavation and before concrete backfilling showed clearly that settlement accelerated wherever the height of the tunnel approached the thickness of the overlying rock.

Instrumentation data showed an increase in vertical deformation as tunnel excavation neared the extensometer, possibly as a consequence of the consolidation of weak material infilling and closure of joints in the discontinuity due to blasting vibrations. Fig. 4.9 shows the typical behavior of the foundation, which initially, under the weight of the dam, underwent a steady rate of settlement. In January 1981, the rate increased, as recorded by the lower anchor of the extensometer, as the tunnelling approached the instrument. After the tunnelling was completed, the settlement rate significantly reduced.

Fig. 4.10 illustrates clearly the effect of blasting on deformations measured by an extensometer crossing shear zone 1. At distances of less than 15 m between blasting and the extensometer, the settlement at each blast increased exponentially even when very low explosive charges were employed.

The rates of settlement recorded varied between 5 mm/100 days for locations where excavation or concrete backfill were still in progress, to 1 mm/100 days or less, for areas already concreted and stabilized.

The purpose of the other instruments was to monitor the performance of the individual shear keys, as well as that of the entire treated foundation as an integral monolith after the treatment and the dam were completed and the reservoir filled. In addition to the extensometers, piezometers, jointmeters and strainmeters installed in the subsurface treatment grid, the two inverted pendulums located in shafts excavated through the grid and anchored about 20 m below the treated zones, also monitored the combined performance of the dam and the strengthened discontinuities in the foundation.

CONSTRUCTION PLANNING, PLANT AND METHODS

CONSTRUCTION PROGRAM	5.3
General Considerations	5.3
Planning for the Diversion of the River	5.4
General Planning	5.8
LAYOUT OF THE CONSTRUCTION FACILITIES	5.13
General	5.13
Design Criteria for Construction Facilities	5.13
CONCRETE SPECIFICATIONS, QUALITY CONTROL AND CONSTRUCTION METHODS	5.16
Concrete Aggregates	5.16
Cement and Fly Ash	5.18
Concrete Mixes	5.19
Quality Control	5.19
CONCRETE PRODUCTION FACILITIES	5.25
Construction Yard Facilities	5.25
Location and Description of the Facilities	5.26
Precooling of Concrete	5.28
CONCRETE PLACEMENT EQUIPMENT	5.35
Monorail	5.36
Aerial Cableways	5.38
Tower Cranes	5.40
PRECAST CONCRETE COMPONENTS AND SLIP-FORMS	5.42
Precast Concrete Components	5.42
Slip-Forms	5.42
STRUCTURAL INSTRUMENTATION AND MONITORING PROGRAM	5.45
Instrumentation Program	5.45
Monitoring Program	5.46

CONSTRUCTION PLANNING, PLANT AND METHODS

CONSTRUCTION PROGRAM

GENERAL CONSIDERATIONS

In 1975, ITAIPU established that the operation of the first power generating unit should commence early in 1983. This allowed 7 years for construction of the civil works and erection of the permanent equipment.

The exceptional magnitude of the construction planning task, as faced in 1975, is indicated by the quantities of work and the heights of the principal structures, as estimated at that time, and shown below:

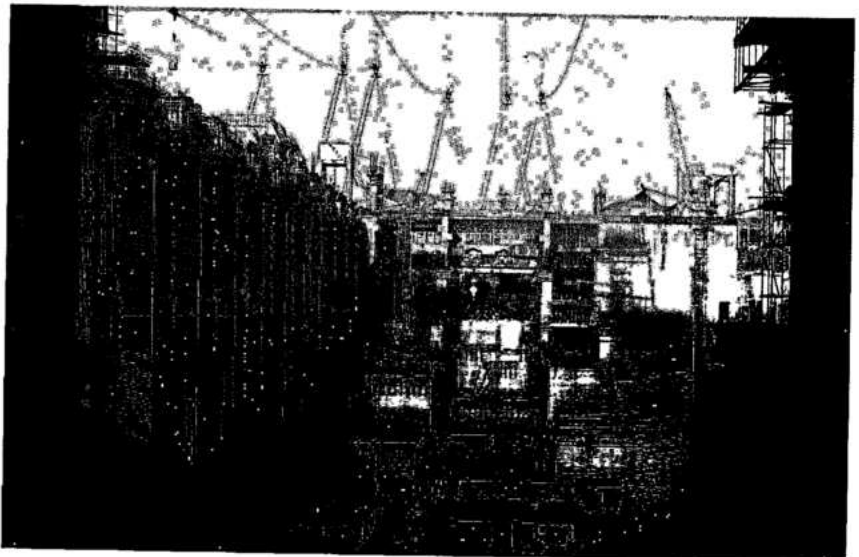
Diversion works

Volume of rock excavation	$20 \times 10^6 \text{ m}^3$
Volume of concrete (part of diversion structure)	$1 \times 10^6 \text{ m}^3$
Volume of cofferdams	$10 \times 10^6 \text{ m}^3$
Height of upstream cofferdam	90 m
Height of downstream cofferdam	70 m

Main permanent works

Volume of rock excavation	$13 \times 10^6 \text{ m}^3$
Volume of concrete	$10 \times 10^6 \text{ m}^3$
Height of the main dam (maximum)	190 m
Height of the powerhouse (maximum)	100 m

*Concrete placement
equipment in operation*



PLANNING FOR THE DIVERSION OF THE RIVER

The simplified Critical Path Method schedule, (CPM), Fig. 5.1, indicates the main activities pertinent to diversion of the river. These activities consisted of excavation of the diversion channel and disposal of the excavated rock, construction of the diversion control structure up to El. 144 and construction of the two main cofferdams.

According to the overall project schedule, this work was hypercritical, that is, a delay in these activities could have resulted in subsequent larger delays. For example the CPM indicated that the latest date by which the safe elevation (approx. El.126) of the closure dike B of the upstream cofferdam had to be reached, was before the flood period of 1979 (January to March). A delay in the opening of the diversion channel which would prevent achieving this safe elevation in time, could have postponed closure of the cofferdams until the dry period of 1979, representing a delay in the general schedule of not less than 6 months.

Diversion channel

Excavation of rock from the diversion channel was scheduled to start in January 1976 and to be completed in 32 months. For planning purposes, the channel was divided into three sections for dry excavation and two areas of underwater excavation at both approaches. Fig.5.2 shows schematic sections indicating stages of construction of the works in the diversion channel, and a histogram of the quantities to be excavated in the various sections.

CPM analyses showed two extremely critical activities. The first was the excavation of the middle section, on which construction of the diversion control structure was dependent. A minimum period of 20 months was allocated for this excavation, with completion in September 1977. The second critical activity was the excavation of the rock masses remaining at the entrance and exit of the channel. For this work, the schedule indicated two conflicting conditions:

- For adequate protection of the diversion structure under construction, these masses had to remain at El.115, which would limit progress of excavation in the dry.
- In order to finish this excavation in 1978, it was essential to take advantage of the May-August dry period of that year when river levels were low, at about El.100. This ensured maximum possible excavation in the dry, including excavation of a trench at the toe of the final rockplug, thereby considerably reducing the volume of underwater excavation.

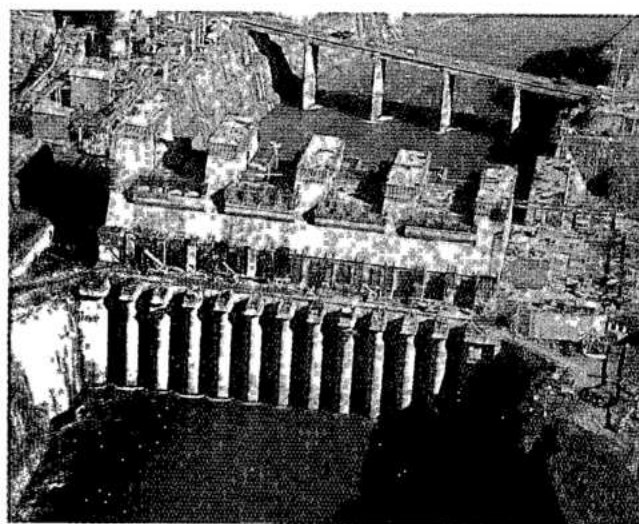
This conflict was resolved by the construction of two thin concrete arch cofferdams upstream and

downstream of the diversion control structure, which was protected by these cofferdams until the last moment before opening the channel in October 1978. The arch cofferdams were removed by virtually instantaneous blasting, see Chapter 6.

Another activity which depended on the excavation of the downstream section was the construction of the service bridge. This bridge provided the only access across the diversion channel after its opening and was essential for the transportation of excavated rock which was stockpiled on the left bank for construction of the main cofferdams. Prior to completion of the bridge a rock bar carrying a road across the channel remained in the downstream section until about 3 months before opening the diversion channel. In order to minimize interference with circulation and access, the construction of a concrete wall, which closed a ravine on the right bank between the middle and downstream sections, was scheduled for the latest possible date.

Diversion control structure

To ensure the construction of the diversion control structure in the shortest possible time, it was essential that in parallel with the excavation of the middle section of the diversion channel, all the industrial facilities of the left bank, including the aerial cableways, be installed. Consequently, it was possible to plan the start and progress of concrete placement in the various blocks without serious restrictions resulting from the installation of the concrete batching and placing equipment. In this manner concrete placement was scheduled to follow immediately after the respective foundations were ready.



Construction bridge of diversion control structure

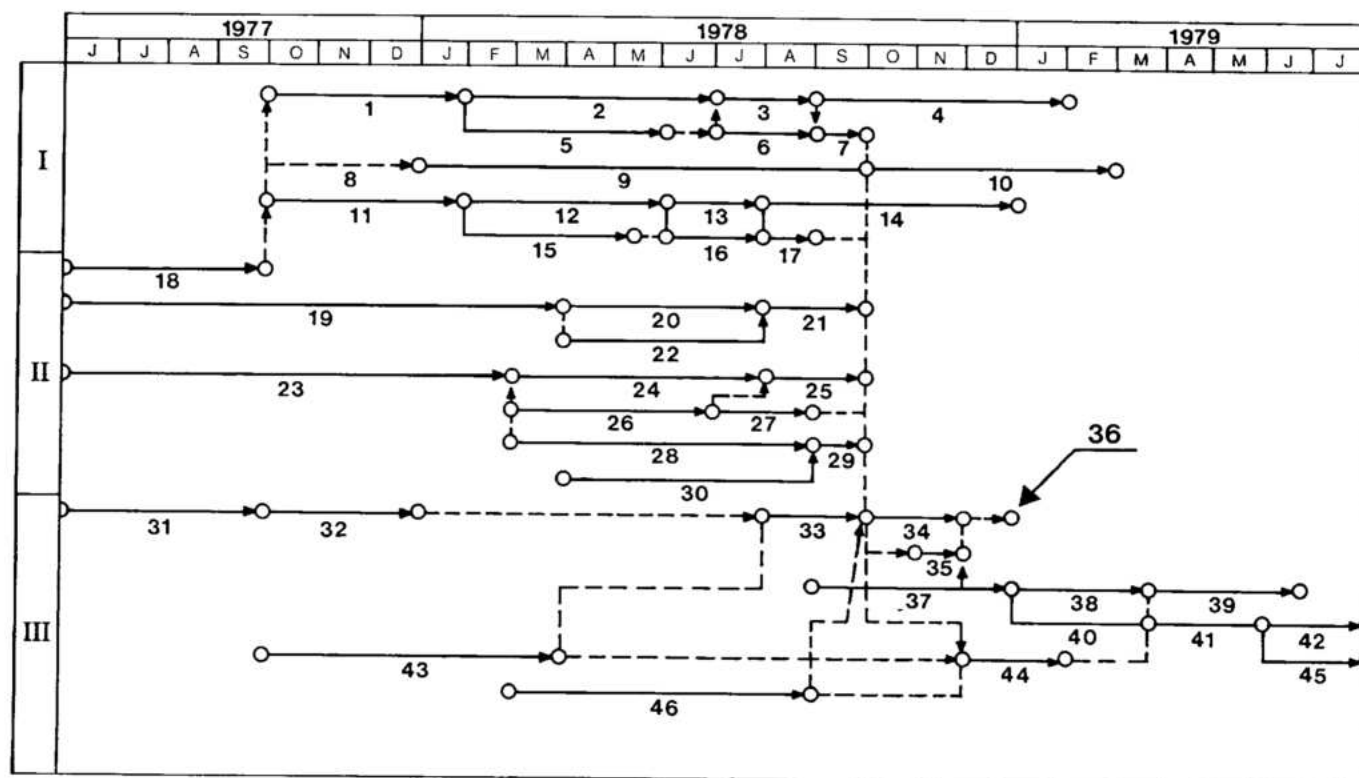


Fig. 5.1 Simplified CPM for diversion of the river

I Diversion control structure

II Diversion channel

III Cofferdams

- 1** Concrete monolith A to invert of diversion sluice
- 2** Concrete leading blocks to El. 116
- 3** Concrete remaining blocks to El. 116
- 4** Concrete monolith A to El. 144
- 5** Install gate and stoplog inverts and concrete 2nd stage
- 6** Install upper sealing beam
- 7** Finish installation
- 8** Dephased concrete placing in monolith B because of construction priority of monolith A and C
- 9** Concrete monolith B to El. 116
- 10** Concrete monolith B to El. 144
- 11** Concrete monolith C to invert of diversion sluice
- 12** Concrete leader blocks to El. 116
- 13** Concrete remaining blocks to El. 116
- 14** Concrete monolith C to El. 144
- 15** Install stoplog inverts and concrete 2nd stage
- 16** Install upper sealing beam
- 17** Finish installation
- 18** Finish excavation middle section of channel
- 19** Excavate upstream section of channel enough to construct upstream concrete cofferdam
- 20** Finish excavation of upstream section
- 21** Remove upstream rock plug
- 22** Construct upstream concrete cofferdam
- 23** Excavate downstream section of channel enough to construct downstream concrete cofferdam and service bridge
- 24** Finish excavation of downstream section except rock passage way across channel
- 25** Remove downstream rock plug
- 26** Construct downstream concrete cofferdam
- 27** Excavate rock passage-way across channel
- 28** Construct service bridge
- 29** Finish right side closure wall
- 30** Construct right side closure wall maintaining channel access
- 31** Construct right bank access to dikes A and B
- 32** Construct partially dikes A and B from the right bank
- 33** Advance dikes B and D with channel still closed
- 34** Close dikes B and D and raise B to El. 126
- 35** Close dike A
- 36** Latest finish time to construct dike B to El. 126
- 37** Dredge between dikes A and B
- 38** Waterproof upstream cofferdam
- 39** Finish upstream cofferdam to El. 140
- 40** Dredge between dikes C and D
- 41** Waterproof downstream cofferdam to El. 110
- 42** Dewatering
- 43** Construct right bank access to dikes C and D and prepare abutments
- 44** Close dike C
- 45** Finish downstream cofferdam to El. 125
- 46** Construct left bank access to dikes A, B, C and D and prepare abutments

Fig. 5.2 Diversion channel rock excavation stages and quantities

Y Elevation (m)

X Years

I Situation in September 1977. Finish excavation of section and start concreting control structure, dry and underwater excavations in the central downstream and upstream sections

II Situation in May 1978. Control structure, concrete cofferdams and service bridge under construction, dry and underwater excavation in the middle central and downstream sections.

III Situation in July 1978. Rock passageway removal and rock trap excavation – finish underwater excavation. Diversion structure under construction. Finish concrete cofferdams. Install service bridge

IV Situation in October 1978. Diversion structure reaches minimum elevation for diversion, finish excavations

1 Underwater excavation

2 Upstream concrete cofferdam

3 Diversion structure

4 Service bridge

5 Rock passage way

6 Downstream concrete cofferdam

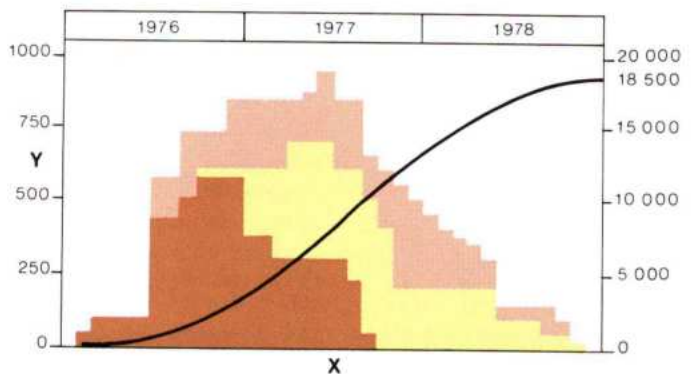
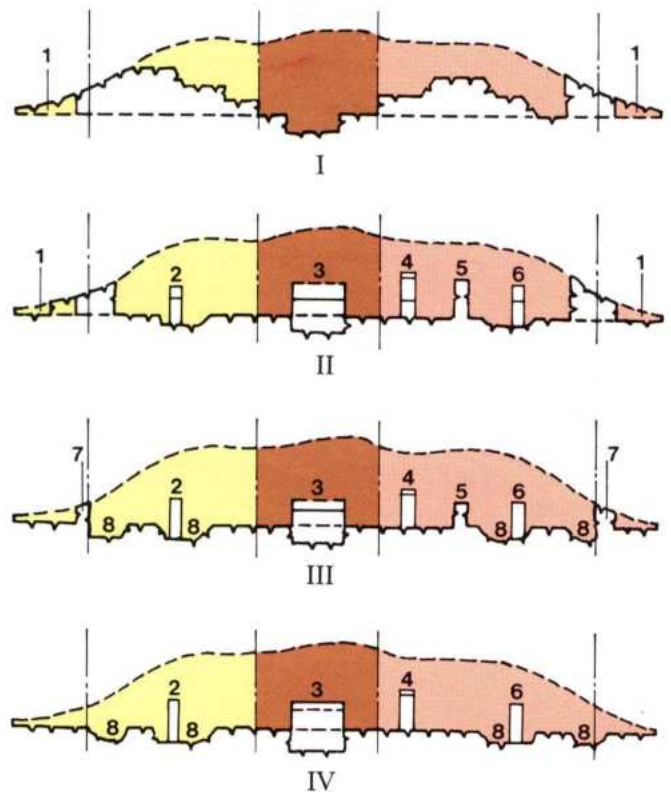
7 Rock plug

8 Rock trap

Upstream section

Middle section

Downstream section



Since the completion of the middle section excavation was planned for September 1977, construction of the diversion structure up to the minimum elevation required for opening the channel was scheduled from October 1977 to October 1978.

Fig.5.3 shows the minimum configuration of the diversion structure for river diversion. It was estimated that a minimum of 12 months would be required to place the estimated 850 000 m³ of concrete. Longitudinal contraction joints which divided a block into three monoliths are also shown in Fig.5.3. Construction of monolith A was critical in the schedule. Relative to monoliths B and C, not only was the placing rate of concrete in monolith A reduced due to the erection of the steel linings adjacent to the gate and stoplog guides, but

also the time required to install the precast concrete beams in the ceiling of sluiceways and concreting of the second stage was longer. Stoplogs were located only in monolith C, and therefore it was estimated that a shorter time would be required for its completion. The placing rate of concrete in monolith B could be higher, and thus its start was delayed in relation to the other monoliths, which had higher priority.

All concrete placement was scheduled to be done by aerial cableways. Although there would be no difficulty in continuing placement after river diversion, when this work was no longer critical, the maximum design level for the flood period in early 1979, El.126, had to be reached in a short time, starting from the minimum elevation for diversion.

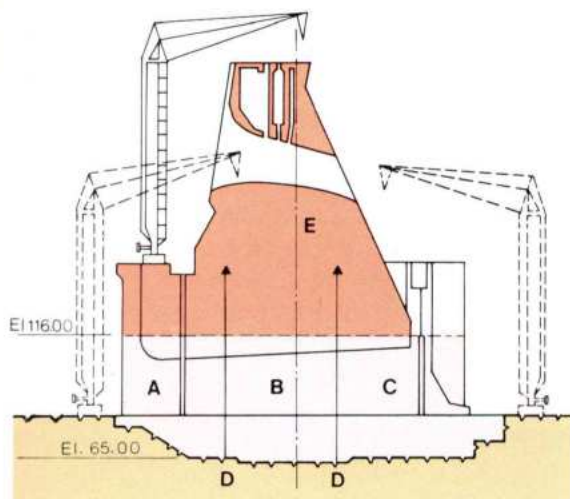


Fig. 5.3 Concrete placement in diversion structure

A, B, C, E Concrete monoliths
D Longitudinal joint contraction

Dense basalt
 Concrete placement with cableways
 Concrete placement with cranes

Main cofferdams

Fig. 5.4 shows the preliminary cross-sections of the upstream and downstream cofferdams used for construction planning. Also shown schematically are the four main stages of their construction.

The truly critical activities were those which commenced after opening of the diversion channel. Prior to that, the following work which was not critical in the general schedule, was to be done:

- Partial placing of dikes A and B, in 1977, so as to restrict the river flow between the left bank and Itaipu Island and cause, during the flood period of the following year, the partial scouring of a large sandbar located in the upstream cofferdam area.
- Preparation of access roads and abutments on both banks.
- Continued placing of rockfill in the closure dikes B and D, during the low flow period prior to opening of the channel. The progress of the dikes was limited only by the river reaching the scouring velocity of the quarry-run rock obtained from the excavations. According to hydraulic model tests, this limit would be reached when rock placed in dikes B and D corresponded to 45% and 30%, respectively, of the total volume of each.

The closing of these dikes immediately after the opening of the diversion channel was estimated to require about $1.2 \times 10^6 \text{ m}^3$ of rock. This work was scheduled in two phases. Initially quarry-run material from the right bank would be placed. When scouring conditions were reached, placing would be carried



Diversion and closed cofferdam dikes

out from both banks with larger selected materials simultaneously in both dikes B and D at a controlled rate so that the loss of head was the same at each dike. As indicated by the schedule, 15 days would be required to place the $400\,000 \text{ m}^3$ estimated for the first phase, and another 15 days for the remaining $800\,000 \text{ m}^3$ of selected rock. This consisted of rock ranging in size from 0.6 m to 1.2 m. To ensure the final phase of closure, large boulders and 4000 tetrahedrons were to be provided. It was estimated that dike B would close at El. 115, assuming that the flow of the Paraná river during closure in early November was about $12\,000 \text{ m}^3/\text{s}$ or less. Immediately thereafter, this dike would be raised to a safe elevation, which might reach El. 126, depending on the river flow. This elevation corresponded with the most unfavorable downstream water levels for a discharge of $22\,000 \text{ m}^3/\text{s}$. The recurrence probability of this discharge was about once in 10 years, which was considered appropriate for the period of cofferdam construction. Simultaneously with raising dike B, rockfill placement would be concentrated on dike A, so as to complete it within one month. This activity was critical to the impermeabilization of the upstream cofferdam since it needed to be completed before dredging could commence between the dikes in the deep channel of the river.

Construction of dike C of the downstream cofferdam and the dredging between dikes C and D were to be carried out simultaneously with placement of the clay core for the upstream cofferdam. However, construction of the clay core of the downstream cofferdam between dikes C and D depended on completion of the clay core for the upstream

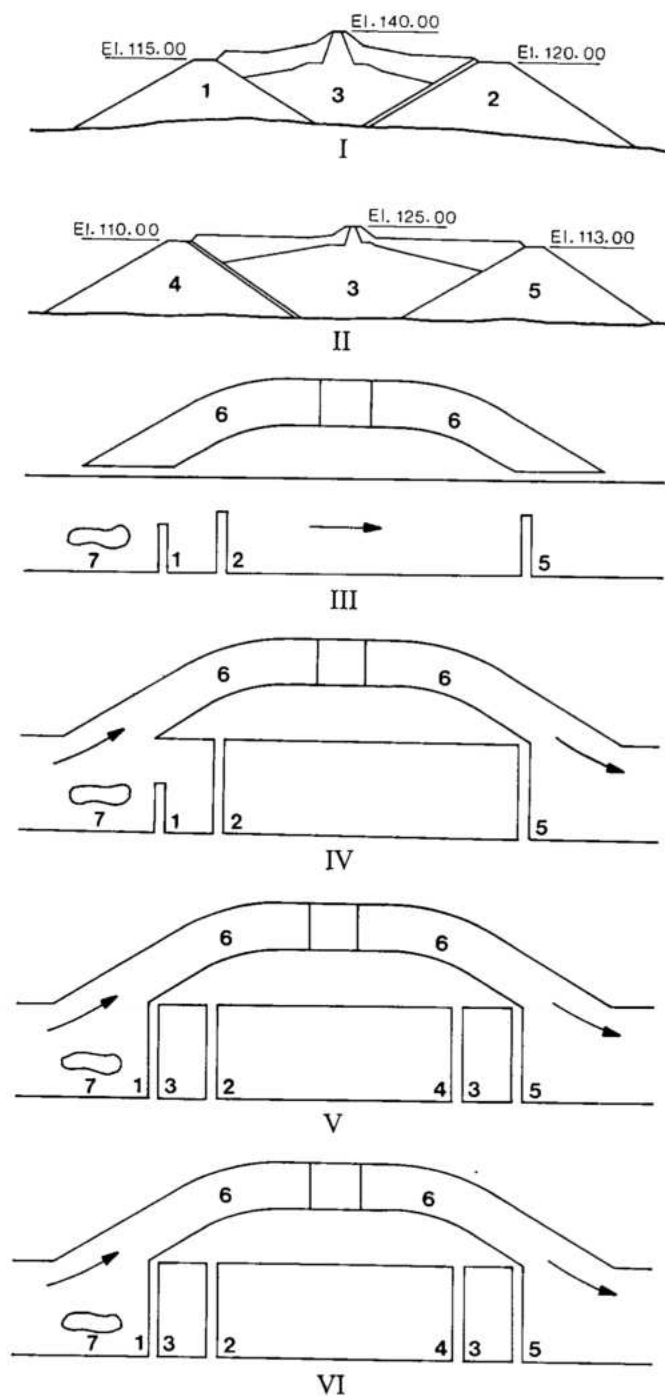


Fig. 5.4 Main stages of river diversion

- | | |
|--|--|
| I Upstream cofferdam | VI 4th stage. Finish waterproofing cofferdams |
| II Downstream cofferdam | 1 Dike A |
| III 1st stage. Partially place dikes A, B and D from right bank, before opening diversion channel | 2 Dike B |
| IV 2nd stage. River closure with dikes B and D after opening diversion channel | 3 Clay core |
| V 3rd stage. Closure of dikes A and C, waterproofing upstream cofferdam | 4 Dike C |
| | 5 Dike D |
| | 6 Diversion channel |
| | 7 Itaipu Island |

cofferdam, since placement of the transition material on the slope of dike C would be feasible only after water flow through the rockfill had been stopped.

Considering the above sequence of activities as mandatory, with normal rainfall and Paraná river flow conditions during cofferdam construction, dewatering of the area between the main cofferdams was scheduled for June 1978. Actually, the cofferdams were completed two months ahead of schedule and dewatering was completed in April 1978, see Chapter 6.

GENERAL PLANNING

The simplified CPM schedule in Fig. 5.5 shows the basic lines of general planning of construction and erection activities up to the start of testing of powerplant unit 1; (for details of the electrical and mechanical equipment manufacturing and erection program see Chapters 12 and 13). Two groups of activities were apparent:

- Activities developed on both banks, which were independent of river diversion and had large floats in the general program.
- Activities which depended on river diversion, and consequently were highly critical.

Activities independent of river diversion

Construction of the spillway, the wing dam and part of the main dam on the right bank, and the rockfill and the earthfill dams on the left bank were the most important activities outside of the river bed. Excluding the main dam blocks on the left bank which interfered with the aerial cableways, all these works could be started considerably in advance of those depending on river diversion. For scheduling, however, it was very convenient to construct the concrete structures and the rockfill dam at the earliest possible dates. The placing of concrete in the year 1979 eliminated the necessity of increasing the production peaks foreseen for the 1980-1981 period, and it was possible to release the tower cranes earlier for use in the powerhouse. Construction of the rockfill dam simultaneously with rock excavation enabled direct placing of rockfill and reduced rehandling. For this reason, the diversion of the Bela Vista and Pomba Quê rivers which crossed the dam area was considered a top priority activity during the initial phase of the work, in parallel with excavation of soil and the start of rock excavation in the diversion channel.

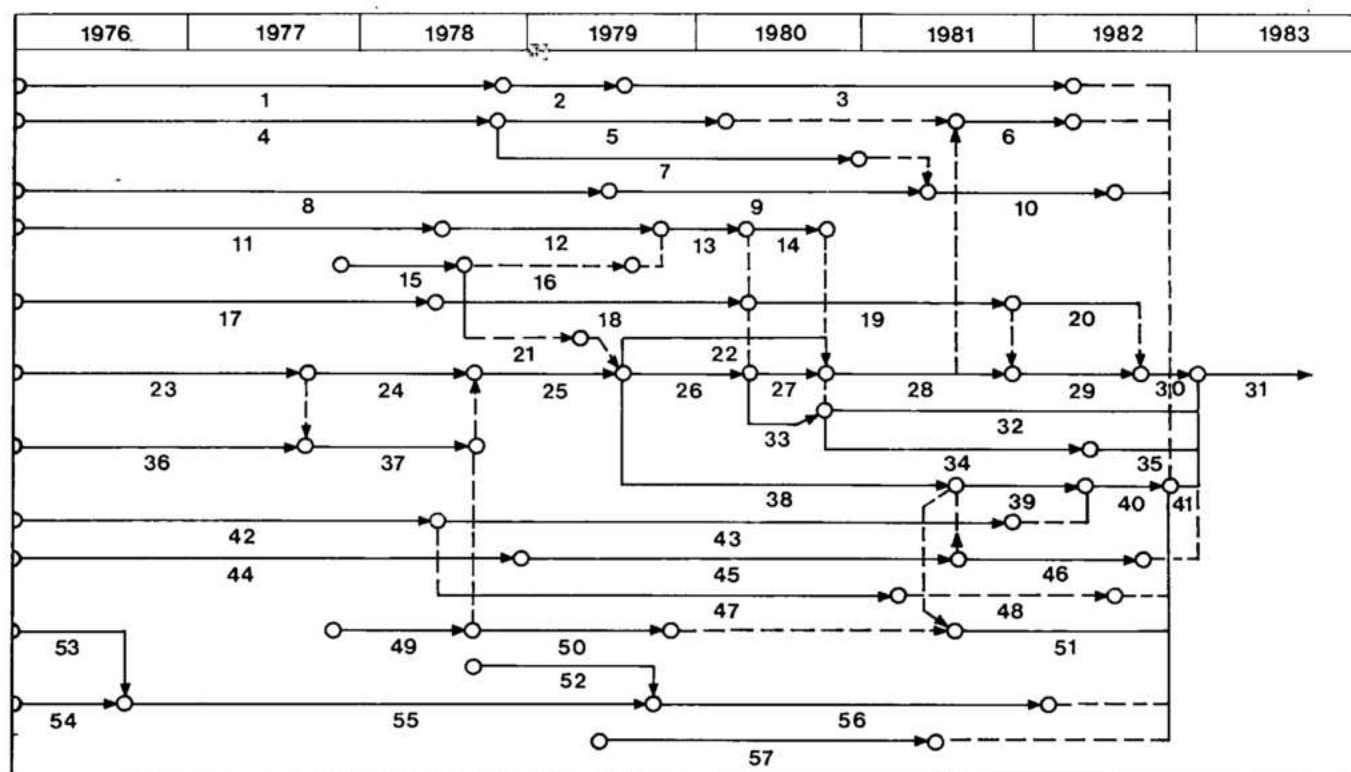


Fig. 5.5 Simplified CPM for construction up to start-up of unit 1

- | | | | |
|---|--|--|---|
| 1 Partially excavate right bank for concrete | 17 Design, specify and purchase turbines and generators | 30 Finish generator installation | 44 Design specify and purchase penstocks |
| 2 Finish spillway chute excavation | 18 Fabricate draft tube, spiral case and staying of unit 1 | 31 Test unit 1 | 45 Supply and erect penstock for unit 1 |
| 3 Construct spillway chute | 19 Finish fabrication of turbine and generator | 32 Construct galleries and install electro-mechanical equipment | 46 Install penstock for unit 1 |
| 4 Construct right bank concrete facilities | 20 Install runner | 33 Concrete powerhouse for passage bridge cranes unit 1 | 47 Fabricate diversion gates |
| 5 Construct partially right wing dam | 21 Excavate part unit 1 | 34 Finish concrete powerhouse and install draft tube stoplogs | 48 Install diversion gates |
| 6 Finish right wing dam | 22 Finish construction at right assembly area | 35 Remove downstream cofferdam | 49 Excavate main dam blocks on river bank |
| 7 Construct spillway crest | 23 Partially excavate diversion channel for concrete | 36 Construct left bank concrete facilities | 50 Continue concrete diversion structure and main dam with cableway |
| 8 Design, specify and purchase spillway gates | 24 Finish excavation at diversion channel | 37 Partially construct diversion structure | 51 Finish concrete main dam and diversion structure with cranes - install stoplogs |
| 9 Fabricate spillway gates | 25 River diversion, finish cofferdams and dewatering | 38 Excavate and construct main dam blocks in river bed with cableways | 52 Excavate and construct abutment wall |
| 10 Install spillway gates | 26 Excavate and construct powerhouse to liberate draft tube 1 | 39 Remove cableways and finish intake of unit 1 | 53 Bela Vista and Pomba-Quê river diversion |
| 11 Design, specify and purchase powerhouse bridge cranes | 27 Install draft tube and concrete 2nd stage | 40 Install intake gate of unit 1 | 54 Excavate partially rockfill dam foundation |
| 12 Fabricate powerhouse bridge cranes | 28 Install staying, spiral case and embedded parts and concrete 2nd stage | 41 Fill reservoir | 55 Finish excavation and construct rockfill dam, except for area next to abutment wall |
| 13 Install bridge cranes | 29 Install turbine and stator | 42 Design specify and purchase penstocks | 56 Finish construction of rockfill dam |
| 14 Erect staying | | 43 Fabricate intake gate for unit 1 | 57 Construct right and left bank earth dams |
| 15 Excavate right assembly area on river bank | | | |
| 16 Construct right assembly area on river bank | | | |

Activities dependent on river diversion

River bed excavation. The rock excavation program to construct the powerhouse and the main dam had two work phases. The first phase was that preceding the dewatering of the area between cofferdams, when maximum progress of excavation in the abutments was desired, the working area being protected by cofferdams on the river banks. This was particularly important on the right bank, since it controlled the start of the concreting operations for powerhouse unit 1. By maintaining a rock plug at El. 115 it was possible to plan the total excavation of the right assembly area and the excavation to El. 75 of the area to be occupied by unit 1. In this phase the partial construction of the right assembly area was begun, this enabled the installation of the bridge cranes and preassembly of the generating units within the required time limit. The second excavation phase started in July 1979 with the dewatering of the area between the cofferdams and the removal of the rock plug. It was estimated that the concrete placement in powerhouse unit 1 would start 2 months after dewatering. Excavation necessary to liberate foundations of the main dam blocks and of the powerhouse units located in the deep channel of the river required a minimum of 6 months. However, the excavation schedule was oriented so that progressive preparation of the intermediary benches proceeded at a maximum rate, which was a significant advantage to the concreting schedule.

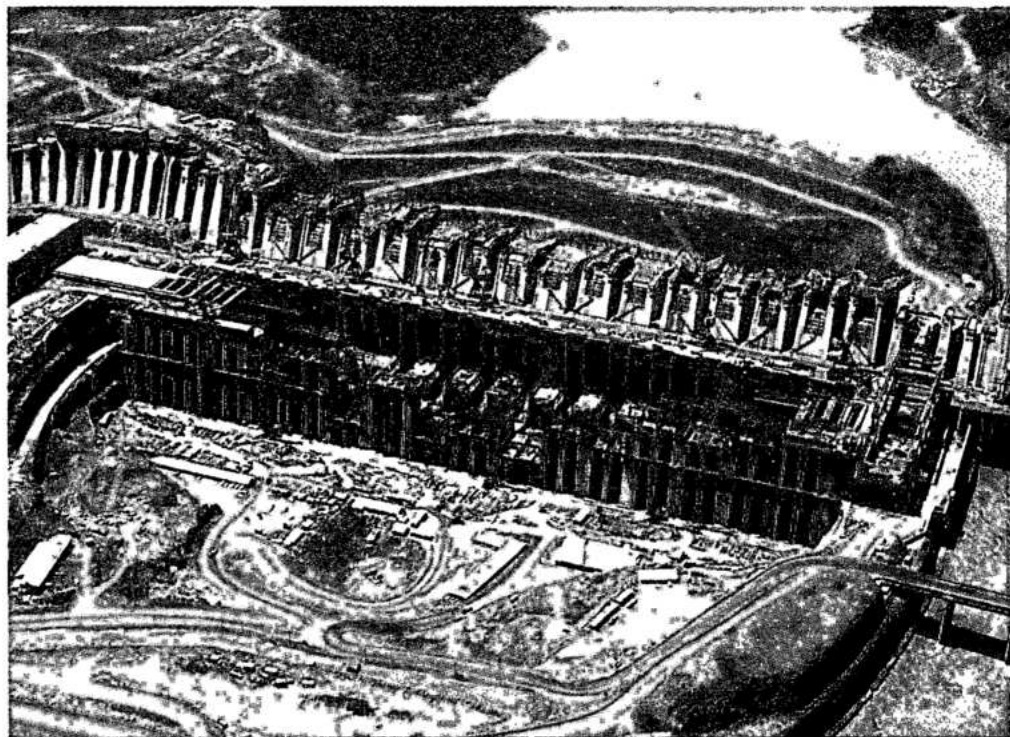
Construction of the main dam. As shown in Fig. 3.2 of Chapter 3, the main dam comprises section E on the right bank, section F in the river bed, section H (the diversion control structure) and section I, including the concrete transition wall forming the abutment of the rockfill dam.

Construction of the section F (hollow gravity blocks) was critical from three aspects:

- The power intake block of unit 1 was required to be ready in time to allow installation of the intake gate.
- The highest blocks located in the deep channel of the river required high rates of concrete placement.
- Concrete placement required total utilization of the handling equipment.

Construction of the main dam was programmed in three separate phases:

- Concrete placement starting in the abutment blocks with higher foundations, simultaneously with excavation proceeding towards the river. The main objective was to reach El. 144 in the blocks corresponding to the first units, since the platform at this elevation on the downstream side of the dam was needed to support the equipment for erection of the lower reducing bend of the turbine.
- The second phase corresponded to the period between the end of excavation and removal of the cableways from the main dam area. Concrete placement in the blocks in the river bed was given priority so that El. 144 was reached as early as



Powerhouse and main dam under construction

possible; it was at this elevation that the tracks for the tower cranes required for the next stage were located. At the same time the abutment blocks were raised at a slower rate, until the limit of placement by aerial cableways was reached.

- In the third phase the power intake structures were concreted using tower cranes operating at El. 144.

Construction of the powerhouse in the river bed.

Construction and erection of unit 1 was the most critical item; schedule for the other units contained adequate floats. The only exception was the downstream structure which had to reach final elevation to permit the erection of draft tube gates and the removal of the downstream cofferdam.

The following important stages were identified:

- First stage concrete to reach El. 82 in unit 1 in May 1980, thereby permitting the start of erection of the draft tube liner.
- Erection of equipment and second stage concreting in the unit 1 draft tube, performed by a crane positioned in the right assembly area, to be done in conjunction with the first stage concreting. This was a critical activity until El. 132 was reached in November 1980, when the support for the bridge cranes at El. 125 was completed.
- Then, erection of the permanent equipment became critical. The stay-ring previously assembled in the erection area was transported to the pit, thus

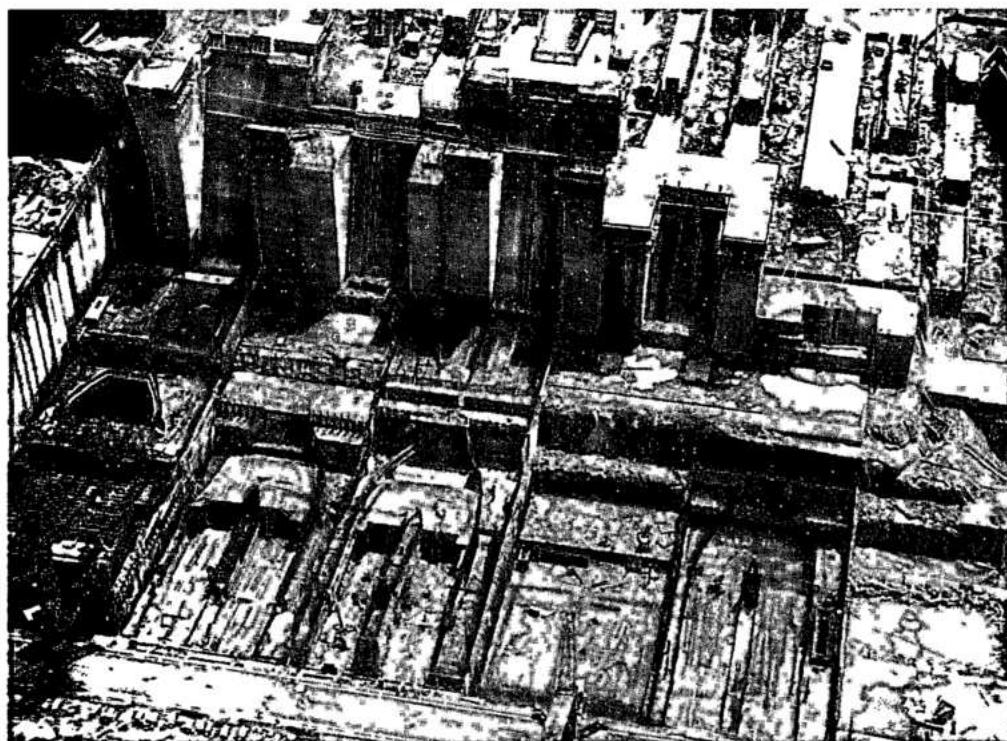
enabling the start of erection of the spiral case. It was estimated that 6 months were required for this activity, followed by 1 month for pressure testing and 6 months for second stage concrete. This allowed the pit of the unit to be ready in November 1981 for erection of the turbine and stator. The stator and the generator rotor were partially and completely assembled, respectively, in the erection area; transportation to the pit in September 1982, required two 10 MN bridge cranes operating in tandem.

- Although not critical, concrete above El. 132 was planned at earliest dates for the first units, in order to complete the roof and obtain the most favorable conditions for equipment erection.

In 1982 the demand for electricity in south - southeastern Brazil was considerably less than the earlier projections. As a consequence, the construction program for the Itaipu units was revised. The date for filling of the reservoir was maintained; however, the start of unit 1 was delayed by about 14 months and that for the other units by up to 3 years, see Fig. 5.6.

- Construction of galleries for the installation of the electromechanical auxiliary equipment was critical for the start up and commissioning of the units.

Construction of powerhouse in the diversion channel. In spite of the downturn in electricity demand in 1982, construction of the units in the



Powerhouse construction in riverbed

Fig. 5.6 Revised program for start up of generating units

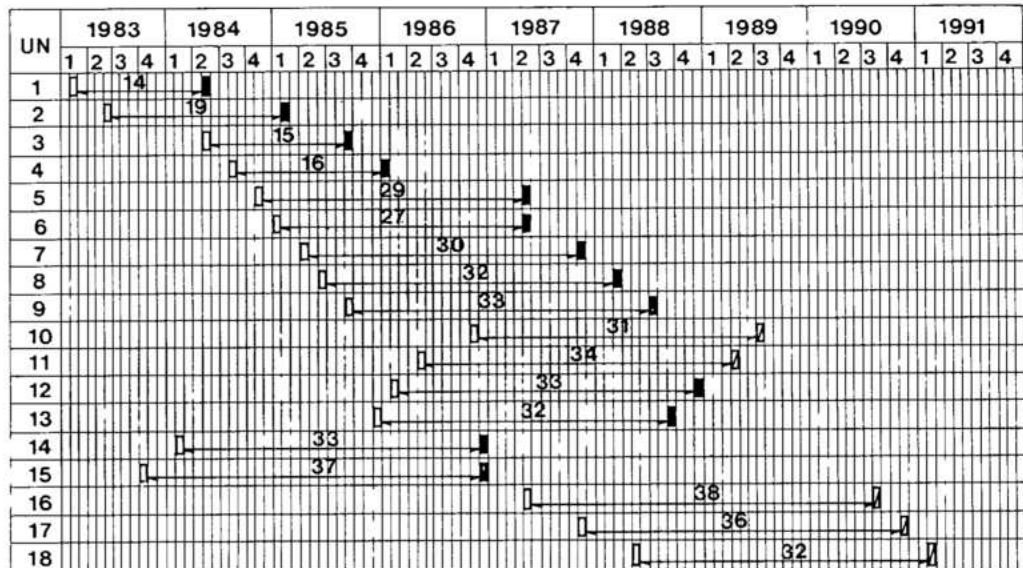
UN Generating unit no.

□ Start foreseen in initial program

■ Actual start

▣ Start foreseen in revised program

□—■ Delay in months



diversion channel, although delayed, was still deemed necessary sequential with completion of the units in the main river bed. Construction equipment and personnel were already on site, and the permanent equipment had been purchased, thus making the units in the diversion channel a low cost option to meet the projected electricity demand, which, by 1985 had begun to increase once more. In fact, by the end of 1985 construction of the 3 units in the diversion channel had become critical and a firm commitment for operation of unit 18 before the end of the first quarter of 1991 was given to FURNAS. This necessitated a fast-track construction program utilizing time saving measures resulting from previous experience in the design and construction of the units in the river bed. These included:

- Reduction in the amount of concrete and reinforcing steel, based upon measurements of actual forces during previous construction and operation of equipment.
- Extensive use of slip-forming first stage concrete in the draft tube piers, unit block and generator pit and all the downstream walls and piers.
- Pre-assembly of large reinforcement cages, to accelerate installation of reinforcement before slip forming.
- Development of special guides and jacking equipment for slip forming.

The construction program had to accommodate several restrictions, the most important of which were:

- Energizing the 7th and 8th 765 kV, 60 Hz transmission lines to the left bank substation was dependent on the installation of SF₆ switchgear in the diversion channel powerhouse structure.



Powerhouse construction in diversion channel

- Demolition of the massive wall between the channel and central assembly area 2 had to be completed before the start of operation of units 14 and 15.
- Early raising of the downstream cofferdam from El. 125 to El. 136 to give greater security to the construction area.
- Crane rails to be completed to transport the stay ring a maximum of 15 months after the start of construction of the unit.
- All units, central assembly area block 3 and block V1, would have to be at El. 144 before removal of the downstream cofferdam.
- Entry into service of a generator 28 months after the lowering of its stay ring.

These constraints together with the proposed completion in the 1st quarter of 1991, resulted in the construction program shown in Fig. 5.7.

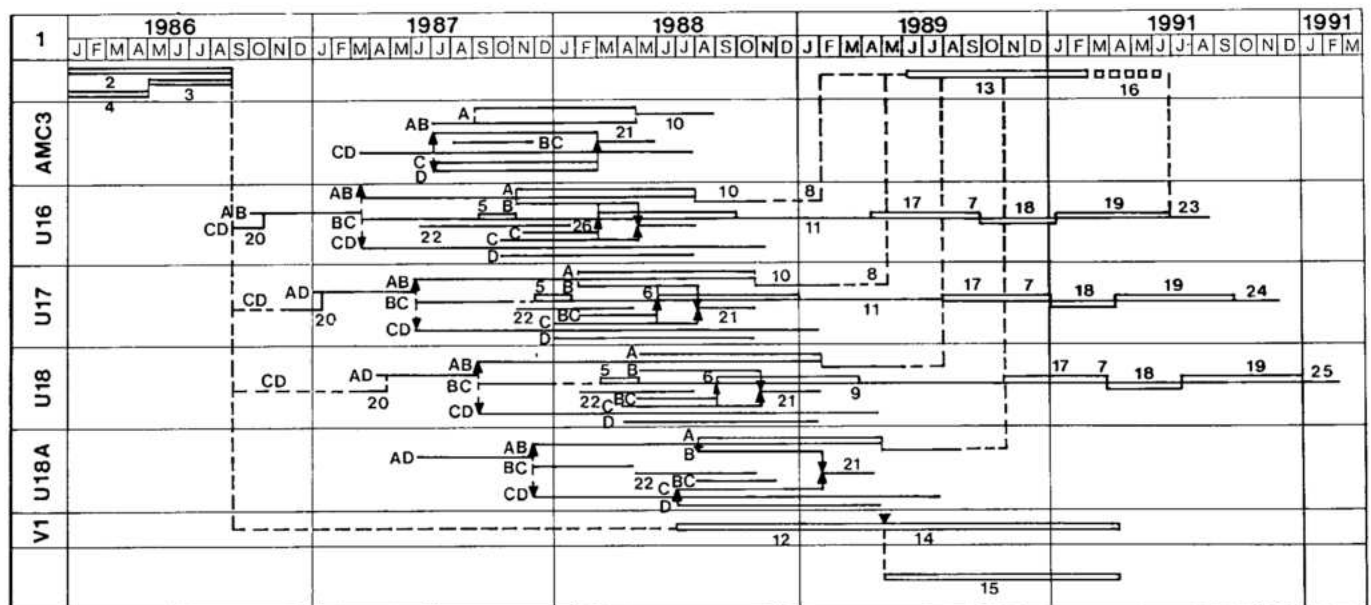


Fig. 5.7 Construction program for units in the diversion channel

- | | | | |
|--|--|------------------------------------|--|
| 1 Block denomination | 8 SF ₆ gallery finishes | 14 Block VI concrete to El. 144.00 | 21 Roof beams BC |
| 2 Excavation U16/U18 A | 9 Spiral case assembly and pressure test | 15 Removal of cofferdam | 22 Penstock sill |
| 3 Ravine wall excavated before start of operation of units 14 and 15 | 10 Beams AB + slab El. 144.00 | 16 Tests of SF ₆ | 23 Tests on unit 16 |
| 4 Cofferdam construction | 11 Turbine pit concreting | 17 Stator assembly | 24 Tests on unit 17 |
| 5 Draft-tubes assembly | 12 Concreting the roof | 18 Lower bearing bracket assembly | 25 Tests on unit 18 |
| 6 Stay ring assembly | 13 Assembly of SF ₆ | 19 Rotor assembly | Note: Letters refer to powerhouse roof beam reference lines |
| 7 Turbine assembly | | 20 Pit | |

LAYOUT OF THE CONSTRUCTION FACILITIES

GENERAL

To obtain the production rates needed at Itaipu construction facilities required specially designed and specified equipment, which was not available from manufacturers' standard production lines. These included various categories of plant, each of which comprised a large industrial unit, see Fig. 5.8. Therefore, the duration of this activity was significant compared with the construction time and it had to be independent of the activities leading to the start of powerplant operation. Thus, ITAIPU decided to design, specify, purchase and install the basic construction equipment and facilities simultaneously

with project design, the call for tenders and the selection of construction contractors. This enabled the contractor to achieve high production rates required by the schedule, within a short period.

DESIGN CRITERIA FOR CONSTRUCTION FACILITIES

For a satisfactory construction program, two aspects of the project had to be balanced: the overall planning of the permanent works and the basic design of the construction facilities. The capacity of the construction facilities was established by production requirements, which were derived from the planning. This apparent contradiction was resolved by evaluating assumed schedule of the permanent works and basic design of the construction facilities, until the most favorable solution was obtained by successive approximations.

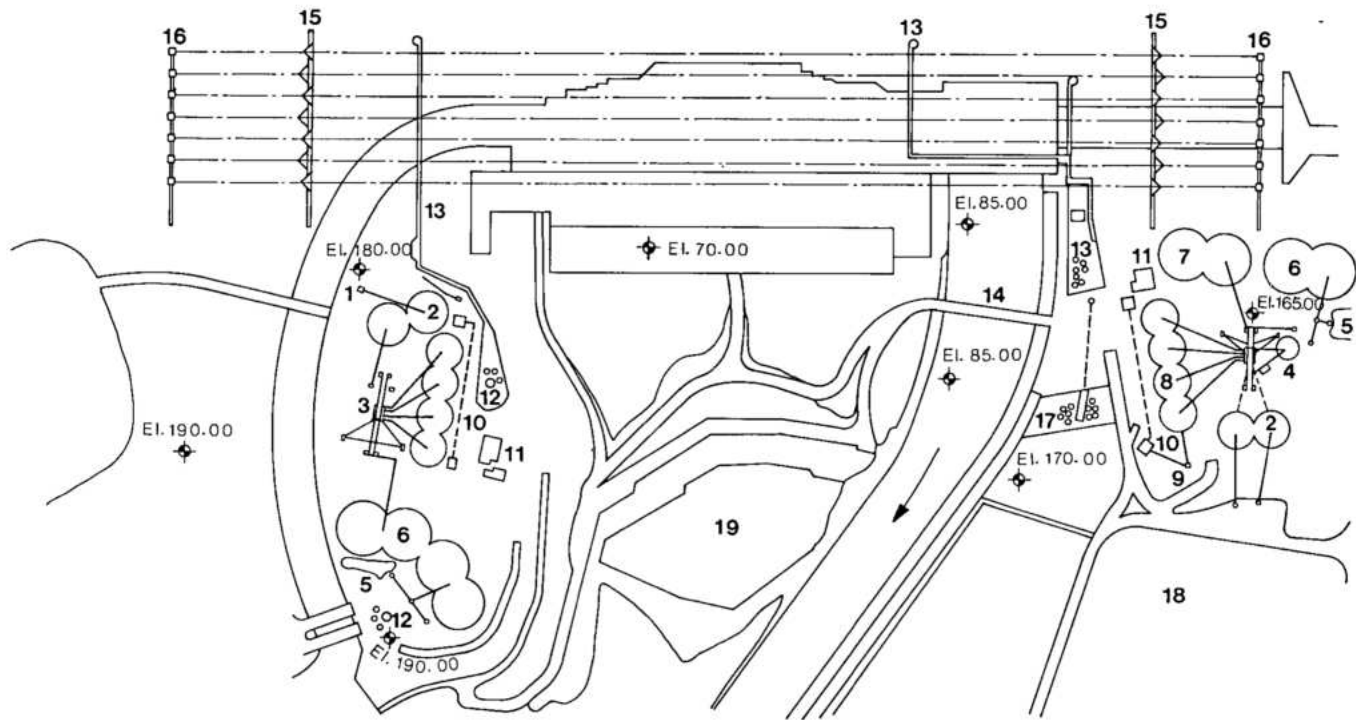


Fig. 5.8 General layout of construction plant and facilities

- | | | | |
|--------------------------|------------------------------|---------------------------|-----------------------------|
| 1 Primary crushers | 6 Natural sand stockpile | 11 Cooling plant | 16 Counterweight cars |
| 2 Compensation stockpile | 7 Artificial sand stockpile | 12 Batching and ice plant | 17 Cement and fly-ash silos |
| 3 Secondary crushers | 8 Coarse aggregate stockpile | 13 Monorail | 18 Sound basalt stockpile |
| 4 Intermediary stockpile | 9 Re-screening and washing | 14 Service bridge | 19 Downstream cofferdam |
| 5 Natural sand reception | 10 Cooling tunnel | 15 Cableways | |

Fig. 5.9 shows the optimized and adopted schedule for concrete placement, in which five major periods were evident:

Period 1: It was from October 1977 to October 1978. It allowed for construction of the diversion control structure up to the minimum elevation which would permit opening of the diversion channel. It was a critical path activity during which nearly 750 000 m³ of concrete had to be placed, averaging 60 000 m³/month, with a peak of 110 000 m³/month.

Period 2: It started with the opening of the diversion channel (October 1978) and ended in October 1979 when the foundations for the main dam in the river bed were ready for concrete placement. During this period, almost all the areas available for concreting corresponded to activities with large floats in the project CPM schedule; hence the earliest and latest accumulated production curves diverged sharply.

Within this wide range of possible production levels, the schedule aimed to reach, at the end of the period, an accumulated production corresponding to the earliest date curve, since the maximum concrete placement demand would take place in the following phase. Also, it aimed to establish a gradual increase in the monthly production based on the quantities to be placed by the end of the first period. In this period the total volume of concrete to be placed was 3.15×10^6 m³, averaging 185 000 m³/month, with a production peak of 225 000 m³/month.

Period 3: Maximum production was to be reached in the third period between October 1979 and July 1982; concrete placing concentrating on the main dam, spillway and powerhouse located in the river bed. An average monthly production of 225 000 m³ was estimated, with peaks nearing 300 000 m³ during the most favorable months of 1980/1981 and decreasing to 180 000 m³ for the second half of 1982. Total volume of concrete to be placed during this period was 4.9×10^6 m³.

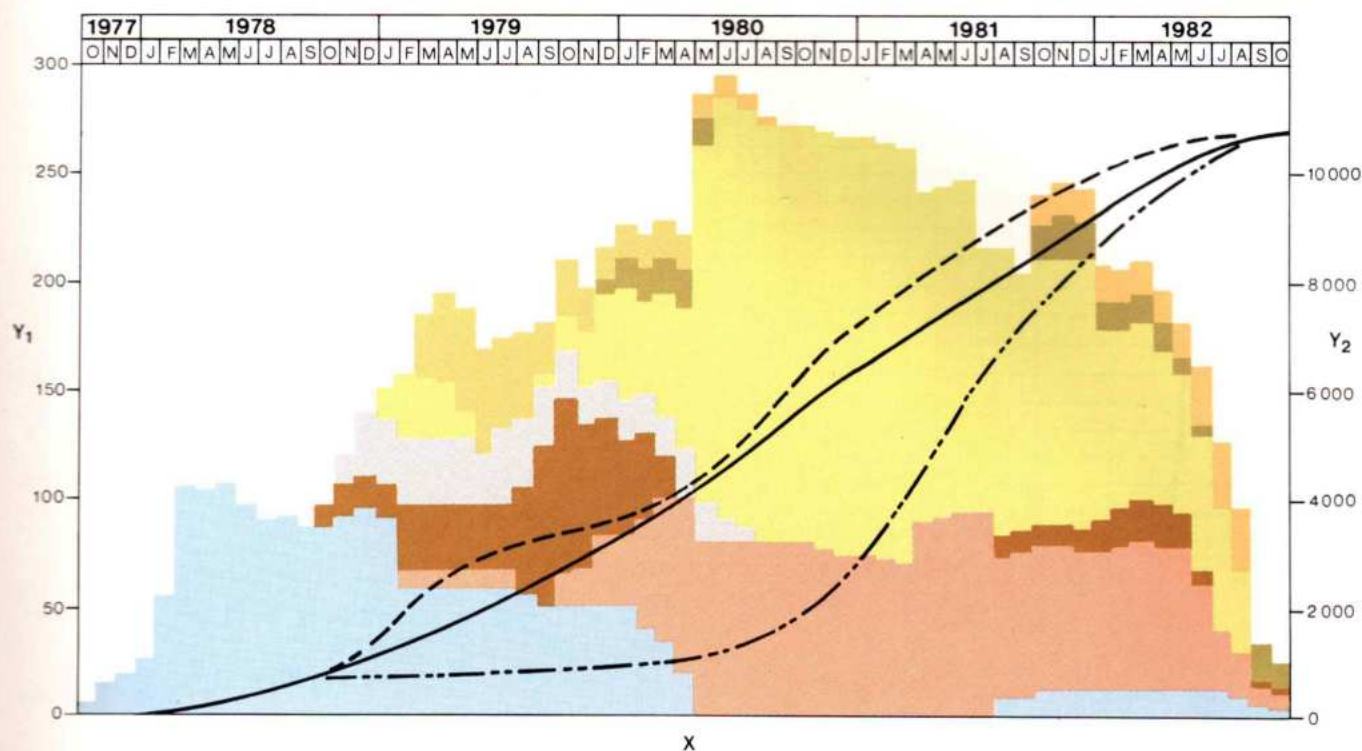


Fig. 5.9 Adopted concrete placement histogram to 1982



Period 4: In the fourth period extending from August 1982 to the second half of 1984, the monthly concrete production was expected to decrease from 180 000 m³ to 30 000 m³/month in the concrete dam, central assembly area, river bed powerhouse units, spillway and substation on the right bank. The total concrete placed in this period was 1.8×10^6 m³.

Other important activities were foreseen in this period, namely: completion of earth and rockfill dams, demolition of upstream cofferdam and plugging of sluiceways in the diversion control structure.

Period 5: The fifth stage of concrete construction began in the main dam blocks adjoining the rockfill dam in January 1986, with concreting of powerhouse units located in the diversion channel including the central assembly area (AMC 3) and closing

structure V1. The total concrete to be placed was in the order of 0.654×10^6 m³ and the first stage work was to be completed by the end of 1989 in accordance with the revised schedule.

In accordance with this schedule, the construction facilities were designed for an overall output of 300 000 m³ of concrete per month, corresponding to the maximum peak in April 1980 – July 1982.

Fig. 5.10 shows a comparison between the volumes indicated in the basic program and the monthly production actually achieved through October 1982, which was the period of maximum production. Actual concrete placement rates were faster than anticipated, especially during 1979–80, mainly because of early completion of the foundations for the main dam and the powerhouse in the river channel. Thus concrete production peaked earlier than anticipated.

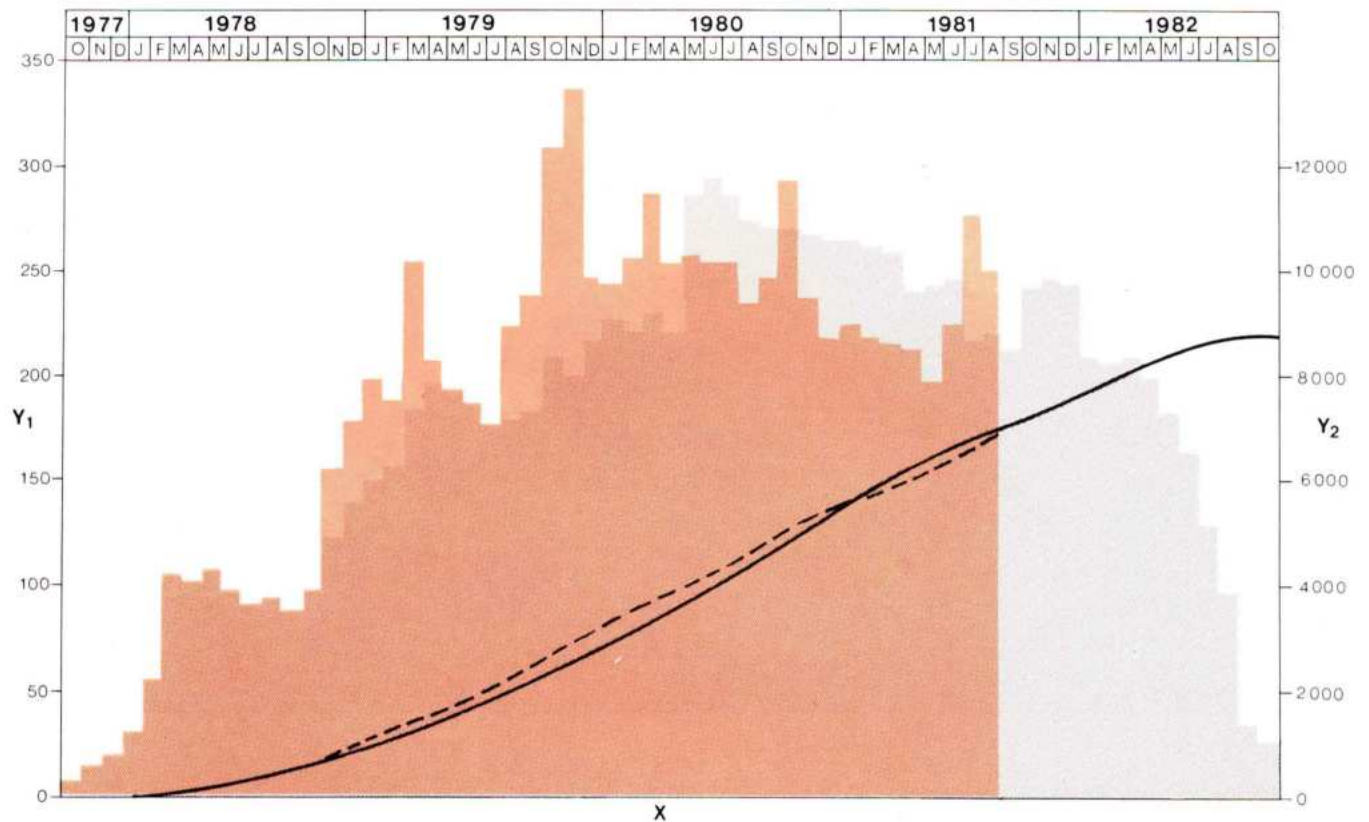


Fig. 5.10 Comparison of programmed and actual concrete placement to 1982

Y₁ Monthly rate
(1000 m³/month)

Y₂ Cumulative volume
(1000 m³)

X Year and month

Actual

Programmed

CONCRETE SPECIFICATIONS, QUALITY CONTROL AND CONSTRUCTION METHODS

CONCRETE AGGREGATES

All coarse aggregate and about 70% of the sand for the concrete was obtained by crushing sound basalt. Breccia and amygdaloidal basalts were not used. Aggregates were designated 1, 2, 3 and 4 corresponding to maximum size, MSA, 19 mm, 38 mm, 76 mm and 152 mm, respectively. The permitted gradation for the coarse aggregate and for the crushed sand was as shown in Tables 5.1 and 5.2. About 30% by weight of the sand was fine natural alluvial sand obtained from deposits along the Rio Paraná. The tests specified for controlling the physical quality of crushed aggregate were: density, absorption, Los Angeles abrasion, natural and artificial weathering (wetting and drying), cyclical ethylene glycol, sodium sulphate and alkali-aggregate reactivity. Typical results of tests are shown in Table 5.3 and Fig. 5.11. Special attention was given to potential alkali-aggregate reactivity. It was

checked not only by the chemical test, (see results in Fig. 5.11), but also by the mortar bar expansion test (ASTM C-227).

Table 5.1 Gradation for coarse aggregate

Sieve opening mm	% passing			
	Aggregate sizes, mm			
	4.8-19	19-38	38-76	76-152
178				100
152				90-100
100			100	20-45
76			90-100	0-15
50		100	20-55	0-5
38		90-100	0-10	
25	100	20-45	0-5	
19	90-100	0-10		
9.5	30-55	0-5		
4.8	0-5			

Table 5.2 Gradation for crushed sand

Sieve no.	Opening mm	% passing
3/8 *	9.5	100
4	4.8	95-100
8	2.4	80-100
16	1.2	50-85
30	0.6	25-50
50	0.3	10-30
100	0.15	2-10

Fineness modulus: $2.30 \leq 3.10$

* Inches

Fig. 5.11 Concrete aggregates potential alkali reactivity chemical method

Y Decrease of alkaline reaction (millimoles/l)
 X Diluted silica (millimoles/l)
 1 Aggregates considered innocuous
 2 Aggregates considered potentially deleterious
 3 Aggregates considered deleterious

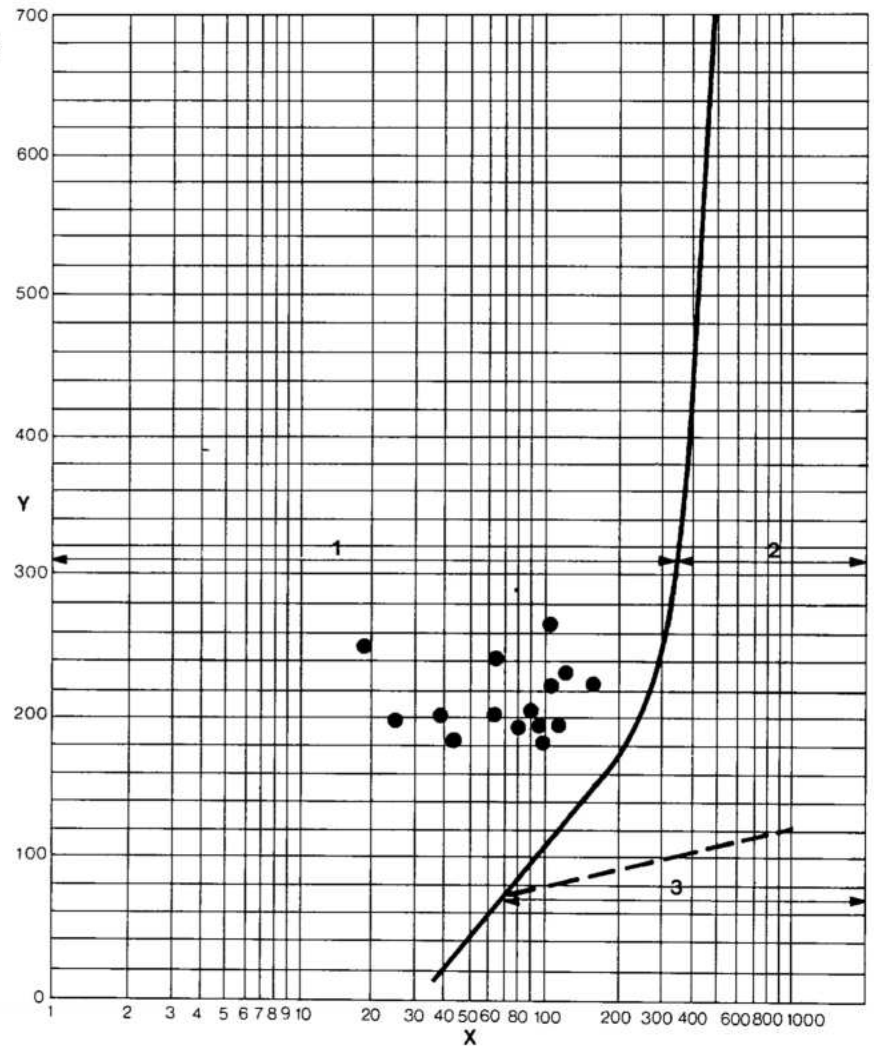


Table 5.3 Crushed aggregate – physical properties of random samples

Natural unit weight	Absorption	Abrasion Los Angeles	Cyclic tests								Alkali-aggregate reactivity	
			Natural Weathering cycles (1 year)		Cycles in water-stove		Ethylene glycol cycles		Na ₂ SO ₄ cycles		Physical method	Chemical
kN/m ³	(%)	Loss (%)	Affected particles (%)	Loss by weight (%)	Affected particles (%)	Loss by weight (%)	Affected particles (%)	Loss by weight (%)	Affected particles (%)	Loss by weight (%)	90 days shrinkage (%)	24 hours
29.28	0.4	8	4	0.03	2	0.8	3.6	1	0.1	0.8	0.01	(1)
29.00	0.6	6	8	0.1	2	0.2	6.7	1	0.3	2.2	0.01	(1)
29.50	0.3	6.5	4	0.06	2	0.2	6.6	1.3	1	0.4	0.01	(1)
29.39	0.3	6.2	12	0.07			13.4	3.8	0.2	0.5	0.02	(2)
29.65	0.2	4	24	0.11	10	5.4	2.5	0.1	0.1	0.4	0.01	(1)
29.51	0.3	4	30	0.13			7	0.3	0.4	1	0.01	(1)
29.34	0.4	9.8	10	0.15	4	0.2	5.9	0.8	0.1	0.7	0.02	(2)
28.87	0.9	10.3	22	0.13	2	0.8	1.2	4.5	0.2	0.7	0.01	(1)
29.30	0.4	5.6	12	0.1	8	0.2	18.0	0.3	1.1	3.3	0.01	(1)

(1) Innocuous (2) Potentially deleterious

CEMENT AND FLY ASH

The cements used in concrete were the equivalent of ASTM type II. They were obtained from four different plants: Itambé, Sta. Rita, and Votoran in Brazil and Vallemí in Paraguay. Fly ash was obtained from the Candiota and Tubarão thermal powerplants in Brazil.

The more significant specified properties of cement were as follows:

Specific surface, Blaine not less than	3200 cm ² /g
Material retained on no. 200 sieve max.	15 %
Initial set minimum	60 min
Final set maximum	10 hours
Autoclave expansion maximum	0.8 %
Heat of hydration, 7 days maximum	314 kJ/kg
Heat of hydration, 28 days maximum	356 kJ/kg
Compressive strength, 3 days minimum	800 N/cm ²
Compressive strength, 7 days minimum	1.5 kN/cm ²
Compressive strength, 28 days minimum	2.5 kN/cm ²
MgO maximum	6.5 %
SO ₃ maximum	3 %
Equivalent alkalis (Na ₂ O) maximum	0.6 %
C ₃ S maximum	35 %
C ₃ A maximum	8 %

For the fly ash the physical properties were as shown below:

Specific surface, Blaine minimum	3500 cm ² /g
Material retained on no. 325 sieve maximum	34 %
Autoclave expansion or shrinkage maximum	0.8 %
Alkali reaction, expansion maximum	0.02 %
MgO maximum	5 %
SO ₃ maximum	5 %
Moisture maximum	3 %
SiO ₃ + Al ₂ O ₃ + Fe ₂ O ₃ minimum	70 %
Equivalent alkali maximum	1.5 %

Pozzolanic activity index:

Water required maximum	105 %
With cement (at 28 days) minimum	75 %
With lime (at 7 days) minimum	560 N/cm ²

The main physical characteristics of the fly ashes and the cements were as shown in Table 5.4.

Table 5.4 Physical characteristics of fly ashes and cements

Properties	Material				Fly ash	
	Cement					
	Votoran	Itambé	Vallemi	Santa Rita	Candiota	Tubarão
Blaine fineness (cm ² /g)	3368	3259	3417	3586	3190	2830
Sieve 200 (%)	6.2	2.4	13.8	13.2		
Sieve 325 (%)	13.3	6.4	18.6	19.4	27.1	41.2
Autoclave expansion (%)	0.09	0.02	0.03	0.08		
Alkali equivalent (Na ₂ O)	0.5	0.47	0.54	0.69		
Free lime (%)	1.04	0.81	1.39	0.7		
C ₃ S (%)	46.7	57.5	52.1	49.5		
C ₃ A (%)	6.7	6.6	6.2	8.7		
Expansion reduction (%)					64.3	68.9
Lime reaction (kg/cm ²)					36	31

CONCRETE MIXES

The specifications designated concrete classes on the basis of three parameters:

1. Maximum size of aggregate, MSA.
2. Minimum strength of concrete in compression (f_{ck})
3. Age.

The designation legend for a concrete with 152 mm maximum aggregate and a specified minimum strength of 1.4 kN/cm^2 (140 kg/cm^2) at 365 days, was as shown in Fig. 5.12.

Table 5.5 shows the classes of concrete used for the various structures and the maximum water/cement + fly ash ratio permitted for mixes with or without entrained air.

Table 5.5 Classes of concrete

Class of concrete	Typical use	Maximum size of aggregate mm	Maximum ratio water:cement & fly ash	
			Concrete with air	Concrete without air
A-100-f	Non-structural backfill concrete	152	0.75	0.85
A-140-f	Mass concrete, dams	152	0.65	0.8
A-180-f	Mass concrete, dams	152	0.55	0.75
A-210-f	Mass concrete, dams	152	0.43	0.7
A-240-f	Mass concrete, dams	152	0.42	0.68
A-280-f	Mass concrete, dams	152	0.4	0.65
B-140-f	Mass concrete, lifts near foundations	76	0.64	0.7
B-180-f	Mass concrete, dams and massive walls	76	0.55	0.68
B-210-f	Mass concrete and structural concrete for massive walls	76	0.5	0.65
B-240-f	Ditto	76	0.45	0.7
B-280-f	Mass concrete, near upstream face of dams, piers of diversion structure	76	0.4	0.65
C-140-c	Structural concrete; thin members	38	0.55	0.65
C-180-c	Ditto	38	0.47	0.6
C-210-c	Structural concrete and concrete exposed to high velocity flow of water	38	0.48	0.55
C-280-c	Ditto	38	0.4	0.58
C-350-c	Ditto	38	0.35	0.5
D-100-f	Porous concrete	19	0.85	
D-210-c	Thin structures and blockouts	19	0.45	0.55
D-280-c	Precast beams and slabs	19	0.4	0.52
D-350-c	Precast beams and slabs and prestressed concrete	19	0.35	0.5
E-210-c	Shotcrete	13	0.5	0.65

QUALITY CONTROL

Sampling

From each 300 m^3 of concrete produced by each plant, a sample was taken sufficient for making six job cylinders $15 \times 30 \text{ cm}$ in size, wet screened by a 38 mm sieve. Also, from each 5000 m^3 of concrete with MSA of 76 mm (aggregate no.3) and 152 mm (aggregate no.4), a representative sample was obtained to make the following test specimens:

- Six cylinders, $15 \times 30 \text{ cm}$, wet screened by a 38 mm sieve.
- Six specimens, $25 \times 25 \times 12.5 \text{ cm}$, wet screened by a 38 mm sieve.

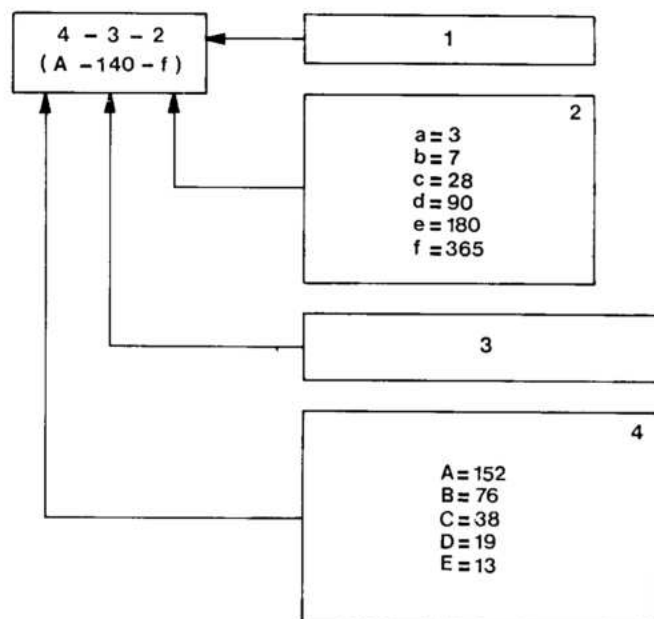


Fig. 5.12 Specifications of concrete classes

- 1 Mix designation
 2 Age (in days)
 3 Minimum strength of concrete in compression - f_{ck} in kg/cm^2
 4 Specified classes, MSA (mm)

- Two cylinders, unscreened:
 For 76 mm MSA, 25 x 50 cm.
 For 152 mm MSA, 45 x 90 cm.

Unmolded samples were taken from placed concrete and tested for: slump, air content, density and temperature. The molded samples (job cylinders and specimens) were tested for unconfined compressive strength at various ages, as indicated in the table below:

Designated age of specified concrete (days)	Age of test (days)
3	3, 7, 28
7	3, 7, 28
28	7, 28, 90
90	7, 28, 90, 180, 360
180	7, 28, 90, 180, 360
360	7, 28, 90, 180, 360

Additional tests on some specimens included: permeability, modulus of elasticity and Poisson's ratio.

Laboratory testing for concrete properties

A comprehensive program of laboratory tests for the various physical properties of concrete was initiated before the start of concrete placement and continued in parallel with the construction. Included were tests for the following properties of concrete: compressive strength, modulus of elasticity, heat of hydration, specific heat, thermal diffusivity, thermal expansion, tensile strength, ultimate tensile strain, creep and relaxation and autogenous volume change.

Analysis of quality control test results

Compressive strength. Results of tests on the job cylinders and specimens were subjected to statistical analyses and were correlated with the results of tests on the laboratory specimens, leading to various correction factors which were applied to the strengths obtained from the job cylinders. The first correction factor was for "wet screening", since the job cylinders were made from samples with all aggregate larger than 38 mm removed. The strength of the job cylinders was compared with those of large cylinders containing concrete exactly like that in the structure, the job cylinder being stronger. Other corrections to the strength of job cylinders were made for variations in strength and loss in strength due to sustained loading. Some plus factors, which were considered only after about 50% of the concrete had been placed, were the extra load-carrying ability due to relaxation of highly stressed zones when failure is near, the shape of the specimen being less favorable than the highly stressed portion in the structure, and the testing error involved in reporting the average stress, which was lower than the maximum stress at failure.

The correction factors as they were employed before and after January 1981 were:

Item	Correction factors %	
	Before 1/81	After 1/81
Wet screening	-8 to -21	-8 to -21*
Variations	-15	-5
Sustained load	-5	-5
Relaxation	0	10
Testing error	0	5

* -8% for 152 mm MSA and -21% + for 76

Modulus of elasticity. Table 5.6 and Fig. 5.13 show the average results of modulus of elasticity, Poisson's ratio and densities obtained from the 15 x 30 cm job cylinders made by "wet screening" aggregate larger than 38 mm,

Table 5.6 Modulus of elasticity of concrete

MSA (mm)		Age (days)		Elasticity modulus kN/cm ²			Poisson ratio		Specific gravity kN/m ³							
				Full mix		Wet screened		Full mix		Wet screened		Full mix				
				Samples	Average	V.C.	Samples	Average	V.C.	Average	V.C.	Samples	Average	V.C.	Samples	Average
38	7	48	2514	29			0.17	16.1			250	24.440	1.9			
	28	56	3354	16.8			0.2	13.5								
	90	38	3568	17.3			0.19	17.5								
	180	23	3550	19.2			0.19	12.2								
	360	34	3708	19.5			0.2	14.8								
76	7	03	2786	25.4	19	2634	22.3	0.2	8.2	0.17	20.8	88	26.03	2.3	24.16	2.3
	28	12	3689	16.3	45	3308	19.6	0.21	12.1	0.19	12.5					
	90	03	4442	7.1	29	3668	13.8	0.21	8.2	0.2	9.8					
	180	07	4384	1.1	17	3647	13.1	0.22	2.4	0.2	12.1					
	360	29	4600	8.7	41	3886	13.3	0.21	13.2	0.2	14.3					
152	7	02	2628	22.2	28	2305	21.8	0.17	14.3	0.18	18.3	141	26.57	1.5	23.66	1.9
	28	12	3783	14.7	47	2986	14.1	0.18	12.9	0.19	15.2					
	90	25	4278	8.9	61	3386	11.6	0.21	12.2	0.19	14.7					
	180	15	4370	8.9	42	3547	7.8	0.22	6.7	0.20	11.4					
	360	19	4508	5.9	73	3595	10.9	0.2	11.8	0.19	12.3					

V.C. = Variation coefficient of the aggregate

V.C. = Variation coefficient of the aggregate

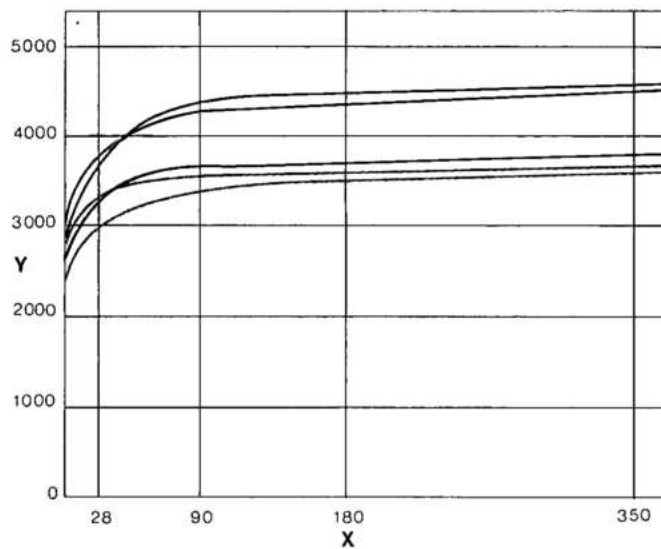


Fig. 5.13 Modulus of elasticity of concrete

Y Modulus of elasticity
(kN/cm²)
X Days

— MSA 38 mm wet screened
— MSA 76 mm wet screened
— MSA 76 mm full mix
— MSA 152 mm wet screened
— MSA 152 mm full mix

as well as those obtained from larger cylinders (25 x 50 mm and 45 x 90 mm), for the full mix without wet screening. The full mix specimens showed moduli higher than 4000 kN/cm². The high unit weight of concrete was attributed to the use of basalt aggregate which had a specific gravity of 2.9.

Efficiency of concrete mixes. The efficiency (η) of a concrete mix is defined as:

$$\eta = \frac{\text{Average compressive strength, N/cm}^2}{\text{Weight of cementitious materials, N/cm}^3}$$

Table 5.7 shows a summary of the average values of efficiencies of concrete mixes used through the end of 1980. The efficiencies are shown for mixes which used cement plus 15% substitution by fly ash and for pozzolanic cement which was used in some parts of the spillway and the right wing dam. The efficiencies are given at different ages for various maximum size aggregates.

Tensile strength and strain capacity of concrete.

Two series of tests were conducted to determine the tensile strength of concrete in flexure and in direct splitting, and its tensile strain capacity at failure.

Table 5.7 Efficiency of concrete mixes used in Itaipu

Average efficiency of mixtures used in the main structures (cement + fly ash)

MSA	3 days			7 days			28 days		
19	0.27	0.29	0.34	0.29	0.47	0.65	0.54	0.84	1.13
38				0.3	0.4	0.59	0.55	0.72	1
76				0.44	0.6	0.8	0.79	1.02	1.16
152				0.51	0.57	0.62	0.9	1.08	1.17

MSA	90 days			180 days			360 days		
19	0.73	1.16	1.47	0.91	1.32	1.67			
38	0.79	1.02	1.30	0.86	1.13	1.52	0.93	0.96	0.98
76	1.17	1.33	1.46	1.34	1.5	1.64	1.45	1.48	1.51
152	1.29	1.41	1.49	1.37	1.54	1.67	1.48	1.53	1.58

MSA (*)	3 days (*)			7 days (*)			28 days (*)		
19				0.71	0.78	0.84	1.08	1.15	1.3
38				0.55	0.64	0.72	0.93	1.02	1.11
76					0.64			1.03	

* For concrete with pozzolanic cement

Flexural strength tests were conducted on mixes with designated (f_{ck}) strengths of 1.4 and 2.1 kN/cm² at 365 days. These tests were made on beams of three sizes: 15 x 15 x 60 cm, 25 x 25 x 100 cm, and 45 x 45 x 180 cm, depending upon the maximum size of the aggregate. The splitting strength tests were made on cylinders of sizes 15 x 30 cm and 25 x 50 cm. The basic data for the eight concrete mixes used for the flexural

tests are given in Table 5.8. From strain gages installed on various beam specimens, the strain capacity at 95% of the rupture strength, was calculated. Typical results are shown in Table 5.9. Table 5.10 shows, for various mixes, the flexural strength at rupture of the beam samples at various ages, the splitting tensile and comparable unconfined compressive strengths at ages of 7, 28 and 90 days.

Table 5.8 Flexural strength data of concrete mixes

Components DSS N/m ³	Test mixes							
	19-I-02	19-Q-01	38-F-01	38-M-01	76-D-03	76-J-01	152-B-03	152-G-01
MSA (mm)	19	19	38	38	76	76	152	152
f_{ck} (kN/cm ²) at one year	2.1	1.4	2.1	1.4	2.1	1.4	2.1	1.4
Cement	1750	1130	1840	1190	1690	1060	1620	1090
Fly-ash	210	130	220	140	200	130	190	130
Water	1600	1550	1340	1340	1080	1080	860	850
W/C	0.78	1.17	0.62	0.96	0.54	0.85	0.45	0.67
Entrained air wet screened %	4.5±0.5	4.5±0.5	4.5±0.5	4.5±0.5	6.5±0.5	6.5±0.5	7.5±0.5	7.5±0.5
Natural sand	2930	3170	2740	2940	1940	2160	1550	1740
Artificial sand	6840	7400	6380	6870	4530	5030	3630	4050
Aggregate no.1	11 250	11 250	6920	6920	5290	5290	4000	4000
Aggregate no.2			5680	5680	4360	4360	3290	3290
Aggregate no.3					6500	6500	4650	4650
Aggregate no.4							6430	6430

Table 5.9 Tensile strain capacity at 95% rupture

Mixture identification				Beam number	Test set	Age	Beam dimensions	Strain capacity at 95% of modulus of rupture (10 ⁶ cm/cm)	
Symbols	MSA mm	W/C+P	Aggregate N/m ³	no.		days	cm	Individual values	Average
152-B-03	152	0.45	1810	8619	1st	28	45 x 45 x 180	56	64
152-G-01	152	0.67	1210	8403	1st	28	45 x 45 x 180	90	
152-G-01	152	0.67	1210	8404	1st	28	45 x 45 x 180	90	90
152-G-01	152	0.67	1210	8405	1st	90	45 x 45 x 180		
152-G-01	152	0.67	1210	8406	1st	90	45 x 45 x 180	95	95
76-J-01	76	0.85	1190	20 442	2nd	28	15 x 15 x 60	79	79.5
76-J-01	76	0.85	1190	20 440	2nd	28	25 x 25 x 100	31	55
76-J-01	76	0.85	1190	20 438	2nd	28	45 x 45 x 180	72	68
152-G-01	152	0.67	1210	20 131	2nd	28	15 x 15 x 60	75	
152-G-01	152	0.67	1210	20 132	2nd	28	15 x 15 x 60	85	80
152-G-01	152	0.67	1210	20 129	2nd	28	25 x 25 x 100	68	
152-G-01	152	0.67	1210	20 130	2nd	28	25 x 25 x 100	73	70.5
152-G-01	152	0.67	1210	20 127	2nd	28	45 x 45 x 180	64	
152-G-01	152	0.67	1210	20 128	2nd	28	45 x 45 x 180	67	65.5

Assumptions: strength values from tests at Itaipu's Concrete Laboratory



General view of concrete production facilities

CONCRETE PRODUCTION FACILITIES

CONSTRUCTION YARD FACILITIES

The construction yard facilities were designed for production of 300 000 m³/month of concrete, cooled to a temperature of 6°C. These facilities comprised two large equivalent industrial plants located on each bank of the river, each consisting of an aggregate crushing plant, cooling plant and concrete batching plants. In addition to these plants, which were the basic source of concrete production, a clinker grinding plant was erected at the site to assure continuity of cement supply in case of an interruption in production at the Brazilian or Paraguayan cement plants during the period of peak demand at Itaipu.

Modulation of the units

The facilities were designed as identical modules coupled in parallel, which avoided the use of mega-units, and offered the following advantages:

- Increased reliability of the whole complex, due to a reduced probability of complete failure and greater flexibility for maintenance.

- Better distribution of the units in locations which were close to the center of demand, which reduced transportation costs.
- Higher probability of salvage and sale at the end of the construction.

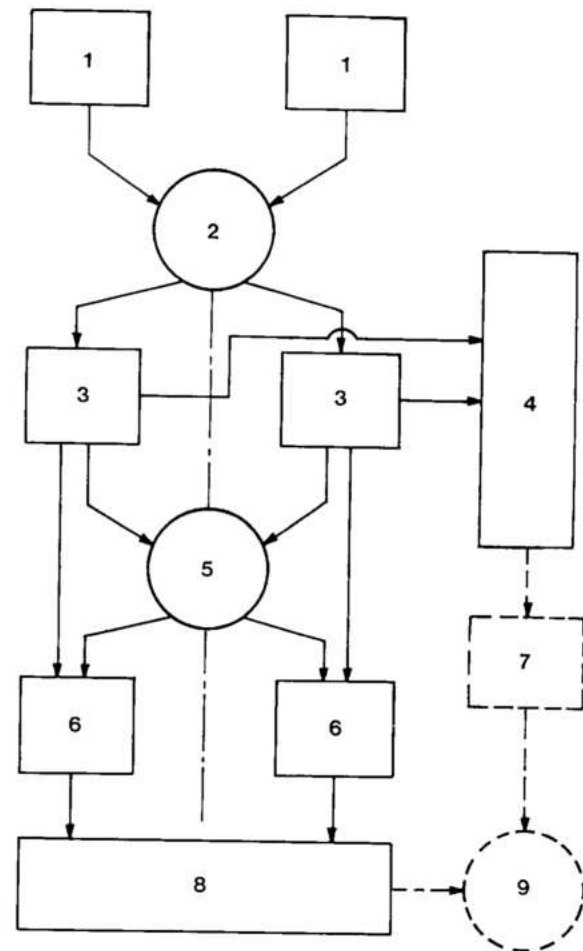
Capacity of the units

The facilities were designed so that the typical production of each unit was consistent with the flow chart sequence, see Fig. 5.14. Thus, the crushing plant, the cooling plant and the concrete batching plants on each bank had rated capacities of 540 m³/h of concrete, or 270 000 m³ for a 25-working-day month with two 10 hour shifts per day. As the estimated maximum demand on each bank was 150 000 m³/month, the ratio of installed capacity to demand was 1.8.

Breakdown into independent sub-units

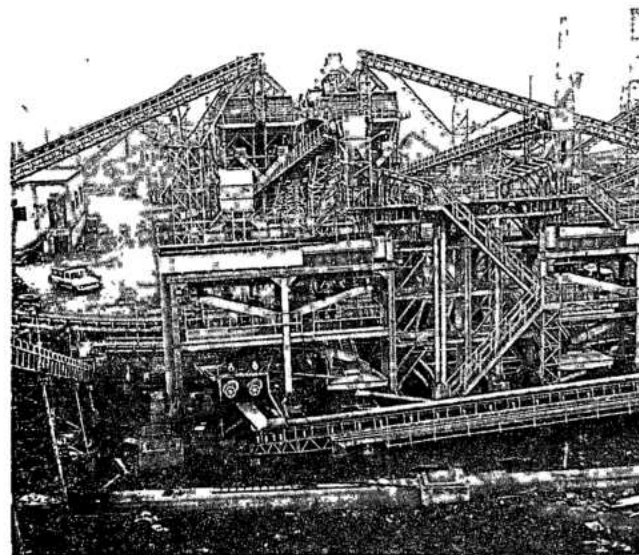
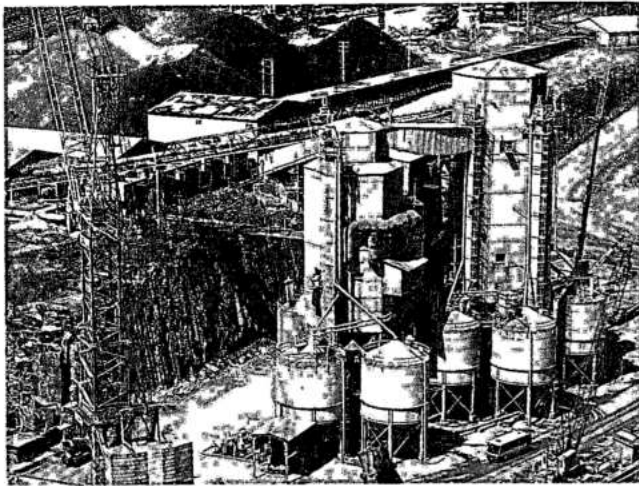
The circuits of the main concrete production plants were relatively large. For reliability, they were split into identical sub-units which worked independently in parallel. Thus if a sub-unit failed, this would not jeopardize the operation of the complete plant. An example of this is shown in Fig. 5.15. The crushing plant was subdivided into two complete units, arranged in parallel. Each of these units

- 1 Sound basalt stockpile
- 2 Clinker stockpile
- 3 Fly-ash silos
- 4 Ammonia compressor plant
- 5 Crushing and screening
- 6 Coarse aggregate stockpile
- 7 Sand grinding
- 8 Grinding and cooling
- 9 Water cooling
- 10 Washing and rescreening
- 11 Artificial sand stockpile
- 12 Natural sand stockpile
- 13 Air cooling
- 14 Coarse aggregate cooling by water sprinkling
- 15 Coarse aggregate no. 2, 3 and 4 cooling by cold air
- 16 Aggregate silos
- 17 Ice plant
- 18 Concrete batch plant
- 19 Monorail
- 20 Dumpcretes
- 21 Silo cars
- 22 Cableways
- 23 Tower cranes
- 24 Concrete placement



- 1 Primary crushing
- 2 Stockpile 1
- 3 Recrushing
- 4 Yard 1 (rock)
- 5 Stockpile 2
- 6 Sand grinding
- 7 Cooling
- 8 Yard 2 (sand)
- 9 Concrete batch plant

As shown in the layout in Fig. 5.8, the concrete production facilities were located downstream of the dam, so that their removal was not necessary prior to the filling of the reservoir. This would have added a new activity to the critical path for the civil works.



Left bank concrete production facilities

Left bank facilities

Concrete batching plants. On the left bank three concrete batching plants were installed, each having a rated capacity of $180 \text{ m}^3/\text{h}$, with four 3 m^3 mixers in each plant. The plants were located on the platform at El. 144 as close as possible to the dock supplying the aerial cableways, and conveniently placed to supply the tower cranes during construction of the power intakes. To avoid overcrowding the area, fourteen 1000 t cement and fly-ash bins were installed on the platform at El. 168. These were equipped with a pneumatic system for transportation of the cement and fly ash to the batch plants.

Crushing plants. The layout of the equipment facilities on the platforms at El. 160 and El. 165 was dependent on the position of the concrete batching plants. The supply area for the primary crushers, at El. 172, was conveniently located in relation to the rockfill stockpiles. Each production line had a capacity of 900 t/h in the primary system, and 600 t/h for the secondary crushing and aggregate classification. After delivery from the stockpiles, coarse aggregate was rescreened, cooled and dried during transport to the batching plants. Storage facilities were provided for both crushed and natural sands, both types of sand being transported and blended in one tunnel, for delivery to the batching plants.

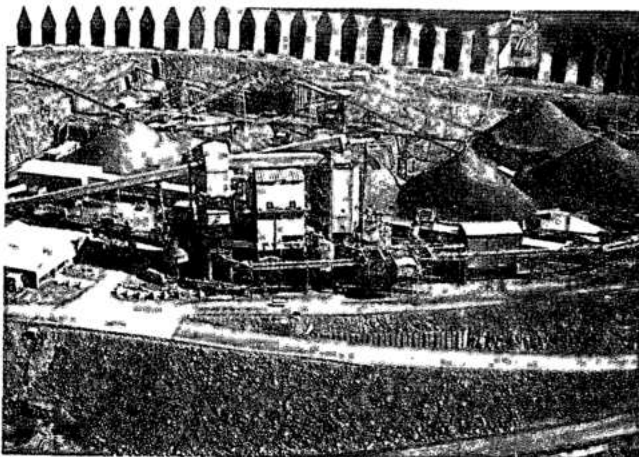
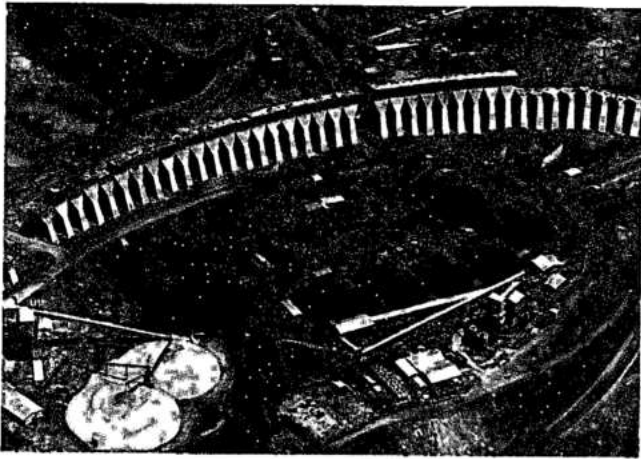
Cooling plant. For cooling concrete from the ambient temperature to the specified temperature of 6°C , three systems were utilized:

- Cooling of all crushed rock carried on a belt conveyor by spraying with water at 2.5°C .
- Cooling of large aggregate (nos. 2,3 and 4), in the operating bins of the batch plant by circulating air at -17°C .
- Use of ice chips instead of water in batching.

These facilities were located partly on the platform at El. 165, adjacent to the aggregate reclaiming assembly and partly on a steel structure adjacent to the batch plants.

Right bank facilities

The concrete production facilities on the right bank were designed to practically the same basic concepts and had the same overall capacity as those on the left bank. The only difference was the positioning of the concrete batch plants, and part of the cooling facilities, as shown in Fig. 5.8. The location of the spillway and the right wing dam at considerably higher elevations justified the separate installation of one of the batch plants on a



Right bank concrete production facilities

bench at El.190, conveniently positioned for supplying the tower cranes used for these structures. The layout on this bank, particularly with respect to the excavation and circulation area required for construction of the right assembly area of the powerhouse, determined the position of the bucket dock for the cableways and the concrete batch plants at El.165.

PRECOOLING OF CONCRETE

Basic data for design of concrete cooling plants

Because setting of the concrete is an exothermic process, substantial quantities of heat are generated in the concrete structure. This makes control of temperature during setting extremely important wherever very large volumes of concrete such as for Itaipu dams are involved. Without artificial cooling the placement volumes will have to

be uneconomically small in order to prevent cracking due to thermal differences in the placement. Of the two artificial cooling methods available, at Itaipu precooling the components of the concrete mix before placement had definite economic, technical and programming advantages over post-cooling with embedded pipes.

The basic factors governing design of the cooling system were:

- the heat transfer coefficient of the finished concrete
- the ambient conditions at the jobsite
- the river water temperature
- the thermal properties of concrete components like aggregate and sand. Because project planning data could change during construction, flexibility was required within certain limits, which in turn meant that all components of the cooling system had to be conservatively sized. Listed below are the average temperatures and the specific heats of the concrete components as delivered to the concrete cooling plants:

Components	Temperature (°C)	Specific heat (kJ/kg/°C)
Water	27	4.2
Cement	40	0.85
Fly ash	40	0.85
Natural sand (dry)	27	0.74
Artificial sand (dry)	27	0.76
Basalt aggregates (dry)	32	0.76

Four different concrete mixes were specified, and it was assumed for cooling capacity calculations that 95% of the concrete would have maximum aggregate nos. 3 or 4, see Table 5.11. The placement temperature of concrete was prescribed as 7°C. A rise of 1°C in concrete temperature between the batch plant and the forms was assumed, because of the large buckets (6 m³), and fast transport equipment. Thus, concrete temperature at delivery from the batch plants had to be 6°C.

Design and operation of the concrete cooling facilities

Refrigeration plants of the same basic design were erected on both banks. The plants, supplied by Sulzer do Brasil, consisted of a chilled-water system for cooling the gravel in a tunnel (wet-belt system), a cold-air system for pre-cooling the gravel in the bins of the concrete batch plants, a water system for cooling the batch water, and an ice production and conveying system. The sand was not cooled. In each

Table 5.11 Concrete mix composition

Components	Concrete compositions in parts by weight			
	Mix 1 aggr. MSA 19 (N/m ³)	Mix 2 aggr. MSA 38 (N/m ³)	Mix 3 aggr. MSA 76 (N/m ³)	Mix 4 aggr. MSA 152 (N/m ³)
Water	1650	1400	1100	900
Cement	2400	2000	1450	1000
Fly ash	600	500	350	300
Natural sand	2400	2300	2100	1800
Artificial sand	5600	5200	4900	4200
Aggregate no. 1	11 250	5000	3000	2500
Aggregate no. 2		7500	3600	3500
Aggregate no. 3			7400	4300
Aggregate no. 4				5400
Total	23 900	23 900	23 900	23 900

of the refrigeration plants, the components of the chilled-water systems were built together with the ammonia refrigeration system. The cold-air and ice systems were housed in the ice plant. On the right bank of the river, where the concrete batch plants were installed at two separate locations, it was necessary to split the ice plant in similar fashion (ice plants 2 and 3). Ice plant 2 was supplied by the main refrigeration plant, while ice plant 3 had its own refrigeration plant.

The cooling plant was built with simplicity, reliability and ruggedness suited to the rough service conditions involved. Complex, automatic control systems were omitted wherever possible, (particularly in the case of the water and air cooling systems); the operating crews preferring direct manual control.

Typical heat balance data for two concrete mixes are shown in Table 5.12. Fig. 5.16 shows the temperatures of various components during concrete production.

Cold water system for aggregate cooling

A closed loop chilled water system was used initially to cool the aggregates. Although the aggregate was washed before entering the cooling tunnel, large quantities of sludge and rock residue still entered the cooling water, and had to be removed from the circuit. Thirty spray water chillers were used to cool the circulating water. One of the reasons for selecting spray chillers was that they are not susceptible to freezing. Each chiller

consisted of nine rows of tubes arranged side by side, with a water distributing pan located above them. The water was sprayed on the outside of the chilling tubes through which the refrigerant at -3°C flowed; below the tubes it was collected in a large 1400 m³ common concrete water tank. The water tank was dimensioned generously to permit a certain amount of refrigeration storage and to eliminate the need to clean the tank too frequently. Fig. 5.17 shows a simplified flow diagram of the chilled water system.

The cooling tunnel consisted of a 200 m long steel structure insulated with prefabricated elements. The tunnel had a slight slope for draining the cooling water. Aggregate was carried through the tunnel on two conveyor belts, each with a capacity of 650 t/h. Chilled water at 2.5°C supplied by three pumps was sprayed on the aggregate during the entire trip. The spray system arranged above each conveyor belt comprised four individually switchable sectors, which were turned on or off from the control room. This system largely prevented the washing away of the fine aggregate. Some cooling water which dripped off the edges of the conveyor belts was collected in the channel running the length of the cooling tunnel. From there, it passed through a concrete channel into a thermally insulated treatment plant, first passing through screens to remove the coarse aggregate and then into five settling tanks. From the settling tanks the water was channeled to an intermediate tank and then pumped to the water chillers.

Table 5.12 Heat balance for various concrete mixes

Component	Weight (N/m ³)	Moisture (N/m ³)	%	Specific heat (kJ/kg/ °C)	Multiplier 2 x 5 (kJ/m ³ /°C)	Temperature (°C)	Enthalpy (kJ/m ³)
Mixture 1							
Cement	2400			0.92	221	40	8840
Fly ash	600			0.92	55	40	2200
Natural sand	2400	168	7	0.84/4.2	272	27	7344
Artificial sand	5600	392	7	0.84/4.2	635	27	17 145
Aggregate no. 1	11 250	56	0.5	0.84/4.2	968	6	5808
Make up water	144			4.2	60	5	300
Flake ice/water	890/616	616		2.1/4.2	187/374	-5/0	-935/0
Latent heat of ice				-335			-29 815
Mechanical heat							4200
Total	23 900				2585		15087
Resulting temperature						5.84	2585
Mixture 4							
Cement	1000			0.92	92	40	3680
Fly ash	300			0.92	27	40	1080
Natural sand	1800	126	7	0.84/4.2	204	27	5508
Artificial sand	4200	294	7	0.84/4.2	476	27	12852
Aggregate no. 1	2500	125	0.5	0.84/4.2	215	6	1290
Aggregate no. 2	3500			0.84	294	-2	-588
Aggregate no. 3	4300			0.84	361	-7.5	-2708
Aggregate no. 4	5400			0.84	454	-2	-908
Makeup water	1475			4.2	62	5	310
Flake ice/water	320/432	432		2.1/4.2	67/134	-5/0	-335/0
Latent heat of ice	432	432		-335			-10 270
Mechanical heat							4200
Total	23 900				2319		13 661
Resulting temperature						5.89	2319

Aggregate leaving the cooling tunnel also carried some cooling water which was then separated by vibrating screens. The water fell into pans below the screens, where sediment up to 0.5 mm size was settled out and delivered into a bin by conveyor screws and belts. The partially clarified water returned to the circuit via the settling tanks. Water losses were made up in the large cold-water tank by means of a float valve.

At exit from the tunnel the following temperatures were achieved:

Aggregate no. 1	6° C
Aggregate no. 2	7° C
Aggregate no. 3	8° C
Aggregate no. 4	9° C

Feedwater systems for concrete and ice production

The batch water for the concrete and the feedwater for the ice plant were pre-cooled; the former because of the heat balance, and the latter to obtain higher efficiency and improved ice quality. The schematic diagram of Fig. 5.18 shows the system. Three spray chillers were installed in each of the buildings housing the aggregate water chillers. The feedwater was introduced at about 27°C via a float valve in the storage tank, circulated through the chillers and cooled to 5°C. A temperature-controlled suction pressure valve on the refrigerant side prevented the water temperature from falling below 4°C, which was necessary to prevent the water in the distribution systems of the ice plants from freezing. For the physically separated ice plants and concrete batch plants on the right bank, the feedwater was cooled centrally in refrigerating plant no.2 and then pumped to the consumers by separate feed pumps. The concrete batch plants were equipped with insulated holding tanks for chilled water, from which the necessary water for each batch was drawn. Each ice maker had a small recirculating tank into which pre-cooled water was fed by float valves. Before entering the recirculating tank, the feedwater was pre-cooled in the ice maker. Circulating pumps supplied the water distribution system of the ice makers; excess water that was not frozen flowed back into the recirculating tanks. The feedwater systems worked largely automatically, the temperatures at the consumer inlets being signalled to the control rooms by remote indicators.

Ice production plants

To meet the peak demands of various concrete mixes, ice production capacity on either river bank was set at 650 t/day. This ensured a high degree of reliability in the event of failure of individual components. Flake ice is ideal for mixing concrete, because the large surface areas of the flakes ensure complete melting, and excessive water in the concrete mix can be avoided. The ice flakes averaged 30 mm in length and 2 mm in thickness and were supplied to the concrete mixer at -5°C. The facilities on the left river bank had to supply three concrete batch plants, which were located close to one another and so could be supplied by one central ice plant. Ice was produced and stored independently for each concrete plant. Three insulated wooden ice storage bins, 100 t capacity each, were installed at the 26.2 m level of the steel high-rise structure. Arranged over each ice bin were nine flake ice makers, each with a capacity of 1 t/h. The ice makers consisted of a cylindrical refrigerant evaporator of steel, the inner wall of which was sprayed with pre-cooled water by a rotating water distribution system. A rotor with steel scrapers removed the ice, which was subcooled to -15°C. The ice flakes fell directly into the ice bins and were stored in layers spread evenly by mechanical ice rakes, spaced 3 m apart, driven by chains on

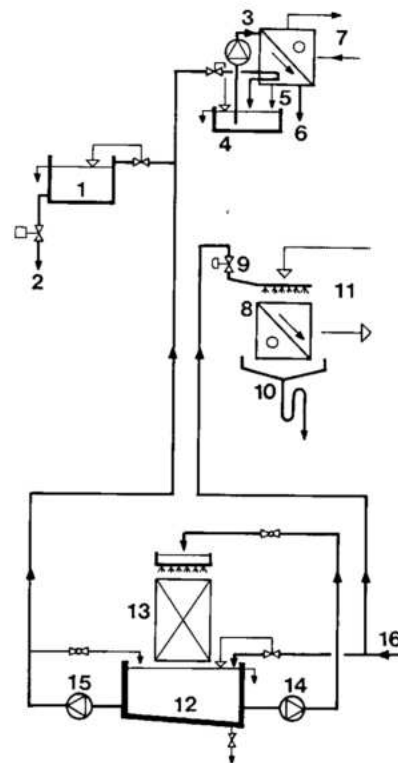


Fig. 5.18 Simplified diagram for feedwater systems

- | | |
|---|--|
| 1 Holding tank for chilled water in a batch plant | 9 Water spray system for defrosting and cleaning |
| 2 To the concrete mixers | 10 Water collecting trough |
| 3 Ice maker with water circulating pump | 11 Cold air circuit |
| 4 Recirculation tank for pre-chilled water | 12 Chilled water tank |
| 5 Surplus water return | 13 Water chillers |
| 6 Flake ice discharge | 14 Circulating pump |
| 7 Refrigerant circuit | 15 Feed pump |
| 8 Finned-tube heat exchanger for cooling air | 16 Fresh water supply |

a steel frame, covering the entire width of the bin. Each batch plant had an insulated holding silo with a capacity of 2 t, from which the necessary quantity of ice for each batch was drawn and weighed. When the ice level in a holding silo fell below a certain minimum, the ice rake in the respective ice bin switched over from filling to discharging. The door at the end was raised automatically by pivot arms on the bin wall and the ice rakes pushed ice from the surface into a lower twin screw, which conveyed the flake ice through a trap door to a metering screw which moved it to the holding silo. The metering guaranteed a constant filling level in the twin screw conveyors, so that clogging in the connecting ducts or screws was prevented. The entire ice installation was automatically controlled and monitored from the central control panel in the ice maker room.

Fig. 5.19 Refrigeration plant - Simplified flow diagram

L Level control

P Temperature control

E Pressure control

1 Piston compressor

2 High-voltage electric motor

3 Auxiliary lubrication pump

4 Oil cooler

5 Ammonia separator

6 Intermediate expansion vessel

7 Ice maker

8 Finned-tube heat exchanger

9 Water chiller for raw water

10 Water chiller for treated water

11 Ammonia circulating pumps

12 Condenser

13 Ammonia collecting tank

14 Automatic deaerator

15 Cooling tower

16 Water collecting tank

17 Pump sump

18 Water circulation pumps

19 Raw water cooling

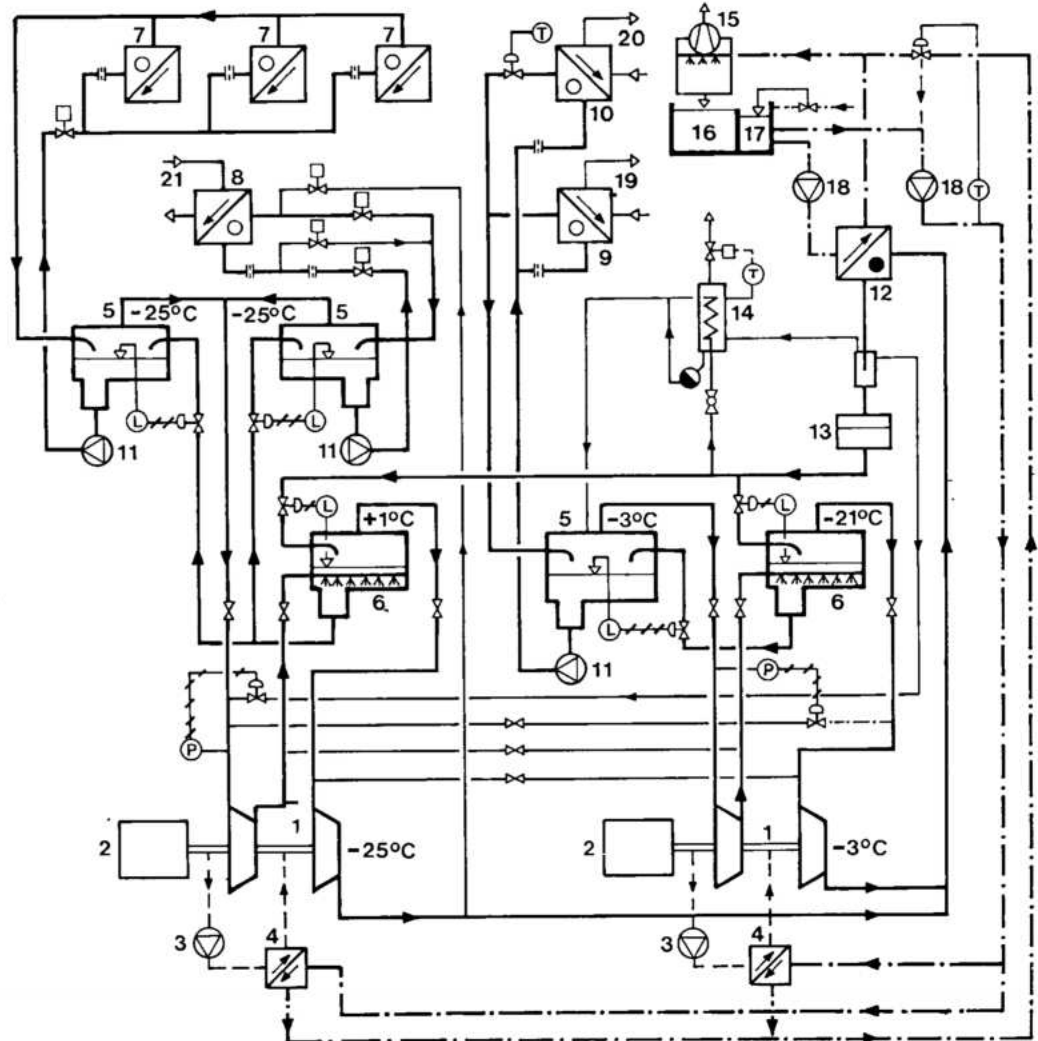
20 Treated water cooling

21 Air cooling

— NH₃

--- Cooling water

--- Oil



Cold-air systems

Aggregates nos. 2, 3 and 4 pre-cooled in the cooling tunnel were transported by insulated conveyor belts to the bins of the batch plant and further cooled with cold air.

Average temperatures of the aggregate which discharged into the concrete mixer were:

Aggregate no. 1	7° C
Aggregate no. 2	- 2° C
Aggregate no. 3	- 7° C
Aggregate no. 4	- 2° C

The fine aggregate no. 1 was not pre-cooled with air because of the danger of its freezing.

The bins area had a hexagonal floor plan divided into a central round bin for cement and fly ash, surrounded by six bins for sand and aggregate. The compartments for aggregate were thermally insulated from the other bins and from the outside. An insulated air cooling chamber was installed in the high-rise steel structures on the ice plants for each batch plant. Housed in these chambers were heat exchangers, each consisting of fifteen finned-tube elements. Ammonia at -25°C

evaporated in the heat exchanger tubes; the air, which flowed from top to bottom in the heat exchangers, left at -17°C. For air circulation, each circuit was equipped with a centrifugal blower rated at about 220 000 m³/h, which blew the air into the bottom of the individual bin compartments. Each air inlet location was fitted with a manually actuated air-flow regulating flap. An extended booster blower was fitted in the supply duct to the compartment for aggregate grade no. 2 in order to overcome the large pressure drop in this compartment. All aggregate bins were open at the top and were joined together in the form of a common return air chamber, from which the return air in the -3°C to +10°C range was sent back to the air cooler chamber. The only automatic feature was the reduction of blower speed when the return air temperature fell below a preset figure. Other changes were made with the air-flow regulating flaps as required; remote indicating thermometers detecting air temperatures.

Refrigeration plants

Three independent ammonia refrigeration plants supply the various cooling systems of the concrete cooling

Table 5.13 Design data for various systems and refrigeration plants

Design data for feedwater systems	Plant 1	Plant 2	Plant 3
For concrete and ice production			
Feedwater rate (m ³ /h)	40	27	13
Water flow rate over water chillers (m ³ /h)	273	273	0
Chilled water temperature (°C)	5	5	5

Design data for ice plants

Ice production rate (t/h)	27	18	9
Ice temperature at concrete mixer inlet (°C)	-5	-5	-5
Storage capacity (t)	3 x 100	2 x 100	1 x 100
Discharge rate (maximum) (t/h)	3 x 24	2 x 24	1 x 24

Design data for cold air systems

Quantity of air (circulated maximum) (m ³ /h)	3 x 220 000	2 x 220 000	1 x 220 000
Air temperature at gravel bin intake (minimum) (°C)	-17	-17	-17

Allocation of holding bins in batch plants

	Bin volume (m ³)	Useful capacity (kN)
Cement	50	1500
Cement substitute	25	500
Aggregate no. 1	96	1120
Aggregate no. 2	96	1120
Aggregate no. 3	144	1690
Aggregate no. 4	48	560
Natural sand	96	1120
Artificial sand	96	1120

Design data for the refrigeration plants

	Evaporation temperature (°C)	Plant 1 (kW)	Plant 2 (kW)	Plant 3 (kW)	Total (kW)
Chilled water for cooling gravel	-3	6395	6395		12 790
Chilled water for concrete and ice production	-3	990	660	330	1980
Air cooling for aggregate bins	-25	2800	1870	935	5605
Ice production	-25	2800	1870	935	5605
Reserve capacity	-3/-25	2790	4050	880	7720
Total installed capacity		15 775	14 845	3080	33 700

facilities. A typical plant schematic is shown in Fig. 5.19 and its performance summarized in Table 5.13. All three plants were basically alike, but refrigeration plant 3 had only a -25°C circuit for its particular duty.

The ammonia system comprised two evaporation circuits of -3°C and -25°C , respectively. All consumers were supplied with expanded ammonia from central separators by hermetic circulating pumps. Orifice plates controlled the distribution of liquid to the consumers. The ammonia vapors resulting from evaporation were returned to the liquid separator together with the surplus liquid ammonia. Evaporation vapors were piped to the piston compressors and compressed to condensation pressure in two stages, with interstage cooling in the intermediate pressure vessels. After condensation in the water cooled condensers, the condensate at 35°C flowed from the condensers via de-aerating bottles into the collecting tanks. From there it went through two expansion steps as it flowed back through the intermediate pressure vessels into the separators. The liquid level in the intermediate pressure vessels and in the separators was maintained constant by controlling the condensate return flow. Refrigeration plant 3 worked the same as refrigeration plant 2, but plant 1 used single stage screw-type compressors. Cooling water for the shell-and-tube condensers, the compressors and oil coolers was cooled in counter-flow, suction-ventilated cooling towers. Because the cooling towers operated in extremely dusty surroundings, adjacent to rock and earth excavation as well as aggregate processing equipment, the concrete water collecting tanks were oversized to allow the dust scrubbed from the air to settle out. Water

losses were made up with treated water from the site supply system via a float valve in the pump sump.

CONCRETE PLACEMENT EQUIPMENT

Analyses of the various alternatives capable of performing the critical phases of the work led to the selection of aerial cableways as the main delivery system, supplemented by tower cranes, see Figs. 5.20 and 5.21. Because of the size of the main dam blocks, the specified lift heights and desired rate of concrete supply, the alternative of employing cranes would have required the construction of large auxiliary structures, both to support the cranes, and for the circulation of the concrete delivery equipment. Because the start of erection of these supports would depend on the completion of the foundations of the permanent structures, an extra activity would be added to the critical path. Therefore, the time required for procurement and construction of the temporary structures (which was significant, considering their size) would be added to the total project time schedule, jeopardizing the established completion date. Conversely, since the installation of aerial cableways was independent of completion of the excavation, high concrete placing rates in the diversion structure, the main dam and the

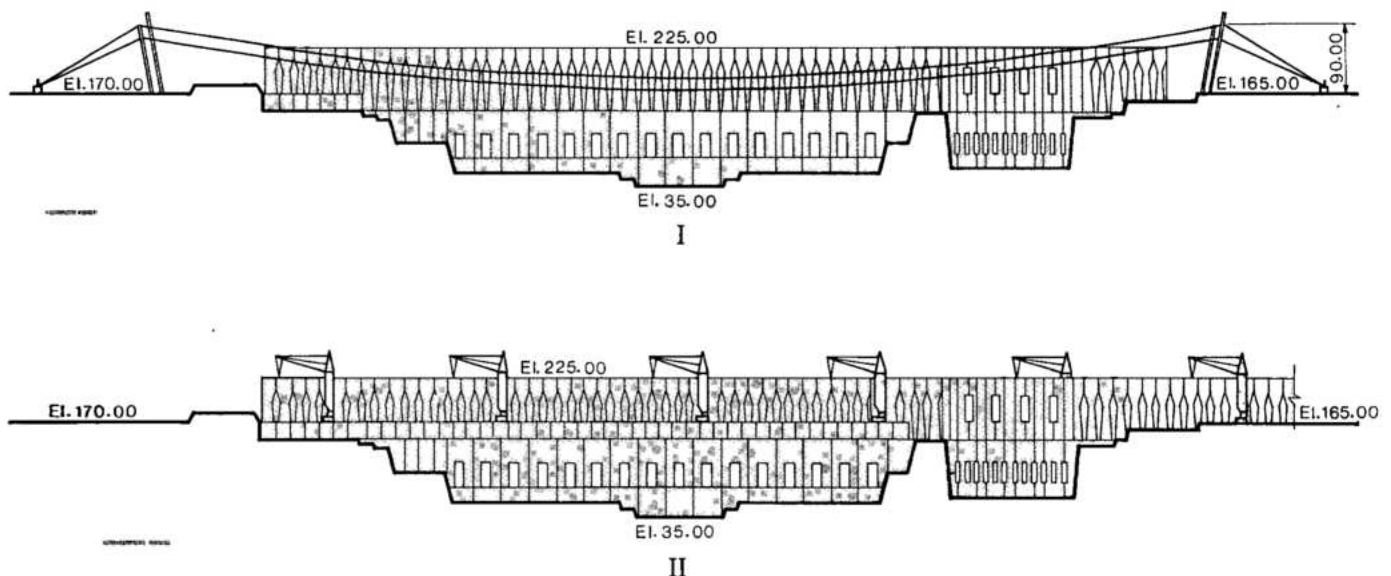


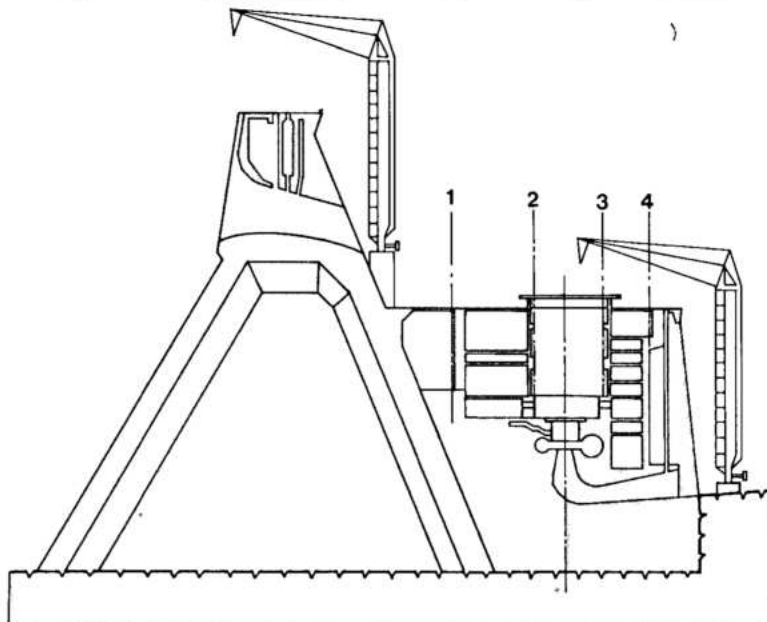
Fig. 5.20 Concrete placement in main dam and powerhouse equipment and stages

I Concrete placement by cableway in main dam and powerhouse

II Concrete placement by crane in main dam and powerhouse

Fig. 5.21 Concrete placement in main dam and powerhouse

1, 2, 3, 4 Reference lines
A, B, C, D
— Dense basalt
— Concrete placement with cableways
— Concrete placement with cranes



powerhouse could be reached soon after the foundations were ready. For the spillway crest structure, the right wing dam and the powerhouse in the diversion channel, their layout did not allow the use of cableways, and tower cranes on rails was the most suitable solution. The reuse of tower cranes was planned in successive phases of the project, for example in the powerhouse, to supplement the cableways during the peak period of concrete placement and in placing concrete in the uppermost portion of the main dam.

For the horizontal transportation of concrete there had to be accommodated in restricted areas both an exceptionally heavy flow of concrete and intense road traffic of the trailers and trucks required for the transportation not only of formwork, steel reinforcement and embedded parts, but also of the parts and materials for assembly of the permanent equipment.

Continuous transportation of buckets by monorail, although unprecedented in heavy civil construction, was the only method which adequately assured continuity and regularity of supply to the cableways without obstructing traffic. This was especially so in the winter when visibility could be impaired by early morning fog.

MONORAIL

As shown in Fig. 5.22 the monorail systems installed on both banks comprised:

- An elevated rail 11 m above the road level, extending underneath the concrete batching plants and along the cableways dock.
- Individually motorized cars with 6 m³ buckets, suspended from the elevated rail. These cars stopped automatically at three points:

1. Under the batch plants, to load concrete.
 2. At the control station, to receive instructions regarding the destination of the load.
 3. At the unloading points, spaced 20 m along the dock, where the load was transferred to the silo-cars.
- Silo-cars to receive the concrete from the monorail cars at the unloading stations along the dock. These cars were moved along the rails to the position where they could directly supply the buckets carried by the cableways.
 - Control station where the control of the entire operation was centralized.
 - Servicing and bucket washing shop.

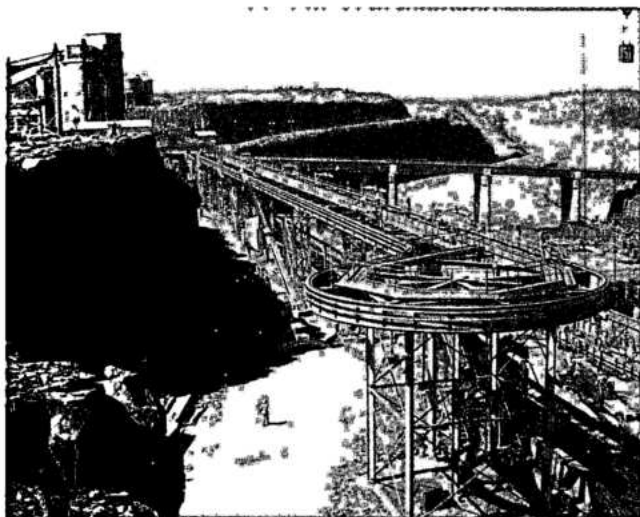
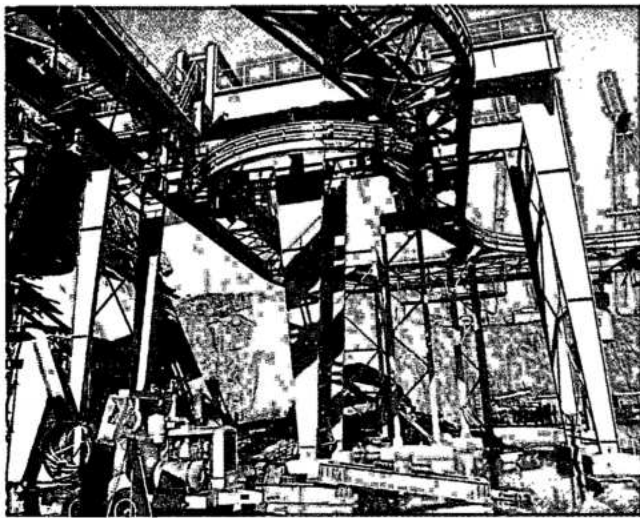
The number of cars operating on the monorail at any time was a function of the demand for concrete. Under conditions of maximum production, the system transported 540 m³/h of concrete on the left bank and 360 m³/h on the right bank.

The configuration of the monorail was adapted to the phase of the construction. Two phases were used for the left bank:

- Supplying the cableways along a straight dock on the left bank of the diversion channel during the first phase of construction.
- During construction of the central blocks the portion of the dock corresponding to the main dam was moved to the right bank of the diversion channel. The portion of the dock corresponding to the powerhouse remained in its original position.

On the right bank, only one configuration was utilized, with the monorail installed along a continuous dock at El. 165.

Dumpcrete trucks. Dumpcrete trucks were used for transportation of all concrete placed by the tower cranes.



Monorail in operation

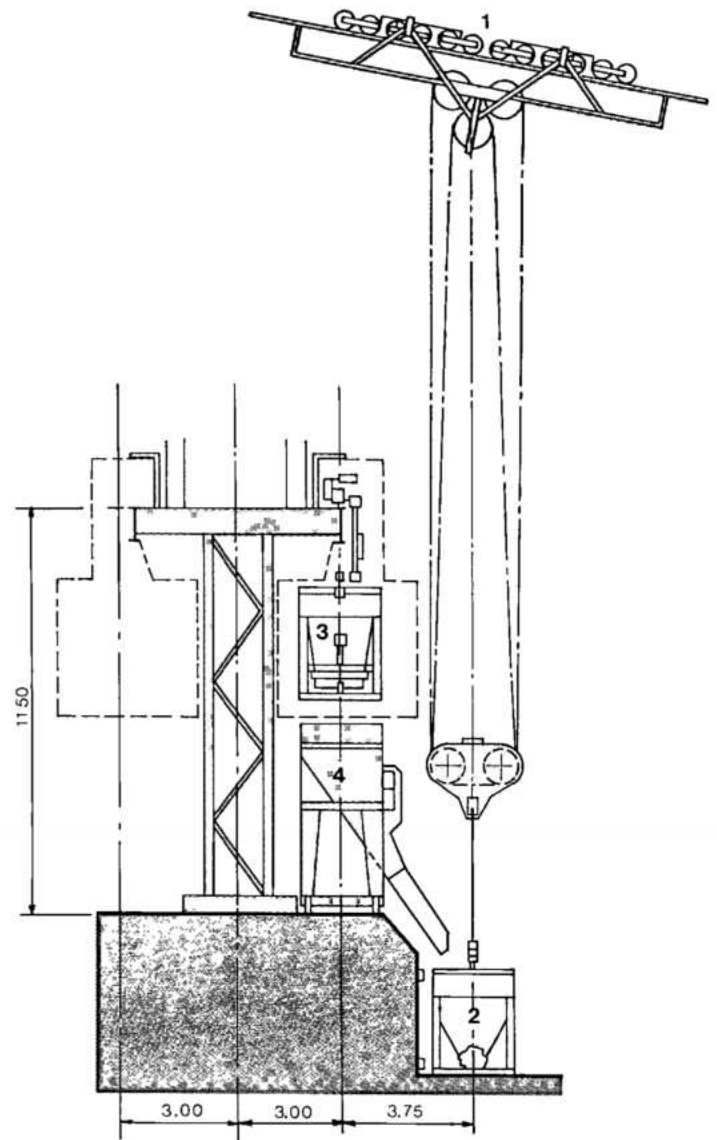


Fig. 5.22 Concrete transfer

- | | |
|----------------------|---------------------------------|
| 1 Aerial cableway | 3 Monorail bucket |
| 2 Bucket of cableway | 4 Intermediate bucket and chute |

AERIAL CABLEWAYS

General arrangement and characteristics

The cableways were designed with movable towers on parallel tracks, one tower on each bank of the river, so that they covered the entire powerhouse and main dam area including the diversion control structure, but excluding the blocks adjacent to the rockfill dam, see Fig. 5.8.

The A-frame towers were raked backwards towards the rear counterweight carriages which ran on rails fixed to a concrete beam anchored to the rock. The movement of the counterweight carriages was synchronous with that of the towers. Two sets of parallel rails on each bank supported the towers, so that adjacent towers mounted on different tracks overlapped each other, thus reducing the gap between cables, see Fig. 5.23. Main characteristics of the cableways were:

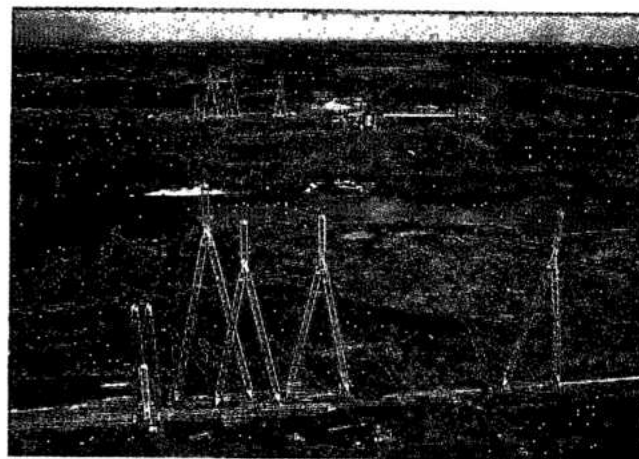
Tower height, 4 units	75 m
Tower height, 3 units	90 m
Span between towers	1360 m
Maximum sag of supporting cable	68 m
Load capacity	250 kN
Bucket capacity	6 and 3 m ³
Hoisting speed with a 250 kN load	104 m/min
Translation speed	450 m/min
Average concrete placing rate	90 m ³ /h

The peak production of concrete to be handled by the cableways was estimated to be 200 000 m³/month. The height of the towers was determined by the elevation which the main dam blocks would reach by the time the cableways would have to be dismantled to allow for the construction of the left bank blocks. This corresponded to the elevation of the sill of the power intakes.

Design details

The cableways as supplied by PHB Watersheim AG of West Germany, with motors and controls by Siemens AG, had the following principal features:

Track and stay ropes. The fully enclosed track and stay ropes consisted of a 91 round wire core with a 220 wire and Z wire cover divided into five layers. At 140 mm diameter these were the largest fully enclosed ropes ever manufactured for cable cranes. Twenty tons of track rope, on which the twelve wheeled crab of the cable crane ran, was required for the 1360 m span.



Aerial cableways

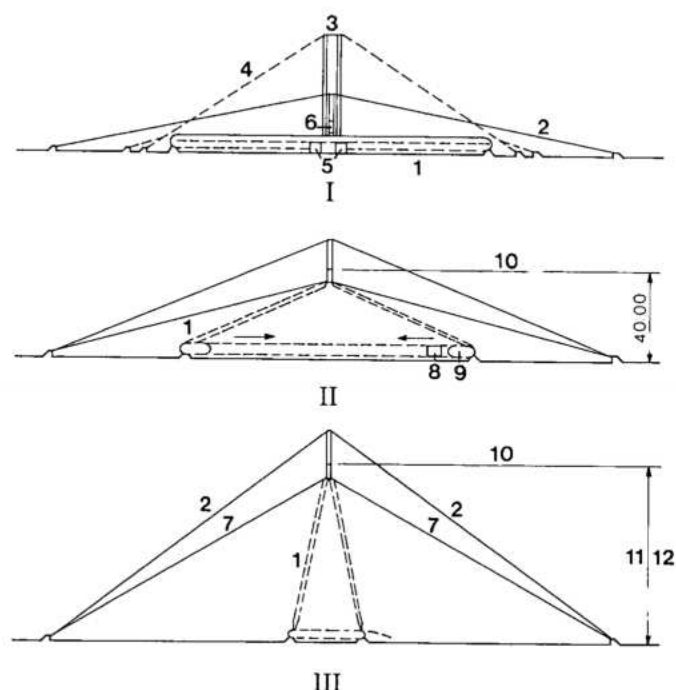


Fig. 5.23 Erection of aerial cableways towers

- | | |
|---|--|
| I Stage 1 | 7 Guy rope of the support halves |
| II Stage 2 | 8 Counterweight |
| III Final position | 9 Tensioning strands and hydraulic puller |
| 1 A-support half | 10 Centre track rope hinge suspension |
| 2 Guy rope of the mast tower | 11 Three cranes (90.00) |
| 3 Two bottom blocks | 12 Four cranes (15.00) |
| 4 Lateral guying of the erection masts | |
| 5 Erection auxiliary supports | |
| 6 Lifting transverse | |

Lattice girder towers. The track ropes were suspended from A shaped square cross-section lattice towers which in turn were braced by the stay ropes attached to the countercarriages. The A-towers ran on a single rail, there being twelve wheels for the 90 m and ten wheels for the 75 m towers. Crane travel was effected by the travel gears and their three-phase motor drive units at the A-towers and at the countercarriages. The travel gear of the countercarriages was subdivided into a vertical gear with two driven wheels and a horizontal gear with twelve non-driven wheels. The countercarriages were welded box structures supporting the concrete block counterweights.

Hoisting and crab-traverse units. Ropes used for the hoisting and crab-traversing mechanism were Warrington Seal type and were attached to the track rope at 50 m intervals by folding carriers. Opening and closing rails fixed to the crab released the folding carriers as the crab passed. Both the hoisting and crab-traversing systems required finely tuned speed control which was achieved by means of a Ward Leonard drive system, with thyristor controlled generator excitation. The hoisting gear which had a thyristor regulator of the motor field had 7-0-7 speed steps, whereas the crab-traversing gear, which was without motor field regulation, had 6-0-6 speed steps. The induction motor and generator of the Ward Leonard drives, together with controls and the transformer for the tower and counter carriage drive motors, were installed in a machine house located on the left bank. Hoisting and traverse units, that is the dc motors, rope drums, gear boxes couplings and safety brakes, were located in a winch house mounted on the left bank A-towers.

Load carrying equipment. The load carrying equipment consisted of a bottom block with pulleys through which the hoisting rope ran, stranded attachment ropes, a rotary load hook and the round concrete bucket which was protected against damage by a timber frame, see Fig. 5.22. The largest concrete buckets had a capacity of 6 m³ and were equipped with a bottom gate which was operated by means of a hydraulic servomotor. The hydraulic accumulator for the system was charged by the action of filling the bucket, each charge being sufficient for three opening and closing cycles of the gate, thus permitting dosed unloading.

Operation. The cable cranes could be operated from control stations located 40 m above the track in the A-towers, one on each bank. From this position the crane driver had an excellent view over the bucket

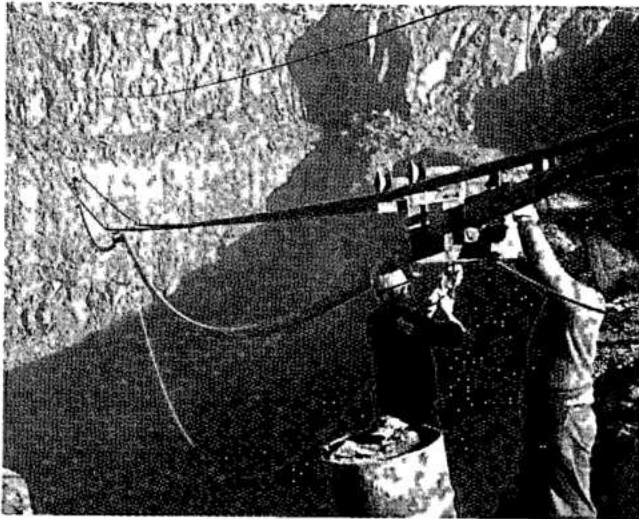
loading point and could watch the entire operation area of the cableways. However, the dual control stations meant that all signals required for control had to be transmitted over a radio relay link simultaneously from one winch house to the other and also to the machine house. The same applied for the return signals for the control and interlocking systems, so that each crane had two radio relay links making fourteen independent links in total. The crane drivers communicated with the receiving stations by radio telephone. Digital displays were used in the control room to show the crab and hoist positions, using signals from digital transmitters mounted on the respective winches.

Erection

After the general clearing of the site area and other preparatory work, such as mounting the winches and auxiliary lifting devices and connecting the site power supply, the erection work began on both banks of the river. First the crane rails were laid on the concrete tracks. Then the countercarriages and A-towers were assembled, the components of the latter having been pre-assembled at the manufacturer's works in units suitable for road transport. The track and both stay ropes were then pulled out and cut to the required lengths; the ends were inserted into cone-shaped sockets, untwisted to form a bunch and cast in a Zamak compound.

A nylon rope was first pulled from one river bank to the other and this was then used for pulling a steel rope. With the latter, two auxiliary track ropes were then pulled across, one after the other, and their ends anchored. The track rope was laid onto erection carriers mounted on the auxiliary track ropes and pulled from the left to the right bank. As there was an extra length of track and stay rope as it lay on the ground, the rope end sockets could immediately be secured after being pulled into the hinged suspensions of the countercarriages and A-towers. Finally the crab was mounted on the track rope and the lifting of the A-towers was effected in stages, see Fig. 5.23.

Erection winches mounted on the two erection masts were used to lift the apex of the A-tower to 40 m above the rails. As it was lifted the two feet of the tower rolled together on the rails, closing like scissors. A wire rope tied to one foot of the tower and to a hydraulic puller attached to the other foot, was used to pull the legs together and thus lift the tower into its final position. Ballast weights were placed on the counter carriage as the A-tower was lifted, and the stay rope was tensioned to give the tower the required 10° backward lean. The winch house, including the hoisting and crab-traversing winches and electrical equipment was pre-assembled separately, away from the erection track, and installed in the A-tower immediately after its erection. As soon as the main erection work had



been completed, the crane was run out of the erection track to make room for the next cableway to be erected.

The aerial cableways were partially demolished before filling the reservoir in October 1982, after all electromechanical equipment had been removed. The remaining structures were demolished by explosives early in 1983.

TOWER CRANES

Virtually all concrete located out of reach of the cableways, and about $4 \times 10^6 \text{ m}^3$ of the concrete in the powerhouse had to be placed by tower cranes. This work was carried out in six successive phases, each with a different arrangement of cranes. Prior to the placement of concrete, the same cranes were used for the erection of steel linings and gate guides in the diversion control structure, and for construction of the service bridge across the diversion channel. This meant that the tower cranes would operate in four different locations, which restricted the selection of the tower cranes to those which could be easily assembled and dismantled.

The characteristics of the tower cranes are given in Table 5.14.

The plan adopted for optimum utilization of the cranes was as follows:

1st Phase – October 1977 to October 1978

During this period, two cranes upstream and two downstream of the diversion control structure assisted in the erection of the sluice linings and gate and stoplog guides. Simultaneously, two other cranes were used for construction of the service bridge.

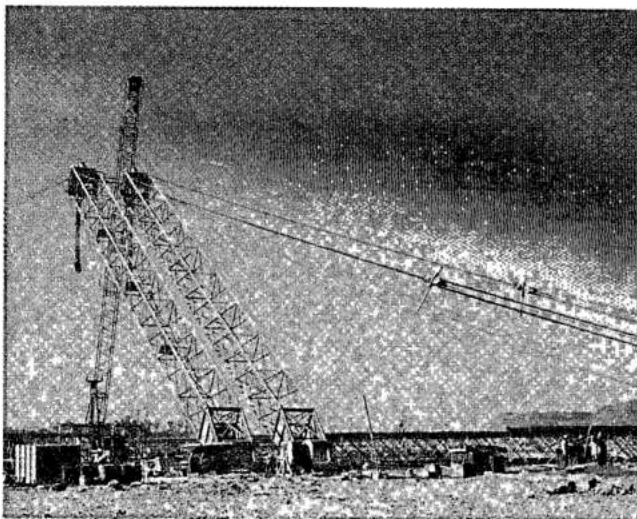
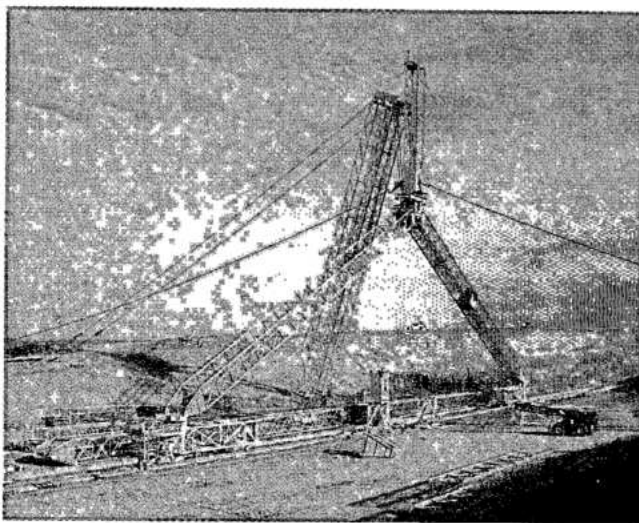
The positions of the cranes in the diversion channel prior to diversion of the river and for placing concrete in the power intakes are shown in Fig. 5.3. Figure 5.21 also shows the positions of the cranes downstream of the powerhouse, and the cranes installed at El.144 downstream of the main dam.

2nd Phase – November 1978 to December 1979

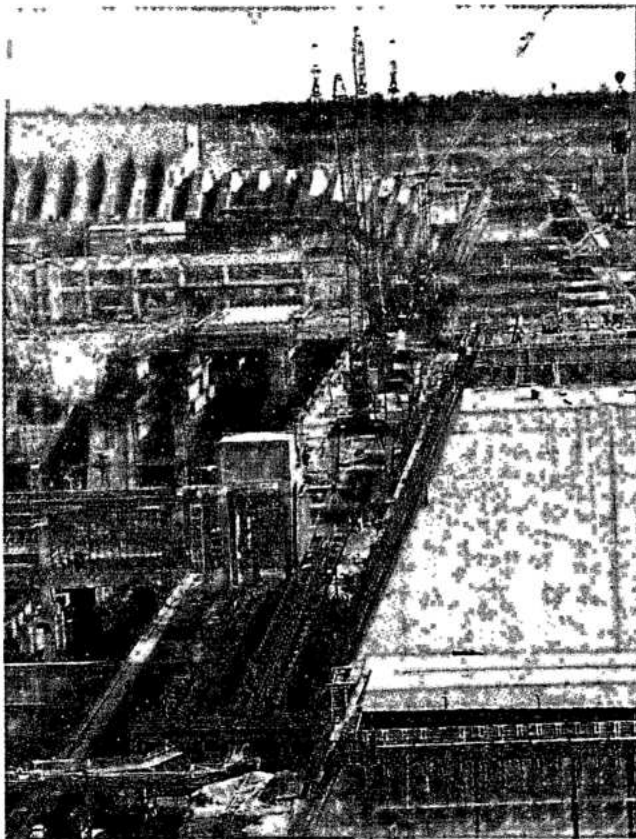
Eight cranes were used to place about $1 \times 10^6 \text{ m}^3$ of concrete in the spillway, the right wing dam and the end walls of the rockfill dam.

3rd Phase – January 1980 to July 1981

Seven cranes were used in the equipment assembly areas and downstream of the powerhouse in the riverbed to supplement the aerial cableways, and place about $600\,000 \text{ m}^3$ of concrete. One crane was used in the spillway and the right wing buttress dam.



Erection of the aerial cableways



Tower cranes

4th Phase – August 1981 to September 1982

During this period about $2.5 \times 10^6 \text{ m}^3$ of concrete was placed in the upper portion of the main dam, the buttress blocks between the diversion control structure and the rockfill dam, the right wing buttress dam and the powerhouse in the river bed.

During the 4th phase the aerial cableways were decommissioned and concrete was placed by eight tower cranes. Construction of the power intakes was a critical activity during this phase, and five dockside rail mounted cranes, with very long reach were used for this purpose. These cranes were installed at El.144, downstream of the main dam, and arranged so that the traffic of dumpcrete trucks was routed under their towers.

The main characteristics of these dockside cranes were:

Type	1	2
Height	84 m	88 m
Maximum reach, at 200 kN	32 m	59 m
Maximum reach, at 100 kN	62 m	80 m
Average placing rate with 6 m ³ bucket	60 m ³ /h	90 m ³ /h
Average placing rate with 3 m ³ bucket	40 m ³ /h	60 m ³ /h

Table 5.14 Characteristics of the tower cranes

Type of crane	Model	Maker	Principal characteristics
Tower crane on rails	IN-710-T	Peiner	Inclined boom, radius of operation 75.6 m (max.) and 19.5 m (minim.). Lifting capacity 8.8 MN (880 t). Lifting velocity 200 m/min.
Tower crane on rails	TN-1401-IT	Peiner	Inclined boom, radius operation 80 m (max.) and 19.5 m (minim.). Lifting capacity 15.58 MN (1558 t). Lifting velocity 200 m/min
Tower crane on rails	550-C	Liebherr	Horizontal boom, radius operation 60 m (max.) and 19.5 m (minim.). Lifting capacity, 4.4 MN (440 t). Lifting velocity 74 m/min.
Tower crane on rails	200-C	Torque	Horizontal boom, radius of operation 50 m (max.). Rotation angle 360°. Lifting capacity 2 MN (200 t). Lifting velocity 75 m/min
Crane on caterpillars	4100 W	Monitowoc	Inclined boom, radius of operation 67 m (max.) and 10.97 m (minim.). Rotation 360°. Lifting capacity 26.32 MN (2632 t)
Crane on wheels	8115-TC	P & H	Inclined boom, radius of operation 67 m (max.) and 15.2 m (minim.). Rotation 360°. Lifting capacity 3.35 MN (335 t)
Crane on wheels	RT-75-5	Grove	Inclined boom, radius of operation 33.5 m (max.) and 3 m (minim.). Rotation 360°. Lifting capacity 1.35 MN (135 t)
Crane on wheels	R-200	P & H	Inclined boom, radius of operation 19.76 m (max.) and 8.75 m (minim.). Rotation 360°. Lifting capacity 550 kN (55 t)
Crane on wheels	714-S	Clark	Inclined boom, radius of operation 18.23 m (max.) and 8.05 m (min). Rotation 360°. Lifting capacity 381 kN (38.1 t)
Crane on tyred wheels	H-80-I	Hyster	Boom load capacity 40 kN (4 t), velocity of lifting 0.3 m/s. Moving velocity 28 km/h.

5th Phase – November 1982 to August 1984

Placing of concrete in the main dam power intakes and powerhouse units in the river bed was diminishing during this phase of construction. The eight tower cranes operating during phase 4 of concreting were gradually reduced to two cranes.

6th Phase – September 1985 to end of 1989

Construction of structures located in diversion channel powerhouse units 16 to 18A, central assembly block 3 and closing block VI was carried out by means of five downstream tower cranes which were used to place a total of $2 \times 10^6 \text{ m}^3$ of concrete.

During construction of the powerhouse units in the diversion channel the critical activity was concreting of the units to the minimum configuration, such as to permit safe passage of the bridge cranes with the heaviest generation components.

PRECAST CONCRETE COMPONENTS AND SLIP-FORMS

PRECAST CONCRETE COMPONENTS

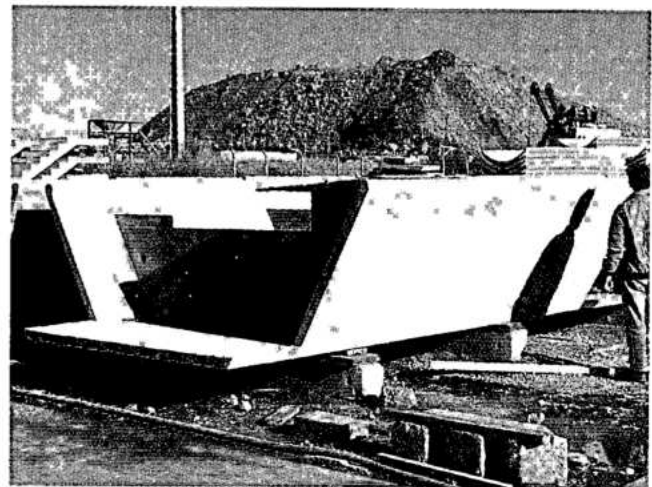
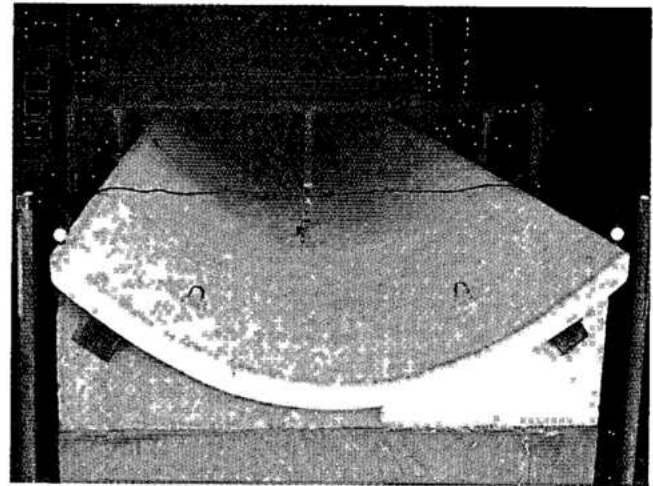
To improve the rate of concrete construction and because of the large volume of concrete involved, precast elements were used extensively. The precast elements were in some cases complete structural units, while in others they were self-supporting and substituted for formwork. The minimum strength of concrete at 28 days was generally 2.8 kN/cm^2 , except for bigger pieces for which it was 3.5 kN/cm^2 . Steam curing for about 10 hours was employed for all pieces, followed by wet curing with a sack cloth cover for a total of 21 days.

Examples of precast elements used as replacement for formwork are as follows:

- Roof of the draft tube.
- Roof of the diversion sluice.
- Roof of the upstream portion of the power intake.
- Roof slabs for galleries in the dams and the powerhouse.
- Truncated-conical members for forming the concave upstream face.
- Polyhedral elements for forming the downstream face of the cavity in the hollow gravity dam blocks.

Some of the large structural pieces which were precast were:

- Stairs.



Precast elements

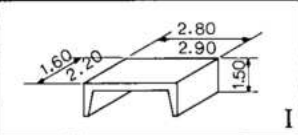
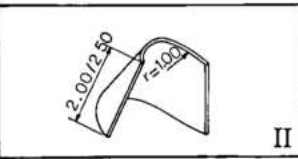
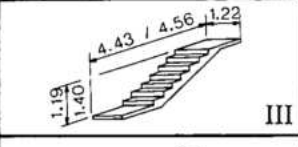

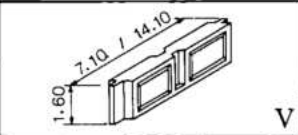
- Beams for bridges over the diversion channel and the spillway.
- Blocks for shafts for elevators and staircases in the main dam.

Fig. 5.24 shows the shapes and dimensions of some of the precast elements used and Table 5.15 the typical quantities.

SLIP-FORMS

Where there was a possibility of continuous concrete placement, slip-forms were used for construction with considerable savings of labor and time. They were used not only for slender structures of a uniform section and for some massive structures with a sectional plan varying with height, but also for structures directly exposed to high velocity flow.

Table 5.15 Precast elements

	Location	Stretch	Quantity of piece types	Quantity of constructed pieces	Concrete volume
	Spillway	A	46	13 724	6961
	Right wing dam	D	32	2083	1165
	Main dam	E & F	479	20 436	33 499
	Diversion structure	H	94	6884	7618
	Left buttress dam	I	22	696	1085
	Powerhouse and erection area	U1 to U15	292	15 517	18 494
	Powerhouse units of diversion channel	U16 to U18A	196	1539	2639
	Operation and administration building	U1	23	96	363
	Total		1161	60 879	71 461

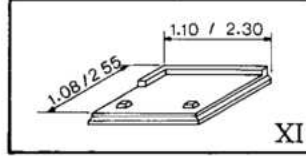
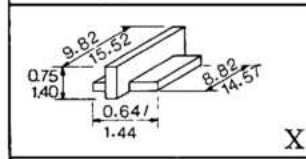
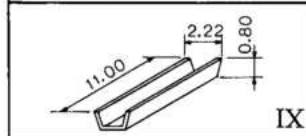
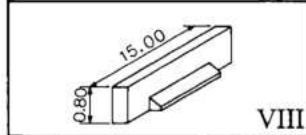
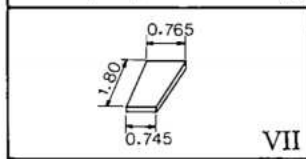
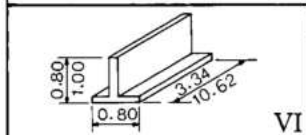
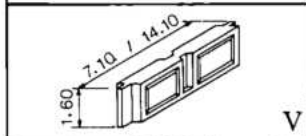
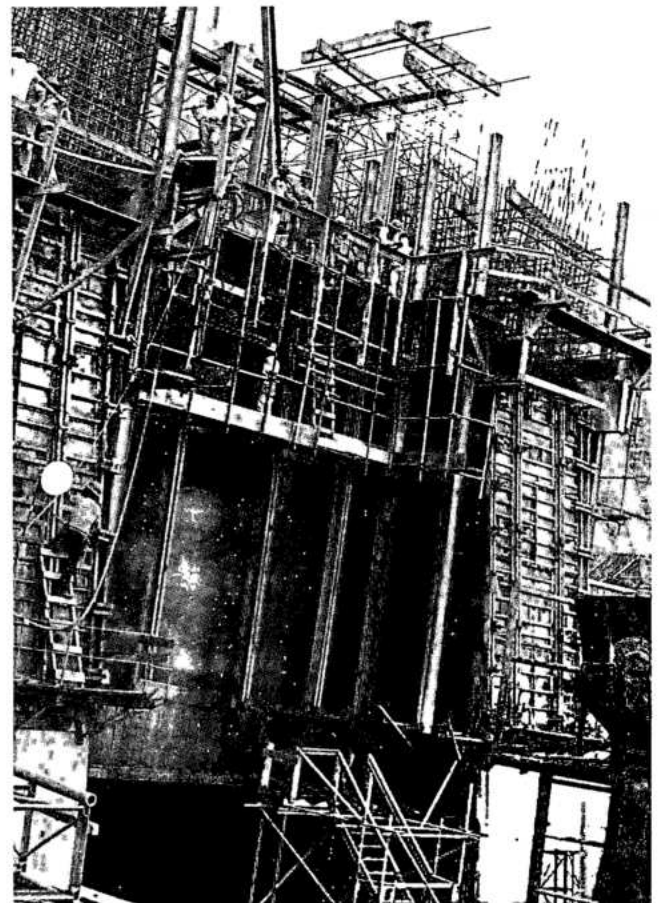
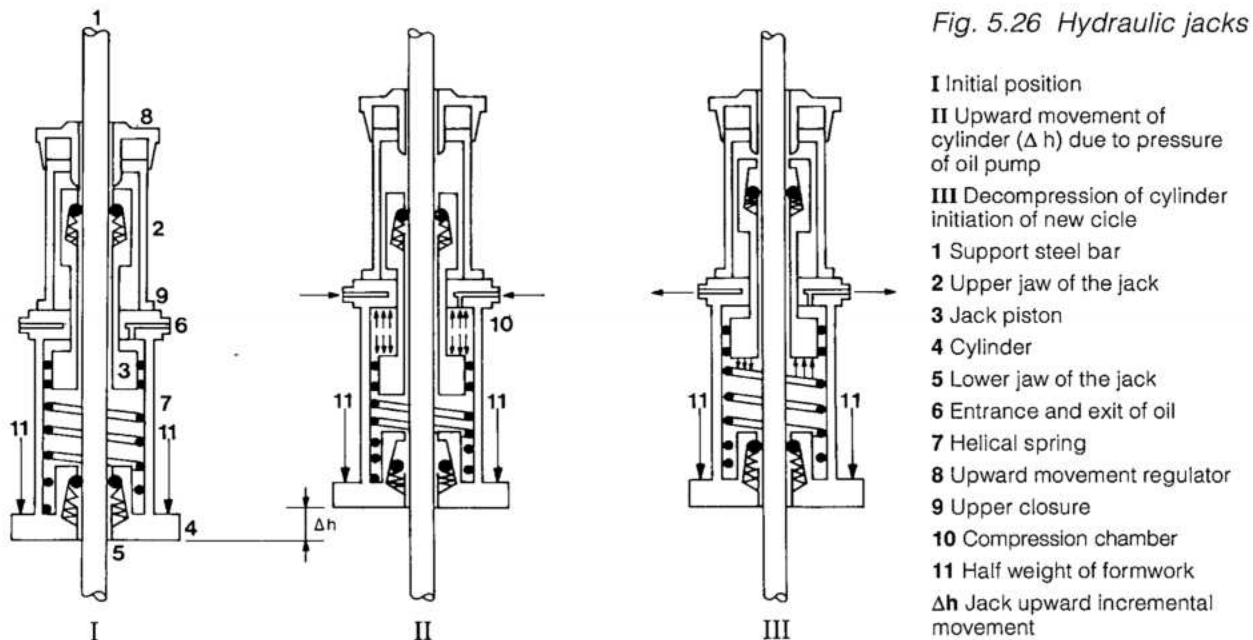
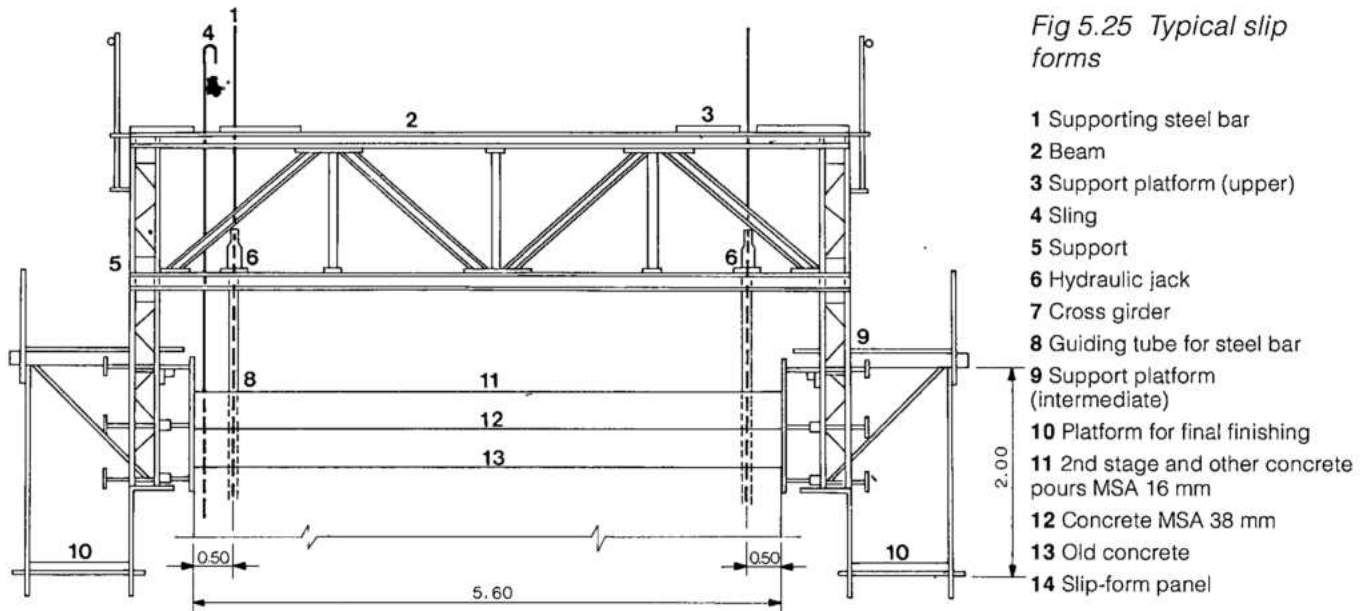


Fig. 5.24 Typical precast components

- I Roof of drainage gallery
- II Upstream end of cavity in main dam
- III Upper extension of piers
- IV Staircases and elevator shafts
- V Beams in power intakes
- VI Side walls
- VII Roof of powerhouse
- VIII Power intakes and draft tube roof
- IX Roof of diversion sluices



Slip-forms



The slip-forms consisted basically of two rigid formwork panels 1.1 m high, with the capability to adjust and develop the geometric shape desired, see Fig. 5.25. They were attached to the steel truss which via special hydraulic jacks, with gripping jaws, see Fig. 5.26, were supported on steel bars. Upward movement of the forms was effected by the jacks climbing the steel bars by means of sequential opening and closing of the upper and lower jaws of the jacks, while the jack piston moved. Initially the forms sustained the fluid pressure of the

fresh concrete, which decreased as the concrete hardened. With a proper rate of placement, the concrete poured at the bottom began to set and harden, permitting the exposure of surface as the form climbed. In order to avoid cold joints, the process had to be continuous.

Slip-forms were employed for construction of the following features:

- Arch cofferdams.
- Piers of the bridge across the diversion channel.
- Sluiceway piers in the diversion control structure.

- Walls and columns of the right and central equipment assembly areas.
- Piers of the downstream powerhouse wall.
- Walls, columns and piers of the powerhouse units in the diversion channel.

For best performance, it was necessary to place the slip-forms precisely on supporting guides. To decrease friction between the freshly placed concrete and the panels, and also to facilitate movement of the forms, an inclination was given to the formwork giving a small variation in the opening width of the top and the bottom of the form. This way the lower end was kept to the design dimensions and the top end was from 0.5 to 2 cm less. Before start of concrete placement, all forms were topographically checked, and during concreting the level, vertical alignment, and dimensions of the formworks were continuously monitored. Reinforcement and embedded parts were installed as the forms climbed. To avoid interruption or slipping of forms in the piers of the service bridge, and also to avoid splicing of bars by overlapping in the same section, the points of splicing were arranged in two alternating rows, and thus the pier reinforcement could be installed without stopping the slip-form. The speed of the slip-form depended in general on the characteristics of the concrete and the ambient temperature. Normally the use of slip-forms is feasible only for rich concrete mixes with accelerator agents, and in an ambience that permits quick setting of the concrete. At Itaipu, however, slip-forms were used for mass concrete with large aggregate at a placing temperature of 7°C, as well as at relatively unfavorable conditions of air temperature and relative humidity. For example, in the massive sluiceway piers of the diversion structure, in order to minimize problems of stability, concrete with a 76 mm aggregate and 2 cm slump with a water-reducing agent was used. Placed at 7°C, this concrete had good workability and consistency and very little bleeding of water. Concrete in the slip-forms was placed in nearly level layers 30 cm high, and was consolidated by immersion vibrators. Great care was taken to ensure that the vibrators did not touch the forms and damage the freshly exposed concrete. The speed of slip-forming varied according to the size and complexity of the structure. The actual maximum and minimum rates achieved at Itaipu were 6.97 and 2.53 m/day. For hydraulic surfaces exposed to high velocity flow, for example the spillway chutes which can be exposed to a maximum water flow velocity of 37 m/s, special care was taken to control the undulation and rugosity of the finished slab. The utilization of a steel levelling template,

weighing 6 t and travelling on guides of steel trestles resulted in hydraulic surfaces practically free from irregularities.

STRUCTURAL INSTRUMENTATION AND MONITORING PROGRAM

INSTRUMENTATION PROGRAM

A comprehensive program of instrumentation for monitoring the behavior of all major concrete and embankment structures and their foundations was planned and executed as construction progressed. Over 2000 instruments were installed, about 90% being considered permanent. After 8 years of project operation, most of the instruments were functioning or useable.

Except for bench marks or survey targets and pins for measuring joint or crack openings at the surface, all other instruments were either embedded or located in the body of structures, or placed in holes drilled in the foundations. Types and functions of the instruments are:

FOUNDATIONS

- Piezometers to measure pore pressures and hydraulic uplift at selected joints or contacts in the rock mass, or at dam-foundation contact.
- Drilled drains to measure total seepage and hydraulic uplift pressures downstream of the main grout curtains.
- Multiple extensometers to measure total and differential deformations, both vertical and horizontal, of the foundations relative to the structures.

EMBANKMENT DAMS

- Piezometers for measuring pore pressures in the clay core and the core-foundation contact.
- Bench marks and targets for high precision surveys to measure horizontal and vertical displacements relative to permanent undisturbed reference bench marks at the distant banks.
- Settlement gages to monitor settlement during construction, after completion and during project operation.
- Pressure cells embedded in the embankment to measure pressures against the concrete transition walls with the concrete structures.

CONCRETE STRUCTURES

- Pendulums, of the direct and inverted types, to measure horizontal deflections of concrete structures, as well as the absolute horizontal deformations of the rock foundation and the structure above it.

- Bench marks and targets for measuring horizontal deflections of the crest of the dam relative to fixed lines of reference between undisturbed bench marks on the distant banks.
 - Pins installed across the surface of contraction joints, and cracks which occurred in some buttress blocks, to measure the openings with removable joint-meters.
 - Embedded jointmeters, installed across longitudinal contraction joints to measure opening before and after joint grouting.
 - Thermometers embedded in concrete to measure its temperature during construction and operation.
 - Rosettes of strainmeters of the Carlson type, were embedded in concrete for measuring autogeneous volume changes, creep and elastic strain, and temperature. Stresses were calculated from strainmeter data.
 - Stressmeters of the Carlson type, to directly measure compressive stresses in the concrete.
- To measure the seepage flow through the structures and their foundations, thirty one discharge weirs were installed in flumes in the galleries in the concrete structures, in tunnels and downstream of the embankment dams.

MONITORING PROGRAM

During construction most instrument readings or measurements were taken at intervals of 1 to 2 weeks. As the reservoir was filled rapidly in only 2 weeks, the instruments were read more frequently:

- Piezometers, seepage discharge and the pressure cells: daily.
- Pendulums and multiple extensometers: every other day.
- Strainmeters, stressmeters, thermometers, jointmeters and settlement gages: twice a week.

The interval between readings was increased from seven to fourteen days during the first year of project operation with essentially full reservoir.

Under normal operating conditions all instruments are monitored once a month, except for piezometers and seepage discharge weirs which are read twice a month. Precision surveys of the benchmarks to measure crest deflections are made at 3-months intervals.

Performance of each structure monitored by instrument readings and measurements is discussed in relevant chapters.

RIVER DIVERSION

RIVER DIVERSION AND COFFERDAMS	6.3
Hydrology and Diversion Flood	6.3
Selection of the Diversion Scheme	6.3
River Diversion Works and Stages	6.4
The Diversion Channel	6.5
Main Cofferdams	6.7
The Arch Cofferdams	6.23
DIVERSION CONTROL STRUCTURE	6.27
Basic Criteria	6.27
Layout of the Diversion Control Structure	6.27
Hydraulic Design of the Sluices	6.29
Structural Design of the Diversion Control Structure	6.30
CONSTRUCTION OF DIVERSION CONTROL STRUCTURE	6.33
Excavation and Foundation Preparation	6.33
Concrete Placement	6.34
DIVERSION GATES AND CLOSURE	6.35
Hydraulic Model Tests and Studies	6.36
Gate Component Design and Manufacture	6.37
Testing and Final Closure	6.43
Recovery of the Gates	6.44
STOPLOGS AND MAINTENANCE GATES	6.46
PERFORMANCE OF DIVERSION CONTROL STRUCTURE	6.47
Instrumentation Arrangement	6.47
Foundation Response	6.48
Structural Performance	6.50

RIVER DIVERSION

RIVER DIVERSION AND COFFERDAMS

HYDROLOGY AND DIVERSION FLOOD

The hydrology, meteorology and the hydrological analysis of the Paraná river basin pertaining to the design of the project are presented in Chapter 2.

For design of the diversion facilities at Itaipu a maximum flow of 35 000 m³/s was selected, which corresponds approximately to a 100-year recurrence, see Fig. 2.12 of Chapter 2.

This criterion was selected as that giving adequate security against overtopping of the diversion works during construction, coupled with acceptable economies in construction.

SELECTION OF THE DIVERSION SCHEME

The general arrangement of the diversion works is shown in Fig. 6.1. This arrangement was selected during the feasibility stage because of favorable topography, and the following technical and economic considerations:

- Rock excavated from the diversion channel could be utilized in the construction of the left bank rockfill dam, the main cofferdams and also to make aggregate for concrete.
- Construction of the rockfill dam could proceed concurrently with excavation of the diversion channel.



General view of river diversion

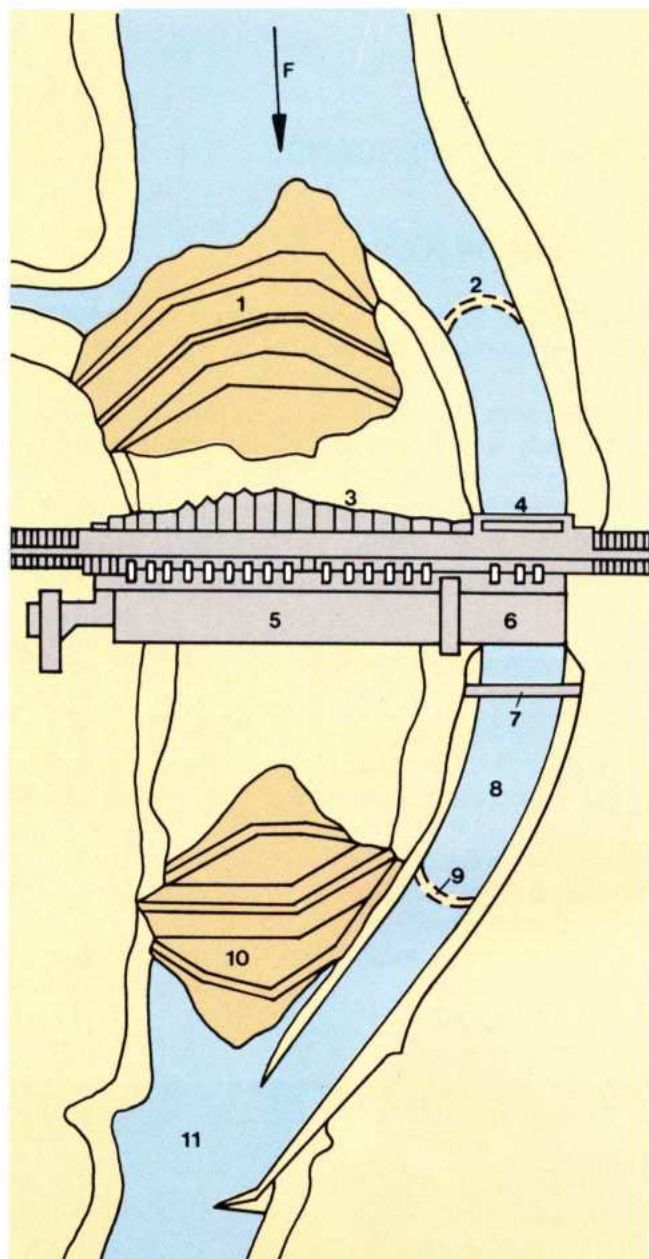


Fig. 6.1 General arrangement

- | | |
|---|---|
| 1 Upstream cofferdam | 8 Diversion channel |
| 2 Upstream arch dam (blasted at diversion time) | 9 Downstream arch cofferdam (blasted at diversion time) |
| 3 Main dam | 10 Downstream cofferdam |
| 4 Diversion control structure | 11 Paraná river |
| 5 River bed powerhouse | F Flow direction |
| 6 Diversion channel powerhouse | Note: Itaipu island was covered by upstream main cofferdam |
| 7 Service bridge | |

- Work on the spillway could proceed independently of the diversion and thus rock excavated for the spillway foundations and approach channel could also be used for the main cofferdams and aggregate.

Total excavation required for the foundations of the diversion structure, was $22.1 \times 10^6 \text{ m}^3$, of which $18.4 \times 10^6 \text{ m}^3$ was rock excavated in the dry, $2.8 \times 10^6 \text{ m}^3$ common material and $0.9 \times 10^6 \text{ m}^3$ underwater rock excavation. Of the excavated rock, $9.3 \times 10^6 \text{ m}^3$ was utilized in the rockfill dam, the remainder being used for production of concrete aggregates, transition and filter materials for the rockfill dam and rockfill for the dikes of the main cofferdams. From the right bank, rock excavated for the foundations of the right wing buttress dam and the spillway and its approach channel provided a significant portion of the $6.6 \times 10^6 \text{ m}^3$ rockfill required for the main cofferdams. Two other alternatives were also studied:

- Two-stage construction of the dam and the powerhouse in the channel of the river, the diversion being made through openings in the blocks of both the dam and the powerhouse.
- Diversion of the river via tunnels through both abutments.

The final layout was selected for reasons of safety, economy and compatibility with the established schedule for completion of the Itaipu project and the start of power generation.

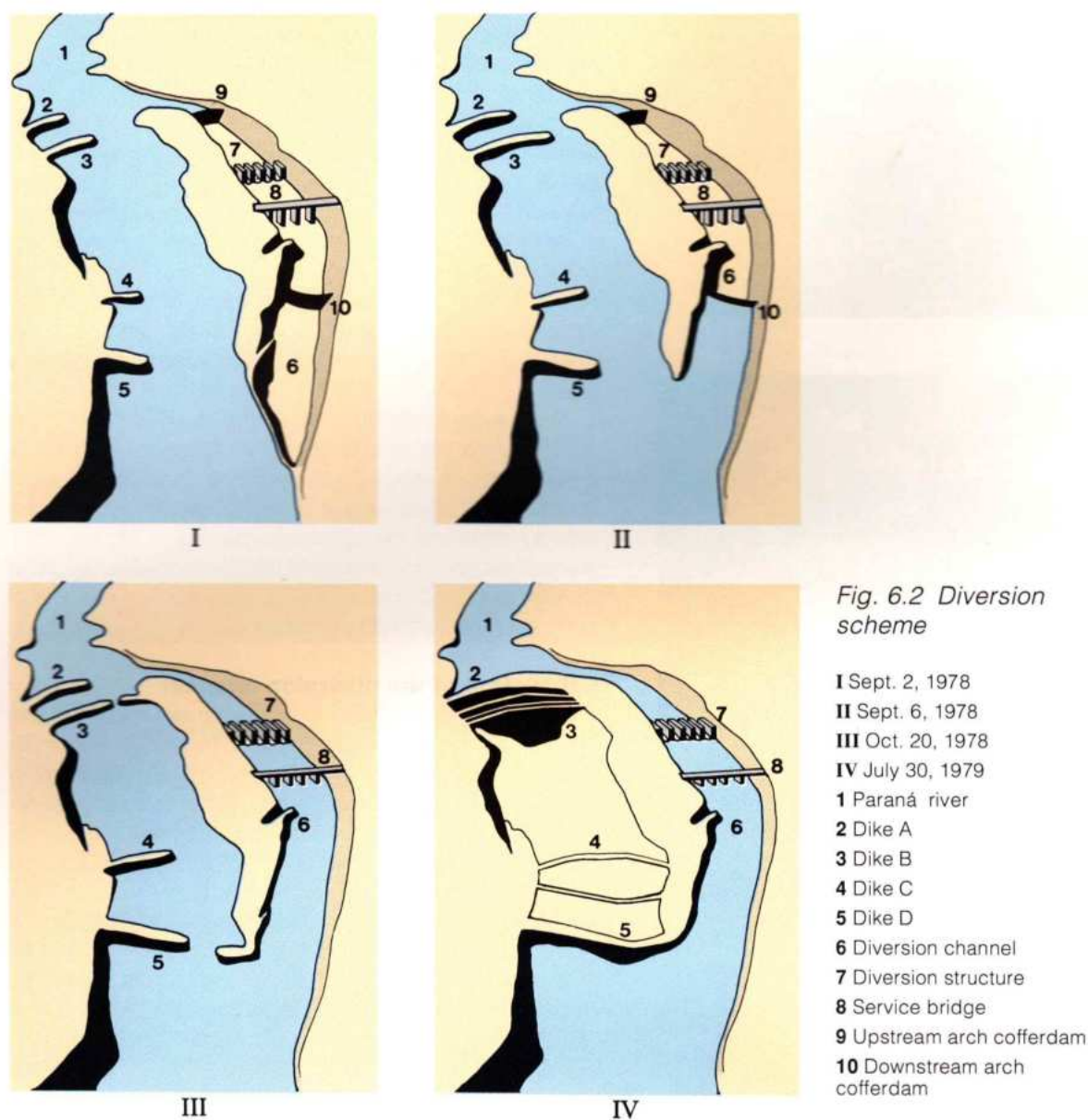
RIVER DIVERSION WORKS AND STAGES

The principal features of the Itaipu diversion works, see Fig. 6.1, were the following:

- Diversion channel.
- Diversion control structure.
- Auxiliary arch cofferdams in the diversion channel.
- Main cofferdams in the river.

Diversion of the Paraná river, to permit the construction of the main dam and the powerhouse during the period 1978-82, consisted of the following steps, see Fig. 6.2:

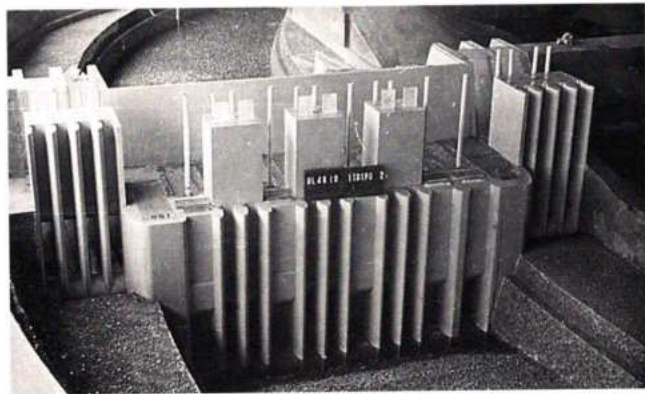
- Excavation of the diversion channel.
- Construction of the first stage of the diversion control structure to El. 120.
- Underwater excavation at the entrance and exit of the diversion channel.
- Construction of the first stages of dikes A, B and D of the main upstream and downstream cofferdams.
- Construction of the upstream and downstream arch cofferdams in the diversion channel.
- Demolition of the natural rock walls or plugs at the entrance and exit of the diversion channel.



- Demolition of the arch cofferdams and diversion of river flow through the diversion channel.
- Closure of dikes B and D.
- Closure of dikes A and C.
- Dredging of sand deposits between dikes A and B and between C and D.
- Placement of clay, for the cores of the main cofferdams by the "squeeze displacement" method in nearly still water.
- Completion of the two main cofferdams to their full heights.
- Unwatering of the work area between the main cofferdams.

THE DIVERSION CHANNEL

The geometric layout of the diversion channel, the configuration of its entrance and exit, the elevations and the grade of its bed were established after a series of tests on a 1:100 scale hydraulic model at CEHPAR (Centro de Hidráulica e Hidrologia Prof. Parigot de Souza) Laboratory in Curitiba, Paraná, Brazil. The model represented a 3000 m stretch of the river and included the main cofferdams, the diversion channel and the diversion structure. The width of the bed of the channel tested was 150 m from its entrance up to the diversion structure,



Hydraulic model, scale 1:100

narrowing thereafter to 100 m at its exit. The elevations of the bed varied as follows:

- El. 90 at the entrance
- El. 87 upstream and
- El. 85 downstream from the diversion structure until the exit.

The sills of the sluices through the diversion structure were located at El.83. The entrance of the diversion channel was designed so as to limit the velocities along the upstream cofferdam to approximately 3 m/s for discharges up to 35 000 m³/s.

The depths of excavation for the diversion channel ranged from 20 to 80 m. The excavation slopes were 1H:20 V (H = horizontal distance and V = vertical height) with 4 m wide berms at 20 m height intervals. The exposed surfaces of basalt along the excavated slopes were compact up to El.135, above which they were fractured and of columnar shape. The predominant fractures in the basalt were vertical, spaced at 5 to 7 m. The measures taken to protect the stability of the excavated slopes were: control of blasting, installation of rock bolts, deep prestressed anchors and drilled drains, mainly in the neighborhood of the diversion structure. Accelerographs, inclinometers, joint-meters and monuments were installed to monitor the behavior of the rock surfaces during blasting.

The average velocity of the water diverted through the channel during its operating life, for all discharges, did not exceed 5 m/s. To ensure the stability of the slopes, the exposed zones of breccia and weak rock were treated by replacement with concrete and the systematic placing of anchor bolts. Prestressed anchors, wire mesh and grouting were utilized in the weakest zones or where the blasting and the rapid relief of stress had caused fracturing of the rock.

Excavation of the diversion channel

The schedule for the diversion channel required the excavation and removal of 2.8×10^6 m³ of common material and 18.4×10^6 m³ of basalt and breccia in 32 months. Priority was given to the central section of the channel, where a total of 6×10^6 m³ of rock was excavated in 18 months, in order to reach the foundations of the diversion structure and start the placement of concrete while the excavation of the rest of the channel was still in progress.

Excavation of the diversion channel commenced in the middle, near the location of the diversion control structure. Other fronts of excavation were subsequently opened from the middle towards the entrance and the exit of the channel. As the excavation neared completion, two rock plugs were left at the entrance and the exit of the channel, as shown in Fig. 6.3. See Chapter 5 for the detailed program of excavation.

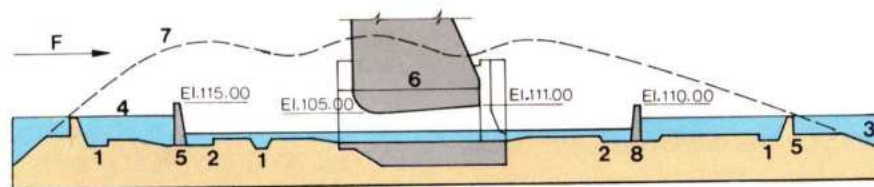


Fig. 6.3 Diversion channel profile at demolition

- 1 Rock trap
- 2 Trench
- 3 River

- 4 Natural rock plug
- 5 Upstream arch cofferdam
- 6 Diversion control structure

- 7 Original ground
- 8 Downstream arch cofferdam
- F Flow direction



Excavation of diversion channel



Underwater excavation

Concurrently with the excavation of the diversion channel in the dry, underwater excavation lowered the river bed at its entrance and exit. Approximately 900 000 m³ of material was excavated by drilling and blasting in up to 10 m of water. The excavated material was removed by a barge-mounted backhoe and hauled to designated areas away from the location of the permanent works.

MAIN COFFERDAMS

Location of the main cofferdams

The locations of the main cofferdams relative to the diversion channel are shown in Fig. 6.1. In selecting

the actual alignments for the two cofferdams, the principal considerations were: total volumes of the embankments, access for placement of the first two closure dikes, the amount of rockfill required for the closure dikes and the required working space between the cofferdams.

The clear distance between the main cofferdams was about 800 m. This provided enough working space for construction of the main dam, the powerhouse and the excavated tailrace. Natural cross-sections of the river along the axes of the two cofferdams are shown in Fig. 6.4. The average water

surface elevations at the locations of the two cofferdams, for flows ranging from 5000 to 35 000 m³/s passing through the diversion channel, are as follows:

Flow in m ³ /s	Water surface elevation (m) at	
	Upstream cofferdam	Downstream cofferdam
5000	99.2	95.2
8000	103.5	99.5
12 000	109.4	104.8
15 000	113.2	108.0
20 000	119.5	113.5
35 000	131.0	120.5

At the location of the upstream cofferdam, the river was about 500 m wide. From the right bank, for the first 350 m to Itaipu Island, the river bed was relatively flat and shallow but, between Itaipu Island and the left bank, there was a deep trench. The location of the axis of the upstream cofferdam was governed by the configuration of the entrance to the diversion channel and by the limits of excavation for the foundation of the main dam. It utilized Itaipu Island and was arched

on the right side to avoid interference with a small stream which flowed into the river from the left bank, just upstream from the cofferdam.

The location of the downstream cofferdam was governed by the exit of the diversion channel. At the chosen site of the downstream cofferdam, the river was about 400 m wide. The site was a wide V, with the deepest part in the middle of the river channel.

The location of the downstream cofferdam was governed by the exit of the diversion channel. At the chosen site of the downstream cofferdam, the river was about 400 m wide. The site was a wide V, with the deepest part in the middle of the river channel.

Deposits of fine alluvial sands and loose boulders on the river bed were detected by bathymetric surveys and drill holes at the sites of the main cofferdams. At the upstream cofferdam, sand deposits averaging 2 m covered the shallower part of the bed to the left of Itaipu Island. The deeper channel, near the left bank, was covered with 4 to 6 m of boulders and 2 to 4 m of sand deposits. Sand and boulder deposits at the downstream cofferdam were located mainly in the area of the foundation of the upstream rockfill dike. Periodic bathymetric checks also showed that the sand deposits shifted from one location to the other with the changes in the flow of the river; this was confirmed by visual inspection of river banks over several seasons. The probable movements of these alluvial sand deposits particularly under the clay zones were thoroughly investigated by hydraulic model tests. As discussed later, an important phase of the construction of the main cofferdams was the dredging of alluvial sand and the removal of boulders from the contact areas of the two clay cores with the bedrock.

Design of the main cofferdams

During the relatively low flow season, from May to November, the average discharge of the Paraná river is 6500 m³/s. For this flow, at the sites of the main cofferdams, river depths ranged from 30 to 35 m at the upstream cofferdam and from 40 to 45 m at the downstream cofferdam. From October to April, when the average river discharge is about 10 000 m³/s, the water at the sites of the cofferdams was 5 m deeper.

The great depths of water and high flows meant that conventional types of cofferdams, consisting of dumped rockfill with a dumped impervious zone on the outer or inflow side, would not be feasible. Also, because of the time limitations of the low flow season, construction of the cofferdams would have to be undertaken in stages in order to protect them if, because of delays or other uncontrollable factors, the partially completed embankments were overtopped.

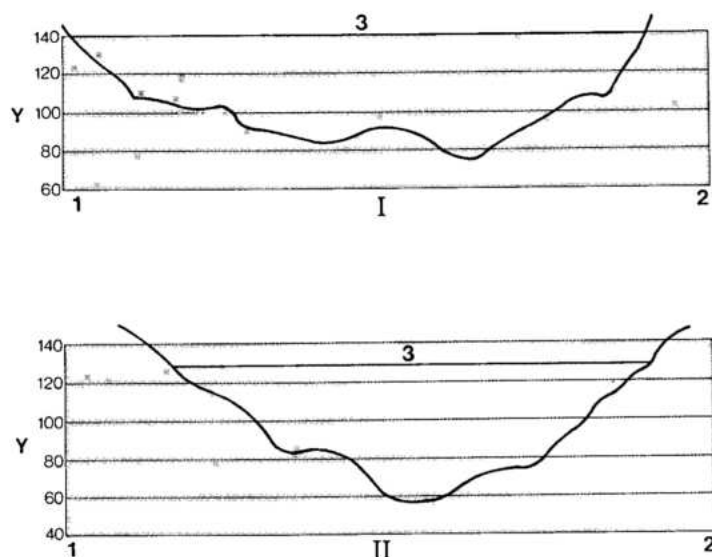


Fig. 6.4 River cross section at main cofferdams

- I Upstream cofferdam
- II Downstream cofferdam
- Y Elevation (m)
- 1 Left bank
- 2 Right bank
- 3 Crest of cofferdam

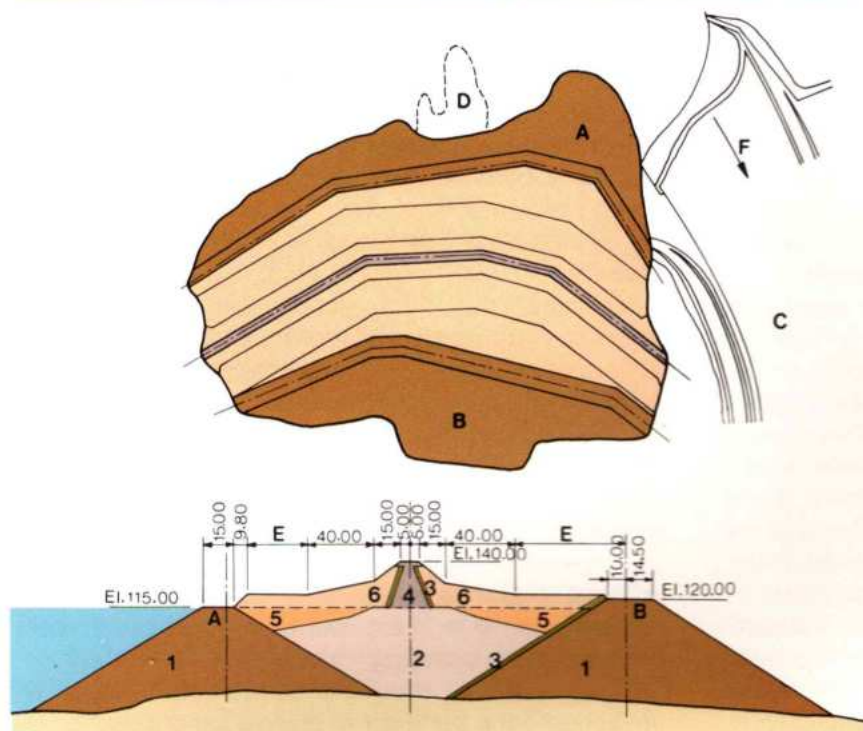


Fig. 6.5 Upstream main cofferdam

- A Dike A
- B Dike B
- C Diversion channel
- D Itaipu Island
- E Random fill
- F Flow direction
- 1 Rockfill placed in water
- 2 Clay placed in water
- 3 Transition
- 4 Compacted clay
- 5 Random placed in water
- 6 Compacted random

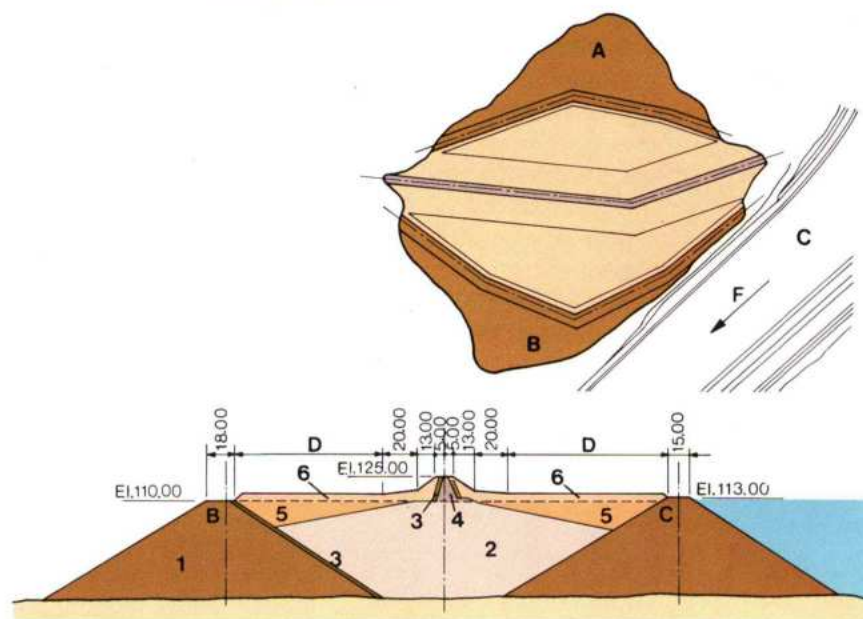


Fig. 6.6 Downstream main cofferdam

- A Dike C
- B Dike D
- C Diversion channel
- D Random fill
- F Flow direction
- 1 Rockfill placed in water
- 2 Clay placed in water
- 3 Transition
- 4 Compacted clay
- 5 Random placed in water
- 6 Compacted random

An extensive series of hydraulic model tests was conducted to check the feasibility of the various concepts and stages of construction of the two cofferdams from the view point of construction and stability. The conceptual features investigated, and later adopted, were:

- Each cofferdam would have two rockfill dikes, which could be built during the low flow seasons.
- Adequate space would be provided between the two rockfill dikes of each cofferdam for the impervious clay core.

- The clay in the two cores would be placed in the water by the "squeeze displacement" method.
- The upper portions of the cofferdams would have the section of a conventional central-core rockfill dam, and be constructed of compacted material.

The plans and cross-sections of the two main cofferdams are shown in Figs. 6.5 and 6.6. Starting from the upstream, the four rockfill dikes were labelled A, B, C and D.

The concept of design of both main cofferdams was the same, and incorporated the following considerations:

- The portion of the cofferdam above the water level would have to rest, partially, on the clay placed in the water and should be stable under various stages of construction and various river water levels, during and after dewatering between the cofferdams.
- The partially completed cofferdams would be designed to withstand overtopping without excessive damage during the early stages.

The cross-sections of the rockfill dikes were selected with conservative slopes and a crest width adequate for two-way traffic of equipment. Model tests had shown that the transverse slopes of the dumped rockfill, depending on the discharge in the Paraná and Iguaçu rivers at the time of construction, may be as flat as 1.6 H:1 V. This slope was therefore used for design purposes together with a crest width of 15 m at the elevation for dike closure; these being El.115 and El.113 respectively for the upstream and downstream cofferdams.

To assure a good seal between the clay and river bedrock, a criterion was established that the minimum width of the clay contact should be 40 m. This conservative criterion was necessary to allow for the possibility of cracks in the bedrock and the presence of boulders and pockets of sand.

Hydraulic model tests

The various concepts and stages of construction of the main cofferdams were verified on the 1:100 scale model at the CEHPAR Laboratory.

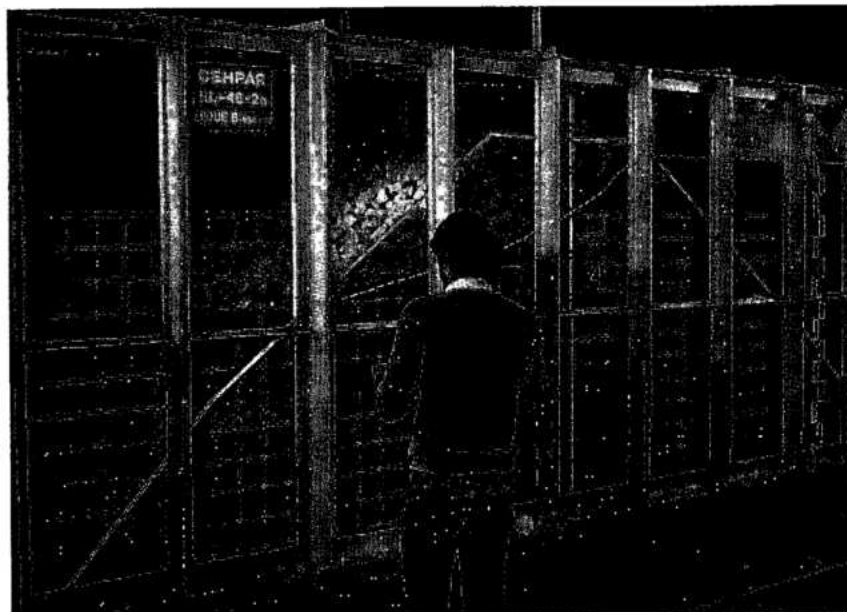
For the study of the stability of the slopes of the rockfill dikes for various flows, as well as when overtopped, a 1:12 scale flume model was used. This model was also used to study the efficacy of the transition between the clay cores and the rockfill in the prototype cofferdams.

To develop a scheme for closure of the river with the rockfill dikes, the following aspects were checked on the 1:100 scale model:

- The sequence of construction of dikes. Should closure be made with only one dike or with the simultaneous completion of two?
- Should closure be made against a bank, or in the river by building dikes from both banks?
- To minimize damage in case of overtopping, what should be the top width and cross-section of the dikes during the first stage of construction and after closure?
- What should be the sequence of closure of the dikes, including the size of material required in the different phases, for flows ranging from 5000 to 17 000 m³/s?

The hydraulic model tests were also used to investigate the behavior of alluvial sand deposits as the rockfill dikes advanced across the river. The tests showed that as the dikes for the upstream cofferdam advanced from the right bank toward the left, with the increase in velocity, the sand in the deeper part of the channel would be flushed downstream. However, there would be no significant movement of sand from near the right bank, in the area between the dikes of both cofferdams.

Principal conclusions drawn from the hydraulic model tests, incorporated into the design and the specifications and adopted for construction, were:



Dikes stability model test

- River closure should be made simultaneously with dikes B and D advancing from the right bank.
- Dikes A, B and D could be partially built before opening of the diversion channel, but the first two should not advance past Itaipu Island. All three dikes could be built during that stage with quarry run rock of any size.
- For protection against damage due to overtopping during that first stage of construction, dikes A, B and D should be 25 m wide between El. 110 and El. 115.
- Additionally the crest and downstream slopes of dikes A and B should be capped with 60 to 120 cm rocks.
- For final closure of dikes B and D, rock from 60 to 120 cm in size was required with minimum width of 15 m at the top. The tops of the closure dikes B and D would be between El. 115 and El. 113, respectively, for a maximum flow of 17000 m³/s with low backwater from the Iguazu river.

Downstream, the construction of dike C and the dredging between dikes C and D were carried out in conjunction with the construction of the clay core between dikes A and B.

The waterproofing between dikes C and D, however, depended on completion of the clay core of the upstream cofferdam, since the placement of the transition material of the slope of dike C was feasible only after water flow through the rockfill had been stopped.

Construction of the main cofferdams

From the design analysis and the hydraulic model tests, the following program for construction was established:

December 1977 to September 1978. Partial construction of dikes A, B, C and D from the right bank, prior to the opening of the diversion channel.

October 1978. Closure of dikes B and D, following the opening of the diversion channel.

December 1978 to March 1979. Closure of dikes A and C. Dredging and cleaning of river bed between the dikes of each cofferdam. Placement of clay in water to complete the cores to just above the water level.

January to May 1979. Completion of the above-water portions of the cofferdams to their final crests at El. 140 for the upstream and at El. 125 for the downstream cofferdam, and start of dewatering.

Construction of rockfill dikes

To construct the dikes, rock obtained from excavation which was not suitable for aggregate for concrete was used. The rock was classified in four grades according to its size:

Grade I <30 cm

Grade II 30-60 cm "tout venant"(as excavated)

Grade III 60-120 cm selected rock

Grade IV >120 cm large blocks of rock.

There was no shortage of grade II material as obtained from excavations for structures. However, to obtain the 800 000 m³ of grade III material required, some special controlled blasting was necessary. A total of 150 000 m³ of large blocks of grade IV rock were stored on both banks. In addition, to provide for unforeseen problems at the time of final closure, 4000 concrete tetrahedrons of 8 t each were cast and were deployed on each bank of the river.

Fig. 6.7 shows the layout of the dikes, as well as a summary of data obtained during their closure. The various stages of construction of the rockfill dikes were:

Stage 1. After removal of the common material from the abutments of the cofferdams, in 1977 dike A and B were advanced 250 m and 150 m from the right bank respectively. The objective was to facilitate flushing of the alluvial material deposited in the deep portion of the river channel and also to utilize, without rehandling, rock from excavations on the right bank. "Tout venant" material was used, protected with grade III material over the crests and at the front ends of the dikes. This protected the dikes against erosion during the flood period early in 1978. Also during the first stage, dikes C and D of the downstream cofferdam were advanced from the right bank for 85 and 110 m, respectively.

The first stages of these dikes were constructed to the full width of the section, about 5 m above the river level. Afterwards, dikes A and B were raised to El. 115 and dikes C and D to El. 110, in 60 cm lifts.

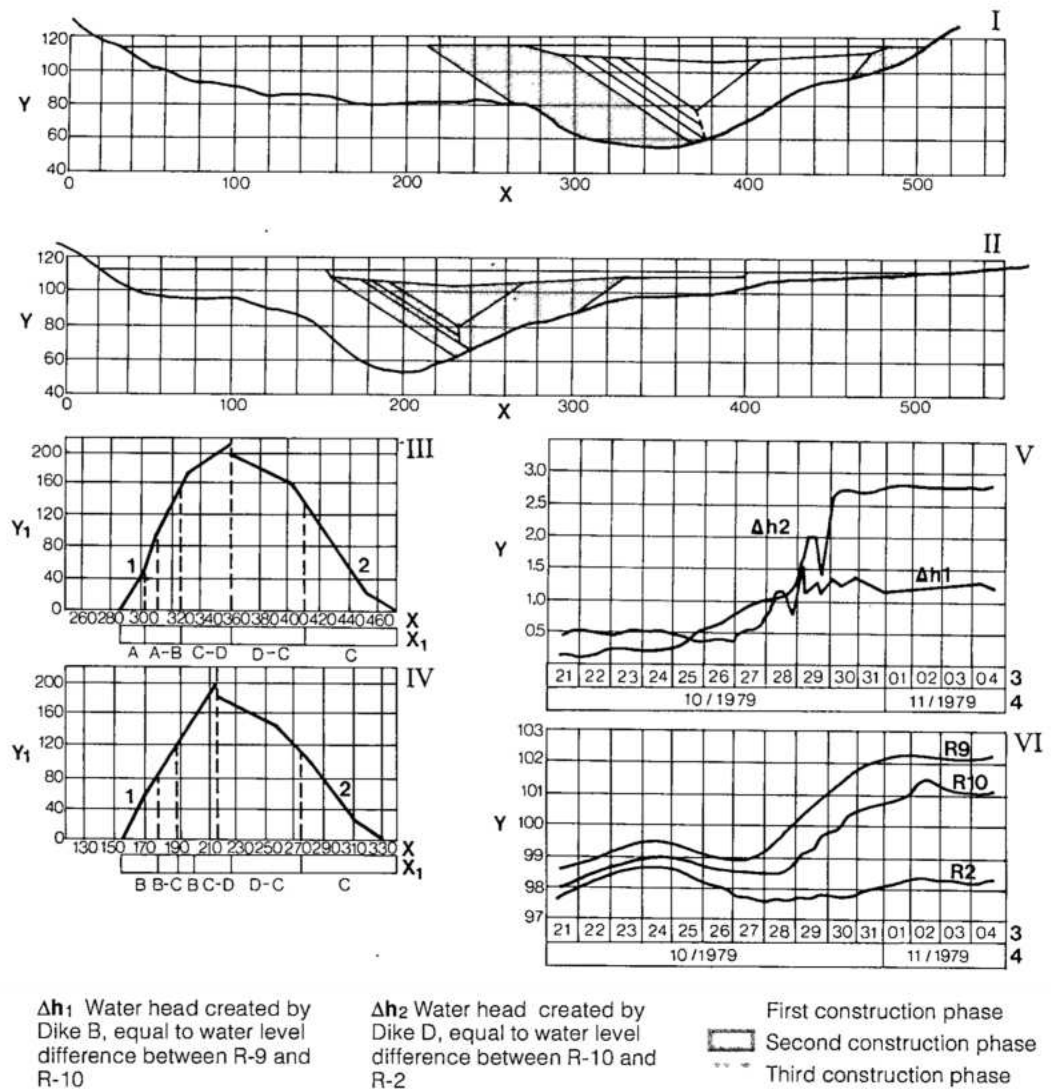
Stage 2. Five months before the opening of the diversion channel in October 1978, during the low flow period, dikes B and D were advanced further. Only grade II material was used during this stage. At the same time, some compacted clay core was constructed in the dry, in the exposed part of the abutments of the cofferdams.

Stage 3. Construction of dikes B and D was resumed immediately after the opening of the diversion channel. Model tests had indicated the practical feasibility of advancing these two dikes from both banks for parallel closure, which would minimize the loss of material due to the concentration of flow. Also, it was considered that closure should be possible with rock no larger than grade III.

For closure of dikes B and D, the work proceeded around-the-clock. Closure was made on October 30, 1978, with dike B at El. 107 and dike D at El. 104.

Fig. 6.7 Dikes band D
- material and
construction

- I Dike B - profile
II Dike D - profile
III Third phase construction evolution for Dike B
IV Third phase construction evolution for Dike D
V Water level evolution
VI Water head evolution
Y Elevations (m)
Y₁ Volume of placed material (10³ m³)
X Stations
X₁ Class of placed material
1 Material placed from the right bank
2 Material placed from the left bank
3 Day
4 Month and year
A Quarry material up to 30 cm size
B Quarry material up to 60 cm size
C Quarry material from 60 to 120 cm
D Selected material larger than 120 cm
R-9 Gage installed upstream of Dike B
R-10 Gage installed between Dikes B and D
R-2 Gage installed downstream of Dike B



Thereafter, both dikes were rapidly raised to their full heights; dike B to El. 115 and dike D to El. 110. For this portion only grade II material was used.

Stage 4. During stage 4 dikes A and C were completed to their full lengths across the river. Also, the slopes of dikes B and C were covered with grade I material to minimize the volume of transition material to be placed between the rockfill and the clay core.

At the time of the closure of dikes B and D, the following conditions prevailed:

Discharge of Paraná river	8100 m ³ /s
Discharge of Iguaçu river	1000 m ³ /s

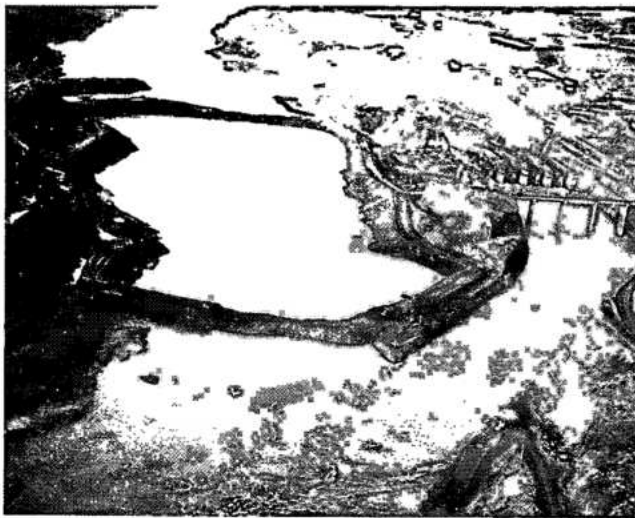
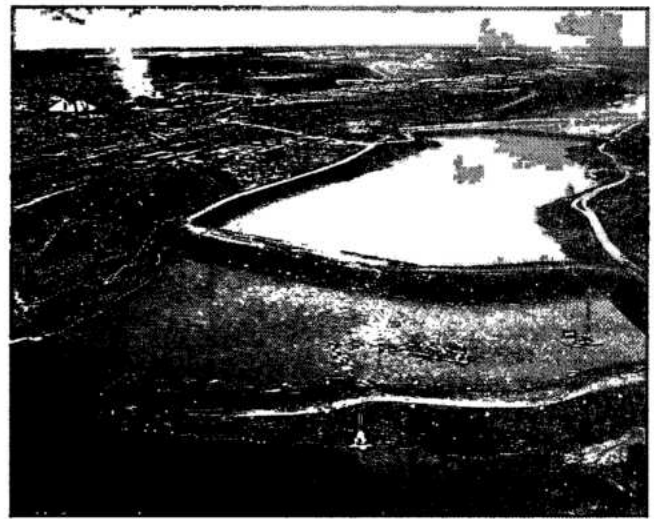
Corresponding water levels, (see Fig. 2.9 of Chapter 2):

At R - 9, upstream of dike A	El. 101.50
At R - 10, between cofferdams	El. 99.52
At R - 2, downstream of dike D	El. 97.74

The successful closure of dikes B and D, ahead of schedule, was attributed to the favorable flow conditions in both the Paraná and Iguaçu rivers and the excellent performance of the construction equipment.

Removal of alluvium from clay core foundations

With all dikes closed, a crucial step was the removal of alluvial sand and boulders from the foundations,



Sequence of construction of the dikes for the main cofferdams

Dredging between dikes

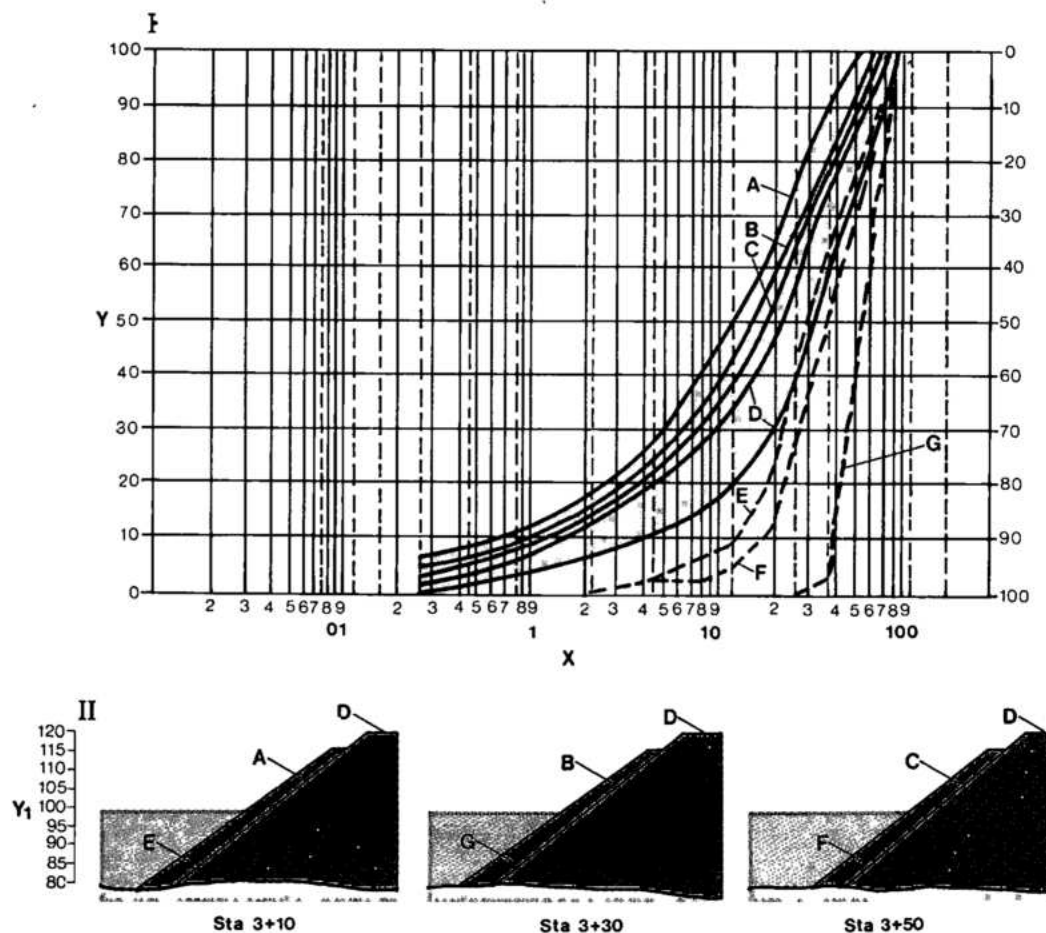
before the placement of clay in the water could commence. This operation consisted of the removal of large boulders by a clamshell and of the sand by dredging. For dredging, a hydraulic suction dredge with a 610 mm suction diameter, a 508 mm delivery diameter, and a 1262 l/s centrifugal pump powered by a diesel engine of 808.82 kW was used. It was supplemented by a 294.12 kW high pressure jet pump of 126.2 l/s, to allow the nozzle to pick up a high concentration of solids at depths up to 60 m. The dredge had a 610 mm diameter, a 70 m long suction line and up to 600 m of flexible pipe discharge line, which delivered the sand upstream of dike A and downstream of dike D. The total capacity of the dredge was 8330 l/s. A barge-mounted crane with a 3.8 m³ clamshell and orange-peel buckets removed the larger boulders from the river bed ahead of the suction dredge. For dredging the sand, two or three passes were required, the work proceeding from toe to toe of the dikes in a direction normal to the axis of the cofferdam. Between dikes A and B, a 29 400 m² area was dredged. In the final pass a 40 m wide strip along the axis was swept clean of the sand.

The efficacy of the dredging operation was checked by side-scan sonar, as well as with a television camera complete with video recorder. With the use of high-intensity lights and injection of clear water, the TV camera gave an excellent picture of a 1 m² area showing fist-size boulders. Jet probing and soundings near the toes of the dikes, and checks by a diver supplemented the sonar and television surveys.

After completion of dredging between dikes A and B, the dredge barges were floated through a shallow breach excavated in the latter to commence

Fig. 6.8 Upstream cofferdam transition material

I Grading curves
II Cross sections
Y Percentage
Y₁ Elevation (m)
X Opening of sieve (mm)
A,B,C Samples collected from the slope, above water level
D Samples collected from the top of dike
E,F,G Samples collected from the slope, under water level
Sta Station
 — Grading of samples collected from the slope, above water level
 --- Grading of samples collected from the slope, under water level
 [Water symbol] Water
 [95% reliability strip symbol] 95% reliability strip from samples collected on top of dike
 [Transition material symbol] Transition material
 [Rockfill symbol] Rockfill



dredging between dikes C and D. Dredging between dikes C and D followed the same procedures as used for the upstream cofferdam. During the last 35% of the operation in the deepest part of the channel, the river level fluctuated over 7 m in one week. This required operating at a depth of 60 m of water which tended to collapse the suction line.

Placement of transition material

Transition material between the clay core and the rockfill was placed on the upstream slope of dike B and the downstream slope of dike C. It was composed of processed breccia less than 7.6 cm in diameter. This gradation being essentially governed by the crushing operation. The breccia was pushed down the slope by bulldozers from windrows placed at the top of the dike.

Some field tests were first made to observe the behavior of transition material placed in this manner. It was found that underwater, as well as in the dry, the slope of repose of the transition material was essentially the same as the slope of the rockfill. The transition material was placed after the alluvial deposits on the river bed had been dredged.

The material was transported by trucks to the crest of the dike and piled 3 m from the edge of the slope. After two truckloads had been accumulated, the material was pushed by a bulldozer, first to the edge and then very slowly downward in order to avoid segregation as much as possible. Grading of the material thus placed was constantly analysed. Placement of the transition material was made in two stages. The first, with a 3 m wide layer at the top; bathymetric surveys checked its progress along the whole slope. In the second stage, an additional layer 2 m wide at the top was placed up to El. 115 in the upstream cofferdam, in order to assure the 3 m minimum specified thickness.

After the placement was concluded, gradation of the material was checked at different depths, as shown in Fig. 6.8. These checks showed that:

- Above the water level there was no significant segregation.
- At about 10 m above the foundation, the material was partially segregated, but its grading curve was still within the specified range.
- Samples collected at the foundation level in the deepest channel of the river showed considerable segregation. The difficulty of collecting samples at

great depths of water did not permit a definitive conclusion on whether segregation occurred only on the surface of the slope or in the full thickness of the transition layer. Thus as a safety measure, a layer about 2 m thick of artificial sand, 12.7 mm maximum size, was placed in the deepest channel. Later, from samples collected by a diver, it was proved that the segregated portion of the transition had been totally covered by this fine material.

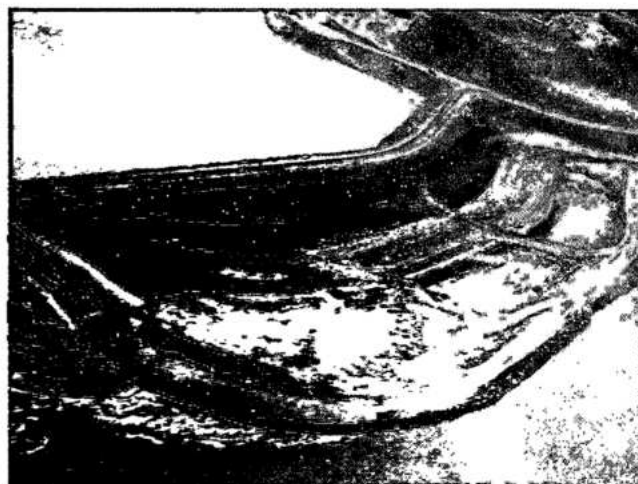
Placement of clay in water

Experience with other projects in placing large amounts of clay in deep water to obtain an impervious core indicated that the "squeeze displacement" method would be the more practical one for the Itaipu cofferdams. In this method, large masses of clay are steadily pushed into the water, without breakdown or dispersal of the material. Among others, this method had previously been employed at Arrow dam in Canada, Loussajarvi dam in Sweden and for a roadway embankment in the Billings reservoir in Brazil. In the first two examples the material used was glacial till, but in the third it was clayey material. However, in none did the water depth exceed 20 m.

Since at Itaipu the material to be placed in water for the cofferdams was a residual clay, it was decided to conduct a large scale field test to study the placement technique and to evaluate the properties of clay before and after placement. About 20 000 m³ of clay were used in the test which was conducted upstream of the partially completed dike A and extended about 50 m into a maximum depth of 12 m of water.

Important conclusions obtained from these tests, and later incorporated into the specifications and techniques actually employed for placement of the clay in water for the two cofferdams, were:

- The placing level of the clay at the front should not be more than 1 m above the water.
- Windrows of two or three truck loads or of about 50 to 60 m³ would be sufficiently large.
- Two or four heavy bulldozers working in pairs could adequately handle this size of windrow.
- The bulldozers should drop their blades and push downward to squeeze the material and make it slide down "en masse".
- For the first 2 or 3 days after the start of continuous placement a thin layer of material would extend along the river bed for about 150 m from the front. This material would be almost slurry and be pushed away by the advancing clay. About 2% of the material could be lost in this manner.
- The following characteristics of the clay should be expected after placement: high air content and negative pore pressures, moisture content 5 to 8%



Placing clay in water

higher than before placement, high compressibility and continuous long-term settlement and relatively high impermeability.

Initial estimates indicated that about 3.7×10^6 m³ of clay would have to be placed underwater at an average rate of 1570 m³/h. Since completion of the cofferdams had priority, earthmoving equipment was transferred from foundation excavation activities. The sequence was as follows, see Fig. 6.9:

- The material excavated in the borrow areas, at its natural moisture content, was hauled by the dump trucks, which piled it up on top of the already placed clay about 3 m from the edge. When about 60 to 90 m³ of material had accumulated in the windrow, a pair of bulldozers working 1 to 1.5 m above the water level, pushed the material downward. All precautions were taken to avoid sliding of the material over the slope, and its consequent saturation and dispersal.

Fig. 6.9 Upstream cofferdam clay placement into water

- I Plan view
 II Scheme of placement
 1 Dike A
 2 Dike B
 3 Center lines
 4 Progressing clay core placed into water
 5 First phase; clay delivery
 6 Second phase
 7 Third phase

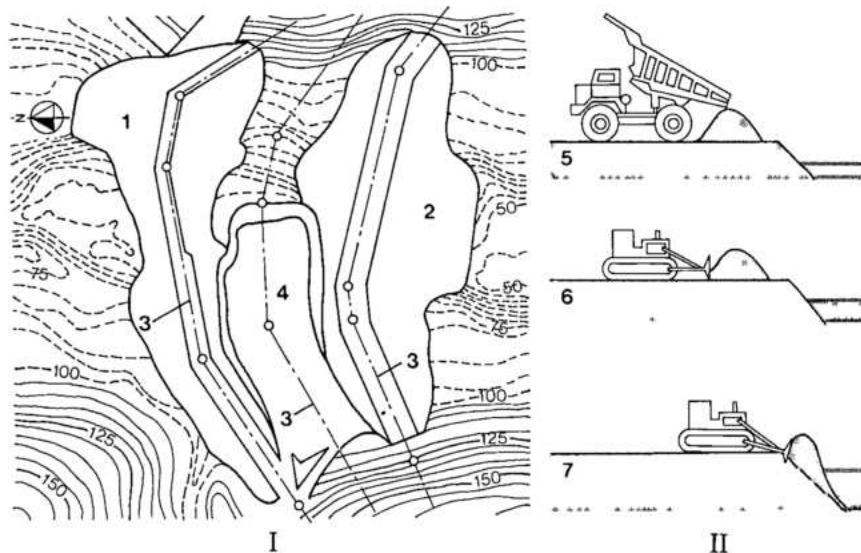


Table 6.1 Equipment used for placement of clay

Equipment		Capacity	Quantity					Total
			A	B	C	D	E	
Loading	Bucyrus 195	10 m ³	1		1			2
	RH 75	7.5 m ³	1			3		4
	CAT 992	7.5 m ³	4		3	1		8
Transportation	Wabco 75	75 t	19		17			36
	Terex 3309	52 t	6	10	5	10		31
	Scrapers	15 t	8	7				15
Excavation and Spraying	D7		2					2
	D8		6	2	1	3	7	19
	Patrol 16:6		1				1	2
	Patrol 120		1					1

A = Borrow area "E"
 E = Core

B = Borrow area "D"

C = Stock pile 13

D = Stock pile 18

- As the front was advanced, the core portion already placed was raised to El. 110 in 10 cm lifts compacted by pad type tamping rollers.

- Simultaneously, the lateral fills in Fig. 6.5 and 6.6, were also advanced by the placing random rock, so as to confine the clay already placed. Because of the exceptionally favorable water levels, it was possible to place the clay in water at an elevation 5 m lower than expected. Besides accelerating placement, the low water levels resulted in the upper part of the core, which was assumed in design as placed in water, being dry and compacted. This confined the underwater clay and improved the stability of the cofferdam.

- At the upstream cofferdam, clay placement started from the right abutment on December 20, 1978, with the water level at El. 100, and was concluded on January 12, 1979, with the water level

at El. 105. The volume of clay placed during this period was about $1.8 \times 10^6 \text{ m}^3$, with a maximum daily production of more than 100 000 m³. This work was completed in about half the scheduled period, principally due to the favorable water levels, excellent performance of the equipment, and strict control of the work.

- At the downstream cofferdam, the clay placement work started on February 16, 1979, and was concluded on March 9, 1979, with production rates of the same order as those for the upstream cofferdam. During this period the water level varied from El. 102 to El. 108. The only difference in the work at the two cofferdams was that at the downstream cofferdam, clay placement proceeded from both banks simultaneously.

A summary of the equipment used for placement of clay is indicated in Table 6.1.

During the in-water placement of clay for the upstream cofferdam, samples were collected for laboratory tests. However, due to the rapid pace of placement, the scheduled investigation program had to be substantially reduced and limited to sixteen percussion holes, thirteen holes for "Shelby" tube samples, and one inspection pit.

On the basis of experience acquired at the upstream cofferdam, the inspection wells and percussion holes originally scheduled for quality control of the downstream cofferdams were canceled. The quality control was limited to the collection of samples during clay placement and the execution of four holes for "Shelby" tube samples.

Characteristics of clay placed in water

To evaluate the strength characteristics of the clay placed in water, the following tests were made on the samples collected from the inspection pits and with "Shelby" tubes through the bore holes: Atterberg limits and index properties, quick undrained triaxial

compression (Q), unconfined compression, consolidation and permeability.

Fig. 6.10 shows the location of boreholes in the upstream cofferdam. Figs. 6.11 and 6.12 show the Atterberg limits, the compaction test results and the variation of moisture content. The variation in strength (deviator stress) against the moisture content is shown in Fig. 6.13, and Fig. 6.14 shows the variation in moisture content with depth.

The material was essentially a dark-brown residual plastic clay, classified as CH (see Fig. 6.11). The average value of the optimum moisture content was 32% and the average moisture content of the material just before placing in water was 2.3% above optimum. Fig. 6.14 shows that for the material sampled from the four boreholes, the upper 7 m of the clay placed in water gained very little moisture. However, below that depth, the moisture content increased to 10% or more above optimum. As it is evident in Fig. 6.12, at moisture content of 45% or more, the shear strength of the clay is about 5 N/cm^2 or less.

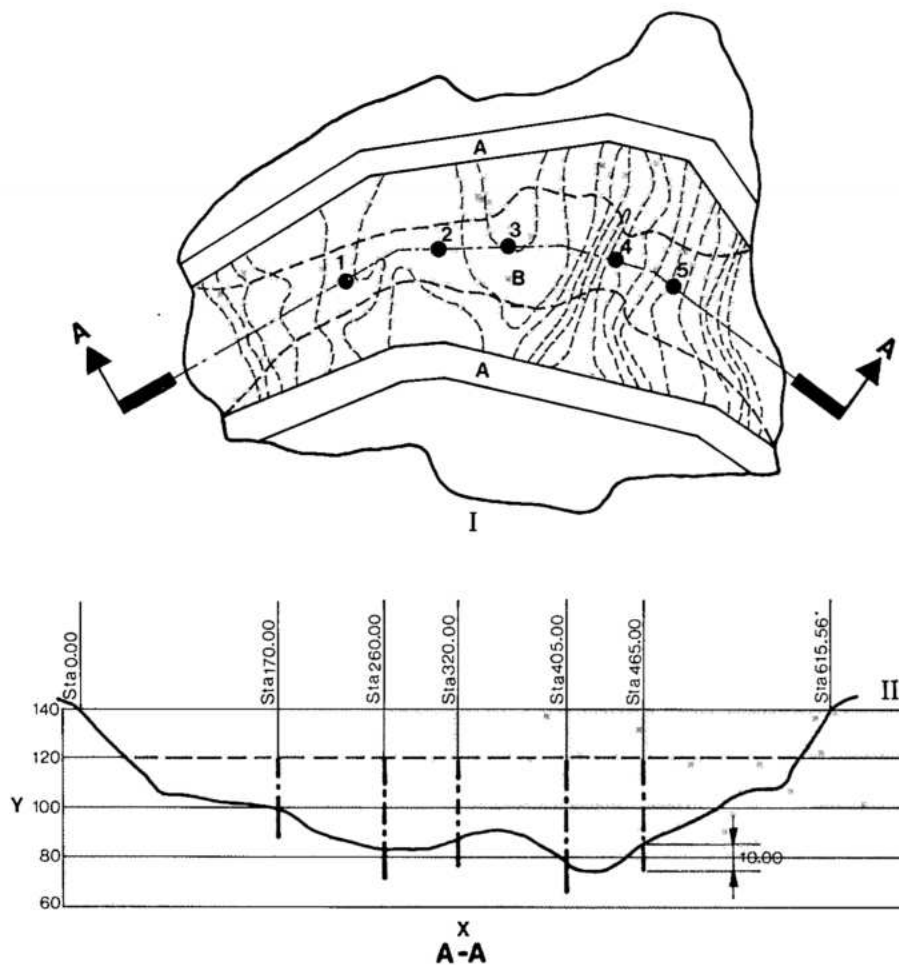


Fig. 6.10 Upstream cofferdam boreholes locations

- I Plan view
- Y Elevation (m)
- X Station (m)
- A Rockfill dikes
- B Clay core
- 1, 2, 3, 4, 5 Boreholes for "Shelby" tubes

Fig. 6.11 Upstream cofferdam material properties

- I Plasticity chart
 II Compaction chart
 Y Plasticity index
 X Liquidity limit
 Y₁ Maximum dry specific weight of soil (g/cm³)
 X₁ Optimum water content (%)
 1 U line
 2 A line
 3 Average value

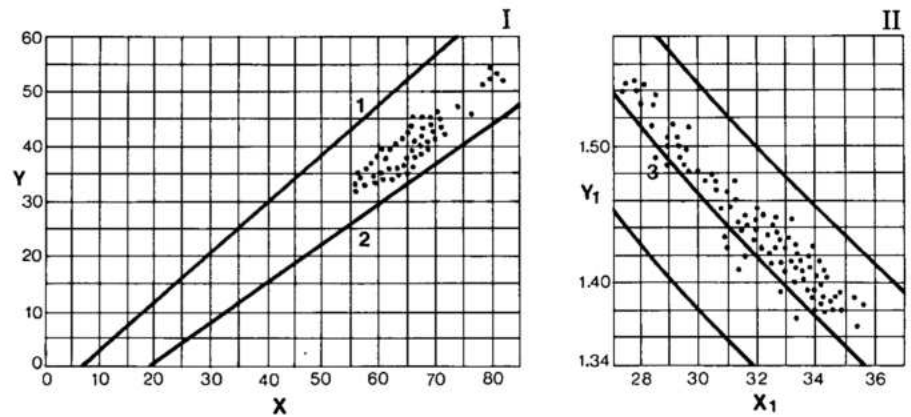
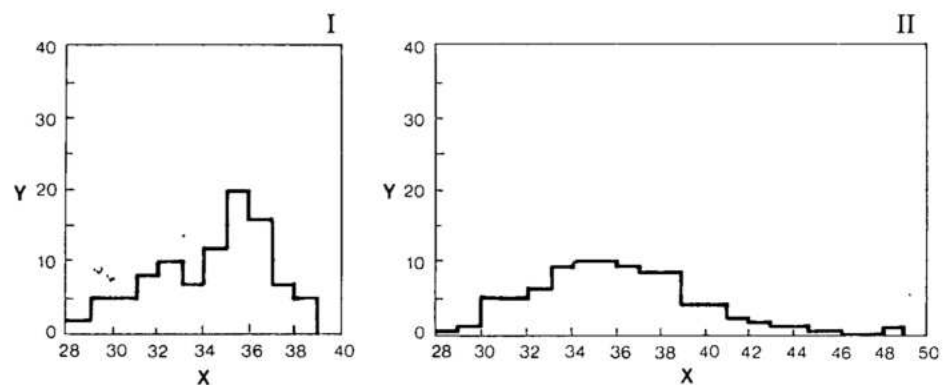


Fig. 6.12 Upstream cofferdam water content variation

- I Samples collected in the dry during placement
 II Samples collected under water after placement
 Y Relative frequency (%)
 X Water content (%)



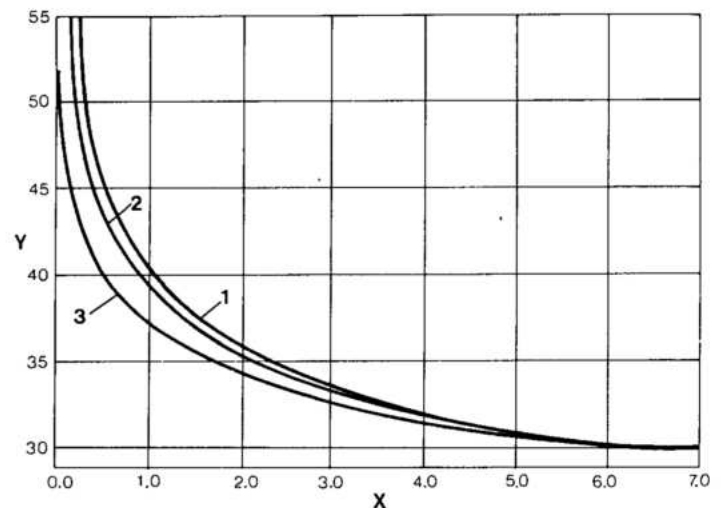
N = 140
 $\bar{X} = 34.3$
 $\sigma = \pm 2.6$

N = 451
 $\bar{X} = 36.9$
 $\sigma = \pm 4.3$

Fig. 6.13 Upstream cofferdam results of triaxial tests

A	B	C		D
		$\sigma_1 - \sigma_3$	\bar{Y}	
1	Triaxial $Q - \sigma_3 = 10 \text{ N/cm}^2$	2.34	36.56	0.85
2	Triaxial $Q - \sigma_3 = 5 \text{ N/cm}^2$	2.01	36.90	0.85
3	Compression simple	1.33	37.24	0.74

- Y Water content (%)
 X Increase of failure axial stress ($\sigma_1 - \sigma_3$) - 10 N/cm²
 A Curves number
 B Type of test
 C Average
 D Correlation factor
 Q Quick triaxial compression



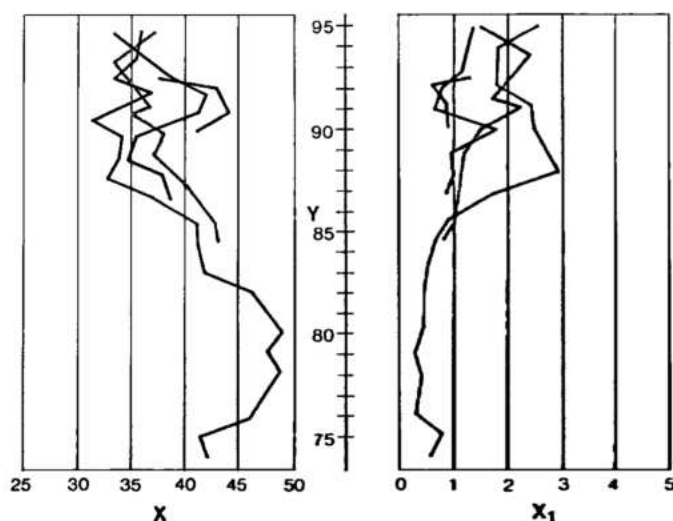


Fig. 6.14 Upstream cofferdam strength and water content variation with depth

Y Elevation
 X Average water content (%)
 X₁ Average increase of failure axial stress ($\sigma_1 - \sigma_3$) - 10 N/cm²

— Borehole 1
 — Borehole 2
 — Borehole 3
 — Borehole 4

Completion of the main cofferdams

The final stage of construction of the two main cofferdams was the completion of the portion above water level which ranged from El. 115 to El. 140 for the upstream cofferdam and from El. 108 to El. 125 for the downstream cofferdam. Construction procedures and specifications for these portions of the cofferdams were the same as for the permanent earthfill and rockfill dams, see Chapter 7.

Total volumes of various materials in the main cofferdams were as follows:

Material	Upstream cofferdam (m ³)	Downstream cofferdam (m ³)
Rockfill	4 238 000	2 471 000
Transition and filters	86 000	73 000
Clay and impervious	1 422 000	1 291 000
Total	5 746 000	3 835 000

Monitoring instrumentation of the main cofferdams

To monitor their performance during construction, as well as after completion, the following types of instrumentation were installed in both main cofferdams:

- Electric piezometers M-600 Geonor, 98 N/cm² capacity and digital counter readings.

- Stand-pipe piezometers.
- Single-plate settlement devices.
- Surface bench marks.

Items of special interest monitored by the instruments were:

- Seepage and pore pressures in jointed bedrock near the contact with the clay.
- Development of piezometric pressures in the clay cores.
- The rate and total settlement of various zones of the embankments at various depths.

Fig. 6.15 shows the location of instrumentation in both cofferdams. Several difficulties were encountered and dealt with in installing the piezometers in the soft clay placed in water. Among them were:

- Difficulty in boring holes in the soft clay, which sometimes had the consistency of mud. Bentonite slurry had to be used to complete these holes.
- Instruments were sometimes moved or made inoperative by the inflow of soft clay. The electric piezometers were protected by a galvanized pipe as the casing was withdrawn.
- Clogging of holes with mud prevented the placement of the seal and sand filter around the piezometers.

Because of these difficulties, several piezometers had to be withdrawn and reinstalled. The installation of these instruments was further complicated by the very rapid placement of the clay in the water.

Performance of the main cofferdams

Fig. 6.16 shows the development of pore pressures in the upstream cofferdam, commencing with the closure of the clay core across the river. At both stations, there was a rapid rise in piezometric pressures in the clay placed in water, as the compacted clay surcharge was added. The maximum values attained at the end of construction indicated in some cases neutral pressures equal to the total pressure. Several months after completion of construction, there was extremely slow dissipation of pore pressures. The settlement of its clay cores of both cofferdams was initially observed by single-plate settlement devices installed at the top of the material placed in water. Later, three lines of surface bench marks were installed: one along the center line of the clay core and the two others parallel to the center line at a distance of 40 m upstream and downstream. The purpose of the bench marks was to measure the differential settlements along the embankment which would indicate the start of transverse cracks.

The rate of settlement of the clay placed in water for the downstream cofferdam is shown in Fig. 6.17.

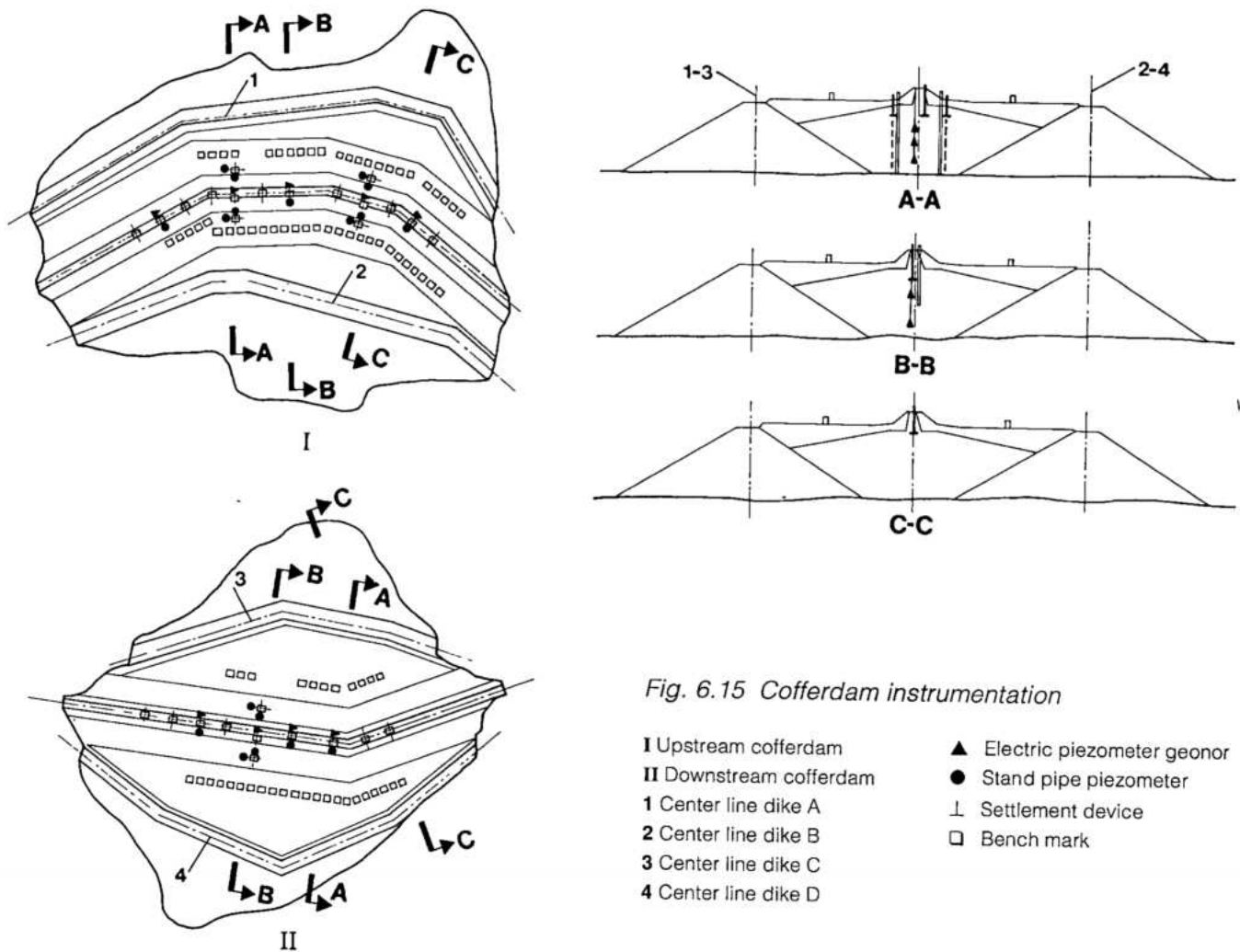


Fig. 6.15 Cofferdam instrumentation

These charts do not include the initial plastic deformation which occurred just after placement. The settlement of clay was more significant at the downstream cofferdam, since dewatering started just after the closure of its clay core. The large settlements between Sta. 4 + 20 and 4 + 70, were related to the shape of the channel, which was narrow and very deep at the downstream cofferdam. As newly placed clay advanced, the slurry at the front was trapped in the depression, forming a mass of very soft and highly compressible material.

Three years after completion of the cofferdams, settlement was still continuing, but at much reduced rates. It was noticed that the settlement measured along the center line of the portion placed in water was equal to the total indicated by the surface benchmarks. The measurements of the superficial benchmarks showed that the settlements were proportional to the fill height and generally

corresponded to the shape of the surface of the bedrock. Thus differential settlements were not great, reducing the probability of transverse cracks.

The following conclusions regarding the performance of the main cofferdams are pertinent:

- The clay cores placed in water provided an excellent seal along their contact with the bedrock.
- Both cofferdams were water-tight; the total infiltration into the work area averaging only about 5 l/s.
- No transverse or longitudinal cracks were observed in the clay cores, indicating that the deformation and the differential settlement were accommodated by the flexible core.
- The rate of consolidation of the clay placed in water was extremely slow and the strength of this soft clay was very low. Because of the confinement provided by the rock dikes and the cap of compacted material on top, the soft clay did not affect the stability of the cofferdams.

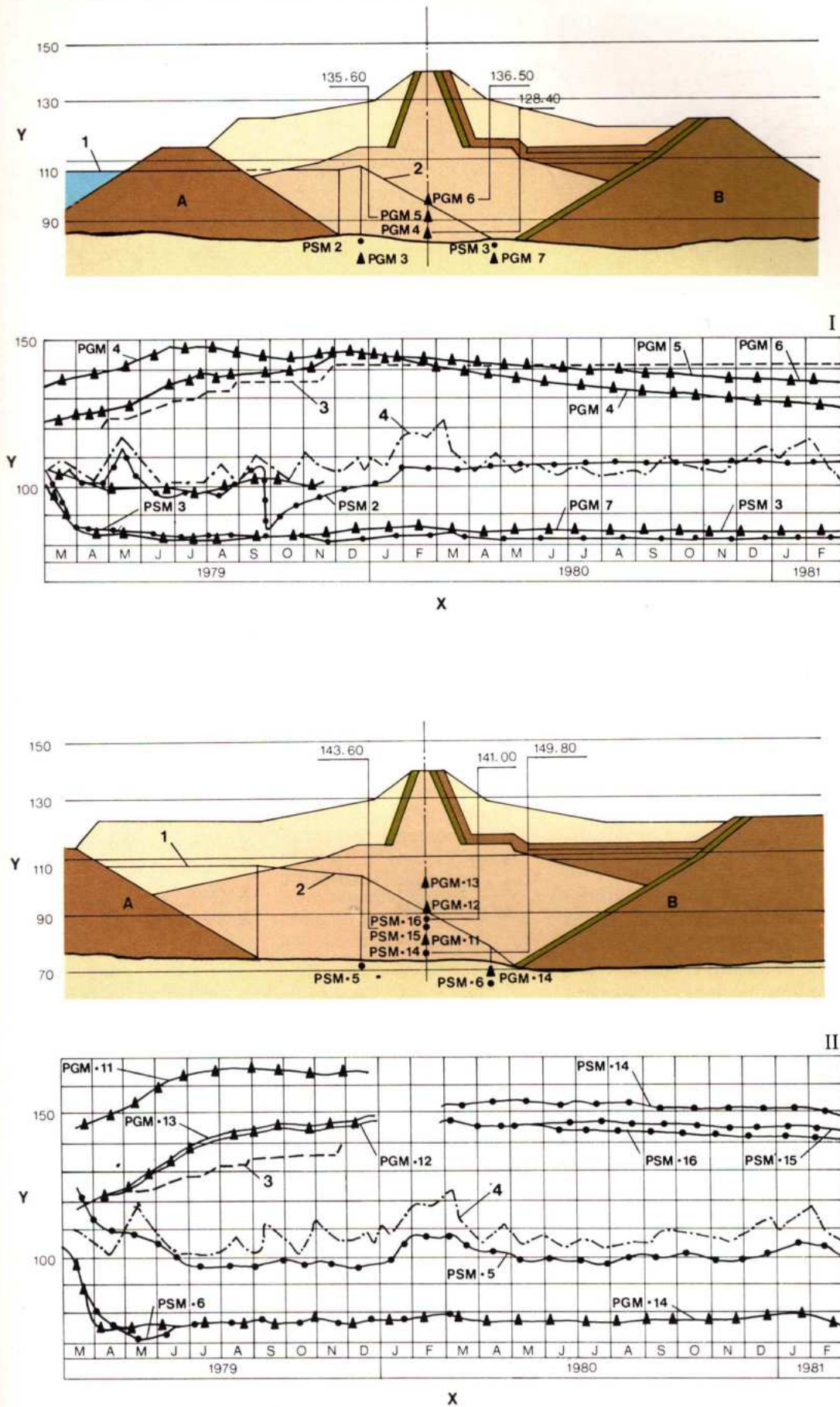


Fig. 6.16
Upstream
cofferdam -
piezometric
pressures

I Upstream cofferdam
sta. 2+55

II Upstream cofferdam
sta. 4+9

Y Elevation (m)

X Year

A Dike A

B Dike B

1 Water level on
Feb. 6, 1981

2 Piezometric level in
the foundation

3 Embankment elevation

4 Water level

PMG Electric pipe
piezometer

PSM Stand pipe
piezometer

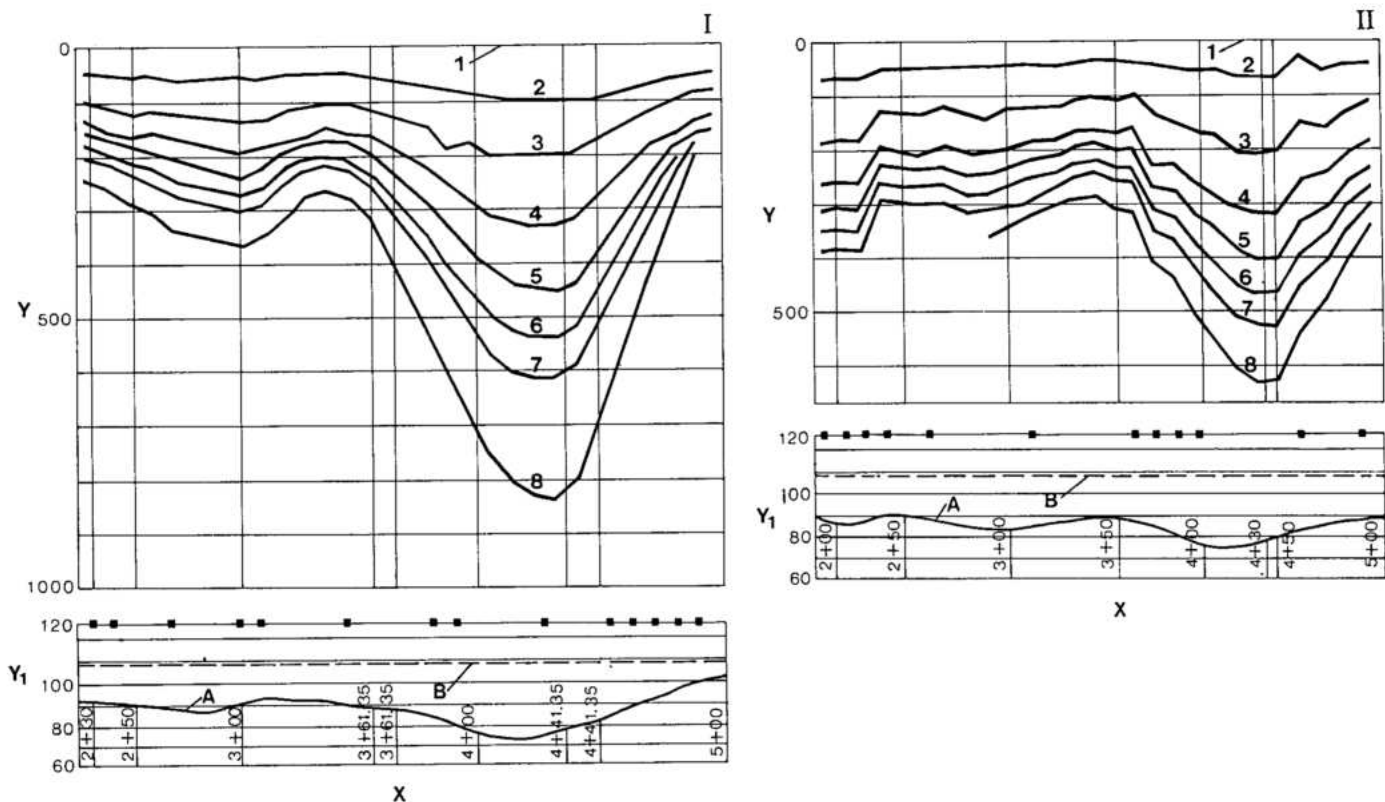


Fig. 6.17 Downstream cofferdam - settlements of clay core placed into water, longitudinal section along center line

I Longitudinal section 40 m upstream of center line

5 Jul. 21, 1980

6 Jan. 13, 1981

1 Oct. 4, 1979

7 Jan. 19, 1981

2 Jan. 9, 1980

8 Feb. 4, 1982

3 Jan. 11, 1980

Mar. 3, 1982

4 Apr. 14, 1980

II Longitudinal section 40 m downstream of center line

7 Jan. 19, 1980

8 Aug. 20, 1981

1 Oct. 4, 1979

A Rock foundation

2 Nov. 9, 1979

B Rockfill

3 Dec. 10, 1979

Y Settlement (mm)

4 Ago. 14, 1980

Y₁ Elevation (m)

5 Jul. 21, 1980

X Station

6 Oct. 13, 1980

■ Bench mark

• The overall performance of the main cofferdams at Itaipu was excellent, including during a period when flows exceeded 20 000 m³/s for 40 continuous days in 1980.

Dewatering between the cofferdams

Since the construction of the clay cores of the main cofferdams up to the water level was concluded ten weeks before the estimated time, the seven pumps specially ordered for dewatering were not yet available. Therefore, it was decided that the dewatering was to begin with the dredging equipment, after small modifications to its two pumps, which had a total pumping capacity of about 3280 l/s with the water level above El.100.

Two curves were plotted for estimating the pumping duration, one with no seepage through the cofferdams and the other with seepage ranging from 380 l/s (above El.90) to 1390 l/s (at El.55). The estimate of seepage was made theoretically, assuming the efficacy of dredging work and the absence of unlikely factors such as seepage through the foundations of the cofferdams. If the hypothesis were incorrect, the seepage could have been substantially higher, perhaps make dewatering impossible with the available equipment and necessitating costly measures such as cutoff grouting.

Fig. 6.18 shows a graph of the theoretical drawdown of water, assuming the continuous operation of the two pumps. The actual pumping operation started on March 9, 1979, with both

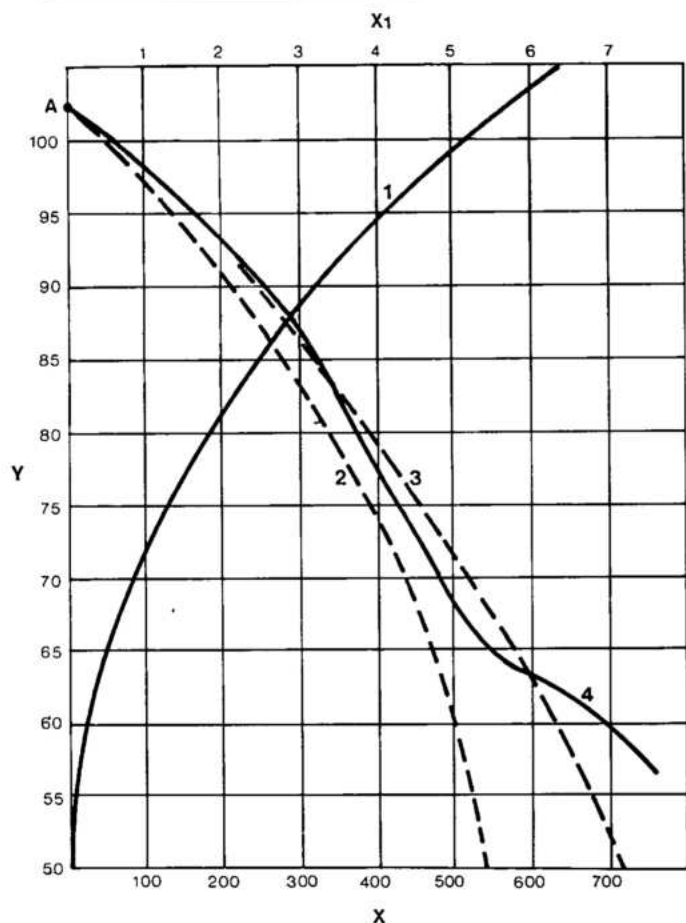


Fig. 6.18 Dewatering curves

- Y** Water level elevation (m)
X Time (hours)
X₁ Volume of pumped water (10^6 m^3)
A Start of pumping (Sept. 3, 1979)
1 Elevation/volume curve of water contained between cofferdams
2 Theoretical dewatering curve assuming nil seepage inflow
3 Theoretical dewatering curve assuming seepage inflow
4 Actual dewatering curve

dredging pumps. When the water level had reached El.84, an additional set of pumps with a capacity of about 700 l/s was used. When the water level reached El.65, the two dredging pumps were demobilized, since below this elevation the schedule made it possible to proceed slower.

To estimate the rate of seepage, pumping was interrupted for 8 hours when the water level had reached El.87 and the rise in water level measured. The seepage thus estimated was less than 3 l/s, which was confirmed after completion of dewatering.



Rock plug at entrance of diversion channel

THE ARCH COFFERDAMS

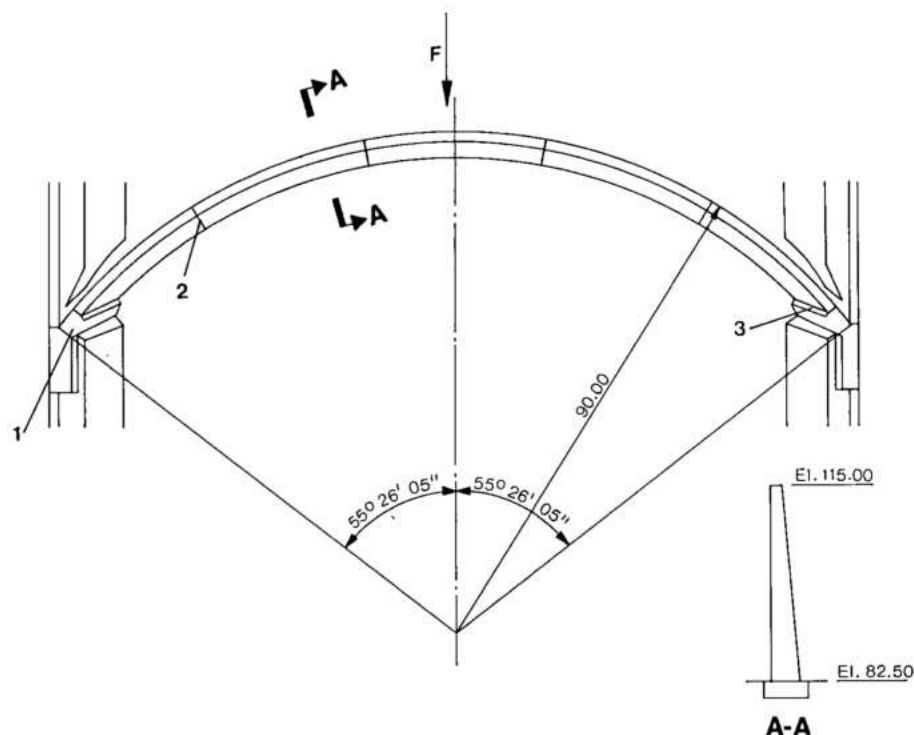
Two natural rock plugs were left at the entrance and the exit of the diversion channel. If there were a delay in the completion of the first stage of the diversion control structure and consequently river diversion deferred to November 1978 – January 1979, the natural rock plugs would not be high enough to protect the work in progress in the sluiceways of the diversion control structure. Also, the removal of the rock plugs and of the blasted rock were two critical activities, which should be completed before the diversion of the river through the sluices of the diversion control structure. Consequently, it was decided to build two auxiliary cofferdams in the diversion channel, one on each side of the diversion control structure. Construction of these auxiliary cofferdams would permit the removal of submerged blasted rock in still water in the entrance and exit portions of the diversion channel. Fig. 6.3 shows the profile of the diversion channel and the relative locations of the auxiliary cofferdams, the rock plugs and the diversion structure.

Concrete arches were selected for the auxiliary cofferdams instead of earth or rockfill, for the following reasons:

- Tight working space in the diversion channel would make access for earthmoving equipment very difficult.
- Nearby vertical banks of the channel may not be suitable for impermeable abutments for embankments.
- Demolition of an embankment by blasting may not be successful and a large amount of rock would have to be removed by barge in rapid flow.

Fig. 6.19 Upstream arch cofferdam

- 1 Pulvino (concrete thrust)
2 Contraction joint (typical)
3 Peripheral joint
F Flow direction



- The risk that some rock would not remain in the rock traps and subsequently get lodged in sluices of the diversion control structure.

Both arch cofferdams were designed as circular arches of uniform thickness assuming that the horizontal arches would carry the external loads. The central angle of the arches was 110° and the upstream face was vertical. Fig. 6.19 shows the typical plan and cross-section of the upstream arch cofferdam as well as the principal dimensions.

Maximum permissible stress in the arches was 900 N/cm^2 for a combination of water pressure and temperature change. Minimum specified strength of the concrete when 90 days old was 1.8 kN/cm^2 , with 7.6 cm maximum aggregate. Placing temperature of concrete averaged 7°C .

Construction of the arch cofferdams

Abutments for the arches were excavated in the form of notched slots in the steep slopes of the diversion channel, by line drilling and low-charge blasting. Loose blocks of rock were removed mechanically, without blasting. In locations where there were indications of potential instability, the rock abutments were anchored by 3 to 5 m long rock bolts and drains drilled on the downstream side. However, consolidation or curtain grouting was not done.

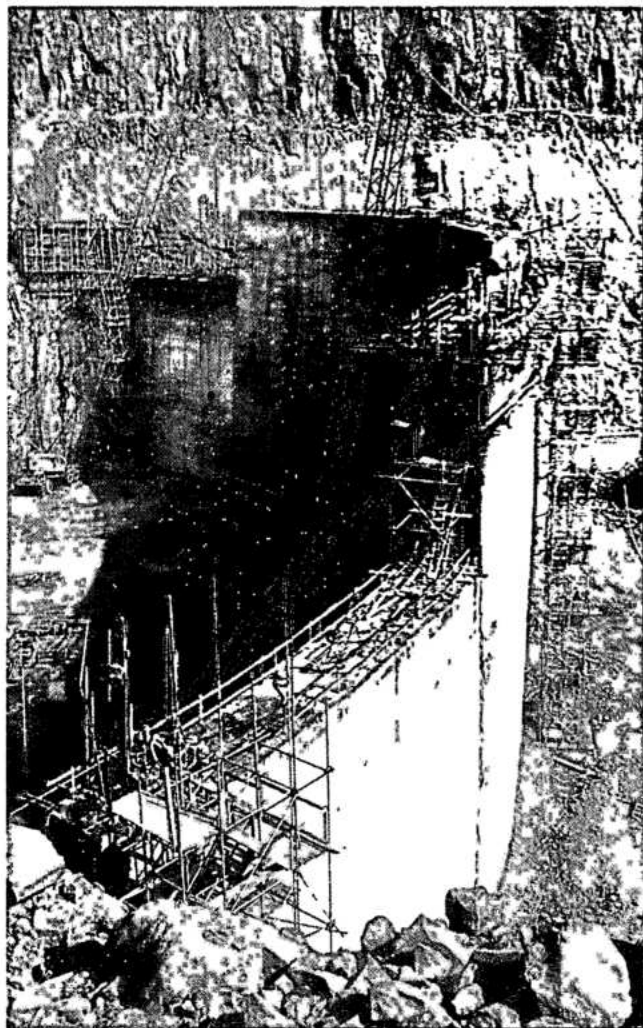
In the horizontal bed of the diversion channel, along the axis of each arch dam, a 3 m deep x 7 m wide trench was

excavated and backfilled with concrete to provide a base for the arch. For better distribution and orientation of the load transmitted by the arches to the steep abutments, pulvinos or thrust blocks of concrete were constructed along each of the four abutments, before concreting the arches, see Fig. 6.19.

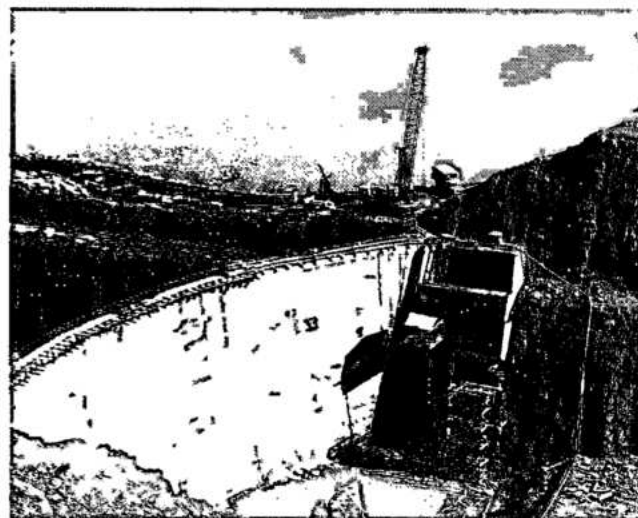
Wooden formwork for the abutment pulvinos was fabricated at the site and the concrete placed in 2.5 to 3 m lifts. Concrete was hauled from the main batch plant on the left bank, about 1 km to the arch dam sites in transit mixer trucks travelling along the bed of the diversion channel. Two mobile cranes were used to lift the buckets from the channel floor and deliver concrete to all blocks of each arch dam.

Each arch cofferdam was constructed in seven blocks formed by vertical radial contraction joints, 20 m apart at the crest. The joint surfaces were formed with vertical keys and piping and outlets were embedded in concrete for grouting them. PVC waterstops were installed on both faces of each joint and embedded in concrete in the base slab.

In the two end blocks of each arch dam, concrete was placed in 2.5 m lifts and vibrated. Construction joints were roughened by high pressure water jets. The surface of the pulvinos and the horizontal base slab, against which the arch concrete was placed, were also roughened by water jet blasting. Straight steel panel cantilever forms were used for forming the curved surface of the end blocks. The forms were stripped after 48 hours, and lifts placed at 72 hour intervals.



Construction of arch cofferdams



The five central blocks of each arch dam, were slip-formed except for the top 2.5 m. The average rate of progress of the slip-forms was 10 cm/h. Details of the slip-forming technique are discussed in Chapter 5 and in Chapter 11.

Other than the joint grouting piping and waterstops, the only embedments in the arch dams were the plastic pipes in which explosives were inserted for demolition. The arch dams, containing 22 000 m³ of concrete in the upstream dam and 13 000 m³ in the downstream dam, were completed in 4.5 months. Because of the relatively thin sections of both arches, see Fig. 6.19, by July 1982 the concrete had cooled to near ambient temperatures and the contraction joints had opened sufficiently for grouting at pressures of about 35 N/cm². A month later, the channel between the rock plugs and arch cofferdams was filled with water.

Demolition of the arch cofferdams

In August 1978, the rock plugs had been trimmed to the following final dimensions:

- Entrance plug: 6 m thick, 18 m high.
- Exit plug: 8 m thick, 12 m high.

When the arch cofferdams had been completed, construction of some features of the diversion control structure became decisive in selecting an appropriate date for diversion of the river by demolition of the arches. It was decided that diversion should be made only after:

- All sluiceways had been completed with a minimum of 5 m of concrete over the roofs.
- All guides and related embedded parts for the diversion gates and stoplogs were installed to at least 5 m above the soffit of the sluiceways.

Several alternatives were studied for the sequence of demolition of the arch cofferdams. Experience gained from the final blasting of the rock plugs at the entrance and exit of the diversion channel was utilized in evaluating the various factors involved. Basic considerations were as follows:

- Debris from demolition of the arches should fall into the rock traps around the arches. It should not pile up in heaps which could form hydraulic controls. No large pieces should enter the sluices of the diversion control structure.
- Waves resulting from the sudden removal of the arches, should not cause excessive hydrodynamic pressures against the roofs of the sluiceways.
- Vibrations in the relatively young concrete of the diversion control structure, caused by shock waves due to blasting, should not be excessive.

The remains of the rock plug at the entrance of the diversion channel were demolished under nearly balanced water levels. Soundings indicated that a large portion of the blasted rock had formed a big pile in the original location of the plug, and had not spread into the trench provided for it, see Fig. 6.3. After this experience, it was decided to demolish the remains of the exit plug under about 10 m differential head; the channel between the plug and the downstream arch being empty. This demolition was successful because most of the blasted rock fell into the trench at the back of the plug. It took 43 seconds for the wave of water to travel the 300 m distance to the downstream arch. The first wave to hit the arch was only about 1 m high and the resulting vibrations did not register on a seismograph located on the crest of the arch.

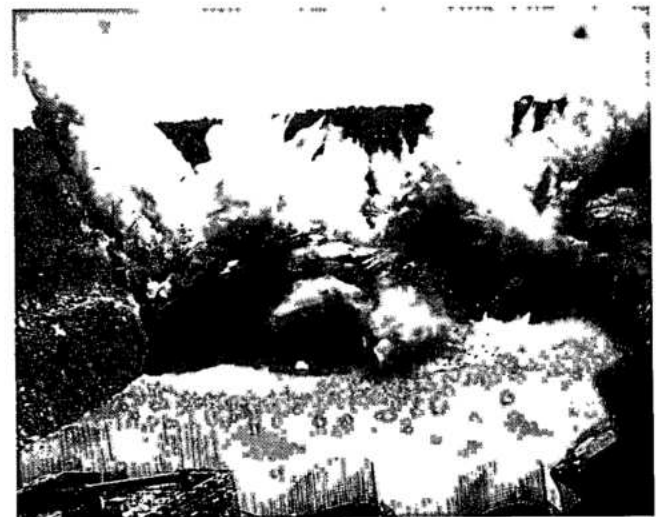
Hydraulic model tests and theoretical studies supplemented by the observations made during the blasting of the rock plugs established the following criteria for the simultaneous demolition of the two arch cofferdams:

- There should be a cushion of water, minimum 2 m deep, between the two arches.
- There should be cushion of water, minimum 2 m deep, between the two arches.
- The differential head of water against the arches at the time of demolition should not exceed 10 m.

The studies indicated that the wave front from the upstream side would pass through the sluices and meet the other front coming from the downstream side about 30 m downstream of the diversion control structure. Also, it was established that the turbulence caused by the impingement of the two wave fronts would not hit the soffits of the sluiceways, up to a river water level at El. 110 at the time of demolition.

Three alternative techniques for demolition of the arches were studied:

- Undercutting the toe of the arch and demolishing it in large panels.
- Blasting the arch into large fragments.



Blasting of arch cofferdams

Fig. 6.20 View of the diversion control structure from upstream

- 1 Top of the dam
- 2 Power intakes
- 3 Servomotor V2
- 4 Servomotor V1
- 5 Diversion gates in the open position
- 6 Diversion gates in the closed position
- 7 Upstream stoplogs in the closed position
- 8 Panels
- 9 Hydraulic units

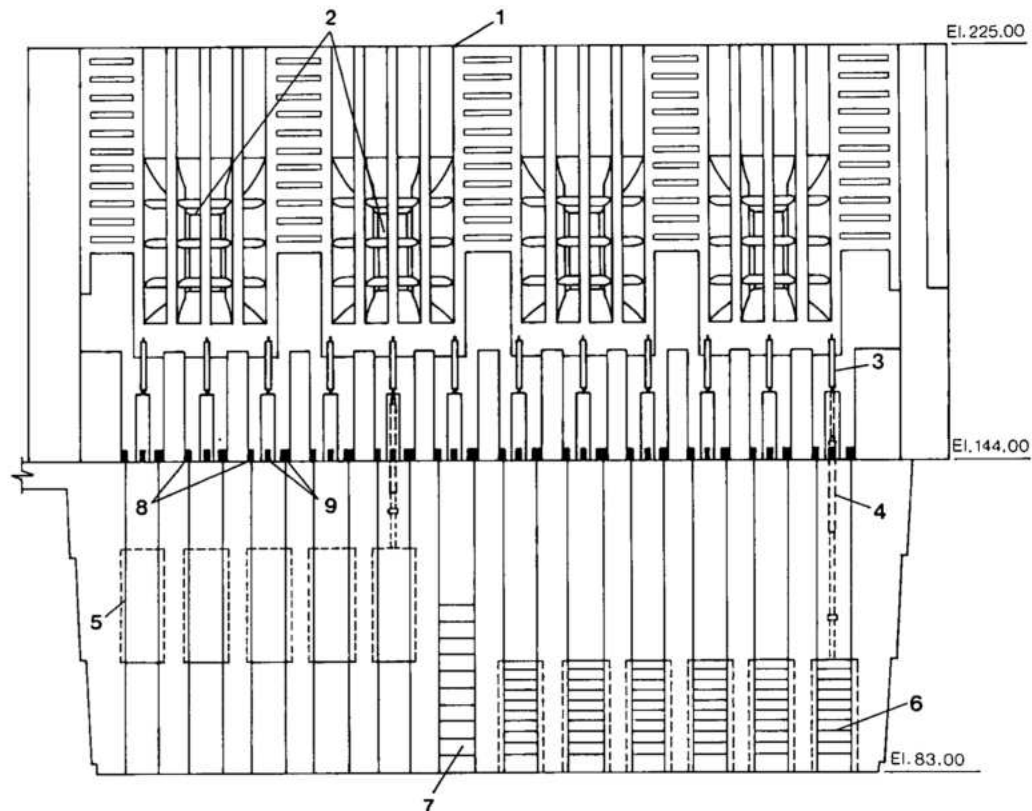
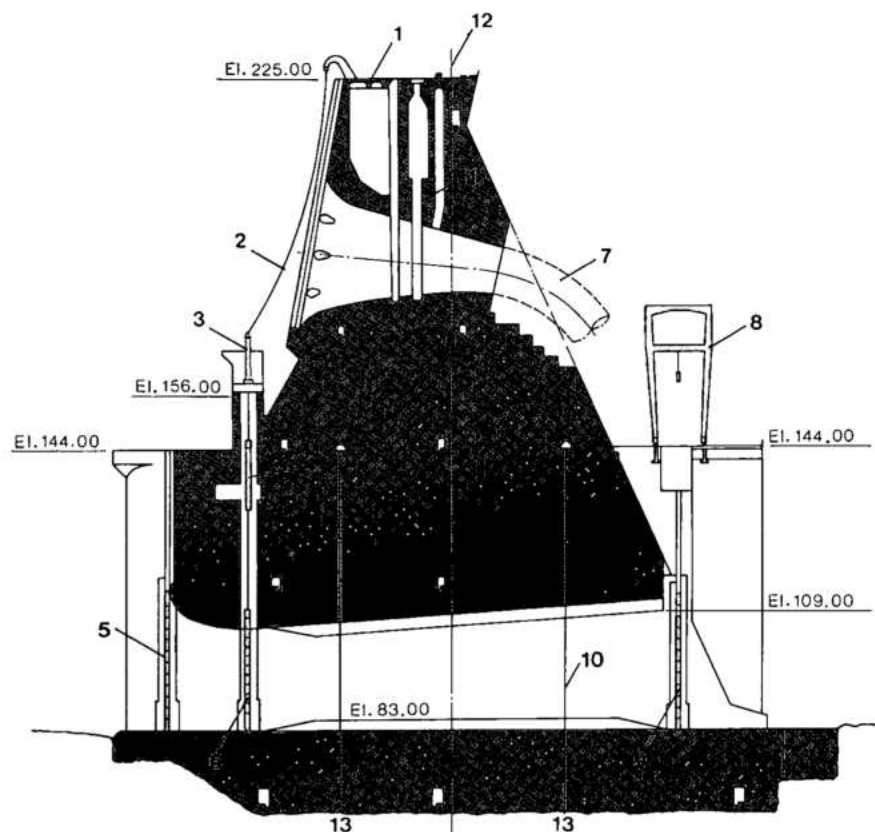
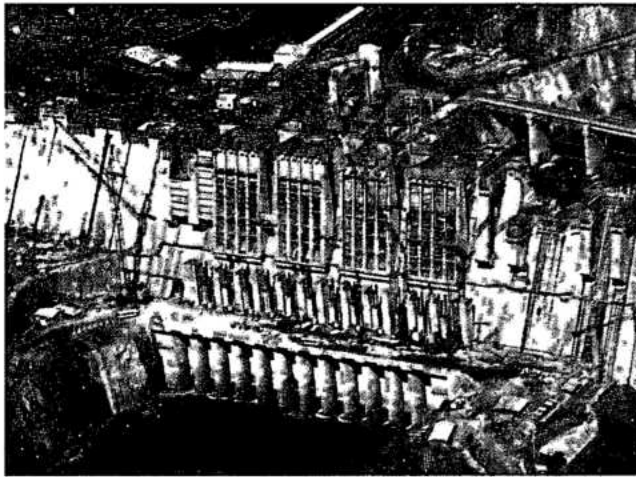
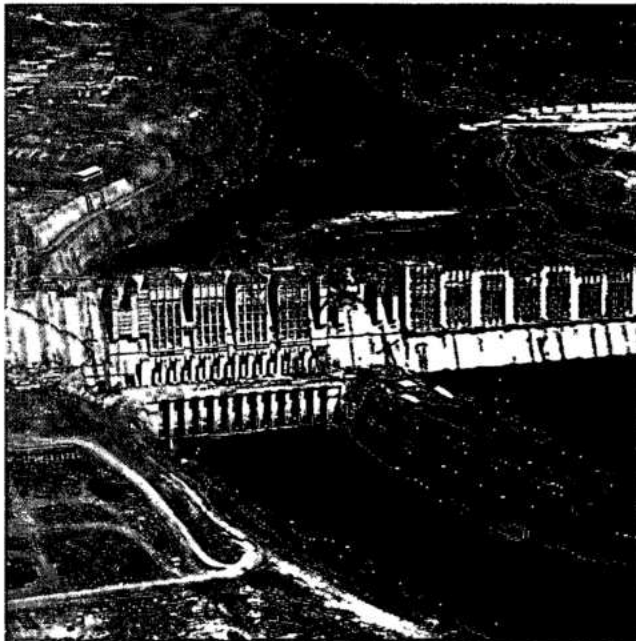


Fig. 6.21 Diversion control structure

- 1 Top of dam
- 2 Recuperation cable
- 3 Servomotor V2
- 4 Servomotor V2/V1
- 5 Upstream stoplog
- 6 Diversion gate
- 7 Penstock
- 8 Downstream gantry crane
- 9 Downstream stoplog
- 10 Diversion sluiceway
- 11 Intake gate slot
- 12 Dam axis
- 13 Longitudinal joint





Diversion control structure

Four of the blocks are 24.6 m wide and have the power intakes located in the upper part. Each of these blocks had one diversion sluice located in the middle. The five intermediate blocks are 12.3 m wide and their transverse contraction joints straddled eight diversion sluices.

The diversion control structure was mostly founded on massive basalt at El.65, except for portions of the central part of the blocks which were lowered another 2 m to eliminate some breccia and amygdaloidal basalt encountered in the area. On the upstream side, starting from the location of the diversion gate, the foundation was sloped up at 45°.

The main foundation grout and drainage curtains on the upstream side were continued from the main dam and fanned into the steep abutments. Galleries were located in the structure near the foundations, at El.70, to control and pump out the seepage flows from the foundations and to facilitate future treatment, if it should become necessary.

Platforms were located at El.144 on both the upstream and downstream side, which provided access during construction and also facilitated the installation and operation of the gates and other equipment. After the final closure, the downstream bridge and platform were partially demolished for installation of the penstocks of the powerhouse in the diversion channel.

HYDRAULIC DESIGN OF THE SLUICES

Hydraulic passages through the structure consist of twelve sluices, each 6.7 m wide and 22 m high at the gate control section, with their floor at El.83. Downstream of the gate, fillets were provided in the four corners of the rectangular sluices, mainly for structural reasons.

The hydraulic design of the diversion sluices was tested and optimized on a 1:100 scale comprehensive hydraulic model of the diversion works. The model tests indicated the following:

- For discharges of less than 12 000 m³/s, the sluices would not be submerged and the control would be provided mostly by the diversion channel.
- For low discharges (<12 000 m³/s), the tailwater levels and the backwater effects of the Iguaçu river would have a critical influence on the head losses through the sluices and the diversion channel.
- For discharges of up to 20 000 m³/s, no significant turbulence would occur at the exit of the sluices.
- For high discharges (>20 000 m³/s), the sluices would be submerged and the head losses would be mostly governed by the geometry of the sluiceways.
- Some instability of flow and turbulence would occur at the exit when flows exceeding 30 000 m³/s were passed and the flows in the Iguaçu river were lower than normal.
- The designed section of the sluiceways would be essentially free of erosion and cavitation for flows up to 25 000 m³/s.

The sluices would pass a flow of 35 000 m³/s, with the water level at El.137 at the upstream cofferdam, with a freeboard of 3 m.

As described in detail earlier, the Paraná river was diverted through the diversion channel on October 20, 1978. During more than three years of operation,

which included river discharges ranging from 20 000 to 28 000 m³/s for a continuous period of 40 days in 1980, the hydraulic performance of the diversion sluices was excellent. For all discharges ranging from 8000 to 28 000 m³/s, the actual head losses and water levels were lower than anticipated and the turbulence at the downstream end was much less than that indicated by the hydraulic model.

All sluices were closed for test purposes, one to three at a time, during the low flow periods from August through November, 1980 and from April through September, 1981. Only the first sluice, near the right abutment of the diversion control structure, had a minor amount of erosion of concrete at the junction of the right wall and the floor. The others had no erosion or other damage.

STRUCTURAL DESIGN OF DIVERSION CONTROL STRUCTURE

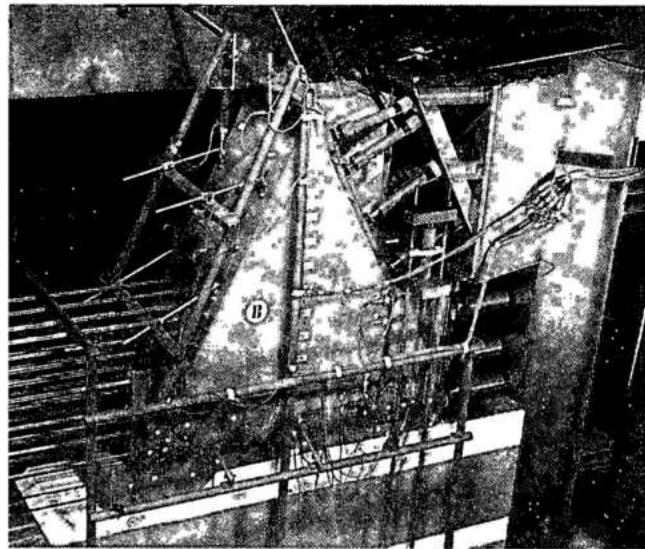
With a maximum height of 162 m and a concrete volume of 2.4×10^6 m³, the diversion control structure is a major concrete gravity dam. To control cracking, the blocks were divided into monoliths by two longitudinal contraction joints between the foundations and El.144, see Fig. 6.21. Above that level the blocks became one monolith. The longitudinal contraction joints were formed with horizontal keys and provided with an embedded pipe system to permit grouting from the galleries.

Mass concrete in the diversion control structure was mostly class A-140-f, meeting a specified minimum compressive strength of 1.4 kN/cm² at 365 days using 152 mm maximum aggregate, see Chapter 5. It was placed in 2.5 m lifts and the maximum placing temperature was 7°C. Near the foundations and for larger pours, the lift height was reduced to 1.25 m.

Stress and stability analyses were made by conventional methods. FEM analysis were made for the portion with the sluiceways.

A structural model of the diversion structure was tested at IPT, Instituto de Pesquisas Tecnológicas do Estado de São Paulo, Brazil. The model, designated model 2, was part of a series of tests which included similar models for the blocks of the hollow gravity dam described in Chapter 9.

The main purpose of the experimental model study was to verify, in the elastic range and up to collapse, the behavior of the region of the solid structure weakened by the diversion openings. The rock foundation was represented with similar



Diversion structure model

deformability but with higher strength, to ensure that the collapse would occur in the concrete structure and not in the rock foundation. For the same reason, it was not necessary to apply loads to the foundation simulating its own weight. The hollow parts of the structure above the water intake were, for ease of construction, modelled as massive parts, although the loads applied to simulate the weight of these parts were proportioned to reflect the real hollow geometry. A vertical crack was assumed to develop, under water load, below the upstream part of the structure. Its location was determined from the interpretation of FEM computations.

Considerations analogous to those for the structure of the hollow gravity dam described in Chapter 9, including the requirement of considerable depth and downstream extension of the foundation, led to selection of a geometrical scale $\lambda = 90$. Fig. 6.22 gives all the significant characteristics of the model, from which it is evident that the model had a thinner foundation slab than the final one shown in Fig. 6.21, because of the limited foundation data available at the time of model testing. Considering the materials available and the geometric scale, the degree of efficiency of the model was fixed as $\zeta = 4.8$ according to the ISMES (Istituto Sperimentale Modellie e Strutture, from Italy) technique described in Chapter 9. Concrete and basalt were simulated by a cementitious micro-concrete with pumice and diatomite, and the breccia layers by two epoxy-resin mortars. The general proportions of these materials were as indicated in Table 6.2

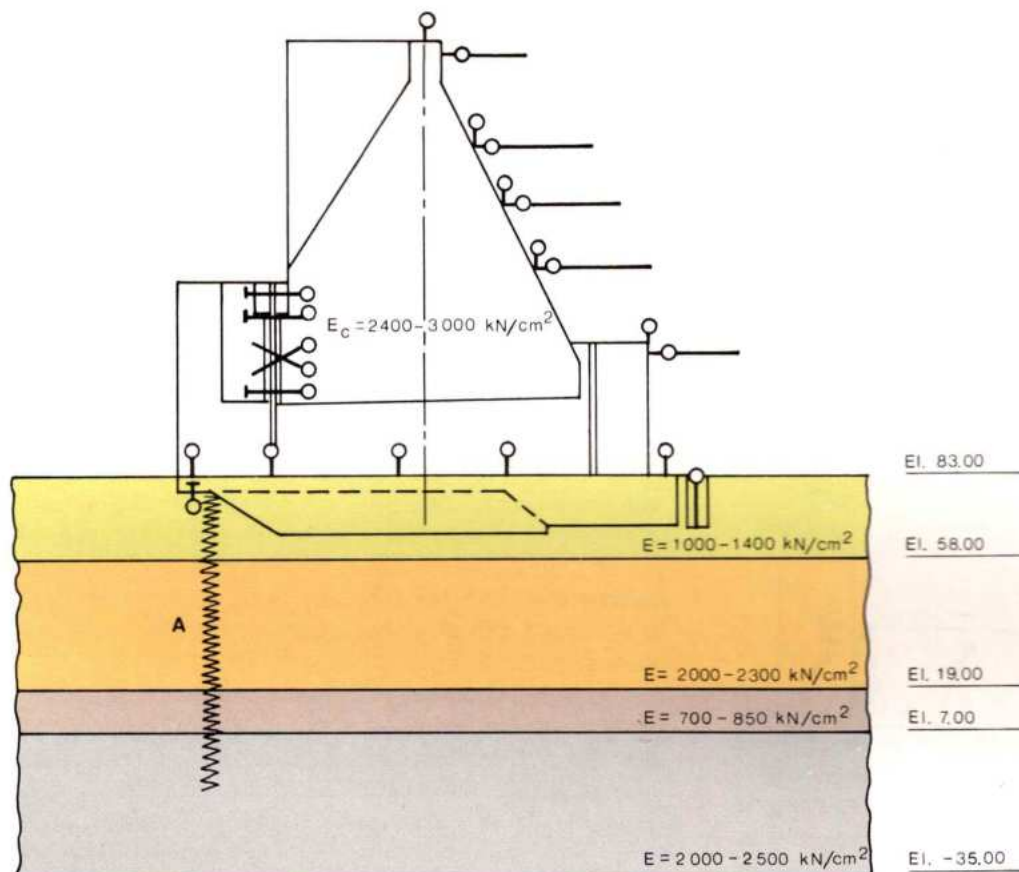


Fig. 6.22 Model 2, for the diversion structure

A Assumed upstream crack
E_c = Elasticity modulus of concrete
E = Elasticity modulus of rock

Table 6.2 Model material

Component	Concrete	Foundation		
		Basalt	Breccia layer 1	Breccia layer 2
Pumice (l)	50.0	50.0		
Pumice powder (l)	10.0	10.0		
Diatomite (kg)	2.0	2.2		
Cement (kg)	48.0	40.0		
Water (kg)	12.3	12.2		
Araldite M (kg)			0.60	0.50
Hardener (kg)			0.12	0.10
Polystyrene crystals (kg)			1.20	3.25
Sand (kg)				0.80

The weight of the concrete structure was simulated by 236 tensioned steel wires suitably distributed throughout the model structure. Each wire passed through a PVC sleeve; the volume occupied by these sleeves was only 0.4% of the total volume of the concrete structure. They were

arranged so as to go through the openings and not through the corresponding walls. The simulated water load on the concrete structure was applied directly by hydraulic jacks, while the thrust on the gates and on the crack in the foundation, as well as the uplift, were simulated by steel wires tensioned by hydraulic jacks. Horizontal and vertical displacements were measured, at the points shown in Fig. 6.22, by means of inductive Hottinger gauges of 10^{-3} mm sensitivity. Hottinger inductive strainmeters of 45 mm gauge length and 1.3×10^{-6} sensitivity were utilized to read the strains in four directions at the points shown in Fig. 6.22.

During the tests in the elastic range, some of the loading cases were studied separately, their effects being subsequently superimposed. However, for the pre-failure and failure phases, all the pertinent loads were applied simultaneously. The successive loading cases were as follows:

- In the elastic range: weight of the concrete structure, first without and then with the powerhouse excavation; weight of structures plus water load; foundation uplift; water load acting on an upstream vertical crack assumed in the rock between El.40 and El.77; and then with the crack between El.7 and El.77.

Fig. 6.23 Model 2: significant displacements during tests under increased loads

I Horizontal displacement
13, 11, 7, 3 Measurement points

Y Gravity and water loads

II Vertical displacement

1, 19, 13, 13, 11, 7 Measurement points

X Displacement in the prototype (mm)

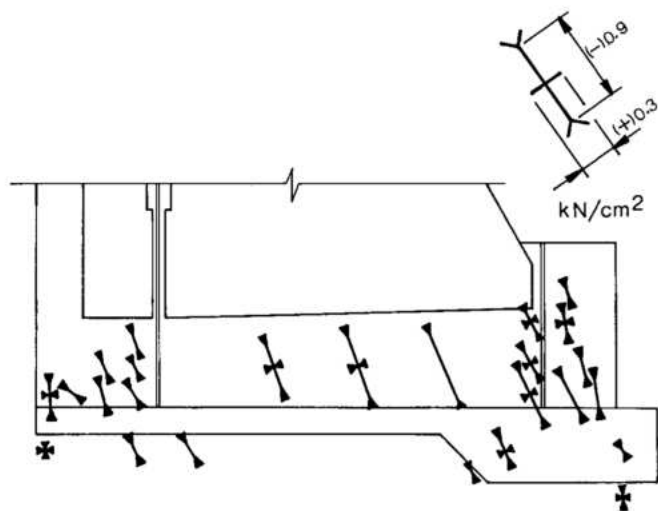
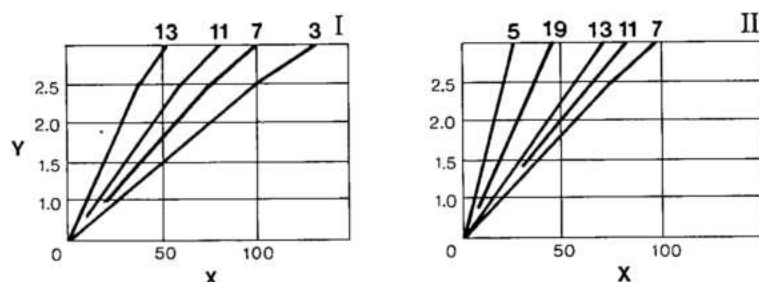


Fig. 6.24 Model 2: Principal stresses referred to prototype under combined dead and water loads (normal values)

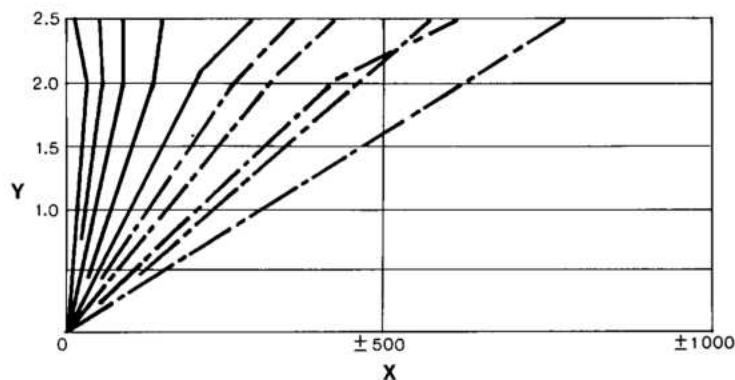


Fig. 6.25 Model 2: Progression of significant stresses increasing the combined action of dead and water load up to 2.5 times their normal values

Y Gravity and water loads
X Stresses (kN/cm^2)

— Tensions
--- Compressions

• Collapse tests: tentative collapse test (Test 2.5 G & 2.5 W, see Chapter 9 for terminology), gradually increasing up to 2.5 times the normal values of both the weight and the water load, all of which did not collapse the structure; final collapse test (Test 2.5 G & 4.5 W), keeping the weight at 2.5 times the normal value and gradually increasing the water load up to 4.5 times normal value, at which point collapse occurred. During the collapse tests, neither the uplift nor the water load on the upstream foundation crack were applied, as these did not contribute to the required mode of failure.

Fig. 6.23 shows the progression of the horizontal and vertical displacements at some significant points during the test with loadings increased up to 2.5 times their normal values. Although the structure did not show any sign of collapse, an increase in the rate of deformation was already evident. Fig. 6.24 shows the principal stresses, referred to the prototype, under the combination of dead and water loads at their normal values and Fig. 6.25 shows the progression of significant stresses, either tension or compression, in the same test as both dead and water loads were increased 2.5 times. Indications of local failures can be observed in these results. Summarizing what was visually observed and measured during Test 2.5 G & 2.5 W, up to approximately 1.7 to 2 times the normal load the model behavior was linearly elastic; from then up to the maximum loading applied (2.5 G & 2.5 W) nothing relevant could be observed, but measurements of strains and displacements suggested an appreciable decrease of the deformability modulus in highly stressed zones and an initial cracking at the top of the gate slots (El. 144). In general, the load carrying capacity of the model was still almost unaffected at the end of this test, at which point the limit of the capacity of the model dead load steel wire system had been reached.

Thus, the only way of reaching the ultimate loading was to further increase only the water load, while maintaining the dead load at 2.5 times the normal value. This resulted in higher tension and compression stresses at the upstream and downstream faces of the model respectively, thus creating a critical situation not only at the downstream face, but also at the upstream gate slots, because of the configuration of the structure.

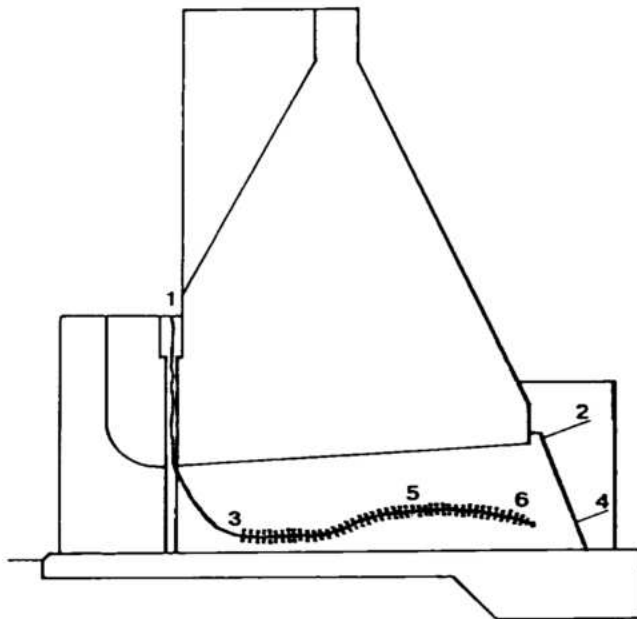


Fig 6.26 Model 2: Failure mechanism

1, 2, 3, ... 6 Indicate points where cracks occurred

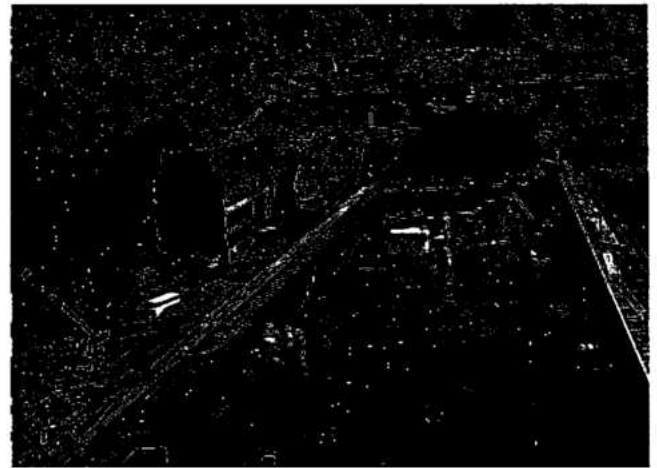
In this way, collapse was finally reached at a maximum water load 4.5 times the normal value combined with a dead load of 2.5 times normal value. The failure mechanism, neglecting secondary cracking, is shown in Fig. 6.26. A shear-tension crack began at point 1, progressing towards point 3, thus separating the main structure from the upstream platform at the slots, while at point 2 another shear-tension crack began and progressed towards point 4 to sever the structure from the downstream platform. With no further increase in load, and after a short interval of time, the wall of the sluiceway was crushed as rupturing progressed initially from 5 towards 6 and finally from 5 to 3.

Thus, from both tests, it could be concluded that the safety factor of the diversion structure against collapse was at least 2.5.

CONSTRUCTION OF DIVERSION CONTROL STRUCTURE

EXCAVATION AND FOUNDATION PREPARATION

To reach the designated foundations and abutments of the diversion control structure, excavation was carried out in three stages as follows:



First concrete monoliths of diversion structure

Stage 1. It was part of the primary excavation for the diversion channel, when the rock was drilled and blasted in 5 to 10 m lifts depending on its condition.

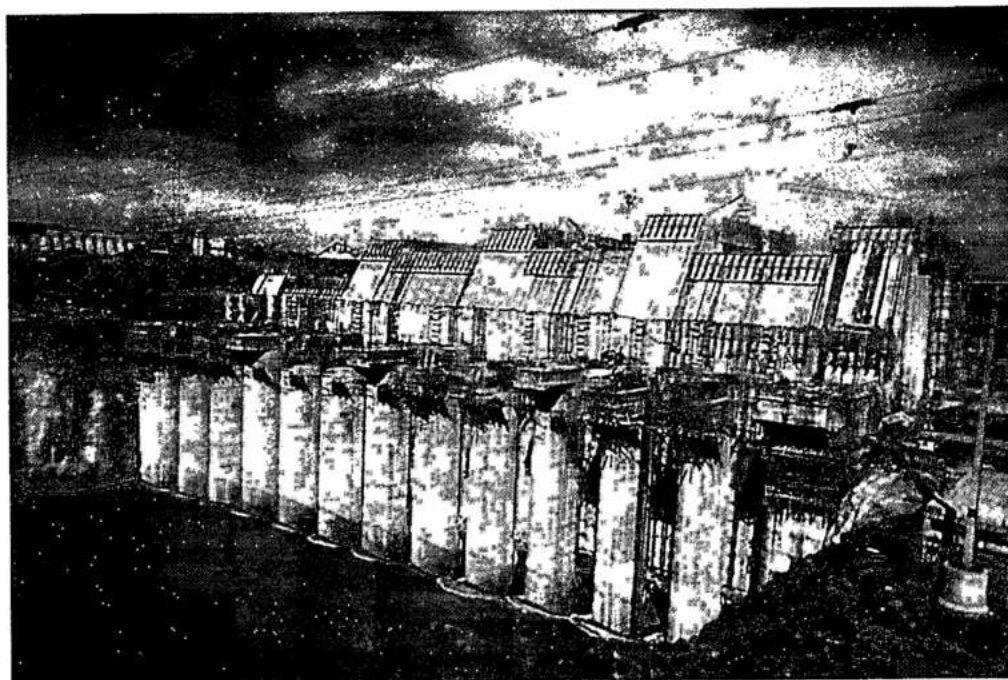
Stage 2. The last 3 m of the rock above the foundation level was excavated in 1 m lifts, with closer spacing of drill holes and controlled blasting. Along the abutments, blocks of columnar basalt which appeared to have been destabilized were removed without blasting. In the areas of the abutments, where there was concern about instability of the slope, rock bolts were installed within 15 days of completion of the excavation.

Stage 3. Excavation for the foundations consisted of the removal of pockets of loose and weak rock by jack hammers. The final clean-up of the foundation was carried out just before the forms were set, such that sound fresh rock was available for receiving concrete.

Low pressure consolidation grouting was carried out by a grid of holes spaced 3 m apart when 2 or 3 m of concrete had been placed. The grout holes were drilled through the concrete to a depth of 5 m into the rock.

Foundation treatment

Drilling of holes for, and grouting of the main upstream curtain was carried out from the gallery at El. 67, after the structure was nearly complete and before filling of the reservoir in October 1982. Along the steep abutments, curtain grouting was carried out from the two shafts formed in the structure. Procedures and sequence for pressure grouting the rock were the same as those for the other concrete dams discussed in Chapter 4. After completion of the curtain and before reservoir filling, foundation drain holes were also drilled from the same gallery and shafts.



Concrete placement in diversion structure

Formwork

Cantilever steel forms were used for concreting the monoliths of the dam, except for the piers of the sluices, which were slip-formed. Where the contraction joints had keys, special panels were bolted on the standard smooth forms when concreting the "low" blocks. PVC waterstops across the contraction joints were folded and attached to the forms, and when the forms were removed, the waterstops were unfolded to embed their free portion in the concrete of the adjoining blocks. At the foundations, the PVC waterstops were embedded in 50 cm deep cavities excavated in sound rock.

CONCRETE PLACEMENT

To meet the river diversion schedule, as discussed in Chapter 5, concrete placement in the upstream and downstream monoliths was given priority over placement in the central monoliths. The installation of embedded guides for the gates and stoplogs in the upstream and downstream monoliths slowed the progress of the concrete. Therefore, all steps of concrete delivery and placement, removal of forms and clean-up, were sequenced as to keep the upstream and downstream monoliths ahead of the central monoliths, which had no embedded parts and only one longitudinal gallery.

The first concrete lift on the foundation was 0.5 m thick, followed by 1 m, 1.5 m and the standard 2.5 m. Mass concrete was placed directly on the rock and an intermediate layer of mortar was not used.

Concrete delivered in 6 m³ buckets was discharged from a height of not more than 2.5 m. In each pour, the sequence of placement was from the downstream towards the upstream, spreading the concrete in 0.3 m layers. Manually operated pneumatic vibrators were used for consolidation of the concrete. However, where working space was adequate, concrete was spread by a bulldozer and consolidated by vibrators mounted on it.

The construction joints were roughened or cut using water jets under a pressure of 4 kN/cm². Forms were stripped 36 to 48 hours after completion of a pour. Concrete buckets were delivered to the location of placement by the cableways. Travelling tower cranes were used for handling the forms and transporting equipment from one monolith to another. The arrangement of the tower cranes and other concrete placement equipment are discussed in Chapter 5.

The roofs of the sluiceways were formed by 12.3 m wide double-T shaped precast concrete beams which extended from one transverse contraction joint to another. A total of 748 such precast units were used in the twelve sluiceways. The use of these precast beams facilitated the rapid placement of concrete during the crucial pre-diversion period.



Slip forming of diversion structure pier

Preparatory to river diversion, the finish of the surfaces of the sluiceways was improved by chipping out poor concrete and irregular construction joints, and then patching the area with epoxy mortar. Where necessary, surface irregularities were ground and smoothened.

Between El. 110 and El. 170 below the floor of the power intakes, concrete pours in 2.5 m lifts were essentially free of embedments and reinforcing steel. In volume, the largest pours were 2 952 m³ between El. 110 and El. 144 and 4300 m³ above El. 144. At El. 144, where the two longitudinal contraction joints terminated, heavy reinforcement was placed in the first two lifts, extending 6 m on either side of the joints. Maximum placement temperature of concrete was 7°C.

Construction of the four power intakes in the diversion control structure was similar to that of the main dam, and is discussed in Chapter 9.

Roller Compacted Concrete

Roller Compacted Concrete (RCC) was placed in 0.3 m lifts in the approximately 10 m wide x 12 m deep trench at the downstream toe of the diversion control structure below El. 83 in the bed of the channel. The lean RCC was used because it would be easier to remove when excavation for the powerhouse was carried out and because it could be placed rapidly prior to river diversion. A total of 26 000 m³ of RCC was placed.

DIVERSION GATES AND CLOSURE

The general arrangement of the diversion gates in the diversion sluice is shown in Fig. 6.21. The twelve gates

were mounted on base of the upstream face of the diversion structure, with the servomotors situated at El. 156.

Three sets of upstream stoplogs and three sets of downstream stoplogs were provided to isolate the gates for dewatering during testing and inspection. The stoplogs could only be deployed in still water. Hence, three maintenance gates (one per sluice) sealing between El. 83 and El. 109, were provided for use on the downstream to control flow, thus enabling a stoplog to be placed or removed. The upstream and downstream stoplogs were used later as permanent maintenance equipment for the power intake gates and are described in detail in Chapter 10.

A 1100 kN gantry crane was used to handle the downstream stoplogs and maintenance gates. This gantry crane was used later, without modification, as permanent maintenance equipment for the intake gates, servomotors and stoplogs; see Chapter 10. The upstream stoplogs were handled by a 1000 kN mobile crane.

In the initial scheme, the diversion gates were to be used solely for diversion, and left in place after the closure and the placing of the permanent concrete plugs in the diversion sluices. However, as the design of the gates progressed, it was realized that savings of about US\$ 30 million (1976 values) could be made if the gates were recovered and subsequently used in the power intakes. This, in turn, meant that the hydraulic servomotors needed to actuate the intake gates could also be used to raise and lower the diversion gates, providing a far safer and more flexible system of operation than that offered by the alternatives considered. Also, some of the gate design features and quality controls employed in the manufacture and testing of the gates could not have been justified had they been destined only as disposable diversion gates rather than permanent equipment. This provided for the diversion gates a greater safety margin and predictability of operation, without incurring any additional cost.

However, the maintenance gates, which had been designed and manufactured before the final decision regarding recovery of the diversion gates had been made, had no top seal, and a downstream water level above El. 109 would overtop them. Isolation of a sluice with a maintenance gate was an integral part of the closure sequence, in case a diversion gate became stuck and overtopping of the gates occurred. At the time of closure, the flow in the Iguaçu river would be low because of upstream storage requirements; hence, the limitation of El. 109 for the maintenance gates corresponded to a maximum flow of about 12 600 m³/s in the Paraná river, which statistically would occur in the months of June through November.

Hence all programming for the manufacture and erection of the diversion gates was directed towards diversion closure in the relatively narrow mid temporal "window" of September-October 1982, in the knowledge that should closure not be achieved during this period for any reason, a 1 year delay in completion of the project could result.

The gates were designed by BVS (Neyrpic) under the supervision of IECO-ELC. The design started in mid 1975, the manufacturing specification being issued by Itaipu in November 1977. Included in the same specification were stoplogs, diversion maintenance gates and the intake gantry crane. The contract for the manufacture and supply of this equipment was awarded to a Joint Venture of the following companies:

Mecanica Pesada S.A.

Bardella S.A. Indústrias Mecânicas

BS Indústrias Mecânicas

BVS (Neyrpic).

HYDRAULIC MODEL TESTS AND STUDIES

Model tests

Tests were conducted on a 1:100 scale hydraulic model to obtain basic design data for the gates and their closure sequence. The model tests took place in the laboratory of SOGREAH, France, during 1976 through 1978. The gate model represented three of twelve sluiceways of the diversion control structure, together with short upstream and downstream sections of the diversion channel. The main objectives and findings of these model tests were as follows:

Vertical forces on the gate. Pressure measurements were taken at a large number of tapping points across the face and the bottom surface of the model at various openings and differential heads. These pressures were integrated to compute the vertical hydraulic forces acting on the gates, as shown in Fig. 6.27 and Table 6.3. The pressure measurements made on the initial design indicated a negative pressure region on the upstream sloping section of the gate bottom, from which the flow was observed to separate at low tailwater levels. It was considered that this separation could be a potential source of gate vibration and the gate profile was modified to eliminate it. Also, the skin plate of the lower section of the gate was relocated on the upstream face, thus reducing the hydraulic vertical loading.

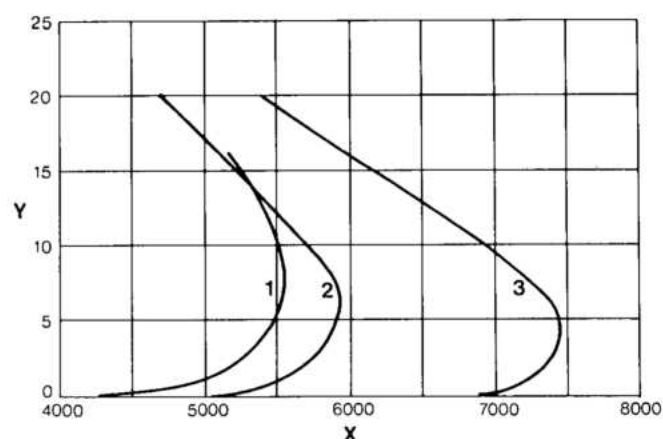


Fig. 6.27 Forces acting on the servomotors

Y Opening (m)
X Force (kN)
1 Intake gate closing at 45 m head
2 Diversion gate closing at 30 m head
3 Diversion gate opening at 30 m head

Table 6.3 Breakdown of maximum forces

Force component	Forces in kN (positive acting down)		
	Intake gate closing at 45m head (7.5 m open)	Diversion gate closing at 30m head (6m open)	Diversion gate opening at 30m head (4m open)
Weight			
Gate	2452	3434	3434
V1 Servomotor		481	481
Piston and links	80	130	130
Thrust (from model test)	3236	2207	2788
Friction	-218	-372	587
Total force	5550	5880	7420

Flow conditions in the sluiceway. The model bellmouth intake and the discharge sluiceways were equipped with pressure taps to evaluate the possibility of cavitation and undue pressure fluctuations during diversion and final closure of the gates. The pressures indicated that there was no risk of cavitation, which was later confirmed by the well preserved state of the concrete walls of the sluiceways when inspected during test

closure of individual gates and after final closure. Pressure measurements and visual observation through the transparent side walls of the model indicated that the flow in the sluiceway downstream of a partially closed gate was highly unstable and agitated when the downstream level was high enough to drown the jet issuing from the bottom of the gate. A separate series of tests was, therefore, conducted to investigate the amplitudes and frequencies of hydraulic pressure fluctuations due to vortex shedding from the lower face of the gate during drowned flow, and to ensure that in both the diversion and intake gate applications these did not coincide with the natural frequency of the gate and its suspension. Readings from pressure transducers located on the bottom face of the model gates were put onto a spectral analyser, which demonstrated that no dominant exciting frequency existed.

Limiting conditions for drowned and undrowned flow, as obtained from the model tests, are shown in Fig. 6.28. Whether the gate flow is drowned or not determined the net head used for computation of the horizontal force on the gate. For drowned flow the downstream level used for this computation was the actual water level, and for undrowned flow it was the lower face of the gate. This consideration was important for the design of the elastic pad supports for the gate wheels.

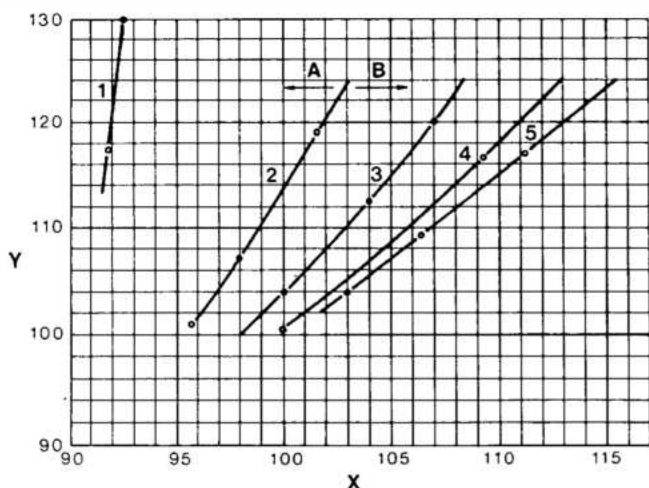


Fig. 6.28 Condition of freeflow

Y Upstream level (m)	1 1 m
X Level 20 m downstream of gates (m)	2 5.5 m
	3 11 m
A Gate undrowned	4 16.5 m
B Gate drowned	5 20 m

The need for an air vent. The tests proved that with the sluiceway geometry employed, sufficient air was naturally supplied to the downstream face of the gate at all gate openings, eliminating the need for an air supply vent for the diversion gates. Tests with and without an air vent gave the same results for the unstable flow conditions with drowned exit flow.

Debris in the gate grooves. Sand and fine gravel particles introduced into the model flow showed, at least qualitatively, that bed load material would not have a marked tendency to accumulate in the gate slots with the design adopted.

GATE COMPONENT DESIGN AND MANUFACTURE

Guides and rolling surfaces

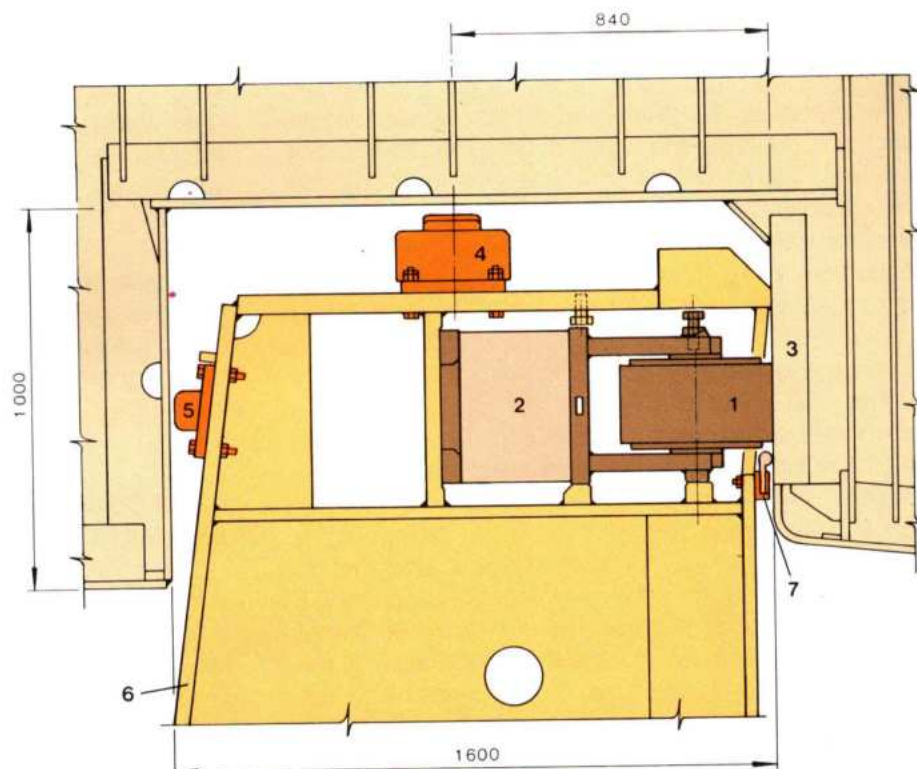
The side guides took three forms. The guides used in the sluice opening are shown in Fig. 6.29. Between El.156 and 133, and 105, the gate was held tightly between the two side stops, both of which had an elastic pad construction and were each compressed 10 mm against a side plate. Any upstream movement of the gate was restricted by means of a 5 mm clearance between the back stop and the embedded parts. In this manner the gates were well braced to resist the forces resulting from turbulence around the gate slot when in the standby position for closure. Below El.105, see Fig. 6.29, the gate was unguided other than for contact between the wheels and the rolling plate, thus minimizing the possibility of the gate jamming. To restrict cavitation damage in the sluice, the embedded metal side parts between El.105 and El.83, extended from 2.2 m upstream of the gate center line to 2.4 m downstream, and included the gate slot and the hydraulic flaring from the slot to the downstream part of the sluice. The combined rolling and bearing plate was 90 mm thick and was embedded in second stage concrete, having a minimum 28 day strength of 40 N/mm².

The rolling and bearing surface was designed for a hydrostatic load of 4.9 kN/mm², which corresponded to the horizontal force applied by the gate with the reservoir at maximum level. An instrumented structural model to a scale of 1:4 tested at the Instituto de Pesquisas Tecnológicas do Estado de São Paulo (IPT), Brazil, proved the validity of the design of the embedded parts and the materials specified. Significant cracks were not evident in the structural model until the loading exceeded 2.5 times the design load.

All sealing surfaces were made from medium strength carbon steel plate, 550 N/mm² tensile strength.

Fig. 6.29 Cross section of the diversion gate

- 1 Wheel
- 2 Elastic pad
- 3 Rolling plate
- 4 Side stop
- 5 Back stop
- 6 Gate
- 7 Side seal
- F Flow direction



The design of the gate rolling and sealing components called for tight tolerances for the respective embedded parts. The combined rolling and bearing plate had to be located to a tolerance of $+2\text{ mm}$, -0 mm and have a planeness tolerance of $\pm 2\text{ mm}$ over its length. Planeness tolerances of $\pm 0.5\text{ mm}$ and $\pm 1\text{ mm}$ were required over the length of the lintel and bottom seal, respectively. Because of the condensed construction program it was decided to erect the parts with the greatest accuracy possible without using any special construction devices; finish concreting the diversion structure, and then grind the surfaces to the required tolerances with a sluice dewatered during the relatively long period between start of diversion and final closure. For this operation, a special grinding machine was developed, comprising a compressed air driven grinding wheel operating on 2.5 m long vertical guides, held to the embedded rolling surfaces by magnets.

Gate structure

A general view of the diversion gate is shown in Fig. 6.30. The gate was designed as a flexible structure such that each element could adjust itself to the embedded parts both during closure when the horizontal loads were reacted by the wheels, and after compression of the elastic pads when these loads were transferred in part to the bearing beam. By making the gate flexible in the upstream/downstream direction, the loading of the

embedded parts could be made relatively uniform. This consideration resulted in a gate constructed of ten separate panels 8230 mm wide. The upper nine panels were each 2050 mm high, weighing 294 kN, with downstream skin plates. For reasons of gate stability and to reduce downpull forces, the lower panel was 4050 mm high, weighed 657 kN and had an upstream skin plate. The gate members were made from medium strength steel, with a minimum yield strength of 360 N/mm^2 and tensile strength between 550 N/mm^2 and 630 N/mm^2 . The allowable structural stresses were limited to 55% of the yield strength for the normal case as defined by DIN 19704.

Individual panels were joined by two sets of bolted flanged connections, each set consisting of 36 mm diameter prestressed high tensile strength bolts. The inter panel joint was sealed with J seals and the movement of the joint resulted from the flexibility in bending of the flanged connection. All high tensile bolts were subject to the same stringent controls as those used for the elastic pad studs, to avoid any problems with stress corrosion cracking. The twenty four bolts were prestressed by means of a hydraulic device to 75% yield strength, resulting in a prestress force of 10.8 MN for the complete panel joint. The pressure required in the hydraulic device to guarantee the correct amount of prestress in the bolt was obtained from a test at site on a sample joint, using strain gauged bolts.

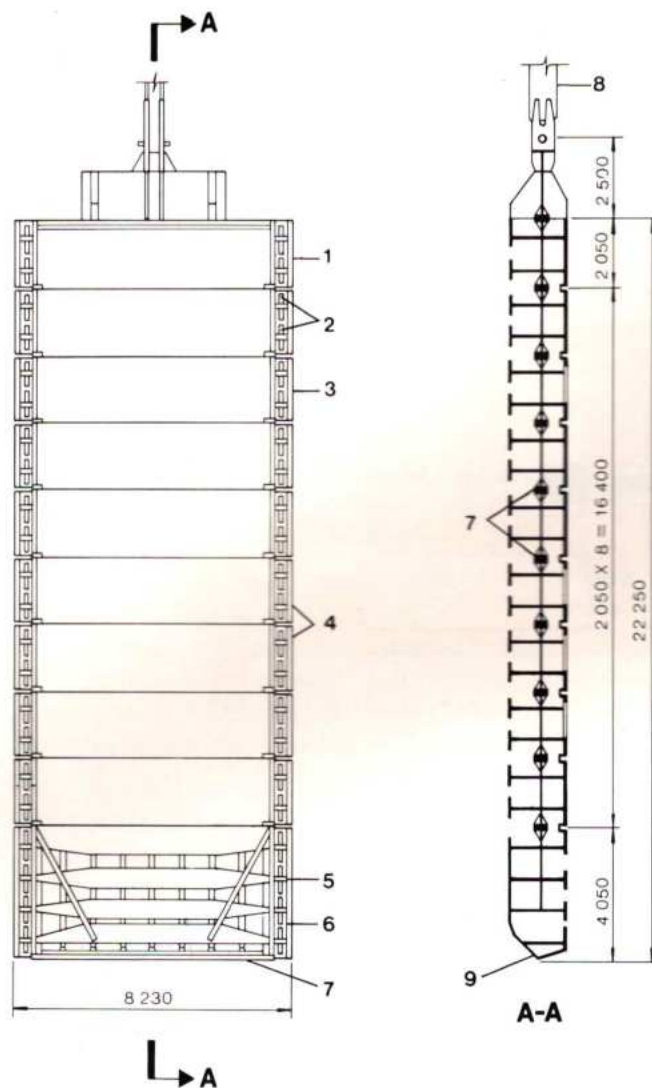


Fig. 6.30 Diversion gate

- | | |
|-----------------------|----------------|
| 1 Upper panel | 6 Side seal |
| 2 Gate wheels | 7 Panel joints |
| 3 Bearing beam | 8 Lifting link |
| 4 Intermediate panels | 9 Bottom seal |
| 5 Lower panel | |

Seals

Details of the top, side, bottom and interpanel seals are shown in Fig. 6.31. Solid rubber U section compression seals were used at the bottom, and inflatable rubber caisson seals at the top. Side and interpanel seals were J type with a 50 mm diameter bulb. Nominal compression of the side seals as determined by the set of the wheels was 0 during lowering of the gates and a maximum of 10 mm after compression of the elastic pads. The effectiveness of

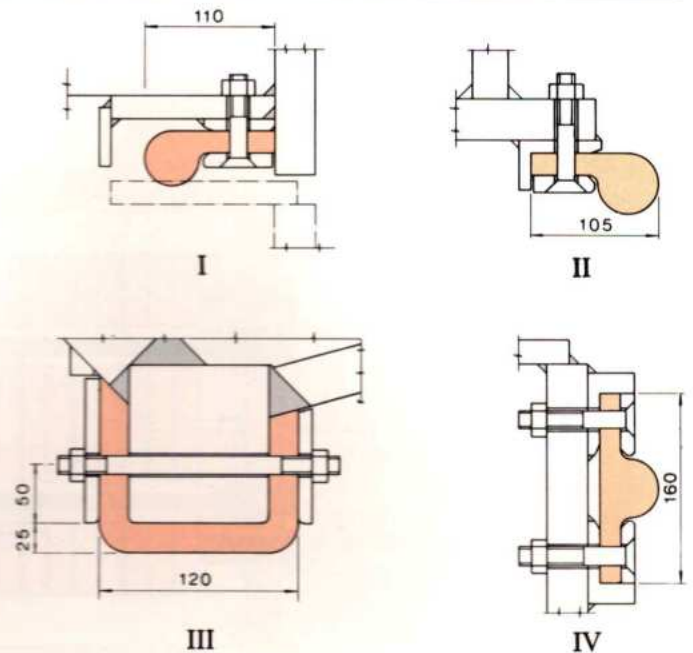


Fig. 6.31 Details of the gates seals

- | | |
|-------------------|-----------------|
| I Interpanel seal | III Bottom seal |
| II Side seal | IV Top seal |

the J type side seal was tested in a hydraulic model under a maximum hydraulic head of 200 m. Retaining bolts for the seals were made from cadmium plated carbon steel (replaced later by stainless steel for use in the intake).

All seals were uncoated and a friction coefficient of 1 between the seals and the embedded parts was assumed.

The quality of the rubber to be used for the seals was assured by testing its hardness, tensile strength, elongation, tear resistance, aging under oxygen, propensity for water absorption and resilience after aging.

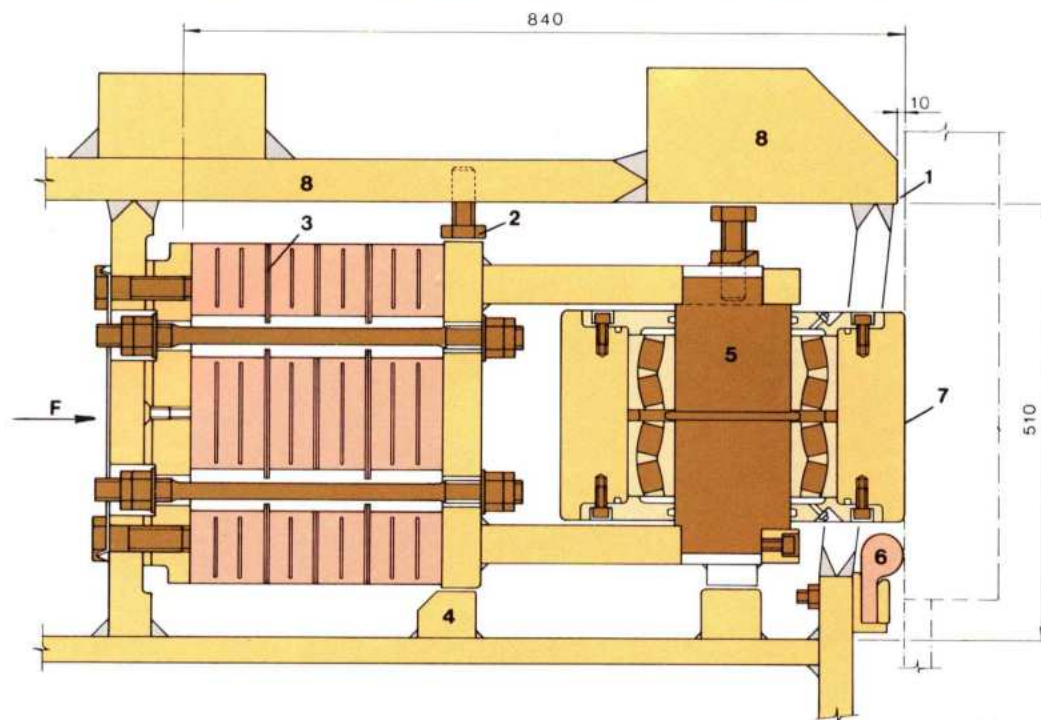
Wheels and attachments

With the stipulated flow conditions at final closure, the differential head across the diversion gate sluices would be about 3 m. This would rapidly increase as simultaneously the reservoir filled and the tailwater level dropped; the final maximum differential head, with the reservoir completely full, being 140 m.

To design the diversion gate wheels and supports to withstand the maximum head was clearly impractical, as was to design the gate operating mechanism to raise the gate under this head. What was required was a system in which the hydrostatic

Fig. 6.32 The wheel assembly

- 1 Wheel rim
- 2 Side guide for pads
- 3 Elastic pads
- 4 Fixed side guide for pads
- 5 Wheel axle
- 6 Side seal
- 7 Radius of wheel surface = 6 m
- 8 Bearing beam
- F Flow direction



force to be reacted by the wheels would be limited to a certain design value, consistent with the need to operate the gates under an acceptable differential head. The limiting reservoir level for gate operation was determined by the design operating conditions for future use in the power intake, and the need to give sufficient time after closure of the diversion to verify that the closure was successful and to allow the gates to be reopened in the event of problems. The chosen solution, as shown in Fig. 6.32, was to mount the wheels on elastic pads which would start to compress at a differential head of 30 m. At a differential head of 45 m, the movement would be such as to permit the gate bearing beam to come into contact with the embedded parts, thus reacting to the further increase in hydrostatic loading. The differential head of 30 m, coupled with the conditions of drowned or undrowned flow from the gates, see Fig. 6.28, with the maximum reservoir filling rate, gave approximately five hours to determine whether the closure had been successful, after which time the gates could not be reopened. This was considered to be conservative. As shown in Fig. 6.32, the elastic pads have a sandwich construction of rubber and stainless steel reinforcing plates. While controlling the deformation of the rubber, the plates also acted as guides for the pretensioned studs. Five and ten layered pads were considered initially, but after a preliminary series of tests, the ten layered pads were chosen because

their greater elasticity resulted in a larger gap (10 mm) between the bearing beam and embedded parts for the same limiting load, and hence implied less stringent tolerances for the manufacture of the gates and the erection of the embedded parts.

The pad material and the pad assemblies were manufactured in Brazil and were subjected to an extensive series of tests and controls, as follows:

Materials. The quality of the rubber was assured by acceptance testing of its hardness, tensile strength, elongation, tear resistance and shear modulus in the received condition and after quick aging in an oven at 100°C. In addition, a quick aging test in ozone was conducted, along with a compression set test in air.

The studs for the pads in the diversion gates were made from hardened and tempered high strength steel with the following specified mechanical properties :

Yield strength	785 N/mm ²
Tensile strength	981 N/mm ²
KCU impact at 20°C	50 J/cm ²

To avoid any possibility of hydrogen embrittlement stress corrosion cracking the studs were left ungalvanized, although they were painted and the maximum hardness was limited to 930 HV. Also a 5% sample of stud threads was subjected to metallographic examination for thread root defects.

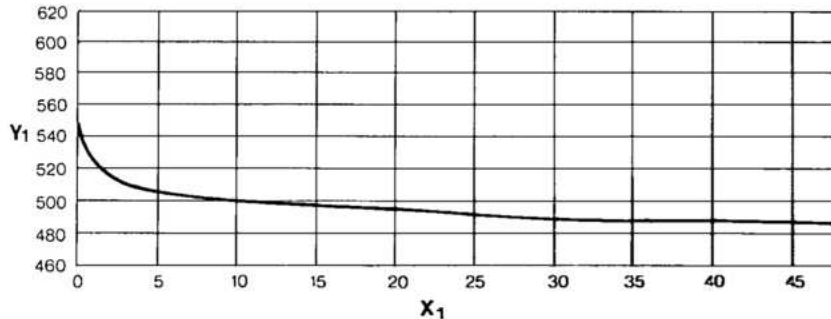
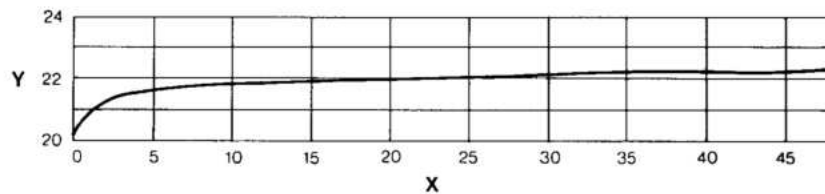


Fig. 6.33 Results of permanent set tests on the elastic pads

Y Deflection (mm)
X Days under constant load of 550 kN
Y₁ Load (kN)
X₁ Days at constant deflection

Adhesion. A representative sandwich of the rubber and steel plates was subjected to cyclic compressive loading of 0 to 1000 kN over 10 000 one-minute cycles, in order to prove the integrity of the adhesion between plate and rubber. This test was supplemented by a test in which the joint between rubber and steel was tested in compression to failure. Separation of 15% of the adhesive surface occurred at a stress of 98 N/mm², which was considered to be acceptable.

Assembly. Sample elastic pad assemblies were subjected to the following tests:

LOAD DEFLECTION TEST IN COMPRESSION. A complete pad was placed in a hydraulic press and loaded progressively. As the load increased, the rubber bulged into the holes for the studs. A pattern made by pouring plastic into the hole with the pad fully compressed showed that, with a 20 mm diameter stud, there would be no interference between stud and rubber.

STABILITY TESTS. A pad was compressed between two central point pivots and the lateral displacement measured. The maximum lateral displacement specified was 3 mm. Lateral stability of the pad was assured by means of the side guides which were adjusted to a clearance of 0.5 mm.

PERMANENT SET. Tests were conducted at a constant temperature of 21°C in order to evaluate the permanent set of the pads under compression loading.

Sample pad assemblies were maintained under a constant load of 550 kN for a period of 120 days and the deflection measured, while other samples were held with a constant deflection and the change in the load of the retaining studs measured. After the 120 day period, an unloading and reloading load

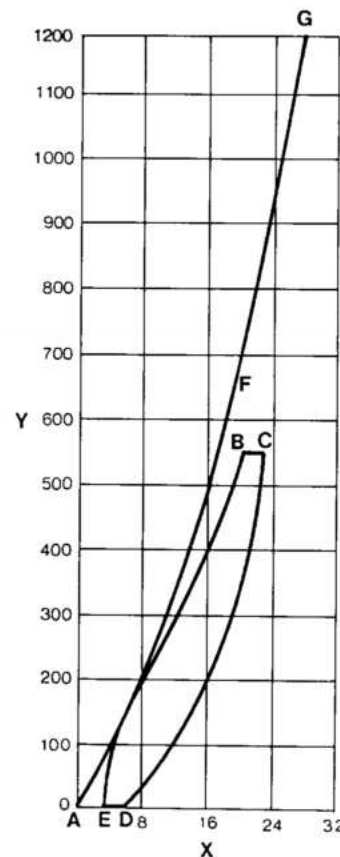


Fig. 6.34 Load deflection curves for the elastic pads

Y Load (kN)
X Deflection (mm)
A-B Initial deflection
B-C Relaxation after 120 days
C-D Unloading after 120 days
D-E Recuparation 1½ hours after unloading (time necessary to return to press)
E-F Reloading to 550 kN
F-G Deflection in service (10 m)

deflection test was performed. The results of these tests are shown in Figs. 6.33 and 6.34. From these results it was concluded that, as the permanent set was virtually established after 45 days, the pads would be initially compressed to 550 kN, held there for 45 days, and then recompressed, lines E, F, G of

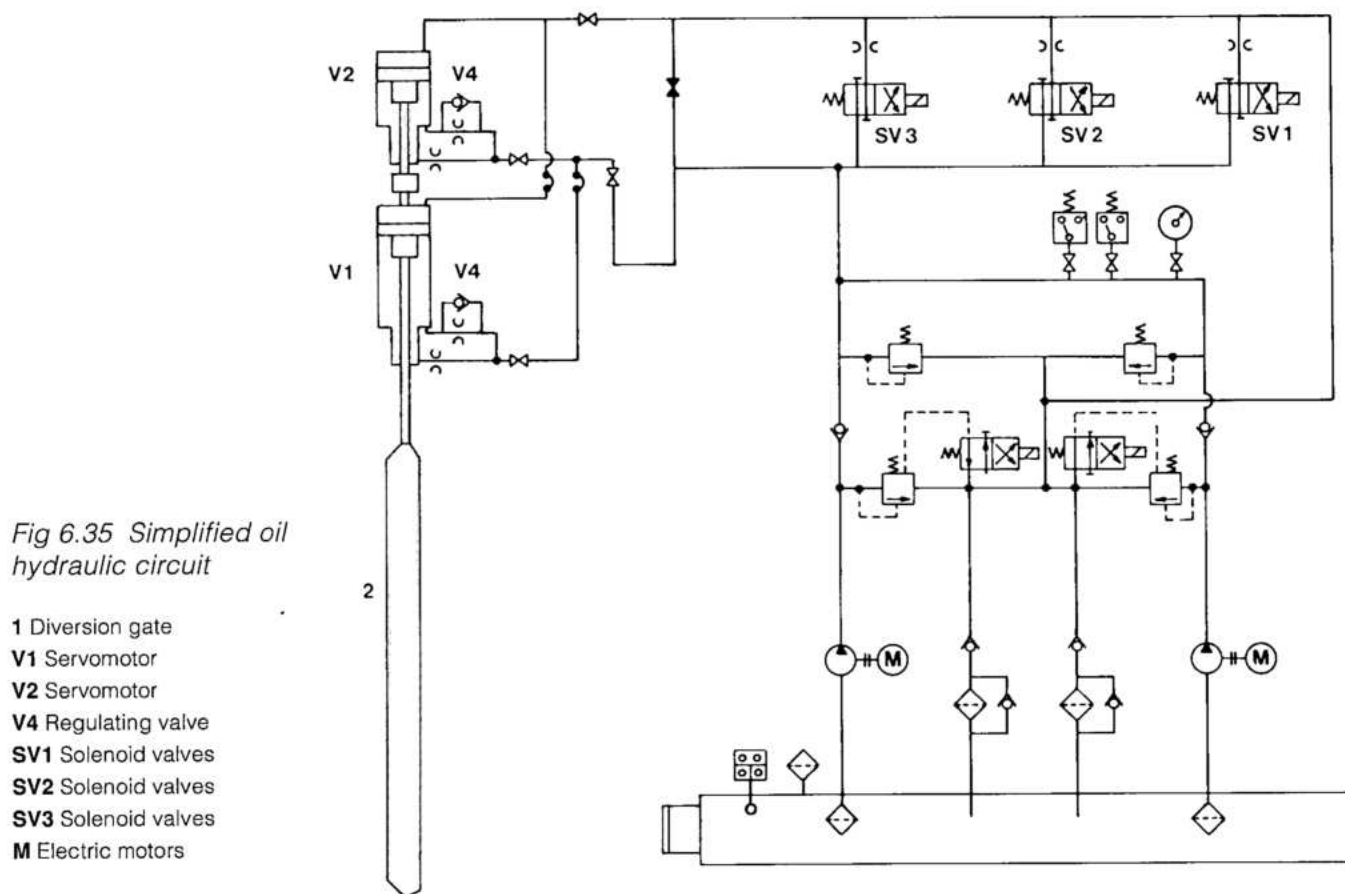


Fig 6.35 Simplified oil hydraulic circuit

Fig. 6.34 being the final design characteristic for the pads. Thus, for the 10 mm gap between beam and embedded parts, the maximum theoretical load is 1200 kN per wheel, which for the wheel dimensions of 410 mm in diameter and 244 mm in width, resulted in a Hertz stress of 1730 N/mm^2 . The wheels were manufactured from forged steel (600 N/mm^2 yield), hardened and tempered to give a rim hardness between 220 to 270 Brinell. There are eight wheels per intermediate panel and sixteen wheels per lower panel, resulting in eighty-eight wheels per diversion gate. Each wheel is mounted upon a forged stainless steel 140 mm diameter axle, equipped with two roller bearings packed with grease and protected with a sealed cover.

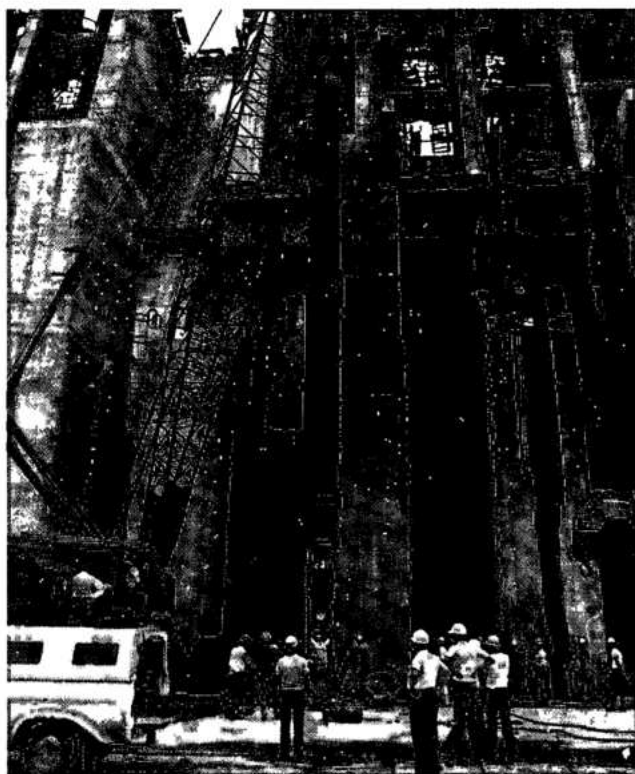
Gate operating mechanism

The course of the diversion gate was 23.9 m, and that of the intake gate was 16.1 m. To facilitate manufacture and to reuse as much equipment as possible for the intake, two servomotors, V1 and V2, connected in series, were used for the diversion. Details of the servomotors are shown in Fig. 6.35. Servomotor V1 has a course of 16.1 m and V2 a

course of 7.8 m, together making the 23.9 m required for diversion closure. The servomotors are single acting, and have a nominal working pressure of 14 N/mm^2 , which corresponds to 8.2 MN pull. Oil connections between the servomotors were made with high pressure flexible hoses.

Servomotor cylinders were fabricated from rolled and welded steel plate, having a minimum yield strength of 360 N/mm^2 , and were made 900 mm diameter, 8.275 m in length; the V1 servomotor being two such cylinders bolted together. The 250 mm diameter piston rods were made from stainless steel, having a minimum yield strength of 650 N/mm^2 . Stresses in the servomotors were limited to 40% of yield strength for normal operation and to 75% of yield strength for the emergency case of a jammed gate.

The two servomotors for each gate were supplied from a common pumping set consisting of two pumps, valves and electric control cabinet. A simplified schematic diagram of the hydraulic system is shown in Fig. 6.35. The gates descended under the influence of gravity, the speed being determined by which solenoid valves (SV1, SV2, SV3) were open. The rate used for the diversion closure was 3 m/min, however, incorporation of other rates was necessary



Installation of a V1 servomotor

for the intake gate application. In order to prevent the gate slamming against the bottom seal, the final part of the closure was restricted to 1 m/min by valve V4 and a dashpot in the servomotor. To compensate for the equivalent oil volume of the piston rod, it was necessary to operate the oil pumps during closure. The opening of the gates was made by closure of the solenoid valves SV1, SV2, and SV3 and operation of the two pumps. Maximum rate of opening was 840 mm/min.

Three separate systems were used to indicate the gate position. One was a cable system attached to the gate and connected to a rotary dial, giving a continuous indication of gate position to an accuracy of 10 mm. The second was a piano wire attached to the gate and, via a pulley and weight, giving the gate position at final closure to an accuracy of 1 mm. In addition to this, final closure could be confirmed by an observer lowered into the gate slot, using a mark on the highest gate panel, which corresponded to a mark on the concrete.

TESTING AND FINAL CLOSURE

After the initial setting up and checking of the control system each diversion gate and its operating mechanism was subjected to the following tests at site:

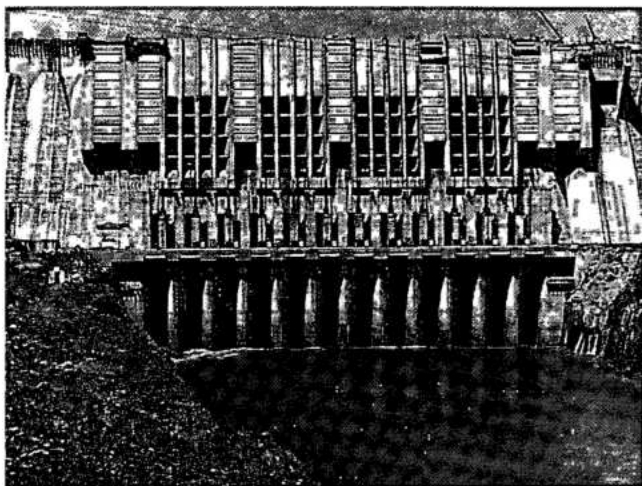
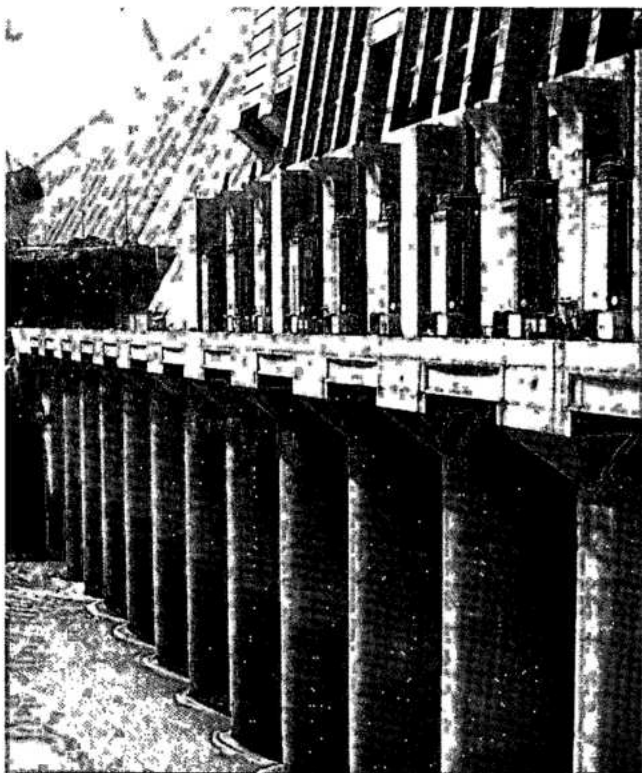
Tests in the dry. The upstream and downstream stoplogs were deployed, and the sluice dewatered. After spraying the seals and guides with water in order to reduce the coefficient of friction and avoid any undue rubbing of the seals, the gate was lowered in the dry, thus checking the operating mechanism and gate clearances. During this test the calibration of the gate position indicator was checked, as was the piano wire indicator and the marks on the concrete.

Provisional check of seal. After the test in the dry, the space between the upstream stoplog and diversion gate was flooded and the effectiveness of the seals checked. It was appreciated that this test was very pessimistic, since the side seal compression was small as determined by the wheel setting and it would increase by 10 mm when the elastic pads compressed. However, even under these conditions the average leakage was of the order of 800 l/s and no local area of exceptionally high leakage flow was evident. This gave a good indication that the seals were effective and that they would function well when compressed in service.

Operation test. Each gate was closed individually into flow in order to check the gate and its operating mechanism under conditions to be expected on the day of closure.

Time to remove equipment. The time available after closure to remove the equipment which was to be reused for the intake gates, and thus would not be drowned, and to prepare the gates for recuperation, was limited to approximately 36 hours. Equipment to be removed was quite substantial and included the oil pumping sets, control panels, continuous gate position indicators, and some hydraulic piping. Hence it was decided to permanently close one of the twelve gates a few weeks prior to the diversion closure proper, to check the time necessary to remove the equipment and to see whether the removal presented any problems. The removal and preparation of the gate for recuperation took 4 hours; hence no problems were foreseen for the operation, and in fact none were encountered during final closure.

Simultaneous trial closure. As a check of the temporary electrical system provided for the diversion gates, a trial simultaneous closure of all eleven gates to the point where the bottom of the gates touched the water surface was made a few days prior to the closure.



Diversion gates in closed position

Final closure

In order to maintain riparian flow in the Paraná river, at the time of closure, the flow at its confluence with Iguaçu river would need to be at least $5000 \text{ m}^3/\text{s}$. Storage in the Iguaçu river system had been made in the weeks prior to closure such as to maintain this flow for the 15 days needed to fill the Itaipu reservoir. Final closure of the Itaipu diversion gates commenced at 5:45 am on October 13, 1982, and was completed eight minutes later. The flow in the Paraná

was $12\,000 \text{ m}^3/\text{s}$, which was the maximum permitted for closure. However, it had been raining heavily in the Paraná basin and higher flows were forecast. To reduce both hydraulic and electrical transients, the eleven gates were closed at 20 second intervals. Eleven hours after closure, the upper four gate panels were visible from the downstream, at which time the differential head at the upper panel was 20 m and the leakage flow was about the same as that seen during the tests in the dry. Twenty seven hours after closure, because of the fall in the downstream level, the upper six panels were visible and with 34 m hydrostatic head on the upper panel and the elastic pads starting to compress, the improvement in sealing was very evident. Pad compression was complete at 45 m head on the upper panel, which occurred 52 hours after closure, when seven panels were visible. At this point, the gates were virtually drop tight.

RECOVERY OF THE GATES

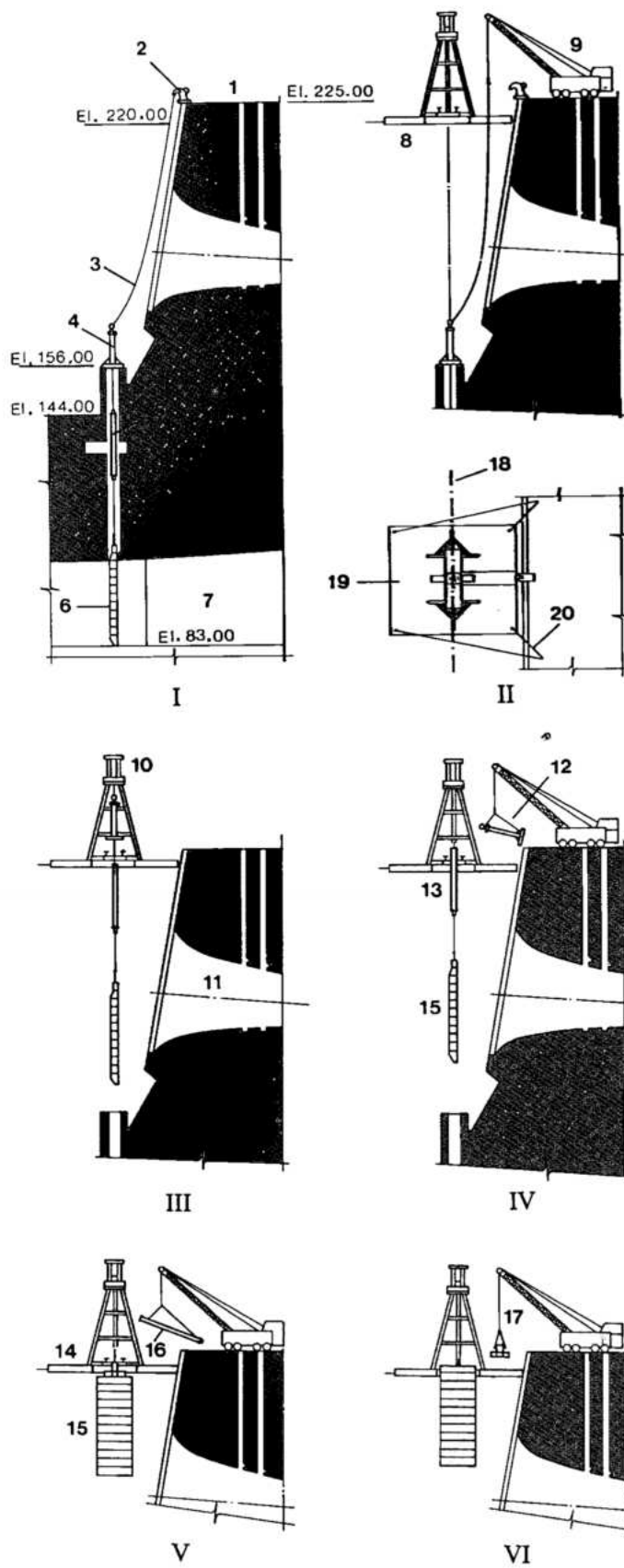
Several schemes for gate recuperation were examined. Originally the proposal was to locate the servomotors on an overhang at El. 225 m, and connect them with the gate via a series of links. This had the advantage that only the gates would be drowned, thus reducing the loss should the recuperation not be successful. Also, with this scheme, the gates themselves could be recovered from El. 225, avoiding the need for a barge, or any underwater work. This scheme was finally discarded because:

- The high cost of providing the overhanging support structure.
- The problem of removing the long link system which blocked the power intakes.
- Fears that the long link system would be susceptible to resonant excitation from the hydraulic forces acting on the gates, both the characteristics of the links and the forces being very difficult to predict with sufficient accuracy.

Several other schemes involving barges and cranes were investigated and finally discarded in favor of the scheme shown in Fig. 6.36.

A 115 mm diameter cable was located between the cover of the V2 servomotor and the top of the dam at El. 225. It is of interest that these cables were originally used for the aerial cable cranes which had been dismantled before diversion closure, see Chapter 5.

Prior to diversion closure, the 21 m wide x 36 m long recovery barge was erected upstream of the Itaipu dam. The barge had a 12 m x 3 m central well which was spanned by a 33 m high steel tower, at the top of which was installed a hydraulic pulling machine with 115 mm diameter cable grippers.



The hydraulic pulling machine is a proprietary equipment which operates using two grips one of which moves vertically, carrying the cable with it on the up stroke and the other holding the cable during the return down stroke of the moving grip. The barge was equipped with a diesel driven electric power generator, lights, and pumping sets to power the hydraulic pulling machine, making it a completely self contained unit. After diversion closure and when the reservoir level had reached the barge, the barge was floated to a prearranged test area, where a 115 mm cable had been anchored. With this cable the barge equipment, its structure and stability were fully tested at forces representative of those required for recuperation of the gates.

The sequence of gate recovery is indicated below and shown in Fig. 6.36.:

Stage 1. The recuperation cable was transferred beneath the barge to the pulling machine by means of an auxiliary cable.

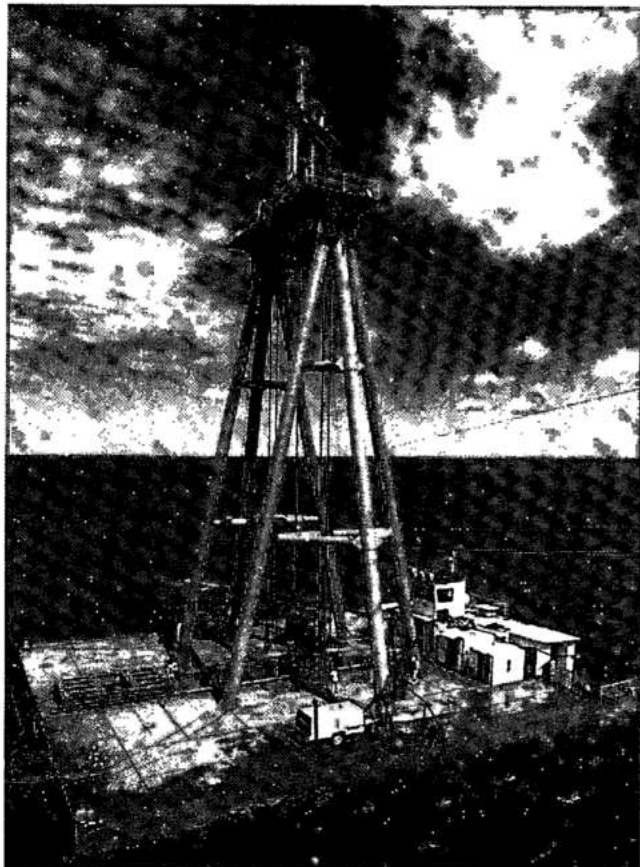
Stage 2. The complete set of equipment, that is, the servomotors and gate, was lifted as a unit until the V2 servomotor was within the tower structure.

Stage 3. An oil pumping unit was then connected to the V2 servomotor and the piston retracted.

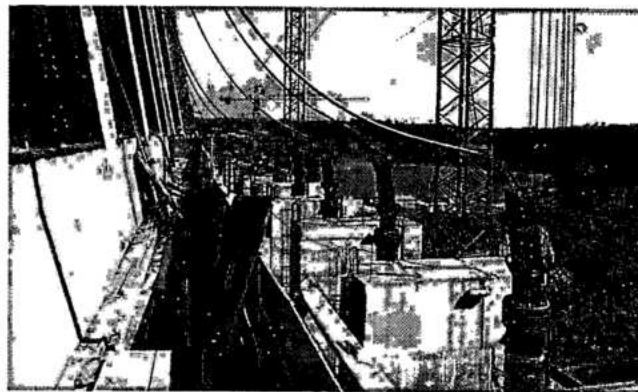
Stage 4. Slings were attached to the V1 servomotor, the cable was disconnected from the V2 servomotor and the V2 servomotor removed.

Fig. 6.36 Recovery of diversion gates

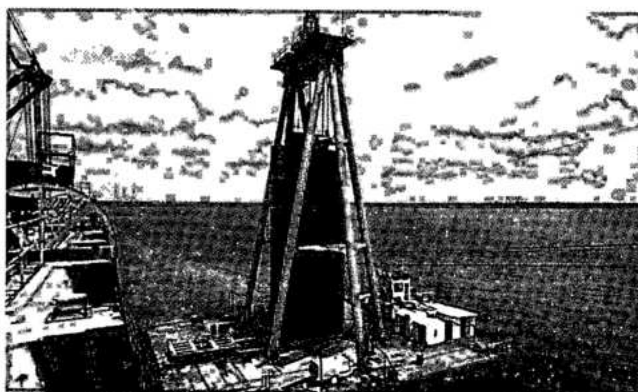
- | | |
|---|-----------------------------|
| I Stage 1 | 8 Barge and lifting tower |
| II Stage 2 | 9 Mobile crane |
| III Stage 3 | 10 Hydraulic pulling device |
| IV Stage 4 | 11 Power intake |
| V Stage 5 | 12 Servomotor V2 |
| VI Stage 6 | 13 Servomotor V1 |
| 1 A top of the dam | 14 Dogging beam |
| 2 Cable anchorage | 15 Diversion gate |
| 3 Recuperation cable | 16 Servomotor V1 |
| 4 Servomotor V2 | 17 Gate panel |
| 5 Servomotor V1 | 18 Gate axis |
| 6 Diversion gate in closed position | 19 Barge |
| 7 Concrete plug (after diversion closure) | 20 Mooring cable |



Recuperation barge



Cable from top of servomotor V2



Diversion gate being removed through barge

Stage 5. The cable was then reconnected to the V1 cylinder and was lifted by the pulling machine into the tower, where the same procedure was repeated to effect its removal (slings, in this case, being attached to the gate).

Stage 6. Finally the cable was attached to the gate, and it too was lifted into the tower to be removed sideways in parts by the mobile crane.

All twelve gates were recovered without any problems.

The refurbishment of the gates for the power intake gate service is described in Chapter 10.

STOPLOGS AND MAINTENANCE GATES

Sufficient upstream and downstream stoplogs were supplied to dewater three diversion sluices concurrently. Each upstream stoplog consisted of one upper panel, with upper side and bottom seals and by-pass valve, and

eleven normal panels, having side and bottom seals only. A downstream stoplog comprised thirteen normal panels, and as with the maintenance gates there was no provision to seal at the top. Upstream stoplogs were handled by a mobile crane and downstream stoplogs and maintenance gates by the 1100 kN gantry crane, which was later used as permanent equipment at the power intakes. The stoplogs and their respective lifting beams were also later used for permanent service at the intakes. Detailed description of these and the 1100 kN gantry crane is given in Chapter 10.

The stoplogs could only be deployed in still water. To stop the flow in a sluice, a maintenance gate was first inserted in the downstream stoplog slot, enabling the upstream stoplog to be placed in position. The maintenance gate could then be removed and substituted by the downstream stoplog, thus freeing the maintenance gate for use in another sluice. Each maintenance gate comprised ten equal panels, a detail of which is shown in Fig. 6.37. The maintenance gate panel was handled by the same lifting beam as used for the stoplogs. Two wheels on each side of the panel ran on grease lubricated roller bearings and side and bottom sealing were effected by simple rectangular rubber seals, see Fig. 6.38.

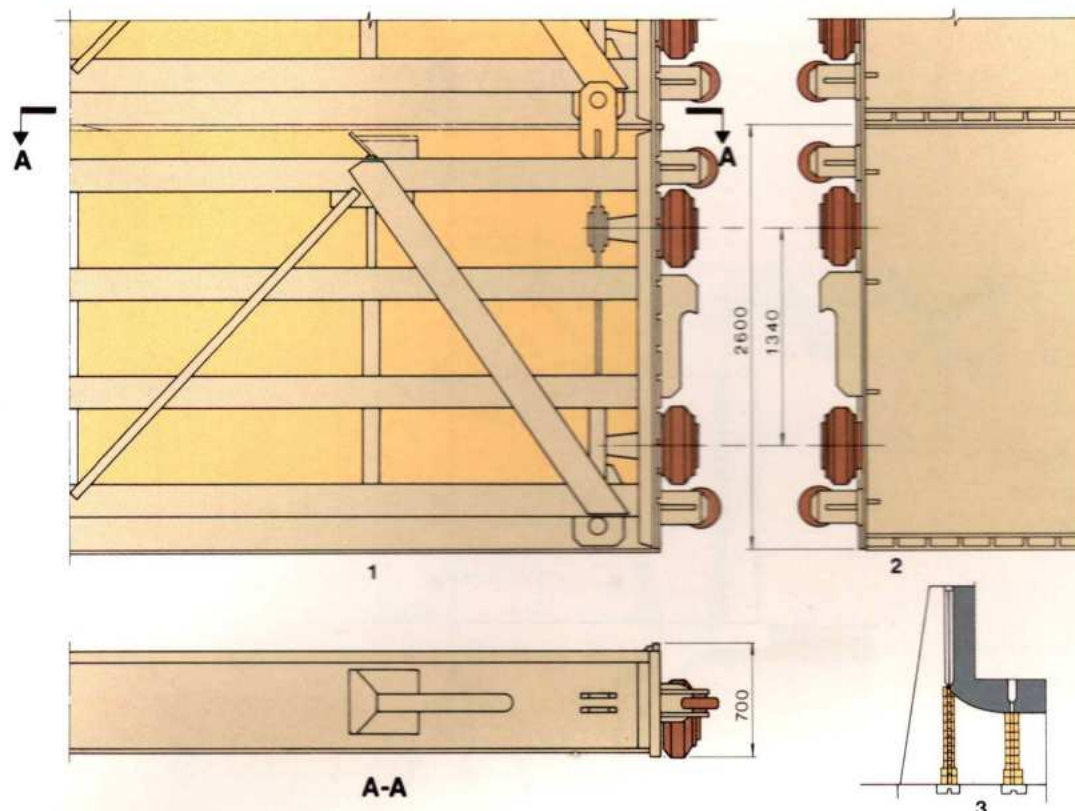
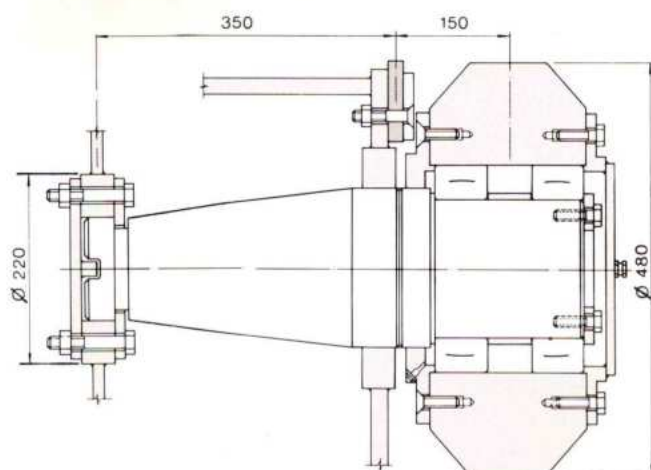


Fig. 6.37
Maintenance gate

- 1 Rear view of gate panel
2 Front view of gate panel
3 Gates in position

Fig. 6.38 Maintenance gate side seal



PERFORMANCE OF DIVERSION CONTROL STRUCTURE

INSTRUMENTATION ARRANGEMENT

The typical arrangement and location of instruments in three central blocks of the diversion control structure are shown in Fig.6.39.

The multiple extensometers penetrate about 70 m of the foundation down to joint A at El.10 approximately. Their orientation is such as to measure the vertical and horizontal deformations of most of the loaded foundation. Four sets of shallow piezometers measure the pore pressures at the dam-foundation contact as well as in the upper part of the foundation which was grouted. Deeper piezometers monitor joint A.

Rosettes of electrical resistance strainmeters were embedded at three elevations:

- In the base slab.
- In a pier between sluices.
- About 10 m above the soffit of a sluiceway.

A total of 27 rosettes comprising 135 strainmeters were installed in the three central blocks. No stressmeters were installed in the diversion structure.

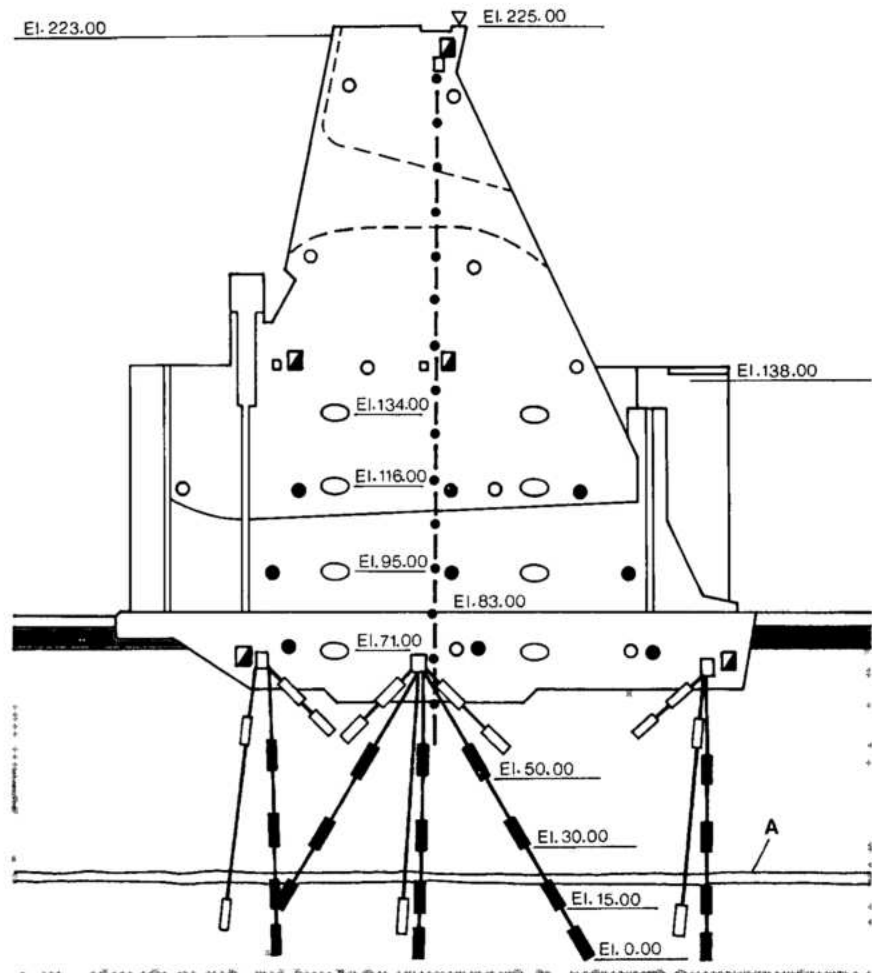
Thirty thermometers were embedded in three central blocks at five levels covering the entire section of the dam.

Since temperatures can also be derived from strainmeter readings, an excellent thermal history of the structure could be readily obtained at any stage.

To measure the openings of the two vertical longitudinal contraction joints which extended from the foundation to El.144, four Carlson type electrical resistance jointmeters were embedded across each joint in blocks H3/4, H8, H12/13 at 20 m height interval.

Fig. 6.39 Typical instrumentation arrangement

- ▲ Joint A
- Piezometer
- Multiple extensometer
- ▣ Group of pins for removable jointmeter
- Rosette of strainmeter
- Jointmeter
- Thermometer
- ⋮ Pendulum
- ▽ Bench mark
- Breccia
- ⋮ Basalt
- ⋮ Discontinuity



In the upstream longitudinal galleries, pins were embedded at four levels on each side of all the transverse contraction joints. Portable joint meters (extensometers) were used to measure the distance between the pins to an accuracy of 0.01 mm.

An inverted pendulum or plumbline, anchored in basalt at El. 51.4, that is, 13.5 m below the foundation of the structure, was installed in the middle of one of the central blocks. The top of the pendulum is in the longitudinal gallery at El. 211.

FOUNDATION RESPONSE

The central blocks of the diversion control structure, each 162 m high, are founded on sound basalt at El. 65. Parts of the foundation for some blocks were lowered an additional 2 m, after excavation of weak breccia and amygdaloidal basalt. The massive foundation slab of the dam, below the invert of the sluice at El. 83, was "keyed" into the foundation

excavated in the bed of the diversion channel. During the first filling of the reservoir in October 1982 and for the next 3 years, this foundation configuration was undisturbed. In 1986, the diversion channel was cofferdamed and excavation for four powerhouse blocks was undertaken adjoining the downstream toe of the diversion control structure.

In October 1978, when the river was diverted through the sluices, the structure had been constructed up to El. 115. During the next 9 months concrete was placed to an average elevation of El. 175 and remained essentially at that level for the next 2 years. From July 1981 through September 1982, the four power intakes were completed and the structure was topped out. During these four and half years prior to reservoir filling, the water level fluctuated between El. 120 and El. 135, and the load imposed on the foundations was primarily composed of the weight of the structure itself. Foundation deformations were essentially all vertical settlement; the extensometers indicated negligible horizontal

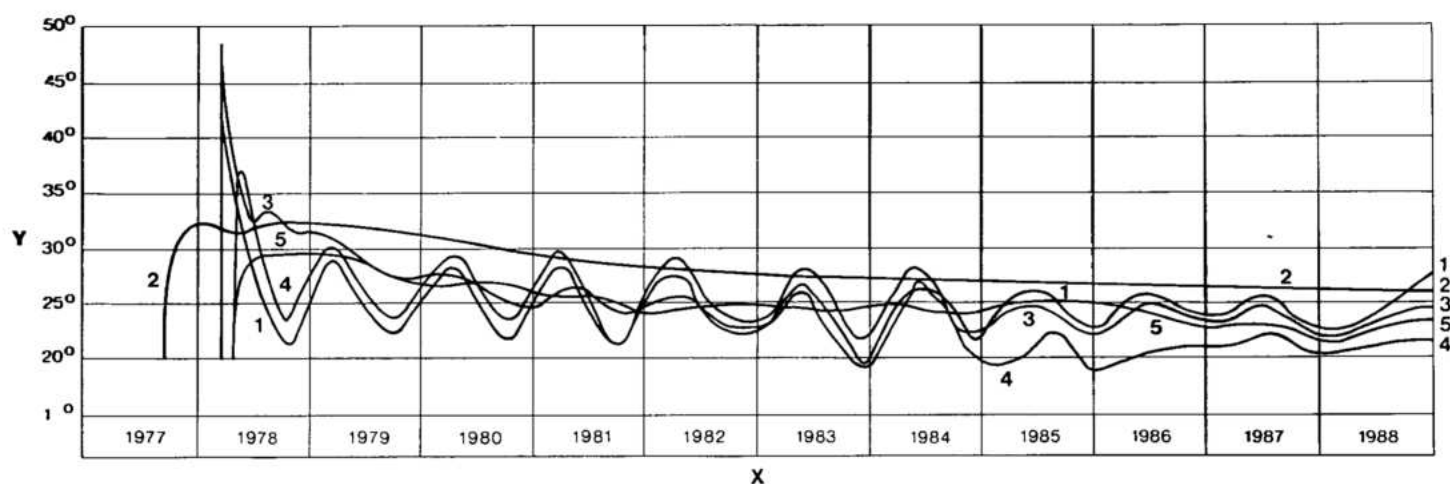
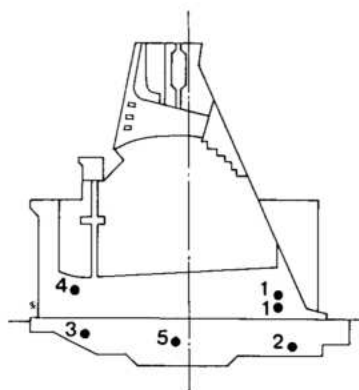


Fig. 6.40 Concrete temperature histories

Y Temperature °C
X Year
1, ... 5 Thermometers



deformation toward downstream. Seasonal ambient temperature changes affected the deflection of the structure, which in turn had insignificant effect on foundation deformation. Since the average temperature of concrete in the 18 m thick base dropped only 5°C in 4 years, see Fig. 6.40, the contraction of concrete did not have an appreciable effect on foundation deformations. It was concluded that in October 1982 the foundation was responding elastically to the imposed loads.

After the diversion gates were closed in October 1982 and the nearly full reservoir load was applied, vertical, as well as, horizontal foundation deformations increased and the distribution changed, reflecting the non-uniform normal, and shear loads transferred to the level foundations and the steep abutments. The measured deformations indicated that as the micro-cracks in the foundation were pressurized and the rock underwent some creep adjustments, a steady state of elastic equilibrium was attained after a period of several months. Thereafter, the structure and the

foundations responded essentially as an elastic integral unit.

The diversion structure and its foundation were both subjected to the maximum lateral load when the diversion channel was dewatered and the rock at its toe excavated down to El.55 for powerhouse construction during January–September 1986. The removal of 28 m of the toe support and the elimination of tailwater pressure disturbed the equilibrium of the diversion structure-foundation complex. While there was no differential displacement between the structure and its abutments and foundations, creep was triggered or re-started which resulted in additional permanent lateral deformation.

Fig. 6.41 shows the vertical foundation deformations measured between 1982 and 1987. Settlement of the blocks was also measured by precise geodetic leveling. Using the October 1982 (reservoir impounding) reading as datum, the maximum crest settlement of 38.3 mm observed in September 1987, in block H 3/4, was less than the calculated value of 50 mm, see Fig. 8.46.

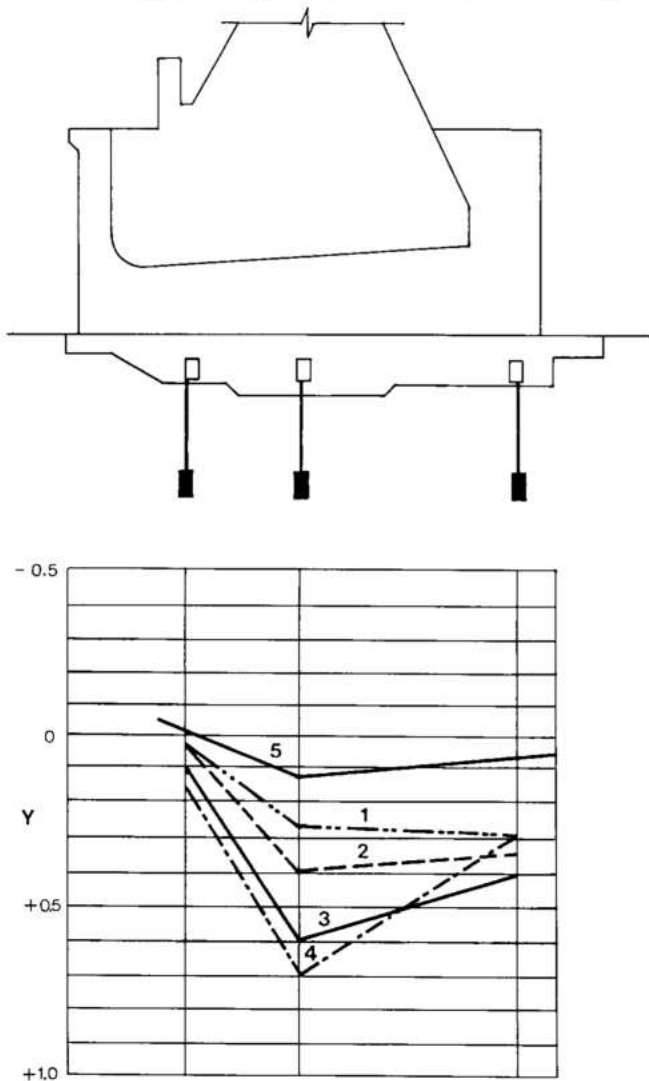


Fig. 6.41 Foundation vertical deformation

Y Deformation diagram (mm)
 ■ Extensometer
 □ Galleries
 1, ... 4 Foundation slab deformations in years 1984, 1985, 1986 and 1987 respectively
 5 Deformations measured between 1982 and 1984
 (–) Denotes upward deformation
 (+) Denotes settlement

Maximum deformation in the downstream direction was about 2 mm under the central part of the structure. It was less towards the abutments. Such displacements occurred at a progressively slower rate and ended in October 1987 when the powerhouse structure had been built to El. 100. The displacements were measured by the extensometers and confirmed by the inverted pendulum.

Foundation drainage and uplift

Uplift pressures at the dam-foundation contact, in joint B at El. 55 and in joint A at El. 10, were measured

by 83 piezometers. Foundation contact piezometric pressures stabilized about 2 years after reservoir filling; the same was true of the pressures in joints A and B. The piezometric pressures remained essentially steady with minor fluctuations due to changes in reservoir and tailwater levels, particularly the latter. The only significant reduction in uplift occurred in November 1987 when the downstream grout and drainage curtains for the powerhouse were completed and the diversion channel was still empty. Fig. 6.42 shows uplift pressure distribution under the structure in 1987.

Flow from drains drilled into the foundation and abutments, including those intercepting foundation joints A and B, was steady from 1983 through 1985, and averaged 15 l/s. Inflow from the abutments was about one-third of the total. In 1986-87, when excavation for the diversion channel powerhouse commenced, there was an increase of about 10 l/s in seepage flow from the left abutment drainage system, some of it being flow through cracks in the concrete in gallery corners. Grouting, crack treatment and new drill holes were undertaken to reduce and control the seepage.

The low uplift pressures and drainage flow attest to the effectiveness of the grout curtains and the foundation drainage system.

STRUCTURAL PERFORMANCE

Thermal behavior of the structure

Concrete in the diversion control structure was placed at temperatures averaging 7°C. There was no provision for post-cooling. Concrete in the piers and the invert of the sluiceways had a higher cement content than the mass concrete in the structure. This was necessary to provide strength, as well as higher resistance against hydraulic erosion.

Concrete temperature histories at seven locations in a typical block of the diversion control structure are shown in Fig. 6.40. While concrete in the piers and floor of the sluiceway had a maximum rise in temperature ranging from 40°C to 48°C, it cooled rapidly to the ambient temperature in 6 months, and after river diversion in October 1978, temperatures were the same as that of the river water. Concrete in the massive base slab, which had a lower cement content, had a temperature rise of only about 20°C, but it cooled at a very slow rate of about 1°C/year and reached the average ambient temperature of 25°C in 7 years after placement. In the areas of high strain near the foundation, such a slow rate of temperature drop obviated the risk of cracking.

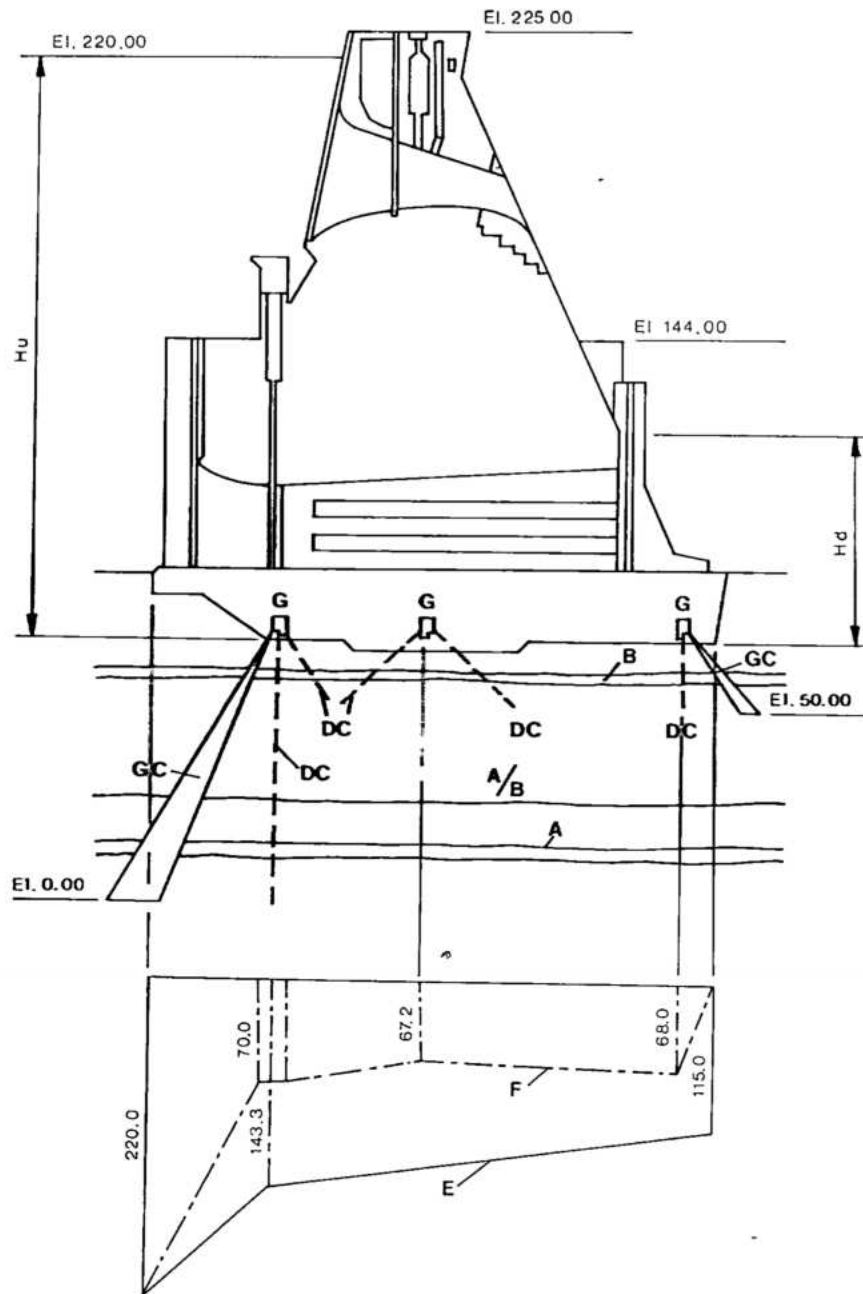


Fig. 6.42 Hydraulic uplift pressure

- Y Uplift (m)
- A Joint A
- B Joint B
- A/B Contact A/B
- DC Drainage curtain
- GC Grout curtain
- Hu Upstream head (m)
- Hd Downstream head (m)
- E Uplift load diagram assumed in normal load criteria, at foundation level
- F Uplift measured on June 30, 1987 at foundation level (m)
- G Drainage galleries

The upper massive part of the structure, between El. 105 and 165, also cooled at a relatively slow rate of about 0.5°C per year. Before the first filling of the reservoir in October 1982, concrete in the lower half of the structure had cooled enough to open about 70% of the longitudinal contraction joints.

Deflections of the structure

Deflections of the structure were measured by the inverted pendulum located essentially in the middle of the structure. The measurements commenced in 1982 and were made at three elevations in the galleries. Fig. 6.43

shows the deflections in the direction of flow for 6 years after reservoir filling and during the peaks of summer and winter.

Since measurements commenced after the structure was nearly finished, the deflections are not the absolute total values. However, prior to reservoir filling, the lateral deflections were very small and fluctuated with the seasonal temperature changes. After the reservoir was filled, the mean annual deflection of the dam crest was about 5 mm in the downstream direction. The pendulum also indicated an axial deflection of the structure of 2 mm towards the left.

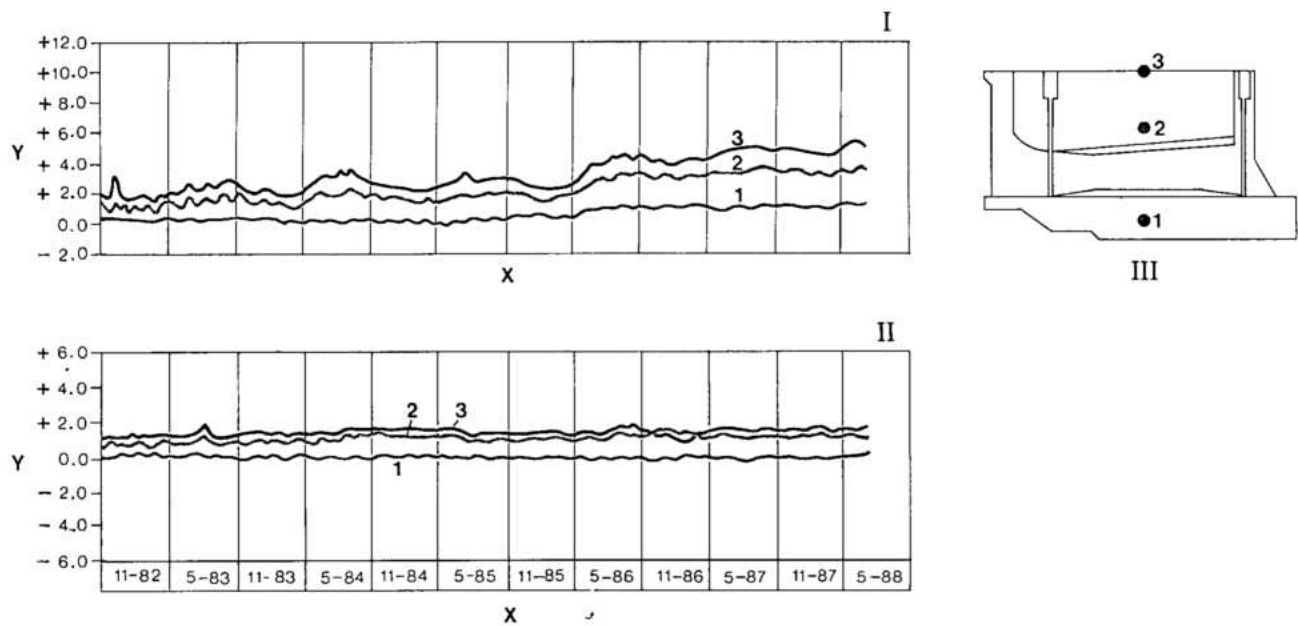


Fig. 6.43 Structure deflections

I Deflections in direction of flow

III Section of the diversion structure

X Month and year

(+) Deflection in upstream direction and to hydraulic right side

II Deflections normal to flow

Y Deflections (mm)

1, 2, 3 Location of inverted pendulum

Through 1985, the average seasonal fluctuations in the deflections of the crest were about 2 mm upstream in the summer (October–February) and about the same amount in the downstream direction in winter (May–August). Following the excavation for the powerhouse in 1986, foundation creep deformation increased the mean annual crest deflection to about 7 mm as the following observations indicate:

Period	Mean annual crest deflection (mm)
December 1986	8.0
July 1987	6.0
December 1987	8.8
November 1988	10.8

These values are much lower than the maximum deflection of 21.8 mm computed by three dimensional FEM analysis for normal loading. The difference can be explained by the following:

- Measured values do not include foundation and structural deformations during construction;
- Actual modulus of elasticity of the foundation rock is higher than that assumed in analysis;

- Because the transverse contraction joints are keyed, there is some interlocking three-dimensional action which makes the structure less flexible;
- The analysis assumed the entire structure cooled to average annual ambient temperature.

Performance of contraction joints

During September–October 1981 and August–September 1982, the longitudinal contraction joints in the piers and in the floor slab of the sluiceways were open 3 to 6 mm. However, about 30% of the upper parts of the joints were closed. The longitudinal joints were grouted in 1982 before reservoir filling. Subsequent measurements during five years indicated that the longitudinal contraction joints were tight and that the structure was acting monolithically in the direction of flow.

Transverse contraction joints between all blocks of the diversion structure, except for the shorter end blocks, have vertical keys and the joints were not grouted. After 5 years of operation the following displacements were measured across transverse contraction joints:

Blocks	Joint opening or closing (mm)	
	EI.67	EI.214
Central	0.08	0.10 – 0.20
End	0.04	1.00 – 1.70

Openings of transverse contraction joints show a seasonal variation of 0.10 to 1 mm near the top of the dam, the larger openings occurring in winter.

Relative displacement between adjoining blocks in the direction of flow was negligible. It appears that the contraction of the blocks due to a drop in body temperature is offset by the axial deformation of the concrete under reservoir pressure. Also the interlocking effect of the keys in the joints transferred some load from the more flexible central blocks to the abutments.

Stresses in concrete

In September 1982, when the diversion control structure was topped out, but before the first filling of the reservoir, concrete in the base slabs and the sluiceway piers was in compression due to the weight of the dam. The maximum vertical normal stresses were in the piers near the downstream end, and ranged from 180 to 290 N/cm². In the thick base slab, the vertical compressions averaged about 100 N/cm². Normal tensile stresses occurred in vertical planes in the axial as well as transverse directions (σ_1 and σ_5) in the base slab and the downstream portion of the piers; these stresses ranged from 30 to 120 N/cm². The principal cause of these tensile stresses was the thermal strain in the highly restrained massive base slab.

Strainmeter measurements taken 20 days after completion of first reservoir filling, showed the following general changes in stresses in the lower portion of the diversion structure:

IN THE BASE SLAB

- Upstream monolith near gate slot: ± 30 N/cm² change in vertical stress; increase in transverse horizontal compressive stress, about 10 to 50 N/cm².
- Central monolith: about 30 N/cm² increase in vertical (σ_3) compression.
- Downstream monolith: 30 to 50 N/cm² increase in vertical (σ_3) compression.

IN THE PIERS

- Upstream portion near gate slot: reduction in compression by 50 to 100 N/cm² in σ_3 .
- Downstream portion: increase of 100 to 120 N/cm² in vertical compression.

Three years after closure of the diversion gates and filling of the reservoir, while the sluiceways were still unplugged, stresses in the diversion control structure had essentially stabilized. Seasonal variations were 30 to 50 N/cm² in the vertical normal stresses, indicating the seasonal response to ambient temperatures and minor fluctuations in reservoir level. The maximum measured compressive values of 450 N/cm² were the principal stresses (σ_4) in the downstream portion of the piers. Maximum tensile stresses of about 150 N/cm² occurred in one

block in the downstream base slab near the foundations. Since instruments located in a similar location in another block were indicating compression, it was decided to attribute these measurements to instrument malfunction.

Fig. 6.44 shows the distribution of vertical normal (σ_3) stresses in the base slab, a sluice pier and in the mass concrete about 10 m above the sluiceways. The stresses are the annual maximum stresses five years after the first filling of the reservoir. Throughout the structure, the maximum stresses are within permissible limits with an adequate margin of safety.

Effects of powerhouse excavation

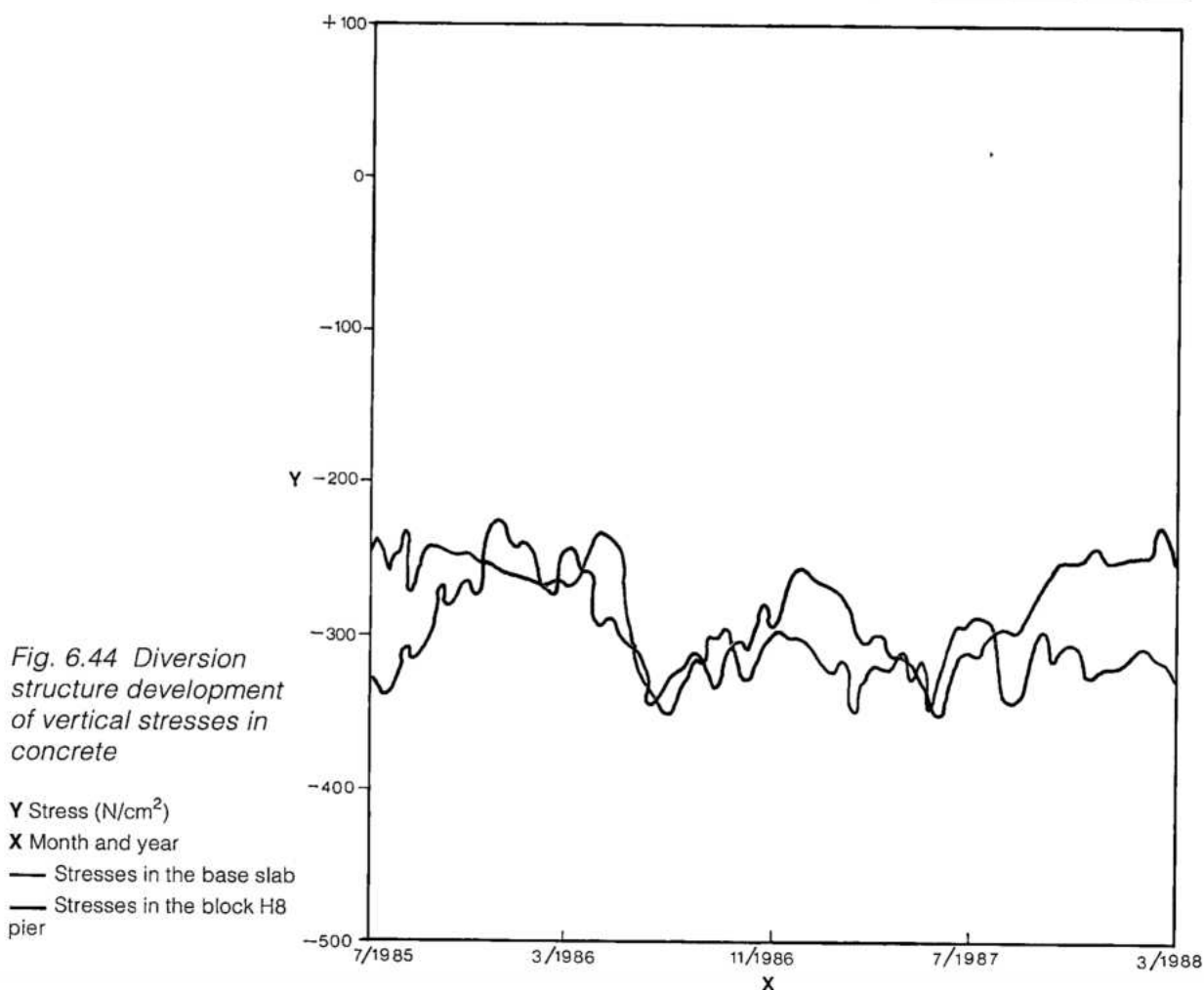
When excavation for the powerhouse at the toe of the diversion control structure was undertaken, some creep-type deformations were triggered in the foundation. Similar phenomenon occurred at the right abutment when some rock was excavated for a powerhouse erection area near the toe of the first block of the structure and the adjoining block F36 of the main dam. The behavior of the structure was affected in the following manner by the additional foundation deformations:

- There was some increase in vertical compression and lateral tension in the downstream monolith and a tendency for the downstream longitudinal joint to open. However, these changes were minor and did not affect the monolithicity or stability of the structure.
- Additional strains along the abutment caused cracking in the concrete around the transverse galleries and at the upstream corners of the lower galleries.
- There was an increase in seepage flow from some formed drains and through the cracks around the galleries.

By the end of 1988, when the powerhouse structure had been substantially completed and the foundation deformations had stabilized again, the structure resumed normal cyclical behavior. The cracks in the galleries were systematically repaired and the drainage restored and augmented.

Seepage through concrete

Drains formed in the concrete near the upstream face worked effectively in keeping the body of the structure free of internal uplift. Maximum total seepage through the concrete in December 1983, one month after reservoir filling, was about 10 l/s. With reservoir and tailwater levels fluctuating only about 2 m, seepage through concrete steadily decreased to 7 l/s by the end of 1985. For the next 18 months there was an increase of about 2 l/s, mainly through the new cracks in the galleries, related to



downstream excavation. After repair of the gallery cracks and provision of a new drainage system, seepage through concrete was steady at about 10 l/s, with some seasonal fluctuations indicating that ambient temperature changes affected seepage through unsealed cracks and joints.

Cracks in galleries

Three types of cracks occurred in the galleries of the diversion control structure:

- Vertical transverse cracks in the upstream gallery at El. 144, which were caused by the rapid cooling of concrete by air convection. This gallery was open at both ends for almost two years while the lower part of the main dam was under construction. These cracks, which occurred in the upstream wall of the gallery, were less than 0.1 mm in opening and were wet or leaking small amounts of water after reservoir filling. Most of these cracks were sealed by lime deposits in about 12 months.

- Corner cracks in lower galleries and cracks in lower transverse galleries near the abutments occurred in 1986. As discussed earlier, these were attributed to foundation creep caused by powerhouse excavation. Pressure grouting was used to seal these cracks and drain holes were drilled to relieve pressure and regulate leakage flow.
- Longitudinal cracks in the upstream foundation gallery (El. 67.25). In a typical block of the diversion control structure, the reservoir load is borne by its massive portion downstream of the sluice gates. The upstream gate structure, resting on a relatively thin base slab, could not be made sufficiently monolithic with the rest of the structure. The upward bending of the tapered base slab caused horizontal tensile stress near the base of the slab. These tensions were higher than the strength of concrete, causing vertical cracks parallel to the gallery, probably starting from the foundation. These cracks were sealed with cement grout.

None of the above three types of cracks affected the stability of the dam.

Summary

The overall performance of the diversion control structure and its foundation was satisfactory and as anticipated during construction, first filling of the reservoir and after 6 years of operation. The only unexpected phenomenon was the secondary foundation creep triggered by downstream powerhouse excavation. However, the structure has responded in a satisfactory manner and achieved a normal state of steady equilibrium and is behaving as a monolithic gravity structure elastically bonded to its foundations. There is also a significant degree of three-dimensional interaction between adjoining blocks.

EARTHFILL

AND ROCKFILL DAMS

GENERAL LAYOUT	7.3
ROCKFILL DAM	7.4
Geological Conditions and Foundations	7.4
Typical Cross-Section	7.4
Rockfill-Concrete Dam Interface	7.5
TRANSITION BETWEEN ROCKFILL DAM AND THE LEFT EARTHFILL DAM	7.8
LEFT EARTHFILL DAM	7.10
Geological Conditions and Foundations	7.10
Typical Cross-Section	7.10
RIGHT EARTHFILL DAM	7.12
Geological Conditions and Foundations	7.12
Typical Cross-Section	7.12
TRANSITION OF RIGHT EARTHFILL DAM AND OVERLAP WITH THE SPILLWAY	7.13
PERFORMANCE OF THE EMBANKMENT DAMS	7.15
Instrumentation and Monitoring	7.15
Performance of the Rockfill Dam and its Foundation	7.16
Performance of the Earthfill Dams and their Foundations	7.17

EARTHFILL

AND ROCKFILL DAMS

GENERAL LAYOUT

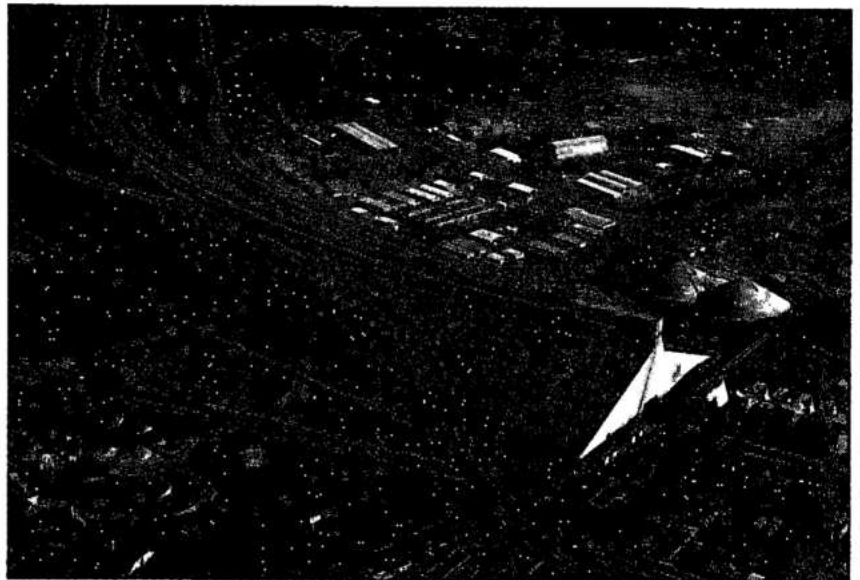
The general plan of the Itaipu project which is shown in Fig. 3.2 of Chapter 3 indicates the location of the principal structures of the scheme, including the rockfill and earth dams on the left bank and the earth dam on the right bank.

Total length of all Itaipu dam structures is 7750 m, of which 1984 m and 2294 m are respectively rockfill dam and earthfill dam on the left bank, and 872 m is earthfill dam on the right bank.

The volume of the rockfill dam is $12.8 \times 10^6 \text{ m}^3$, of which $10.7 \times 10^6 \text{ m}^3$ are rockfill, transition and filter, and the remaining $2.1 \times 10^6 \text{ m}^3$ is clay in the impervious core. Total volume of the left earthfill dam, including its transition with the rockfill dam, is $4.4 \times 10^6 \text{ m}^3$, of which $0.6 \times 10^6 \text{ m}^3$ is rockfill, transition and filter materials. The right earthfill dam has a total volume of $0.4 \times 10^6 \text{ m}^3$ of which $0.3 \times 10^6 \text{ m}^3$ is compacted clay and $0.1 \times 10^6 \text{ m}^3$ rockfill, transition and impervious core.

On both banks, above El.160 approximately, there was an extensive mantle of residual soils formed by the decomposition of basalt. These soils were generally homogeneous clays, of medium to high plasticity, porous, compressible and with low strength. The depth of the overburden increased with the distance from the river.

These factors, together with the low heights necessary for the extreme flanks of the dams, favored the selection of earthfill dams for a long stretch on the left bank and for a shorter portion right of the spillway. For the left



Left bank rockfill

earthfill dam there was no interference with any concrete structure or construction plant, nor were there any constraints of space. Also the borrow areas were at a convenient haul distance.

ROCKFILL DAM

The choice of a rockfill type section for the dam on the left bank was influenced by the supply of a large quantity of suitable material accumulated from nearby excavation of the diversion channel and the ease of transporting it directly to the place of dam construction.

Also, soil excavated for the rockfill dam foundation could be used in part as material for construction of the adjacent earthfill dam and in part for construction of dikes to divert the Pomba Quê and Bela Vista creeks.

To determine the length of the rockfill dam on the left bank and to select the type of fill (rock or earth), a comparative study was made, using for the final evaluation such parameters as volume of rock versus soil to be used for construction, cost of excavation, transport, placing and compacting.

GEOLOGICAL CONDITIONS AND FOUNDATIONS

Natural ground surface in the area of the rockfill dam was sloping gently between El.165 and El.182. The residual soil overlying rock, varied from 5 to 15 m in thickness. All the overburden was removed and most of the embankment was based directly on sound, dense basalt of flow E, see Chapter 4. The thickness of this basalt stratum is about 30 m. It is moderately jointed and generally has very low permeability. Near the surface, the basalt has sub-horizontal joints, which form "onion peel" layers, 25 to 30 cm thick.

At the base of the basalt, at about 30 m depth, there is a zone of breccia about 1 m thick. The permeability of this breccia was found by field tests to range from 0.2 to 0.6 Lugeons.

At a depth of about 40 m below the rock surface, there is joint A discontinuity, which has considerably higher permeability of 10 to 20 Lugeons.

TYPICAL CROSS-SECTION

As shown in Fig. 7.1, the rockfill dam has a central core of compacted clay with a vertical downstream face and 1V:0.6 H upstream face. The thickness of



Clay core of rockfill dam

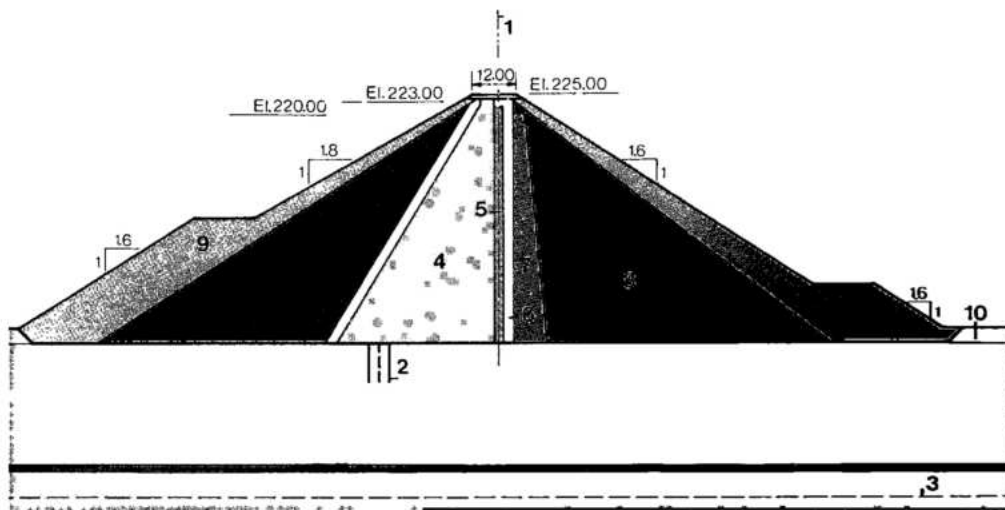
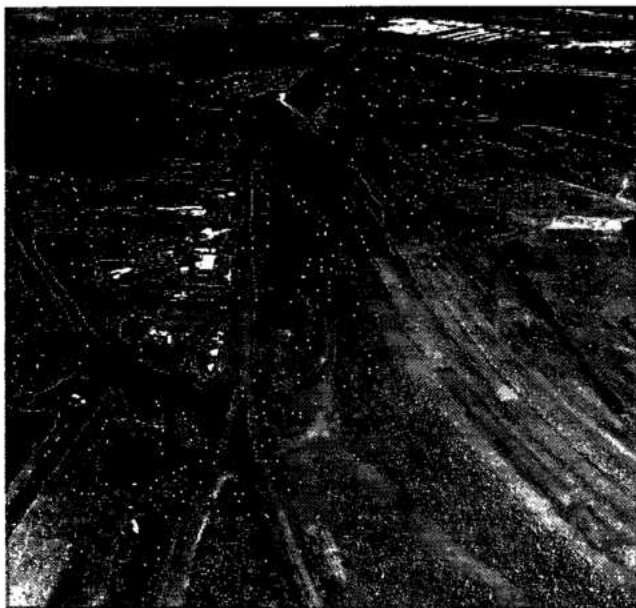


Fig. 7.1 Rockfill dam - Typical cross section



Rockfill dam nearing completion

the core is more than 0.65 of reservoir head. The clay core is protected on the upstream side by a 2.5 m thick zone of fine transition, consisting of crushed rock, minimum size 76 mm. The downstream face of the core is vertical. Protection against piping of clay fines is provided by a 2 m thick sand filter, then a 2.3 m wide fine transition zone of crushed rock, minimum size 76 mm, and finally a coarse transition composed of crushed rock 76 mm to 305 mm in size. The coarse transition zone is 3.2 m thick at the crest with a slight taper of 1 V:0.1 H. The external slopes of the outer shells of rockfill are 1 V: 1.8 H on the upstream and 1 V:1.6 H on the downstream side.

The foundations for the impervious core, the filter and the transition zones were sound rock, while the rockfill shells were based on slightly weathered rock reached after removal of ripable weathered material.

Under the clay core, two rows of 8 m deep low pressure grout holes were provided at 10 m centers to cut off seepage through the superficial portion of basalt. Sub-horizontal joints exposed under the core area and extending 10 m upstream of the core were slush grouted and sealed with cement mortar. Generally, the grout taken in the shallow cutoff holes was nominal.

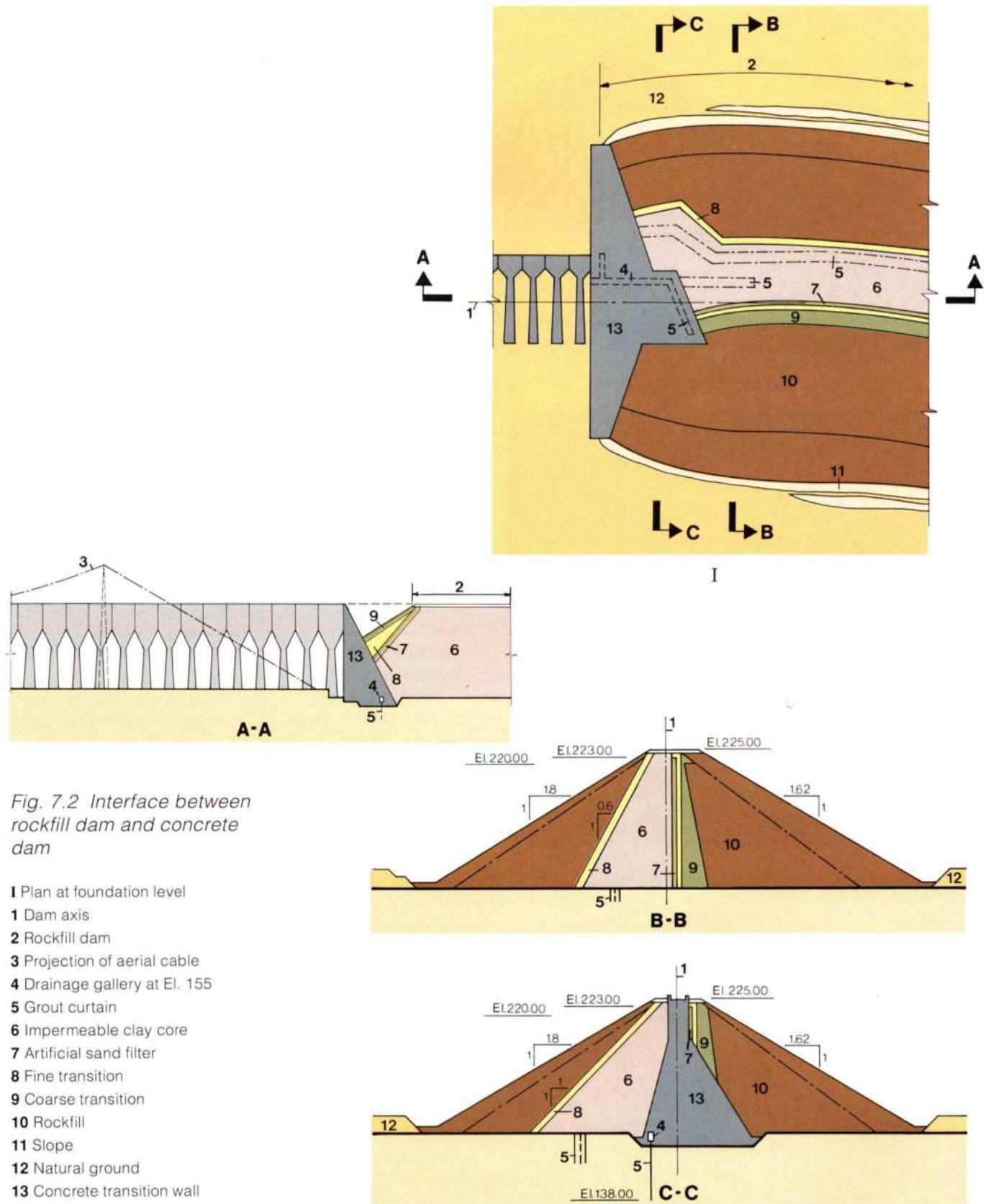
Placement and compacting of the sandy clay in the central core was in accordance with the following specifications:

Maximum layer thickness, after compacting	10 cm
Tamping roller	TC - 15B pad type
Number of passes	6
Moisture content	Range 0.5% above and 2% below proctor optimum

The rockfill was placed in 60 cm lifts and compacted by four passes of an 80 kN smooth vibratory roller.

ROCKFILL – CONCRETE DAM INTERFACE

Determination of the terminus of the left side of the rockfill dam, where it meets the concrete buttress dam, was dictated by the construction schedule and the temporary installations for concreting of the main dam and the powerhouse, in particular the cableways. If the rockfill dam was extended into the



cableway, its construction could have been undertaken only after the dismantling of the cableways in mid 1982. Considering that all the embankment dams were scheduled for completion by the end of 1981, construction of a rockfill portion in this area would have critically interfered with the schedule. For this and other reasons, it was decided that the interface between the rockfill dam and the concrete dam should consist of a transverse concrete gravity end wall located just left and clear of the cableways, see Fig. 7.2

Construction of rockfill-concrete dam interface was programmed to be as short as possible bearing in mind that closure of the diversion and consequent filling of the reservoir depended upon its timely completion.

It was estimated that the construction of a rockfill dam at this section of the embankment would be slower than that of a concrete type dam, due mainly to extended interruptions as a consequence of rain during the construction period.

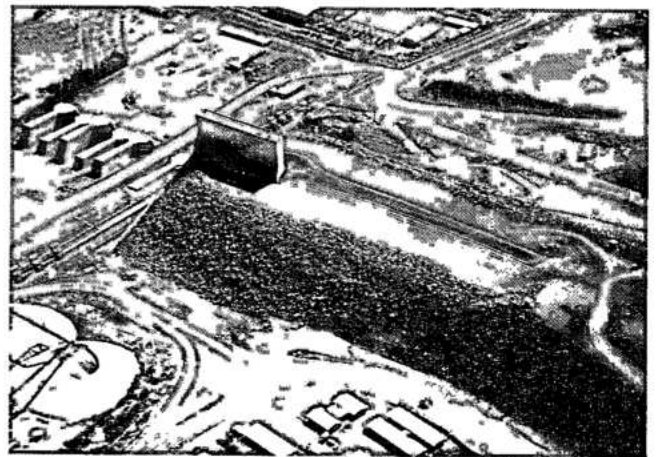
Therefore, construction of the rockfill dam was started near the area of counterweight installations for cableways, and was programmed to be completed before the cableways were dismantled.

That part of the concrete dam which formed the interface with the rockfill dam, was concreted starting from the point of anchorage of the aerial cables. It is a monolithic gravity structure with slopes of 1 V:0.34 H on the upstream side and 1 V:0.46 H on the downstream face and length of approximately 70 m, being entirely overlapped by rockfill structure, see Fig. 7.2. The overlap length was insufficient to develop the final slope of the rockfill dam. To overcome this, two gravity retaining walls were constructed perpendicular to the concrete dam on its upstream and downstream sides. These end walls were designed to retain and support the rockfill dam in the longitudinal direction, see Fig. 7.2. On the external face, the walls are vertical and on the rockfill side, they have a slope of 1 V:0.9 H, variable height of 0 to 25 m and total length of about 200 m.

Efficient contact was achieved by overlapping the clay core of the rockfill dam with the upstream face of the concrete. In the transverse section this overlap is 8 m wide at the crest, increasing with the depth in accordance with the upstream slope of the core which was increased to 1 V:1 H. The transverse contact width between clay core and foundation at the overlap was 0.65 times the reservoir head.

The longitudinal contact between the impervious clay core and concrete, along the upstream face of the concrete interface, is equal to the reservoir head.

External geometry of the rockfill dam was not modified, maintaining the same external slope until



Transition of rockfill dam with concrete dam

meeting with the face of the concrete interface or with the transverse gravity walls.

The end face of the concrete interface was inclined to the vertical as well as to the axis of the dam, so that with the settlement of the embankment the clay would exert positive pressure against the concrete.

Grout and drainage curtain holes were drilled from the gallery in the concrete transition at El. 155. The grout curtain consists of three rows of 75 mm diameter holes (primary, secondary and tertiary) 23 m deep with a minimum spacing of 2.5 m. From the same gallery one row of 100 mm diameter drainage holes were drilled, 15 m deep and 3 m spacing. These drainage holes were topped by 125 mm diameter steel tubes which acted as drill guides and also facilitated measurement of leakage flow. An upstream grout curtain of two rows of 75 mm diameter holes, 6 m deep with 2.5 m maximum spacing extends from the concrete transition beneath the impermeable core to meet with the grout curtain of the rockfill dam.

A second grout curtain under the impermeable core consisting of three rows of 75 mm diameter holes drilled to El. 136 extends from the concrete transition to 40 m upstream, parallel to the dam axis.

In the rockfill dam overlap there is no drainage curtain.

To measure pressure at the clay concrete contact, pressure cells were installed at three different locations on the face of the concrete interface.

TRANSITION BETWEEN ROCKFILL DAM AND LEFT EARTHFILL DAM

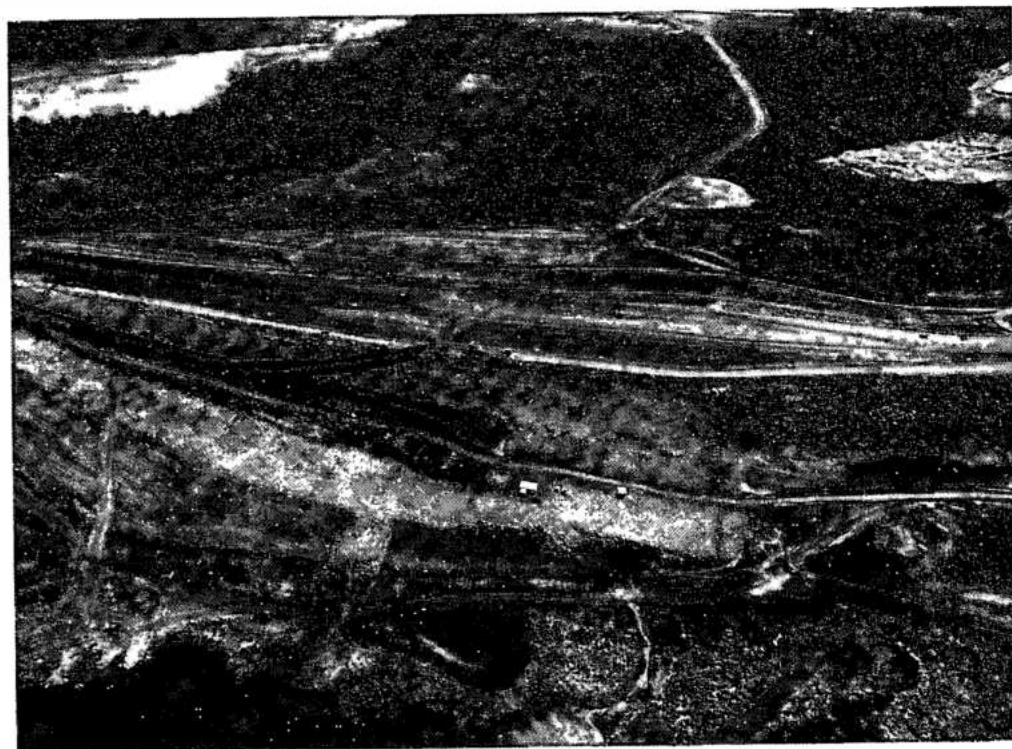
A 300 m long transition from the rockfill dam to the left earthfill dam was necessary to accommodate the differences in foundation conditions and requirements and the cross-sections of these two types of embankment dams. The plan and cross-section of the transition are shown in Fig. 7.3.

On the upstream side, while the rockfill zone was gradually reduced, the clay core of the rockfill dam was widened by increasing its upstream slope from 1 V:0.6 H to 1 V:3 H at the left end of the transition.

Similarly, the downstream vertical filter was progressively replaced by compacted soil which was widened until it matched the 1 V:3.5 H slope of the earthfill dam. The external slopes were also gradually flattened to match those of the earthfill dam at the end of the transition.

The internal system of drainage in the transition portion consists of a 2 m wide vertical filter, which is continuous with the filter zones of both embankment dams, and by a 1.5 m thick filter carpet draining horizontally to the downstream and located directly on the foundation.

For most of the transition portion, the overburden of residual soil was excavated to sound rock. About 100 m from the earthfill dam, the excavation was sloped up to firm soil.



Construction of the transition between rockfill and earthfill dams

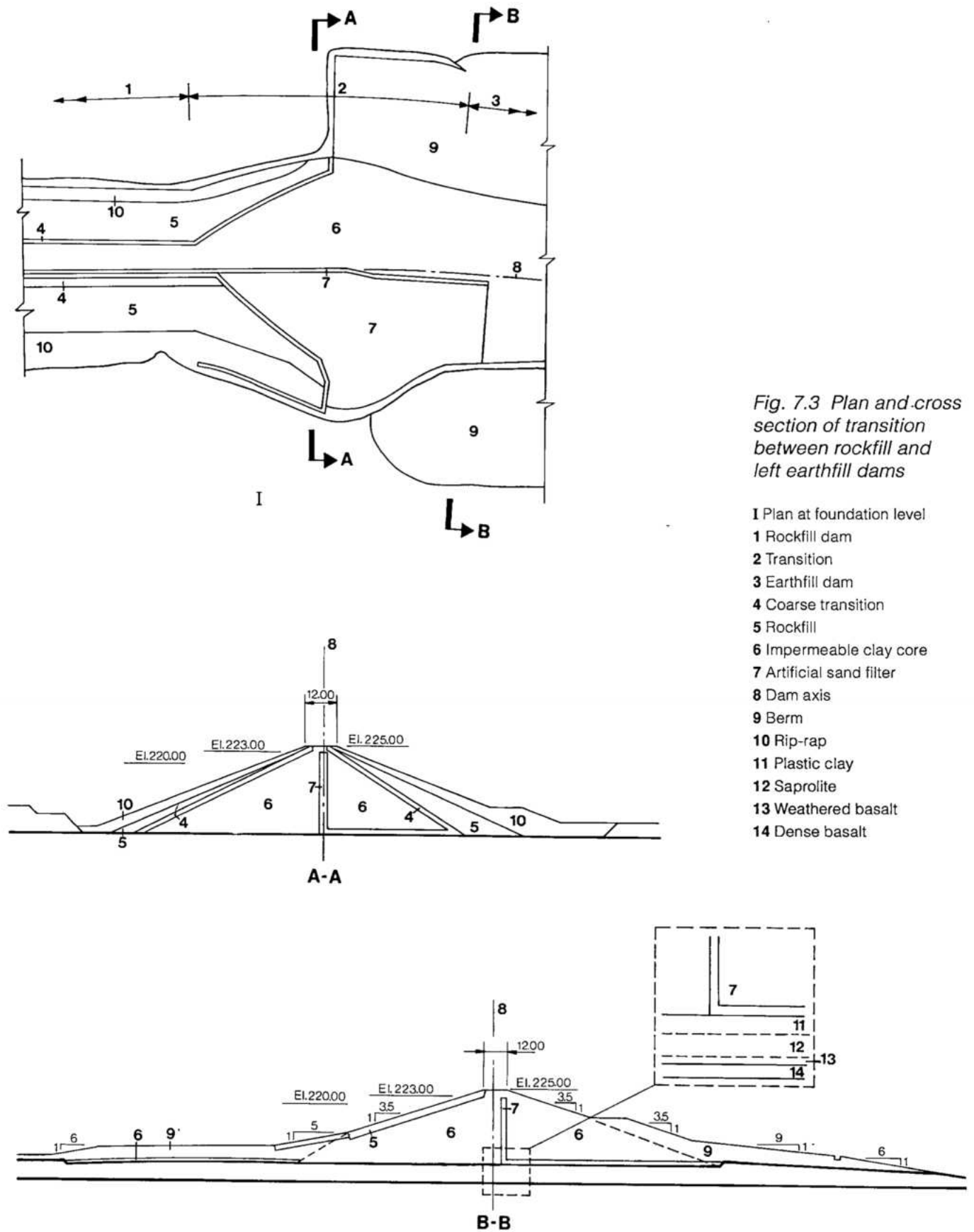


Fig. 7.3 Plan and cross section of transition between rockfill and left earthfill dams

- 1 Plan at foundation level
- 1 Rockfill dam
- 2 Transition
- 3 Earthfill dam
- 4 Coarse transition
- 5 Rockfill
- 6 Impermeable clay core
- 7 Artificial sand filter
- 8 Dam axis
- 9 Berm
- 10 Rip-rap
- 11 Plastic clay
- 12 Saprolite
- 13 Weathered basalt
- 14 Dense basalt

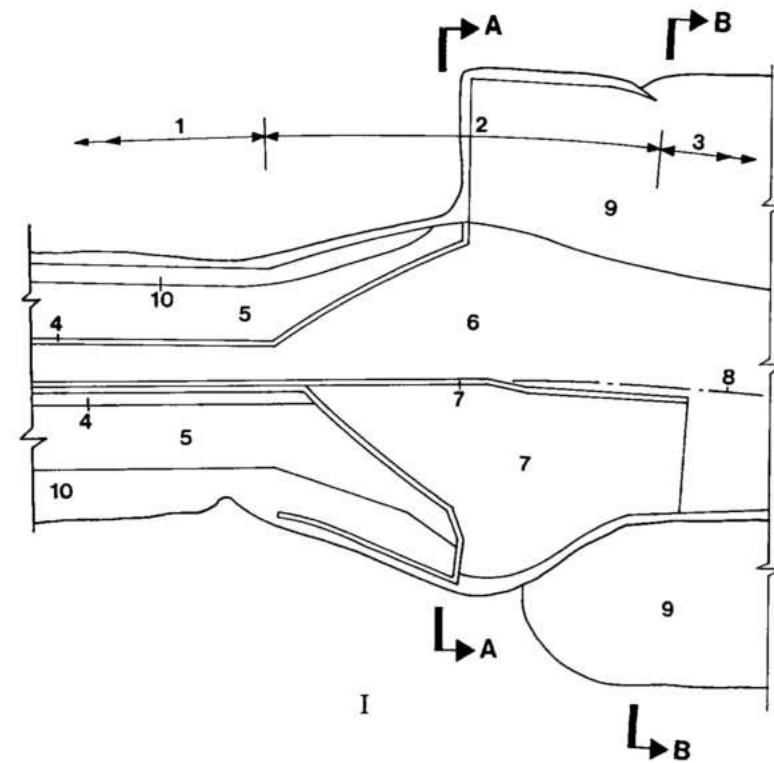
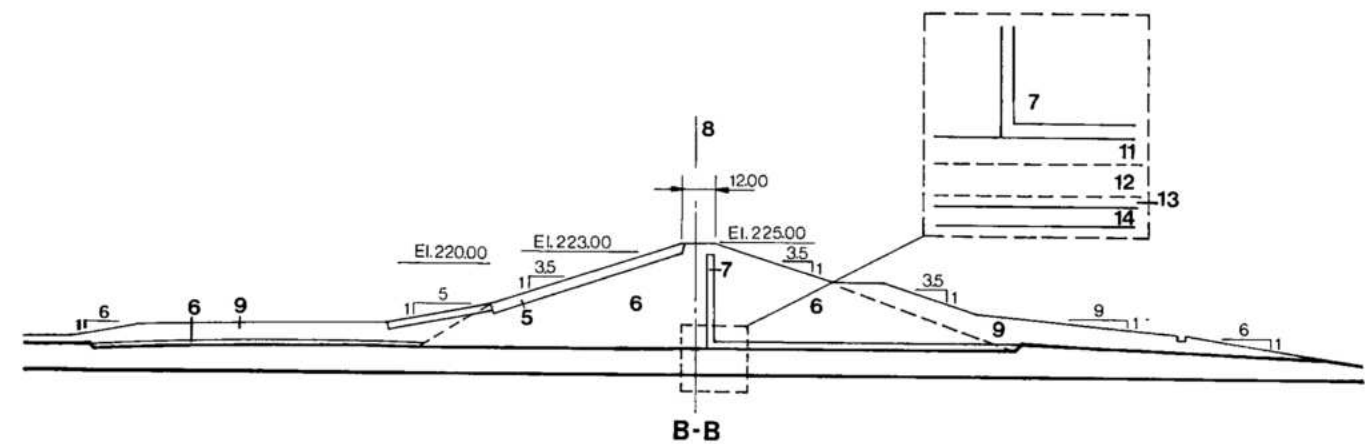
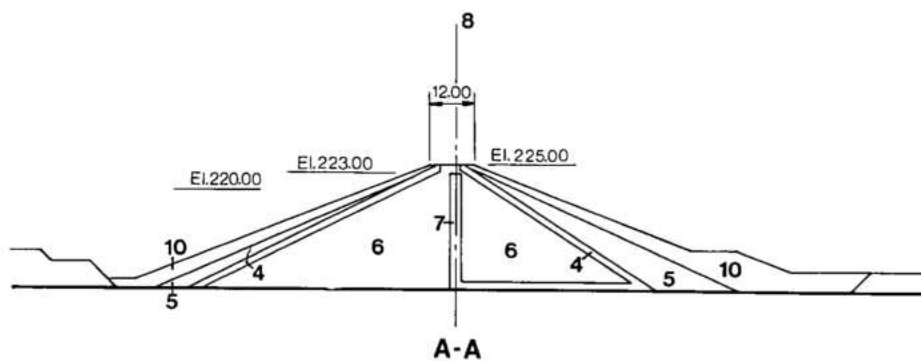


Fig. 7.3 Plan and cross section of transition between rockfill and left earthfill dams



LEFT EARTHFILL DAM

GEOLOGICAL CONDITIONS AND FOUNDATIONS

The foundations for the left earthfill dam are composed of residual soils derived from basalts and breccias.

The plastic clay which belongs to the CH group of unified classification, appeared in a layer of average 6 m depth. At its base it had a layer of continuous weathered and fragmented rock which appeared in all locations along the embankment and was always involved in a clay matrix.

A detailed study was made to determine the behavior of this porous clay in the foundation. It was partially saturated, had characteristics of rapid increase in density and resistance with the increase of superimposed load and, as such, had acceptable properties as a dam foundation. This conclusion was reached after laboratory tests and principally, after analyzing the behavior of the clay in areas of stockpiles and backfills made by the contractors for various construction installations of the project.

All these tests and observations were confirmed by Instituto de Pesquisas Tecnológicas de São Paulo (IPT) type pressure meters installed in the earthfill dam, which showed that the compression of the partially saturated

porous clay was proportional to the increase in height of the dam fill during construction and rapidly stabilized when the final height was reached.

Below the porous clay a saprolite type of soil occurred in a layer of up to 9 m in depth. The saprolite was composed of sandy or silty clays, of plastic consistency, greyish-red in color, with traces of basalt rock matrix together with old fractures, forming paths for seepage of subsoil water.

The saprolite was underlain by sound basalt rock with few joints. At the level of this rock, however, a thin layer of very fractured material was found.

TYPICAL CROSS-SECTION

With the objective of optimizing the design, the left earthfill dam was divided into two stretches:

- 10 to 30 m high.
- less than 10 m high.

The higher stretch of the dam, 10 to 30 m in height, is 630 m long starting from the transition with the rockfill dam. Essentially it has a homogeneous central section of compacted plastic clay with the upstream and downstream slopes of 1 V:3.5 H from crest down to mid-height and then 1 V:2 H to the foundation, see Fig. 7.4. Starting from the points of inflexion of the slopes of the central section, stabilizing berms with very flat slopes were provided on both sides.



*Left earthfill dam
in construction*

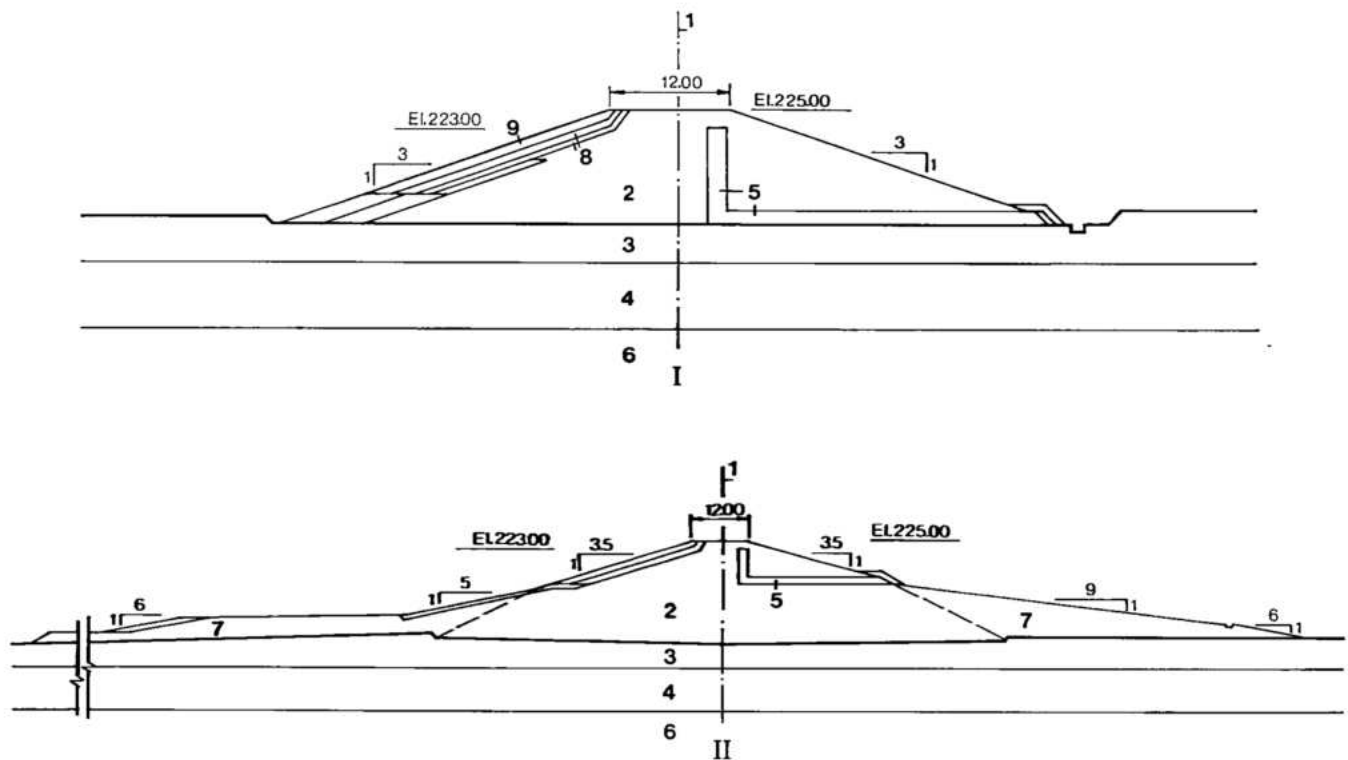


Fig. 7.4 Left earthfill dam cross sections

- | | | | |
|--|-------------------------|--------------------------|---------------------|
| I Left earthfill dam with height less than 10 m | 1 Dam axis | 4 Weathered rock | 7 Berm |
| II Left earthfill dam with height between 10 and 30 m | 2 Impermeable clay core | 5 Artificial sand filter | 8 Coarse transition |
| | 3 Plastic clay | 6 Dense basalt | 9 Rip-rap |

On the upstream side, the berm becomes a 2 m thick impervious blanket. Some portions of the berms were placed before the central section of the dam was started. Random soils, including plastic clay, saprolite and weathered basalt, as obtained from excavation for the foundations of the rockfill dam, were used for constructing the berms. The material was spread by bulldozers in 20 cm layers and compacted by two passes of a smooth vibratory roller.

Compacting of the central clay section was done in accordance with the same specifications as for the core of the rockfill dam. To minimize differential settlements, excavation for the foundation had a trapezoidal section, removing a maximum of 3 m under projection of the crest and 0.5 m at the upstream and downstream extremities of the central section. Under the berms, only the topsoil with organic matter was excavated.

Internal drainage is by a 2 m thick vertical chimney filter linked with a 1 m thick horizontal carpet filter. For the filters, crushed rock was used, which was a by-product or reject from the primary crusher for making concrete aggregate, see Chapter 5.

Seepage captured by the filters, or coming through the foundations, drains through the natural layers of saprolite or weathered rock. Several permeability tests made in bore holes, and the experience from Pomba Quê and Bela Vista dikes, which were constructed nearby and on similar foundations, indicated that the strata of weathered basalt and the saprolite would provide excellent natural drainage.

As an additional safety measure, after the filling of the reservoir, a line of drainage wells was executed near the downstream toe of the dam. These wells were 0.20 m diameter, at 30 m spacing and extended into the weathered basalt.

For the 1360 m long portion of the left earthfill dam, where it is 10 m or less in height, the cross-section has uniform slopes of 1 V:3 H on both faces. It is constructed of compacted plastic clay, see Fig. 7.4. No berms were provided. The internal drainage system is similar to that of the higher portion.

For this portion of the dam excavation was limited to only 1 m of top soil, which contained organic material together with dried-out clayey soil mixed with weathered rock fragments.

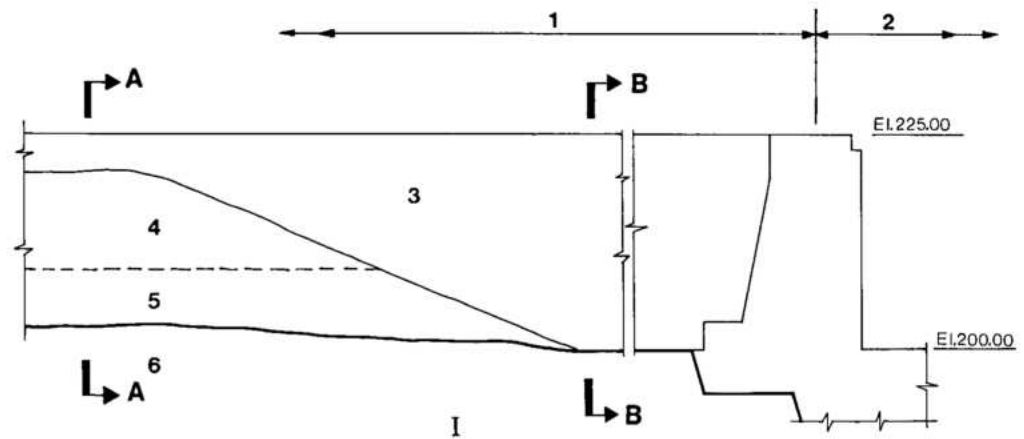
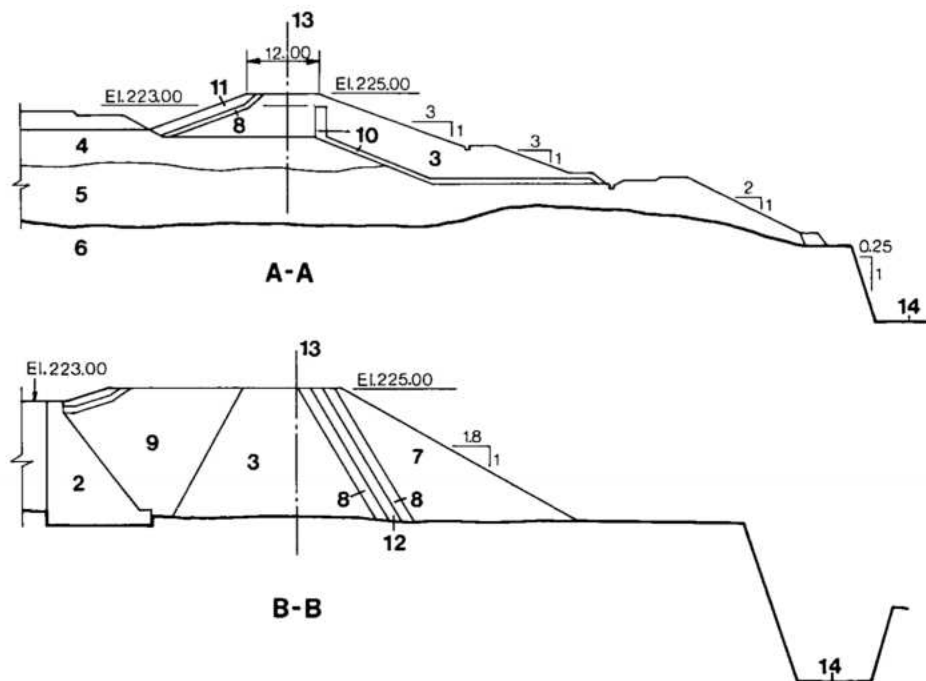


Fig. 7.5 Transition between right earthfill dam and the spillway - longitudinal and transverse sections (for plan views, see Fig. 7.6)

- 1 Longitudinal section
- 1 Right earthfill dam
- 2 Spillway structure
- 3 Impermeable clay core
- 4 Plastic clay
- 5 Saprolite
- 6 Dense basalt
- 7 Rockfill
- 8 Coarse transition
- 9 Backfill with rockspoil
- 10 Artificial sand filter
- 11 Rip-rap
- 12 Fine transition
- 13 Dam axis
- 14 Access road to powerhouse



RIGHT EARTHFILL DAM

GEOLOGICAL CONDITIONS AND FOUNDATIONS

The geology and foundation treatment were identical for both right and left earthfill dams.

The material from borrow pits on the right bank was limited only to highly plastic clay, whereas on the left bank plastic soils and sandy material were available as well, having originated from decomposition of outcrops of basaltic breccia.

TYPICAL CROSS-SECTION

The right earthfill dam is a homogeneous conventional section of compacted plastic clay with uniform upstream and downstream slopes of 1 V:3 H, with maximum height of 25 m and 900 m length, see Fig. 7.5.

The internal drainage system comprises a vertical filter 2 m wide and drainage blanket 1 m thick, both of artificial sand. An important aspect of design is a free outflow of internal drainage along the whole toe of the downstream side of the dam.

Excavations for the dam removed the overburden, to only 1 m in depth in order to eliminate dry topsoil and regularize the ground.

Percolation through foundation is controlled by a drainage blanket composed of sand and by permeable stratum of saprolite outcropping on the downstream side of the dam near the access road to the powerhouse.

To avoid future erosion of slope at this location, graded filters of granular material were provided.

TRANSITION OF RIGHT EARTHFILL DAM AND OVERLAP WITH THE SPILLWAY

The type of contact between the earthfill dam and the concrete structure on the right bank was different in concept than the left side embankment.

The design of the dam in the zone of the overlap at the spillway was determined by hydraulic conditions of the spillway, which required construction of a guide wall with a crest at El. 223.

Thus, on the upstream side, the concrete structure overlaps the earthfill core and acts as its confinement, see Fig. 7.5.

Excavation for the road under the spillway, limited the space available for a massive earthfill, see Fig. 7.5, and in consequence, clay fill on the upstream side and rockfill on the downstream side were retained by the lateral wall of the spillway.

In the transition section, of approximately 50 m in length, a change in external geometry and in zoning of the core was required for proper contact with the concrete structure of the spillway.

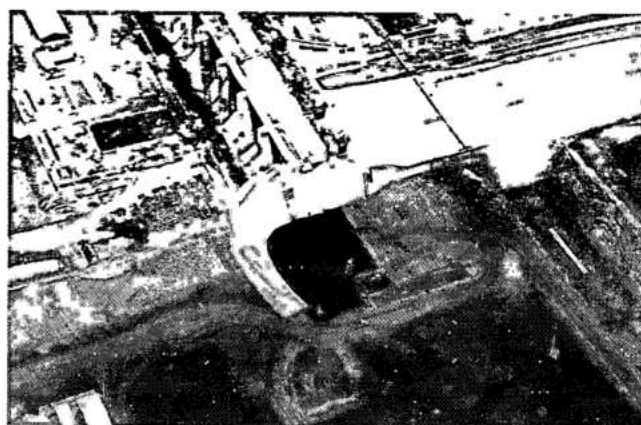
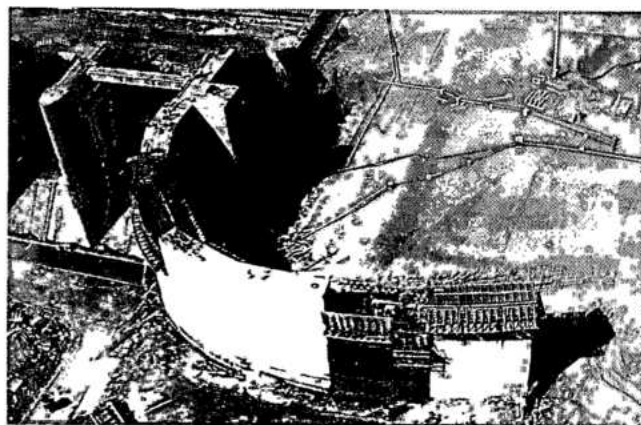
The transverse section changes progressively from a homogeneous section of clayey material founded on soil to a mixed section of earth-rockfill founded on rock.

In this stretch, excavation of the foundation deepens, cutting the plastic clay stratum and saprolite with a much flatter slope of 1 V:4 H, until it reaches sound rock foundation.

A clay fill with a slope of 1 V:3 H, is transformed into an impervious central core 12 m wide at the crest with external slopes of 1 V:0.5 H on the upstream and downstream sides of the dam.

On the upstream side of the dam the crest widens to match the external alignment of the dam with the guide wall.

The space between the impervious clay core and the external upstream slope of the earthfill is filled by clayey material which becomes gradually thicker and higher, with the external slope deviating from the alignment at the earthfill dam and the impervious core decreasing in thickness as excavation of the foundation deepens.



Transition of right earthfill dam with spillway

On the downstream side, starting at the earthfill dam, the rockfill becomes thicker and higher as the core diminishes with the deepening of foundation excavation. At the point where excavation meets the rock, the rockfill reaches its maximum height and width. Accompanying the change of internal zoning, the external downstream slope becomes steeper varying from 1 V:3 H to 1 V:1.8 H.

At this section, the internal drainage system comprises a vertical chimney filter 2 m wide and a drainage blanket 1 m thick which extends from the foot of the vertical filter to the extremity of the downstream fill. It acts also as a transition between the core and foundation soil.

Thus, in the last 50 m of fill which were constructed as an overlap with the concrete structure, the dam is already founded on rock, has a central impervious core, and on the upstream side a

zone of backfill with clay material confined between the central core and the guide wall.

On the downstream side it has a zone of rockfill sloping 1 V:1.8 H.

The impervious core is protected by three zones of transition constructed in granular material. Each zone is 2 m thick.

Plans and sections of the earthfill dam on the right flank, between the right side abutment and the spillway wall, are shown in Fig. 7.6.

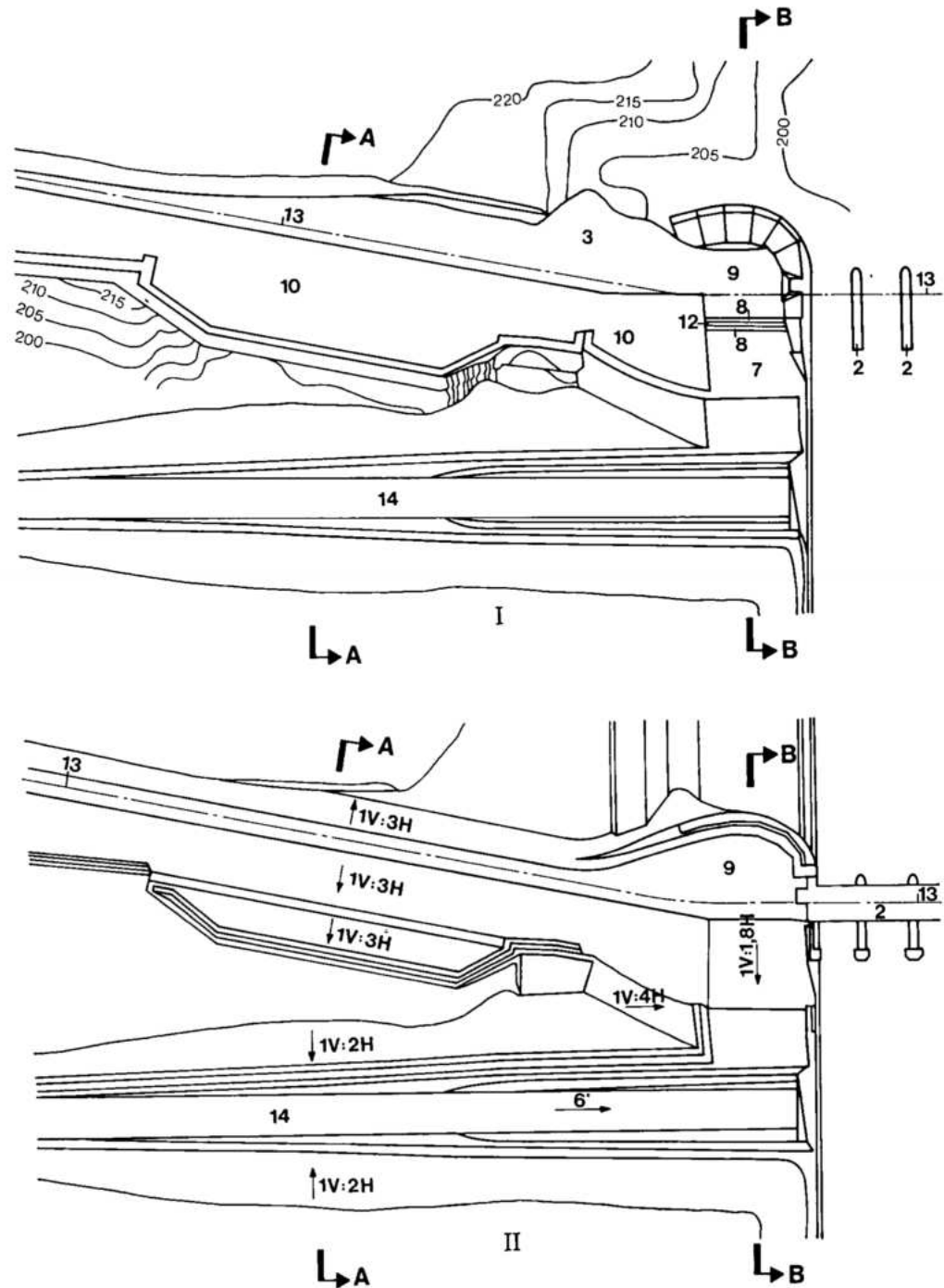


Fig. 7.6 Transition between right earthfill dam and the spillway - Plan view (for nomenclature, see Fig. 7.5)

I Foundation plan
II Plan at El. 225.00

PERFORMANCE OF THE EMBANKMENT DAMS

INSTRUMENTATION AND MONITORING

Rockfill dam

As the rockfill dam on the left bank was of conventional design, based on almost flat sound rock foundation, and all zones of the embankment were compacted, the principal indices of its stability and performance monitored were:

- Pore or piezometric pressures at the contact between the impervious core and the rock foundation.
- Piezometric pressures in the shallow basalt foundation and in the breccia layer and the discontinuity located 30 to 40 m under the sound basalt foundation.
- Embankment settlement.
- Seepage flow through the dam and its foundations.

Interaction at the concrete interface

Interaction between the rockfill dam and the concrete transition wall at the interface with the buttress dam was monitored by measurements of piezometric and earth pressures at the upstream longitudinal and transverse contacts between the concrete wall and the clay core. The instruments were installed at two elevations.

Locations of instruments in a cross-section of the rockfill dam and at the concrete interface are shown in Fig. 7.7. Total numbers of instruments installed in the rockfill dam were:

Piezometers	47
Pressure cells	6
Surface bench marks	43
Seepage discharge weir	1

Deflections of the crest from a reference line along the axis of the dam, as well as the absolute settlement of the crest of the rockfill and earthfill dams, were also obtained from high precision geodetic surveys of the combined Itaipu project structures.

Earthfill dams

Unlike the rockfill dam, the earthfill wing dams were founded either on completely weathered rock (saprolite) or on residual soils. Since these foundations were compressible and permeable, in addition to piezometric pressures, settlement of and seepage through the foundations are of great significance with respect to stability and safe performance of the earthfill dams.

Standpipe and electric type piezometers were installed at the contact between the embankment and the foundations across the full width of the dam at representative locations, in order to obtain the hydraulic gradient profiles in the relatively permeable foundation, see Fig. 7.8. While bench marks along the crest were used in the survey of surface settlement, IPT type settlement gages, capable of measuring incremental settlement from the foundation to the surface were installed both downstream and upstream of the chimney filter in the embankment.

Seepage from the embankment was mostly gathered by the chimney and blanket filter drains, and flow through the foundations was intercepted by vertical drainage wells at the toe of the earthfill dams, and collected by paved ditches running parallel to the toe. Weirs for measuring the discharge were located such that seepage flows from specific sectors of the dam could be monitored separately. The turbidity and the amount of sediment in the seepage flow, which may indicate internal piping, were also measured.

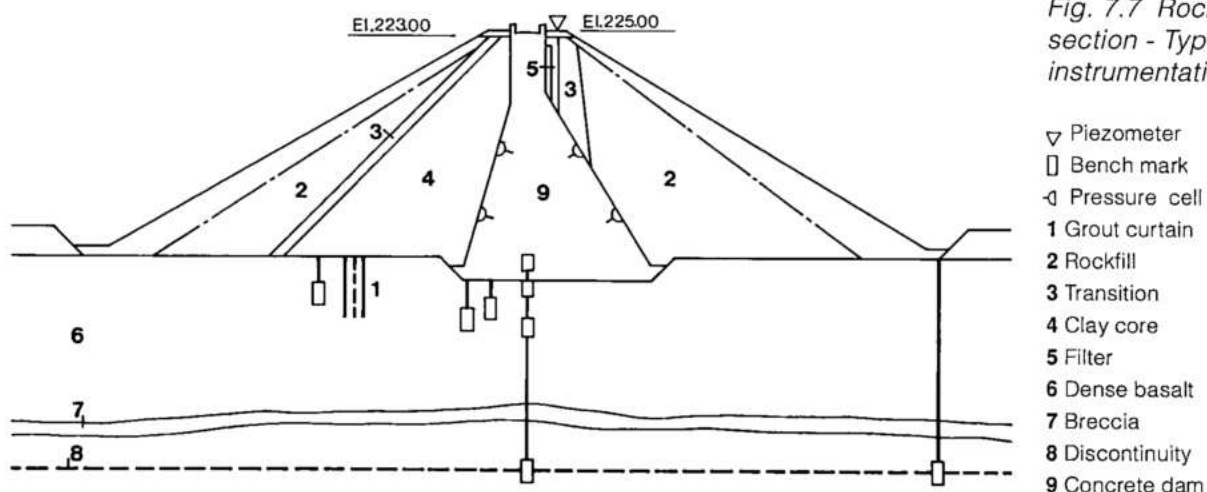


Fig. 7.7 Rockfill dam section - Typical instrumentation

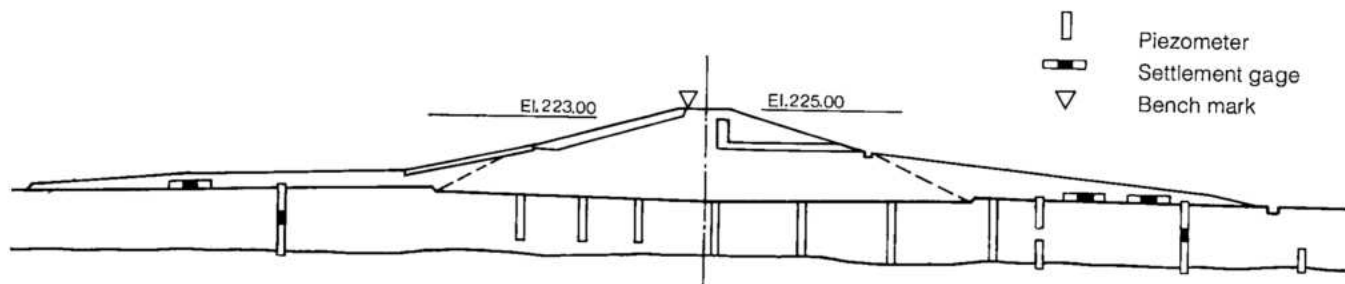


Fig. 7.8 Earthfill dam section - Typical instrumentation

The junction of the right earthfill dam with the spillway was instrumented with pressure cells and piezometers installed at the contact between impervious core and the transverse face of the concrete wall.

Numbers of instruments installed in the two earthfill dams were:

Piezometers	62
Settlement gages	9
Pressure cells	6
Surface bench marks	40
Seepage discharge weirs	4

PERFORMANCE OF THE ROCKFILL DAM AND ITS FOUNDATION

Settlement and deformations

Settlement of the rockfill dam during construction was not measured. However, settlement of its foundations due to the weight of the embankment, was measured just before reservoir filling as part of the overall geodetic survey; it was less than 1 mm. Two years after the reservoir was filled, the surveys showed that the crest of the rockfill dam had settled 10 to 18 mm relative to the foundation; the higher the fill, the greater the settlement. During the next year, the rockfill embankment settled another 3 to 5 mm, and after 5 years of operation, there was essentially no additional settlement.

Settlement of the rockfill dam represented progressive internal consolidation as the reservoir rose at an average rate of 3 m/day. Since it took several months for the water to penetrate and partially saturate the thick clay core, consolidation of the dam continued for 5 years, but at a gradually diminishing rate.

With consolidation of the rockfill shells and the transition zones, the density and the overall shear strength of the embankment improved. The overall deformation

modulus of the rockfill dam was higher than anticipated in the design, because the maximum settlement of the dam (25 mm) was less than the theoretically calculated value. It demonstrated that the rockfill dam was stronger and more durable than anticipated.

Partly due to consolidation and partly due to deformation or bending of the core in response to the reservoir load, the rockfill dam deflected in the downstream direction. From 9 October 1982, before reservoir filling, to 9 March 1987, that is, after 4.5 years of operation, the crest of the rockfill dam had moved about 20 mm downstream. About 30% of the lateral deformation occurred within one month after the first filling of the reservoir. Five years after reservoir filling, with an essentially constant reservoir level, the rockfill dam embankment had completed its consolidation and there was no significant change in lateral deformation.

Piezometric pressures and seepage

The contact between the clay core and the foundations, and the upper 10 m of the basalt foundation, saturated rapidly when the reservoir was filled. Under a head of about 50 m at the base of the clay core, 1 month after the first filling of the reservoir, uplift pressures expressed as percentage of the hydraulic head, were as follows:

At the core foundation contact	10 - 45%
In the shallow foundation	15 - 100%
In foundation joint D at El. 130	18 - 20%

In the shallow foundation and at the core contact, the higher uplift pressures were upstream of the 10 m deep grout curtain. Since the uplift pressures at the contact were generally lower than in the foundation, it indicated that the slush grouting and sealing of the exposed cracks under and upstream of the clay core were more effective than the grout curtain in making the upper portion of the foundation rock completely water-proof. As the permeability of the foundation and the contact was very

low even before grouting, even with high uplift pressure gradients the seepage flow and the risk of piping in the clay core were insignificant. In any case, the graded filter zone downstream of the clay core provided the necessary control of piping and erosion in the clay core.

The relatively low piezometric pressures in the deeper foundation contact showed that, because of the long seepage path from the location where the joint is exposed in the reservoir, the joint will take much longer to saturate, and that as long as there is release of seepage on the downstream side, the uplift pressures in joint D would be of no consequence.

Piezometric pressures at all locations in the foundation continued to increase for about 2 years after the first filling of the reservoir and stabilized at the following values:

At the core-foundation contact	5 – 55%
In the shallow foundation	30 – 100%
In foundation joint at El. 130	25 – 30%

Upstream of the grout curtain, the uplift pressures responded to small fluctuations in the reservoir level. Measurements of the phreatic level in relief wells drilled at the toe of the dam down to the foundation joint D, indicated a steady piezometric level at about 40% of the hydraulic head.

Total seepage through the 1984 m long rockfill dam and its foundation and from the relief drains drilled at its toe was negligible. For the first 6 months after reservoir filling, the seepage was 0.22 l/s. After 5 years, the seepage was practically nil.

Piezometric pressures at the upstream face of the concrete dam interface and at the transverse contact increased progressively, as shown below as percentage of the hydrostatic head:

Contact	El. of instrument	Piezometric pressure (%)	
		12/82	4/87
Upstream	169	45	78
Longitudinal	189	48	86
Transverse	169		14
	189		10

This showed that the contact between the concrete and the clay core was quite impervious. Because effective hydraulic head at the downstream end of the transverse contact was less than 10% of the gross head, there was no possibility of piping of

the clay core, and the seepage flow was negligible. This was confirmed 5 years after reservoir filling.

Before reservoir filling, total pressure at the clay core-wall contact was 40 N/cm² at El. 169 and 15 to 25 N/cm² at El. 189; all were tensile. These represented pore pressures induced during compactation of highly plastic clay with a moisture content higher than the optimum.

The pressures were higher along the upstream face than along the transverse contact.

About 1 year after the reservoir was filled, total pressures at El. 169 had increased to about 60 N/cm² along the upstream and to about 45 N/cm² at the transverse contact. Thereafter, there was a steady decrease in tension, and after 5 years the total pressures ranged between 10 N/cm² tension and 4 N/cm² compression.

The increase in total compressive pressures, the steady piezometric pressures, and the negligible seepage at the contact between the core and the concrete transition wall indicated that there was adequate interaction and load transfer between the two structures.

Summary

Performance of the rockfill dam was excellent. Overall strength of the embankment was better than specified and the materials were highly durable, which indicated a long useful life for the structure with very low maintenance. The embankment had attained almost optimum consolidation and the piezometric pressures at the foundation contact were either stable or slowly reducing. Seepage through the dam, its foundation and at the interface with the buttress dam was negligible.

PERFORMANCE OF THE EARTHFILL DAMS AND THEIR FOUNDATIONS

Left bank earthfill dam

Settlement of the foundation of the left earthfill dam was of special interest, because the foundation material was composed of saprolite or residual clayey soils which were highly porous and weaker than the compacted central core of the earthfill dam. While the core of most of the transition from the rockfill to the left earthfill dam was based on rock or compact material, most of the 2294 m long left earthfill dam was based on the residual soils, 3 to 8 m thick, overlying weathered basalt.

During construction, maximum settlement of the foundation, measured under the 22.5 m high core of the left earthfill dam was 550 mm. Under the berms

and the core where it was less than 17 m high, foundation settlement during construction ranged from 150 to 300 mm. Additional combined settlement of the foundation and the left earthfill dam about one month after reservoir filling, obtained from a survey of the markers on the crest, was as follows:

Transition	15 mm
Dam, 30-15 m high	150 mm
Dam, 15-5 m high	30 mm

In a 630 m long and average 15 m high portion of the left earthfill dam, where the shallow residual soils were excavated and the core was based on partly weathered basalt, the settlement was only about 5 mm.

The large settlement under the average 22 m high earthfill dam was due to the rapid saturation and collapse of the structure of the residual soils. Consolidation of the clay core due to reservoir load was estimated to be less than 5 mm. Settlement of the foundation continued during the subsequent period, and under the higher part of the dam the maximum value was 180 mm. The rate was only about 3 mm/year, 3 years after reservoir filling.

This high foundation settlement was anticipated in design and the central compacted section was made much wider and its slopes flatter than a homogeneous section based on rock would require. Consolidation of the foundation improved its density and strength, and thus the stability of the dam.

Consolidation of the soils foundation and the embankment of the left earthfill dam, also resulted in lateral displacement of the axis. This was verified as a part of the geodetic surveys made 10 days before and after the start of reservoir filling, and at one year intervals thereafter. During the 30 days of reservoir filling, at the right flank of the left earthfill dam, adjoining the transition with the rockfill dam, the crest moved 31 mm in the downstream direction while the left end moved 49 mm upstream, that is, there was a profound counterclockwise rotation of the entire left earthfill dam. During the next 2 years, while the reservoir was essentially steady, the rotation was reversed, with the right end moving 20 mm upstream and the left end shifting 52 mm in the opposite direction. Five years after reservoir filling, the general tendency was for the crest of the dam to move upstream. Such displacements are related not only to the consolidation of the foundation soils, but also to the crustal adjustments due to the weight of the reservoir which can continue for several years. The impervious core of the earthfill dams, as well as the outer berms, are flexible and strong enough to

absorb the strains due to the deformations without affecting the stability of the dam.

Hydrogeologic behavior

Standpipe type piezometers installed in the foundation soils and at the rock contact indicated that the natural water table followed the rock surface and that natural seepage was from the banks towards the river. Electric piezometers installed in the earth dam core registered low negative and positive pore pressures (± 1.2 to 3.4 N/cm^2); the negative pore pressures were in the foundation clay and were attributed to natural drying of the clay which had been exposed for more than 2 years.

Piezometric levels in the foundation soils and at the rock contact rose rapidly as the reservoir filled, and a steady state was reached about 4 months after the reservoir was full and steady at $\text{El. } 214 \pm 1 \text{ m}$. Total seepage flow through the foundations and embankments of the left earthfill dam was 12 l/s at that time. After 5 years, the seepage flow had reached 26 l/s and was essentially stable thereafter.

Seepage flow was significantly affected by rainfall. For example, following heavy rainfall (555 mm) in April and May, 1987, total outflow from the drainage system reached a maximum of 44 l/s, that is about 150% of the average normal amount. Infiltration of surface runoff into the natural banks raised the water table and the gradient towards the river; which in turn increased the seepage through the permeable foundation of the dam. As the seepage flow reduced after the rainy period while the reservoir level remained constant, it clearly established the correlation between rainfall and seepage through the earthfill dams.

To check for piping of fines from the core or the foundation, the amount of suspended solids was regularly monitored. Initially, one year after reservoir filling, the total solids in seepage under and through the left earthfill dam was 54 mg/l. Four years later the amount was only 16 mg/l. Most of the sediment was attributed to the initial saturation of the porous clays and collapse of their structure, and also to infiltration of surface runoff along the banks. The amount of suspended solids and its gradual reduction, demonstrated a steady state of seepage without any piping, and corroborated adequacy of the design with wide berms and upstream blanket.

Piezometric pressures and the phreatic gradient under the left earthfill dam, reached steady levels 1 to 2 years after reservoir filling. While the steady piezometric levels were lower than those assumed in the design, they varied for different sections of the dam, depending upon the properties and depth of the foundation soils overlying basalt. Water levels at

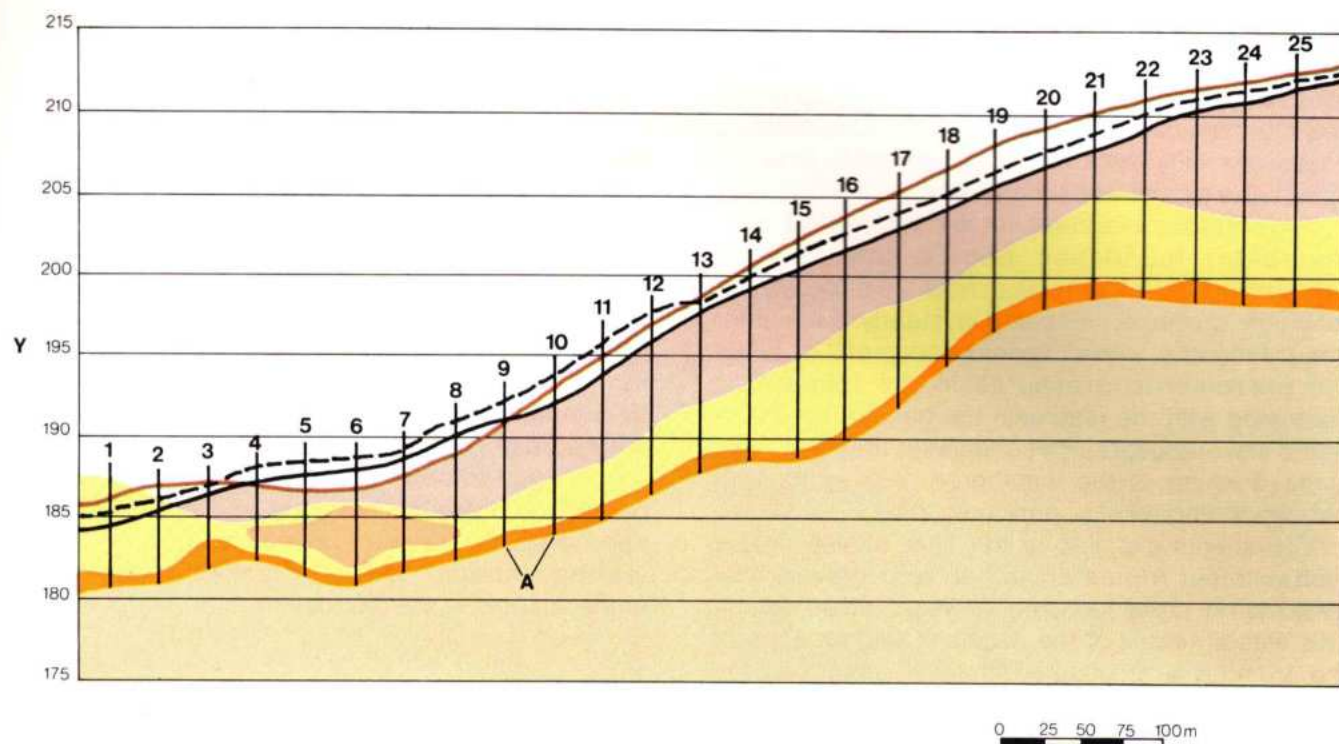


Fig. 7.9 Left earthfill dam longitudinal section at downstream toe of earthfill relief wells

--- Max. piezometric levels
in July 86
— Max. piezometric levels
in June 88

Y Elevation (m)
A DRL relief wells (1,2...25)
Ground surface
Red clay

Fractured rock
Saprolite
Sound rock
Alluvion

Note: As registered in June 1988 only relief wells DRL-5 DRL-8 were flowing at the rate of approx. 4.1 l/s

the downstream toe of the left earthfill dam, which were measured in relief wells drilled between 1986 and 1988, ranged from El.185 to El.211 (with reservoir level at El.219.6); these were also influenced by the same factors as the rest of the piezometric pressures, see Fig. 7.9.

Right bank earthfill dam

While the response of the right bank earthfill dam to the first filling of the reservoir and subsequent reservoir fluctuation was similar in nature to that of the left earthfill dam, quantitatively it was significantly different. The principal factors to which these differences in behavior and performance of the two dams are attributed were the shallower depth of weathered rock or saprolite foundations and the thicker rockfill shells of the higher section of the right bank dam.

Settlement of the foundation during construction of the embankment was about half of that measured under comparably high portions of the left earthfill dam. The maximum values averaged 100 mm or

one-third of that of the left earthfill dam; the reason being a lesser thickness of saprolite as compared to the left bank.

About 2 months after the first reservoir filling, the foundation under the central part of the dam settled an additional 14 mm, which was about 30% of that of the earthfill dam of comparable height. This indicated lesser consolidation and a slower rate of saturation of the clayey soils and saprolite in the foundation.

For the next 3 years, with the reservoir full and with only minor level fluctuations, consolidation of the foundation soils progressed at an average rate of 15 mm per year, reaching a maximum of 48 mm under the right higher half of the dam. Five years after reservoir filling, foundation settlement had slowed down to less than 3 mm/year, indicating that the foundation had stabilized almost to its optimum state, with consequential improvement in its density and strength.

The compacted clay core, which is much thicker than that of the left earthfill dam, consolidated only about 2 mm after 5 years of sustaining full reservoir

pressure. The larger consolidation of the foundation as compared to that of the dam would tend to gradually build up strains in the embankment; however, the compacted plastic clay embankment possesses sufficient strength and flexibility to safely absorb the strains without cracking.

Piezometers installed in the weathered rock (saprolite) foundation and at the bedrock responded quickly to the first application of reservoir pressure, reaching a steady state after about 4 months, with a maximum head of 2 m. While the piezometric pressures in the foundation fluctuated with the reservoir, the general tendency was a slow reduction. This indicated that there was some draining of the weathered rock strata with corresponding relief of pore pressures.

Instruments installed in the filter blanket in the embankment indicated either zero or very low piezometric pressures after 5 years of operation. This was an index of the excellent performance of the chimney and blanket filters in protecting the embankment against build up of excessive internal pore pressures.

Seepage through the embankment via the internal filter zones and through the permeable foundation reached a steady range of 12 to 15 l/s four years after first reservoir filling. During the rainy season, there was an increase of 2 to 5 l/s, which represented the surface runoff infiltrating into the ground water and the weathered rock foundation. Over an 8 year period, no sediments were detected in the seepage water, indicating that no internal erosion of fines or piping was taking place.

Behavior of the contact between the clay core of the right earthfill dam and the concrete transition wall with the spillway was monitored by piezometers and pressure cells. As the reservoir was first filled, the piezometric pressures at the contact at El. 205 about 5 m above the foundations were about 27 kN/m^2 ; but at other locations the piezometric pressures were negligible.

A pressure cell near El. 205 measured a contact pressure of 90 kN/m^2 at the start of reservoir filling, which reduced to 55 kN/m^2 later when the reservoir had been nearly full for 2 months. Deducting the pore pressure, the effective pressure against the wall was 28 kN/m^2 , which is well within the design assumptions. Five years after the operation started, contact pressures and the piezometric levels were essentially steady, indicating that there was no separation between the embankment core and the concrete wall.

Monthly and quarterly measurements following the filling of the reservoir showed that in all functional aspects the right earthfill dam and its foundation

attained a steady state after about two years, with the various indicators responding normally to the fluctuations in the reservoir level.

Summary

The performance of the earthfill dams and their response to the imposed reservoir load, was satisfactory and within adequate margins of safety. Substantial consolidation of the porous clay foundation during construction and under reservoir pressure, strengthened the foundation, and the flexible compacted embankment adapted to the deformation without critical strains. Configuration of the stable phreatic surface and the steady seepage discharge indicated that the design of the left earthfill dam with a thick core and flat berms was appropriate. There were no indications of piping or internal erosion of fines from either the dam embankments or the foundation.

SPILLWAY AND OPERATION OF RESERVOIR

BASIC CONSIDERATIONS	8.3
MODEL TESTS	8.3
Hydraulic Models	8.3
Verification of the General Arrangement	8.4
Verification of Hydraulic Design of the Spillway Crest	8.8
Piers	8.11
Tests on Flip Buckets	8.13
Analyses of Erosion Effects Downstream of the Spillway	8.14
FINAL SPILLWAY ARRANGEMENT	8.21
Design of Structures	8.22
CONSTRUCTION OF THE SPILLWAY	8.25
Crest Structure	8.25
Roadway Tunnel under the Spillway	8.29
Chutes, Walls, Buckets and Galleries	8.29
GATES AND ASSOCIATED EQUIPMENT	8.31
Spillway Equipment	8.31
General Arrangement and Layout of Equipment	8.31
Gates	8.31
Gantry Crane	8.40
Spillway Stoplogs and Lifting Beam	8.43
Auxiliary Equipment	8.45
Power Supplies	8.46
Protection, Control, Instrumentation	8.47
OPERATING EXPERIENCE	8.48
Filling of the Reservoir and Maximum Recorded Flood	8.48
Reevaluation of Spillway Design Flood	8.48
Hydraulic Performance of the Spillway	8.49

STRUCTURAL PERFORMANCE OF THE SPILLWAY	8.52
Monitoring Objectives and Instrumentation	8.52
Behavior of the Crest Structure Foundations	8.54
Performance of Spillway Chutes and Guide Walls	8.56
Performance of the Flip Buckets and the Downstream Protection Slabs	8.56
GEOPHYSICAL PERFORMANCE OF THE RESERVOIR	8.60
Crustal Settlement	8.60
Seismic Monitoring	8.61

SPILLWAY AND OPERATION

OF RESERVOIR

BASIC CONSIDERATIONS

Hydrological, geological, powerhouse and dam layout as well as diversion studies made at the feasibility stage had established that the Itaipu spillway would:

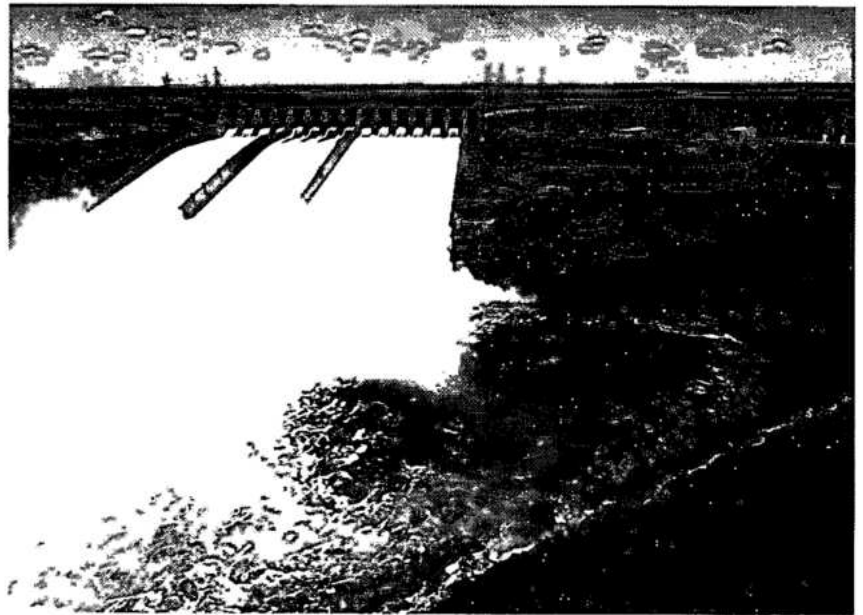
- Pass a maximum flow of 62 200 m³/s with reservoir level at El. 223.
- Be located on the right bank.
- Be of the flip bucket type, discharging into the Paraná river 1.2 km downstream of the power station.

Initial considerations of cost and operational convenience had indicated a five parallel chute configuration with thirteen 20 m x 20 m main gates and three 13 m x 13 m auxiliary gates together with a separate log chute. However, adoption of this arrangement was conditional on the results of further economic analyses and detailed model testing.

MODEL TESTS

HYDRAULIC MODELS

Studies and tests for analysis of the spillway design and operational conditions were performed on two models. A three dimensional one in 1:100 scale, including all features and structures necessary for



*Itaipu spillway in
operation*

verification of the overall hydraulic performance; and a partial model, in 1:50 scale, reproducing three complete bays of the spillway crest structure.

The configuration of the comprehensive three-dimensional model is defined in Fig. 8.1. Basic outlines of the partial model are defined in Fig. 8.2.

VERIFICATION OF THE GENERAL ARRANGEMENT

Verification of the general arrangement commenced with the analysis of the operational conditions of the spillway derived from the feasibility studies, whose basic layout is shown in Fig. 2.17 of Chapter 2. The prototype spillway modelled consisted of:

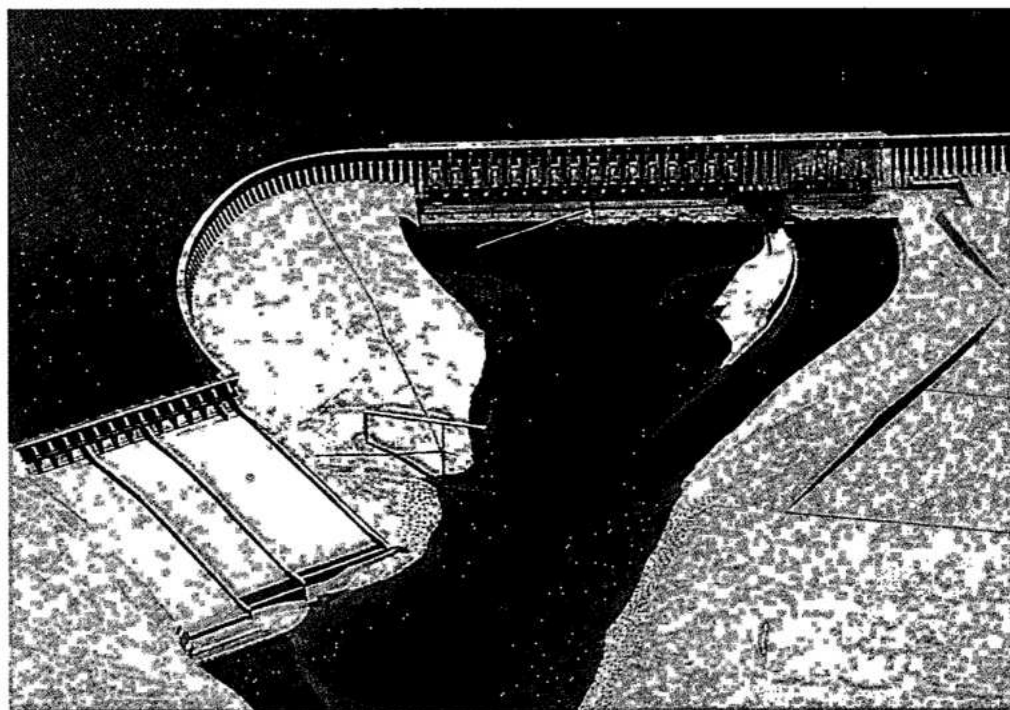
- A chute having three bays, each with 13 m x 13 m gates at the right bank constituting a service spillway, intended to operate almost full-time during the early years of operation.
- Four main chutes, three of which had three bays and the other four bays, each with 20 m x 20 m radial gates, whose discharge capacity when added to that of the service spillway would pass the maximum design flood.
- A narrow chute on the left bank specifically intended for passing logs and floating debris.

The examination of the results of the tests on this model led to the following observations:

- Approach conditions at both flanks of the spillway were not satisfactory during high flows, as the service spillway and the chute for passing logs caused flow restrictions.
- The discharge was lower than that required; the discharge coefficient being in the order of $1.90 \text{ m}^{1/2}/\text{s}$. This low value was partially due to the not completely satisfactory conditions of approach to the spillway, and in particular to the very high position of the chute with reference to the crest.
- Because of the staggered exit ends of the five chutes, the jets impacted close to the foundations of the flip buckets.
- The effect of spillway operation on tailwater levels at the powerhouse was minimal.

Results of model tests on the five chute spillway suggested the following modifications, which were incorporated in the arrangement shown in Fig. 8.3:

- The log chute was eliminated.
- The service spillway was increased to a chute with four 20 m x 20 m gates.
- Main spillway to have two chutes one with four and the other with six 20 m x 20 m gates.
- To eliminate the adverse effect of jet impingement, the discharge buckets for the central and right chute were made at an oblique angle to the river flow.
- Redesign of the crest by increasing its height above the upper edge of the chute, in order to improve the coefficient of discharge, see Fig. 8.4.



*Spillway comparative
model-scale 1:100*

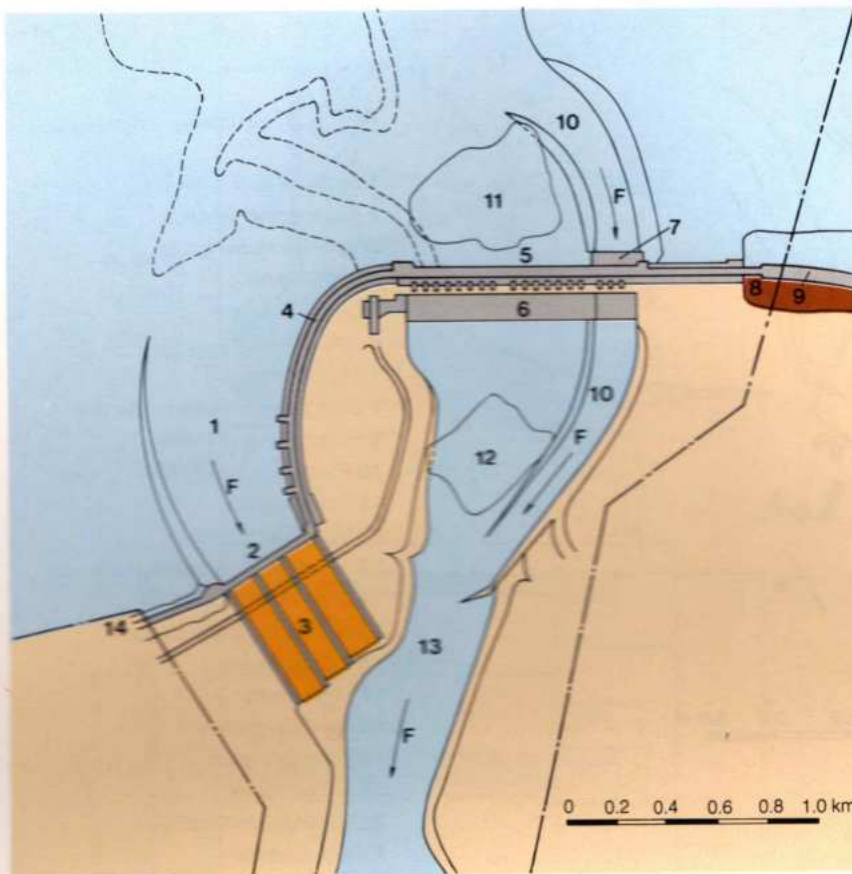


Fig. 8.1 General layout of model

- 1 Approach channel to the spillway
- 2 Spillway - control works
- 3 Spillway - chutes
- 4 Butress dam
- 5 Main dam with water intake
- 6 Powerhouse with 18 x 700 MW units
- 7 Diversion control structure
- 8 Transition
- 9 Rockfill dam
- 10 Channel for river diversion
- 11 Upstream cofferdam
- 12 Downstream cofferdam
- 13 Paraná river
- 14 Right earthfill dam
- F Flow direction
- Limits of the hydraulic model

Selection of the adopted scheme, see Fig. 8.3, was particularly influenced by economic considerations and the anticipated mode of spillway operation. Detailed cost estimates, comparing five, three and two chutes were made to determine the most economic arrangement. The comparative economic analyses considered the following:

- Excavation in the approach channel for the chutes, buckets and guide walls.
- Concrete and steel reinforcement in the crest structure, piers, bridge, chutes, buckets and guide walls.
- Gates, trunnion anchorages and hoists.
- Time required for construction.

This resulted in the following comparative costs:

Selected number of chutes	Cost Index
5	133
3	105
2	100

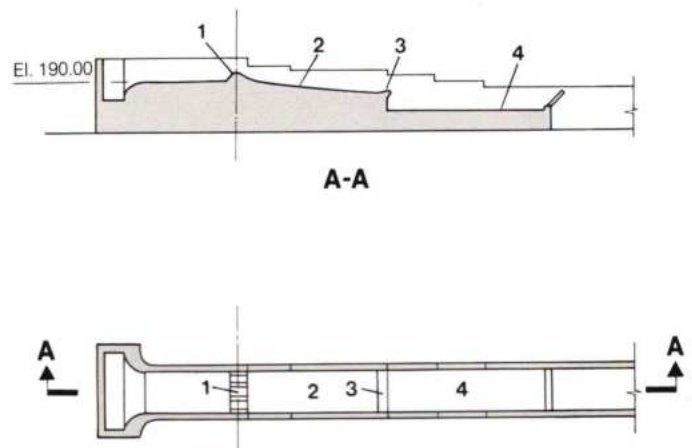
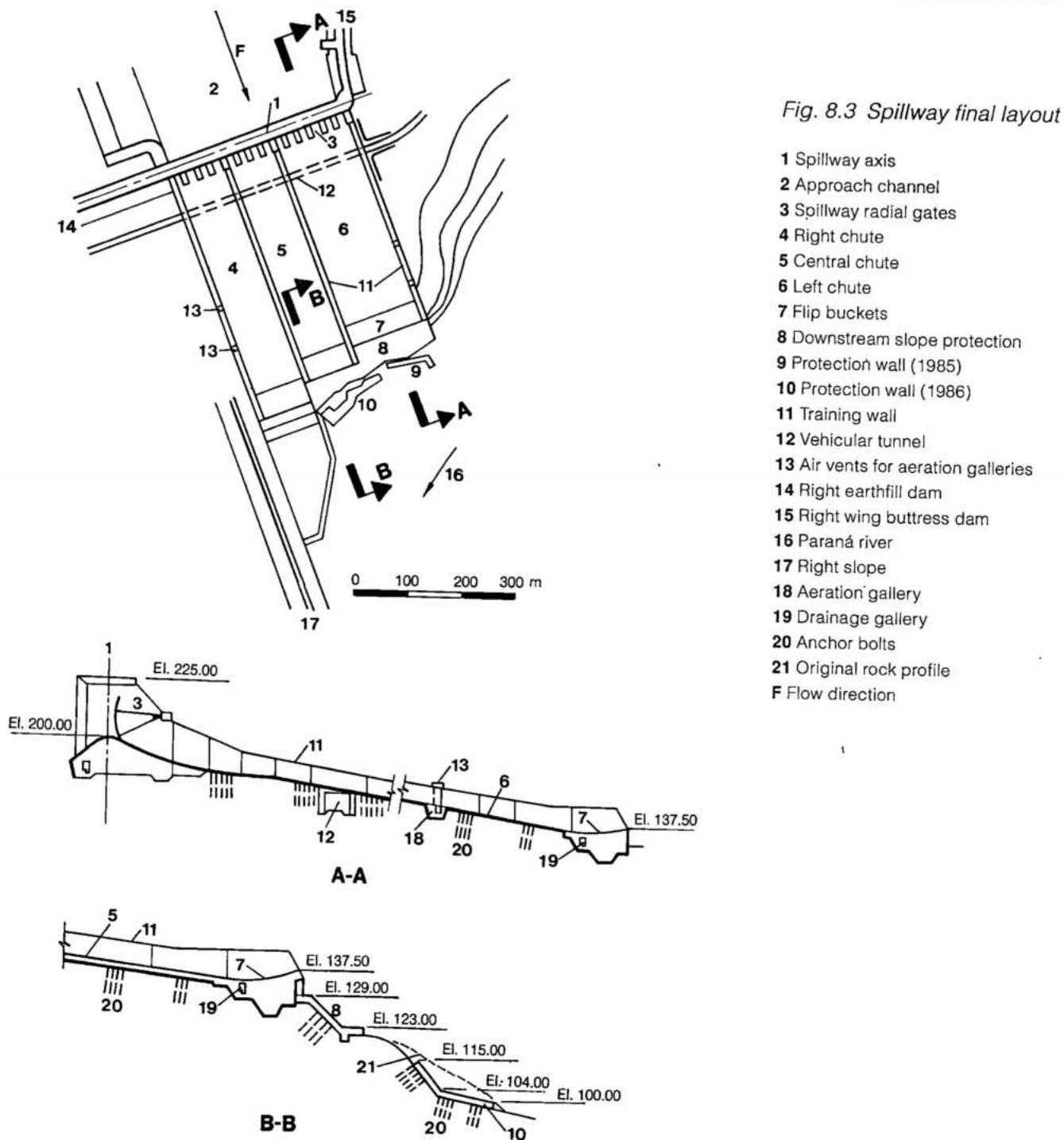


Fig. 8.2 Partial hydraulic model

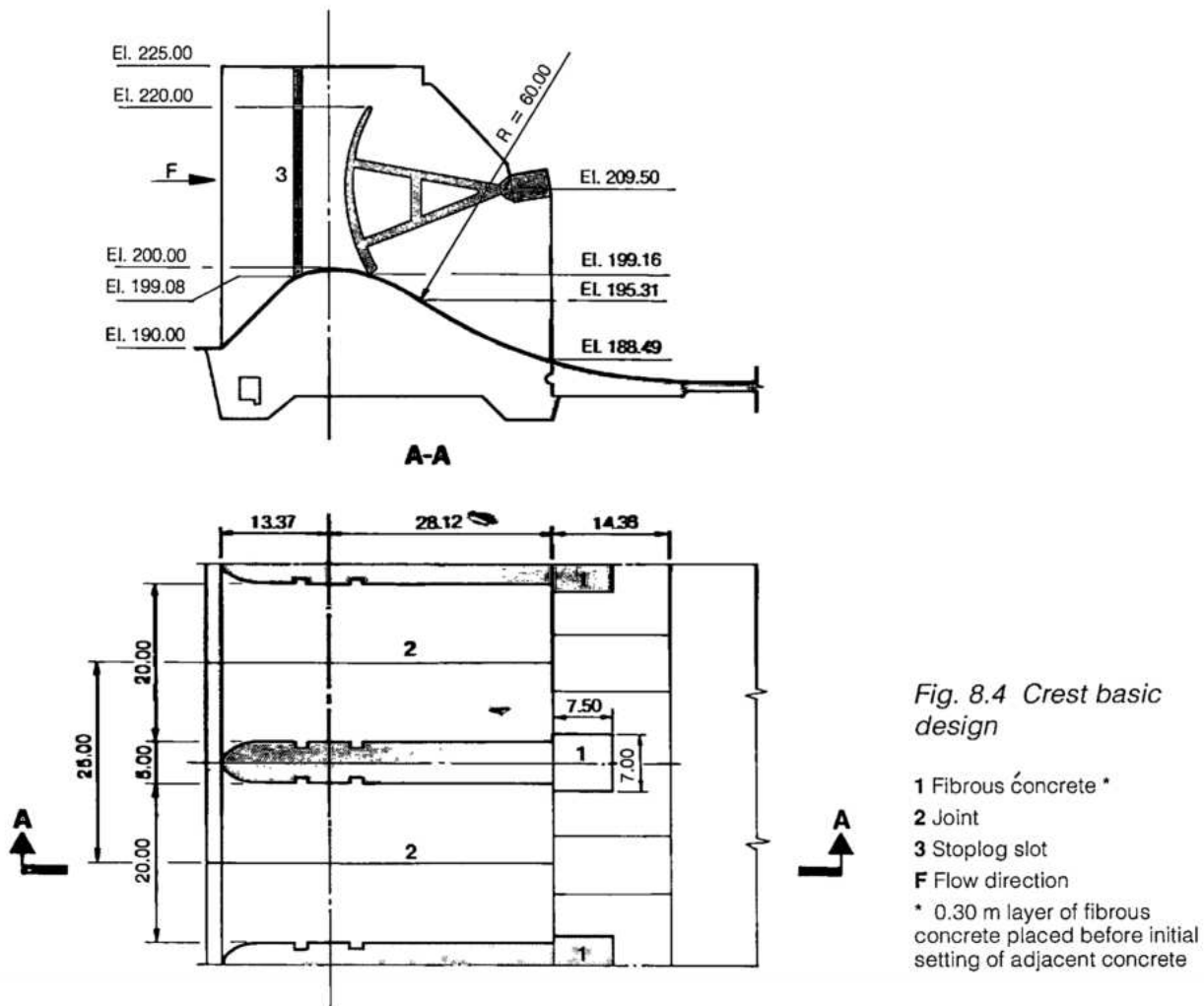
- 1 Spillway crest - three complete passages
- 2 Chutes

- 3 Flip bucket - El. 140
- 4 Movable bottom - El. 90



While the two chute alternative was about 5% cheaper than the three chutes, there was a 50% higher risk with the former in that there might not be enough operational flexibility for repairs to be made during a prolonged high flood period. The unprecedented floods of 1982-83, to be described later, demonstrated in retrospect the far reaching implications of the risks involved if the spillway

had malfunctioned. Thus the three chute arrangement was adopted, the necessity to reduce risk, improve operational flexibility and capability to safely handle emergencies taking precedence over the small economic advantage of the two chute arrangement. Specifically, the advantages of the selected arrangement, as proven during 8 years of operation, are:



- Each chute can discharge more than twice the average annual natural flow of the river; thus only one chute has to be operational during flows up to 20 000 m³/s.
- Greater flexibility in operating the gates and the chutes so as to control downstream erosion.
- Ability to schedule maintenance and repair of chutes and discharge buckets without reducing the degree of protection for the project.

Similar economic analyses of eight different crest elevations indicated that the most economical was El. 200.

Making all gates the same size, while being the most economical solution also had additional advantages of uniformity of design and manufacture, and possible interchange of components and operating mechanisms.

The total width of the three chutes, including the two intermediate guide walls, was constant at 345 m, without convergence, for the entire length of the chutes. Because of the natural topography at the

river bank, the lengths of the three chutes would be different.

The profiles of the chutes essentially followed the available sound rock and were refined to minimize excavation and concrete required for the walls. Curves, transitions and slopes of the floors of the chutes were selected to avoid negative pressures. The profiles of the three chutes were not parallel to each other for their entire lengths.

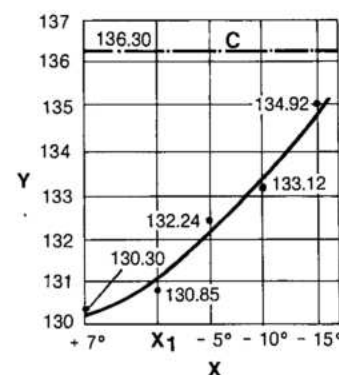
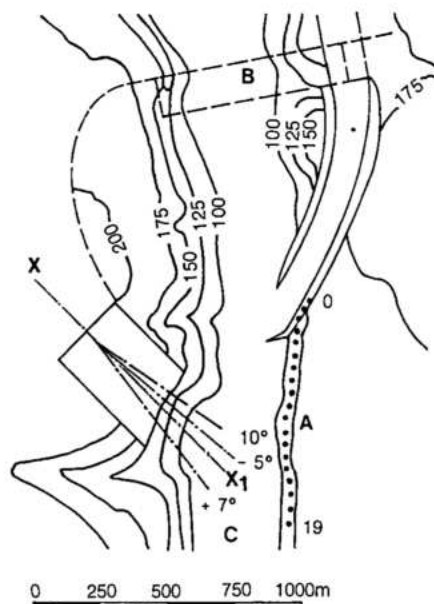
Further refinements of spillway arrangement included optimization of the alignment of the chutes on the basis of three main parameters:

1. Tailwater conditions at the powerhouse.
2. Currents and velocities along the banks of the river and at the discharge end of the spillway.
3. Erosion downstream of the buckets in the river, and formation of bars.

Five longitudinal alignments oriented relative to a reference line X₁ (the preliminary alignment adopted in the feasibility studies) were model tested as shown in Fig. 8.5.

Fig. 8.5 Maximum velocities along the left bank with respect to orientation of spillway

Y Water level at the powerhouse for $Q = 53\,000\text{ m}^3/\text{s}$
X Orientations studied for the axis of the spillway (the + sign means clockwise rotation)
A Points of measurement of velocities
B Powerhouse
C Downstream level
X₁ Orientation of spillway axis in the feasibility design



Results of the orientation tests indicated that:

- Tailwater levels at the powerhouse tended to be lower as the alignment was turned to the right, as the flow from the spillway was turned to follow the river axis. The difference, however, became really important only when the chutes were more than 10° to the right of line X_1 .
- The velocities along the left bank of the river facing the spillway tended to increase as the spillway was turned to the left of line X_1 .
- Erosion in the river increased with rotation of the spillway to the right of line X_1 . When turned to the left, the jets from the spillway landed in the deeper part of the river providing a more efficient dissipation of energy.

This also reduced the piling up of flow against the opposite bank of the river and almost eliminated erosion of that bank. Further rotation to the right would require additional excavation for the right hand chute and for the exit channel.

Analyses of these results led to the selection of an alignment 5° left of line X_1 . With this alignment, the river offered a natural stilling pool in front of the central and the left chute. As shown in Fig. 8.6, only the discharge from the right chute impinges on a relatively shallow part of the river.

The advantages of the selected arrangement were confirmed by later studies of erosion tendencies under different operating conditions. These studies also led to the decision to pre-excavate to El. 95 the area facing the right chute, to the extent that could be done in the dry. This excavation reduced the volume of material likely to cause the formation of bars in the river

bed, which could result in a localized control and a significant rise in tailwater levels at the powerhouse.

The advantages of the selected alignment outweighed the disadvantages. The tailwater levels at the powerhouse would rise significantly only during high floods, when the reduction of head could be offset by increasing the turbine discharge. Erosion along the left bank was considered a secondary problem common to all alternatives, perhaps a little more intense for the selected scheme than for the alternatives turned more to the right.

The heights of the four walls were selected to prevent overtopping for all conditions of gate operation, except for the case when an end gate is closed or partially open and the others are fully open. Head loss along the chute, air entrainment and freeboard were considered in determining heights of the walls.

Performance of the chutes and the walls was checked on the 1:100 scale comprehensive model for a wide range of gate operating sequences. The measured pressure and velocity distributions were considered satisfactory.

VERIFICATION OF HYDRAULIC DESIGN OF THE SPILLWAY CREST

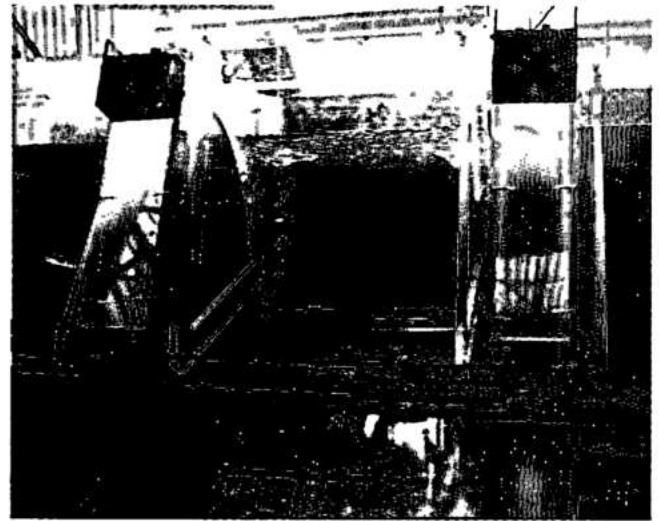
The head over the spillway crest varies between 20 and 23.5 m. A theoretical comparison was made of crests with design heads ranging from 20 to 25 m. Assuming a maximum permissible negative pressure

of 20 N/cm^2 a design head of 20 m was selected to define the geometric profile of the crest.

The theoretically developed shape of the crest was checked and refined on the 1:50 scale partial model simulating three gates. On the model the refinements consisted of testing the effects of the depth of the approach channel, gate sill elevation, trunnion and stoplog locations.

The studies were conventional, including the measurement of pressure distribution and the discharge capacity of the structure through the whole range of operations anticipated for the prototype.

The tests measured the pressure distribution along the centerline of the crest and along the piers, and identified the locations of low pressures for various gate openings.

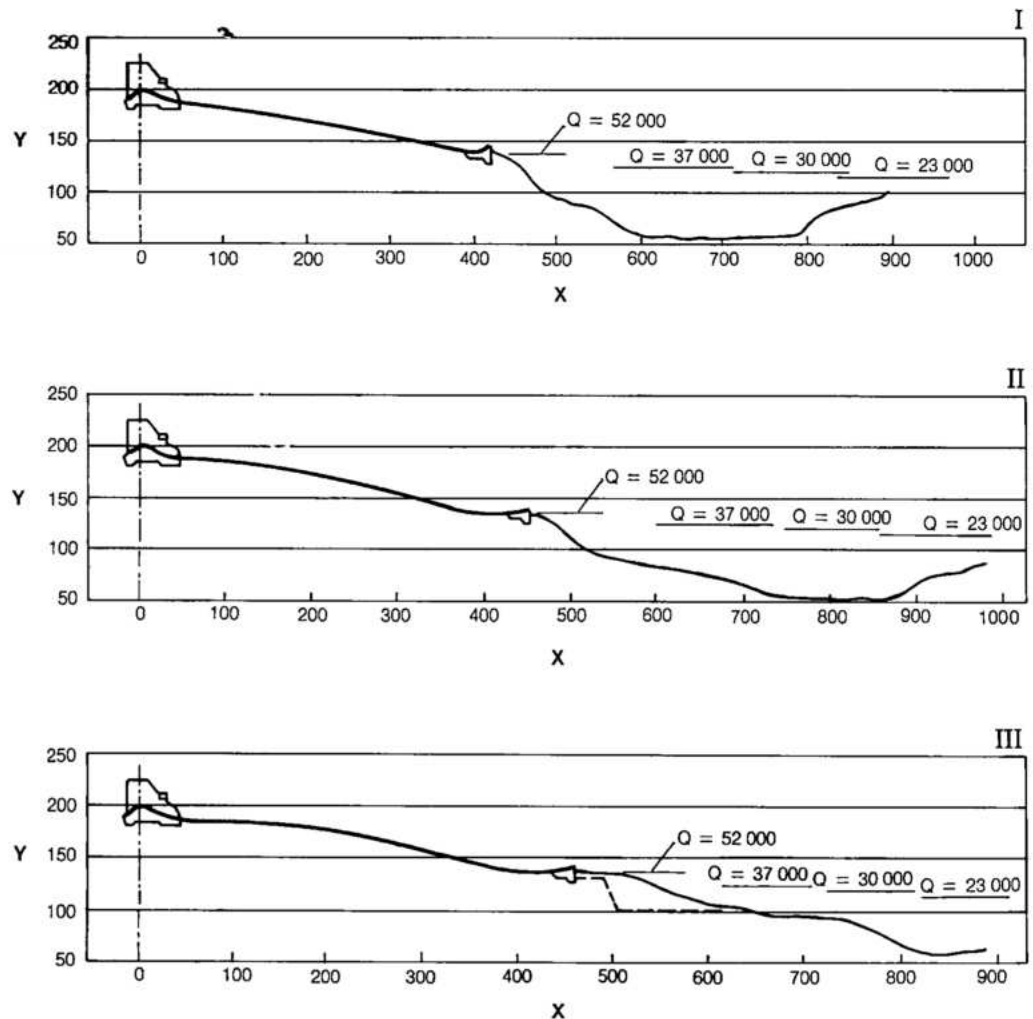


Partial model of spillway crest - scale 1:50

Fig. 8.6 Longitudinal section along in the axis of the chutes

I Left chute
II Central chute
III Right chute
Y Downstream level (m)
X Distance from the crest axis (m)
A Recurrence (years)
Q Discharge (m^3/s)

Y	A	Q
112	10	23 000
117	100	30 000
121	1000	37 000
135	10 000	62 000



The probable areas of incipient cavitation were considered those where negative pressures exceeded 20 N/cm^2 and the average pressure fluctuation was $\pm 9 \text{ N/cm}^2$. To minimize risk of cavitation, the average cavitation factor should be equal to or greater than -0.45 , with a value no less than -0.40 in the more sensitive locations.

The following principal results were obtained:

- The discharge capacity was compatible with that required, see Fig. 8.7.
- Pressures along the centerline of crest and the base of the pier showed sub-atmospheric values under certain conditions of operation, but their magnitude was considered acceptable, see Fig. 8.8.
- Practically all conditions of operation with partially open gates caused vortices to appear, and their intensity and magnitude was accentuated as gate openings increased. The vortices tended to form close to the stoplog slot.

- For fully open gate operation and at nearly maximum heads, the gate trunnions would be submerged.

The following modifications were made on the basis of these results, see Fig. 8.9:

- Relocation of the stoplog slot further upstream from the crest and away from the region where the vortices formed, to avoid the superposition of the factors which tended to cause low pressures.
- Raising the gate trunnion and moving it downstream to keep it out of the flow line for all discharges, and to increase the pressures for operation with partially open gates, and to reduce the frequency and intensity of the vortices.

With these alterations, all the objectives were attained to a satisfactory degree, the only adverse effect being the appearance of a low-pressure point at the base of the stoplog slot at its new location because it was still within an area where the pressures were normally low. This was considered

Fig. 8.7 Discharge capacity

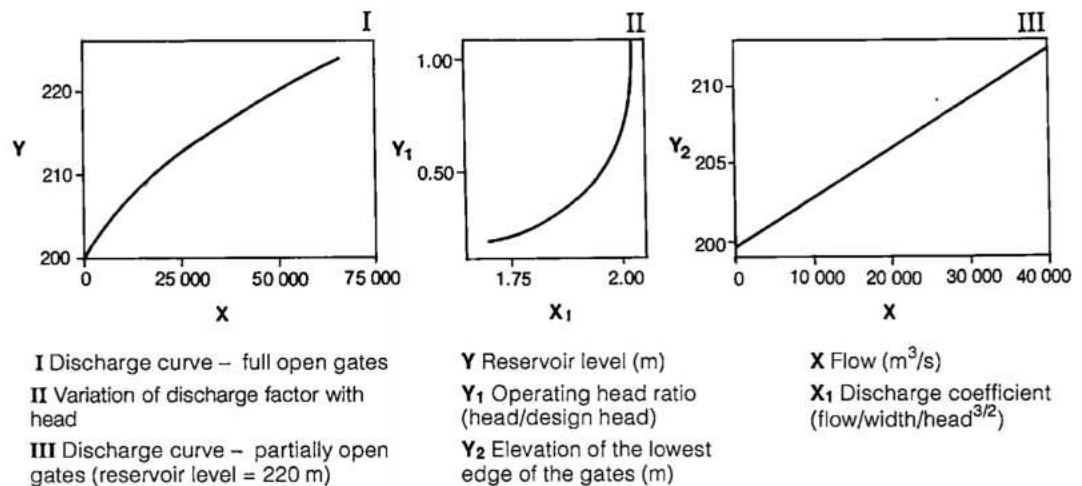
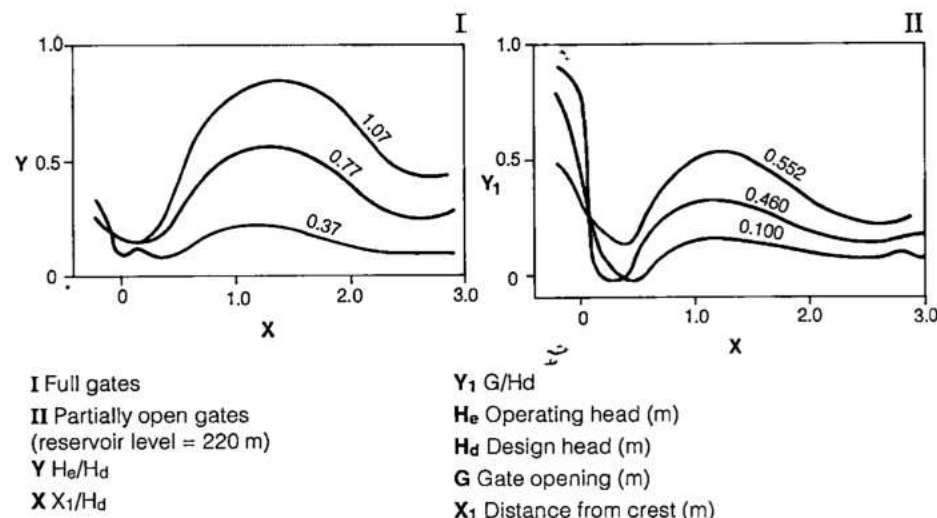


Fig. 8.8 Pressure along the centerline of crest



acceptable since it occurred only for full-gate operation with head near the maximum and the amount of the measured negative pressure (27 N/cm^2) was only 35% more than the 20 N/cm^2 criterion adopted for cavitation free operation.

Theoretical computations for the discharge capacity of a typical bay of the spillway at heads other than the design head of 20 m, considered such factors as the effect of submergence and the tangency. The relationships of these factors are shown in Fig. 8.10. When checked on the model, it was confirmed that with all fourteen gates fully open and reservoir level at El. 223, the spillway would discharge $61\,000 \text{ m}^3/\text{s}$.

PIERS

For the piers, an elliptical upstream nose was selected. Then, various lengths and shapes were tested in the 1:50 scale model jointly with the selected crest.

Factors considered in the evaluation of the hydraulic performance of the piers were:

- Degree of discontinuity and instability of flow immediately downstream of the pier.
- Risk of cavitation at the junction between the downstream end of the pier and the crest surface.

The first tests on the piers were to study the advantages of extending them upstream in order to avoid accentuated flow separation on the crest whenever one chute was operated alone, which created lateral flow at the approach to the spillway.

This solution, however, did not lead to satisfactory results, because the flow conditions over the crest were in fact altered significantly only by considerable uneconomic and difficult elongation of wall. Additional measures taken such as inclining the head of the pier in an upstream direction were also unsatisfactory; therefore, it was decided not to make alterations in this region.

The tail of the pier was subjected to an extensive test program, starting from a shape with the minimum necessary dimensions for structural reasons, see Fig. 8.9, and going to a long streamlined, partially submerged, tapered configuration, shown as III in Fig. 8.11. Parameters for evaluating the performance of each alternative were the water levels along the side walls and the possibility of cavitation immediately downstream of the pier as a consequence of the formation of vortices in the separation zone.

The configuration corresponding to the minimum dimensions i.e., a typical 5 m thick pier, extending 13.37 m upstream and 28.04 m downstream of the axis of the crest, with a square downstream end, see Y₁ of Fig. 8.11, was selected for final design for the following reasons:

- Minimum cost and simplicity of construction.

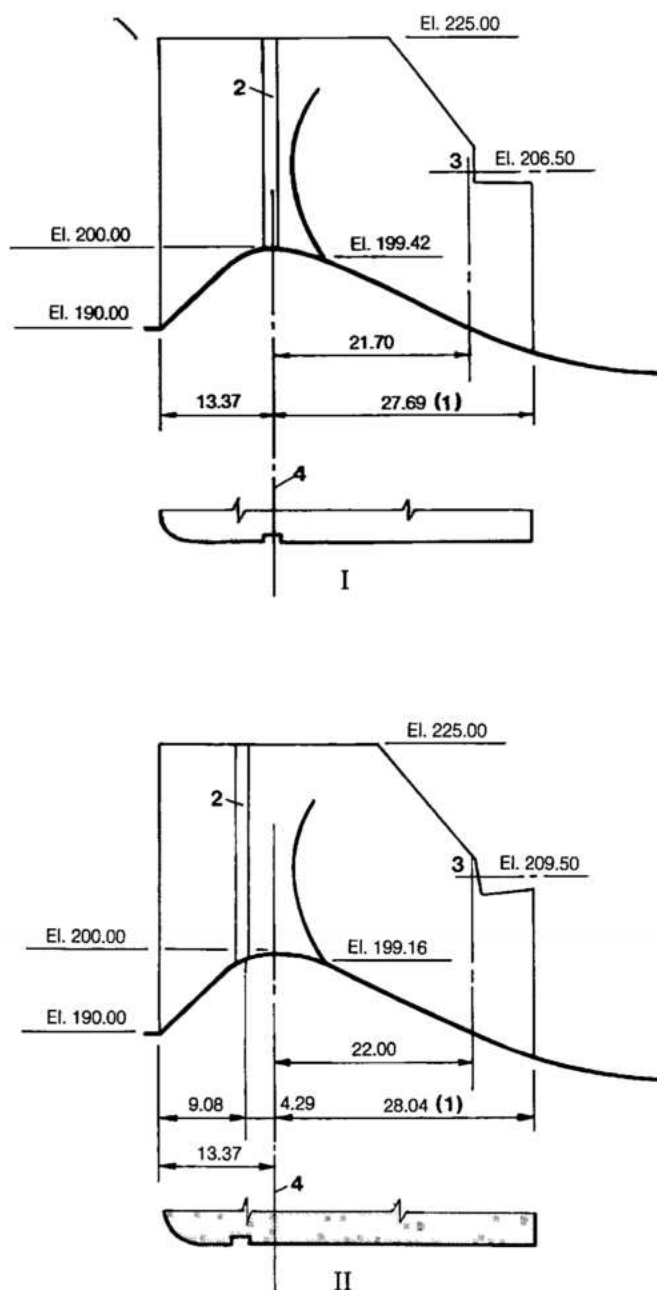


Fig. 8.9 Pier ends studied

- I Initial design
- II Modified design
- 1 Minimum dimension for structural stability
- 2 Stoplog slot
- 3 Spillway gate trunnion
- 4 Crest centerline

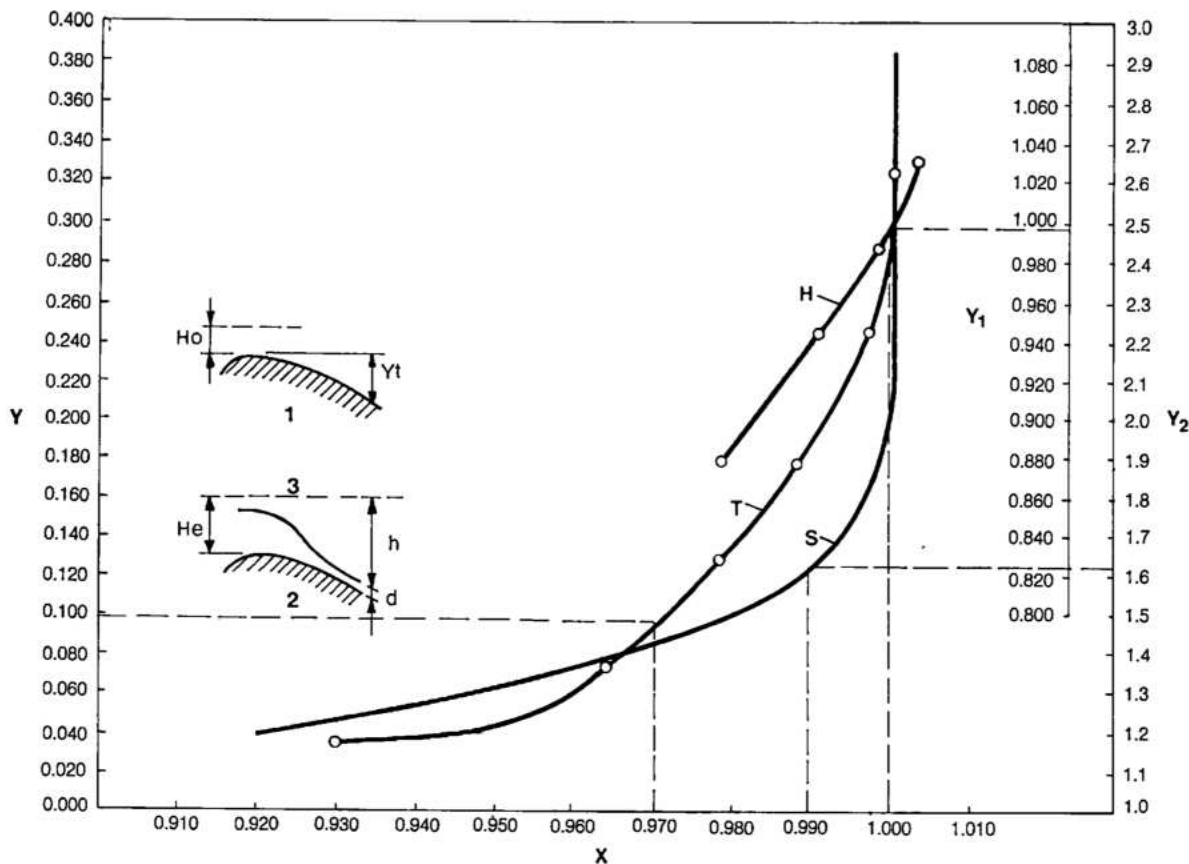


Fig. 8.10 Tangency, head and submergence effect

Y_t Y_t/H_0	H Head effect	1 Tangency
Y_1 H_0/H_0	T Tangency effect	2 Submergency
Y_2 $h + d/H_0$	S Submergency effect	3 Emergency level
X λ effect		

- Water levels at the side walls, resulting from shock waves formed at the separation at the end of the pier, did not result in excessive super-elevations.

There would not be any risk of cavitation or erosion for total spillway discharge of 20 000 m³/s. If it is assumed that all powerplant units are also operating, the total combined outflow would therefore exceed 32 000 m³/s. Considering the low probability of occurrence of such a flow, the square-end piers were considered acceptable.

An additional shape of the pier, see configuration I in Fig. 8.11, was studied as an option for reducing the height of side walls. For this shape also, even though it was longer and tapered, a straight tail was indicated instead of a rounded tail, because it was considered important that the position of flow separation be well defined. The length of the pier in this alternative was limited by the crest dimensions, since it was desirable to keep the pier totally within its monolith.

While standard operating procedures would require that all gates in any chute be opened simultaneously and to the same extent, the possibility of one gate being closed while the others were open, had to be considered as an emergency condition. A series of model tests was made with an end gate fully or partially closed and all the others raised equally to various heights. In Fig. 8.12 the hydraulic profiles in the left chute along the left wall are shown for two types of piers with the left end gate fully closed and all the others fully open and with the reservoir at El. 223. It is seen that for the short square end pier a wave about 7-m high would overtop the wall. With the elongated and partly submerged tapered pier, the shock wave would be much reduced and the wall would not be overtopped. In addition, the inundation at the trailing end of the pier was practically eliminated under all operational conditions of the spillway and the risk of cavitation in this region was also eliminated.

However, an analysis of the risk of overtopping indicated that this problem was significant only for the left chute, where an access road to the powerhouse could be damaged. In the other chutes, the overtopping of side walls would not have serious consequences. Tests showed that one single elongated pier next to the left wall eliminated its overtopping. The evaluation of costs for elongating all piers and their comparison with the costs of repairs in case of cavitation at the end portion of non-elongated piers during infrequent high flows, led to the adoption of the short piers. The final shape adopted for the single elongated pier next to the left wall of the left chute was that of configuration IV, in Fig. 8.11.

TESTS ON FLIP BUCKETS

The specific discharge at maximum flow condition in the Itaipu spillway is $183 \text{ m}^3/\text{s}/\text{m}$. Maximum velocity at the exit is about 40 m/s . Dissipation of the huge amount of energy at the exit without damage to permanent works and without significant surcharge of the powerhouse tailwater were the principal guidelines for design of the discharge buckets of the spillway. To assure accessibility for inspection and maintenance, minimize the risk of damage and for ease of construction, the following additional criteria were used:

- The lips of the discharge buckets should be located above the river level for a flow of $30\,000 \text{ m}^3/\text{s}$, the highest flood of record at that time.

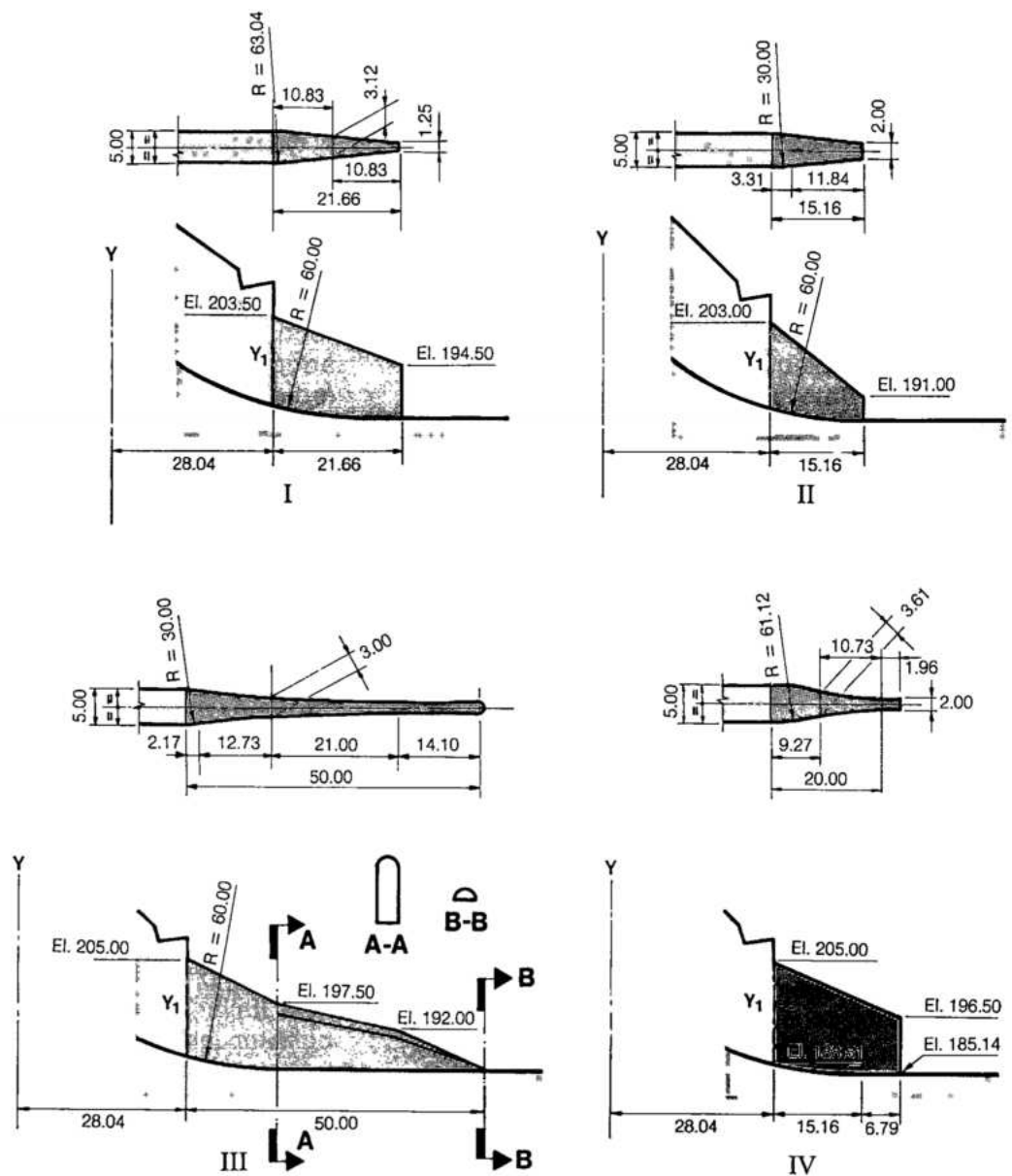
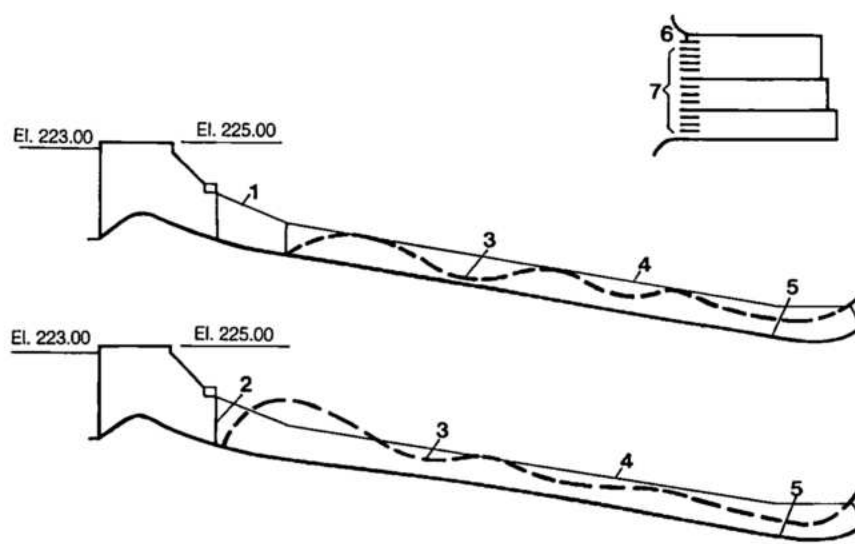


Fig. 8.12 Tests with end gate closed

- 1 Elongated pier
- 2 Square end pier
- 3 Flow profile
- 4 Left wall
- 5 Chute
- 6 End gate closed
- 7 Gates completely open



- The discharge jets should impinge in the deeper parts of the river.
- Energy dissipation within the buckets, that is, formation of hydraulic jumps, should be avoided except for very low flows.

A comprehensive study of energy dissipation consisted of a program of tests on the 1:100 scale model using a cohesionless erodible (movable) bed in the river. This series supplemented an earlier test program with a fixed bed, and provided comparative qualitative data regarding the tendency for regressive erosion at the toes of the buckets, erosion and formation of bars in the river channel, and tailwater surcharge at the powerhouse.

Initial tests were carried out on a simple conventional circular bucket. For the layout with the oblique ends of the central and right chutes, two alternative solutions were analyzed, one with a variable radius bucket and the second with a horizontal triangular bucket with curved edges. Tests on these two alternatives indicated that hydraulically both were feasible. However, in the final layout as shown in Fig. 8.13, all buckets were made circular with a radius between 27.54 m and 46.25 m depending on the bucket.

To improve dissipation of energy dispersion blocks were tested in the flip bucket to spread the jet and reduce energy concentration in the impact area. The block arrangement shown in Fig. 8.13 was tested in the three-dimensional and partial models. The test results confirmed the following:

- The amount of erosion in the river bed was reduced, but not to an appreciable degree, see the Table in Fig. 8.14.
- To eliminate cavitation at the dispersion blocks under all operating conditions, a highly elaborate

and complex design of the blocks would be required.

On the basis of model test results, considerations of construction complexity, the possibility of damage by floating material and the difficulties of repair and maintenance, it was decided not to adopt the dispersion blocks.

In the plain circular buckets an elongation with a rectilinear deflector was also tested and later adopted to obtain a better defined jet without reducing pressures at the extremity of the structure, a region naturally subjected to localized negative pressures. This detail is shown in item II of Fig. 8.13.

The exit angle of the buckets was then tested for the three chutes. The studies showed that exit angles of 25° for the right and central chutes and of 30° to 25° for the left chute, would be the most appropriate for proper orientation of the jets.

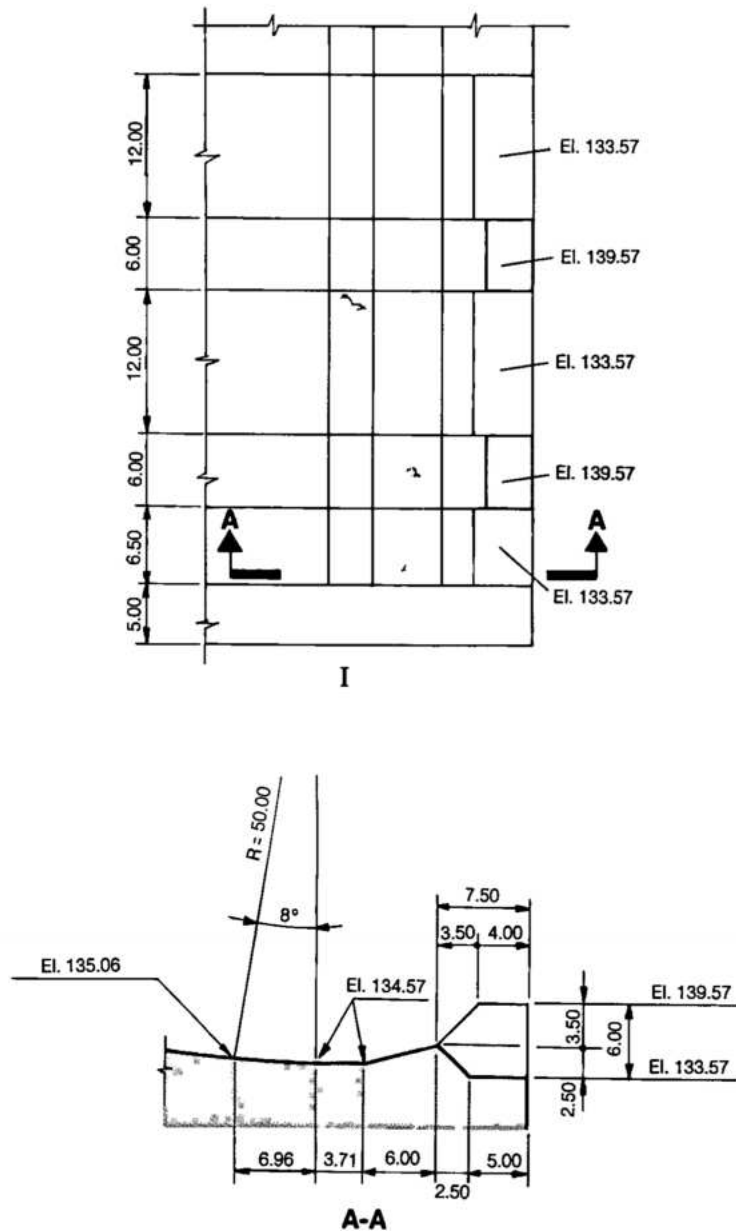
ANALYSES OF EROSION EFFECTS DOWNSTREAM OF THE SPILLWAY

Normally the following parameters are considered for evaluation of downstream erosion:

- Terminal velocity.
- Specific discharge.
- Downstream water depth.
- Angle of incidence of the jet on the water surface downstream.
- Quality of rock in the plunge area.

At Itaipu, the following additional factors had to be taken into account:

- High frequency of operation of the spillway during the first ten years of project operation.
- High concentration of energy in the discharge jets.



- Inability to impact the jets into deep water in the river for the entire width of the spillway, some areas of plunge being relatively shallow.

Energy concentration in the exit jets is essentially a function of the specific discharge. At Itaipu, this could reach a maximum value of 150 MW/m in the buckets ($q = 183 \text{ m}^3/\text{s/m}$ at El.140). Such a high concentration of energy could also occur at flows less than the maximum, when only one or two chutes would be operating as shown in Fig. 8.15.

Therefore, the sequence of operating the chutes was a vital factor for reducing downstream erosion.

Because of the large width of the spillway only the jet from the left chute would impinge into very deep water, while the central and right jets would impact in medium depth to shallow water. Fig. 8.16 shows the original and the eroded profiles of the river in front of the three chutes, as obtained in the model.

The method used was based on the reduction of the dynamic action of the impinging liquid surfaces

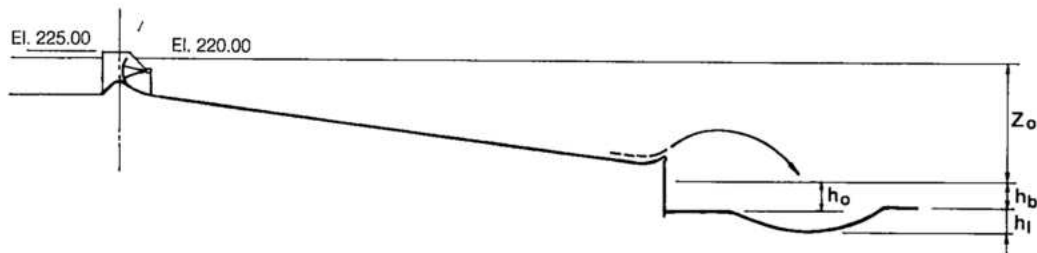


Fig. 8.14 Comparison between erosions: conventional flip bucket and flip bucket with blocks

A Test performed

B Basic parameters

 q Specific discharges ($\text{m}^3/\text{s}/\text{m}$)

Z_o Water level difference (m)

h_o Groundwater depth at the beginning of the test (m)

h_i Maximum depth operation for conventional flip bucket (m)

h_b Maximum depth after operation flip bucket with blocks (m)

B	A						
	1	2	3	4	5	6	7
q	61.4	80.9	88.7	88.7	120.7	147.8	182.7
Z_o	101.0	101.0	89.0	94.0	106.5	108.0	84.0
h_o	49.0	49.0	55.0	51.0	41.0	44.0	69.0
h_i	54.0	56.0	61.0	59.0	52.0	61.0	77.0
h_b	49.0	49.5	55.0	51.0	50.0	57.0	73.0

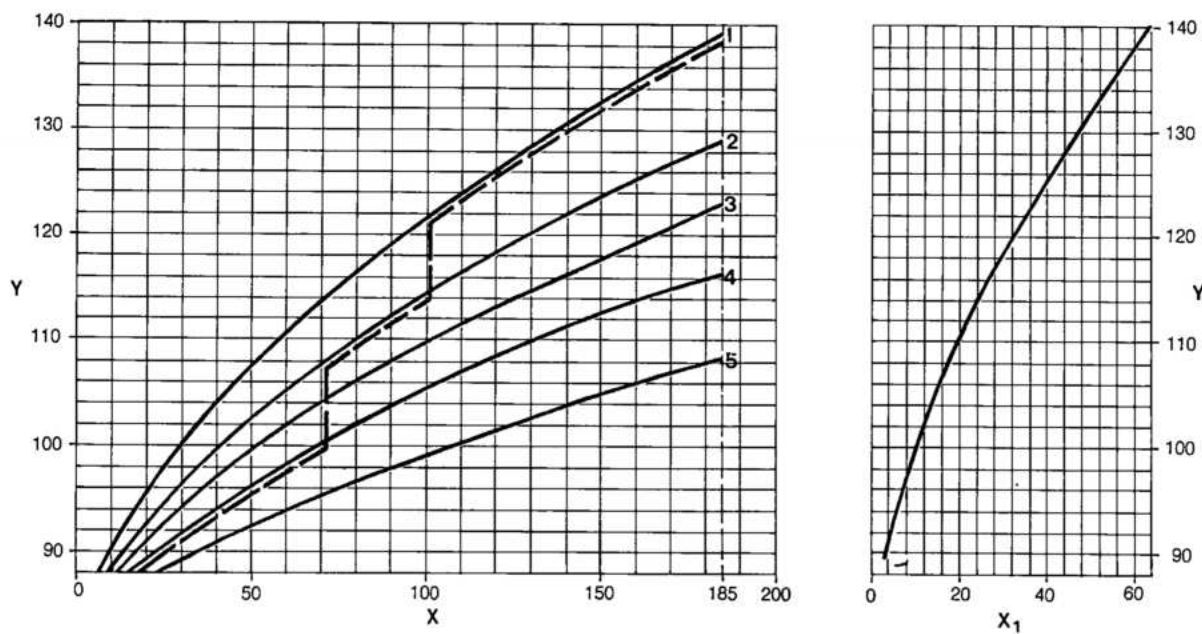


Fig. 8.15 Operation and specific discharge curve

Y Downstream water level (m)

 X Discharge per meter of width (m^3/s)

 X_1 Total discharge (m^3/s)

 1 All chutes = $61\,975\text{ m}^3/\text{s}$

 2 Left and central (or right) chutes = $44\,400\text{ m}^3/\text{s}$

 3 Central and right chutes = $35\,150\text{ m}^3/\text{s}$

 4 Left chute = $26\,825\text{ m}^3/\text{s}$

 5 Central (or right) chute = $17\,575\text{ m}^3/\text{s}$

--- Spillway variable operation curve

of the jets along the depth. The following simplifications were made:

- Determination of head losses in the chutes was made by the conventional method using gradually varied flow.
- Dissipation of dynamic energy after impingement was assumed to be linear, and a function of the angle of incidence of the jet without deviation along its course under water.
- Thickness of the jet was assumed constant from the lip of the bucket i.e., neglecting the acceleration from the edge of the bucket down to the water surface and the effects of air resistance and dispersion.

Results of the analysis are shown in Fig. 8.17, for the following situations:

- Combined operation of all chutes with uniformly distributed discharge.
- Individual operation of the left chute, from the initial minimum to the maximum discharge.

These results were considered conservative, because in addition to the above simplistic approach, the method did not consider that any dynamic action existed near the bed before it had attained its final stable profile.

Initial studies with a movable bed model compared the plain circular bucket and one with a dentated sill. The dentations aerated the lower nape of the jet, dispersed it and reduced the concentration of energy, producing less scour and bars considerably lower than those resulting from the use of the plain flip bucket. For normal operations of the spillway, however, which are generally characterized by the area on the left of the dashed line on Fig. 8.15, the difference in results for the two types of buckets was not important, as for these conditions the adopted plain flip bucket also showed acceptable results.

The selected configuration was subjected to a series of tests for evaluating both the scour effects and the consequent formation of bars.

To estimate scour the flood shown in the hydrograph of Fig. 8.18 was synthesized assuming no flow through the powerhouse, and maximum discharge in the Iguaçu river. This synthesis represented the most adverse conditions for downstream water levels. The movable bed was simulated by cohesive material (natural gravel, powdered gypsum, and portland cement in

Fig. 8.16
Downstream
erosion model
results

- I Left chute
II Central chute
III Right chute
Y Elevation (m)
X Distance -
downstream
from spillway flip
bucket
1 Original profile
2 Eroded profile

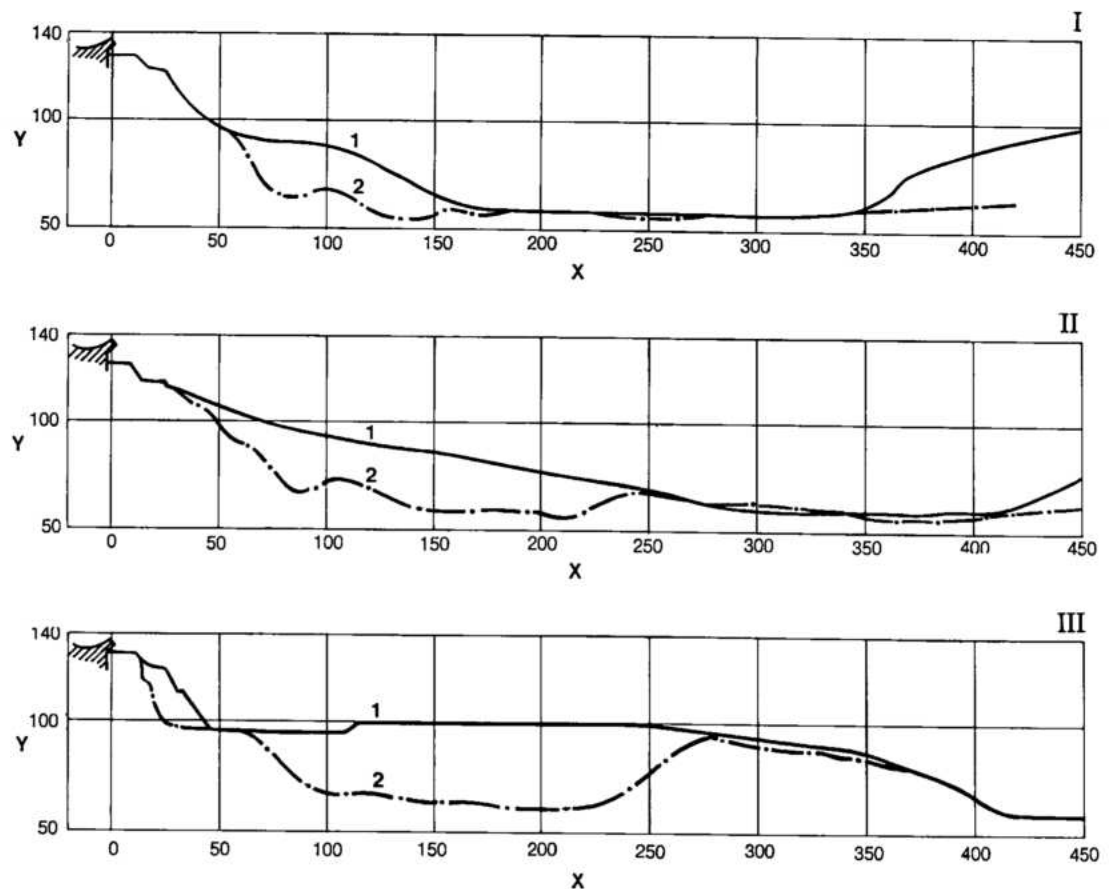


Fig. 8.17 Results of erosion analysis

- Y Elevations (m)
 X Distance downstream from spillway flip bucket (m)
 1 Approximate trajectory of the jets
 2 Downstream levels. All chutes
 3 Downstream levels. Left chute only
 4 Eroded profile. All chutes
 5 Eroded profile. Left chute only
 q Specific discharge ($\text{m}^3/\text{s}/\text{m}$)

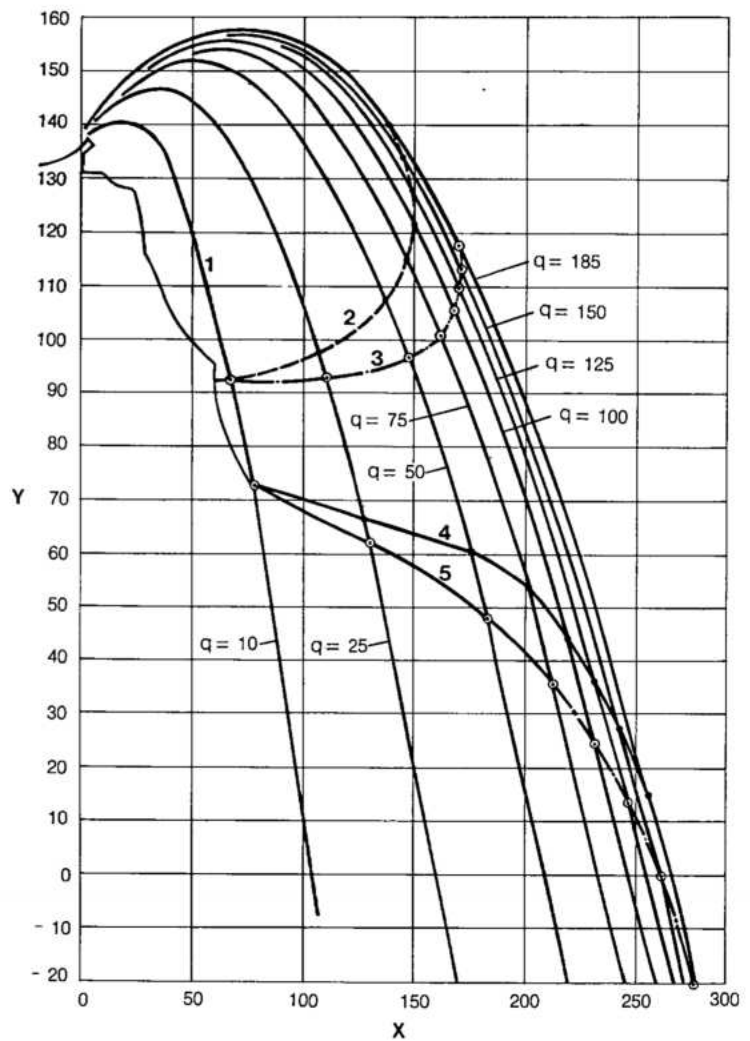
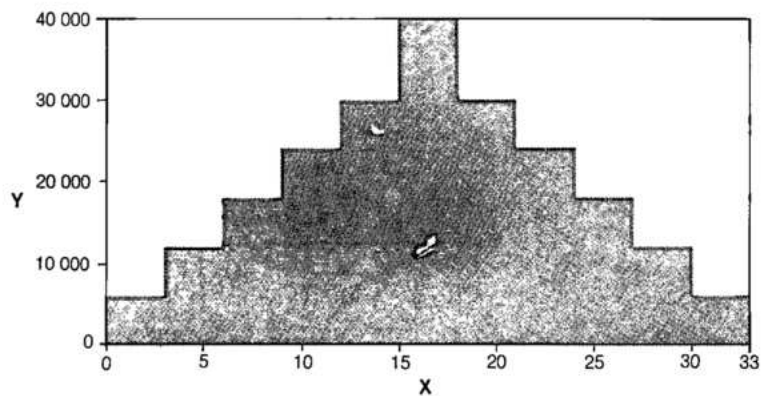


Fig. 8.18 Simulated hydrograph

- Y Discharge (m^3/s)
 X Elapsed time (hours)



pre-established proportions), whose scour limit was determined by a test performed in a rectangular channel at an average velocity of 0.8 m/s (model).

To aid the interpretation of model results a theoretical analysis of the probable erosion was conducted.

The following main observations resulted from this test.

- Due to return currents and superficial and deep instability of the flow, heavy scour may occur, particularly in front of the right chute and against the excavated right-bank of the spillway.
- During the highest discharges, scour would occur on the left bank of the river opposite the spillway.
- No regressive tendency of erosion was noticed in front of the left and central chutes. In front of the right chute there was a weak, but significant, attack against the excavated slope by the same return current and surges that scoured the right bank.
- A large volume of eroded material settled on the original river bed generally downstream of the central and the right chutes, in an area not affected by the impact of the jets. The sediment deposits reduced considerably the natural section of the river; therefore, their effects on river control had to be considered.
- For a maximum discharge concentration of $120 \text{ m}^3/\text{s}/\text{m}$, scour measured on the model reached El. 60 for all chutes in operation. This compared with scour down to El. 40 calculated theoretically (see Fig. 8.16). The difference being attributed to the limited operation time of

the model and the steep incidence of the jet on the downstream cushion at higher discharges.

Another series of tests was conducted to study the control exercised by the bars. In the model, channel shape resulting from the bars was set with cohesive material after removal of all loose material. The original, natural form of the bed was restored with non-cohesive material with a gradation simulating fractured rock in the prototype; the gradation was also modified to study effects of various degrees of fracturing.

To compensate for the increase in volume due to the voids in the fractured material, additional material equivalent to 20% of the original volume of the bed material was added during the test. The gradations of the materials used are shown in Fig. 8.19. The simulated hydrographs are shown in Fig. 8.20, which also shows how the spillway discharge was distributed between the three chutes.

The following test procedure was adopted:

- Separate operation of the power units in the river channel at the minimum and mean tailwater levels of the Paraná river.
- Identification of the effect of the bars having submitted the river bed to a series of flood discharges up to $40\,000 \text{ m}^3/\text{s}$ (cycles 1, 2, 3 on the II hydrograph of Fig. 8.20).
- For the bar which corresponded to the whole sequence of the simulated operation, evaluation of the effects of its removal to El. 100, El. 95 and El. 85, and an estimate of the respective volumes to be removed.

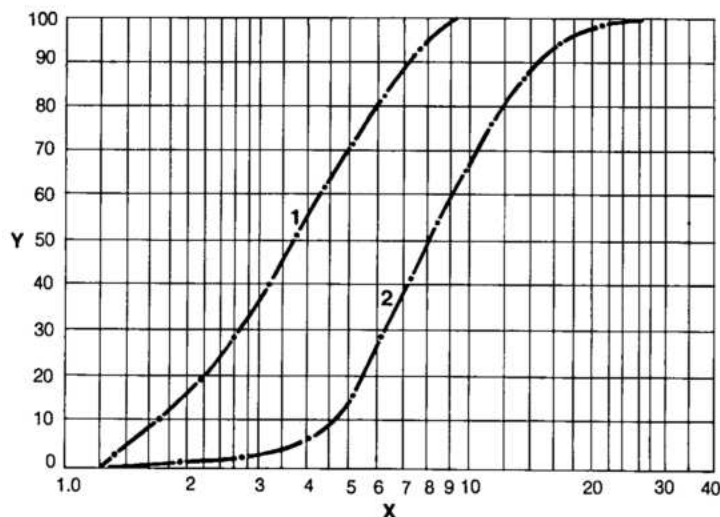


Fig. 8.19 Grain size - test with cohesive material

Y Percent finer than
X Opening of sieve (mm)

1 Grain size - tests A, B
2 Grain size - test C

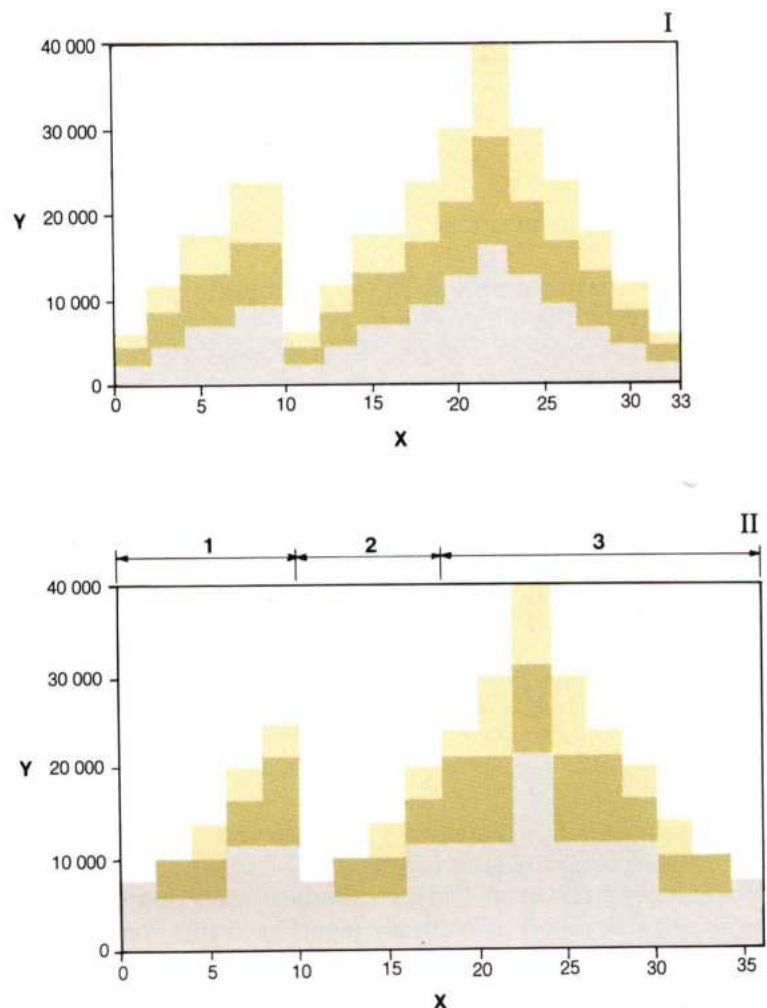


Fig. 8.20 Simulated hydrographs

I Test A

II Test B, C

Y Discharge (m^3/s)

X Elapsed time (hours)

Left chute

Central chute

Right chute

1, 2, 3 Cycles

Test A, B = Distribution of discharge between chutes differently

Test C = Modification of gradation of non-cohesive material

The results are shown on Fig. 8.21. While the results are only qualitative, they did indicate that the formation of bars in the river bed could cause a significant surcharge in the tailwater at the powerhouse. The maximum value measured by the model was 1.34 m, which is the equivalent to a 1.14% reduction in the average available head at the powerplant. Water level in the river had a substantial effect on the degree of control exercised by the bars. For the same operating conditions, surcharge at the powerhouse was 1.34 m with downstream river level at El. 101.25, but only 0.85 m when the river level was at El. 105.

The spillway operating mode also influenced the results. It was indicated that the preferred order of operation should be the left, the central and then the right chute, in successive stages without excessive concentration of discharge in any chute.

The more frequent floods, up to 25 000 m^3/s , corresponding to cycles I and II of the simulated hydrograph, would not erode enough material to

form large bars and the effect on powerhouse tailwater would be insignificant.

The tests demonstrated qualitatively that the degree of fracturing of river bed rock had a great influence on erosion. They also showed the importance of proper simulation of the physical quality and condition of the rock for quantitative evaluation.

It was concluded that the problem of the bars could be approached in two ways:

1. Advance excavation of the material likely to be eroded or
2. Removal of the bars at a convenient time.

The first option would involve underwater excavation and related high cost and early investment.

The second option, as adopted at Itaipu, was to observe the phenomena for several years of project operation, evaluate the economic implications of tailwater surcharge, and then decide if any remedial action was necessary or justified.

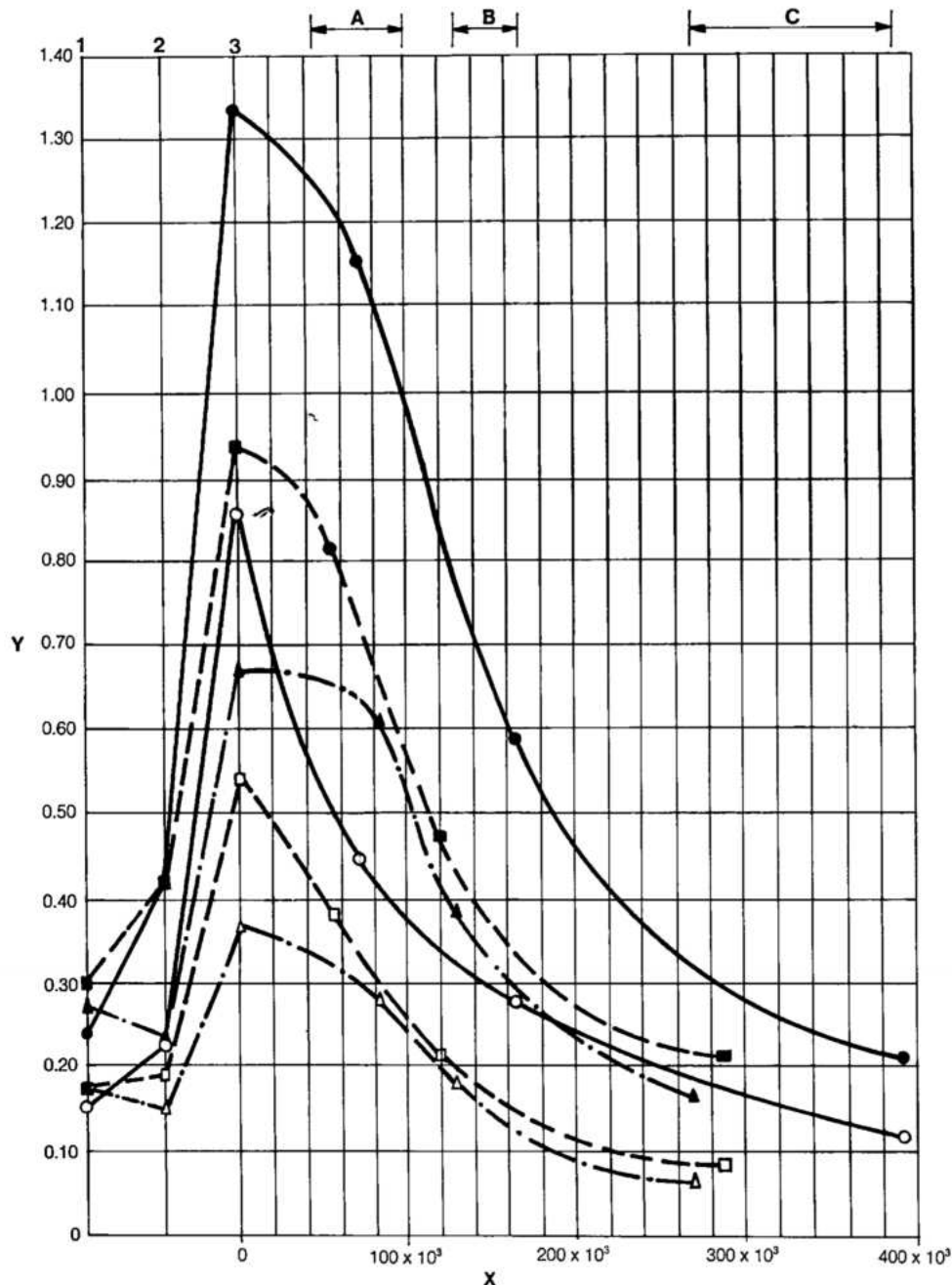


Fig. 8.21 Effects of the bars on levels near the powerhouse

Y Additional differences in levels (m)
 X Volume removed (m³)
 1 Cycle 1; first flood of 24 000 m³/s
 2 Cycle 2; second flood up to 24 000 m³/s
 3 Cycle 3; second flood up to 40 000 m³/s
 A Removal of volume at El. 100
 B Removal of volume at El. 95
 C Removal of volume at El. 89
 —○— Test A
 - - -□- - Test B
 ····△···· Test C

FINAL SPILLWAY ARRANGEMENT

In its final form the Itaipu spillway is a conventional sloping channel spillway with an ogee shaped control structure, divided into three chutes each with its own flip bucket, see Fig. 8.3.

The left side of the approach channel was bordered by the right wing buttress dam and the right side by an inclined slope to natural ground level which was protected

by rip rap and concrete walls. The spillway section is a mass gravity structure with its foundation at El. 180, the crest at El. 200 and the top of the structure at El. 225. There are fifteen blocks, with fourteen radial gates, separated and supported by 5 m wide piers. Each chute is separated by a reinforced concrete gravity wall anchored to the foundation by steel rock bolts. The chute profiles are at different levels following the rock contour to minimize foundation excavation. The right and central chutes have four 20 m x 20 m gates each and the left chute has six 20 m x 20 m gates.

The dimensions of the chutes including flip bucket as measured from the spillway crest are: left, 430 m long x 145 m wide; central, 450 m long x 95 m wide; and right, 470 m long x 95 m wide.

The lower end of each chute is provided with a flip bucket type energy dissipator with the flip at El. 140 for the right chute, and at El. 137.5 for the other two chutes.

The total discharge capacity with reservoir water level at El. 223.24 is 62 200 m³/s, the right and central chute contributing 17 706 m³/s each and the left chute contributing 25 558 m³/s.

Total concrete volume of the structure is 700 000 m³.

DESIGN OF STRUCTURES

Crest structure

The gated crest structure was designed as a concrete gravity dam, divided into fifteen blocks by plain transverse contraction joints located in the center of each bay. Except for the two end blocks, A1 and A15, the other thirteen blocks are identical, 20 m wide, and symmetrical about the pier on the crest.

Stress, stability and design analyses considered each block to be monolithic and elastically bonded to the sound rock foundation. The design loadings included:

- Maximum reservoir pressure with gates closed, as well as raised
- Loads transmitted through the gate trunnions and their anchorages
- Weight of the structure
- Foundation uplift with drains working, as well as inoperative.

It was assumed that the structure received no support from the chute slabs or guide walls, from which it was separated by a contraction joint at the downstream end of the piers. Allowable factors of safety and stresses in the concrete were the same as for the concrete dams, see Chapter 9.

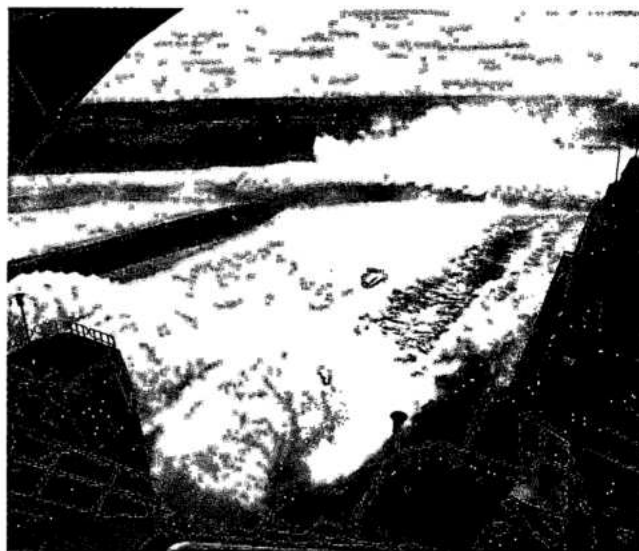
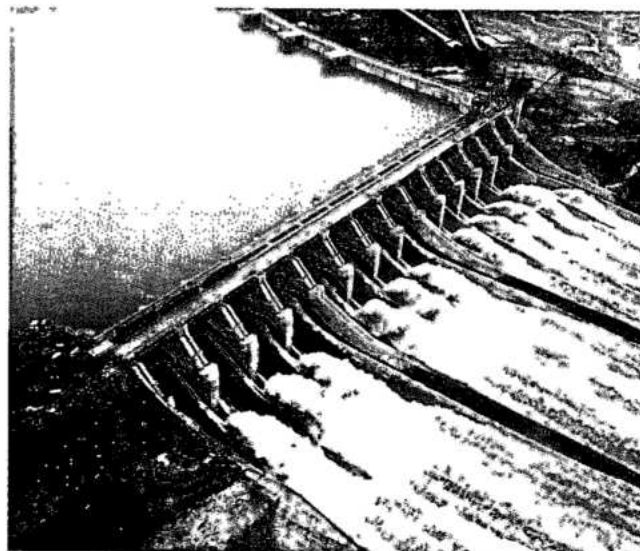
A longitudinal gallery along the entire length of the structure was provided near the foundations and the upstream face. Curtain grouting was performed from this gallery and foundation drains were drilled to depth of 15 m to control uplift.

Mass concrete in the crest structure was class A-140-f, with a 50 cm overlay of D-350-f concrete for the overflow crest. The latter was reinforced with two layers of 25 mm diameter bars at 20 cm spacing at each way. Otherwise, the crest structure was essentially unreinforced.

Piers

The 5 m thick piers which support the gate trunnions were designed as reinforced concrete walls subjected to both bending and torsion. The most critical loading combination being full reservoir pressure, with one gate closed and the other open.

The piers are of D-350-f concrete and are anchored into the massive crest structure with reinforcing steel. Transmission of the thrust from the gates through the trunnions and its distribution in the concrete piers was by means of prestressed cables anchored at the upstream end of the pier.



Spillway gate piers

Chute slabs

The chute floor consists of 1 m thick concrete slabs, reinforced with two layers of steel bars, 25 mm in diameter in a 20 cm x 20 cm grid. To improve bond, 32 mm diameter 3 m long steel dowels were drilled and grouted into the foundation at 2 m spacing. The embedment length of the dowels was between 3 and 7 m and they were distributed as shown in Fig. 8.22 which was based on their resisting half the hydrostatic head, assuming drains to be inoperative. Half-round porous concrete tiles were placed along the rock surface in a pattern to daylight into drainage galleries excavated in rock along the middle of each chute. Because of the effective drainage provisions and excellent bond with concrete, there was no need to design the slab against uplift or bending. Instead, it was designed as a 1 m thick lining with nominal reinforcement for temperature effects. The lower 0.6 m of the slabs was in class A-140-f concrete and the upper 0.4 m in D-350-f concrete with two layers of 25 mm diameter bars at 20 cm spacing in both directions. The concrete in chute floor slabs was placed continuously with slip-forms, in 20 m wide strips. Transverse contraction joints were spaced 60 m apart. The two layers of concrete were placed less than 4 hours apart, thus preventing a cold joint between them.

To obtain a hydraulically smooth finish, the following tolerance limits were specified and strictly enforced during construction:

In direction of flow	5 mm in 3 m
Normal to flow	10 mm in ≥ 10 m
	5 mm in ≤ 10 m

Guide walls

The end guide walls were designed as concrete gravity structures, subjected to the head of water on one side, as indicated by the hydraulic model tests for maximum discharge conditions. Typical joint spacing was 10 m. Only temperature distribution steel reinforcement was provided near the surface.

For the central guide walls, the critical load was lateral water pressure with one chute running full and the other empty. These walls were inverted T shaped reinforced concrete cantilevers, 5 m thick, with the toe slab anchored to sound rock with steel rock bolts:

Flip buckets

The flip buckets were designed as mass concrete gravity structures bonded to the rock foundation. The foundation was trenched to form a 5 m deep key under each bucket. Since the lateral loads which the bucket structure had to

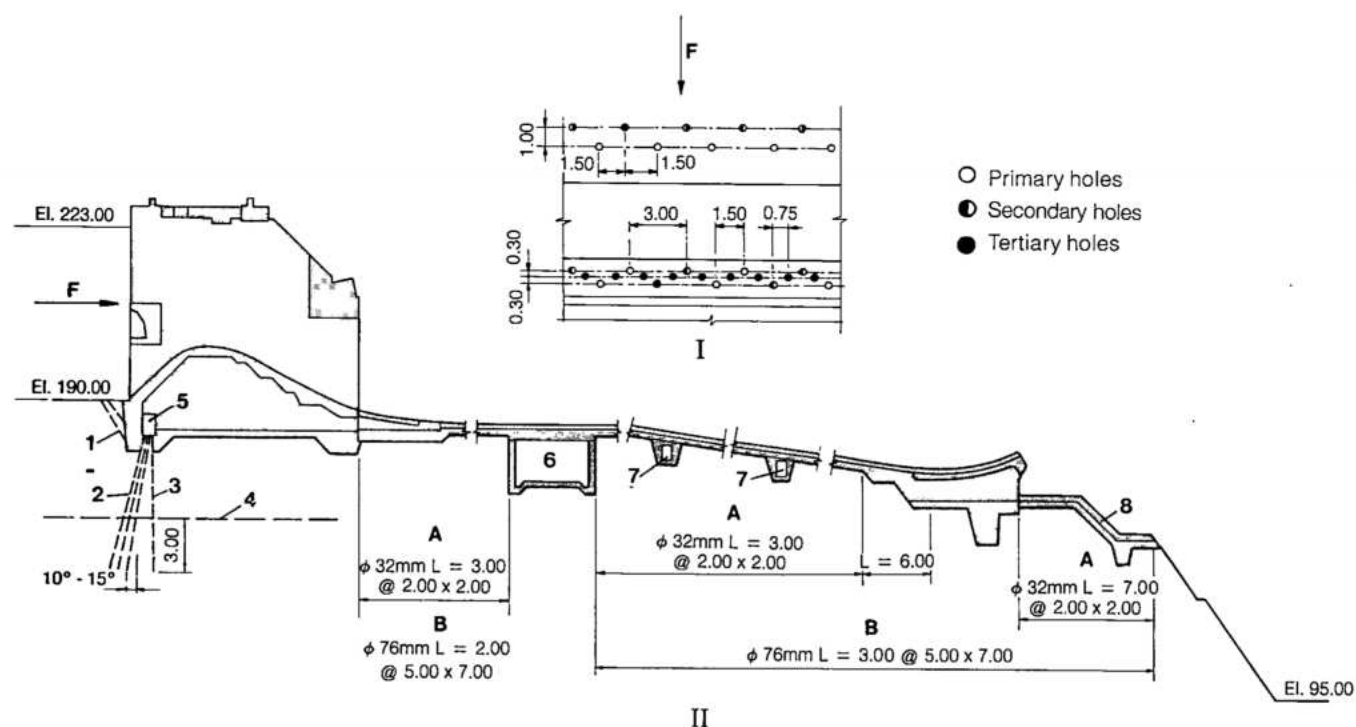


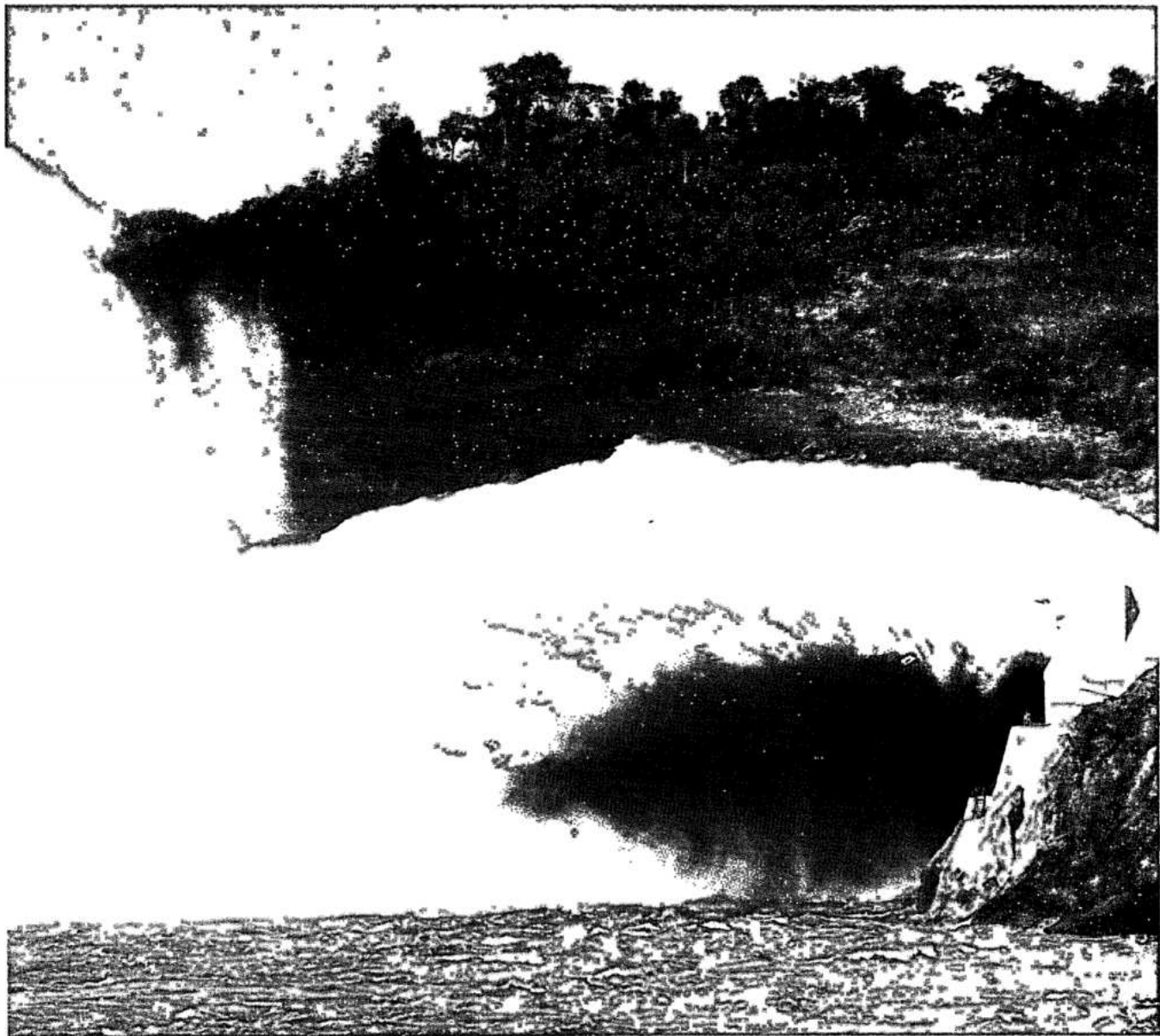
Fig. 8.22 Foundation treatment and concreting

sustain were relatively modest, the body of the bucket is of A-140-f class mass concrete. Contraction joints 20 m apart divide the bucket into monolithic blocks.

A 0.5 m thick layer of D-350-f concrete covers the surface of the bucket. This layer is reinforced with two layers of 25 mm diameter bars at 20 m spacing to provide resistance to hydraulic tractive forces.

A concrete slab is provided downstream of the flip bucket to protect the slope. This slab is firmly bonded and anchored to the rock. Further downstream, the slope is covered with two layers of shotcrete and wire mesh anchored to the rock with 3 m long rock bolts placed at 2 m intervals. Half round drains are provided at the contact surface.

Flip bucket in operation



Aeration galleries

With a maximum head exceeding 80 m, specific discharge of $183 \text{ m}^3/\text{s}/\text{m}$ and flow velocity of about 40 m/s, the lower parts of the chutes and the buckets were considered vulnerable to cavitation. In 1978, excessive cavitation damage to a spillway in Iran raised the question of similar risk at Itaipu, particularly during the early years of operation, even though model tests had shown the Itaipu design to be cavitation free.

Considering the consequences of the potential risk, it was decided to make provisions for aerating the flow from under the chutes, should it become necessary during operation. Consequently, two galleries, each $2 \text{ m} \times 2 \text{ m}$ were constructed under each chute normal to the direction of flow. The galleries were connected to air intake shafts, built into the guide walls. At each end the two galleries were spaced 90 m apart, with the lower gallery about 25 m upstream of the start of the bucket. If in the future there is damage in the buckets or chutes due to cavitation, slots could then be cut through the floor slab to the aeration galleries. As discussed later such a situation had not arisen after 8 years of operation.

breccia of flow B, see Fig. 8.23. Permissible bearing resistance of the foundation material was $100 \text{ N}/\text{cm}^2$, which was easily accommodated by the proposed design under maximum loading conditions, including earthquake forces.

The principal concern was the permeability of flow D which was resolved by a series of grout and drainage curtains as shown in Fig. 8.22.

The upstream main grout curtain is composed of three rows of 76 mm diameter primary, secondary and tertiary holes, inclined 10° – 15° upstream.

Drilling of these grout holes was done from the drainage gallery on the upstream side of the spillway at El. 183.75, with the following spacing:

- Primary holes at 6 m intervals in the first and third rows
- Secondary holes at 6 m intervals in the first and third rows
- Tertiary holes at 1.5 m intervals in the second row

The gallery from which the holes were drilled was narrow which restricted the distance between the lines of holes to 0.3 m at the gallery level. However, because each line of holes has a different inclination relative to the vertical, they are 3 m apart at discontinuity D. The holes reached 3 m below discontinuity D, averaging 27–30 m in length.

Outside the upstream end of the spillway, 18 m from its axis, an additional consolidation curtain with 76 mm diameter holes in two rows was provided through the platform at El. 190.

The spacing of holes was arranged as follows:

- Primary holes, in the downstream row, at 3 m centers
- Secondary holes, in the first row upstream, at 3 m centers.

The spacing between these rows was 1 m.

Next to the grout curtain in the upstream gallery at El. 183.75 a drainage curtain was provided, 0.7 m

CONSTRUCTION OF THE SPILLWAY

CREST STRUCTURE

Excavation and foundation preparation

The spillway structure is sited on dense basalt, the chutes are on flows C, D and E which are composed of vesicular basalt and breccia and the foundation slab of the flip bucket is on

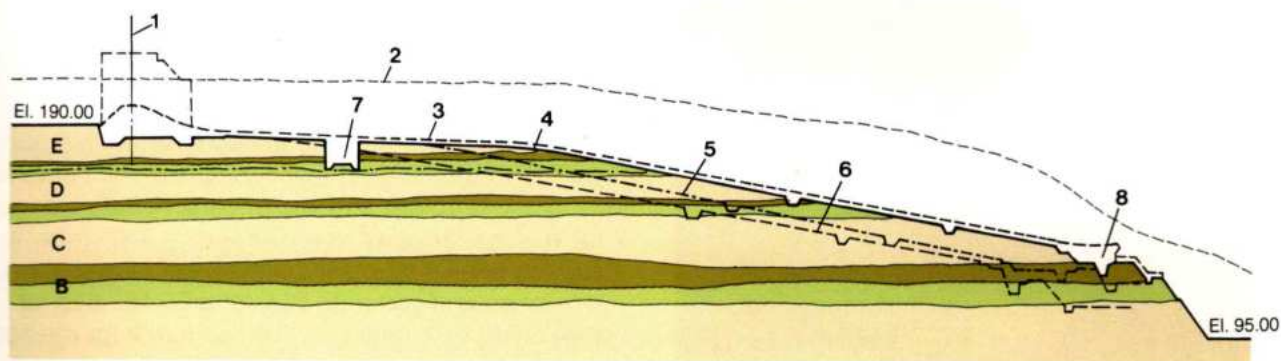


Fig. 8.23 Spillway excavation profile

B, C, D, E Flows

1 Spillway axis

2 Natural ground profile

3 Typical profile of the structure

4 Right chute

5 Central chute

6 Left chute

7 Road tunnel

8 Flip bucket

--- Joint flow D

Breccia

Dense basalt

Vesicular amygdalite

from the last downstream row of grout holes and reaching 3 m below discontinuity D.

Under the chutes there are 76 mm diameter drainage holes with spacing grid of 5 x 7 m extending a minimum of 3 m from the surface of the excavation.

Also 100 mm diameter deep drainage holes, up to 10 m long, were located in vertical rock faces on both sides of the spillway. They were drilled inclined 15° to the horizontal and were spaced at 5 m centers coincidentally with half-round drains of 200 mm diameter at the rock surface.

Excavation for the foundations of the gated crest structure was a continuation of excavation for the approach channel. Drilling and blasting was done in 2 to 3 m lifts; the shallower lifts being used near the structure and at the bed of the channel at El. 190. Excavation of rock for another 5 m to the foundation of the central part of the structure proceeded in 1 m lifts. At the upstream end, a line of holes was drilled at 0.5 m spacing down to El. 181, the base of the cutoff trench, and controlled blasting was used to avoid disturbing the foundation rock. Excavation for the downstream cutoff trench, between El. 185 and El. 181, also used line drilling of the slopes. The rock foundation was prepared for concrete by removing loose material with high pressure water jets. Consolidation grouting was not required for foundations of the spillway crest structure.

Concrete placement in crest and piers

Two tower cranes traveling on rails parallel to the axis of the crest structure, located at El. 190 in the approach channel, were used for concreting. They

handled the transfer of materials and equipment from block to block, the delivery, erection and removal of forms, and the pickup and delivery of concrete buckets. Concrete was hauled in dumpcrete trucks from the right bank batch plant via a road through a gap in the right wing dam and then up the spillway approach channel.

Two 1.25 m thick lifts of C-210-f concrete were first placed in the upstream and downstream cutoff trenches. Each lift was placed for the full width of the 25 m block with end steel and wood forms. The concrete in each lift was placed in 0.3 m layers, spread manually or by tractor blades, and consolidated by immersion vibrators. Two parallel upstream PVC waterstops, located at the transverse contraction joints, were embedded in a 0.5 m deep cavity excavated in foundation rock and mounted on the end forms to permit their embedment first in one and then the next adjoining block.

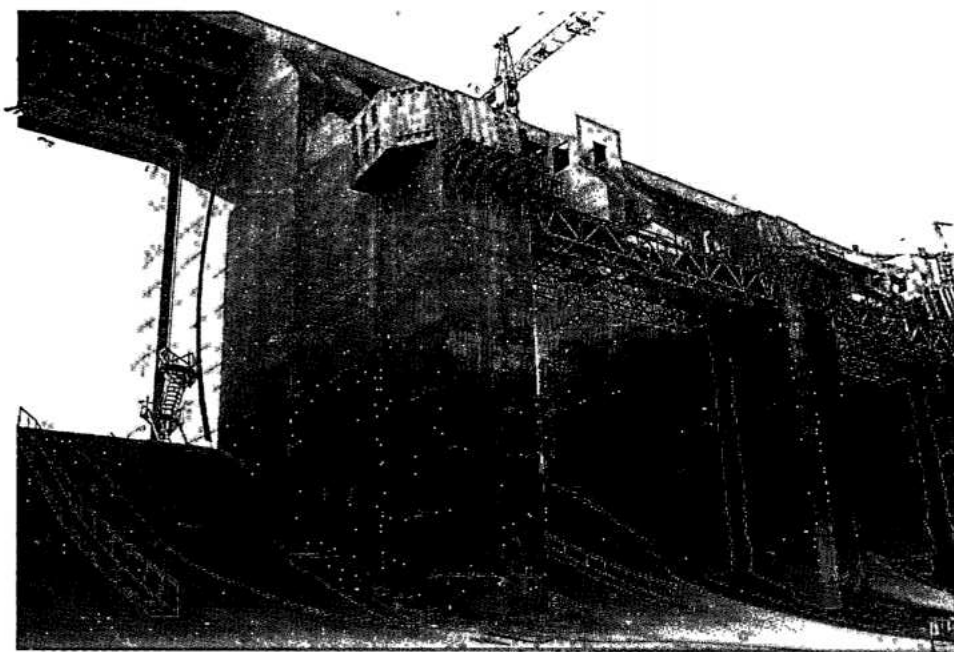
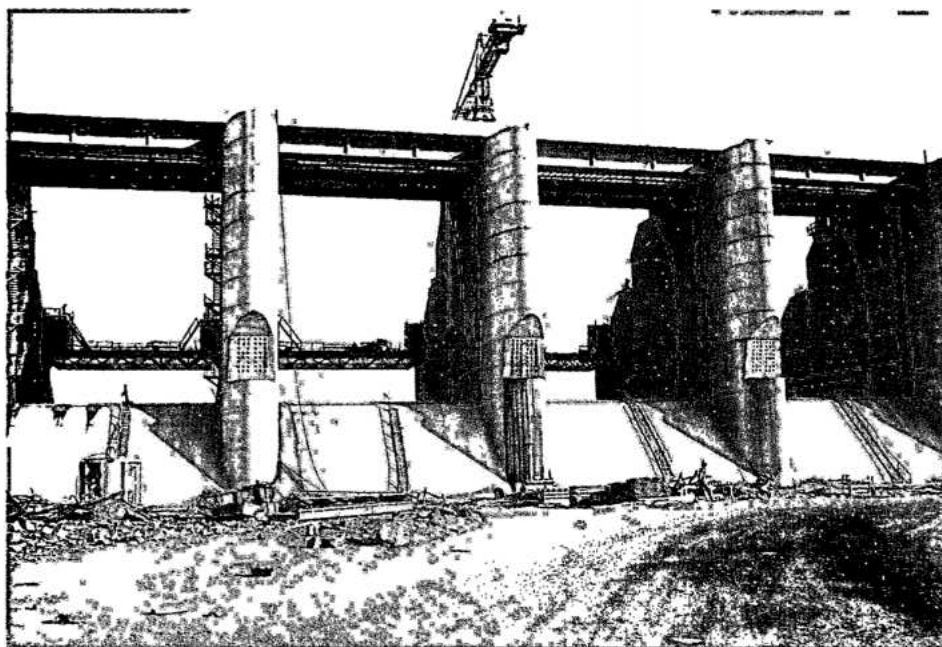
The third lift, also in C-210-f concrete, covered the entire base of the block, and was 1.25 m thick in the cutoffs and 0.5 m over the foundation between them. Since this lift covered about 1050 m², its placing temperature was kept below 7° C and 38 mm aggregate was used. The forms were stripped and each old lift was covered with new concrete within 72 hours. In winter, these measures were effective in preventing cracks in the lifts placed on rock foundation. Construction joints were cut by high pressure water jets and cleaned before new concrete was placed.

The walls of the 2.5 m wide x 3.75 m high upstream gallery, with its floor on top of the second lift, were formed by steel forms. At the contraction joint a PVC waterstop and steel reinforcing bars were installed around the gallery. Flat precast concrete slabs were used to form the roof of the gallery at El. 182.5. The next two lifts to the top of the gallery were also 1.25 m high. Except for the portion upstream of the gallery where C-210-f concrete was placed, these two lifts were of A-140-f concrete, which was leaner and used 152 mm aggregate. The downstream face of these two lifts formed the vertical contraction joint between the crest structure and the chutes. A 0.2 m deep x 1.2 m high keyway was formed in this face with wooden panels mounted on the steel forms.

Subsequent concrete lifts, from El. 182.5 to 197.5, were 2.5 m high and in A-140-f concrete for the body of the structure, with a 1.5 m thick outer shell of C-210-f concrete on the upstream face. On the downstream curved face, the concrete was formed in sloping steps for placing the richer D-210-f second stage finishing concrete. Fig. 8.24 shows the details of the concrete stages.



Excavation of spillway foundation



*Construction of crest
and piers*

The upstream 1.5 m thick concrete, sloping at 45° , was placed behind wooden forms in 3.5 m lifts to El. 198.5. The concrete with 2.5 cm slump was poured through a rubber trunk attached to a bucket. Because of the sharp curvature and tight finish requirements for the finishing layer of concrete on the downstream face from El. 188.5 to the crest, sliding steel forms, 0.6 m wide, 10 m long, and loaded with precast concrete beams, were used. The D-210-f concrete, with 19 mm aggregate and 2.5 cm

slump, was poured about 2 m ahead of the sliding form, and consolidated by 70-90 mm diameter vibrators with long hose in front of and under the form; this prevented the formation of pockets. Excess concrete which piled up in front of the form was removed periodically and placed on the next higher bench. Concrete placement proceeded uphill from downstream to upstream at an average rate of 40 cm/h. Before commencing concreting, the heavy steel reinforcement was cleaned with compressed air jets.

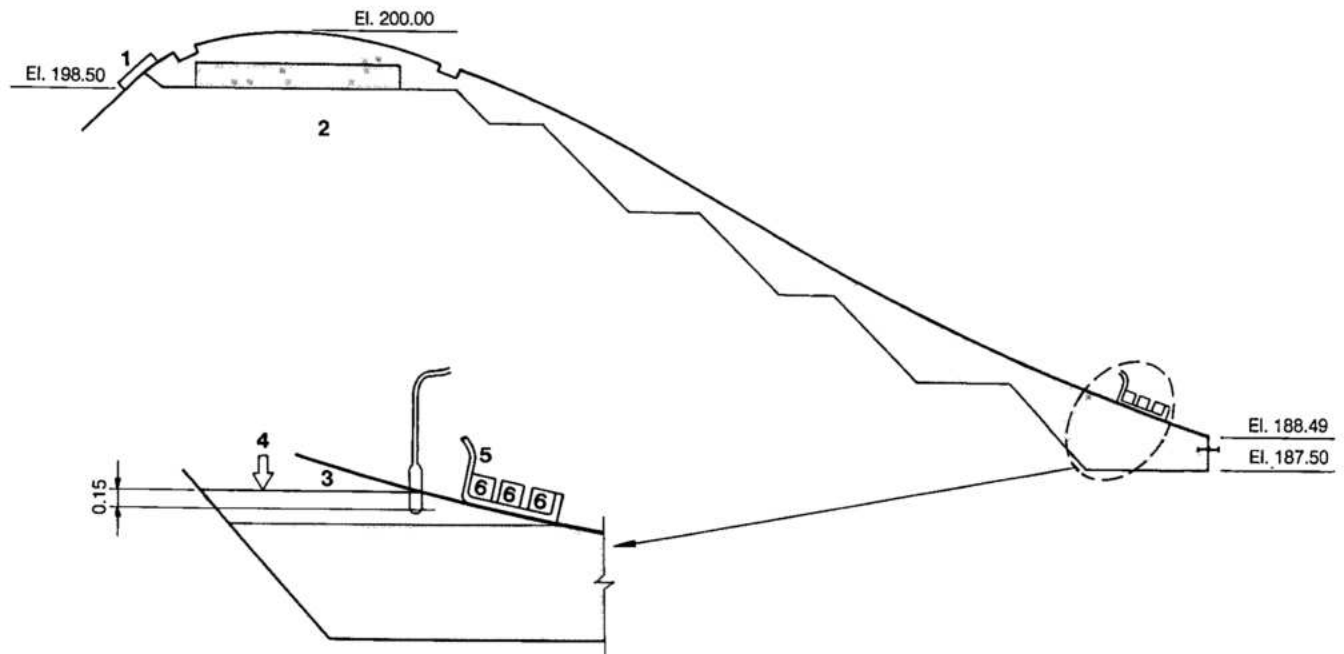


Fig. 8.24 Concrete placement in the crest

- | | |
|-------------------------------|------------------------------------|
| 1 Wood form work | 6 Precast concrete beams (weights) |
| 2 Old concrete, A-140-f | 7 Detail |
| 3 Concrete maximum level | D-210-f concrete - slump 2.5 cm |
| 4 Point of concrete placement | C-210-f concrete - slump 2.5 cm |
| 5 Slip form | |

The top 10 cm wide portion of the crest between the block-outs for sills of the radial gate and the stoplogs, was ground to a smooth finish.

In the center of each block, vertical rebars were embedded as part of the reinforcement required to integrate the 5 m thick pier with the massive crest structure. From the surface of the crest to El. 205, the C-210-c concrete in the piers was placed in 2.5 m lifts between steel and wood forms. Concrete placement essentially followed the techniques used in other mass concrete structures, with careful vibration of concrete between the reinforcing steel and near the formwork.

Between El. 205 and El. 212.5, post-tensioning cables in 100 mm diameter sheaths, were installed in the pier, extending from blockouts in the upstream nose to the downstream face, where the concrete anchor beam was constructed separately from the pier. The structural steel support and welded steel housing for the gate trunnion bearing shaft at El. 209 was also embedded in these lifts.

To protect the embedments from damage and for better consolidation and workability, the construction of the piers used the same procedures as other massive structures, such as the buttress dam. Blockouts were left in both faces of the pier for the curved side seal plates of the gates.

Construction of the 5 m wide x 3.5 m high and 8.4 m long concrete beam for post-tensioning anchorage for the trunnions required special concreting procedures. The 105 m³ of concrete in the beam had to be placed continuously, since no construction joints were permitted. In addition to the sheathed main post-tensioning cables, the beam contained heavy reinforcement in two directions and transverse post-tensioning rods. The entire beam was enclosed by steel forms; to prevent damage to the forms, concrete rise was limited to 50 cm/h. D-350-c concrete was poured from the bucket through a rubber trunk reaching down through the reinforcement. To avoid pockets of segregation and for better workability, a slump of 9 cm was used for the first 1 meter and then reduced to 6.5 and 4.5 cm in two steps in the upper part of the beam.

ROADWAY TUNNEL UNDER THE SPILLWAY

Excavation for the 13 m wide, 345 m long and varying height roadway tunnel under the spillway chute was carried out in 3 m lifts, with line drilling along the near vertical walls. Portions of the steep slopes were stabilized with 5 m long, 25 mm diameter steel rock bolts within a few days after excavation. Near the top, 1 m below the base of the spillway chute slab, notches were excavated in rock for the supporting precast concrete beams and roof slab.

The walls of the tunnel were lined with 0.3 m thick concrete with light two-way reinforcement. The concrete was delivered by dumpcrete trucks and placed in 2.5 m lifts and 5.0 m wide panels. Precast concrete beams, 15 m long and 0.8 m deep were installed to form the roof of the tunnel, as well as the base for the chute slab.

Drain holes were drilled through the walls, 5 m into rock, to alleviate seepage pressures at contacts and discontinuities between various strata of the rock.

CHUTES, WALLS, BUCKETS AND GALLERIES

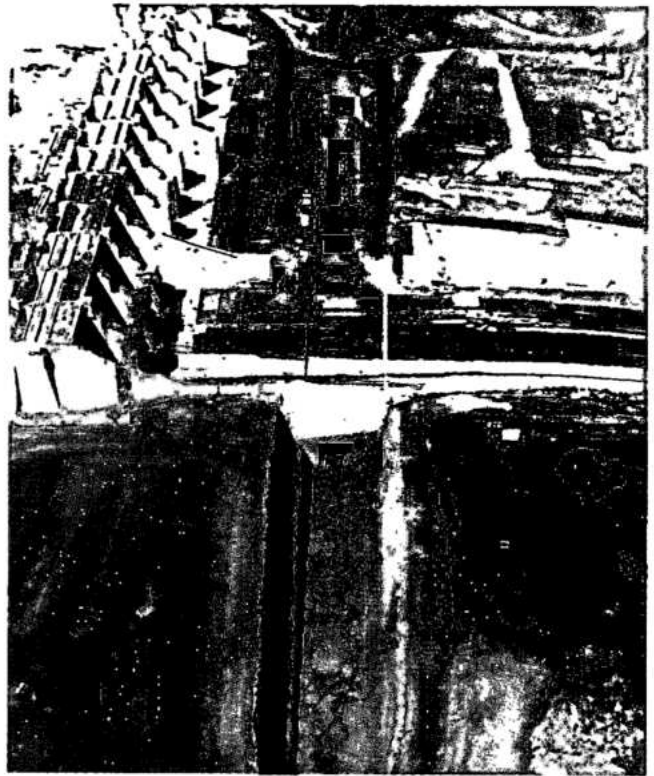
Excavation

Excavation of rock for the 155 000 m² area covered by the chutes was carried out in three stages.

The first stage, which involved drilling and blasting of rock to within 5 m of the designated foundation, proceeded from upstream to downstream as continuation of excavation for the crest structure and from the right bank to the left. Depth of excavation at the right bank ranged from 30 to 80 m and, at the left flank of the spillway from 5 to 10 m. Most of the massive excavation was carried out in 10 m lifts, with holes drilled by down-the-hole percussion drills at 2 m spacings.

The drilling and blasting lifts were reduced to 1 m in the second stage of excavation. Line drilling was adopted for excavation of the right bank slopes, for the four drainage galleries located under the chutes, for the two transverse aeration galleries under each chute and for the longitudinal cuts between adjoining chutes. The latter cuts were up to 10 m in depth between portions of the right and central chutes. Excavation for cutoff trenches and foundations of the flip buckets was executed in the same sequence as for the chutes.

The final stage of excavation comprised the trimming of slopes, cuts and foundations to the design grades. The right bank slope was finished with 2 to 4 m wide berms at 20 m height intervals. In general, the excavated material was hauled out towards the left and either stockpiled for making aggregate or disposed in designated spoil areas.



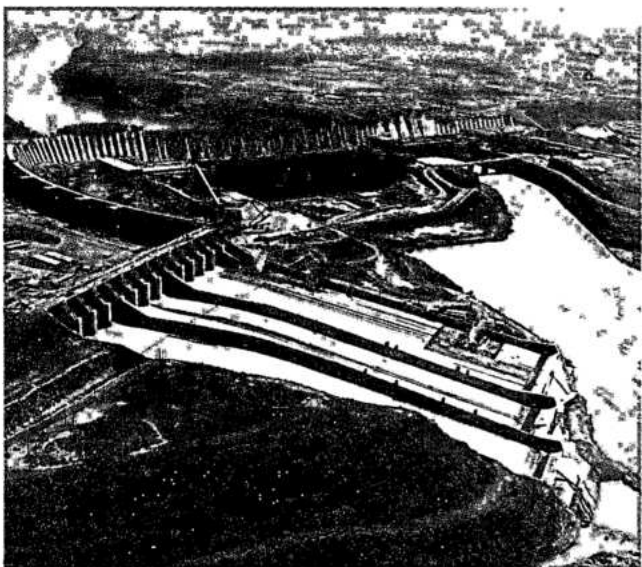
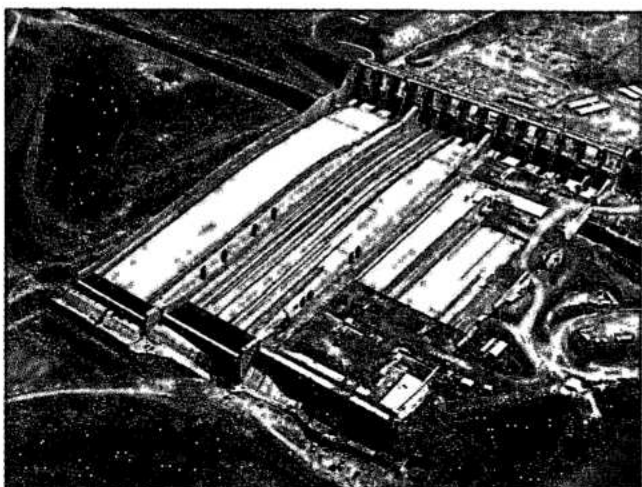
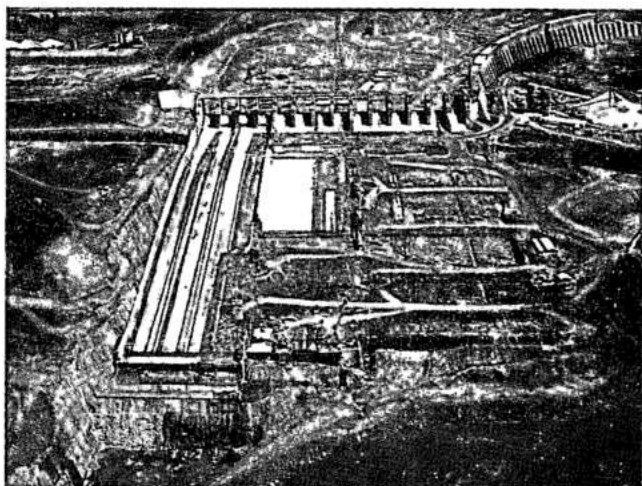
Construction of roadway tunnel under the spillway

Slope and foundation treatment

Deep cuts such as at the right bank or below the right bucket, where indicated were stabilized with rock bolts installed within 2 weeks of completion of excavation. Shotcrete was then applied to the right bank cut above the right wall, the entire right bank above El. 95 downstream of the right chute and the transverse slope downstream of the bucket protection slabs.

After removal of loose material from the foundation of the chute slab, 3 m deep holes were percussion drilled at 2 m spacing, and 38 mm diameter steel dowels grouted in. Next, 150 mm diameter half-round drainage tiles of porous concrete were placed at 2 m spacing in a herringbone pattern, terminating at the four drainage galleries, two under the left chute and one each under central and right chutes.

Other locations, where dowels or anchors were installed, were the foundations of the protection slabs downstream of the flip buckets and the longitudinal cut between the right and central chutes. In the latter case, 38 mm diameter CA-50 steel bars embedded 3 to 5 m into the rock at 2 m spacing, were installed to anchor the wall lining.



Spillway construction

Concrete placement

The sequence of concrete placement was from downstream to upstream and from the right bank to the left. First, the flip buckets were constructed in average 20 m wide monoliths. Except for the 0.3 m thick and reinforced finishing layer for the flip bucket surface, concreting of the massive flip bucket structures followed the same procedures as mass concrete in the crest structure. Concrete in the surface lift was shaped by a straightedge travelling on wooden guides in the shape of the designed circular surface of the flip bucket.

Concrete in the chute floor slab was placed in 20 m wide and 60 to 72 m long panels, with 8.5 m wide panels used along the guide walls. In the right and left chutes, panels starting from the flip bucket were placed first, followed by the next upstream panel. However, in the central chute, slab construction was started from the middle of the chute and completed to the crest structure, followed by the lower downstream portion. The panels along the guide wall were placed after the walls had been completed.

Final finish of the concrete surface was done with a straightedge screed mounted on a steel frame cart with two wheels on each side. The wheels ran on steel tracks the level of which was adjusted with screw jacks. Class A-140-f concrete was used in the bottom 50-60 cm thick layer and class D-350-f concrete was used for the final 40-50 cm layer concrete in the top layer. Concrete in this top layer was placed and vibrated 6 m ahead of the screed which was then pulled 3 m forward at a slow and steady rate such that excess concrete could be pushed ahead without breaks in the finished surface. On the trailing side of the traveling screed cart the concrete surface was trowelled where necessary.

Concreting a slab panel was a continuous operation. Interruptions in concrete placement never exceeded 2 hours, and thus no cold joints were formed either between the two layers or in the surface.

Floors and walls of the drainage and aeration galleries were lined with concrete pumped into the forms. They were covered by flat precast concrete slabs, before concreting of the chute floor slab over them.

Blocks of the divide walls were constructed in 2.5 m lifts, following the procedures for other massive structures.

The surfaces of the chute slabs and the walls were closely inspected and checked for surface irregularities, offsets at joints and pockets of poor concrete. Poor concrete was chipped out in rectangular shapes and replaced by plaques of epoxy mortar, an average of 10 mm thick. Where necessary, surface irregularities were ground to allowable tolerances.

GATES AND ASSOCIATED EQUIPMENT

SPILLWAY EQUIPMENT

General considerations

The crest structure houses the spillway gates, stoplogs and associated electro-mechanical equipment, see Fig. 8.25. The bridge over the spillway crest structure provides truck access from the right bank to the road at El. 225, which is continuous across the top of the spillway, the main dam and the embankment dams, to the left bank. A tunnel under the spillway provides truck access from the right bank to the right assembly area and the powerhouse at El. 144. Both roads can accommodate heavy duty trailers carrying the widest and heaviest single piece of Itaipu equipment, which is the 8.65 m diameter, 3000 kN turbine runner.

GENERAL ARRANGEMENT AND LAYOUT OF EQUIPMENT

Each two gates share an oil pumping set located in the local gate control room in the pier between the gates at El. 223. Also located in the room are the gate position indicator and the local control panel. The central control panel for all the gates and the local electrical substation are located in a room in the left end spillway block (A15) at El. 214.9. Electrical cables and oil piping for the gates run in a gallery located in the downstream side of the bridge between El. 222.6 and 224.7. Access to the gallery is from steps leading from El. 225 at the right and left ends of the spillway. Access to the control rooms is via this gallery or through downstream doors accessible from El. 225 by external vertical ladders with safety cages, leading to a platform at El. 223. Stairs from this platform give downstream man access to the servomotor upper bearings at El. 216. Equipment in the local control room at El. 223 can be removed through hatches at El. 225 which are normally closed with sealed hatch covers.

Centerline of the stoplog slots is located 4 m upstream of the spillway crest centerline and the sill is at El. 199.58. Stoplogs are deployed by means of a 785 kN gantry crane running on rails at El. 225 along the full length of the spillway.

In the left end block (A15) the following equipment is installed:

- Sewage treatment plant.
- Ventilation fans.

- Electrical substation, potable water tank and pumps, and batteries.
- Standby diesel generators, main and day diesel oil storage tanks, batteries for the diesels and central control panel for the gates.
- Toilets and service rooms.

In the future an observation tower may be constructed at the left end of the spillway. The tower will provide access by cable car from the left and right banks of the project. Access to all levels in block A 15 is via stairs; however, an elevator will be installed when the observation tower is completed.

GATES

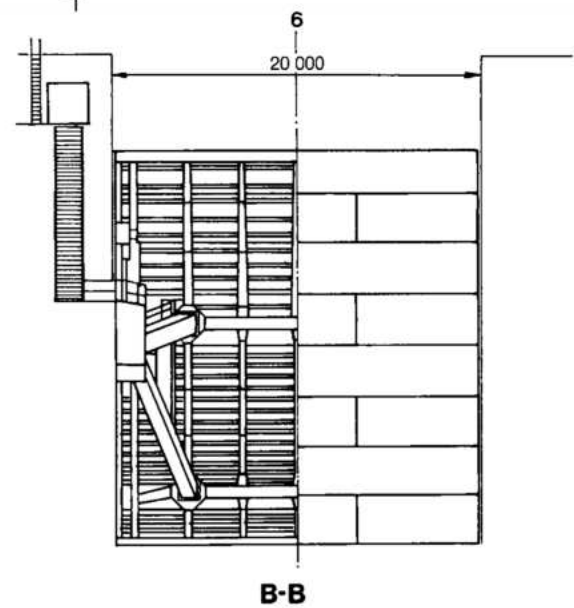
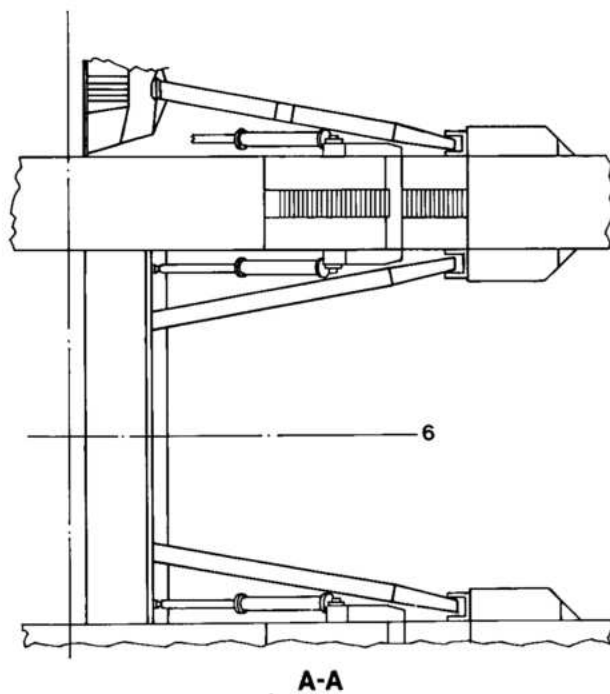
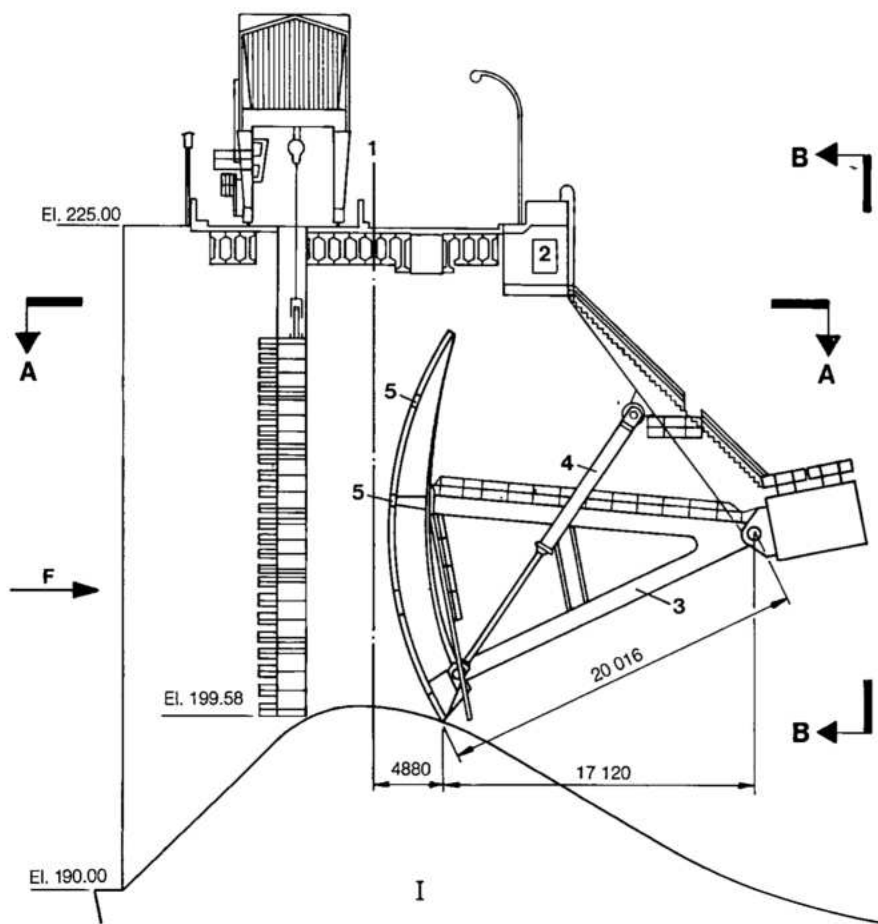
Radial type (tainter) gates between piers operating on trunnion bearings were the obvious and indisputable selection for the spillway at Itaipu. This type of gate had proved itself in similar applications worldwide and precedents of similar dimensions were already in successful operation at many installations, particularly in Brazil, as follows:

Spillway and location	Number of gates	Height above crest (m)	Width (m)
Itaipu, Brazil - Paraguay	14	20.0	20.0
Guri, Venezuela	9	19.8	15.2
John Day, U.S.A.	20	18.3	15.2
Maxwell, U.S.A.	5	18.3	25.6
Malpaso, México	4	18.7	15.0
Salto Osório, Brazil	4	20.0	15.3
São Simão, Brazil	9	20.1	15.0
Tarbela, Pakistan	16	18.6	15.2
Wanapum, U.S.A.	12	19.8	15.2

The radial type gates have the following advantageous features over alternatives such as slide or fixed wheel gates:

- Continuous control of flow.
- Virtually vibration and cavitation free.
- Hydrostatic and dynamic forces can be conveniently reacted in the typical spillway design.
- Sealing is reasonably straightforward.
- Operation can be easily observed.

Although winch and cable operation is sometimes used for tainter gates, it was discarded for Itaipu in



favor of hydraulic servomotor operation for the following reasons:

- The hydraulic servomotor is far more compact and gives freedom in arrangement i.e. the pumping set can be placed virtually anywhere.
- Winch houses would obstruct the upper platform at El. 225 and to place them in alternative locations would involve difficult pulley arrangements.
- Reserve capacity and redundancy can easily be incorporated into hydraulic systems by interconnecting sumps and pumps between units.
- Synchronism of twin hydraulic servomotor systems is simple to achieve, compared with synchronizing cable and winch systems.

Also the hydraulic servomotor systems had already been proven reliable in radial gate service, at many operating facilities.

Basic characteristics

Salient dimensions, weights and characteristics of the spillway gates are given below and the general arrangement is shown in Fig. 8.25.

Number of gates	14
Gate height	21.34 m
Gate width	20 m
Sill beam elevation	199.16 m
Gate radius	20.016 m
Normal opening and closing velocity	0.20 m/min
Maximum opening of gate	16.34 m
Total weight of gate without fixed parts	3185 kN
Weight of gate arm	52 kN
Weight of gate servomotor (full of oil)	142.12 kN

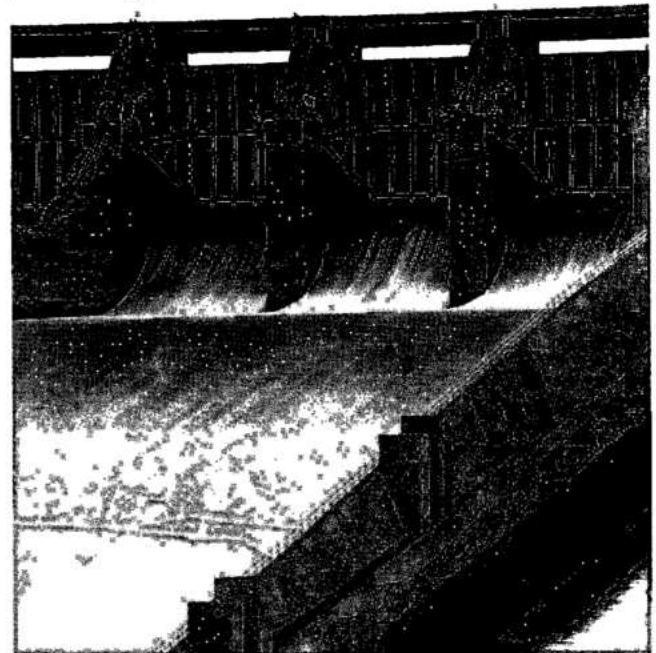
The gates were designed to DIN-19704 for three loading cases, namely "normal" (NB), "specific" (BB) and "exceptional" (AB).

The "normal" case considered the gate subjected to frequently occurring loads, together with the most favorable frictional forces. In the "specific" case less frequently occurring loads, such as flood conditions were considered together with loads due to impeded movement, temperature effects and wind. Finally, in the "exceptional" case all unusual loads during transport and installation are considered in addition to those resulting from malfunctioning safety devices.

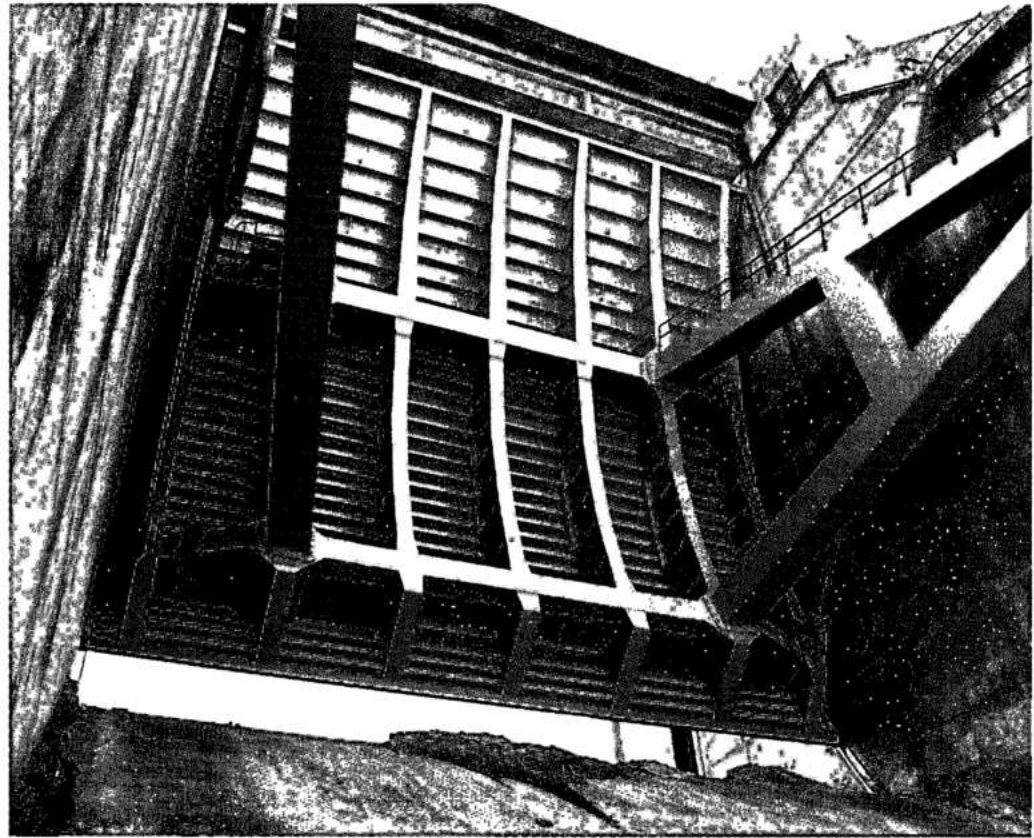
Allowable stresses and other criteria were as follows:

Normal	Tension and bending 55% yield; shear 38% yield point
Special	1.15 normal
Exceptional	1.32 normal
Minimum allowable plate thickness	9.5 mm
Corrosion allowance for stress calculations	2 mm
Impact loading multipliers	1.05 for gate opening from the closed position; 1.25 for all supports
Normal reservoir water level	El. 220
Exceptional reservoir water level	El. 223
Design wind velocity	100 km/h

The gates were designed and manufactured by a Consortium of the Companies Badoni-ATB, Ishibras and Coemsa, Brazil, the oil pumping sets being supplied by Sperry Vickers, Brazil under subcontract to the Consortium.



Spillway gates



Spillway gates

Gate component manufacture and design

Structure. The gate panel consists of a curved skinplate reinforced by T shaped horizontal stringers at approximately 550 mm spacing, and backed by seven vertical beams of welded plate section which in turn are supported by two horizontal beams to which the gate arms are bolted. The panel was transported in eight sections which were welded together at the site.

At its lateral ends, the bottom panel has housings for the lower bearings of the two hydraulic servomotors. The lower part of the bottom panel was filled with concrete to give additional weight and increase rigidity. The gate arms have a welded box section and are formed in an A-shape, the two feet being bolted to the gate panel and the main trunnion bearing forming the apex. Transport limitations dictated delivery of each arm in four parts (the apex, two bottom legs and the center section) for site welding. Lubrite, self lubricating radial and side thrust bearings thermally shrunk into the arm forged housing, were used for the main trunnions.

The stainless steel main trunnion bearing shaft is supported in a welded steel housing which in turn is bolted to a steel structure embedded in the first

stage concrete. Positional adjustment of the shaft support was effected with bolts attached to the embedded structure. When positioned, the support was welded in place.

The maximum force transmitted through each trunnion bearing is 23 700 kN in the radial direction and 4560 kN laterally.

Four bearing pads on each side of the gate limit its lateral movement, the clearance between the pads and the embedded bearing plate being 5 mm. As shown in Fig. 8.26, each pad has two bronze bearing strips attached by stainless steel countersunk bolts to the pad support structure, which in turn is bolted to the side of the gate. The two upper pads are 1250 mm long and are shaped to the curve of the gate, whereas the two lower pads are 660 mm long and are rectangular.

The gate was designed for the "exceptional" condition of the pads being jammed against the embedded bearing plate with the servomotor force corresponding to the setting of the second relief valve of the hydraulic pumping set, see Fig. 8.28.

Metal walkways along the gate arms and down the structure provide man access to the lower servomotor bearing and gate bottom seal.

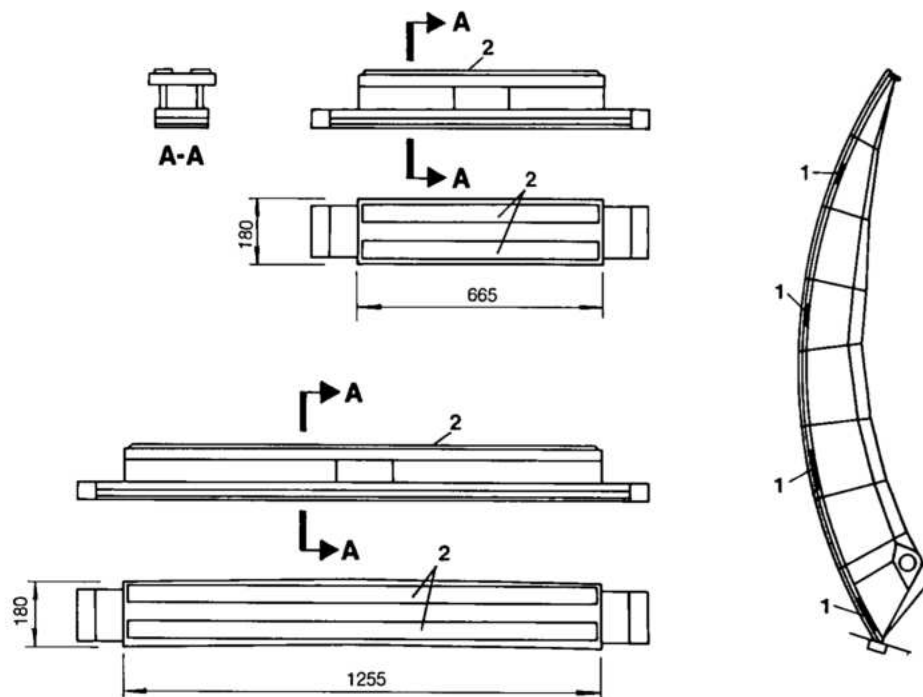
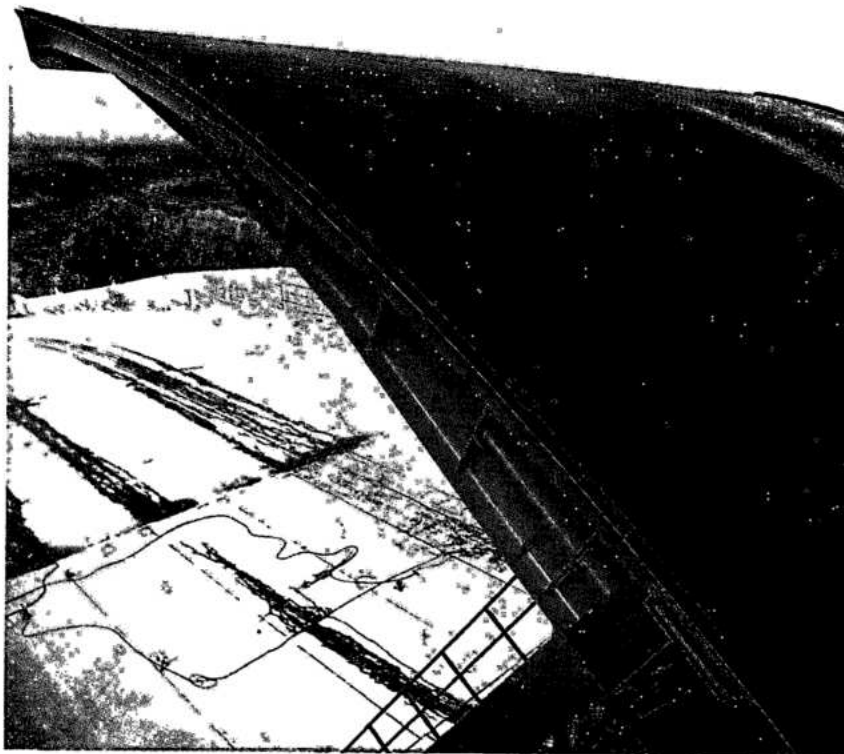


Fig. 8.26 Bearing pads

- 1 Bearing pads
- 2 Bronze strip



Spillway gates bearing pads

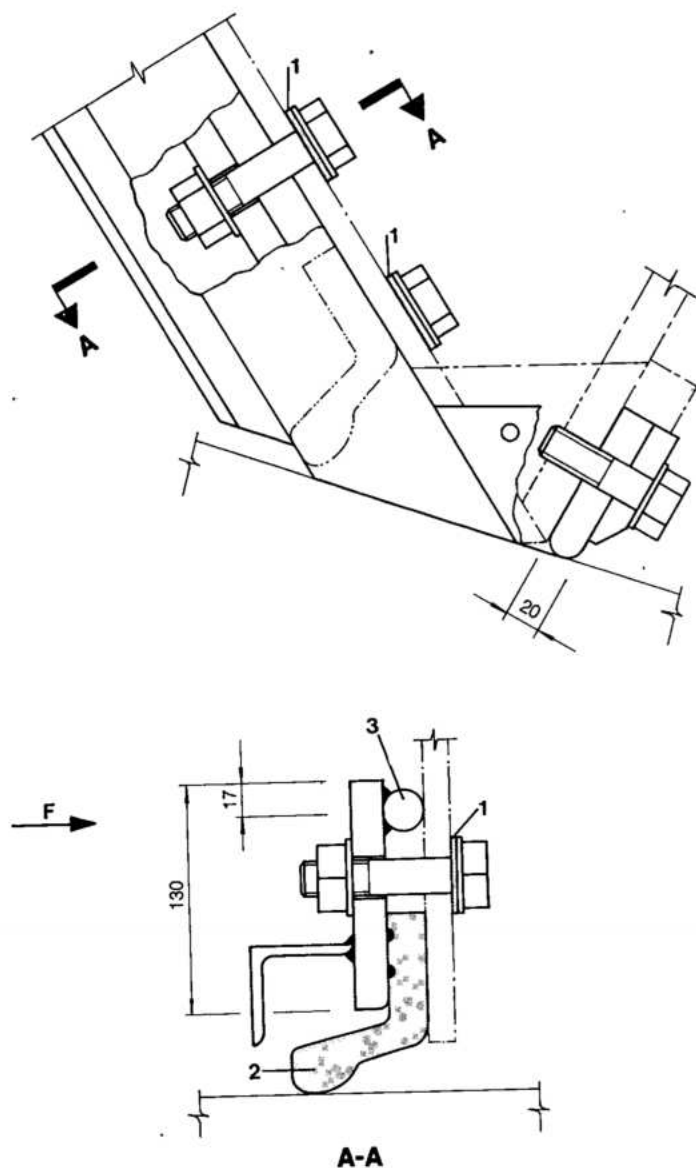


Fig. 8.27 Details of seals

- 1 Rubber washer
- 2 Lateral seal
- 3 Wedge
- F Flow direction

Seals. Details of the side and bottom seals are shown in Fig. 8.27. The L type side seal is held in place by a 19 mm thick retaining plate which is attached to the gate skin plate by 20 mm diameter stainless steel bolts at 110 mm spacing. There are eight separate curved retaining plates with a 3 mm gap between them when in place. Welded to the front of the plates is an L shaped section, which acts as a protection for the seal, and, at each bolt location, a spacer bar. Weld beads were applied to the retaining plate to assist in the lateral retention of the seal.

Pre-compression of the seal after erection was 5 mm. The rectangular type bottom seal also has a 5 mm compression with the gate closed and is secured in position by a 16 mm thick retaining plate held by 16 mm diameter stainless steel bolts at 110 mm spacing. The seals have 60-70 shore hardness, 2.06 kN/cm^2 tensile strength and were subjected to the usual aging and compression testing.

Embedded parts. Blockouts were left in the first stage concrete for the side seal and guide plates, the bottom sole plate and the hydraulic servomotor trunnion supports.

Steel support plates were embedded in the first stage concrete and the holding and adjusting bolts of the embedded parts were welded to them. The side seal and guide plates shared a common blockout, the support consisting of a welded embedded box structure on to which the two stainless plates were welded. An embedded "I" beam was used to support the stainless steel sole plate.

The support for the servomotor upper trunnion is an embedded 11.25 mm diameter steel tube with seven welded lateral thrust rings and two welded horizontal reinforcing plates, which also counteract torque.

Oil hydraulic mechanism. The system consists of single acting servomotors on either side of the gate and associated connecting piping to the oil pumping set located in the local control room.

There are seven oil pumping sets in all, each one serving two adjacent gates. A simplified schematic diagram of the system is shown in Fig. 8.28 and consists of, for each gate:

- A 4000 l oil sump tank with visual and electric level indicators and alarms.
- An electric motor driven positive displacement pump with suction filter, designed for 114 l/min at a normal pressure of 1440 N/cm^2 .
- Two discharge relief valves one at a set pressure of 1459 N/cm^2 and the other at a set pressure of 1471 N/cm^2 .
- Changeover valves.

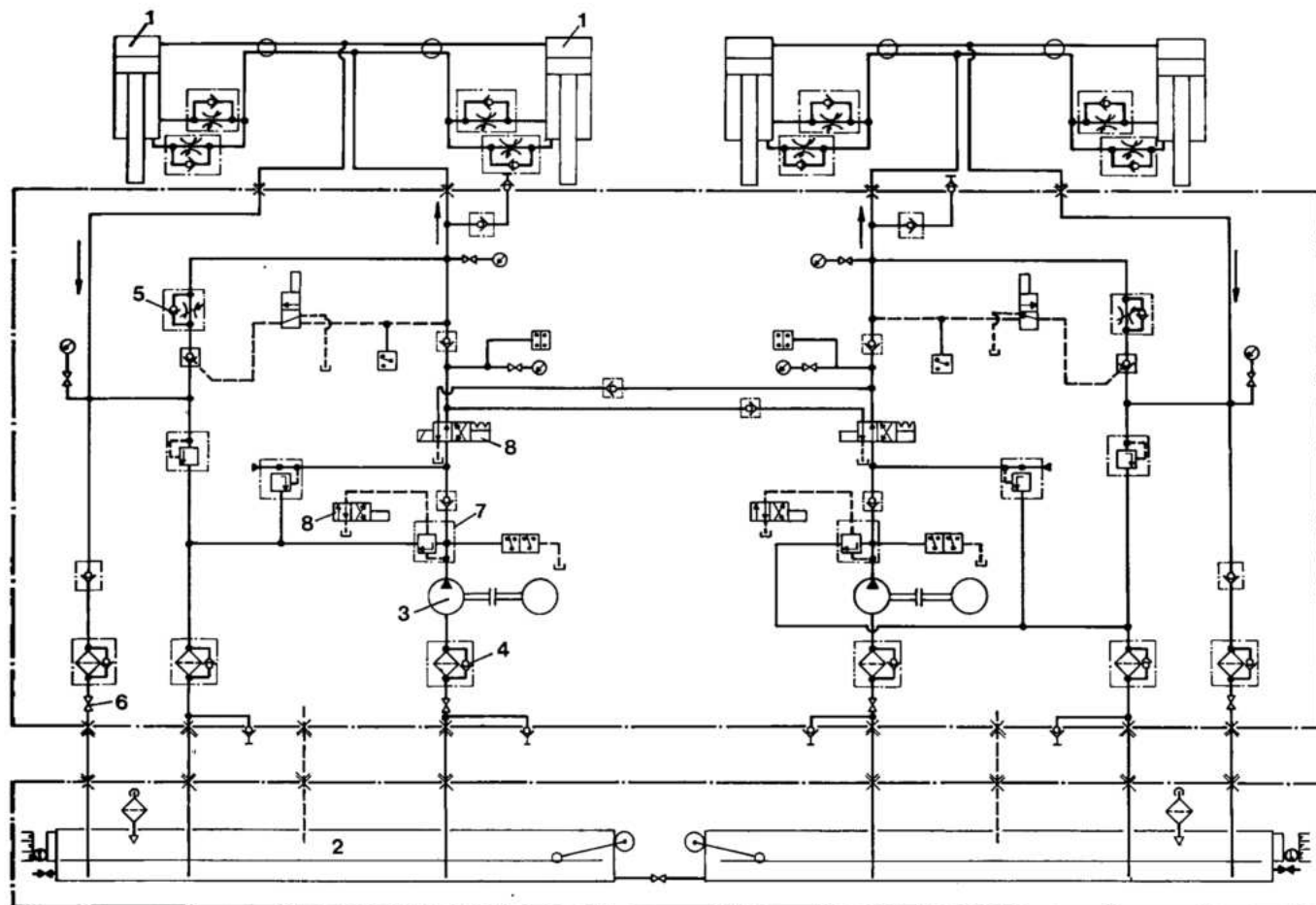


Fig. 8.28 Oil hydraulic system

1 Gate servomotor
2 Oil sump tank

3 Electric oil pump
4 Suction filter

5 Valve V1
6 Valve V2

7 Relief valve
8 Changeover valve

There are interconnections between the sump tanks of each gate and between their respective oil discharge lines such that either pumping set and/or sump tank can be used to operate either gate as necessary.

A portable electrical motor driven pumping set is available in the unlikely event that both motor driven pumps of any one hydraulic unit are inoperative.

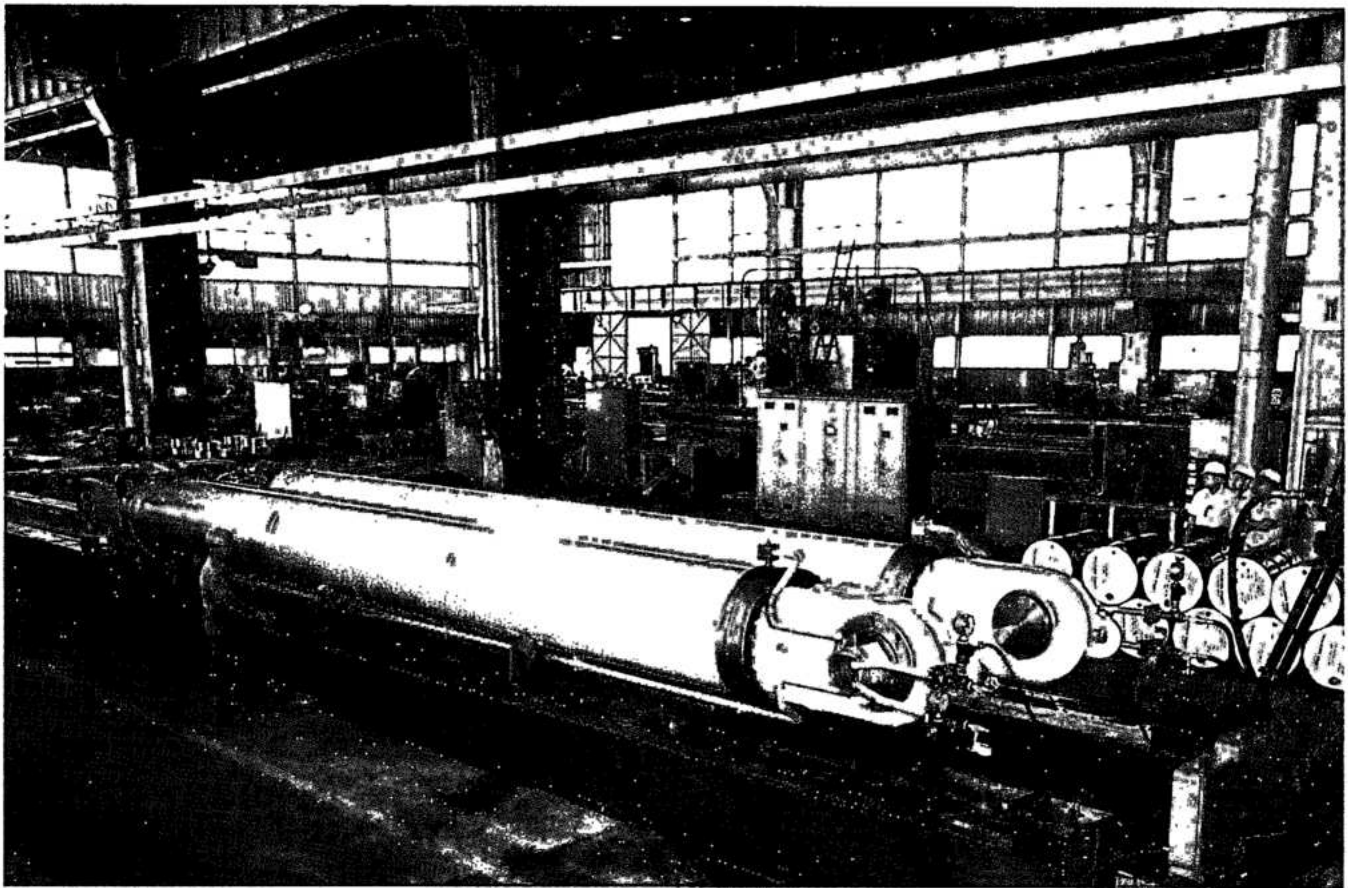
Each sump tank is sized to store the volume of oil in one servomotor plus 20% of the oil in the complete hydraulic system of one gate.

The gate is opened at a rate of 0.2 m/min by operating the oil pump. Closure of the gate is effected by connecting the lower side of the servomotor to the upper side through valve V1, and allowing the gate to close by gravity. Speed of closure is controlled by orifices to 0.2 m/min and the difference in oil volume due to the piston rod is compensated by natural aspiration from the oil sump via valve V2.

A cross-section of the servomotor is shown in Fig. 8.29. The servomotor body is made from rolled and welded steel plate welded to forged steel flanged ends. Forged steel covers are attached with stainless steel bolts to the flanged ends.

The forged steel piston is fixed to the 8570 mm long stainless steel piston rod by means of a retaining nut; the piston seal being a Chevron "V" type, held by a bolted retaining plate. Grease lubricated spherical plain bearings are used for the attachment to the upper and lower shafts at the pier wall and gate structure respectively, the lower eye fitting being screwed to the piston rod. Oil supply and discharge pipes are fed through an articulated distributor at the upper bearing and the pipe supplying the lower chamber of the servomotor has a shut off orifice to limit the speed of final closure to 0.1 m/min.

Servomotors were designed to the ASME Boiler and Pressure Vessel Code and were hydrostatically and functionally tested in the workshop.



Testing of spillway gate servomotor in manufacturer's works

Position indicator. A cable attached to the gate arm near the main trunnion bearing encircles a heavy pulley and is tensioned by a counterweight moving in a protective tube mounted on the pier wall. A second continuous loop cable transmits the movement of the pulley shaft to the position indicator cabinet in the local control room.

Changes in length of the first cable are negligible and those of the second cable are compensated by a spring supporting one of its pulleys, thus maintaining tension in the cable. In the position indicator cabinet, movement of the second cable is used to drive an analogue clock type visual indicator and a continuous cam belt which, via limit switches, control gate opening and closure. The position indicator also supplies remote signals to the central gate control in block A15 and the central control room in the powerhouse.

Gate operation. To comply with the requirements of downstream navigation and other river functions, releases from Itaipu reservoir are carefully regulated. The hourly fluctuations of the Paraná river levels

below the mouth of Iguaçu river should not exceed 0.5 m and the maximum variation within 24 hours should not exceed 2 m.

Itaipu power generation is essentially on run-of-the-river basis, without large changes in the reservoir level for peaking operations. Therefore, to maintain a fairly constant and highest possible head for power generation, the Itaipu reservoir is kept near full and fluctuations are normally limited to 0.6 m, between the normal maximum water level at El. 220 and normal minimum at El. 219.4.

During floods the spillway gates are gradually opened to maintain the normal full reservoir elevation as long as possible. When it is no longer possible to hold the reservoir level, all the gates are gradually opened further. Surcharge will only occur when the flood inflow is larger than the spillway discharge capacity at normal reservoir level. When the flood begins to recede, the gates are gradually closed to maintain the normal full reservoir level once again.

From the model test results, an operational priority was established as follows:

Gate opening and closure. Within each chute, the gates are opened automatically at 10 second intervals starting from both ends and progressing to the center; this sequence avoids excessive forces and overtopping flows on the guide walls. The actual sequences used are as follows:

Chute	Gates
Left	12, 11, 9, 13, 10, 14
Central	8, 5, 7, 6
Right	4, 1, 3, 2

All gates within the same chute normally have equal openings. The closure of the gates in any chute can be simultaneous or follow the reverse sequence of opening.

Chute operation. Discharges into the chutes must be in the following sequence to minimize erosion downstream of the spillway:

- Operate the left chute first.
- Next, operate both the left and central chutes together.
- Use all three chutes for flood discharges exceeding 20 000 m³/s.
- Discontinue individual chute operation in the reverse order.

Minimum gate openings. The minimum initial gate openings at reservoir water levels higher than El. 219.5 are as follows:

1 m for the left chute gates.

2.75 m for the central chute gates.

0.75 m for the right chute gates.

The specified minimum initial openings for gates of the left and right chutes ensure minimum discharges such that the hydraulic jump will not occur within the flip bucket. The larger initial openings of the central chute gates cause the jet trajectory to fall farther into the river, away from the protection slabs at the chute's right edge.

Operation of the fourteen gates is normally effected from the central gate control room in block A15, the individual local control rooms being used normally only for test purposes. Individual gates can be operated from the central gate control room, but as explained previously all gates in any one chute are normally operated concurrently.

The operation of each chute is commanded manually, but once called, the gates of the chute in question are operated in sequence at 10 second intervals.

The cam actuator is programmed with the following steps:

- 25 cm: up to 12 m opening
- 100 cm: between 12 and 15 m opening
- 134 cm: between 15 and 16.34 m opening

Hence, once the button to operate is pressed, all gates in a chute (with the 10 second interval) will move either to the minimum opening or the next step and there stop, awaiting further commands.

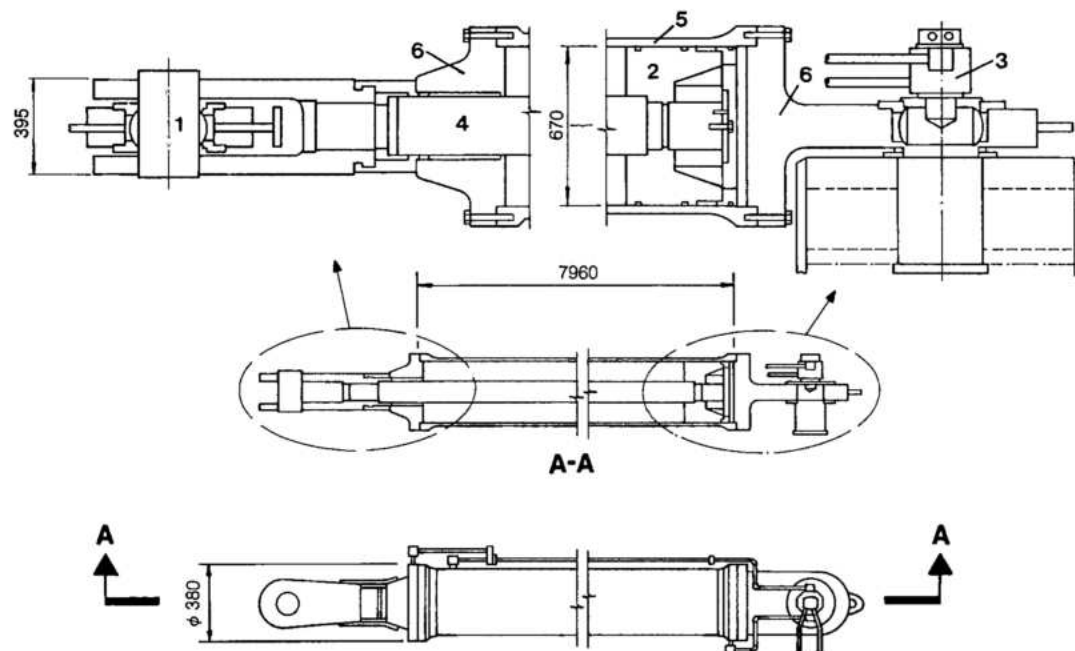


Fig. 8.29
Spillway gate
servomotor

- 1 Coupling pin
- 2 Piston
- 3 Hydraulic oil piping set
- 4 Shaft
- 5 Cylinder
- 6 Cylinder head

GANTRY CRANE

Basic characteristics and general arrangement

The basic characteristics of the spillway gantry crane are given below:

Basic characteristics

Nominal capacity	785 kN
Width between rails	5 m
Vertical course of lifting beam	27 m
Height of crane	13.5 m
Maximum width of crane	6.6 m
Length between buffers	11 m
Weight of crane (without lifting beam)	879 kN

Hoisting mechanism

Maximum velocity	2 m/min
Minimum velocity	0.2 m/min
Diameter of cable	25.4 mm
Type of cable (fiber core, galvanized)	6 x 37
Type of motor	Induction slip ring rotor; resistance speed control

Travel mechanism

Maximum speed	30 m/min
Minimum speed	3 m/min
Type of motor	Induction-slip ring rotor; resistance speed control

The minimum amount of civil structures required for the gantry design and its ideal suitability for the spillway service made it the obvious and indisputable choice. Crane capacity was determined by the weight of a single stoplog panel plus lifting beam.

The crane was specified for outdoor operation with the upper machine housing completely enclosed, containing motors, gearing, cable drums and electrical equipment. Travel of the crane is along the stoplog line only, there being no necessity for travel in the upstream/downstream direction. Power supply, 460 V, 50 Hz, is through a trailing cable, which is wound onto a holding drum on the crane and connected to one of two electrical supply points at piers 4 and 11, respectively.

Design and manufacture of the crane was to the FEM (Federation Europeenne de la Manutention) Standard – Section I, with the following classifications for component parts:

Structural parts

Class of utilization	B	Regular use on intermittent duty
State of loading	2	Moderate – appliances which hoist the safe working load fairly frequently and, normally between 1/3 and 2/3 of safe working load
Group	4	

Hoisting and translation mechanism

Class of operation	V2	Operating hours per day >2<4
State of loading	3	Mechanisms and components subjected for the most part to loads close to the maximum
Group	3m	

The group is derived automatically from the class and state. Class and state were defined by taking into consideration the most extreme use of the crane for stoplog deployment during the maintenance of the spillway gates.

The design wind speeds were (in km/h):

Normal service	100
Without load	150
Out of service	288 in parking position with bracing cables

The crane runs on rails 5 m apart, 355.7 m long between end bumpers, over the fourteen spillway stoplog slots. Parking area for the crane when out of service is at the right end of the spillway, where there are four holding blocks for anchoring the crane.

Component design and manufacture

Structure. A general arrangement of the spillway gantry crane is shown in Fig. 8.30. The frame consists of four welded box girder legs connected to an upper platform on which the hoisting equipment is mounted. At the bottom, the two upstream legs are connected to a welded box girder beam as are the two downstream legs. The enclosure for the hoisting mechanism and associated electrical equipment is of galvanized steel sheeting attached to a welded steel framework. Access to the enclosure is via a caged

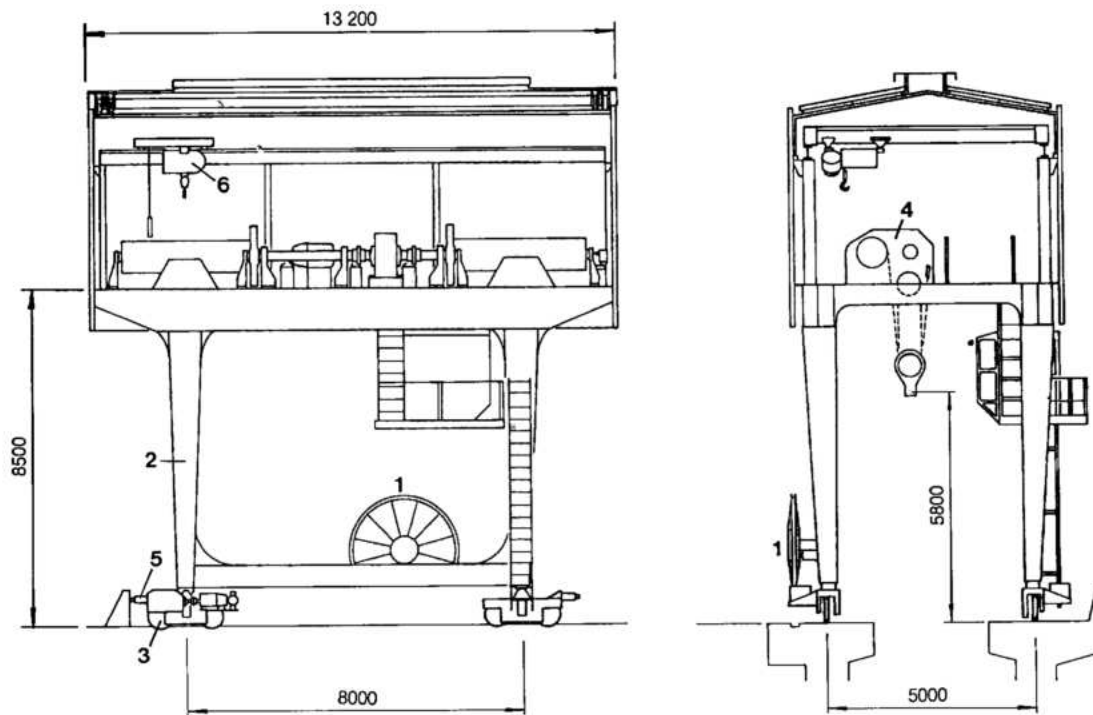
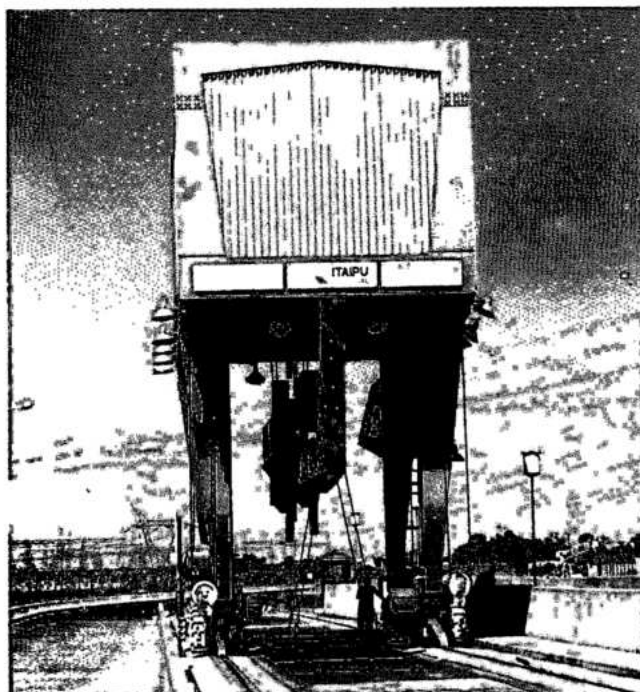


Fig. 8.30 Spillway gantry crane arrangement

- | | | |
|--------------------|----------------------|---------------------|
| 1 Rolling cables | 3 Travel mechanism | 5 Hydraulic buffer |
| 2 Gantry crane leg | 4 Hoisting mechanism | 6 Maintenance hoist |



Spillway gantry crane

ladder from the control cabin which is under the steel platform. The control cabin is reached by a caged ladder attached to the upstream right leg. The steel platform was specified to support 5000 N/m^2 . Pipes installed in the crane legs drain rain water from the roof of the machine enclosure to El. 225.

Travel mechanism. The crane moves on four wheeled trolleys, one attached to each leg, the upstream and downstream right side trolleys being motorized, see Fig. 8.31. Each trolley has two wheels, a hydraulic buffer and is pin connected to the leg of the crane. The two motorized trolleys are also equipped with motor, gear reducer and electric/hydraulic brake. The electric /hydraulic brake has dual actuation, one by pressurized oil supplied from a foot pedal operated master cylinder in the control cabin and the other by solenoids. The former is used for slowing the crane and the latter for automatic emergency stops and temporary parking. The motor is stepless speed controlled by slipring connected variable rotor resistances, electronically modulated. When in position, the gantry crane is secured in place by two handwheel operated locking mechanisms which grip the crane rail, see Fig. 8.32.

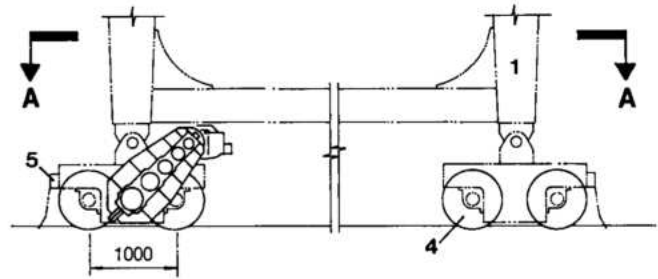


Fig. 8.31 Gantry crane travel mechanism

- 1 Gantry crane leg
- 2 Gear reducer
- 3 Motor
- 4 Wheel
- 5 Hydraulic buffer

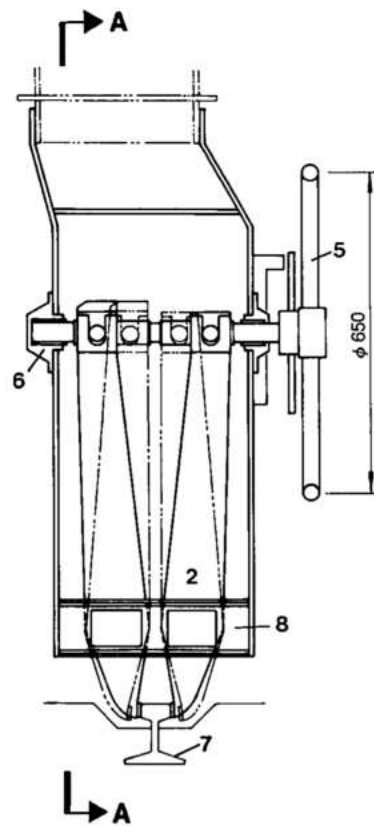
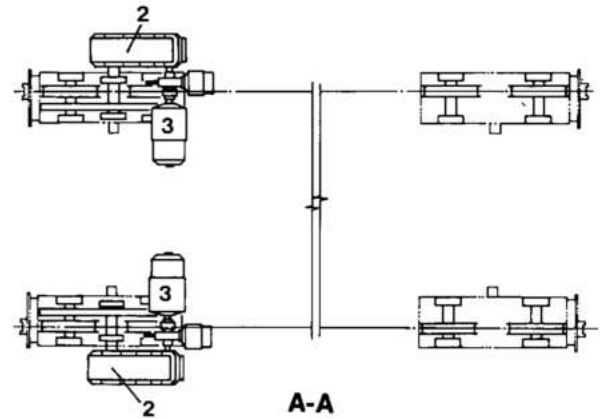
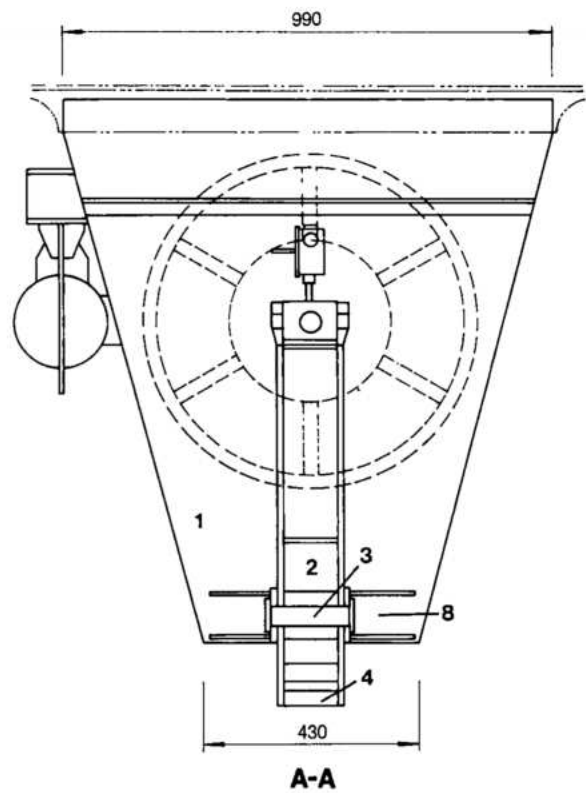


Fig. 8.32 Gantry crane locking mechanism

- 1 Grippers box
- 2 Gripper
- 3 Guide pin
- 4 Gripping jaw
- 5 Hand wheel
- 6 Bearing
- 7 Rail
- 8 Guides



Hoisting mechanism. The stoplog lifting beam is permanently attached with stainless steel pins to the two pulley blocks of the hoisting mechanism. A steel lifting cable runs through the pulley block passing around the intermediate pulleys to the hoist drum on which it is secured. The two winch drums are synchronously rotated by an electric motor through a gear reducer, see Fig. 8.33. Two electromagnetic drum brakes act on the input shaft to the reducer and the speed of descent is controlled by a dynamic electric brake located between the motor and first brake. Stepless speed control of the motor is by slipring connected variable rotor resistances, electronically modulated. The motor and dynamic brake can be removed with the load maintained in position by the magnetic brakes. The hoisting mechanism has the following safety features:

- Overload device which is activated and stops the hoist at 10% to 20% above nominal load in the raising direction.
- Loose cable device which stops the hoist in the lowering direction.
- Limit switch which stops the hoist when the pulley blocks rise above an upper limit.

- Limit switches controlling the upper and lower positions of the stoplog lifting beam.
- Overvelocity switches which activate the brakes.

A 29.4 kN electric motor driven hoist attached to the structure of the cabin is used for maintenance of the crane hoisting mechanism. Travel of the maintenance hoist is manual.

The gantry crane used to handle the spillway stoplogs and associated hatch covers was supplied by Villares S.A. - Brazil.

SPILLWAY STOPLOGS AND LIFTING BEAM

There are two sets of stoplogs to serve the fourteen spillway gates. Stoplogs are used to isolate the spillway gate from the reservoir when the gate needs to be repaired, maintained or inspected. An assumption was that no more than two gates would need to be isolated at the same time. Each stoplog comprises six identical panels, see Fig. 8.34. These panels, when not in use, are individually stored in a stoplog slot, held by a retractable support. Design was in accordance with DIN 19704, DIN 4114 and

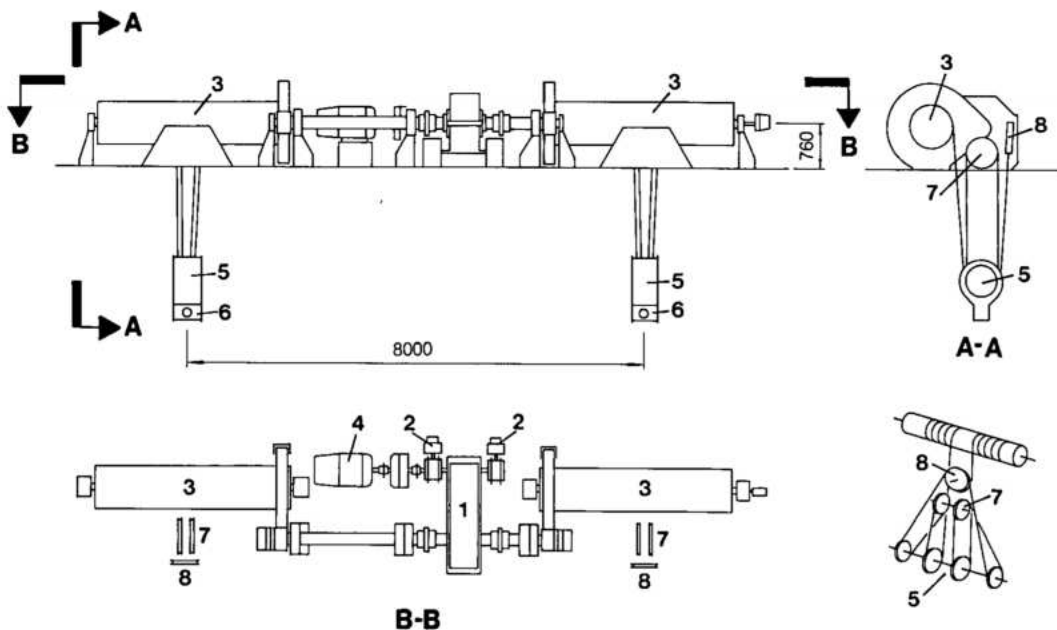


Fig. 8.33 Gantry crane hoisting mechanism

- | | |
|-----------------|--------------------------------|
| 1 Gear reducer | 5 Pulley block |
| 2 Dynamic brake | 6 Pin for stoplog lifting beam |
| 3 Hoist drum | 7 Transverse pulley |
| 4 Motor | 8 Lateral pulley |

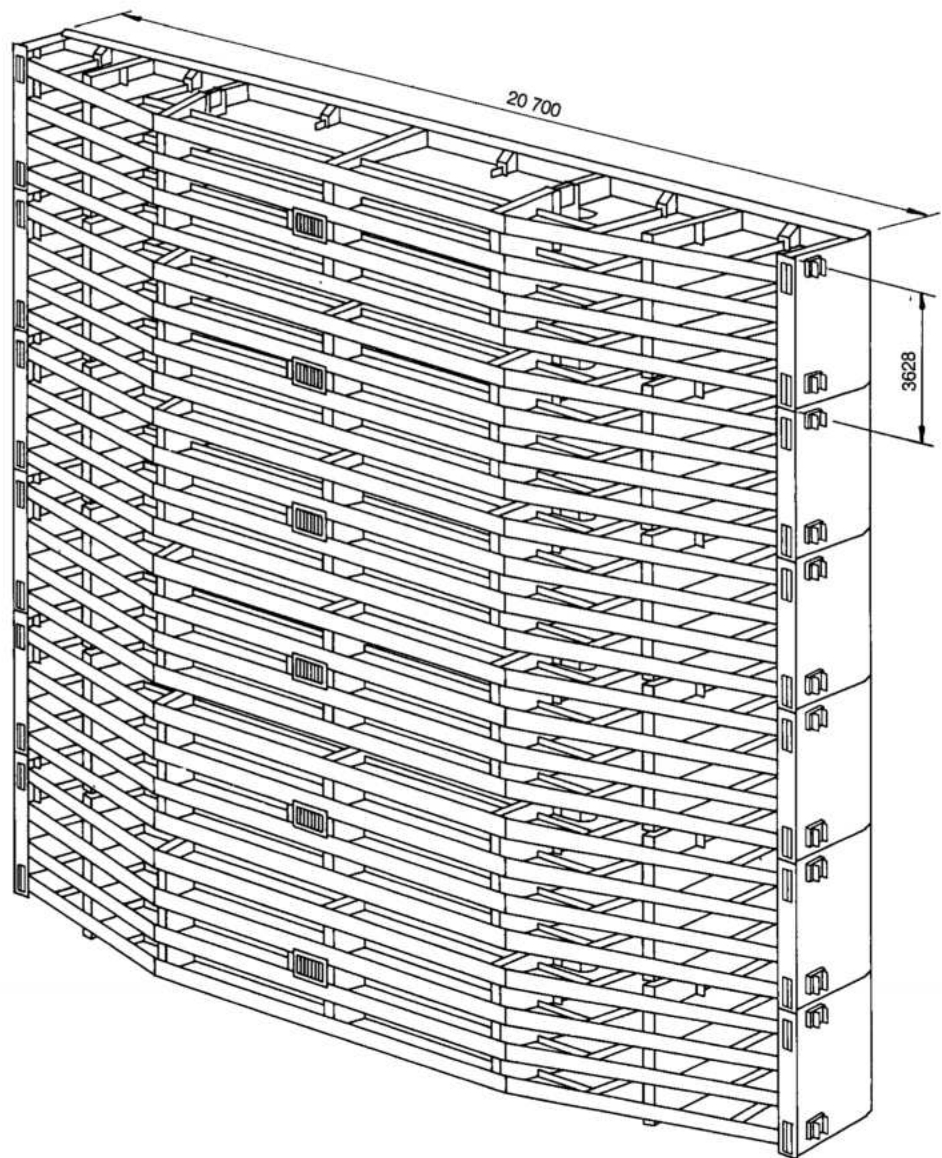


Fig. 8.34 Spillway stoplog arrangement

DIN 4101 with the bottom seal specified at El. 199.58 and upstream water levels of El. 221.18 "normal" and El. 223 "exceptional". Deployment of the stoplogs is made under balanced water conditions. Each panel has a by-pass valve, the valve of the top element being actuated by the lifting beam, thus watering the space between stoplog and spillway gate automatically. Dewatering of this space is done by slightly opening the spillway gate. All parts were designed with a 2 mm corrosion allowance, the minimum specified plate thickness being 9.5 mm.

In addition to the normal structural compliance, it was specified that the lifting beam and elements of the stoplogs support a load of 1962 kN with stresses not exceeding 75% yield.

The basic characteristics of the stoplogs and lifting beam are as follows:

Width of stoplog slot	20 m
Height of complete stoplog (six panels)	21.6 m
Weight of complete stoplog	3828 kN
Weight of lifting beam	119.2 kN

The general arrangement of a complete spillway stoplog is shown in perspective in Fig. 8.34. Each panel, see Fig. 8.35, is made from welded mild steel plate and has music note side seals on the downstream face and rectangular bottom seals,

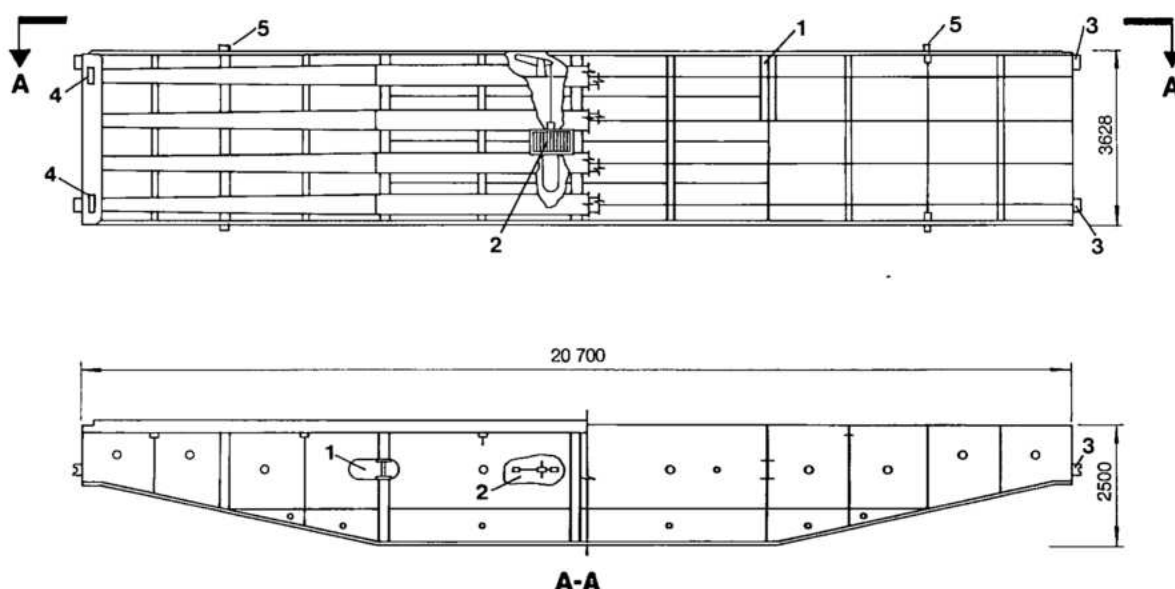


Fig. 8.35 Detail of stoplog panels

- 1 Lifting lug
- 2 By pass valve
- 3 Side guides
- 4 Retaining spring
- 5 Location pin

whose retaining plates are held by stainless steel bolts. Seal compression is 5 mm. Details of the 254 mm by-pass valve are shown in Fig. 8.36.

Each panel has two guides on each side to ensure lateral alignment when being deployed and two pins on the lower face which engage bushings on the upper face to ensure accurate coupling between two stacked panels. The two hooks of the lifting beam engage pins on the upper face of each panel.

Details of the lifting beam are shown in Fig. 8.37. The counterweight of the grappling mechanism is placed in one of two positions, engage and disengage, depending on the operation to be made. Alignment of the beam in the stoplog slot is maintained by the two wheels on either side.

Lateral guides, side and bottom seal plates were embedded in blockouts left in first stage concrete, steel plates being provided in the first stage concrete to facilitate erection. Parts in contact with seals have a stainless steel overlay.

The spillway stoplogs and lifting beam were supplied by a Consortium composed of the Companies Badoni-ATB/Ishibras/Coemsa, Brazil.

AUXILIARY EQUIPMENT

Ventilation

The ventilation system for the equipment rooms of the spillway comprises air admission for the diesel and battery room and air exhaust for the battery room, kitchen, toilets and sewage treatment plant. Fans for the air admission system are located in the ventilation room at El. 214.9. Ambient air drawn through an outside grill is filtered to 10 micra before entering the room. The air from the exhaust systems is discharged into the atmosphere through the equipment access room at El. 219.8.

Sewage

The spillway sewage treatment plant has a capacity of 3850 l/d, which is designed to accommodate fifty-five operation and maintenance personnel plus visitors to the future observation tower. Sewage from the various toilets is piped to a 7.44 m³ concrete septic tank, the overflow of which is dosed with chlorine before being discharged into the river downstream.

Fig. 8.36 Details of by pass valve

- 1 Lever
- 2 Push rod
- 3 Spring
- 4 Inlet grid
- 5 Valve seat

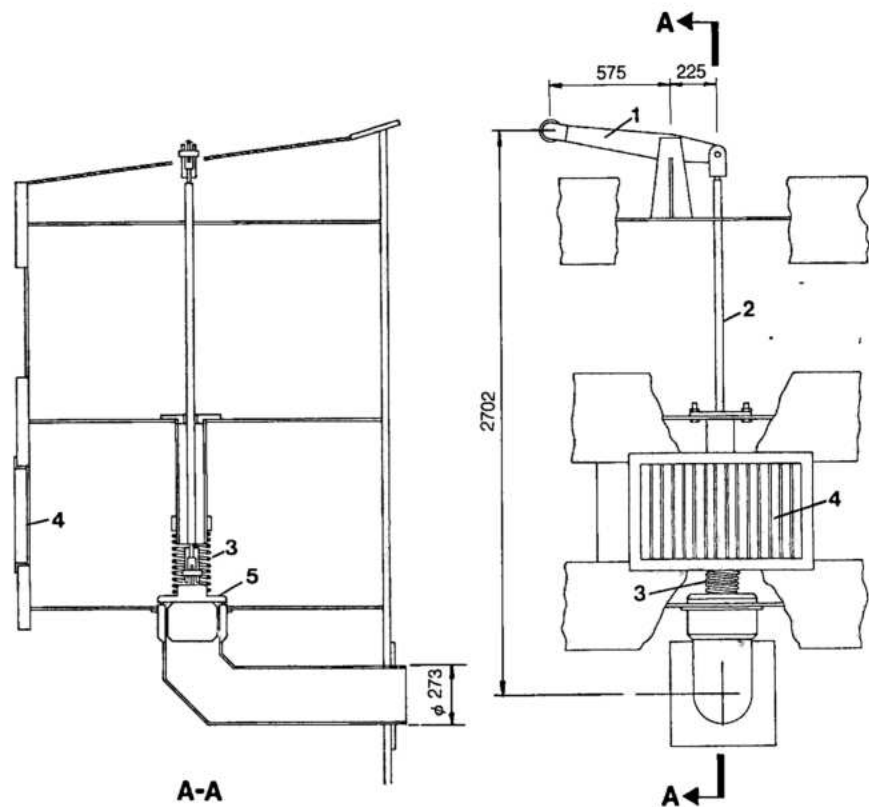
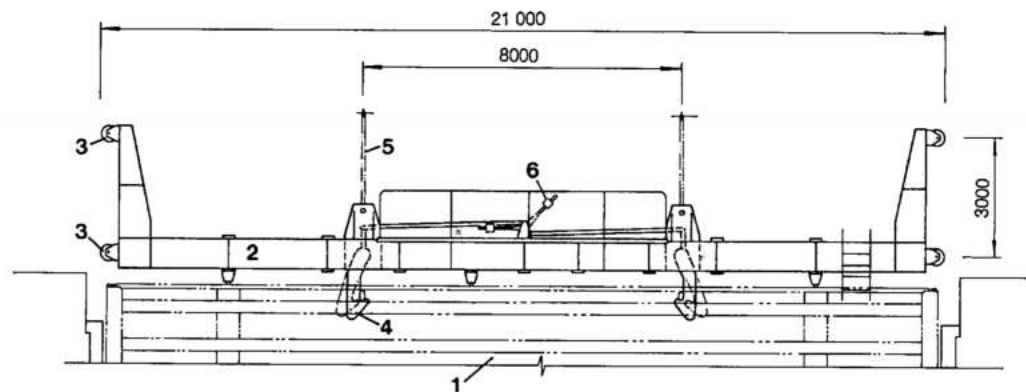


Fig. 8.37 Details of lifting beam

- 1 Stoplog
- 2 Lifting beam
- 3 Guide wheels
- 4 Hook
- 5 Cable of gantry crane
- 6 Counterweight



Potable water

Potable water piped from the treatment plant ETA 1 located in the main dam, see Chapter 10, fills an 8 m^3 holding tank located in block A15 of the spillway at El. 214.9. From there it is pumped to an 8 m^3 holding tank in the base of the observation tower at El. 238.1, as well as being piped by gravity to the rooms below. The holding tank in the observation tower supplies water to the rooms at El. 214.9 and above, as well as to the right bank substation.

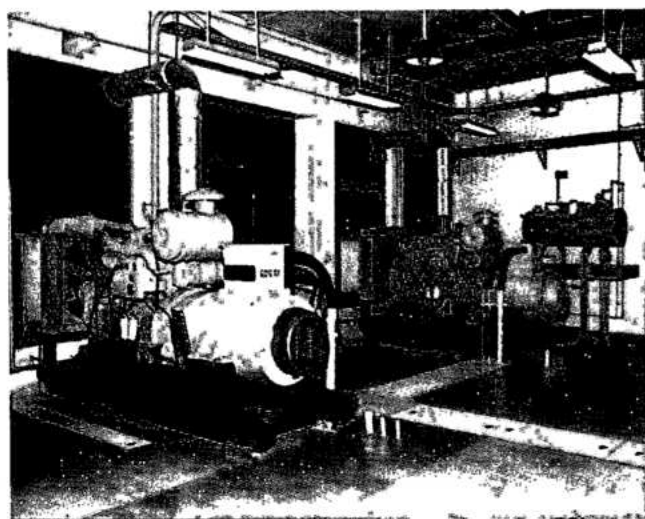
POWER SUPPLIES

The requirement to be able to control the spillway gates under all conditions to ensure the safety of the project, placed the loads for the area in a Class I category. This resulted in the 50 Hz auxiliary power being supplied by two separately sourced 13.8 kV feeders from the powerhouse, backed by two local emergency diesel generating units. The 125 V dc system is supplied by two independent battery and charger groups.

50 Hz auxiliary power

The spillway substation (QK), located at El. 214.9 in block A15, consists of two 500 kVA dry type transformers, 13.8 kV-460 V (delta star), each connected through a low voltage circuit breaker to a 460 V bus section. The two bus sections can be connected together through a bus-tie circuit breaker. Each bus section can also be supplied by a 200 kVA diesel generator located at El. 219.8 in block A15. A simplified single line arrangement is shown in Fig. 8.38.

In normal operation, both 13.8 kV sources are available and both transformers are energized,



Diesel generating units

supplying their associated 460 V bus section with the tie breaker open. In the event of failure of one source the secondary (460 V) breaker opens and the tie breaker closes automatically. In the event of failure of both sources the secondary (460 V) breakers open and the diesel generator is started to supply the required loads.

125 V dc system

The system, located at El. 214.9 in block A15, consists of two chargers and two sets of batteries 96 Ah each and a distribution panel. Either charger/battery group is capable of supplying the required loads. Suitable switching is supplied to allow high reliability and availability during operation, maintenance and emergencies.

PROTECTION, CONTROL, INSTRUMENTATION

Extensive use of local annunciation/alarm units has been made for each of the main auxiliary service groups (i.e. 50 Hz, 125 V dc, and diesel generators). All critical values of voltage and temperature are monitored along with the status of the main circuit breakers and protection.

Because the powerhouse units were installed in stages, control of the spillway was duplicated in the local control room of generating units 1 and 2, the central control room of the plant and in the SCADA system, as each became available, see Chapter 14.

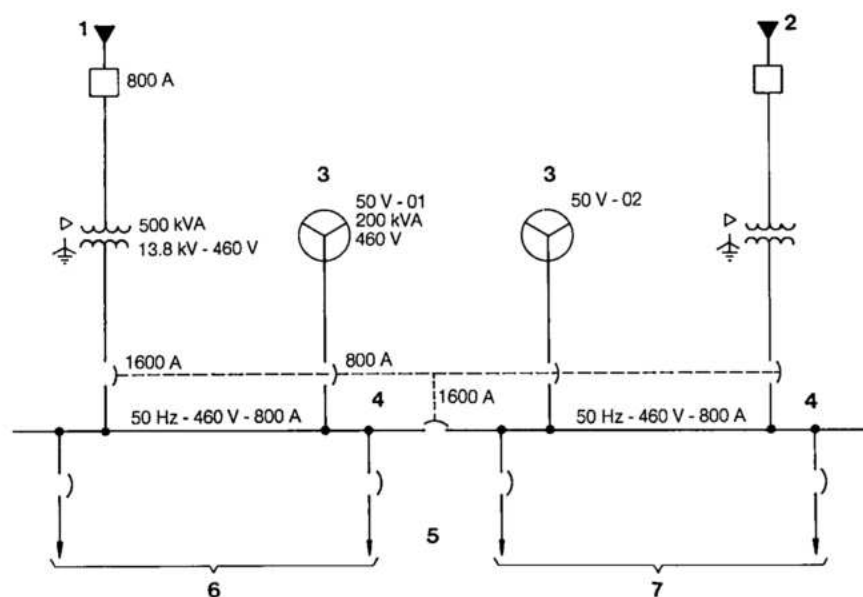


Fig. 8.38 Spillway 50 Hz auxiliary power

- 1 From powerhouse 13.8 kV switchgear QP-01
- 2 From powerhouse 13.8 kV switchgear QP-02
- 3 Diesel set
- 4 Class I pads
- 5 Spillway substation QK
- 6 Sixteen feeders
- 7 Fifteen feeders

Fire detection

The area has an extensive fire detection system utilizing detectors of combustion products (ionization), rate of rise of temperature, and absolute temperature. These work through a fire detection cabinet to give audiovisual alarms and actuate local and remote annunciation. They also act to shut-down the ventilation system in the area affected.

OPERATING EXPERIENCE

FILLING OF THE RESERVOIR AND MAXIMUM RECORDED FLOOD

During the reservoir filling period releases at Jupia, the next upstream dam, and the Parana river inflow into Itaipu reservoir were communicated to Itaipu. Also data from an automatic water level recording gauge on the Iguaçu river at Capanema were telemetered to Itaipu. This had the dual purpose of determining the amount of gate openings required to pass a targeted flow, and to throttle back reservoir outflows when Iguaçu floods occurred, thus minimizing high tailwaters at Itaipu and ensuring that total flow of the Paraná below the confluence of the Iguaçu did not exceed a predetermined amount.

On October 13, 1982, see Chapter 6, the diversion gates were completely closed and the Itaipu reservoir filled in three stages as follows:

Stage I. From river water level at El. 109 to reservoir at El. 205.8, without making any releases from Itaipu. A minimum flow of 5000 m³/s was maintained downstream in the Paraná river by releases from

reservoirs on the Iguaçu river. This stage was completed in only 15 days, the rapid first filling being an integral part of the diversion closure plan, see Chapter 6.

Stage II. From October 27, 1982 until April 1984, spillway gate operation was such as to allow the reservoir to rise to El. 210, and then fluctuate up to El. 217, by balancing the inflows and outflows.

Stage III. Final filling of the reservoir up to the normal maximum water level at El. 220. During this period, the maximum rate of rise in reservoir level was limited by operation of the spillway gates to 1 m/day.

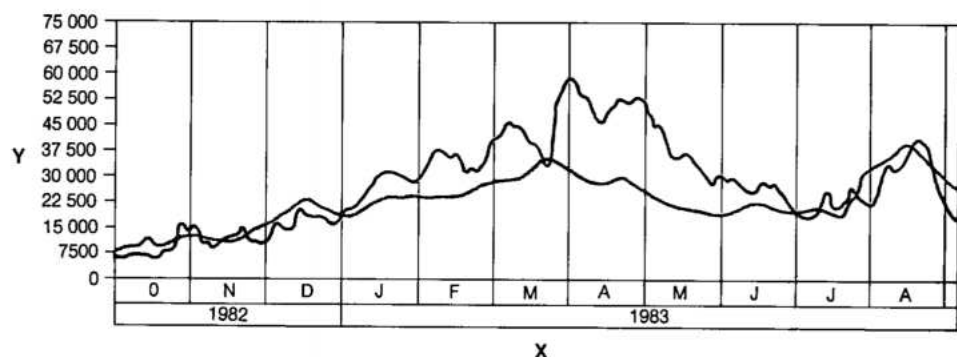
The two highest flood peaks of the 62 year record at Guaíra occurred during 1982-83, see Fig. 8.39. The spillway gates were fully opened at the end of November 1982, when inflow reached 20 000 m³/s, and were kept open through August 1983, when the inflows receded to about 15 000 m³/s. During this 9 month period, flows over the spillway were controlled, except for a brief period at the peak flows. At the end of February 1983, some four months into the continuous operation of the spillway and shortly after the first high peak discharge of 36 200 m³/s had passed, the gates for each chute were closed for about 1 hour for inspection of the chute. After that, the gates were fully opened again until August 1983. During this period, the spillway performed satisfactorily. The 40 000 m³/s flood peak of record was reduced to a routed outflow of 38 000 m³/s, and delayed about two days. The fluctuations of the reservoir water level during the 9 month flood period were kept within 3 m.

RE-EVALUATION OF SPILLWAY DESIGN FLOOD

Itaipu experienced continuous high Paraná river flows from October 1982 through September 1983. The 1982-83 average annual rainfall over the

Fig. 8.39 Flood and PMF hydrograph of Guaíra (pattern C)

Y Discharge (m³/s)
X Month and year
— Simulated PMF hydrograph at Guaíra (without Ilha Grande reservoir)
— 1982-83 flood



820 000 km² watershed was 2230 mm, about twice the long-term basin average. In light of this occurrence, a comprehensive review of the spillway design flood was made.

Daily discharges at Guaíra exceeded 20 000 m³/s from November 23, 1982 until July 1983, a period of 238 days. There were two unprecedented flood peaks: a maximum daily discharge of 36 200 m³/s on February 21, 1983; and the highest historic record of 40 000 m³/s on June 15, 1983. If the two flood peaks were analyzed as single-peak events on an annual frequency basis, the February peak would have a return period of 1 in 150 years, and the July event 1 in 500 years. Frequency analyses had not been made either for the two highest recorded flood peaks occurring consecutively in the same year, or the 40 000 m³/s maximum happening in June, which is usually one of the months of lowest flows. However, their recurrence probability could be much smaller than the 1000-year frequency.

The Iguaçu river also experienced its two highest floods of record: 28 600 m³/s and 27 500 m³/s in July and September 1983, respectively. These were very high discharges from the Iguaçu basin (68 000 km²), compared with 40 000 m³/s in the Itaipu watershed (820 000 km²). The floods from both the Paraná and the Iguaçu rivers caused unusually high tailwater levels at Itaipu during the entire 1982-83 water year.

Due to these very high floods in the two river systems, a re-evaluation of the spillway design flood was made by including all the available rainfall data and by extending the flood simulation over a period longer than the seven months used in the previous studies. This PMF update followed the original procedures and methodology and used the previously developed computer programs discussed in Chapter 2.

Three meteorologically possible PMF sequences of a 12 month period were used in developing the inflow hydrographs. Pattern A contained the seven

months from October through April used in the earlier studies and included March 1928 data. The design sequence was extended to include May through September, forming a complete water year. Patterns B and C were the same as pattern A, except for March, where 1982 and 1983 data were substituted for March 1928. For all three patterns the maximum peak inflow of 72 000 m³/s occurred in February, as in the original PMF. The second highest peak inflow was in March for all three rainfall patterns. Pattern C, with March 1983 rainfall data, produced a higher peak inflow than patterns A and B, see Fig. 8.39 and Table 8.1. Therefore, the 12 month hydrograph computed from pattern C rainfall was adopted as the new Itaipu PMF. After routing the new PMF through the reservoir, the inflow at the spillway was essentially the same as that of the spillway design flood, confirming the adequacy of the spillway to safely handle the updated PMF.

HYDRAULIC PERFORMANCE OF THE SPILLWAY

Overall performance

As anticipated during design, all chutes of the spillway operated almost continuously during the first 3 years after filling of the reservoir. Thereafter, for the next 3 years, one or two chutes were in continuous operation. It was estimated that during the first 5 years of operation the Itaipu spillway had passed the equivalent of 500 000 GWh of energy, and more water than many major spillways pass in 50 years.

Overall hydraulic performance of the spillway including handling the unprecedented floods of 1982-83, was entirely satisfactory and essentially flawless.

Crest and piers

For all discharges up to 38 000 m³/s, the flow over the crest with gates fully open was smooth. Hardly any vibrations could be felt while standing on the piers.

Table 8.1 Average basin rainfall (mm) of the 12-month probable maximum precipitation (PMP) sequence

	Oct	Nov	Dec	Jan	Feb	Mar	Apr	May	Jun	Jul	Aug	Sep
Pattern A	257	284	378	364	295	247	191	202	108	144	100	188
Year	1930	1939	1926	1951	1964	1928	1956	1983	1983	1957	1957	1957
Pattern B	(same for all patterns)					271	(same for all patterns)					
Year	(same for all patterns)					1982	(same for all patterns)					
Pattern C (*)	(same for all patterns)					222	(same for all patterns)					
Year	(same for all patterns)					1983	(same for all patterns)					

* See simulated hydrograph of pattern C in Fig. 8.39

There was turbulence downstream of the square ends of the piers when the separated flows from adjoining bays intermingled. As expected, a considerable amount of air was entrained in the water during the turbulent merger.

After 8 years of operation, no cavitation damage or erosion had occurred either along the piers, or at their downstream faces, or in the adjoining surface of the crest or the chute.

Chutes and flip buckets

Flow profiles in the chutes and along the guide walls at all discharges experienced, were comparable to those predicted by the hydraulic model tests. There were noticeable longitudinal rollers and submerged mini jumps or waves along the middle of the chutes, with the water surface relatively smooth before entering the flip buckets. Even at flows above 30 000 m³/s, there was no splashing over the guide walls or any tendency to climb up the walls due to cross flows. When the gates were first opened, the hydraulic jump formed in each bucket was swept away within about 5 minutes when flow exceeded 3000 m³/s.

Considering the amount of energy discharged through the spillway, there was evidence of only nominal erosion of concrete surfaces. Before the first operation of the spillway in November 1982, the chutes and flip buckets were thoroughly inspected for finishing defects. Epoxy mortar was used to replace defective concrete which was chipped out. Surface irregularities were ground and polished to the allowed tolerances. The repaired areas were regularly inspected during operation. About 10% of the epoxy patches were dislodged during the first 6 months of operation and were replaced by new epoxy mortar. After 2 years of operation, including the high floods of 1983, the need for repairs was less frequent and dry pack mortar was used for patching the eroded areas. At some locations where rough mortar surfaces were observed, an epoxy-cement mix was applied to smooth them.

Some minor cracks, both longitudinal and normal to the flow, occurred in the surfaces of the chutes and flip buckets. However, after 8 years of operation the cracks had neither deteriorated nor progressed further.

With the exception of one incident, no cavitation damage such as pitting, spalling or erosion of concrete surfaces exposed to the high velocity flow had been observed after 8 years of operation. Also, at joints and cracks normal to the flow, there was no cavitation damage. The absence of cavitation damage was attributed to good hydraulic design,

the excellent finish of the surfaces, strict enforcement of quality control standards during construction and to the large amount of entrained air in the water in the chutes.

The only incidence of cavitation damage was the spalling of concrete at the downstream end of the right wall of the left chute, which was first observed in February 1983. The alignment of the face of the wall converged towards the flow. It was rectified in June 1985 by removing some concrete, making the face divergent to the flow, and providing a smooth finish. Since the repairs and modifications, no new cavitation damage had occurred.

The excellent performance of the chutes and buckets, and the lack of cavitation damage indicated that the flow was well aerated. Therefore, there was no need to introduce air from the aeration galleries by making slots in the chute slabs.

As planned, there was minimal energy dissipation within the chutes and buckets, and the river served as the principal dissipator. While scour in the river was essentially as predicted, some damage to the slopes at the toes of the buckets occurred.

Downstream slopes

The combination of high flood discharges in 1982-83 and the continuous operation of the spillway for over 3 years caused some erosion on the slopes downstream of the concrete slab which protects the toes of the flip buckets. The hydrodynamic forces produced by the jet impinging upon the river produced strong eddy currents and high waves against the right bank. The erosive action started at the base of the shotcreted area at about El.100 downstream of the left and center buckets. The loose and weathered rock blocks underlying the treated surface were progressively undercut and dislodged and the rock bolts were exposed. Downstream of the left chute, this erosive action reached some parts of the concrete slab.

The central chute was operated for a shorter period. Therefore, the erosion was less severe. The more gentle slope at this location also provided a wider protective strip. However, severe erosion occurred in the area downstream of the dividing wall between the right and central chutes. The area between the excavated rock, the rock ridge, and the natural ground slope was severely damaged up to El.115. The eroded areas with typical sections of the damaged slope and the treated areas are shown in Figs. 8.40 and 8.41.

The right bank deflected the cross-currents and the surges scoured out columnar basalt to a depth of 5 to 10 m for a length of about 100 m. Since this scour terminated about 50 m downstream of the right bucket, it did not endanger the structure.

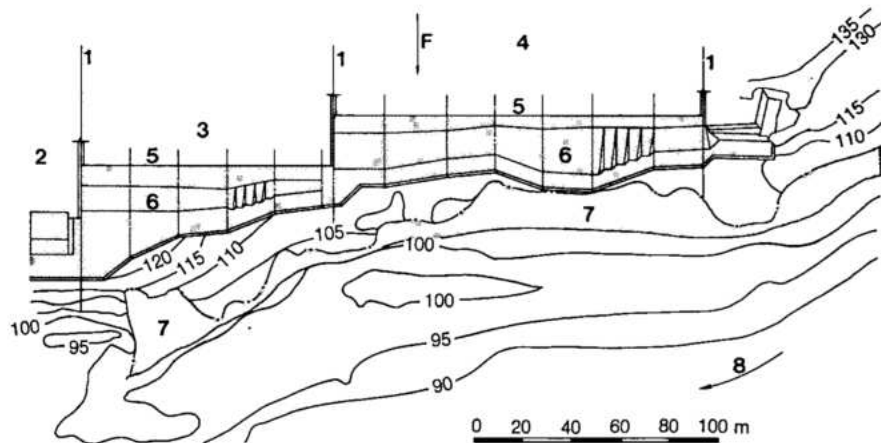


Fig. 8.40 Spillway downstream slopes eroded regions

- 1 Wall reference line
- 2 Right flip bucket
- 3 Central flip bucket
- 4 Left flip bucket
- 5 Downstream end of flip bucket
- 6 Downstream slope protection slab
- 7 Eroded regions
- 8 Paraná river
- F Flow direction

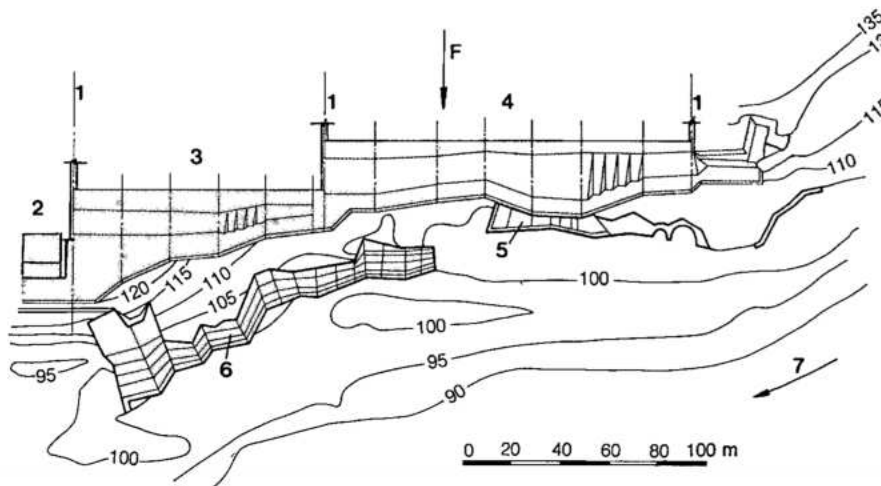


Fig. 8.41 Spillway downstream slopes protection walls

- 1 Wall reference line
- 2 Right flip bucket
- 3 Central flip bucket
- 4 Left flip bucket
- 5 Protection wall (1985)
- 6 Protection wall (1986)
- 7 Paraná river
- F Flow direction

Repair of eroded downstream slopes

The eroded downstream slope of the left chute was first detected in August 1985 during a routine inspection. Since the scoured area extended to the toe of the concrete slab, immediate remedial measures were needed to protect the slab. It was estimated that the repair work would require 30 to 45 days, when the chute would be closed and the tailwater levels maintained below El. 98. This was not easy to accomplish during the flood season because:

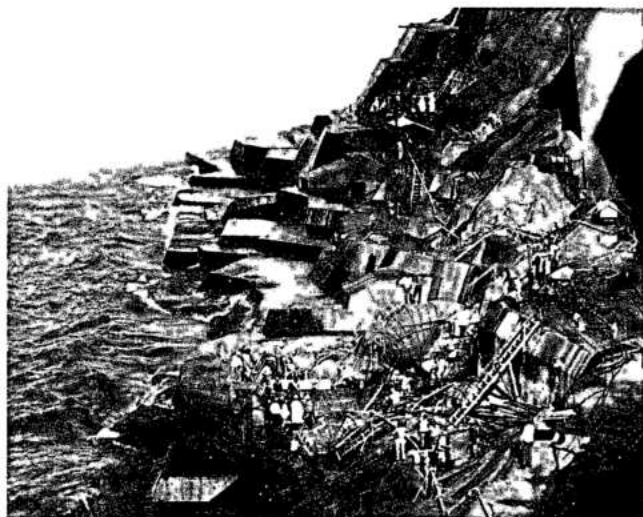
- With one chute closed, the spillway capacity would be reduced and the reservoir may rise above the maximum allowable surcharge level.
- High tailwater levels caused by flood discharges from both the Paraná and the Iguaçu rivers could occur.
- Difficulties may arise in maintaining the downstream flow fluctuations within the mandatory limits.

Repair work for the area downstream of the left chute was carried out during the low-flow season in September 1985. The reservoir was first drawn

down to El. 217 to allow for storage of an inflow of $9000 \text{ m}^3/\text{s}$ for 30 days. The left chute gates were then closed. Discharges into the central and right chutes were regulated to maintain a tailwater level of El. 98, or lower, at the spillway toe. Actual repairs took 30 days, while the entire operation, including the reservoir drawdown, lasted about 40 days.

A reinforced concrete wall, 1 m minimum thickness, was built on the eroded slope, and was anchored to the rock with 32 mm diameter, 9 m long steel anchors in a $2 \text{ m} \times 2 \text{ m}$ grid. The concrete mix had a minimum specified strength of 2.8 kN/cm^2 at 28 days, 19 mm maximum aggregate size, and water cement ratio of 0.52. It was pumped from El. 140 to El. 100 and the total volume of concrete, placed in two phases, was 3380 m^3 .

The damaged area below the central chute was discovered during the remedial work on the slope below the left chute, the damage being obscured while the left chute was in operation. During the dry season of 1986, the



Repair of eroded downstream slopes



discharge through the left chute was decreased to allow a thorough inspection of the slope below the central chute. It was found that the erosion was extensive, but it was decided that the need for repairs was not immediate. Repairs were carried out from October to December 1986, using the same procedures as for the left chute area. Work conditions at this site were extremely difficult. The adjacent left chute was always operating, creating persistent spray and strong winds, caused by negative pressure under the spillway jets together with eddy currents and rough waves in the river. A 1 m high cofferdam was built with sandbags to protect the personnel and the work area. Ropes were attached to rock bolts along the water line for safety of personnel.

STRUCTURAL PERFORMANCE OF THE SPILLWAY

MONITORING OBJECTIVES AND INSTRUMENTATION

To assess the stability and safety of the principal structures of the spillway, namely the gated crest dam, the three chutes and the discharge buckets, the following items were monitored by instruments installed during construction:

- Crest structure: deflections, seepage, foundation settlement and deformations, joint openings, hydraulic uplift, and temperatures and stresses in concrete.

- Chutes: piezometric (uplift) pressures, seepage flow from contact and drilled drains under the slab and into the galleries, and joint openings.
- Buckets and downstream protection slabs: piezometric pressures under the buckets, seepage into galleries, opening of joints between bucket and chute slab and walls, and deformation of foundations under the bucket and downstream protection slabs.

The walls and ceiling of the highway tunnel passing under the spillway chute were regularly inspected, and seepage through the ceiling measured. Also, stresses in the beams supporting the post-tensioned anchorages for the trunnions of the radial gates were measured by embedded stressmeters.

Typical arrangements of instruments installed in the crest structure and the flip buckets are shown in Figs. 8.42 and 8.43, respectively. The following instruments were initially installed in the spillway:

Piezometers	72
Multiple extensometers	
Under crest dam	8
Under buckets	4
Direct pendulums	2
Embedded pins for removable joint meters	32
Embedded thermometers	10
Rosettes of strainmeters	2
Embedded stressmeters	2
Bench marks	2
Discharge weir	1

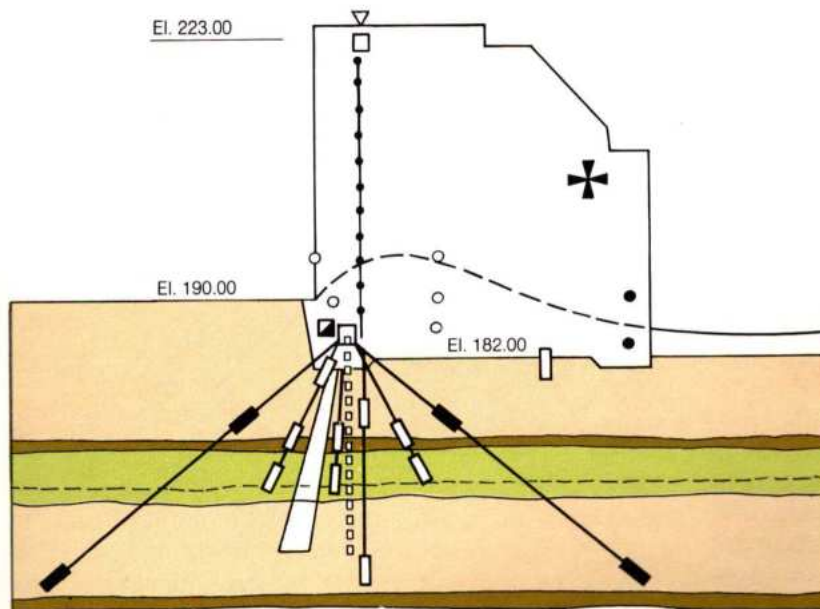


Fig. 8.42 Spillway crest structure typical instrumentation arrangement

- Grout curtain
- Piezometer
- Multiple extensometer
- ▣ Group of removable pins for jointmeter
- Rosette of strainmeters
- ⊕ Stressmeter
- Thermometer
- ⬮ Pendulum
- ▽ Bench mark
- Drainage holes
- Basalt
- Breccia
- Vesicular amygdalite
- Joint D

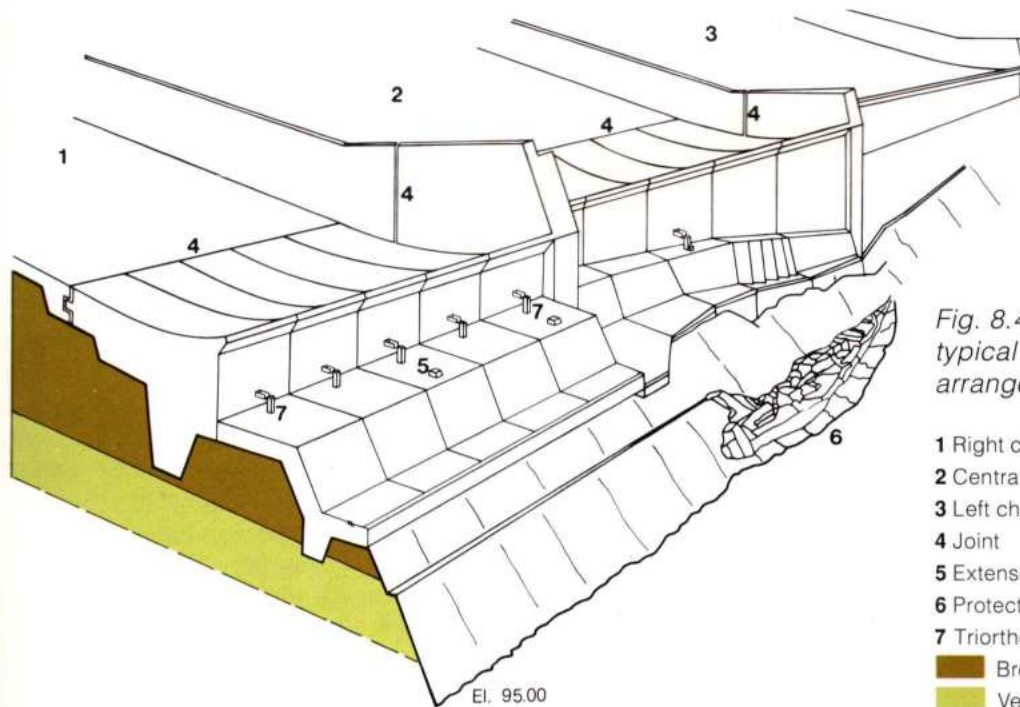


Fig. 8.43 Spillway bucket typical instrumentation arrangement - isometric view

- 1 Right chute
- 2 Central chute
- 3 Left chute
- 4 Joint
- 5 Extensometers
- 6 Protection walls of eroded area
- 7 Triorthogonal markers
- Breccia
- Vesicular amygdalite

While most of the instruments were installed during construction, two multiple extensometers were installed in the protection slabs and under the right and central buckets in 1987. At the same time, pairs of pins were installed across various joints of the same buckets.

BEHAVIOR OF THE CREST STRUCTURE AND FOUNDATIONS

Settlement and deformations

Foundation settlement about one month after first filling of the reservoir and with the spillway gates closed, averaged 7 mm. The settlement was more pronounced under the higher blocks towards the left. Over the next 5 years, foundation settlement fluctuated, increasing in summer and with some reduction in winter with an eventual increase to about 8.5 mm. These settlement values were obtained by the comprehensive geodesic surveys, and were mostly due to the crustal settlement under the weight of the reservoir.

Deformations in the upper 30 m of the foundation, relative to the structure, were measured by multiple extensometers, see Fig. 8.42, located under a central and the two end blocks of the spillway crest dam. About 1 month after the first filling of the reservoir, maximum lateral deformation in the downstream direction and the settlement measured only 0.1 mm and 0.07 mm, respectively. After 5 years of operation, with the reservoir level between El. 210 and El. 219.6, discharge ranging from 8 000 m³/s to 38 000 m³/s, and one to three chutes operating, foundation deformations had stabilized to the following:

Lateral deformation (downstream)	0.15 – 0.30 mm
Settlement	0.02 – 0.07 mm

This confirmed that the structure and the foundations functioned integrally and elastically.

Uplift pressures and seepage

Uplift pressures were measured by piezometers located in the concrete-rock contact, in the upper 10 to 15 m of the breccia foundation, in the contact between two breccias, and at a joint 20 to 25 m below the structure. Piezometers were located under eight spillway blocks, upstream of the grout curtain, between the grout and drainage curtains and downstream of the line of drains.

Within 6 months after first reservoir filling, uplift pressures at the concrete-rock contact had stabilized as follows:

Location	Average uplift pressure (% hydrostatic head)	
	Actual (1987)	Design limit
Upstream of the grout curtain	77	95
Between the grout and drainage curtain	20	50
3 m downstream of the drainage curtain	12	37
25 m downstream of the drainage curtain	10	22

Upstream of the grout curtain, uplift pressures at the foundation contact fluctuated with the reservoir level; but downstream of the curtain, the fluctuations were seasonal and less than 1%.

Uplift pressures in the joints or contacts, 10 to 25 m below the structure, took about 4 years to stabilize. Since some of these deeper foundation features daylighted under the chutes, where they were intercepted by drains or galleries under the slabs, pore pressures in these joints were spread over an area wider than the base of the crest structure. In joint D, which is in breccia about 18 m below the structure and was not intercepted by either the grout or the drainage curtain, the average stable uplift pressure at the axis of the dam was 33% of the hydrostatic head.

Seepage flow from the 20 m deep drilled foundation drains into the longitudinal gallery of the crest structure peaked at about 200 l/min within 2 months after first filling of the reservoir. Eight months later, with nearly constant reservoir level and steady uplift pressures, the flow had reduced to 70 l/min. Over the next 4 years, when the reservoir level was raised about 3 m to the normal maximum, the seepage discharge was 75 l/min, and essentially constant.

Structural deflections

Before reservoir filling, the pendulums installed in the middle block and the left end block showed that the completed structure was deflecting upstream in summer and downstream in winter. In the direction of flow, the annual range of deflection at the top of the structure was 0.8 to 1.2 mm upstream; in the axial direction, the range was 0.4 to 1.3 mm towards the left.

About 30 days after reservoir filling, with all spillway gates open, there was a slow trend for reversal of deflections towards the downstream and the right abutment. Since it was still summer, reservoir pressure had not fully offset the deflections caused by the rise in ambient temperatures.

During the next year, changes in deflections were seasonal due to temperature changes and were not affected by the closure or opening of the gates. Average seasonal deflections of the top of the structure for 5 years of operation were:

In direction of flow

Block	Deflections (mm)		
	Upstream	Downstream	Amplitude
Middle	0.5	- 2.0	2.5
Left end	0.6	- 1.5	2.1

In axial direction

Block	Left	Right	Amplitude
Middle	- 0.6	0.2	0.8
Left end	- 3.3	- 0.1	3.2

The amplitude of cyclic transverse deflections was about 20% higher for the central block compared to the left end block, which is partly explained by the greater rigidity of the latter in the axial direction. However, the axial amplitude for the left end block was 4 times that for the central block, because it is exposed to solar radiation and air over a much greater area than the central block.

Average body temperatures in the crest structure stabilized at 25°C about 6 months after placement of concrete; thereafter, the seasonal fluctuations were about $\pm 2^\circ\text{C}$. The effect of thermal stability was reflected in the seasonal fluctuation of ± 0.25 mm in opening of the smooth transverse contraction joints between the blocks.

Magnitude of the deflections and joint openings were as anticipated. Since the differential deflections in both planes between adjoining blocks were very small, no difficulties were encountered in raising or closing the radial gates.

Stresses in the crest structure

Near the gate sill or crown of the ogee crest, post construction stresses were tensile in all directions, with a tendency to increase in winter. After reservoir filling, the stresses showed an average fluctuation of about 150 N/cm²; the vertical stresses peaking at about 50 N/cm² compressive at the end of summer, and about 150 N/cm² tensile in winter. The transverse horizontal stresses were very similar to the vertical stresses; but the longitudinal stresses continued to be tensile, from 100 to 250 N/cm² for 5 years of operation.

Tensile stresses near the surface of the overflow crest were partly caused by the complex transfer of loads from the pier to the massive structure and partly reflect the ambient temperature changes. Because of heavy steel reinforcement provided near the surface, tensile stresses did not cause any cracking in the concrete.

Stresses in the structure near the foundation and under the downstream one-third of the pier, as measured by a rosette of five strainmeters in the central block, were also tensile at the completion of construction. These were attributed to the rapid cooling of the concrete. After the reservoir was filled and all spillway gates opened, and for 8 years thereafter, the stresses in N/cm² were as follows:

Vertical, σ_3	20 - 80	Tensile
Inclined 45° \rightarrow , σ_4	0 - 50	Compressive
Inclined 45° \leftarrow , σ_2	100 - 120	Tensile
Longitudinal, horizontal, σ_5	50 - 80	Tensile

Seasonal fluctuations of 30 to 50 N/cm² were measured in the vertical and inclined stresses, with minor fluctuations in others. However, starting from July 1987, one of the coldest winters, stresses in all directions showed a substantial increase in compression, and by November 1987 and start of the summer, the total stresses in all directions were compressive 150 to 250 N/cm².

The reason for this difference in stresses is that the spillway gates in the central chute were closed November 1987 through March 1988.

Stresses in trunnion support beams

Stressmeters installed in the central and left end blocks measured the stresses in the beams supporting the gate trunnions. The beams had been in compression throughout the 8 year period of operation. However the stresses are strongly affected by ambient temperatures. The average maximum and minimum values of the measured stresses were: 320 N/cm² and 60 N/cm². The annual stress variation was consistent with the ambient temperatures, indicating that there was no relaxation in the pre-stressed anchorages and that the loads from the gates were being shared by the anchorages and the concrete without overstressing the bond.

Summary

With one or more chutes of the spillway in continuous operation for more than 8 years, performance of the gated crest structure was excellent. The foundations and the structure were functioning normally, with uplift, seepage, deformations and stresses well within safe limits.

PERFORMANCE OF SPILLWAY CHUTES AND GUIDE WALLS

Guide walls

While the deflections of, and stresses in, the four guide walls separating the chutes were not measured by instruments or planimetric surveys, periodic inspections checked the joints in the walls. No noticeable offsets in the direction of flow were observed in the joints during 8 years of operation, including those in the central walls with one chute operating and the other dry.

Chute floor slabs

The stability of the floor slabs of the chutes, which were constructed in long continuous strips of heavily reinforced concrete, could be affected if high pressures developed and separated the slab from its rock foundations. Therefore, piezometric pressures were monitored where relatively permeable joints or contacts in the foundation rock daylight under the slabs. Seepage flows from the half-round pipe drains placed on the rock surface and from some drilled drains, which is collected in the longitudinal galleries under the chutes was also measured. The three transverse contraction joints in each slab were visually inspected to check for offsets against the direction of flow.

At the roadway tunnel, where the chutes form the roof, seepage through the contraction joints was monitored. For the first eight months of operation flow through the joints which leaked into the roadway tunnel, ranged from 77 to 93 l/min. In August 1983 (winter) the contraction joints in the chute slabs were sealed with epoxy. Two months after the treatment, the leakage through joints in the slabs had reduced to 6 l/min and 6 months later it was less than 0.3 l/min. Similarly, the leakage through a contraction joint in the slab into the longitudinal gallery under the chute, just downstream of the roadway tunnel, gradually reduced after surface treatment of the joints, from a peak of 154 l/min to virtually nothing 3 months after treatment.

Between July 1987 and June 1988, foundation piezometers, located in the rock-concrete interface continued to show reduced levels of uplift. Piezometers, monitoring the foundation of central chute upstream and downstream of the road tunnel, recorded in 1988 seasonal uplift oscillations of less than 3 m.

On the left chute along the joint D, in gallery 4, piezometers showed variation in uplift in the range of 3 to 4 m. The piezometric pressures in this area stabilized about 6 months after reservoir filling. Sensitivity of uplift pressures to ambient temperatures indicated that some water was

infiltrating through fine cracks in the concrete contact. However, the uplift was not sufficient either to separate the concrete slab from the rock or to lift it by overstressing the steel dowels.

Periodic inspections of the dry chutes after prolonged operation, did not show any indication of either lifting or warping of the chute slabs. During 8 years of operation, no structural cracks had occurred in the floor slabs of the three chutes between the crest structure and the buckets. Total seepage under the chutes and the walls, collected in the galleries, was about 15 l/min.

Summary

The floor slabs of the three chutes were elastically bonded to the foundation rock. There was no separation between the two and the drainage system was efficient in controlling seepage and uplift.

PERFORMANCE OF THE FLIP BUCKETS AND THE DOWNSTREAM PROTECTION SLABS

Foundation behavior

Deformations of the buckets, their foundations and of the downstream protection slabs, were monitored by:

- Multiple extensometers installed through the downstream protection slab of central and right chutes, see Fig. 8.43.
- Openings of the contraction joints between the chutes and the buckets. These measurements were made on top of the guide walls, on the floor slabs when chutes were dry, and in the galleries in the buckets.
- Openings of the joints between the buckets and the downstream protection slabs.

From the start of spillway operation in November 1982 through November 1986, when all three chutes were operating over 85% of the time, the contraction joints in the walls between the chutes opened about 0.6 mm in winter and closed in summer. Such cyclical behavior was uniformly repeated through six seasons, indicating that only very small elastic deformations of the foundation had taken place.

However, in November 1986 during summer, it was observed that the contraction joints in the walls, instead of closing, continued to open further. At that time inspection of the right and central buckets showed that the joints between the buckets and the downstream protection slabs had an opening of 10 and 3 mm, respectively. To monitor these joints, five sets of triorthogonal markers were installed, four along the width of the right chute and one in the middle of the central chute, see Fig. 8.44.

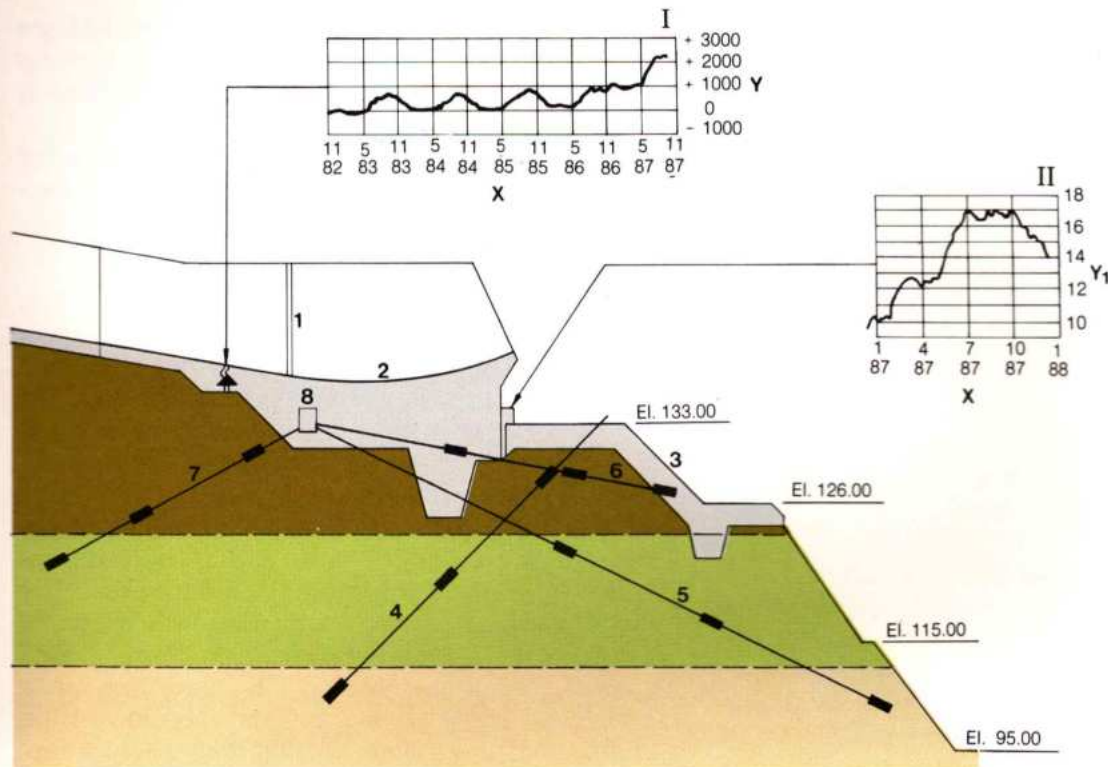


Fig. 8.44 Instrumentation of joints between buckets and protection slabs (right chute)

I Reading from strainmeters

II Reading from triorthogonal markers installed in December 87

Y Movements (10^{-3} mm) (+ opening; - closure)

Y₁ Dislocation (mm)

X Month and year

1 Opening 2.5 mm

2 Flip bucket

3 Slope protection slab

4 Extensometer initially installed in 1982

5 Installed in 1989

6 Multipoint installed in 1989

7 Extensometer installed in 1989

8 Drainage gallery

Breccia

Vesicular amygdbasalt

Dense basalt

From January to August 1987 with the right chute operating less than 20% of the time, the opening of the joints between the buckets and the downstream protection slabs reached a maximum of 17 mm for the right and 5 mm for the central chutes. Joints on top of divide walls and between the bucket and the chute slab in the galleries under the latter also showed some increase in lateral deformation in the downstream direction. During the subsequent 5 months of summer, there was about 30% reduction in all joint openings.

In June 1988, the right chute was operated at different flows with water falling on the protection slab and with the jet falling beyond into the river. Joint openings were measured after each test operation. Analysis of data obtained from the extensometers, of the geological data obtained during excavation and

from drill holes, and from the various joint opening measurements indicated the following:

- During construction of the buckets and excavation of the 30 m deep steep slope for the plunge pool downstream of the right chute, there was stress relief and relaxation of the rock ledge under the protection slabs.
- Before operation, there was a permanent lateral deformation of about 1 mm under the central right buckets.
- Relaxation and creep of the foundation rock, particularly in the breccia under the downstream protection slab, continued after the start of spillway operation. The rate of permanent deformation steadily increased during the first 4 years of operation, and then slowed down considerably during the fifth year.

- During operation at all discharges a considerable amount of water flowed into the breccia through the open joint between the bucket and the protection slab. This created substantial hydrostatic pressure in the rock and contributed to the permanent deformation of the breccia. Therefore, the joints were sealed and the breccia drained in 1989.
- Maximum permanent deformation of about 12 mm towards downstream had occurred in the ledge under the downstream protection slab. However, permanent deformation under the bucket structure was less than 3 mm.

Average permanent deformations downstream of the central and left buckets were 3 and 1 mm, respectively. It was concluded that substantial stress relief relaxation of the rock under the downstream protection slab had probably weakened the ledge in front of the right chute. Since the permanent deformations under the buckets were small, it was concluded that the stability of the buckets had not been impaired. However, progressive weakening or loss of the downstream protection slabs and their rock foundations could expose and undermine the bucket structures.

Therefore, in 1986 remedial works comprising walls and buttresses of 1 m thick concrete were constructed to support the rock face below the left and central chutes. The bathymetric surveys of the plunge pool in front of the right chute showed no major erosion or undercutting of the rock face in front of the bucket. In conclusion, it was decided to further analyze the behavior of the deeper foundation on the basis of a longer record of measurement extensometers. If the non-elastic deformations continued to increase or there was other evidence of excessive weakening of the rock ledge, remedial measures to strengthen the rock, similar to that in front of the other two chutes, would be required.

Erosion of the plunge pool

Bathymetric surveys of the plunge area were made in October 1988.

The results of the survey are shown in Fig. 8.45, the major erosion and transportation of material being as follows:

- Below the right chute the surface was eroded to El.67. Based upon the model test results it is expected that a stable depth of El. 60 will be reached in this region.
- In the triangular area downstream of the right chute there was only minor erosion. Two scour holes about 30 m deep were found in front of the right and central chutes.
- Columnar basalt blocks were found in the central area at a depth of 4 to 10 m.

- The deepest erosion was found in front of the right and central chutes. Downstream of the left chute there were deposits of eroded material comprising sand, clay and rock fragments.

In general, the erosion and transportation of material were as predicted from the model tests.

Structural performance of the buckets

The blocks of the flip buckets were designed as gravity structures of mass concrete, which were separated from each other, from the chute slabs and from the guide walls by smooth contraction joints. Steel reinforcement was provided in the surface layer of concrete to resist hydraulic traction and accommodate temperature changes without cracking.

Principal forces exerted on the bucket structures were hydrodynamic, with radial and lateral centrifugal and longitudinal components. The blocks were founded on sound rock, with a central 6 m deep key, normal to the direction flow.

Joint measurements had indicated that, while there was some permanent deformation of the foundation, there was no differential movement between the buckets and the foundation and their combined behavior was elastic. In other words, the buckets were stable, with adequate margins of safety against sliding.

After the first year of operation, a crack was detected in a block of the right bucket. It was in the middle of the block, in the direction of flow, and about 5 m long in the bucket floor. The crack was first detected in the gallery under the bucket because of minor leakage when the chute was in operation. Therefore, it was concluded that the crack extended through the 2.5 m thick concrete. The most probable cause of the crack was a cold joint in the surface 1 m thick layer of reinforced concrete. Rapid cooling of the concrete above, because of air convection through the gallery, opened the cold joint and extended it into a crack. The crack was sealed with epoxy; no other cracks had occurred in the buckets after 8 years of operation.

Summary

In spite of the extensive operation of the spillway, the structural performance of the buckets was excellent. Relaxation and substantial non-elastic deformation of the rock ledge, which had weakened the foundation of the slab downstream of the right chute, had not affected the stability of the bucket structure. Remedial treatment of the rock slopes downstream of the left and central chutes had been satisfactory; similar treatment may be necessary in the future for the area in front of the right chute.

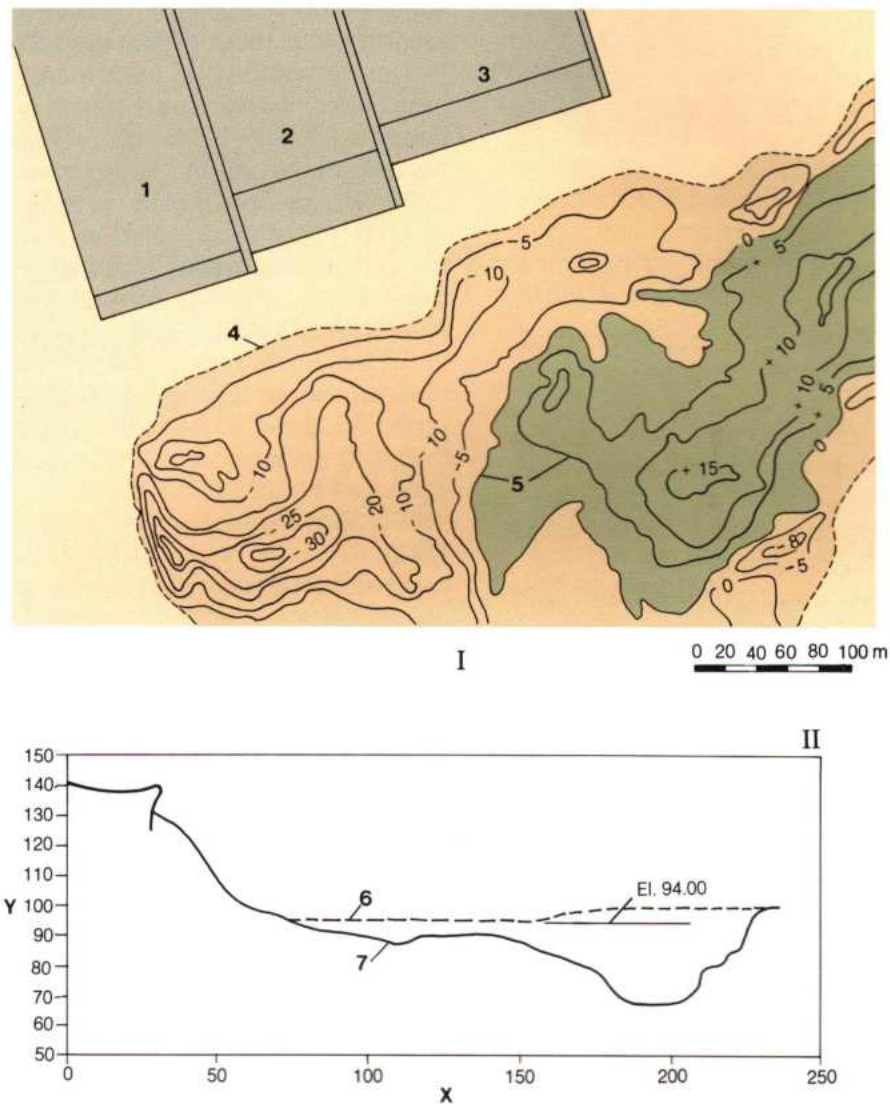


Fig. 8.45 Bathymetric survey downstream

- | | |
|--|---|
| Y Elevations (m) | 5 Comparative topography lines of erosion and sedimentation between Oct. 1982 and Oct. 1988 |
| X Distance (m) | 6 Profile measured in Oct. 1982 |
| I Plan of survey results | 7 Profile measured in Oct. 1988 |
| II Profile of eroded river bed downstream of the right chute-water level El.94 | Area of erosion |
| 1,2,3 Chutes of the spillway | Area of sedimentation |
| 4 Assumed bathymetric limit of survey | |

GEOPHYSICAL PERFORMANCE OF THE RESERVOIR

For assessing the response of the reservoir area to the rapid rate of filling, the following phenomena were of special interest:

- Rate and amount of crustal settlement due to weight of the water.
- Reservoir-related seismic activity.

CRUSTAL SETTLEMENT

Crustal settlements due to weight of reservoir water were deduced from the periodic geodetic surveys of the bench marks on the crest of the dam. Settlements of the crests of the various structures with respect to reference stations on each bank, included internal consolidation of the dam, deformation of the upper (about 20 m deep) foundation and crustal settlement.

Deformation of the upper foundation was measured by extensometers. Internal consolidation of the embankment dams, which was considerable,

was measured by settlement gauges. The settlement of the concrete dam crest as measured in the geodetic survey is due mainly to crust deformation. Settlement of the structure and foundation is about 10% of the crest settlement.

The largest crustal settlements occurred in the main river channel, where the depth of water at normal full pool level is 180 m. Fig. 8.46 shows crest settlement curves for the concrete dams, including the buttress and hollow gravity blocks and the diversion control structure, over 5 years after first filling of the reservoir. The settlements are relative to the measurement one week before the start of reservoir filling. Making allowances for the variations in internal adjustment and deformation of the upper foundations, which were affected by the type of dam and foundation configuration, the following general conclusions were drawn:

- About 50% of the crustal deformation occurred within 30 days of completion of the first reservoir filling.
- Crustal settlement had continued to increase during 5 years of operation with essentially constant reservoir level, but at a gradually slower rate. In the

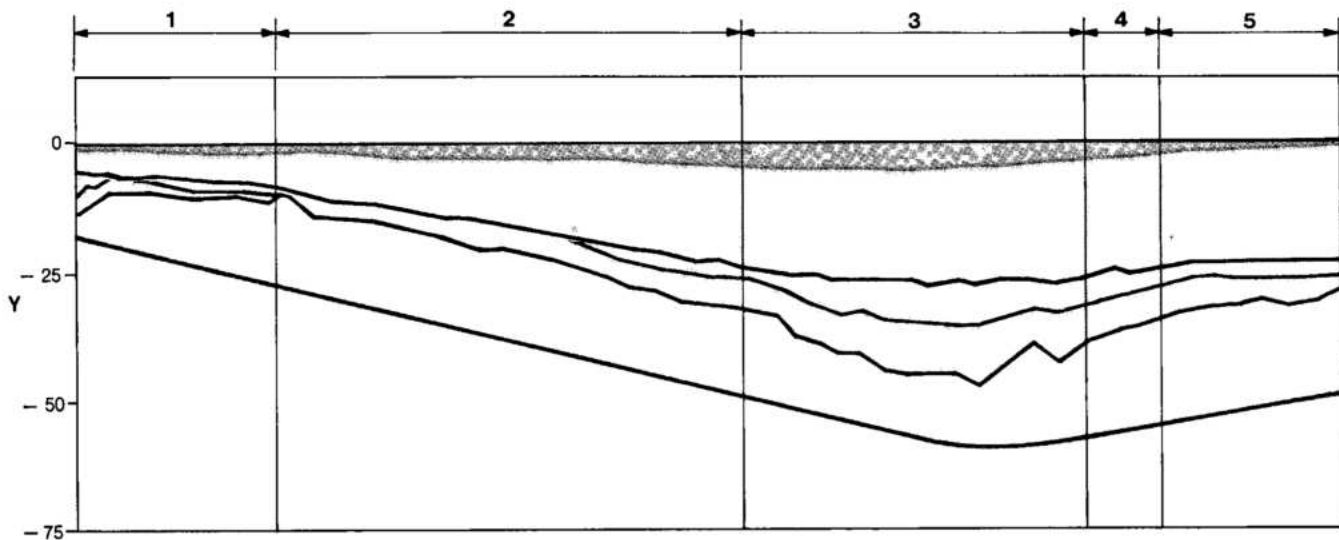


Fig. 8.46 Reservoir crustal settlement

Y Crustal settlement (mm)

1 Spillway

2 Right wing buttress dam

3 Main dam

4 Diversion structure

5 Left buttress dam

— Reference crest datum on Oct. 7, 1982

— Crest settlement on Nov. 29, 1982

— Crest settlement on May 21, 1984

— Crest settlement on Sept. 3, 1987

— Maximum theoretical crustal settlement

▨ Foundation settlement

Crustal settlement

deepest part of the reservoir the rate was about 5 mm/year, which is significantly more than the incremental deformation of the upper foundation. It also indicated that creep type deformation of the deep crust was likely to continue for several more years.

- Crustal settlements were proportional to the depth of water, varying gradually in the axial direction. Any abrupt changes in crest settlement reflected deformation of the upper foundation and not that of the crustal continuum.
- The measured crustal settlements were not the absolute values since the settlement extended towards the banks and under the permanent bench marks of reference stations.
- There were no differential crustal settlements which could occur along a deep buried fault.

Crustal settlements were also estimated assuming the reservoir bed to be a flat semi-infinite elastic medium. The formula used considers deformation directly proportional to the weight of the water and average width of the loaded area, and inversely proportional to the modulus of deformation of the rock mass. The curve of theoretical crustal settlement shown in Fig. 8.46 assumed the reservoir loaded area to be 1.5 km wide and 100 km long and the modulus of deformation of 5×10^3 kN/cm².

Comparison of the theoretically estimated values with the measured settlements indicated that there were no anomalies in the behavior of the bedrock over the entire reservoir area. It confirmed that the crustal response was elastic and within the expected range, which did not adversely affect the safety and stability of the Itaipu project structures.

the data were recorded on drums which were replaced at 1 to 2 day intervals. By the time of reservoir filling, the data were telemetered to a central receiving station in the Itaipu laboratory on the right bank near the dam.

Instrumentation data were analyzed by seismologists at the University of Brasília with weekly reports to the project management. The instruments recorded distant earthquakes, as well as vibrations due to blasting. During reservoir filling, seismologists were present at the site and reviewed the recorded data every day.

The following observations were based on data gathered by the seismographic network over a period of 8 years:

- No seismic activity originating in the reservoir area or within 200 km from the project was detected during the 18 months prior to filling of the reservoir.
- During the 15-day rapid filling of the reservoir there was no indication of micro-seismics in the reservoir area or vicinity.
- No seismic activity originating in the reservoir area or within 200 km of the project was detected during 8 years of operation.
- The accelerographs, which were set to measure accelerations greater than 0.01 g, were not triggered during reservoir filling or 8 years of operation.
- The downstream seismograph recorded vibrations due to spillway operation, particularly when the discharge exceeded 20 000 m³/s.

Continuous scientific monitoring and analysis of the instrumentation data had not only confirmed the aseismic nature of the project area, but also provided the reassurance that there was either none or an extremely low probability of reservoir induced seismicity at Itaipu.

SEISMIC MONITORING

On basis of historic earthquake records and regional geological data, the Itaipu project and reservoir area was considered to be aseismic. However, there was considerable interest in the probability of reservoir induced seismic activity similar to that experienced at some large reservoirs in various countries. An additional concern was the unknown correlation between the rapid rate of reservoir filling, crustal instability and seismic activity.

A seismic monitoring network was installed and operational about 18 months before first filling of the reservoir. The network consisted of five seismographic stations located around the reservoir, one seismograph located near the confluence of Monday and Paraná rivers about 2 km downstream of the spillway, and two accelerometers located on the crest of the dam. Initially,

HOLLOW GRAVITY AND BUTTRESS DAMS

SELECTION OF TYPE OF CONCRETE DAMS	9.3
DESIGN OF THE HOLLOW GRAVITY DAM	9.5
Shape of the Hollow Gravity Dam Blocks	9.5
Longitudinal Contraction Joints in Hollow Gravity Blocks	9.10
Transverse Contraction Joints	9.12
Concrete Characteristics	9.12
Stress and Stability Analyses Criteria	9.13
FEM Mathematical Model Studies	9.14
DESIGN OF THE BUTTRESS DAM	9.18
Buttress Block Configuration	9.19
Contraction Joints	9.19
Concrete Specifications	9.20
Stress and Stability Analyses Criteria	9.20
FEM Analyses	9.20
STRUCTURAL AND GEOMECHANICAL MODEL TESTS	9.21
CONSTRUCTION OF THE HOLLOW GRAVITY AND BUTTRESS DAMS	9.39
Construction Sequences	9.39
Foundation Excavation and Preparation	9.39
Concrete Construction	9.44
PERFORMANCE OF THE HOLLOW GRAVITY DAM	9.47
Instrumentation and Monitoring	9.47
Tests Prior to Reservoir Filling	9.50
Foundation Response	9.51
Structural Performance	9.55
Seepage Through Upstream Head	9.58

PERFORMANCE OF THE BUTTRESS DAM

Instrumentation and Monitoring

9.62

Foundation Response

9.62

Structural Performance

9.62

9.64

HOLLOW GRAVITY

AND BUTTRESS DAMS

SELECTION OF TYPE OF CONCRETE DAMS

The feasibility report recommended that for the concrete dams of Itaipu, the final selection between solid gravity and hollow gravity types should be made after the geotechnical investigations then in progress were completed, see Chapter 2. There are two sub-types of the hollow gravity dam. In one type a large longitudinal opening or cavity is formed inside a conventional solid gravity dam. The second group consists of several variations on the buttress dam.

For Itaipu main dam, only the double buttress cell type, also called the Marcello type, was considered, the other types being eliminated at an early stage. Hence the studies made for Itaipu compared a conventional solid gravity dam with a double buttress hollow gravity main dam, with single massive head buttress wing dams.

Layout studies of the typical power intake and powerplant unit blocks showed that a 34 m wide single buttress block was not structurally feasible and two 17 m wide single buttress blocks could not accommodate the large penstock and a monolithic intake structure. The cellular shape of the double buttress hollow gravity dam with a structurally monolithic top portion, was the most convenient and economical for the transverse alignment of the power



*View of main dam
under construction*

intake and powerhouse blocks. For the blocks on the wings of the main dam, where there were no power intakes, the single buttress type dam was more economical. Two hollow gravity blocks were adopted for the left wing between the last power intake block of the main dam and the diversion control structure principally for convenience during construction, when a temporary work platform was constructed on the partly complete blocks, and heavy vehicular traffic routed over them.

Inherently, the solid gravity and the hollow gravity types belong to the same group of concrete dams, because for stability both are dependent upon their weight and shape. Not only are the two types essentially similar in principles of structural function and behavior, permissible stresses and factors of safety, but also, both types are constructed in mass concrete of essentially the same quality, using the same methods of concrete placement and consolidation and treatment of construction joints.

The hollow gravity type has the following advantages over the solid gravity dam:

- About 25 to 30% less volume of concrete.
- Better stability against overturning because of the flatter upstream slope and the greater base width.
- Better dissipation of heat of hydration in the relatively thinner stems of the block or cell.
- Less hydraulic uplift in the foundation and a more effective foundation drainage system.

Structurally, the hollow gravity concept represents a more efficient utilization of concrete. Since the stresses induced in the foundations, both normal and shear, are of the same order of magnitude for both, there is no difference in the quality or treatment of foundation required for either type of dam.

For a thorough analysis of the two types, the following disadvantages of the hollow gravity dam were also taken into account, which offset to some extent the factors in its favor:

- A higher cement content in the concrete in some parts of the dam.
- More formwork required.
- Complexity of shape of upstream and downstream heads may slow down placement of concrete.
- Complexity of benched excavation for blocks on the sloping abutments.
- Some steel reinforcement required in areas of stress concentration at the terminals of contraction joints.
- Because the structural details of a hollow gravity dam are more complex than for a solid dam, a greater amount of engineering study, analyses and model testing were required for the former, resulting in higher cost of engineering.

However, the collective negative impact of the above factors implied a relatively small increase in the unit cost of concrete. In Fig. 9.1 are shown the actual volumes of concrete in the Itaipu hollow

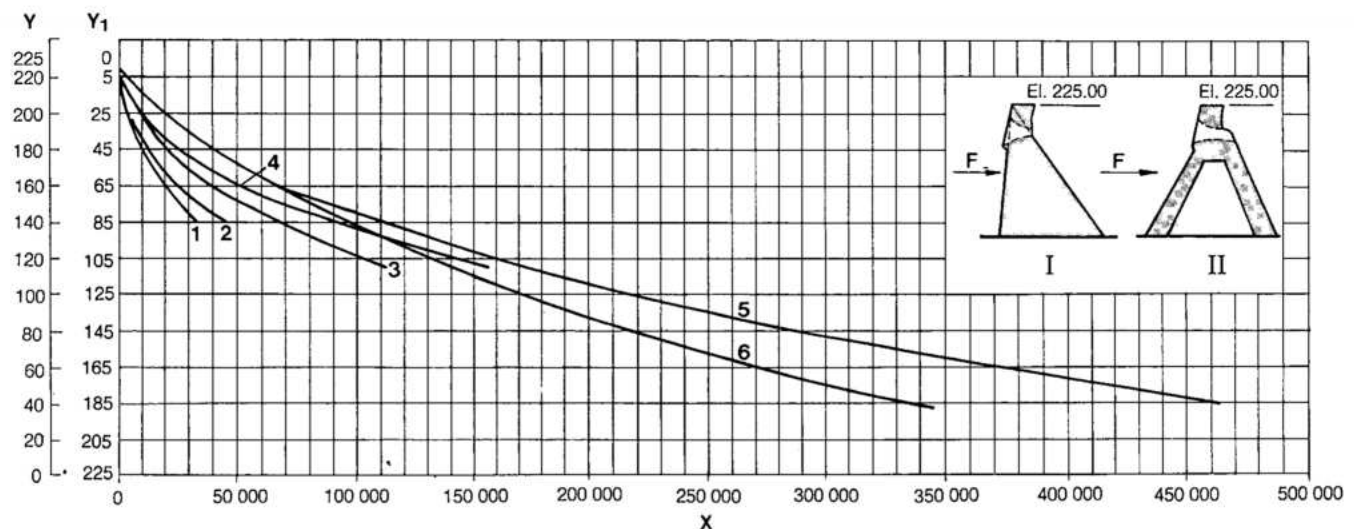


Fig. 9.1 Comparative concrete volumes - Hollow gravity, buttress and solid gravity dams

I Solid gravity block
II Hollow gravity block
Y Foundation elevation (m)

Y₁ Block height (m)

X Accumulated volume of concrete per block (m³)

1 Buttress block (17 m)

2 Solid gravity block (17 m)

3 Hollow gravity block without power intake (34 m)

4 Solid gravity block without power intake (34 m)

5 Solid gravity block with power intake (34 m)

6 Hollow gravity block with power intake (34 m)

F Flow direction

gravity and buttress dams, and the comparison with an equivalent theoretical solid gravity dam. The formwork area and the excavation for foundations were also computed; the total comparative quantities being:

	Hollow gravity and buttress dams	Solid gravity dam	
	Actual (m ³)	Estimated (m ³)	Savings (m ³)
Concrete	5.12×10^6	6.76×10^6	1.64×10^6
Formwork	1.25×10^6	1.04×10^6	-0.21×10^6
Excavation	1.96×10^6	1.60×10^6	-0.36×10^6

At Itaipu, the reduction of 1.64×10^6 m³ of concrete not only represented a saving of about US\$ 160 million in direct costs (1974 prices), but also substantial savings in financial charges and interest. In addition, it represented a reduction of about 6 months in the time required for construction of the crucial lower 60% of the dam located in the main river channel. These substantial economic advantages were the principal justification for the

adoption of the hollow gravity type for the main dam and buttress types for the wing dams. For a general arrangement and identification numbers of the main and wing dams and connections with the diversion structure and spillway see Fig. 9.2.

DESIGN OF THE HOLLOW GRAVITY DAM

SHAPE OF THE HOLLOW GRAVITY DAM BLOCKS

The blocks of the hollow gravity dam are monolithic cells, each consisting of an upstream head supported by two buttress stems and enclosed by a downstream face slab, see Fig.9.3. Each block is a cantilever, elastically affixed to the foundations and structurally independent of the adjoining blocks. Adjoining blocks abut against each other at the upstream head, at the downstream face slab and in the upper portion, but are separated by transverse contraction joints.

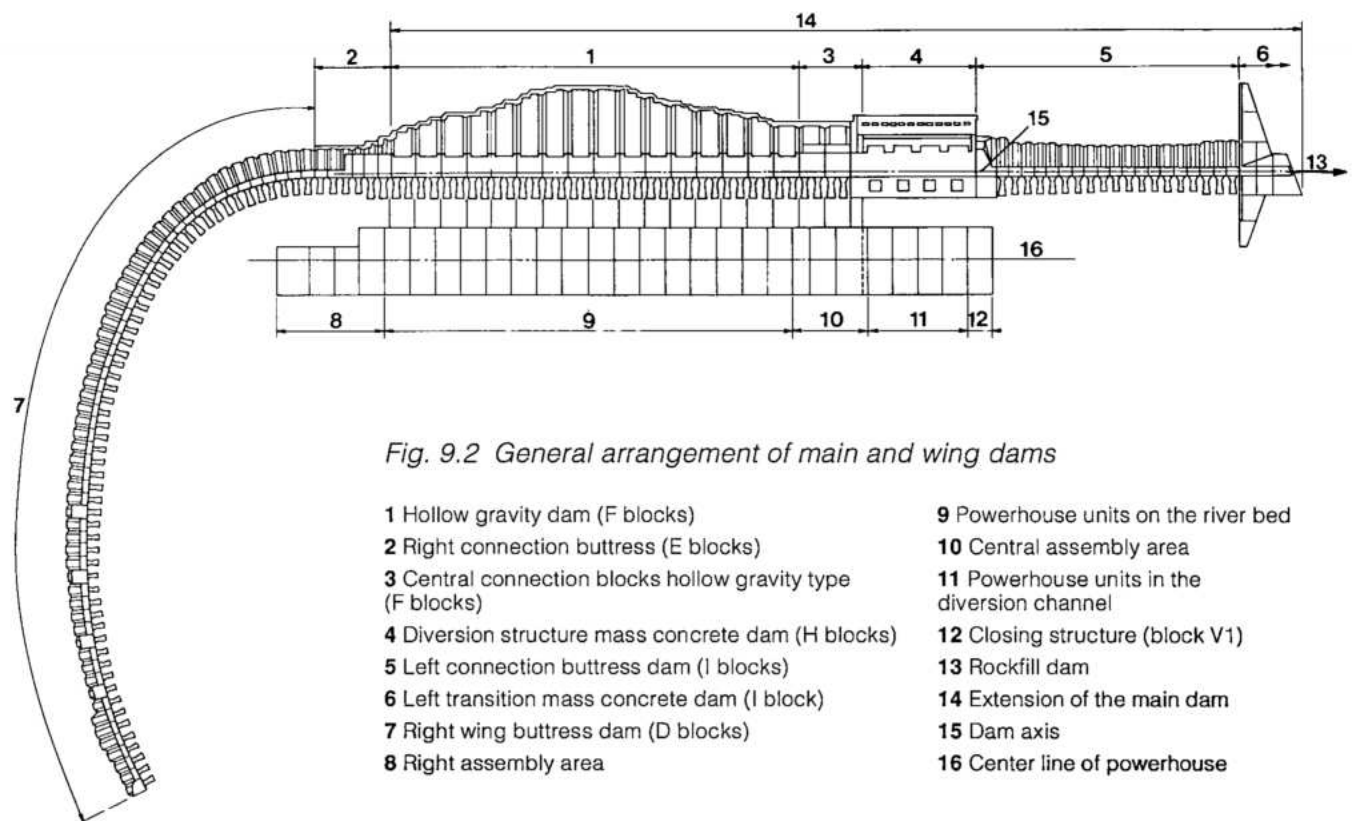


Fig. 9.2 General arrangement of main and wing dams

- 1 Hollow gravity dam (F blocks)
- 2 Right connection buttress (E blocks)
- 3 Central connection blocks hollow gravity type (F blocks)
- 4 Diversion structure mass concrete dam (H blocks)
- 5 Left connection buttress dam (I blocks)
- 6 Left transition mass concrete dam (I block)
- 7 Right wing buttress dam (D blocks)
- 8 Right assembly area
- 9 Powerhouse units on the river bed
- 10 Central assembly area
- 11 Powerhouse units in the diversion channel
- 12 Closing structure (block V1)
- 13 Rockfill dam
- 14 Extension of the main dam
- 15 Dam axis
- 16 Center line of powerhouse

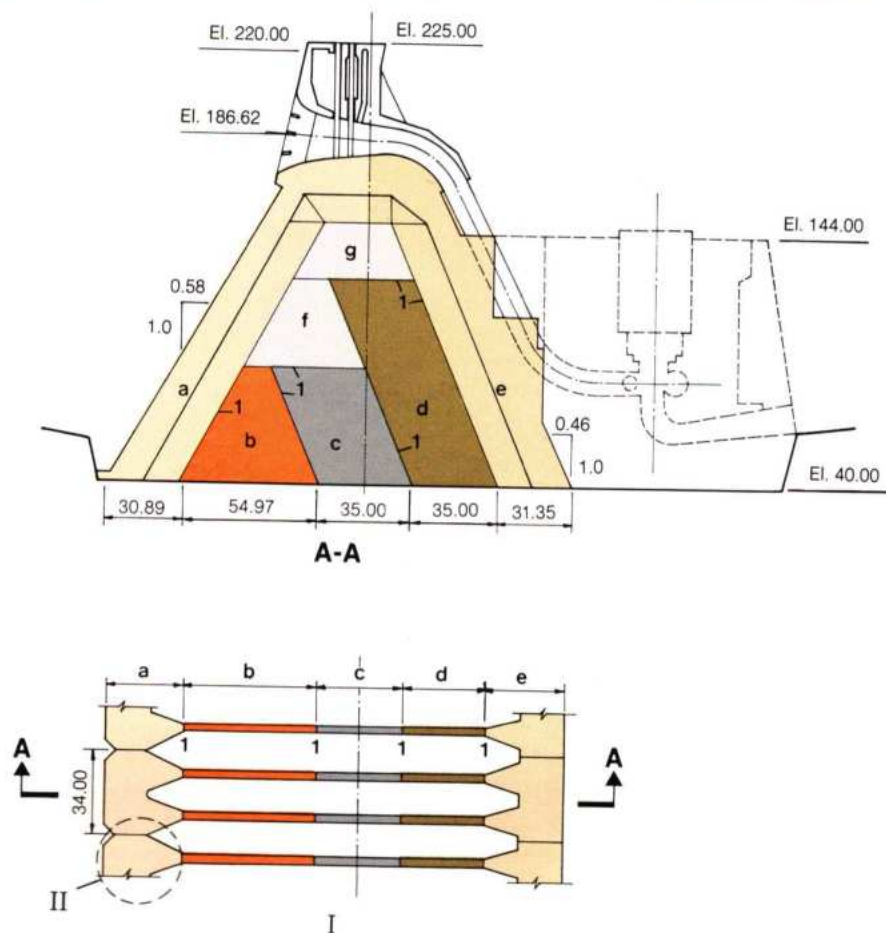


Fig. 9.3 Hollow gravity dam - details of typical hollow gravity block

I Plan and section at El. 40

II Detail

a, b, ... g Monoliths

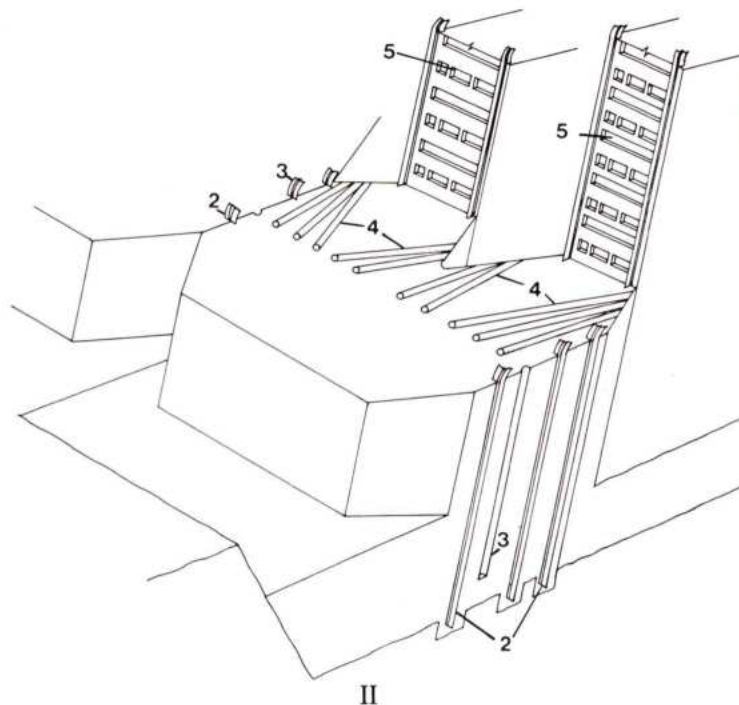
1 Contraction joints

2 Water stops

3 Drain at joint

4 Internal dewatering pipes

5 Keys



At the time of design of Itaipu, the highest hollow gravity dam was the José María de Oriol (Alcantara) dam in Spain, which is 130 m high and was completed in 1969. The Itaipu dam being 100 to 196 m high was an increase of 46% necessitating analysis not only by conventional methods, but also with finite element methods (FEM) and by structural model tests. In addition, comparative studies of the design and performance of existing hollow gravity dams were made in determining the various structural details of the Itaipu dam.

In Fig. 9.4 are shown the more important dimensional data for Itaipu and other hollow gravity dams existing at the time. The width of each Itaipu block is 34 m, which was determined by the spacing of the power generating units located at the toe of

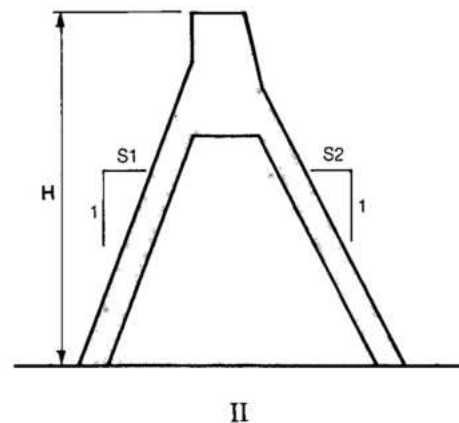
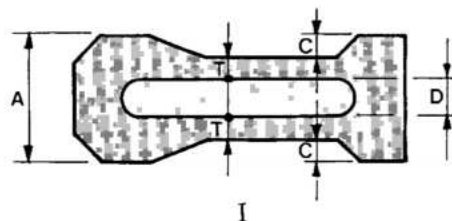
the dam and was 55 % more than the 22 m width of blocks in Alcantara, Ancipa and other dams. Also, the upstream and downstream slopes of the Itaipu blocks were flatter than most of the hollow gravity dams in existence. The hollowness index, defined as the ratio of the net volume of concrete to the gross volume of the solid cross-section, for various dams is also shown in Fig. 9.4. The typical Itaipu block is about average in massiveness as compared to the others.

Of the eighteen hollow gravity blocks of Itaipu dam, sixteen have a power intake located on the top and a 10.5 m diameter penstock supported on the downstream face. Cross-section and plan of a block with the power intake are shown in Fig. 9.5. The remaining two blocks, which are without any power

Fig. 9.4 Comparison of hollow gravity dams

I Plan

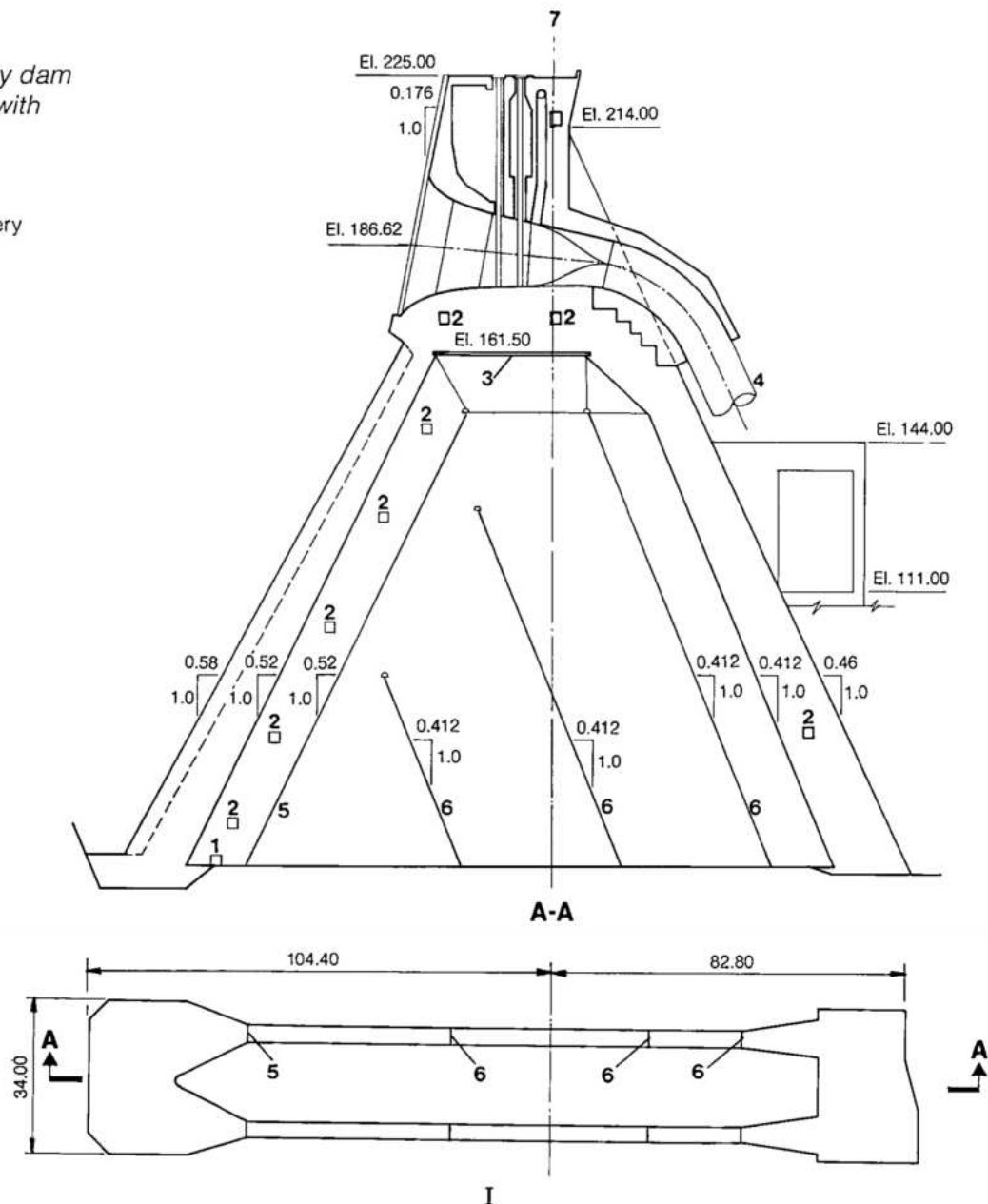
II Cross section



Dam	Country	Year completed	Max. height H (m)	A (m)	S ₁	S ₂	C (m)	D (m)	T (m)	Hollowness Index
Itaipu	Brazil/Paraguay	1982	196	34.0	0.58	0.46	4.8	12.4	6.0	0.57
Alcantara	Spain	1969	130	22.0	0.45	0.45	2.5	7.0	5.0	0.61
Ancipa	Italy	1952	112	22.0	0.45	0.45	3.5	7.0	4.0	0.55
Malga Bissina	Italy	1957	87	22.0	0.45	0.45	2.85	7.0	4.65	0.6
Latiyan	Iran	1967	87	28.0	0.45	0.48	5.38	5.75	5.75	0.56
Dixence	Switzerland	1937	81	26.0	0.04	0.81	4.0	8.0	5.0	0.6
Sabbione	Italy	1952	66	22.0	0.45	0.45	3.0	7.0	4.5	0.61
Pantano D'Avio	Italy	1956	65	22.0	0.45	0.45	2.88	7.0	4.62	0.61
Bau Muggeris	Sardinia	1949	63	22.0	0.45	0.45	3.5	7.0	4.0	0.57
Trona	Italy	1942	58	24.0	0.05	0.64	3.7	7.4	4.6	0.62
Inga	Zaire	1977	48	18.0	0.55	0.4	1.75	7.5	3.5	0.65

Fig. 9.5 Hollow gravity dam typical highest block with power intake section

- I Plan at El. 45
 1 Foundation drainage gallery
 2 Access gallery
 3 Precast concrete slab
 4 Penstock
 5,6 Contraction joints
 7 Dam axis



intake are shown in Fig. 9.6. In configuration, they are similar to the blocks with power intakes for the lower 50 % of the height; with the downstream face slab eliminated in the upper part.

The large power intakes through the upper part of the block considerably reduce the weight and stabilizing force. This was partly compensated by the flatter slopes of the upstream and downstream faces and consequent greater transverse width of the Itaipu blocks as compared to other dams.

The shape of the upstream face of the hollow gravity block, which withstands the reservoir

pressure, was refined by a series of two-dimensional FEM studies, which considered the influence of the following variables on the stresses in the massive head, see Fig. 9.7:

- Chamfers to trim the upstream corners, which affect the resultant force due to reservoir pressure.
- Location of waterstops in the transverse joints, which determines the amount of balancing lateral hydrostatic pressure on the head.
- Net minimum thickness at the crown, and downstream slope of the head.
- Thickness of the buttresses supporting the head.

LONGITUDINAL CONTRACTION JOINTS IN HOLLOW GRAVITY BLOCKS

For large hollow gravity dams concrete cannot be placed over the entire block in continuous lifts without contraction joints. To eliminate contraction joints, very heavy steel reinforcement would be required in each lift. The configuration of a hollow gravity block is too complex for continuous placement of concrete and, for the Itaipu dam the volume of concrete in each pour was so large that cold joints would have been unavoidable. An additional factor was that the uneven cooling of concrete in the various parts of the block causes temperature gradients between the massive head and the slender buttress stems, producing high tensile stresses and potential cracking, starting near the foundation where restraint is maximum. The provision of longitudinal contraction joints was a practical solution for avoiding cracking and, at the same time, facilitating rapid construction. For selection of arrangement of longitudinal (parallel to axis of the dam) contraction joints in the hollow gravity dam, four different joint arrangements were analyzed, see Fig. 9.8. All these alternatives had actually been used in other hollow gravity or buttress dams. The sloping contraction joints were essentially parallel to the curvilinear trajectories of the principal stresses in the dam after application of the

reservoir load, and had an advantage over vertical joints in that the shear stresses would be much lower. In the adopted system, the contraction joints are parallel to the upstream and downstream faces of the dam, see Fig. 9.5. The lower portion of the highest block consists of eight monoliths with six contraction joints. This joint arrangement had the following practical advantages:

- Concrete could be placed in as many as four monoliths per block at the same time.
- Layout of the monoliths was compatible with the aerial cableways used for concrete placement.
- A partially complete block was stable against water pressure to the top of the completed upstream head.
- The largest concrete pour (upstream head, 2200 m^3 , in 2.5 m lift), could be placed by one cableway in about 24 hours.

These advantages were proven during construction, permitting placement of an average of $135\,000 \text{ m}^3$ of concrete per month in the hollow gravity dam during 1979-81.

To provide sufficient shearing resistance between the monoliths, two types of unreinforced concrete keys were formed along the longitudinal contraction joints:

- Trapezoidal in the joint parallel to the upstream face.
- Triangular in other joints, see Fig. 9.9.

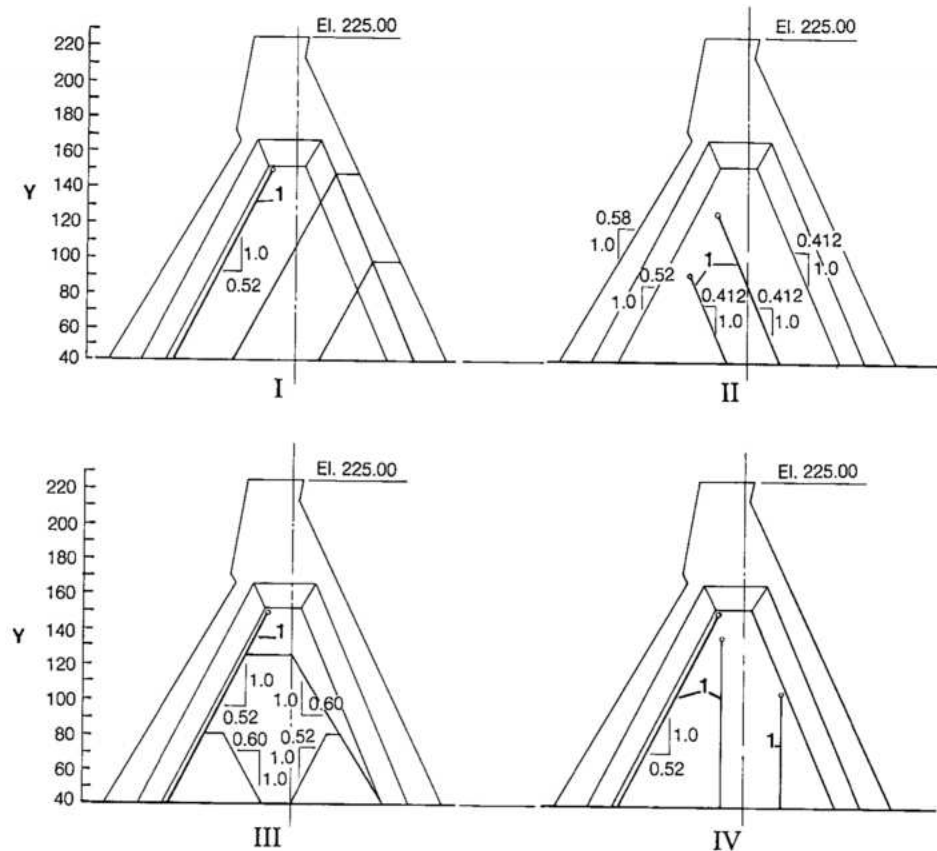


Fig. 9.8 Hollow gravity dam longitudinal contraction joints arrangement alternatives

I..., IV Location alternatives for contraction joint

Y Elevations (m)

1 Contraction joints

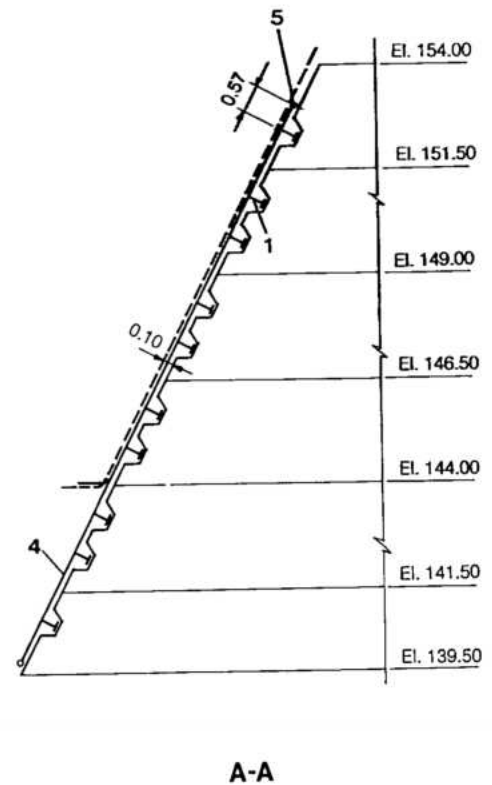
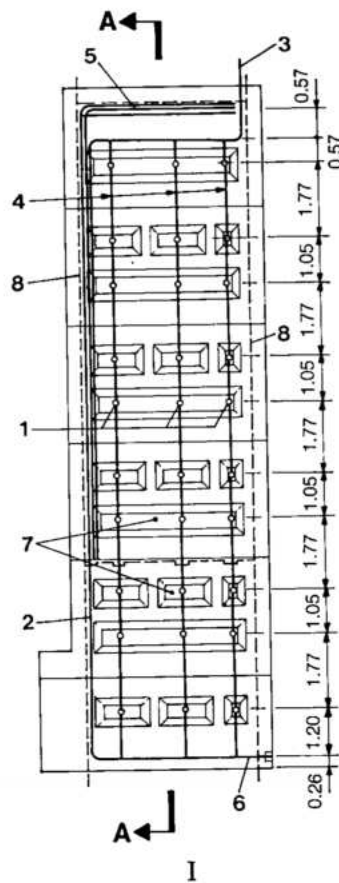
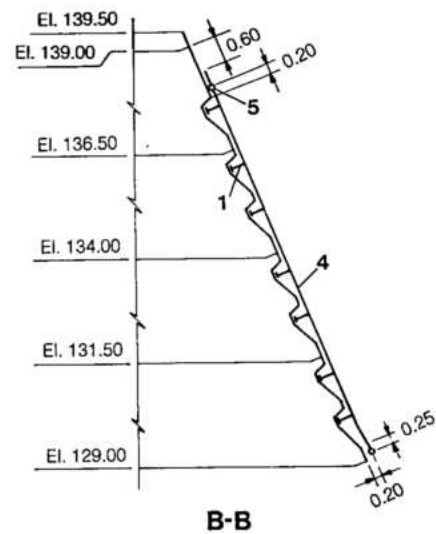
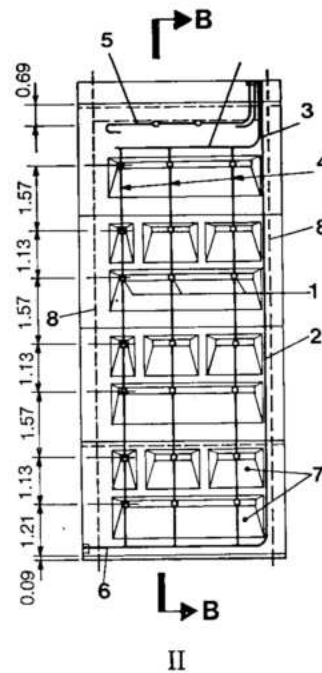


Fig. 9.9 Longitudinal contraction joints-keys and grouting systems

- I Joint 5
- II Joint 6
- 1 Grout outlets
- 2 38 mm diameter supply header
- 3 38 mm diameter return header
- 4 25 mm diameter risers
- 5 Air vent
- 6 38 mm diameter emergency grout inlet
- 7 Shear keys
- 8 PVC waterstop



To obtain partial or full monolithic action of the hollow gravity block, the longitudinal contraction joints were grouted before the reservoir was filled. The degree of monolithic action attained depended on the opening of the joint at the time of grouting and the penetration and coverage by the grout.

The longitudinal contraction joints were sealed by water-cement grout forced through a pipe system embedded in the face of the higher monolith at each joint. The joint surfaces were circumscribed by polyvinylchloride seals embedded along both exposed faces. Joint grouting was performed in 12.5 m high lifts after washing and testing the joint and the pipe system with air and water under pressure. During grouting in a joint of a particular lift, adjoining joints and lifts of the same joint were filled with water. Grouting specifications limited the grout pressure measured at the vent at the top of each grouting lift to 50 N/cm².

FEM analyses showed that contraction joint B, in the lower 50 m of the blocks would open between 0.5 and 1 mm about 12 months after start of concreting of the lowermost lifts, see Fig. 9.5. Fourteen series of grouting in contraction joints B in blocks F11/12 through F21/22 were executed between the foundation and El. 89.5, during the colder months of 1980 and 1981. From the grout take it was estimated that the coverage of these joints was about 70 %.

FEM analyses also indicated that the probability of joints C opening about 0.5 mm was approximately 30% of its extension, but other longitudinal contraction joints namely A and D would not open sufficiently in the greater part of their length to permit grouting. The reason was that the joint opening due to temperature drop was more than offset by the deformation of the monolith due to its own weight or that of the adjoining monolith.

A simple system for regrouting the longitudinal contraction joints after the reservoir was filled and in case they reopened, was also provided. It consisted of short 55 mm diameter PVC pipes embedded in concrete and extended from the surface to within 20 cm of the joint. Holes drilled through these pipes could be used to inject grout into the joint.

TRANSVERSE CONTRACTION JOINTS

Transverse contraction joints between the heads of adjoining hollow gravity or buttress dam blocks were not keyed. This permitted independent movement between adjacent blocks in a direction perpendicular to the axis. As shown in Fig. 9.10, the transverse joints between hollow gravity blocks have three PVC

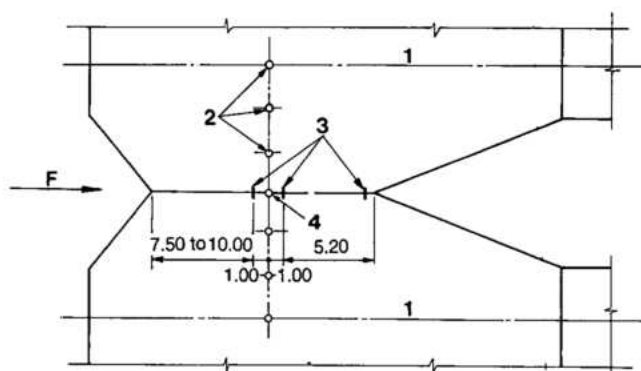


Fig. 9.10 Transverse contraction joint

- 1 Reference line
- 2 200 mm diameter to 300 mm diameter head drains
- 3 PVC water stops
- 4 250 mm diameter joint drain
- F Flow direction

waterstops. Between the two upstream waterstops a drain was formed to handle percolating water and carry it through the galleries to sumps and pumping plants described in detail in Chapter 10. The joint space between the two downstream waterstops was to be grouted at a later date, if considered beneficial or necessary.

To ensure water tightness and better consolidation of concrete in the congested area, concrete with maximum aggregate of 38 mm was used adjoining the transverse contraction joint and the waterstops. The upstream seals were located 2.5 m downstream of the upstream face to let the lateral water pressure in the open joint reduce lateral tensile stresses which might occur in the massive head. In order to relieve pore pressures in the concrete, a series of 200 mm diameter drains were formed in the head parallel to the upstream face at 3 m spacing. These drains exit into the galleries at various elevations and the seepage water flows by gravity into a collector system.

CONCRETE CHARACTERISTICS

The specified strengths of concrete in the various parts of a typical hollow gravity dam block and the heights of lifts are shown in Fig. 9.11. The standard lift of concrete placement was 2.5 m.

The predominant class of concrete used in the dam was A-140-f, which signifies a characteristic compressive strength of 1.4 kN/cm² at 365 days age

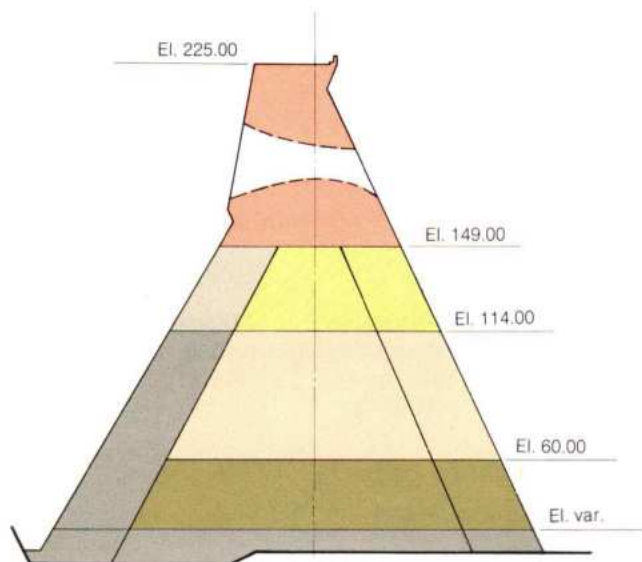


Fig. 9.11 Hollow gravity dam concrete classification

A Maximum aggregate size 152 mm

B Maximum aggregate size 76 mm

B-180-f

B-210-f

A-140-f

A-180-f

A-210-f

Various

and aggregate MSA of 152 mm. To obtain low permeability and higher tensile strength, concrete in the upstream head used smaller (75 mm) size aggregate and a higher cement content.

Concrete temperature control

In addition to the provision of contraction joints, construction specifications included three other requirements to control temperature of the concrete and reduce the risk of cracking. These were:

- Temperature of concrete when placed in the forms should not exceed 7°C.
- About 12 to 25 percent of portland cement in the concrete mix should be replaced by fly ash.
- Concrete on and near the foundations should be placed in relatively thin lifts (50 to 70 cm).

Initially about 25% of the cement was replaced by fly ash. After about 20% of concrete had been placed in the dams, serious difficulties were encountered in obtaining adequate quantity of fly ash conforming to the specifications. It then became necessary to reduce fly ash to about 12% of the cement content by volume.

Composition of typical mass concrete mixes, concrete quality control and the plant for cooling, batching, mixing and placing concrete are discussed in greater detail in Chapter 5.

STRESS AND STABILITY ANALYSES CRITERIA

Loading conditions

The loading conditions used for the stress and stability analyses of the hollow gravity dam were divided into four classes:

Normal loading conditions (NLC). All loading combinations during normal project operation and routine maintenance for average hydrological conditions.

Exceptional loading conditions (ELC). All statistically possible but infrequent cases during project operation and major maintenance.

Ultimate loading conditions (ULC). Highly improbable combination of events (gross overloads, catastrophic floods, major equipment malfunction and accidental loads) during construction or operation.

Construction loading conditions (CLC). Temporary loads applied during construction, such as construction equipment loading, loading during erection of permanent equipment, or any temporary condition on an incomplete monolith or block.

Earthquake acceleration

Although the project region is considered to be aseismic or of very low seismic activity, horizontal and vertical seismic acceleration of 0.05g was included in NLC and 0.08g in ELC, in the most unfavorable directions.

Uplift pressure distribution

Hydraulic uplift pressure distribution assumed along the foundation contact of the highest blocks of the main dam and the adjacent powerhouse for loading conditions NLC, ELC and ULC was as follows, see Fig. 9.12:

- Upstream of the dam and downstream of the powerhouse as far as the grout curtains, uplift pressure equals the upstream and downstream hydrostatic head column (H_u and H_d) respectively, down to the rock discontinuity at El. 20.
- Between the upstream and downstream longitudinal drainage tunnels at El. 20, the uplift pressure H_0 is constant and equals the distance between foundation surface at El. 35 to El. 40 and the discontinuity at El. 20.
- Between the upstream grout curtains and the drainage tunnel uplift pressure varied linearly from H_u to H_0 .

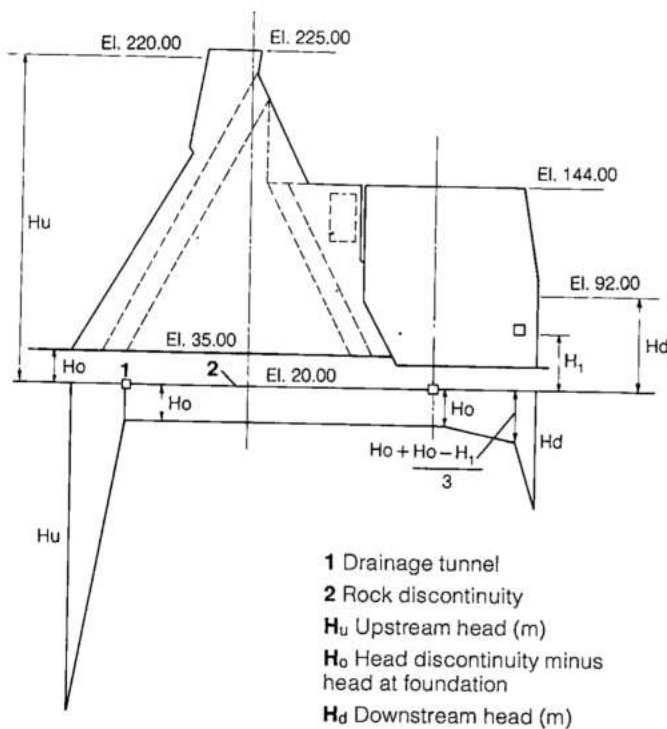


Fig. 9.12 Main dam - Uplift criteria

- At the downstream drainage curtain the uplift equals $H_o + 0.33(H_d - H_o)$, and from there the uplift pressure varied linearly to H_d at the downstream grout curtain and to H_o at the downstream drainage tunnel.
- Drainage water from both tunnels was to be pumped, making $H_o = 0$; but assuming damage to the pumps, the value of $H_o = (\text{El. at discontinuity minus El. at foundation surface})$ was used in the analyses.

Factors of safety against shearing and sliding

The following table shows the minimum permissible partial factors of safety against shearing-sliding which were used in the analyses for Itaipu concrete dams for the various loading conditions.

	Normal loading conditions	Exceptional loading conditions	Ultimate loading conditions
Y_c	4.0 3.0*	3.0	1.5
Y_ϕ	2.0 1.5*	1.4	1.1

* In case of adequate knowledge and good quality of the foundation.

Y_c = partial safety factor for shear strength

Y_ϕ = partial safety factor for frictional resistance

Maximum allowable stresses in the dam for the various classes of concrete used were determined by the field laboratory of ITAIPU. The following table shows the various classes of mass concrete used in the hollow gravity and buttress dams, the specified characteristic compressive strength at 365 days and the allowable compressive and tensile stresses.

Characteristic strength of concrete in compression (kN/cm^2)	Allowable compressive stress (N/cm^2)	Allowable tensile stress (N/cm^2)
21	700	70
18	600	60
14	460	46

FEM MATHEMATICAL MODEL STUDIES

FEM computer programs were used for the following design studies:

Location and grouting of contraction joints between monoliths

Since the base length of the highest hollow gravity dam blocks is about 192 m, the buttresses had to be divided by contraction joints into monoliths not longer than 60 m to control the tensile stresses caused by temperature changes in the mass concrete. These joints were keyed and were to be grouted before filling of the reservoir, but if they did not open sufficiently to permit grouting, then there would not be a full transfer of load between the monoliths. FEM computations were made for this case to check the stresses under different loading conditions with the joints open and compared with the results for full monolithicity, see Fig. 9.13.

Stress patterns in the highest hollow gravity block

Principal stresses were calculated in two vertical planes; one inside and the other outside the center line of the counterfort. Figure 9.14 shows the results for the inside plane and a combination of own weight and hydrostatic load.

Stress patterns in the block with the "leg"

These FEM analyses included the adjacent rock mass, different loading conditions and uplift forces, see Fig. 9.15. Deflections of the dam were also determined.

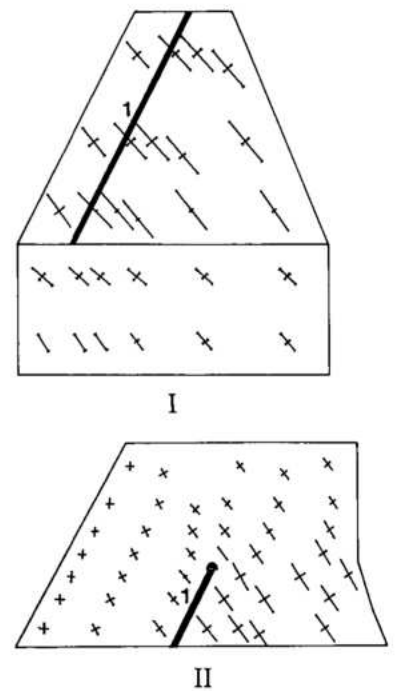
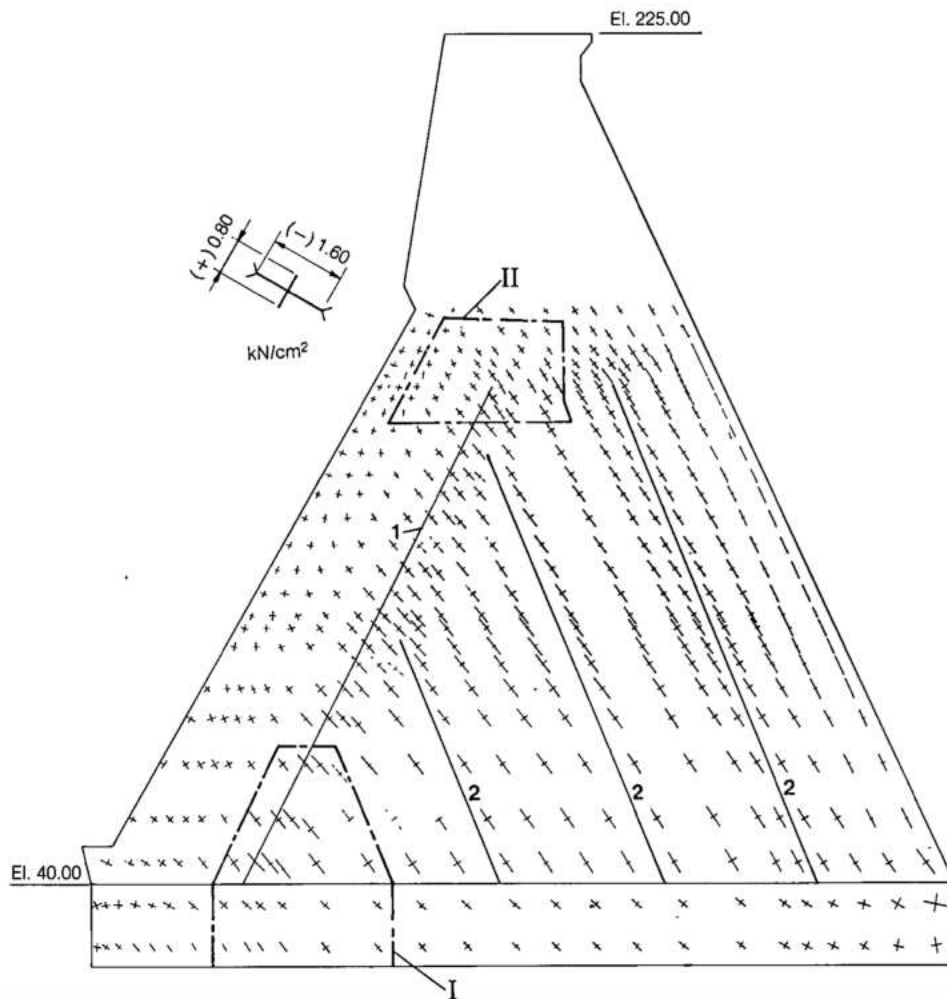


Fig. 9.13 Contraction joints FEM analysis of stress concentration

I Detail
II Detail
1, 2 Contraction joints

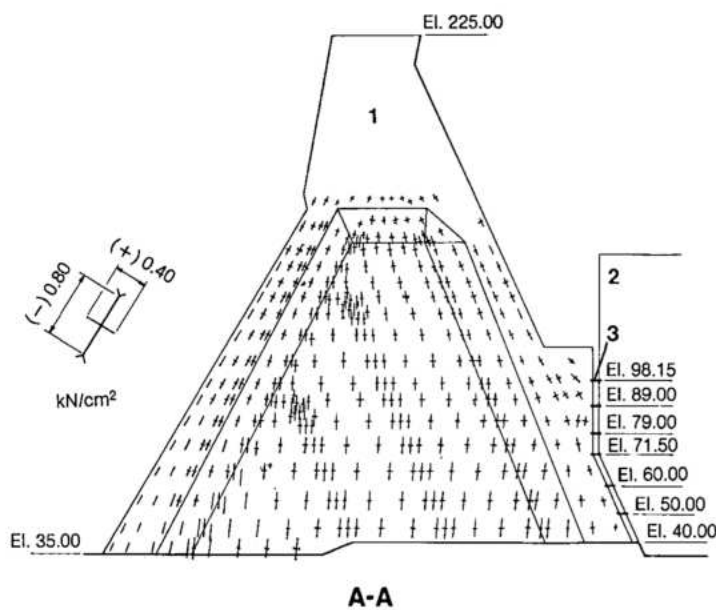
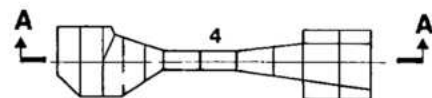


Fig. 9.14 FEM stress analysis of highest hollow gravity block

1 Section of the main block located on center of gravity of elements situated externally to the counterfort
2 Powerhouse
3 Simulation of contact by bars between dam and powerhouse
4 Location of section
(-) compression
(+) tension



Minimum time intervals between concrete lifts and stresses caused by the heat of hydration in heads of the block

Because of the large size of the upstream head, FEM calculations were made for various seasonal ambient temperatures and concrete mixes to determine the rate of cooling and time-temperature histories, see Fig. 9.16.

Stresses in buttress stems caused by hydration temperature changes

For 4.6 to 6 m wide and 60 m long monoliths in the stems and for 2.5 m concrete lift, the FEM analysis indicated that the concrete in the buttresses would cool to the ambient temperature in about 6 months.

Tensile stresses in the upstream head due to reservoir load

FEM computations helped locate the waterstops, so that lateral water pressure would counterbalance the internal tensile stresses.

Stability against sliding at the foundation and at a discontinuity underneath

Such studies were made for various blocks and loading conditions and included the effective properties of the foundation rock.

Analysis of seepage under some dam blocks with a gouge filled contact in the foundation

Uplift forces determined by FEM were used in the analysis of stability of the dam and the foundation.

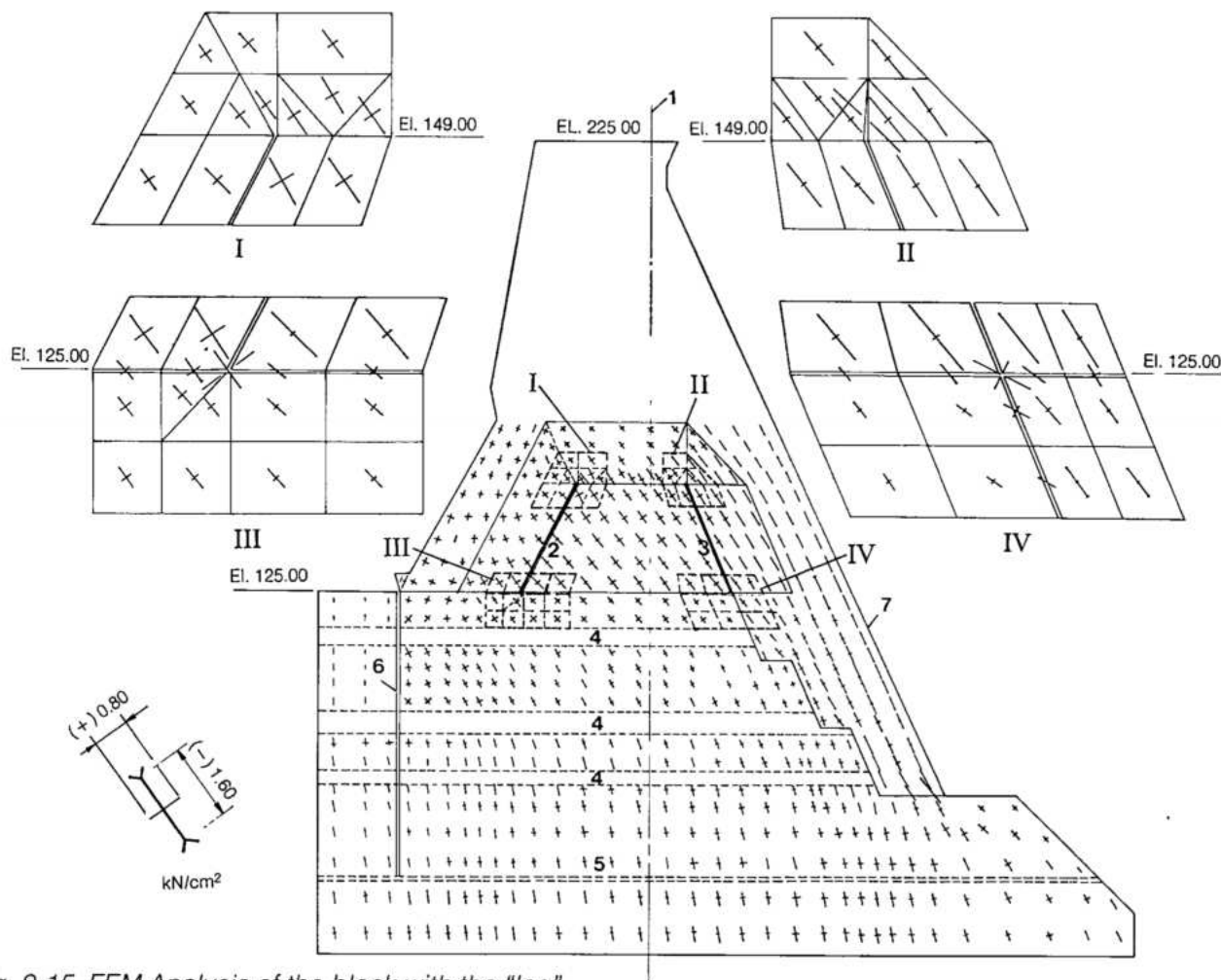


Fig. 9.15 FEM Analysis of the block with the "leg"

I, II Details at top of contraction joint 2 and 3
III, IV Details at base of contraction joint 2 and 3

1 Dam axis
2,3 Contraction joints
4 Fractured zone
5 Joint in rock stratum

6 Crack in rock
7 Leg of the hollow gravity block
(+) Tension
(-) compression

Stability of permanent rock cuts

These calculations were used for establishing the criteria for slope treatment such as benching, rock bolting and shotcrete.

Distribution of normal and shear stresses in the shear keys in the foundations of the highest blocks

FEM analyses were used for establishing the scope, layout and dimensions of the subterranean treatment.

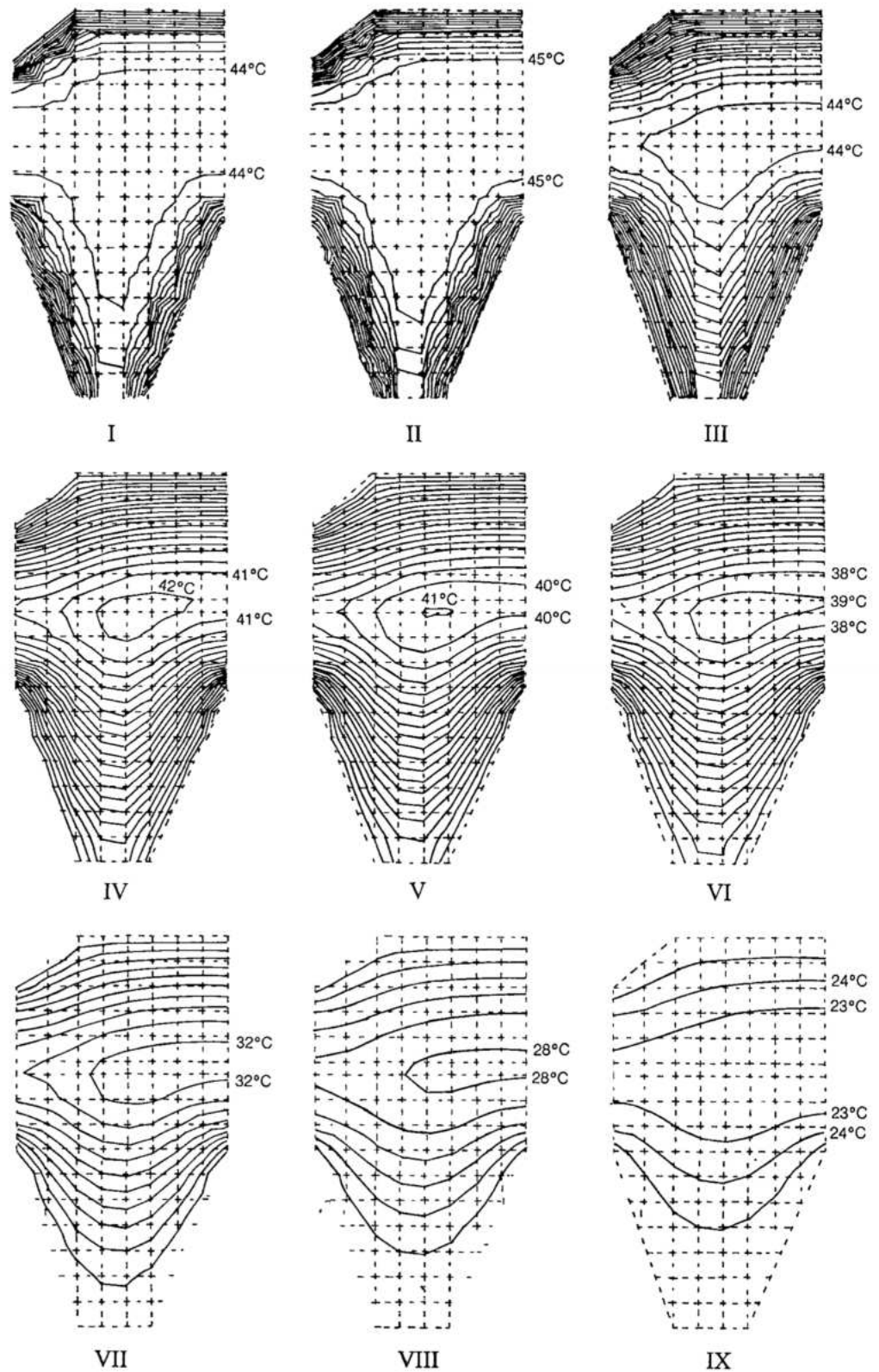


Fig.9.16 FEM analysis of rate of cooling of hollow gravity dam-upstream head

- I 10 days
- II 27 days
- III 90 days
- IV 270 days
- V 330 days
- VI 390 days
- VII 750 days
- VIII 1100 days
- IX 1410 days

DESIGN OF THE BUTTRESS DAM

On the right bank, between the spillway and the hollow gravity main dam, there are sixty-four buttress dam blocks, and, on the left side, between the diversion control structure and the rockfill dam there are nineteen buttress dam blocks. All eighty-three blocks are identical in structural configuration and profile, and are 17 m wide at the axis.

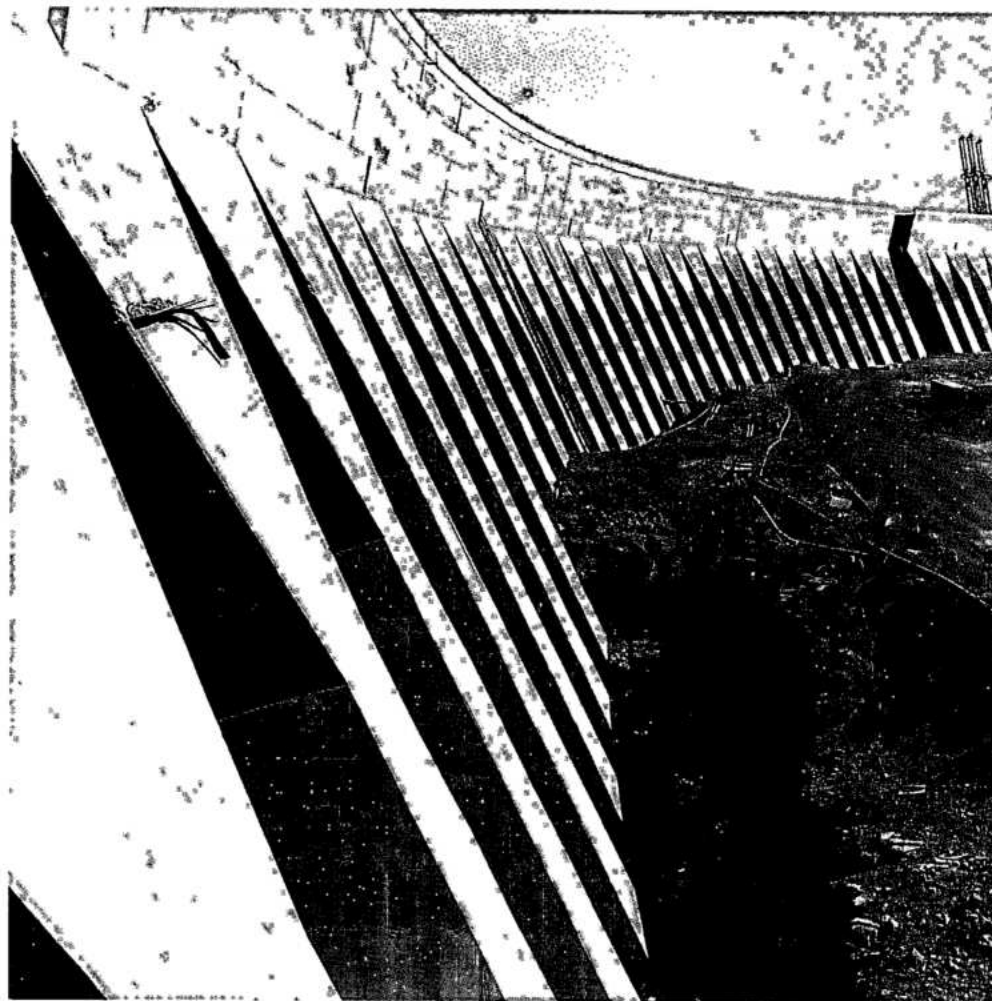
The polygonal head mass concrete buttress type was selected for the wing dams for the following main reasons:

- Economy: a typical block of the adopted buttress design contains 30% less concrete than a comparable solid gravity block.
- Adaptability for construction of a forebay and power intakes for a possible future powerhouse.
- Suitability for interface with the main hollow gravity dam and the diversion control structure.
- Optimization of concreting operations, which

would be adversely affected if an embankment type dam was adopted.

- Since no power intakes or penstocks were to be located in the wing dams, the buttress type was preferred to the hollow gravity, because of simplicity of forming and construction.

A plan and cross-section of a typical buttress dam block are shown in Fig. 9.17. Heights of the buttress dam blocks range from 35 to 85 m. Three of the blocks on the right wing of the hollow gravity dam have stepped massive concrete legs supporting the downstream portion of the structure above the deep excavation for the powerhouse. Except for galleries near the crest of all blocks and near the foundations of the left wing blocks, the buttress dams do not have any large openings through them. The only major appurtenances on the buttress dams are three platforms for the transmission line towers on the right bank and, adjoining the main dam, storage chambers for stoplogs.



Right wing buttress dam

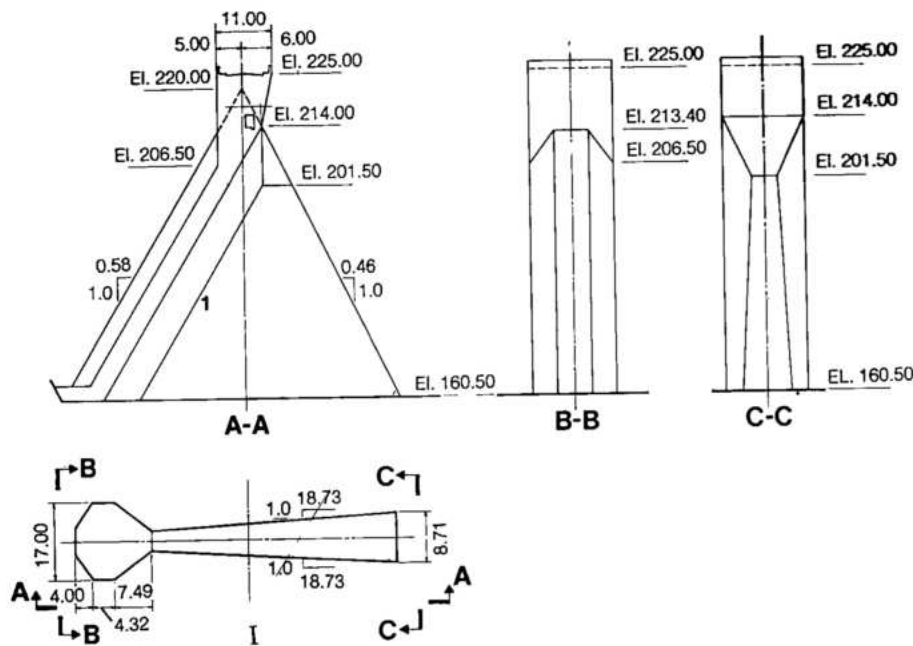


Fig. 9.17 Typical block on the right wing buttress dam

I Plan

1 Contraction joint

BUTTRESS BLOCK CONFIGURATION

To maintain visual continuity, as well as for adequate stability, the upstream and downstream slopes of the buttress dam blocks were the same as those of the hollow gravity dam. The three components of a typical block, namely, the upstream head, the buttress stem and the crest have the same configuration for all buttress dam blocks.

The upstream head is essentially the quadrant of a circle, with three straight chords substituted for the arc to form the upstream face, see Fig. 9.17. Normal to the upstream face the section of the head is constant from the foundation to El. 201.5, where it meets the rectangular wall of the crest. The polygonal head was developed after FEM stress analyses of various shapes. The adopted shape of the head is free of internal tensile stresses and easier to construct because the flat faces are simpler to form than a curved one.

The buttress stem increases in thickness horizontally from the neck to the downstream face and vertically from El. 201.5 down to the foundation.

CONTRACTION JOINTS

Several FEM analyses were made to study the possibility of building buttress dam blocks monolithically, that is without any longitudinal contraction joints. The thermal tensile stresses which would occur in a monolithic block were

studied using variations in the modulus of elasticity of concrete, placing temperature of concrete, concrete mixes, cement and pozzolan content, lift height and time interval between lifts. These analyses indicated that blocks up to 50 m in height could be constructed without contraction joints if concrete temperatures were kept within certain limits during the first four months after placing and if abnormally cold winters were not encountered.

Blocks higher than 50 m had one or two keyed contraction joints parallel to the upstream face, the first joint separating the head from the buttress stem. Design of the keys and provisions for grouting the contraction joints were similar to those for the longitudinal contraction joints in the hollow gravity dam.

No cracking occurred in any buttress dam blocks built with longitudinal contraction joints, either during construction or after the reservoir was filled. On the other hand, in several blocks built without contraction joints, vertical cracks occurred in the buttress stems and the neck or underside of the head, 12 to 18 months after concrete was placed and the blocks already completed to or near the top. These cracks which commenced from the foundation were detected during a relatively cold winter about 2 years before reservoir filling.

The cracking was attributed to three departures from design assumptions:

1. The heat of hydration was considerably higher
2. The amount of fly ash was less and the cement content higher in the lower lifts of concrete

3. The actual modulus of concrete was higher. The cracks were grouted with high pressure epoxy injections during the colder months of 1981. In the incomplete buttress blocks, contraction joints were introduced between the head and the stem and reinforcement steel placed on the already complete lifts to control the extension of the cracks. Treatment of the cracks is discussed in detail in the section on performance of the buttress dam.

The transverse joints between the heads of adjoining blocks had two formed drains and three waterstops. For internal drainage of the heads, 200 mm drains at 3 m spacing were formed parallel to the upstream face. The internal and joint drains exit near the base of each block.

CONCRETE SPECIFICATIONS

In a typical buttress dam block, B-210-f concrete was specified for the first 5 m above the foundations, with the lifts increasing from 50 cm to 2.5 m in height. Above that, B-180-f concrete was used in the heads and A-140-f for the stems. The standard lift height was 2.5 m.

The specified maximum placement temperature of concrete was 7° C and the specified fly ash content was 25 % of cement by weight. Certain flexibility in placement temperature was permitted and in the early stages of construction, the average placement temperature was about 9°C for right wing dam blocks near the spillway. Also, for later pours the actual average fly ash content was 12% of the cement.

Specifications for methods of mixing and placing concrete and quality control of construction of buttress dam blocks were the same as for the hollow gravity dam.

STRESS AND STABILITY ANALYSES CRITERIA

The loading conditions used for the stress and stability analyses of the buttress dam blocks were identical to those for the hollow gravity dam, with the exception of uplift. Uplift pressure distribution differed from that for the hollow gravity dam (see Fig. 9.12), in that the pressure H_0 at the drainage curtain or the drainage tunnel was equal to 0.33 H_u and from there it varied linearly to zero at the downstream toe of the block.

Factors of safety against shearing and sliding, and maximum allowable stresses in the dam for the various loading conditions were identical to those for the hollow gravity dam.

FEM ANALYSES

A series of FEM analyses using bidimensional computer programs were performed for two typical buttress dam blocks, one on horizontal foundations and the other with a downstream leg support.

These studies investigated the following:

- Rate of cooling and temperature distribution, assuming different concrete properties, placing temperature and ambient conditions.
- Thermal and total stresses in a monolithic block for different loading combinations.
- Effects of various locations and configurations of cracks or joints on the stresses for different loading conditions.

Results of some of the more extensive FEM analyses made for the hollow gravity dam and the structural and geomechanical model tests were also applicable and utilized in the stress and stability studies of the buttress dam.

Typical examples of distribution of principal stresses in a buttress dam block without any joints and with two vertical cracks are shown in Fig. 9.18.

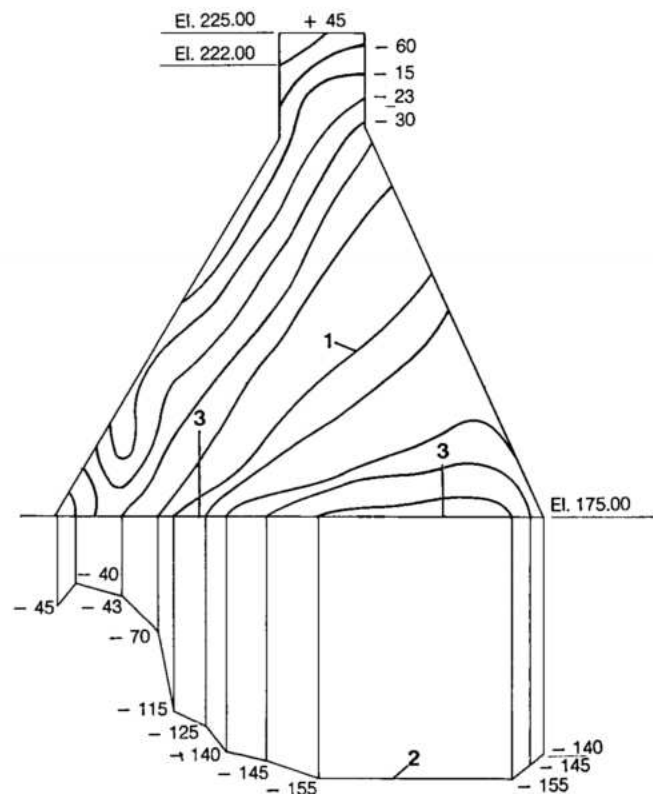


Fig.9.18 Distribution of principal vertical stress in buttress dam block - FEM analysis

- 1 Lines of equal stress (N/cm^2) (-) compression (+) tension
- 2 Stress diagram by FEM at base El. 175
- 3 Cracks

STRUCTURAL AND GEOMECHANICAL MODEL TESTS

Structural and foundation safety assessment with physical models

Because the Itaipu hollow gravity dam was unprecedented in size, independent methods were utilized to ascertain its safety. In addition to mathematical analyses by conventional and finite element methods, the integrity and safety of representative individual blocks of the dam were experimentally verified, in the elastic range as well as to the stage of collapse, by means of physical (structural) models. Also, a comprehensive geomechanical model of the complete dam was used to determine the weakest points in the combined system, and to ascertain potential failure mechanisms.

In particular the structural models showed how the structures responded to non-linearities, cracking, deformations and stress redistributions and provided an insight into the behavior beyond the elastic range up to the point of collapse.

Structural model technique

Four models were tested for the Itaipu dams as follows:

Model 1. Maximum height hollow gravity block, at Istituto Sperimentale Modelli e Strutture (ISMES), Bergamo, Italy.

Model 2. Diversion structure, at Instituto de Pesquisas Tecnológicas de São Paulo (IPT), Brazil.

Model 3. Hollow gravity dam block with downstream sloping strut at IPT.

Model 4. Comprehensive geomechanical model of complete dam at ISMES.

Models 1, 3 and 4 are described in this Chapter. Structural model 2 of the diversion structure is described in Chapter 6.

ISMES technique was followed throughout the tests, with some adaptations made to suit IPT testing facilities or local availability of suitable materials.

The controlling parameters are geometric scale $\lambda = L/L'$ (the affix denotes model quantities), and the "degree of efficiency", $\zeta = \sigma/\sigma' = E/E' = \rho/\rho'$ where:

L = length

σ = stress

E = modulus of elasticity

ρ = specific gravity

Once λ and ζ are chosen, all the remaining relationships are fixed. The simplest choice for models to be tested up to collapse would be $\zeta = 1$ (same materials in model and prototype); however in some cases this greatly complicates modelling if weight is an important factor affecting the state of stress. This was so for models 1 to 3 and, for these, model materials had to be different from those of the prototype, with a relationship linking the Mohr's envelopes of the prototype and the model materials. Microconcretes with pumice or expanded clay aggregate with ζ of 1 to 15 were used and the weights in the model were simulated by a system of small point loads distributed in the mass and applied by means of steel wires anchored at selected points and passing through embedded PVC sleeves. The set of wires, each of them in series with a dynamometer rubber ring, was tensioned by hydraulic jacks. Water loads were applied by hydraulic jacks. Strains and displacements were measured by means of Hottinger inductive gages.

Ideally the structural model should be tested up to collapse by gradually increasing, at a constant rate, all the loads involved. However due to physical limitations with the steel wires, weight could not be simulated beyond more than 3 times the design value. As none of the three models collapsed under 3 times the normal loads, failure was achieved either by maintaining the weights at their normal value and increasing only the water load (model 1, tested at ISMES), or increasing the water load while maintaining the model weights at their maximum feasible value (2.5 times the normal value for model 3, tested at IPT). Although this was recognized as a distortion of the actual conditions it did give a good indication of the structural safety factors.

The structural models did not verify stability against sliding in the foundation; this was studied with the geomechanical model.

Structural model 1: maximum height hollow gravity block.

Model 1 was built and tested by ISMES in October 1975. It represented a hollow gravity block of maximum height, with the geometrical dimensions established in the feasibility stage, see Fig. 9.19. These were, height = 182 m, foundation at El. 42; the crest at El. 224, maximum water load at El. 222 and block width = 37 m. In the final design the dimensions were: block width = 34 m, foundation at El. 35 for the upstream half of the block and at El. 40 for the downstream half, maximum water level at El. 223, and the crest at El. 225.

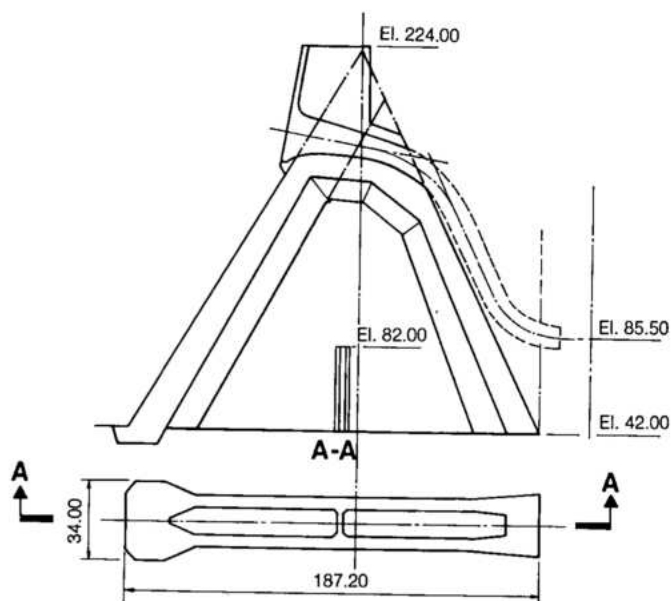
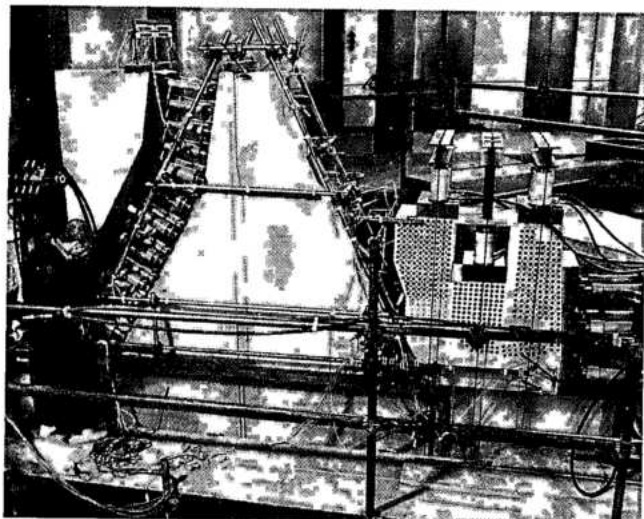
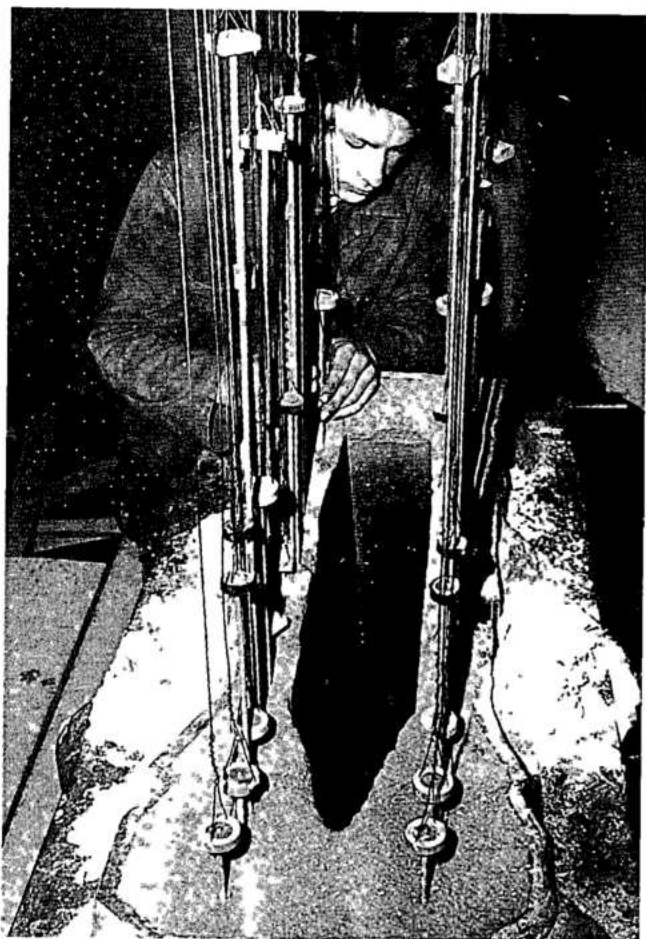


Fig. 9.19 The maximum height hollow gravity block represented by model 1



Structural model 1

Since the results of tests on the preliminary design did not indicate either excessive stresses or weak members which could fail prematurely, and because the dimensional changes in the final design were either minor or conservative, it was decided not to model test the final design.

The model was built to geometric scale $\lambda = 90$. As in this model only the concrete structure was examined, weight forces were applied only to the dam and the foundation was simulated only to provide appropriate boundary conditions. Concrete was simulated by a pumice-cement mortar with modulus $E = 515 \text{ kN/cm}^2$ and a Poisson's ratio $\nu = 0.2$. Basalt layers were reproduced by an analogous mortar, with $E = 550 \text{ kN/cm}^2$ and $\nu = 0.2$, while the foundation breccia layers were made of an epoxy-resin mixture with $E = 370 \text{ kN/cm}^2$ and $\nu = 0.3$, see Fig. 9.20.

The strength of the breccia was made deliberately higher to ensure that premature collapse of that layer would not occur, which would prevent the investigation of the structural behavior of the dam during the failure tests. The powerhouse was represented by a block cast with an epoxy-resin mixture, suitably perforated to simulate the mean deformability of the various parts of the powerhouse structure.

A series of ten tests was initially performed under normal loads, as shown in Fig. 9.21. A sample of the results, whose agreement with the results of FEM computations was very good, is given by Fig. 9.22.

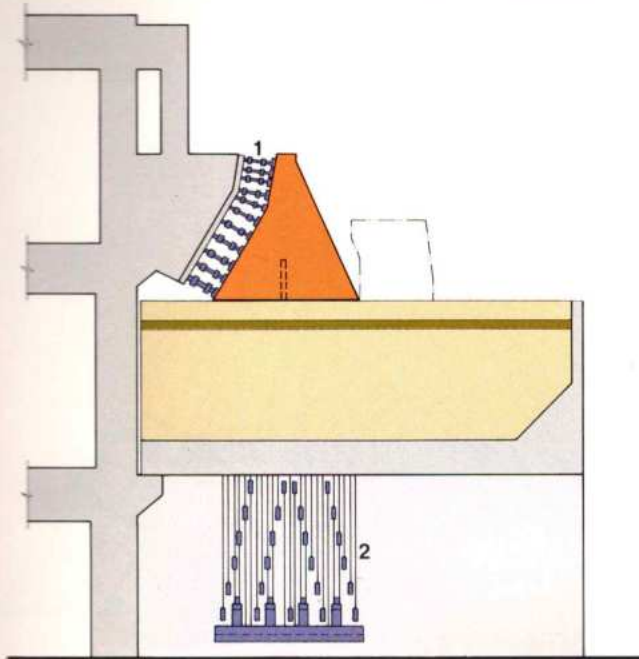


Fig 9.20 Model 1 and its loading equipment

- 1 Water load jacks
2 Dead load jacks and steel wires
Basalt
Breccia

no.	Test	no.	Test
1		6	
2		7	
3		8	
4		9	
5		10	

Fig. 9.21 Model 1 tests under normal loads

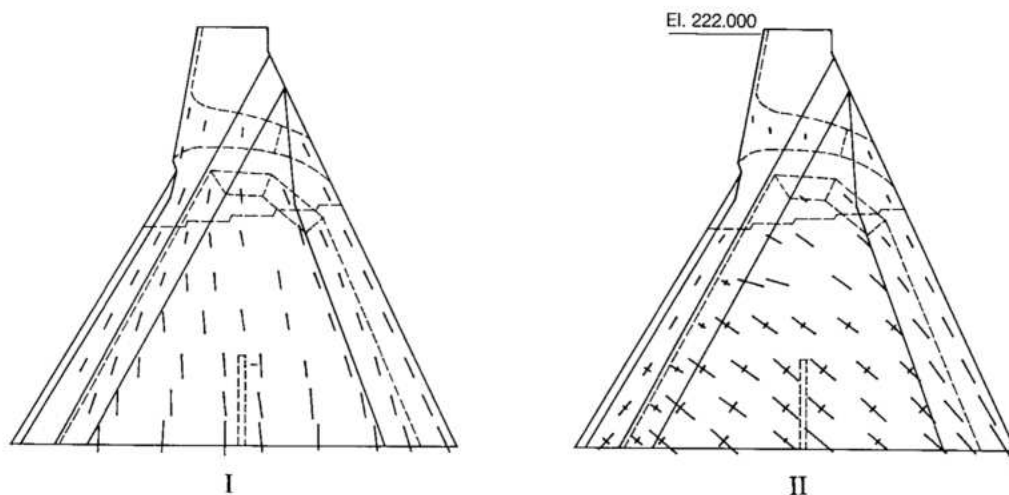
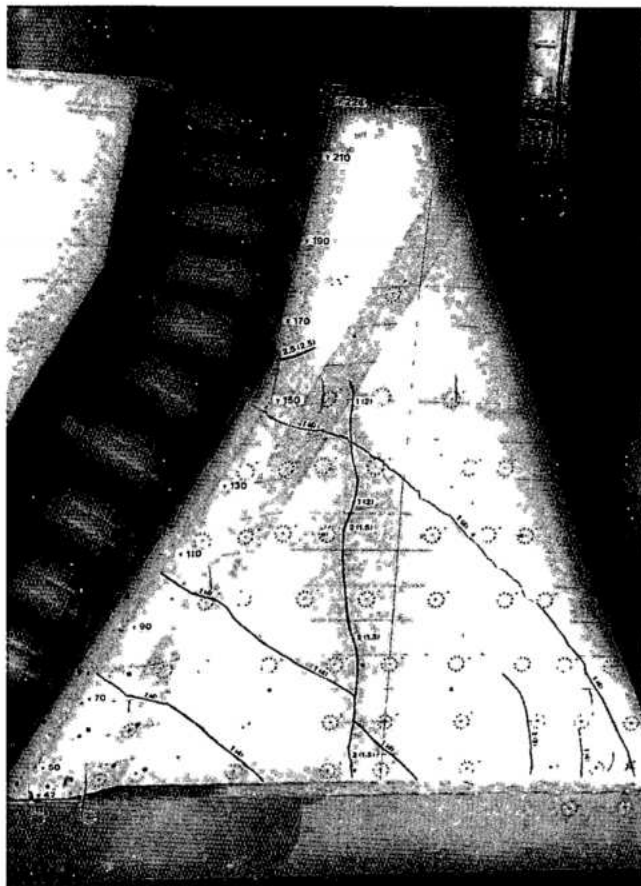


Fig. 9.22 Model 1 typical stress results under normal loads

I Principal stresses with dead load (test no. 1)

II Principal stresses with water load (test no. 2)



Model of main dam blocks, showing cracks

After the first series, tests A and B under increased loads were conducted. Test A consisted of increasing both the weight and the hydrostatic thrust, in increments representing 1.5, 2 and 3 times the normal values of the loads and by applying first the weight increase and then the corresponding hydrostatic thrust increment. During this test, under twice the weight and 1.5 times the thrust, two sub-vertical micro-cracks were detected, from the foundation plane up to El. 120 on one buttress stem, and up to El. 140 on the other, see Fig. 9.23. Both micro-cracks closed upon application of the subsequent increment of the hydrostatic thrust to twice its normal value, and did not progress during the next loading increase. The cracks were ascribed to the influence of the dead load applied through the buttresses, on a diaphragm wall connecting the two stems from the foundation plane to El. 82. This diaphragm was initially considered necessary to improve the lateral stability of the buttresses during their construction; after the model tests the diaphragm wall was deleted. The presence of the two micro-cracks did not affect the performance of the model. For test B, the dead load was first reduced to its normal value and thereafter maintained constant. Then the hydrostatic thrust was gradually stepped up to 4 times its normal value. At this stage, the three cracks, I, II and III of Fig. 9.23 developed, one immediately after the other, approximately following the compression isostatics, causing total collapse of the model.

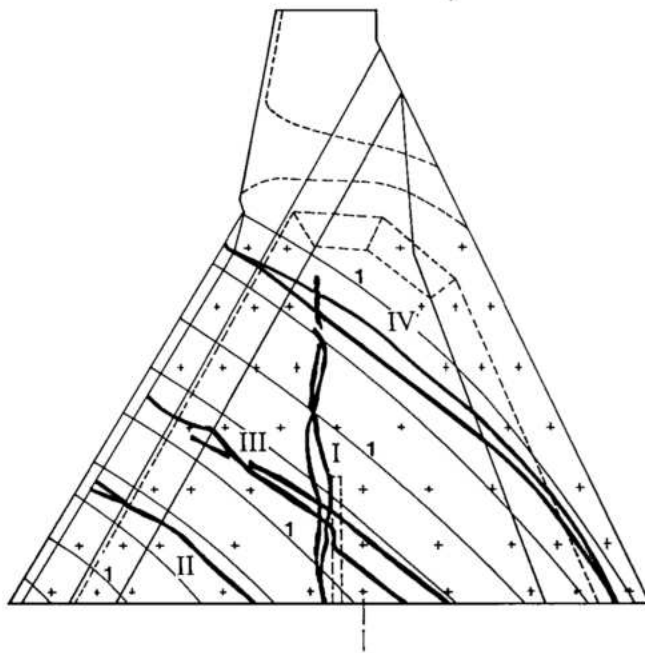


Fig. 9.23 Model 1 cracks developed during tests under increased loads

- I Secondary cracks formed during test A
 II, III, IV Failure cracks formed during final test B
 1 Approximate isostatics for 1G and 4W
 G Weight of structure
 W Hydrostatic thrust

Structural model 3: block with the downstream sloping strut

Some hollow gravity blocks of the main dam were founded immediately upstream of deep excavations for the central assembly area and for the first blocks of the powerhouse on the right bank. Part of the rock slope, from the foundation of these blocks down to the bottom of the excavations, was replaced by sloping, mass-concrete struts, of different heights. Model 3 was of the block with the highest strut (F1/2) and was to scale $\lambda = 75$. The two stems of this block were founded at different levels, El. 115 and El. 125, as shown in Fig. 9.24, in which the mechanical properties of the concrete and the rock layers as used in the model are as indicated in Table 9.1.

Table 9.1 Material properties "As Built" in the model

Material	E (kN/cm ²)	f _{cm} (kN/cm ²)
1 Concrete	1620	2.17
2 Concrete	1980	2.31
3 Basalt	1340 - 1500	1.23 - 1.40
4 "Breccia" (*)	1080	1.00
5 Basalt	1900	1.98
6 "Breccia" (*)	1000	1.00
7 Basalt	2190	2.20

(*) In the model "Breccia" means Breccia + vesicular and/or amygdalobasalt; E = Elasticity modulus, f_{cm} = average compressive strength.

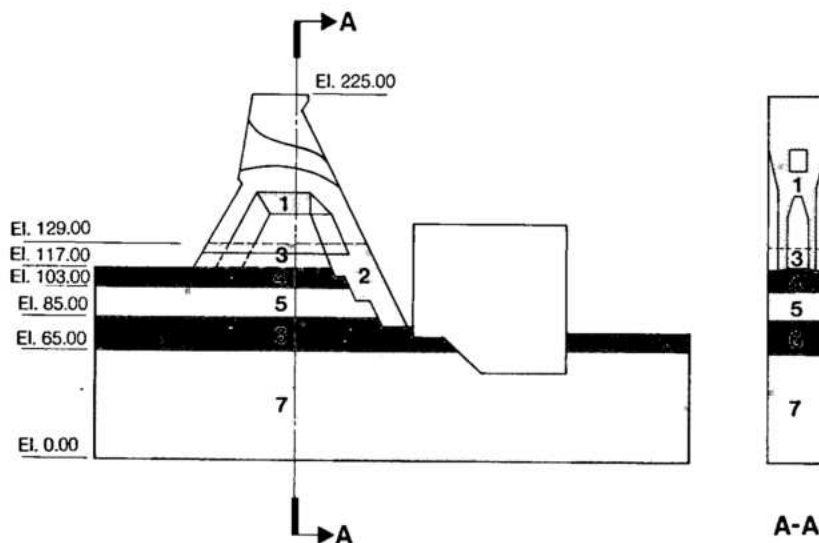


Fig. 9.24 Model 3 for the block with the sloping mass-concrete "strut"

- 1, 2 Concrete
 3, 5, 7 Basalt
 4, 6 Breccia

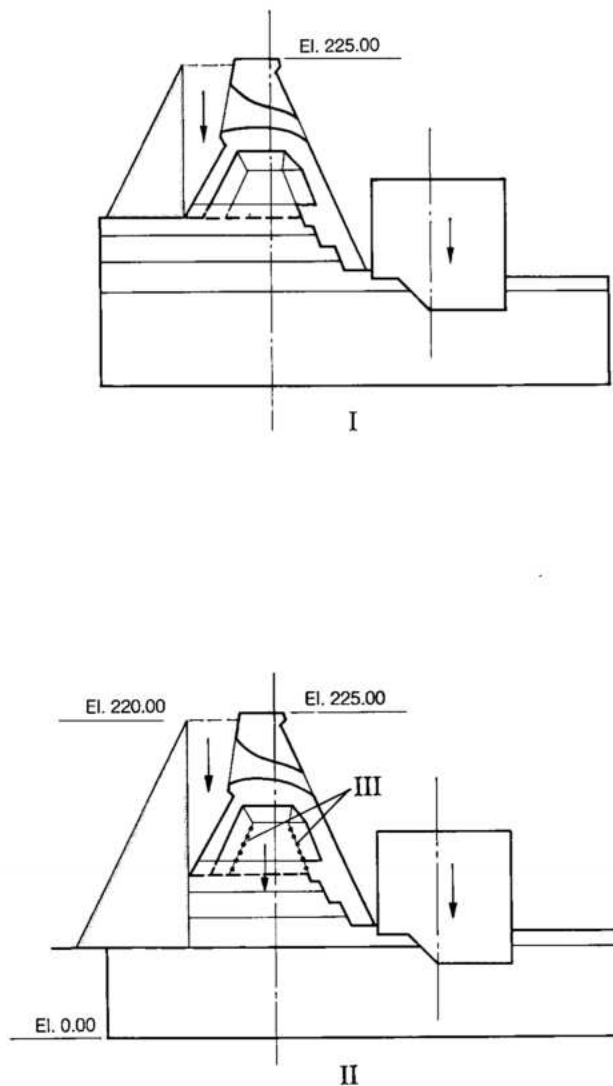


Fig. 9.25 Model 3: principal normal load cases

- I** Configuration 1: initial configuration (no contraction joint simulated)
- II** Configuration 2: simulating the contraction joints, with an upstream vertical crack in foundation, and worst conditions from the models
- III** Configuration 3: same as II above including holes drilled along the alignments of the contraction joints

Model 3 examined the behavior of the combined system comprising the dam block and the rock foundation down to El.65. Appropriate strength characteristics and deformabilities were simulated in the rock layers, together with simulation of the weight of the whole system.

Twelve tests were performed during March-May 1979, with loadings corresponding to the normal values of the dead load of both the structures and the foundation rock, together with water thrust applied to three different geometrical configurations, namely:

1. Without any vertical cracking of the rock at the upstream toe of the dam;
2. Simulating an upstream vertical crack down to El. 65 by removing from the model all the upstream rock down to El. 65.
3. Same as 2. above, plus the simulation of the longitudinal contraction joints "I" and "II" by means of holes drilled along the alignment of the joints to give a 50% reduction of the concrete section, see Fig. 9.25.

Tests to failure were conducted with configuration 3. Fig. 9.25 shows the loading for the test with configurations 1 and 2 under normal loads.

On completion of the tests under normal loads, a prefailure test was performed under loadings corresponding to 1.5 times the normal values of configuration 2 in Fig. 9.25. This test confirmed the results obtained under normal loads. Finally, three more tests were performed under progressively increasing loadings, which were aimed at eventual failure either of the concrete structure or the foundation, or both.

Fig. 9.26 gives representative principal stresses measured during the tests under normal loads. They correspond to the worst conditions for the concrete and rock foundation system. These tests showed the following:

- There were significant differences between principal stresses measured on each side of the block, in the lower region of the strut, which were attributed to the lack of symmetry of the structure.
- The 50% weakening of the concrete sections by the holes drilled along contraction joints "I" and "II" had no significant influence on the stresses and displacements.
- Maximum principal compressive stresses measured were:
 - Stem: < 400 N/cm²
 - Strut: < 550 N/cm²
 - Foundation: < 550 N/cm²

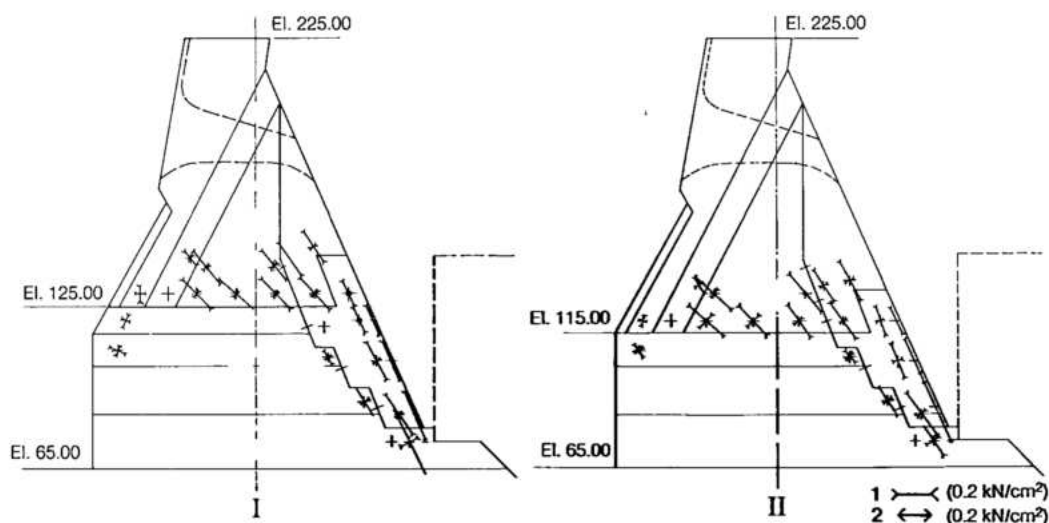


Fig. 9.26 Model 3: a representative set of the principal stresses under normal loads (configuration 2 of Fig. 9.25)

I Left side II Right side 1 Compression (0.2 kN/cm^2) 2 Tension (0.2 kN/cm^2)

• Maximum principal tensile stresses were less than 20 N/cm^2 in the concrete structures and less than 40 N/cm^2 at isolated points in the foundation, e.g. at the bottom of the upstream vertical crack near El. 65. Generally, the model stresses and displacements were consistent with the result of the FEM computations. Fig. 9.27 shows the measured displacements for various water loads, together with those from FEM results for the loading case nearest to that shown in configuration 2 of Fig. 9.25.

Three tests for failure were performed:

1. Application of the dead load G of concrete and rock foundation, combined with hydrostatic thrust W (El. 65 to El. 220), both being increased in parallel, from zero to a maximum of 2.5 times their normal values. In this test, shear failure of the contraction joint occurred in the right stem of the concrete structure, commencing at load $1.5G$ and $1.5W$, see Fig. 9.28.

2. Increasing in parallel, dead load G and hydrostatic thrust W (El. 65 to El. 220), from zero up to 2.5 times normal value; thereafter, while maintaining dead load at $2.5G$, progressively increasing hydrostatic thrust W up to a maximum

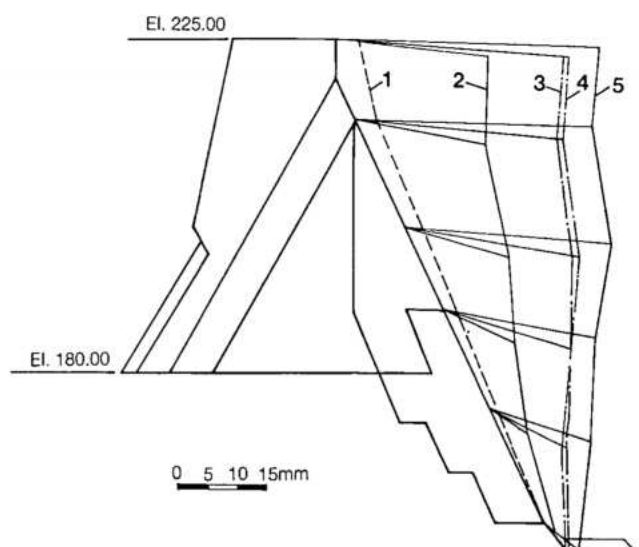


Fig. 9.27 Model 3: horizontal displacements measured and computed

- 1 Water load from El. 115 to El. 180
- 2 Water load from El. 115 to El. 220
- 3 Water load from El. 65 to El. 220
- 4 Water load from El. 65 to El. 220
- 5 Results from FEM computation (water load from El. 61 to El. 220)

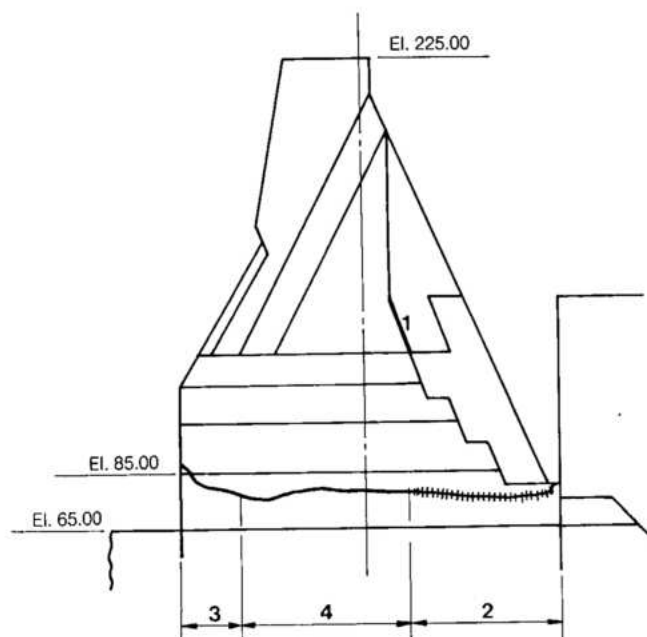


Fig. 9.28 Model 3: crack pattern for 1st and 2nd test for failure

- | | |
|------------------------------------|---------------------------------|
| 1 Contraction joint shear collapse | 3 Tension crack |
| 2 Crushed zone | 4 Compression and shear failure |

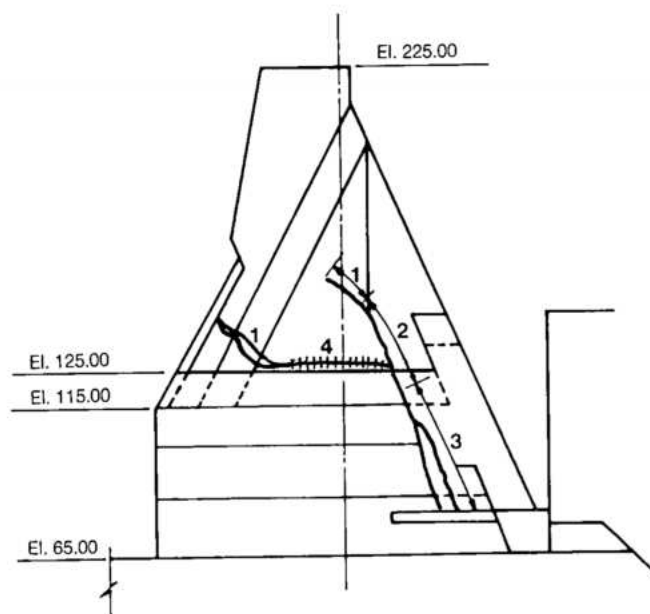


Fig. 9.29 Model 3: final collapse mechanism (3rd test)

- | | |
|---|----------------|
| 1 Tension cracks | 3 Shear cracks |
| 2 Relative movements along the contraction joint, already sheared in the previous failure tests | 4 Crushed zone |

of 3.25 times normal value. In this test, shear failure progressed over the full length of the contraction joint in the right stem, while similar shear failure in the left stem commenced at load 2.5G and 2.5W. At the maximum load for this test (2.5G and 3.25W), crushing failure commenced under the concrete strut and progressed upstream in breccia B, see Fig. 9.28. After the failure in breccia B, hydrostatic thrust W was applied only from El. 115 to El. 220, but was increased to 3.75 times its normal value. This only increased the extent of failure in breccia B and did not produce any new zones of failure.

3. Performed after replacing a considerable portion of the previously crushed breccia B by a polymetric mortar of the same elastic modulus E but of much higher strength. For this test, hydrostatic thrust W was applied only between El. 115 and El. 220. Dead load G and hydrostatic thrust W were both initially increased from zero to 2.5 normal. Thereafter, load G was kept constant and thrust W was progressively increased to 4.75 times the normal. At this last stage (2.5G and 4.75W), the ultimate limit of the strength of the concrete and foundation rock system was reached. Thus, replacement of the weak breccia permitted an increase in the value of W, applied between El. 115 and El. 220, from 3.75 (in the second test) to a maximum of 4.75 times normal value. The failure mechanism finally developed during this test is shown in Fig. 9.29.

Model 3 indicated that for the combined system of the concrete structure and rock foundation including breccia B (with assumed $E = 1 \times 1000 \text{ kN/cm}^2$ and $f_{cm} = 1000 \text{ N/cm}^2$), the global safety factor should lie between 2.5G and 3.25W (thrust between El. 65 and El. 220) and 2.5G and 3.75 W (thrust between El. 115 and El. 220). However, taking into account the particular characteristics of the model and the loading for the second phase of the second test to failure, the global safety factor obtained from the tests was taken to be approximately 2.5G and 3.25W.

The elastic range results obtained from model 3 were consistent with those obtained by means of FEM calculations, confirming the validity of stresses and strains obtained by the latter. The model, in conjunction with FEM calculations, demonstrated satisfactory behavior of the structure under normal loads. The failure mechanism observed in the third IPT test for failure was consistent with the one recorded at ISMES when testing structural model 1 (maximum height main dam block), as illustrated in Fig. 9.23.

The geomechanical model and the prototype

The Itaipu geomechanical model represented almost the entire concrete dam, ensuring appropriate boundary conditions for the central part, see Fig. 9.30. The foundation was simulated down to 110 m below the lowest foundation plane, see Fig. 9.31. The upstream part of the foundation was defined by a surface corresponding to the assumed upstream crack in the foundation. Downstream, the model was extended to a distance corresponding to the outcrop of joint J1, the lowest major joint in the rock mass. Fig. 9.31 gives a schematic representation of the excavation profiles as well as foundation layers and joints, whose parameters for the model are summarized in the accompanying tables.

In addition to simplifications in the geological simulation there were some differences of geometry

between the final design of the structures and the model, which were either insignificant or conservative. These were mainly: excavation profiles, sixteen powerhouse blocks in river channel instead of the fourteen in the model, and excavations for the right and central assembly areas were smaller than those in the model.

Geological features were simplified to permit a suitable simulation at the geometric scale $\lambda = 130$, mainly replacing some groups of non-critical layers by single model layers with the same weight, deformation and strength characteristics. The major joints were simulated as cohesionless friction planes, an assumption which was both conservative for normal conditions and consistent with the investigation to failure. Fractured zones were conservatively replaced by a cohesionless friction joint located at the top of the fractured zone.

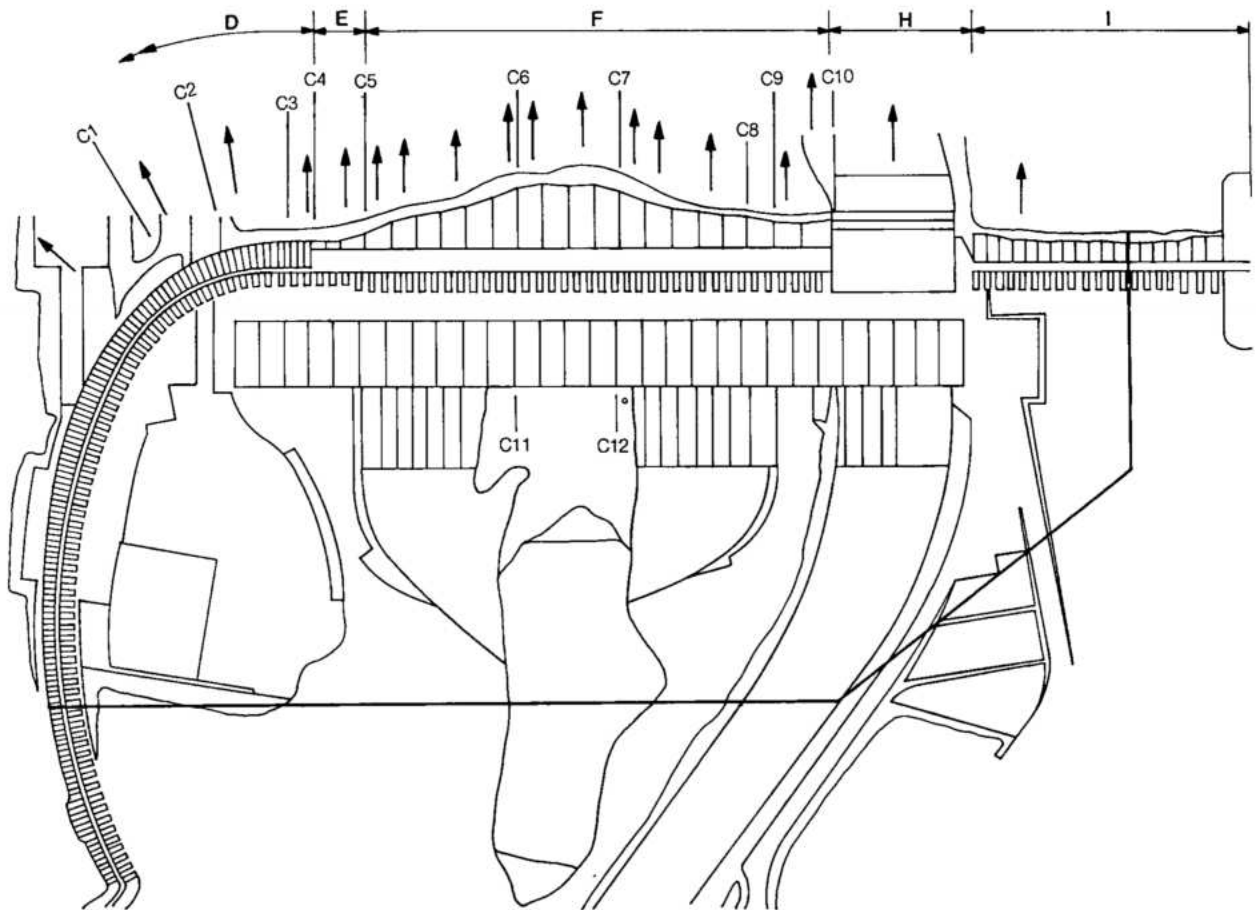


Fig. 9.30 Geomechanical model - model 4

— Project area represented by model
 ↑ Instrumented section

C1 to C12 Cuts between model structural blocks
 D,E,F,H,I Identification of dam blocks

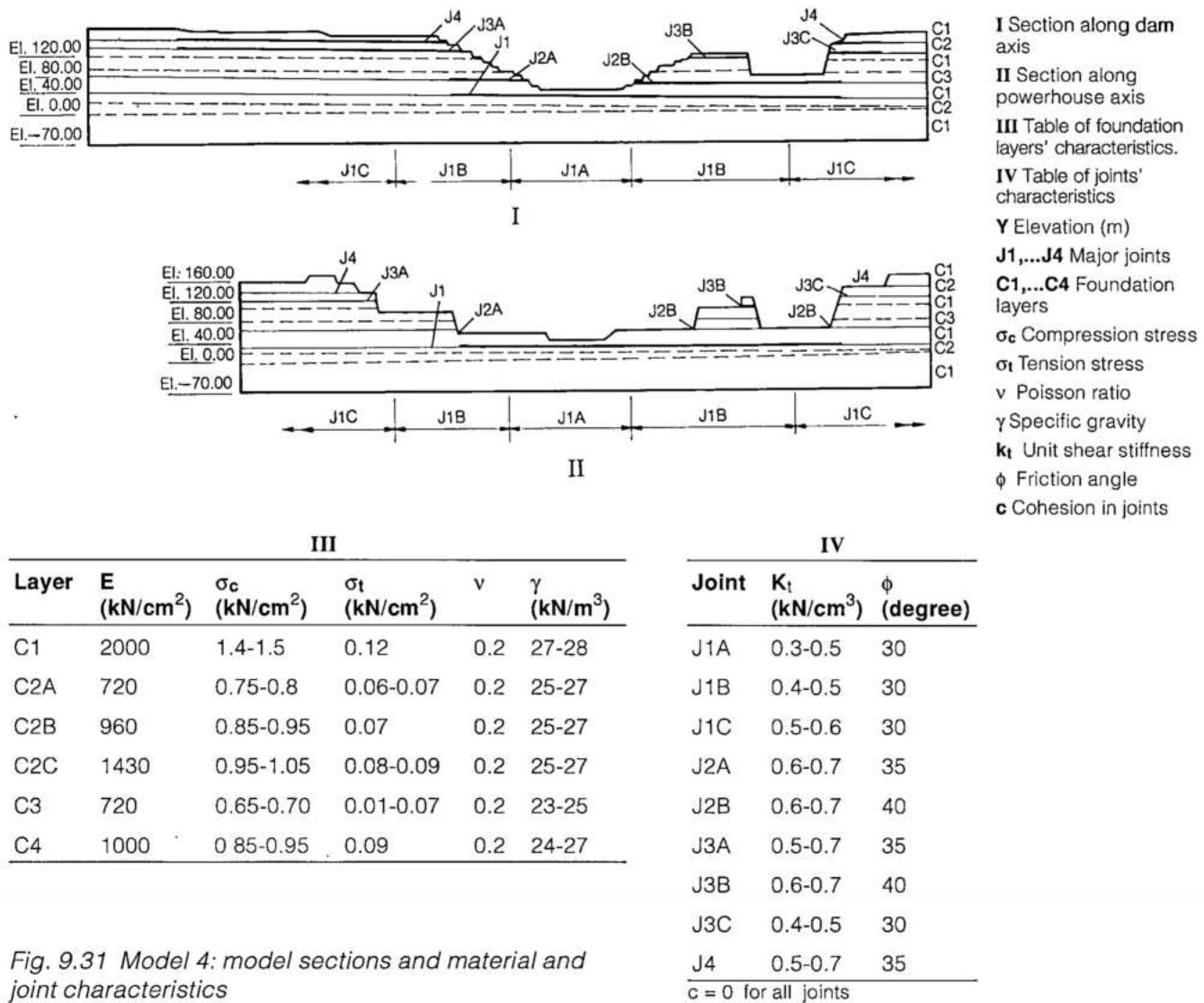


Fig. 9.31 Model 4: model sections and material and joint characteristics

Fig. 9.32 shows the typical transposition to the model of the characteristics of the rock foundation, all of which were conservative.

Correct simulation of the loading of this model demanded that the specific gravity of model and prototype be the same, leading to $\zeta = \lambda = 130$. Therefore, the ultimate compression and tension stresses were also reduced by 130, as well as the modulus E of every material involved. The relationships between Mohr envelopes and stress-strain curves in model and prototype are shown in Fig. 9.33.

For representing concrete with appropriate weight, deformability, and strength to assure that failure would occur in the rock mass and not in the concrete structures, a mixture of powdered

limestone and baryte bonded with resin emulsions was used. These materials had a deformability modulus of 20 to 25 kN/cm² and compressive strength of 30 to 40 N/cm². The addition of glycerine stabilized the water content of the material, thus reducing shrinkage. For the rock layers mixtures of powders bonded with dielectric oils were used. These mixtures, when suitably compressed produced materials having low mechanical characteristics: compression modulus with a minimum value between 50 and 70 kN/cm² and compressive strength between 6 and 10 N/cm². Even at such low values, these mixtures gave a good simulation of the deformation and strength characteristics of the modelled rocks. The lower rock layer from El. - 70 to El. 0, was cast in place.



Geomechanical model

To further ensure compliance with the specified parameters, all the upper layers from El. 0 up to El.180, were built with bonded pre-cast blocks. Each block of concrete structures (dam and powerhouse) was cast in place; so that it would be structurally independent from the adjoining blocks, a varnish coat was applied to its sides.

For the four principal joints in the rock mass, unit shear stiffnesses and friction angles were simulated in the whole extent of each joint, by means of appropriate combination of polyethylene sheets. In the more significant parts of the joints, shown in Fig. 9.31, shear stiffness and friction together with the application of uplift pressures was made by air-pressurized rubber bags filled with monogranular materials. Fig. 9.34 shows the typical results of a shear test with the rubber bag.

Figs. 9.35, 9.36 and 9.37 show some representative sections with the corresponding load

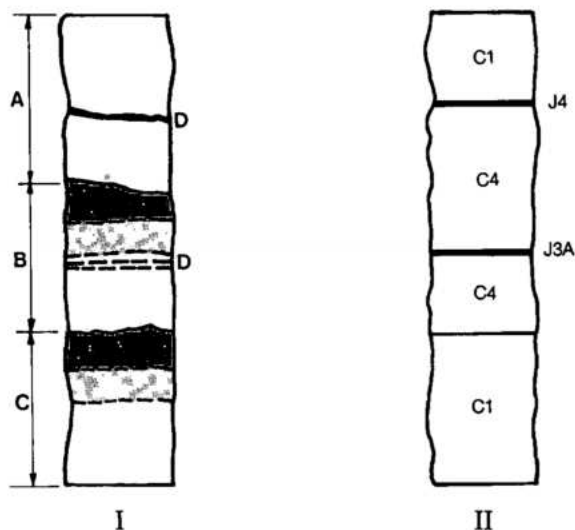


Fig. 9.32 Model 4: model representation of foundation

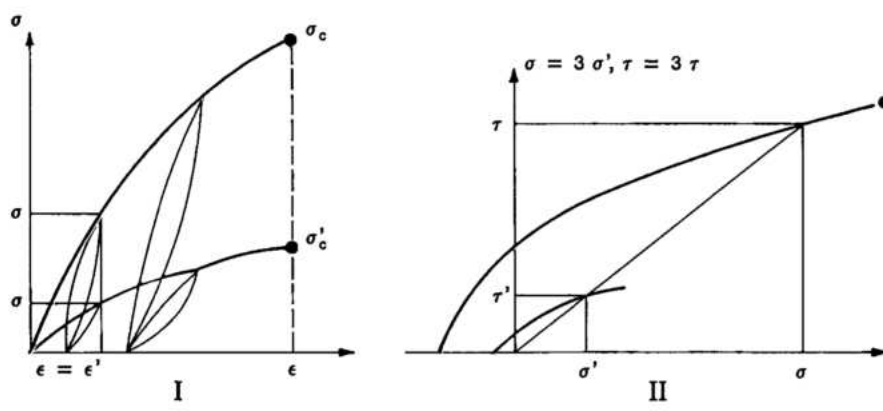


Fig. 9.33 Model 4: stress strain curves and mohr envelopes

diagrams. The hydrostatic thrust was applied by means of small specially built hydraulic jacks, arranged vertically and horizontally, to permit independent control of both components of the thrust for the tests beyond normal loads. The depth of the vertical upstream crack in the foundation was assumed variable according to the characteristics of the foundation layers and joints, their relative location, and the geometry of the excavations. The assumptions were pessimistic, to obtain an experimental estimate of the safety factor against sliding at certain sections of the dam-foundation system. The pressure acting in the vertical crack was assumed either as linearly increasing with depth or as constant, the latter being for deeper zones of the upstream crack.

The triangular or trapezoidal uplift diagrams were transformed into equivalent rectangular diagrams, adapted to the three or two series of uplift bags placed in each of the four joints of the model. Three uplift loadings, shown in Fig. 9.37, were included in the model tests:

- Design uplift representing normal project operation conditions;

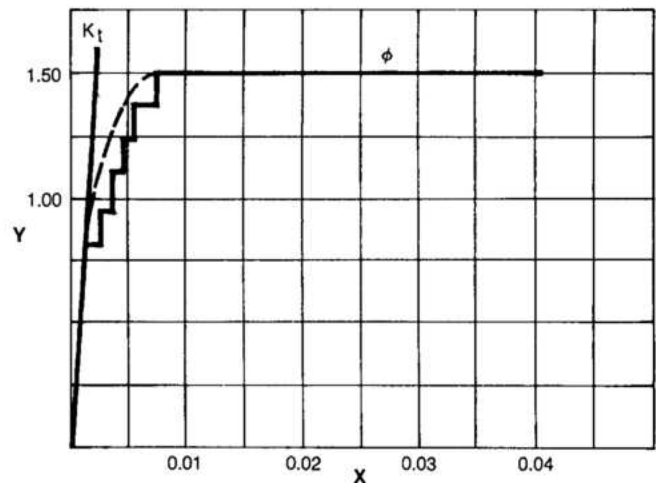


Fig. 9.34 Shear tests with uplift bag

Y Shear stress (N/cm²)

X Displacement (cm)

K_t Unit shear stiffness taken as 685 N/m³

φ Friction angle, taken as 36.5°

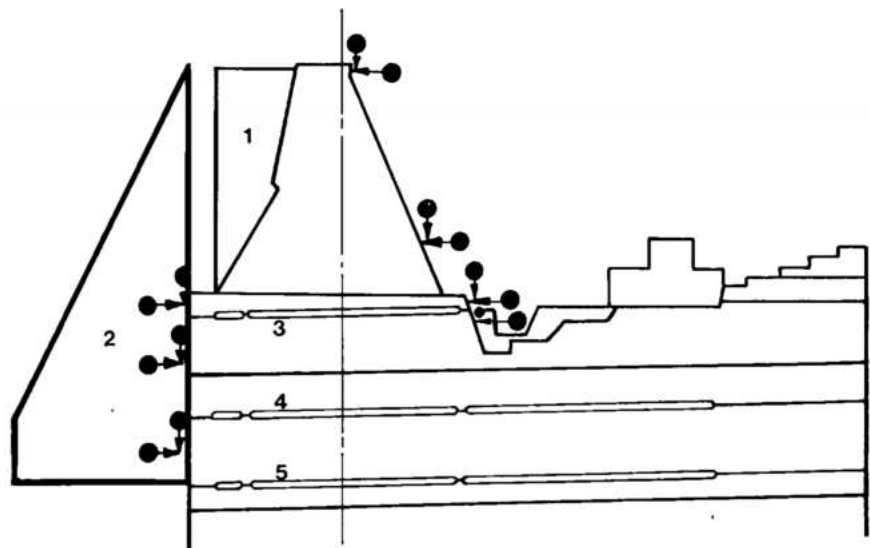


Fig. 9.35 Model 4: typical section of dam blocks upstream of central assembly area

1 Vertical water loads

2 Horizontal water loads

3 Joint J3B

4 Joint J2B

5 Joint J1B

For joints see Fig. 9.31

• Measuring points

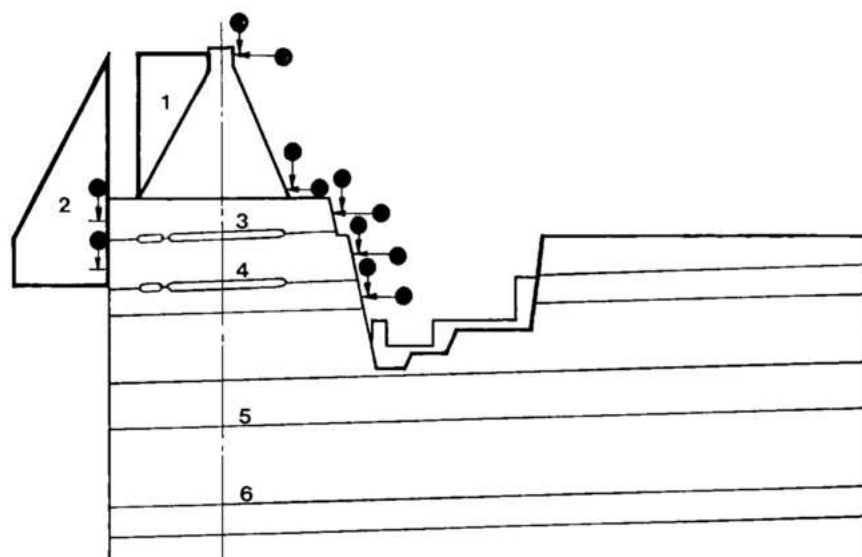


Fig. 9.36 Model 4: typical section of dam blocks upstream of right assembly area

- 1 Vertical water loads
- 2 Horizontal water loads
- 3 Joint J4
- 4 Joint J3A
- 5 Joint J2A
- 6 Joint J1B
- For joints see Fig. 9.31
- Measuring points

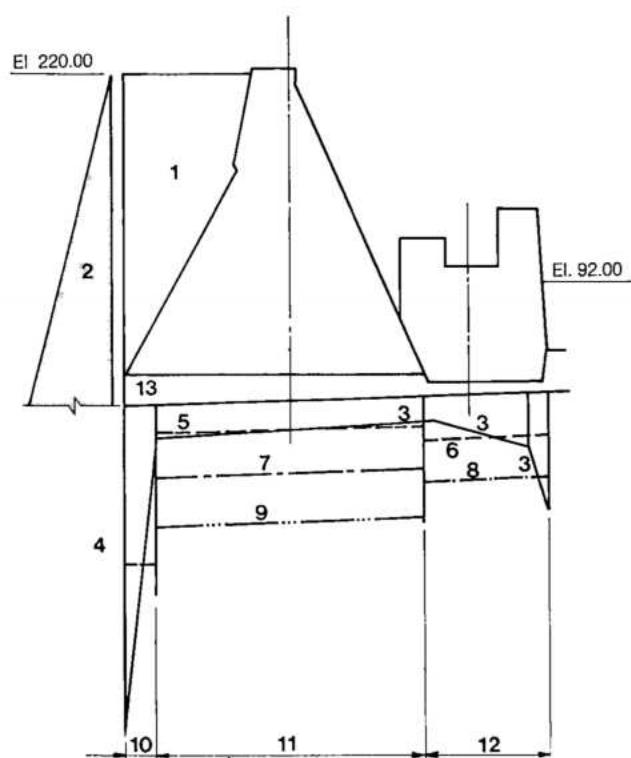


Fig. 9.37 Model 4: typical section of blocks in river channel

- 1 Vertical water loads
- 2 Horizontal water loads
- 3 Actual design uplift
- 4, 5, 6 Model "design" uplift
- 4, 7, 8 Model "friction reducing" uplift
- 9, 8 Model "special" uplift
- 10, 11, 12 Uplift bags
- 13 Joint J1A
- 13 Joint J1A

- Extra uplift for more severe loading conditions;
- Friction reducing uplift.

The last condition was introduced at joint J1 to obtain an effect equivalent to reducing the friction angle of the joint from 30° to 25° . An angle of 30° was considered appropriate when the model was started; later in-situ shear tests made at the site indicated that 25° would be more representative. Later, a fourth condition, called the special uplift, was used in one of the tests.

To ensure conceptual consistency with the computed values of the shear friction factor, only the horizontal component of water thrust was increased during any particular test beyond normal loads, the vertical component being held at its normal value. The same was done with all other vertical loads and uplift. About 200 displacement meters were distributed in nineteen transverse sections, as shown in Fig. 9.30; the instrumentation of several sections is shown in Figs. 9.35 and 9.36. The displacement meters were inductance strain gages of different sensitivity, fixed to a rigid steel structure. To keep dimensional changes to a minimum the testing hall was kept at $20^\circ \pm 0.5^\circ\text{C}$ with 65 to 75% relative humidity. Each set of 200 readings was automatically scanned and recorded at intervals not exceeding 600 seconds on punched tape and subsequently processed.

Tables 9.2 and 9.3 list the series of tests performed on the geomechanical model at ISMES during July to September 1978.

Table 9.2 Preliminary tests

Test	H	Joints with uplift *	"Design" uplift	"Extra" uplift
1	1.0	None		
2	1.5	None		
3	1.5	J3	X	
4	1.5	J3		X
5	1.5	J4	X	
6	1.5	J4		X
7	1.5	J2	X	
8	1.5	J2		X
9	1.5	J1	X	
10	1.5	J1		X
11	1.5	J1-J2-J3-J4		X
12	1.5	J1-J2-J3-J4	X	

Table 9.3 Pre-failure and failure tests

Test	H	Joints with uplift *	"Design" uplift	"Extra" uplift
13	2.0	J1-J2-J3-J4	X	
14	2.0	J1-J2-J3-J4	X	
15	1.75	J1-J2-J3-J4	X	
16	1.0	J1-J2-J3-J4	X	
17	1.75	J1-J2-J3-J4		X
18	2.0	J1-J2-J3-J4	X	
19	2.0	J1-J2-J3-J4		X
20	2.25	J1-J2-J3-J4	X	
21	2.25	J1-J2-J3-J4	X	
22	2.5	J1-J2-J3-J4	X	
23	2.8	J1-J2-J3-J4	X	
24	3.5	J1-J2-J3-J4	X	

* J3 implies J3A, J3B and J3C, etc...

The first test observed model behavior under normal loads without any uplift in the joints. In test 2 the horizontal load was then increased to $H = 1.5$. In these basic reference tests the model behavior was

virtually elastic. The next series of tests (3 to 10) evaluated the individual behavior of each joint when subjected to load $H = 1.5$ combined with either design or extra uplift, a combination which could indicate any unsuspected potential weakness at the joints. This did not occur, and the almost elastic and quasi-linear behavior of the model up to $H = 1.5$ indicated that failure of any part of the model was still remote, see Fig. 9.38. Indeed, the first collapse occurred only at load $H = 2.5$, in blocks F31/32 to F35/36, upstream of the central assembly area.

Tests 11 to 12 were performed, under load $H = 1.5$, with design and extra uplift conditions applied at all four joints simultaneously. They confirmed that after nine tests performed at more than the normal horizontal thrust and under various uplift conditions the model was still reliable.

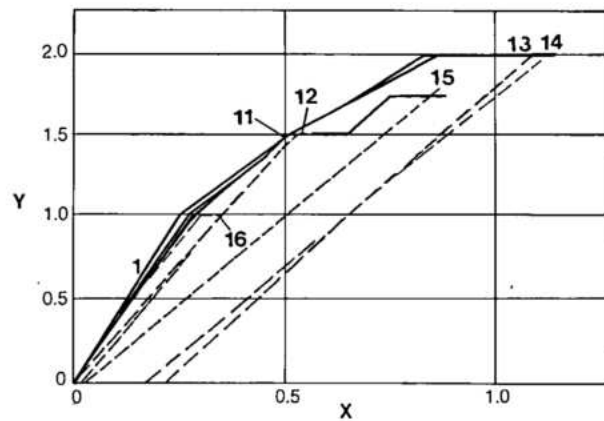
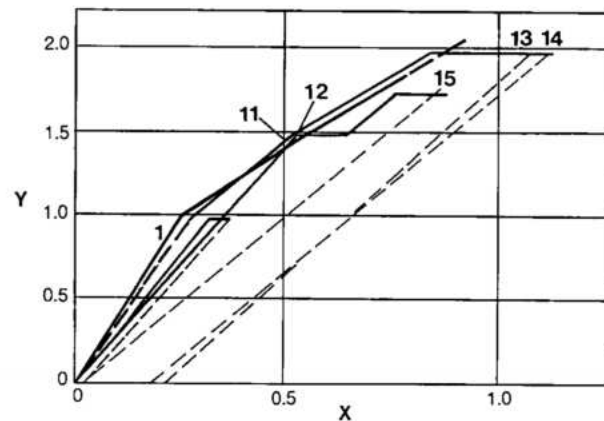


Fig. 9.38 Crest displacements of two model blocks in the river bed during tests 1-11-12-13-14-15-16

Y Horizontal water load
X Displacement (mm)

Some displacements from tests 1 to 16 are shown in Fig. 9.39.

After test 12 the horizontal thrust was increased to $H = 2$ with design uplift on all four joints. In test 13 the deformations increased sharply, especially in the zones upstream of both assembly area excavations, where failure occurred first at $H = 2.5$ for the central assembly area, and then at $H = 2.8$ for the right assembly area. Fig. 9.40 shows progressive displacements recorded at four significant sections during tests 13 and 14 ($H = 2$). In view of the increased rate of deformation which was recorded under $H = 2$, test 14 was a repetition of test 13, but with loading sustained until the approximately 200

recorded displacements were completely stabilized. Final readings for test 14 were only slightly higher than for test 13, but they served to give a clearer indication of the time during which the load should be sustained. From test 15 on, all tests (with the sole exception of test 16 as discussed later), had the friction reducing uplift condition applied at joint J1 (which had been modelled with $\phi = 30^\circ$) in order to simulate a possible lower value of the friction angle ($\phi = 25^\circ$) at this joint. At test 15, with this more severe uplift, the maximum thrust applied was $H = 1.75$, although $H = 2$ had been applied at tests 13 and 14. The displacements measured during test 15 in the central part of the main dam, which were directly

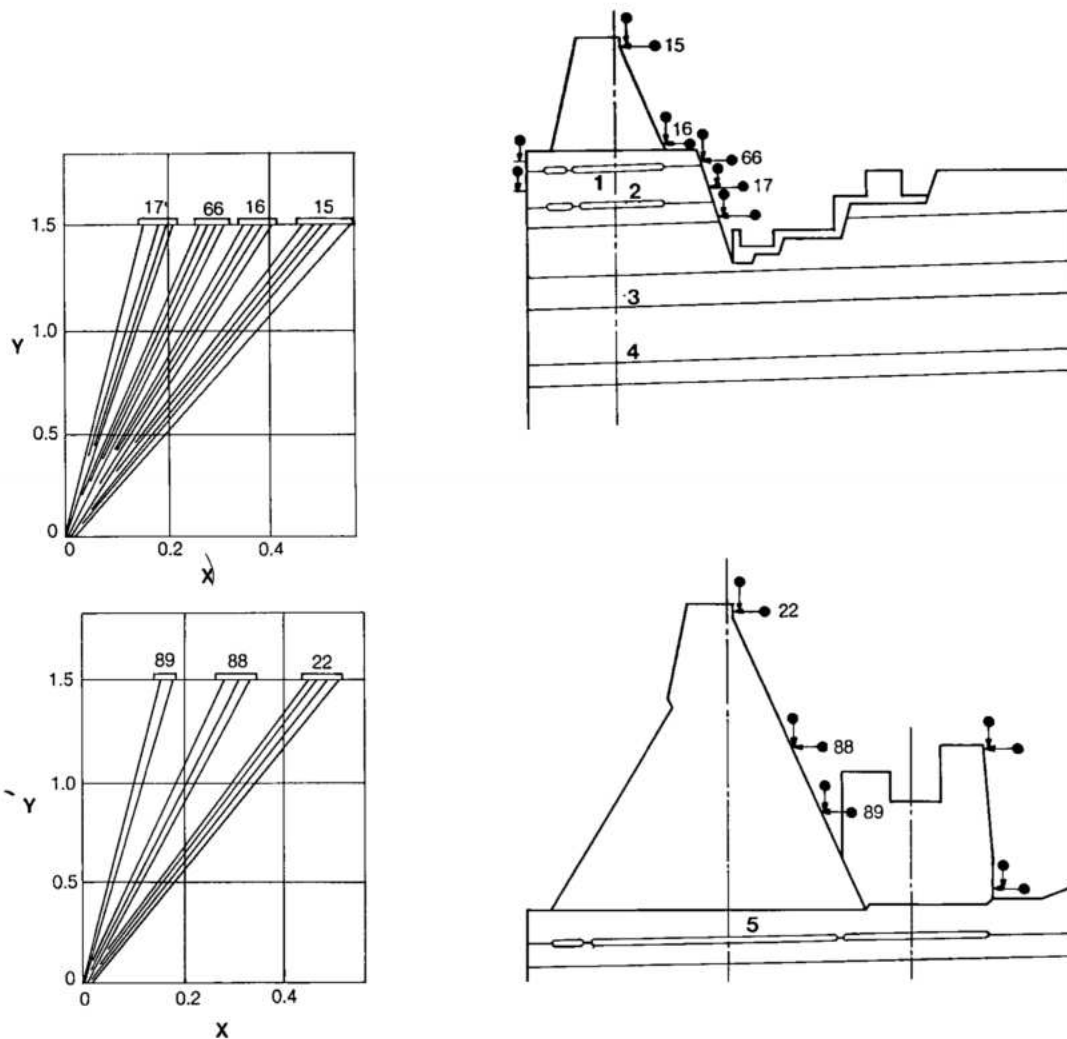


Fig. 9.39 Model 4: typical results from tests 3 to 12

Y Horizontal water loads
X Displacement (mm)
1 Joint J4
2 Joint J3A

3 Joint J2
4 Joint J1
5 Joint J1A
Measuring points

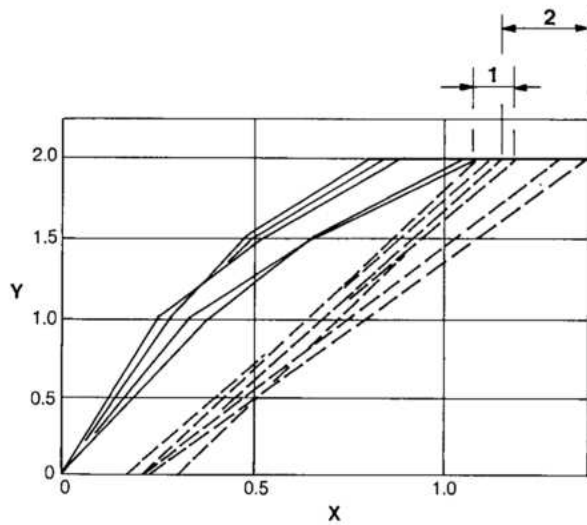


Fig. 9.40 Model 4: dam crest displacements of four representative sections

Y Horizontal water load

X Displacement (m)

1,2 Final readings for tests 13 and 14

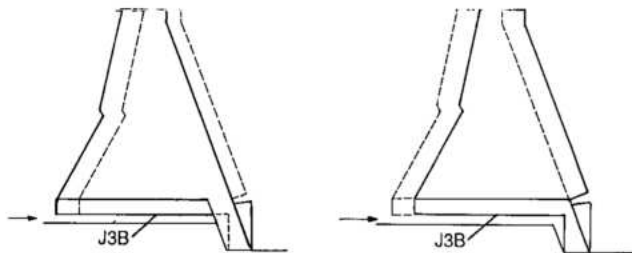


Fig. 9.41 Model 4: collapse mode of block with strut

affected by the friction reducing uplift in joint J1, were not significantly different from those extrapolated from test 12, or obtained at the same loading in tests 13 and 14 ($H = 2$) with no friction reducing uplift. These displacements were subsequently confirmed by all the other tests which included the friction reducing uplift.

Although each block of the model dam and powerhouse was cast independently from the adjoining blocks, twelve cuts were made between concrete blocks down to rock surface at different phases of testing, to further ensure the complete independence of groups of similarly founded blocks with the large displacements typical of tests with increased H , especially in the failure phase. Cut locations are shown in Fig. 9.30. Cuts 1 to 4 were made before test 15, to eliminate any possible arching effect between the D and E buttresses, thus restricting the possibility of an arching contribution to the rock layers. Comparison of displacements observed at test 15 with those previously recorded did not show any significant variation.

In test 16 with the special uplift and $H = 1$, no significant variation of the displacement was observed in comparison with the previous tests with considerably smaller uplifts, see Fig. 9.39.

Test 17 was similar to test 15, but with the extra uplift instead of the design uplift. The displacements were about the same as those for test 15, and no other special effects were noted. Tests 18 to 21 were made to cautiously approach failure, which was expected first under the three F blocks upstream of the central assembly area. Test 19 ($H = 2$) was done under the extra uplift condition. In test 20, complete stabilization of joint displacements was observed under $H = 2.25$, this being subsequently confirmed with longer sustained load at test 21.

Before commencing test 22, cuts 5 to 10, see Fig. 9.30, were made, assuring complete independence of all dam blocks. At test 22, under $H = 2.5$, the ultimate resistance of joint J3B was reached. The whole rock layer above joint J3B under the three blocks upstream of the central assembly area slid. Of those three blocks, one had a concrete strut, whose liaison with the block itself was destroyed by the push of the upper rock layer, resulting in conspicuously independent movement of the block, see Fig. 9.41. Fig. 9.42 shows the horizontal displacements recorded at joint J3B during test 22 up to the collapse. Also shown is the median of the corresponding movements of joint J3B measured during the previous 21 tests. The difference between the median displacements from tests 1 to 21 and the displacements from test 22 is

almost entirely due to cuts 8, 9 and 10 between blocks executed after test 21.

Tests were resumed after disconnecting the hydrostatic thrust jacks above the already collapsed joint J3B, and performing the last two cuts (11 and 12), between powerhouse blocks. For test 23, maximum hydrostatic thrust was increased to $H = 2.8$ and sustained for approximately 8 hours. Continuous displacements of joints J4 and J3A along the whole segment upstream of the right assembly area excavation, and with local surface failures, clearly indicated that resistance of joint J4 and J3A had been overcome. Fig. 9.43 illustrates the development of displacements at both joints up to failure.

After disconnecting the loading jacks of D and E blocks, the final test, no. 24, was performed to reach the collapse of F and H blocks with the exclusion of the already collapsed F portion upstream of the central assembly area. Although the maximum thrust applied was $H = 3.5$, on a conservative basis, $H = 3.25$ was taken for the shear friction factor of joint J. Collapse was initiated under the blocks at the left abutment and continued under the river blocks towards the right abutment, accompanied by local rupturing of the strata downstream of the powerhouse. Maximum thrust $H = 3.25$ to 3.50 also overcame the resistance of joint J2B ($\phi = 40^\circ$) under the diversion control structure. Figs. 9.44 and 9.45 show the significant displacements.

Table 9.4 summarizes the final results. The column, "Inferred SFF ϕ (shear friction factor)" was obtained from analyses of the values of the increased horizontal thrust both at the beginning of plastification and at collapse, together with the corresponding progression of the significant displacements. The values 3 to 3.25 for blocks F1 to F30 are roughly twice the FEM computed values; this is because of the strong arching resistance of the deep sound rock strata between the foundation surface and joint J1.

Analyses of the approximately 5000 load displacement curves had shown a remarkable degree of consistency, both in the various transverse sections and all along the dam axis. Additional confirmation of dependability of ISMES technique and the geophysical model was the consistency of the model test displacements in the elastic range with those computed by conventional bidimensional mathematical analyses. In view of the three dimensional strength reserve of the foundations, the model tests indicated higher shear-friction factors of safety than the numerical stability analyses.

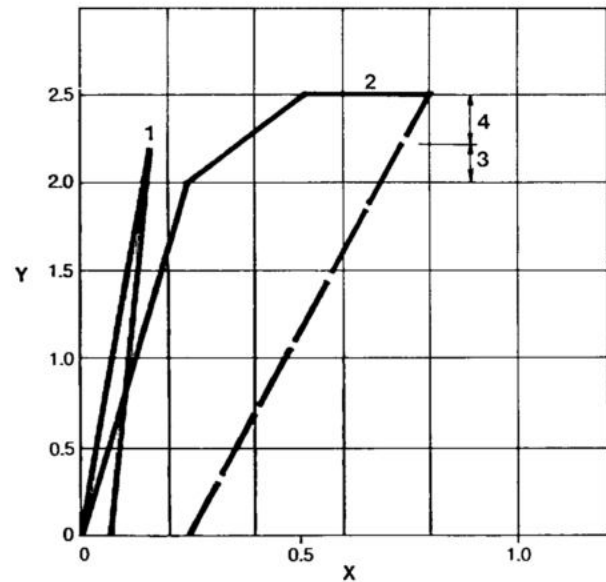


Fig. 9.42 Model 4: horizontal displacements of joint J3B

- Y Horizontal-water load
- X Displacement (mm)
- 1 Median of tests 1 to 21
- 2 Test 22
- 3 Beginning of large displacement
- 4 Failure

Table 9.4 Displacement test results.

Blocks involved	H at initial plastification	H at failure	Failure features	Inferred SFF ϕ
F31 to F36	~ 2.0	2.5	J3B $c = 0$ $\phi = 40^\circ$	~2.25
D51 to E6	~ 1.75	2.8	J4 and J3A $c = 0$ $\phi = 35^\circ$	~2.25
F1 to F30	> 2.30	3.5	J2 $c = 0$ $\phi = 35^\circ$ $c = 0$ $\phi = 40^\circ$ J1 $c = 0$ $\phi = 25^\circ$	3.0-3.25
Stretch H	> 2.5	3.5	J2 $c = 0$ $\phi = 40^\circ$	3.0-3.25

CONSTRUCTION OF THE HOLLOW GRAVITY AND BUTTRESS DAMS

CONSTRUCTION SEQUENCES

Principal sequences for construction of the main hollow gravity and the two wings of the buttress dams were as follows:

- For the eighteen hollow gravity blocks.
- Excavation for the stepped dam foundations proceeding from top of each bank to about El. 140.
- Foundation excavation below El. 140 after completion of the cofferdams, river diversion and dewatering.
- Consolidation grouting of the foundations for the upstream heads.
- Concrete placement first in two blocks on the left bank to El. 144, then simultaneously in several blocks proceeding from top of both abutments towards the river bed.
- Subsurface treatment and construction of shear keys under the river bed and in one discontinuity in the right abutment, concurrently with construction of the dam blocks.
- Construction of the power intake and trashrack structures on top of sixteen blocks.

For the buttress dams.

- Excavation for the foundations of the right wing dam at the right end, as continuation of spillway approach

channel, and for the last six blocks simultaneously with excavation for the main dam blocks.

- Excavation of foundations for the nineteen buttress blocks between the diversion control structure and the rockfill dam.
- Consolidation grouting of the foundation of the heads prior to concrete placement.
- Concreting of eight to ten blocks at the same time, proceeding from right to left. The last six E blocks were completed concurrently with the hollow gravity blocks.
- Construction of the left wing blocks and the concrete wall at the interface between the rockfill and the buttress dam.

FOUNDATION EXCAVATION AND PREPARATION

Foundation Excavation

The excavation profile of the foundations for the main dam blocks was stepped at different levels between El. 30 in the river channel and El. 160 above the river banks, so that the structure is founded entirely on physically sound rock, see Fig. 9.46. The disposition of horizontal platforms and almost vertical steps, see Fig. 9.47, permitted a more uniform support for the stems of the hollow gravity blocks and facilitated access during construction. The total volume of rock excavated for the foundations of the main dam was about $2.2 \times 10^6 \text{ m}^3$.

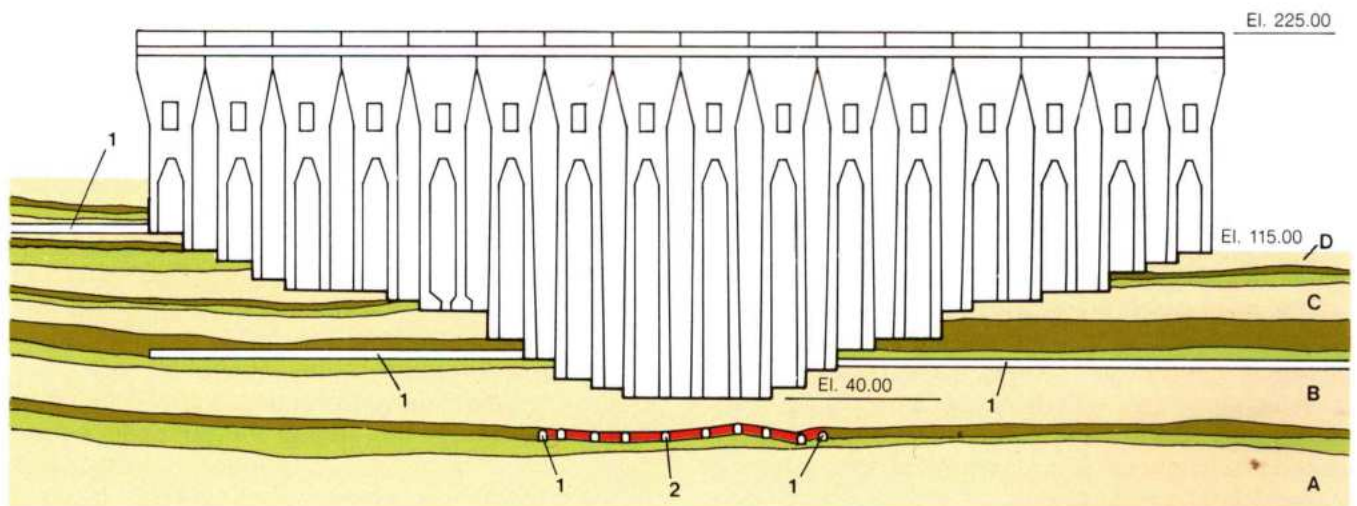


Fig. 9.46 Main dam foundation and excavation profile

1 Drainage tunnel

2 Shear keys

A, B, C and D Flows

— Flow contact

Dense basalt

Vesicular amygdalobasalt

Breccia

Shear zone

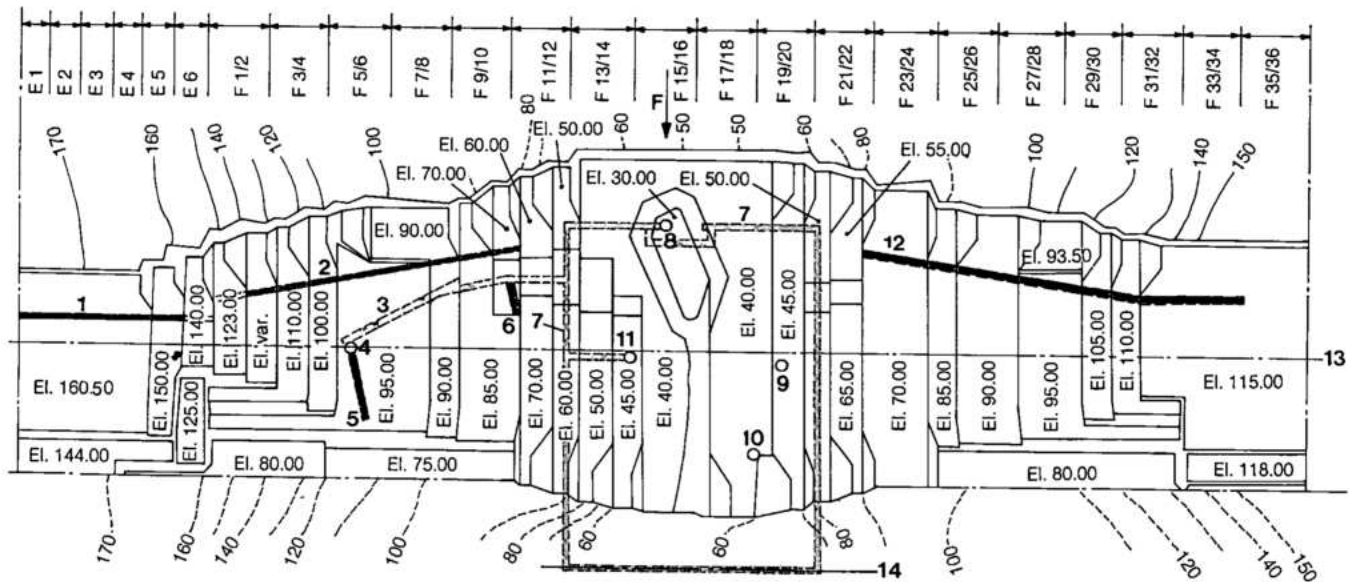


Fig. 9.47 Main dam excavation plan

- | | |
|--|--|
| 1 Exploration and drainage tunnel at El. 125 | 7 Exploration and drainage tunnels at El. 20 |
| 2 Exploration and drainage tunnel at El. 60 | 8,9,10,11 Exploration shafts to Els. 20 and 12 |
| 3 Exploration and drainage tunnel at El. 12 | 12 Exploration and drainage tunnel at El. 55 |
| 4 Exploration shaft at the right bank at El. 7 | 13 Dam axis |
| 5 Exploration tunnel at Els. 76 and 61 | 14 Centerline of powerhouse units |
| 6 Exploration tunnel at El. 20 | F Flow direction |

The axis of the main dam is approximately perpendicular to the river channel. In the upstream areas of the dam, the contour lines of the abutments diverge, and consequently the foundation of the heads had to be excavated deeper. To minimize the excavation, as well as the volume of concrete, longitudinal steps were adopted in the excavation of the upstream area, the slopes were reduced to 1 V:2 to 3 H and the height was, in general, limited to 10 m. These steps coincided with the longitudinal contraction joints in the stems. Also, this was done to minimize differential settlements of the monoliths and concentrations of stresses in the dam structure.

The configuration and location of the steps allowed the stems to be concreted against rock, giving protection to the excavated rock slopes. To avoid significant differential settlements between contiguous stems, these transverse steps were limited to a height of 15 m. Under the upstream heads of the hollow gravity blocks the vertical steps were reduced to a slope of approximately 1 V:2.2 H when located in the middle of the block and 1 V:0.4 to 1 H between blocks. This gave a more gradual profile to the excavation, avoiding concentrations of stresses

in the dam and permitting a better contact between the concrete and the rock. Additionally, because the foundation of the head was partially below the foundation elevation of the stems, a certain horizontal interlink of the block was achieved.

Some foundations of the hollow gravity blocks were immediately upstream of the deep excavation for the powerhouse. Therefore part of the stepped rock slope was reinforced by an inclined mass concrete strut in order to improve the stability of the foundations, see Fig. 9.48.

Primary drilling and blasting was carried out in 10 m lifts. As the excavation approached within 5 m of a designated foundation or slope, depth of the drill holes was reduced and the blasting controlled to minimize disturbance of the foundation rock. Low pressure consolidation grouting with 10 m deep holes was done in the area of the upstream heads prior to the final cleanup with high pressure water jets and erection of forms for the concrete.

From the foundation area of the main dam the excavated rock was hauled out mostly from the upstream side and taken to the stockpiles on both banks.

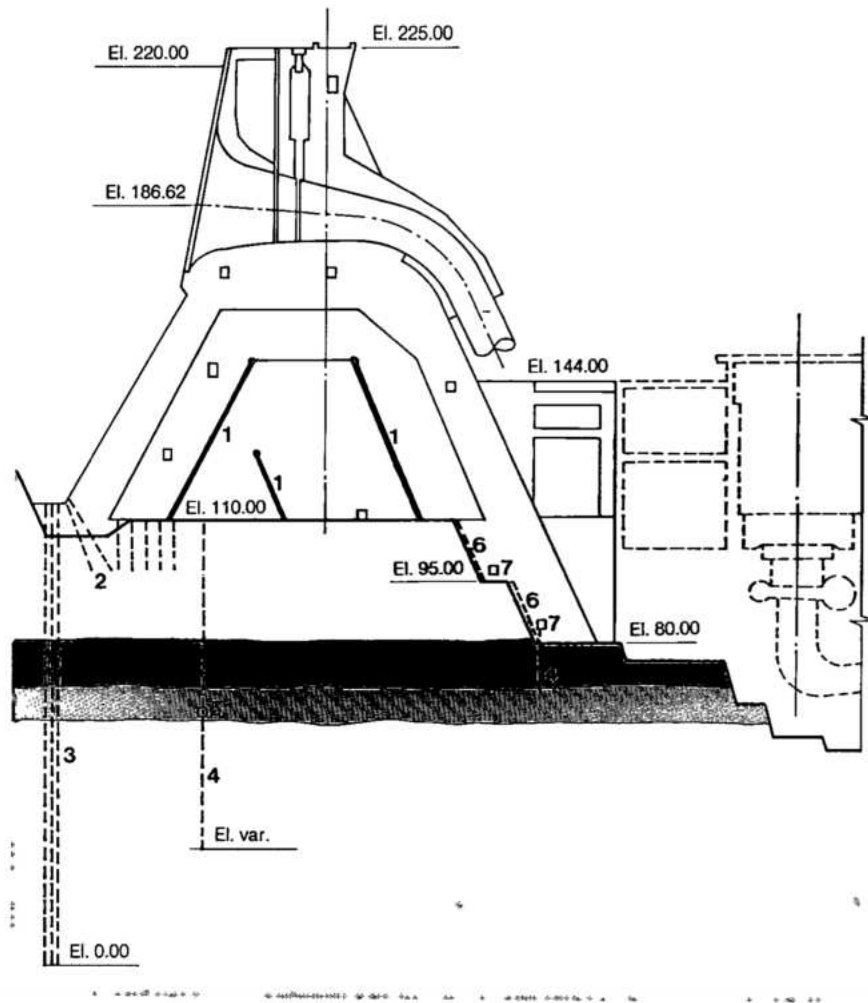


Fig. 9.48 Foundation treatment of blocks with stepped downstream rock slope

- 1 Contraction joints
- 2 Consolidation grouting
- 3 Grout curtain
- 4 Drainage holes
- 5 Drainage tunnel
- 6 Halfround tile drains
- 7 Drainage gallery
- Dense basalt
- Breccia
- Vesicular amygdbasalt

Excavation for the foundations of most of the wing buttress dam blocks was relatively shallow, 5 to 15 m. Also, the differential levels between the adjoining blocks were from 0 to 5 m only. For two blocks on each bank, it was necessary to excavate 5 to 10 m deep shafts to remove rock unsuitable for foundations.

Foundation grouting

The design of the grout curtain and the drainage systems of the main dam was governed principally by the fractured zones or the pervious discontinuities in the foundation. As some of the relatively pervious discontinuities or zones daylighted upstream of the dam in the area of the reservoir and the others downstream of the powerhouse, there was a possibility of substantial seepage flow into the dam area. To reduce and control seepage, complete isolation of the foundation area of the highest blocks of the dam by a grout curtain was necessary. In addition, drainage tunnels were excavated to effectively reduce uplift pressures in the foundation strata.

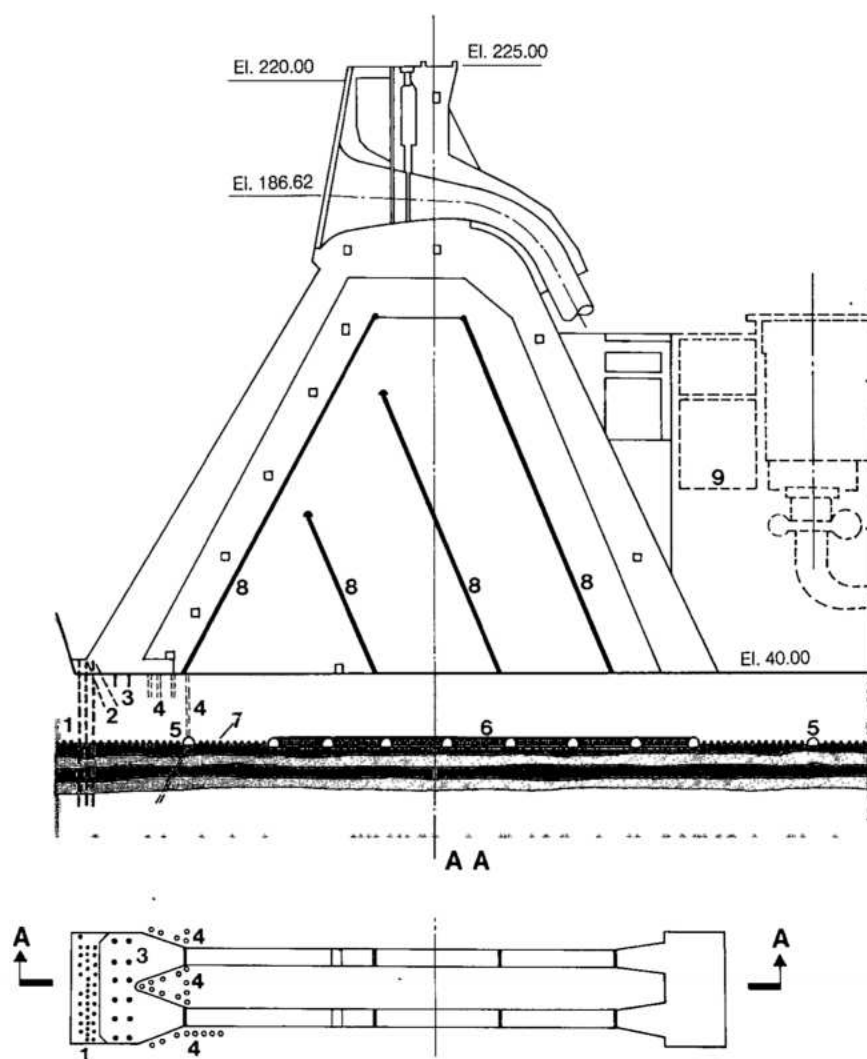
The main grout curtain is located upstream of the dam blocks and interconnects with the downstream grout curtain of the powerhouse through transverse curtains at the abutments, see Figs. 9.49 and 9.50.

Two rows of holes spaced at 3 m centers were drilled and grouted from a platform upstream of the dam. First, the downstream row holes were grouted by split-spacing sequence. Then the holes in the upstream row were grouted in the same manner. An additional central row of holes was drilled and grouted in areas where the grout absorption in holes of either of the first two rows exceeded 12.5 kg/m. Where very pervious zones were encountered, additional holes were drilled and grouted. The transverse curtains connecting with the powerhouse were made in a similar fashion.

The depth of the curtain in the different stretches of the dam depended on the geological characteristics of the foundation. In the river channel it was 40 m under the highest blocks of the dam, intercepting contact A/B and joint A.

Fig. 9.49 Foundation treatment of hollow gravity block in the river channel

- 1 Grout curtain
 - 2 Contact grouting
 - 3 Consolidation and contact grouting
 - 4 Drainage holes
 - 5 Drainage tunnel
 - 6 Shear keys
 - 7 Discontinuities
 - 8 Contraction joints
 - 9 Powerhouse
- Dense basalt
 Breccia
 Vesicular amygdbasalt



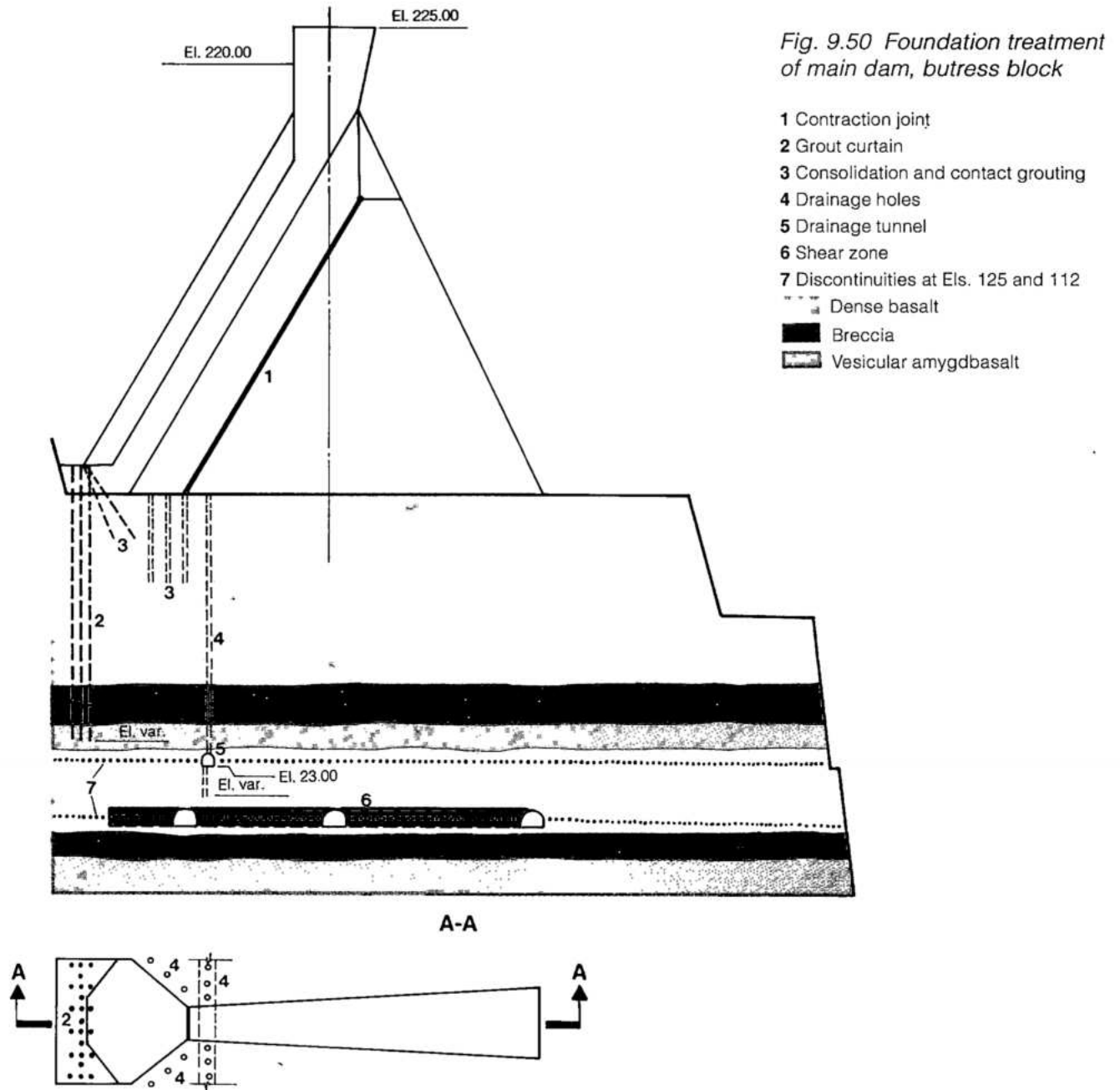
In the highest blocks situated in the river channel, galleries were located downstream of the transverse contraction joints between blocks to provide access for supplementing the grout curtain, should it become necessary. In addition, contact grouting was executed from the upstream platforms of the blocks, consisting of two lines of holes inclined downstream, reaching 6 m below the block foundation level at 3 m spacing, see Fig. 9.48. The purpose of this grouting was not only to ensure adequate impermeability of the upper rock foundation levels under the upstream, but also to reinforce the upstream grout curtain, if necessary, by regrouting from behind the head between the stems.

Under the upstream heads of the blocks' consolidation grouting and impermeabilization treatment was performed after pouring the first concrete lift. It consisted of 3 m deep holes on 6mx6m centers injected by the split spacing method; the spacing was reduced if grout

absorption was higher than 12.5 kg/m. The grouting was to plug any fractures in the upper zone of the foundation which might have been opened by blasting during excavation.

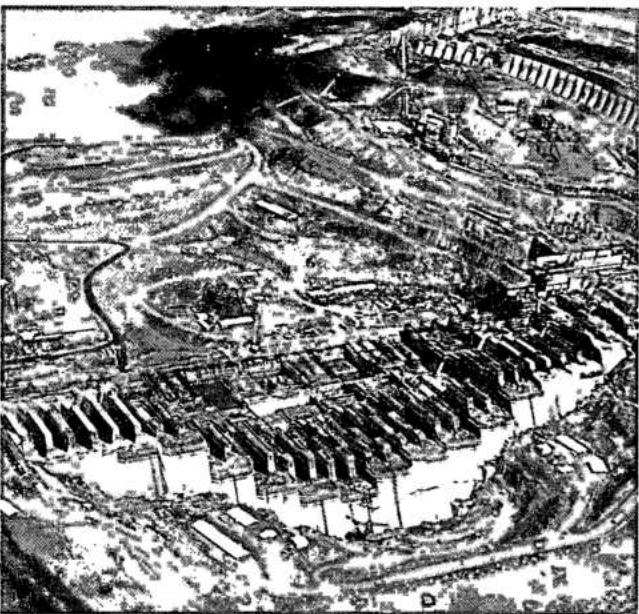
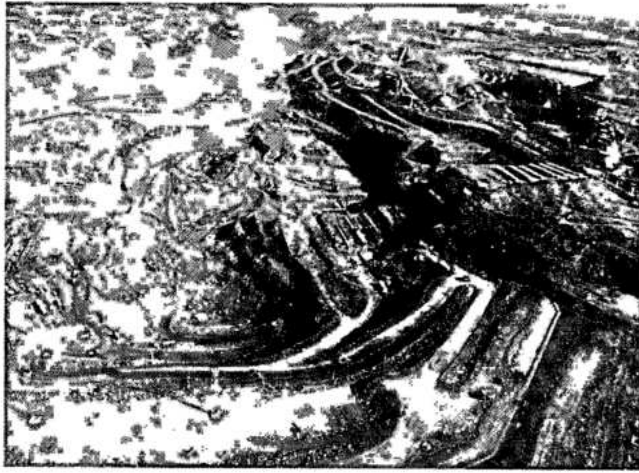
Foundation drainage system

The foundation drainage system is particularly important for the main dam because of a sliding tendency along the sub-horizontal discontinuities in the foundation. Behind the upstream drainage lines these discontinuities had to be maintained free of seepage flow, with piezometric levels below the elevation of the foundation of the concrete blocks. Therefore the exploratory tunnels excavated along the principal discontinuities were incorporated into the foundation drainage system, see Figs. 4.3, and 9.46. These tunnels were located along the discontinuities at El. 125 and El. 60 in the right abutment, at El. 20 in the river bed and at El. 55 in the left abutment.



Between the stems, next to the upstream heads of the hollow gravity and wing buttress blocks, a line of fan-shaped vertical drains 102 mm in diameter, spaced at 2 m, connected the foundation surface with the drainage tunnels. This drain curtain further extended from the drainage tunnels into the lower levels of the rock corresponding to the depth of the grout curtains.

In the river channel area, in addition to the upstream drainage tunnel at El. 20, a downstream longitudinal tunnel under the powerhouse and two transverse tunnels were excavated, isolating an area of approximately 145 m x 185 m. These lateral tunnels were also connected to the surface through 102 mm diameter drain holes, spaced 6 m apart drilled upward from the tunnels.



Main dam construction sequence

The drainage system in the foundation benches of the dam consists of one or two lines of approximately horizontal holes drilled through the buttress stems at 5 m spacing.

The pumping system which handles the drainage water is described in Chapter 10.

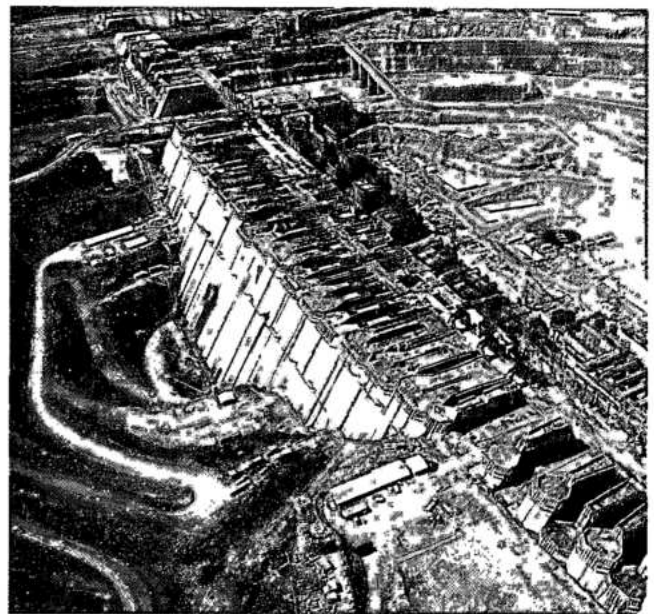
CONCRETE CONSTRUCTION

Hollow gravity blocks

A typical high hollow gravity dam block was divided into eight monoliths formed by the longitudinal contraction joints for about 60% of its height, see Fig. 9.5. Concrete was first placed in the first two monoliths of the buttresses, between contraction joints A and B. After these monoliths had reached a height of 5 to 10 m, the next downstream monoliths between contraction joints B and C were concreted to one or two lifts below the first monoliths. Concrete placement in the massive upstream head was then done with concrete in the first buttress monoliths at least 5 m higher.

The monolith forming the downstream head was the last to be constructed. In the abutment blocks where a strut extended below the downstream head, concrete in the strut was placed before any in the block itself.

Typical lift heights commencing from the foundations were 0.5, 1.5 and 2.5 m; thereafter the standard 2.5 m lift was used up to the base of the power intakes.



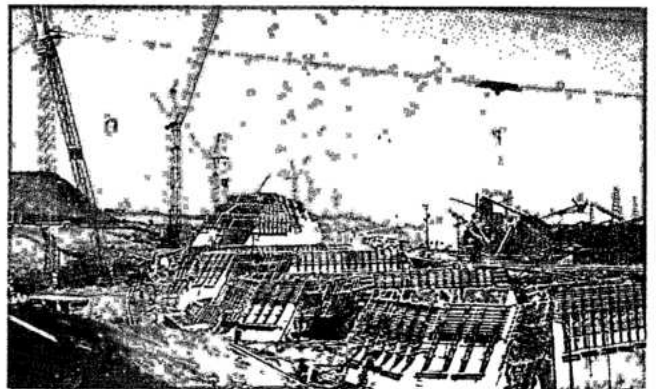
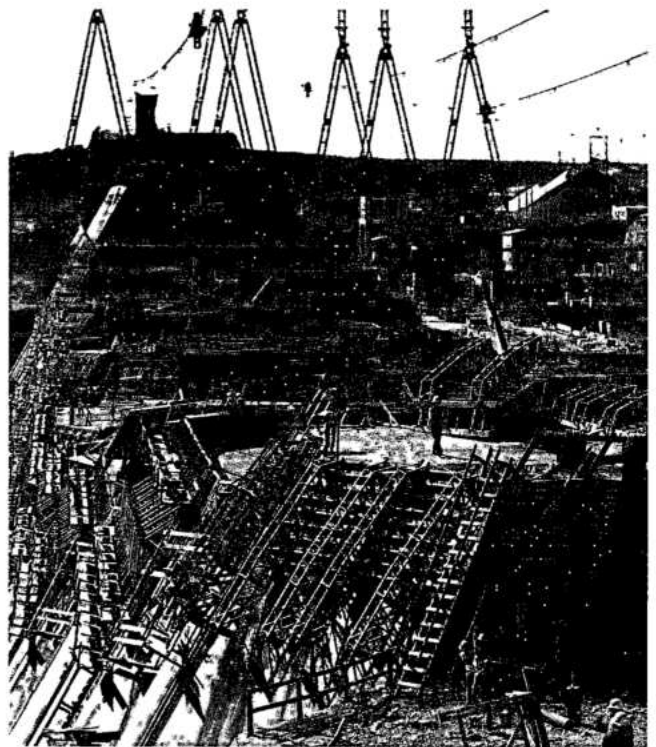
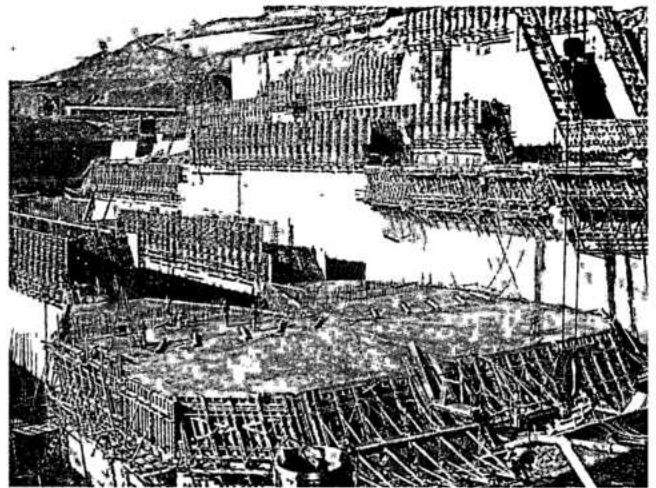
Cantilever steel forms were used throughout, with wooden forms for notches and corners near the foundations. Curvilinear precast concrete elements were used to form the underside of the upstream head. Wooden panels were mounted on the steel forms for the two types of keys formed in the longitudinal contraction joints. Piping for joint grouting was also attached to these forms. At El. 161.5, where the buttresses and the heads converge to form the ceiling of the cell, precast concrete slabs served as forms for the concrete placed above.

As discussed in Chapter 5, concrete for the hollow gravity dam, the diversion control structure and six buttress dam blocks on either wing was delivered in 6 m^3 buckets by the aerial cableways to El. 155. Above that elevation, the buckets were handled by the tower cranes.

As the main dam rose above El. 140, where there was interference between the various operations carried out by the cableways, ROTEC belt conveyor swinger systems were used for placing concrete in the interior monoliths. The 6 m^3 buckets poured concrete into 9 m^3 hoppers which discharged it onto the belt on a swinger boom capable of 360° rotation. In the forms, the concrete so delivered had the same consistency with respect to segregation as that discharged from the buckets lowered from the cableways.

Typical steps in placing concrete in a standard 2.5 m lift, after the forms had been erected, were:

- Roughening and cleanup of the surface of old concrete with high pressure water jets.
- Installation in each lift, or where required, of embedments such as waterstops at contraction joints, metal forms for drains in the upstream head and at transverse contraction joints, piping and outlets for grouting along longitudinal joints and instruments and their cables.
- Buckets filled with 6 m^3 of concrete were picked up by the cableway from the left bank dock and laterally transported to, and lowered about 3 m above, the surface of the monolith being poured.
- Concrete was spread in 0.3 m layers in the upstream downstream direction by tractor blades, or in restricted spaces manually with immersion vibrators. Vibrators mounted on a backhoe were also used to consolidate concrete.
- The consolidated parts of a 0.3 m layer were covered by new layers, forming steps, until the full 2.5 m lift was completed.
- Wet curing of the completed lift commencing 12 hours after completion, and stripping the forms after 72 or more hours.



Wooden forms and concrete placement

Except for the galleries, at some sharp re-entrant angles in the foundations of the upstream heads, at the downstream knees of some blocks, and at the upper ends of the longitudinal contraction joints, no reinforcement steel was placed in the hollow gravity blocks from the foundations to El. 161.5. Thus, concreting of the lower 70% of the high hollow gravity blocks was repetitive in technique, efficient and relatively rapid.

Construction above El. 161.5, comprising the power intakes and structures for the trashracks, gates, stoplogs, servomotors and inlets to the penstocks, was more complex and slower than in the lower parts of the hollow gravity blocks.

The major steps of construction of the structure above El. 161.5, and the techniques employed, were as follows:

- Precast concrete slabs were placed at El. 161.5 to form the roof of each hollow gravity cell, see Fig. 9.5. The first 1.5 m lift above the roof had two layers of two-way reinforcement and was constructed as a single monolith almost rectangular in shape. Concrete placement technique and sequences were the same as for the lower monoliths.
- Between El. 163 and 169, four lifts, each 1.5 m high and containing about 3000 m³, were placed as mass concrete. On the upstream side, a 4 m cantilever was formed for the seat of the trashracks and on the downstream face stepped blockouts were formed for second stage concrete for penstock embedment. Wood formwork was used on the downstream side because of dowels for steel reinforcement and vertical keys formed on the transverse vertical faces.
- Above El. 169, concrete for the curved and sloping invert, with reinforcement near the surface and for the vertical piers and walls, was placed in 1 to 0.5 m lifts. The surface layer was screeded to design shape and blockouts formed and anchor bolts and embedded metalwork installed for the sills of gates and stoplogs.
- Above the invert, the thick end walls of each intake were constructed in 2.5 m lifts using steel panel forms. These walls were generally 5 to 10 m higher than the intake piers and had blockouts for horizontal cross-beams of the intake, and steel dowels where the second stage concrete for the transition from the gate to the penstock was placed.
- For the concrete transition, wood formwork covered with plywood panels and finished close to the designed warped surface was fabricated and erected at each intake between the end walls completed to about El. 186. Because of the heavy

reinforcement and restricted accessibility, concrete with a slump of 4 to 6 cm was placed in 0.5 m lifts and consolidated with long-hosed vibrators which could reach under the formwork. For some intakes the concrete was pumped into the transition areas.

- For the reinforced concrete cross-beams and piers of the intake, specially fabricated steel forms were used. Each span of the beams was placed without construction joints.
- The soffit of the intake upstream of the gate, was formed by precast inverted T beams.

Above the soffit, the construction of the breast wall, the gate maintenance chamber and the rest of the dam to the crest roadway, utilized the same technique as used for other massive structures.

Buttress dam blocks

The methods of concrete placement in the D, E and I wing buttress dam blocks were essentially the same as for the buttresses of the hollow gravity blocks. After consolidation grouting of the foundation of the heads and final cleanup, standard steel panel forms were used for most of the pours, with some wooden forms for the underside of the head for the first lift. Lift heights off the foundation were the same as for the hollow gravity dam.

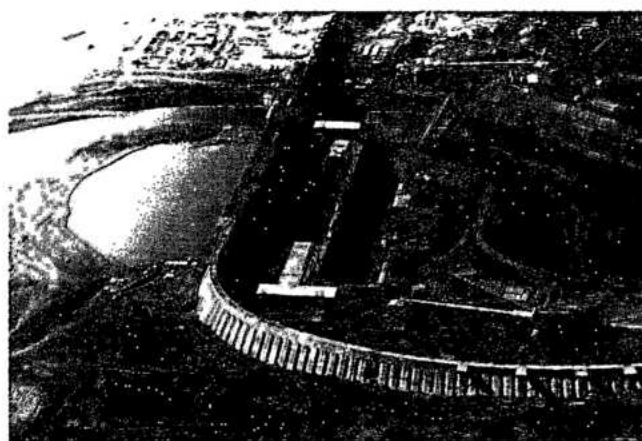
Initially, several D blocks lower than 50 m were constructed as single monoliths combining the head and the stem. After cracks were observed in these blocks during the winter of 1980, as discussed later in this chapter, an inclined contraction joint was introduced between the head and the buttress stem.

For the D, E and I buttress blocks with the contraction joint, the buttress was constructed first. When the buttress had reached a height of 5 to 7.5 m above the last lift in the head, concreting was resumed in the latter. Keys were formed in the upstream face of the buttress.

Except for six E and I blocks on each flank, which were covered by the aerial cableways, concrete for all buttress dam blocks was hauled to the location by dumpcrete trucks, discharged into buckets, which were then delivered by the tower cranes to the formed lift.

Because of their smaller size, ease of access and simplicity of the structural shape, concrete construction of the buttress dam was faster than the hollow gravity dam. There was some reinforced concrete construction near the top of three D blocks

which had platforms for transmission line towers and some E and I blocks which had chambers for storing stoplogs and other equipment.



Right wing dam construction sequence

PERFORMANCE OF THE HOLLOW GRAVITY DAM

INSTRUMENTATION AND MONITORING

Layout of instrumentation

As the eighteen blocks of the Itaipu main dam, designated F1/2 through F35/36, constitute the highest and largest hollow gravity dam in the world, four representative blocks were heavily instrumented to monitor their performance. Typical layout of instrumentation in a hollow gravity block is shown in Fig.9.51. The blocks were selected for instrumentation for the following reasons:

- Blocks F13/14 and F19/20, with foundations at El.45 and El.40, respectively, are representative of the highest hollow gravity blocks in the river channel. Some weak zones, about 20 m below the foundations of these blocks were strengthened by constructing concrete shear keys.
- Block F5/6, with foundation at El. 95, is one of the shorter blocks with a power intake and a penstock located in it. There is a steep, 22 m deep cut at its toe.
- Block F35/36, is a 110 m high block without a power intake or penstock, and is not an enclosed cell. At its toe, there is a 30 m deep cut to the powerhouse erection area. On its left it adjoins an abutment block of the diversion control structure and the 60 m deep steep bank of the diversion channel.

The functions of the monitoring instruments were the same as those in the diversion control structure, see Chapter 6.

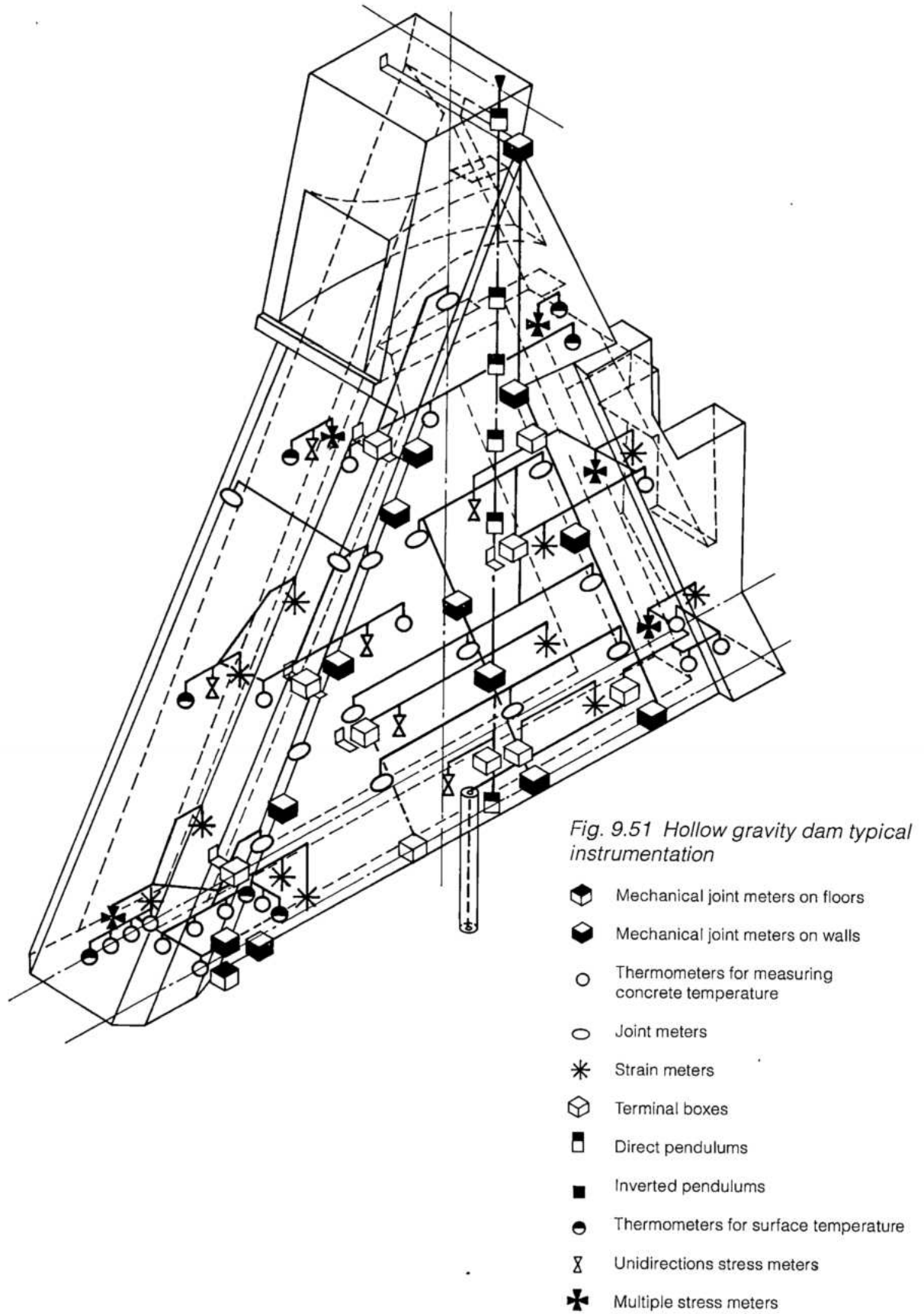
Instrumentation in the foundation of the main dam

Instrumentation in the foundation of a typical hollow gravity block is shown in Fig. 9.52. It comprises multiple extensometers, inverted pendulums and piezometers. Vertical and horizontal movements of the foundations are monitored in order to evaluate the performance and structural stability of the dam. Shear key instrumentation is described in Chapter 4.

Characteristics monitored

Fundamentally, the stability and satisfactory performance of the dam depends on each block acting as a monolithic structure which is bonded to its foundations.

The cellular block distributes the imposed and internal loads elastically to the different parts of the structure and the foundation. The designs assumed that the distribution of loads would occur without cracking, rupture, or shearing, and that no part of the structure would be over-stressed or strained beyond the elastic limit.



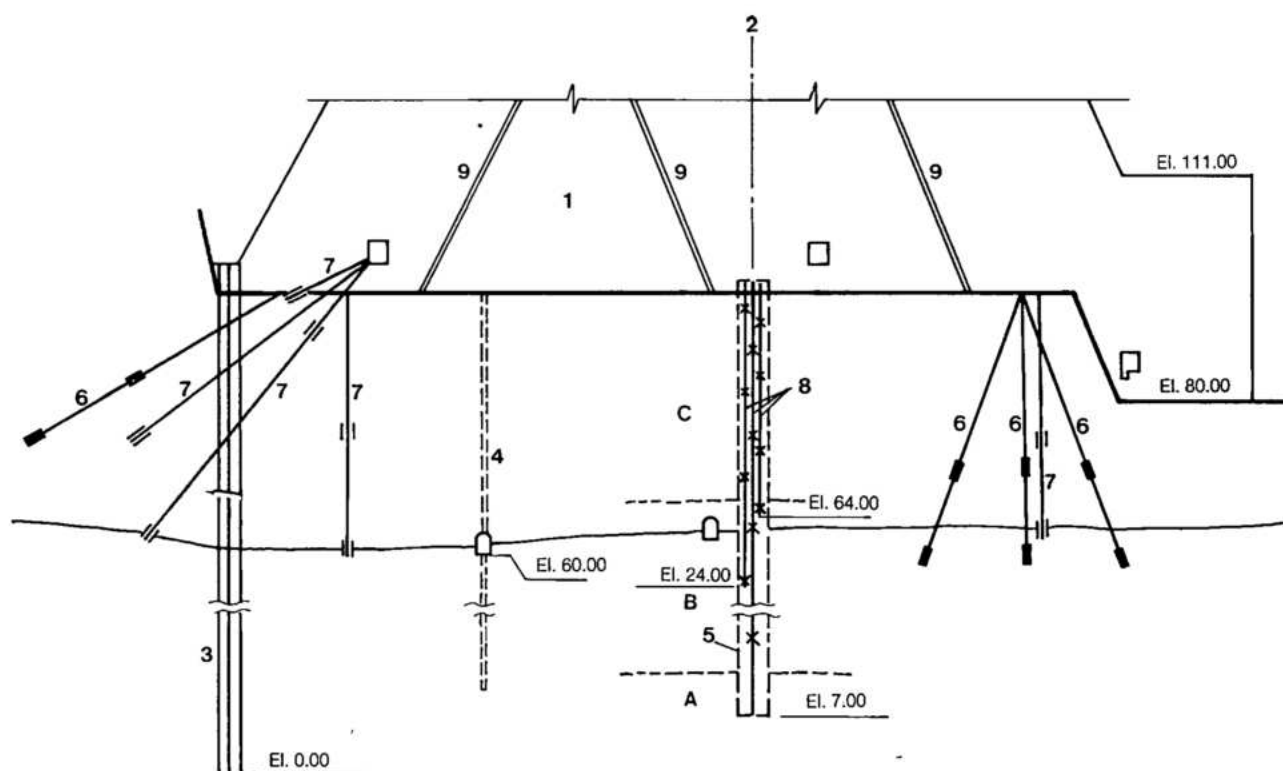


Fig. 9.52 Instrumentation of foundation in a typical hollow gravity block

- | | |
|---------------------------|--------------------------|
| A, B, C, ... Basalt flows | 5 Large diameter shaft |
| 1 Hollow gravity block | 6 Multiple extensometers |
| 2 Dam axis | 7 Foundation piezometers |
| 3 Grout curtain | 8 Inverted pendulums |
| 4 Drainage curtain | 9 Contraction joints |

Since the hollow gravity dam is complex in articulation and constructed in stages, the following characteristics and factors were of special interest:

- Transfer of dead load from the upstream head to the buttresses during construction. Opening of the contraction joint in the neck, which is parallel to the upstream face, is an indicator of this action.
- Possibility of internal cracking in the head, particularly near the foundation. Measurements of discharge from the formed drains and particularly rapid increase in flow, rate of temperature drop and the strainmeter and stressmeter readings were useful in assessing this factor.
- Opening of longitudinal contraction joints and the feasibility of grouting them. Embedded and surface jointmeter measurements and concrete temperature readings provided the data required for selecting the time for joint grouting.
- Cracking of the foundation near the upstream grout curtain, which was indicated by the FEM analyses. Rapid and abnormal increases in piezometric pressures, flow from the drilled drain holes and increase in horizontal deformations measured by the extensometers, were useful in evaluating possible cracking.
- Permanent and elastic deformations of the foundation, particularly in the direction of flow. These were of special interest for blocks with deep cuts at their toes and for blocks with shear key treatment under their foundations. Inclined extensometers installed in the foundations and inverted pendulums provided the data necessary for evaluating foundation behavior.
- Monolithic response of each completed block of the dam after filling of reservoir and the achievement of a steady elastic state. Data obtained from

foundation extensometers, inverted and direct pendulums, stressmeters and strainmeters provided the clues for ascertaining this aspect of behavior of the dam.

TESTS PRIOR TO RESERVOIR FILLING

Two series of tests were performed on the hollow gravity dam blocks 10 to 15 months before reservoir filling:

1. Watertightness of the upstream head was checked by filling the formed drains with water. The drains were capped at their bottom exit, and filled in stages to a height of average 100 m. Similarly, the watertightness of the transverse contraction joints was tested during July-September 1981, by capping the exits of the joint drains near the bottom and filling them with water to about El. 140. In this manner the joints were subjected to hydrostatic heads of as much as 100 m. Any leakage detected through construction joints or pockets of concrete itself, was sealed with epoxy mortar on both the upstream and downstream faces of the heads before first filling of the reservoir.

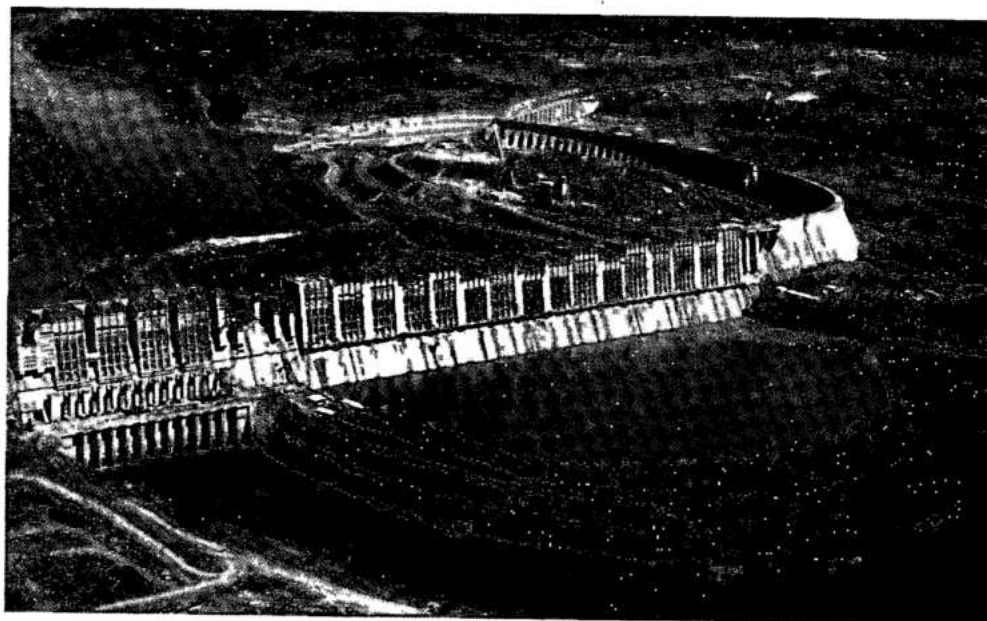
2. Pre-loading test. The space between the dam and the upstream cofferdam was filled with water to El. 134.5 in stages. This permitted the application of 100 m of head on the central blocks and of 120 m on the shear keys in the foundation. From measurements of foundation deformation, stresses in the dam, and piezometric and uplift pressures, it

was possible to project the response of the dam and the foundation when the full reservoir load was applied. The pre-loading test also provided a second check of the watertightness of the heads.

Principal results indicative of the structural performance of the highest blocks of the hollow gravity dam under the pre-loading condition were:

- Horizontal deformation at the foundations of the central blocks was less than 0.2 mm near the upstream end and not measurable near the downstream toe.
- Foundation settlement was significant as measured by extensometers; for central blocks it averaged 7 mm under the upstream head and 5 mm under the downstream toe of the dam.
- Horizontal deflection of the crest of the dam in the direction of flow was less than 0.4 mm.
- Longitudinal contraction joints parallel to the upstream face at the neck, were open 0.3 to 0.9 mm in the lower one-third and closed for the rest of the height.
- Second upstream longitudinal contraction joints were open 0.9 mm for half their height.
- Other longitudinal joints were essentially closed.
- Vertical normal stresses in the buttress stems near the foundation averaged 300 N/cm² compressive, and the distribution was essentially uniform.

In summary, at the end of the preloading test and before the rapid filling of the reservoir in October 1982, the hollow gravity structure was still adjusting and its response was not yet entirely monolithic. It was also concluded that external loads had not been fully transferred to the foundations.



Main dam pre-loading test

FOUNDATION RESPONSE

Settlement

Vertical multiple extensometers provided data regarding settlement and consolidation of the foundation to a depth of 40 m. Relative settlements between various strata, contacts and discontinuities were also measured by the same instruments.

Fig. 9.53 shows the history of foundation settlement under one of the highest hollow gravity blocks (F17/18). The foundation had settled from 5.5 to 7.5 mm during the pre-loading. During October 1982, the response to reservoir filling was rapid, with the settlement increasing by 1 to 1.5 mm in about 20 days. After December 1982 for the next 5 years, with the reservoir level between El. 215 and El. 220, foundation settlement increased at a rate of about 0.25 mm per year at the upstream end and less than 0.1 mm per year in the downstream part. This extremely slow rate of increase in settlement is attributed to internal consolidation of the foundation,

particularly in the zone of discontinuities, where the shear keys were constructed. Such consolidation improved the strength and stability of the foundation.

Foundations of some abutment blocks, particularly F35/36, demonstrated a different pattern of settlement from that of the central blocks. Before reservoir filling, settlement under the upstream head was about 0.2 mm, zero in the middle and about 1 mm under the downstream toe of the block. After the full reservoir pressure was applied, the foundation of this block tilted, with a rise of about 1 mm at the upstream and increase in settlement in the middle and near the downstream toe of about 2 mm.

Lateral deformation of the foundation in the direction of flow was measured by the inclined extensometers and inverted pendulums. Extensometers under the heads of six hollow gravity blocks were inclined 60° to the vertical and extended 30 to 80 m upstream into the foundations. In two abutment blocks, extensometers inclined 30° to the vertical and extending both towards the

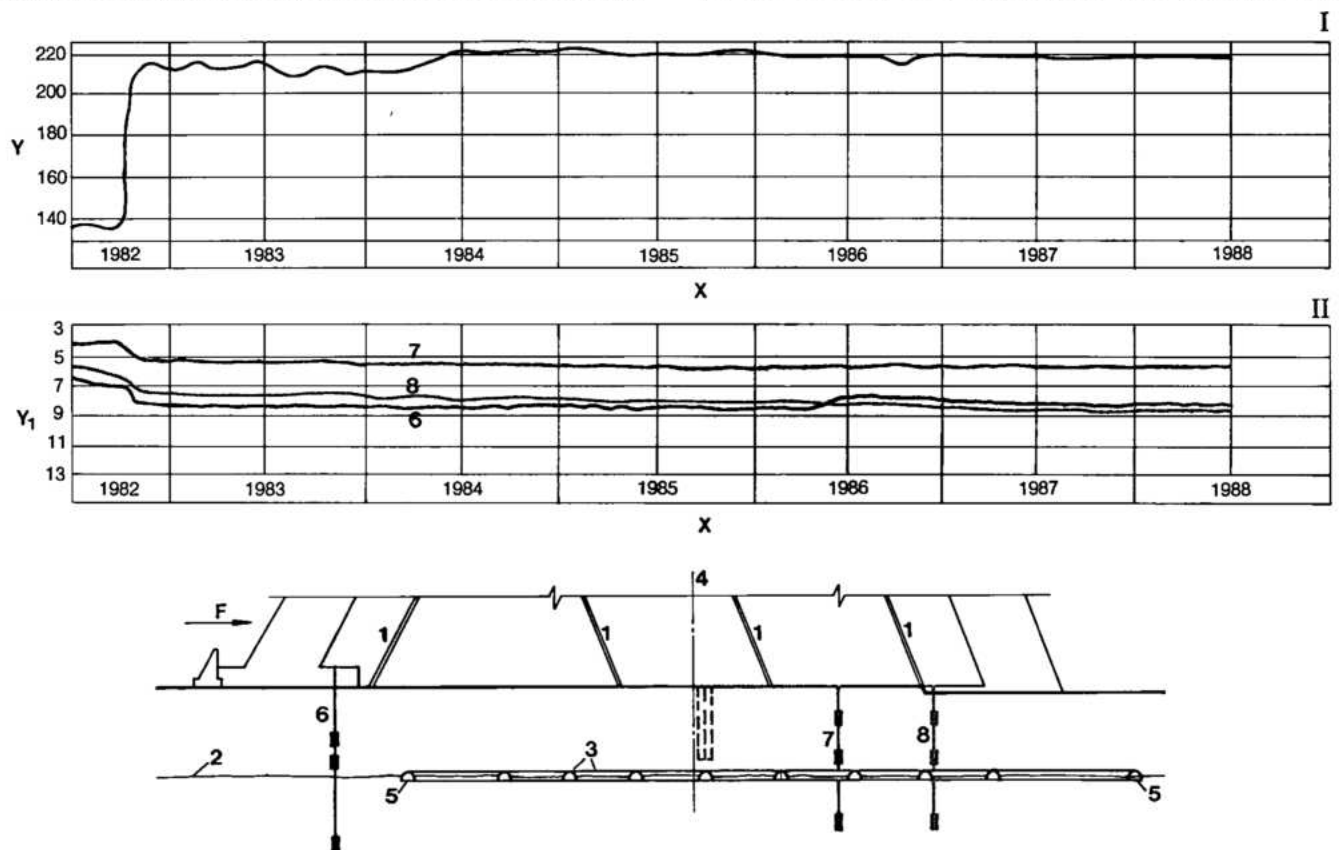


Fig 9.53 Hollow gravity dam foundation settlement

I Reservoir water level

II Settlement of block F17/18 as measured by extensometers in position 1

Y Elevation (m)

Y₁ Foundation settlement (mm)

X Years

1 Contraction joints

2 Contact between basalt flows A and B

3 Shear keys

4 Dam axis

5 Drainage tunnels

6 Extensometer EM-F-19

7 Extensometer EM-F-18

8 Extensometer EM-F-20

F Flow direction

upstream and downstream were located in the middle or near the downstream toe.

At the upstream end of all hollow gravity blocks the foundation deformed 1 to 1.5 mm in the downstream direction in about 15 days as the reservoir was filled to El. 215. In the downstream area lateral deformation of the foundation was of the same order. For almost 2 years after reservoir filling the lateral deformations of the foundation were essentially unchanged. During April-June 1984 when the reservoir was raised from El. 210 to El. 219.6, the foundation deformed an additional 1.5 mm towards downstream. After that the lateral deformations increased from negligible to 1 mm in 5 years.

Foundations of the end block F35/36 were affected by excavation for the powerhouse in the diversion channel in 1986. While there was no measurable increase in settlement, the lateral deformation increased about 0.7 mm in the downstream direction over a period of 12 months. As was the case for the diversion control structure, foundation creep induced by the downstream excavations petered out in about 1 year and the foundation stabilized.

In summary, 8 years after reservoir filling the foundations of all hollow gravity dam blocks had essentially stabilized.

Performance of foundation strengthened by shear keys

Because the extensometers in the key grid were installed when excavation of tunnels and concrete placement in the dam had already advanced, total deformation of the treated foundation zone could not be measured; however, the instruments measured the incremental changes and indicated trends from which the performance could be analyzed. Foundation deformations were affected by tunnel excavation, blasting and weight of the dam, the amount of consolidation also depending on the nature and thickness of the discontinuity and the softer infill material. Extensometer readings, made after excavation and before concrete backfilling, showed clearly that settlements accelerated wherever the height of a tunnel approached the thickness of the overburden.

From instrumentation data it was established that blasting vibration also was one of the main causes of settlement of the rock mass. Field data showed an increase of vertical deformation as the excavation approached the instrument location, possibly as a consequence of consolidation of clay infilling and closure of joints in the discontinuity. Fig. 4.9 shows typical behavior of the rock mass, which initially

under the weight of the rising dam underwent a steady rate of settlement. In January 1981, the rate increased when tunnelling operations were nearby, as recorded by the lower anchor after the opening of the tunnel. Later this extensometer resumed the previous settlement rate.

Fig. 4.10 shows the effect of blasting on readings of an extensometer crossing shear zone 1. It was observed that at a distance less than 15 m between blasting and the instrument, the settlement measured at each blast increased exponentially even when very low explosive charges were employed.

The rates of settlement recorded varied between 5 mm/100 days, for locations where excavation or concrete backfill were still in progress, to 1 mm/100 days, or less, for areas already concreted and stabilized.

Typically, foundation deformations during construction of the shear key grid ranged from 1.5 to 3.5 mm, the difference of 2 mm being consolidation of the treated zone.

During the subsequent 15 months, when the subsurface treatment was completed and preloading of the central blocks carried out, settlement almost doubled in magnitude, the large amounts being in the upstream area and towards the left bank. Total consolidation of the material in the treated zone between contact A/B and joint A, where the shear keys were located, was 2 to 3 mm or about 50% of the foundation settlement.

The rate of consolidation slowed down considerably after the treatment tunnels were concreted. In one month after reservoir filling, average additional settlement of the keyed zone was 0.3 mm, and a lateral deformation of 0.4 mm occurred in the downstream direction. These values are about 30% of the total foundation deformations and were measured by triorthogonal markers located in the perimetral gallery around the shear key grid. Three months after first filling of the reservoir and during the next 6 years, there were no measurable incremental deformations, either vertical or lateral, in the shear keyed zone.

Two rosettes of strainmeters were embedded in concrete of longitudinal keys and two in transverse keys. Before reservoir filling, tensile stresses in horizontal and sub-horizontal directions were observed in most locations. These were attributed to the heat of hydration, subsequent cooling and shrinkage of concrete. After reservoir filling, over a period of 6 years stress development in the keys showed the following trends:

- Vertical stresses were compressive in all locations and continued to increase at an annual rate of 10 to 15 N/cm².

- Vertical compressive stresses were about 270 N/cm^2 in the upstream area in both the longitudinal and transverse keys. In the downstream part of the treated foundation these stresses were about 130 N/cm^2 .
- Tensile horizontal stresses were dissipating and compression increasing in the upstream portion of the keyed foundation at an annual rate of 15 to 20 N/cm^2 .

There were almost no piezometric pressures in, or seepage through, the shear key treated foundation. The perimetral tunnel around the treated zone was highly effective in intercepting seepage through the discontinuities.

Analysis of the deformations and the stresses in concrete indicated that foundations in the treated area had fully consolidated and adequately strengthened. While the stresses in concrete were still changing, the increase in compression indicated that the vertical and lateral shear loads were being shared between the strengthened rock and the concrete. It was concluded that the keyed foundation had the same degree of stability as the sound rock foundation of the dam.

Foundation uplift and drainage

Typical arrangement of foundation piezometers, the grout curtain, and shallow and deep drain holes for two hollow gravity blocks is shown in Fig. 9.54.

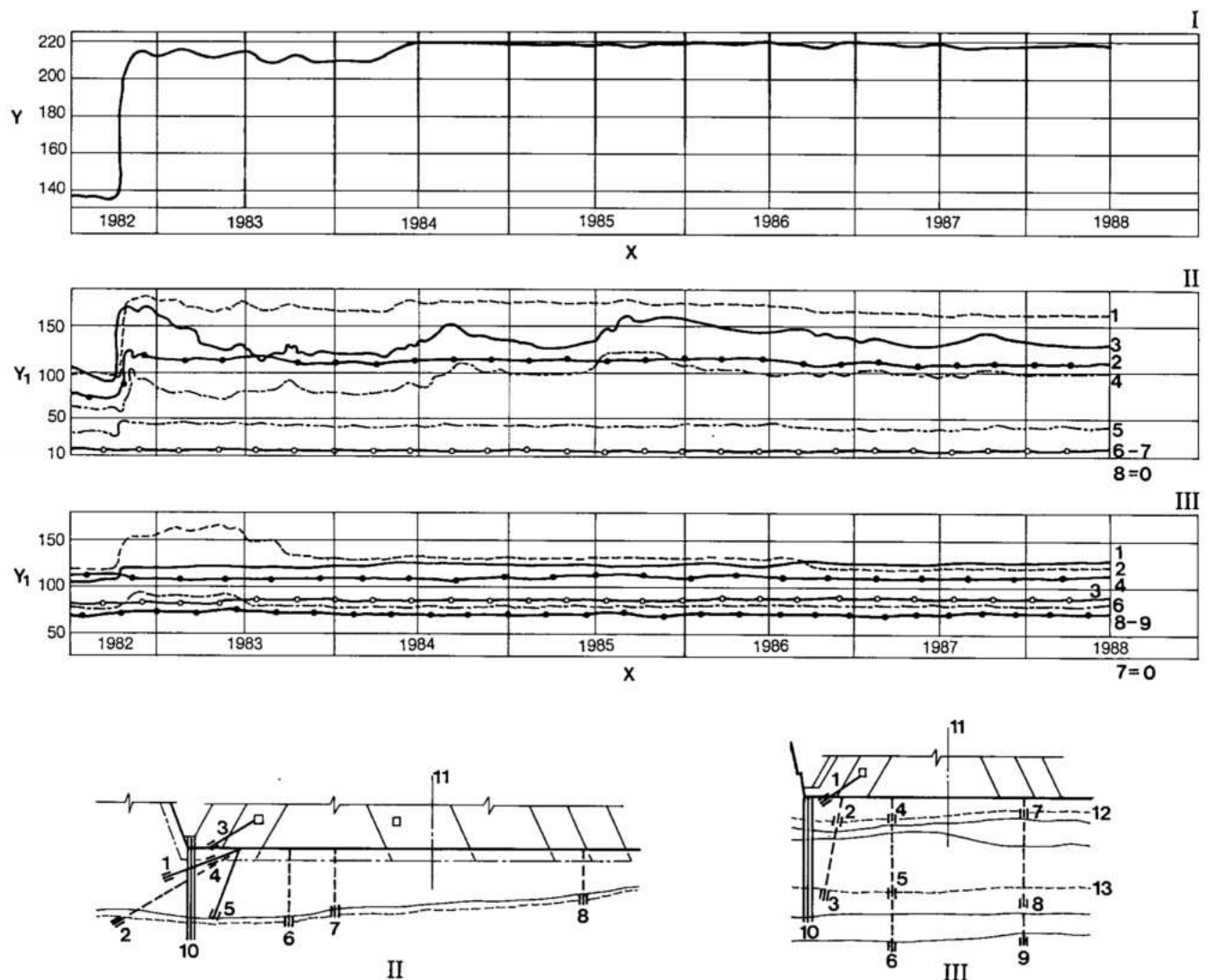


Fig. 9.54 Hollow gravity dam blocks: foundation piezometric and measured pressures with time

I Reservoir water level
II Block F19/20
III Block F35/36

Y Elevation (m)
Y₁ Piezometric level (m)
X Years

1 to 9 Piezometers
10 Grout curtain
11 Dam axis

12 Contact C/D
13 Contact B/C

Piezometers were located upstream of the grout curtain at major foundation joints and contacts, and also downstream of the curtain in the same features. Others were located at the concrete-rock contact downstream of the grout curtain.

As anticipated, upstream of the grout curtain the piezometric pressures built up to 60 to 100% of the reservoir level as micro cracks in the rock were saturated. Downstream of the grout curtain, the uplift pressures averaged about 10% of the reservoir head and were essentially unchanged after 8 years of operation.

Uplift pressures at the concrete-rock contact under the upstream half of the head were 60 to 100% of the reservoir head. Since the shallow drain holes were drilled into the foundation along the downstream trace of the head and the deeper drainage curtain was also located downstream of the head, uplift at the foundation contact was not appreciably relieved by the drains. However, there was a small gradual reduction in the uplift under the head over a period of 4 years.

Fig. 9.55 shows the uplift pressure in 1987 at the foundation contact of block F19/20, which is typical of the high blocks. With the reservoir level essentially steady for 3 years, the uplift pressures had become generally stable. The uplift pressure distribution assumed in design and stability analyses is also shown in Fig. 9.54. The actual uplift pressures are generally lower than those of the design criteria.

Flow from shallow foundation drains downstream of the heads gradually increased as the reservoir level reached its maximum steady level at El. 219.6 in 1984. Total flow from the shallow drains in June 1984 was 199 l/min. After that for the next 3 years there was a steady reduction of 30 l/min per year, indicating a gradual closure of seepage paths. The drainage flows also showed some influence of seasonal temperatures, increasing in winter and reducing in summer.

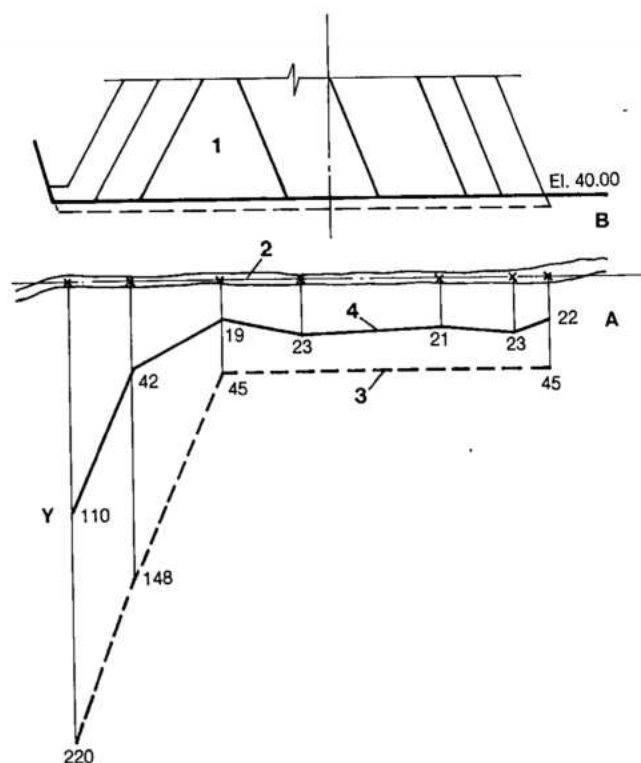
Total flow from the deeper drainage curtain holes and from the drainage galleries, including the galleries at El. 20 around the zone of shear key treatment, also peaked in 1984 at about 3000 l/min. This included drainage from 6 buttress blocks on the right abutment. During the next 5 years the total drainage flow had reduced to about 1920 l/min.

Observation and analysis of foundation piezometric pressures and drainage flows indicated that:

- The grout curtain is effective in reducing seepage through the foundation and its more permeable features, to a nominal and controllable amount. Since the seepage flows are reducing with time, the efficacy of the grout cutoff is not being impaired.
- Shallow and deep foundation drains are very effective in reducing the uplift pressures which are less than those assumed in design criteria, indicating adequate margins of safety and stability of the dam.

Fig. 9.55 Uplift pressure at foundation contact of typical hollow gravity block

- Y Uplift (m)
 A,B Basalt flows
 1 Block F19/20
 2 Contact A/B
 3 Theoretical uplift diagram
 4 Uplift pressure measured by instruments in December, 1988



- Total seepage from the foundations is less than that predicted by mathematical analysis and compares favorably with the experience at other high concrete dams on similar foundations. There is no indication that significant soluble materials are being leached out of either the rock or the grout curtain.

STRUCTURAL PERFORMANCE

Deflections of the hollow gravity dam

Deflections of the dam in the axial and transverse planes are indicative of its response to the external loads, principally reservoir pressure, and the degree of internal monolithic action of the hollow gravity cells. During construction various monoliths of a block deformed and deflected due to their own weight, in particular the upstream head which leaned on the buttress stems. Later as the central blocks were completed nearly to the top with the buttresses confined by the two massive heads to form the cupola, and the dam was pre-loaded, the entire block deflected as a whole with minor internal adjustments. Before the reservoir was filled in October 1982, the longitudinal contraction joints

open were grouted. As the reservoir was filled, the entire block deformed and deflected as the loads were distributed to the various structural members by bending and shear.

For measuring deflections of the crest of the dam a base line along the axis was first established on October 9, 1982, before reservoir filling, by high precision geodetic surveys. After reservoir filling, the deflections in axial, as well as transverse directions were measured both by geodetic surveys and direct pendulums. While the geodetic survey measured total deflections from the base line, that is, they included the deformations of the foundations, the direct pendulums measured deflections of the structure only relative to the foundation. The pendulums also measured deflections of the dam at several elevations, including El. 223.9 near the crest.

Downstream horizontal deflections of the crest of the main hollow gravity dam relative to the fixed axis from June 1985 through June 1988 are plotted in Fig 9.56. It was observed that:

- The higher blocks deflected more than the shorter ones.

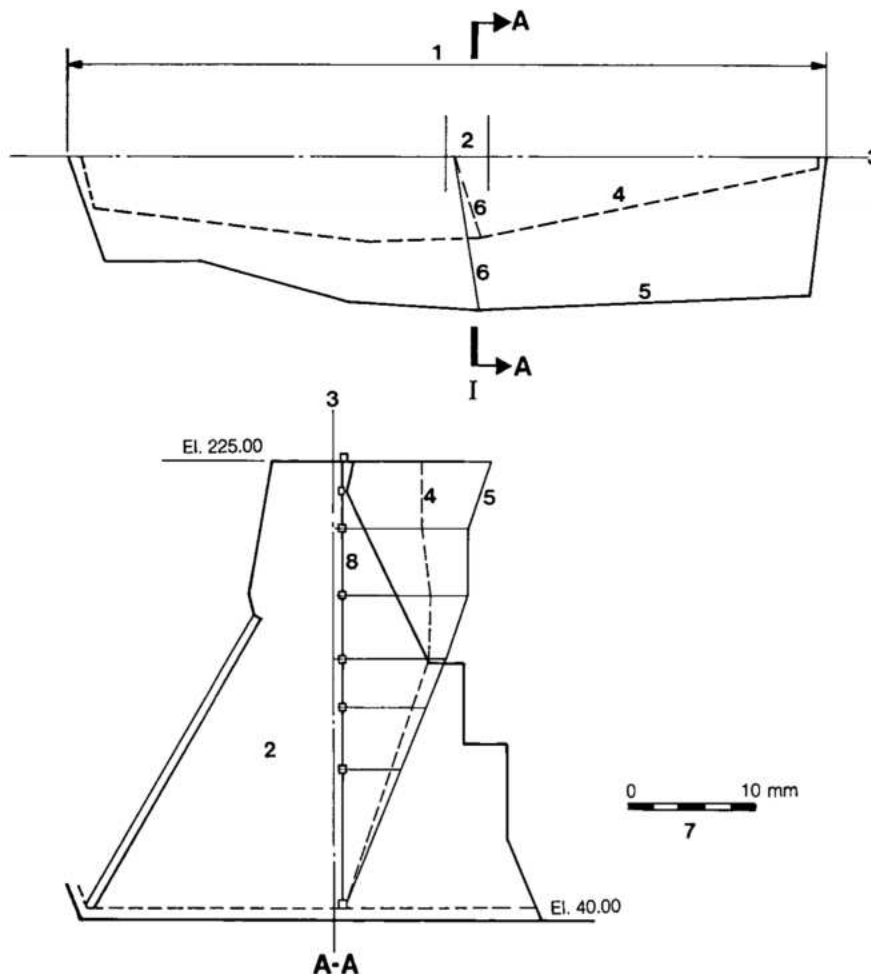


Fig.9.56 Hollow gravity dam-deflections measured by direct pendulums

- 1 Horizontal displacements at crest, El, 225
- 2 Extension in plan of the main dam
- 3 Highest block F 19/20
- 4 Dam axis
- 5 Crest deflection in June 1985
- 6 Crest deflection in June 1988
- 7 Vectors of horizontal angular deflection
- 8 Deflection scale
- 9 Direct pendulum

- In the axial direction most blocks leaned towards the left abutment with the last three blocks leaning in the opposite direction.

Changes in deflections of block F19/20 over a period of 3 years are shown in Fig. 9.55.

Principal observations regarding performance of the hollow gravity dam, as indicated by the deflections, are:

- Maximum downstream deflections occur during winter (June-August). Maximum crest deflection observed so far was 11.8 mm for block F13/14, (one of the highest blocks), in June 1987 during an abnormally cold winter.
- During a normal winter (June 1986), deflection of the crest of block F19/20 was 9.6 mm. This compares with a deflection of 9.8 mm computed by the FEM for a monolithic elastic dam block and foundation. With a vertical crack in the foundation, the FEM model indicated a crest deflection of 23 mm. Therefore, it was concluded that the dam and its foundation are elastically integrated and there was no cracking in either the foundation or the upstream head of the hollow gravity dam.
- During summer (December-February), the downstream exposed face of the dam warms up and expands and it moves upstream, reducing the crest deflection by about 35% from that in winter.
- Blocks which have the powerhouse at their toe are protected from downstream exposure below El. 144. Below this elevation there are very small seasonal changes in deflections.
- Comparison of summer (January 1985) deflections of two shorter blocks F5/6 and F35/36 demonstrated that the complete hollow gravity cell block is more rigid and less sensitive to ambient temperature changes than the double buttress type with a downstream open face.
- Maximum deflection in the axial direction so far observed was 4.2 mm in block F5/6 in June 1987. It was towards the left bank. Because of lateral relaxation of the rock, the abutment blocks tend to lean towards the river channel. Some axial deflection is also attributed to the two-step foundation levels for a single hollow gravity block, e.g. F5/6. However, axial bending has not caused excessive tensile stresses.

Differential deformations between adjoining hollow gravity blocks were monitored by measuring the movements of transverse contraction joints at the foundation and in the galleries at various elevations. Over a 2 year period from July 1985 to June 1987 the average differential movements were as follows:

Joint opening, axial direction

At the foundations	0.25 mm
At El. 214	1.04 mm

Transverse differential deformation

At the foundations	0.10 mm
At El. 214	0.30 mm

Differential settlement at upstream head

At the foundations	0.12 mm
--------------------	---------

During the same period, differential movements between the first and the last hollow gravity blocks and the adjoining buttress dam on the right, and diversion control structure on the left, were generally about double the above average values. This was to be expected because the adjoining blocks are more flexible than their hollow gravity neighbours.

The very small differential movements between the hollow gravity blocks was another confirmation that the dam and its foundation had attained elastic equilibrium. For the blocks with shear key treatment, the differential movements were about 20% of the average values and the settlement essentially zero, which indicated that the shear keys were acting integrally with the foundation rock.

Thermal behavior of the hollow gravity dam

Structural performance of the hollow gravity dam, reflected in deflections and stresses, is significantly affected by the distribution of body temperatures within the block. Because of its box shape and articulated construction, the massive upstream head and downstream face slab and the different concrete mixes used, the various components of the block cool at different rates. Temperature gradients within the monoliths can cause appreciable tensile stresses, particularly in areas of high restraint. Rates of cooling of, or temperature changes in, the various structural components also depend on exposure to water on the upstream side, air circulation within the hollow block, and exposure of the downstream face.

Typical histories of temperatures observed in the high blocks over a period of 8 years are shown in Fig. 9.57. The temperatures were measured by thermometers located near the foundations and at about mid-height, and embedded in the upstream head, buttress stem and the downstream head.

Functioning of the contraction joints

Prior to pre-loading and reservoir filling, the longitudinal contraction joints were monitored and the indications of opening verified against calculations based on temperature data. As indicated by FEM analyses, the contraction joints in the necks of the upstream and downstream heads (A and D) were generally closed, but the two joints in the buttress stems (B and C) opened up to 1 mm for the lower 50 m of their heights. The open joints were tightly interlocked to permit flexure of the monoliths as a structural unit.

After reservoir filling, seasonal fluctuations averaging about 0.1 mm were measured in the opening and closing of the various longitudinal contraction joints. In some blocks, observed joint openings were partially attributed to foundation creep and adjustment. In such instances the joints were tested by water circulation, and when the opening exceeded 0.2 mm, they were filled with cement grout under low pressure. The keyed longitudinal contraction joints served their dual function of crack prevention and load transfer between monoliths, as anticipated.

The transverse contraction joints between the blocks functioned as planned, and permitted independent movement of each hollow gravity block without interfering with the next block. As concreting progressed and the heads cooled and contracted, the transverse joints opened. Further, as the structure as a whole adjusted and deformed, and the foundation also consolidated and deformed, the joint openings changed and stabilized. Seepage flow from joint drains in the transverse contraction joints was another performance indicator. Six months after reservoir filling, the flow from the joint drains ranged from 0 to 8 l/min, except for joint drain F36/H1 which was discharging about 25 l/min. Two years later flow from five joint drains had increased to the range 38 to 191 l/min, with a tendency for further increase. Since the reservoir level was essentially constant during this period, explorations and tests, comprising drill holes in the vicinity and sealing the drain with bentonite in stages, were performed. In most cases the sources of leakage were found to be either the foundation contact, permeable construction joints, cracks, or porous concrete around the water stops. Drilled drains intercepting the identified areas of percolation or cracks often reduced the drain discharge. Some joint drains were plugged with bentonite. Efficacy of the remedial treatment in controlling the excessive joint drain flow is evident from the following data:

Joint (drain)	Flow in l/min				
	10/85	2/86	11/86	2/87	6/87
F8/9	106	122	157	107	23
F10/11	38	26	13	9	7
F22/23	148				
F24/25	101	61	40	27	32
F34/35	191	117	80	81	64

Five years after reservoir filling, flow from joint drains had stabilized and they were functioning as designed.

SEEPAGE THROUGH UPSTREAM HEAD

Each hollow gravity block had twenty-one drains formed in its head. Out of the 378 drains in these blocks, only six drains in five blocks discharged more than 2 l/min after reservoir filling, as shown below:

Block (drain)	Flow in l/min					
	11/82	1/83	6/83	10/85	11/86	9/87
F9/10 (9)	4.4	3.3	1.4	25.8	6.0	0.6
F17/18 (7)	2.2	1.8	0.9	0.8	S	S
F21/22(4)	4.2	4.2	4.1	S	S	S
F34/35(3,5)	15.0	520.0	S	S	S	S
F35/36 (10)	S	S	S	115	112	110

S = flow less than 0.5 l/min

Generally, high flows occurred in heads adjoining joint drains with excessive flows. Rapid increases in flow through internal drains of F34/35 occurred 2 months after reservoir filling, while those in F35/36 drains occurred after 3 years. Investigations showed that the principal causes were the same as for high flows through the joint drains. For blocks F35/36 another contributory factor was additional foundation deformation attributed to new excavation at the toe of the block and for the powerhouse in the diversion channel. Remedial treatment similar to that for the joint drains was successful and the drains functioned properly and effectively reduced pore pressures in the heads.

Cracking incidents

Cracks in buttresses. With the exception of blocks F33/34 and F35/36, there were no cracks in the buttresses of the hollow gravity dam. A 2.5 m x 2.5 m vehicular access gallery was constructed through these four buttresses. It was located at foundation level near a contraction joint in the middle monoliths. In the winter of 1981, vertical and subvertical hairline cracks were detected; one set started from the corner of the gallery and another about 12 m upstream. The cracks did not appear to extend through the buttresses. Cracks which were open 0.10 mm or more were injected with epoxy before the pre-loading test. The gallery was plugged with concrete before the reservoir was filled.

The principal cause of these cracks was determined to be the large and rapid drop of temperature. Concrete in the lowest lifts was placed in January-February (the height of summer), 1979, and attained a maximum temperature of 36°C. Then it cooled rapidly to 18°C in 6 months, which is about 50% faster than the cooling rate observed for most other hollow gravity blocks. The rapid cooling combined with stress concentrations around the access gallery, induced tensile stresses of about 260 N/cm² near the foundations, leading to the start of cracks and alleviation of tension.

In December 1986, four years after reservoir filling, new vertical and inclined cracks were observed in buttresses of block F35/36. While their configuration was similar to the earlier cracks, they were 10 to 15 m long, 0.2 to 0.6 mm open and some extended through the buttresses. Since no new cracks occurred in the adjoining block F33/34, the new cracks could not be attributed to thermal factors. It was established, by comprehensive analysis of the measured foundation deformations, deflections of the block and differential movements at the transverse contraction joint with the adjoining block of the diversion control structure, that relaxation and tilting of the foundation, due to the new excavations downstream of the block and in the diversion channel, induced excessive tensile strains in the buttresses. Incipient cracks and residual stress concentration in the critical areas also contributed to the cracks. These cracks were repaired by epoxy grouting. After completion of the downstream construction and the end of foundation creep, the structural performance of the block was restored to normal.

Cracks in upstream heads. Two semi-vertical cracks were detected in the heads of two blocks during pressure testing of the internal drains; one daylighted

on the upstream face and the other on the downstream side of the head. These cracks were attributed to either deformation of the stepped foundations of the dual head, or a combination of other factors. Possibly minor thermal cracks were aggravated and extended by the hydraulic pressure in the drains. Epoxy grouting effectively sealed these cracks and restored the integrity of the head, before the reservoir was filled.

Three years after reservoir filling, cracks were observed on the downstream side of the upstream heads of blocks F8 and F9, on either side of the transverse contraction joint F8/9 and starting from the foundation. The crack in F9 was essentially dry, and was sealed with epoxy injections. However, there was leakage through the F8 crack and it was increasing with time. It was suspected that the crack extended to the joint drain F8/9, because the flow through that drain exceeded 100 l/min at that time and was increasing. Exploratory drill holes confirmed this and indicated that the crack had formed a prism about 4 m high, 1.5 m wide and 3.5 m deep at the base. The contraction joint formed one face of the prism. It was concluded that the prism had essentially separated from the rest of the head and was unstressed. Drain holes were drilled into the crack. Epoxy grouting, performed in stages, was only partially successful because of some clayey sediment deposits in the crack. The latter evidence and tests on adjoining joint and formed drains confirmed that the seepage into the crack was coming through the foundations. With adequate drainage and partial grouting of the crack which stabilized the prism, the dam block was adequately restored and functioning normally.

Development of stresses in the dam

Stresses in the concrete were measured directly by embedded stressmeters or converted from strains indicated by rosettes of strainmeters. Most stressmeters were placed to measure vertical and 45° inclined stresses. But the strainmeter rosettes could also measure strains in the horizontal axial and transverse directions.

Before reservoir filling. Initially, as the individual monoliths were built up to 50 m above their foundations, the stresses were mainly due to their own weight. Above that height there was transfer of some weight from both the upstream and the downstream heads to the buttresses. At the end of 1981, when most blocks had been completed to about El. 200, and before the pre-loading test, the vertical stresses near the foundations of the high

blocks (El. 53), were all compressive and averaged the following values:

Upstream head	100 N/cm ²
Buttresses	250 N/cm ²
Downstream head	100 N/cm ²

Vertical stresses in the thin buttresses fluctuated 70 to 100 N/cm² responding to ambient temperatures, compressions increasing in winter and reducing in summer. Stresses in both heads were not affected by ambient temperatures.

Some lateral stresses were also detected, and were less than 50 N/cm².

Effect of pre-loading. During the gradual application of up to 100 m water pressure on the central blocks the vertical compressive stress in the buttress near the foundation of the high blocks increased by 70 to 100 N/cm². There was little change in the stresses in the downstream head. In the upstream head, there was an increase of about 50 N/cm² in compression.

The stresses increased progressively, with some seasonal fluctuations. This indicated that the monoliths were adjusting to each other and that there was continuous change in load transfer patterns across the contraction joints and via the cupola roof joining the two heads under the power intake.

Effect of reservoir filling. The embedded stressmeters showed changes in stresses almost as rapidly as the reservoir level rose above the pre-loading level, El.135. Depending upon the location, there was an increase of 50 to 70 N/cm² compression in vertical and principal stresses parallel to the upstream and downstream faces of the dam.

Fig. 9.58 shows the vertical stresses in the upstream and downstream heads, and in the buttresses of a typical hollow gravity block, before and after reservoir filling (1979-82 and 8 years later, 1990).

After the rapid increase in stress following reservoir filling, there was a reduction of 10 to 30 N/cm² in compression in the upstream head. This was partly due to the increase in pore pressure in the head (which reduces the stress measured by a stressmeter), and partly due to the transfer of load from the upstream to the downstream head via the cupola roof.

Distribution of vertical stresses in a typical block at three elevations in 1985 are shown in Fig. 9.59. These are stress values measured by strainmeters. On the same diagram, principal stresses are shown with the values obtained from the FEM mathematical model.

After 5 years of operation, with the reservoir full and fluctuating only about 4 m, stresses in all hollow gravity blocks and their structural components were all compressive. Maximum vertical stresses, as measured by the instruments near the foundations of the highest blocks were:

Upstream head	200 – 250 N/cm ²
Buttresses	350 – 400 N/cm ²
Downstream head	150 – 350 N/cm ²

Seasonally, the interior stresses fluctuated 30 to 50 N/cm² only; but near the exposed downstream face the fluctuations were 100 to 150 N/cm².

Development of stresses in the upstream head were of special interest, because high tensions could cause cracking and leakage. Even with working internal drains, pore pressures can build up along construction joints and around the embedded instruments. Stressmeters installed parallel to the upstream face particularly reflected the effect of pore pressures on principal stresses. While no tensions were detected, some principal stresses were about 100 N/cm² compressive.

Summary

Deformations, settlements and deflections of the hollow gravity dam and its foundations, which are measured by the instrumentation and systematically analyzed, indicated normal and stable behavior. All stresses in the concrete dam are compressive, and are less than 33% of the corresponding concrete strength. The structure underwent internal adjustment, and as anticipated, the dam blocks and their foundations perform as an integral elastic complex.

There were no indications of foundation cracking near the upstream grout curtain. Remedial treatment of the few cracks which occurred in some blocks, had fully restored their structural integrity. The grout curtain and the foundation drainage system were effective in controlling seepage and uplift pressures, within adequate margins of safety.

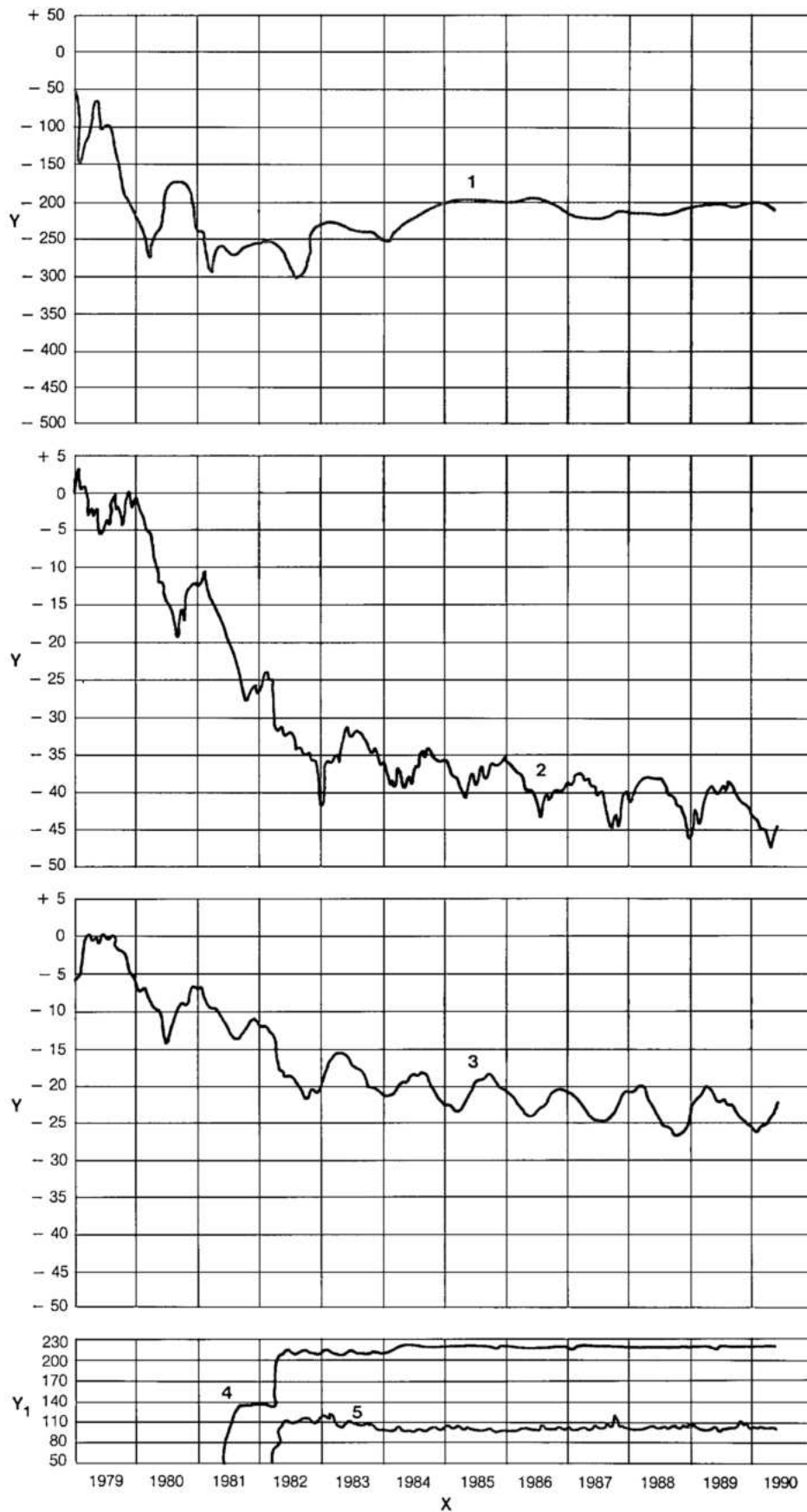


Fig.9.58 Hollow gravity dam - Development of vertical stresses in concrete at El.53

Y Stress (N/cm²)

Y₁ Elevation (m)

X Years

1 Stress in upstream head

2 Stress in middle of counterfort

3 Stress in downstream head

4 Upstream water level

5 Downstream water level

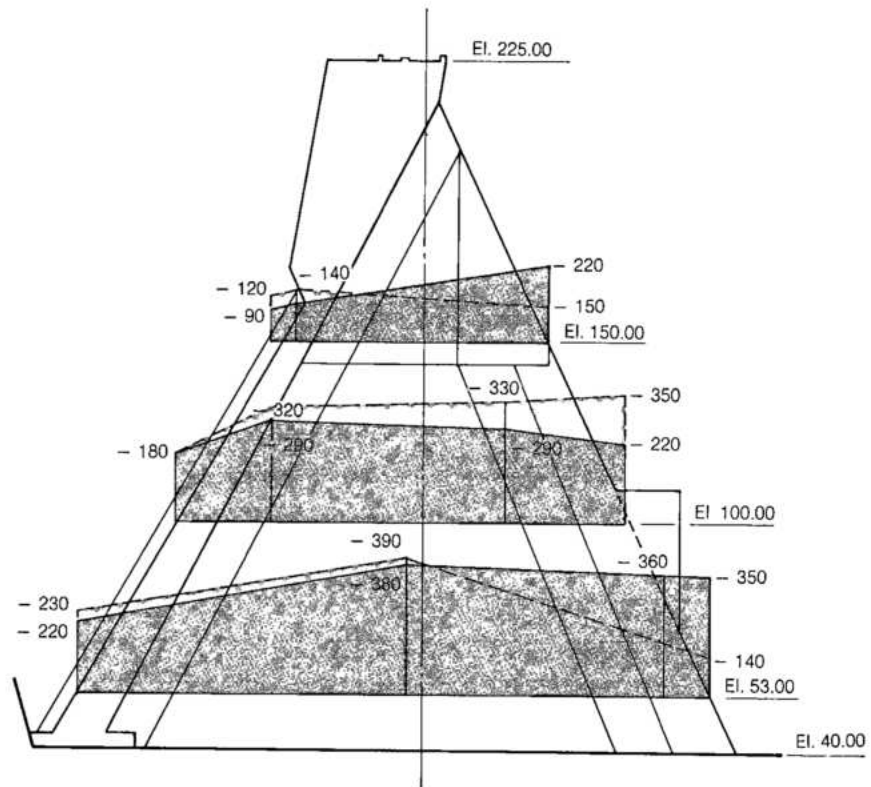




Fig. 9.59 Vertical stresses distributed in a typical hollow gravity block (F19/20)

 Theoretical stress distribution (N/cm^2)
 Stress distribution measured in 1985
 (–) compressive (N/cm^2)

FOUNDATION RESPONSE

PERFORMANCE OF THE BUTTRESS DAM

INSTRUMENTATION AND MONITORING

Instrumentation arrangement

Nine blocks were selected as representative and instrumented to monitor the behavior of the buttress dam. Fig. 9.60 shows the typical layout of instruments in a buttress dam block. In addition, the following types of instruments were installed in the foundations:

- Vertical and inclined multiple extensometers under the head, which penetrated 50 to 70 m into the foundations, including some discontinuities and contacts between different strata.
- Multiple extensometers in the steep rock cut downstream of some of the blocks on the right bank.
- Piezometers under the upstream heads to measure uplift.

High precision geodetic surveys for deflections and settlement of the crest of the entire Itaipu dam included the two wings of the buttress dam.

Settlement

Settlement and lateral deformation of the foundations, and of steep cuts downstream of the nine blocks were monitored by the multiple extensometers. During construction and prior to reservoir filling, the maximum settlement under the highest buttress block was only about 0.1 mm. When the reservoir was filled, settlement of about 1 mm occurred near the downstream part but there was a foundation rise of about 0.8 mm at the upstream head. This indicated a downstream tilting of about 2 mm of the highest buttress dam blocks which stabilized about 2 years after reservoir filling without any measurable increase from the initial values.

Lateral foundation deformations in the directions of flow were negligible prior to reservoir filling, with the exception of deformation of the downstream cut slopes, which is discussed later. Simultaneously with reservoir filling, horizontal deformation of 0.5 to 1 mm in the downstream direction was measured under the heads of two of the highest buttress dam blocks (E6 and I1); at the same time, under the stem in the

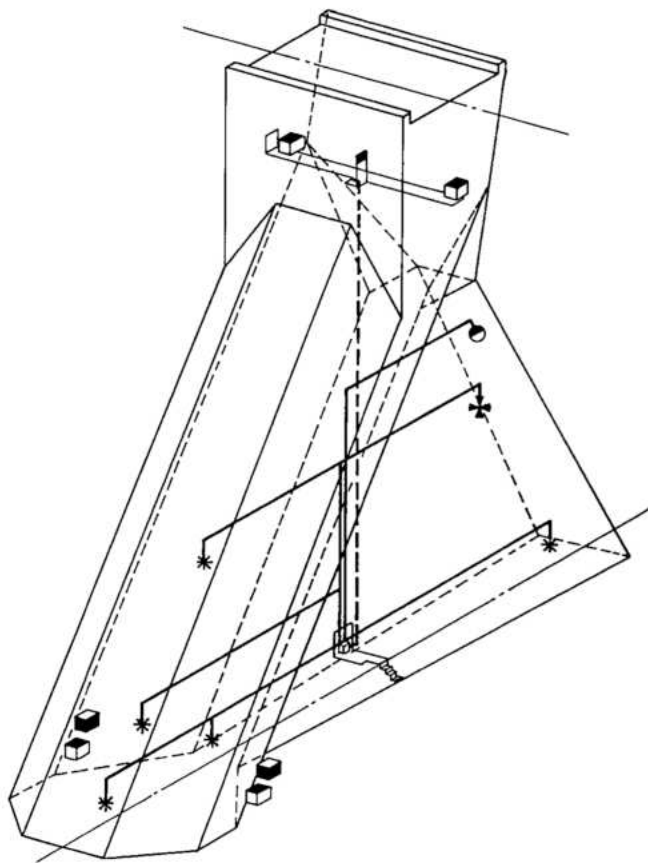









Fig. 9.60 Buttress dam typical instrumentation

-  Mechanical joint meters on floors
-  Mechanical joint meters on walls
-  Strain meters
-  Terminal boxes
-  Direct pendulums
-  Thermometers for surface temperature
-  Multiple stress meters

downstream part it was only about 0.3 mm. The maximum lateral foundation deformation under these high blocks gradually increased to 3 mm in 2 years after reservoir filling, and thereafter remained steady. However, these deformations show a cyclic variation of ± 1 mm in response to the seasonal ambient and water temperature changes. Under the buttress stems the lateral foundation deformations remained unchanged. The lateral deformations under the two highest buttress blocks were attributed to the shearing strains in the contact between basalt and breccia which is located 7 to 10 m under these blocks and has high pore pressures upstream of the main drainage curtain. Since the deformations stabilized, the response of the foundation was elastic and the margin of safety against shearing-sliding adequate.

Behavior of the rock cut and bench downstream of four blocks on the right bank was monitored by near horizontal extensometers installed in the face of the slope and extending 10 to 25 m into the foundations of the dam. Lateral deformations of 1.5 to 2.5 mm occurred as the dam was constructed and before the reservoir was filled. Since there were no similar deformations under other buttress blocks due to

their own weight, these were attributed to stress relief and relaxation of the cut slopes. With the filling of the reservoir and for 5 years afterwards, deformation of the slope increased to and steadied at 4.5 mm in the downstream direction. Analysis of the differential deformation between anchors on the same extensometer and measurements from newer and longer extensometers installed through the dam indicated that:

- Foundation creep was localized in the downstream part of the exposed foundation and had stopped;
- Foundation under the dam blocks was stable and its strength was unimpaired by the permanent deformations that had occurred.

Piezometric and uplift pressures were monitored at the concrete-rock contact and in various foundation joints and discontinuities up to a depth of 30 m under about one-third of the buttress blocks. The pressures were measured both upstream and downstream of the drilled drainage curtain located just downstream of the head. Uplift pressures at the foundation contact developed rapidly following reservoir filling and attained values averaging from 20 to 60% of the hydraulic head. Under the heads of eight buttress blocks the uplift pressures were

almost 100% of the reservoir head. Downstream of the drainage curtain, uplift was less than 10% of the reservoir head. Uplift pressures under the buttress heads showed seasonal fluctuations: increasing in winter and reducing in summer. Otherwise, they had stabilized after four years of operation. While the uplift pressures under eight blocks were higher than predicted, indicating that the grout and drainage curtains were not fully effective in controlling uplift, seepage flow from the drains was small and steady. No remedial treatment was considered necessary, because adequate margins of safety against sliding were available even with the higher uplift.

The grout and drainage curtains were effective in reducing flow through and piezometric pressures in the basalt-breccia contacts which were located 10 m or more under the buttress dam foundations. Uplift pressures in these contacts, between the two curtains averaged 50 to 60% of the hydraulic head.

STRUCTURAL PERFORMANCE

Thermal behavior and cracking

Typical thermal history of a buttress dam block is shown in Fig. 9.61. In the massive head, maximum concrete temperature in the range 30° to 32°C was reached in about 30 days after placement and remained in that range for about 3 months. After that it cooled at the rate of about $1^{\circ}\text{C}/\text{month}$. In the relatively thin buttress, because of exposure to air

on both sides, the maximum temperature was 27° to 30°C , and the rate of cooling about $1.5^{\circ}\text{C}/\text{month}$.

For a concrete lift placed in summer (December), the average temperatures at the end of winter (August) were as follows:

Feature	Maximum temperature($^{\circ}\text{C}$)	Winter temperature($^{\circ}\text{C}$)
Head	32	28
Buttress	30	20

A temperature differential of 8 to 10°C between the head and the buttress and the relatively rapid rate of cooling of the buttress would cause tensile stress concentrations of 150 to $200\text{ N}/\text{cm}^2$ in the areas of high restraint near the foundation and the neck where the buttress stem flares into the head:

In thirty of the highest buttress dam blocks, contraction joints were provided between the head and the stem and in the buttress itself. In these blocks, the tensile stress conditions were alleviated by the joints and no cracking occurred in the buttresses. Some hairline surface cracks, parallel to the upstream slope, did occur on the underside or neck of the head. These cracks, which were shallow and caused in winter by large daily ambient temperature fluctuations, were not of structural consequence.

In the buttress dam blocks shorter than 50 m, which were constructed without contraction joints,

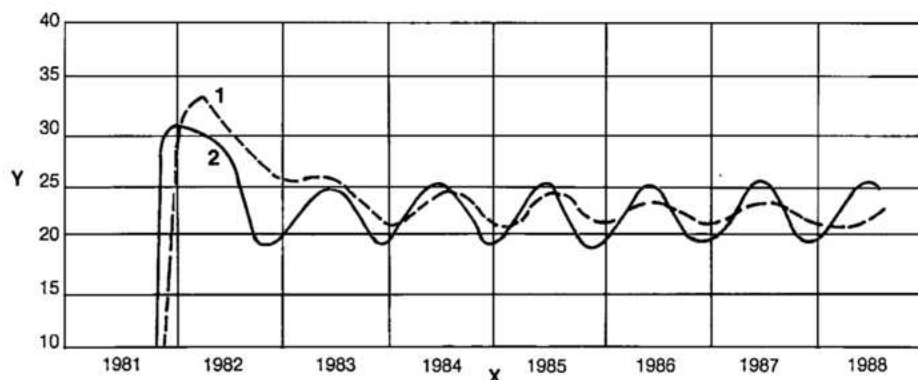


Fig.9.61 Thermal history of a typical buttress block

Y Temperature ($^{\circ}\text{C}$)

X Years

1,2 Thermometers embedded in concrete



vertical and subvertical cracks were first detected in August (winter) 1980, when most of these blocks were either complete or built to more than half their heights. Cracking was not predicted by mathematical analyses because the actual heat of hydration was higher, buttress concrete cooled more rapidly, and the modulus of elasticity of concrete was higher than assumed.

Typical cracks in a 45 m high block are shown in Fig. 9.62. Most cracks were 2 to 25 m in length and 0.1 to 1 mm open in the winter and commenced at the foundations. Investigations, including core hole drilling along and across major cracks during a one year period, (September 1980/August 1981), indicated that about 30% of the cracks in the buttresses were deep and penetrated through the stem. Also, there was a general tendency for the major cracks to progress upwards during each winter. Cracks in the neck of the head were generally shallow.

All cracks which were more than 3 m long and 0.3 mm or more open, were injected with epoxy in September 1981, one year before reservoir filling. Thereafter, the cracks were systematically monitored each winter, and their lengths and openings measured. Seven years after treatment, only two grouted cracks had extended significantly such that they required supplementary injections of epoxy.

Deflections of the dam

Structural performance of the buttress dam blocks was evaluated on the basis of deflections measured by pendulums and stresses and strains measured by embedded instruments. Before reservoir filling, the blocks were responding to seasonal

temperatures, deflecting upstream in the summer and downstream in the winter. The maximum amplitude of cyclical crest deflection of the highest buttress dam blocks was 2 mm in the direction of flow and about 1 mm in the axial direction. These deflections were less than the theoretical values, indicating that the blocks were more rigid than assumed in design, but acting elastically and monolithically before water load was applied.

One month after reservoir filling, and in the middle of summer, all buttress dam blocks had deflected upstream, the maximum crest movement being 2.8 mm. The highest buttress block on the right bank adjoining the hollow gravity dam was an exception: its crest deflected 1.5 mm downstream. This indicated that the weight of reservoir water and expansion of the buttress due to high ambient temperatures and solar radiation, tilted a typical buttress dam block towards upstream, offsetting the downstream bending and deflection due to water pressure. For the highest abutment block, higher foundation deformation and settlement due to the deep cut at its toe, contributed to larger downstream deflection which offset the effect of water weight and ambient heat.

After 5 years of operation, deflections and deformations of all the buttress dam blocks had stabilized, the crest deflections varying within a normal seasonal pattern. For the highest blocks, the seasonal fluctuations in crest deflections were about 4 mm downstream and 2 mm upstream. During this period, there was no relative transverse deformation at the contraction joints between adjoining blocks.

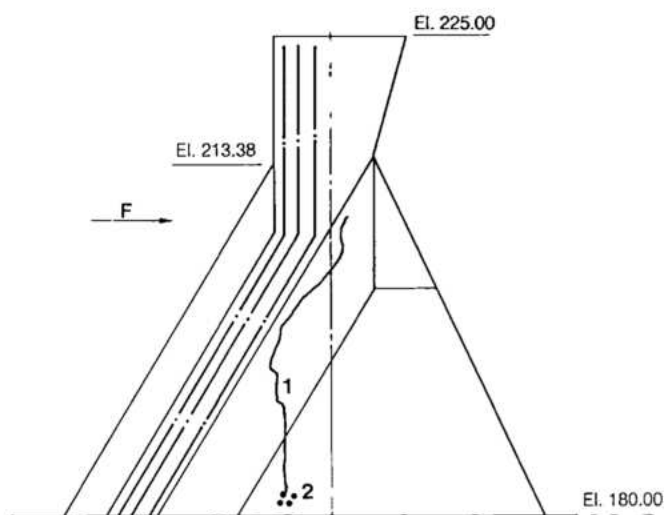


Fig 9.62 Buttress dam - typical cracks

- 1 Vertical crack
- 2 Core holes drilled along the crack
- F Flow direction

Stress development

Development of vertical stresses in the highest buttress block, (E6), were continuously monitored commencing with the start of construction, by six stress meters embedded in the head, the stem and the downstream strut, and located 6 m above the foundations. Fig. 9.63 shows the history of the vertical stresses from 1980 through 1988, when the block was topped out in June 1982, the vertical stresses were due to the weight of the dam and the thermal effects, and averaged as follows:

Location	Before reservoir filling, June/82 (N/cm ²)	After 5 years of operation, June/87 (N/cm ²)
Head	150	280
Buttress stem		
Upstream	100	120
Middle	150	180
Downstream	150	180

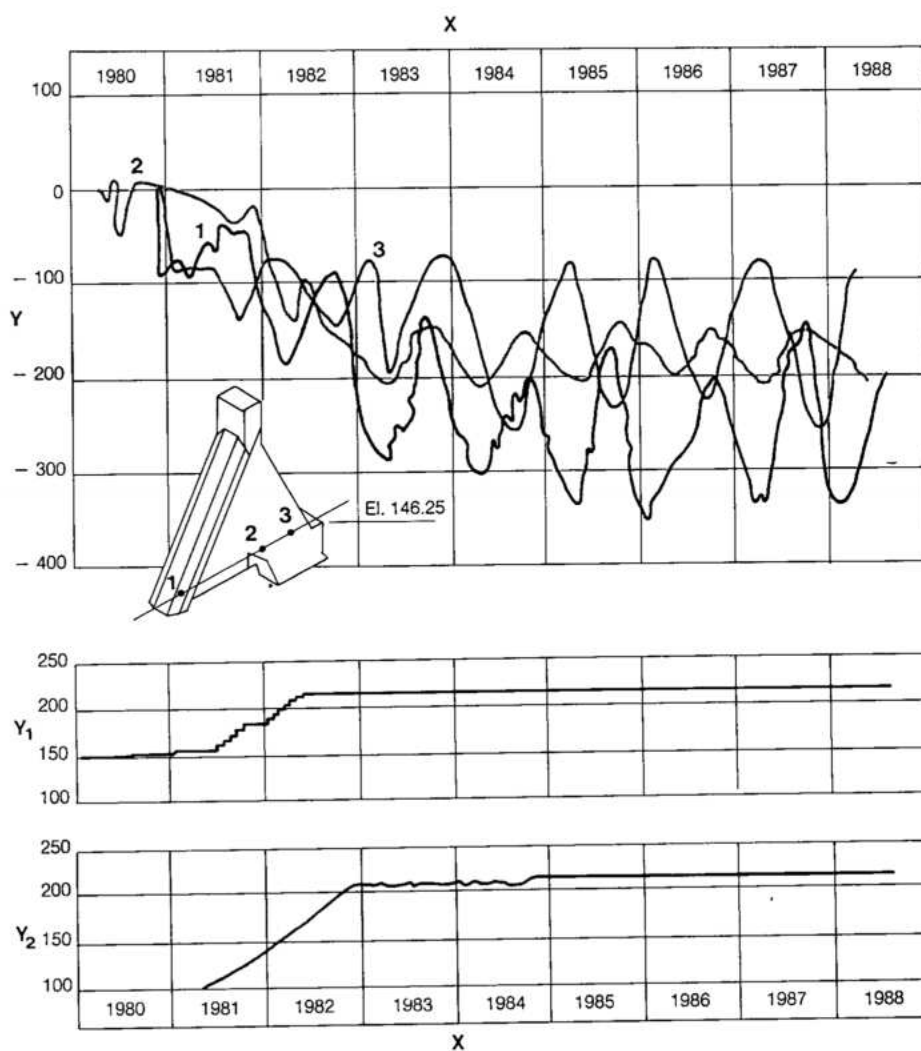


Fig.9.63 Stress history of buttress block E6

Y Stresses (N/cm²)

X Years

Y₁ Concrete elevation (m)

1,2,3 Stress meters

Y₂ Reservoir level (m)

Even before reservoir filling, the vertical stresses were responding to seasonal ambient temperature cycles. In the summer, the buttress expanded, introducing counter-clockwise bending moment in the dam. This increased the compressive stress in the head and upstream part of the buttress by 50 to 70 N/cm² from the average and reduced the stresses in the downstream part of the buttress by about the same amount.

One month after the reservoir was filled, (which was in summer), there was an increase in compression of about 50 N/cm² in the buttress. After 5 years of operation, as the foundation deformations stabilized, the average vertical stresses had also achieved a steady state. While the average stress in the head almost doubled, there was only a small increase in the buttress. The steady stresses compare reasonably well with the theoretically computed values and confirm satisfactory structural performance of the buttress dam.

Seasonal fluctuations in the vertical stress are 150 N/cm² near the toe of the buttress. In the upstream and middle part of the buttress the amplitude of stress changes is only 30 to 50 N/cm². The cyclical stress changes attest to the very high influence of ambient temperature changes on the behavior of the structure, and also indicate that the buttress dam blocks are functioning as stable elastic monolithic structures with stresses well within the limits of safety.

Stresses in the heads of three buttress dam blocks were also monitored by rosettes of five strainmeters embedded near the foundation. No tensile stresses were detected in any direction, either during the first 2 years when the concrete cooled down to the average ambient temperature, or after the reservoir was filled. After 7 years of reservoir operation horizontal stresses near the foundation in the axial direction were compressive and ranged 100 to 150 N/cm². No transverse cracks or leakage through the heads of any of the buttress dam blocks had occurred, which also indicated satisfactory and safe performance of the structure.

Watertightness of the wing buttress dams

Internal drains formed in the heads of the buttress dam were pressurized and tested for leaks, before the reservoir was filled. Six months after reservoir filling 90% of the internal and joint drains were functioning; while most drains were wet, the flow was generally less than 3 l/min per drain. In one block on the left bank, two drains were discharging 10 to 20 l/min, but the flow was steady 2 to 7 years after reservoir filling, with seasonal fluctuations related to the cyclical bending of the block.

Another exception was the flow from joint drains of a block at the right abutment and two joint drains on the left flank. In 1989, these joint drains were each discharging between 10 and 30 l/min. The total seepage flow through the buttress dam was less than 150 l/min in 1989. Also, there was a noticeable tendency of reduction in overall seepage.

Summary

All individual blocks in the three buttress dam wings D, E and I were performing satisfactorily. Treatment of cracks with epoxy had adequately restored the integrity of the blocks and they were responding as elastic and monolithic structures in sustaining the reservoir and thermal loads within the required safety limits. The foundation had attained a state of elastic equilibrium and the uplift pressures were effectively controlled by the foundation drainage system.

POWER INTAKES, PENSTOCKS AND EQUIPMENT IN THE CONCRETE DAM

EQUIPMENT ALLOCATION	10.3
Right Wing Buttress Dam (D and E Blocks)	10.4
Main Hollow Gravity Dam (F Blocks)	10.4
Diversion Control Structure (H Blocks)	10.4
Left Buttress Dam (I Blocks)	10.5
POWER INTAKE DESIGN	10.5
Hydraulic Design	10.5
Hydraulic Model Tests	10.6
Structural Design	10.8
TRASHRACKS	10.9
TRASHRACK CLEANING MACHINES	10.11
INTAKE GATES	10.15
General	10.15
Conversion of the Gates	10.16
Operating Experience	10.20
STOPLOGS	10.21
GANTRY CRANES	10.23
Basic Characteristics and General Equipment	10.23
Component Design and Manufacture	10.25
PENSTOCKS	10.27
AUXILIARY EQUIPMENT	10.31
Dam Drainage Pumping System	10.31
Sanitary Services	10.33
Water Treatment Plants	10.33
Potable and Chlorine Free Water	10.33
Evaporative Cooling Ventilation System Make-up Water	10.33
Ventilation	10.34

POWER SUPPLIES	10.35
General	10.35
50 Hz Auxiliary Power	10.35
60 Hz Auxiliary Power	10.36
125 V dc Systems	10.36
PROTECTION, CONTROL AND INSTRUMENTATION	10.36

POWER INTAKES, PENSTOCKS

AND EQUIPMENT

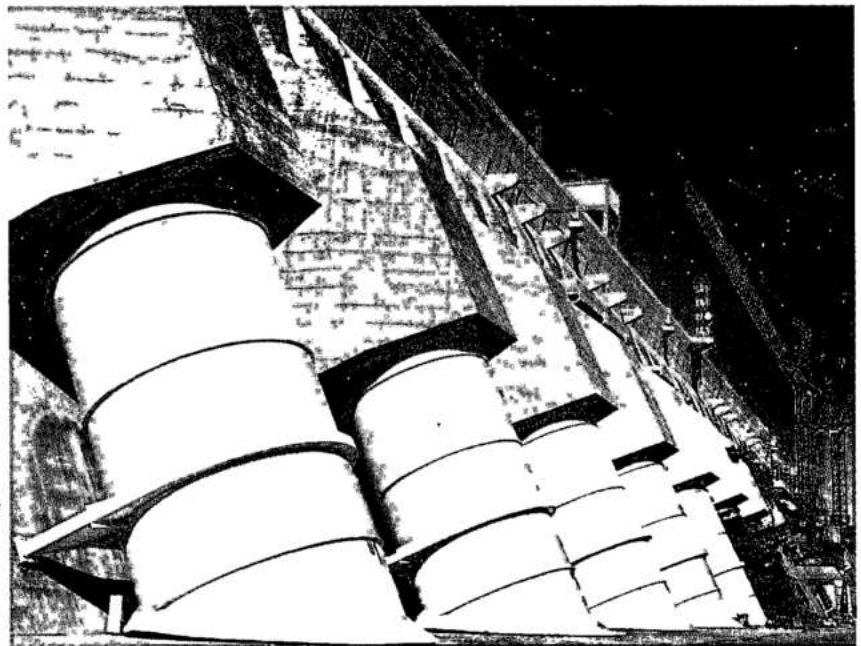
IN THE CONCRETE DAM

EQUIPMENT ALLOCATION

In addition to the power intake equipment such as gates, hoists, stoplogs, trashracks, gantry cranes, and the penstocks, the following electromechanical equipment is located in the various parts of the concrete dam:

- Elevators and access ladders.
- Drainage pumping stations.
- Ventilation systems in the enclosed galleries and foundation tunnels.
- Sewage collection and pumping systems.
- Domestic water treatment plant.
- Telecommunication stations.
- Electrical substations and control panels.

The various sections of the concrete dam between the spillway on the right bank and the rockfill dam on the left bank have a common crest at El. 225 which provides continuous road access between the two banks. Because of location and differences in structural configuration, the concrete dam blocks have a widely differing allocation of equipment. The distribution of equipment in the various parts of the concrete dam is thus presented separately.



*View of penstocks
from El. 144*

RIGHT WING BUTTRESS DAM (D AND E BLOCKS)

This part of the concrete dam, comprising sixty four buttress blocks, is 1088 m long and extends from the spillway to the main hollow gravity dam. A gallery at El. 214 runs continuously through the entire concrete dam; manual access to the gallery is via steps from the crest road at El. 225 at several locations. This gallery gives access to the various structural instruments embedded in concrete or their panels. A drainage pumping station, which forms a part of the system for handling seepage through the dam and its foundations, is located at El. 176, in buttress block D7, about 110 m from the end of the spillway.

A second access gallery at El. 169 commences in the last two blocks of the right buttress dam and continues through the hollow gravity dam; steps from El. 225 lead to this gallery and the lower downstream part of the dam is accessible via external metal ladders. Three towers for 500 kV transmission lines to the right bank substation are located on a platform on the upstream face of three blocks of the dam at El. 195, which are accessed through a transverse gallery.

The last two blocks adjoining the hollow gravity dam (E5 and E6) house the stoplog storage chamber and a room at El. 213.50 in which the upstream water level transmitter is located; this room is reached by steps from El. 225.

When not in use, a stoplog gantry crane and a trashrack cleaning machine are anchored on top of blocks E3 and E4. The right bank water treatment plant for the project area is at El. 160.5 between blocks E3 and E4.

MAIN HOLLOW GRAVITY DAM (F BLOCKS)

Sixteen power intakes are located in sixteen 34 m wide hollow gravity blocks. The two left end blocks (F33/34 and F35/36) which do not have power intakes, are located upstream of the central assembly area of the powerhouse.

Power intake equipment consists of trashracks, stoplogs, intake gates and hoists, by-pass valves and penstock filling lines, and penstocks for each intake. Two intake gantry cranes and two trashrack cleaning machines serving all the power intakes are stationed on the main dam.

The intake of the tenth block (F19/20) has no power intake equipment; it is intended for future expansion of generating capacity if required, and is currently sealed with concrete stoplogs. Spacing of

intakes at 34 m centers is the same as generating unit spacing in the powerhouse.

Also installed in the main dam is the following auxiliary equipment:

- Drainage pumping plants at the base or in the foundations of the dam, which are a composite part of the dam drainage scheme.
- Sewage collection and pumping system for the various toilets located in the main dam.
- A water treatment plant at El. 161 near the left bank (block F33/34) for the project area.
- Reservoir level transmitters at El. 213.50 in left end block F35/36.
- Telecommunication rooms, together with the necessary ventilation and local air conditioning system, potable water reticulation, access elevators and electrical substations and control panels.

The road across the top of the dam at El. 225 gives vehicular and pedestrian access to the intake gate servomotors, gantry cranes and trashrack cleaning machines, which are all mounted or operate at this level. Stairs located in towers lead from El. 225 to galleries at eight levels ranging from El. 214 to El. 56.5. These galleries are also accessible from the El. 144 road upstream of the powerhouse. Metal walkways at selected locations give access between galleries and to instrumentation and other equipment in the dam. The intake gate by-pass valves and penstock access doors are located in blockouts at El. 179 which are reached via steps and metal walkways from the El. 169 gallery. Intake gate hydraulic pumping sets are located in rooms adjoining the El. 214 gallery.

When not in use two sets of stoplogs are stored in a chamber in the left end block (F35/36).

DIVERSION CONTROL STRUCTURE (H BLOCKS)

Four power intakes are located in the upper part of the diversion control structure, but only three have intake equipment. The extra intake could be outfitted with equipment if an additional generating unit were installed in the future. The two blocks without power intake equipment correspond to unit blocks 9A and 18A which are without generating equipment.

Because of the constraints of the narrow and deep diversion channel, the central blocks of the diversion structure with the four power intakes are 24.6 m wide as compared to 34 m generating unit spacing. To adapt to this difference, a lateral curve was provided in the lower reducing bend to ensure alignment of the penstock with the turbine spiral case, see Chapter 12. However, the

internal configuration of the power intakes on the diversion control structure is identical to those of the sixteen intakes on the main dam.

After the closure of the diversion gates and filling of the reservoir at the end of 1982, the twelve sluices were plugged with concrete. The four power intakes were completed before reservoir filling and the structure of the four powerhouse blocks at the toe of the diversion control structure was constructed in 1986-89.

Track rails for the intake gantry cranes and trashrack cleaning machines are continuous to the left end of the diversion control structure where there is a parking area for the machines when out of service. Longitudinal access galleries are located at El. 214, El. 169, El. 144, El. 114.20 and El. 67.25, and are connected by transverse galleries leading to instrumentation recesses.

A drainage pumping sump in the lowest gallery at El. 67.25 in the left end block is an integral part of the system for controlling drainage through the entire concrete dam and its foundations. Another drainage pumping sump, with pump platform at El. 118.5 and sump bottom at El. 76.7 is located in block H8 at the powerhouse - dam interface and drains leakage water of penstock joints and from adjoining galleries. The galleries are ventilated by a mixture of forced fan and natural ventilation and elevators and stairs provide vertical access.

LEFT BUTTRESS DAM (I BLOCKS)

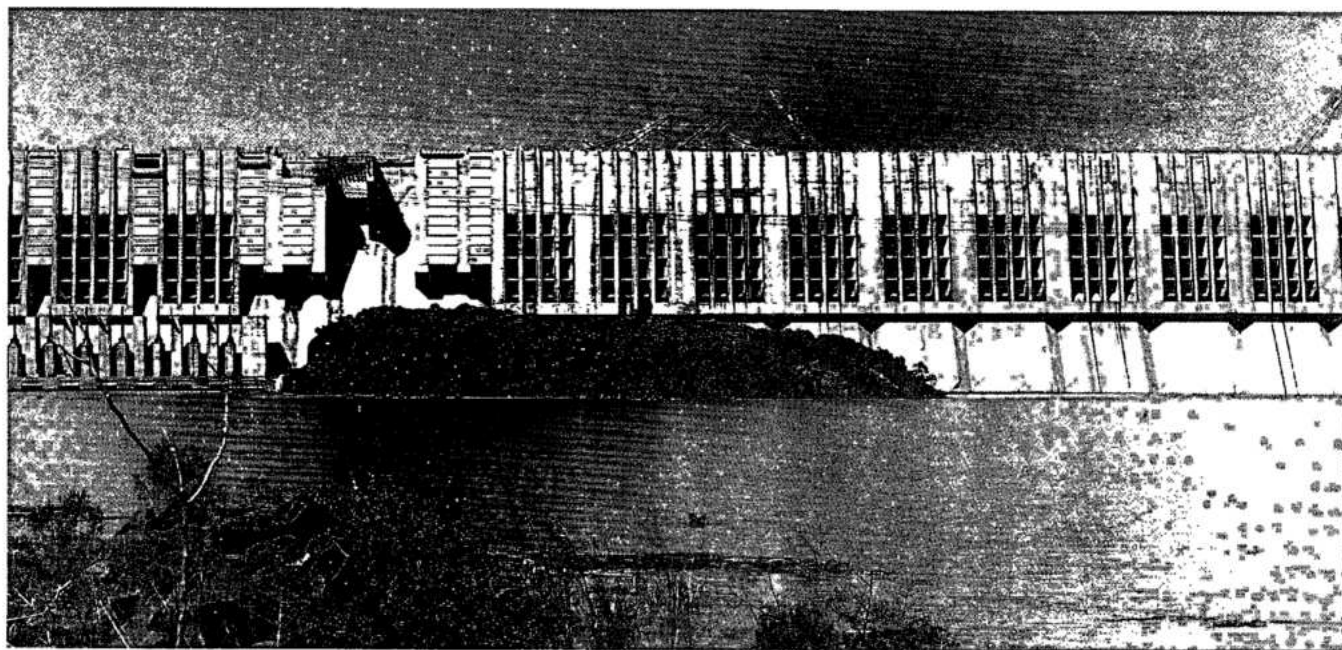
The accesses in the dam blocks between the diversion control structure and the rockfill dam are similar to those in the right wing dam blocks. There is a continuous access gallery at El. 214, which is reached from El. 225, and several local galleries which are accessible at El. 144 from the powerhouse area. A pumping plant is located at El. 164 in a central block.

POWER INTAKE DESIGN

HYDRAULIC DESIGN

All the power intakes are identical in configuration, design and equipment. The following considerations governed the determination of the shape and dimensions of the water passages:

- Velocity of flow should increase gradually from the trashracks to the gate location.
- Head losses at the trashracks and in the entire intake should not be excessive.
- Negative pressures should not develop in corners at stoplog or gate slots.



Intakes before flooding of reservoir

- During operation at normal or minimum reservoir levels, suction of air into the penstock should not occur.
- Vortex formation under various reservoir levels and unit operation sequences, particularly at intakes on the right bank, should not be excessive and cause trashrack vibrations.
- The structural design should be simplified to facilitate rapid construction.
- Width of the intake gates should be the same as that of the diversion gates.

The last criterion was established in 1976 after extensive studies of the practical feasibility and economic justification for reuse of the diversion gates in the power intakes. Thus the width of the power intake throat at the gate slot was fixed at 6.7 m, and the area of the opening is 100 m² or 115 % of the penstock area.

The level of the intake gate sill was established at El. 177.56, to permit power operation with the reservoir at El. 200. While it is planned to operate Itaipu as a run of river plant with a drawdown of less than 1 m, under certain emergency conditions such as major repairs to the spillway, it may be necessary to operate the powerplant at reservoir drawdown to the spillway crest level. The soffit at the stoplog slot is at El. 194.15, which provides enough submergence at reservoir level El. 200 to prevent air suction during operation. Hydraulic profile and section of a typical intake are shown in Fig. 10.1.

The gross area of the intake opening is 792 m² and net area is 600 m². For normal turbine discharge of 660 m³/s, the average velocities are 1.1 m/s at the trashracks, 6.4 m/s at the intake gate and 7.6 m/s in the penstock.

The 2 m diameter air vent shaft necessary for air supply when filling and draining the penstock is located in the roof 3 m downstream of the intake gate.

HYDRAULIC MODEL TESTS

Design of the power intakes was tested and optimized on two hydraulic models:

- A comprehensive 1:100 scale model including all intakes, concrete dams and the spillway.
- A 1:50 scale model of a single intake, penstock, lower bend and the turbine spiral case.

The main objective of the tests on the comprehensive model was to study the formation of vortices, and approach and return flow conditions for various unit operating sequences. Various physical provisions for the reduction or elimination of vortices were also tested.

The following powerplant unit operation conditions were considered:

20 units in operation	no. 1 to 20
18 units in operation	no. 1 to 18
16 units in operation	no. 1 to 16
12 units in operation	no. 1 to 8 and 17 to 20
8 units in operation	no. 1 to 8, or 4 groups of 2 units each
4 units in operation	no. 1, 2, 7 and 8

In the test series the following reservoir elevations were used: 220, 215, 212.5, 210, 207.5, 205 and 202.5. The spillway was not in operation during the tests.

The principal results and conclusions obtained from the tests were:

- In the dead water between adjoining power intakes, horizontal rollers occurred, causing lateral flow. The intensity of roller and lateral flow increased with lower reservoir levels (El. 205 – El. 210), and eventually turned into a vortex discharging into the intake.
- Oblique or lateral currents from one side to the other occurred at the end blocks and for a few isolated units in operation.
- Uniform approach flow conditions, which occur when sixteen to twenty units are in operation, do not facilitate vortex formation.
- There is a definitive risk of vortex formation when reservoir level is below El. 215.
- There is a possibility of vortex formation with reservoir at El. 220, when units are operated in isolated groups, e.g. eight units operating as follows: no. 1, 2, 7, 8, 13, 14 and 19, 20. But no vortices occurred when units 1 through 8 were in operation simultaneously.

Fig. 10.1 Hydraulic profile of power intake (page 10.7)

1 Dam axis	10 Intake gate
2 Curve $x^2+9y^2=16.73$	11 Distance from the axis of the main dam to the powerhouse centerline, 111.5 m
3 Curve $x^2+9y^2=17.8$	12 Width of dam blocks, 34 m for dam blocks: F 1/2 to 31/32; 24.60 m for diversion structure blocks H 3/4, H 6/7, H 9/10 and H 12/13
4 Intake	13 Tangency point
5 Ventilation duct	14 Flow direction
6 Transition in concrete	
7 Steel penstock, 10.50 m diameter	
8 End of 1st stage concrete	
9 Stoplogs	

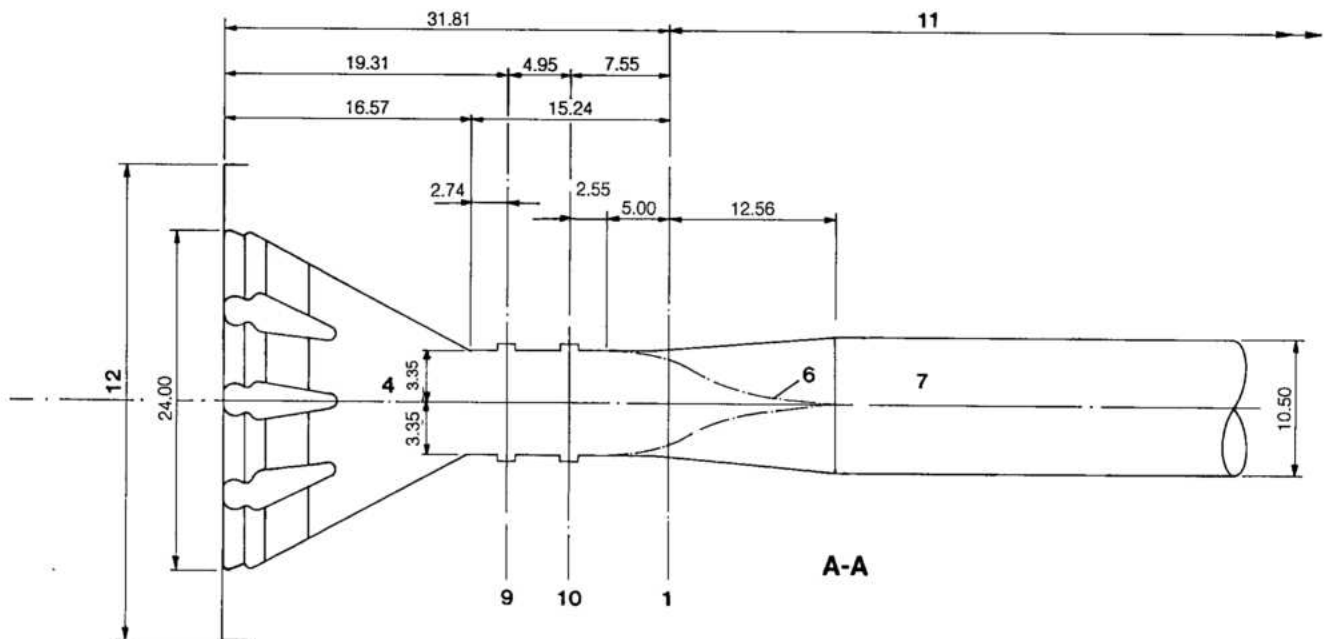
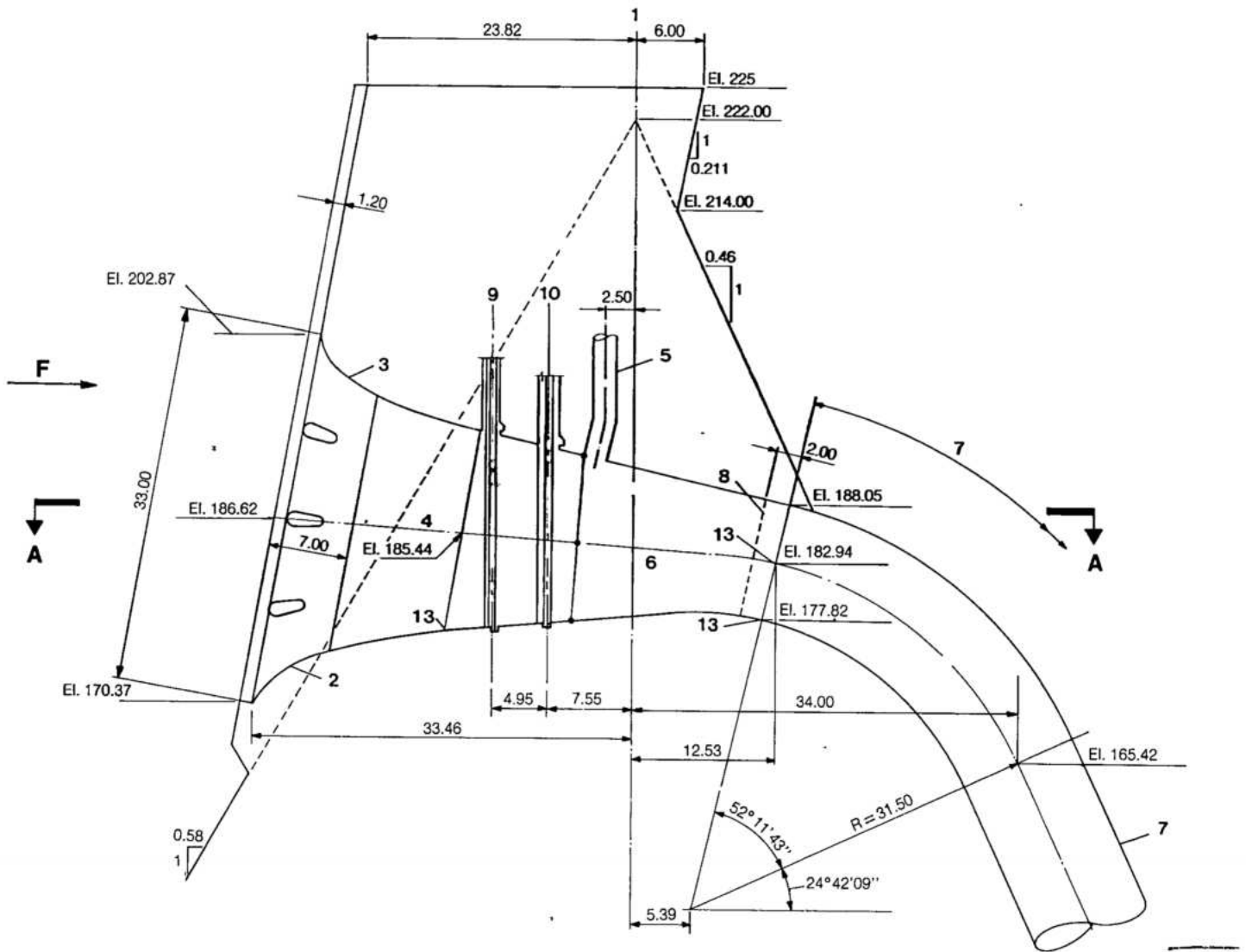
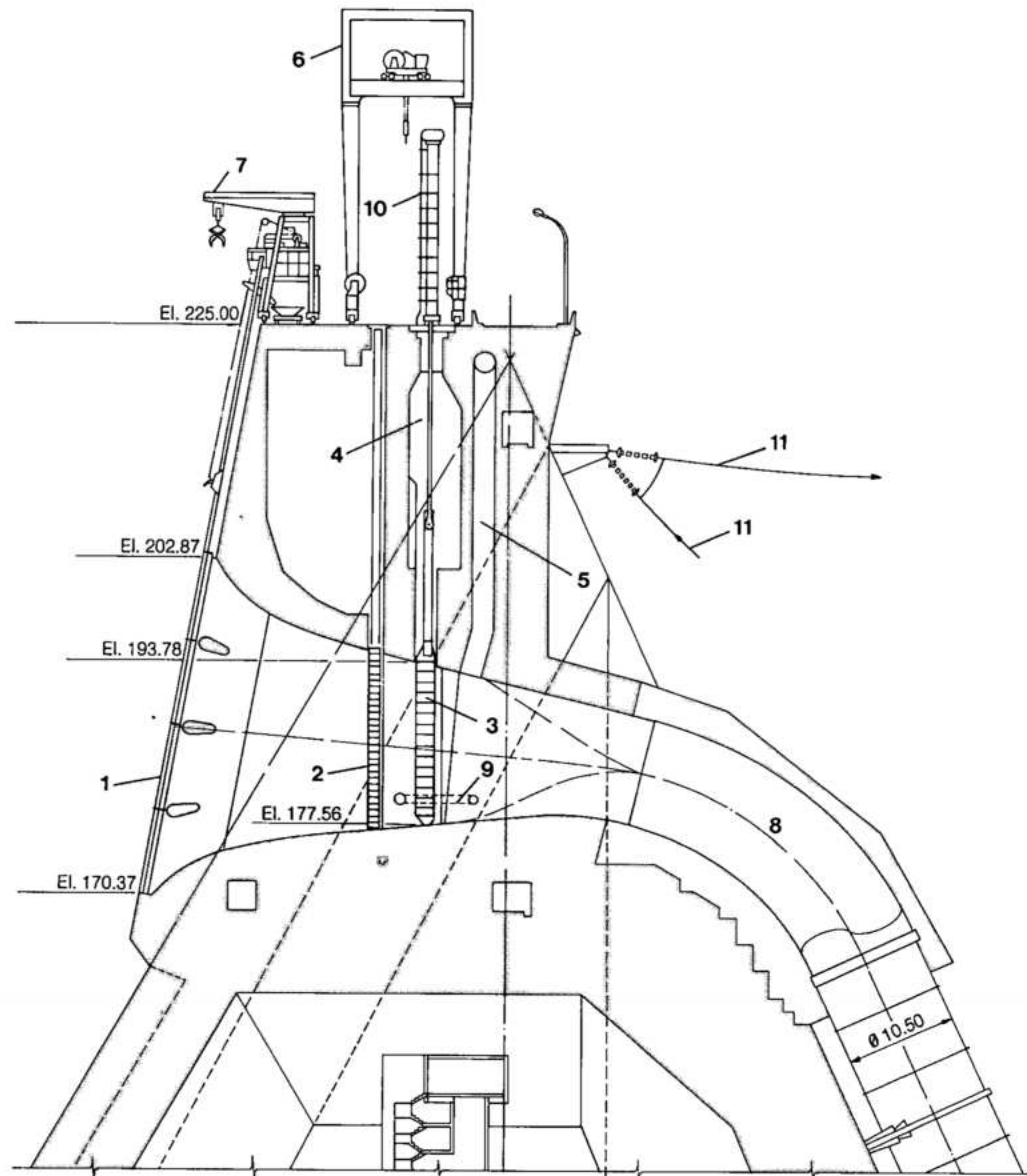


Fig. 10.2 Typical power intake

- 1 Trashracks
- 2 Stoplog
- 3 Intake gate
- 4 Gate maintenance chamber
- 5 Air vent
- 6 1100 kN gantry crane
- 7 Trashrack cleaning machine
- 8 Penstock
- 9 By-pass valve
- 10 Intake gate servomotor
- 11 Transmission lines



To eliminate lateral rollers and cross flow between intakes, which facilitated the formation of vortices, the following remedial provisions were tested and implemented:

- The breast wall was extended into the space between the intakes.
- For one end block on either side of the main dam and the diversion control structure, piers were extended from the face of the dam to the same configuration as the end walls of the power intakes. Precast concrete panels were used to build a face parallel to the trashracks and the breast wall. A 30 cm horizontal slot was left open between the panels.

Vertical slots and circular orifices in the breast wall, which would circulate water behind the trashracks, were tested on the models to check their

efficacy in preventing vortex formation. Circular orifices were more effective than the slots. However, these provisions were not implemented, because it was considered that the probability of occurrence of vortices is small and can be eliminated by avoiding operation of units in isolated groups.

STRUCTURAL DESIGN

The power intake structure, including the water passage, the breast walls, piers and beams, was designed and built of reinforced concrete, to act as a monolithic part of the block of the dam on which it is located. Structurally, each power intake is separated from the adjoining ones by plain transverse contraction joints.

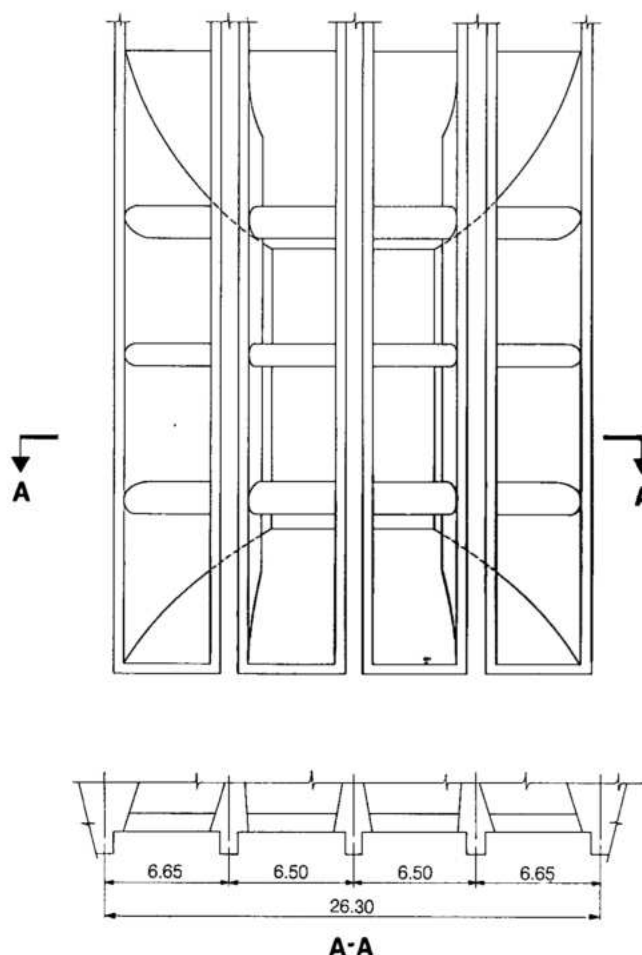


Fig. 10.3 Power intake : view from upstream

Cross-sections of a typical power intake are shown in Fig. 10.2 and front elevation in Fig. 10.3. Three concrete piers and three concrete beams support the trashracks. The end walls of the bellmouth are massive with minimum thickness of 1.2 m for the intakes on the diversion control structure and 2 m on the main dam. The 25 m high breast wall, rising from the roof of the power intake entrance, protects the stoplog slot, and provides a base for extension of trashrack guides to top of the dam at El. 225.

The vertical piers and the horizontal beams supporting the trashrack panels, like the trashracks, were designed for a maximum normal differential head of 7.5 m and a maximum exceptional differential head of 10 m. Reinforcement around the bellmouth, the throat and the unlined transition, was provided for the most critical combination of internal hydrostatic pressure and the stresses induced by the weight and deflection of the structure. At the

base, reinforcement was also provided for adequate anchorage into, and elastic continuity with, the mass concrete structure of either the hollow gravity dam or the massive gravity diversion control structure.

A special site-fabricated formwork was used for placing concrete in the transition between the intake gate and the penstock to the close finish tolerances required by the specifications. However, to expedite construction, precast concrete beams, inverted T in shape, were used to form the soffit of the intake bellmouth upstream of the stoplogs.

TRASHRACKS

As shown in Figs. 10.2 and 10.3 the intake is divided into four equal parts by the vertical concrete piers with five identical lower trashrack panels and one upper panel in each. Trashrack construction is such as to give a free water passage 150 mm wide by 700 mm deep, the width corresponding approximately to the turbine wicket gate opening for 10% output. Trashracks were designed to DIN 19704 for a differential head of 7.5 m in normal case and 10 m in exceptional loading. The vertical bars of the trashrack panels are supported by fish belly type horizontal beams constructed of mild steel plates strengthened with extruded rectangular steel section, welded to the plate edge. Bronze surfaced pads mounted on the downstream face of the beams transmit forces to the embedded parts and two similar pads on each side of the panel at its extremities ensure lateral positioning of the panel during deployment. Two stainless steel pins on the upper horizontal beam mate with bushes on the lower beam to ensure accurate alignment of two panels. Each lower and upper panel has nine horizontal beams, the only difference between the two types of panel being that the upper panel has the bars of the racks extended on a welded structure to form a cage at the top of the intake opening. The hooks of the lifting beam engage pins welded to the upper horizontal beam of each panel. The design was checked for resonant coincidence of the frequency of shedding vortices from the bars, with the natural frequency of the bar.

Blockouts were left in the first stage concrete for the mild steel guides, which were subsequently embedded in second stage concrete. Embedded steel plates, positioned at intervals in the first stage concrete, facilitated the erection of the guides. The guides position not only the trashrack panels and lifting beam but also the



*Manufacture of
trashracks at CIE in
Asunción*



Installation of the trashracks in the intake



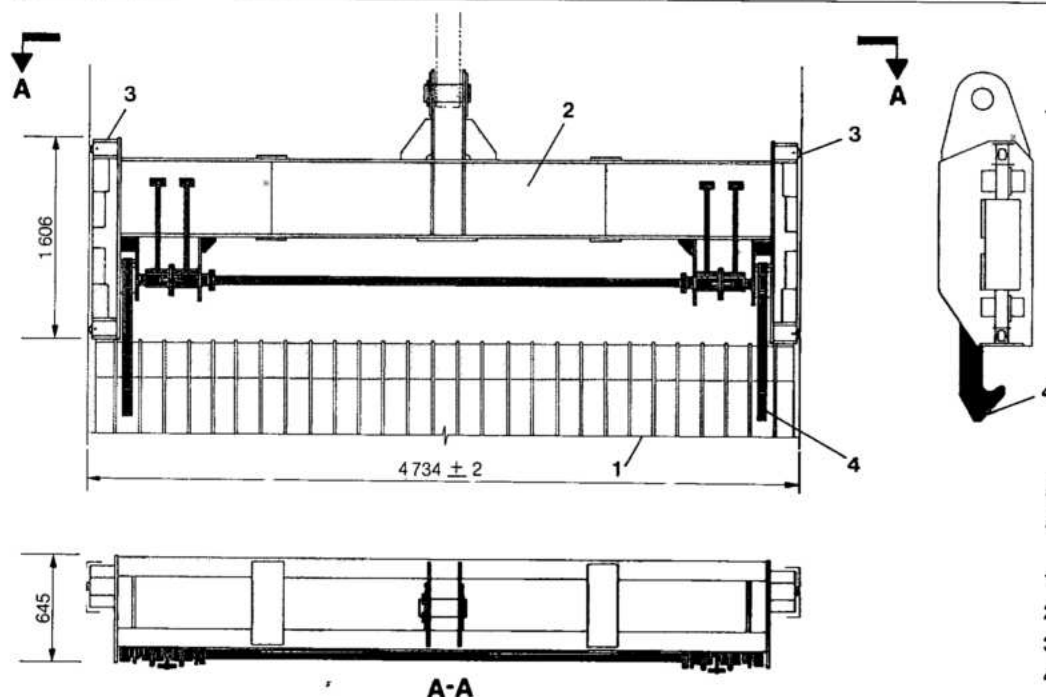
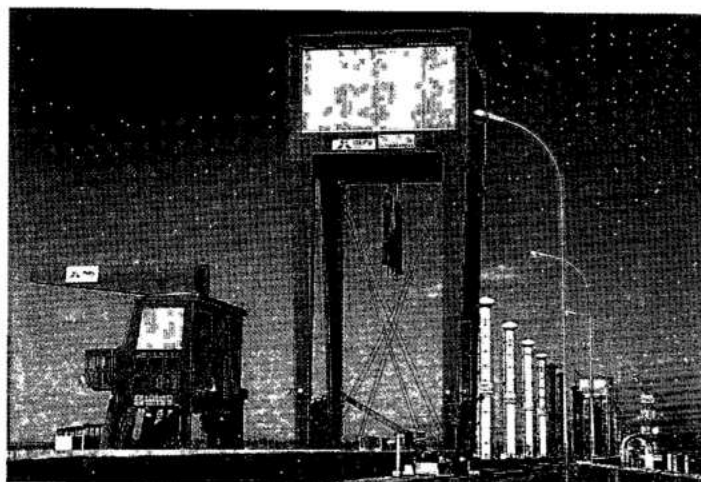


Fig. 10.4 View of lifting beam

- 1 Trashrack
- 2 Lifting beam
- 3 Wheels
- 4 Hook



Trashrack cleaning machine, gantry crane and intake gate servomotors at EL. 225

grab of the trashrack cleaning machine and were erected to an accuracy of $+1/-3$ mm on the guiding surface before embedment. Two wheels on each side of the lifting beam run in the guides and the hooks of the beam either engage or release a panel depending on the position of the hand-operated counterweights, see Fig.10.4.

Operation of the lifting beam is from the auxiliary hook of the trashrack cleaning machine from which it is suspended by a centrally positioned horizontal shaft. A system of embedded pipes in the concrete columns of the intake opening attached to differential pressure transducers measure pressure differential across each set of panels, the signal from which is used to give local and remote alarm when it exceeds 4.9 m head. The trashrack cleaning

machine is then used to remove the obstructing material.

Intake trashracks and embedded parts were fabricated by the consortium of Brazilian and Paraguayan companies Badoni, Ishibras, Coemsa and CIE.

TRASHRACK CLEANING MACHINES

Floating vegetation, logs and other debris which accumulate on the trashracks is removed by the trashrack cleaning machines, which are also used to handle the trashrack panels.

There are two machines operating from El. 225, each of which can serve the twenty intakes. When not in service the machines are parked and tethered in designated areas, one on each side of the dam.

The leading dimensions, weights and characteristics of the trashrack cleaning machine are:

Size

Length	15 m
Height	12.7 m
Width	4.5 m

Weight (complete)	838.7 kN
--------------------------	----------

Maximum translation speeds

High velocity	28 m/min for 50 Hz
	33.6 m/min for 60 Hz
Low velocity	2 m/min for 50 Hz
	2.4 m/min for 60 Hz

Grab

Maximum speed descending	28 m/min for 50 Hz
	33.6 m/min for 60 Hz
Maximum speed ascending	14 m/min for 50 Hz
	16.8 m/min for 60 Hz
Maximum capacity	2.5 kN
Maximum volume	2 m ³

Jib crane

Maximum capacity	200 kN
Hoist speed	8 m/min for 50 Hz
	9.6 m/min for 60 Hz

Wheeled cart

Number	5
Capacity	98.1 kN
Maximum volume	8 m ³

Tractors

Number	2
Type	Mercedes Benz with hydraulic operated front loader

The trashracks can be cleaned with a turbine in operation at maximum wicket gate opening. Mounted on a common wheeled structure, the machine is split into two functionally different sections, one a grab which combs

the racks clean and the other a pillar jib crane which is used to remove large items, such as logs, from the water and also handle the trashrack panels. The two machines are serviced by five tractor pulled carts in which the trash is hauled to designated disposal areas. Power supply to the machines is through a flexible cable which runs in a trench at El. 225. There are two power feederplugs in block F23/24, downstream of the machine approximately at the center of its operating range. The left feeder supplies power at 60 Hz and the right at 50 Hz. However as the machines can operate at both frequencies (although at different speeds) this does not restrict their interchangeability. The specification called for design and manufacture to the standard of the Fédération Européenne de la Manutention (FEM) Section I, with the following specific requirements:

Structure

Class of utilization	B	Regular use on intermittent duty
State of loading	2	Appliances which hoist the safe working load frequently and normally load between 1/3 and 2/3 of the safe working load
Group	4	

Grab and translation mechanism

Class	V2	Average daily operating hours 2, and theoretical life 6300 hours
State of loading	3	Mechanisms or components subjected for the most part to loads close to the maximum
Group	3 m	

Crane

Class of operation	V2	Average daily operating hours 2, and theoretical life 6300 hours
State of loading	2	Mechanisms or components subjected to moderate and maximum loads for substantially equal periods
Group	2 m	

The group is automatically determined by the preceding class and state which in turn were obtained from a study of the maximum use of the machine.

During the first 6 years of project operation the machines were scarcely used because, except during the first filling of the reservoir, the water had

been virtually free of debris. Obviously this could change with changing climatic conditions and use of the reservoir.

Specified maximum design wind velocities were 100 km/h in service and 150 km/h with the machine parked and tethered. As shown in the general arrangement of Fig. 10.5, the structure of the cleaning machine comprises six box girder legs made from welded mild steel plate, three supported on the downstream rail and three on the upstream. The center legs divide the machine into the two functional sections, trashrack cleaning and log and trashrack handling. The upstream legs are inclined at 10° corresponding to the slope of the trashracks. Horizontal platforms connected to the legs support the mechanical and electrical equipment for the various drives. There are two separate control cabins mounted on each of the upstream end legs, trashrack cleaning being controlled from left cabin and the handling crane from the other. Travel of the machine along the rails can be controlled from either cabin. When one cabin is in service the controls of the other are automatically disconnected. The control cabins are totally enclosed with ample windows for visual monitoring of the operations. There are multiple lamps for night use of the machine.

The trailing cable which supplies electrical power to the machine is wound on to a large drum located between the left and center downstream legs. A variable speed induction motor driving through a gear reducer, rotates the drum. Speed control is by

variable resistances in the supply to the stator, controlled by the setting of the travel speed of the machine. The same motor, via chain drives, indexes the cable feed horn along the drum, see Fig. 10.6. Power from the cable is supplied from the center of the drum to the machine, through slip rings.

Travel of the machine is by one of two electric motors, mounted on the internal platform which, via a gear reducer and two shafts, drive the wheel units attached to the two left legs, see Fig. 10.7. The wheel units of the center and right legs are free wheeled. One of the electric motors is for high velocity translation and the other is for inching movements when the machine is near its final position at the trashrack. Both motors are slip ring rotor resistance speed controlled, the resistance switching sequence being automatic up to the final speed as selected by the operator. Switching from the high speed motor to the low speed is automatic from sensors attached to the machine, which respond to the change in inductance when they pass over embedded steel plates. There are two sets of sensors, one for positioning the machine for trashrack cleaning and the other for positioning for use of the crane. For fast travel to the selected trashrack, the sensors are disconnected by the operator and reconnected when approaching the chosen trashrack. During operation at the trashrack the machine is manually chocked-in position by a Vee block, the underside of which is forced onto the rail, and the upper Vee portion via a free wheel, impeding any movement of the machine in either direction. Hydraulic buffers on the end legs protect the machine from collision damage.

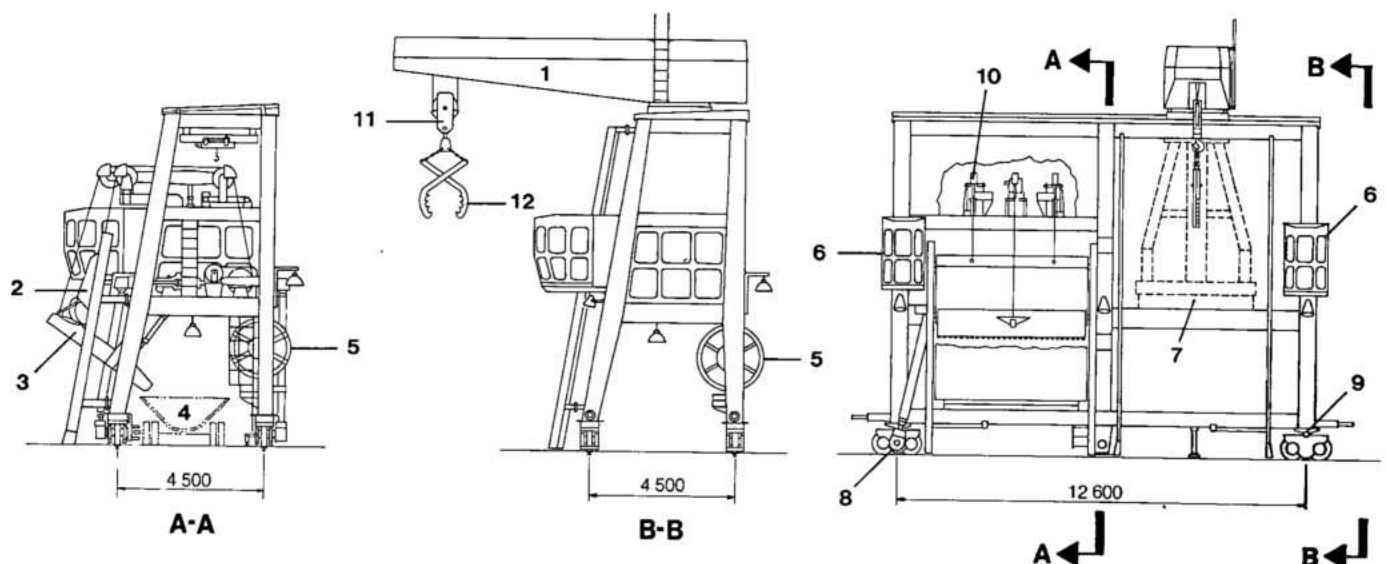


Fig. 10.5 Trashrack cleaning machine: general arrangement

- | | | | |
|--------------------|---------------------------|----------------------------|----------------------------------|
| 1 Pillar jib crane | 4 Wheeled cart | 7 Crane rotation mechanism | 10 Rocker arm activator for grab |
| 2 Grab | 5 Drum for trailing cable | 8 Machine travel mechanism | 11 Crane hoist |
| 3 Chute | 6 Control cabin | 9 Hydraulic buffer | 12 Pincers |

Fig. 10.6
Trashrack
cleaning machine
trailing cable drive

- 1 Cable drum
- 2 Motor
- 3 Gear reducer
- 4 Chain
- 5 Cable guide
- 6 Trailing cable
- 7 Slip-ring housing
- 8 Fixed cable

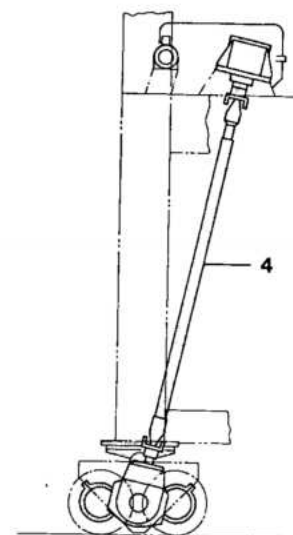
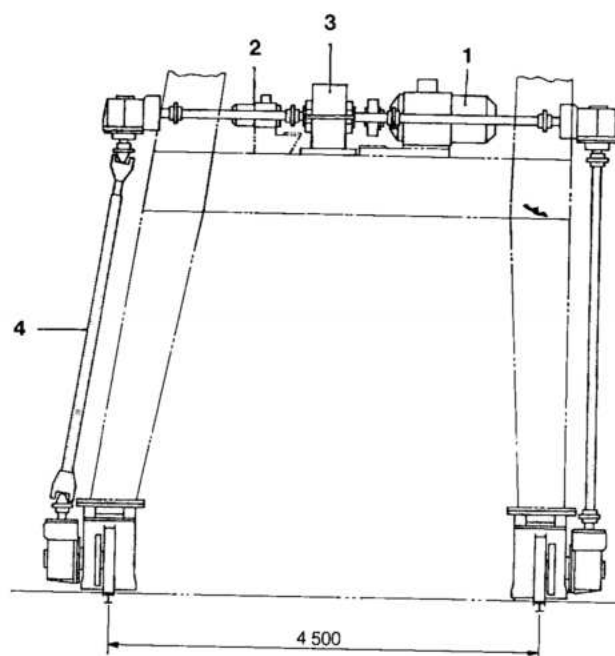
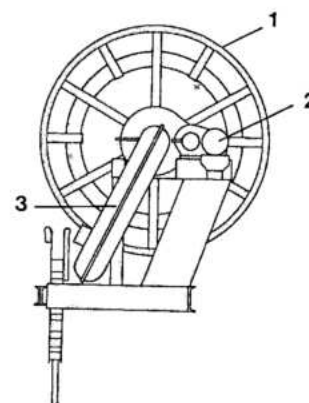
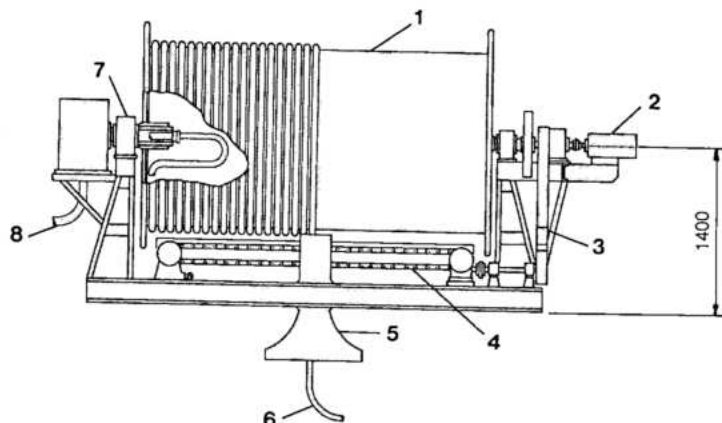
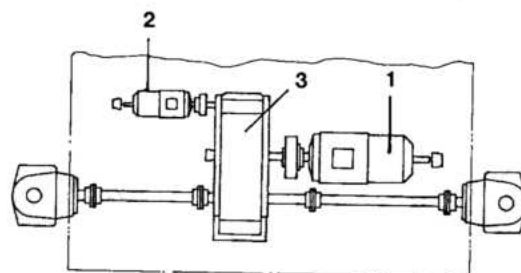


Fig. 10.7 Trashrack
cleaning machine:
travel mechanism

- 1 Main motor
- 2 Inching motor
- 3 Gear reducer
- 4 Drive shaft



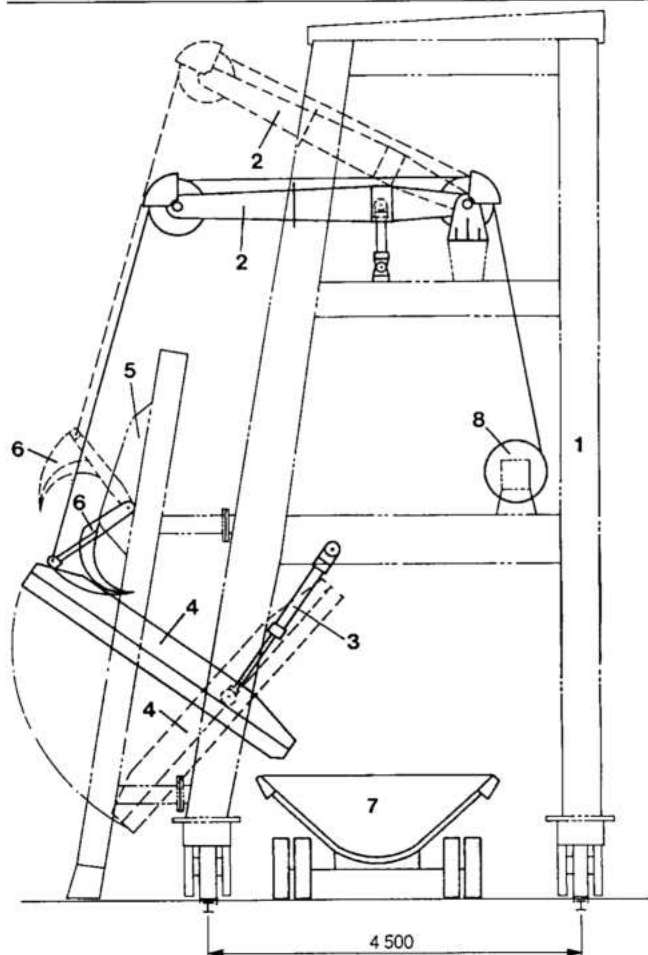


Fig. 10.8 Grab/chute of trashrack cleaning machine

- | | |
|--------------|----------------|
| 1 Main frame | 5 Grab |
| 2 Rocker arm | 6 Grab comb |
| 3 Servomotor | 7 Wheeled cart |
| 4 Chute | 8 Winch motor |

As shown in Fig. 10.8, the grab is a wheeled trolley with a front scraper and clamshell lid. Its vertical movement is controlled by three cables attached to a winch, the rotation of which is by a variable speed electric motor, acting through a gear reducer. The two side cables are attached to the platform of the grab. The center cable is attached to the clamshell lid and is used to open and close the lid via a hydraulic servomotor operated rocker arm.

Winch motor speed is controlled by variation of the stator current frequency by a thyristor bank and via slip rings by a variable rotor resistance. The stator current is under control of the machine operator whereas the rotor resistance control is automatic and is used to decelerate the grab slowly at the end of its travel. The hoisting mechanism is equipped with all necessary safety features such as electromagnetic brakes, overload and slack cable devices. The grab is programmed to clean trash

first from El. 186 and then from El. 170; however, if necessary, this order of operation can be manually overridden. After the grab has been lowered to the set level the clamshell closes on the trash and the grab is raised. When it reaches the upper point the chute tray is automatically rotated by two hydraulic servomotors, the clamshell opens and the trash falls down the chute to the bucket of the wheeled cart.

The pillar jib crane section of the machine, used for handling the trashracks and large debris, consists of a welded steel jib mounted on a three-legged support, the whole of which rotates through 270° on a central thrust ball bearing. Two horizontal platforms mounted between the legs house the crane mechanisms, the upper platform, the jib trolley travel mechanism and the lower, the hoist and rotational mechanism.

The trolley of the jib crane which carries the hoist pulleys, runs on two rails mounted on the jib. There are two running wheels and two guide wheels on each side of the trolley, and movement is by cables attached to the trolley, winding onto an electric motor driven winch. Like the grab mechanism the electric motor of the crane hoist is speed controlled with thyristors on the stator supply and variable rotor resistance, the latter being for controlled starting and stopping. A hook attachment to the trashrack lifting beam is used when deploying trashracks, and the pincers are used when pulling logs or heavy debris from the water. The pincers are armed by pulling open the geometric locking device which collapses when they encounter an object, allowing the pincers to close. Rotation of the pillar support is by a vertical electric motor driven pinion, mounted on the lower platform of the support, engaging a large diameter gear wheel attached to the machine structure.

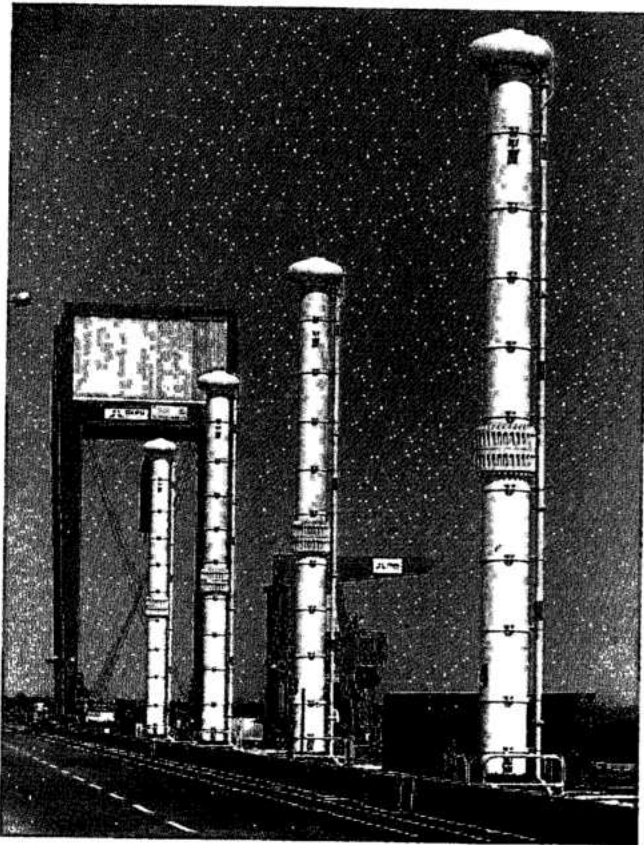
Both the grab and the jib crane mechanisms are serviced by a small bridge crane running beneath the upper beam of the machine.

The trashrack cleaning machine was designed and manufactured by Bardella S.A. – Indústrias Mecânicas, São Paulo.

INTAKE GATES

GENERAL

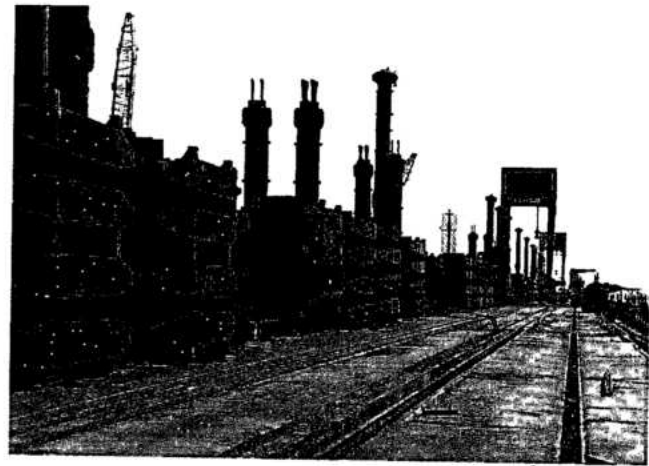
The intake gates have the same basic design as that used for the diversion closure, see Chapter 6. The majority of the intake gates were made from parts recovered from the diversion control structure after filling of the reservoir. As such, the type of gate and hoisting mechanism chosen for the intake gate was dictated in part by their initial use for closure



Intake gates servomotors and gantry crane

of the diversion sluices. An essential feature of the diversion closure gates was that the individual wheel supports collapsed at a set upstream water level and, after that, the loading was sustained by the gate end beam bearing on the embedded parts. Thus a fixed wheel gate was the only choice for diversion closure, as well as being eminently suitable for the power intake. For diversion, the hoisting mechanism had to be compact enough for rapid removal after closure, or suitable for submergence and later recovery and use with no ill effects. This precluded cable and winch mechanisms, leaving hydraulic hoists as the only viable solution. Also, hydraulic hoists were obviously a better choice for the intake, in that the pumping sets could be conveniently located in the access galleries in the dam, with the servomotors above the gates at El. 225. This arrangement had the slight aesthetic disadvantage of having the servomotors exposed above the top of the dam, but it was completely outweighed by the obvious operational and maintenance problems involved in the alternative of having the servomotors in chambers in the dam below El. 225.

After recovery, the diversion gates were dismantled, parts refurbished and replaced as necessary, and modifications were made in order to create fourteen intake gates from the twelve diversion gates. In all there are



Recuperated gates

eighteen intake gates, but to allow sufficient time after closure for the recovery and modification of the diversion gates, new intake gates for the first four units to enter into operation were procured separately and not made from the diversion gates.

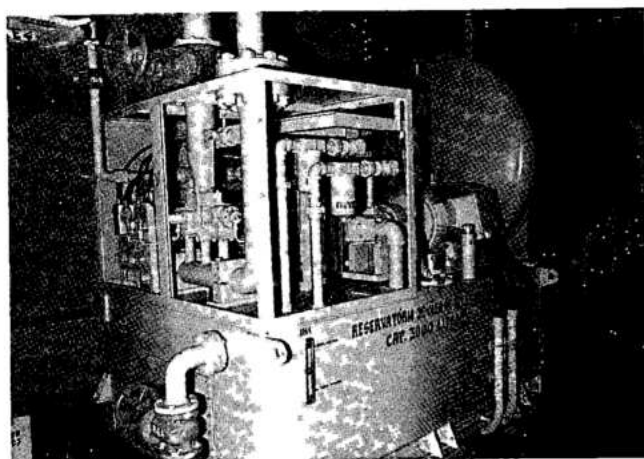
CONVERSION OF THE GATES

The differences between an intake gate and a diversion gate are shown schematically in Fig. 10.9 and salient details of the intake gates are:

Type	Fixed wheel gate
Number of gates	18
Height of gate	16.35 m
Width of gate	8.23 m
Maximum depth of gate beams	1730 mm
Maximum thickness of skin plate	50 mm
Minimum thickness of skin plate	35 mm
Number of wheels per gate	64
Weight of one gate	2420 kN
Sill beam elevation	177.56 m
Operation	By hydraulic servomotor

The principal steps of conversion, and differences between the diversion and intake gate applications were as follows:

- The only modification to servomotor V1 was to remove the upper cover and replace it with a compensating chamber. This chamber compensated for the difference in oil volume of the servomotor in the open and closed positions and hence deleted the operation of oil pumps



Pumping set for the intake gate servomotors

during closure of the diversion gate; it also allowed for thermal expansion of the oil, and compensated for any leakage.

- Two V2 servomotors were bolted together to produce a single V1 servomotor and a new piston rod was required for the composite V1 servomotor.
- Suspension couplings were reused with no modifications.
- Fourteen new suspension rods and servomotor supports together with two new bottom panels were obtained.
- To avoid vibration of the gates due to vortex shedding from the gate slot when the gate is open and from the bottom edge when the gate is descending, rubber mounted pads were used to restrain the gate. Details of the pads are shown in Fig. 10.10. In the maintenance chamber where there is no rolling surface, the gate is held in the direction of flow by compression of rubber mounted pads (detail 6) on the upstream fixed part reacted by the front angle beam pressing against the downstream guide. Between the maintenance chamber and conduit, the gate is held in direction of flow by compression of the rubber pads (detail 5) mounted on the gate reacted by the wheel against the rolling surface and in the lateral sense by compression of the rubber mounted at the left of the pads. When the gate is in the conduit, these pads are not compressed, the gate being held only in the upstream/downstream direction by compression of pads (detail 5).
- The diversion gate pumping sets were reused for the intake gate without modification, except for an additional tank of 7000 l capacity which was connected to the pumping set to store the system oil during maintenance of the servomotor.
- Control circuitry was revised to accommodate the different requirements for the intake gate application. A schematic diagram of the revised system is shown in

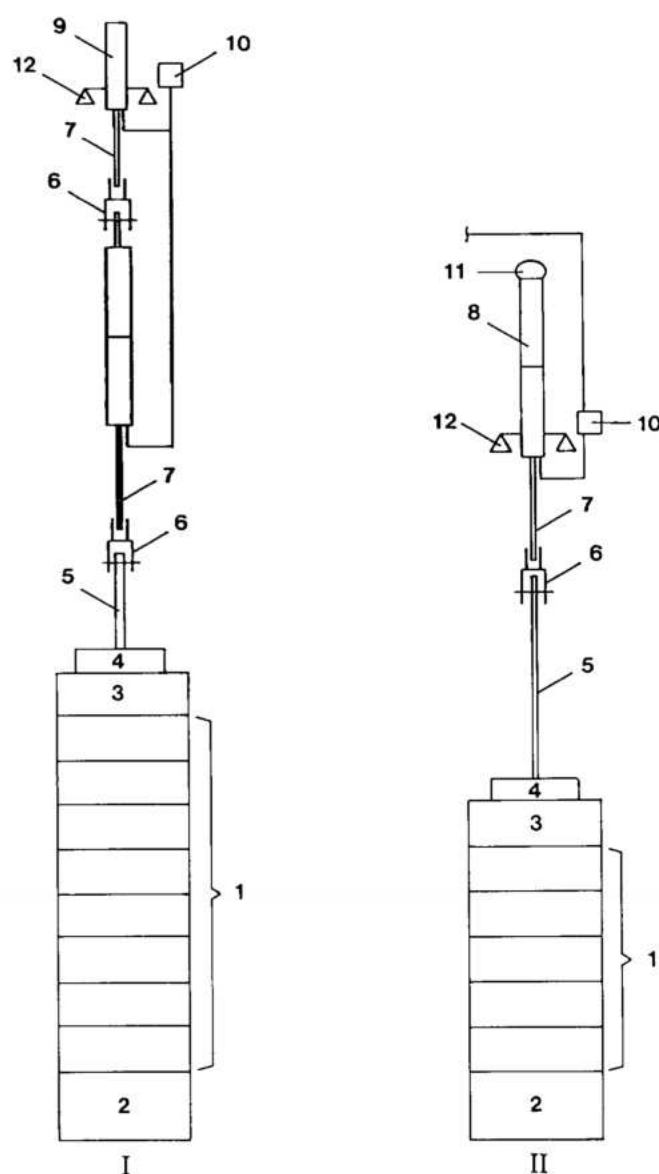


Fig. 10.9 Diversion power intake gates-schematic diagrams

- | | |
|-----------------------|---|
| I Diversion gate | 7 Piston rod |
| II Intake gate | 8 Servomotor V1 |
| 1 Intermediate panels | 9 Servomotor V2 |
| 2 Lower panel | 10 Pumping set, control panel and indicator |
| 3 Upper panel | 11 Compensating chamber |
| 4 Lifting beam | 12 Support beam |
| 5 Link | |
| 6 Coupling | |

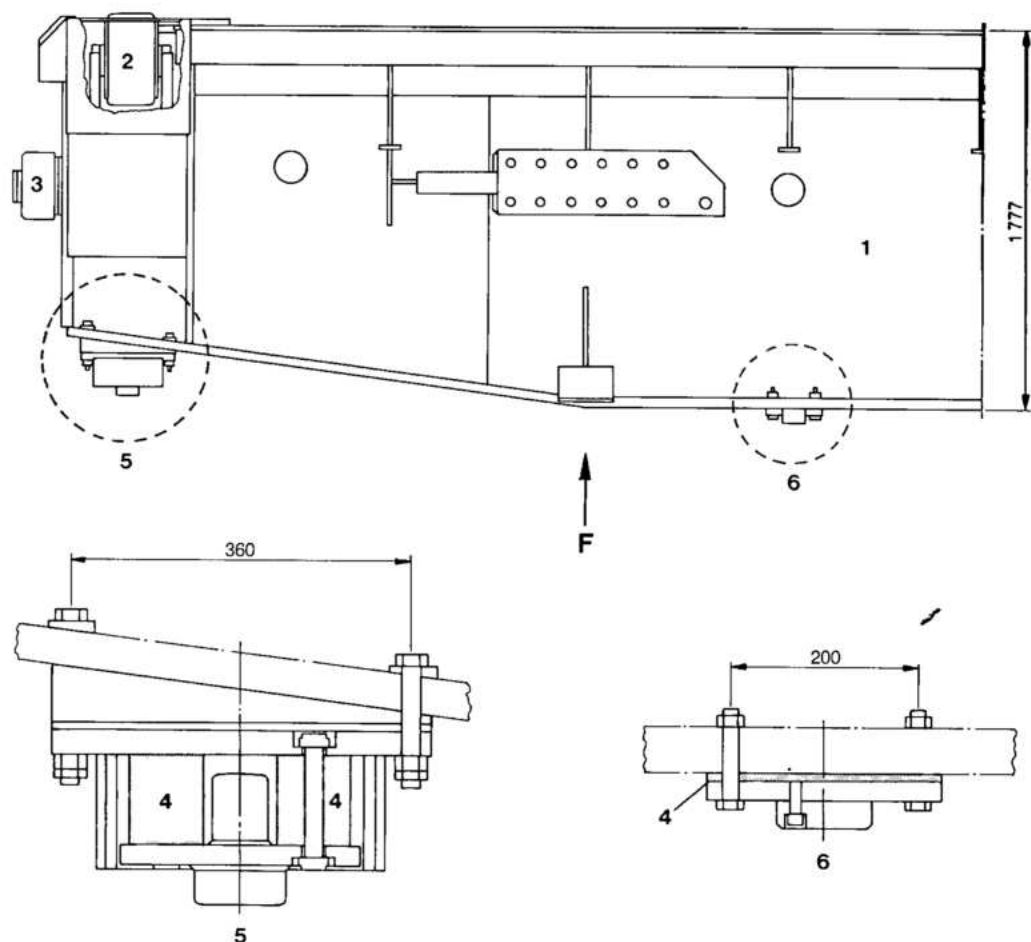


Fig. 10.10 Details of the gate restraining pads

- 1 Gate
- 2 Wheels
- 3 Side pads
- 4 Rubber pads
- 5 Detail
- 6 Detail
- F Flow direction

Fig. 10.11. In addition to the deletion of pump operation during closure, the main differences between operation of diversion and intake gates are:

1. Closed intake gates are completely opened only under balanced head. First the penstock is partially filled through the by-pass system and then the gates are cracked open to 80 mm to balance the head across the gate. Partial prefilling by the by-pass valve is to avoid the vibration and cavitation which would result if the gate were cracked open to fill an empty penstock.

2. The intake gate is kept in the open position by oil pressure in the servomotor. The gate closes when this pressure is released via the hydraulic circuits. Release can be instigated from a manual order, or as a signal from the powerhouse control system. By various combinations of opening solenoid valves SV1, SV2, SV3, the closure rates can be 3 m/min normal (as used in the diversion), 5 m/min emergency and 8 m/min maximum.

3. In order to prevent the bottom seal of the gate slamming against the sill beam, in the final part of the closure the velocity is restricted, by an orifice, to

1 m/min. Whilst the gate is closing, the downstream side of the gate is supplied with air to prevent a partial vacuum forming in the penstock. Air supply is from the 2 m diameter air vent leading from the penstock to the top of the dam at El. 225.

• For reuse in the intake gates, the elastic pads were prestressed such that if the hydraulic loads are distributed evenly between the wheels of the gate there will be no compression of the pads. Only in the event of additional load on a wheel due to slight misalignment inherent in the manufacture and erection tolerances of the gate and guides, would the pad function as an elastic unit. The hydrostatic forces, as calculated for the intake gate, distributed evenly between the wheels resulted in a prestress load of 850 kN for the pads, i.e., considerably higher than the 550 kN employed for the diversion. Hence the fastening studs of the pads employed in the diversion gate could not be reused for the intake gate. For the intake gate, interference between the stud and the rubber pads when compressed was accepted in the knowledge that the elasticity of the pad assembly in this application was less critical.

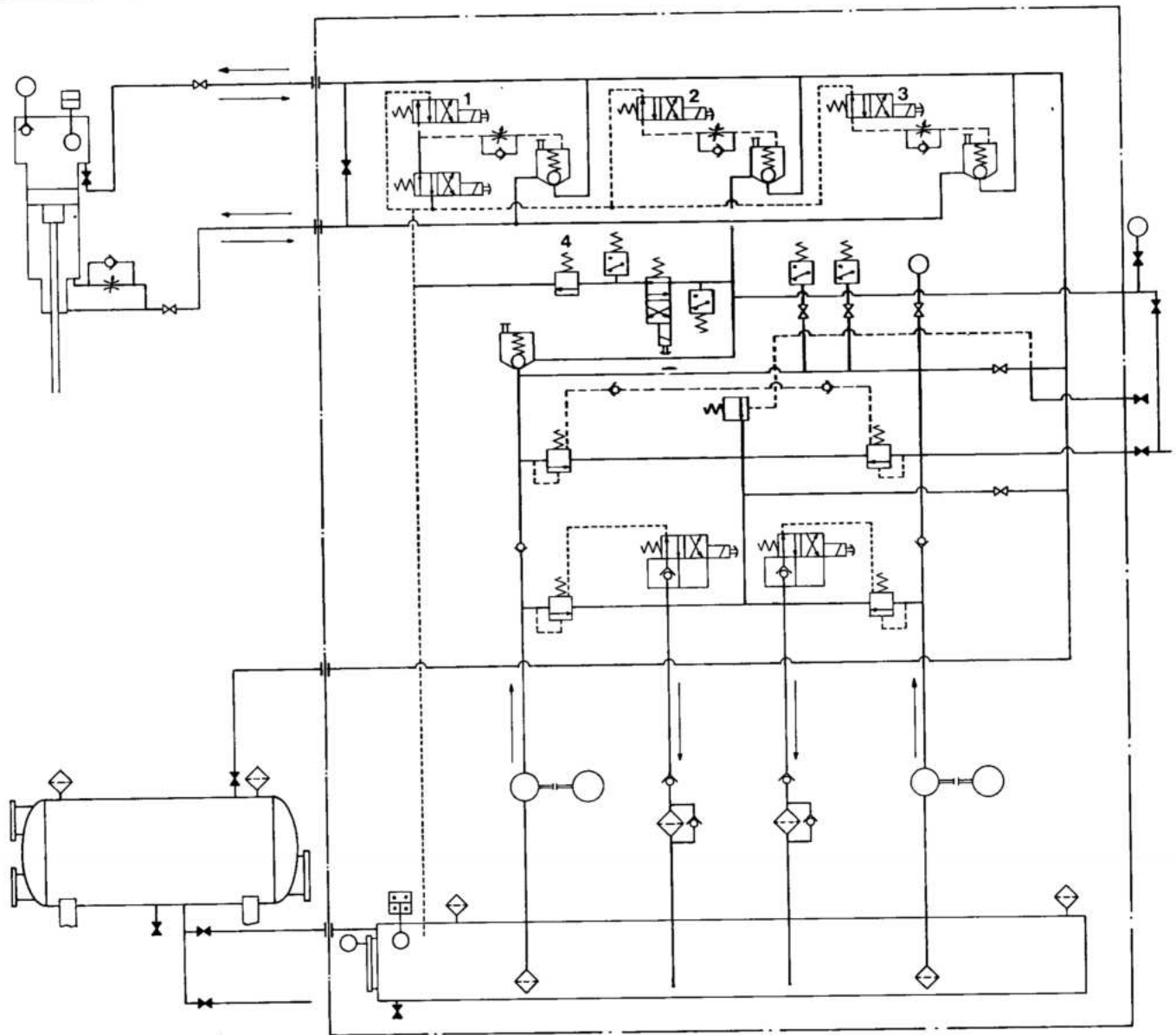


Fig. 10.11 Schematic diagram of the revised control circuitry for the intake gate

1 Solenoid valve SV3

2 Solenoid valve SV2

3 Solenoid valve SV1

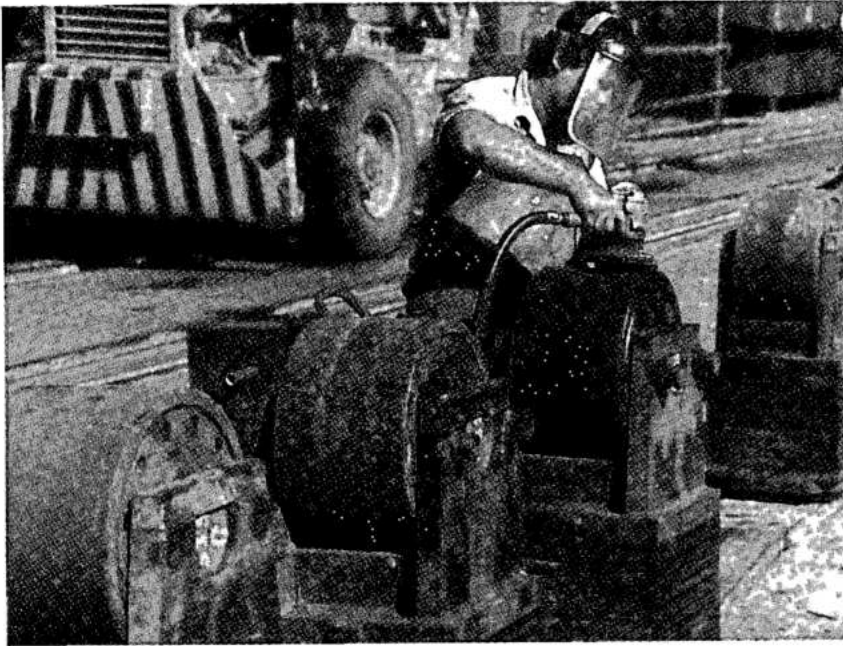
4 Pressure valve VLP5

It was also decided that these studs for the intake gates should be of stainless steel. Load deflection tests were conducted with various sized studs, and the stud diameter was optimized at 28 mm. This diameter was the minimum which could be used with readily available stainless steel, and with which the effects of interference were still negligible, there being only a 1 mm difference in pad deflection at 850 kN load with the 28 mm studs, compared with the same load on a pad with 20 mm diameter studs. Permanent set tests at a load of 850 kN and tests with the corresponding deflection, gave results

similar to the tests conducted at 550 kN, i.e., that permanent set was established after 45 days.

- The rubber seals have a precompression of 3 mm, and all sealing and rolling surfaces were manufactured from stainless steel treated to 270 HB. Retaining bolts for the seals were replaced by ones made from stainless steel.

Maintenance of the intake gate is performed in the maintenance chamber, with the stoplogs in place. In this chamber, routine maintenance such as painting, replacement of wheels and seals, is conducted. If necessary, the gates and servomotors can be completely removed by the 1100 kN gantry crane.



Cleaning of intake gate wheels after recuperation from the diversion structure

OPERATING EXPERIENCE

Both in diversion closure and power intake service, the performance of the gates has been virtually trouble free. Diversion closure occurred as programmed and recuperation of the gates was completely successful. In the power intake, the gates have operated with no significant problems for several years. Described in this section are some of the minor problems which were encountered and resolved; however, at no time did these impede either the construction program, or operation, or in-service availability of the gates.

After removal from the diversion structure, some of the elastic pads were found to be damaged with cracks or tears in the rubber outer surface, usually in the bulges between the stainless steel plates. A concern was the stability of these cracks in service and the possibility of growth with time. The following criteria were used for acceptance or rejection of the individual component pads for service in the intake. Rejection of a component pad did not imply rejection of the complete pad, as the pad could be dismantled and complete pads made from individual acceptable component layers.

- Cracks or tears, longitudinal or oblique, in the rubber face should not be more than 3 mm deep and 30 mm in length.
- Lack of adhesion between the internal stainless steel plate and side rubber leading to bubbles in the rubber could be accepted.
- Lack of adhesion between the rubber and external stainless steel plates of individual pads could be accepted.

Gate wheels as recovered from the diversion were severely corroded and there was concern that this would continue in intake gate service, eventually leading to damage of the stainless steel embedded parts. As an initial precaution the wheels for the first two gates made from recovered parts, were sand blasted and painted with zinc rich epoxy. At the same time some unpainted wheels were put into intake gate service and their diameters monitored over several months to assess the degree of corrosion and subsequent wear. Total reduction in diameter after 2 years service was about 0.1 mm only and the rate of loss was slowing. It was therefore concluded that the initial severe corrosion was due to unfavorable water conditions at the bottom of the reservoir during early operation at the diversion structure and this was not indicative of future service. Painting of the wheels was therefore discontinued; in any event, the painting was not a great success because of loss of paint in operation.

During erection, solar heating of the oil in a servomotor caused the piston to rise and, when it reached the flange of the compensating chamber, to break the flange bolts. This unexpected occurrence

- All servomotors were painted white to reduce solar heating.
- During erection when the valves of the hydraulic system leading to and from the servomotor were often closed, the piston would always be at 200 mm minimum from the compensating chamber flange.
- In service, when the gate is open, the pressure in the hydraulic system would be controlled to only 55 bar by a separate relief valve which would be

switched on by solenoid valve VLP5, in response to the gate open limit switch, see Fig. 10.11.

Very low leakage rates were adopted for the solenoid valves of the hydraulic system in order to reduce to a minimum the number of gate repositions. This resulted in tight valve clearances and subsequent sticking of the valve in service. The original spool valves were substituted with spring loaded ball type, resolving the problem.

The original system of limit switches taken from cams operated by a wire activated position indicator was found to be inaccurate due to changes in the length of the wire resulting from thermal variations. The important limit switches, e.g. for pump shut off, were therefore transferred to a rod activated system mounted on the servomotor beam support. The rod is lifted by the rising gate and falls under its own weight as the gate descends.

Water was found in the majority of the recovered diversion gate wheels. Initially it was thought that the water was entering via the spring loaded grease nipples and these were replaced for the intake gates by stainless steel plugs. However water was again found in the wheels during routine maintenance and, although water proof grease was used, this was found to be deteriorating. A series of tests were therefore conducted at IPT - Instituto de Pesquisas Tecnológicas - in São Paulo in which various wheel seals and grease filling methods were tested in a pressurized water tank. It was found that the X wheel shaft seal as used was perfectly adequate provided the wheel bearing space was completely filled with grease without air bubbles, under a high internal pressure. This could not be guaranteed with the grease nipple system and a simple apparatus was found to be successful in which the wheel was mounted on a grease filled cylinder and the wheel uniformly and completely filled with grease by means of a jack activated piston in the cylinder.

STOPLOGS

The stoplogs and lifting beams used in the power intakes are those originally used in the diversion sluices. The stoplogs are used to isolate the intake from the reservoir for maintenance of the intake gate, penstock and turbine. The intake gate also isolates the penstock and turbine from the reservoir but the stoplogs are normally deployed during maintenance for additional security. As used in the diversion, each

upstream stoplog consisted of one upper element with an upper lintel seal and by-pass valve and eleven normal elements. Each downstream stoplog consisted of thirteen normal elements, there being no need for an upper seal. From the three sets of stoplogs for the diversion sluices, there were available for the power intakes seventy-two normal elements and three upper elements, as well as three lifting beams. Three sets of stoplogs are normally used for maintenance in the power intake, each stoplog comprising one upper element and six normal elements. The remaining diversion stoplogs were used for temporary sealing of four intakes during construction, four of the normal elements being provided with an upper seal. Hence, should it be necessary, these additional stoplogs can also be used for maintenance of the intake gates, after pumping water into the space between stoplog and intake gate to equalize pressures.

The seven stoplog elements are normally handled in two bolted assemblies, the upper four and lower three, weighing 489.4 kN and 359.5 kN, respectively. However, if necessary, each element can be handled separately. When not in use the stoplogs are stored in chambers in blocks E5/6 and F35/36. Both the storage chambers and stoplog slots have checker plate covers.

Principal data of the stoplogs and lifting beams are:

Number of sets in service	3 normal 4 modified
Number of elements per set	7 (6 normal elements + 1 top element)
Height of one normal element	2.46 m
Height of one top element	3.10 m
Width of elements	7.49 m
Maximum depth of stoplog beams	900 mm
Thickness of skin plate	26 mm
Sill beam elevation	177.18 m
Weight of one top element	119.32 kN
Weight of one top element	140 kN
Operation	By a gantry crane with a lifting beam

They were designed and manufactured in accordance with DIN 19 704 and DIN 4114 and welds were inspected and tested to the French standard CM 1966.

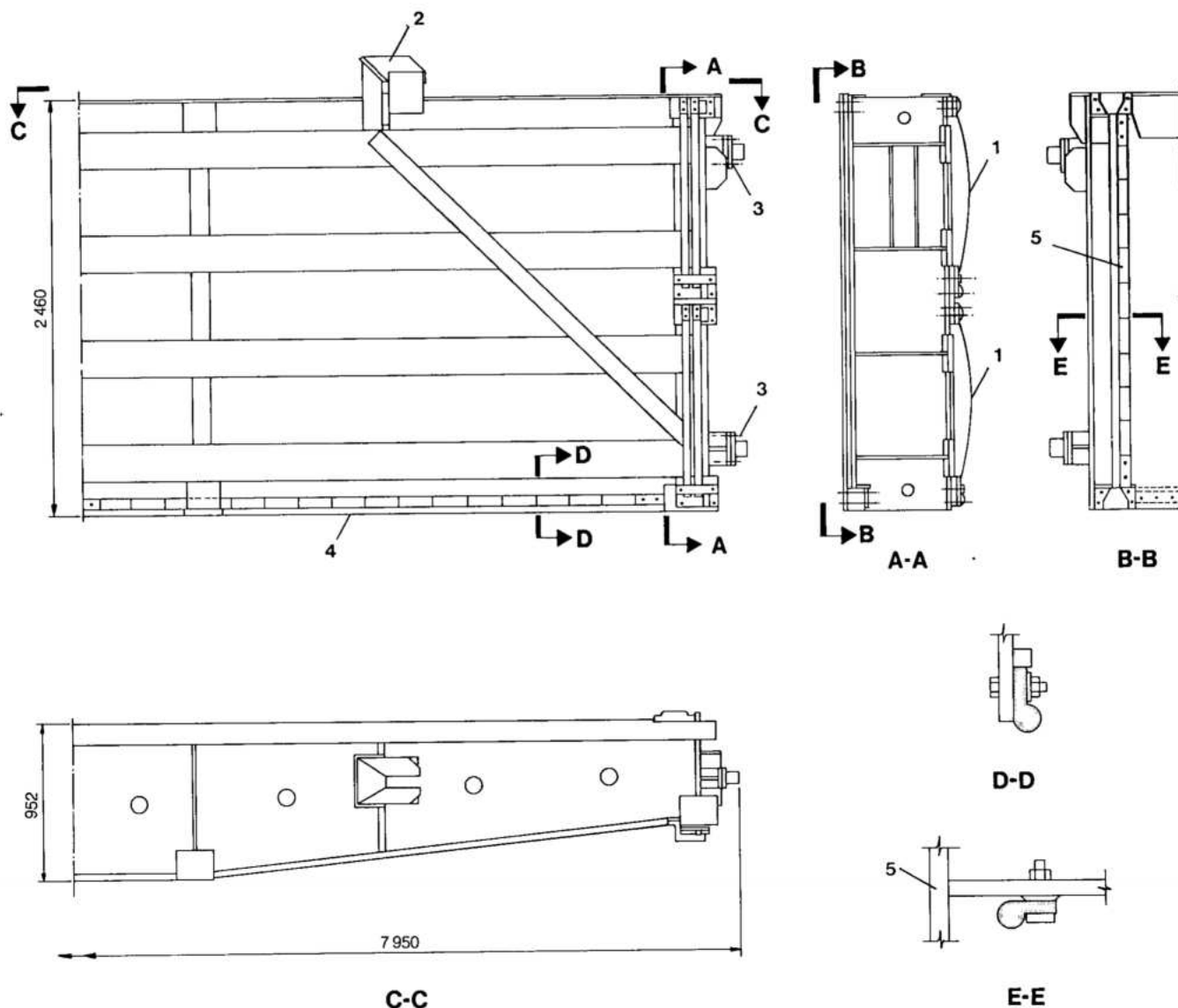


Fig. 10.12 Stoplog normal element

- 1 Restraining springs 2 Lifting lug 3 Side guides 4 Interpanel and bottom seal 5 Side seal

Lifting beams, lifting lugs and stoplog element connecting bolts were all designed for 2750 kN (2.5 times the nominal capacity of the gantry crane).

A normal element is shown in Fig. 10.12. These were made from welded mild steel plate and consist essentially of four horizontal beams welded to the downstream skin plate, which transmit the forces to the vertical side beams, the end pads of which are supported by the embedded parts. Music note seals are secured by pressure pads held by stainless steel bolts to the skin plate.

Four springs, two on each side, precompress the seals to ensure adequate sealing at the start of dewatering when the upstream and downstream pressures are almost equalized. Stainless steel facings are provided on the embedded parts where the seals contact, there being two such facings at the lintel, one for the upper element and the other for the normal element when used as an upper. Each element has lifting lugs to engage with the lifting beam and the upper element has two 350 mm diameter by-pass valves which are automatically opened by the weight of the lifting beams. Two lugs on each side guide the elements.

As shown in Fig. 10.13 the lifting beam has two guide wheels on each side. The lifting hooks are armed to engage by the manual positioning of the counterweight lever.

The stoplogs and lifting beams were manufactured by the same Joint Venture that manufactured the intake gates, with designs by BVS-Neyrpic, Grenoble, France.

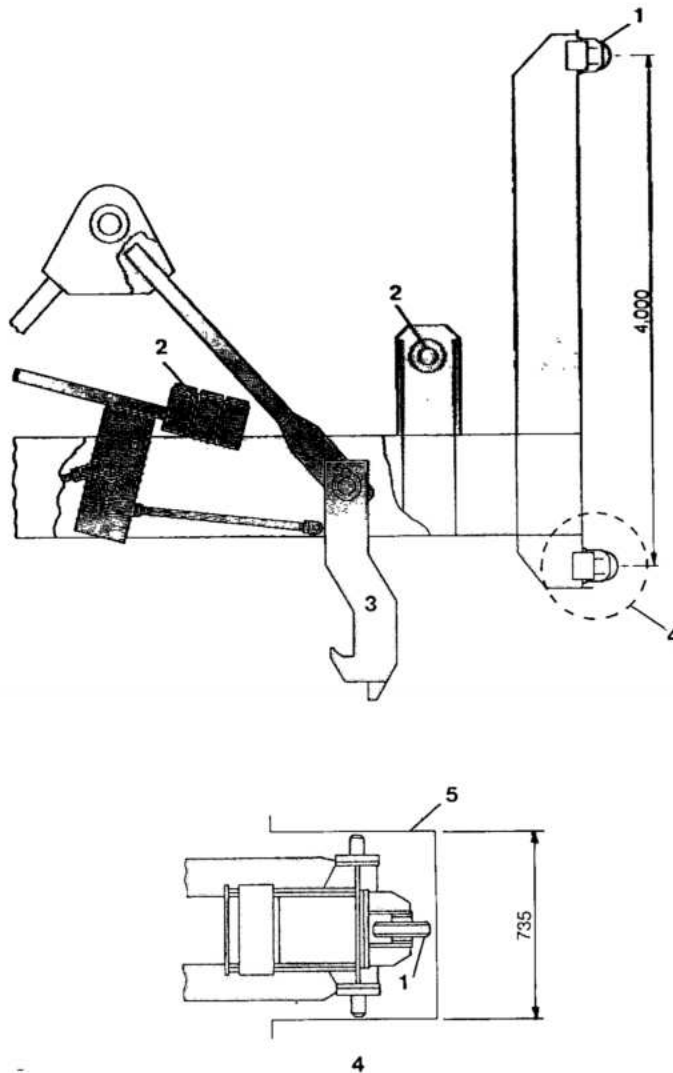


Fig. 10.13 Stoplog lifting beam

- | | |
|------------------------|-------------------------|
| 1 Wheels | 4 Detail, inferior view |
| 2 Release lever weight | 5 Stoplog slot |
| 3 Hook | |

GANTRY CRANES

Two 1100 kN gantry cranes are used to handle the intake gates and their hydraulic servomotors, and the stoplogs. One of the cranes was used initially on the downstream side of the diversion control structure to handle the maintenance gates and stoplogs, see Chapter 6. This crane was later dismantled and re-erected on the top of the main dam.

Crane capacity was determined by the weight of the four normal panel stoplogs plus the lifting beam. The specified speeds were based upon operating experience at other major hydroelectric stations.

The gantry design was chosen because it is virtually self contained requiring minor support structures as compared to a bridge crane. This permitted a relatively simple transfer from the diversion structure to the intakes. Also, it was comparatively simple to design a gantry to straddle the high intake gate servomotors, whereas any alternative would have required extensive auxiliary structures above the servomotors.

BASIC CHARACTERISTICS AND GENERAL ARRANGEMENT

The basic characteristics of the intake gate gantry cranes are:

Number of cranes in service	2
Height of crane	30 m
Maximum width of crane	12.39 m
Length between buffers	16.9 m
Rail span	10 m
Length of railtrack	857.55 m
Top of crane rail elevation	225 m
Weight of gantry crane	1864 kN

Hoisting mechanism

Maximum nominal velocity	4.58 m/min for 50 Hz 5.5 m/min for 60 Hz
Minimum nominal velocity	1.67 m/min for 50 Hz 2 m/min for 60 Hz
Capacity at maximum velocity	400 kN
Capacity at minimum velocity	1100 kN
Lift height	81.2 m
Diameter of cable (nominal)	32 mm
Hoist motors	Slip ring induction type
Motor	2 x 61.8 kW for 50 Hz 2 x 71 kW for 60 Hz

Car travel mechanism

Nominal velocity	8.33 m/min for 50 Hz 10 m/min for 60 Hz
Travel motor	Slip ring induction type
Motor	8.9 kW for 50 Hz 10 kW for 60 Hz

Crane travel mechanism

Nominal velocity	25 m/min for 50 Hz 30 m/min for 60 Hz
Travel motor	Slip ring induction type
Motor	16.3 kW for 50 Hz 18.7 kW for 60 Hz

Maintenance hoist

Nominal travel speed	20 m/min for 50 Hz 24 m/min for 60 Hz
Nominal capacity	98.1 kN
Maximum nominal lifting velocity	10 m/min for 50 Hz 12 m/min for 60 Hz
Minimum nominal lifting velocity	1 m/min for 50 Hz 1.2 m/min for 60 Hz

The cranes were specified for outdoor operation with the upper machine housing containing motors, gearing, cable drums and electrical equipment completely enclosed with galvanized steel sheeting. Electrical supply to the cranes is through a trailing cable connected to one of two points in a single pit, midway along the length of the crane

rails. The left side point supplies 440 V, 60 Hz and the other 440 V, 50 Hz, both cranes being capable of working with either frequency.

Design and manufacture of the cranes was to the FEM (Fédération Européenne de la Manutention) Standard - Section I, with the following classification for component parts:

Structural parts

Class of utilization	B	Regular use on intermittent duty
State of loading	2	Appliances which hoist the safe working load frequently and normal load between 1/3 and 2/3 of the safe working load
Group	4	

Hoisting and translation mechanism

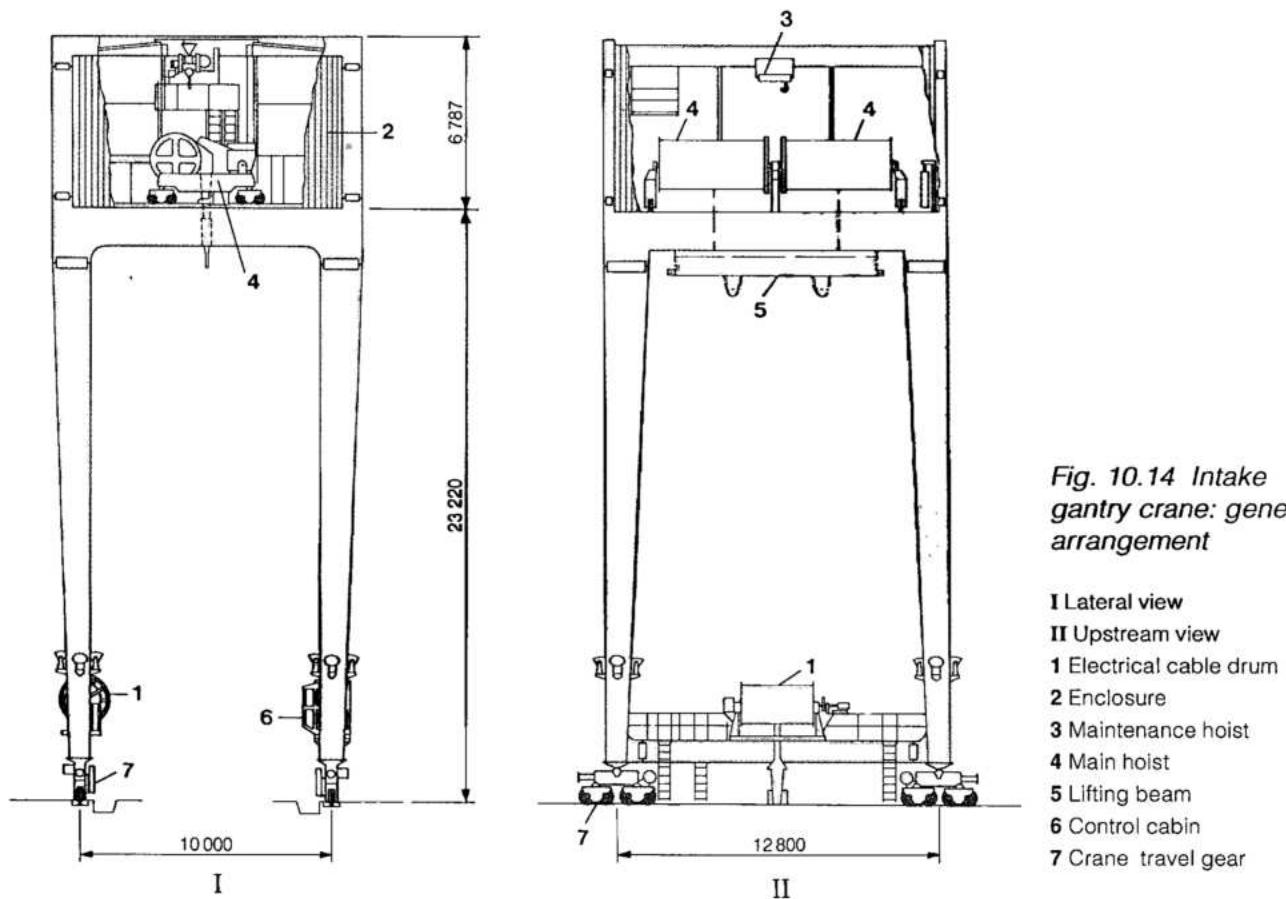
Class of operation	V2	Average daily operating hours > 2 and theoretical life > 6300 hours
State of loading	3	Mechanisms or components subjected for the most part to loads close to the maximum
Group	3 m	

In each case the group is determined automatically by the preceding class and state. Specified classes and states were determined from a detailed analysis of the use of the cranes in the construction phase and were adopted in the knowledge that this phase would be far more arduous than in subsequent operation of the powerhouse.

Design wind velocities were:

Normal service	100 km/h
Out of service (in parking position with bracing cables)	150 km/h

It should be noted that the out of service wind velocity is less than that used for the other gantry cranes, see Chapter 8. This was due to a re-evaluation of the project design wind velocities after the contract for the intake gantry crane had been awarded, which had to be done early in order for the crane to be used in the diversion. It was decided that the risks involved in maintaining the 150 km/h out of service wind velocity were minimal and no changes were made to the gantry crane structure, or, more important, to the cladding of the machine housing.



Rails for the crane extend the length of the main dam and the diversion control structure at El. 225, and straddle the stoplog and intake gate slots. At 20 m the cranes are high enough to pass over the intake gate servomotors. When out of service the cranes are parked at either end of the rails where there are anchor blocks to which the cranes are tethered with bracing cables.

COMPONENT DESIGN AND MANUFACTURE

Structure

The general arrangement of an intake gantry crane is shown in Fig. 10.14. Hoisting equipment is mounted on a platform 23.2 m above the rails. The platform is supported on a frame carried by four box girder legs made from welded steel plate, which in turn are pin mounted on the wheeled travel trolleys. Access to the platform is by a ladder in the downstream left side leg which in turn is accessed from the control cabin, which is mounted on the lower beam connecting the downstream legs. The electrical cable drum is mounted on a similar beam connecting the upstream legs. Pipes in the crane legs drain rain water from the roof of the machine housing to El. 225.

Travel mechanism

Crane travel is effected by an electric motor acting through a gear reducer on each of the four wheeled trolleys, see Fig. 10.15. Continuous speed control of the motors is by thyristor control of the stator supply and, for starting, stepped resistors connected through slip rings to the rotor windings. After decelerating with the motor speed control the crane is brought to a standstill with hydraulic disc brakes acting on each motor shaft. Oil supply to the brakes is piped from foot pedal operated master cylinders in the control cabin. For emergency stopping the motors are additionally equipped with electromagnetic brakes. The double braking system was an extra safety feature specified for all the important mechanisms of the crane.

Hydraulic buffers attached to the outside of each trolley encounter stops at the extremes of the rails to absorb the shock in the unlikely event of overrun.

Hoisting mechanism

Two electric motors drive the main cable drums of the hoisting winch through a shared planetary gear reducer, see Fig. 10.16. One motor operates at high speeds for loads up to 400 kN and the second at

Fig. 10.15 Intake gantry crane travel gear

- 1 Motor
- 2 Gear train
- 3 Hydraulic buffer
- 4 Pinned joint
- 5 Gantry crane leg

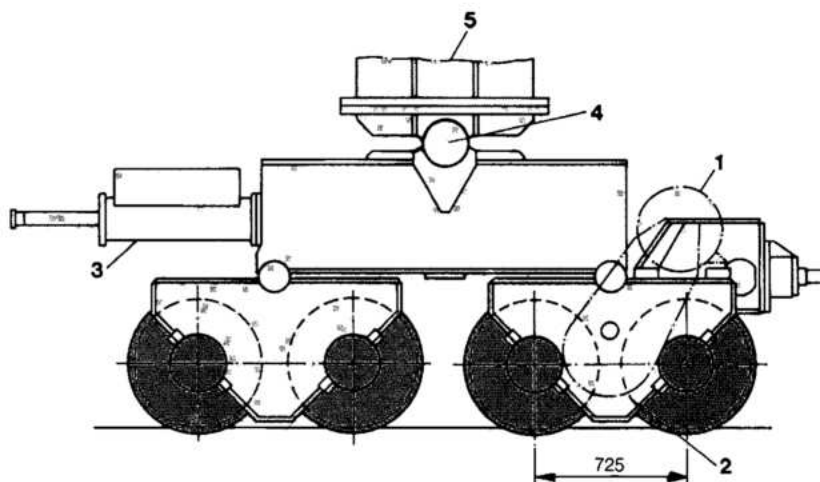
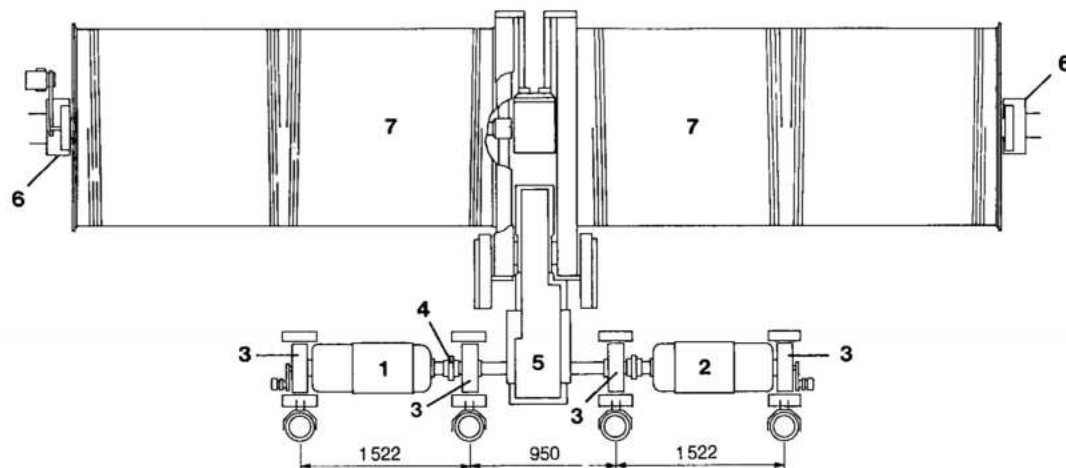


Fig. 10.16 Intake gantry crane - main hoist

- 1 High speed motor
- 2 Low speed motor
- 3 Electromagnetic brake
- 4 Coupling
- 5 Gear reducer
- 6 Bearing
- 7 Cable drum



lower speeds for loads not exceeding 1100 kN. Protection relays ensure that only one of the motors can be operated at a given time. Both motors have rotor resistance speed control with thyristor modulation in the 0 to 30 % speed range, permitting continuous inching operation at low speeds. Above 30% speed control is stepped, being a function of the number of resistors in circuit. Each motor has two electromagnetic brakes, one on a shaft extension from the rear of the motor and the other between the flexible coupling and the gear reducer.

The hoisting mechanism has protection against overvelocity and slack cable. Fibre core cable was specified in preference to steel core because of its better flexibility. For stoplog service the bottom pulleys are

connected to the stoplog lifting beam and, for use in the intake gate slots, they are attached to a special handling beam which fits the gate elements.

Cable drums and their mechanisms are mounted on a wheeled trolley which moves between the stoplog and gate slots on rails in the machine enclosure, see Fig. 10.17. The trolley is driven by an electric motor operating through a gear reducer train and drive shafts on to the two downstream wheel trains. Speed control of the motor is by the same system as used for the crane travel motor.

A small electric hoist, not shown in this figure, fixed to the roof of the machine housing is used to maintain the hoisting equipment (see Item 3 of Fig. 10.14).

The cranes were part of the supply contract for the diversion gates.

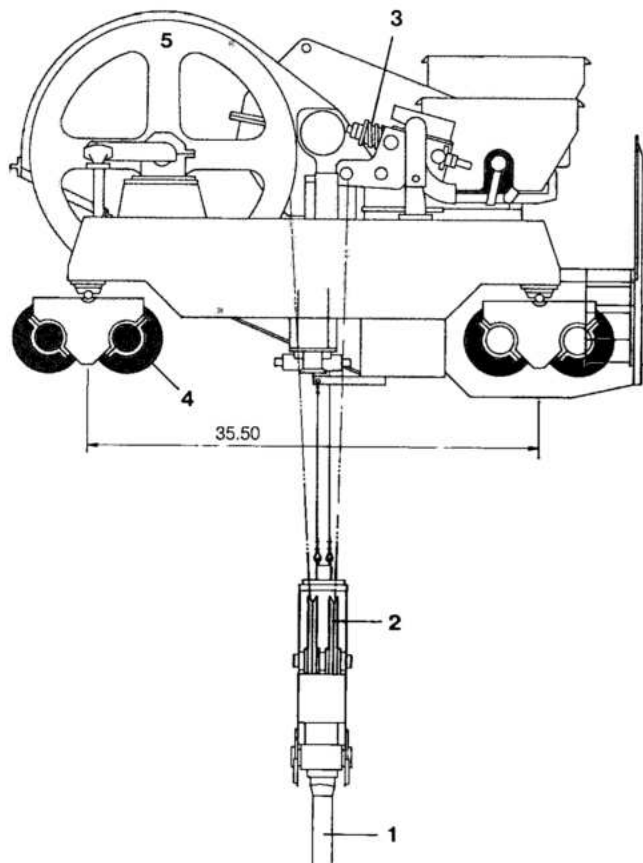


Fig. 10.17 Intake gantry crane - travel car

- | | |
|---|-------------------|
| 1 Hook | 4 Car wheels |
| 2 Pulleys | 5 Main hoist drum |
| 3 Cable fixed point and overload device | |

PENSTOCKS

A uniform diameter welded plate steel penstock conveys water from the concrete intake to the lower reducing bend of the turbine. Internal penstock diameter, 10.5 m, was determined on the basis of detailed economic analyses and comparison with current world-wide practice for large powerplants.

The upper bend of the penstock, 31.5 m radius and 32.19 m long, is anchored to the dam and embedded in concrete. A 47.41 m long straight portion is exposed and located on the downstream face of the dam. At its lower end it connects to the lower bend with a coupling designed to accommodate thermal expansion and any

movement between the powerhouse and the dam, which are independent structures, see Fig. 10.18.

The penstock was designed and manufactured to the French SHF standard for pressure conduits "Données techniques annexes au cahier des charges pour la fourniture et le montage des conduites forcées en acier et de leurs accessoires", without a hydrostatic pressure test at higher than working pressure, as specified for the lower bend and spiral case, which were designed to the ASME code. Although the two codes give almost the same design for normal loadings, without an elevated hydrostatic pressure test considerably thinner plate could be used for the penstock. This apparent inconsistency, and the omission of the elevated pressure test, were justified because stresses in the exposed penstock could be calculated accurately, while the stress distributions in the lower bend, which is an integral part of the spiral case and was pressurized before encasement in concrete, were more complex. In the upper bend of the penstock, the relatively thinner plate is adequate because it was embedded in concrete. The French standard provides an additional margin of safety because it demands more stringent quality control of fabrication than the ASME code, together with lower allowable weld and material defect levels.

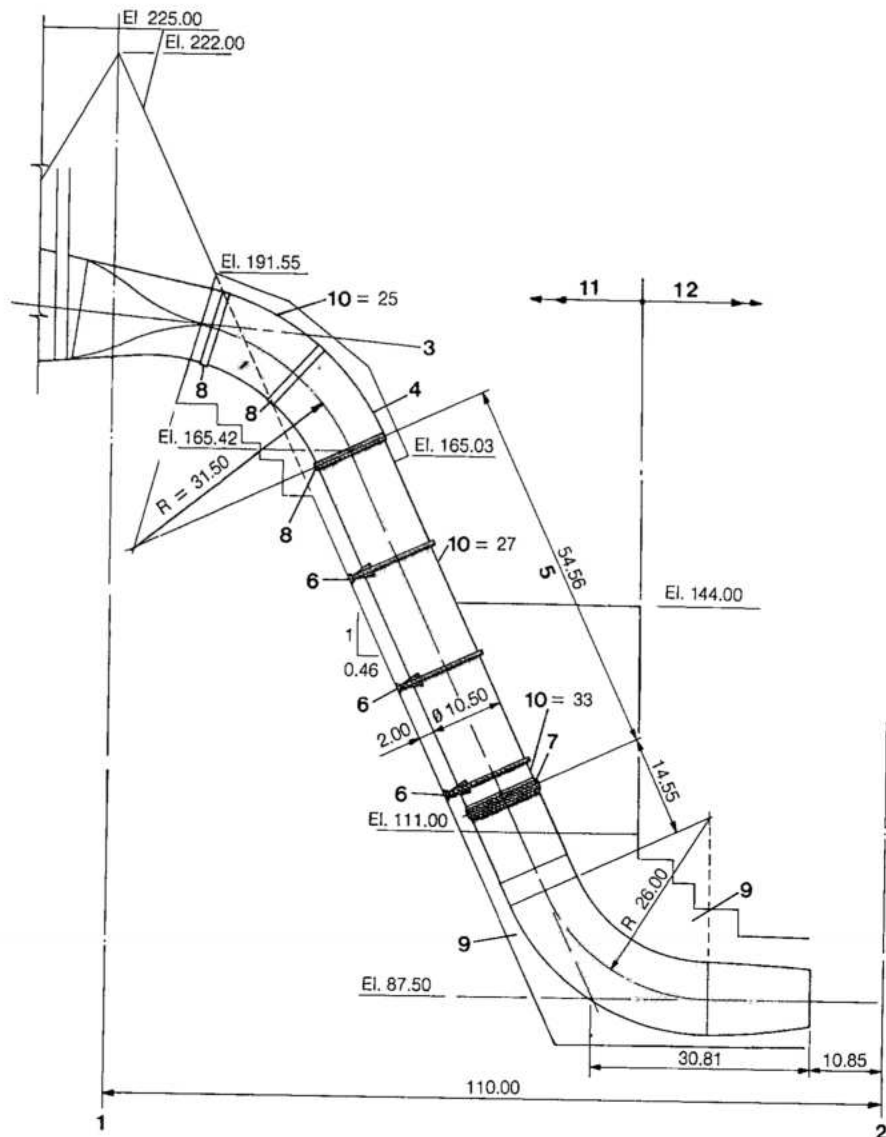
The upper bend was designed to resist the hydrodynamic forces due to internal pressure, change of direction of the flow and water hammer, as well as axial loads due to ambient temperature changes. It is anchored to the dam and embedded in second stage concrete placed in a large blockout in the face of the dam. The transverse faces of the blockout were formed with vertical keys which improved bond as well as resistance to the transverse shear forces.

Circumferential and horizontal transverse steel reinforcement, connecting with dowels embedded in first stage concrete, resist internal pressure and the lifting components of the thrust, as well as elastically integrating the anchored bend to the dam. High strength prestressed cable anchors were initially considered in lieu of a concrete anchor block, but were not used because of concern about the relaxation of cables and concentration of stresses in the dam. To ensure proper transmittal of the forces from the upper bend to the concrete, it has three thrust rings one at each extremity and one in the center.

The initial pour of the encasement concrete was supported by a temporary platform mounted at El. 144. This initial pour encased the lower thrust ring and when set it was self supporting and could, in turn, support the bend and subsequent concrete pours, allowing removal of the platform.

Fig. 10.18 General arrangement of penstock

- 1 Dam axis
- 2 Powerhouse centerline
- 3 Intake centerline
- 4 Penstock bend embedded in concrete blockouts
- 5 Straight part of penstock
- 6 Supports
- 7 Expansion joint coupling
- 8 Thrust rings
- 9 Concrete embedment of penstock at the powerhouse
- 10 Plate thickness (mm)
- 11 Intake
- 12 Powerhouse



The penstocks were fabricated from SAR-50 Brazilian steel plate varying in thickness from the minimum allowed 25 mm to 42 mm maximum at the coupling. These thicknesses included a specified corrosion allowance of 2 mm for the straight section and 3 mm for the upper bend. Plate was supplied to the site cut and rolled and was welded in an assembly plant on the right bank. All penstock welds, both axial and circumferential were manually executed. An automatic process was considered and in fact qualified for the axial welds, but was not used as the manual welds gave better and more consistent mechanical properties. The welds were not stress relieved or normalized, adequate impact resistance being obtained by the welding procedure used. In accordance with the SHF code, production run-off plates were made for all welds and weld properties

continuously monitored, with special attention being given to impact values which were specified as minimum of 3.5 kgm average at 0° C. All welds were initially ultrasonically tested and finally X-rayed. Dimensional conformity was ensured during erection by use of wheel spoke type internal supports.

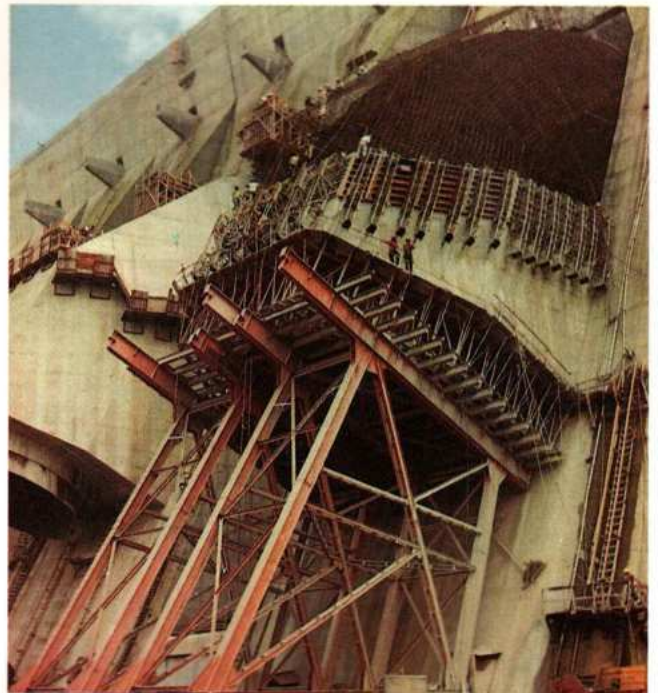
Cement grout was injected through nipples left in the upper bend to fill the voids, and drainage was provided at the thrust rings for any leakage along the steel contact. As a precaution against stress corrosion cracking, the inner surface of the penstock was sandblasted and painted with zinc rich epoxy primer and coal tar epoxy finish coat. Zinc rich primer and alkalyde white finish were used for the exposed outer surface. A rainproof cover was used where the penstock entered the powerhouse deck at El. 144.



Aerial view of penstock welding facilities on right bank



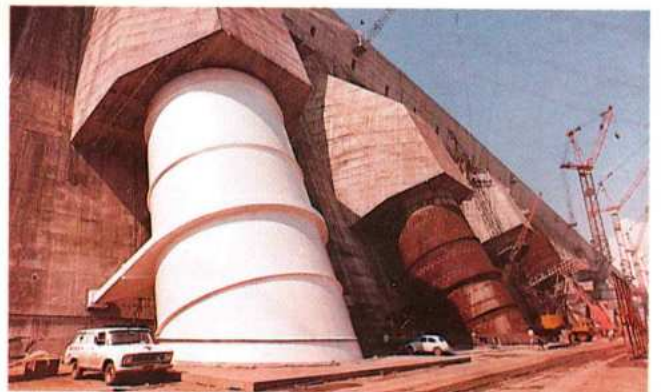
Transport of penstock segment from yard



Penstock concreting of upper bend. First pour of concrete supported by temporary support



Erection of penstock upper bend



Penstock of unit 1 completed. Others in various stages of construction

Three hoop strap braces, sliding on two legs, support the exposed straight section of the penstock. The lower surface of the feet are stainless steel which is in contact with two lubrite coated steel pads bolted to the embedded parts, see Fig. 10.19. A stainless steel overlay was used on the penstock and lower bend at the coupling seal. The welded two way coupling was designed for ± 30 mm axial movement and ± 4 mm radial. Sealing was effected by rubber seal rings on both the mating parts, compressed by multiple bolt adjusted seal rings. Axial movement of the coupling is limited by a central tongue welded to the coupling sheath, see Fig. 10.20. Problems were encountered in unit 1 coupling, and the seal design was modified to that shown in Fig. 10.20.

A 700 mm diameter pipe embedded in first stage concrete conveys water from the upstream of the intake gate to fill the penstock. Flow in the pipe is controlled by a 700 mm diameter butterfly valve located at El. 179.6. When the sealing surfaces in the turbine wicket gates are new, the flow through the valve is much more than the leakage, and it is capable of filling the penstock in approximately 2 hours, to a stage where the intake gate can be opened. However, as wear occurs the wicket gate leakage increases, producing an unacceptably long

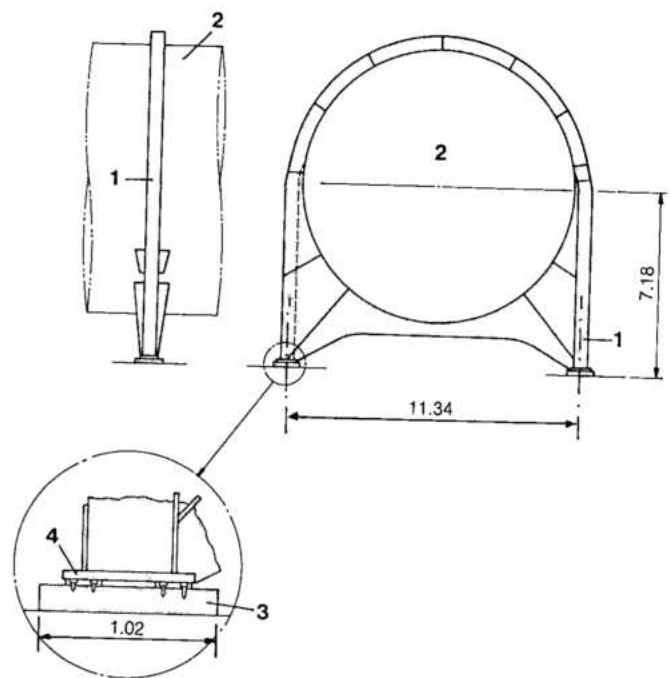


Fig. 10.19 Penstock support

1 Support
2 Penstock

3 Steel base pad
4 Self lubricating pads

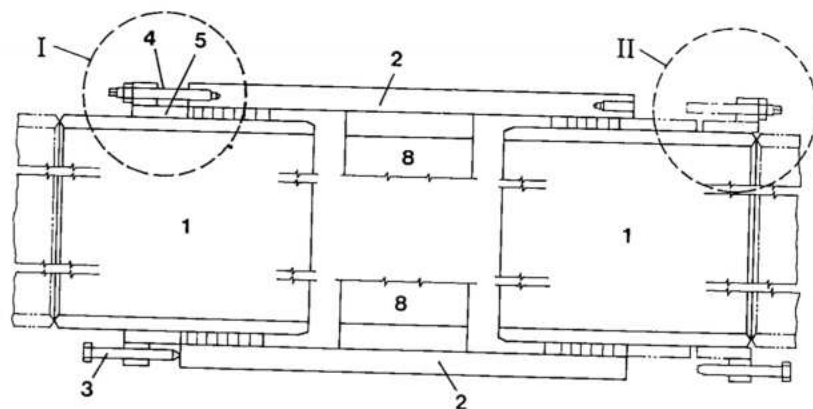
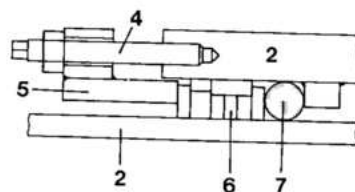
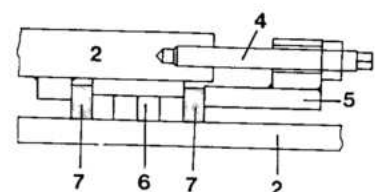


Fig. 10.20 Penstock coupling

I Original seal
II Modified seal
1 Penstock
2 Coupling sheath
3 Distance bolt
4 Seal tightening bolt
5 Pressure plate
6 Asbestos cotton seal
7 Rubber seal
8 Central tongue



I



II

penstock filling time. Since a larger by-pass valve would have been uneconomic and difficult to accommodate, the normal procedure is to fill with the intake gate by-pass valve until the wicket gate bottom seal is well drowned (to minimize cavitation) and then open the gate to 80 mm to complete the filling.

A protective steel plate is embedded in the concrete at the point where the jet from the by-pass impacts and the pipe at exit is narrowed to 600 mm, not only to direct the jet, but also to provide back pressure in the valve to prevent cavitation. For security and reliability the by-pass valve is opened by oil servomotors and closed by its own weight.

Pressure oil for the valves is supplied from two pumping sets at El. 179, one at intake no. 7 for the 50 Hz units and the other at intake no. 15 for the 60 Hz units. Central pumping sets were chosen in preference to individual sets at each valve for reasons of economy and reliability. The oil is supplied via a nitrogen charged pressure vessel and the electric motor driven pumps are automatically operated in response to changes in the vessel pressure. There is a normally closed interconnection between the two systems and, if necessary, the pressure vessels can be primed with an emergency pump. The valves are manually operated from a local control panel.

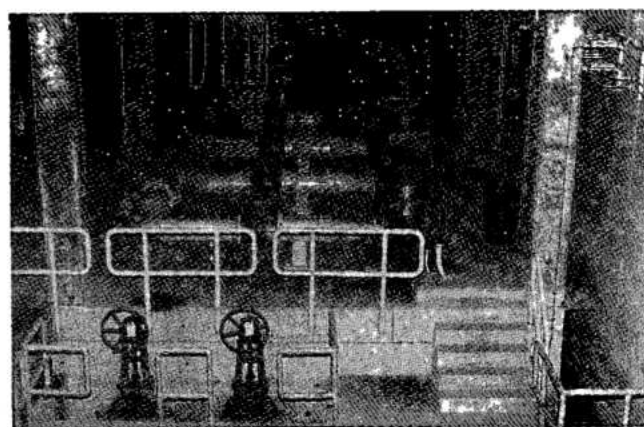
Penstocks were fabricated by Badoni-ATS, Indústria Metal Mecânica S.A., Brazil which, under the same contract, also supplied the intake gate by-pass valves and the penstock couplings.

AUXILIARY EQUIPMENT

DAM DRAINAGE PUMPING SYSTEM

Seepage from the foundations of the dams and the powerhouse, and leakage through the dams and structures is channeled to drainage pumping stations in the concrete dams, where the water is pumped through the powerhouse to discharge into the tailrace. As shown in Fig. 10.21, the drainage pumping stations are arranged in a cascading fashion such that the overflow from the higher stations will discharge into the lower.

Pumping capacities are given in Table 10.1. Capacities were calculated using liberal



Pumping stations in the main dam

Table 10.1 Pump characteristics

Sump number	Location (block number)	Number of pumps per sump				Pump characteristics	
		Normal	Reserve	Future	Total	Head m	Flow m ³ /min
1	F 3/4 – F 5/6	2	1	1	4	51	2.1
2	F 11/12 – F 13/14	2	1	1	4	93	3.33
3	F 15/16 – F 17/18	6	2	2	10	113	3.33
4	F 19/20 – F 21/22	2	1	1	4	95	3.56
5	I 20	1	1		2	12	1.5
6	F 15/16	2	1	1	4	39	5.25
7	H 14	2	1		3	94	3.17
8	D 7	1	1		2	19	3
9	H 8	2	1		3	75	1.8

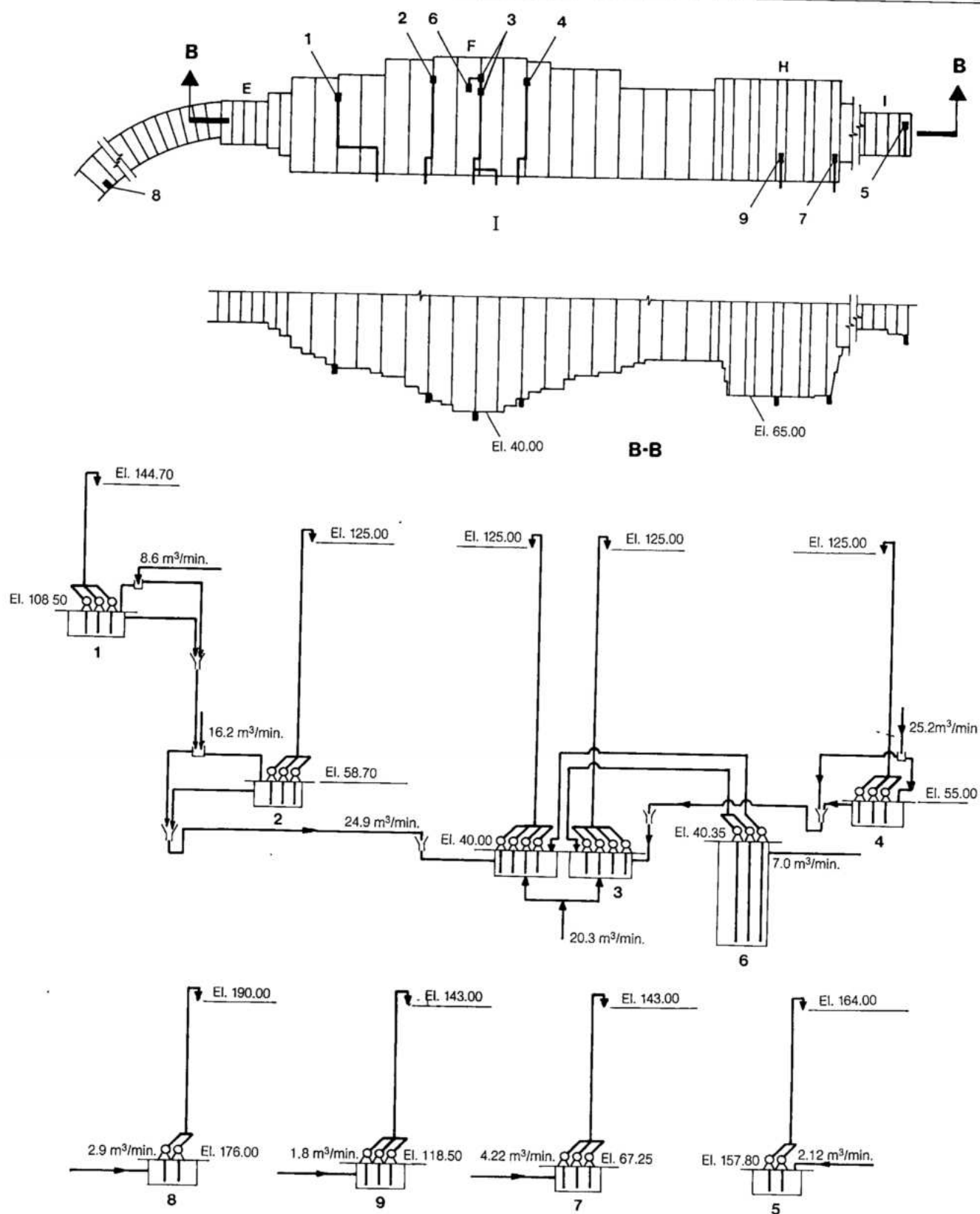


Fig. 10.21 Pumping stations in dam; schematic

I Plan view E, F, H, I Dam blocks 1, 2, 3, ...9 Pumping stations

assumptions for seepage through contraction joints, internal drains and the foundations, together with estimates of the maximum rainfall which could enter through the exposed portions of the buttress and hollow gravity blocks. All this was necessary to ensure that sufficient pumping capacity was installed to deal with the most extreme conditions possible. During 8 years of operation, only about 33 % of the pumping capacity was employed, with the maximum inflow occurring just after the reservoir was filled.

SANITARY SERVICES

Sewage and waste water from the toilets and wash rooms in the dam is collected in tanks and pumped to the holding tanks of the powerhouse sewage treatment facilities described in Chapter 13.

WATER TREATMENT PLANTS

The Itaipu project area has its own potable water supply, independent of the municipal systems of Foz do Iguaçu and Ciudad del Este. Two water treatment plants located in the concrete dam, ETA1 between blocks E3 and E4, El. 161 and ETA2 between blocks F33 and F34, El. 161, purify water obtained from the powerhouse cooling water system to supply the powerhouse with:

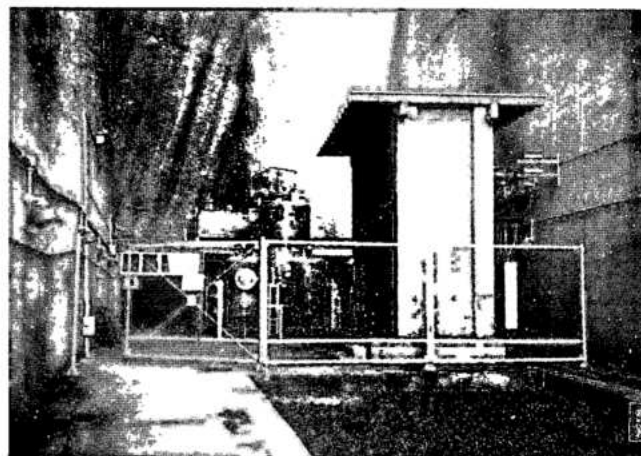
- Potable water
- Chlorine free make-up water for the deionized water generator winding cooling system.
- Make-up water for the evaporative cooling plants of the powerhouse ventilation system.

Other than some differences in layout, treatment plants ETA1 and ETA2 are similar and hence the following descriptions apply to both.

There are two completely separate systems at each station. One produces potable and chlorine free water and the other make-up water for the evaporative cooling plant. Both systems were supplied by Degremont, Brazil.

POTABLE AND CHLORINE FREE WATER

The system can produce a maximum of 15 m³/h of potable water to Brazilian standard ABNT PB-19. Normally 2.5 m³/h of the water is further processed to give chlorine free water for make-up to the generator deionized water systems. A schematic of the system is shown in Fig.10.22, which consists of subsystems as follows:



Water treatment plant - ETA 1

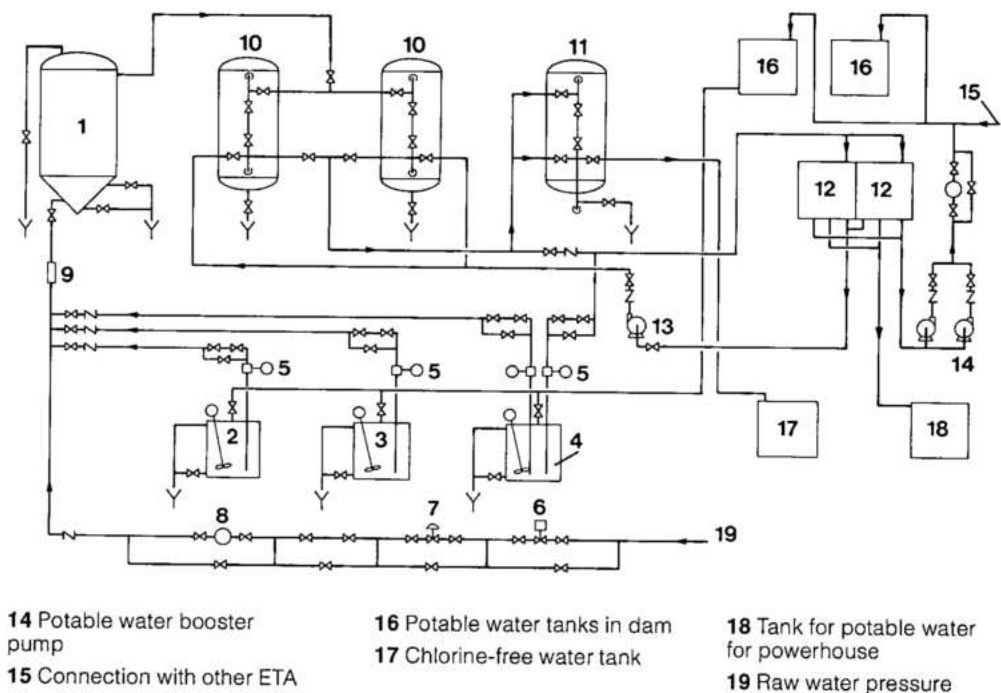
- Mixing tanks for aluminium sulphate, sodium carbonate and sodium hyperchlorate, complete with dosing pumps to inject these chemicals into the incoming raw water. Aluminium sulphate coagulates fine particles to a size which either settles or can be filtered, sodium carbonate softens the water and sodium hyperchlorate kills water borne organisms.
- A pressurized clarification tank in which the heavier coagulated particles settle. There is a premixing tank ahead of the clarifier to ensure an even distribution of the chemicals in the water. Deposited particles are periodically discharged to drain from the clarification tank.
- Two sand filters with back washing facilities to filter the particles remaining after clarification.
- A 200 m³ holding tank which receives the potable water after passing through the sand filters. The holding tank is split into 100 m³ separate compartments such that one half of the tank can be cleaned while the other remains in service. Water is gravity fed from the tank to the powerhouse tank and to the two pumps which fill the elevated water tanks in the dam.
- An activated carbon filter which removes the chlorine from the water destined for the generator winding deionized water system. This water is piped to a 2 m³ holding tank from where it is distributed to the generator systems on demand.

EVAPORATIVE COOLING VENTILATION SYSTEM MAKE-UP WATER

This system receives water from the powerhouse cooling water system and purifies it to slightly less than potable quality, suitable for make-up to the tanks of the

Fig. 10.22 Schematic diagram of potable and chlorine-free water treatment plants

- 1 Clarifier
- 2 Sodium carbonate mixing tank
- 3 Aluminium sulphate mixing tank
- 4 Sodium hyperchlorate mixing tank
- 5 Chemical feeder
- 6 Solenoid valve
- 7 Pressure reducing valve
- 8 Flow meter
- 9 Hydraulic mixer
- 10 Sand filters
- 11 Activated carbon filter
- 12 Potable water holding tank
- 13 Back wash pump



evaporative cooling system. Maximum capacity of this water purifying system is $30 \text{ m}^3/\text{h}$; a schematic is shown in Fig. 10.23. Aluminium sulphate, sodium chloride and sodium hyperchlorate are added to the incoming raw water before it passes through a mixing tank to ensure adequate flocculation, and then it is conveyed to a gravity clarifier. Coagulated particles settle in the bottom of the clarifier and are regularly discharged to drain. Clarified water of the required quality passes to a holding tank from where it is distributed to the evaporative coolers on demand from the float valves in the tanks of the coolers.

VENTILATION

Equipment rooms at El. 214 are forced fan ventilated. All toilets and the sewage pumping station have automatically operated exhaust fans, with air ducts to the ambient. The upper galleries are naturally ventilated. Lower galleries at El. 20 and El. 74 are forced fan ventilated with air drawn from and exhausted to the higher galleries.

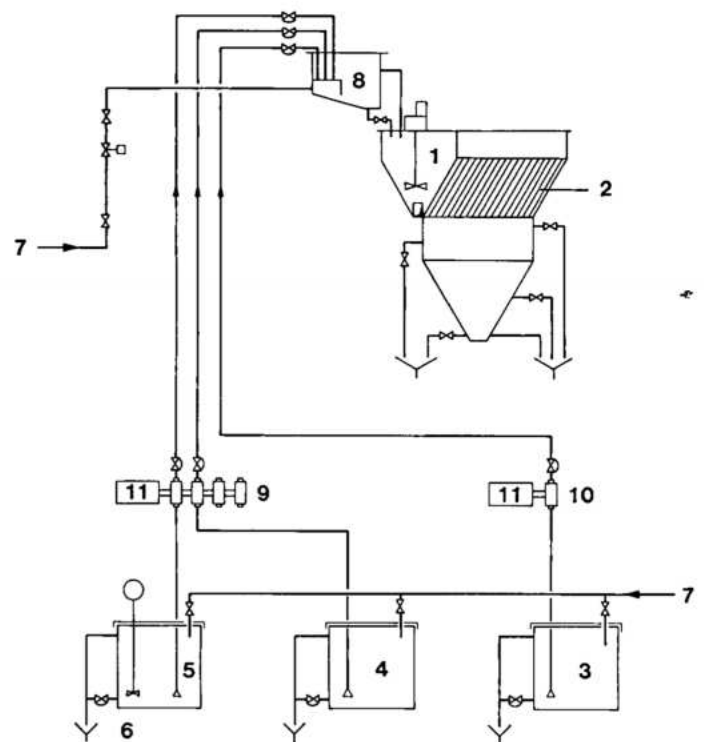


Fig. 10.23 Simplified schematic diagram of water treatment of evaporative coolers

- 1 Mixing tank
- 2 Clarifier
- 3 Sodium hyperchlorate dosage tank
- 4 Sodium carbonate dosage tank
- 5 Aluminium sulphate dosage tank
- 6 Mixers
- 7 Water inlet
- 8 Pre-mixing tank
- 9 Quadruplex dosage pump
- 10 Simplex dosage pump
- 11 Electric motor

In normal operation both regular 13.8 kV sources are available and their associated transformers are energized and supply a 460 V bus section with the tie breaker open. In the event of failure of one source, the secondary (460 V) breaker opens and the tie breaker closes automatically. In the event of failure of both sources, the secondary (460 V) breakers open and the breaker of the emergency diesel source, as well as the tie breaker, close automatically.

The general load substations QT-01 and QT-04, located at El. 214 in block F7/8 and El. 144 in block F5/6, consist of two 750 kVA transformers, 13.8 kV-460 V (delta-star), each connected through a low voltage circuit breaker to a sectionalized 460 V bus with a bus-tie circuit breaker. A second bus-tie circuit breaker allows shedding of Class III loads if required. In normal operation both regular 13.8 kV sources are available and their associated transformers are energized and supply a 460 V bus section with the first 460 V bus tie breaker open and the second one (for Class III loads) closed. In the event of failure of one source the secondary (460 V) breaker opens and the first tie breaker closes automatically. No emergency diesel source is available.

60 HZ AUXILIARY POWER

The pump substation QQ-03 located at El. 144 in block I-1, consists of three 500 kVA dry type transformers, 13.8 kV-460 V (delta star), each connected through a low voltage circuit breaker to a sectionalized 460 V bus. The operation is the same as for the similar panels at 50 Hz.

The general load substations QT-02, QT-03, and QT-05 located at El. 214 in blocks F25/26, H9/10 and H12/13 (split station), and El. 144 in block F29/30 consist of two 750 kVA (500 kVA for QT-03) dry type transformers, delta-star, each connected through a low voltage circuit breaker to a sectionalized 460 V bus with a bus-tie circuit breaker. The Class III load shedding and the operation are the same as for the similar panels of the 50 Hz system.

125 V dc SYSTEMS

In the main dam area there are four, basically separate, 125 V dc systems. Each system consists of two nickel cadmium batteries, two static type chargers, and two distribution panels with switching and interconnections to allow operating flexibility

while maintaining high reliability. The main functions of the systems are to supply power for the controls of the auxiliary equipment, alarm and annunciation, communications and emergency lighting.

Within the 50 Hz sector, one system is located at El. 214 in blocks F9/10 and F11/12 to service the intake gate areas for blocks 1 to 9A, and another at El. 144, block F17/18, for the dam drainage areas. In the 60 Hz sector, a system at El. 214 in blocks F21/22 and F23/24 services the intake areas for units 10 to 15, and another in blocks H3/4 and H6/7 services units 16 to 18.

The four systems are basically the same, with the exception that the equipment associated with units 16 to 18 are rated 152 Ah and the others 272 Ah.

PROTECTION, CONTROL AND INSTRUMENTATION

In general the protection used is fairly standard for this class of switchgear consisting of phase, neutral, and ground overcurrent relays on the main supply transformer with thermal/magnetic breakers on the feeders. One temperature detector with alarm and trip functions is provided on each transformer. Lock-out tripping relays are used to prevent transfer in the event of a fault.

Extensive use of local annunciation/alarm units has been made for each main auxiliary service group (i.e. 50 Hz/60 Hz substation and 125 V dc system). All critical values of voltage and temperature are monitored along with the status of the main circuit breakers and protection.

Because of the installation of generating units and the development of centralized control in stages, the controls and alarms were duplicated in the local control rooms of units 1 and 2 for the 50 Hz sector and units 14 and 15 for the 60 Hz sector, the central control room, and in the SCADA system for use as each became available.

POWERHOUSE ARRANGEMENT, DESIGN AND CONSTRUCTION

GENERAL CONSIDERATIONS	11.3
GENERAL ARRANGEMENT	11.4
General	11.4
External Access	11.6
Equipment Arrangement in a Typical Unit Bay	11.7
Equipment Arrangement in the Assembly Areas	11.12
CIVIL AND STRUCTURAL DESIGN	11.15
General Design Considerations	11.15
Design Criteria and Methodology	11.16
Unit Blocks in the River Bed	11.18
Unit Blocks in the Diversion Channel	11.24
OPERATION AND ADMINISTRATION BUILDING	11.28
PERFORMANCE OF THE POWERHOUSE STRUCTURES	11.30
Functions Monitored and Instrumentation	11.30
Foundation Response	11.30
Structural Performance	11.32

POWERHOUSE ARRANGEMENT, **DESIGN AND CONSTRUCTION**

GENERAL CONSIDERATIONS

The analysis of different project layouts investigated during the feasibility studies concluded that the most suitable location for the powerhouse would be at the toe of the main dam in the river channel and at the toe of the diversion control structure in the diversion channel. The principal factors which favored this location were:

- Relatively short length of penstock signifying good turbine regulation.
- Continuity of the powerhouse floors.
- Easy access for erection of equipment.
- Operation and maintenance.
- Case of accommodating the proposed number and size of generating units and their auxiliaries.

On conclusion of the feasibility studies the powerhouse arrangement was tentatively established with the following salient features:

- Eighteen turbine generator units of which fourteen were to be installed in the main channel of the Paraná river and four in the diversion channel.
- Unit bay spacing of 37 m; units to be installed in pairs within structurally independent and individually watertight blocks.
- Three erection and service buildings, two at the extremes and one between the main powerhouse and the diversion channel.



*Interior view of the
powerhouse -
generators hall*

- Semi-outdoor type powerhouse with removable roof sections over the unit bays at the upper deck elevation, which would be serviced by 2 x 2.5 MN and 1 x 19 MN (2 x 250 t and 1 x 1900 t) gantry cranes.
- All service galleries located downstream of the units.

Subsequent detailed studies of the requirements of a fast-track construction schedule, equipment installation, operation and maintenance, coupled with a more detailed analysis of equipment characteristics, resulted in the following refinements in the powerhouse arrangement:

- More detailed studies of project and regional systems resulting in the elimination of drawdown, together with the resolution of the dual frequency problem, led to an increase in the net head and rotational speed of the turbines. This permitted a reduction in unit spacing from 37 m to 34 m, which subsequently meant that the number of unit bays in the river channel could be increased to sixteen.
- After further study of the final construction program and operation and maintenance requirements the outdoor type design was considered inappropriate. An indoor type design was adopted with standard bridge cranes operated at two levels in the powerhouse; the number of cranes being increased to accommodate the anticipated peak rates of equipment installation.
- Rapid advances in the state of the art and sufficient experience at 500 kV of gas insulated switchgear (GIS) permitted consideration of this equipment for Itaipu.

The compact nature of the GIS design enabled the switchgear to be incorporated in an upstream gallery in the indoor powerhouse and the main transformers to be installed in a gallery upstream of the generators at El.108, allowing substantial shortening of the 18 kV generator isolated phase buses.

- Access requirements to the powerhouse both during construction and operation necessitated the elimination of the left bank assembly area and a subsequent increase in the size of the central one.
- The introduction of the upstream galleries permitted the incorporation of a downstream anti-flooding gallery above the draft tubes, which in turn dispensed with the need for the double unit watertight block design and its attendant constructional and operational disadvantages.

GENERAL ARRANGEMENT

GENERAL

A general plan of the Itaipu powerhouse, and operation and administration building is shown in Fig. 11.1. It comprises an independent 968 m long structure at the toe of the main dam and the diversion

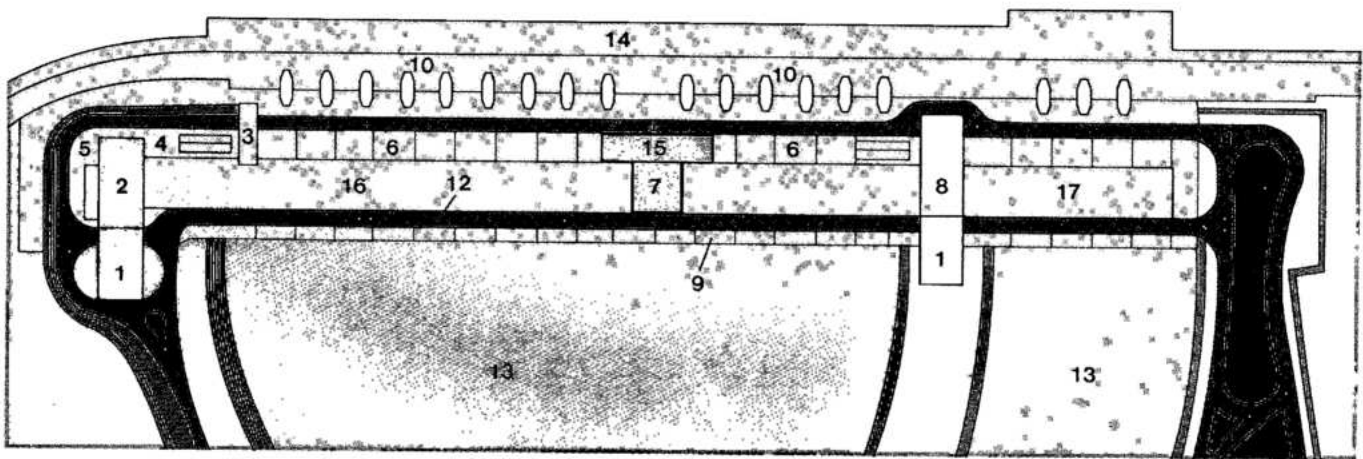


FIG.11.1 General plan of powerhouse

- | | | | |
|----------------------------------|-------------------------------|------------------------------|--|
| 1 Equipment unloading building | 5 Vertical circulation access | 9 Draft tube stoplog hatches | 14 Dam and power intakes |
| 2 Right assembly area | 6 Transmission line take-offs | 10 Penstocks | 15 Central operation and administration building |
| 3 Transformer unloading location | 7 Central control room | 11 Upstream road | 16 River bed powerhouse |
| 4 Auxiliary service transformers | 8 Central assembly area | 12 Downstream road | 17 Diversion channel powerhouse |
| | | 13 Tailrace | |



*Powerhouse roof and
central operation and
administration building*

control structure, containing all the equipment necessary for generation, control and dispatch of Itaipu power. The facility can be conveniently split into the following major sections:

Right assembly area. The right assembly area consists of:

- An unloading, unpacking and pre-assembly area at El. 144.
- 2 x 2.5 MN (2 x 250 t) cranes accessing to the main assembly area at El. 108, and
- A structure extending from El. 92.4 to El. 144 housing the 50 Hz general station electrical and mechanical services, 50 Hz standby diesel generators and transformer detanking facilities and workshops.

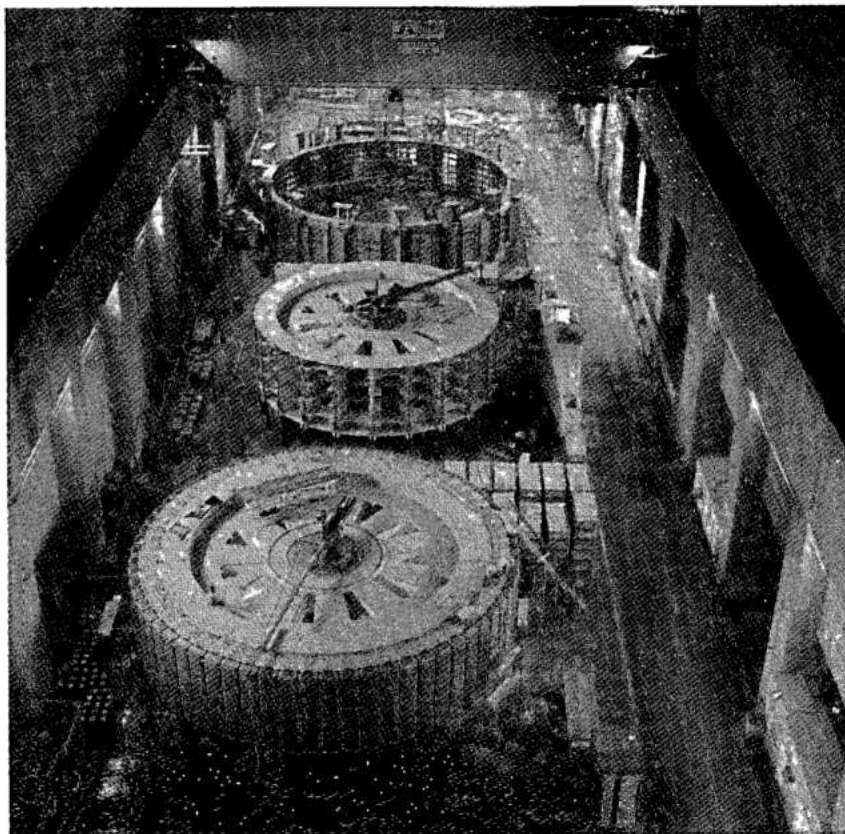
Also in the right assembly area is a reception room and tourist viewing facilities of the powerhouse main hall at El. 108.

The preassembly area at El. 144 is located between 37.65 m upstream and 98.85 m downstream of the units' center line and is in total 136.5 m long and 30.7 m wide. The main assembly area at El. 108 is 141.3m long (more than four unit bay widths) and

29 m wide, which together with the central assembly area provided sufficient space for erection of major turbine and generator parts to meet the programmed entry of three to four units in operation annually.

Unit bays 1 to 15. Unit bays 1 to 15 (plus an extra bay, block 9A) are located in the powerhouse structure constructed in the original bed of the Paraná river. The structure is 544 m long and extends from the right assembly area to the central assembly area. Each unit bay is 34 m wide, and extends from El. 50 to El. 144, and houses a turbine/generator unit, three unit main step-up transformers, switchgear and mechanical and electrical auxiliaries. In essence, the bays are identical in respect of the arrangement of major items of equipment. There are fifteen generating units installed; the central unit bay 9A being without any equipment or embedded parts.

The central control room is downstream at El. 135 between unit bays 9A and 10 with a viewing area above at El. 139. Adjacent to the viewing area in unit blocks U8, U9, U11 and U12 are offices and areas for technicians and operators.



*Right assembly area -
rotor assembly*

Central assembly area. Like the right assembly area, the central assembly area also has an unpacking and pre-assembly area at El. 144 with 2 x 2.5 MN (2 x 250 t) cranes accessing to a 98.15 m long and 29 m wide main assembly area at El. 108. The pre-assembly space is 144 m long and is located between 62.35 m upstream of the centerline of units and 81.65 m downstream and is 32.8 m wide. Below El. 144 the structure houses the 60 Hz electrical and mechanical services, the 60 Hz standby diesel generators, spare transformer areas and workshops.

Central operation and administration building .

The five storey central operation and administration building is located between units 9 and 11. The building houses the main entrance hall, auditorium, visitors' reception center, load dispatch center for 50 and 60 Hz frequencies, administration offices and rooms for technicians.

Unit bays 16 to 18A. The powerhouse constructed in the excavated diversion channel has four 34 m wide unit bays, which are virtually identical in arrangement to unit bays 1 to 15. Three of the unit bays contain turbine-generator units, the bay on the extreme left (18A) is empty.

V1 block. The powerhouse on the left bank is closed with block V1, which is 39.3 m wide at El. 144 and 99 m long. There is a draft tube stoplog storage pit at El. 144 downstream and the area inside at El. 108 is used for additional erection and pre-assembly space. All crane rails extend to the end of block V1.

The roof over the units in the powerhouse, 30 m wide and 902.5 m long, is made of precast concrete elements supported by cast in place concrete girders each 2 m wide x 6.1 m deep and 32.7 m long. The girders at maximum spacing of 9.1 m were constructed of C-210-c concrete placed in steel forms. On top of the girders, semi-cylindrical precast shell elements, 152.5 m radius, 2.5 m wide and of varying length between 7.3 and 12.83 m were placed to form a concave corrugated roof.

The roof over both right and central assembly areas has a length of 280.5 m and is also made of similar precast elements.

EXTERNAL ACCESS.

As shown in Fig. 11.1, vehicle access to the powerhouse is via roads leading from the right and left banks to the deck at El. 144. There are two roads extending the whole length of the powerhouse at this elevation, one upstream between the powerhouse

and the dam and the other downstream between the powerhouse and the draft tube gantry crane rails. Truck access into the powerhouse is via the roller doors of the right and central assembly areas and the respective cargo reception level of each area.

Access for light cargo and personnel is also available from top of the main dam at El. 225, via elevators and stairs leading to the upstream road at El. 144. Personnel access to the inside of the powerhouse is through smaller doors

in the roller doors in the right and central assembly areas and via entrances along the length of the powerhouse as shown in Fig. 11.1.

EQUIPMENT ARRANGEMENT IN A TYPICAL UNIT BAY.

The cross section of a typical unit block is shown in Fig. 11.2. The turbine-generator unit is in the middle of the block and is

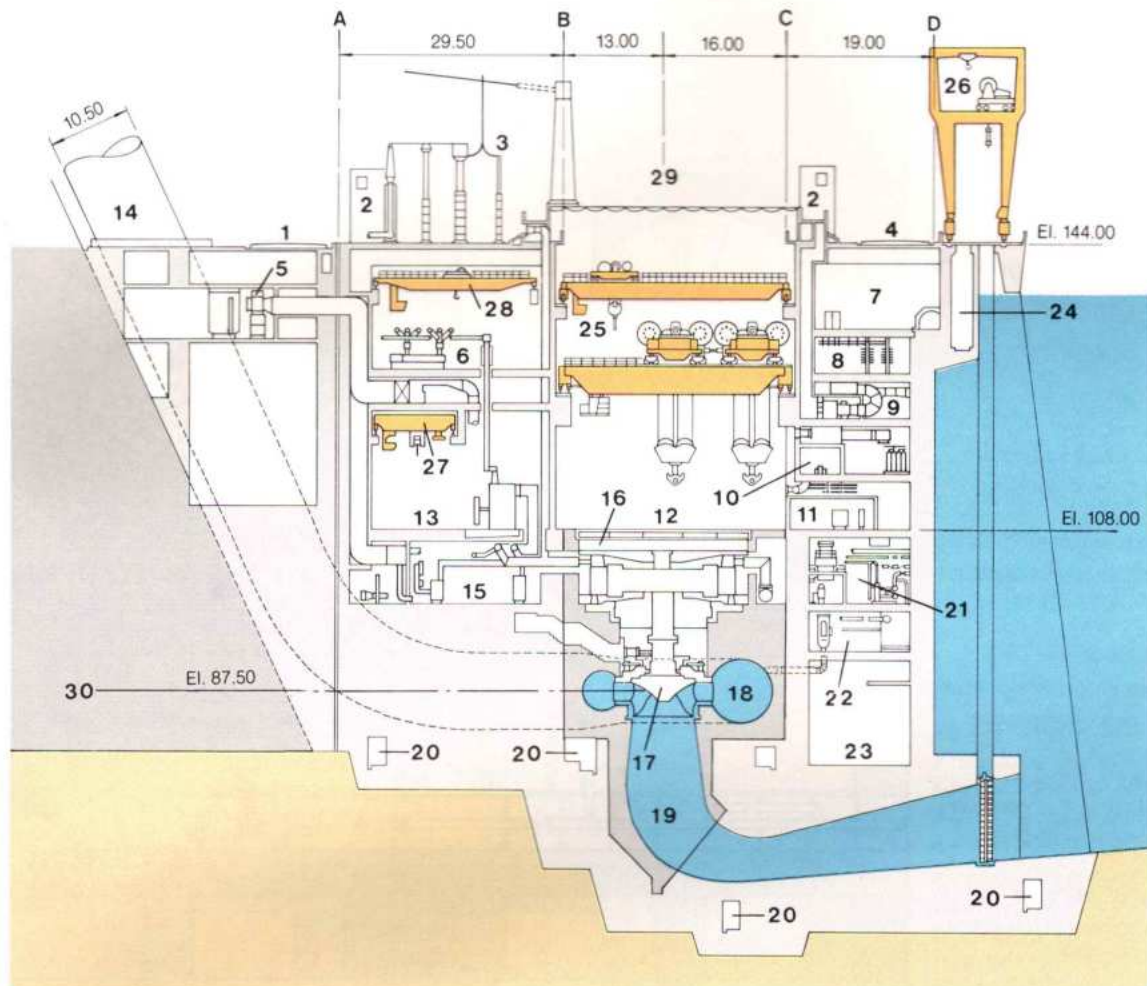
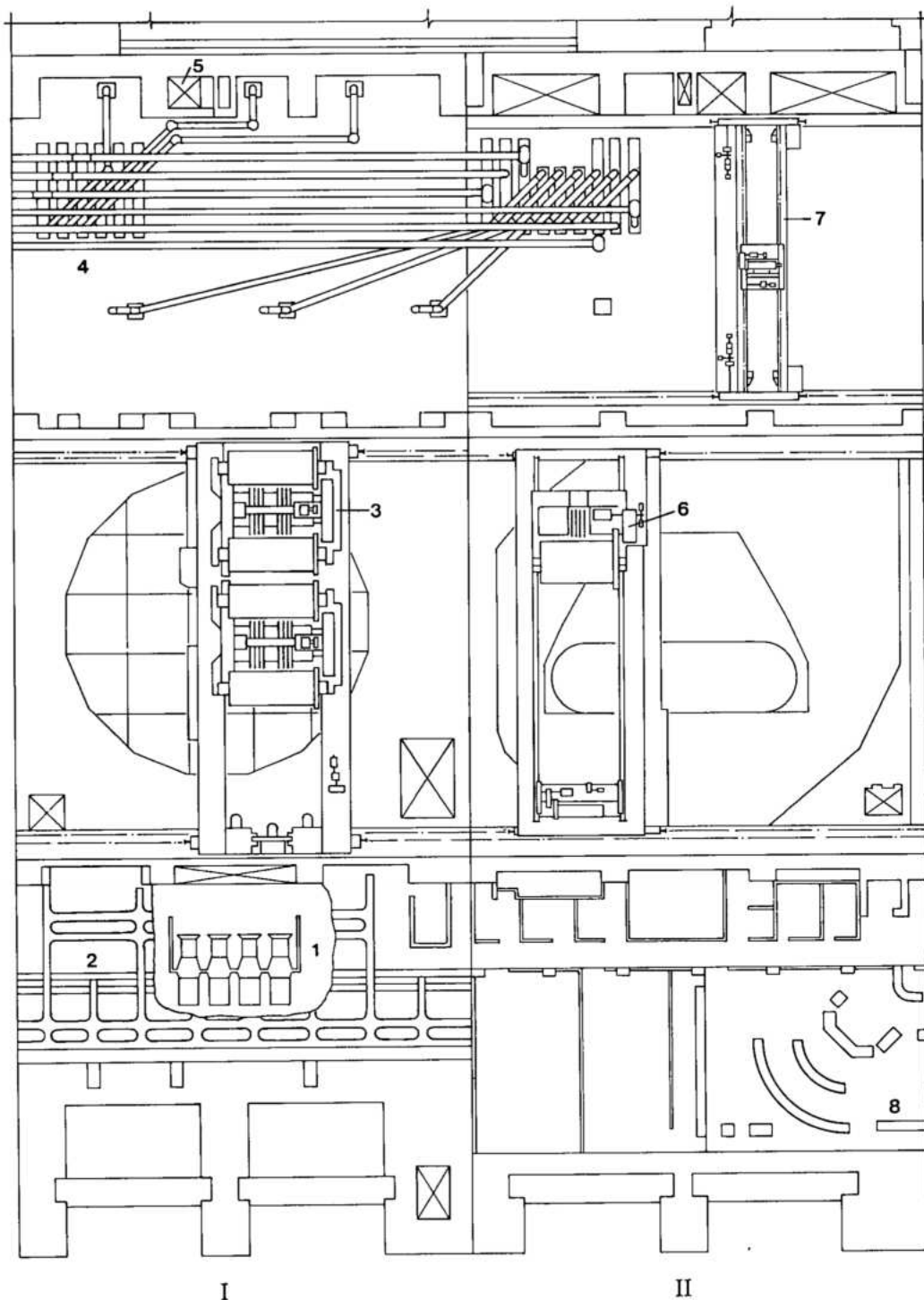


Fig. 11.2 Powerhouse section general arrangement

- | | | | |
|--|---|--|--|
| A, B, C, D Reference lines | 9 Ventilation equipment gallery | 18 Spiral case | 26 Gantry crane, 1.4 MN (140 t) |
| 1 Upstream road | 10 Battery room | 19 Draft tube | 27 Main transformers crane, 2.5 MN (250 t) |
| 2 Elevators | 11 Local unit control room | 20 Drainage gallery | 28 SF ₆ equipment crane, 100 kN (10 t) |
| 3 Transmission line take-offs | 12 Generator hall | 21 Mechanical equipment gallery | 29 Units' centerline |
| 4 Downstream road | 13 Main transformers gallery | 22 Pumps, strainers and piping gallery | 30 Turbine centerline |
| 5 Powerhouse upstream ventilation equipment rooms | 14 Penstock | 23 Anti-flooding gallery | First stage concrete |
| 6 SF ₆ switchgear | 15 Electrical auxiliary and excitation equipment gallery | 24 Draft tube stoplog storage | Second stage concrete |
| 7 Electrical equipment gallery | 16 Generator | 25 Main powerhouse crane, 10 MN (1000 t). | |
| 8 Electrical cable gallery | 17 Turbine | | |

Fig. 11.5 Powerhouse equipment arrangement floors at El. 122, and El. 128.2

- I Unit 9
II Unit 9A
- 1 Downstream ventilation plant
 - 2 Electrical cable gallery
 - 3 Main bridge crane, 2 x 5 MN(1000 t), four units
 - 4 SF₆ switchgear
 - 5 Elevator
 - 6 Bridge crane, 2.5 MN (250 t), two units
 - 7 Bridge crane for SF₆ equipment
 - 8 Central control room



- El.57.5 downstream . Draft tube unwatering valve.
- El.77.4 . Access to the draft tube upstream and downstream manholes and penstock spiral case drainage valves.
- El.77.4 downstream . Anti-flooding gallery leading to pump sumps between El.89 and El.68 in five units. The gallery provides an emergency retention

reservoir, which will give powerhouse staff time to rectify a potential flooding situation.

- Between El.89 and El.80 downstream . Pump sumps in two units for general powerhouse drainage.
- El.92.4 downstream . General mechanical services including powerhouse cooling water supply, sewage pumps and pump motors for the drainage systems listed

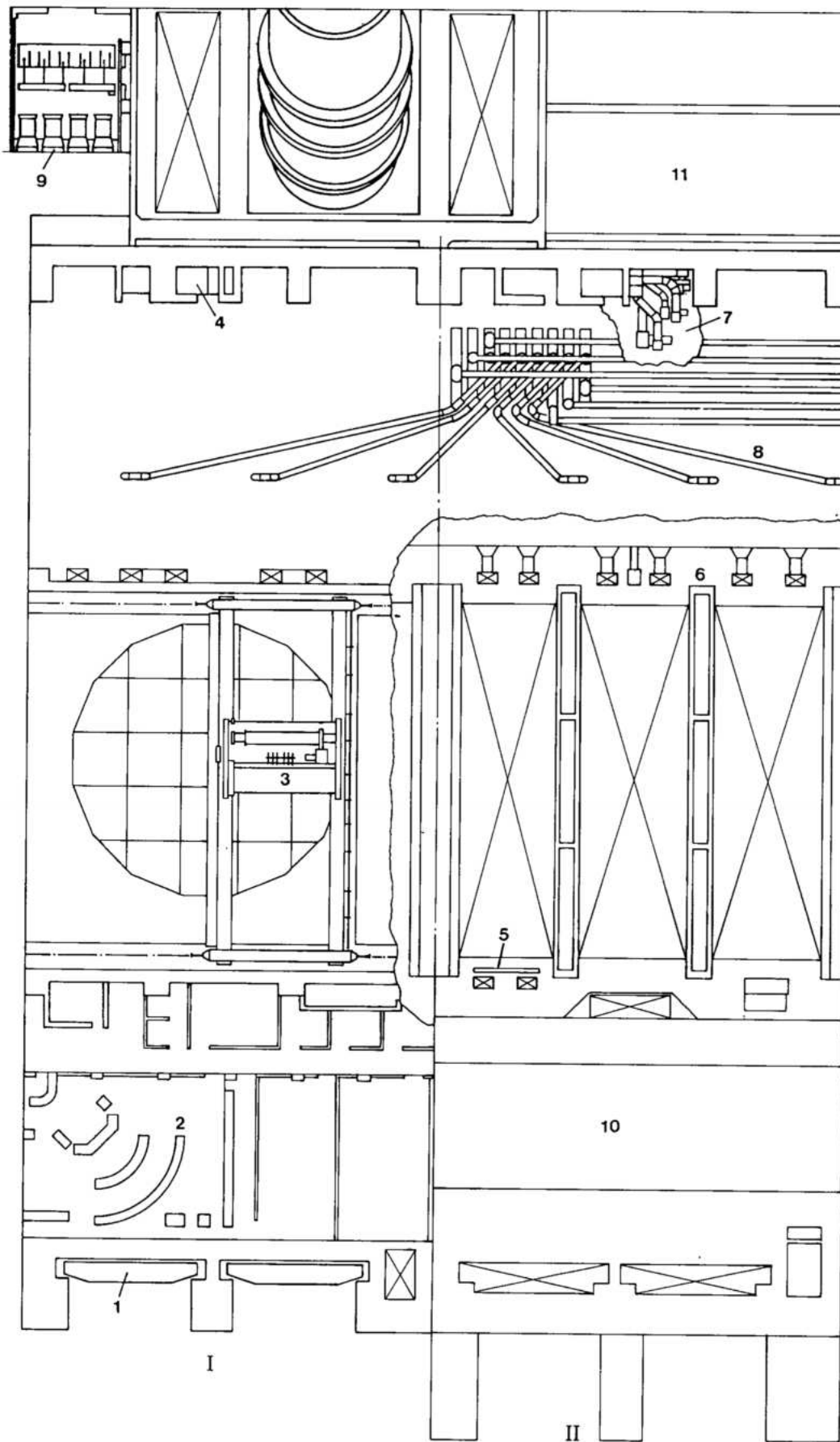


Fig. 11.6 Powerhouse equipment arrangement floors at El. 135.6 and El. 144.55

- I Unit 10
- II Unit 11
- 1 Draft tube stoplogs (five sets)
- 2 Central control room
- 3 Auxiliary bridge crane 1000/200 kN (100 t/20 t)
- 4 Elevator
- 5 Ventilation exhaust
- 6 Exhaust fans
- 7 Exhaust fans for turbine pit and generator
- 8 SF₆ Switchgear
- 9 Upstream ventilation equipment
- 10 Downstream road
- 11 Upstream road

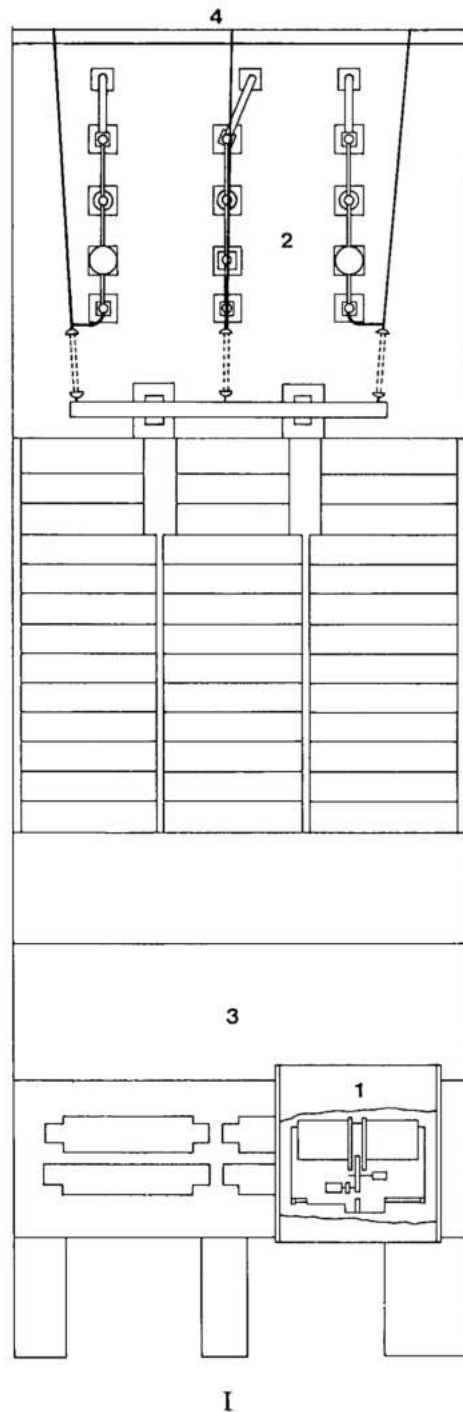


Fig. 11.7 Powerhouse equipment arrangement floors at El. 144 and 144.3

- | | |
|--|------------------------|
| 1 Unit 12 | 2 Power line take-offs |
| 1 Gantry crane for draft tube stoplogs | 3 Downstream road |
| | 4 Upstream road |

above. In units 2, 12 and 17 there are the collection tanks and pumps of the powerhouse sewage system.

- El.98.5 downstream . Turbine governor, pumps and heat exchanger unit for cooling water for stator of the generator, air compressor for partial load operation of turbine, air compressor for the governor, governor compressed air tanks and oil/air tank, control panels for the unit motors, generator brakes, air receiver and generator thrust bearing lift pumps, generator neutral equipment.
- El.98.5 upstream . Unit terminal cubicles, cubicles for excitation equipment and bus bars from the generators to the step-up transformers.
- El.108 downstream . Local control room (one per two units), protection panels for the units and for the 500 kV line take-offs.
- El.115 downstream . CO₂ cylinders and fire-fighting equipment, distribution switchboards for the ac and dc auxiliary services and the battery room.
- El.122 downstream . Ventilation plant for the downstream galleries and air conditioning plant (units 8 and 9 only).
- El.127 downstream . Cable trays, cubicles and auxiliary electrical equipment.
- El.133 downstream . Ventilation equipment and distribution panels. Central control room located in unit bays 9A and 10.
- El.108 upstream . Main unit step-up transformers located in individual cells protected by transverse fire protection walls and fire doors.
- El.124 upstream . Upstream ventilation equipment.
- El.128 upstream . GIS (SF₆) 500 kV switchgear.

Transverse access at each unit is via galleries at El.77.4, El. 95, El.98.5 and at the generator floor level at El.108.

The upstream evaporative cooling and ventilation equipment is located outside of the powerhouse wall at El.132, and the transformer cooling water tank at El.111. As the upstream wall of the powerhouse is designed to be water-tight up to El.144, there is no access across this wall.

Vertical access in the powerhouse is via the elevators and stairs as indicated in Fig. 11.1. The 50 Hz auxiliary service transformers are located near the right assembly area upstream at El.144 and the 60 Hz auxiliary service transformers are at the same level near the central assembly area.

EQUIPMENT ARRANGEMENT IN THE ASSEMBLY AREAS

Arrangement of equipment in the right and central assembly areas is shown in Figs.11.8 and 11.9.

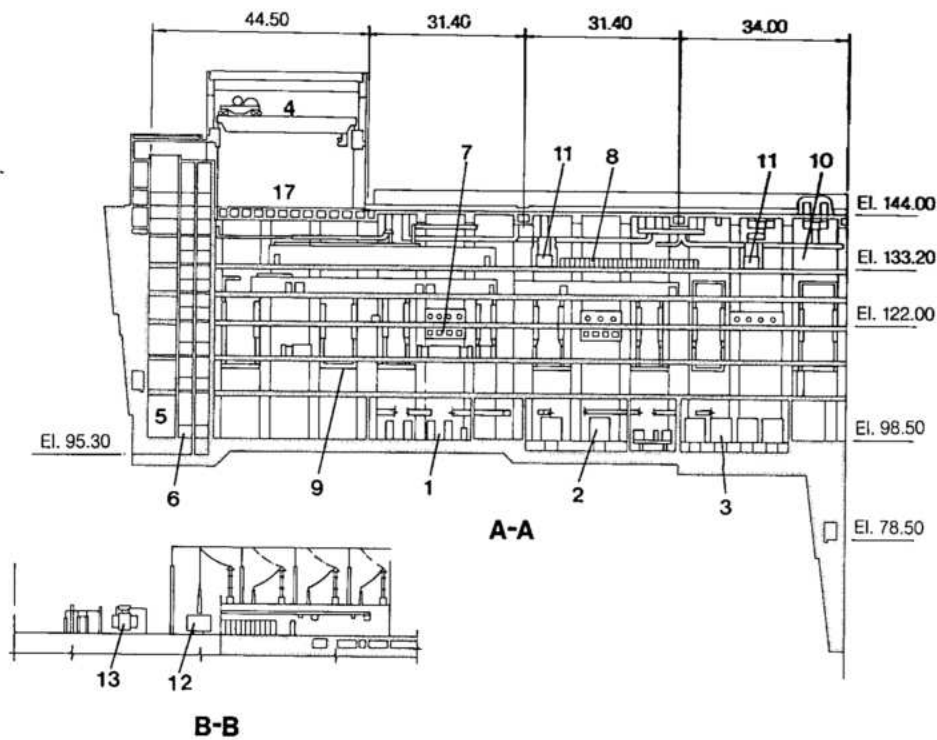
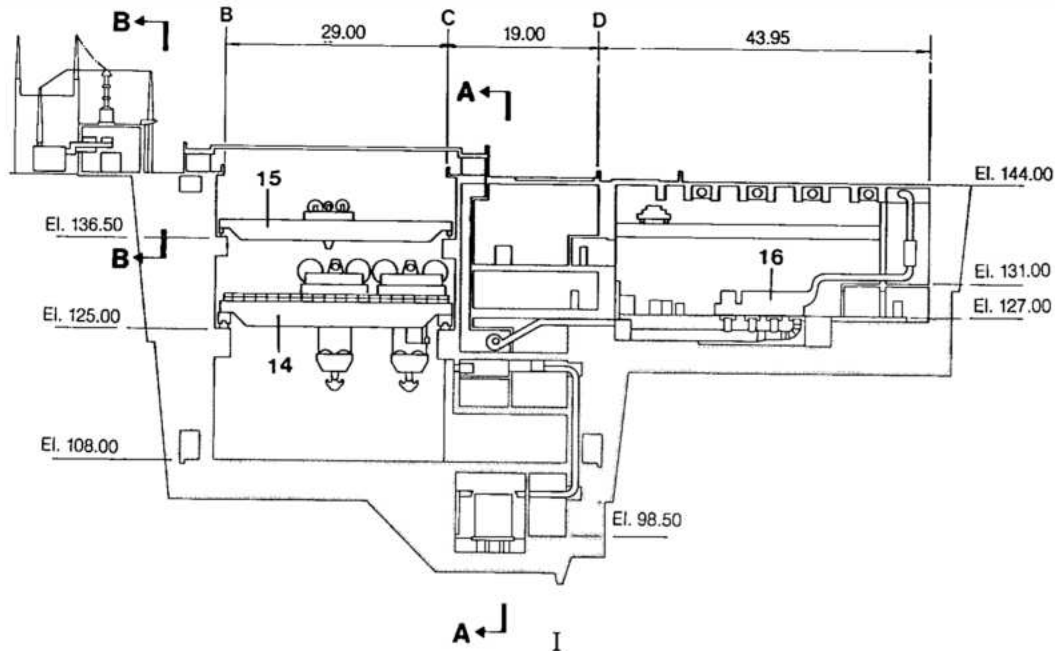


Fig. 11.8 Right assembly area - cross sections



- 1 Transversal section
- 1 Powerhouse compressed air
- 2 Lubricating oil plant
- 3 Transformer oil plant
- 4 Bridge cranes, 2.5 MN (250 t), two units
- 5 Cargo elevator
- 6 Passenger elevators
- 7 Ventilation fans
- 8 Control cubicles for standby diesel generators
- 9 Ventilation ducts
- 10 Lighting cubicle
- 11 Transformers for standby diesel generators
- 12 Auxiliary services transformer
- 13 Emergency power transformer
- 14 Main bridge cranes, 10 MN (1000 t), four units
- 15 Main bridge cranes, 1 MN (100 t), two units
- 16 Standby diesel generators
- 17 Equipment unloading building

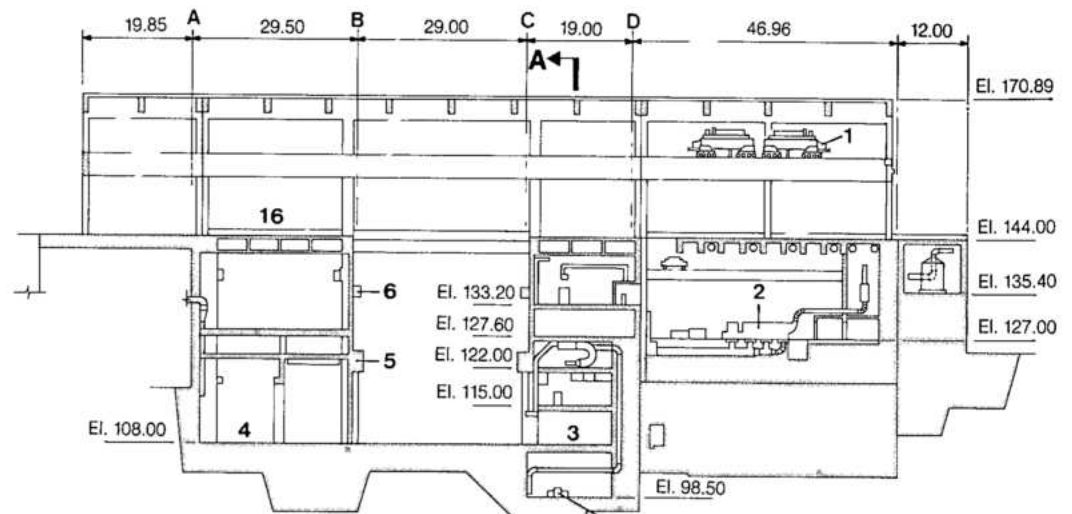
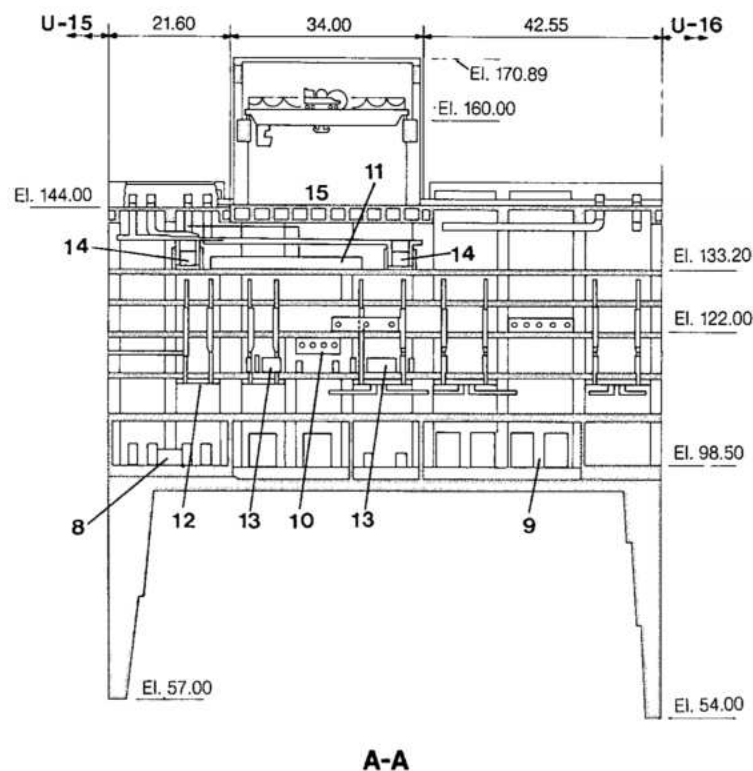


Fig. 11.9 Central assembly-area cross sections

I Transversal section

- 1 Bridge cranes, 2.5 MN (250 t), two units
- 2 Standby diesel generators
- 3 Workshop/Machinshop
- 4 Main step-up transformers gallery
- 5 Beams for 10 MN (1000 t) main bridge crane
- 6 Beams for 1 MN (100 t) bridge crane
- 7 Lubricating oil plant
- 8 Powerhouse compressed air plant
- 9 Transformer oil plant
- 10 Ventilation fans
- 11 Control cubicle for standby diesel generators
- 12 Ventilation ducts
- 13 Auxiliary service control cubicles
- 14 Transformer for standby diesel generators
- 15 Equipment unloading building
- 16 SF₆ gallery



Location of the major equipment in the right and central assembly areas is as follows:

Equipment	Location	El.
Lubricating oil storage and treatment	Downstream	98.5
Transformer oil storage and treatment	Downstream	98.5
Powerhouse compressed air	Downstream	98.5
Workshops/Machinerieshops	Downstream	108
Diesel generators	Downstream	127
Oil tanks for diesel	Downstream	135
Transformer detanking	Upstream	108

Sewage treatment facilities are located away from both assembly areas at El.144.

CIVIL AND STRUCTURAL DESIGN

GENERAL DESIGN CONSIDERATIONS

The following general considerations guided the design of the twenty blocks of the powerhouse:

- Each block shall be an independent structural unit, separated from the dam and adjoining powerhouse blocks by contraction joints.
- Each block should be capable of safely resisting the hydraulic loads transmitted through the spiral case and draft tube, the tailwater pressure, the weights, torques and thrusts imposed by the electromechanical equipment, within the limits of stresses and deformations set by the design criteria.
- Structural components, separated by construction joints, should be articulated to facilitate rapid construction and interface scheduling. Also, each component must be capable of safely handling any temporary loads which may be imposed during the various stages of construction.
- Structural components must not be susceptible to vibration and resonance induced by operation of the permanent equipment.
- After completion, and before, as well as after installation of the generating equipment, each block should perform as an integral elastic structure, without overstressing any area or component.

Several studies were made to select the distance between the axis of the dam and the centerline of the powerhouse units. Three factors governed this selection:

1. Powerhouse structure to be independent of the dam and not overlap the toe of the latter;
2. The straight length between the lower bend of the penstock and the spiral case to be the minimum required for satisfactory operation of the turbine.
3. The radius and angle of the lower bend of the penstock should be acceptable to turbine manufacturers.

After extensive reviews with the turbine manufacturers, the combined length of the lower bend and the transition to the spiral case was shortened. The structural studies showed that the upstream wall of the powerhouse could be located at the toes of the main dam blocks with foundation at El.70. While portions of five powerhouse blocks (U7-U10) would overlap the toes of the dam blocks whose foundations were lower than El.70, it did not significantly affect the structural performance of either the dam or the powerhouse. In the final design, the distance between the axis of the dam and centerline of the powerhouse units is 111.5 m, about 15 m less than in the initial layouts.

The longitudinal contraction joint between the dam and the powerhouse is vertical between El.144 and El.70 and follows the downstream face of the dam down to the foundations for five unit blocks. Powerhouse structure upstream of the joint, where some secondary galleries are located, see Fig.11.2, structurally functions as a part of the dam.

Transverse contraction joints, at 34 m spacing, separate the powerhouse unit blocks. The joints are plain and open to permit independent flexure of the super-structure without transfer of loads from one block to the other.

Structural concepts

Equipment assembly areas. The right assembly area was mostly carved out of sound rock and is almost entirely rigidly confined. The foundation slab has a thickness varying between 1 and 5 m. The upstream and downstream walls, 36 m high (El.108 to El.144), were placed directly against the excavated faces of the rock. Because of the average 0.1 H:1 V slope of excavation, thickness of these walls varied from 6 m at the base to 10 m at the top.

The 150.5 m long right assembly area was divided into four structurally independent blocks by transverse contraction joints. Because the walls and floor slabs of the U-shaped structure are massive and in bonded contact with sound rock, structural members were not designed as frames, and reinforcement was provided for

temperature changes and the heavy load of the assembled generator rotors.

While the central assembly area is similar in layout to that of the right bank, its structural concept was different because it was not excavated into the abutment. In fact, it is completely free on the upstream side, and was therefore designed as a composite structural frame.

Typical unit block. To establish the general structural configuration of a typical unit block, a three-dimensional finite element mathematical model was made with the estimated dimensions of the principal load-carrying members, i.e. the substructure, the external walls and the main floors, including foundation rock down to El.0. Using the normal loading condition, the principal objective of this analysis was to understand the tendencies of behavior of the various structural components of the block and the pattern of distribution of loads among them.

The results of the initial analysis indicated that while the bulk of the forces transmitted through and due to the generating equipment would be resisted by the central massive core of the substructure (below El.98), the 100 m high downstream wall and piers will resist the tailwater pressure by flexure. The relatively slender transverse walls share some of the tailwater pressure. Considering the above pattern of load distribution, a typical unit block was divided into three sections by two vertical construction joints. The location of the construction joints was also influenced by the required stages of construction, schedule of installation of equipment, and the concrete placement methods to be employed.

The portion of the unit block downstream of the central core around the unit consists essentially of an L-shaped structural monolith, with the substructure slabs and the draft tube forming the horizontal part of the inverted L and the downstream breast wall and the counterfort piers forming the vertical member. This monolith was designed as a dam to resist hydrostatic pressure from tailwater at El.142.5, which may occur during a probable maximum flood, after the impounding of a future downstream reservoir. The downstream walls and piers were constructed ahead of the floor slabs of the downstream galleries, in order to protect the incomplete unit blocks when the first unit started operation.

Loading conditions

For structural design and stability analyses of the various blocks of the powerhouse and the equipment assembly areas, the following four classes of loading conditions were used:

Construction loading. Included various possible combinations of loads during construction, such as exceptional live loads due to movement or installation of construction or permanent equipment, loads imposed during testing of permanent equipment, and loads imposed by fresh concrete on existing lifts or incomplete members. Special consideration in design was given to the loads during encasement of the spiral case and the stay ring, during installation of the turbine and the generator while the powerhouse structure was only partially completed, from external hydrostatic loads and abnormal temporary uplift pressures on parts of structure during construction.

Normal loading. Covered various combinations which would be imposed on the structures during normal operation of the powerhouse, such as hydrostatic loads with reservoir level at El.220 and the tailwater varying between El.92 and El.110.85, temperature changes, uplift pressures, normal wind loads and dynamic loads due to mobile equipment, such as water pressure in penstock and spiral case, without load rejection overpressure.

Exceptional loading. Along with normal loading conditions, they included combinations of loads of statistically low frequency of occurrence, such as hydrostatic loads due to the reservoir at El.223 and tailwater at El.122, seismic loads due to earthquake acceleration of 0.05g horizontal, and dynamic loads on penstock and spiral case with load rejection overpressure or due to short-circuit in the generator.

Limiting loading. Combined highly improbable loads, such as reservoir level at El.223 and tailwater at El.142.5 corresponding to the passage of a probable maximum flood through the Itaipu reservoir after the impounding of the proposed Corpus Dam, 150 km downstream, extremely severe wind loads, a seismic event equivalent to earthquake acceleration of 0.08g horizontal and limiting dynamic loads on turbine and generator.

DESIGN CRITERIA AND METHODOLOGY

Methodology

For the design of the reinforced concrete structural elements the following general approach was used:

- Massive components, such as concrete under the penstock bend upstream of the unit and the generator pedestal were analysed by the FEM method to determine the stress distribution and the amount of reinforcement required.

- Downstream structure, comprising the downstream wall, the piers and portions of the substructure were considered a cantilever monolith and designed by conventional flexural method, assuming that all the tailwater pressure was borne by the downstream wall and the counterfort piers, without any support from the downstream gallery walls and the transverse outer walls of the unit block.
- Superstructure frames, comprising columns and beams, such as for the crane tracks in the various equipment galleries, were designed as two dimensional frames, wherever appropriate.
- Encasement concrete, such as the second stage concrete for embedment of the spiral case, was designed to sustain a portion of the internal hydrostatic pressure which would be transmitted due to elastic deformation of the steel liner. Before embedment the spiral case was pressurized equivalent to 90% normal reservoir head, and the concrete was placed at a temperature not exceeding 10°C and a rate of 0.12 m/h. The reinforcement was designed for the induced shrinkage and thermal stresses, as well as the load transferred from the spiral case.

Design loads

The following uniformly distributed loads (in kN/m²) were used in the design of principal slabs, beams and frames:

Main step-up transformer gallery floor slab	15
GIS (SF ₆) gallery floor	15
Downstream roadway	20
Cable gallery floor	10
Ventilation gallery floor	10
Battery room floor	15
Anti-flooding gallery floor	120
Assembly area floors	80
Generator floor	50
Turbine floor	15
Oil storage room	25
Precast roof elements	0.5

For design of reinforcement, Brazilian standards ABNT NB-1 and NB-49 were employed. In special cases, foreign codes were used (ACI, DIN, CEB). For design of upstream galleries where vehicle loading was considered, Brazilian code NBR 7188 was also employed.

Concrete characteristics

Types of concrete used in the structural components of the powerhouse and the equipment assembly areas were:

Structural component	f _{ck} N/cm ²	Days	MSA mm
Massive structures	2100	365	76
Superstructure (in general)	2100	28	38
Roof structures with long spans	2800	28	38
Corners of frames (densely reinforced)	2800	28	38
Downstream piers, external walls (slip-formed)	2100	28	38
Interior walls; floor slabs and columns	2100	28	38
Concrete exposed to high water velocities	2800	28	38
Pre-cast elements			
Bridge beams, beams of roof structure – long span	3500	28	19
Beams and slabs	2800	28	19
Covers, stairs, roof elements in galleries	2100	28	38
Spiral case encasement (pumped concrete)	2100	28	38
Concrete for draft tubes	2100	28	76
2nd stage concrete			
Slabs, columns, beams, blockouts	2100	28	19
Thin structures	1800	28	19

Interaction between main dam and powerhouse.

The interaction of the main dam and powerhouse blocks in the river bed was studied with the computerized Finite Element Method for both two and three dimensional models having the following features:

- The joint between the main dam and powerhouse was assumed to transmit horizontal forces only.
- Deflections were assumed to be entirely elastic.
- Loading comprised the weight of the structure at various stages of construction and hydrostatic loads from the reservoir and tailrace, see Fig. 11.10.
- The reservoir was assumed to fill instantaneously.
- The tailrace was assumed to be at El.92 and uplift pressure on the fractured rock of joint A was included. For uplift pressures all drains were assumed to be operative.

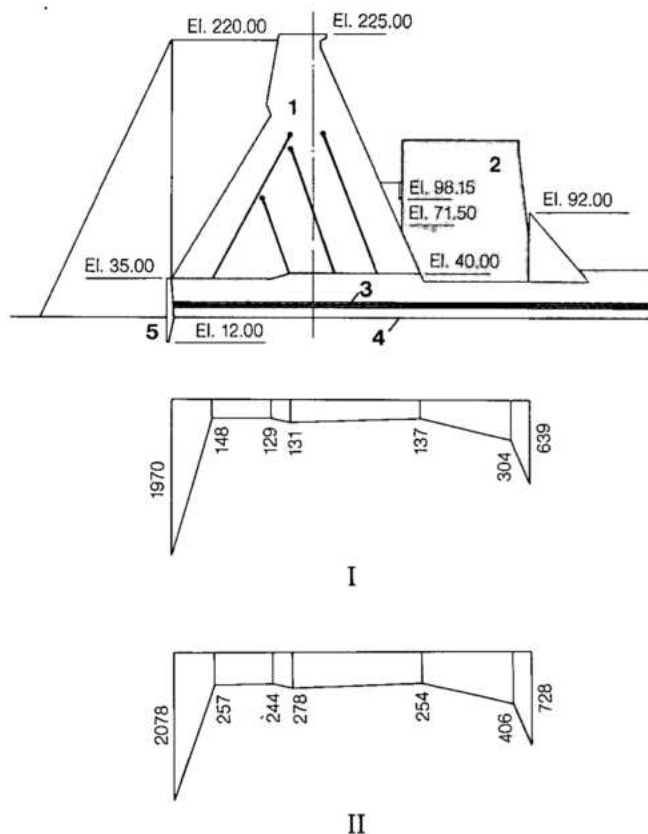


Fig. 11.10 Load diagram for main dam - blocks with intakes and the powerhouse

- | | |
|---|-----------------------------|
| I Uplift pressure on fractured zone (kN/cm ²) | 2 Powerhouse |
| II Uplift pressure on joint A (kN/cm ²) | 3 Fractured zone |
| 1 Dam | 4 Joint A |
| | 5 Vertical foundation crack |

- A vertical crack in the foundation was assumed to extend from the heel of the dam to El. 12.
- For the three dimensional model the joint was simulated by horizontal axial bars 10 cm in diameter; see Fig 11.11.
- Foundations were assumed to be a series of almost horizontal basalt flows sloping 2° from upstream to downstream.
- Concrete aging was simulated by a modulus of elasticity of 3×10^6 N/cm² when loaded only by the weight of the structure and 4×10^6 N/cm² when hydrostatic forces were applied.

The first mathematical model studied was for the hollow gravity dam blocks sited on the river bed at El. 35 and in contact with the powerhouse at the same elevation.

Principal results of the analysis are shown in Fig. 11.11 and the main conclusions were:

- A zone of tensile stresses, in the range of 68 to 72 N/cm², exist in downstream head of the dam at El. 98 as a result of temperature changes.
- At the location where the lower penstock bend enters the powerhouse, compressive stresses of 1630 N/cm² are present near the joint.
- Maximum horizontal deformation at the joint between dam and powerhouse is 9 mm at El. 98.15, tending to close the joint.
- Thermal contractions due to cooling of the concrete tend to open the joint whereas the loadings resulting from the weight of the structures and hydrostatic forces close the joint, see Table 11.1.
- Joint movement calculated by the three dimensional model was about 0.2 mm less than that obtained from the two dimensional one.

The two dimensional mathematical model was used to study the performance of the joint for the blocks with foundations above El. 40 and gave a maximum relative deformation of 8.2 mm between El. 98 and El. 113. Based upon the results of the study, a contraction joint of 10 mm was allowed between the dam and powerhouse at line A between the foundation and El. 111 for units 1 to 15 and the assembly areas. On the inclined part of the contact between El. 80 and El. 111 the joint gap was 100 mm.

As the diversion structure had already stabilized before the units in the diversion were built, no joint was provided for this part of the powerhouse.

Height of concrete lifts

In the more massive areas the lifts ranged from 0.5 to 1.5 m in height. The exterior walls of the unit block were placed in 2 to 2.5 m lifts. For slip-formed downstream piers the rate of placement was restricted to 0.12 m/h.

UNIT BLOCKS IN THE RIVER BED

Foundations and stability analysis

Foundation conditions. Foundation conditions for almost all the powerhouse structures were similar to those for the central blocks of the main dam and the diversion control structure. Except for the central six blocks, U6 to U10, all powerhouse blocks are founded on sound, dense basalt of flow B. For the six central blocks, where the river bedrock was about 25 m lower, backfill concrete was placed to El. 55, so that all sixteen blocks in the main river channel had a nearly horizontal foundation.

The dense basalt of flow B has excellent geomechanical properties, characterized by a high modulus of deformability $E > 20\,000$ MPa and by the

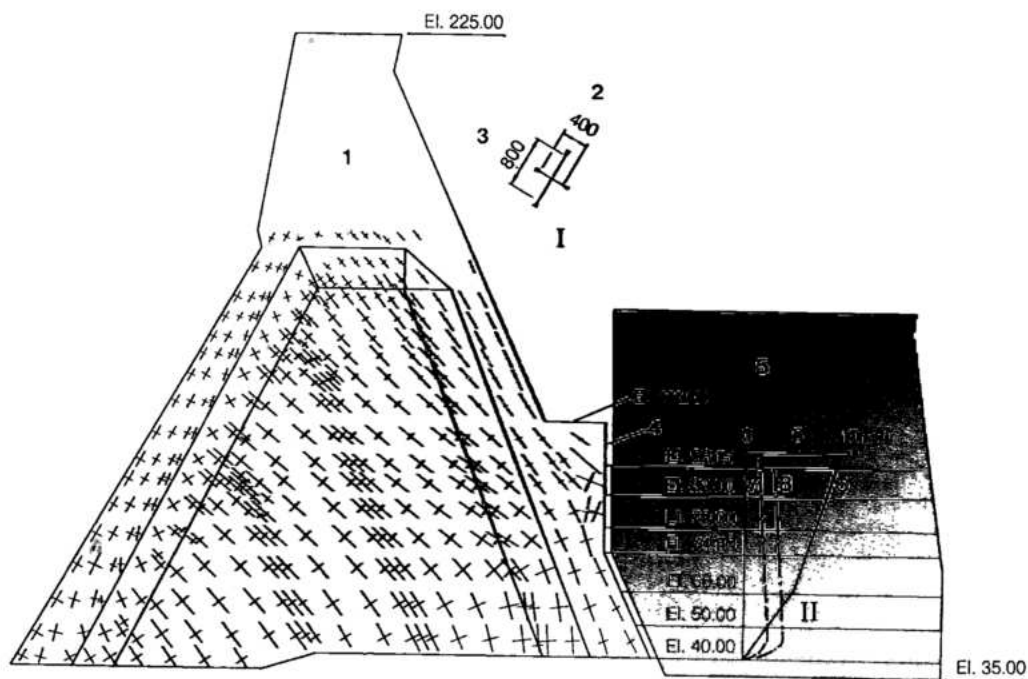


Fig. 11.11 Three - dimensional FEM model of the dam and the powerhouse - principal stresses, joint deformation

- I** Scale of principal stresses
II Diagram of joint movement between main dam and powerhouse
1 Main dam
2 Tension (kN/cm^2)
3 Compression ($-\text{kN/cm}^2$)
4 Bars simulating contact between main dam and the powerhouse
5 Powerhouse
6 Closure of joint (combined forces)
7 Thermal contraction on September 30-1981
8 Thermal contraction on June 30-1982

Table 11.1 Measured joint movements for temperature changes and effect of weight of structures (mm)

Elevation (m)	30 September 1981		30 June 1982	
	Closure due to structure weight	Opening of joint due to temperature	Closure due to structure weight	Opening of joint due to temperature
45	1.2	2.3	1.2	3.1
60	4.2	2.0	4.2	2.9
79	6.7	1.7	6.7	2.7
98	9.0	1.3	9.0	2.0

absence of weaker zones which might impair the stability of the powerhouse. Only in the central blocks located in the deepest part of the river channel the following foundation features required careful stability analysis, as well as beneficiation treatment:

- Contact between flows A and B at El.20 approximately, comprised of extensive joint and fracture zones and dipping upstream, see Chapter 4.
- Lack of downstream confinement
- Discontinuity A, located at about El.12.






Stability analysis and uplift control. The stability of the central powerhouse blocks and their foundation against shearing-sliding was studied in conjunction with the central blocks of the main dam as follows:

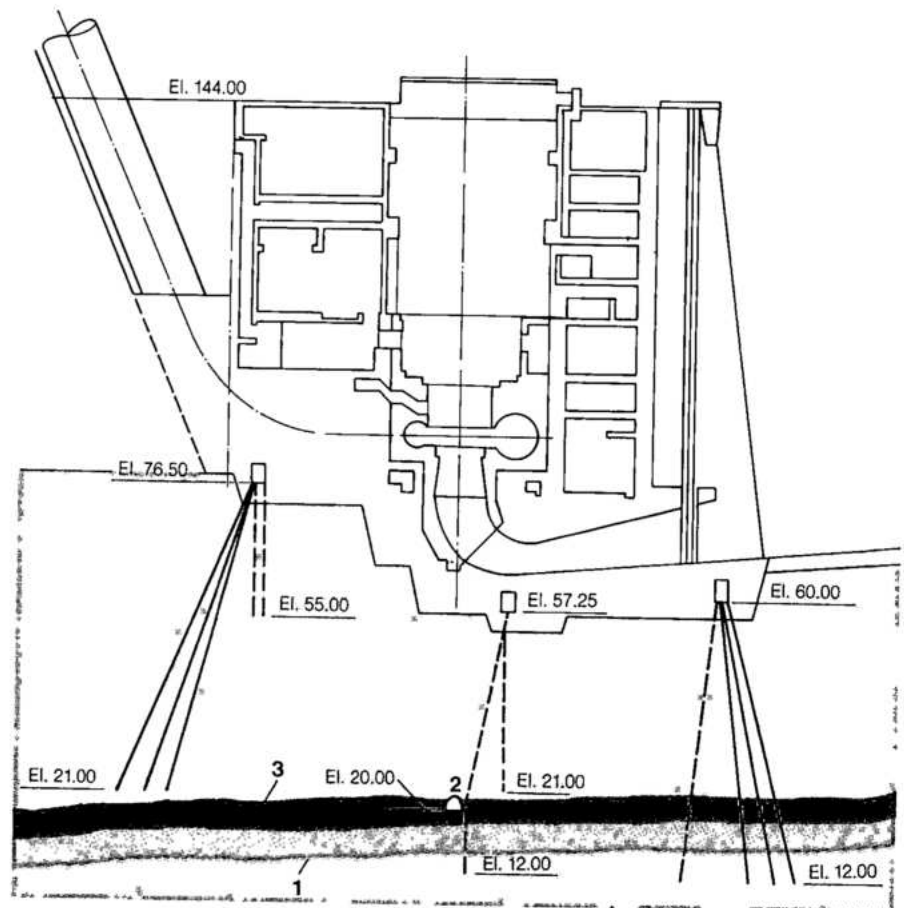
- Conventional sliding stability analysis in which the blocks of the powerhouse were considered to be rigid, independent of the main dam or the diversion control structure.
- Verification of the stability by means of geomechanical and mathematical models.

The comprehensive geomechanical model evaluated the stability of the powerhouse jointly with the dam, particularly with respect to the weaker zones in the foundation, as discussed in Chapter 4.

Safety against flotation was also checked for such unit blocks as U9A, where the units might not be installed and the second stage concrete not placed for several years. For such analysis the critical criteria assumed maximum tailwater level, foundation drains

Fig. 11.12 Grout curtains and drainage holes

- 1 Discontinuity A
- 2 Drainage gallery
- 3 Contact between flows A and B
-  Dense basalt flow B
-  Breccia
-  Vesicular - amygdbasalt
-  76 mm diameter grout hole
-  100 mm diameter drainage hole



inoperative and no effective bond at foundation contact A/B.

To improve the margins of safety against shearing-sliding and flotation at the weaker foundation features, it was necessary to provide specific treatment for reducing seepage through the relatively pervious zones or discontinuities of the foundation and to reduce uplift pressures and keep them within the criteria assumed in stability analyses and design. As shown in the Fig. 11.12 the treatment basically consisted of:

- A curtain of grout holes drilled from the downstream gallery at El. 60. This grout curtain consisted of 76 mm diameter holes as follows:
 - Primary inclined at 15° to vertical and spaced at 3 m.
 - Secondary inclined at 7° to vertical and spaced at 3 m.
 - Tertiary inclined at 11° to vertical and spaced at 1.54 m.

For consolidation of the backfill concrete and rock foundation of U6 to U10, extra holes were drilled to El. 1.

- A grout curtain drilled from the gallery at El. 76.50 to reach El. 21, with grid spacing of 3 m.

- Inclined drainage holes behind the downstream grout curtain drilled from the downstream gallery at El. 60.
- A vertical line and a line at 64° to the vertical of 100 mm diameter drainage holes drilled from the

gallery at El. 57.25. These were spaced at 3 m and reached El. 34 and in the case of U7 El. 19.

- A vertical line of 100 mm diameter drainage holes behind the grout curtain drilled from the gallery at El. 76.5 spaced at 3 m centers and reaching El. 55.
- Grout and drainage holes between blocks AMC2 and AMC3 and between U18A and block VI drilled vertically between El. 108 and El. 50.

At the concrete-rock contact a network of half-round concrete pipes was provided to collect any contact seepage and carry it to the galleries.

Two transverse grout and drainage curtains were provided at the extremities of the powerhouse, to complete the cut-off of lateral seepage flows under its foundation. These transverse curtains were connected with the grout curtains of the main dam.

The depths of the grout and drainage curtains were determined on the basis of permeability characteristics of the various strata and their contact zones, in particular the contact between flows A and B (about El. 20) and the discontinuity A (about El. 12). A drainage tunnel parallel to and under the centerline of the units was located to intercept contact A/B. In turn, this drainage tunnel joins the

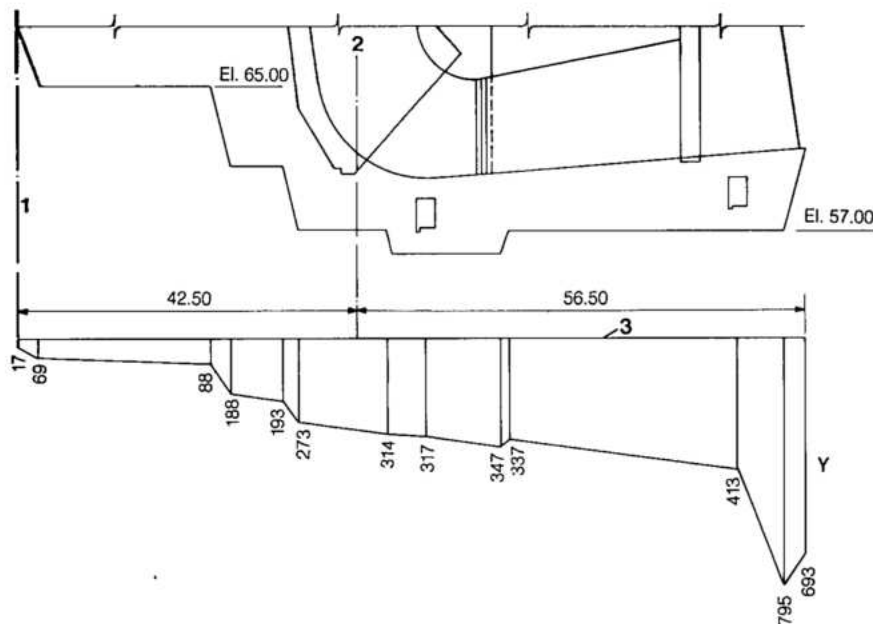


Fig. 11.13 Uplift pressure diagram (units U1 to U15).

Y Uplift pressure (kN/m²)
 1 Contraction joint between main dam and the powerhouse
 2 Centerline of units
 3 Base line at El. 57

transverse drainage tunnels provided under the central blocks of the main dam, see Chapter 10. The tunnel roof was reinforced with 3 m long rock bolts and the tunnel was lined with mesh reinforced gunite. Drainage holes were drilled from the floor of the tunnel to discontinuity A.

Uplift pressure distribution under the powerhouse blocks in the main river channel, as used in stability analysis, is shown in Fig. 11.13. It was assumed that the foundation drains would effectively reduce the piezometric pressure at the drainage gallery to 33% of the difference between the upstream and the tailwater heads.

Construction

For the sixteen unit blocks of the powerhouse in the main river bed and for the right and central assembly areas, the sequence of excavation was as follows:

- For the right and central erection areas and for block U1 to El. 115, excavation was finished before completion of the main cofferdams.
- After the main cofferdams were completed and the river bed dewatered, excavation for the powerhouse block was a continuation of the foundation excavation for the main dam.
- About 120 000 m³ of backfill concrete was placed for six central blocks where the bedrock was below El. 50.

To meet the critical program described in Chapter 5, the following construction sequence was adopted:

- Concreting of the floor and walls of the right assembly area proceeded ahead of construction of blocks E5, E6 and F1/2 of the dam.
- After dewatering of the river bed, concrete backfill was placed to El. 54, under blocks U6 to U15.

- Proceeding from both the right and left banks towards the middle, mass concrete was placed up to El. 62 in the central and downstream monoliths separated by the construction joint along line C.
- Concrete upstream of the contraction joint between the dam and the powerhouse (line A) was placed monolithic with the dam and ahead of that in the powerhouse blocks.
- In the upstream monoliths (between lines A and B), up to El. 85, leaving the space for the penstock, concrete was placed either simultaneously with or following first stage concrete in the central core monoliths.
- Draft tubes were constructed and the first stage of the core block poured.
- Following the completion of the roof of the draft tube, the transverse and longitudinal walls and the piers of the downstream monolith were constructed rapidly to El. 130 with the extensive use of slip-forming.
- Next, the massive first stage portions of the central and upstream monoliths were brought up to the main deck at El. 108.
- While the other powerhouse blocks were much lower, in U1, U2 and U3 blocks the columns and beams for supporting the main powerhouse cranes were completed to El. 125, concurrently with the downstream wall.
- The final stages of construction for each unit block were completion of the superstructure, internal floors of the downstream galleries, precast roof of the powerhouse and second stage concrete around the spiral case and other equipment.

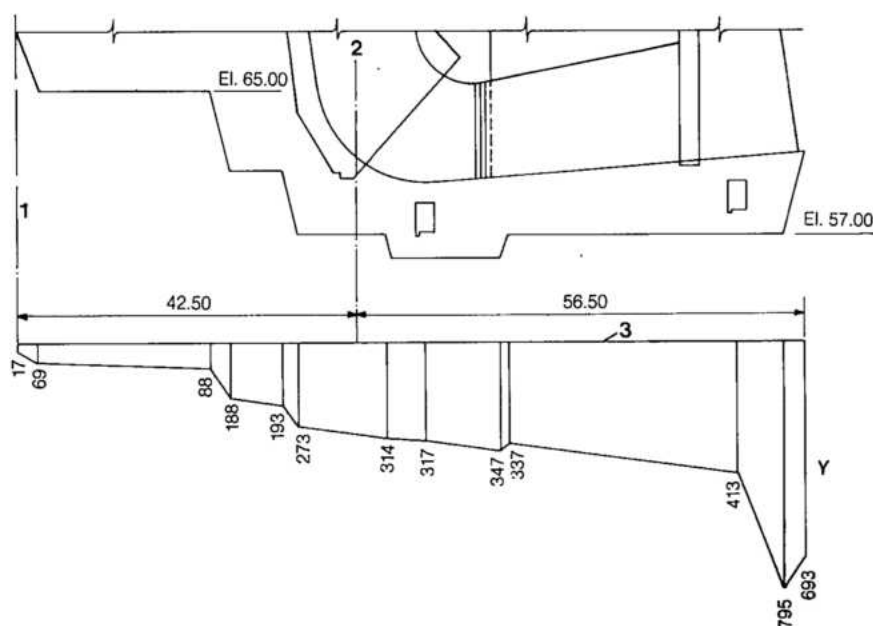


Fig. 11.13 Uplift pressure diagram (units U1 to U15).

Y Uplift pressure (kN/m²)
 1 Contraction joint between main dam and the powerhouse
 2 Centerline of units
 3 Base line at El. 57

transverse drainage tunnels provided under the central blocks of the main dam, see Chapter 10. The tunnel roof was reinforced with 3 m long rock bolts and the tunnel was lined with mesh reinforced gunite. Drainage holes were drilled from the floor of the tunnel to discontinuity A.

Uplift pressure distribution under the powerhouse blocks in the main river channel, as used in stability analysis, is shown in Fig. 11.13. It was assumed that the foundation drains would effectively reduce the piezometric pressure at the drainage gallery to 33% of the difference between the upstream and the tailwater heads.

Construction

For the sixteen unit blocks of the powerhouse in the main river bed and for the right and central assembly areas, the sequence of excavation was as follows:

- For the right and central erection areas and for block U1 to El. 115, excavation was finished before completion of the main cofferdams.
- After the main cofferdams were completed and the river bed dewatered, excavation for the powerhouse block was a continuation of the foundation excavation for the main dam.
- About 120 000 m³ of backfill concrete was placed for six central blocks where the bedrock was below El. 50.

To meet the critical program described in Chapter 5, the following construction sequence was adopted:

- Concreting of the floor and walls of the right assembly area proceeded ahead of construction of blocks E5, E6 and F1/2 of the dam.
- After dewatering of the river bed, concrete backfill was placed to El. 54, under blocks U6 to U15.

- Proceeding from both the right and left banks towards the middle, mass concrete was placed up to El. 62 in the central and downstream monoliths separated by the construction joint along line C.

- Concrete upstream of the contraction joint between the dam and the powerhouse (line A) was placed monolithic with the dam and ahead of that in the powerhouse blocks.

- In the upstream monoliths (between lines A and B), up to El. 85, leaving the space for the penstock, concrete was placed either simultaneously with or following first stage concrete in the central core monoliths.

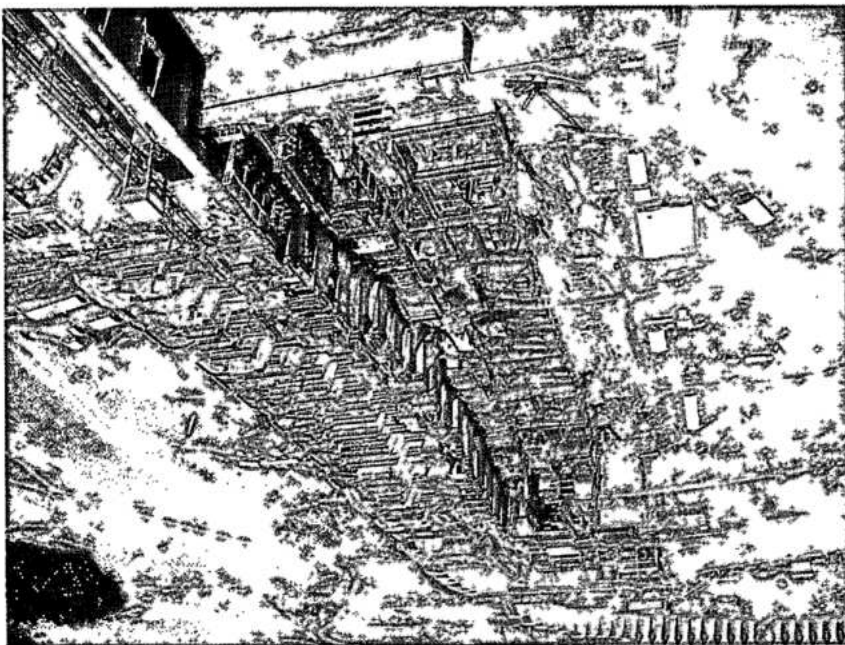
- Draft tubes were constructed and the first stage of the core block poured.

- Following the completion of the roof of the draft tube, the transverse and longitudinal walls and the piers of the downstream monolith were constructed rapidly to El. 130 with the extensive use of slip-forming.

- Next, the massive first stage portions of the central and upstream monoliths were brought up to the main deck at El. 108.

- While the other powerhouse blocks were much lower, in U1, U2 and U3 blocks the columns and beams for supporting the main powerhouse cranes were completed to El. 125, concurrently with the downstream wall.

- The final stages of construction for each unit block were completion of the superstructure, internal floors of the downstream galleries, precast roof of the powerhouse and second stage concrete around the spiral case and other equipment.



Construction of the
powerhouse



Backfill concrete below El. 54. In the central part of the powerhouse, over an area approximately 155 m x 45 m, the bedrock was 5 to 20 m below El. 54, the lowest nominal foundation of the powerhouse. Considering the large volume of backfill concrete required, it was decided that the concrete would be placed continuously without any contraction joints or treatment of joints between layers.

The concrete was delivered in dump trucks, placed at 6 m intervals and spread by bulldozers in 0.5 m layers. Compaction and consolidation of concrete was with backhoes with internal vibrators. Some immersion type vibrators were also employed. Concrete placement averaged 15 000 m³/day.

Core samples were taken from the backfill concrete 30 to 60 days after placement, and a series of in-situ permeability tests were made in the drill holes. The tests showed that the strength of concrete was adequate for powerhouse foundations, but it was quite pervious with coefficients of permeability ranging from 10⁻² cm/s to 10⁻⁴ cm/s as compared to an average permeability of 10⁻⁵ cm/s for the foundation rock. Consequently, a downstream grout curtain comprising three rows of holes was executed from the foundation gallery at El. 60 to seal off the backfill concrete from the tailrace. A curtain of drain holes was drilled through the backfill concrete upstream of the grout curtain.

Additional drain holes were drilled from the draft tube drainage gallery at El. 57.25 and from the perimetral drainage tunnel at El. 20 which is under the centerline of the units, see Fig. 11.12. Thus seepage into and uplift pressures in the backfill concrete were adequately controlled.

Substructure construction. Typical configuration of the powerhouse foundation surface, as shown in Fig. 11.2 was:

- At El. 57 extending from the unit center lines to 57 m downstream, with a section 14 m long, further excavated to El. 54.
- Local excavation for drainage sumps to El. 46.
- Upstream four stepped benches at El. 57, El. 65, El. 75 and El. 80 to meet the contraction joint between the dam and the powerhouse at line A.

After final cleanup, half-round 0.15 m diameter porous concrete pipe was placed at 2 m centers along the cut upstream slopes parallel to the axis, as well as along the near vertical upstream walls of the right assembly area. These contact drains were connected to headers leading to the various drainage galleries.

A 0.30 m thick regularizing layer of concrete was placed on the horizontal benches or foundation, 7 to 15 days before commencement of mass concrete placement.

In the three monoliths formed by longitudinal construction joints along lines A, B and C, mass concrete was placed to about El. 62 under the draft tube and in the core block, and to El. 82 in the upstream monolith under the penstock. This was poured typically in a 0.5 m lift on the foundation, followed by 2.5 m lifts. The lifts in each monolith were continuous between transverse contraction joints.

The techniques of formwork, placing and consolidation of concrete, and of construction joint treatment were the same as for the massive portions of the main dam, as described in Chapter 9. For the two upstream monoliths, concrete in buckets was delivered by the cableways. For the downstream portion including the piers, four tower cranes travelling on tracks located just downstream of the powerhouse, handled the delivery of concrete buckets, forms, and precast elements used for roofs of the draft tube and embedded steel.

Special site-fabricated forms were used for the faces of first stage concrete where a large number of dowel bars were embedded for better bond with second stage concrete. These forms were faced with fine mesh expanded metal supported by timber frames. Holes for the dowel bars were formed through the expanded metal; there was a negligible amount of concrete mortar lost through the fine mesh. Such forms were effectively used around the draft tube throat and the turbine pit.

Special plywood lined forms were fabricated at site for placement of concrete for the unlined portion of the draft tube elbow. The roof of the straight portion of the draft tube was formed by inverted T precast concrete beams. In heavily reinforced areas and around steel liners where accessibility was restricted, concrete was poured through chutes or flexible pipes and consolidated with vibrators on long hoses.

The following structural elements were constructed by slip-forming: downstream breast wall above the draft tube and the piers or counterforts supporting it and walls of the central and right assembly areas. For some large slip-formed blocks with a large amount of reinforcement, concrete was delivered by pumping; D-210-c concrete with 9 cm slump and a retarder admixture was used. Where pumpcrete was employed the average speed of the slip-forms was restricted to 5 cm/h.

Superstructure construction. Construction of the superstructure, comprising walls, columns and floor slabs above El. 108, followed conventional forming and concrete placement procedures for reinforced concrete structures. In the slip-formed walls, blockouts with dowels were provided for the later

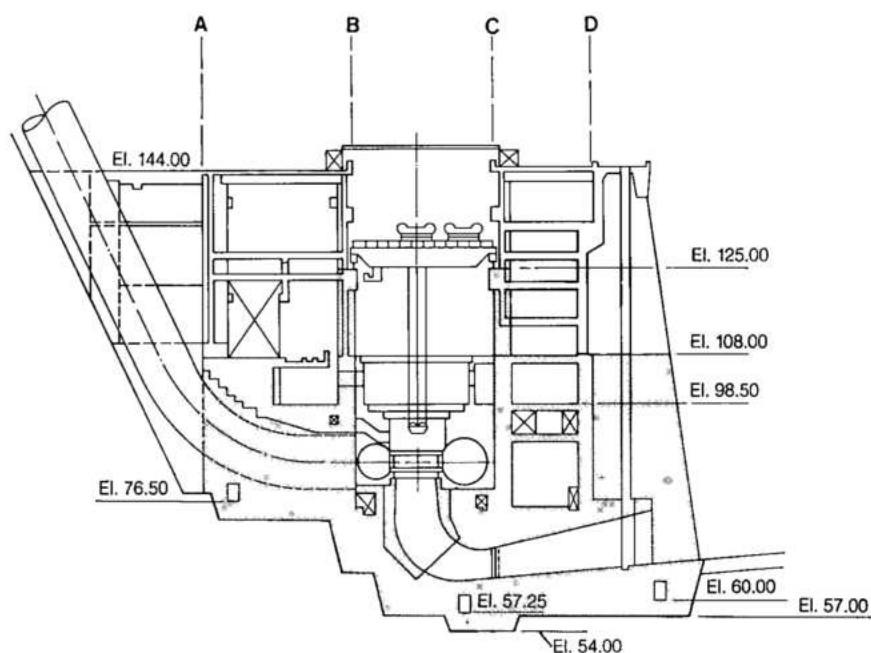


Fig. 11.14 Minimum configuration of concrete in the powerhouse unit required for lowering of stay ring into the turbine pit

construction of floor slabs or installation of precast stairs or beams. Due to very tight construction schedule, transport and assembly of turbine and generators heavy components had to be carried out before construction of powerhouse was completed.

Thus, a minimum economic configuration of concrete elements in the unit blocks was established to avoid overstressing of concrete when handling of this equipment should take place. Fig. 11.14 shows this configuration defined as follows:

- Axis A-B

All components including transformer support slab constructed to El. 108.

- Axis B-C

External side walls between axis B and C concreted to El. 98.50.

- Axis B and C

Columns and main crane beams constructed to El. 125.

- Downstream of line C.

Slabs and counterforts constructed to El. 108.

Economy on reinforcement was also an additional advantage of this configuration.

Initially, concrete for superstructure construction was delivered by the tower cranes located downstream of the powerhouse. After the upstream deck at the toe of the dam and the deck downstream of the generator hall were completed, delivery of concrete was handled by tower cranes operating at El. 144.

UNIT BLOCKS IN THE DIVERSION CHANNEL

Utilizing the large amount of data gathered by instrumentation and the evaluation of structural behavior of the powerhouse blocks in the river bed during construction, filling of the reservoir and tailrace, and five years of operation, the design criteria for the four unit blocks in the diversion channel were modified as follows:

- Uplift criteria. Piezometric pressure measurements during the first five years of project operation indicated that the foundation drains under both the dam and the powerhouse blocks were highly efficient. Therefore, for the unit blocks constructed in the diversion channel during 1986-88, the uplift distribution criterion was less severe. As shown in Fig. 11.15, it assumed the piezometric drop at the drainage gallery to be 66% of the difference between the upstream level and the elevation of the floor of the drainage gallery. This permitted a reduction in the depth of the foundation slab of the diversion units resulting in 63 000 m³ less excavation and 27 000 m³ less concrete for the four unit blocks. Work on the foundation slab was further facilitated by utilizing 30 000 m³ of rollcrete already existing in the diversion channel at downstream and of the diversion structure.

- Interaction with the diversion control structure. Since the diversion control structure had already been subjected to full reservoir pressure, (with its tailrace empty) for four years, its deformations had already stabilized. Therefore, it was assumed that no forces would be

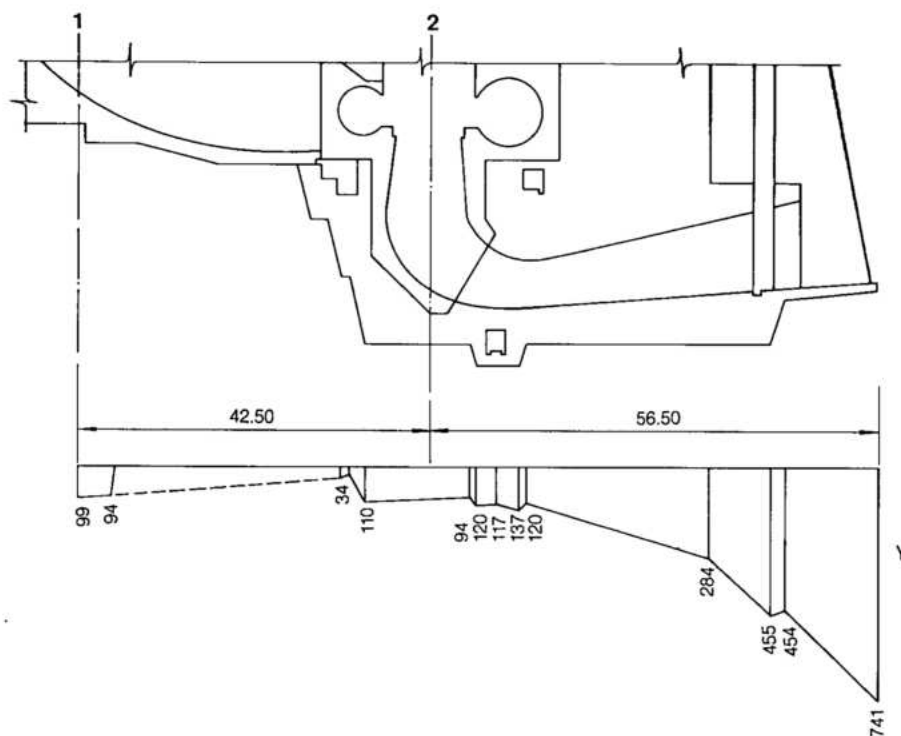


Fig. 11.15 Uplift pressure diagram (units U16 to U18A)

Y Uplift pressure (kN/m²)

1 Contraction joint between main dam and the powerhouse - reference line A

2 Centerline of units

transferred from the dam to the powerhouse. This criterion was also justified by the stresses, deformations, and joint openings measured at the contact between U9A and the main dam, which indicated that there was no significant transmission of load from the dam to the powerhouse.

- Massive concrete members in contact with rock. Deformations and stresses were determined by two and three-dimensional FEM analysis assuming the concrete and the rock elastically bonded together, but with different moduli of deformability.
- Equipment loads obtained from installed equipment and actual operational data were generally less than those assumed in the earlier design.
- Allowable tensile strength of concrete was increased, and the strict criterion for reinforcement required for crack control was relaxed. These revisions were justified because instrumentation data indicated generally lower tensile stresses than originally anticipated.
- Because of the more favorable hydraulic conditions in the diversion channel, the slope of the tailrace for the diversion units could be made 18° compared with 12° necessary for the river bed units. This saved 60 000 m³ of rock excavation and, at the same time, avoided excavation in the vicinity of the piers supporting the bridge across the diversion channel.

The above modifications in design criteria and concepts also resulted in a reduction of reinforcement from approximately 1 kN/m³ to 0.81 kN/m³ and a reduction in the thickness of structural walls to the extent of a saving of 56 250 m³ of concrete for the four unit blocks.

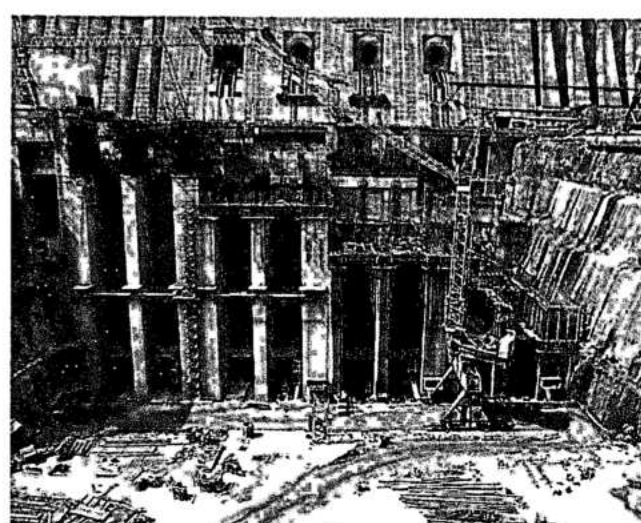
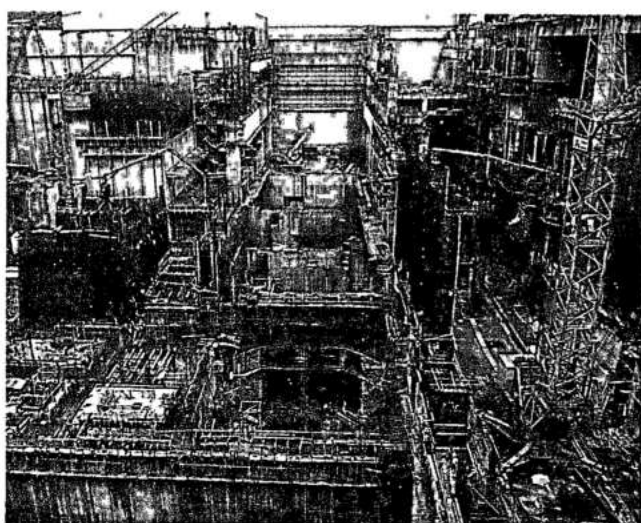
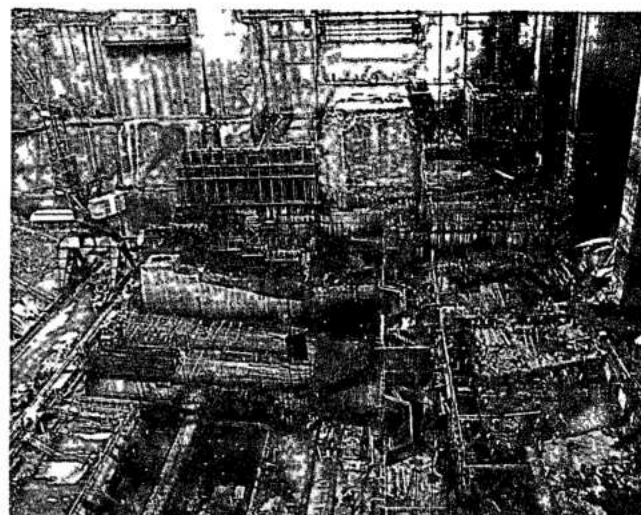
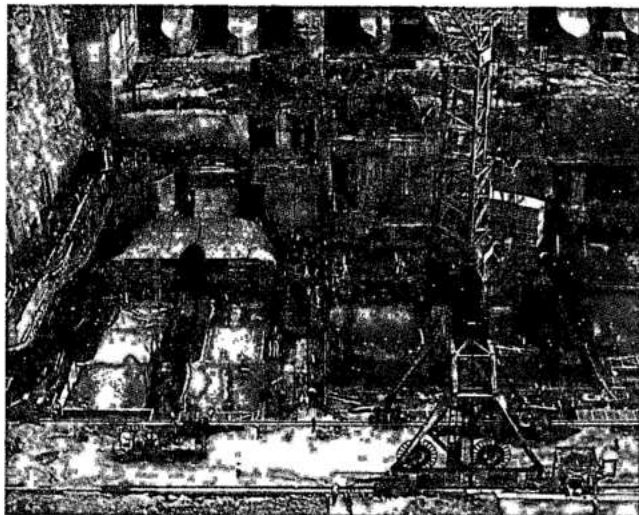
Since there was a substantial reduction in required rock excavation, and concrete volume, it accelerated the pace of construction of the unit blocks in the diversion channel as compared to those in the main river channel, while maintaining the same standards of quality and safety.

Construction

Construction of the four powerhouse blocks and related structures in the diversion channel commenced in January 1986, three years after filling of the reservoir, and was completed in 1991.

It proceeded in the following sequences:

- Excavation for powerhouse foundations at toe of the diversion control structure from the bottom of the diversion channel at El.85 to sound basalt of flow B at El.49. Excavated material was hauled to and compacted in the upper part of the cofferdam in the diversion channel, for its completion to El. 136. Total excavated material was 457 000 m³.
- Demolition of the gravity wall in the ravine between the central assembling area and the diversion channel. Blasting was carefully controlled



Construction of the powerhouse in the diversion channel

because of the close proximity of the generating units in the powerhouse in the river bed. Particle velocities resulting from blasting at the units were limited to less than 2 cm/s up to 30 Hz, achieved by having blast holes no more than 76 mm diameter. Permissible particle velocities with respect to age of concrete given in Chapter 4 for subsurface treatment were rigidly adhered to:

- Demolition of portion of the downstream piers and bridge of the diversion control structure at El. 144, for installation of penstocks.
- Placement of foundation slabs below the draft tubes and on the penstock benches.
- Construction of the draft tube walls and roof in lifts by conventional concrete placement methods up to El. 79.5.

- Construction of the structure above El. 79.5 in central and downstream monoliths mostly by slip-forming methods.

Excavation for powerhouse in the diversion channel was influenced by the existence of the access ramp to the diversion structure. The ramp was excavated in breccia of flow B from El. 85 to El. 65 and, when the diversion structure was completed it was backfilled with rollcrete. When re-excavated for the new powerhouse this breccia was found permeable and it was excavated to El. 65, together with the backfill concrete. Grouting and drainage was similar to that for the powerhouse in the river bed. The principal grout curtain was drilled from the downstream gallery at El. 61.25 to reach about El. 5.

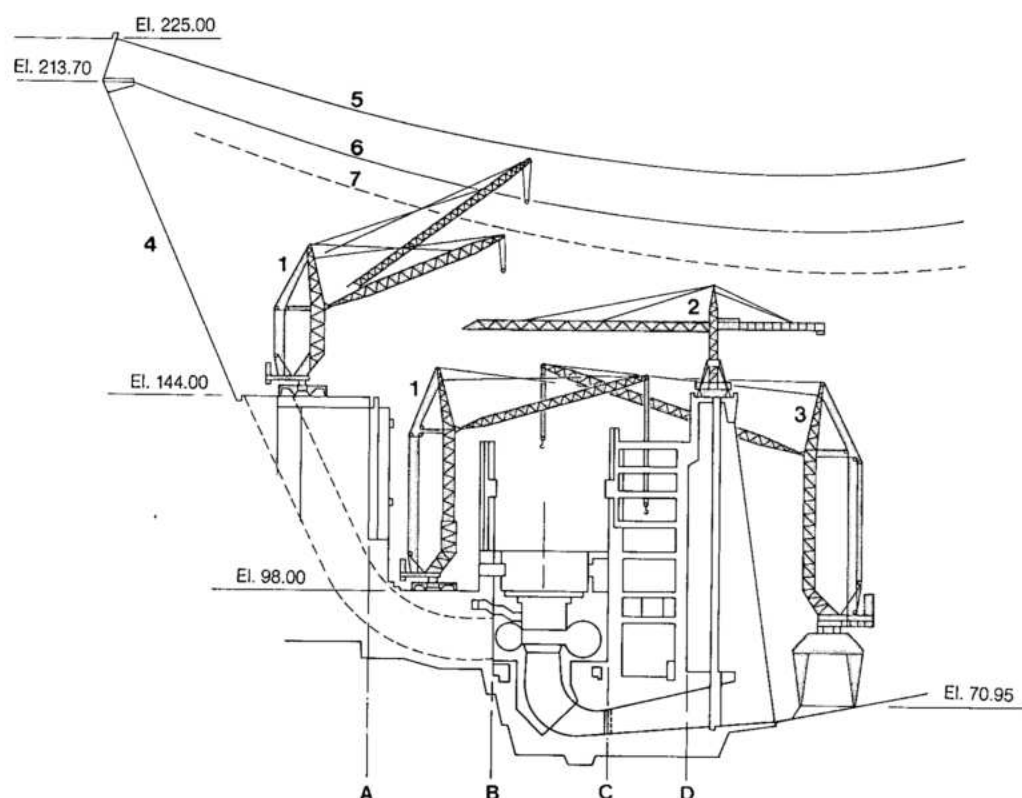


Fig. 11.16 Location of tower cranes in the powerhouse units in the diversion channel

A,B,C,D Reference lines

- 1** Tower crane Peiner
- 2** Tower crane Liebherr
- 3** Tower crane Painer heavy duty
- 4** Intake and diversion structure
- 5** Lightning conductor
- 6** Transmission line
- 7** Safe limit line

Drainage holes were drilled from the central gallery at El. 58.5, one line vertically and the second at 64° to the vertical. These holes reached discontinuity B and penetrated the rock at least 3 m inside flow B. Another grout curtain was made during construction of the powerhouse from El. 67.25 on the upstream side, reaching El. 50. Additional grout and drainage holes were made between the central assembly area block AMC 2 and AMC 3 and between unit 18A and block V1. At the concrete rock contact half round concrete pipes were arranged in a network to collect contact seepage and convey it to the drainage galleries.

The construction of the powerhouse in the diversion channel essentially followed the same general procedure as used for the powerhouse in the river bed. However, there was considerable difference in detail because of the extensive use of slip forms for structures which, in the river bed, were constructed with conventional formwork. Restricted movement of tower cranes because of their interference with transmission lines, see Fig. 11.16, was a major influencing factor in the decision to use slip forms, as was the limited time available for construction. However, there were other advantageous factors:

- Pre-assembled cages of reinforcement had to be used with considerable savings in construction time. For example, installation of reinforcement in the forms for a column required 3600 man-hours, while with pre-assembly in the yard only 2400 man-hours were required. On the other hand, pre-assembly of the large reinforcement cages required more welding and additional steel "towers" to support them. However, the time saved by slip-forming, which was made possible by the use of large pre-assembled reinforcement cages, offset such disadvantages.
- Because the slip-forms climbed on their own, support and external craneage were minimal.
- The number of construction joints was reduced.

Fig. 11.17 shows the area of first stage concrete where slip forming was used: concreting was done in sublayers of 20 cm at 4 hour intervals. The concrete was transported to the pumps by trucks. Jets of water were used to clean and cure the concrete after removal of the forms. Concrete mix frequently used codified as 38D-29, was equivalent of C-210-c, see Fig. 5.12.

Characteristics of this concrete are given in Table 11.2.

Table 11.2 Concrete characteristics

Code description			fck (N/cm ² /days)	W/C	Slump(cm)	Entrained air(%)		
38 D-29 (C210c)			2060/275	0.54	14 ± 1	4 ± 0.5		
Weight of materials in kg								
Cement	Fly-ash	Water	Air entrain- ment agent	Plastic additive	Natural sand	Artificial sand	Aggregate 1	Aggregate 2
268	31	170	Variable	Variable	509	340	720	400

Test results (Conditions: Temp.=5.9 ° C; Slump=14.4 cm; Entrained air=4.2 %)

3 days			7 days			28 days		
fck (N/cm ²)	C.V (%)	fck (N/cm ²)	fcj (N/cm ²)	C.V (%)	fck (N/cm ²)	fcj (N/cm ²)	C.V (%)	fck (N/cm ²)
883	23.2	608	1560	14.9	1256	2541	10.9	2188

W/C = water/cement ratio fcj=average concrete strength in compression after j days fck = characteristic resistance of concrete in compression
C.V.=coefficient of variation

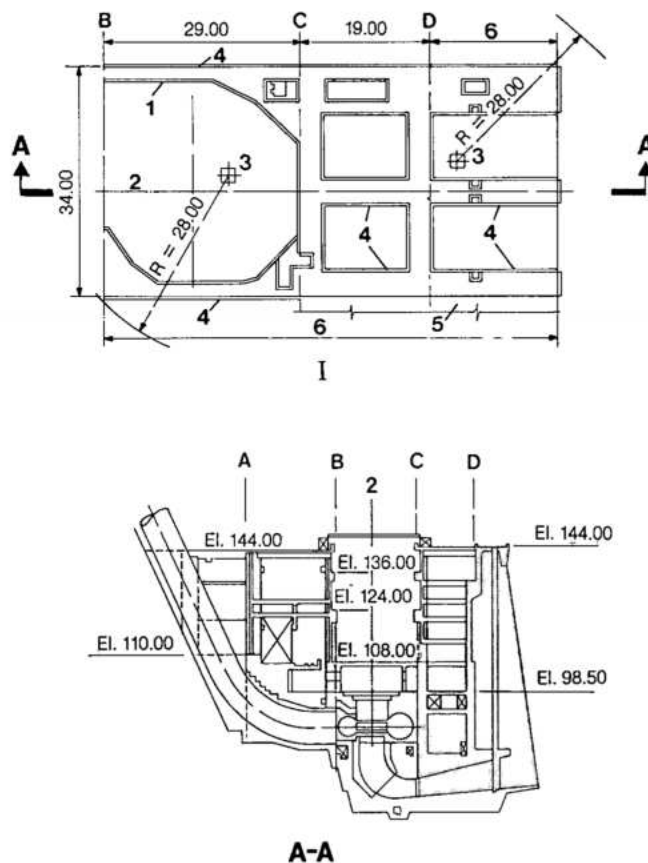


Fig. 11.17 Slip formed areas

- I Plan of unit
A, B, C, D Reference lines
1 Fixed board form
4 Slip formed area
5 Wall of adjacent unit
2 Centerline of units

OPERATION AND ADMINISTRATION BUILDING

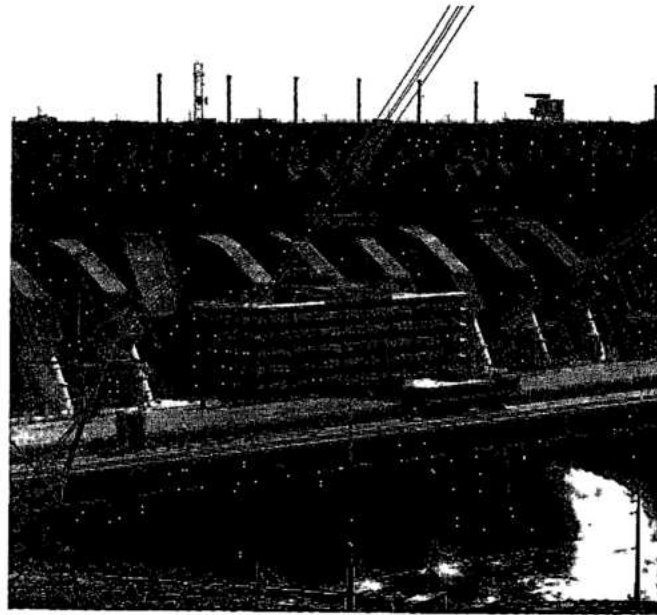
General

The operation and administration building lodges operating staff, administration offices, and visitors' reception. It is located between unit blocks U8 and U11 on the upstream side of the powerhouse, and is accessed from the upstream and downstream roads at El. 144.2. The downstream access is the main entrance and used for formal occasions,

The building was constructed in reinforced concrete and the outside faces were made from precast elements with facing in finished concrete, to match with adjacent concrete structures. A general view of the operation and administration building is shown in Fig. 11.18.

The six story building is 98.5 m by 64 m in plan and has floor arrangement as follows:

Ground floor at EL.145.2. Upstream there are two car parks on either side of a hall containing an eighty seat auditorium, elevator and stairs. The auditorium has complete facilities for lectures and discussions. The hall extends downstream across the powerhouse to the main entrance and is used for reception of visitors. In the hall is the load dispatch center and two escalators which lead to the viewing area above the central control room at El. 139.50. The hall is open at the sides to the powerhouse but comfort air conditioning is provided.



Operation and
administration building

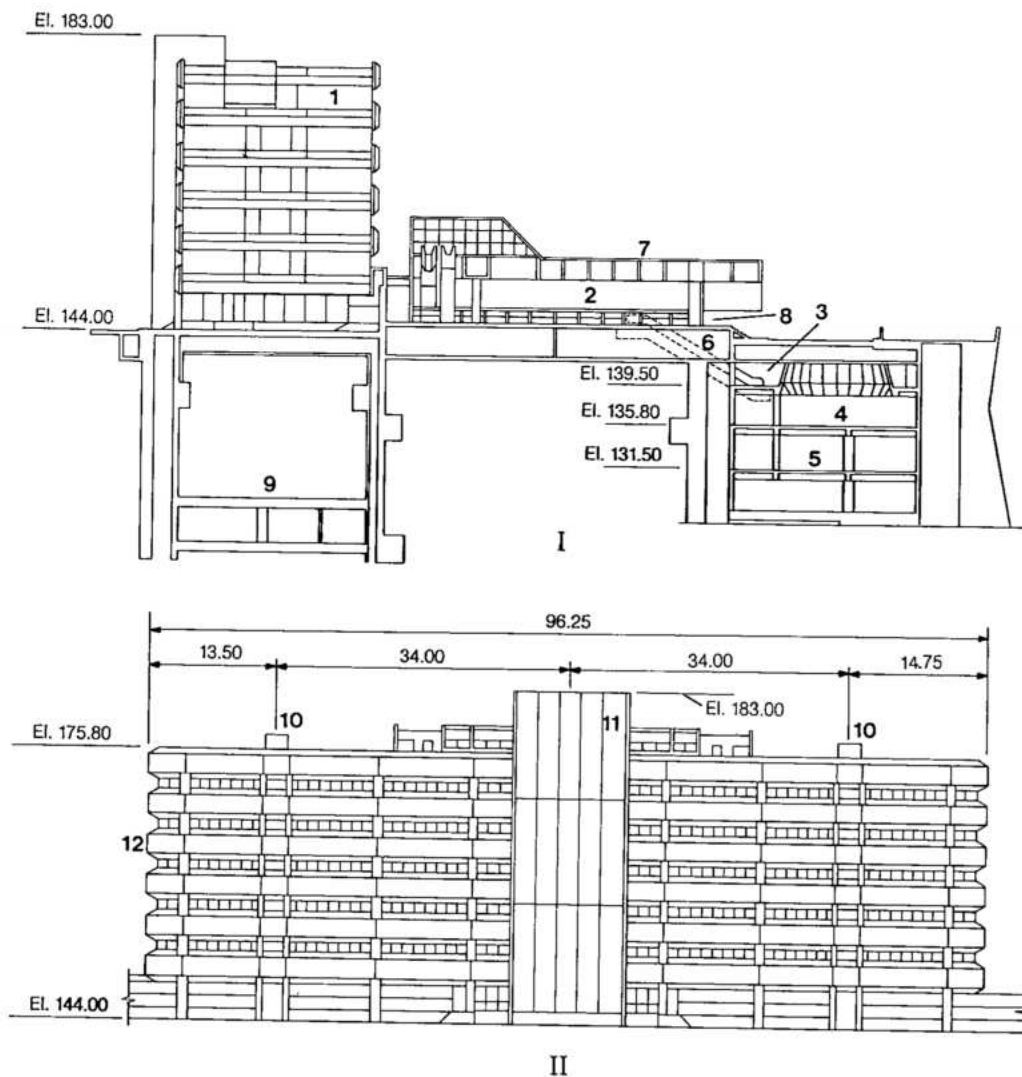


Fig. 11.18 General
view of operation and
administrative
reception and control
area

I Transversal section on line
9A of the powerhouse

II Upstream view

1 Operation and
administration building,
reception and control area

2 Main hall and visitors'
reception area

3 Viewing gallery for central
control room

4 Central control room

5 Cable spreading room,
TADMIC and control room
auxiliaries

6 Escalators

7 Terrace

8 Main entrance to visitors'
area

9 GIS (SF₆) 500 kV
switchgear gallery

10 Staircase

11 Precast vertical elements

12 Precast horizontal

Floors one to five. Office areas with central toilet facilities. These floors are air conditioned.

Upper level. Entertainment area for guests, partly open air. This level also houses the elevator machine rooms and ventilation exhaust fans. The covered areas are air conditioned.

Mezzanine floor (EL.179). Two water tanks, 22 000 l each, and access to elevator machine rooms.

Structural design criteria

The design criteria adopted were as follows:

Uniform loads

Slabs only	5000 N/m ²
Beams and columns	4000 N/m ²
During construction	5500 N/m ²
At El.144	
On projection of building	5000 N/m ²
On remaining area	10 000 N/m ²

Temperature variation

Maximum increase	
Top floors	19° C
Floors 1 to 5	6° C
Maximum drop	
Top floors	30° C
Floors 1 to 5	17° C

Wind velocities

Basic	50 m/s
Maximum	55.6 m/s

Seismic

Exceptional	0.05 g
Limiting	0.08 g

- Response of the powerhouse unit structure to internal and external loads such as thermal changes, foundation adjustment, load transfer from or to the dam, hydraulic load transmitted through the turbine spiral case and tailwater pressure. For this purpose the following were monitored by instruments: movements at transverse contraction joints and longitudinal contraction joints between the dam and the unit blocks; stress and strainmeter measurements at various locations of the structure below the generator deck; concrete temperatures in the massive portions of the structure.

Typical arrangement of instruments in a unit block is shown in Fig. 11.20 and in the powerhouse foundations in Fig. 11.19. The number of instruments installed in the powerhouse, the assembly areas and in their foundations in 1982 (more instruments were installed later) was:

Multiple extensometers	22
Piezometers	79
Direct pendulums	2
Pins for joint movement	156 pairs
Embedded jointmeters	24
Embedded thermometers	10
Rosettes of strainmeters	8
Strainmeters on reinforcement bars	8
Stressmeters	10
Discharge weirs	9

The direct pendulums were installed in U3 block downstream of main dam block F5/6 on the right abutment and in U9A downstream of main dam block F19/20 in the middle of the river channel. The pendulum in U3 measured the relative deflections of the structure between the foundations (El.61) and top deck of the powerhouse (El.142). Since block U9A was reserved for a unit to be installed in distant future, the second stage structure was not completed and the pendulum measured deflection only to El.126.

Extensometers were installed in the foundations of eight blocks. Of particular interest were the blocks located downstream of the four central blocks of the main dam, because the discontinuities under the powerhouse were not strengthened with shear keys.

FOUNDATION RESPONSE

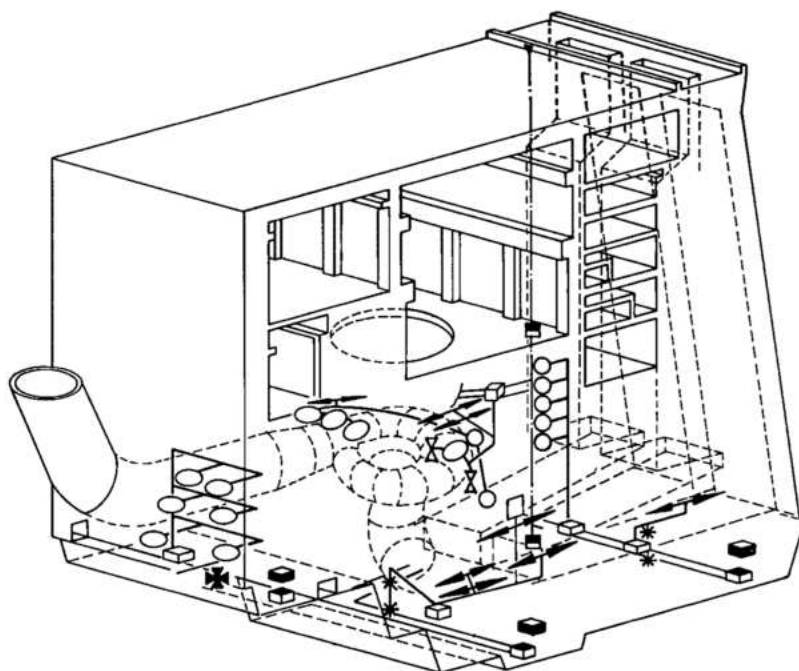
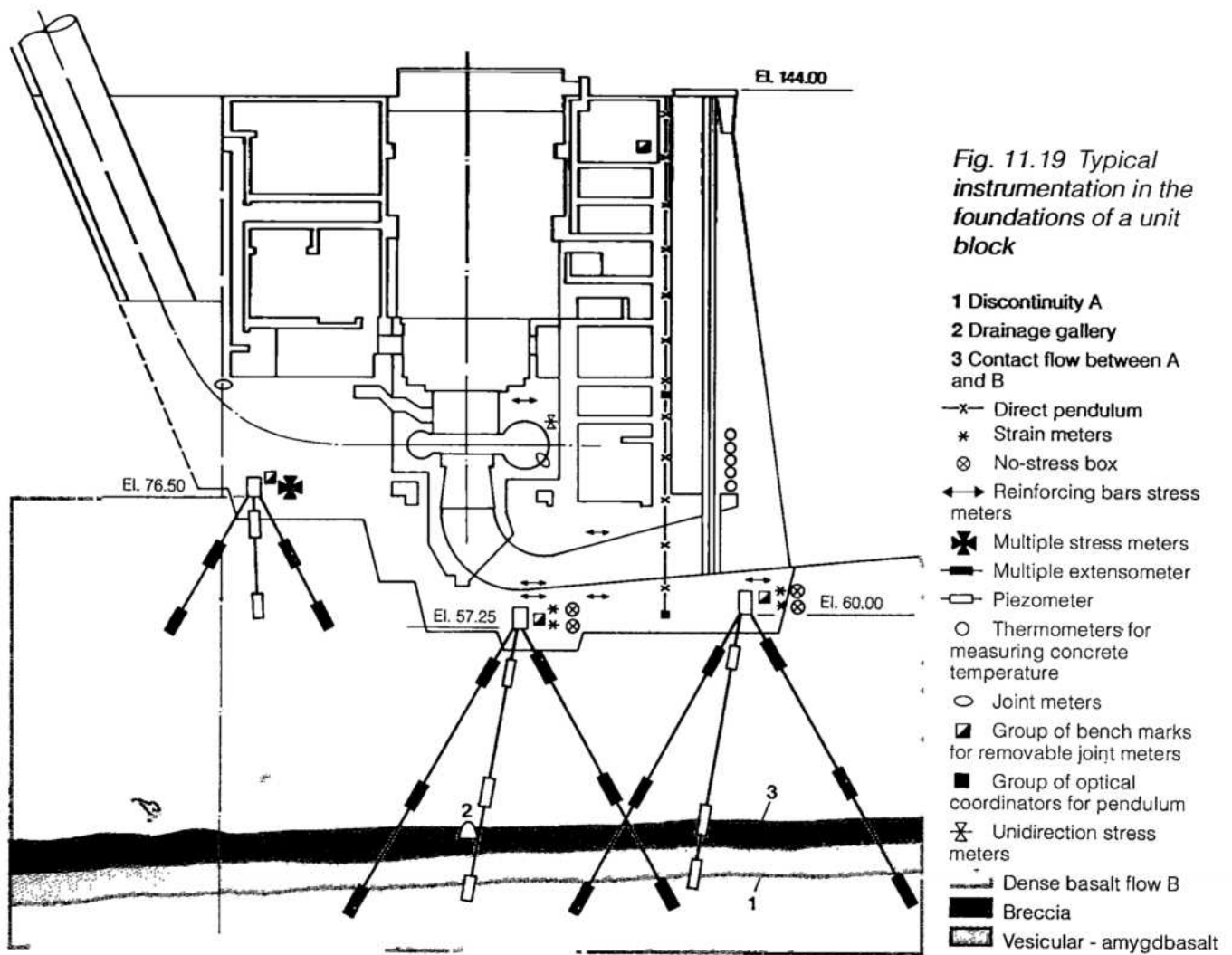
During construction and prior to filling of the reservoir and the tailrace, average settlement of the foundations of the central unit blocks was 0.7 to 2.7 mm. One month after reservoir filling and with

PERFORMANCE OF THE POWERHOUSE STRUCTURES

FUNCTIONS MONITORED AND INSTRUMENTATION

Performance of the unit block structures was analysed by monitoring the following functions:

- Response of the foundations to weight of the structure, reservoir filling and tailwater pressures. Measurements of deformations, piezometric pressures and seepage provided the necessary data, see Fig. 11.19.



tailwater pressure there was additional settlement of 1.2 to 2.5 mm. About 1 mm of the incremental settlement was due to consolidation of the weaker material in the untreated discontinuities between El.10 and El.20. Compression and consolidation of the foundation continued at a very slow rate for about 6 months after reservoir filling, adding an average of 0.15 mm to settlement.

Behavior of the foundation of four unit blocks constructed in the diversion channel in 1986-87, was similar to that discussed in Chapter 6, except that the settlements were about 30% of those for the unit blocks in the main river channel. Lateral deformation of the foundation also occurred under the unit blocks, but it did not affect the concrete structure because most of it occurred during excavation.

After one year of operation, foundations of the powerhouse blocks, including those completed with units in operation, were acting elastically. This was confirmed by fluctuations of 0.1 to 0.3 mm in foundation deformations in response to bending of the structure with changes in tailwater level.

Piezometric pressures in the foundations, particularly in such discontinuities as contact A/B and joint A responded rapidly as the tailrace was inundated for the first time. The behavior of piezometric pressure in these discontinuities of units U1, U3 and U5, recorded in May 1987, indicated variations between 8 to 10 m, when the tailwater level rose to El.120.5, from 97.2 m recorded in January 1987. Foundation uplift pressures stabilized about 6 months after first filling of the tailrace, the average values being within the limits anticipated in design. Total seepage flow from foundation and contact drains averaged 500 l/min.

Analysis of data gathered by instrumentation over a period of 8 years showed that the foundations of the powerhouse were performing satisfactorily and were providing adequate support to the structures. Consolidation and elastic response of the foundations of the central unit blocks confirm the adequacy of the untreated discontinuities which underlay about 20 m of sound rock and the 25 m thick concrete backfill and reinforced concrete slab. Efficient control of uplift pressures by drilled downstream and transverse drainage curtains, and by the perimetral drainage tunnel under the central blocks of the main dam, further contributed to stability of the powerhouse foundations.

STRUCTURAL PERFORMANCE

Deformations, deflections and behavior of joints

Deflections which were measured by pendulums, and deformations measured at the various

contraction joints were two indicators of the functioning of the unit block structure. While a typical powerhouse block was designed to act as a monolithic unit, it was constructed in three monoliths separated by vertical joints with reinforcing steel connecting them. Also concrete around the spiral case and other equipment supports was placed in a second stage. Therefore, the reception and internal distribution of loads imposed on the block, which depended upon the rigidity and flexural modulus of the various components of the structure, was analytically indeterminate.

Since various powerhouse blocks were at different stages of completion when the reservoir and the tailrace were filled, their response, as indicated by deformations and deflections, was expected to be different. Another factor affecting block deflections was the start of operation of the generating unit.

Deflections measured by direct pendulums which were installed in the downstream monoliths of blocks U3 and U9A indicated the following behavior trends over a period of 8 years of project operation:

BLOCK U3

- Six months after the first filling of the reservoir and the tailrace, the substructure at the generator deck level had deflected about 0.5 mm upstream, while at the top deck (El.142.3) the deflection was about 5 mm. With the advent of summer, for the next 8 months, the superstructure moved 8 mm downstream while the substructure deflected only about 1 mm.
- For the first 2 years of operation the cyclical movements were repeated. Correlations and mathematical analysis confirmed that the changes in ambient temperatures and tailwater level were the principal causes of this behavior, which was normal. Since the foundation of the main dam block upstream of U3 is at El.100, the substructure did not receive any load from the dam.
- From the middle of 1985 when unit 3 was put in operation, there was a distinct downstream movement of the structure and for the following 2 years the net movements were all towards downstream, 0 to 1.5 mm at generator deck and 0 to 6 mm at the top deck of the superstructure.
- The block had also tilted axially toward the left, about 1 and 1.5 mm at the generator and top deck levels, respectively. This deflection remained essentially unchanged during 8 years.
- Since the pendulum was located in the downstream monolith, its measurements could not be used to estimate deflection of the core block. Because there was no evidence of an uneven pressure distribution in the guide bearings, it was concluded that the

deflections of the core block had been insignificant and verticality of the shaft of the power generating unit had not been affected.

BLOCK U9A

- In the incomplete block, where neither a unit had been installed nor second stage concrete placed in the substructure, the deflections at the deck level ranged between 1 and 2 mm in the upstream direction, with a cyclical pattern conforming to seasonal temperatures.
- At a higher level, El.126.4, the upstream deflections ranged from 2 to 5 mm.
- In the axial direction there was no measurable deflection of the substructure but at El.126.4 there was a steady tilt of about 0.8 mm to the right.
- Since no deflection in the downstream direction occurred, it appears that there was little or no load transferred from the dam, whose foundation is at about the same elevation as block U9A.

Opening and closing and the relative lateral movement of the transverse contraction joints were monitored to study the interaction between adjoining blocks. While the powerhouse unit blocks were designed to act independently of each other, vertical shear keys formed in the contraction joints in the right assembly area between El.98 and El.141 provided some linkage between them. No relative movement in the transverse plane, either horizontal or vertical, was observed between any adjoining unit blocks, indicating that there may be some structural continuity between the blocks. On the other hand, maximum joint opening and closing ranged 0.3 to 0.5 mm in a cyclical pattern corresponding to the seasonal ambient temperatures, which indicated little load transfer between the blocks.

Comparing the structural characteristics, stages of construction and deflection records of monitored blocks U3 and U9A, it was concluded that the hydraulic load transmitted through the turbine spiral case was distributed through and resisted by the entire substructure, and that it offset the effects of tailwater pressure and deflected the structure downstream.

Stresses in the structures

Because of richer mixes and higher cement content, concrete in the powerhouse structures attained a maximum temperature of 50°C to 55°C. In most locations in the structures the concrete cooled to the average ambient temperature in 6 months. Such rapid cooling introduced tensile stresses of the order of 50 to 100 N/cm²; because steel reinforcement was provided, in general there was no structural cracking.

Within a few days after filling of the reservoir and the tailrace, stresses measured by strainmeters and stressmeters in block U3 and U9A had become

compressive. Stresses in block U3, in which the unit had been in operation since mid-1985, were continuously measured by instruments embedded at five locations. Except for lack of structural contact with the dam because of its higher foundation, this block was considered typical for evaluating the stress distribution in the powerhouse structures. Analysis of the extensive data showed the following:

- Stresses in concrete at all locations had remained stable for 3 years of operation when both the reservoir and tailwater levels were nearly constant. Only the axial horizontal stress (σ_5) in the more massive concrete upstream of the draft tube elbow fluctuated 50 to 100 N/cm² with seasonal temperature changes.
- Stresses in all planes were compressive, with following values (N/cm²):

Upstream of unit near foundation

Principal stresses in transverse plane	200 – 300
Axial horizontal stresses	50 – 150

Draft tube base slab, downstream

Principal stresses in transverse plane	50 – 300
--	----------

Draft tube wall and pier, downstream

Principal stresses in transverse plane	350 – 400
--	-----------

- The actual stresses in various parts of the massive, as well as structural concrete were well within the design limits. This was also confirmed by the modest deformations observed in the structure.

Two stressmeters were installed in the concrete surrounding the spiral case of unit 3. With the unit operating, the stresses in concrete were only 20 to 60 N/cm², compression, with cyclical variation reflecting ambient temperature changes. These stresses were about the same as calculated by Finite Element Analysis. Two jointmeters installed around the same spiral case showed that the gap between steel and concrete was completely closed when the unit was in operation. This confirmed that the spiral case steel was sustaining most of the internal hydraulic pressure and only a very small amount was transferred to the encasing concrete, as anticipated in design.

Eleven strainmeters were installed in reinforcement bars in four unit blocks at locations around the draft tube and in second stage concrete around spiral cases. Due to the method of embedment of the spiral case, see Chapter 12, tensions measured over a period of 6 years were very low, the maximum being only 30 N/cm².

Incidences of cracking in concrete

No structural cracks had occurred in the powerhouse structures after completion and during 8 years of project operation. However, there were four incidences of cracking during construction, as follows:

- Second stage concrete around spiral case, blocks U9 and U13. Concrete around the spiral case and for the shaft pit above it was pumped and slipformed at a rate of 0.12 m/h. Radial cracks, 1 to 5 mm open at the surface and about 0.4 m deep, were discovered at top of the lift at El.95. These cracks were attributed to a combination of factors related to slipforming technique, the high slump and cement content and rapid cooling. They were controlled by using a net of steel reinforcement at top of the lift, before resuming concrete placement. Since this was an area of low stress, cracks were of no structural significance.
- Downstream lateral wall above draft tube; blocks U16 and U17. Vertical and subhorizontal cracks were observed in the lateral (axial) walls above the

draft tube, after about 3 m had been slipformed. Seen from the downstream face and top of the lift, the vertical cracks were 1 to 3 m long, about 1 mm open at the surface and about 0.1 m deep. The subhorizontal cracks were minor and similar to construction joints. The vertical cracks were caused by rapid cooling and were controlled by additional reinforcement placed on top of the lift. Since the wall of the anti-flooding gallery where the cracks occurred is 2 m thick and the cracks did not extend through it, no additional treatment was considered necessary.

Summary

Overall structural performance of the powerhouse unit blocks and other structures was as anticipated in design, and within the desired margins of safety and durability. The absence of structural vibrations in blocks where the units were operating and the efficient control of seepage through and uplift pressures in the foundations were also indicative of a long, safe and low maintenance operating life for the powerhouse structures.

POWERHOUSE GENERATION

EQUIPMENT

TURBINE / GENERATOR UNIT	12.3
General Arrangement of the Turbine Generator Unit	12.3
Specifications and Contracts	12.5
Shaft Stability	12.5
TURBINES	12.12
Basic Characteristics	12.12
Model Tests	12.18
Component Design and Manufacture	12.24
Erection Testing and Commissioning	12.38
Operating Experience	12.46
TURBINE GOVERNORS	12.48
General Considerations and Basic Characteristics	12.48
Component Design	12.51
GENERATORS	12.55
Basic Characteristics	12.55
Component Design and Manufacture	12.59
Erection	12.81
Commissioning and Testing	12.88
Operating Experience	12.91
GENERATOR EXCITATION SYSTEM	12.92
General Requirements	12.92
Configuration	12.93
GENERATOR TERMINAL EQUIPMENT	12.96
Isolated Phase Bus	12.97
Generator Neutral and Terminal Cubicles	12.99
GENERATOR STEP-UP TRANSFORMERS	12.100
Basic Characteristics	12.100
Component Design and Manufacture	12.101
Installation, Testing and Commissioning	12.102
Operating Experience	12.102

500 kV SWITCHGEAR (SF₆ – GIS)	12.103
Basic Characteristics	12.103
Arrangement	12.104
Component Design and Manufacture	12.105
Testing and Commissioning	12.109
Operating Experience	12.110
 ORGANIZATION OF CONTRACTS FOR PERMANENT EQUIPMENT	 12.111
 QUALITY CONTROL OF MANUFACTURE	 12.112
Manufacturer's Quality Control Organization	12.112
Quality Control Documentation	12.113

POWERHOUSE GENERATION

EQUIPMENT

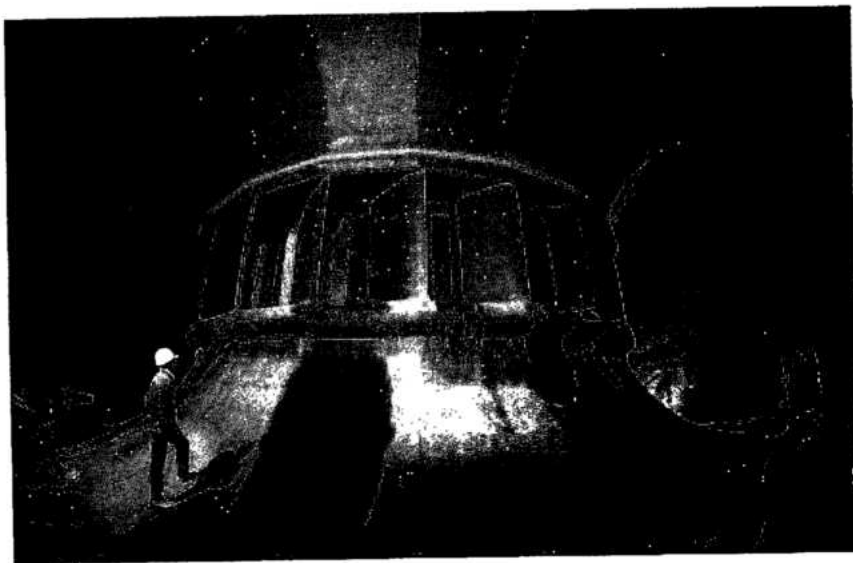
TURBINE / GENERATOR UNIT

GENERAL ARRANGEMENT OF THE TURBINE GENERATOR UNIT

The arrangement of the turbine/generator unit was re-evaluated after the feasibility study, in the light of the changes to powerhouse layout described in Chapter 11.

Alternative arrangements with two and three guide bearings were re-examined, together with those having the thrust bearing mounted on a lower generator bracket or on the head cover using a support cone.

At the feasibility stage a unit with head cover mounted thrust bearing and two guide bearings was recommended; however, a three guide bearing arrangement with the thrust bearing mounted on the lower bracket was finally adopted. Three guide bearings give a margin of safety against shaft vibrations under fault and runaway conditions. The alternative of a thrust bearing on a lower generator bracket offered better access to the turbine pit and facilitated general maintenance. The major advantage of the head cover mounted design (to reduce the length of the shaft) could not be exploited because of civil considerations. In addition, it was considered that the arrangement with a bottom bracket would give a



*Inside the spiral case of
the Itaipu turbines*

more natural break in contractor design and supply responsibility, should, for commercial or technical reasons, the generator and turbine be supplied by separate manufacturers rather than those of a consortium.

It was recognized that the decision to use a lower bracket would mean a more massive head cover to limit deflections and inclination at the wicket gates and turbine bearing; however this was accepted in the light of the above considerations.

The final general arrangement of the turbine generator units is shown in Fig. 12.1.

Turbine

The spiral case (with the stay ring), draft tube liner, pit liner and lower reducing bend are embedded in concrete, with the center line of the stay ring at El. 87.5.

The direction of rotation of the unit when viewed from above is clockwise.

Practically all parts of the turbine are contained within the confines of the turbine pit, the only items outside being:

- Governor pumping set and governor pressure tanks alongside the generator enclosure at El. 98.5.

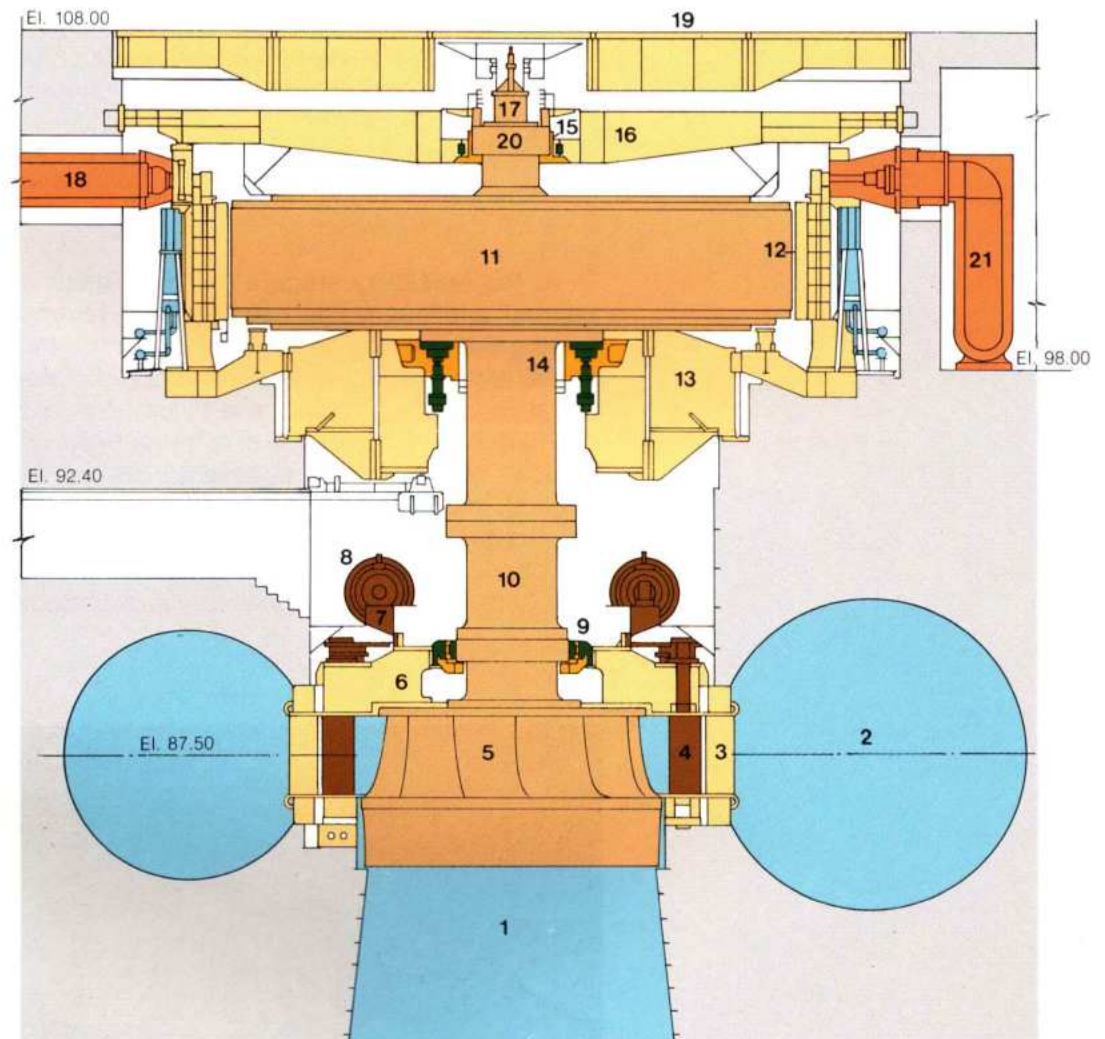


Fig. 12.1 Sectional view of turbine generator unit

- | | | | |
|--------------------|--------------------------|--------------------------------------|--|
| 1 Draft tube liner | 7 Operating ring | 13 Bottom bracket | 18 Isolated phase bus bar (line side) |
| 2 Spiral case | 8 Wicket gate servomotor | 14 Combined thrust and guide bearing | 19 Generator top cover |
| 3 Stay vane | 9 Lower guide bearing | 15 Upper guide bearing | 20 Upper guide bearing collar |
| 4 Wicket gate | 10 Turbine shaft | 16 Upper bracket | 21 Isolated phase bus bar (neutral side) |
| 5 Runner | 11 Generator rotor | 17 Air admission valve | |
| 6 Head cover | 12 Generator stator | | |

- Governor compressors and part load compressors for the 50 Hz low load units, in a separate compressor room at El.98.5.
- Governor control panel in the local control room at El.108.
- Turbine electrical control cabinets and instrument cabinet in the downstream access way at El.92.4.

Generator

The main parts of the generator including the stator, rotor and support brackets are contained in a concrete enclosure approximately 22 m in diameter and 10 m deep. The generator top cover is an integral part of the operating floor at El. 108, and the bottom cover is attached to the underside of the lower bracket at El. 95.3.

Ancillary equipment located outside the generator enclosure are:

- High pressure oil lift pumps for the thrust bearing.
- Unit auxiliary service transformers.
- Motor control centers.
- Generator neutral cubicle, downstream of the generator enclosure El.98.5.
- Excitation transformers and cubicles, in a gallery upstream of the generator at El.98.5.
- Dionized water cooling system for stator bars, in a gallery downstream of the generator at El.98.5.

Erection and disassembly of the unit is done mostly from above through the top of the generator enclosure at El.108, using the main powerhouse cranes. However, smaller turbine components can be transported in and out of the turbine pit by means of a 100 kN circular monorail mounted beneath the generator lower bracket, connecting with an extension rail into the downstream access way at El.92.4.

SPECIFICATIONS AND CONTRACTS

Resulting from the feasibility and subsequent studies the final specifications were issued for international bidding in February 1977. Included in the bid package with the turbines and generators were the bus-ducts, local control boards and motor control centers. Before it was issued, the specifications were reviewed by a number of eminent consultants, and opinions were also sought from leading manufacturers of hydroelectric equipment.

Bids for the specifications were received from the following four consortia:

- Consortium General Electric (GE), comprising: General Electric do Brasil, Canadian General Electric and Dominion Engineering Works.

- Consórcio Itaipu Electromecânico (CIEM), comprising: Brown Boveri, Alsthom Atlantique, BSI, Bardella, Creusot Loire, Consórcio Ingeniería Electromecánica, Voith, Mecânica Pesada, Neyrpic and Siemens.

- Japan Consortium for Itaipu (JCI), comprising: Ishikawajima, Toshiba, Hitachi and Mitsubishi.

- Consortium Paraná, comprising Westinghouse, Allis-Chalmers, Consórcio Ingeniería Electromecánica and Coemsa Construções Eletromecânicas S.A.

After an extensive review of the bids by ITAIPU Binacional, IECO-ELC and a panel of consultants, the contract was awarded to the CIEM consortium in October 1978.

The contract encompassed the design, manufacture and supervision of erection and commissioning of the equipment. Transport from factory to site was arranged by ITAIPU and erection was done by the Consortium Itamon under the direction of ITAIPU.

SHAFT STABILITY

General

For the reasons stated previously, the Itaipu turbine/generator unit has three guide bearings and a lower thrust bearing mounted on a separate thrust bracket.

The turbine and generator manufacturers were held jointly responsible for the determination of bearing flexibility and shaft stability. At the tender stage, the guaranteed value for turbine bearing flexibility was 1 $\mu\text{m/kN}$, including head cover and concrete flexibility; however this was decreased to 0.7 $\mu\text{m/kN}$ after the bearing/head cover assembly was analyzed in detail.

The shaft line calculations were therefore made with the following bearing flexibility values:

- Turbine bearing: 0.7 $\mu\text{m/kN}$
- Intermediate bearing: 0.8 $\mu\text{m/kN}$
- Generator upper bearing: 1.2 $\mu\text{m/kN}$

Specification requirements

The specifications required the following in respect of shaft stability:

- The critical speed of the forward whirl of the first order to be a safe margin above the maximum runaway speed.
- The critical speed of the counter whirl of the first order to be a safe margin above the maximum speed at load rejection.

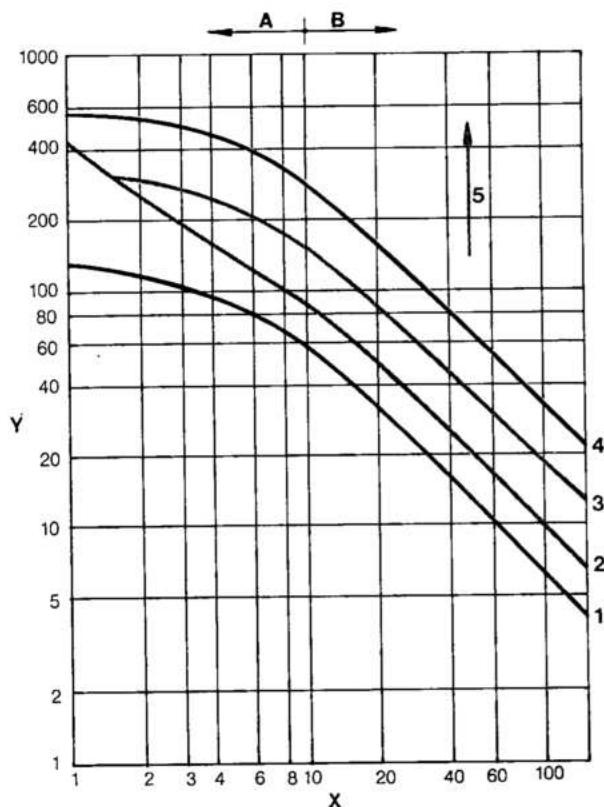


Fig. 12.2 Vibration frequency

Y Vibrational amplitude peak to peak (μm)

X Vibration frequency (Hz)

A Based upon USSR standards

B Based upon ISO 3945

1 Good

2 Very acceptable

3 Acceptable

4 Satisfactory

5 Unsatisfactory

- The point of resonance of the fundamental torsional with the fundamental whirling speed to be a safe margin above the maximum runaway speed.
- There was to be no danger of combination resonance between natural bending frequencies in the range normal speed to maximum speed resulting from a load rejection.
- The vibration amplitudes not to exceed those given in Fig. 12.2 coupled with Table 12.1.
- There was to be no possibility of the turbine stationary and rotating wearing rings touching under any possible condition, including runaway.

Mathematical model and input data

The mathematical models for the calculation of bending, torsional and axial frequencies are shown in Figs. 12.3, 12.4 and 12.5.

In these models the bearings and their supports were considered as single springs, the constants of which were a sum of the flexibilities of the individual components of the bearing as shown in Fig. 12.6 and Fig. 12.7. Oil film stiffness was established in the manner shown in Fig. 12.8. Magnetic pull in terms of magnetic stiffness was included.

Using the mathematical models, the calculations were made with a computerized transfer matrix program for computation of both natural frequencies and forced vibrations. For the forced vibration calculations the cases in Table 12.2 (see pag. 12.12) were considered together with the appropriate sources of excitation. Group 1 cases were used for basic design and to show complicity with the normal specification requirements, Group 2 to show complicity with extreme specification requirements and Group 3 for limit case (no damage) complicity.

Table 12.1 Limits for vibrational displacements

	Guide bearings		Other parts of the turbines
	Vibrations between shaft and guide bearing pad	Vibrations between guide bearing pad and concrete	
Outputs greater than 75% of rated output	Curve 2	Curve 4	Curve 4
Outputs 0 to 30% and 60% to 75% of rated output	Curve 4	Curve 4	Curve 4
See Fig. 12.2 for curves 2 and 4			

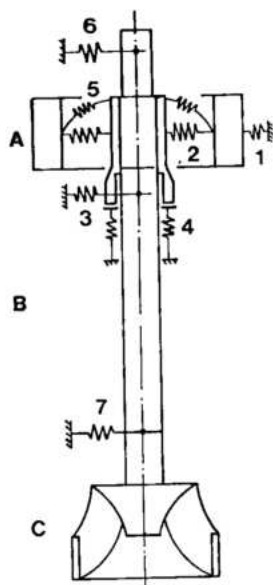


Fig. 12.3 Model for calculation of bending natural frequency

- A Generator rotor
B Shaft
C Turbine runner
- 1 Lateral magnetic stiffness
2 Lateral stiffness of generator-rotor spider
3 Lateral stiffness of generator lower guide bearing
4 Axial stiffness of thrust bearing
5 Bending/torsional stiffness of generator-rotor spider
6 Lateral stiffness of generator upper guide bearing
7 Lateral stiffness of turbine guide bearing

Exciting forces were as follows:

- Unbalance forces in accordance with ISO 1940 (the factor G representing the balance quality grade):

Generator G 6.3 at rated speed 90.9 rpm.

Turbine G16 at runaway speed 170 rpm.

Hydraulic forces as obtained from model test and experience as shown in Fig. 12.9.

- Magnetic forces due to rotor short circuit, rotating at rotor speed:

4.5 MN for case 7 of Table 12.2,

16.81 MN for cases 8 and 9 and data of Fig. 12.10 for time speed dependency in the case of speed rise.

Results of the analysis of natural frequencies (critical speeds)

Natural Bending frequencies. Because of the large rotational inertias of the machine, especially of the generator rotor, the natural bending frequencies depend considerably on the running speed.

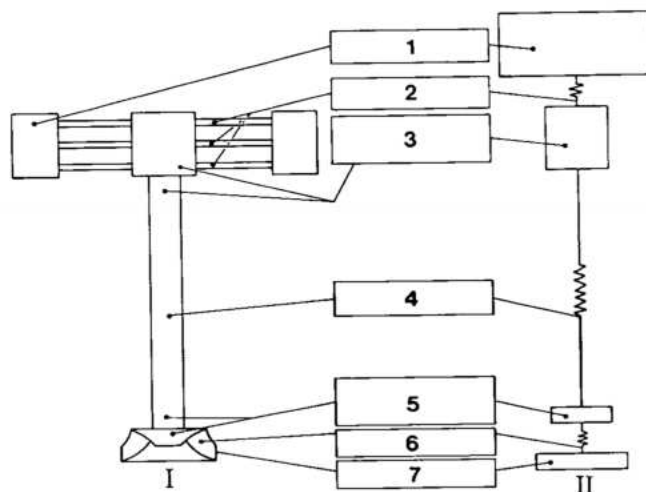


Fig. 12.4 Torsional vibrations, model for calculation

- I Real system
II Model for calculation
- 1 External rotating mass of generator rotor
2 Torsional flexibility of generator-rotor spider
3 Internal rotating mass of generator runner including shaft
4 Torsional flexibility of shaft
5 Internal rotating mass of turbine runner including shaft
6 Torsional flexibility of turbine runner
7 External rotating mass of turbine runner

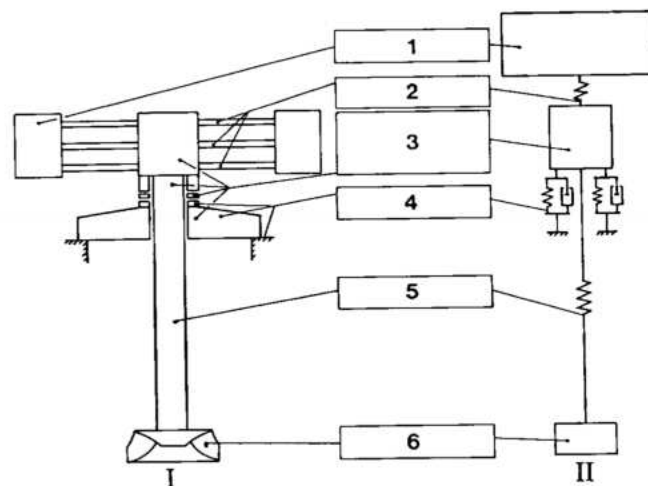


Fig. 12.5 Axial vibrations, model for calculation

- I Real system
II Model for calculation
- 1 External mass of generator rotor
2 Flexibility of generator-rotor spider
3 Internal mass of generator rotor including portions of shaft, bearing and bracket
4 Flexibility of bearing, bracket and concrete
5 Flexibility of shaft
6 Mass of turbine runner including shaft portion

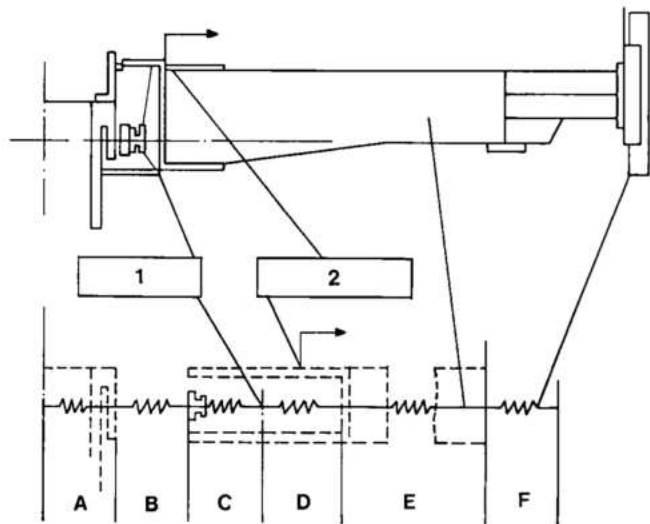


Fig. 12.6 Effective flexibilities of bearing

- A** Shaft
B Oil film
C Pads and supports of bearing
D Residual parts of bearing
E Bracket and bearing housing
F Foundation
1 Pickup for shaft vibration
2 Pickup for vibration of bearing body

Part of construction	A	B	C	D	E	F	Total
Flexibility of part in $\mu\text{m/kN}$	0.2	0.15	0.3	0.15	0.34	0.06	1.2
Effective flexibility for vibration measurement in $\mu\text{m/kN}$		Shaft vibration			Vibration of bearing body		
		0.45			0.40		

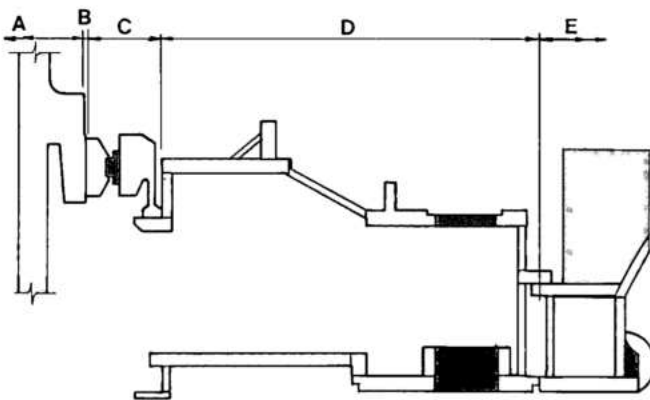


Fig. 12.7 Turbine bearing flexibilities

	$\mu\text{m/kN}$
A Turbine shaft	0.08
B Oil film	0.15
C Bearing ring	0.07
D Head cover plus connection	0.18
E Spiral case embedded in concrete	0.22

Fig. 12.11 shows this influence; both first forward whirl and counter whirl natural frequencies are represented as functions of speed, with and without magnetic pull and with the residual magnetic pull at undisturbed rapid de-excitation.

Torsional and axial. The calculated torsional and axial fundamental natural frequencies exhibited a considerable safety margin, being respectively 4.06 and 3.07 times runaway speed.

Combination frequencies. In gyroscopic systems with non linear elements, combination resonances may occur if the speed of the unit is coincident with the sum or difference of two natural bending frequencies, or the sum of a natural bending frequency and a natural torsional frequency and any harmonic thereof.

The results for the calculation of the combination bending frequencies are given in Fig. 12.12. As is evident, the combination bending frequencies are

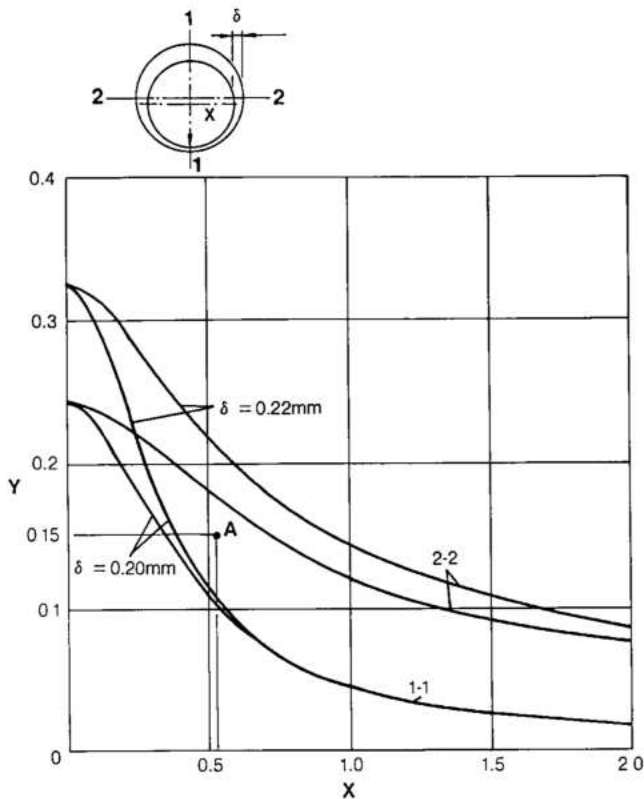


Fig. 12.8 Oil film flexibility

Y Oil film flexibility ($\mu\text{m/kN}$)

X Load (MW)

A Resultant flexibility of oil film for calculation

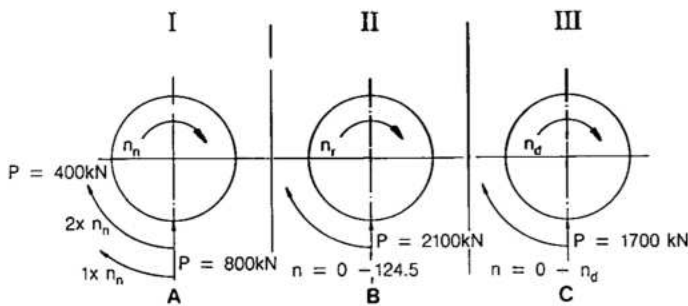


Fig. 12.9 Radial hydraulic forces acting in the mean plan of distributor

I Normal operation

II Load rejection transient

III Runaway condition

A Rotating with $1 \times n_n$ relative to shaft

B Spacefixed or rotating with runner speed

C Spacefixed or rotating with runner speed

n_n Rated speed (90.9 rpm)

n_r Load rejection speed (124.5 rpm)

n_d Runaway speed (170 rpm)

coincident with the possible shaft speeds only at high orders, which is of no consequence in practice. Likewise there was no danger of resonance resulting from combined bending and torsional frequencies, as the worst combination gave a minimum of 2.3 times runaway speed.

Results of the analysis of forced bending vibrations

Here only the results of cases 1 and 3 are presented, as these governed the design, it being proved that the forces resulting from the other cases could be accommodated without damage.

Fig. 12.13 shows the maximum absolute shaft deflections as calculated for both cases.

A direct comparison between the guaranteed and the calculated values of the absolute shaft deflections shown in Fig. 12.13, is not possible for bearings, since the guaranteed values are relative, as shown in Table 12.1. However they do have meaning for the calculations of wearing ring clearances. The corresponding calculated relative values for the deflections are compared with the specified guaranteed values in Fig. 12.14, together with the calculated values of the absolute shaft deflection and the contributions of the individual exciting components.

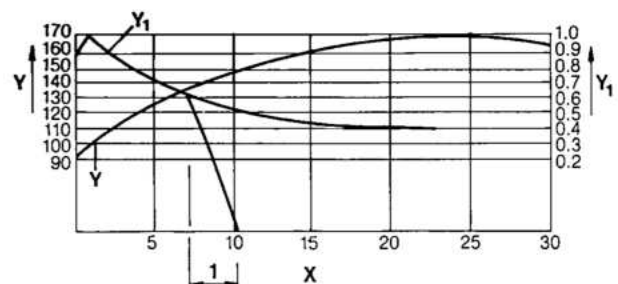


Fig. 12.10 Magnetic pull in case of speed rise up to runaway speed after load rejection

Y Speed (rpm)

Y_1 $C_e/C_{e_{max}}$

X Time (s)

1 Rapid excitation

$C_{e_{max}}$ 600 kN/mm

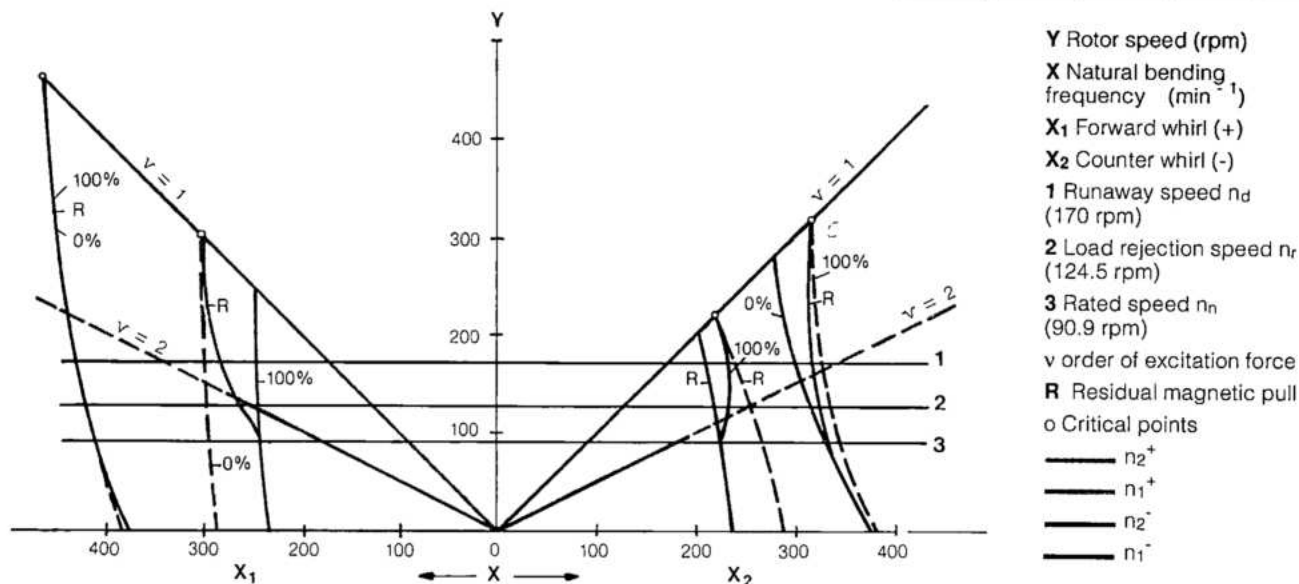


Fig. 12.11 Natural bending frequencies as function of rotor speed and magnetic pull

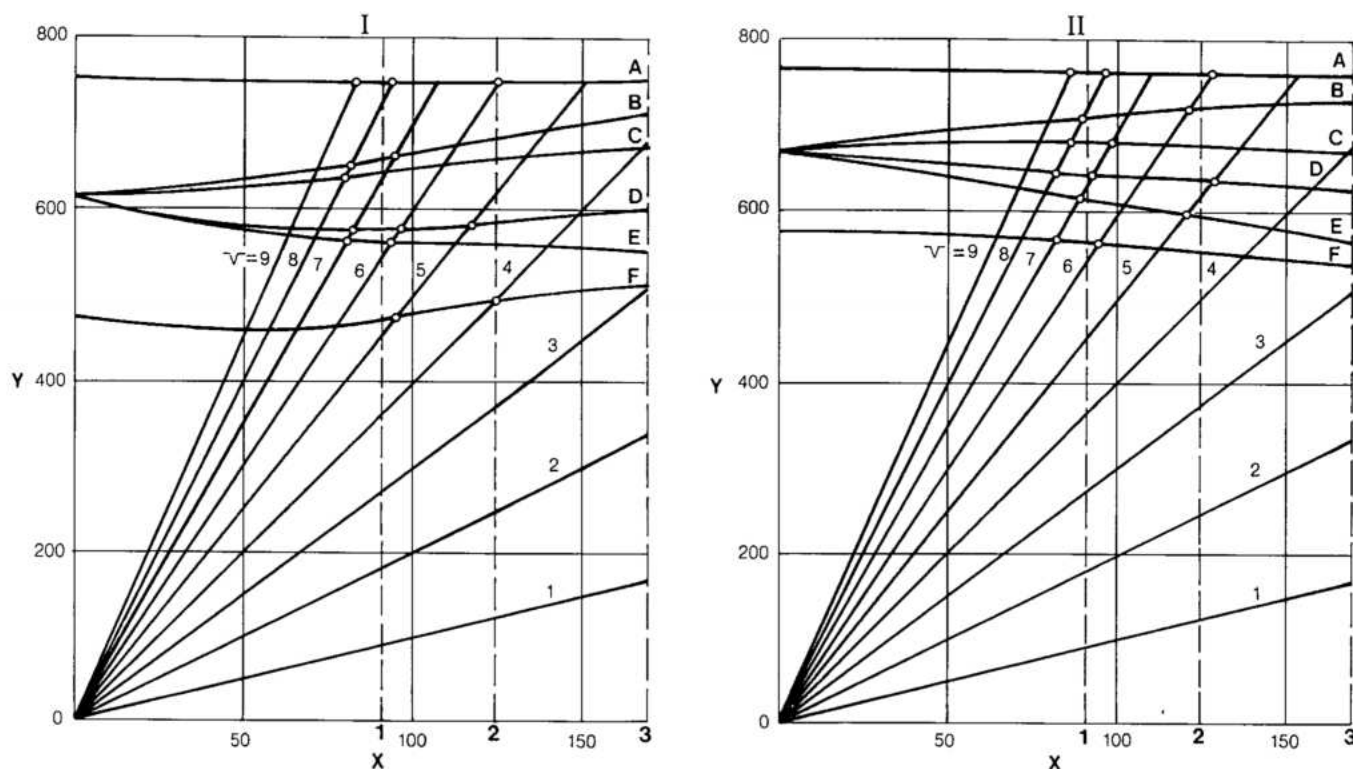


Fig. 12.12 Combined natural bending frequencies

I Magnetic pull = residual magnetic pull for overvoltage control and faulty de-excitation

II Magnetic pull = 0

Y Natural bending frequency (min^{-1})

X Shaft speed (rpm)

v Order of excitation force

A $\Sigma 2^+, 2^-$
B $\Sigma 2^+, 1^+$
C $\Sigma 2^+, 1^-$
D $\Sigma 2^-, 1^+$
E $\Sigma 2^+, 1^-$
F $\Sigma 1^+, 1^-$

1 Rated speed $n_n = 90.9$ rpm

2 Load rejection speed $n_r = 124.5$ rpm

3 Runaway speed $n_d = 170$ rpm

2⁺ 2nd harmonic forward whirl

1⁻ 1st harmonic counter whirl

2⁻ 2nd harmonic counter whirl

1⁺ 1st harmonic forward whirl

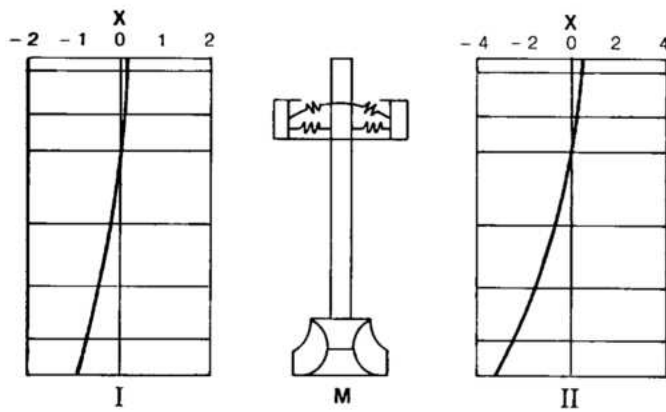


Fig. 12.13 Maximum lateral shaft deflection

- I** Normal operation ($n_n = 90.9$ rpm, CM = 100 %)
II Runaway condition ($n_d = 170$ rpm, CM = 0%)
M Model for calculation
X Deflection (mm)

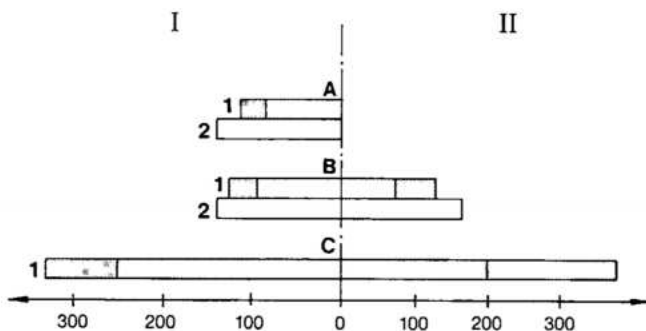


Fig. 12.14 Calculated and acceptable vibration

- I** Normal operation
II Runaway speed
1 Calculated
2 Acceptable
A Bearing housing-absolute
B Shaft-relative
C Shaft absolute
 [Pattern] due to unbalanced hydraulic forces

The importance of the hydraulic forces on the turbine runner is very evident, not only for the turbine supports, but also for the generator supports. In order to absorb the resulting forces, a direct support of the upper generator bearing to the structure was necessary, although not intended originally.

Because of the strong influence of the hydraulic forces which contained a large safety margin, along with the large safety margin used in the computation of the dynamic radial stiffness of the system, the calculated vibrational amplitudes at the turbine guide bearing were outside those permitted by the specifications. In order to show compliance CIEM conducted a more detailed practical analysis using actual results from operating turbines, resulting in the curve in Fig. 12.15, which was confirmed by measurements made at site during commissioning.

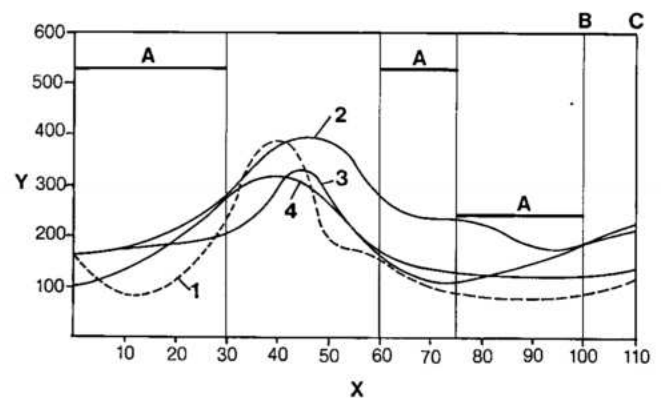


Fig. 12.15 Vibration amplitudes (peak-to-peak) of shaft vibrations

Itaipu

Effective head = 118.4 m
 Speed = 90.9 rpm
 Rated output = 740 000 kW

Paulo Afonso IV

Effective head = 115 m
 Speed = 120 rpm
 Rated output = 417 000 kW

Cabora Bassa

Effective head = 118.5 m
 Speed = 107 rpm
 Rated output = 415 000 kW

- Y** Shaft runout peak-to-peak (μm)
X Output (%)
1 Itaipu measured
2 Itaipu expected
3 Cabora Bassa
4 Paulo Afonso IV
A Guarantee limits
B Rated load
C Overload

Table 12.2 Possible cases of operation and coherent excitation forces

Group no.	Case of excitation		Condition of system			
	Case no.	Frequency	Operating condition	Governor defect		
				Turbine	Voltage	Rapid de-excitation
1	1	Permanent	Normal operation			
	2	Often	Full load rejection			
	3	Seldom	Fault case+ full load rejection	x		
2	4	Very seldom	Fault case+ full load rejection	x		x
	5	Very seldom	Fault case+ full load rejection		x	
	6	Very improbable	Fault case+ full load rejection	x	x	x
3	7	Very improbable	Fault case + double short circuit of rotor			
	8	Extremely improbable	Fault case + double short circuit of rotor+ full load rejection		x	x
	9	Extremely improbable	Double short circuit of rotor+ full load rejection		x	x

TURBINES

BASIC CHARACTERISTICS

The turbine characteristics resulting from the feasibility study as listed in Chapter 2 were all determined in the knowledge that they were preliminary and would be subject to change with further study.

At the time of the feasibility study the turbine was tentatively sized for 715 MW at 108 m rated net head, rotating at 85.7 rpm (60 Hz) and 71.4 rpm (50 Hz).

More comprehensive power studies, incorporating integrated operation of all the reservoirs and power projects in the Rio Paraná basin, including those already in operation or proposed for the future,

confirmed that the most beneficial mode of operation would be for Itaipu to operate as a base-load plant with a very small drawdown of the reservoir.

Possible daily peaking modes for Itaipu were considered together with limitations imposed by downstream conditions, a typical curve being shown in Fig. 12.16. The final turbine rated head was thus higher than that assumed in the feasibility study and was chosen, as shown in Fig. 12.17, so that the rated turbine output could be achieved 50% of the time. This took into consideration the possibility of a downstream hydroelectric development. Turbine rotational speeds were also re-evaluated with leading manufacturers and it was decided that, with no further increase in turbine setting, the speeds could be safely increased and still be well within the experience curve of Fig. 2.15 of Chapter 2. This increase in speed was consistent with the decision being taken in parallel regarding dual frequency and

Table 12.2 (Continued)

Speed n in rpm	Magnetic pull CM in kN/mm	Kind of excitation			
		Generator unbalance G 6.3 (n_n) $e = 662 \mu\text{m}$	Turbine unbalance G 16 (n_d) $e = 889 \mu\text{m}$	Hydraulic force at turbine runner according to Fig. 12.9	Double short circuit of rotor
90.9	- 600	x	x	x	
124.5	- 440	x	x	x	
170	0	x	x	x	
170	- 240	x	x	x	
124.5	- 600	x	x	x	
170	- 600	x	x	x	
124.5	0	x	x	x	x
90.9	0	x	x	x	x
124.5	0	x	x	x	x

n_n = rated speed n_d = runaway speed e = residual excentricity (ISO 1940)

resulted in an optimization of the generator and turbine design to serve both electrical systems.

The specification of the Itaipu turbines is as follows:

Type

Francis.

Rating

The final specified rating was 715 MW at a rated head of 112.9 m. The head for overall best efficiency was 118.4 m. It was also initially specified that the turbine would normally be wicket gate limited to 740 MW with operation above this only being permitted for limited periods.

Heads

As Itaipu is essentially a run-of-river plant, the level of the upper reservoir is maintained practically constant, at El. 220. The tailwater levels however are

a function of the station flow, as shown in the estimated tailwater rating curve given in Fig. 12.17. The hydrological data together with the tailwater rating curve gave the specified probable operational heads given in Table 12.3.

Setting

The minimum plant cavitation coefficient at the runner outlet established during the feasibility studies was confirmed to be 0.137, maintaining the centerline elevation of the turbine at El. 87.5. Minimum, normal and maximum turbine submergences are given in Table 12.4, with the respective values of the cavitation coefficient (relative to the runner outlet elevation). Again it should be emphasized that as the upper reservoir level is virtually constant both net head and sigma are a function only of the tailwater level and thus there is a unique value of sigma for each head.

Fig. 12.18 Turbines - operating range

Y Discharge (m^3/s)

X Net head (m)

X₁ Minimum head (82.9 m)

X₂ Rated head (112.9 m)

X₃ Design head (118.4 m)

X₄ Maximum head (126.7 m)

1 10% output

2 30% output

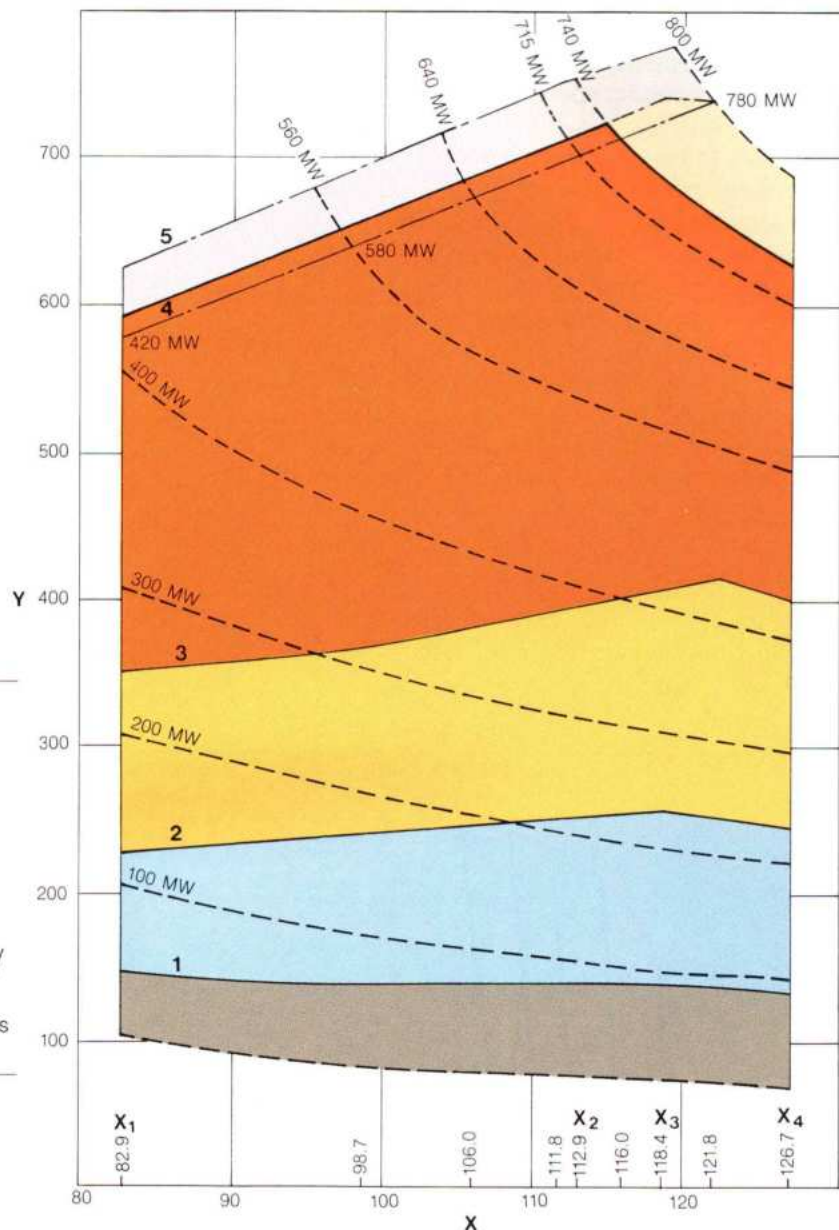
3 60% output

4 Rated opening

5 Max. opening (592 mm)

	Units 1 to 3	Other Units
No load	240	240
Very low load operation	No limit	800
Low load operation	400	800
Normal operation	No limit	No limit
Normal operation	Limited by generator thermal restrictions	Limited by generator thermal restrictions
Overload	50	50

* Operating time restrictions (in hours) during guarantee period



Normal and overload operation. Initially it was specified that unlimited operation, within the guarantee period (8000 hours) would be possible only in the normal region, operation in the overload region having an operating time restriction. However, negotiations with CIEM resulted in an extension of unlimited operation to the overload range, establishing the following new maximum outputs at which the cavitation, vibrational and power fluctuation guarantees applied.

- 800 MW at 126.7 m net head
- 800 MW at 121.8 m net head
- 780 MW at 118.4 m net head

However, nominal turbine rating remained that corresponding to rated wicket gate opening, i.e.,

715 MW at 112.9 m rated head, and the guarantees of efficiency and output were still restricted to the region of normal operation.

Limited operation to the maximum wicket gate opening of 592 mm was permitted for testing.

Low-load operation. The low-load region is defined as between 30 and 60% of the load corresponding to the rated wicket gate opening. It was recognized that draft tube pressure fluctuations would be experienced in this region, and that problems might be encountered with continuous low-load operation. Hence the specified time of operation in this region was left open, subject to the results of the model tests.

Operation of the model in this range was fully investigated during the model test, and based on these studies it was agreed with CIEM that the time of low-load operation during the guarantee period should be limited to 5% of the total.

Very low-load operation. To meet the requirement that the Paraguayan network could be energized by the Itaipu units independently of the Brazilian system, it was specified that the 50 Hz units should operate continuously, without contractual restrictions, in the region between 10 and 30% of the load corresponding to the rated wicket gate opening.

This stipulation is not usual for Francis turbines of the specific speed and size of those of Itaipu, and so the following measures were taken, to minimize cavitation damage:

- Extension of the stainless steel protection on the suction side of the runner blades and band.
- Continuous injection of air into the vaneless space between runner and wicket gates, through the head cover and bottom ring.
- Complete inspection after 1000 hours' operation between 10 and 30% load to investigate the extent of the cavitation damage and to repair and, if necessary, extend the stainless steel protection.

Taking into consideration the additional costs of these measures, and the mode of operation of the Paraguayan network, it was finally decided to adopt the above modifications for only three of the nine 50 Hz units.

Speed no-load to 10% load. To meet the requirements of testing and synchronizing it was agreed with CIEM that the turbine guarantee should be valid for up to 3% of the total operational time in the region of speed no-load to 10% of the load corresponding to rated wicket gate opening.

Cavitation damage

The allowable loss of metal, resulting from cavitation over the first 8000 hours operation, was specified as 59 kg, with the requirement that the loss in metal thickness in this period should be no more than 20% of the total thickness, and any stainless steel overlay should not be pitted through to the base metal.

Turbine efficiency

To ensure the overall efficiency of the unit, that part of the penstock downstream of the expansion joint called the lower reducing bend, was made part of the turbine contract and included in the turbine efficiency guarantee.

The proposed mode of operation of Itaipu was investigated using characteristic curves of turbines of the same specific speed as the Itaipu machines. These studies resulted in the specified peak and weighted efficiency guarantee for the turbine and lower reducing bend as follows:

- At 118.4 m net head and 715 MW: $\geq 92.5\%$
- At best efficiency point (b.e.p.): $\geq 94.5\%$ where b.e.p. is at not less than 610 MW and 118.4 m net head.
- And weighted average efficiency calculated at the operating points of Table 12.5 by the formula:

$$\eta E = \Sigma(T\eta_p)/100$$

where:

η_p = efficiency at point

ηE = weighted average efficiency

T = time factor

Table 12.5 Calculated weighted average efficiency

H net head (m)	Gate position	T time factor (%)
121.8	b.e.p.	38
	740 MW	2
118.4	b.e.p.	36
	715 MW	9
111.8	b.e.p.	2
	656 MW	13

The weighted average efficiency as calculated by this method was specified to be not less than 93.8%. CIEM in fact guaranteed higher values of efficiency than those specified, as shown in Table 12.6.

Regulation

Pre-specification transient studies with the proposed penstock configuration and turbine characteristics gave the load rejection values for various unit inertias, penstock diameters and wicket gate closure times.

Optimizing penstock costs and costs of machine inertia additional to that normally obtained in the design, together with electrical stability requirements, led to the specification of transient speed rises of 35% for the 60 Hz machines and 37% for the 50 Hz machines, coupled with 30% head rise, for load rejections from a maximum output of 740 MW. Load rejections from the overload region were excluded from the speed rise guarantee, the additional speed rise being accepted considering the low frequency of operation in this region.

Table 12.6 Efficiencies guaranteed, measured and predicted for prototype

Efficiency	Guaranteed (%)	Measured on model (%)	Predicted for prototype (%)
Best efficiency point at 118.4m net head (design)	95.3	93.3	96.2
Efficiency at 118.4m net head (design) and 715 MW output (rated)	94.1	92.3	95.2
Weighted average efficiency	95		95.9

The final combined inertia (GD^2), of the Itaipu machines to meet these requirements is $332 \times 10^6 \text{ kgm}^2$ which corresponds to turbine/generator inertia constant H of 5.3 kWs/kVA referred to 737 MVA of the 60 Hz generator and $H = 4.6 \text{ kWs/kVA}$ referred to 823.6 MVA of the 50 Hz generator. These H values are coupled to a wicket gate fast closure time of approximately 9 s from an output of 740 MW. Cushioning at the end of the servomotor stroke is provided to accommodate part load rejections.

A general arrangement of the turbine is shown in Fig. 12.19 and the basic parameters, dimensions and weights of the main turbine parts are given in Table 12.7

MODEL TESTS

Hydraulic model tests were specified to be conducted in a laboratory of the manufacturers' choice and were to be generally in accordance with the International Code for Model Acceptance Tests of Hydraulic Turbines IEC 193/1965 and 193A/1972, where applicable. The model tests were witnessed by ITAIPU personnel.

In the specification, ITAIPU reserved the option of performing a further series of tests in a laboratory of their choice, should there be any doubts regarding the manufacturers' tests. It was not found necessary to exercise this option.

The following parameters were to be confirmed by model tests:

- Efficiency and output guarantees.
- Runaway speed.
- Existence of adequate margins for the cavitation guarantee.
- Draft tube and spiral case pressure oscillations.
- Shaft torque oscillations.
- Hydraulic thrust (together with sizing of the balance pipes).

- Hydrodynamic forces acting on the wicket gates. Influence of air admission through the shaft and to the vaneless space.

The model tests were conducted in the Hydraulic Machines Institute of the Federal Institute of Technology of Lausanne, Switzerland, during March/April 1979.

The model scale was 1:1.97 giving a model runner exit diameter of 416 mm, compared with the specified minimum of 300 mm. The standard Lausanne test circuit was used, modified to incorporate the lower bend.

The following measurements were made:

- Flow. "In circuit" electromagnetic flowmeter calibrated by a volumetric tank.
- Head. Differential manometer, calibrated with a dead weight tester.
- Spiral case and draft tube pressures. Pressure transducers calibrated with a dead weight tester.
- Torque. Load cells on the stator of the dynamometer.
- Torque fluctuations. Strain gauge torquemeter mounted on the turbine shaft.
- Speed. Toothed wheel on the shaft, and magnetic pickup.
- Axial thrust. Pressure difference across the hydrostatic bearing.
- Wicket gate torque. Strain gauges on the wicket gate shaft.

For simplification, the rotating speed for computing prototype values from the model results, was the design speed of 91.6 rpm.

Model test head was chosen as follows:

- 12 m constant test head for tests without aeration.
- Thoma similarity for cavitation testing using, as a pressure reference, the runner exit, to best account for the two phase flow.
- Froude similarity for aeration tests.

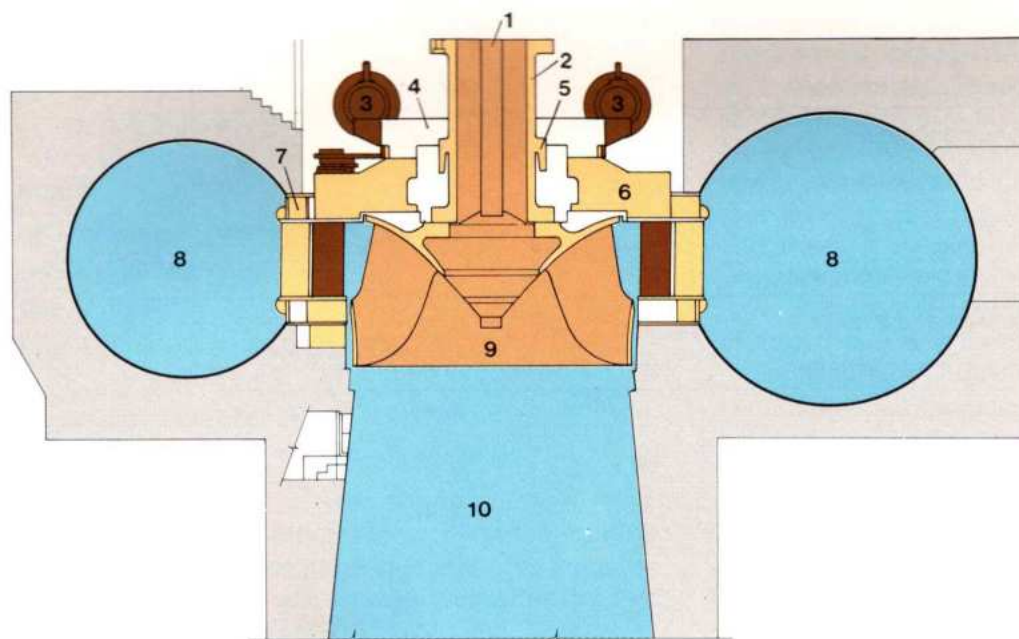
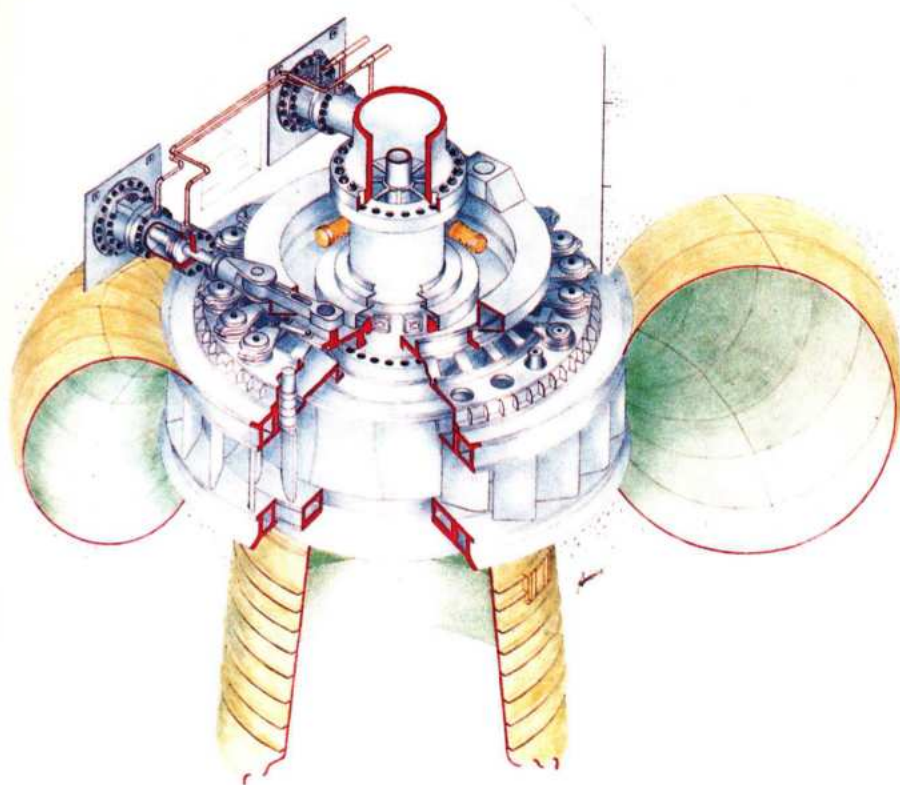
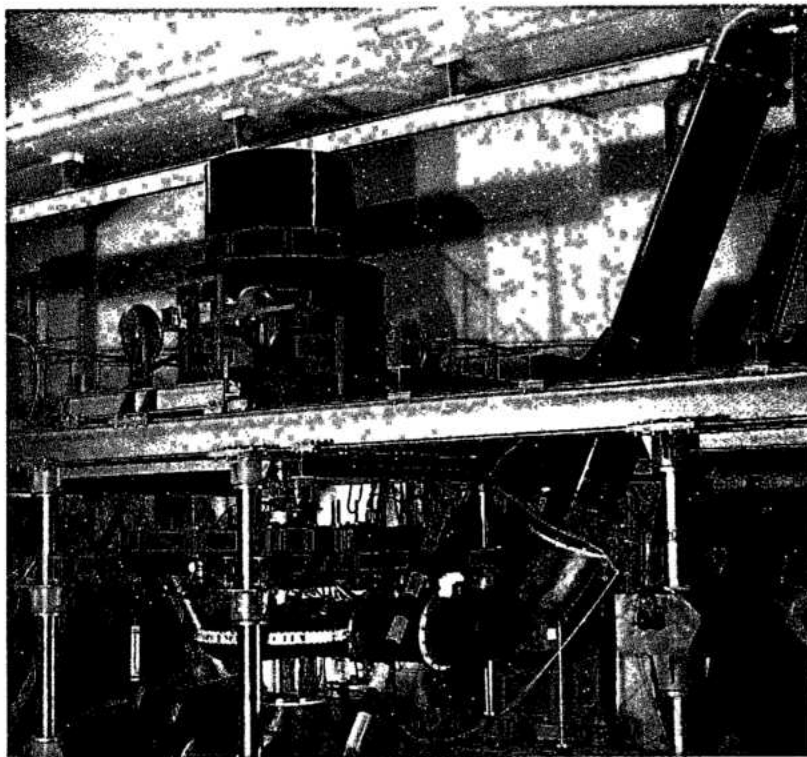


Fig. 12.19 Turbine general arrangement and sectional view

- 1 Shaft aeration piping
- 2 Turbine shaft
- 3 Servomotor
- 4 Operating ring
- 5 Lower guide bearing collar
- 6 Head cover
- 7 Stay ring
- 8 Spiral casing
- 9 Runner
- 10 Draft tube liner

Table 12.7 Turbines – salient data

Item	Leading characteristic	Unit	Dimensions	Weight (kN)
Runner	Height of blades	m	4.207	2902
	Outside diameter	m	8.6	
	Height of runner	m	4.5	
Runner shaft	Length	m	5.52	1255
	Inside diameter	m	2.1	
	Outside diameter	m	2.6	
	Diameter of flanges	m	3.7	
	Bearing collar diameter	m	3.2	
	Height of bearing collar	m	1.015	
Head cover	Maximum diameter	m	11.17	2371
	Maximum plate thickness	mm	150	
Head cover wearing ring	Wearing ring diameter	m	7.89	24.2
	Height	mm	231	
	Hardness	HB	260 ± 30	
Bottom ring wearing ring	Wearing ring diameter (max.)	m	8.83	42.4
	Wearing ring diameter (min.)	m	8.61	
	Height	mm	424	
	Hardness	HB	260	
Bottom ring	Maximum diameter	m	10.76	785
	Inside diameter	m	8.66	
	Height	m	742	
	Maximum plate thickness	mm	102	
Spiral casing	Entrance diameter	m	9.64	5817
	Number of strakes		29	
	Heaviest segment			460
	Maximum plate thickness	mm	77	
Lower bend	Largest inner diameter	m	10.50	8423 (average)
	Minimum inner diameter	m	9.64	
Stay-ring	Inside diameter of vanes	m	10.975	3825 (160 mm vanes)
	Outside diameter of vanes	m	12.678	4158 (200 mm vanes)
	Height of vanes	m	2.222	
	Number of vanes		24	



Turbine model test at Lausanne

The main findings of the model tests were as follows:

Efficiency and output

The values of model efficiency evaluated from the head, flow and torque measurements are given in Table 12.6. Conversion of model to prototype efficiency was specified to be made with a modified Hutton formula as follows:

$$\eta_p = X(1 - \eta_m)[1 - (\text{Rem}/\text{Rep})^{0.2}] + \eta_m$$

where:

η_p = prototype efficiency

η_m = model efficiency

Rem = model Reynolds number

Rep = prototype Reynolds number

$X = 0$ at $Q = 0.25 Q_{\eta\max}$

increasing linearly to $X = 0.75$ at $Q_{\eta\max}$

$Q_{\eta\max}$ = flow at point of maximum efficiency

The Hutton formula was thought to be more applicable than the Moody formula (reference IEC Code), because of the large size of the Itaipu units. Predicted prototype efficiencies calculated by this formula are shown in Table 12.6 and Fig. 12.20.

The model results also demonstrated that the guaranteed values of output could be met.

Maximum prototype runaway speed as scaled from the model test results was 170 rpm.

Cavitation

Flow conditions were observed at the inlet and exit of the runner, through viewing ports in the spiral case and draft tube. Photographs were taken and sketches made of visible cavitation, see Fig. 12.21. These observations confirmed the extent of the stainless steel overlay on the runner, see Fig. 12.22, and the need, or otherwise, for air admission.

Curves of efficiency, and discharge versus σ plotted for operation in the overload range demonstrated acceptable margins of σ plant to σ critical, as defined in the IEC Code.

For all turbines, stainless steel was applied to the suction side of the blade outlet and to the band as protection against the possibility of cavitation damage in these areas at high turbine outputs. It should be noted that cavitation bubbles at this location were not evident in the model at any normal operating point, bubbles only being induced by operating at much lower than contractual sigma values.

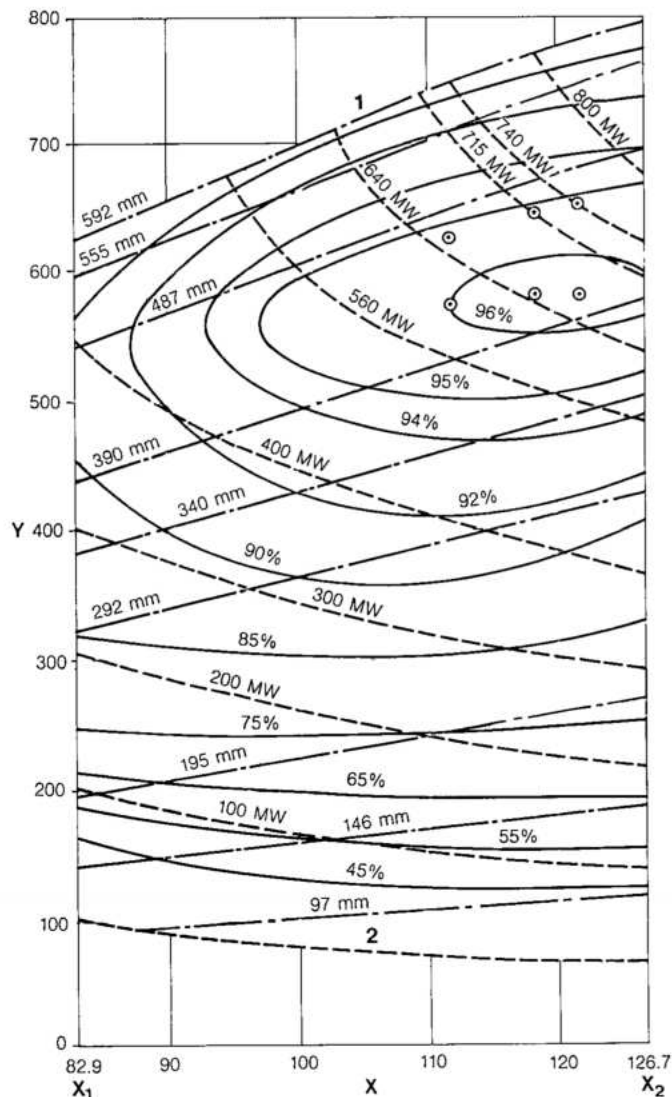


Fig. 12.20 Turbine efficiency

- Y** Discharge (m^3/s)
X Net head (m)
X₁ Minimum head
X₂ Maximum head
1 Maximum opening
2 No load
 — Efficiency
 - - - Wicket gate opening
 - - - Turbine output
 ⊙ Weighted efficiency

Particular attention was paid to the very low-load operating range, to determine the additional stainless steel protection for the three 50 Hz units which were guaranteed to operate in this region. Strong cavitating vortices passing through the blade channels were observed starting at the crown and contacting the band, but not the blades. Air admitted to the vaneless space significantly attenuated these vortices, and for these three turbines stainless steel protection was applied to the crown at the origin of the vortex. Additional stainless steel was also applied to the suction side of the blade to protect against damage, should the vortices touch the blades in the prototype.

Also evident were the runner cone vortices at part load and at high output, resulting from off design flow conditions at the runner leading edge. Air applied through the runner was seen to attenuate these vortices.

Operating stability

Draft tube pressure fluctuations are experienced in all Francis turbines operating at other than best efficiency. In the past, the main concern has been at partial loads (equivalent to Itaipu's designated "low load" operation), but problems have occurred in recent turbines at outputs greater than best efficiency. The draft tube fluctuations can be particularly troublesome when they are strong and cause variations in net head, especially if these are in resonance with the hydraulic or electrical system such as to cause large swings in generator output.

Typical measurements from the model test are shown in Fig. 12.23 from which the following is evident:

- All draft tube fluctuations are less than the 7% of rated head permitted by the specifications.
- Comparing measured draft tube and spiral case fluctuations, there is no indication of strong changes in turbine net head which would lead to large swings in turbine output. This observation was reinforced by the torque measurements.
- At very low load operation the fluctuations are disorganized and are typical of the "white noise" produced by the cavitating crown vortices evident in the cavitation tests. Compressed air admitted in the vaneless space was shown to be effective in reducing this noise.
- As seen in Fig. 12.23, at low load operation there is a strong vortex in the draft tube rotating at $\frac{1}{4}$ to $\frac{1}{5}$ turbine speed, giving rise to substantial draft tube and spiral case pressure fluctuations. The model tests defined the gate opening at which this vortex was strongly evident. These were in turn used to mark the boundaries of the low load operation region in which the turbine would not normally be operated.

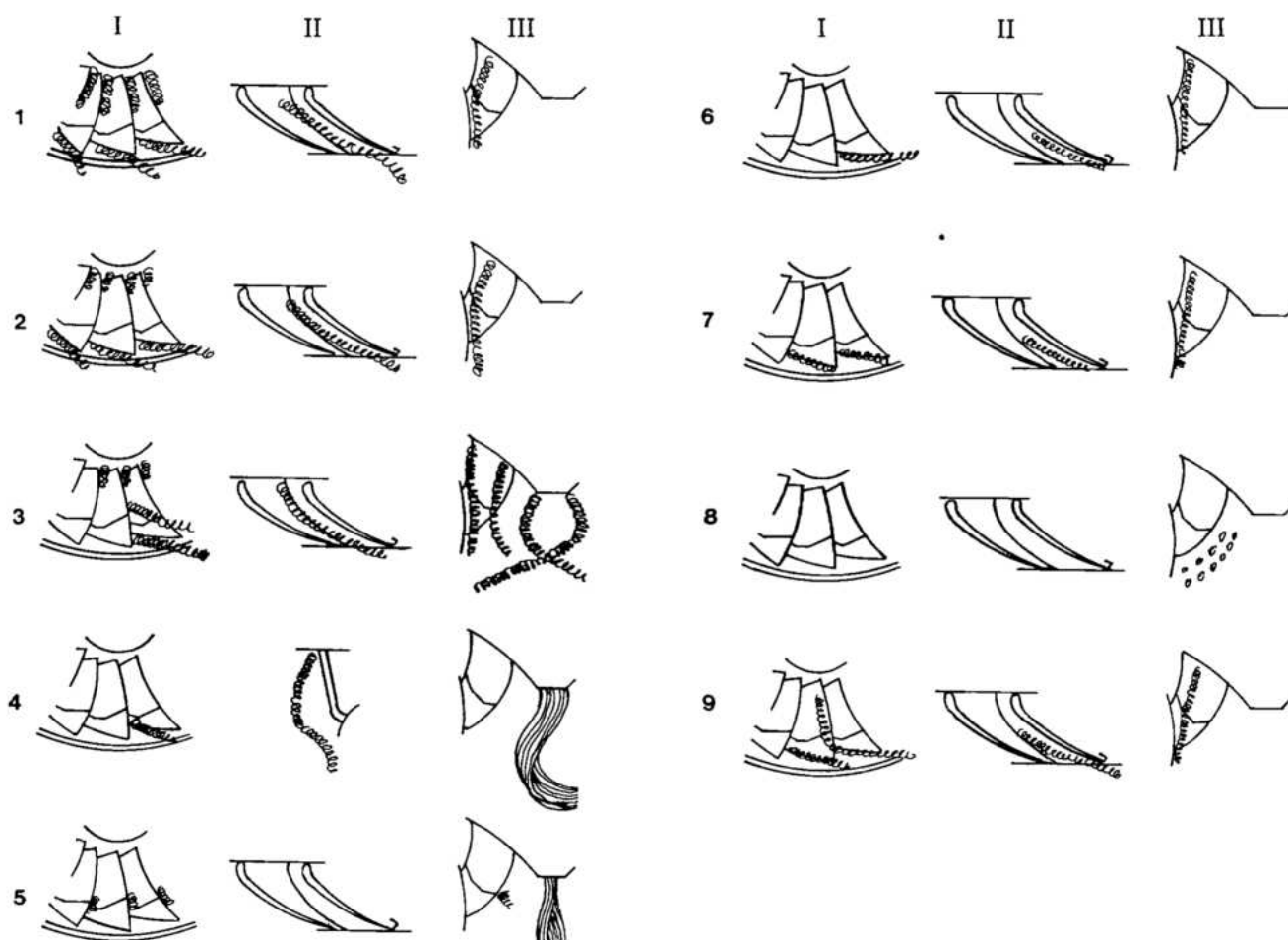


Fig. 12.21 Cavitation test observations

I Blades exit

II Band

III Blade channel

1, 2, ... 5 $\sigma = 0.137$ 6, 7 $\sigma = 0.475$ 8, 9 $\sigma = 0.268$

Air admitted through the shaft was found in the main to be effective in reducing the amplitude of the draft tube pressure fluctuations due to the rotational vortex, and hence would be of use at the low gate end of the normal operation region to quell any remaining fluctuations.

- In the region of best efficiency point there are no fluctuations or signs of vortex activity.
- At outputs beyond the point of best efficiency, generally small draft tube fluctuations reappear but are disorganized, having in the main a frequency of between 0.8 to 1 rotational speed and amplitude of about 0.5% head. These fluctuations are due to a central vortex in the draft tube, which could be seen in the cavitation observations and were of particular concern because of possible resonance with the penstock. Air admitted through the shaft completely quelled these fluctuations.

Hydraulic thrust

The hydraulic thrust measured on the model hydrostatic bearing required corrections to give prototype values, as follows:

- Geometric discrepancies between model and prototype resulted in differences in the projected area acted on by various internal pressures.
- Atmospheric pressure acting on the top surface of the model shaft does not follow the scaling head ratio.
- Weight of the runner and weight of water in the model runner do not comply with the axial thrust similarity law.
- Because of differences between model and prototype wearing rings the leakage through the rings to the space between the top cover and runner crown, and hence the pressure there, is not homogeneous.

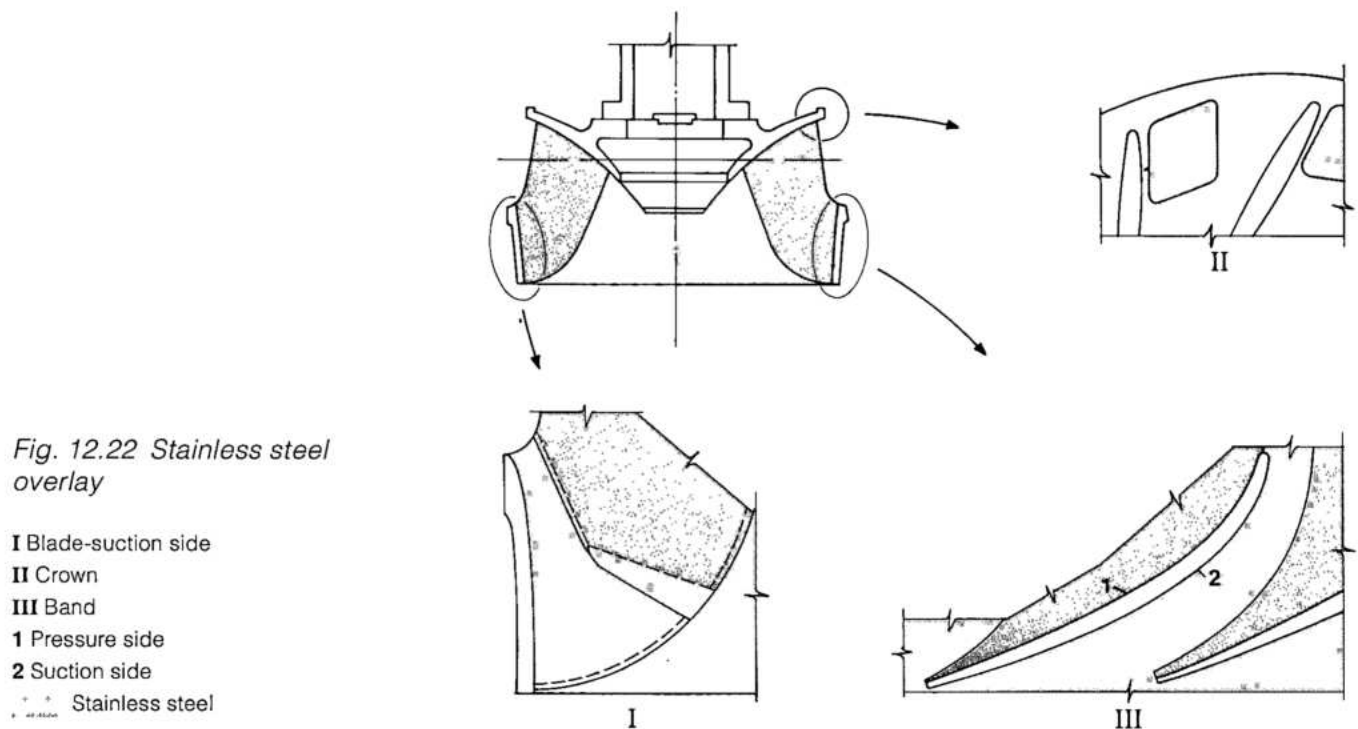


Fig. 12.22 Stainless steel overlay

After correction, the maximum hydraulic thrust measured on the model and converted to prototype was 5.98 MN compared with the guaranteed conservative value of 16.31 MN. Measurements made on the generator thrust bearing confirmed the value obtained from the model test.

Wicket gate torques

Measured wicket gate torques with the wicket gates aligned and misaligned, which were used in the design of the regulating mechanism, are shown respectively in Figs. 12.24 and 12.25. The specification required that at speed no load the net torque on the individual gates should be near zero, thus preventing runaway and slamming of the gates should the oil system fail. From Fig. 12.24 it is evident that this requirement is fulfilled if the dynamic friction is taken into consideration.

COMPONENT DESIGN AND MANUFACTURE

General

The overriding principle of the specifications was to use a conservative approach. Where possible, well tried designs and arrangements were defined with

very little departure from accepted practice. Because Itaipu has eighteen units, characteristics which would not be economically feasible in a smaller powerplant could be considered for Itaipu.

The following maximum stress levels were specified for all parts of the turbine when subjected to the most severe loading condition experienced during steady state operation or load rejection:

- Cast iron: 10% of the ultimate strength; but in any event the compressive stress should not exceed 69 N/mm^2 .
- Cast steel: 20% of the ultimate strength or 33% of the yield strength whichever is the less.
- Plate steel for principal parts: as allowed by the ASME Boiler and Pressure Vessel Code Section VIII.
- Other materials: 20% of the ultimate strength or one-third of the yield strength whichever is less.

In addition to those general requirements the following particular considerations were to be met:

- For the rotating parts of the turbine when subjected to maximum runaway speed or with locked runner, maximum combined stresses should not exceed 67% of yield.
- For the wicket gate stems and levers at loads causing failure of the shear pin, maximum combined stress should not exceed 67% of yield.

- Steel for important parts to have approved minimum impact value at 0°C (normally in the range 25 J to 30 J).

Calculations were to be submitted by the contractor, proving the compliance to specifications of all major parts of the turbine. In accordance with modern practice CIEM used mainly the finite element technique for these calculations, together with correlation with measurements taken on operating turbines to support the validity of the computer programs and input data used.

Stay ring

The stay ring consists of two box type rings of rectangular section connected by twenty-four stay vanes, see Fig. 12.26. The box plates are 100 mm thick with link plates of 61 mm to 90 mm thick.

In accordance with ITAIPU's specifications, the yield stress of the material for the stay ring, spiral case and lower reducing bend does not exceed 353 N/mm². This was to avoid the use of specially processed steels which would result in complicated welding and heat treatment procedures.

The stay ring was manufactured in four sections, each section being welded by the MIG and submerged arc processes.

Great care was taken to ensure that problems of cracking in the stay vanes as a result of vortex shedding from the stay vanes and residual stresses in the welds were avoided. The following measures were therefore adopted:

- Average stress of the vane to be as low as possible, consistent with the hydraulic design requirements.

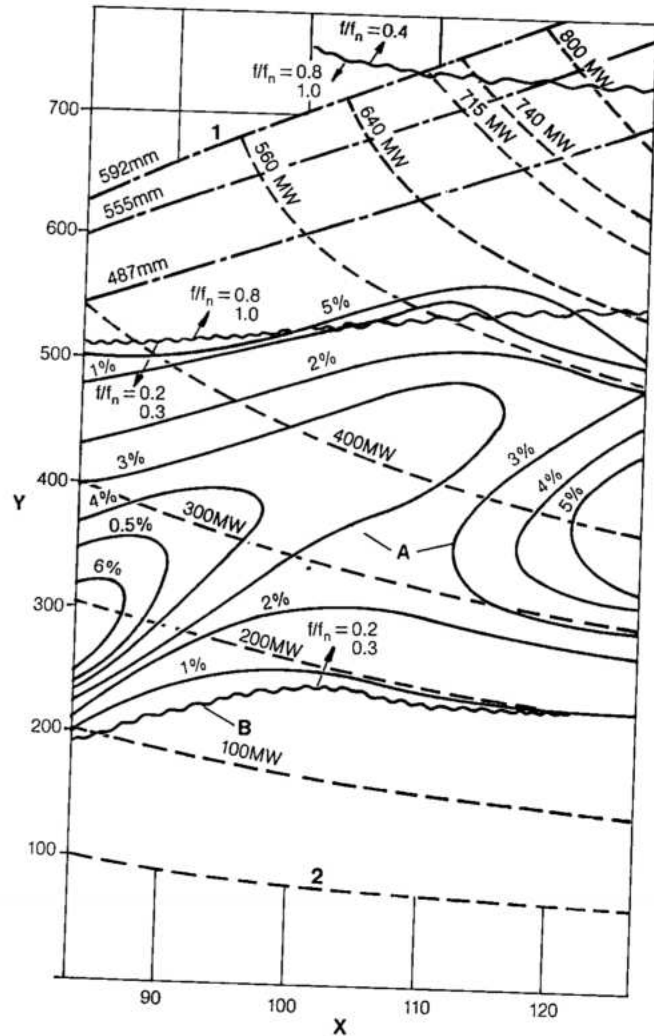
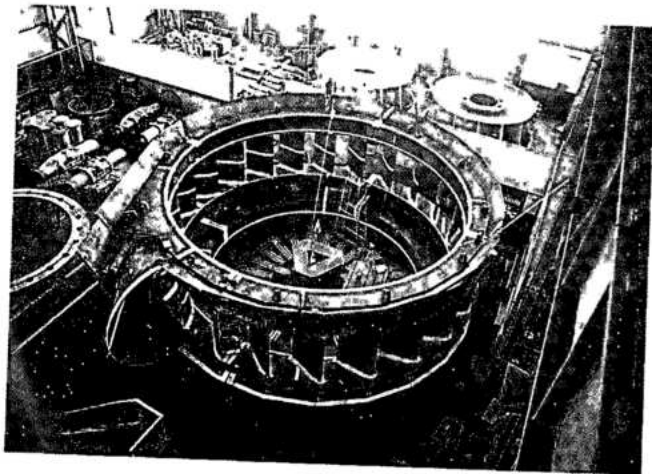


Fig. 12.23 Draft tube pressure fluctuations

- Y Discharge (m³/s)
- X Net head (m)
- 1 Maximum opening
- 2 No load
- A Peak-to-peak values as % of head
- B Non organized fluctuation
- Pressure fluctuations
- Frequency boundaries



Turbine stay ring in manufacture

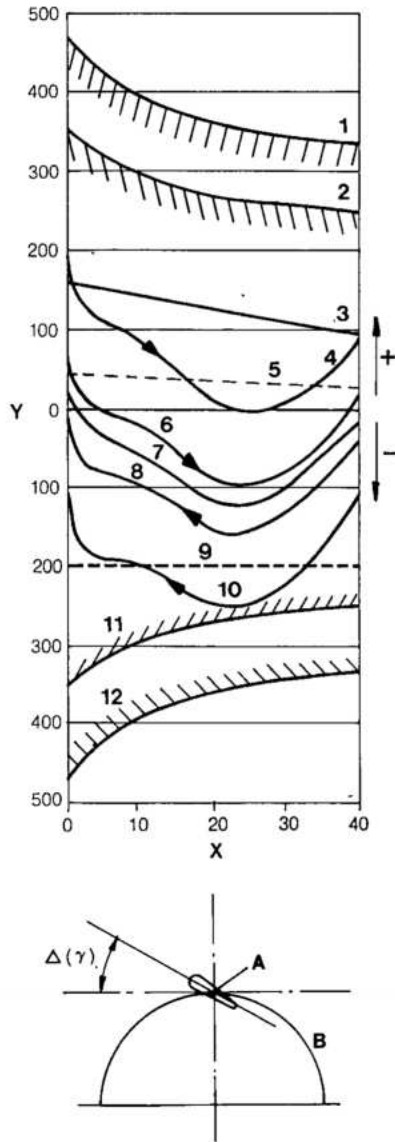
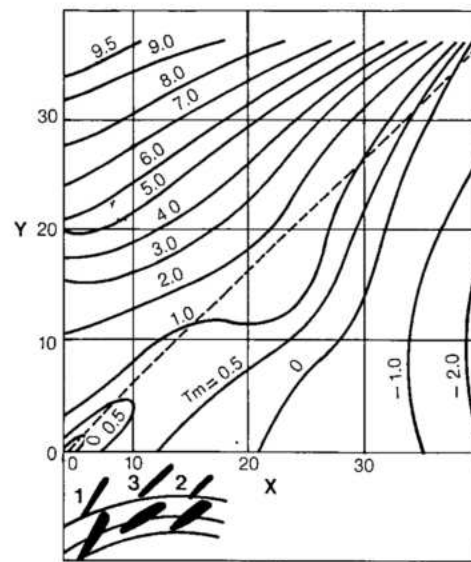


Fig. 12.24 Wicket gate torques all gates aligned

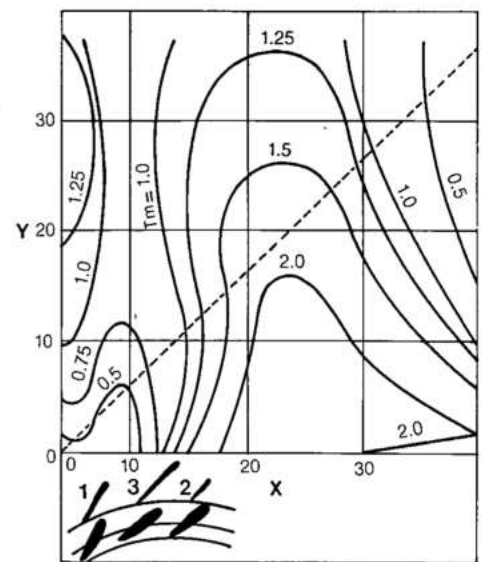
Y Wicket gate torque (kNm)
X Opening angle of wicket gates $\Delta \gamma$ (degrees)
1 Servomotor torque available to open wicket gates at maximum oil pressure (640 kN/cm²)
2 Servomotor torque available to open wicket gates at minimum oil pressure (480 kN/cm²)
3 Servomotor torque available to close wicket gates at minimum oil pressure (480 kN/cm²)

4 Servomotor torque available to close wicket gates at maximum oil pressure (640 kN/cm²)
5 Static friction torque on wicket gates (friction coefficient for impending motion only $M_r = 0.15$)
6 Dynamic friction torque on wicket gates (friction coefficient during movement only, $M_{rd} = 0.04$)
7 Hydraulic resisting torque developed by wicket gates
8 Hydraulic plus dynamic friction torque required to open wicket gates

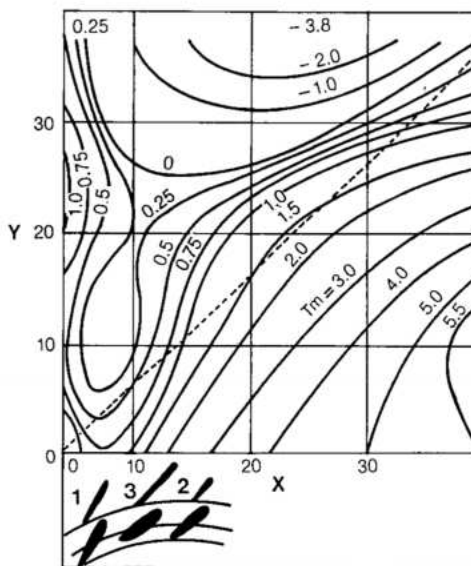
9 Hydraulic plus dynamic friction torque required to close wicket gates
10 Hydraulic plus static friction torque required to open wicket gates
11 Hydraulic plus static friction torque required to close wicket gates
12 Friction break operating torque
A Wicket gate
B Wicket gate pitch circle
 + open tendency
 - tendency



I



II



III

Fig. 12.25 Out of synchronization wicket gate torques

I Wicket gate no. 1 misaligned
II Wicket gate no. 23 misaligned
III Wicket gate no. 24 misaligned
Y Angle of misaligned gate
X Angle of aligned gate
Tm = Wicket gate operating torque on a per head per unit diameter basis
1 Wicket gate no. 1
2 Wicket gate no. 23
3 Wicket gate no. 24
 + Closing tendency
 - Opening tendency

- First natural frequency of the blade to be substantially higher than the vortex shedding frequency.
- Profile of the blade trailing edge to be such as to keep the intensity of the dynamic stresses resulting from vortex shedding to a minimum.
- Stress concentration at the welded junctions of vanes and upper and lower rings to be minimized by ample transitions.
- Residual stresses after shop welding to be kept to a minimum by thermal stress relieving. To this end stress relieving was conducted in two stages, the first after 50% weldment and the second after completion of the welding.
- Residual stresses after alignment and welding of the quadrants at the site to be reduced by accurate shop fitting of the pieces, controlled, balanced welding procedures and dimensional control during and after site welding.
- Quality control of the welds using ultrasonic examination and checking by dye penetrant and magnetic particle tests, and polishing and painting the welds, to improve the fatigue characteristics.

In the initial CIEM design the vane thickness was 160 mm and the first three 50 Hz and first two 60 Hz units were made with this thickness. However, by agreement between CIEM and ITAIPU, in order to give further security against vortex shedding problems, the vane thickness for all thirteen subsequent units was increased to 200 mm.

Spiral case and lower bend

As explained earlier, the penstock downstream of the penstock expansion joint (the lower bend) was included in the turbine supply.

The lower bend, spiral case and stayring were all specified to be designed for the maximum hydraulic transient pressure of 1.68 N/mm^2 and to be pressure tested at 2.52 N/mm^2 . Design conformed to the ASME Boiler and Pressure Vessel Code with the following specific requirements:

- The membrane stresses to be calculated by the appropriate Torus formulae and in no case to exceed 25% of the ultimate stress (ASME Section VIII, Division 1).
- The total combined stress resulting from the summation of principal, bending and secondary stresses at the design pressure, should remain below the minimum yield strength (ASME Section VIII, Division 2).

The lower bend is made of fine grained steel with twenty-two segments, for units 1 to 15 and unit 18 (twenty-three segments for units 16 and 17), see

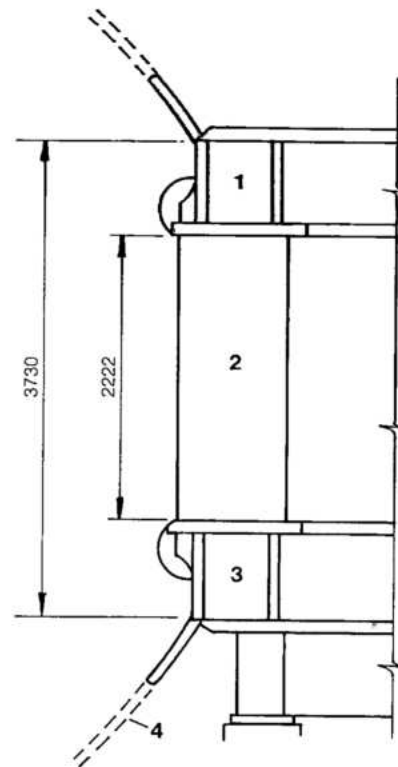


Fig. 12.26 Stay-ring

- | | |
|--------------|-----------------|
| 1 Upper ring | 3 Lower ring |
| 2 Stay vane | 4 Spiral casing |

Fig. 12.27. The lower bend of units 16 to 18 are also curved in plan view in order to compensate the slight difference in design of units in the diversion structure compared with that of the main dam. Embedded thrust rings of the lower bend provide a fixed point for pressure testing and pressurization during embedment of the bend and spiral case. The lower bend has tapings for the Gibson and thermodynamic flow measurement methods for site efficiency tests.

The penstock and spiral case are drained through a 590 mm diameter pipe with a grided entrance and butterfly valve, connecting the lower bend and draft tube.

The spiral case is made of twenty-nine segments, each segment consisting of fine grained steel plates of different thickness rolled and trial fitted in the manufacturer's works. The thickest plate is 77 mm.

A 750 mm-diameter outlet is provided in each spiral case for water supply to unit cooling, station service and station fire protection systems, see Chapter 13.

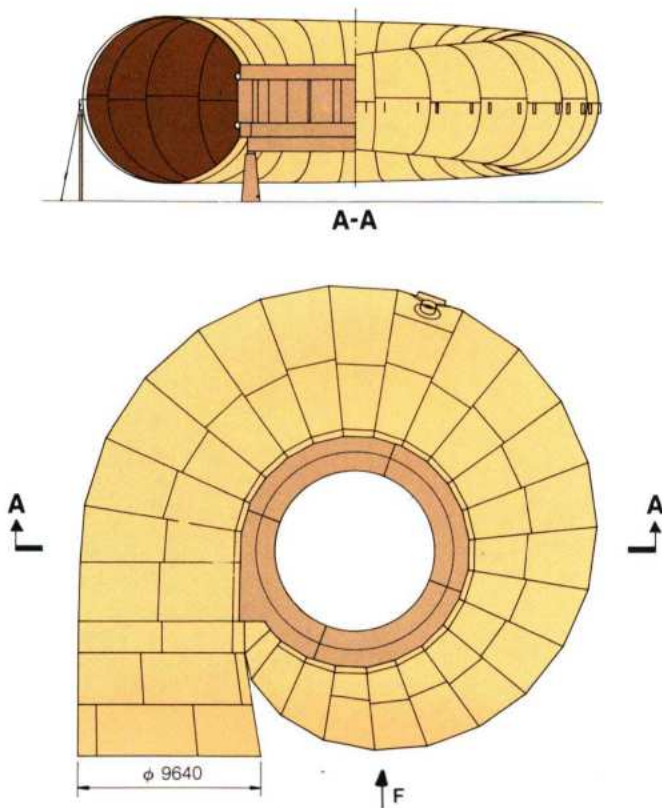


Fig. 12.27 Spiral case

F Flow direction



Transport of spiral case segment along powerhouse

There is also a 1.2 m diameter mandoor for access to the inside of the spiral case from the downstream gallery. The mandoor opens inward and is flush with the inside surface of the spiral case when closed. It is instrumented to prevent opening of the power intake gate when the mandoor is open.

Pressure taps corresponding to those used in the model tests are provided in the lower bend and spiral case, including Winter-Kennedy taps whose differential pressure is used to continuously monitor turbine flow.

Head cover and bottom ring

The head cover and bottom ring each consist of two semicircular shop welded plate structures with flanges for bolting together the two halves. This form of construction was necessary because of transport limitations. Welded in the lower skin plates of the head cover are twenty-four cast steel cylinders which retain the intermediate bearings for the twenty-four wicket gates. Likewise the bottom ring is equipped with twenty-four cast steel cylinders for the lower wicket gate bearings, see Fig. 12.28.

The upper wicket gate bearing is held in a circular plate bolted to the head cover and the wicket gate up thrust ring is bolted to this plate.

For the first two units, for which the regulating gear was trial shop assembled, the bottom ring and head cover were supplied to the site with their respective wicket gate bearings installed. For all other units only the head cover was supplied with the intermediate wicket gate bearings installed and at site the cylinders in the bottom ring were reamed with the head cover and bottom ring mated. Wicket gate bearings were then shrunk in the bottom ring.

As the Itaipu machines have a separate lower bracket to support the thrust bearing, the head cover must resist, with acceptable deflections, the hydraulic forces acting on the lower surface of the cover. Calculations were made by the finite element method giving the following radial deflections at the turbine guide bearing attachment:

- 0.22 mm for normal operation.
- 0.45 mm for transient conditions.

These deflections, coupled with those resulting from thermal deformation, necessitated a special turbine bearing design to be described later.

The finite element analysis also confirmed that, with an erection clearance between wicket gate and head cover of 0.4 mm, there would be no problems with binding under the most extreme operating conditions. On the bottom face of the head cover

and top face of the bottom ring in the general area of the wicket gates, is a welded layer of stainless steel 6 mm thick, to ensure that wear is minimal over a long period of operation and that the leakage remains within the guaranteed value of $3.5 \text{ m}^3/\text{s}$.

Leakage water through the upper wearing ring is drained to the draft tube through six 300 mm diameter equalizing pipes to reduce the pressure in the chamber between the runner and head cover and the resulting down thrust on the runner. The required area of the equalizing pipes was based on values obtained from model tests.

There is bronze overlay comprising six segments 500 mm long, 6 mm thick, on the bottom face of the head cover to act as an upthrust ring in the unlikely event of the runner lifting during transient conditions.

Stationary wearing rings, made from chrome steel with a hardness of $260 \pm 30 \text{ HB}$, were delivered to the site in segments and bolted to the head cover and bottom ring. The segments were welded together and all edges seal welded to prevent rusting of the underlying steel and the associated problem of expansion of corrosion products. Four 26 mm diameter inspection holes with removable plugs in the head cover allow measurement of the clearance between the rotating and stationary wearing rings. The head cover has three pumps for wicket gate seal leakage. One small pump is for normal leakage and the other two of approximately $130 \text{ m}^3/\text{h}$ each, for emergency conditions. Also there is a gravity drain via a vertical hole drilled in a stay vane at a level higher than that of pump operation.

The head cover and bottom ring are attached to the upper and lower plates of the stay ring respectively by flanged and bolted connections, the mating surfaces on the stay ring being spot faced at

site. The exact seating of the head cover and bottom ring is achieved by means of spacer washers for each bolt.

The hold down bolts are tensioned hydraulically.

Regulating mechanism

Initially three types of servomotor systems were considered for the turbine:

- Individual servomotors for each wicket gate.
- Multiple servomotors mounted on the head cover and operating through an operating ring.
- The traditional concept of two servomotors mounted in the pit liner and operating through an operating ring.

Although thought viable in the feasibility study, (see Chapter 2,) individual servomotors were finally precluded for the following reasons:

- Each servomotor is required to react to the transitory hydraulic moment of each gate, whereas the operating ring system averages these moments.
- The operating ring system has been adopted and used in many operating turbines while the individual servomotor system is still at development stage for units of the size of Itaipu.
- Additional maintenance requirements.

Multiple servomotors mounted on the head cover or back of the pit liner were made difficult by the specifications requirement for the locking devices to resist maximum servomotor forces. Hence the final choice was that of twin servomotors and operating ring.

The two servomotors are located on the upstream side of the pit liner at El.92.1 and each is bolted to a steel structure embedded in the turbine pit concrete.

The servomotors, which operate at an oil pressure between 3.9 N/mm^2 and 5.9 N/mm^2 consist of a

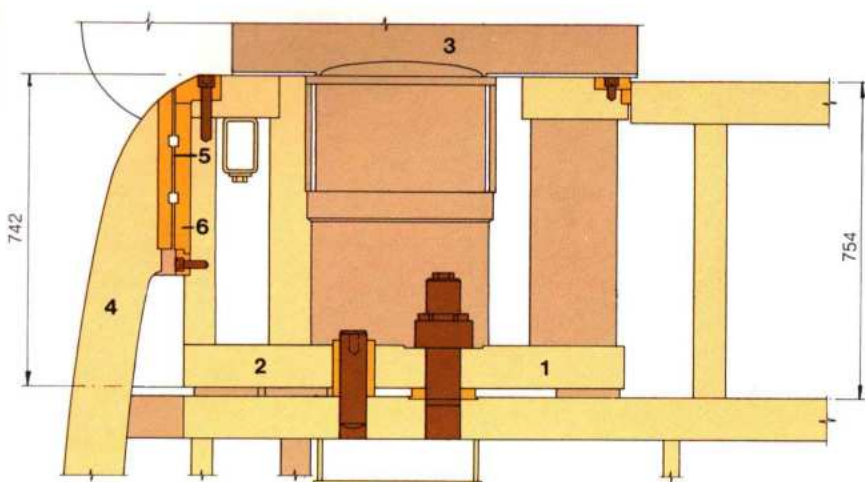
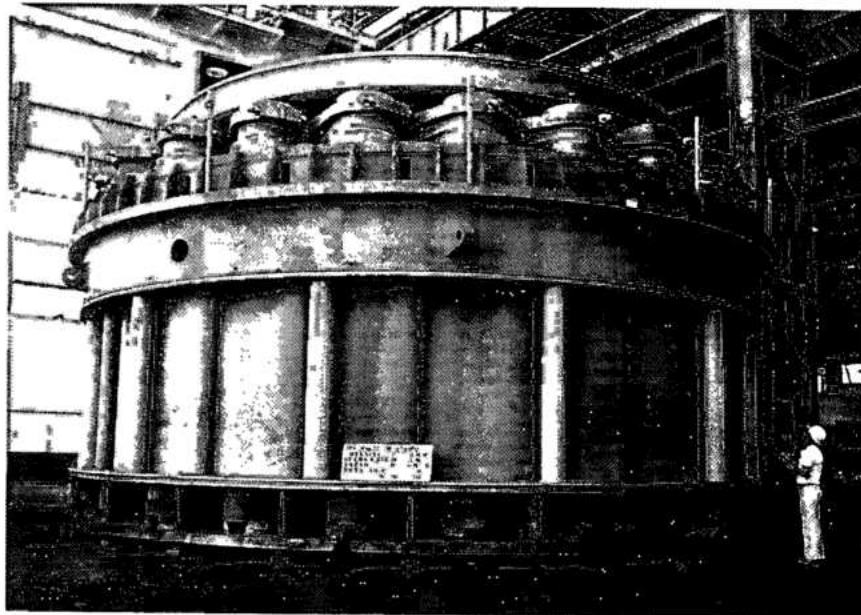


Fig. 12.28 Section of bottom ring wicket gate lower bearing

- 1 Stay ring
- 2 Bottom ring
- 3 Wicket gate
- 4 Runner
- 5 Rotating wearing ring
- 6 Fixed wearing ring



Shop assembly of regulating mechanism

acting on the gates is less than the resistance of the shear pin/clamp combination at any opening of the turbine distributor, as is the full servomotor force on the gate.

If during closing movement of the distributor an obstacle prevents closure of a wicket gate, the shear pin will break, but since the hydraulic torque acting on the free gate is always smaller than the reactive torque of the clamp, even though the gate may slip out of synchronism it will not slam or flail and, should the obstacle be flushed out, it will then follow the movement of the upper lever. The hydraulic torque on the gates neighboring the misaligned gate never exceeds that of the shear pin/clamp combination.

In the unlikely event that during opening movement of the distributor an obstacle, whose size is normally limited by the trashrack, is caught between a wicket gate and a stay vane and prevents further opening of the gate, the shear pin will also break, but the lagging of the free gate relative to the opening of the synchronized gates has to be about 10 degrees before the hydraulic torque on the free gate exceeds the slipping torque of the friction brake. Thus the shear pins have a compressed air monitoring system which initiates unloading of the unit and shutdown should the shear pin break. If breakage is accompanied by slipping of the friction brake then this too is monitored by a limit switch which instigates the closing of the power intake gate. Finally the pin (7) provides an additional security, in

that large hydraulic closing torque in excess of the reactive friction torque only acts on a misaligned gate when it is at a smaller opening than the other gates. With pin (7) intact, a free gate cannot reach this position, regardless of the initial reason for its free movement.

The regulating mechanism of the first two turbines to be supplied was shop assembled (with the respective top and bottom covers) in order to check dimensional tolerances.

Turbine shaft

The turbine shaft is manufactured from a forged steel cylinder welded to two forged flanges, one for coupling to the turbine runner and the other to the lower generator shaft, see Fig. 12.31.

Coupling between the turbine shaft and runner is made by twenty-four coupling bolts 210 mm in diameter, pretensioned during erection by a hydraulic device.

Stresses in the shaft were calculated by the finite element method for all possible loading conditions.

The shaft seal as detailed in Fig. 12.32 consists of a six segment stainless steel ring bolted to the runner flange. Effecting the seal are carbon rings held in a ring holder. Pressure between the carbon ring and the stainless steel ring is maintained by twenty-four stainless steel springs which automatically compensate for seal wear. Wear is

minimized by filtered water supplied to the seal gap through hydrocyclones.

For maintenance there is an emergency seal which with the application of powerhouse service compressed air, seals on the side of the runner coupling flange.

Turbine guide bearing

The stiffness of the turbine guide bearing was defined by the line shaft stability studies.

The radial deflection of the head cover in the region of the bearing was calculated to be 0.22 mm for normal operation and 0.45 mm for operation under transient conditions. These deflections together with those resulting from thermal expansion of the bearing in service (18°C differential) necessitated a special design of the bearing support, see Fig. 12.33. This has a necked

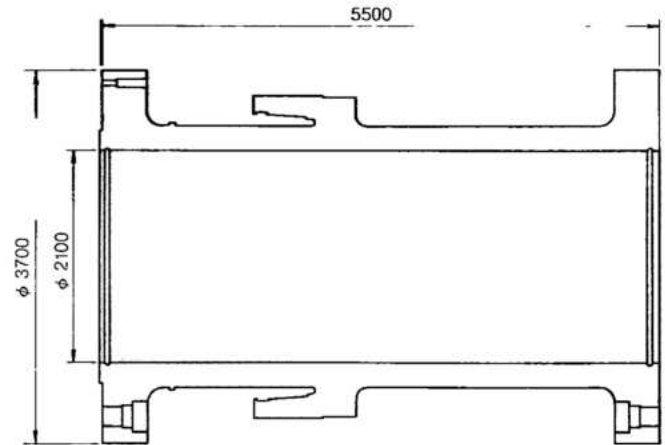
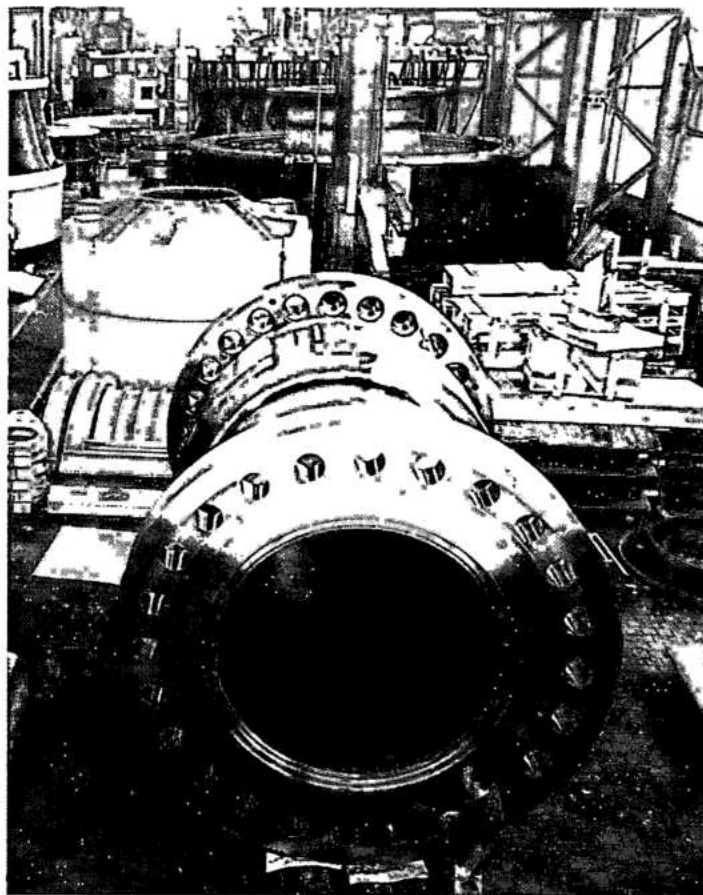
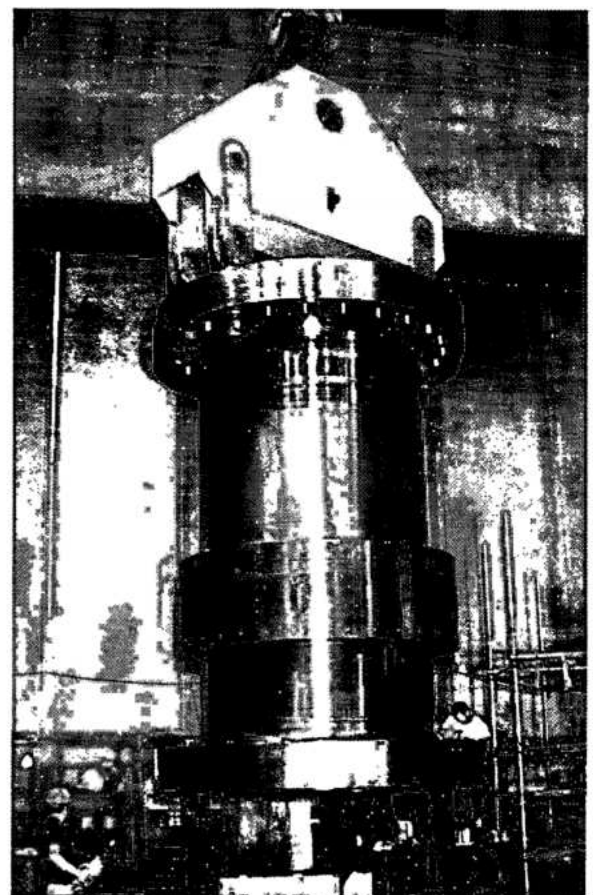


Fig. 12.31 Turbine shaft



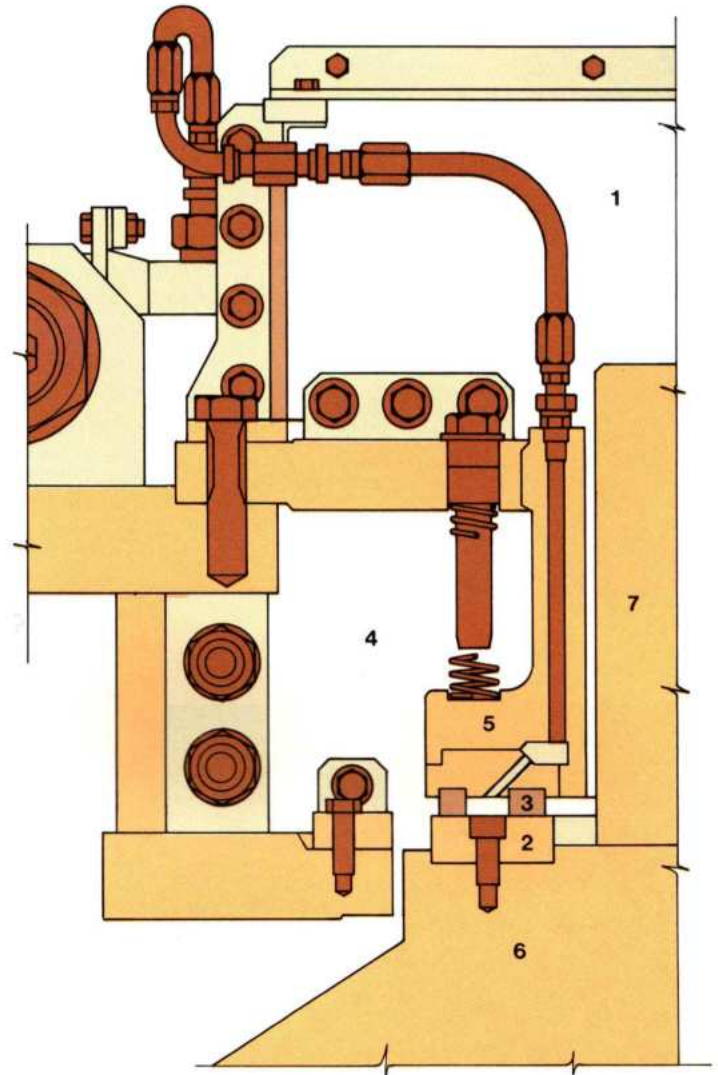
Turbine shaft at manufacturer's works



Transport of turbine shaft inside powerhouse

Fig. 12.32 Shaft seal

- 1 Steel water pipe
- 2 Stainless ring
- 3 Carbon ringers
- 4 Springs
- 5 Ring holder
- 6 Runner crown
- 7 Turbine shaft



cylindrical support, which isolates head cover deflection from the bearing (to a factor of 0.23) while providing radial stiffness. Also the support is attached to the head cover at a point 500 mm below the bearing, where the radial deflections of the head cover are 0.1 mm for normal operation and 0.18 mm under transient conditions.

The bearing stiffness is a combination of the flexibilities of all components back to the pit liner, see Fig. 12.7.

The bearing is the self-lubricating type with oil circulation to the bearing segments effected by the centrifugal pumping action of radial holes in the shaft bearing collar. After passing through the bearing, the oil is cooled in four oil/water coolers mounted on the head cover. Only three of these coolers are necessary for

normal operation, the fourth is a reserve. There are twelve white metal coated cast steel bearing segments, each radially adjustable by adjusting screw positioned vertical wedges behind the segments. The running clearance of the bearing at operating temperature is $400\text{ }\mu\text{m}$ and bearing velocity is 15.46 m/s (60 Hz) and 15.23 m/s (50 Hz). The bearing was designed for a maximum temperature of 70°C for the white metal and 60°C for the oil, under the following specified conditions:

- With oil cooling:
 - Continuous operation between 50% and 105% normal speed.
 - Operation for 5 minutes at runaway speed.
- Without oil cooling:
 - Load rejection.
 - Rated load for 15 minutes.

The bearing is drained through a pipe in the bottom of the bearing pot which connects with similar drains from the generator bearings and the governor tank. From there the oil enters a 210 l/min motor driven pump located in the head cover, which feeds it out of the turbine pit.

The oil can be cleaned by cycling through a portable purifier at the turbine/generator unit itself, or pumped to the central oil system, see Chapter 13.

The bearing is equipped with high/low oil level switches, pad and oil temperature transducers, "water-oil" transducers and cooling water flow switches.



Turbine guide bearing

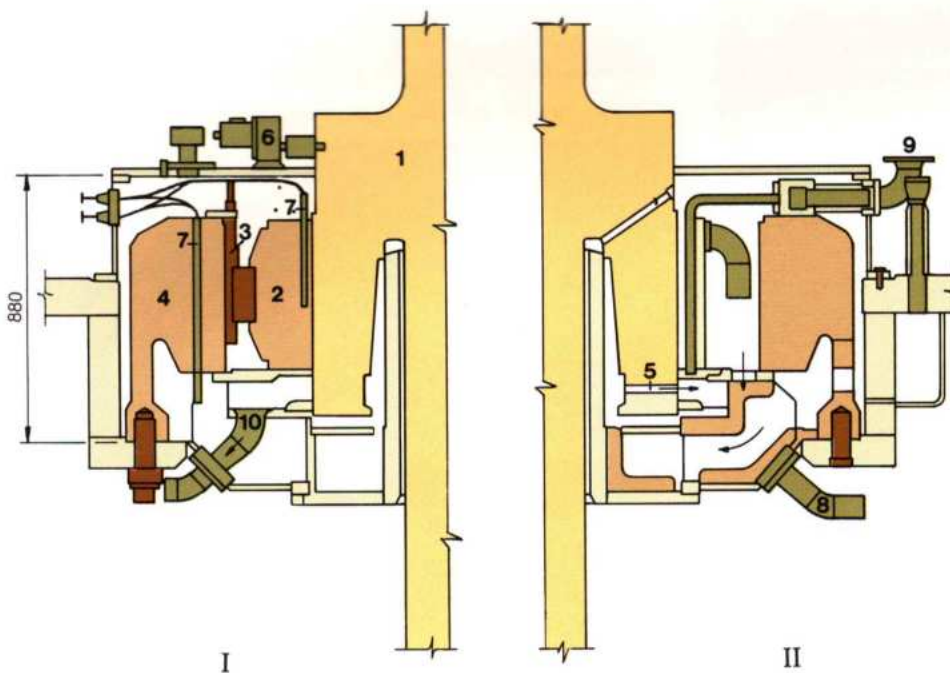
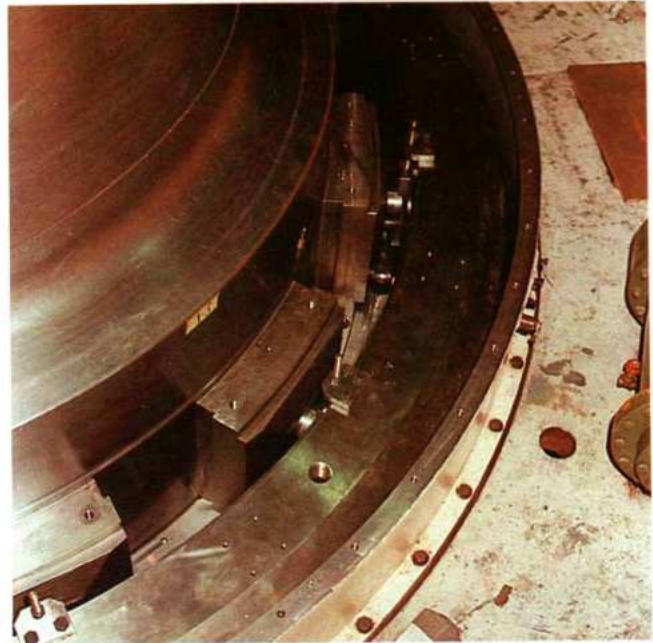


Fig. 12.33 Different section of turbine guide bearing

- 1 Turbine shaft
- 2 Bearing pad
- 3 Adjustment shims
- 4 Bearing support
- 5 Radial pump
- 6 Overvelocity device
- 7 RTD's
- 8 Oil drain
- 9 Oil from coolers
- 10 Oil to coolers

Runner

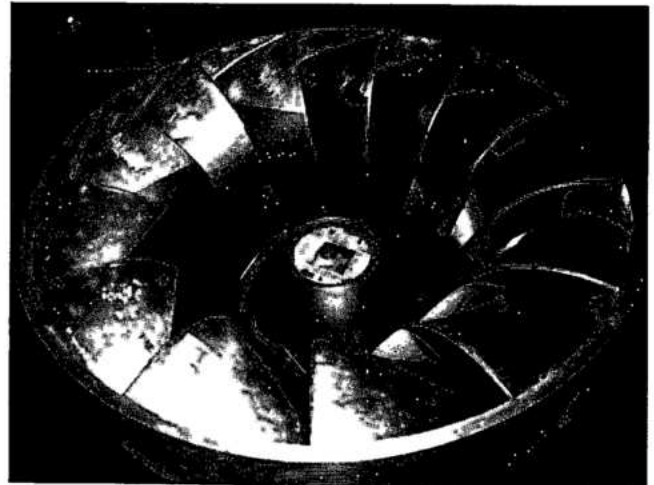
The hydraulic profile of the turbine runner was determined using modern computational fluid dynamic methods and confirmed by model tests in order to:

- Attain a high wicket best efficiency without sacrificing efficiency at full wicket gate.
- Eliminate any cavitation at the blade inlet under high loads without causing unstable flow separations under low heads.
- Minimize partial load fluctuations without inducing instability at high loads.

Model tests also served to establish the areas to be protected by the 5 mm thick stainless steel overlay as shown in Fig. 12.22, as well as the necessity for natural and compressed air admission.

During pre-specification studies, the feasibility of site-fabricated, and completely shop-fabricated runners, was evaluated, and it was decided that a shop-fabricated runner would be preferable, to maintain maximum quality control and adherence to schedules even though this implied special provisions for transportation.

The runner is manufactured from cast steel crowns and bands and thirteen cast steel blades, see Fig. 12.34. Runners supplied by Mecânica Pesada were manually welded, whereas those from Voith were welded with the electro-slag method, using consumable welding wire guide tubes. With the electro-slag method the joint is enclosed by shaped water cooled copper shoes which are moved manually as the weld progresses. Welding wire is fed vertically into the weld via the guide tube; the runner assembly being positioned by a manipulator to ensure the correct orientation of the runner relative to the welding head. The maximum thickness of the vane is 171 mm. The lengths of the



Turbine runner showing extent of stainless steel overlay

groove to be welded was 3500 mm at the crown and 4300 mm at the band.

One of the concerns with the electroslag method was the grain size and hence the impact strength of the weld. Therefore great care was taken in execution of weld, supervision of weld parameters and in subsequent testing, to ensure that a Charpy V impact value of 24 J at 0°C was maintained.

With the electro-slag method each weld took approximately 1 day to execute; about 10 hours for the actual welding and 14 hours for preparation. However, after this, back gouging and manual welding was required for repairs and filling the edge radius of the weld. This required about 6000 hours for the first runner, reducing with experience to 3000 hours for the last. Hence the total minimum

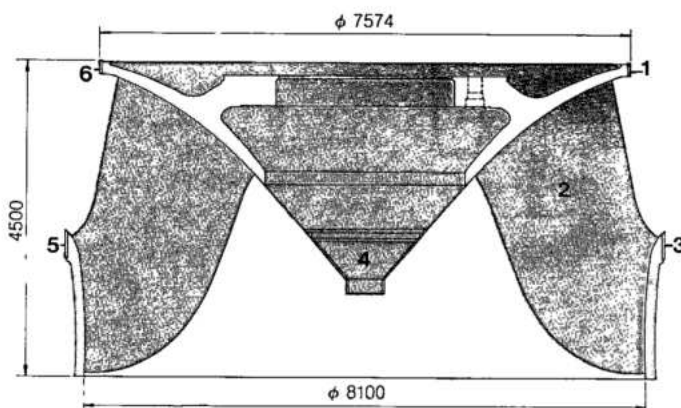


Fig. 12.34 Turbine runner

- 1 Runner crown
- 2 Runner blade (13 blades)
- 3 Runner band
- 4 Runner nose cone
- 5 Lower rotating wearing ring
- 6 Upper rotating wearing ring

time to weld a Voith runner was about 3700 hours. A completely manually welded runner required a minimum of six welders and a maximum of twelve with the following approximate welding time in hours:

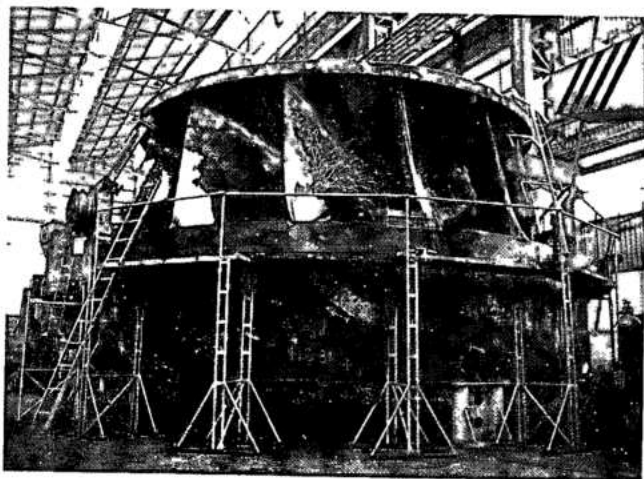
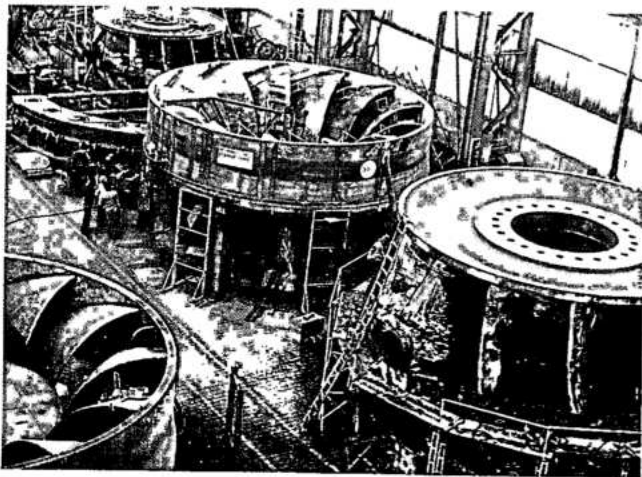
Preparation of crown	970
Preparation of band	600
Each blade to crown weld	4300
Each blade to band weld	3900

Because of the combination of welders, each manually welded runner took about 8000 hours to weld.

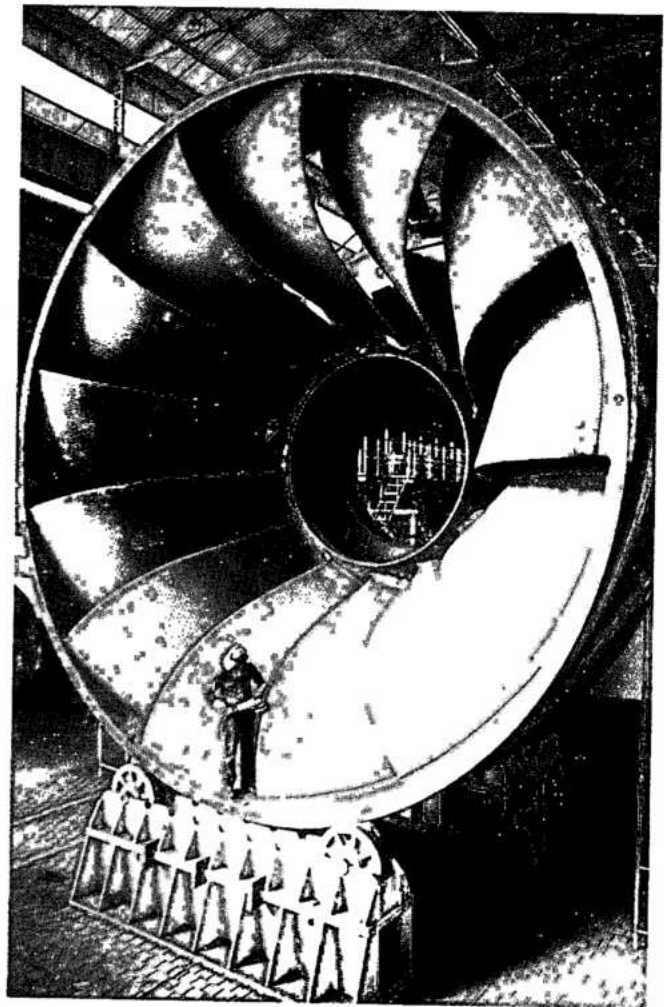
After stress relieving and nondestructive testing, the runner hydraulic surfaces were ground smooth and given two coats of zinc epoxy primer.

The runner was then machined and the stainless steel wearing rings shrunk on. Following normal practice, a hardness difference between the stationary and rotating wearing rings of 50 HB was specified, to avoid galling in the unlikely event of the rings touching.

Any possibility of the rings contacting was extremely remote, as the radial clearance between the rings with the unit stationary was 6 mm and the maximum calculated radial movement of the rotational ring was 4.7 mm. The 4.7 mm movement would occur at runaway, and comprised 3.02 mm shaft deflection (determined from the line shaft calculations) and 1.68 mm radial expansion of the runner band due to centrifugal forces, calculated by a finite element analysis of the runner.



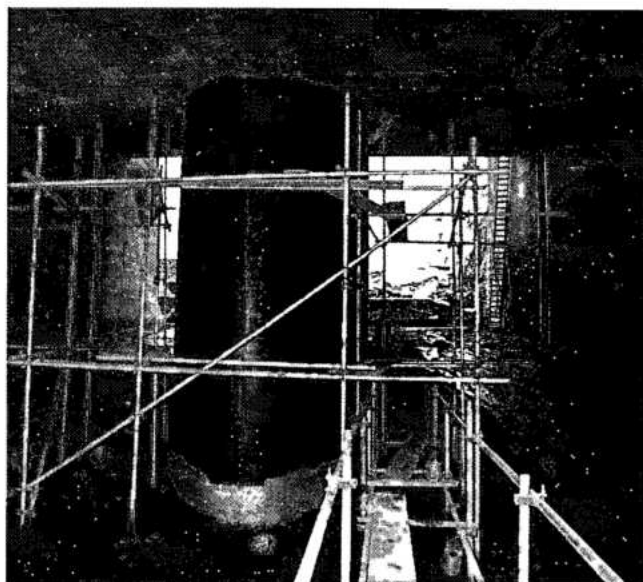
Manufacture of turbine runner



The runner was statically balanced by mounting it on a special hydrostatic balancing ring and removing metal as necessary from the runner band.

Air admission

The model tests indicated that air admission was necessary to improve hydraulic stability at the upper and lower boundaries of the normal operation region, and on the first three 50 Hz units to reduce noise and cavitation when operating in the very low load region. Air admission to improve hydraulic stability is effected via a tube extending from the top of the generator to the center of the runner cone, see Fig. 12.1. The aeration valve at the top of the generator automatically admits atmospheric air when the pressure at the runner drops below a set value. Should the valve fail for any reason and in the event that the tailwater is above El.106.35, water is prevented from entering the generator by a system of labyrinths and drainage pipes. The effectiveness of the labyrinths was confirmed at speeds up to runaway by full scale shop tests. The air admission pipe was coated internally with hot sprayed zinc and painted to prevent rusting. Compressed air admission for low load operation is via the top cover and bottom ring into the vaneless space between the wicket gates and runner. There is one compressor for each low load 50 Hz unit, supplying 2300 m³/h air at a working pressure of 1.25 N/mm².



Draft tube central pier

Draft tube liner and pit liner

The concrete part of the draft tube is split into two sections by a central pier, the nose of which is lined with steel. Two draft tube bulkhead gates are required to isolate the turbine from the tailrace, see Chapter 13.

The draft tube has a steel liner extending from the stay ring to the point where the average velocity of the water is 6 m/s at full load, just short of the draft tube elbow. The draft tube liner is embedded and anchored in the second stage concrete, and was designed to resist buckling from the maximum external water pressure with the turbine dewatered. It is formed from nine field welded segments. Segment number one is welded to the stay ring and has a shoulder which can support the runner during maintenance when uncoupled from the generator shaft. The first draft tube liner was shop assembled to verify plate alignment.

Two inward opening mandrels, each 760 mm wide and 1000 mm high, located on opposite sides of the draft tube liner provide access for inspection of the runner. There are three removable platforms for the eighteen units, which are supported by two beams which pass through holes in the draft tube liner. The beams are permanently stored near the draft tube access of each unit.

The turbine pit has a plate lining, which prevents the ingress of leakage water from the concrete and also serves as formwork for placing the concrete. Attached to the liner are electrical wires and pipes. These ensured alignment of the embedded pipelines to the pipes which run inside the turbine pit. The pit liner also has two access openings to the turbine pit and blockouts for the servomotor supports. It is formed from eight segments assembled and welded in the powerhouse assembly bays.

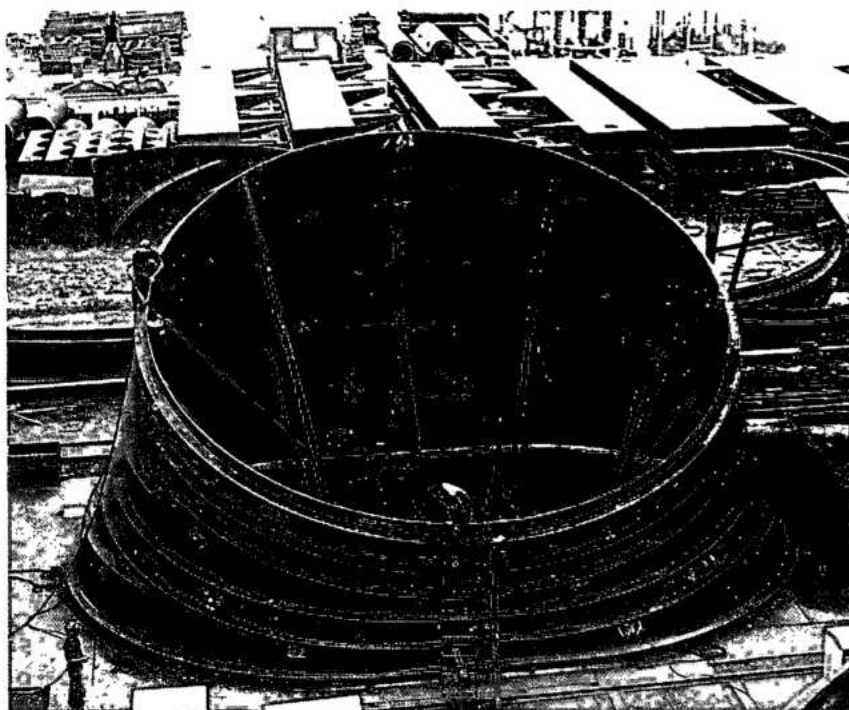
Attached to the upper part of the pit liner is a flange with a circular track, on which there is a 100 kN crane used for maintenance of the equipment in the turbine pit.

ERECTION TESTING AND COMMISSIONING

Erection

Because of transport limitations some of the major parts of the Itaipu turbines were assembled at site, the component parts leaving the manufacturer's works in sections for coupling or welding.

A large blockout was provided in the first stage concrete for the complete turbine generator unit. In this

*Draft tube liner*

way the powerhouse could be constructed independently of the generating units and in particular, the powerhouse crane rails could be laid to provide crane access to the units under construction.

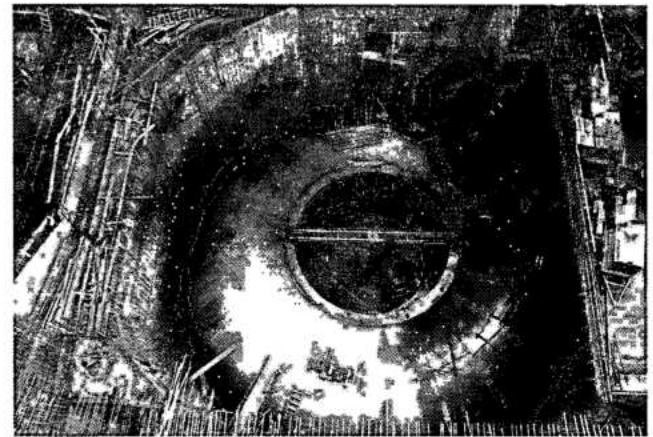
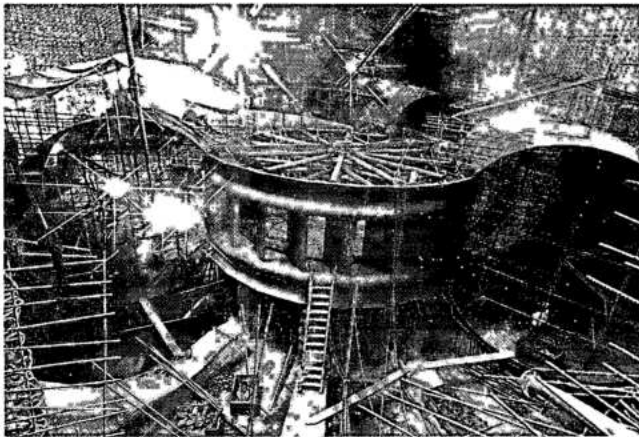
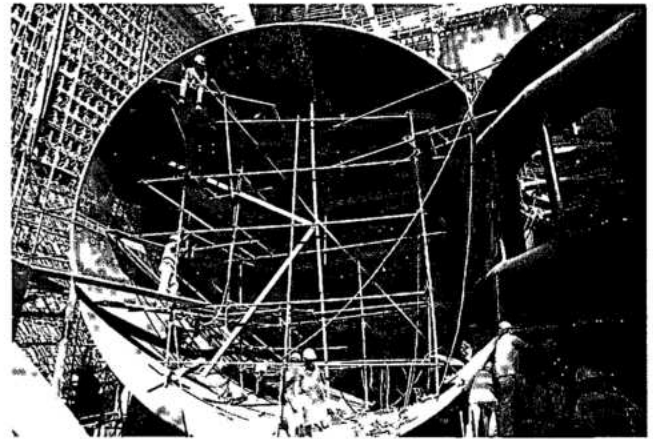
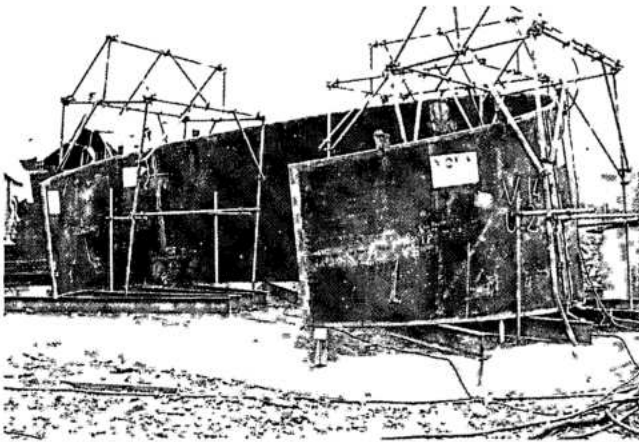
Draft tube liner

The rolled plates which formed the draft tube liner were lowered into the block out and manually welded in situ with full penetration double V welds, making the individual segments of the liner. Each segment was supported by the one below and the circumferential welds progressively made. During erection, the liner assembly was tied back to the first stage concrete with turbuckle rods, and anchor bars were welded to the structure to provide the keys for second stage concreting.

Spiral case and lower bend

After the draft tube liner was embedded, the concrete plinths for the spiral case and lower bend were formed. The individual shop rolled and cut plates which formed the spiral case and lower reducing bend were welded together into segments in a pre-erection area on the left bank, away from the

powerhouse. Welds were ultrasonically tested and X-rayed before the segments were moved to the powerhouse. Stay ring quadrants were mounted on their concrete supports and welded. Great care was taken in levelling and welding the stay ring to minimize residual stresses. To this end the fit of the stay ring was made as accurately as possible and pre-and post-weld heating was used with balanced welding techniques to control the difference in weld shrinkage between the top and bottom rings to within 1 mm. Erection and welding of the stay ring required about 25 days. The spiral casing segments were manually welded, to each other and to the stay ring. Before welding, the segments were preheated to about 150°C. The interpass temperature was limited to 250°C and after weld completion the structure was maintained at the preheat temperature for approximately 2 hours. The welding of the circumferential seams was started simultaneously at the spiral case inlet and the small end of the casing. The top and bottom joints of the spiral case to the stay ring were welded concurrently. Welding of the spiral case with a team of about twenty welders took approximately 100 days and required 16.5 tons of electrodes.



Erection of turbine spiral case

The completed segments for the lower bend were reinforced with an internal spider for transport and welding. Segments were lowered by a 3 MN crane operating from El. 144 on to a rail-mounted trolley which was used to convey the segments from El. 144 down the blackout to the spiral case area. Segments were mounted on supports and the circumferential joints welded manually, starting from the spiral case. All spiral case and lower bend welds were first tested ultrasonically, dye checked and then 100% X-rayed. The joint between the stay ring and the top section of the draft tube liner was made at the assembly area and transported to the turbine pit and carefully fitted to the next draft tube lower section. After pressure testing a seal plate was welded between the two sections and then the scroll case was pressurized and concreted. The make up joint between the two draft tube sections was finally welded from inside the draft tube. Plastic sheets were placed between the plinths and the assembly

to ensure free movement during the pressure test and mastic was inserted at the corners of the plinths to guarantee an even distribution of loads. The end plates of the stay ring were flame cut ready for the test ring, with a rig mounted on a temporary support in the draft tube. The reusable test bulkhead was welded to the upper end of the lower reducing bend, and the hydrostatic test pressure sequence of Fig. 12.35 was achieved by a pumping set. All welds were monitored for water-tightness. The pit liner, which was erected outside the powerhouse, was welded to the stay ring and the embedded supports for the servomotors attached. The spiral case and lower bend were surrounded with distribution reinforcing bars, embedded piping was installed and then all was embedded in concrete with an internal pressure of 120 N/cm^2 maintained by an elevated water tank. Thus, in service the spiral case (and lower bend) support most of the internal pressure, with only a small percentage transferred to

the concrete. Concrete was poured in layers as shown in Figs. 12.36 and 12.37.

Above El. 87.5 the pour was straightforward and done at 25 cm/h. However, below this elevation the pour was conducted in three stages with two concrete pumps. Plastic and galvanized steel pipes were led from possible void areas to the outside, for pressure grouting after the pour. The three stages were as follows:

Stage 1. Between El. 81.2 and 82. Region between powerhouse B line and supports 84 and 85, see Fig. 12.36.

This concrete was fed through funnels on the outside of the spiral case.

Stage 2. Between El. 82 and 82.9. The area between B line and support B11. Concrete was fed through funnels on the outside of the spiral case and holes in the stay ring.

Stage 3. Between El. 82.9 and 87.5. At a concrete pour velocity of 12 cm/h around the complete spiral case, through funnels and holes in the stay-ring Vibrators of 90mm diameter were used through the same holes to consolidate the concrete.

To avoid any possibility of stress corrosion cracking the inside surfaces of lower reducing bend, spiral case and draft tube liner were sandblasted and painted with zinc rich epoxy primer and coal tar epoxy finish coats.

Installation of the bottom ring

The two halves of the bottom ring were levelled to an accuracy of 0.1 mm in the assembly area and the mating surfaces cleaned and coated with silicon grease and bolted together. Roundness of the bottom ring to an accuracy of $+ 0.6 \text{ mm} - 0.0 \text{ mm}$ was ensured with a centrally mounted spider support.

For all units, other than the first two 50 Hz units, bottom ring wicket gate bearing holes were finally reamed using the top cover as a template. For these units the fibreglide wicket gate bearings were shrunk in at $- 80^{\circ}\text{C}$ and secured with loctite. The bottom ring was lowered into the turbine pit and, after positioning it on the stay ring, holes were drilled and tapped for the holding down bolts, through the hole for each wicket gate bearing. The bottom fixed wearing ring was attached to the bottom ring and seal welds made.

Preparation of the head cover

Two halves of the head cover were bolted together in the assembly area with the mating surfaces sealed with silicon grease.

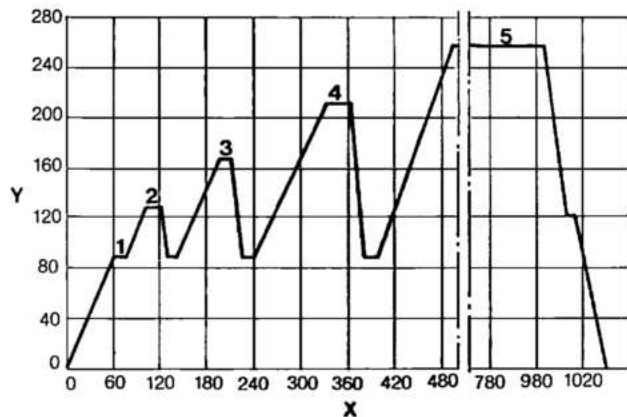


Fig. 12.35 Hydrostatic test pressure

Y Pressure (N/cm ²)	X Time (minutes)
1 90	
2 130	
3 170	
4 215	
5 252	

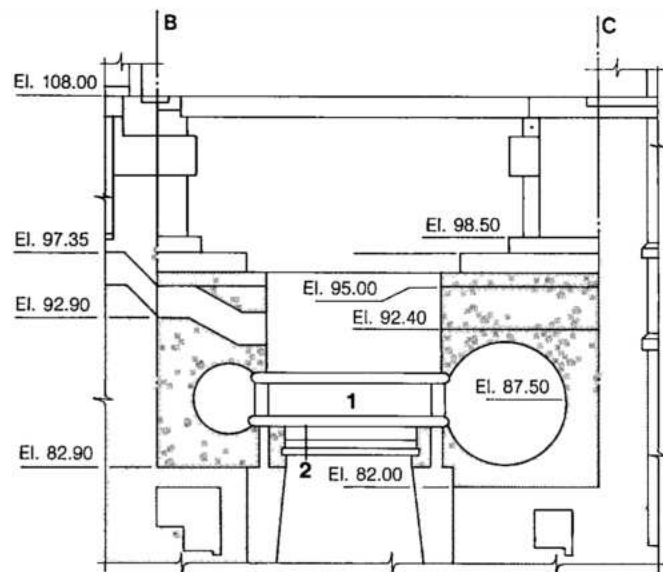


Fig. 12.36 Layers of concrete poured around the spiral case and generator's pit up to El. 96

First stage concrete
 Second stage concrete

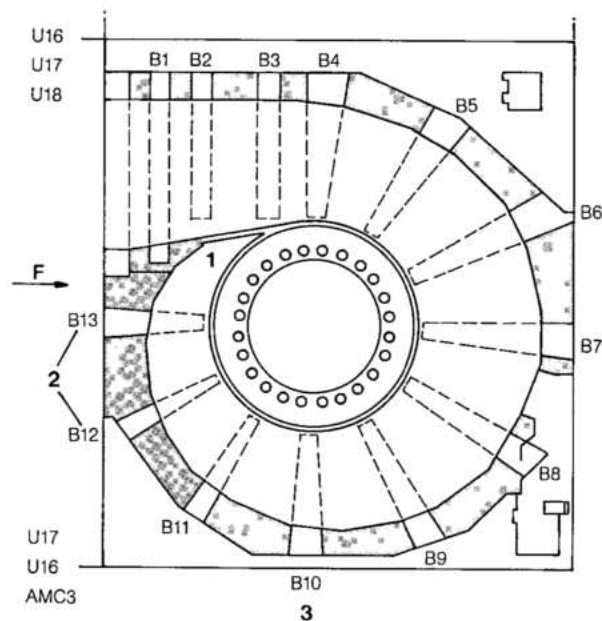
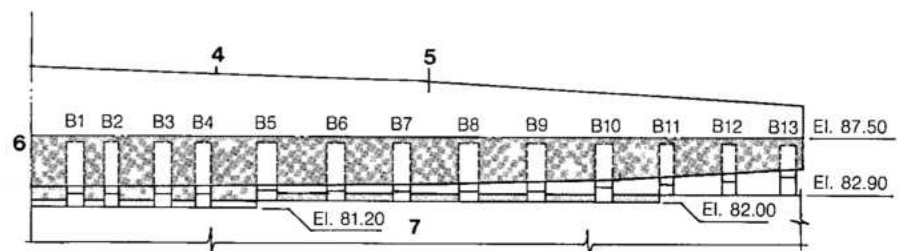


Fig. 12.37 Concrete phases of layer "87" poured around the spiral case

- 1 Extreme end of the spiral case
- 2 Supports
- 3 Plan at El. 82.2
- 4 Upper level of spiral case
- 5 Invert level of spiral case
- 6 Concrete layer "87"
- 7 Developed length of spiral case
- F Flow direction



Eight wicket gates were then provisionally installed in the bottom ring and the head cover supported on them. After positioning checks, holes for the head cover holding bolts were drilled and tapped using the head cover as a template.

The head cover was then removed and in it were installed piping, oil pumps, and drainage pumps. At this stage the upper stationary wearing ring was bolted to the head cover and seal welded. Also the emergency seal was installed, as well as the retaining plate for the main shaft seal.

Installation of the turbine runner

The turbine shaft was mounted on the runner in the assembly area and the holes for the coupling bolts in

both items finish reamed. The runner was transported to the turbine pit and supported on the ledge in the draft tube liner. After installation of the twenty-four wicket gates the turbine shaft was coupled to the turbine runner in the pit, the head cover lowered into position and levelled by spacer washers at the holding down bolts. Up to this stage, total erection had taken about 3 years from the start of draft tube erection.

Other turbine parts

Servomotors and the operating ring were installed and the turbine was ready for coupling to the lower generator shaft. Installation of the turbine shaft seal, guide bearing and servomotor linkage could then proceed in parallel with generator erection.



Lowering of runner



Equipment in turbine pit

Commissioning and testing

The measurements made during commissioning confirmed the results of the model tests and calculations, in that all contractual values were complied with. Of particular interest:

- The guaranteed output values were reached and, depending on wicket gate opening, exceeded by about 1% to 3%.
- Pressure fluctuations in the spiral case showed a negligibly small amplitude over the entire load range, see Fig. 12.38.
- The amplitudes of the pressure fluctuations, measured in the draft tube cone, confirmed the values scaled from the model tests, see Fig. 12.39.
- In the part-load range, the frequencies of the draft tube vortex correspond to those found in the model test. As shown in Table 12.8, the supply of stabilizing air resulted in a further reduction of the noise level during operation. No interaction between the pressure fluctuations and the dynamic characteristics of the plant was observed at any load.

Table 12.8 Noise level in the turbine pit

Output %	Noise level in db A	
	With air	Without air
100	95.5	97.5
60	90	93
30	92	98.5

- As is evident in Fig. 12.40, the pressure and speed rises measured during load rejections confirmed those calculated.
- The shaft and bearing vibration amplitudes measured at the various measuring points of the turbine were less than the contractually guaranteed values, see Fig. 12.15.
- Measured turbine bearing temperatures at full load operation were 43° C for the oil and 52° C for the pads.

Fig. 12.38 Measured spiral case pressure fluctuation

Y Pressure fluctuation
X Unit output (MW)
X₁ Wicket gate opening (mm)

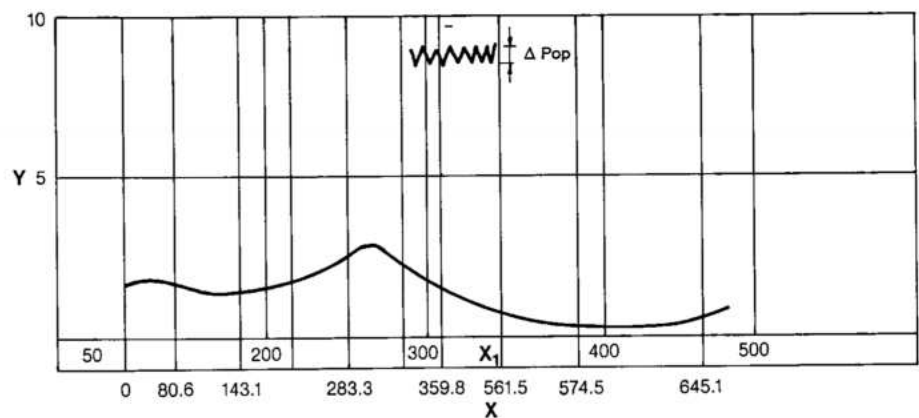
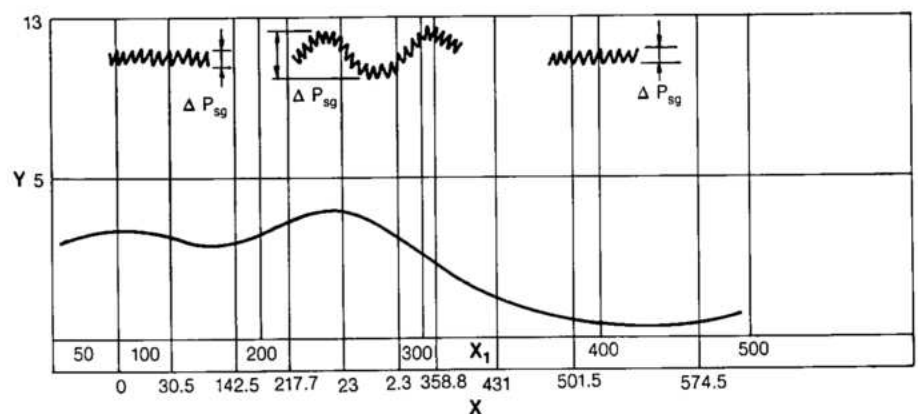


Fig. 12.39 Draft tube cone pressure fluctuation

Y Pressure fluctuation
X Unit output (MW)
X₁ Wicket gate opening (mm)



• Torque fluctuations measured at the turbine shaft by means of strain gauges were less than the guaranteed value of $\pm 2^\circ$ of the rated torque.

In addition, special tests were conducted as follows:

Strain gauging of unit 1 during the pressure test.

Strain gauges were placed on the stay vane welds and on the attachment of the spiral case to the stay ring. Apart from a few extraneous results which could be attributed to strain gauge errors, in general the stay vane stresses were within 10% of those calculated.

Measurement of the dynamic stresses in the stay vanes by strain gauges. The results of strain gauge measurements taken during operation of the turbine are shown in Fig. 12.41. As the measured stresses were low, it was concluded that there was little possibility of cracking of the vanes as a result of fatigue. This was also evidenced by the complete absence of in service cracks, as confirmed by regular dye and ultrasonic checks of the welds between the stay vanes and stay ring.

Head cover deflection under pressure. The head cover deflection was accurately measured and

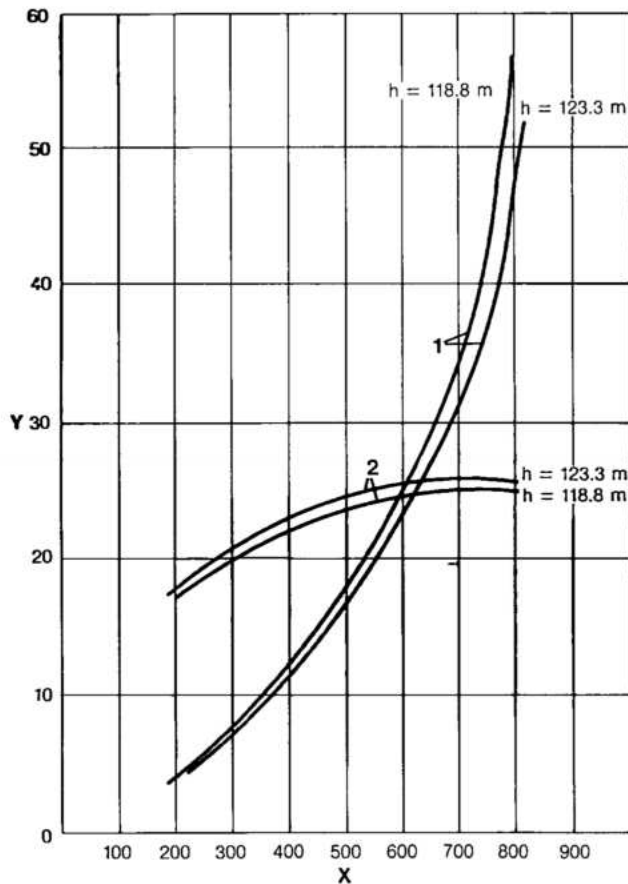


Fig. 12.40 Load rejection tests

Y Speed and head rise (%)
X Generator output (MW)
1 Head rise
2 Speed rise

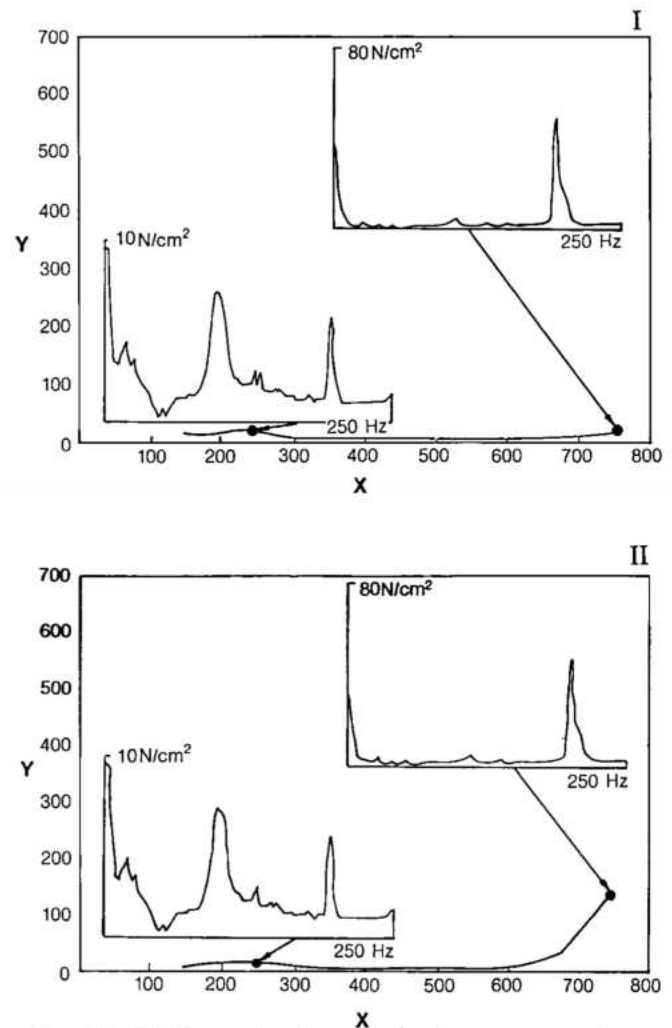


Fig. 12.41 Dynamic stresses in stay vane no. 4

I Amplitude at 108 Hz
(lowest bending critical frequency)
II Amplitude at 196 Hz
(lowest torsional critical frequency)

Y Dynamic stress
($N/cm^2 \cdot 2\sqrt{2} \text{ rms}$)
X Turbine flow (m^3/s)

compared with the results of the finite element analysis. This is an important factor because wicket gate end clearances should be minimal to avoid excess leakage and high residual torque, but adequate to prevent touching when the cover deflects under pressure. The measured deflection was 0.73 mm compared with the 0.74 mm calculated.

The measured leakage rate with wicket gate end clearances of 0.5 mm at the top and 0.9 mm at the bottom (measured after an initial settlement period) was 1.65 m³/s compared with 3.5 m³/s specified. A valve lower than the specified value was necessary to ensure that the residual speed of the unit with the wicket gates closed would be less than the specified 20%, an important factor in minimizing the wear of the generator brakes.

OPERATING EXPERIENCE

Performance of the Itaipu turbines has been excellent. They were commissioned without any problems and have been in continuous trouble-free operation for many years. The only repair work

conducted has been on minor cavitation damage to runners through 1988.

The extent of the stainless steel protection on the runner surface was based upon observations made on the turbine model. Such observations could only account for regions of large underpressure which were evidenced in the model by bubble trails and vortices. In respect of large cavitation effects, the information obtained from the model was complete and the cavitation guarantees in operation were fulfilled. However, localized cavitation, which could not be identified in model test, was experienced in the first operating units as shown in Fig. 12.42. The cavitation damage, as shown, started to become apparent at approximately 4000 hours operation and could be divided into specific areas as follows:

- Cavitation damage on the crown in areas A due to low load operation, especially without admission of air. As shown in Fig. 12.43, swirling vortices are formed in the channel, giving rise to low pressure areas at A.

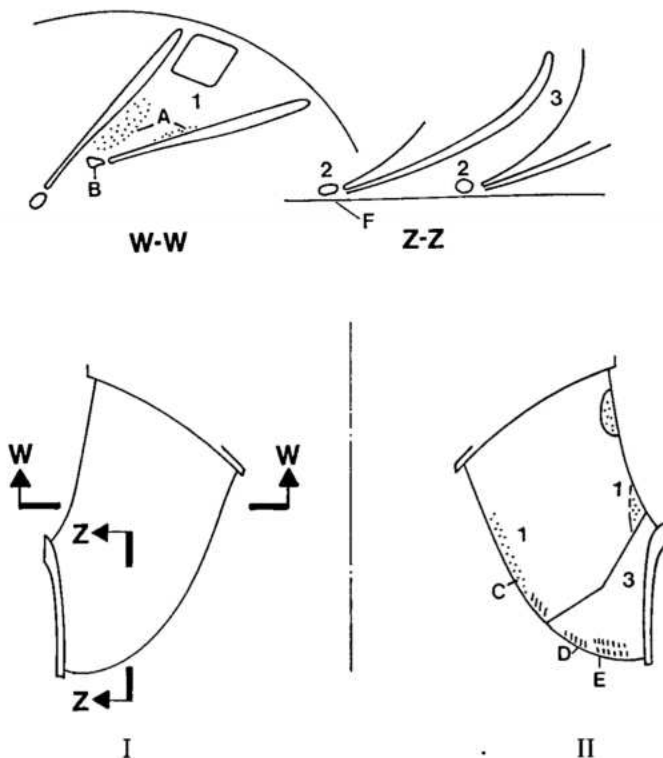


Fig. 12.42 Cavitation damage on runners

A, B, C, D, E Cavitated areas
I Pressure side
II Suction side

1 Minor cavitation to carbon steel
2 Major cavitation to carbon steel
3 Stainless steel

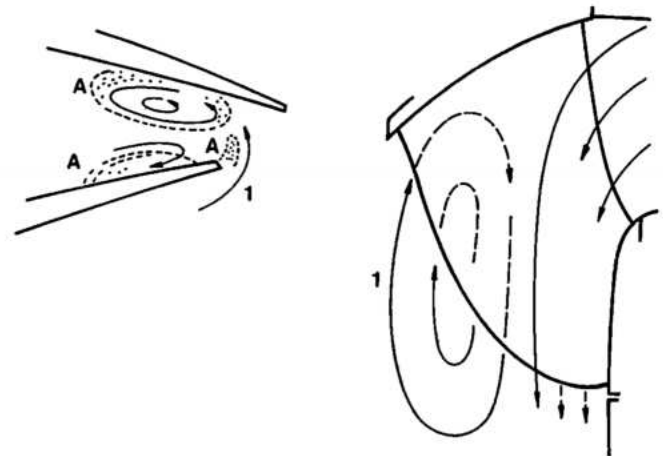


Fig. 12.43 Vortex formation

A Cavitated areas 1 Upflows around the blade

- Cavitation damage on the crown in area B is a direct result of Karman vortices as shown in Fig. 12.44, as is the damage on the blade outlet edge (areas C, D and E) and the runner band (area F), see Fig. 12.45.

Although the damage was slight, in order to avoid difficult repairs in service it was decided to extend the stainless steel protection on the units then in erection or manufacture, as shown in Fig. 12.46.

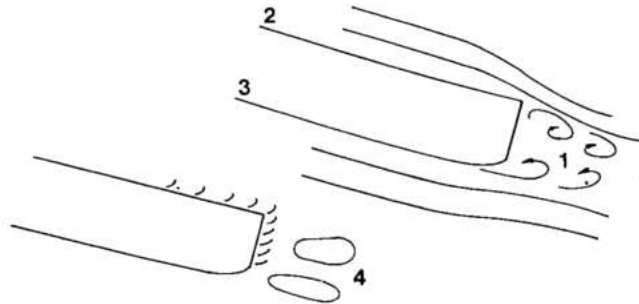


Fig. 12.44 Vortex formation

- | | |
|-----------------|--------------------------|
| 1 Vortex | 3 Suction side |
| 2 Pressure side | 4 Highly cavitated areas |

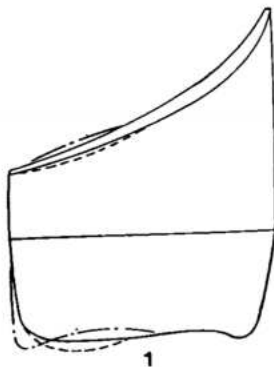


Fig. 12.45 Cavitation damage at the blade outlet

- | | |
|---|--------------------------|
| 1 Depression along the profile in the blade outlet area | 3 Implosion area |
| 2 Vortex imploding in the fluid area | 4 Vortex attachment area |



Cavitation damage

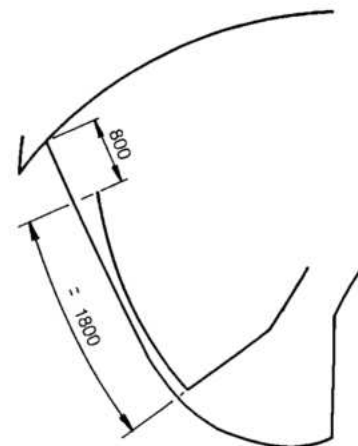
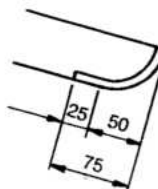
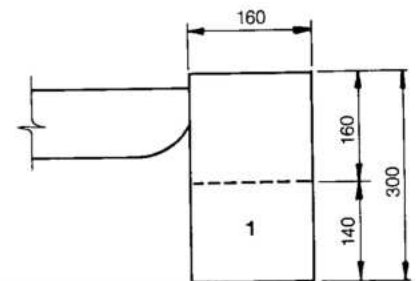


Fig. 12.46 Stainless steel protection

- 1 Runner band

TURBINE GOVERNORS

GENERAL CONSIDERATIONS AND BASIC CHARACTERISTICS

The functions to be performed by a turbine governor are basically those of controlling the starting phase of the unit by assuring a stable and precise speed control at no-load conditions, permitting a fast synchronization with the electrical system, and assuring stable operation of the unit under various network and load conditions. The latter necessitates sharing the generator power with other units on the system according to previously established load-frequency characteristics of the unit in steady-state conditions, and keeping the transient frequency deviations resulting from load disturbances to within acceptable values.

In the wider task of the frequency and active power regulation in an interconnected system, the role of the turbine governor may be extended to participation in secondary regulation in a power/frequency inter-areas load exchange scheme under the control of a network central authority.

At Itaipu, because of its importance in the Brazil-Paraguay interconnected system, all these functions have to be accomplished within particularly stringent values, which is made more difficult by the differing requirements of the two national electrical systems.

The 60 Hz feeds the Brazilian network through a relatively long ac transmission system, whose characteristics are subjected to change during its development period, starting from a single uncompensated line to a final scheme of four lines, series and parallel compensated.

The 50 Hz sector is connected to the smaller Paraguayan system and to a high voltage dc (HVDC) transmission system, which in the first approximation is equivalent to an isolated passive load without inertia and with no intrinsic auto-regulation and in which the frequency oscillations are to be kept within small limits so as not to detune the HVDC filters.

The characteristics needed to fulfil these requirements are:

- Precise, stable and low-drift speed value.
- Small dead-band.
- Fast response to speed changes.
- Great adaptability to different system conditions, which implies wide ranges for the setting of the main parameters of the governor.
- Possibility of participating in joint-control operation.

- Possibility of accepting external signals for dynamic stabilization purposes, or to participate in a general power/frequency or load exchange regulation scheme depending on external network requirements.

The turbine governor chosen to meet the requirements of both the 60 Hz and 50 Hz systems is the electronic Proportional, Integral, Derivative (PID) type with hydraulic amplification. The settings of the various sections of this governor are individually adjustable, thus giving the high degree of flexibility required for the Itaipu application.

Structure

The Rapid 77 governor has a two tier structure in which the speed and load governing section and the positioner section are physically and functionally separate. Feedback for the PID is taken from the electrical signal supplied to the main oil distributing valve, and the hydraulic positioner/wicket gate servomotor circuit has its own feedbacks via a signal taken from transducers on the wicket gate operating mechanism and on the spool of the main distributing valve, see Fig. 12.47. This two tier structure facilitates the layout of the governor, assists maintenance and improves operational reliability. For small displacements the variables can be assumed to be linear, and thus the system can be expressed in terms of linear differential equations and their respective transfer functions which are shown for the speed governor and hydraulic positioner/wicket gate servomotor circuits in Figs. 12.48 and 12.49.

With reference to Fig. 12.48 the speed governor has the three PID terms as follows:

Proportional (P). It gives a signal proportional to the difference between actual turbine speed and that required (speed error). Because of the high inertia of the water column and lags in the oil hydraulic circuit, this speed error signal has to be moderated by a proportional constant ($1/b_t$); b_t is equivalent to the temporary speed droop, its inverse being necessary in this case because it is acting directly on the input signal, rather than on the feedback signal as was normal in earlier governors (both mechanical and electronic). As with any temporary speed droop, if acting alone the proportional signal (P) would produce an unacceptable error in steady state speed as a function of wicket gate position.

Integral (I). It is a signal dependent on the integral of the speed error and eliminates the permanent speed error inherent in the proportional action. It is equivalent to the dashpot action of a mechanical

governor, the inverse of T_d subscript again being used because of its position in the input circuit rather than the feedback.

Summation of the proportional and integral actions at exit signal gives the normal PI transfer function in terms of temporary speed droop (b_t) and dashpot constant (T_d).

Differential (D). It is a signal dependent on the differential of the speed error, and makes the initial wicket gate movement fast in response to a system perturbation, hence improving the response of the governor without adversely affecting its stability. The

differential action of the governor is placed ahead of the proportional ($1/b_t$) and integral action ($1/T_d P$), which is advantageous in that the phase advance due to the differential action contributes to de-saturate the effect of the integral action.

Some idea of the effect of the variables b_t , T_n and T_d on the speed response of the unit to small disturbances at the no-load condition is given in Fig. 12.50.

The changeover switch from the frequency set-value to the network frequency is provided to permit a rapid synchronization of the unit. Load sharing of Itaipu with the rest of the electrical system

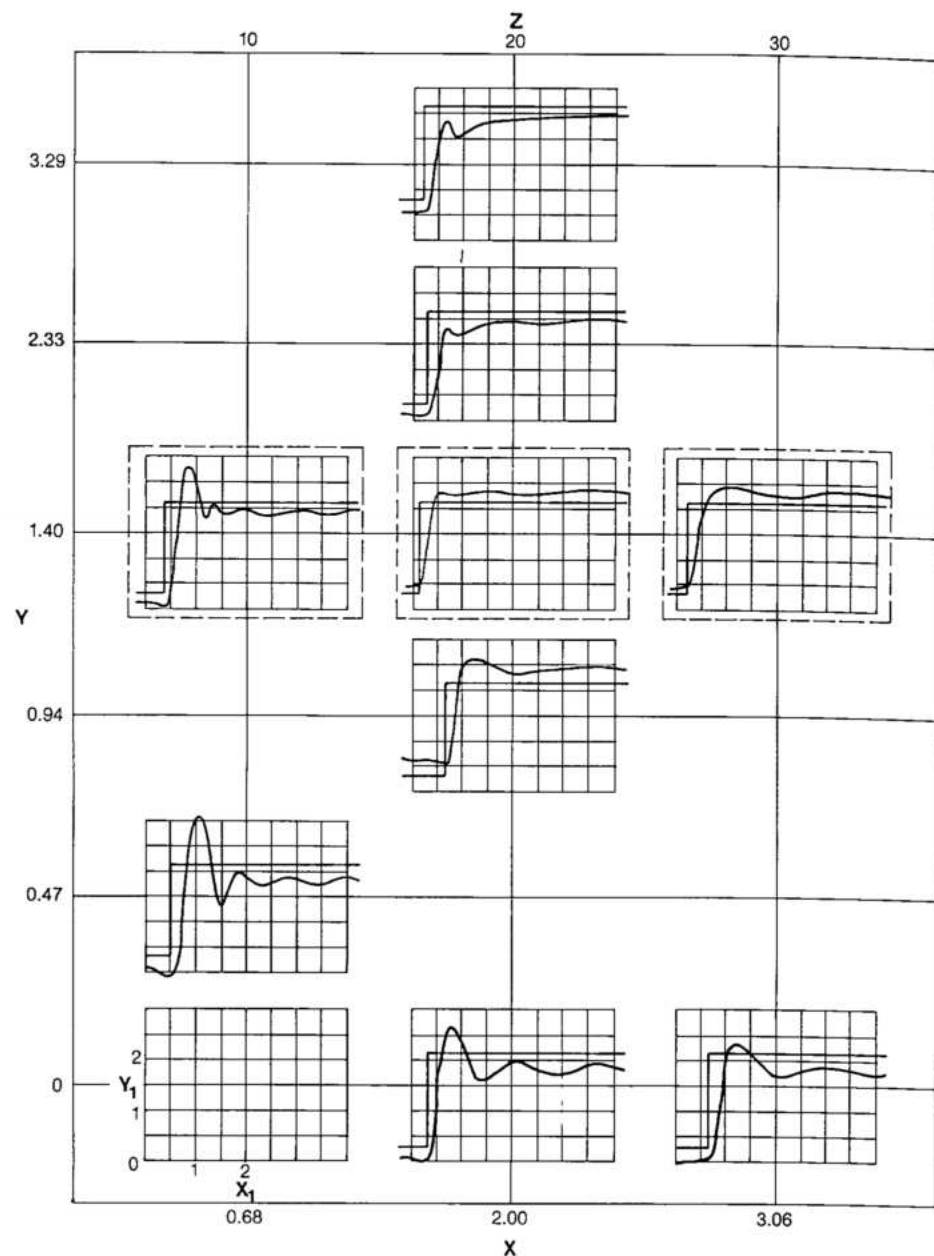


Fig. 12.50 Governor powerhouse tests

Y T_n (s)
 Y₁ f_n (%)
 X T_d (s)
 Z b_t (%)

is achieved via its relative permanent speed droop (b_p), unless under joint load control, see Chapter 14.

For detailed calculations of the Itaipu governor in the case of big disturbances, the main non-linearities present in the electric and mechanical elements of the regulating system were modelled, including a non-linear representation of the turbine.

Basic characteristics

The governor has the following basic adjustments and characteristics:

- Standard range for parameter adjustment:
- Permanent speed droop b_p : 0 to 10%
- Temporary speed droop b_t : 20 to 200%
- Time constant of the damping device T_d : 1 to 11 seconds.
- Derivate time constant, T_n : 0.2 to 2.2 seconds
- Governor characteristics:
- Promptitude time constant T_x : $0.05 \text{ s} < T_x < 0.5 \text{ s}$
- Speed dead band, $i_x < 10^{-4}$
- Command signal dead band $i_c < 2 \times 10^{-3}$
- Governor inaccuracy relative to the servomotor position $i_y < 2 \times 10^{-3}$ for $b_p = 5\%$.
- Typical set values for Itaipu (50 Hz units):
- $b_p = 3\%$ to 5%
- $b_t = 40\%$
- $T_d = 8$ seconds
- $T_n = 1$ second.

COMPONENT DESIGN

A simplified diagram of the speed control element of the Rapid 77 governor is shown in Fig. 12.51, and for the hydraulic positioner/wicket gate servomotor in Fig. 12.52.

Governor cubicle

The governor control cubicle for each unit, incorporating the components of the speed governor (shown inside the dotted line of Fig. 12.51), is located in the local control room at El.108. The cubicle is 600 mm x 600 mm by 2.1 m high and contains:

- Vertically mounted printed circuits.
- Selector switch for permanent speed droop.
- Graduated potentiometers and selector switchings for changing governor PID parameters.
- Unit frequency analog indicator.
- Governor fault indicator.
- Voltmeter and test points.

The other governor controls and indications are mounted in the panels of the local and central control rooms, see Chapter 14.

There are two types of circuits in the governor:

- Main speed governing circuits.
- Auxiliary circuits such as remote indication signals, speed switches and other sensor switches.

Each of these two types of circuits has its own power supply.

Main speed governing circuit

The power supply for the main speed governing circuits is from the powerhouse 120 V ac auxiliary supply through an internal transformer and a rectifier, giving $\pm 24 \text{ V dc}$ which supplies the relays controlled by the flip-flops of the load frequency setting and wicket gate opening limit setting. In the event of a failure of the powerhouse 120 V ac supply, the supply switches to two 20 V nickel cadmium batteries, kept under permanent charge. These batteries have sufficient capacity for up to 1 hour of operation.

The $\pm 15 \text{ V dc}$ supply is obtained from the $\pm 24 \text{ V dc}$ supply for the operational amplifier static change-over switches, transistors, etc. and by means of an oscillator, the 50 V 400 Hz which supplies each the variometer, and the 12.7 V 400 Hz which supplies the galvanic separators and electronic circuits of the power transducer. Also obtained from the 24 V dc supply via an oscillator is the $2 \times 20 \text{ V 400 Hz}$ feed which after rectification gives the 24 V fault signal.

Auxiliary circuit power supplies

Power for the auxiliary circuits is taken from the 125 V dc station power supply through dc to dc converter to give the following:

- 15 V dc for the auxiliary frequency measuring circuit and the remote indication circuits of load frequency setting wicket gate opening limit setting and power.
- 48 V dc for the speed relay.
- 10 V dc for the remote indication of wicket gate position, and via oscillators to give 127 V ac 400 Hz for remote indication galvanic separators and the digital voltmeter.

Frequency sensing

The signals for unit and network frequency are taken from voltage transformers on the generator 18 kV bus and the main 500 kV bus. The frequencies are converted to a dc signal and compared, the difference being fed into the PID section of the governor. A reference signal can be used instead of the network frequency in the event of an isolated start. There is always enough residual magnetism in the generator to produce a signal, even before the initial excitation of the generator.

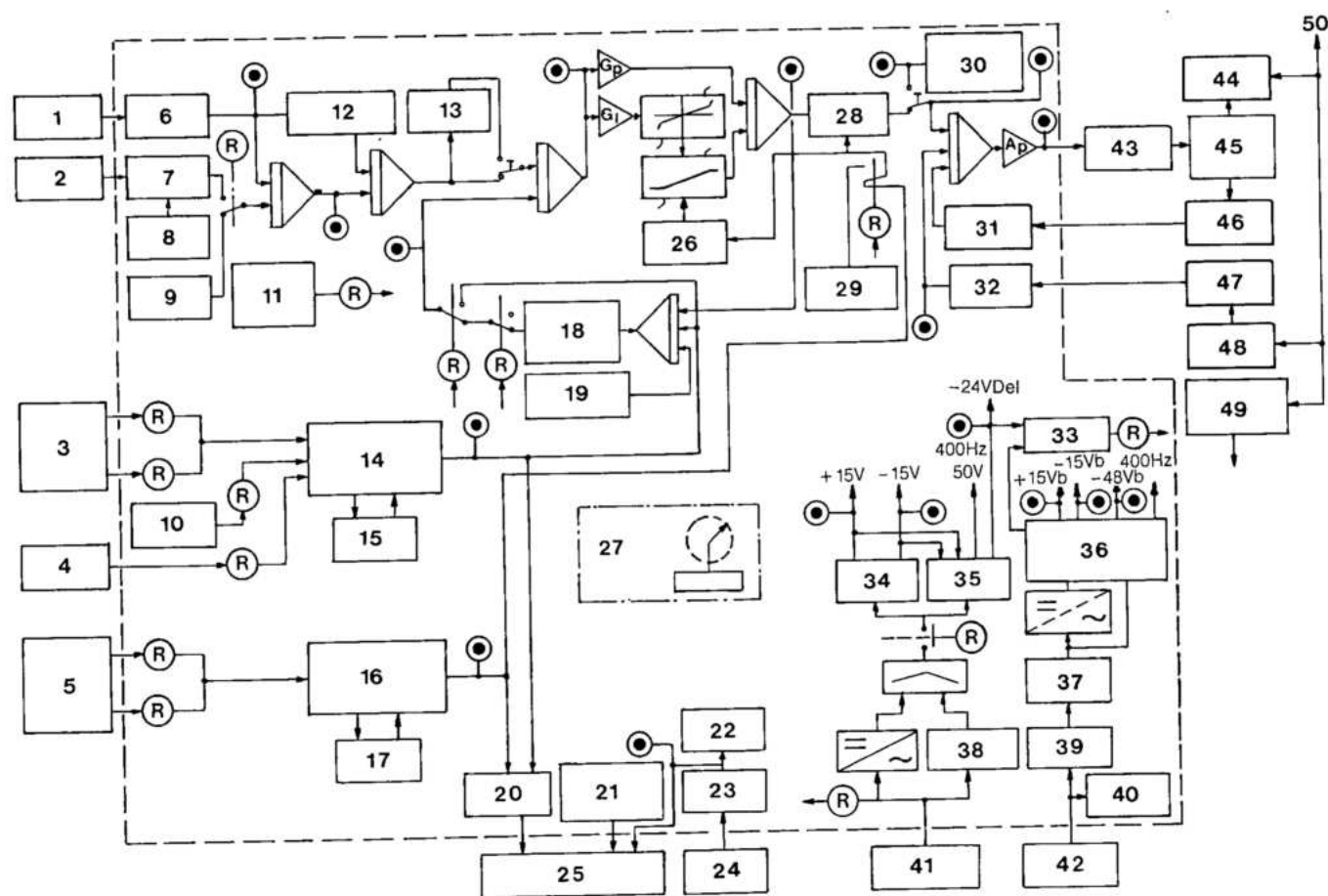


Fig. 12.51 Rapid 77 simplified diagram

- | | | | |
|---------------------------------|---|--|------------------------------------|
| 1 Unit frequency | 14 Digital load frequency | 26 Clipping | 38 Battery and maintenance |
| 2 Network frequency | 15 Position detection | 27 Voltmeter and switch for test | 39 Protective cell |
| 3 Load frequency control | 16 Digital opening limiter | 28 Minimum selection | 40 Relay supply |
| 4 Zero resetting | 17 Position detection | 29 Starting bias voltage | 41 ac auxiliary supplies |
| 5 Opening limiter control | 18 Permanent speed b _p droop | 30 Wicket gate manual control | 42 Power plant battery |
| 6 Converter F/U | 19 Speed no load bias voltage | 31 Detection | 43 Actuator |
| 7 Converter F/U | 20 Galvanic separators | 32 Detection | 44 Servomotor |
| 8 Shifting | 21 Governing unit potentiometer | 33 Supply failure | 45 Oil distributing valve |
| 9 Reference frequency | 22 Speed switches | 34 Electronic supply | 46 Variometer |
| 10 Speed selector | 23 Converter F/U | 35 Oscillator 400 Hz | 47 Variometer |
| 11 Frequency transducer failure | 24 Unit frequency | 36 Speed switch and remote indication supply | 48 Linear cam |
| 12 Accelerometer | 25 Remote indications CF L.O. wicket gate frequency | 37 Oscillator 400 Hz | 49 Remote indication potentiometer |
| 13 Dead band for testing | | | 50 Wicket gate |
| | | | • Test points |

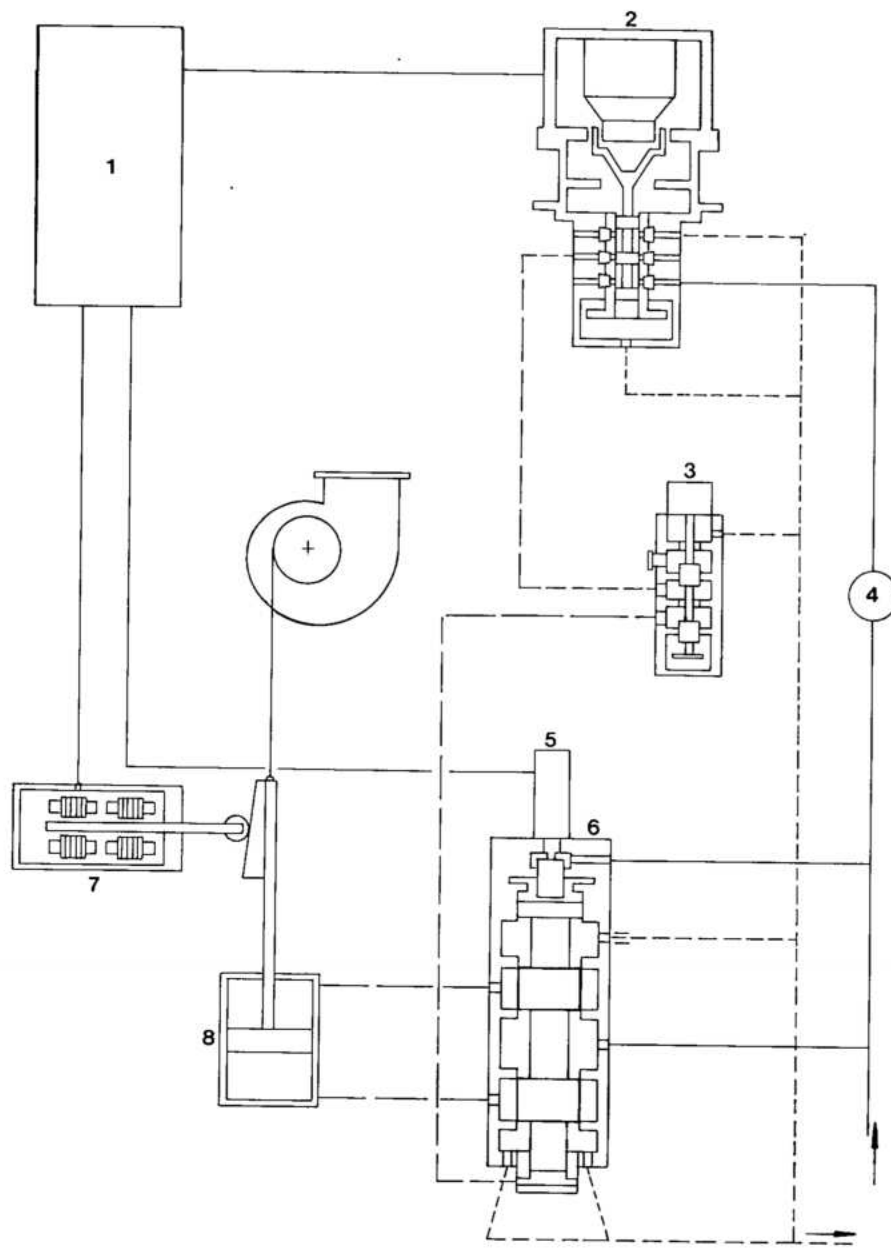


Fig. 12.52 Simplified diagram of governor's hydraulic system

- 1 Speed governor
- 2 Actuator
- 3 Shutdown solenoid valve
- 4 Filter
- 5 Distributing valve
- 7 Variometer
- 8 Servomotor

During startup, before the unit circuit breaker is closed, the governor adjusts the speed of the unit until the two frequencies are equal, but not necessarily in phase. Synchronization can then be done automatically or manually, as selected by the manual/automatic selector switch. To assist the synchronizer the governor automatically sets the unit frequency 0.1 Hz lower than the network frequency, corresponding to a beat period of 10 seconds.

Hydraulic equipment

Hydraulic equipment including the hydraulic positioner, the governor pumping set and the

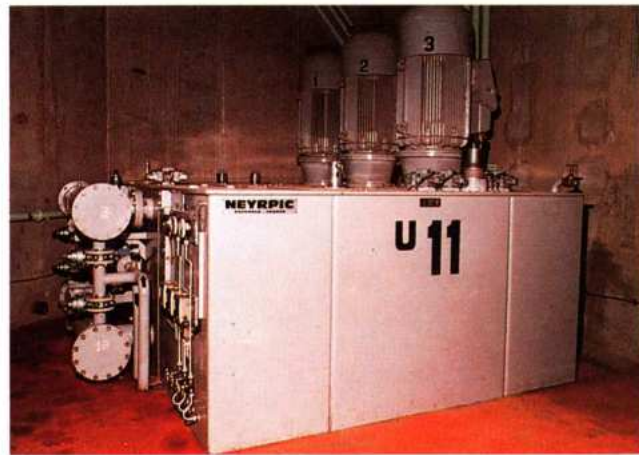
oil/air pressure tanks are located at El. 98.5. The governor compressors are located in the compressor room on the downstream side of the generator, at the same elevation. A simplified schematic of the system is shown in Fig. 12.52.

Hydraulic positioner

Mounted on the tank of the pumping set, are the actuator, the shut down valve, and the distributing valve. Oil under pressure is supplied from the pressure tanks which are kept charged by the oil pumping set.



Governor pressure tanks



Governor oil pump set

A signal from the electronic governor activates a coil in the actuator which moves in a permanent magnetic field. This moves the spool of the pilot actuator valve, permitting the oil pressure to move the spool of the distributing valve. The distributing valve controls the flow to the main servomotors, which, in turn, move the wicket gates via the operating ring and levers. The variometers on the regulating ring and the spool of the distributing valve provide the necessary electrical feedback to the positioner part of the electronic governor.

For security there are two independent shutdown solenoids which are activated on the command to shut down the unit. These override the governor speed control permitting the exhaust of oil from the lower side of the actuator, which in turn shifts the

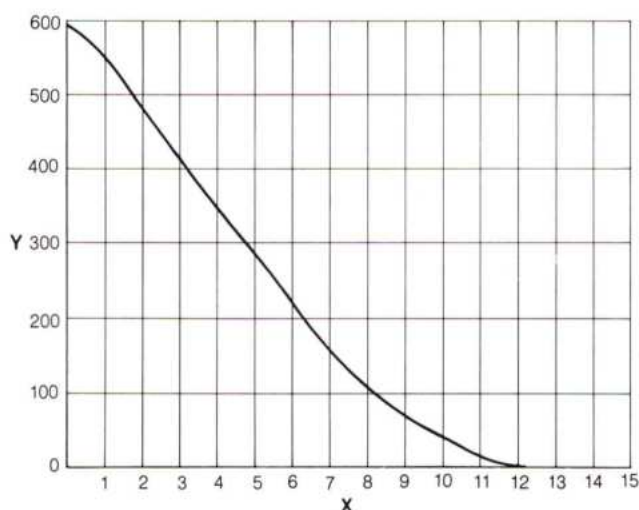
distributing valve to close the wicket gates at their maximum rate. The allowable closure rate is determined by the specified speed and pressure rise during load rejection, which for Itaipu necessitated a two stage curve as shown in Fig. 12.53. Cushioning during the last portion of the stroke is provided by orifices in the main servomotor.

Oil pumping set

The three three-phase induction-motor driven screw pumps mounted on the pumping set sump tank supply oil to the oil/air pressure tank, from which it is piped to the hydraulic positioner. During operation of the turbine, one pump is constantly in service, the pressure controlled idler valve determining whether the oil is pumped to the pressure tank or returned to

Fig. 12.53 Wicket gate closure law

Y Wicket gate opening (mm)
X Time (s)



the pumping set sump tank. The two other pumps are started sequentially in response to pressure tank mounted pressure switches. The 1000 l/min oil pumps are rated to have a combined per minute flow of at least 2.5 times the total volume of the wicket gate servomotors. The pumping set sump tank is sized for 110% of the oil volume of the entire governor system, which results in a storage volume of 4800 l. Two oil/water straight tube type heat exchanges on the side of the pumping set sump tank cool the governor oil; only one of these is normally used, the other acting as reserve. The pumping set sump tank has a level gauge, level switches, oil temperature thermometers, drain pipes and air breathers. Pump suctions have replaceable filters.

The three 8900 l pressure tanks, one containing oil and compressed air, and the other two only compressed air, are sized such that the volume of oil between the maximum pressure of 640 N/cm² and minimum pressure of 480 N/cm² allows five consecutive opening closing strokes of the wicket gate servomotors, without the pumps in operation.

Make up air for the pressure tanks comes from two air cooled compressors, each with 52 m³/h capacity, which supply a 1400 l auxiliary receiver. The compressors operate in response to pressure switches on the receiver and are rated so that the three pressure tanks can be charged from atmospheric pressure up to maximum operating pressure within 15 hours. Air is supplied from the auxiliary receiver to the pressure tanks via a solenoid valve which is operated from an oil high level switch in the oil/air pressure tank.

The pressure tanks auxiliary receiver and pumps are equipped with pressure relief valves. The supply pipe from the oil/air pressure tank has a quick acting valve which closes in response to a low oil level switch in the tank, to prevent air entering the system. Leakage oil from the main servomotors is collected in a small sump tank and pumped back to the pumping set sump tank.

turbine parameters resulted in nine 50 Hz and nine 60 Hz units each with identical turbines of 715 MW rotating at nearly the same speed, consistent with the integer pole ratios required for the two frequencies and the same moment of inertia.

The compensated 60 Hz transmission lines and the reactive compensation for load at the receiving end permitted a relatively high rated power factor of 0.95 resulting in a generator rated output of 737 MVA (0.98 generator efficiency). The 50 Hz generators supplying the HVDC transmission system also had to supply the reactive power corresponding to the balance between the reactive absorption of the converters plus filters at full load, with one filter out of service, resulting in a power factor of 0.85 and generator rating of 823.6 MVA.

The relatively long 60 Hz transmission lines requires good generator performance to assure system stability, that is relatively low reactance, high moment of inertia and high exciter ceiling voltage ratio.

The optimal overall generator characteristics were obtained adopting the maximum bore diameter with the maximum allowable stress for the rotor at the runaway speed and direct water cooling for stator winding, which permitted the 60 Hz units to have a synchronous reactance of 0.9 p.u. and an overload capacity of 766 MVA within relatively low temperature limits.

The synchronous p.u. reactance and the moment of inertia for the 50 Hz generators were made the same as those of the 60 Hz units, considering the long term expansion plans of the ANDE system and the advantages of uniformity of design.

The specified moment of inertia for both 50 Hz and 60 Hz generators was the same, consistent with the overpressure limits of practically equal penstocks and unit overspeed limits of equal diameter rotors.

Generators of both frequencies are capable of operating at terminal voltages from 5% above to 10% below the nominal 18 kV within the limits as shown in the generator capability curves of Figs. 12.54 and 12.55. These capability curves are for the generator only and do not include the limits imposed by the exciter in the leading, i.e. under excited area, which are described in the exciter section of this chapter. Table 12.9 gives unit ratings, temperature limits and basic parameters. The principal dimensions and weights of the main components of the 50 Hz and the 60 Hz generators are indicated in Table 12.10.

GENERATORS

BASIC CHARACTERISTICS

The economic and operation studies on the optimum installed capacity, the dual frequency study and the investigations into acceptable

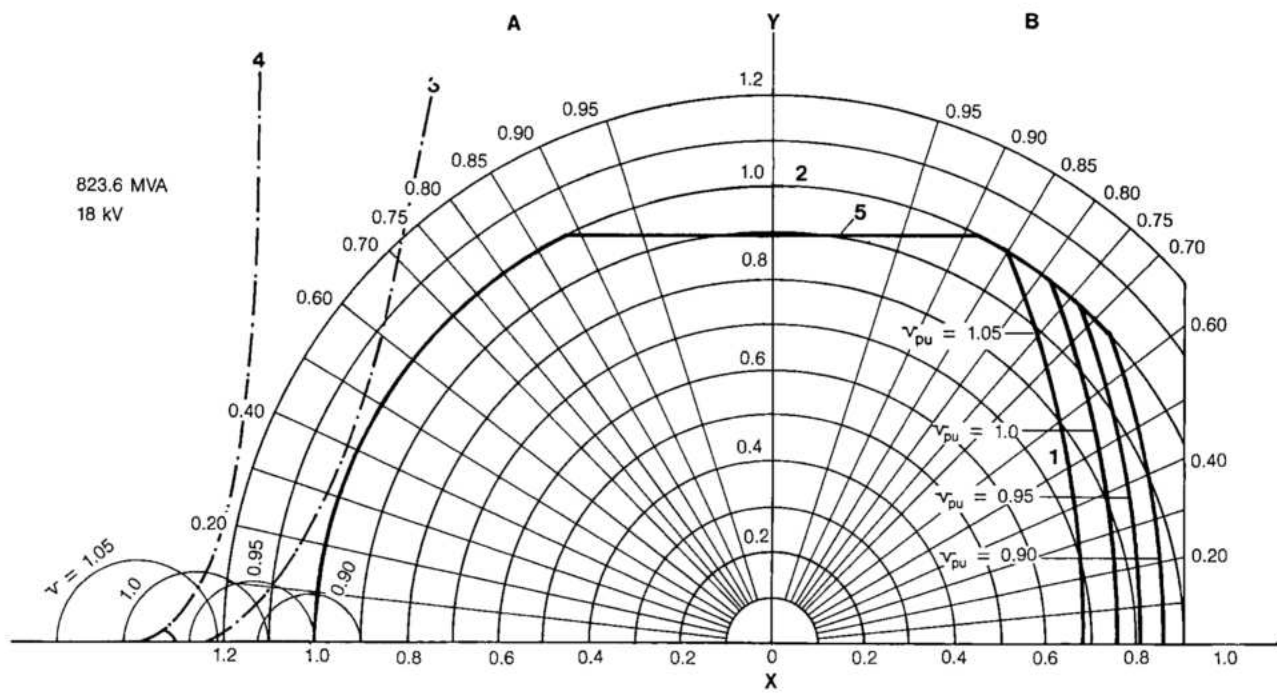


Fig. 12.54 Generator capability characteristics - 50 Hz

Y Active power (p.u.)
X Reactive power (p.u.)

A Underexcited
B Overexcited

Limits:
1 Rotor current
2 Stator current (contractual limit)

3 Practical stability (at 1 p.u. voltage)
4 Theoretical stability (at 1 p.u. voltage)
5 Turbine output

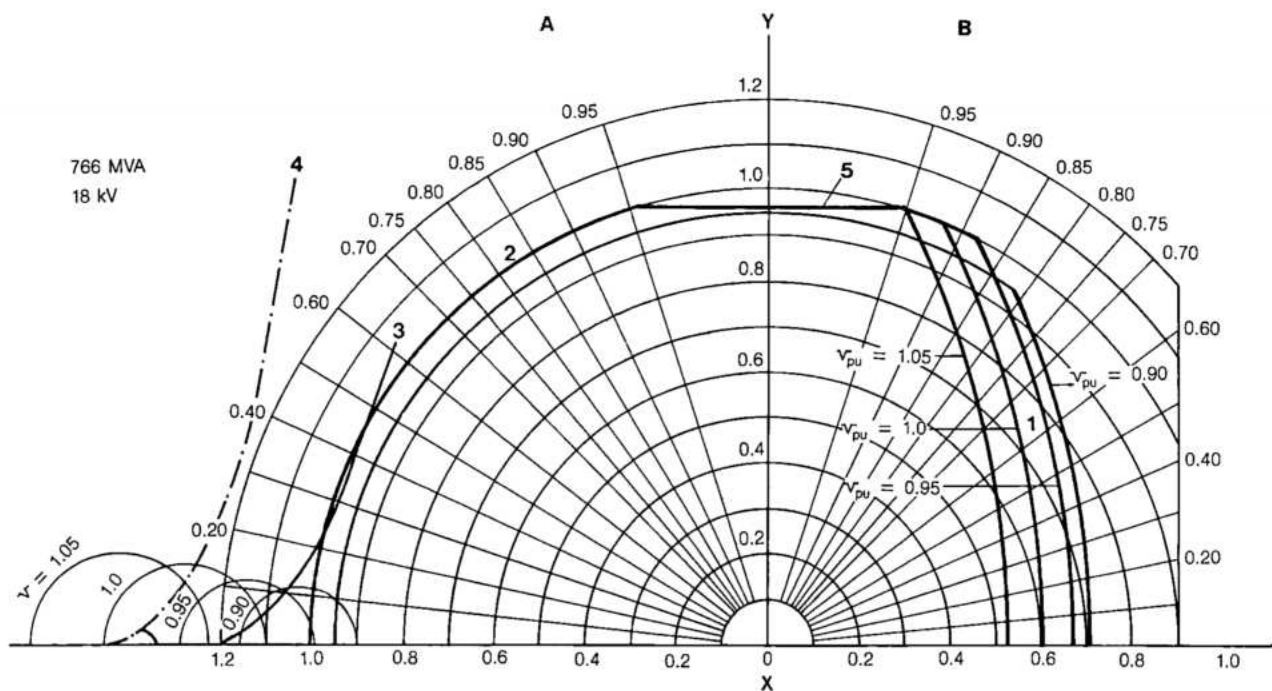


Fig. 12.55 Generator capability characteristics - 60 Hz

Y Active power (p.u.)
X Reactive power (p.u.)

A Underexcited
B Overexcited

Limits:
1 Rotor current
2 Stator current (contractual limit)

3 Practical stability (at 1 p.u. voltage)
4 Theoretical stability (at 1 p.u. voltage)
5 Turbine output

Table 12.9 Generator – basic data

Item	Unit	50 Hz	60 Hz
Nominal power output	MVA	823.6	737
Maximum power output	MVA	823.6	766
Stator copper temperature	°C	85	85
Rotor copper temperature	°C	100	100
Power factor		0.85	0.95
Nominal voltage ($\pm 5\%$)	kV	18	18
Nominal current	A	26 417	23 639
Nominal running speed	rpm	90.9	92.3
Load rejection speed	rpm	124.5	124.5
Runaway speed	rpm	170	170
Moment of inertia (GD^2)	kgm ²	320×10^6	320×10^6
"H" factor	kWs/kVA	4.4	5.07
Synchronous reactances			
Direct axis, saturated (X_d)	p.u.	0.85	0.85
Direct axis, unsaturated (X_{du})	p.u.	≤ 0.9	≤ 0.9
Quadrature axis, unsaturated (X_{qu})	p.u.	≤ 0.705	≤ 0.68
Transient reactances			
Direct axis, saturated (X'_d)	p.u.	0.3	0.26
Direct axis, unsaturated (X'_d) - contractual	p.u.	0.32	0.3
Quadrature axis, unsaturated (X'_{qu})	p.u.	0.705	0.68
Subtransient reactances			
Direct axis, saturated (X''_d) - contractual	p.u.	0.2	0.18
Direct axis, unsaturated (X''_d)	p.u.	0.243	0.24
Quadrature axis, unsaturated (X''_{qu})	p.u.	0.267	0.27
Ratio of quad/direct axis		1.1	1.17
Negative sequence reactances (X^2)	p.u.	0.255	0.255
Zero sequence reactances (X^0)	p.u.	0.087	0.1
Short circuit ratio		1.18	1.18
Time constants			
Direct axis, transient, open circuit (T'_{do})	s	9.5	7.6
Direct axis, transient, short circuit (T'_d)	s	3.1	2.5
Direct axis, transient, short circuit (T''_d)	s	0.1	0.055

Table 12.10 Generators' dimensions and weights of leading components

Item	Characteristics	Unit	Dimensions/Weights
Stator	Weight of 50 Hz units	MN	6.85
	Weight of 60 Hz units	MN	6.08
	External diameter	m	19.38
	Internal diameter	m	16
	Height of frame	m	6.4
	Height of core	m	3.5
Upper shaft	Weight of 50 Hz units	kN	383
	Weight of 60 Hz units	kN	379
	Length	m	2.33
	External diameter	m	1.65
	Internal diameter	m	1.35
Lower shaft	Weight of 50 and 60 Hz units	MN	1.17
	Length	m	6.02
	External diameter	m	2.6
	Internal diameter	m	2.1
Upper bracket	Weight of 50 and 60 Hz units	MN	1.44
	External diameter	m	22
	Length of arms	m	8.77
	Height of arms (maximum)	m	1.52
	Numbers of arms		16
Lower bracket	Weight of 50 and 60 Hz units	MN	3.73
	External diameter	m	12.71
	Height (maximum)	m	4.41
	Numbers of arms		8
Rotor	Weight of 50 Hz units	MN	20.2
	Weight of 60 Hz units	MN	20
	Diameter of 50 Hz units	m	15.926
	Diameter of 60 Hz units	m	15.946
Poles	Weight of 50 Hz units	MN	4.64
	Weight of 60 Hz units	MN	3.71
	Number for 50 Hz units		66
	Number for 60 Hz units		78

COMPONENT DESIGN AND MANUFACTURE

General

The general arrangement of the generator (50 and 60 Hz) is shown in Fig. 12.56. Although both manufacturers Brown Boveri (BBC) and Siemens had their own procedures and practices, considerable common design was used and interchangeability of components was maximized.

The permitted stress levels were the same as those adopted for the turbine, with the following additional requirements:

- At the runaway speed, the average stresses in the rotating parts should not exceed 70% of the maximum yield of the material.
- The maximum stresses in the non-moving parts of the generator, due to the most severe normal operating conditions, should not exceed 33% of the minimum yield point of the material or 25% of the ultimate tensile strength.
- For transient conditions, i.e. short-circuit, half of the field winding shorted, 120° out-of-phase synchronization, bearing abnormalities and temporary overloads up to and including the maximum output available from the turbine, the unit stress of the materials should not exceed 50% of the minimum yield point of the material.
- Percentage elongation of the rotor rim material should be not less than 12%, based on a 50 mm gauge length and the design should assume no friction between layers of laminations. Maximum circumferential unit stress should be the average stress across the weakest radial section.

In the structural design of the generator stationary components, emphasis was placed on measures to keep the stator cylindrical, both during normal and transient operating conditions. Paramount in the design of all parts was the need to maintain the rotor and the stator centers concentric, and to as soon as possible restore the correct centering if the nature of a disturbance were such as to provoke a temporary relative displacement.

Temperatures selected for the stator core and the stator winding under normal loading provide balanced conditions, such that the heat flow through the insulation from core to winding and vice versa is minimized. The generators have direct water-cooled stator windings and closed circuit air cooled stator cores and rotors. In the event of failure of the stator winding cooling water flow, the unit can be restored to service, without a flow of cooling water, after the time-consuming procedure of drying the hollow winding bars with nitrogen. The air-cooled rating (i.e. without stator cooling water) is in the order of

200 MVA, which is compatible with the low load capability of the three 50 Hz turbines.

In design the emphasis was placed on operational reliability and therefore conservative maximum temperature limits were adopted. The limits are indicated below:

Generator component	Maximum temperature (°C)
Stator winding (hot spot)	90
Deionized cooling water at the exit	75
Stator core at any point including teeth	100
Rotor winding	100
Powerhouse cooling water temperature	30

Stator frame, core and winding

The stator frame is made from welded mild steel plate and consists of eight horizontal rings interconnected by sixteen equally spaced vertical columns. Attached to each column, above and below the end rings, there are obliquely mounted vertical plates which function as torsional springs. This type of design has already been successfully used on several large machines, the torsional flexure of the supports allows an almost unimpeded thermal expansion of the core. The top oblique plates are connected to the upper bearing bracket arms, which are bolted to embedded plates in the concrete wall of the generator housing. The bottom oblique plates are bolted to the embedded lower bearing bracket foundation ring. As a result of the twisting of the plates the stator frame is radially stretched. This reduces buckling forces on the stator core laminations as well as minimizes stator tendency to take a deformed non-circular shape during short circuiting of the half the rotor poles. Also, the oblique plates considerably reduce the forces transmitted to the foundation during transient conditions. Under the worst possible fault conditions stresses up to 90% yield result in the plates, but this was considered acceptable in view of the very low probability of such events. The design was such as to avoid resonance of the elastic support system with any frequency present in normal or transient operation of the units. The design of oblique considered the worst combination of system switching, and particularly being critical for the 50 Hz units connected to the HVDC system with its low impedance.

Finite element analysis techniques, together with conventional analytical methods, were employed in

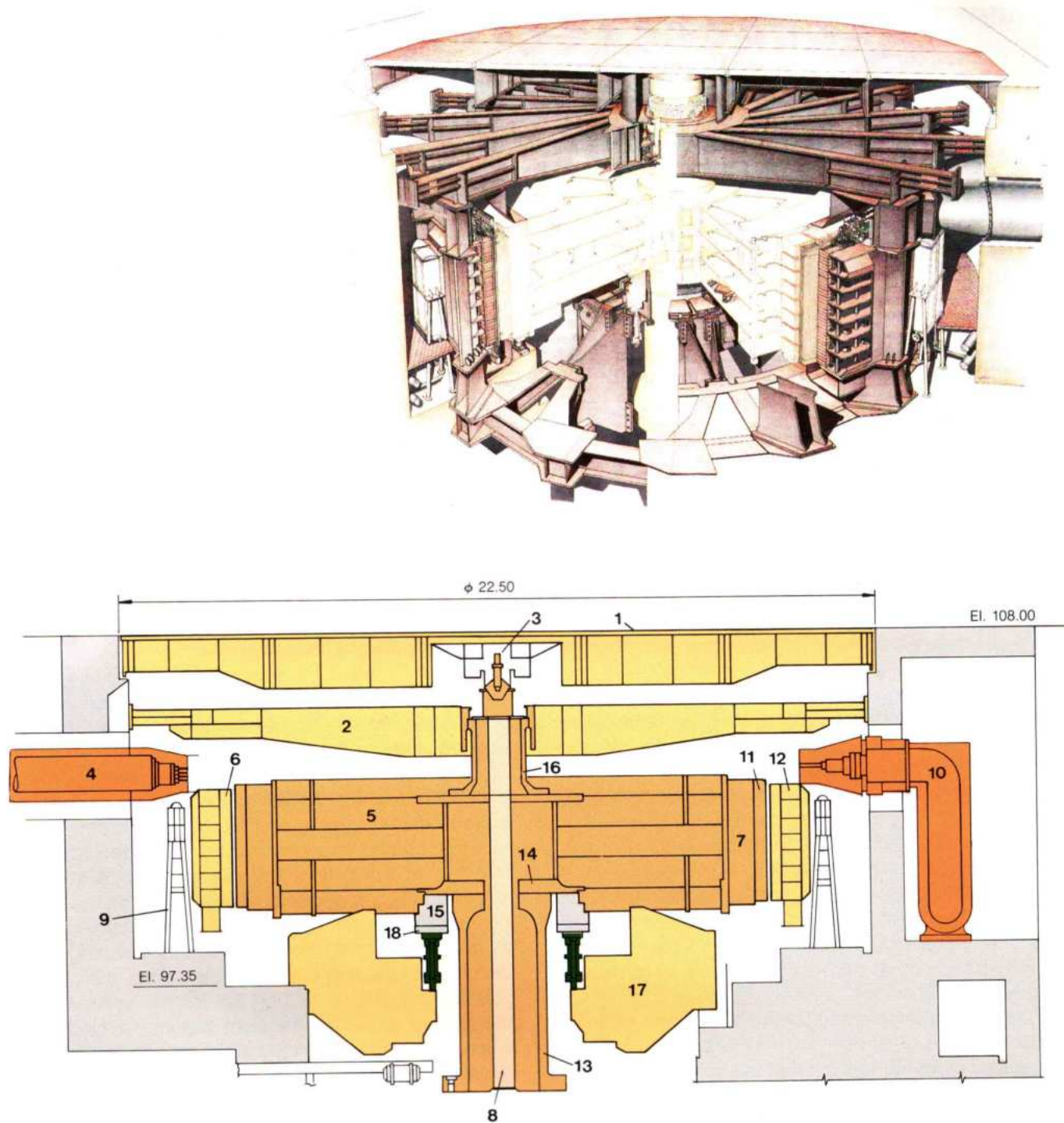
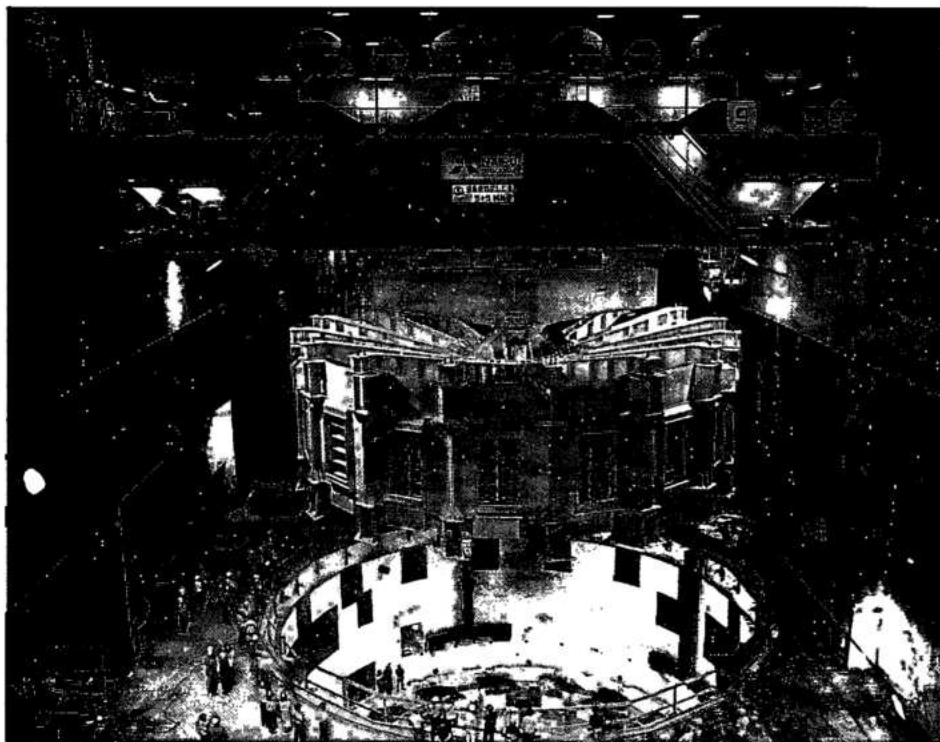


Fig. 12.56 Generator general arrangement and sectional view

- | | | |
|----------------------------------|--------------------------------------|---|
| 1 Generator housing cover | 7 Rotor rim | 13 Generator lower shaft |
| 2 Upper bracket arm | 8 Aeration piping | 14 Rotor hub |
| 3 Shaft aeration valve | 9 Air-water cooler | 15 Thrust block |
| 4 Isolated phase bus (line-side) | 10 Isolated phase bus (neutral side) | 16 Generator upper shaft |
| 5 Rotor spider | 11 Rotor pole | 17 Lower bracket central part with combined bearing |
| 6 Stator core | 12 Stator frame | 18 Thrust bearing upper pad |



*Completed stator
being lowered into
generator pit*

the design of the stator frame. Structural calculations were made for normal and transient loadings and for various temperatures.

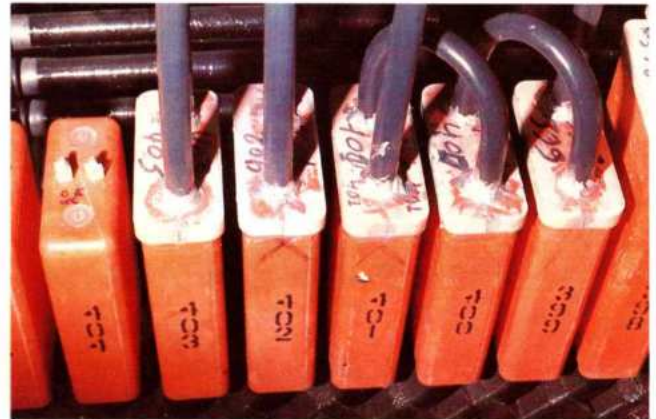
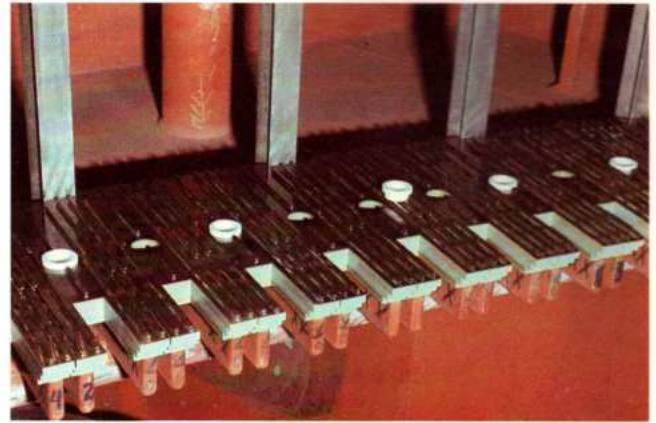
The stator frame was delivered to the project site in eight welded stress relieved segments, ready for assembly and final welding. A shop assembly check was made before delivery. Site stacking of the stator core was done, before lowering the stator into the pit. This method was chosen in preference to joining factory assembled sections having dimensions suitable for transport. This gave a jointless structure which is more resistant to the forces causing deformations.

The stator core was formed by field stacking 0.5 mm thick sheets of silicone steel having high magnetic permeability and low losses. Sheets were stamped in segments with slots for the bar windings, dove-tail slots for the key-bars and holes for the through-bolts. Stampings were deburred, cleaned and coated with special insulating varnish. Core stacking methods were different for the two suppliers, Brown Boveri used a single sheet per layer, whereas Siemens used eighteen sheets packets. Theoretically, the Brown Boveri method provides better resistance to inter-laminar slippage, while the Siemens method is superior in respect to lamination buckling. For both, the layers were overlapped by one third of the sheet length, thus

repeating every third layer. After a packet 54 mm in height was completed, a separator sheet 6 mm thick having stainless steel radial ribs was used to create the cooling air ducts. The core was fastened to the stator frame by double dove-tail key-bars located between the core and the frame. The core was compressed by through-bolts tightened between a heavy bottom end plate, which was part of the frame, and independent segmental clamping plates at the top. Through-bolts were insulated to prevent short-circuiting the core and were tightened to give an average pressure of 189 N/cm^2 .

The stator winding connections are star-connected Roebel bar-type, wave wound with six parallel paths per phase, see Fig. 12.57. Each winding bar has twenty-four solid conductors and six hollow rectangular conductors, which are the same width as the solid conductor, but approximately twice as thick and carry the bar cooling water. The 360° transposed strands are suitably insulated from each other and firmly bonded together. Class F mica based insulation system was used with uniform thickness throughout the bar length and end-turn areas. Bar insulation was impregnated and filled with a thermo-setting resin using a vacuum process, and then temperature-cured under pressure. This resulted in a very solid and dense insulation structure practically free of voids. Overall bar dimensions are 33.4 mm x 57 mm for the 50 Hz units

and 32.5 mm x 54.15 mm for the 60 Hz. The slot portion of the bar surface was treated with a conducting finish to ensure a good contact conductivity. The voltage gradient control for the end turns was different for the two manufacturers. In the BBC design the bar ends were covered by semiconducting paint while Siemens end turns used only a semiconductive collar several centimeters long near the slot. Conductor connections were made with silver soldering and the joints were insulated and covered with molded caps filled with fire resistant compound in the BBC design. Siemens compound is not fire resistant but it prevents fire propagation. As the winding is directly water cooled, the electrical connections were made first nearer the slot, with the six hollow conductors carried on to the top and bottom ends of the bar for cross connections. Connections for supply and return of the deionized water were made at the upper end turns. The method of securing the stator bars in the slots was different for each manufacturer. BBC used a side filler on one side of the bar only, see Fig. 12.57. This was in addition to the normal semiconducting bottom and separator strips. Initially the side filler was a semi-conducting



Detail of lower stator bar connection

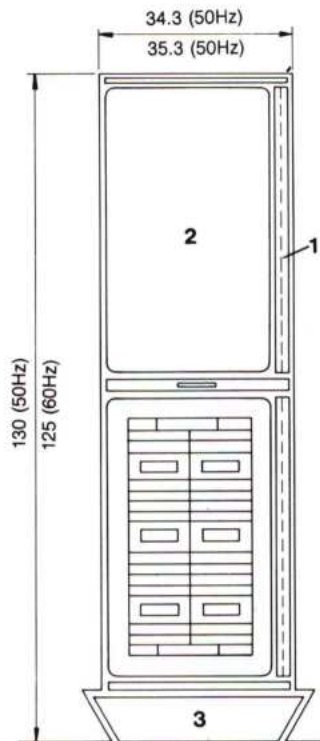


Fig. 12.57 Stator winding slot section

- 1 Side filler
- 2 Winding bar
- 3 Wedge



Rotor hub in manufacture

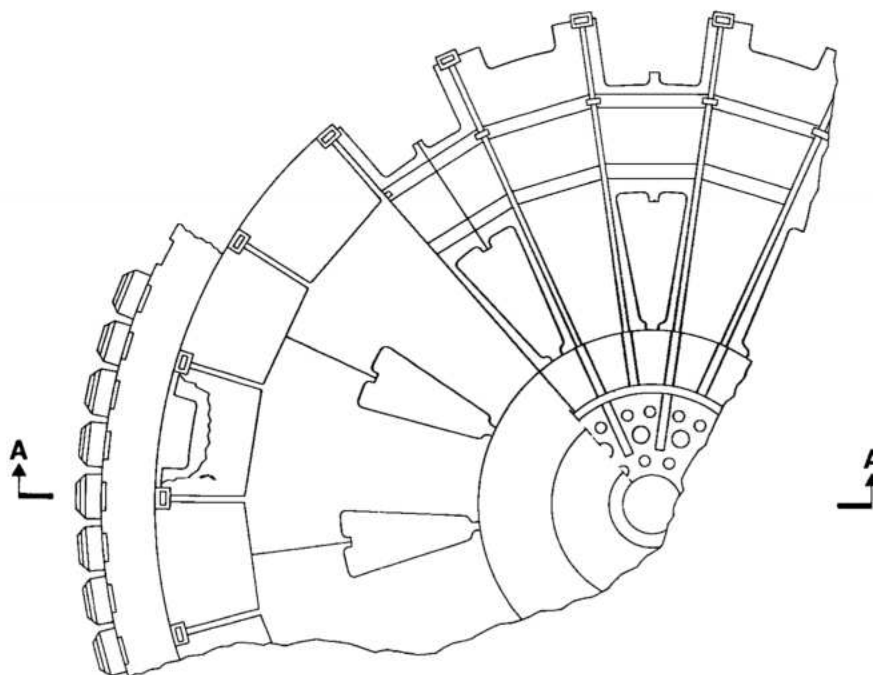
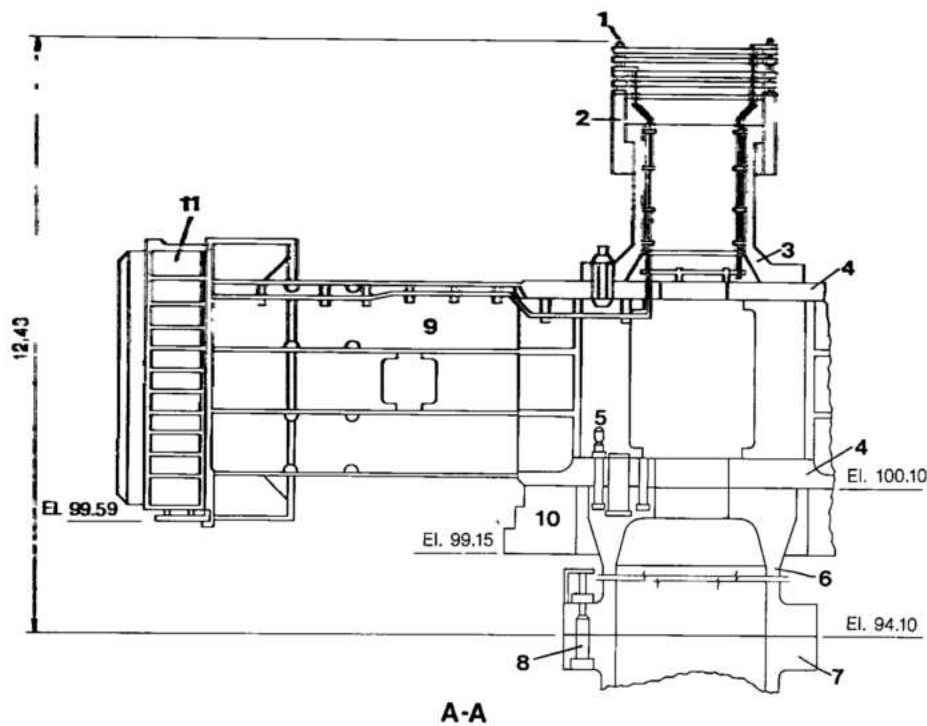


Fig. 12.58 Rotor

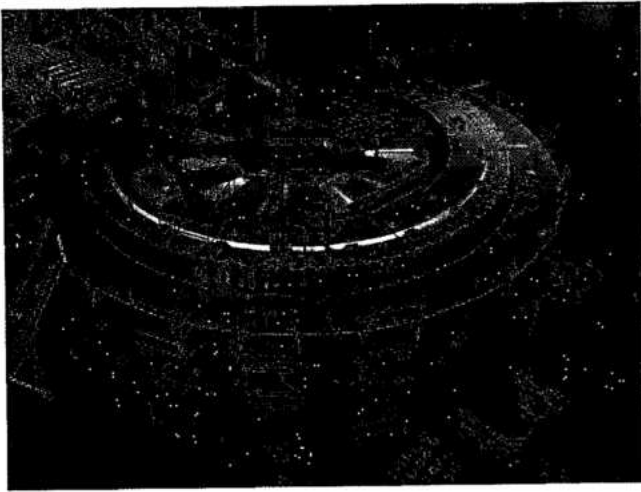
- 1 Slip rings
- 2 Upper guide bearing collar
- 3 Generator upper shaft
- 4 Rotor hub
- 5 Generator shaft rotor coupling bolts
- 6 Generator lower shaft
- 7 Turbine shaft
- 8 Turbine-generator shaft coupling bolts
- 9 Rotor spider
- 10 Thrust block
- 11 Stator frame

synthetic varnish-impregnated fabric. Later this was changed to semi-conducting sheet material in various thicknesses glued at three spots to the bar. Siemens method used a "U" shaped slot liner fabric material with a semi-conducting putty between the bar and the liner. When cured, this putty bonded the liner to the bar and also caused slight bulging

of the liner into the air slots, thereby locking the bar axially.

Rotor

The rotor, see Fig.12.58, is a welded mild steel plate to structure consisting of a rigid central boss, to which the upper and lower generator shafts are



Trial of rotor

bolted and a more flexible outer section which carries the rotor rim and poles. The rotor hub was shop welded and then stress relieved. Rotor arms were shipped to the site in eleven parts for the 50 Hz units and thirteen parts for the 60 Hz units. Before shipping a complete shop assembly was made to check the fabrication. Connections between the arms and between the hub and the arms were welded at site using preheated and balanced welding techniques to minimize distortion.

Calculations were made with the finite element analysis method. In the calculations, as a conservative design feature, the additional support

given by the shrink fitting of the rim on the spider was not included and the total weight of the rim on the spider was assumed to be acting on the bottom support plate.

The rotor rim was made from over 30 000 stacked and bolted steel plates, the majority of which were 2.75 mm thick. These were arranged in eleven basic ring groups to make up a total height of 3536.5 mm for the 60 Hz units and 3820.5 mm for the 50 Hz. During the stacking the plates were compressed in stages and through bolts were used in the final assembly to give compression and to provide linkage for the plates. The stacking and interleaving pattern is designed to create ventilation slots in the rim and to allow the cooling air to pass through the rim and around the field poles. The rotor rim is keyed to the rotor arms to transmit driving torque and to control rim roundness. It is shrunk onto the keys and, to limit stresses in the arms resulting from the shrinking, is designed to float radially off the supports above 115% normal speed. Shrinkage interference between the arms and the rim is 3.8 mm. Torque is transmitted via the wedge "U" section assembly shown in Fig. 12.59.

To obtain the same values for the direct-axis unsaturated synchronous reactance and short-circuit ratio, the operating air gap width between the poles and the stator is 36 mm for the 50 Hz machines, and 27 mm for the 60 Hz.

Maximum axial deflection of the rotor relative to the thrust bearing is 1.15 mm. With the shrunk on design the maximum combined stress of 162 N/mm^2 occurs at stand-still. Stresses in all other operational cases, including runaway speed, are less as the prestress is relieved by the centrifugal forces. A sectionalized steel plate brake ring having a hardness of $175 \pm 25 \text{ HB}$ is bolted to the bottom of the rotor rim.

A special lifting beam was used to transport the finished rotor to the generator pit.

Shafts

The upper shaft is divided in two parts, the upper collar being insulated electrically from the lower part, see Fig 12.60. The lower part of the upper shaft was made from a single forging, whereas it was more convenient to make the lower generator shaft by welding two forged flanges to the forged central cylinder, see Fig. 12.61.

Coupling bolt holes of the lower shaft and turbine shaft were reamed by means of a special tool and the two shafts were coupled at the site. The coupling bolts were hydraulically tensioned to 67% yield stress and transmit a maximum torque of 79.295 kNm, see Fig. 12.62.

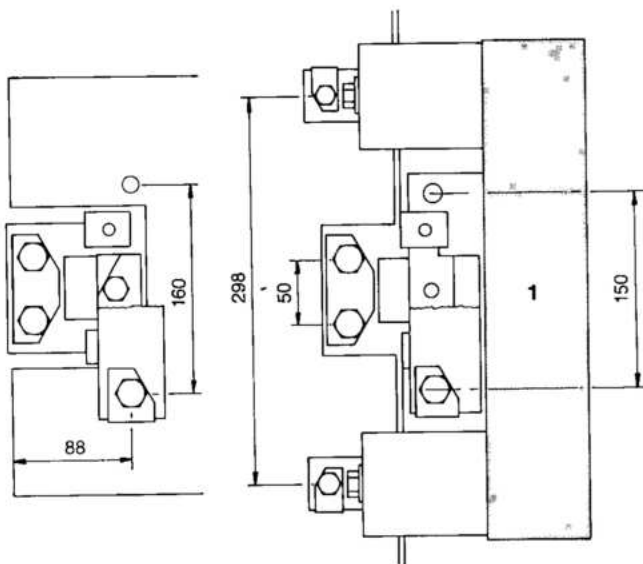


Fig. 12.59 Wedge "U" section assembly

1 Rotor rim

The lower shaft is connected to the rotor hub by means of thirty-three bolts tightened to 67% yield stress and arranged on two pitch circle diameters. The torque is transmitted through eleven shear dowels.

Field poles and winding

The core of the field poles was formed by stacking 1.06 mm thick low loss steel sheets, which were punched, deburred and cleaned. The steel sheets were compressed between the end plates which were welded to five through rivets. On their inner face the poles have a protruding dovetail for mounting into a corresponding slot on the rotor rim. Four key hole slots were provided on the outer face for installation of the damper bar windings. The four bars were brazed to rectangular bars at the top and bottom of the pole. Then they were extended



Detail of brake ring on underside of rotor.
Note seating nuts and holding studs

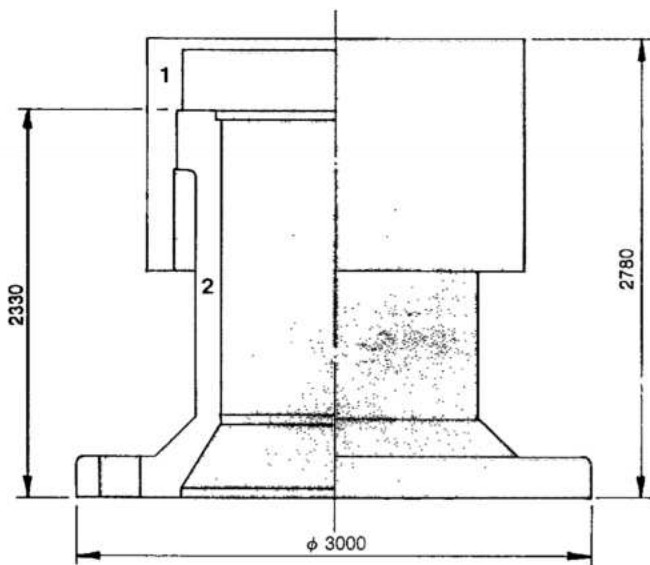


Fig. 12.60 Upper shaft

- 1 Upper guide bearing collar
- 2 Shaft

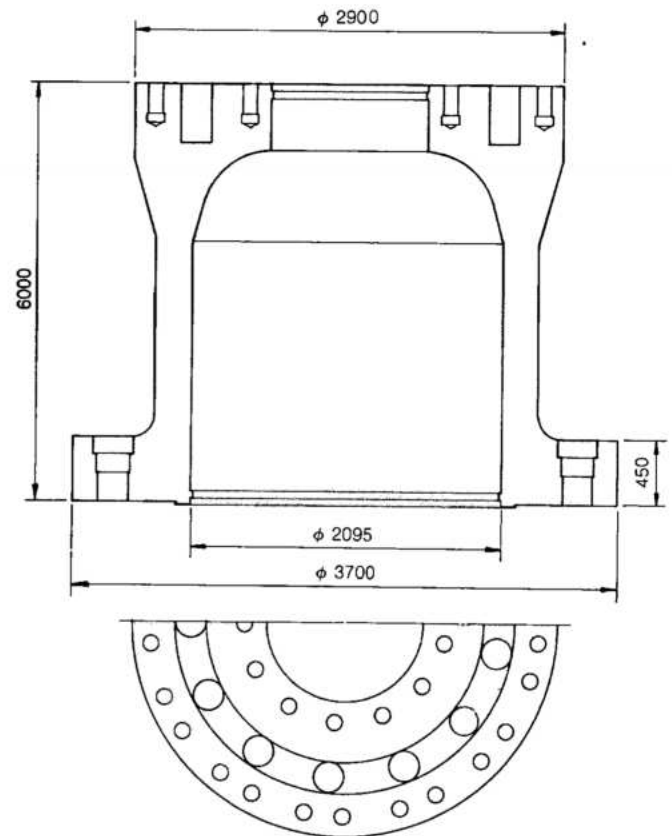


Fig. 12.61 Generator lower shaft



Generator lower shaft undergoing cleaning and visual inspection before coupling to turbine shaft

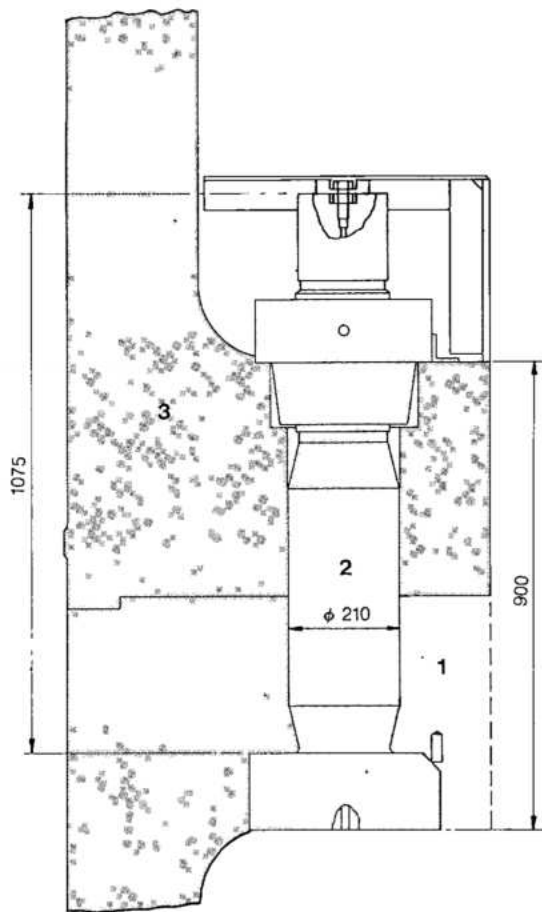


Fig. 12.62 Section through a coupling bolt

- 1 Turbine shaft
- 2 Turbine and generator shaft coupling bolt
- 3 Generator lower shaft

towards the adjacent poles to allow for interconnection of the damper bar winding. The attachment of the poles to the rim is as shown in Fig. 12.63.

Field windings were made from rectangular copper bars, edge-wound, having a fin of reduced section on the outer edge for cooling. The winding was fitted on the core, from the inner dovetail side, over an insulating sleeve. Insulating collars were used between the backside of the pole face and the winding and also between the winding and the retaining metal collar on the dovetail side.

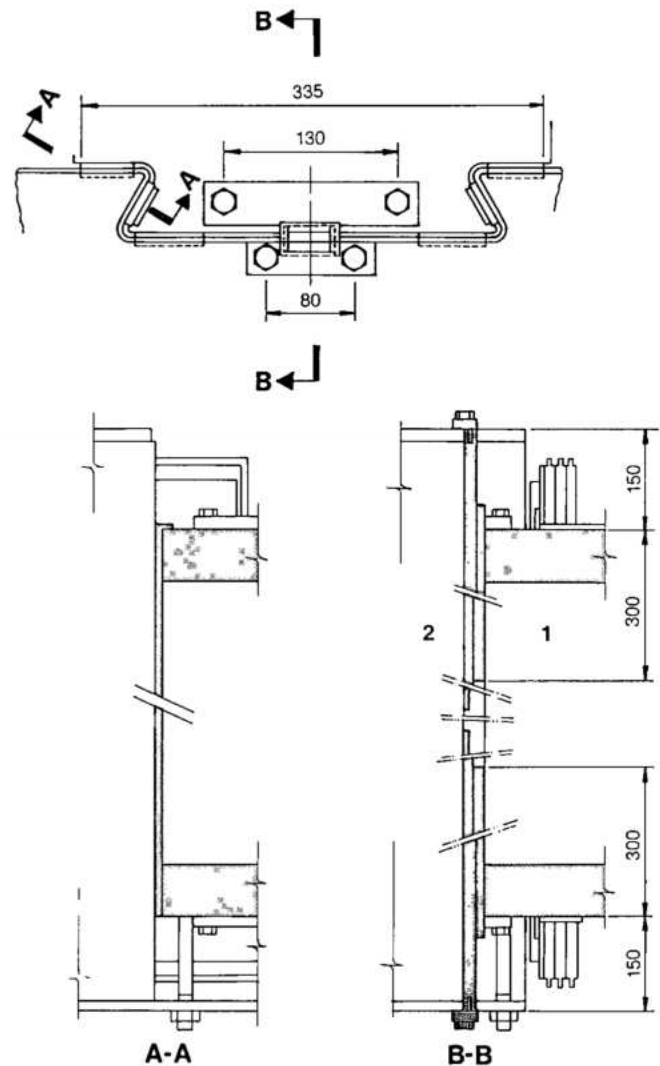


Fig. 12.63 Fixing of poles

1 Rotor pole

2 Rotor rim

Interconnections between poles for the main and damper windings were made directly, by using flexible jumpers. Connections to the slip rings are by flat copper bus bars mounted between the rotor arms and running under the top rotor plate to the rotor center. At the rotor center they are mounted on the inside of the hollow upper shaft where they connect with the slip rings.

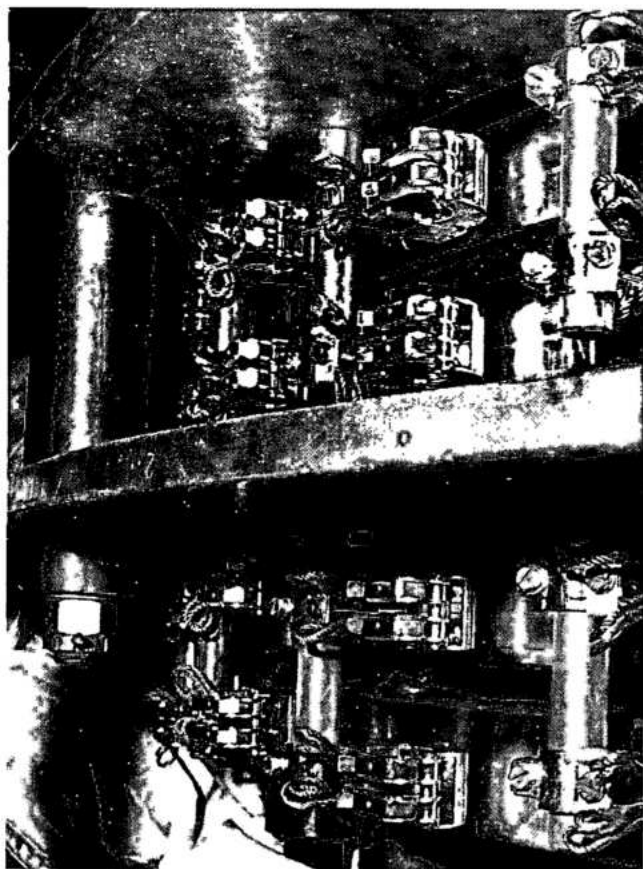
Slip rings

There are four slip rings, two for each of the positive and negative field connections, see Fig. 12.64. They were mounted on insulators from a flange at the top of the upper shaft and are separated by further insulation from each other. The slip rings were spirally machined on the brush contact face to reduce brush wear and to improve contact with the carbon brushes. The brush rigging is supported from the upper bracket and the whole area is enclosed for dust control. Cooling air is supplied from the outside

of the generator housing by a system of fans and ducts. A hatch-way through the generator top cover provides access to the slip ring area.

Lower bearing bracket

Design of the lower bearing bracket considered three basic loadings: the vertical load, the maximum radial force and the thermal stresses. In normal operation the vertical load was calculated as 42.5 MN, being the sum of the weight of the rotating parts, the hydraulic thrust and the contingency allowance. This, however, assumed a rather low value for the hydraulic thrust, which will be explained later. The maximum radial force of 1.014 MN assumed a simultaneous occurrence of full load rejection and short circuiting of half on the rotor poles. Thermal stresses were evaluated assuming a linear temperature gradient along the arms, between the bracket hub and the concrete foundation. In order to avoid high thermal forces acting upon the concrete, the bracket radial elasticity had to be high. On the other hand, high



Detail of slip ring

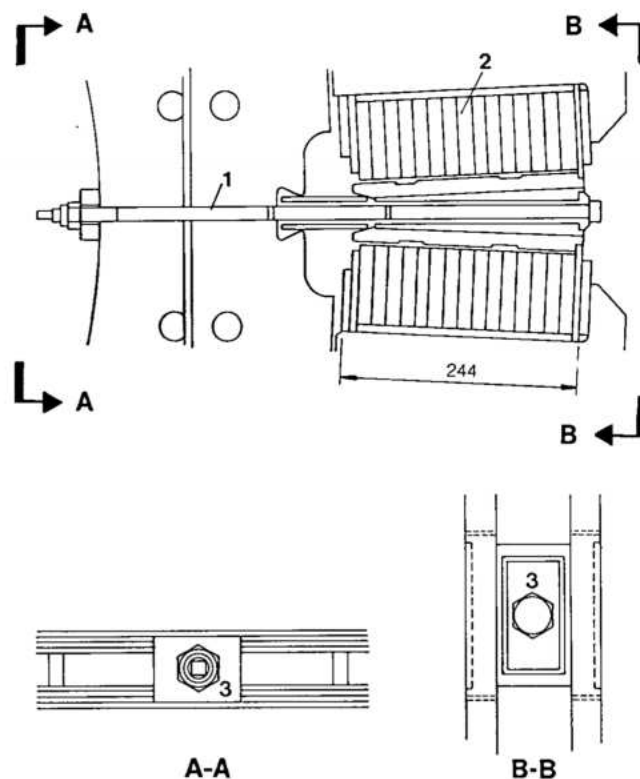
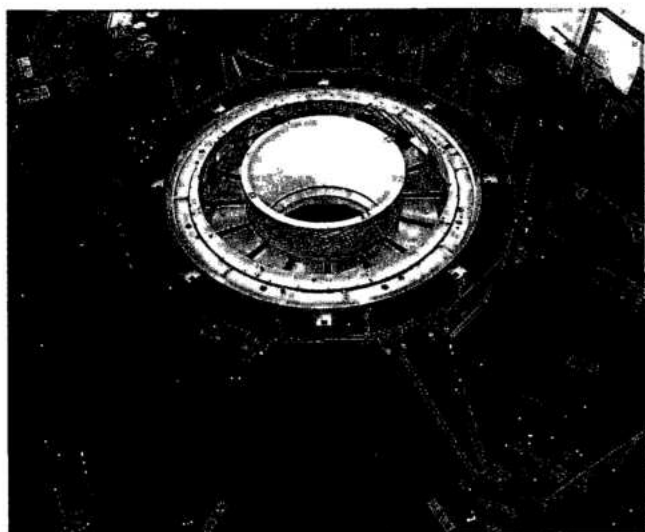


Fig. 12.64 Separation of poles

1 Stud

2 Pole coil

3 Space block



Generator lower bearing bracket ready for transport to generator pit for installation

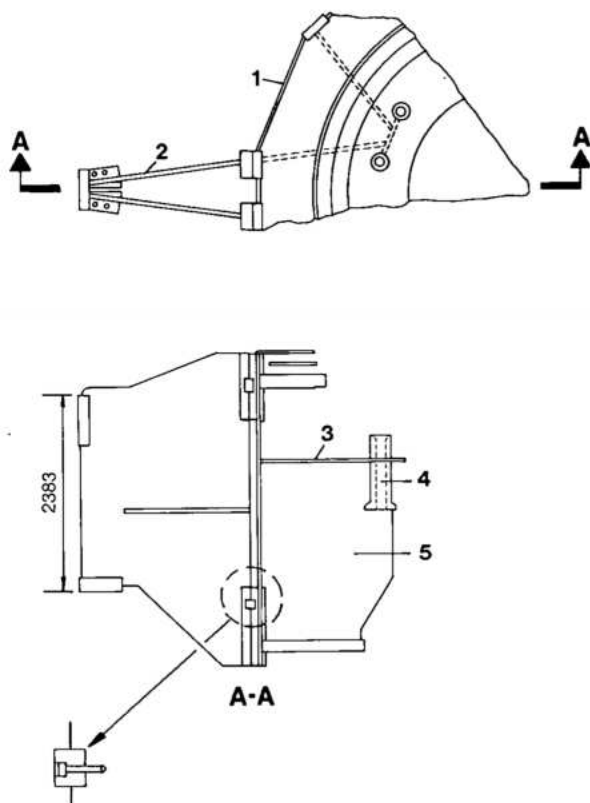


Fig. 12.65 Lower bearing bracket

- 1 Opening for bearing oil to water heat exchanger
- 2 Bracket arm
- 3 Bearing oil sump bottom
- 4 Bearing pad support
- 5 Bracket central part

radial stiffness was necessary to satisfy the requirements of shaft stability and to maintain bearing clearances. These contradictory requirements were satisfied by the welded steel plate design consisting essentially of a central ring which contains the bearing oil reservoir and eight pairs of arms arranged starlike as shown in Fig. 12.65. The central part is made up of three rings interconnected by vertical plates. All the arms are loaded equally in the vertical direction. One arm of each pair is rigidly attached to the foundation, while the other arm is free to move radially. Because thermal expansion is accommodated by a slight rotation of the bracket hub, this arrangement considerably reduces thermal stresses and at the same time maintains the radial rigidity of the bracket. To maximize the radial stiffness of the lower guide bearing, the elevation of the bearing horizontal centerline and that of the points at which the arms transmit the bearing load to the concrete are nearly the same. The stresses and deflection of the lower bearing bracket were calculated by conventional stress analysis, and by the finite element method. The results were verified on a three-dimensional steel model in which all components, including welds, were to a scale of 1:10. This model was subjected to all possible loading combinations, asymmetrical, radial and axial. Instability was not evident at loads 70% above the maximum design loads. The finite element analysis method determined the regions of stress concentrations and local deformations and proved that under the worst possible conditions none of the components or welds would be stressed above 60% of the yield point.

Upper bearing bracket

The bracket is fabricated from mild steel welded plate. It transmits the upper bearing loads to the concrete and also supports the slip ring enclosure and the turbine aeration valve. The sixteen arms of the upper bearing bracket are in the horizontal plane, at an angle to the radial direction, see Fig. 12.66. With the skewed design, thermal expansion of the arms causes a slight rotation of the bracket hub, and thus minimizes the influence which the expansion has on the bearing center and the clearance. The connection of the arms to the stator frame is by the upper oblique plates which isolate the expansion of the stator frame from the upper bracket and thus prevents these movements from affecting the upper bearing clearances.

In the region between the bracket hub and the stator frame, the bearing bracket arms have an "I" beam cross section. In the region between the stator

frame and the concrete wall, the connections are made by horizontal steel plates, which can accommodate vertical thermal expansion of the stator frame while maintaining the stiffness necessary for the guide bearing. Structural calculations were made by conventional methods only, but their accuracy had already been confirmed in previous designs. Arm end support plates were located and embedded in the concrete after the erection of the bracket.

Generator bearings

The generator has two guide bearings, the upper guide bearing mounted on the upper bracket at El.104.7 and the lower guide bearing mounted together with the thrust bearing on the lower

bracket at El. 99.15. As the lower generator guide and the thrust bearing share the same oil system, they are referred to collectively as the combined bearing, see Figs. 12.67 and 12.68. All bearings are designed to the same specification as the turbine guide bearing, i.e.:

- With oil cooling. Operation for 5 minutes at runaway speed and continuous operation between 50% and 105% normal speed.
- Without oil cooling. Overspeed due to full load rejection and rated load for 15 minutes.

In addition, the thrust bearings were specified to be capable of operating without damage under the following exceptional conditions:

- Emergency shutdown with the high pressure oil lift system inoperative.

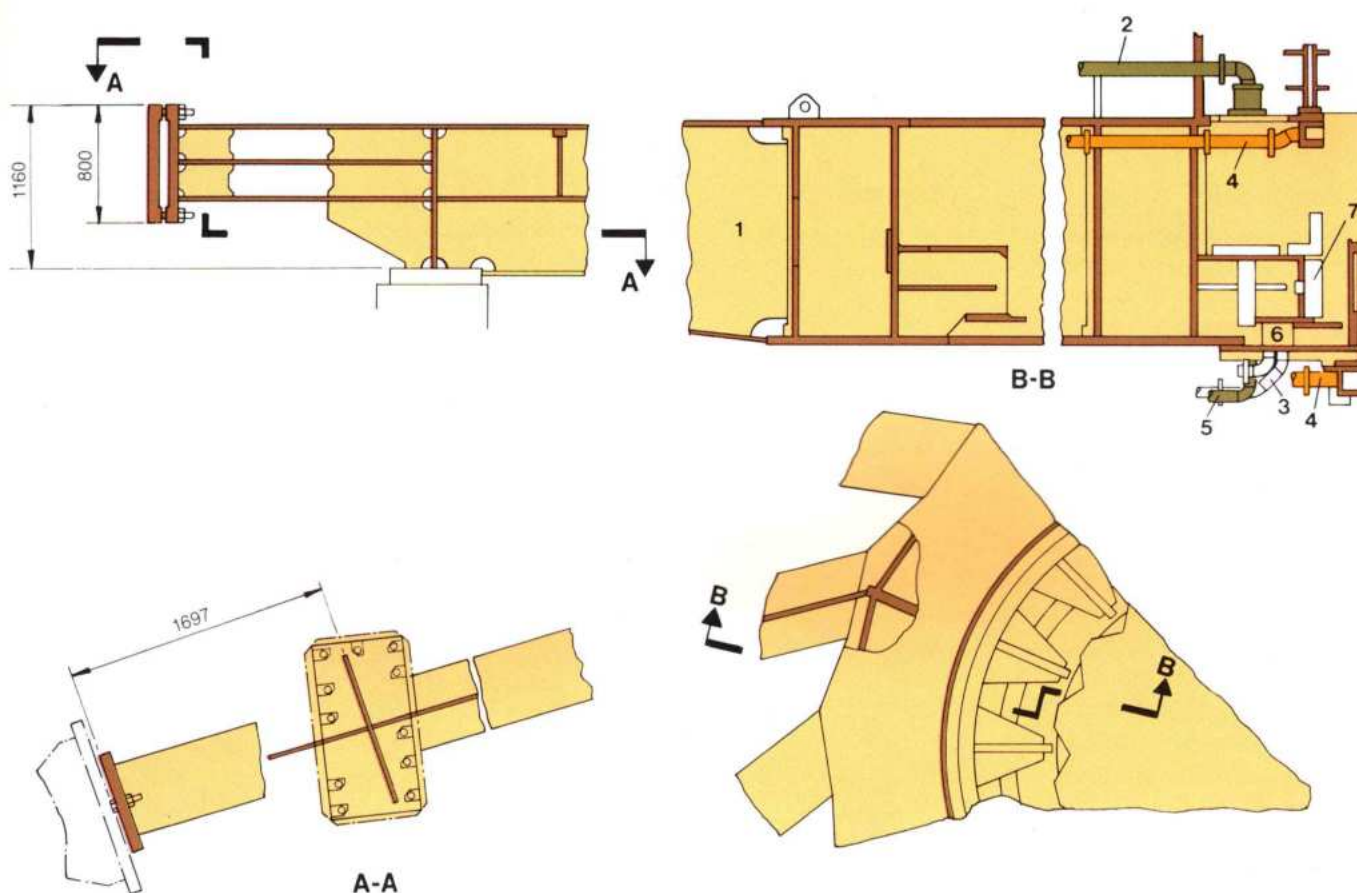


Fig. 12.66 Generator thrust bearing

- | | |
|-----------------------------------|---|
| 1 Upper bracket arm | 5 Bearing oil emptying piping |
| 2 Bearing oil filling piping | 6 Upper guide bearing oil to water heat exchanger |
| 3 Bearing cooling water piping | 7 Upper guide bearing pad (16 pads) |
| 4 Bearing oil vapor drainage pipe | |

- Starting with the high pressure oil lift system inoperative, but with supplementary measures such as jacking the rotor to establish a thin oil film before starting.
- Specified design temperatures are given below:

Item	Temperature (°C)
Maximum oil temperature	55
Maximum hottest spot metal temperature (bulb)	
Thrust bearing	85
Guide bearing	70
Maximum metal temperature measured by RTD	
Thrust bearing	83
Guide bearing	68

All bearings have oil level alarms and trips and oil and bearing pad temperature sensors.

Combined bearing

Total design load on the thrust bearing was 42.5 MN, comprising the following:

Component	Load (MN)
Weight of generator rotor complete including upper and lower shaft and thrust block	19.61
Weight of turbine runner and turbine shaft	4.3
Turbine hydraulic thrust	16
Contingency	2.59

This load together with a pad area of 6640 cm² gives a pad specific pressure of 400 N/cm² (sixteen pads) which was used for all the design calculations. The turbine model tests, however, indicated a maximum thrust of 5.86 MN only, which reduced the thrust bearing load (without contingency) to 29.77 MN. In the interest of security this potential reduction was not considered in the design of the bearings.

The bearings are of the Kingsbury type with the 5.2 m diameter 770 kN steel thrust block mounted on sixteen pads, each pad in turn being supported by a support ring and a jack bolt. The pads and support rings are designed so that the concave deflections resulting from the pressure forces are almost compensated by the convex deformations due to thermal effects. An alternative design of a sandwich pad with a thin upper plate supported on elastic springs was considered. This design had the advantage that thermal deformations would be negligible, because of the thin plate and ease of cooling, and deformations of the plate due to the pressure distribution could be regulated by adjusting the elasticity of the individual springs. However, this alternative was finally discarded, as the deformations of the pad with the adopted manufacturer's traditional design was shown by calculation and precedent to be perfectly acceptable, see Fig. 12.69.

The annular ring support is mounted on the jack bolt via an off center ball support which permits the pad to automatically adopt the correct inclination to create the oil film necessary to support the load. The

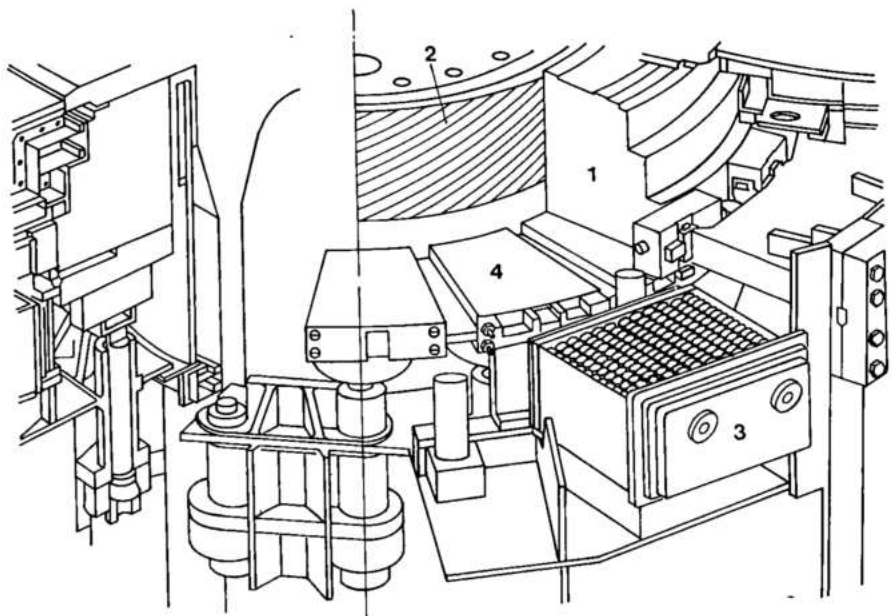


Fig. 12.67 General arrangement of generator's combined bearing

- 1 Thrust block
- 2 Generator lower shaft
- 3 Thrust bearing oil to water heat exchanger
- 4 Thrust bearing pad

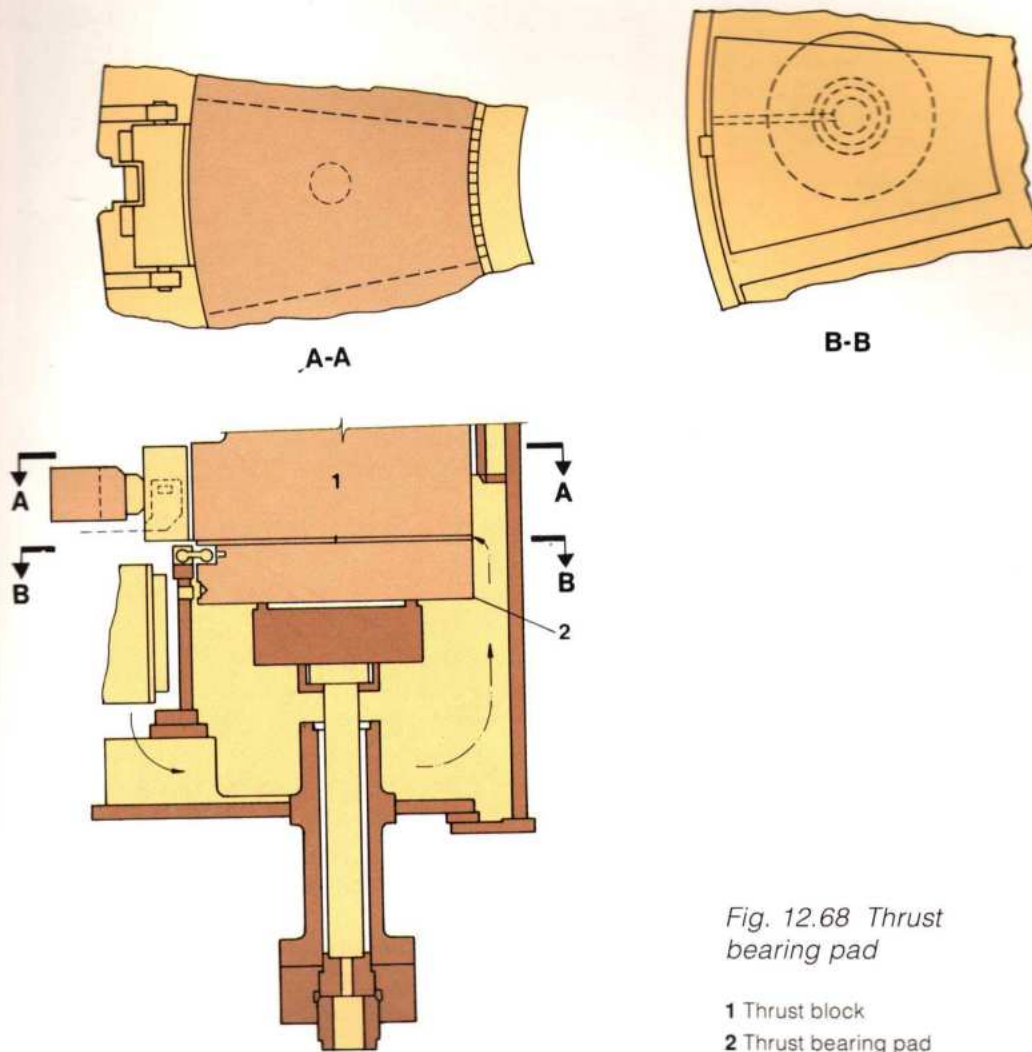


Fig. 12.68 Thrust bearing pad

- 1 Thrust block
2 Thrust bearing pad

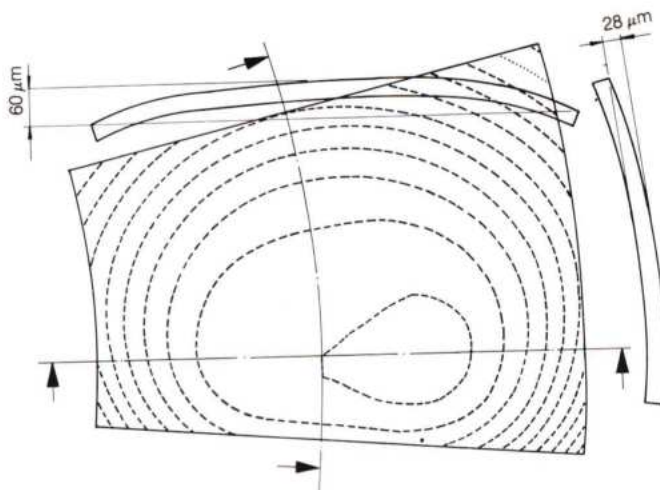


Fig. 12.69 Itaipu thrust bearing pad - deflections in service - calculated

minimum oil film thickness was calculated to be $65 \mu\text{m}$; the calculated oil film profile and pressure distribution in operation are shown in Figs. 12.70 and 12.71 respectively. Calculated friction loss per pad was 31.22 kW. The thrust block also deflects in service due to pressure loading and temperature effects. Deviation from planar of the block above the bearing pads is about $15 \mu\text{m}$ which is easily accommodated in the operating oil film thickness. Radial dimensional changes as a result of temperature, however, are significant, and result in a large initial radial clearance for the lower generator guide bearing, which reduces as the bearing warms. Erection clearance is $730 \mu\text{m}$ which reduces to $350 \mu\text{m}$ after about 15 minutes operation of the generator. During this period the lower generator guide bearing still contributes to the stability of the line shaft, the relevant critical speeds at starting

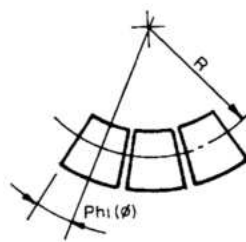
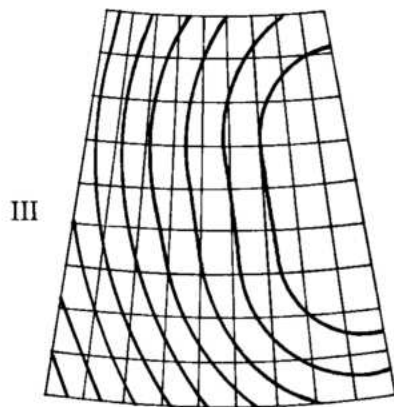
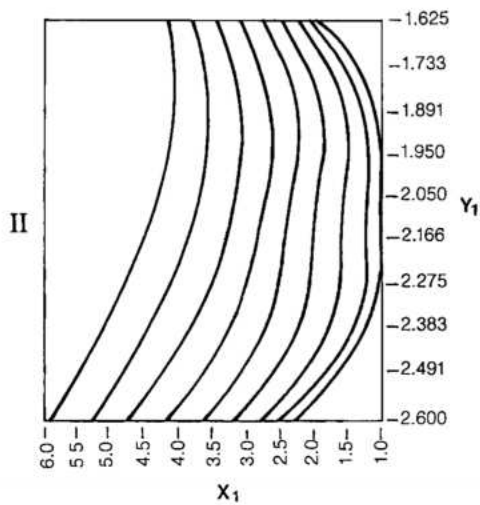
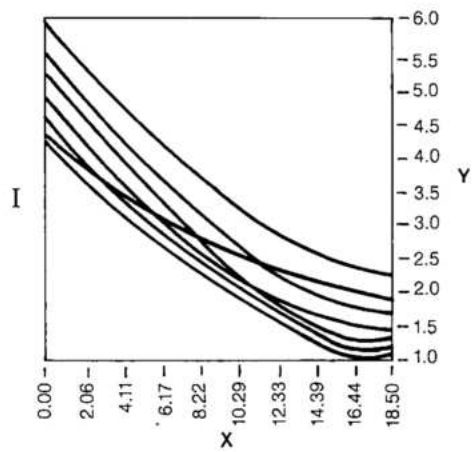


Fig. 12.70 Oil film thickness - calculated

I Tangential variation
II Radial Variation
III Plan of segment showing oil-film thickness contours

Y Gap ratio H/H_{min}
X Angle $\Phi (\phi)$
Y₁ Radius (m)
X₁ Gap ratio H/H_{min}

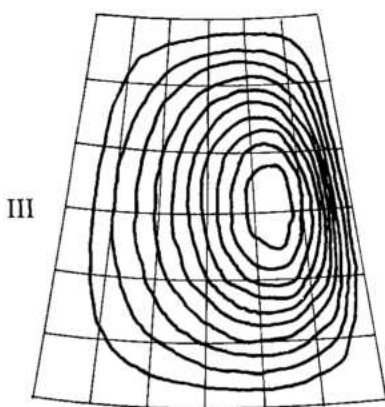
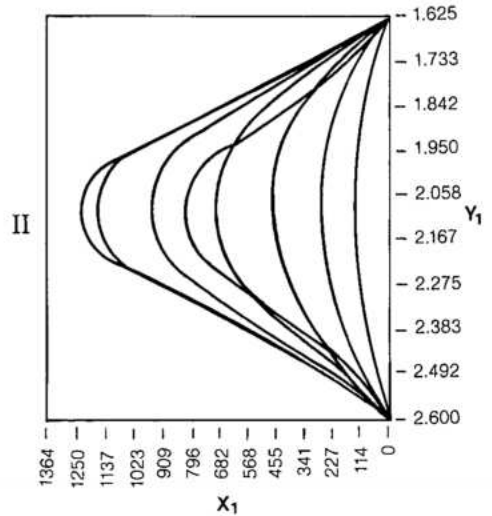
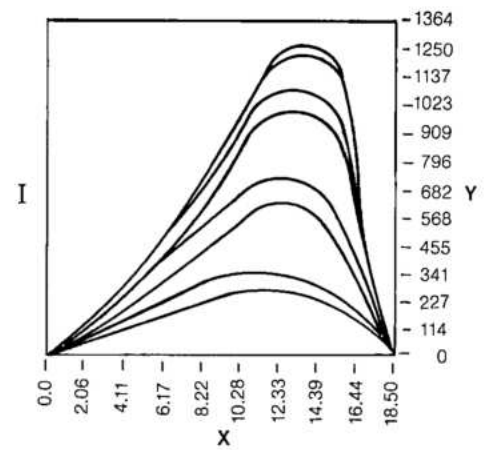
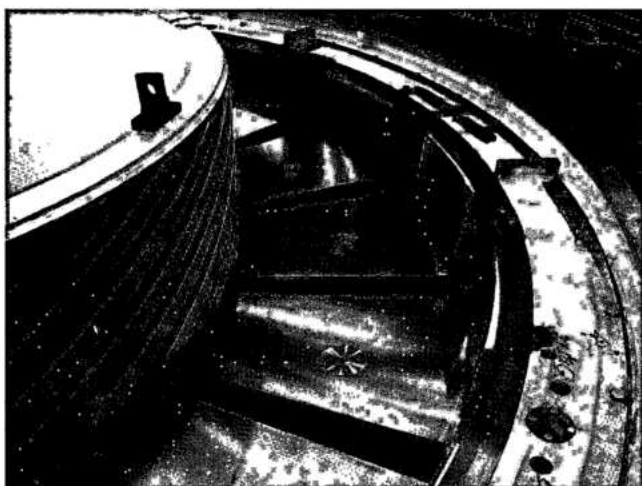


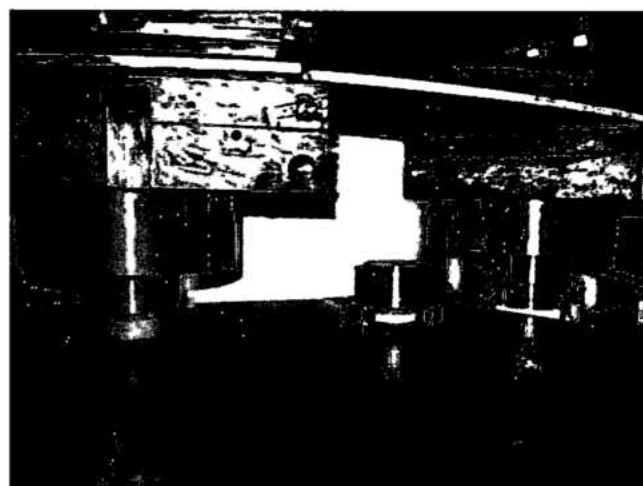
Fig. 12.71 Thrust-bearing pressure distribution calculated

I Tangential distribution
II Radial distribution
III Plan of segment showing isobars

Y Pressure (N/cm²)
X Angle $\Phi (\phi)$
Y₁ Radius (m)
X₁ Pressure (N/cm²)



Combined bearing: thrust pads on their support



being 220 rpm with magnetic pull and 260 rpm without, both well above normal operating speed.

The thrust block was manufactured from forged steel with minimum tensile strength 485 N/mm^2 and minimum yield 250 N/mm^2 and was subjected to ultrasonic examination and liquid penetrant testing. No repair welding was permitted on the thrust block running surface. The running surface of the thrust block was finished to a centerline average of $8 \mu\text{m}$. Attachment of the thrust block to the rotor hub is by means of clearance bolts, so that the block can accommodate the movements due to pressure and thermal expansion. Torque is transmitted from the block to the hub by radial dowels which also permit expansion of the block.

White metal babbitt of the bearing pads was tested for adherence using the shear method and the bond was ultrasonically examined. The pad base material was heat treated at 700°C for approximately 100 hours in order to reduce the hydrogen to a limit of less than $1.2 \text{ cm}^3/100 \text{ g}$ and thus eliminate any possibility of hydrogen bubbling under the white metal.

The lower generator guide bearing comprises sixteen tilting pads bearing on the thrust block outer diameter which has a tangential velocity of 24.74 m/s . It was designed on the assumption that only 25% of the guide bearing segments were operative, under the following specific pressure limits:

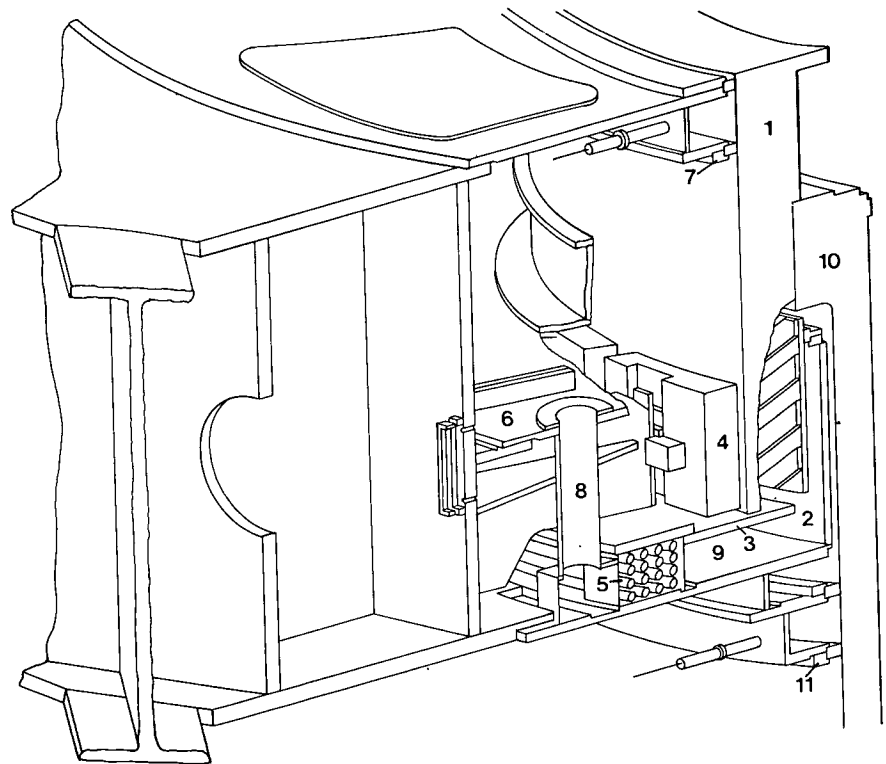
- Continuous operation: 2.4 N/mm^2
- Transient: 4.5 N/mm^2
- Extreme fault cases: 14.4 N/mm^2

The combined bearing is equipped with an air breather system leading to an oil trap outside the generator enclosure. A slight positive pressure is maintained in the bearing pot by a spiral seal, which consists of a helical grooved casing in close proximity to the shaft and thus acts as a viscous pump. The bearing is drained via a pipe in the bottom of the bearing pot. By use of special lifting devices and after jacking the rotor, both the lower guide bearing and thrust bearing pads can be removed laterally and lowered into the turbine pit, without necessitating the removal of the generator rotor. The total heat exchanger capacity of 985 kW is such that adequate cooling can be maintained with one exchanger out of service. Eight oil to raw water heat exchangers are located in the oil pot, each with ten finned single pass water tubes 25 mm in diameter. The oil is circulated through the heat exchanger by the viscous pumping action between the bearing pads and thrust block. Direct water cooling of the thrust bearing pads was considered but not adopted because its major advantage, that of decreasing the size of the bearing and thus increasing specific pressures, did not compensate for the additional complications involved and because, at the time of bidding, there was little experience in the industry.

During starting and stopping of the turbine generator unit, the thrust bearing oil film is established by means of the high pressure oil pumping system. However, if necessary the unit can be stopped without the system. The system pressure is 2.8 kN/cm^2 as provided by two electric motor driven helical screw pumps, one in reserve should

Fig. 12.72 Upper bearing general arrangement

- 1 Upper guide bearing collar
- 2 Radial gap
- 3 Shim plates
- 4 Bearing segments
- 5 Cooler
- 6 Cover
- 7 Spiral seal
- 8 Pipe
- 9 Chamber
- 10 Generator upper shaft
- 11 Spiral seal

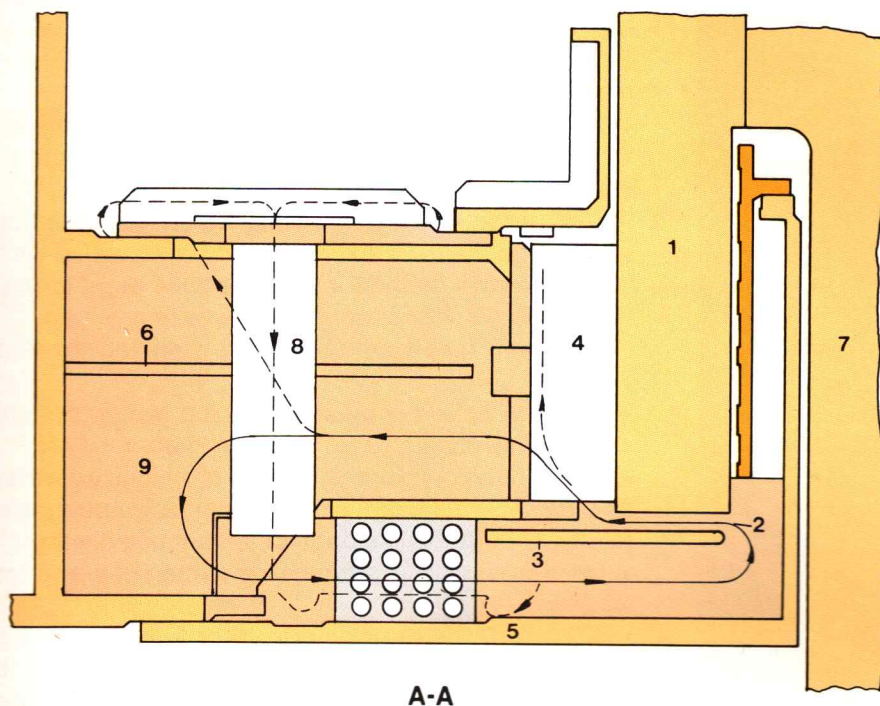


the other fail. For additional operating reliability one pump is supplied from the 50 Hz powerhouse system and other from the 60 Hz. Oil is pumped to a collection chamber from where it is individually piped via equalizing orifices to each thrust pad. Non return valves are located at each pad to ensure that the pad oil film is maintained in the unlikely event of a supply line rupture. It takes about a second to lift the rotor after which the pad pressures stabilize at approximately 1.55 kN/cm^2 , each pad receiving 4.7 l/min oil supply. The supply orifices in each line are sized such that even if three supply lines are broken the general oil pressure drops only to 1.4 kN/cm^2 which is still sufficient to support the generator.

Upper bearing

The upper guide bearing shown in Fig. 12.72 comprises sixteen tilting pads which bear on the shoulder of the upper shaft and are supported by the upper bearing bracket. Calculated specific loadings for the upper generator guide bearing are the same as the lower generator guide bearing. The velocity of the bearing journal is 10.47 m/s and the

erection and running clearance are $350 \mu\text{m}$ (minimum) and $200 \mu\text{m}$ respectively. Fig.12.73 shows the oil circulation of the upper guide bearing. A pumping action is developed in the radial gap above the ring (2), due to the rotation of runner (1). The gap height is adjustable by shim plates (3). The cold oil flows past the bearing segments (4), picks up heat, and then flows through the cooler (5) and back to the collar and bearing segment gap. Pressure in the space upstream of the collar and bearing segment is maintained by the cover (6) and the spiral seal (7). Any leakage oil collects on the loosely fitted cover (6) and flows through the pipes (8) and the chamber (9) between the two cooler halves, back to the pump inlet. This ensures that the pump inlet is always under positive static pressure due to the free oil level above the cover (6). Spiral seal (11) prevents leakage into the rotor or generator space. The pump gap is approximately 7.2 mm resulting in a flow of 3700 l/min at 300 mm oil column. The oil to water heat exchanger shown in Fig. 12.74 is in two halves, each half being sufficient to maintain the necessary cooling (30 kW). Cooling tubes are finless and curved.



A-A

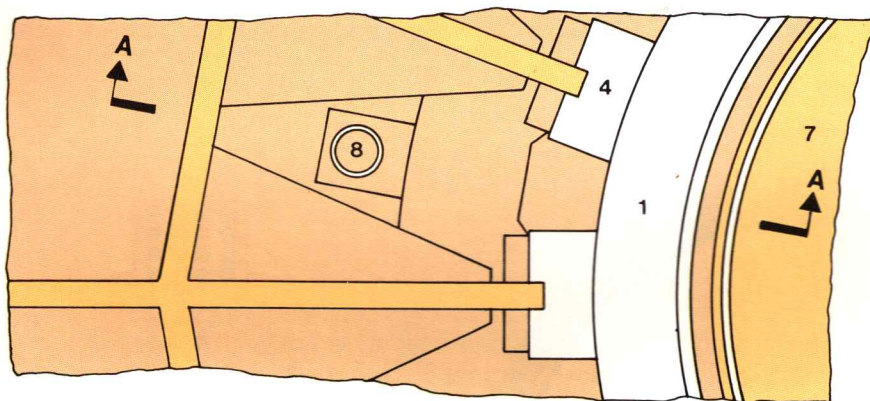


Fig. 12.73 Upper guide bearing oil circulation

- 1 Upper guide bearing collar
- 2 Radial gap
- 3 Shim plates
- 4 Upper guide bearing pad
- 5 Upper guide bearing oil to water heat exchanger
- 6 Cover
- 7 Generator upper shaft
- 8 Pipe
- 9 Chamber

Cooling systems

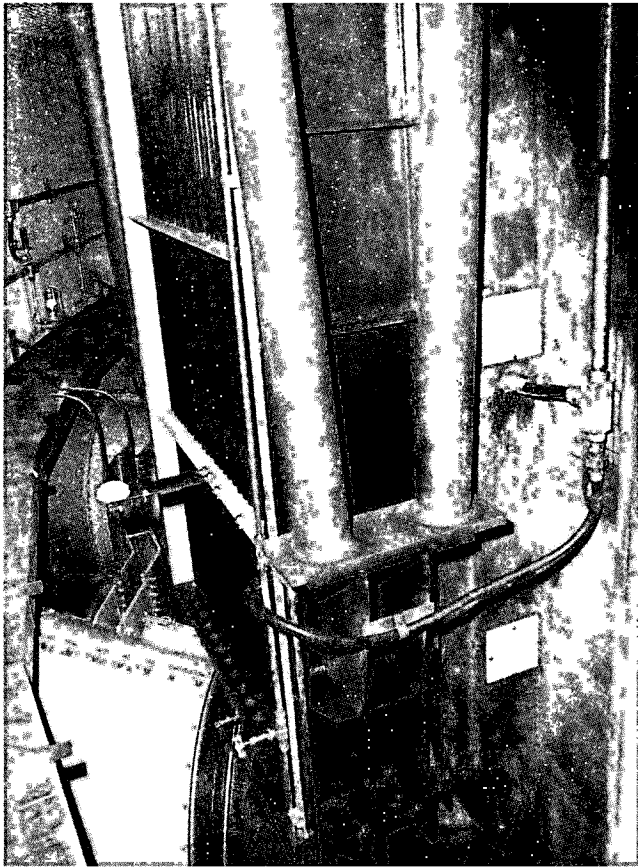
With the exception of the stator winding, which is direct water cooled, the generator utilizes standard air cooling methods. The rotor rim, field poles, stator core and frame, are radially cooled by air circulated by the fan action of the rotor, which in turn is cooled by air to raw water heat exchangers.

A comparative study of generators with direct water cooled stator windings to those completely air cooled showed that the adoption of the direct water cooling method to the stator winding

permitted about 30% reduction in the overall weight and cost of generator and gave a better overall efficiency.

Additionally, the selected method also gives the following advantages:

- Slightly lower airflow resulting in lower noise levels and reduced windage losses.
- Lower temperature of the stator windings, giving extended service life.
- More uniform temperature distribution between the stator winding bar and core, minimizing by



Generator air to raw water cooler

approximately 60 % the relative movements between the bar and core and therefore reducing the risk of loosening of the bars and the subsequent erosion of the semiconducting layers.

- Better monitoring of stator winding temperatures by measuring the cooling water exit temperature at the each conductor group.
- With utilization of direct water cooling, the stator winding consists of six parallel circuits, while with the air cooling method it would require eight to ten, hence the number of connections were reduced.

The main disadvantages of the selected method were:

- Addition of a complex deionized water system complete with deionizers, filters and pumps.
- Loss of unit output in the event of deionized water cooling system failure, although partial output is still available after the drainage of all deionized water.
- Restriction in high potential dc testing of the stator winding.

The direct water-cooled stator windings were finally chosen for Itaipu generators because the advantages substantially outweighed the disadvantages.

The stator deionized water system schematic diagram is shown in Fig. 12.75. The system is designed to dissipate the heat load of 4714 kW. The total water flow through the bars and connectors is $0.042 \text{ m}^3/\text{s}$. Pumps and heat exchangers are located

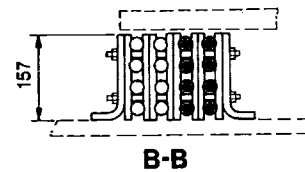
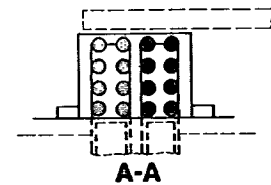
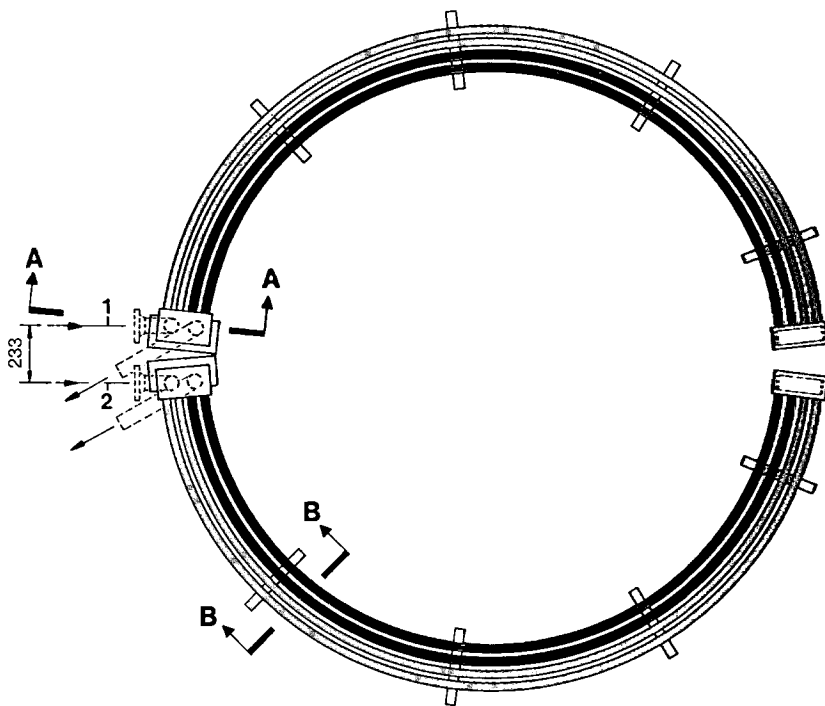


Fig. 12.74 Upper bearing oil to water heat exchanger

- 1 Water in
2 Water out

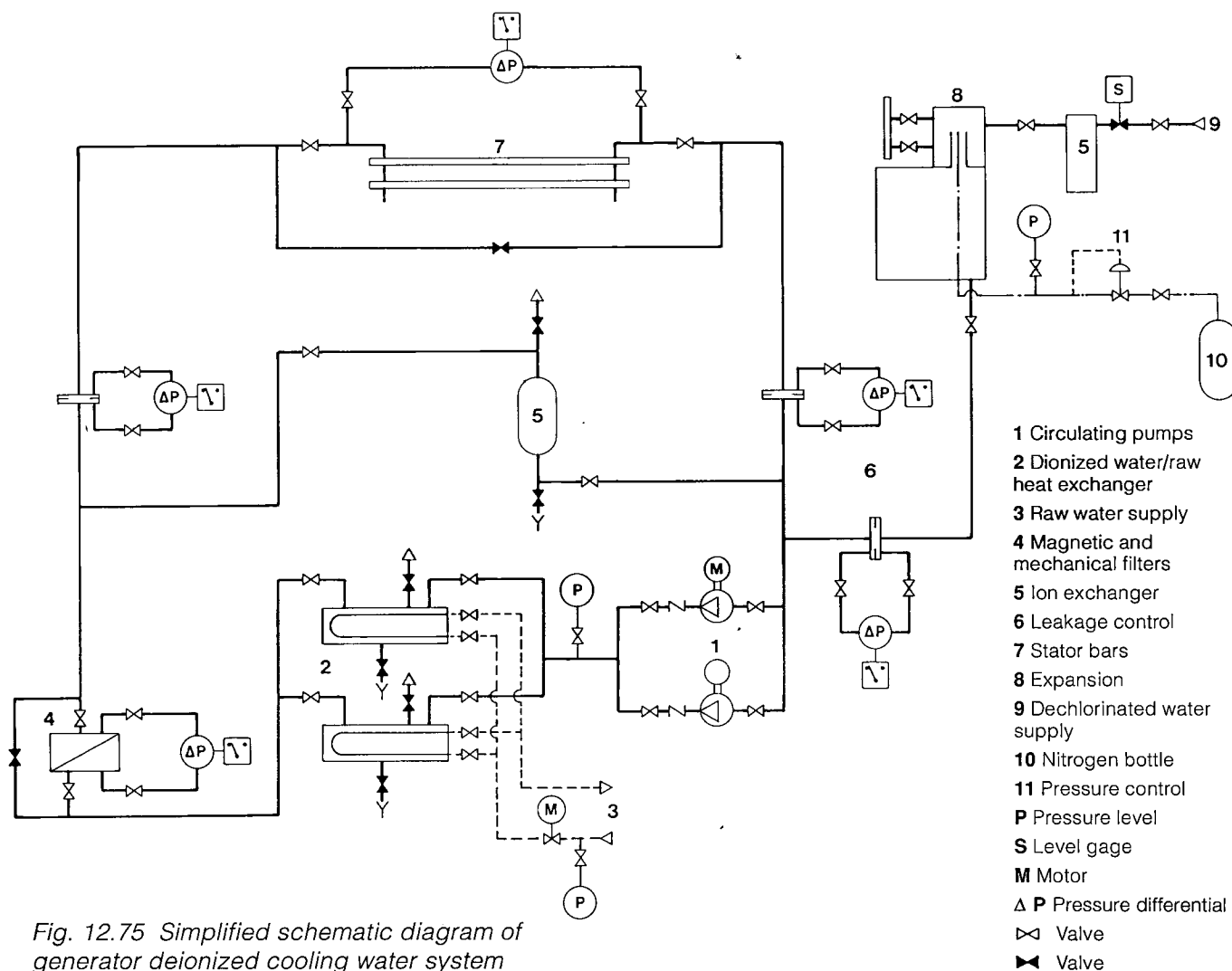


Fig. 12.75 Simplified schematic diagram of generator deionized cooling water system

in the downstream gallery, at El. 98.5 and the water treatment plant is installed on the compressor room roof in the same gallery. The entire deionized water cooling system piping used only copper, stainless steel and plastic, i.e. non-corrosive materials. There are two three-phase ac motor driven pumps, one of them acting as a stand-by which starts automatically should the other fail. Should both pumps fail, the generator is gradually unloaded. Normally two deionized/raw water coolers are operated in parallel to prevent the deionized water in one of the coolers being charged with copper ions should it be shut down for an extended period, but each cooler is designed for the total thermal load thus permitting in-operation maintenance of the other cooler. A motor operated control valve in the raw water inlet

pipe of the coolers regulates the deionized water temperature at the outlet of the winding between 40°C and 60°C with the temperature being proportional to the stator current. Thus, regardless of the operating mode of the generator, an almost constant winding temperature approximately equal to that of the ambient air is maintained. This ensures that there is no condensation on any part of the deionized water circuit. For the same reason, when the machine is stopped for short intervals, the flow of deionized water is continued, the space heaters being switched on only for long stops.

Mechanical micro-filters with 5 μm mesh are used for trapping impurities in the deionized water. They have replaceable filter elements of cellulose fibers which have larger pores on the outside than the

inside. Thus, the coarser impurities are trapped at the surface, while the smaller particles penetrate to different depths in the element according to their fineness, ensuring maximum efficiency of the filter. The degree of filter contamination is monitored by a differential pressure meter with alarm contacts. A magnetic separator traps very fine magnetic particles which, if allowed to pass, would oscillate in the magnetic field of the stator and could cause serious damage to the stator winding. The magnetic separator consists of permanent magnetic bars. All particles containing iron are attracted to and held by the bars, which have protective sleeves made of a non-corroding material. A combined by-pass system permits in-operation cleaning and replacement of the mechanical filter and magnetic separator.

As the deionized water is in direct contact with the high voltage stator winding copper and flows through the earthed piping system, it must be kept at a very low conductivity. The maximum conductivity is $5 \mu\text{S/cm}$. At larger values, there is a danger of flashover between the high voltage circuits and the earthed parts. During commissioning, the deionized water equipment is filled with demineralized water of very low conductivity and oxygen content. During operation however, copper ions are released by the windings, which gradually increase the conductivity of the water and therefore requires a continuous deionization of the water by the use of ion exchanger. The ion exchanger is connected in parallel to the winding cooling circuits and receives only about 0.5% of the total pure water flow, and reduces the water conductivity to $0.1 \mu\text{S/cm}$, which is sufficient to keep the conductivity of the water in the general circuit at approximately $2.3 \mu\text{S/cm}$. Special granular resins are used in the ion exchanger, which are basically polymers into which effective exchanger groups have been incorporated. The cation exchanger contains strongly acidic groups and draws cations from the water and replaces them with the equivalent amount of hydrogen ions; the anion exchanger contains strongly basic groups and takes anions from the water and replaces them with hydroxyl ions. A third resin is used to maintain the pH of the water between 8 and 8.5. Resins have a life of over 8000 operating hours and can be replaced during operation. The conductivity of the water increases very slowly when the ion exchanger is not in operation.

Differences in the volume of the deionized water in the system which result from changes in temperature, are compensated for by an expansion tank installed at the highest point of the system. To avoid oxygen contamination of the water, the tank is

filled with nitrogen at low pressure. Nitrogen for the expansion tank comes from a cylinder via a pressure reducer. The cylinder can be replaced during operation of the unit. Deionized water lost through leakage is made up from dechlorinated water, obtained from the water treatment plants described in Chapter 10. Before entering the expansion tank this water passes through a small deionizer which is attached to the tank.

The rotor rim, field poles, stator iron and frame are cooled by a closed air circulation system. The fan action of the rotor is used to drive the air radially through the slots in the rotor rim laminations and between the field poles. This results in very uniform cooling of the rotor and stator compared with the alternative of using axial fans to drive air in the top and bottom of the air gap. From the air gap the cooling air passes through slots in the stator core, through the air to raw water heat exchangers which are mounted on the outside of the stator and then through air ducts back to the middle of the rotor.

A theoretical model for the generator air flow was developed; the model information was supplemented by the results from other generators in operation, and from a test rig. The volumetric flow of air required was $160 \text{ m}^3/\text{s}$ and, with a 10 mm clearance between the air baffles and the rotor rim, the flow through the heat exchangers was estimated to be $200 \text{ m}^3/\text{s}$, 10% of which is flowing back through the clearance. There are sixteen air/water heat exchangers (6300 kW total) per generator, designed for 77.4°C air in, 40°C air out, with 30°C raw water supply and a 10°C water temperature increase. Each heat exchanger has six rows of triangularly arranged tubes, twenty-eight tubes in one row and twenty-seven in the adjacent row. In the twenty-seven tube row the side plates have a protruding corner piece to ensure an even velocity distribution. The 90/10 copper nickel water tubes have soldered copper fins in a helical configuration, to improve the heat transfer coefficient. The heat exchangers are connected to the stator via flexible type bellows.

Brakes and jacks

Although separate brakes and jacks were initially considered, with the jacks located close to the thrust bearing to minimize structural stress changes during the jacking, the final design adopted the more usual combined brake and jack system, the brake system employing compressed air and the jacking system using high pressure oil.

A simplified schematic diagram of the combined system is shown in Fig. 12.76. There are thirty-two brakes/jacks which, when extended, operate on the

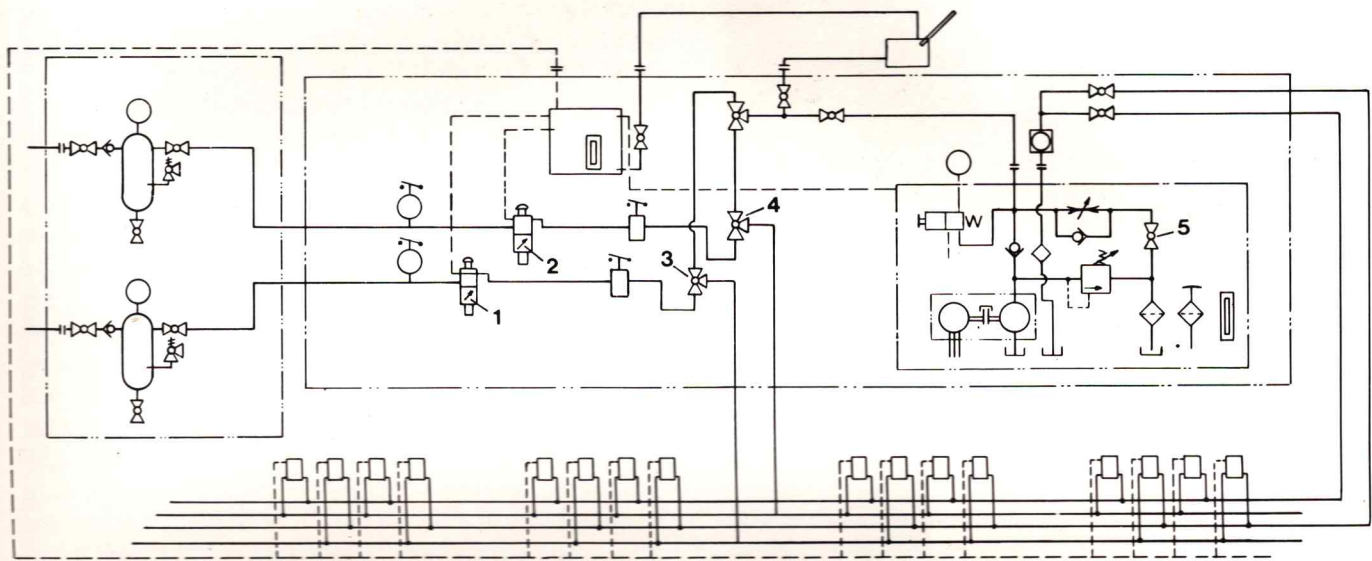


Fig. 12.76 Brakes and jacks schematic diagram

1,2 Solenoid valves

3,4 Three-way valve

5 By-pass valve

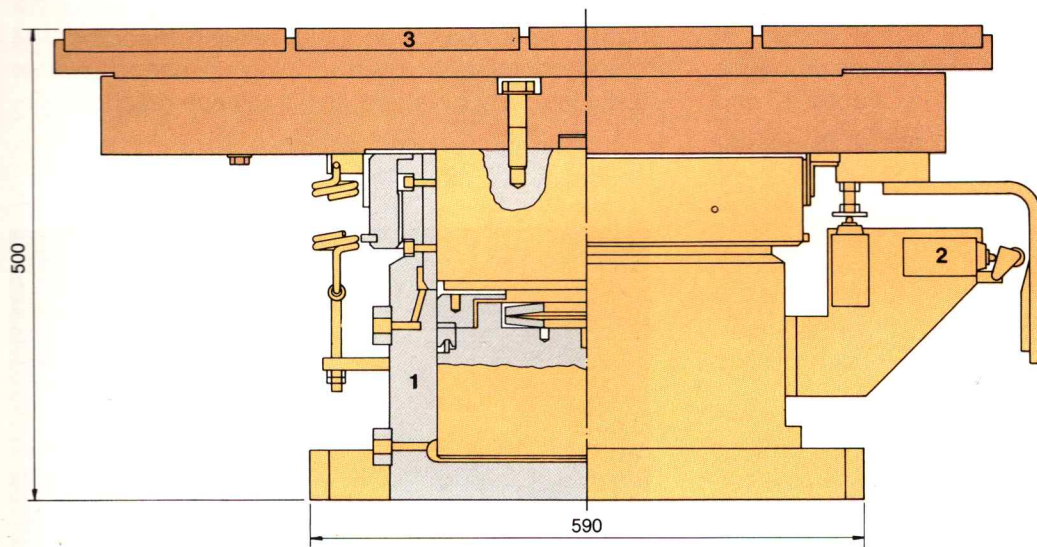


Fig. 12.77 Brakes and jacks detail

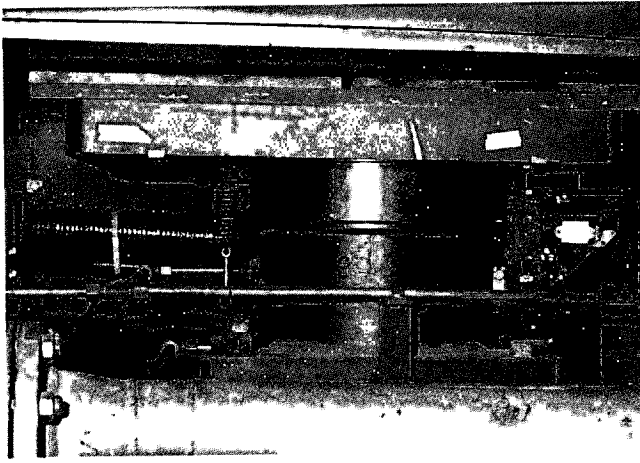
1 Jack cylinder

2 Limit switch

3 Shoe

brake ring, bolted to the underside of the generator rim. A detailed arrangement of the brake/jack is shown in Fig. 12.77. The upper (to which the shoe is attached) is supported on the lower by a Belleville spring washer. Oil or air pressure admitted between

the bottom face of the lower piston and the cylinder casing applies the jack shoe to the brake ring. During braking any unevenness in the brake ring is accommodated by movement of the upper piston in the cylinder, this movement being regulated by the



Generator combined brake/jack

two pre-tensioned springs attached to the shoe on either side of the cylinder compressing the Belleville washer. The same two springs return the combined piston when the air or oil pressure is released. The total travel course of the piston is 30 mm and the maximum permitted wear of the brake lining is 8 mm. The thirty-two brakes/jacks are operated by two separate independent air/oil circuits such that only a bank of sixteen can be applied, the other bank normally acting as a reserve. If necessary, all thirty-two brakes/jacks can be applied simultaneously.

Compressed air is supplied from the powerhouse compressed air system described in Chapter 13 and should the powerhouse air system fail, each brake/jack system is equipped with a 600 l air accumulator which is sufficient for two brake applications. Non-return valves in the supply lines prevent the accumulators back feeding into the powerhouse system. If the thirty-two brake/jacks are deployed, then the combined system is adequate for three applications. The maximum pressure in the system is 88 N/cm^2 and the minimum 66 N/cm^2 .

The new turbine wicket gate clearances are such that the residual speed of the generator unit is around 20 rpm, which results in a total stopping time of 520 seconds when sixteen brake cylinders are used and a brake ring temperature of 50°C . Brake application at the lowest speed practically possible is necessary since it minimizes brake wear and reduces the production of the undesirable brake dust. However, in the case of worn wicket gate clearances it is possible to apply brakes at a maximum speed of 45 rpm, by opening solenoid valves, see (1) and (2) in Fig. 12.76, in which case unit stopping when sixteen

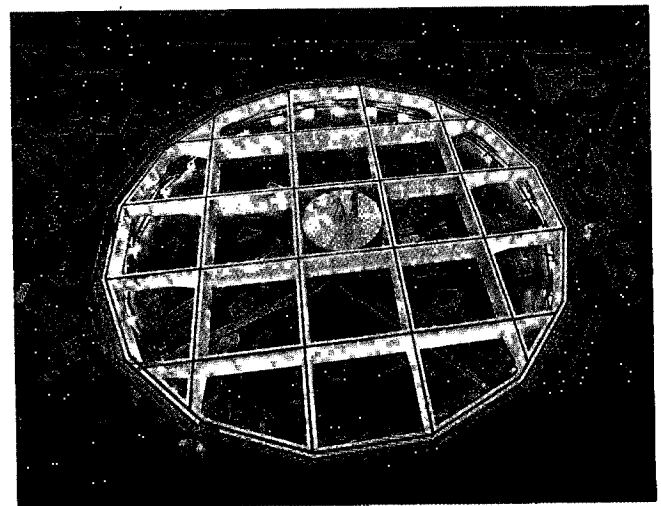
brake cylinders are used is about 325 seconds (total time from full speed) and results in a brake ring temperature of approximately 90°C .

Oil jacking is activated by operation of three-way valves (3) or (4). Sixteen jacks are sufficient to lift the rotor. Oil is pumped to the jacks at 1.95 kN/cm^2 pressure by the electric motor driven pumping set. The jacks are raised and the pump is stopped automatically by a limit switch on the rotor. The rotor is lowered by opening the by-pass valve (5). A manual pump is provided should the motor driven pump be out of service. This manual pump would be used in the event the thrust bearing oil film needs to be established.

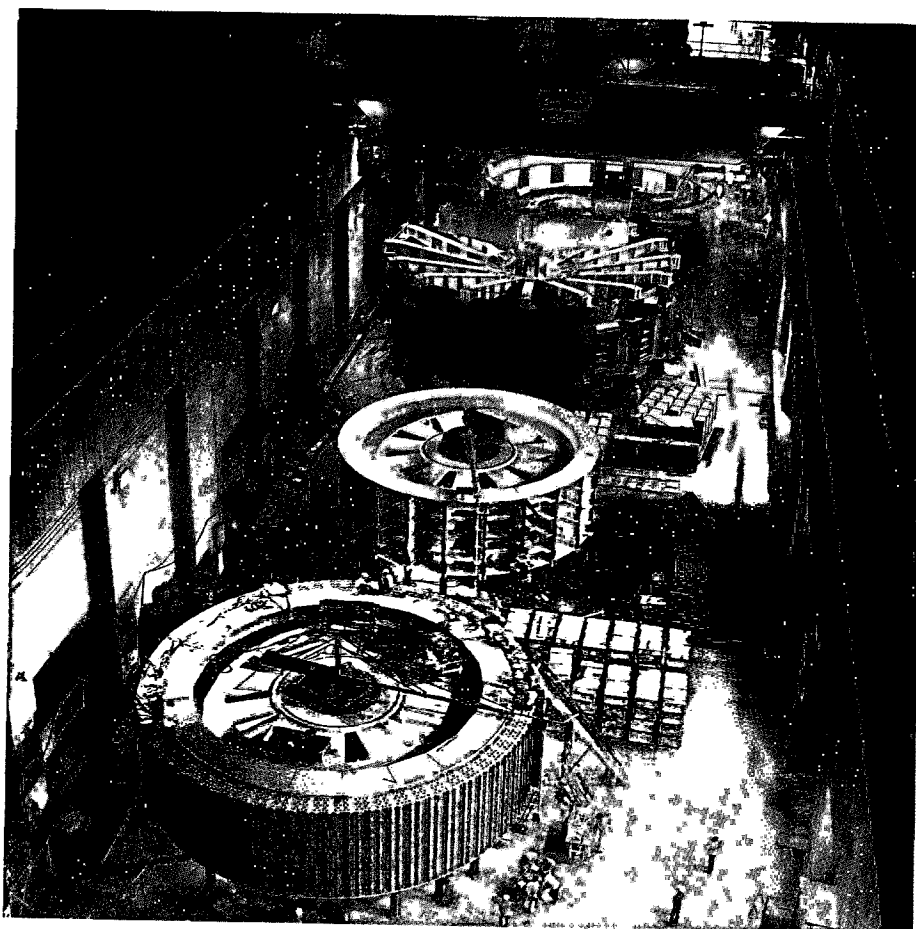
CO₂ fire protection system

Although it was recognized that generators with Class F insulation have been installed without fire protection, or with water sprinkler systems, CO₂ was selected to provide the fire protection with minimum after-effects. The risk of thermal shock to the unit was considered to be acceptable and the safety door interlocks prevent the system from operating when the operating personnel are inside the generator housing.

The 500 N/cm^2 CO₂ system comprises two banks of cylinders, one bank being the principal system and the other acting as a back-up. The cylinder banks are located in the downstream gallery at El.115, each bank serving two generators. Both banks are sized for an initial release (needing 104 cylinders) followed by a topping-up period release requiring sixty cylinders. Initial release reaches CO₂



Generator top cover support structure



Generator erection in right assembly area. One stator with lifting beam ready for placing in generator pit, two rotors in various stages of erection

concentration of 50% in the generator enclosure within 3 minutes and the top-up maintains a concentration of 30% minimum for 20 minutes, approximately the time necessary to stop the unit. A 101.6 mm ring header is used for the initial release period switching to a 38.1 mm ring header for the topping-up period. Activation of the CO₂ system is by ten smoke and sixteen temperature detectors located in the generator housing. If any detector operates, an alarm is initiated and, if at least one of each type operates, the unit shutdown is initiated and the primary CO₂ system discharges after 60 seconds. A dedicated ventilation system is used to exhaust the CO₂ after the fire danger has ended.

Covers and access

The generator has sealed top and bottom covers which contain the circulation of cooling air and serve as a fire-proof enclosure for the CO₂ fire protection system. Checker plates comprising the bottom cover are bolted to the lower bearing bracket, and those of the top cover are supported by a welded

structure which spans the generator concrete housing at El.108.

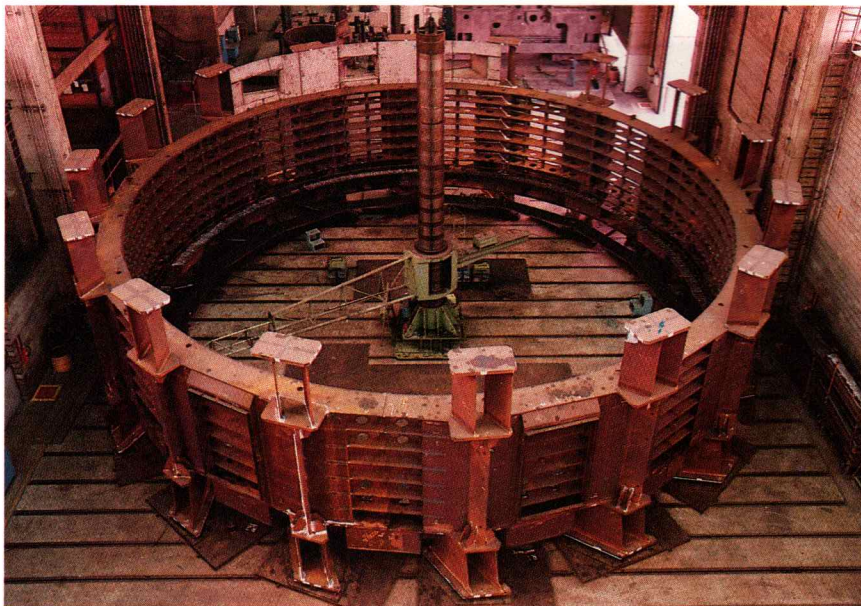
Access to the generator housing is by means of two sealed doors diametrically opposed each at El.98.5. Inside the housing there is a walkway around the stator frame and a space for removing the air/raw water heat exchangers.

Access to the generator lower bracket is by a ladder from the turbine through a lockable man door in the bottom cover. The top cover has a man door for access to the slip ring enclosure and to the turbine aeration valve. The specifications required that the top cover be designed to support a distributed load of 0.49 N/cm² and a point load of 200 kN.

ERECTION

General

Shipping limitations necessitated that the majority of the assembly work of the large components of the generators and all the final erection of the unit take



*Alignment and welding
of stator segments*

place at site. The major items consisting of the stator, rotor, and upper and lower brackets complete with bearing housings, were assembled in the powerhouse assembly areas and then moved to the generator pit where the final erection, including alignment and the connection of auxiliaries, was done. Minor differences exist between the 50 Hz and 60 Hz generators and the procedures of the two suppliers involved; these are noted where they are considered of interest.

Stator

The eight sections of the stator frame were assembled and levelled in the assembly area and rounded to 0 to + 2 mm tolerance using a center-post pivoted beam micrometer. The sequence of welding the sections of the frame together was carefully controlled and adjusted to limit overall distortion of the completed frame.

In preparation for stacking the stator core, the bottom clamping fingers and the vertical dovetail key-bars were installed. The clamping fingers were levelled and welded and a trial fit of core laminations made to the key-bars. The key-bars were aligned and their keeper plates welded.

Stator core stacking was done in eight stages, each consisting of approximately seven core packs. At the end of each stage the core was hydraulically pressed, the height and inside diameter checked and if necessary the key-bars adjusted to maintain the design diameter to ± 0.7 mm. On completion, the stator core was given a magnetization test.



Installation of stator core guides

The primary purpose of this test was to locate, by infra-red sensor, hot spots caused by interlaminar magnetic short circuits. The secondary benefit was the compaction of the core as follows:

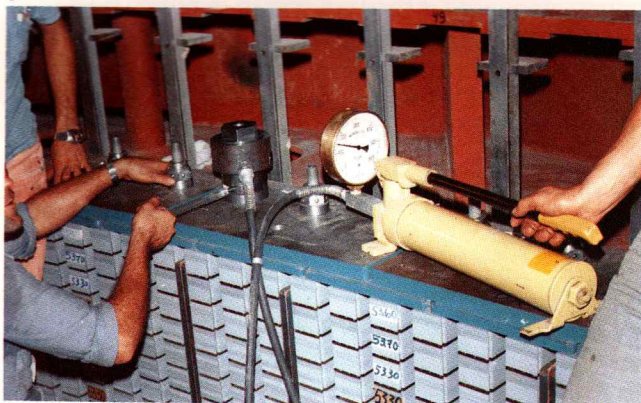
	Before	After
50 Hz	3506 ± 2 mm	$3500 + 4$ mm - 0 mm
60 Hz	3266 ± 2 mm	$3260 + 4$ mm - 0 mm

During the magnetizing test on the first Siemens (50 Hz) generator, a permanent dislocation of some laminations of the lower packet occurred. This was due to the temperature differentials due to lack of preheat of the base plate. The distortion was only 1.5 mm, which was considered acceptable.

The assembly of the complete stator frame and core required approximately 7 months.

The installation of the top and bottom supporting rings which are used to lash the bars was slightly different for each manufacturer. BBC fitted the rings before installing the bars while Siemens installed them afterwards. In either case, the method of blocking and lashing in the winding end-turn areas was similar and was completed before the wedging and making of the winding end connections.

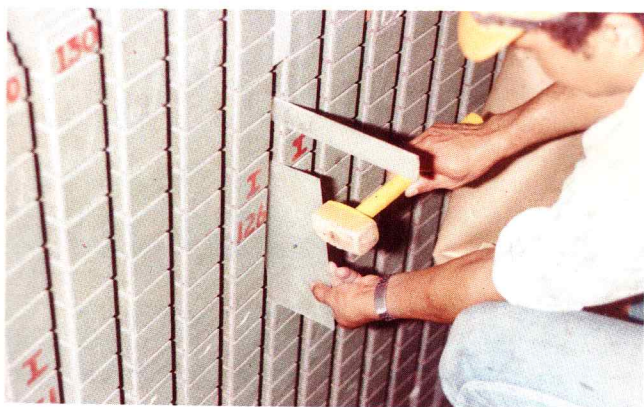
The brazing of the end connections was done using a silver solder at a temperature of 650 to 800°C and currents of 1500 to 5000 A. The bar insulation was protected by thermal paste and nitrogen gas was used to reduce oxidation during the process. The stator was then moved to the generator pit, with the 10 MN cranes using a special multi-arm lifting device to prevent distortion, and centered to ± 0.2 mm tolerance. Main circuit rings were installed



Tensioning of stator core holding bolts with a hydraulic jack



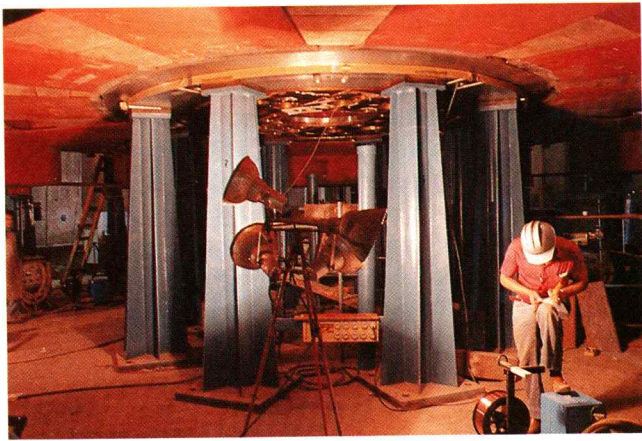
Installation of stator winding. Insertion of side filler (BBC generator)



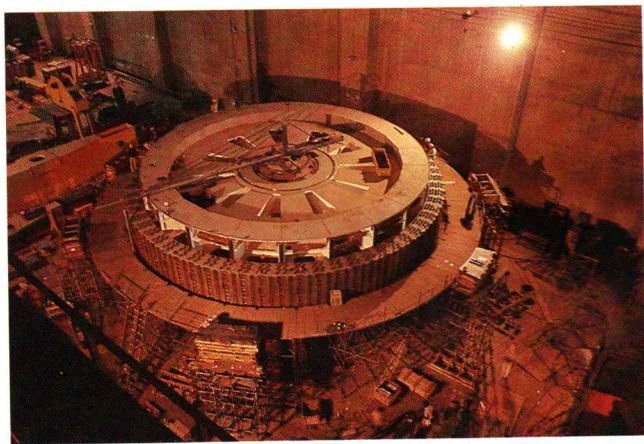
Tightening of the core package with a torque wrench



Lashing of upper bars



Central hub of rotor supported in the assembly area



Rotor rim stacking

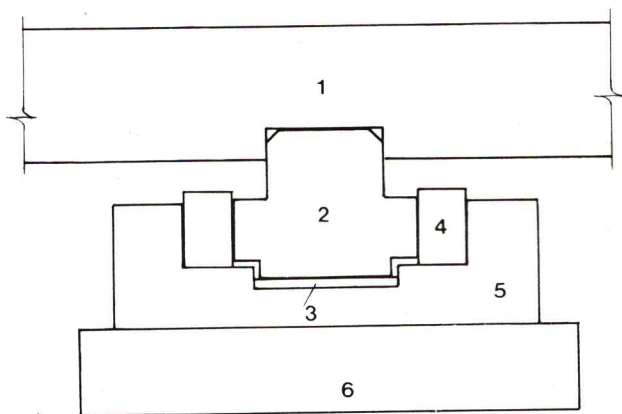


Fig. 12.78 Rotor rim mounting detail

- | | |
|-------------|--------------------|
| 1 Rotor rim | 4 Wedges |
| 2 Key | 5 "U" beam |
| 3 Shim | 6 Spider head beam |

and connected by brazing and then the winding end-caps were installed. Finally the deionized water cooling connections between the stator bars were made, and associated headers and insulated connections between the winding and the headers were installed. The specified location of stacking of the generator core and the placement of winding bars was the generator pit. Later, because of scheduling, this was changed and it was done in the assembly area.

Rotor

In the assembly area, the central hub of the rotor was supported on eight steel pedestals and levelled to 0.02 mm/m. A center-post pivoted beam micrometer was mounted on the top of the hub to control circularity.

Rotor arms were bolted to the hub with their outer end supported by a pedestal under each of the two rim head beams. After all the arms were assembled, a dimensional check was made and the joints at the hub and between the arms were welded. The sequence of welding was carefully controlled to minimize overall distortion and to maintain a level of tolerance to ± 0.3 mm, a radial tolerance to the face of the rim head columns to ± 1.0 mm, and a vertical tolerance of the rim head columns to ± 0.3 mm in the circumferential direction.

In preparation for stacking the rotor rim, the vertical "U" beams were mounted on the head beams, see Fig. 12.78. The bottom compression plates, for the rim laminations, were supported on the head beams step blocks and on separate temporary pedestals. A trial fit of rim laminations, twenty sheets at 3 mm each, was made and the "U" beams adjusted and welded to the head beams.

The rim was compressed vertically with through-bolts at six stages of stacking and, if required, the height of the stack was adjusted for low spots of 2 mm or more, using special shim laminations. The outer face of the rim was maintained within a maximum to minimum range of 0.6 mm on the radial measurements. Final rim compression was made by checking the loading stud elongation.

The assembly of a rotor to this stage of completion required approximately 12 months.

For the shrink fit of the rim, tubular heaters were installed in four stud holes per pole position and a strip heater placed on the underside of the rim. The rim was heated to approximately 60°C higher than the rotor arms and then the radial shims were installed. The tapered tangential wedges, on both sides of the main key, were fitted and driven using hydraulic jacks. When all keys and wedges were in

place, keeper plates were installed on the top and bottom.

Field poles were shipped to site fully assembled and ready for installation on the rotor rim. Mounting utilized a single dovetail connection, with a set of seven shim and wedge locations, to accurately locate to ± 0.3 mm radially and firmly hold the pole. The vertical position was set to ± 1.0 mm by two adjustable studs to the lower rim pressure plate. The final radial tapered wedges, in the center of the dovetail, were driven in with hydraulic jacks, and keeper plates installed. Three wedge shaped longitudinal supports were installed between poles and anchored to the rim by bolts through the ventilation slots.

The main field winding and the damper bar winding were directly connected between poles by bolted connections at the top and bottom of the poles. The main field leads were installed, from the central hub to the top of the rim, inside one of the rotor arms.

The brake ring, consisting of plate segments, was installed on the bottom side of the rim using

extended through-studs and shims to obtain a level tolerance of ± 0.2 mm.

After final painting the rotor was moved to the generator pit using a four hook equalizer beam with the two 10 MN cranes coupled together.

Lower bearing bracket and foundation ring

The lower bearing bracket and the stator base are coupled and supported by a fabricated foundation ring embedded in concrete in the generator pit. The eight sections of the ring were placed, levelled and welded together prior to bolting down and embedding. Also mounted on the ring are the generator brake and jack units.

The central hub of the lower bearing bracket was placed on pedestals in the erection area and accurately levelled. The arms were attached using a system of dowels and keys, for alignment and load transmission, before bolting.

Thrust bearing and lower generator guide bearing components, up to and including the bearing shoes, were installed in the hub. This included the jack bolt assemblies extending through the bottom of the



Installation of a generator pole



Rotor arms ready to be lifted on the supports and welded to the central hub

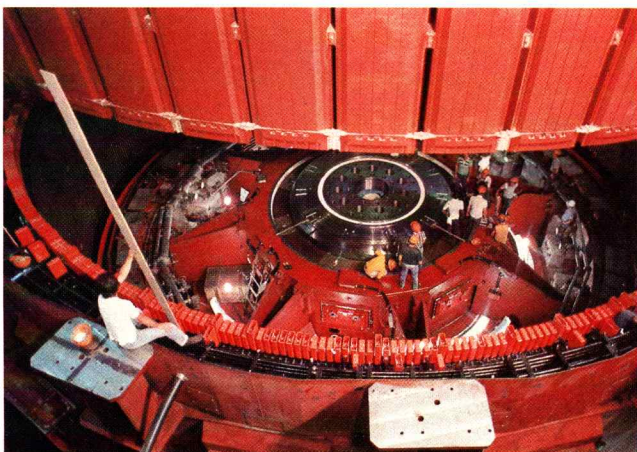


Lower generator and turbine shaft coupling

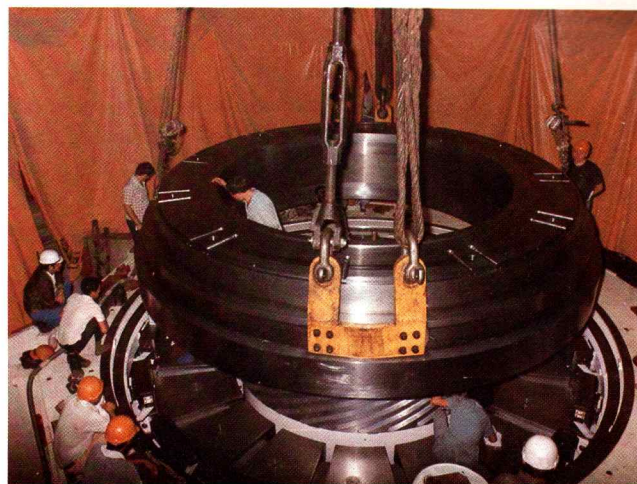
housing to allow load adjustment on each thrust shoe. Also installed were the oil to water heat exchangers and the piping for the high pressure oil lift system of the thrust bearing. The bearing shoes were temporarily removed prior to moving the assembly into the housing.

Lower generator shaft

The lower generator shaft was installed and coupled to the turbine shaft prior to placing the lower bearing bracket in the generator housing. This was done by matching the high and low points on the coupling and pulling the coupling together with six hydraulic jacks. The combined unit was checked for plumb and centering to the turbine lower wearing ring. The



Thrust block



Thrust block being lowered onto thrust pad

coupling holes were reamed and the coupling bolts installed and hydraulically tensioned. The stator, which had previously been placed in the housing, was centered on the shaft and bolted to the foundation ring.

The lower bearing bracket assembly was lifted into the generator housing, levelled and centered on the shaft before final bolting to the foundation ring. The thrust bearing was re-installed and the thrust block placed on the pads, using the high pressure oil system to aid in centering to the shaft. A final check of the shaft center, plumb, coupling face level, thrust block level, and center was made.

Brake and jack unit

Brake and jack units were mounted on the foundation ring. The associated compressed air, and high pressure oil piping and electrical wiring was installed. These units were used to support the rotor after it was moved to the pit from the erection area and coupled to the thrust block.

Coupling of rotor

Coupling of the rotor hub to the thrust block was done initially with the rotor supported by the main powerhouse cranes. Factory match marks were mated and the initial alignment established using four vertical dowel guides. Using temporary hydraulic jacks, the thrust block was raised for final alignment of the horizontal torque dowels. The rotor was then lowered by the cranes and the total load taken on the thrust bearing and the temporary jacks.

The adjustable bearing support nuts were tightened and the load was transferred from the temporary jacks.

After rechecking the alignment, vertical cap bolts, each with a spacer tube and slip washer to allow thermal radial growth of the thrust block, were installed. This was followed by the reaming of the holes for the horizontal torque dowels and the fitting of the dowels and keeper plates to complete the coupling.

Coupling of rotor hub

Initial coupling was made using four hydraulically actuated jacking bolts, four temporary guide dowels with excentric adjustment, and four without. After completing a plumb check, all coupling bolts were installed and hydraulically stretched to approximately 80% of their working stress and a second plumb check was made. The static load on the thrust bearing pads was equalized and a third plumb check was made.

A complete run-out check was made of the combined generator rotor, shafts, and turbine

runner using the thrust bearing high pressure oil system to allow rotation in 45° steps. The shaft coupling bolts were tightened to their final value and the run-out rechecked. The shear dowel holes were finish-bored and the dowels were fitted and keeper plates were installed to complete the coupling process.

Generator upper shaft

The upper shaft was placed on the rotor using a powerhouse crane and centered with horizontal hydraulic jacks. Five temporary bolts were installed and the field slip-rings mounted. A preliminary alignment and run-out check was made and six additional bolts were installed and an alignment recheck was made. Then a full plumb check of all rotating parts was carried out.

Six of the temporary bolts were removed and the bolt holes enlarged. The six permanent bolts were fitted and hydraulically tensioned to approximately 50% load. The remaining bolts were installed and all bolts were tensioned to final values and their nuts locked.



Lowering of rotor onto generator lower shaft



Upper bracket during erection

Upper bearing bracket

The upper bearing bracket hub was placed on pedestals in the erection area and levelled. Bracket arms were spaced and levelled before welding to the hub was made in a controlled sequence to minimize distortion.

Upper guide bearing components, including the sixteen pads, oil to water heat exchanger, spiral seal, shaft and collar seals, and associated seal plates were installed on a trial basis and centered and levelled. The piping for the bearing cooling water, oil vapor control, oil fill and drain connections and the electrical conduits were installed.

In preparation for installing the bracket inside the generator housing, the bracket base plates were placed on the stator supports and levelled by using shim plates. The vertical bracket support plates were trimmed to length to suit the base plate elevations and a trial fit of the bracket in the generator housing was made. Since the bracket must center on the upper shaft and be level at a specific elevation relative to the bearing journal, several adjustments were necessary. Base plates were welded to vertical support plates, fixing the bracket to the stator.

Radial foundation plates, to be embedded in the generator housing wall, were aligned with the arm ends and made ready for grouting. After grouting, the vertical keys were fitted between the arm ends and the foundation plates and a final centering and levelling check were made. Tapered dowels were fitted between the base plates and the stator supports.

Final assembly of the inner parts of the upper guide bearing was completed, bearing shoe clearance adjusted and the various instrumentation

connections made. Piping connections were completed and the system was made ready for filling. At this time the installation of the following systems was completed:

- Stator air to water heat exchangers, complete with piping, headers, valves, and instrumentation.
- CO₂ fire protection system.
- Slip-rings, and brush assemblies, including the field leads from the exciter cubicle and those to the field poles.
- Turbine air admission valve and the top chamber which forms a part of the slip-ring housing.

Generator top cover and support

The generator top cover was assembled, welded and painted in the assembly area and then lifted into the housing. Individual panels of the top cover strips were mounted on gasket material and gaskets were also inserted between them.

Erection time

Total erection time from beginning of the draft tube erection to the start of commissioning was about 3 ½ years. The time from the start of manufacturing of the most critical item (stay ring/spiral case) was about 4 ½ years.

COMMISSIONING AND TESTING

Commissioning

Balancing of the unit was done at speed-no-load. The method used was by filtering and processing of signals generated by the proximeters and the accelerometers installed at the three guide bearings of the units.

The two-plane procedure foreseen in the contract was not feasible due to the relatively high ratio of diameter to height of the rotor. Nevertheless a satisfactory balancing of all the units was obtained with the simple one-plane compensation procedure.

The units were tested at an overspeed of 140%. The rotor rim was checked and it did not float under 110% of the nominal speed.

Stator and rotor winding insulation were dried by circulation of current in short-circuit conditions. Insulation resistance and polarization index were measured and the dielectric tests were made on the armature and field windings.

Generator no-load and short-circuit saturation curves were determined. The units were synchronized and load rejection tests were performed. Bearing temperatures at load were measured and

clearances of the guide bearings adjusted as necessary to meet the contractual temperatures.

Heat-run tests of the generators at full contractual load were performed and then the units were released for commercial operation.

During the commissioning test sequence, all unit monitoring and protective devices were checked and properly adjusted.

Testing

Acceptance tests were performed on four machines; two units of each manufacturer or one at each frequency. The acceptance tests included:

- Measurement of ohmic resistances of stator and rotor windings.
- Determination of short-circuit and no-load characteristics.
- Determination of no-load voltage wave form and TIF.
- Determination of negative sequence reactance and resistance, X_2 and R_2 .
- Determination of subtransient quadrature axis reactance X'' and transient open circuit time constant T''_{do} .
- Performance of sudden short-circuit test at reduced voltage to determine subtransient and transient direct-axis reactances X''_d and X'_d and time constants T''_d and T'_d ; and armature time constant T_d .
- Determination of segregated losses by calorimetric method.
- Performance of heat-run tests.

Typical no-load and short-circuit characteristics are shown in Fig.12.79 and 12.80. The direct-axis unsaturated synchronous reactance X_d was found greater than the guaranteed value; all other parameters were found to be within the specified limits.

The measurements of mechanical losses and heat-run tests were performed at two different conditions of the ventilation circuit: with the inlet-air openings of the upper side of the rotor respectively completely open (RO) and partially closed (RC).

The most significant results of the loss measurements and heat-run tests are shown in Tables 12.11 and 12.12.

The differences in losses found between units of the two manufacturers for the same frequency machines are mainly justified by differences in saturation characteristics, core stacking methods, air-circuit geometry and the air-gap dimension.

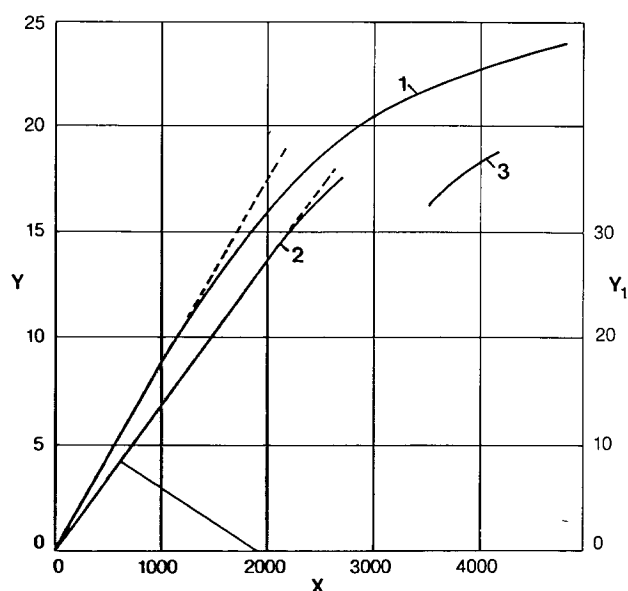


Fig. 12.79 Open and short circuit saturation curves typical for 50 Hz generators

Y V_0 (kV)	1 V_0 No-load curve
Y_1 I_k (kA)	2 I_k Short circuit curve
X I_f (A)	3 Zero power factor, 63% I_n

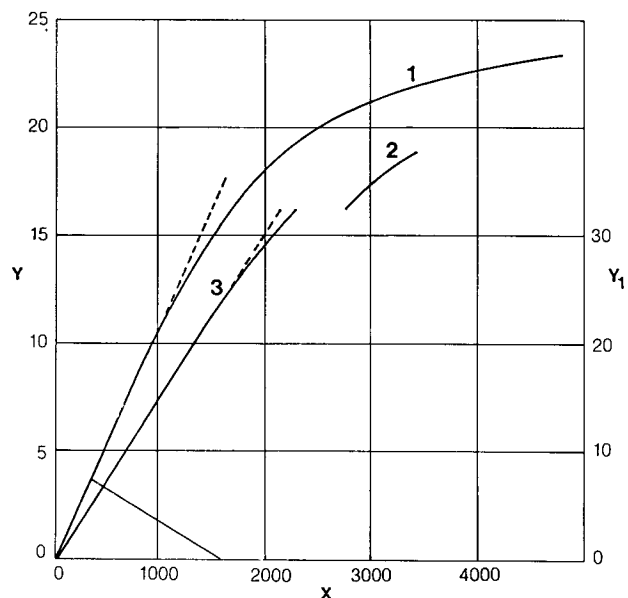


Fig. 12.80 Open and short circuit saturation curves typical for 60 Hz generators

Y V_0 (kV)	1 V_0 No-load curve
Y_1 I_k (kA)	2 I_k Short circuit curve
X I_f (A)	3 Zero power factor, 54% I_n

Table 12.11 Results of segregated loss measurements (kW)

		50 Hz (1)		60 Hz (2)	
		Manufacturer		Manufacturer	
		A	B	A	B
Rotor air ventilation	Openings open	1481	1366	1469	1401
	Openings closed	1128	1013 ^(*)	1191	1106
Voltage dependent		1869	2119	2068	2253
Current dependent	Ohmic	2694	2689	2469	2368
	Additional	1660	1731	1936	1826
Excitation (Field)		1760	1766	1311	1345
Other		1071	1073	1014	1049
Total measured	Openings open	10 535	10 744	10 267	10 242
	Openings closed	10 182	10 391 ^(*)	9989	9947
Total specified		10 477	10 477	10 013	10 013
Difference	Openings open	+ 58	+ 267	+ 254	+ 229
	Openings closed	- 295	- 86 ^(*)	- 24	- 66

(1) Losses in kW at 823.6 MVA 0.85 P.F.

(2) Losses in kW at 766 MVA 0.95 P.F.

(*) Estimated

Table 12.12 Results of heat-run tests (°C)

			50 Hz			60 Hz			
Tests at full rating; 1.05 p.u. voltage reduced cooling conditions			Manufacturer			Manufacturer			
			A		B	A		B	
			RO	RC	RO	RO	RC	RO	RC
Air/raw water heat exchangers	Raw water	in	30	30	30	30	30	30	30
		out	40	39	40.5	40	39.5	39.7	39.5
	Air	in	63.6	66.6	69.6	64.2	67.1	63.8	67.2
		out	42.5	41	41.8	42.8	41.5	39.1	40.4
Stator core (RTDs)		max.	74.6	78.5	83	78.2	81.1	78.7	83.4
		avg.	73.1	76.9	80.1	75.2	78	76.3	80.8
Rotor winding		avg.	97	105.9	104.5	89.5	98.1	85.6	93.5
Stator winding (RTD)		max.	54.3	55	57	60.6	66.2	62.2	63.5
		avg.	51.8	52.3	54.1	52	57.4	56.7	57.9
Pure water/raw water heat exchanger	Pure water	in	57	56.8	59.5	58.2	64.2	60	60.5
		out	36	35.8	37.5	33.9	41	38	38
	Raw water	in	21.8	21.5	18.3	25	26.2	27.5	27.7
		out	38.2	37.5	37.2	35.2	36	39.6	39.4

RO = Rotor air ventilation with openings open

RC = Rotor air ventilation with openings closed

The analysis of the results showed that for all cases, with one exception, the specified limits of losses and temperature can be met with an adequate setting of the rotor inlet air openings.

- Thrust bearing. A special test of the thrust bearing of one unit was extensively instrumented, with embedded sensors for in-service point measurement of metal temperatures and oil film pressures and thickness. During this test the contractual requirement that the units are able to stop without the high pressure pumps in operation, was also verified. The test program included the following conditions:

1. Measurements at steady-state with the unit in different operating modes (loads).
2. Recording of run-up transient conditions.
3. A series of unit stops, starting from the nominal speed and switching on the high pressure oil pump at progressively lower speeds.
4. A stop without high-pressure oil pump and application of the brakes.

The results of all tests were satisfactory and in good agreement with the design values. The results confirmed the value of hydraulic thrust obtained from the turbine model tests and the ability to stop the unit without the high pressure oil pumps; however, this did not influence the normal stopping procedure which continues to be made with the pumps in operation.

OPERATING EXPERIENCE

Several problems were experienced during the commissioning and subsequent operation of the units, as follows:

Generator vibrations

During operation, the BBC 60 Hz generators exhibited higher than specified vibrational levels in the stator core and the end turns. This occurred for a twenty-four node vibration mode of the core at 120 Hz and from the coincidence that the natural frequency of the end windings of some bars was 120 Hz.

The solution to reduce the stator vibrations was to change the space distribution of the armature reaction flux by altering the stator connections. Other electrical parameters were essentially unchanged by this modification.

The Siemens 60 Hz generators did not have the problem of stator core vibration because the natural frequency was different, as a result of all or some of the following factors:

- Varnishing of the stator core lamination packets on one side only instead of both in the case of BBC.

- Different core stacking method.
- Different bar installation procedure.

As far as the high end-turn vibration of some stator bars, a convenient solution was found by improving the fixing of the critical end turns. As the vibrations levels are not sufficiently high to endanger the windings, the required modifications will be made later when operationally convenient.

Rotor rim flotation

The rotor rim is designed to float at rotational speed 15% above the generator nominal speed. Excessive clearance of the rim bolts resulted in insufficient shrinkage of unit 1 rim, which floated at 75% nominal speed. This was corrected in subsequent machines. However, unit 1 was left to float at normal operating speed with periodic inspections of the wedge support system. This was done with a view that correction will be made at a convenient time, in the future or immediately, if the inspection indicated problems. Through 1990 no correction has been deemed necessary.

Brake dust

Excessive dust was produced during braking, even though the rotational speed when the brakes were applied was relatively low. The problem was exacerbated by the large number of start/stops during the early years of operation. The corrective solution was to change the material of the brake lining and to close one side of the generator rotor vents to restrict the circulation of the dust. The latter measure was possible due to excess capacity of the rotor air ventilation system.

Sticking of brake jacks

During erection and commissioning many brake jacks galled when, with application of pressurized oil, they were used to lift the generator rotor. This necessitated replacement of the damaged jacks and gave concern about subsequent similar failures when lifting the rotor for maintenance and inspection. Insertion of an elastic layer between the jack and brake ring was successful in resolving the problem. No problems were experienced when the jacks were used with the compressed air for braking.

Overheating of generator brushes

In the original design the generator brush enclosure was only naturally ventilated. High temperature of the brushes resulted, which was aggravated by inadequate brush design and materials. Different materials were tested and a forced ventilation system was installed, which mitigated the problem.

Deposits in the stator core windings

After several years of operation, deposits of cuprous and cupric oxides were found in the cooling water channels of the stator windings of the BBC generators. The first indication of this were higher water temperature readings at the discharge outlets of the affected channels and, on investigation, these channels were found to be substantially blocked. The propensity for deposits to accumulate is extremely sensitive to the pure water oxygen content, trace elements and pH of the water. A critical change in any of these parameters resulted in accelerated deposits of the oxides. This was particularly evident in the case of Itaipu units where, with essentially the same design and conditions of operation, the BBC generators suffered from the problem whereas Siemens generators did not. Cleaning of the deposits was made by using a chemical method and the problem was solved by flushing the cooling water channels of the stator winding by a slightly acidic solution.

GENERATOR EXCITATION SYSTEM

GENERAL REQUIREMENTS

Requirements for the excitation system for Itaipu generators were as follows:

- High positive ceiling voltage capability to obtain a fast voltage regulation response during transient condition.
- Studies of the 60 Hz system indicated the need for negative excitation current capability to increase the generator line charging capacity to charge the long unloaded transmission lines and to limit the voltage rise in case of full load rejection at the far end of the 60 Hz lines or at the HVDC converter station with reactive unbalance due to the harmonic filters.
- A power system stabilizer was required as a precaution to dampen possible power swings. Theoretical studies established the excitation control needed to limit these power excursions to acceptable values.

All the above requirements could be conveniently met with a static excitation system, which was also the most economical and reliable solution.

The static excitation system for all Itaipu units is the "Unitrol DCN" supplied by Brown Boveri, the characteristics of which are given in Table 12.13.

Control philosophy

The generator and other components are equipped with protection relays which respond to abnormal conditions and trip the machine. The capability curve of the generator in turn, is confined by limiters on the excitation system.

Limit controllers override the voltage regulator and prevent the generator reaching an operating condition which would cause a protective relay to trip. One group of limiters reduce the excitation current in the overexcited region controlling overtemperatures and overfluxing. The other group of limiters increases currents in the underexcited region and maintains minimum excitation currents required for stability of the machine. The action of the limiters is shown in the capability curves of Fig. 12.81 and is as follows:

- **Volt/Herz limiter.** Limits the generator voltages to a preset value to prevent magnetic saturation in the main power transformers, auxiliary and instrument transformers. This limiter is essential during unit starting when the excited generator has not reached adequate speed, and also in the event of severe system overvoltages. The action of this limiter is shown in Fig. 12.82.
- **Rotor current limiter.** Protects the rotor against overloading and overtemperatures in the overexcited operating range. It also protects the positive and negative static converters and supply transformers against overload, when operating in the respective modes, and acts in two stages. The first stage, which is instantaneous, limits the current to a maximum permissible value. The second stage reduces this overcurrent after a certain time to the maximum continuous rotor current. Entering of the second stage is blocked if the generator voltage is low, signifying persistence of an external fault. The rotor current limiter has priority over all other limiters.
- **Rotor angle limiter.** Acts in the underexcited region and prevents the generator from falling out of step with the transmission system. This is accomplished by monitoring the rotor and system phase differences and applying correction to the generator field current to maintain synchronism.
- **Reactive current limiter.** This limiter acts in the underexcited range and takes over from the rotor angle limiter when the nominal active power decreases to about 25% of the rated power.
- **Minimum excitation current limiter.** Maintains the value of minimum field current needed to keep the generator excitation within the practical stability limit.
- **Negative excitation current limiter.** Protects the negative current converter and the associated transformers from an overload.

Table 12.13 Principal characteristics of excitation systems

Principal characteristics	Unit	50 Hz	60 Hz
Positive current converters			
Positive ceiling voltage	V	1380	2250
Negative ceiling voltage	V	1240	2250
Continuous rated current	A	10 000	7100
Negative current converters			
Positive ceiling voltage	V	1380	2250
Negative ceiling voltage	V	1380	2250
Continuous rated current	A	2400	1350
Field voltages			
No load (@ 25° C)	V	205	220
Rated load (@ 100° C)	V	442	405
Voltage response	s	< 0.05	< 0.05
Transformers			
Output for positive converters	kVA	2500	3500
Output for negative converters	kVA	800	1000
Primary voltage	kV	18	18
Secondary voltage			
Positive converters	kV	1150	1850
Negative converters	kV	1850	1950

CONFIGURATION

Layout

Essential components of the static excitation system are the positive and negative excitation current converters, electronic voltage regulator with limiters, stabilizing equipment, converter gate control units, equipment for field flashing, static protective relays and the high speed de-excitation and field flashing circuits.

The excitation equipment is housed in metal cubicles installed upstream from the generator at El. 98.5.

Excitation power is taken from connections on the generator isolated bus through dry type transformer banks, one bank for the positive converters and another for the negative.

The positive and negative excitation currents are generated by fully controlled rectifier bridges (thyristors) connected in anti-parallel by a current

limiter reactor (choke) shown in Fig. 12.83. The choke limits internal fault currents arising from short-circuits, and the anti-parallel configuration ensures certain availability of field current at all times.

The exciter output is connected to the generator field winding through a field circuit-breaker and the shaft slip rings. Overvoltage protection and field discharge resistor are incorporated.

For field flashing, a separate supply is taken from the powerhouse 460 V system through a rectifier bank. Switchover to the normal excitation is done when the generator voltage reaches 70%. For emergency situations when, for any reason, the 460 V system is not available, field flashing can also be done from the powerhouse 125 V dc system.

Arrangement of converters

A total of 144 thyristors are used in each excitation system, 108 in the positive converter and thirty-six in

the negative. Because of the different requirements of 60 Hz and 50 Hz generators, thyristors are connected somewhat differently. The 60 Hz system uses three thyristors in series to give a 2250 V dc output ceiling voltage, with six parallels for the positive and two parallels for the negative converter. The 50 Hz system uses two thyristors in series to give a 1380 V dc output ceiling voltage with nine parallels (in five groups) for the positive and three for the negative converter.

The converters are designed so that with the failure of up to two parallels (groups for the 50 Hz) in the positive bridges as well as one parallel in the negative bridges, the machine can still operate at the rated load. The loss of two parallels in the negative bridge switches it off but operation can continue on the positive bridge without interruption.

The loss of three or more **positive parallel groups** initiates unit shutdown.

Because of the high **excitation equipment** reliability requirements, the **quantity of parallel thyristor branches in reserve totals 100%**, which means that the operation can be maintained at the full level with only half of the number of parallel thyristors.

When a thyristor branch becomes defective it is isolated by a quick-acting fuse without disturbing the excitation system operation, and the defective branch is indicated. By monitoring the current flow in each thyristor branch it is possible to detect faults in the ignition circuit. Individual RC networks for the thyristors ensure uniform voltage distribution between series-connected thyristors while a collective RC network protects against hole storage effect.

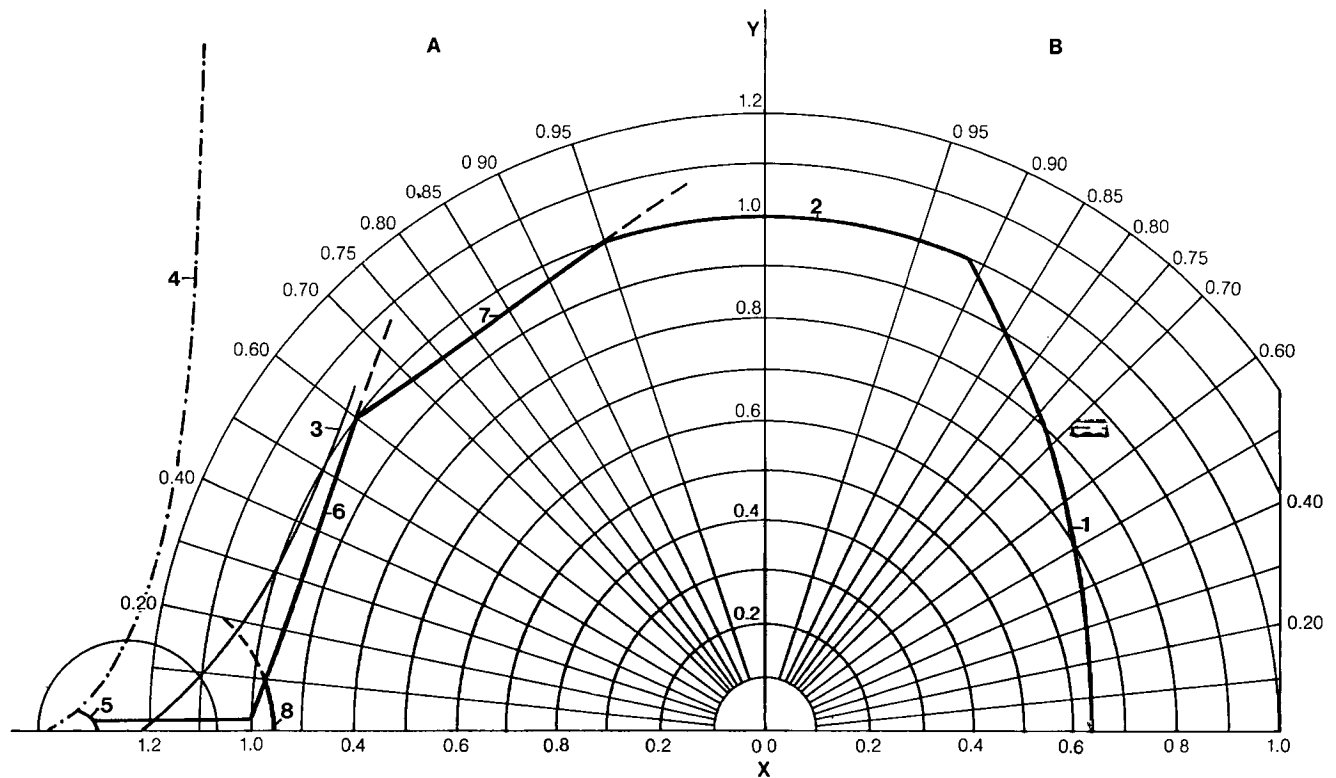


Fig. 12.81 Capability curve of the generator (generic) with limit controllers

Y Active power (p.u.)
X Reactive power (p.u.)
A Leading
B Lagging

1 Field current (max.)
2 Stator current (limited by the capability of the stator. No special limiter provided).
3 Practical stability
4 Theoretical stability
5 Negative excitation current limiter
6 Underexcitation limiter

7 Load angle limiter
8 Minimum excitation current limiter (negative excitation out of service)
 Note: Chart is at nominal voltage

Thyristor banks are cooled by a closed loop air system. This system was chosen to avoid contamination during long plant construction period. The air, which is circulated by fans, is cooled by air/raw water heat exchangers, three per assembly, two of which are necessary when the exciter is functioning, the third being reserve.

Excitation transformers

The transformers are of dry, epoxy cast Class F insulation type. Each bank consists of three single

phase units. Transformer windings are connected into ungrounded wye on the primary side and delta on the secondary side. The wye winding connection combined with the single phase transformer units, suits the phase segregation principle and practically eliminates the possibility of a phase-to-phase fault which would cause an interphase short circuit at generator terminals. Transformer units are naturally cooled with design temperature rise of 90°C for windings and 35°C for the enclosures.

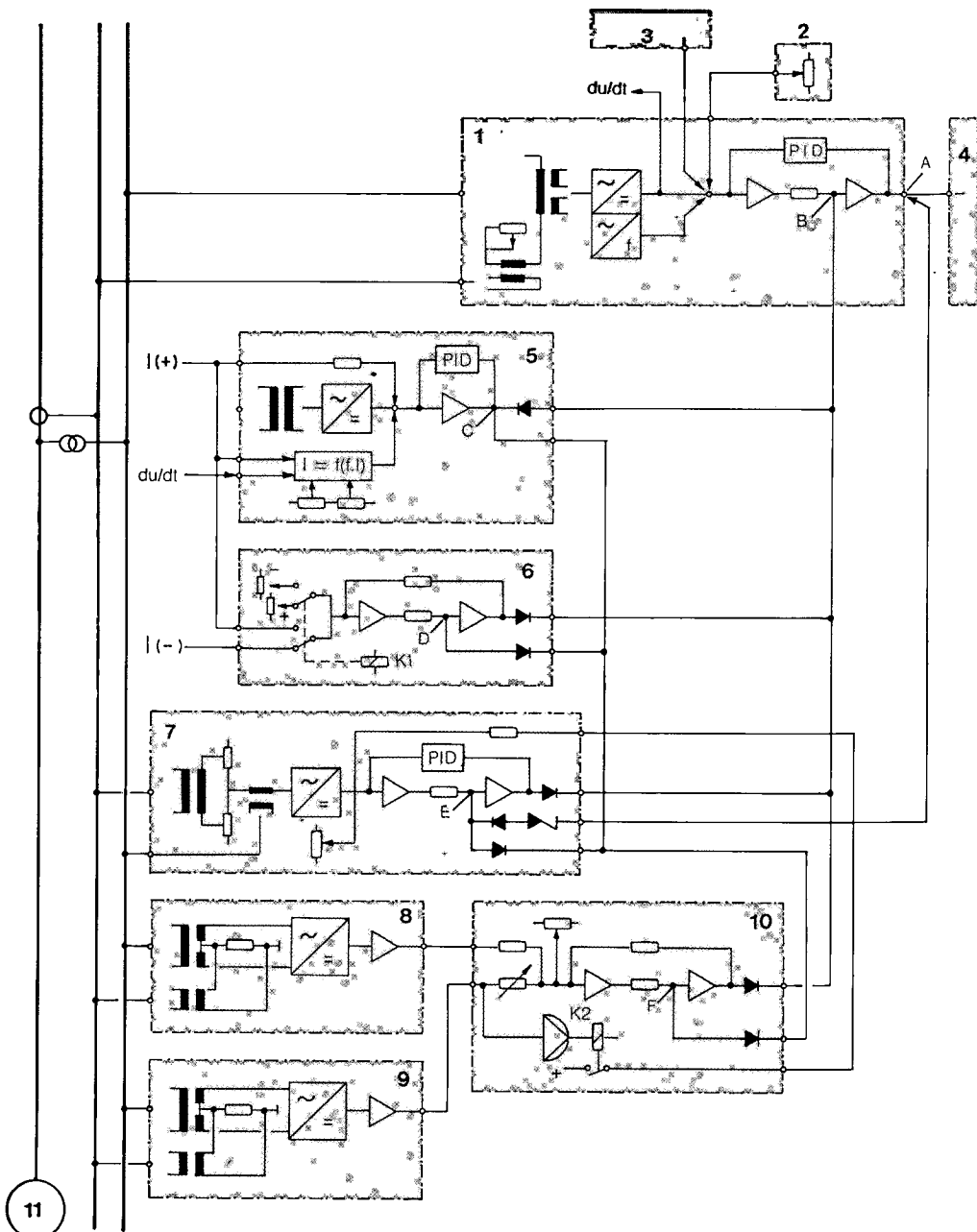
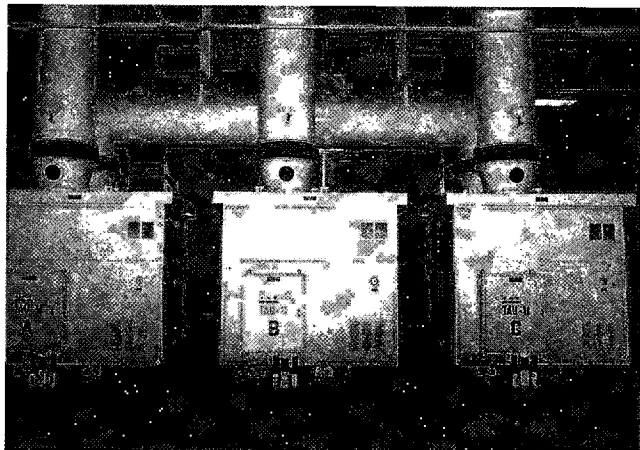


Fig. 12.82 Interaction of the limit controllers and the voltage regulator

- 1 Voltage regulator
- 2 Set-point value for the generator voltage
- 3 Slip stabilization equipment
- 4 Circulation current reactor
- 5 Rotor current limiter (overexcited mode)
- 6 Excitation current limiter (underexcited mode)
- 7 Rotor angle limiter
- 8 Reactive current limiter
- 9 Active current measurement
- 10 Reactive current limitation as a function of active current
- 11 Generator
- A-F Output points
- K1, K2 Relays
- I(+) Excitation transformer for the positive bridge
- I(-) Excitation transformer for the negative bridge
- $I = f(t, I)$ Set-point value as a function of current aid time
- PID Proportional, integral and derivative action-filter
- du/dt differentiation of the generator e.m.f. as function of time



Excitation cubicle

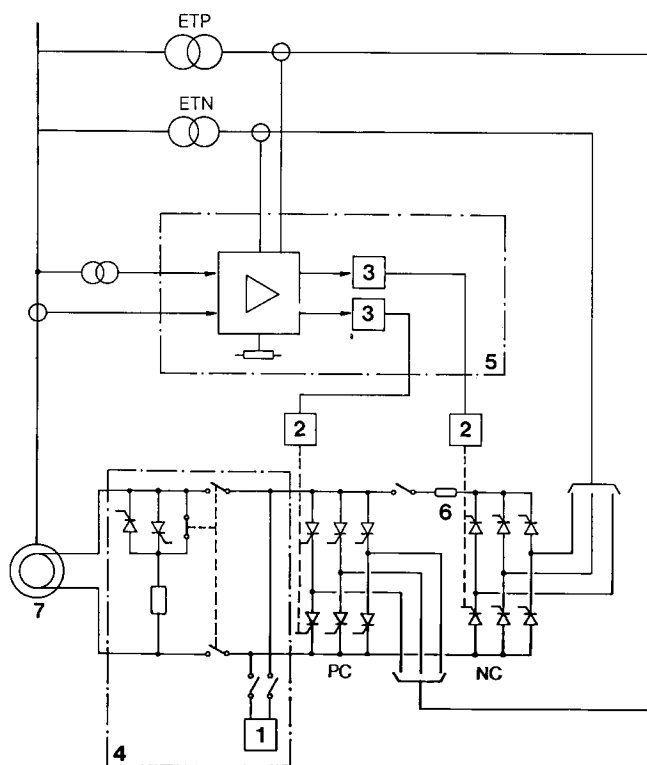


Fig. 12.83 Basic circuit diagram of the static excitation equipment

- | | |
|--------------------------------|--|
| 1 Field flashing unit | ETP Excitation transformer for positive converter |
| 2 Pulse amplifier | ETN Excitation transformer for negative converter |
| 3 Pulse generators | PC Positive converter |
| 4 Field overvoltage protection | NC Negative converter |
| 5 Control and limit circuits | |
| 6 Circulatory current reactor | |
| 7 Generator | |

The high voltage windings are rated at 10 392 V, $\pm 5\%$ 125 kV BIL, 50 kV power frequency voltage withstand. The kVA rating and the secondary voltages vary and are shown in Table 12.13.

Field circuit breaker

This dc circuit breaker is installed in the main excitation circuit on the dc side. The breaker is dry type, with a rated voltage of 2500 V dc and a rated current of 4500 A. The breaker is tripped only for faults within the excitation equipment or for internal generator electrical faults and it is not tripped for normal unit stop or other emergency stops. The breaker has auxiliary contacts which are used to switch-in the field discharge resistor.

Disconnecting switch

The disconnecting switch is three-pole, group operated, with a motor for each pole and a common control box for "gang" operation of all three poles. The switch is common to the positive and negative excitation transformers and it is installed in the secondary bus duct.

Secondary bus duct

Voltage characteristics are same as for the main bus:

Rated voltage	18 kV
Impulse withstand (crest)	125 kV
Rated continuous current	1200 A
Rated momentary current	448 kA (asym)

Insulating neoprene rings are provided between the bus and the transformer enclosures, and insulating pads between the enclosures and the steel supports.

GENERATOR TERMINAL EQUIPMENT

The generator terminal equipment, supplied under the CIEM contract, also includes the 18 kV isolated phase bus and the generator neutral and terminal cubicles. The isolated phase bus is self cooled type and operates under slight positive air pressure. A simplified single line diagram of the isolated phase bus system is shown in Fig. 12.84.

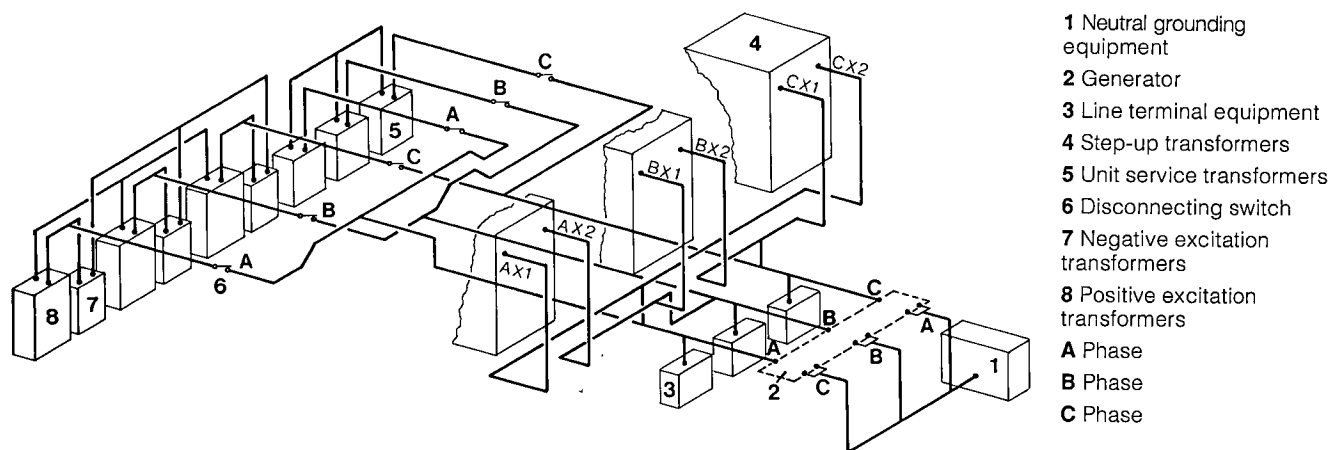


Fig. 12.84 Generator terminal equipment

ISOLATED PHASE BUS

The basic arrangement and rating for the 50 Hz and 60 Hz isolated phase bus is the same, except where it was necessary to accommodate the slightly higher output of the 50 Hz generator. The main characteristics are given in Table 12.14.

The bus aluminum conductor and the enclosure are co-axial, with the aluminum enclosure sections welded to give an airtight system, see Fig. 12.85. To prevent stray circulating currents, the bus enclosures are insulated from their mountings and isolated from the terminal equipment by neoprene rings. A single ground point connection is made at the common interconnection point of the three phases near the generator. This reduces the losses due to the circulating current between the enclosure and the ground. There was no danger of high enclosure voltages because bus lengths are short. Multiple grounds are avoided by insulating the supports of the enclosure by 2 kV rated neoprene insulating pads at the supports.

The bus enclosures are kept under a small positive pressure (0.05 kN/cm^2) to prevent the entrance of dust and moisture. Pressurized air is automatically supplied from the powerhouse compressed air system via condensate separators, a dryer (which also acts as an accumulator), and a pressure reducing valve, see Fig. 12.86.

The bus conductor is made of high conductivity aluminum pipe with braided type joints at selected intervals to absorb thermal expansion. All internal joints, both fixed and expansion type, are welded for low losses and high reliability. The terminations, at

the various pieces of equipment, are of a braided type to allow for thermal expansion and to eliminate transfer of vibrations.

Basic electrical insulation is provided by the air inside the enclosure. The conductor is supported by molded, ribbed insulators, having a creepage distance of 440 mm. The maximum distance between the adjacent supports is 6 m.

Both secondary buses which feed the excitation and auxiliary service transformers, are equipped with disconnecting switches. These are single pole units of the telescopic type having a three-pole gang operated motor mechanism. The disconnecting switches are capable of interrupting the associated transformer magnetizing currents but not the load currents.

The main generator leads pass through an aluminum seal-off plate at the concrete housing and project part of the way into the generator stator. To maintain the positive pressure in the system, a seal-off bushing is used

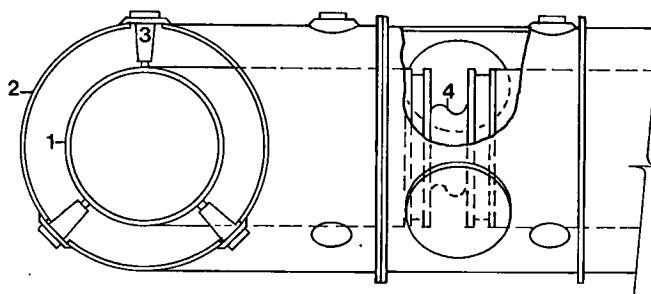


Fig. 12.85 Isolated phase bus cross-section

- | | |
|----------------------|--------------------------------|
| 1 Aluminum conductor | 3 Insulator |
| 2 Enclosure | 4 Flexible disconnecting joint |

Table 12.14 Characteristics of the isolated phase bus

Item	Unit	50 Hz	60 Hz
Normal operating voltage	kV rms	18	18
Maximum operating voltage	kV rms	24	24
Impulse withstand voltage	kV crest	125	125
Power frequency withstand voltage (1min)	kV rms	60	60
Current main bus			
Generator main	kA rms	28	26
Transformer delta current	kA rms	16.1	15.1
Momentary current rating	kA rms	225	246
Four second current rating	kA rms	166	155
Current – secondary bus			
Transformer – exciter/auxiliary	kA rms	4	1.2
Momentary current rating	kA rms	465	448
Four second current rating	kA rms	290	280
Temperature rise above 40°C			
Bus conductor/connector	°C	65	65
Enclosure/supports – accessible	°C	30	30
Enclosure/supports – inaccessible	°C	70	70
Terminations	°C	65	65
Losses / three-phase meter			
Enclosure	kW	77	73.6
Bus	kW	94	92.5
Diameter			
Enclosure – main bus	mm	1430	1560
Conductor – main bus	mm	1000	1000
Enclosure – delta bus	mm	1430	1430
Conductor – delta bus	mm	1000	1000
Enclosure – secondary bus	mm	730	730
Conductor – secondary bus	mm	300	300

between the bus and enclosure in each phase. Enclosures are interconnected to allow the sheath currents to circulate. Generator neutral leads are similar to the main leads except that two sets of bus connections are made for each phase. This allows the

split-phase arrangement used in the generator windings to be separated at the neutral by the removal of the flexible connectors.

Delta leads at the generator step-up transformers have their enclosures connected to the bushing flange.

At each transformer the two phases of the isolated phase bus have their enclosures interconnected to facilitate the circulation of sheath currents.

Secondary lead connections at the excitation and auxiliary transformers are made in a similar manner as the ones at the generator transformer.

GENERATOR NEUTRAL AND TERMINAL CUBICLES

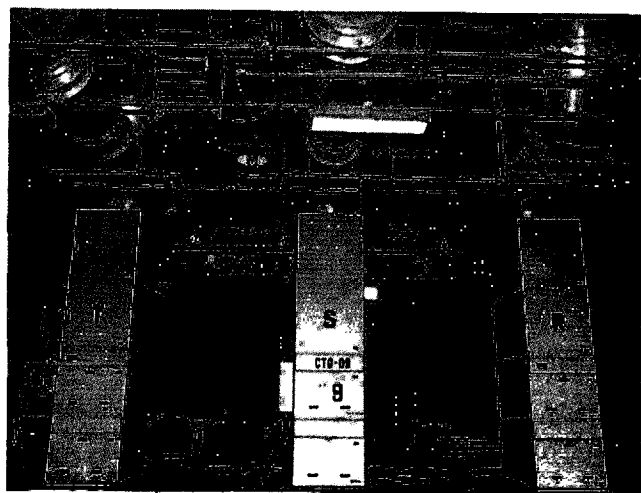
Neutral cubicle

The generator neutral cubicle is installed at El. 98.5 and is located immediately downstream from the generator housing. It is directly connected to the neutral bus and contains the grounding transformer and a disconnect switch. Bus connection is made through the single pole manually operated disconnect switch.

The grounding transformer has a continuous rating of 50 kVA and a 10 second rating of 560 kVA. The secondary resistor is of the cast iron type and has continuous rating of 24 kW and a 10 second rating of 168 kW. Its nominal voltage is 240 V and it has a nominal resistance of 1 ohm and an allowable temperature rise of 140°C.

Terminal cubicle

The generator terminal cubicle consists of three free standing single phase units located upstream of the generator housing and directly under the main



Isolated phase bus

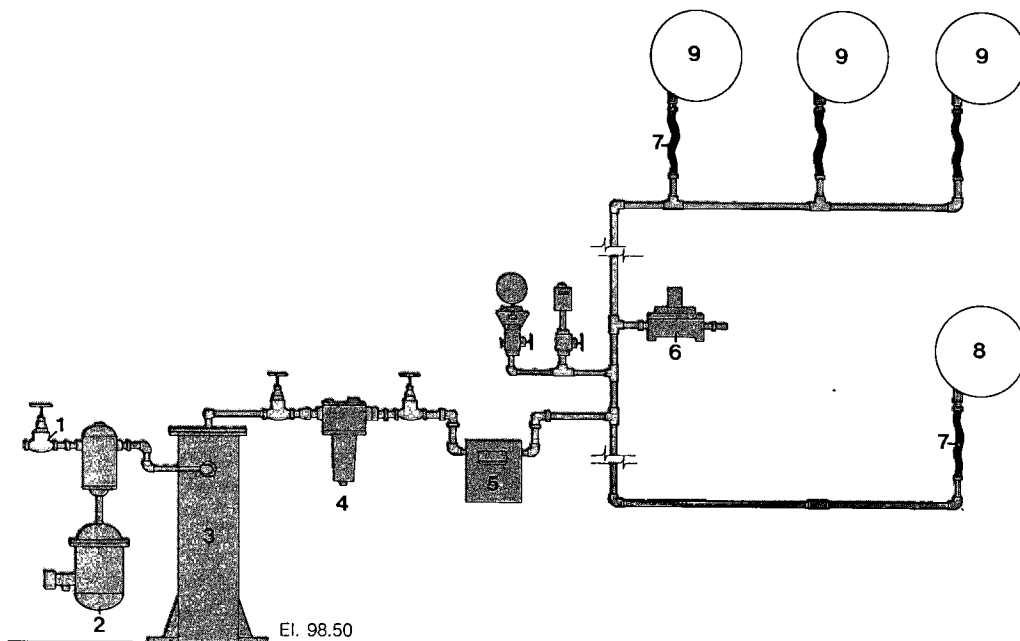
generator isolated phase bus at El. 98.5. The units contain the generator surge protection equipment and potential transformers, with each element located in one of the four separate compartments.

The cubicle is separated from the isolated phase bus by a seal-off bushing.

The two lower compartments have the potential transformers and their primary protection fuses. The potential transformers are connected phase to ground on the primary side.

Fig. 12.86 Isolated phase bus air supply

- 1 Check valve
- 2 Separator and condenser
- 3 Air dryer
- 4 Pressure and safety valve
- 5 Air meter
- 6 Safety valve
- 7 Flexible connection rubber
- 8 Generator neutral bus
- 9 Bus



GENERATOR STEP-UP TRANSFORMERS

The generator step-up transformers were supplied by Consortium Citran (comprising Indústria Elétrica Brown Boveri and TUSA - Transformadores União) and by Coemsa - Construções Eletromecânicas. They are used to step-up the 18 kV generator voltage to the 500 kV transmission system nominal voltage for the right bank and Foz de Iguaçu substations. Each single phase transformer is installed in an explosion-and fire-proof concrete bay, at the upstream gallery at El. 108. Inside the bay, the transformer is mounted over a sump which has a 1.1 m thick layer of 50 mm crushed rock and is drained to concrete tanks at El. 90 near units U3, U7, U10, U14 and U18. Each single phase transformer bay room has forced ventilation and a fire-proof automatically closing front door. Surrounding the transformer is a water sprinkler type fire protection system which is described in Chapter 13.

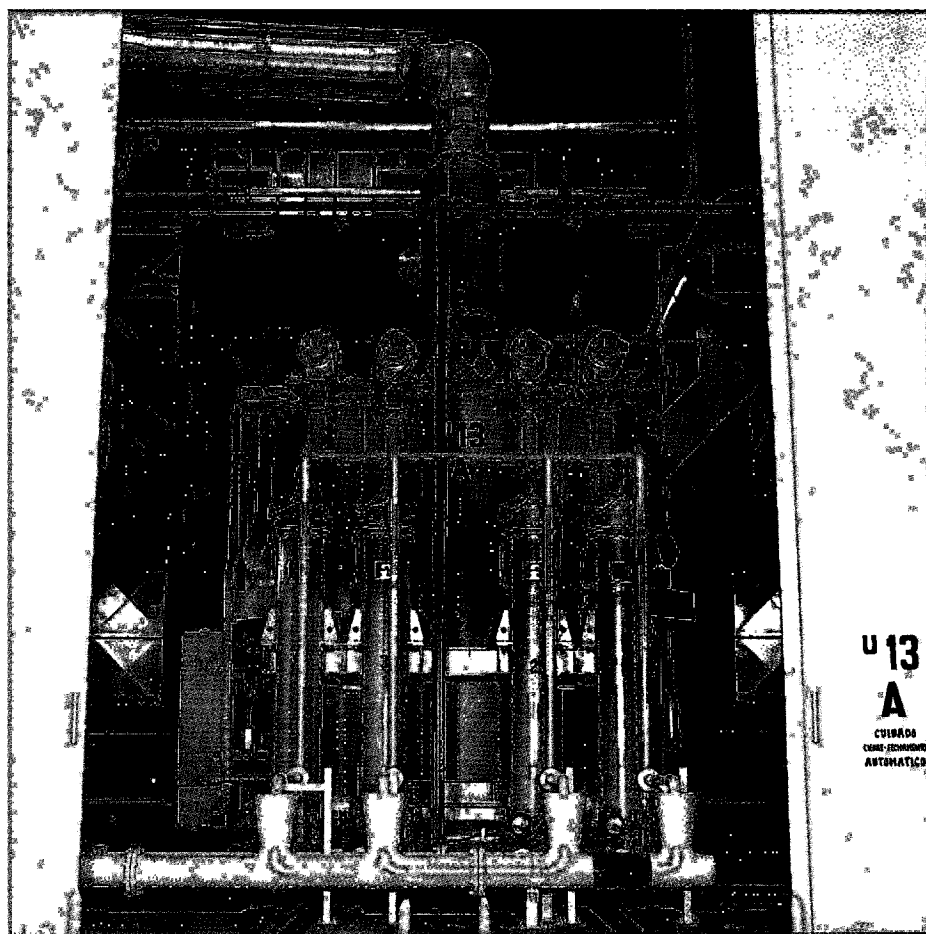
Transformer untanking facilities are provided in the powerhouse right and central assembly areas.

Transformer control and supervisory cubicles are located at El.108 near the upstream wall of the transformer gallery.

BASIC CHARACTERISTICS

The different requirements of the 50 Hz and 60 Hz systems resulted in transformer banks with different ratings; 50 Hz being 825 MVA and 60 Hz being 768 MVA. Banks at both frequencies comprise three single phase units of subtractive polarity, with a transformation ratio of 525 to 18 kV, and $\pm 2 \times 2.5\%$ off-load taps on the neutral side of the high voltage winding.

The transformers are oil insulated, water cooled type (OFWF), each having four oil to water heat exchangers, one of which is redundant. Water for the



Main transformers

cooling is taken from the powerhouse cooling water system described in Chapter 13.

The high voltage test requirements are given below.

Test voltage	HV line (kV)	HV neutral (kV)	LV (kV)
Lightning impulse			
Full wave	1550	110	125
Chopped wave	1780		145
Switching surge	1300		
Inducted voltage at power frequency	680		40.6
Applied voltage at power frequency	34	34	50

The design temperature rise is 65°C over ambient air temperature of 40°C with the cooling water temperature of 30°C.

The high voltage bushing is equipped with four bushing type current transformers for protection. Two of these are linear type with 2000-5A ratios and two are standard type with multiple taps to give 2000 to 300-5A ratios. The high voltage neutral bushing has two bushing type current transformers for thermal imaging, with 3500-5A ratio for 50 Hz and a 1200-2.5A ratio for 60 Hz units. The low voltage bushings do not have current transformers.

The generator step-up transformers are equipped with an oil conservator which has an inner rubber membrane to prevent direct oil contact with the outside air. The conservator tank accommodates the thermal expansion of the oil and allows the use of Buchholz type gas relay.

The transformers are equipped with the usual oil level, oil temperature, winding temperature, cooling water flow indicators with alarm and trip contacts and two pressure relief valves. The permissible transformer noise design level is 85 dB.

COMPONENT DESIGN AND MANUFACTURE

Although the 50 Hz and 60 Hz transformer units are very similar, the difference in frequency and

ratings does result in different weights and dimensions as follows:

	50 Hz	60 Hz
Weights (kN)		
Removable parts	1300	1060
Tank and accessories	410	315
Oil	430	415
Complete with oil	2140	1790
Heaviest piece for transportation (without oil)	1600	1322
Dimensions (mm)		
Height	7260	6835
Width	7000	6565
Depth	6440	6300

Construction of the transformers is of the core-type with both limbs wound. Limbs are bound with fiberglass tape and the core clamps are of steel, made to minimize eddy current losses arising from the stray flux of the basic frequency and harmonics.

An electrostatic cylinder is placed between the core limb and the low voltage (LV) winding to limit the voltage transferred to the LV winding to a reasonable level when the high voltage (HV) winding is subjected to impulse voltage. Because of heavy currents, the LV winding is of the spiral type with multi-conductors in parallel.

The HV bushing lead connects to the midpoint of HV winding, and the neutral leads to the extreme ends of this winding. Transformer optimization resulted in the choice of an interleaved double disc coil winding, giving the required distribution of series capacitances and voltages. Voltage taps are brought out along each half of the winding.

The transformer has two vertically-mounted tap changers, one for each half winding.

The winding conductor is covered with multilayers of thermally stabilized cellulose insulating paper. Between winding are pressboard cylinders. The HV leads from both the winding limbs to the bushing are formed of copper electrodes with moulded pressboard.

The transformer tank has been designed to withstand pressure differential resulting from near internal vacuum during transformer drying-out

process. One of the long sides of the tank has an aluminum plate through which the LV bushings connection are made. Inside the tank, walls are shielded with silicon steel sheets to contain the stray magnetic flux.

The SF₆/oil HV condenser type bushing is made of oil-impregnated paper, and is rated at 1550 kV BIL and 1600 A. The HV neutral and the LV bushings are rated at 150 kV BIL and 2000 A and 25 000 A respectively. Both are drip-proof type mounted in such a way that the porcelain can be changed without reducing the oil level in the main tank.

The four oil/water heat exchangers are made of stainless steel. With the two heat exchangers in operation the transformer can deliver 85% of its rating, and with three, the full rating. Because the control room is remote from the transformer location, the valves of the cooling system are motor operated, and have remote visual indicators.

Cooling oil is pumped to the bottom of the winding from where it flows to the top. Inside the tank the strategically placed baffles direct the oil stream to potentially hot spots to ensure a uniform winding operating temperature.

High-voltage tests were conducted in the factory using an arrangement in which the transformer oil/SF₆ bushing was mounted as in-service together with its SF₆ gas connection chamber. On top of this chamber a second bushing, SF₆/air type, was mounted in such a way that both the SF₆ and oil parts of the transformer bushing were tested together.

For the heat run test (type test) the transformer was supplied with a current which corresponded to the guaranteed load and for the 50 Hz units with additional harmonic currents to simulate the effect of dc converter station influence.

INSTALLATION, TESTING AND COMMISSIONING

The transformer was transported by road to the jobsite, without conservator, HV bushing and heat exchangers, in a special "low bed" truck. To reduce weight and to prevent the entrance of moisture into the tank the oil was replaced by dry nitrogen gas under positive pressure. To avoid shock damage to the core and coils during transportation, the transformer was securely bolted to the bottom of the tank with bolts accessible from the outside. During shipment impact recorders were attached to the units.

After transport to the gallery, the transformers were conveyed along the gallery with the 2.5 MN transformer cranes and wheeled on rails into their respective concrete wall bays. The wheel assembly was then removed, permitting the transformer to rest on its sole plates.

Precise alignment of the transformer with the SF₆ bus connection chamber was made with a teflon sleeve. The sleeve allowed three dimensional adjustment of the transformer position.

After a careful inspection of the unit for shipping damage, the ancillary equipment, which was removed for shipment, was remounted. This included the oil conservator tank, all bushings, and all heat exchangers. The unit was then vacuum tested and filled with the oil using the vacuum method for degassing as described in Chapter 13.

Routine tests were carried out on each unit, these included Doble testing of the high voltage bushing, checking all current transformers for resistance and polarity, dielectric and moisture levels tests of the oil, and an oil chromatograph.

A series of heat runs confirmed the proper functioning of the cooling system and allowed final adjustments of the flow monitoring devices.

OPERATING EXPERIENCE

The initial design required transformer tank grounding at two locations. This resulted in undesirable circulating currents, and later was modified to grounding at a single ground point.

Component failures in the control circuits of the transformer cooling system were caused by high voltage transients generated by the operation of contactors and relays. This problem was corrected by the addition of suitable surge suppressors.

Up to 1990 there had been only one in-service fault, the failure of a high voltage winding in a 50 Hz unit after 6 years of operation. This resulted in a discharge of oil through the pressure relief valve and some tank distortion together with damage to the coil. The transformer was returned to the factory for investigation and repair, but the cause of failure was not clearly established.

Some problems were experienced with the reliability of the cooling water flow monitors. The monitors were replaced with a new type unit.

500 kV SWITCHGEAR (SF₆ – GIS)

The 500 kV switching station has fifty-two circuit-breakers for the protection and switching of eighteen generator transformers, two auxiliary transformers, eight overhead lines and four bus sections, as shown in Fig. 12.87.

The 500 kV gas insulated switchgear (GIS) experience was still relatively limited at the time of preparation of the procurement specification for Itaipu GIS equipment (1978-1979). Therefore the selection of this type of equipment was preceded by an extensive study involving visits to manufacturers' factories and existing installations worldwide, before writing the specifications. Acceptable bids were received from Brown-Boveri, Siemens, Delle Alstom and Mitsubishi Electric Company. Brown Boveri was awarded the contract in 1980.

BASIC CHARACTERISTICS

The basic characteristics of the SF₆ gas insulated switchgear are:

Switchgear general

Maximum service voltage	550 kV rms
Basic insulation level	1550 kV crest
Switching surge withstand	1240 kV crest
Power frequency withstand	740 kV rms 1 min
Continuous current	4000 A rms
Nominal gas pressure at 20° C	420 kPa (absolute)

Circuit breakers

Construction	Horizontal
no. of interrupters per phase	4
Type	Puffer
Interrupting current	63 kA (sym)
Interrupting time	50 ms
Gas pressure at 20° C	620 kPa (absolute)
Operating mechanism	Hydraulic

Surge arresters

Metal oxide type	444 kV
------------------	--------

Disconnect switches

Voltage withstands across open contacts	
Low frequency	960 kV rms
Lightning impulse	1864 kV crest
Switching surge	1700 kV crest

Potential transformers

Type	Wound
Primary voltage to ground	287.5 kV
Secondary voltage	2 x 115 / 66.4 V

Outdoor porcelain bushings for line exit

Basic insulation level	1800 kV
Power frequency withstand	860 kV, 1 min
Nominal gas pressure	250 kPa (absolute)

Grounding switches

General type	Spring operated
Line exit type	Spring operated (motor charged)

Factory routine test voltages

Power frequency withstand (50 Hz and 60 Hz)	740 kV rms, 72 s (20% longer duration than the standard)
---	--

Site test voltages

Applied to ground and across open gaps of disconnect switches and circuit breakers	
Applied for 50 Hz or 60 Hz, phase to ground	570 kV rms 1min* 380 kV rms 5 min 350 kV rms 24 h
Oscillating switching surge	± 940 kV peak three surges each* ± 940 kV peak five surges each**

* Applied across open gaps of disconnectors and circuit breakers (and consequently to ground of the connected GIS equipment).

** Additionally applied phase to ground with disconnectors and circuit breakers closed.

ARRANGEMENT

As already explained in Chapters 2 and 11, one of the reasons for choosing SF₆ GIS was its compact dimensions, enabling it to be installed in the powerhouse and connected directly to the generator transformers, see Fig. 11.2 of Chapter 11. Besides making ideal use of available powerhouse space, this arrangement eliminated the need for a large number of overhead lines, which would have been difficult to install, linking the generator transformers with the two separate switchyards one on each bank of the river. Moreover, with the powerhouse unit spacing it was actually impossible to provide adequate clearance between the eighteen overhead lines required to link the 500 kV generator transformers with the switchyards. Use of the gas insulated switchgear solved all of the above problems. Instead of eighteen 500 kV overhead lines, only eight lines were required, with one line in each frequency group (50 Hz and 60 Hz) providing line spare capacity.

This solution also ensured an optimum arrangement for the unit group comprising the generator, the generator transformer, switchgear and the connection to the transmission lines. All bus

bars and equipment carrying power from the generators to the line terminals were protected by an earthed metal enclosures giving an almost ideal arrangement in which the control and protection equipment could be interconnected by very short cables, contributing not only to the plant's reliability but also to a considerable savings in cost.

The single-line diagram in Fig. 12.87 shows two main bus systems for the 500 kV GIS. The arrangement is the same for both the 50 Hz and 60 Hz sectors. The generator switchbays are in a one-and-one-half breaker arrangement, while a two-breaker arrangement was chosen for the line feeders. This arrangement gives a very high reliability. Connected to each of the two sectors of the switching station is an auxiliary transformer for supplying the 13.8 kV station services.

Short connecting buses were made possible by the switchbays being located close to the generator transformers and to the line terminals. However, since the generators, and therefore the generator transformers also, are 34 m apart, long lengths of bus are necessary to connect the compact switchbay group, see Fig. 12.88. The overall length of the GIS installation along the axis of the powerhouse is 340 m for the 50 Hz sector, and 438 m

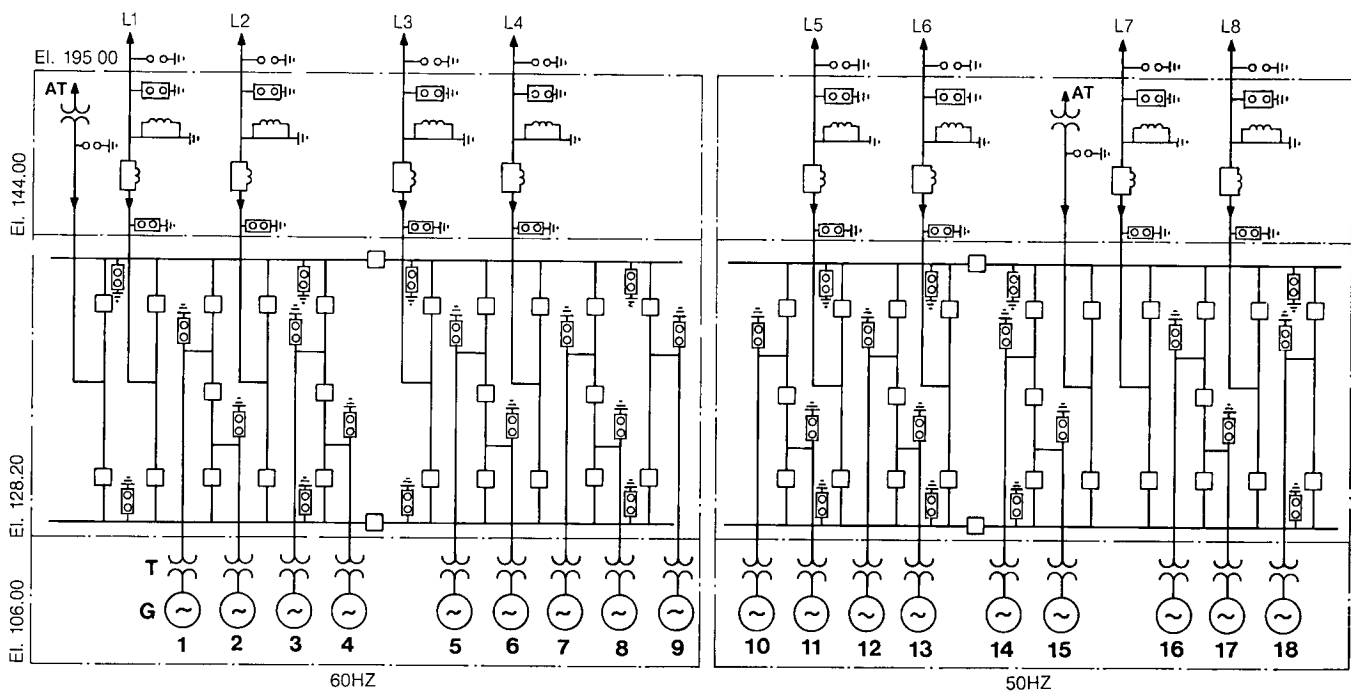


Fig. 12.87 Simplified single-line diagram of 500 kV SF₆ GIS

L1-L8 Overhead feeders

AT Auxiliary transformers

T1-T18 Generator transformers

G1-G18 Generators

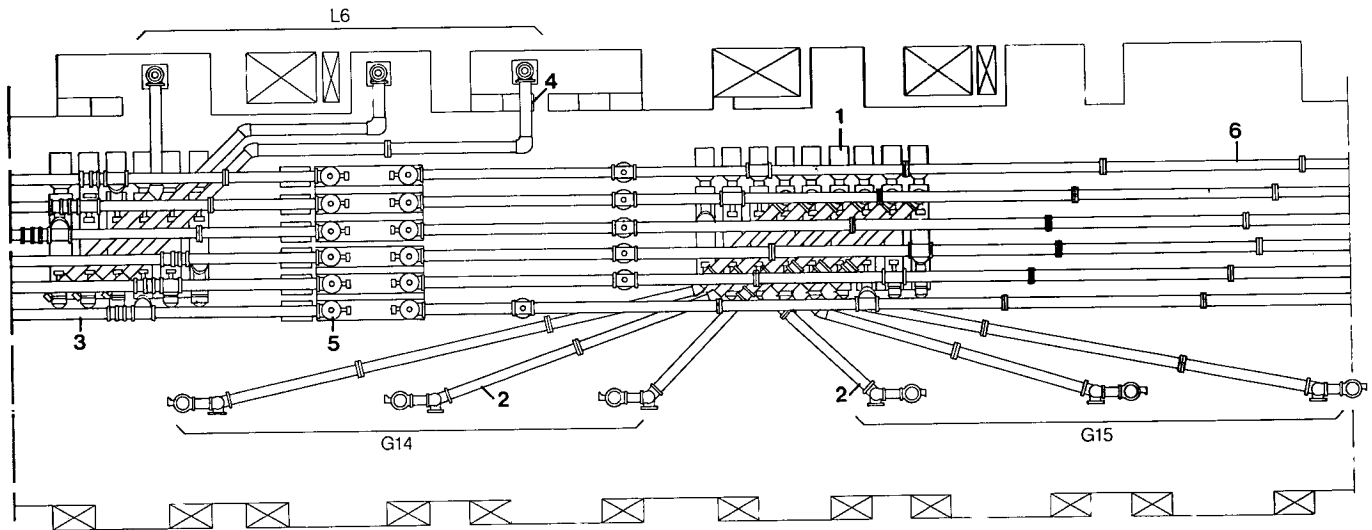


Fig. 12.88 Plan view of the 550 kV SF₆ GIS installation

1 Generator circuit breakers
2 Generator connections G14/G15

3 Line circuit breakers
4 Line connections (L6)
5 Bus sectionalizer breakers
6 Main bus

for the 60 Hz sector. The difference in length is due to the central assembly area which exists in the center of the 60 Hz sector.

All the switchbays have the same layout, with the circuit-breakers at the floor level and the other equipment and bus installed above, see Fig. 12.89. This arrangement enables staff to move freely at the floor level and ensured, despite the large size of the installation, a straightforward layout and good accessibility to all parts during maintenance and the commissioning tests. The overall configuration has been designed to enable any part of the switchbays (including breaker components) or bus sections to be replaced quickly and easily without disturbing the operation of the neighboring bays. All components of the 50 Hz and 60 Hz sectors of GIS are interchangeable.

Oil/SF₆ bushings connect the generator transformers directly to the GIS. Transformer protection against surge overvoltages is provided at these transition points by metal-enclosed metal oxide surge arresters.

Close to each switchbay are the control cubicles for operating the switchgear. These cubicles contain all devices necessary for local operation and also include mimic diagrams. The integrated signalling system is provided for the SCADA facility which is described in Chapter 14. The GIS equipment protection includes electronic busbar protection systems, which are installed in cubicles near the local control cubicles.

Lightning in the area can cause severe surge stressing, and hence also very steep-front impulse voltages. This concern required detailed studies of insulation coordination. Careful design of the plant earthing system, to ensure the lowest possible surge impedance, improved lightning protection for the lines in the sections near the installation and surge arresters at the terminals and certain points along the bus were essential features of a protection system that ensured the specified safety margin of 20%. Calculations were based on a current rate of rise of 100 kA/us for atmospheric discharges in the immediate vicinity of the powerplant.

COMPONENT DESIGN AND MANUFACTURE

The entire GIS is made up from standardized modular components. All grounded enclosures are made of aluminum and have bolted flange connections. See Fig. 12.90, for a cross-section of the bus.

Bus design

In optimizing the design, the distance between insulators supporting conductors (spacers) was increased from 6 m to 10 m. To maintain the required stiffness, the conductor diameter was also increased from 160 mm to 246 mm. The smaller diameter was kept only on short runs.

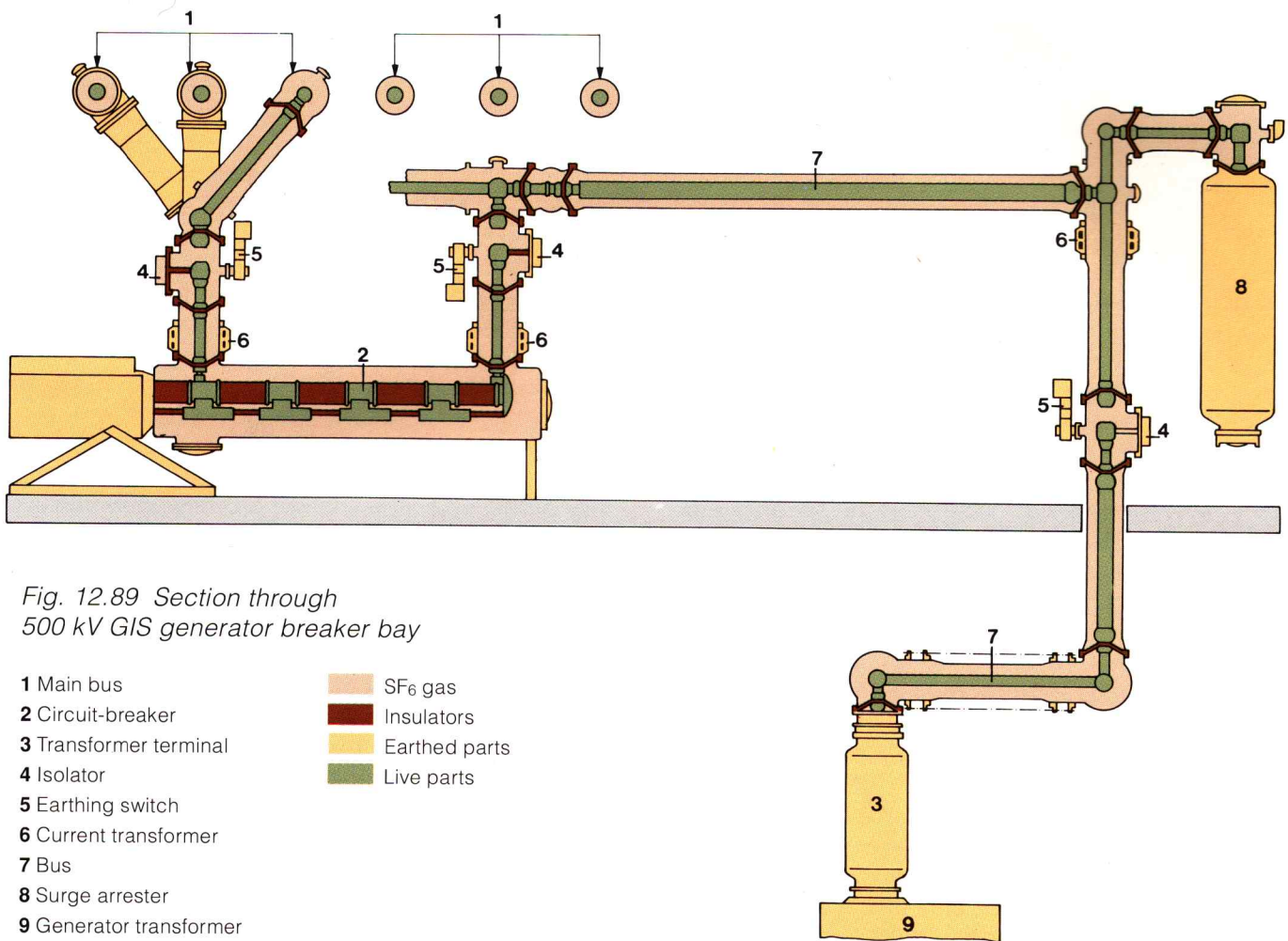
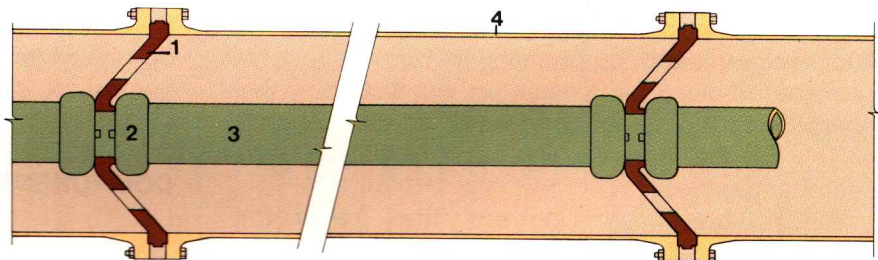


Fig. 12.89 Section through 500 kV GIS generator breaker bay

- | | |
|-------------------------|-----------------------|
| 1 Main bus | ■ SF ₆ gas |
| 2 Circuit-breaker | ■ Insulators |
| 3 Transformer terminal | ■ Earthed parts |
| 4 Isolator | ■ Live parts |
| 5 Earthing switch | |
| 6 Current transformer | |
| 7 Bus | |
| 8 Surge arrester | |
| 9 Generator transformer | |

Fig. 12.90 SF₆ GIS busbar longitudinal view

- | |
|--------------------|
| 1 Spacer insulator |
| 2 Bus connector |
| 3 Conductor |
| 4 Bus enclosure |

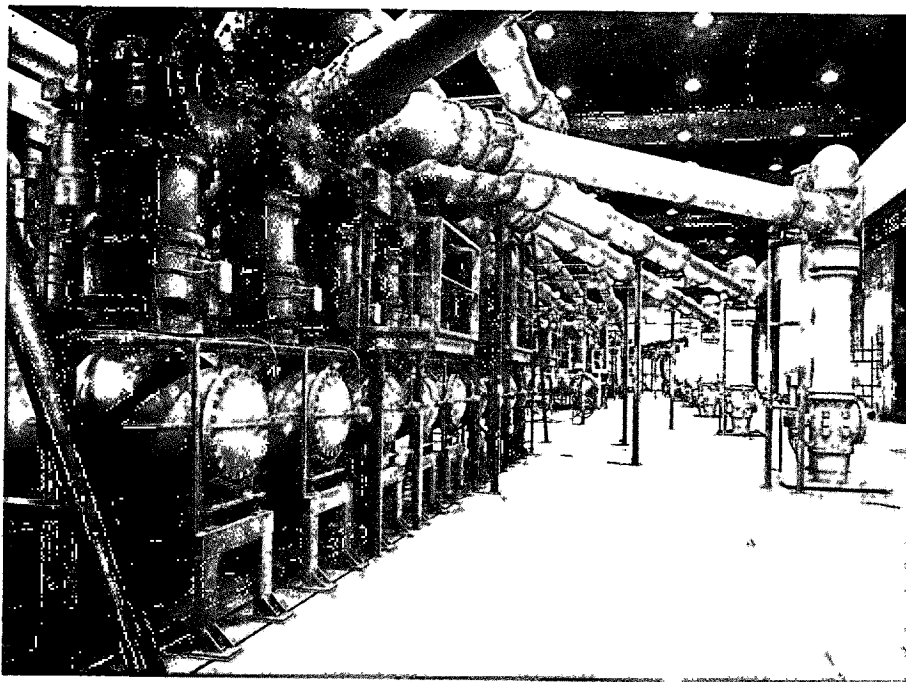
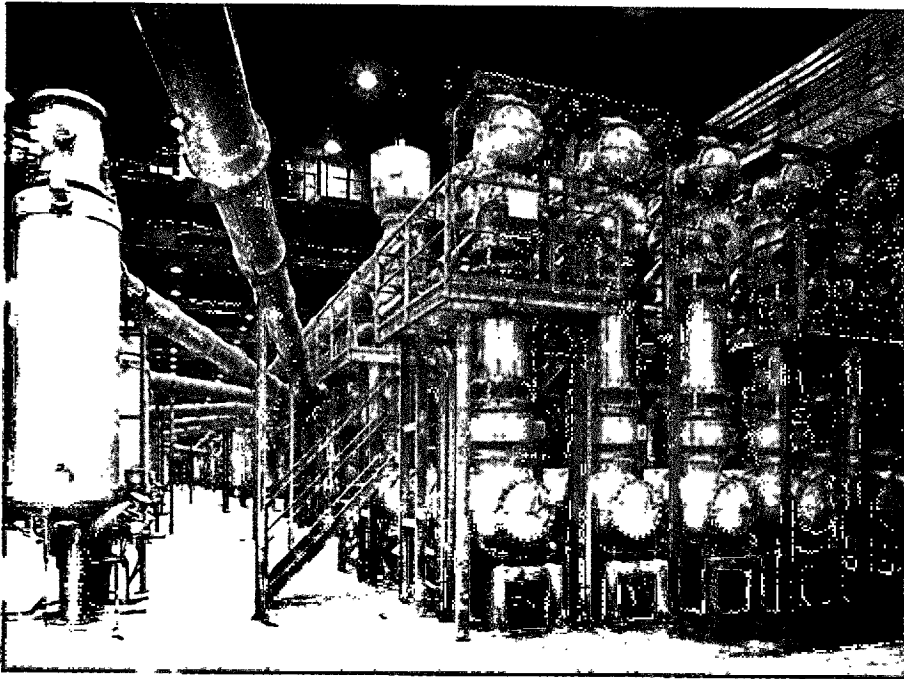


Increase in the conductor diameter was possible without proportional change in the housing diameter. However, it had the following effects:

- Lowering of the surge impedance and increasing the capacitance of test sections, which resulted in more severe tracking damage to the spacers during flashovers.
- Increase of electric field stresses at the enclosure and, at least theoretically, the equipment became

more sensitive to the presence of conducting particles and to surface imperfections of the enclosure.

The conductors and all shielding electrodes in the buses were covered with a coating of dielectric paint, which gave a marginal increase of the breakdown voltage not only under clean conditions, but also in the presence of conducting particles.

*SF₆ gallery***Provision for transformer Doble testing**

In spite of wide acceptance of transformer chromatography as a reliable maintenance tool, many users still insist on periodic application of transformer Doble tests. Contrary to conventional air-insulated systems, where access to transformer terminals requires some preparatory work, GIS

offers a convenient way to perform such tests by means of readily built-in equipment.

An isolating switch is provided between the GIS conductor and the transformer terminal, which permits disconnection of the transformer from the GIS conductor. A ground switch at the transformer side of the isolator is terminated at the GIS enclosure

with a 10 kV bushing, which permits connection of the Doble test equipment to the transformer terminal without opening the GIS enclosure.

Theoretically, the best location for these switches would be right at the transformer high voltage bushing, since in this case the measurements would be direct without need for any corrections. At Itaipu this location was considered inconvenient, because the access to the switches which are mounted above unit transformers would become very difficult. As a consequence it was decided to utilize isolating and grounding switches already provided at El.129.2. The only required change was replacement of the standard 2 kV bushing associated with the corresponding grounding switch by a 10 kV bushing compatible with the contemplated Doble testing. However, the results of the testing had to be corrected for effects of approximately 12 m of GIS bus to enclosure capacitance.

Transformer to GIS flange connections

Flange connections between the GIS enclosures and the single phase unit step-up transformers are made through a 2 kV insulating ring. This was required by ITAIPU in order to prevent induced currents GIS enclosure, in approximately 600 A, circulating through the transformer tanks in parallel with the current in ground connections. The transformer manufacturer limited the circulating current to 50 A maximum. To avoid the possibility of arcing across the insulation during transient voltage conditions, four 660 kV metal oxide surge arresters were provided at each phase connection.

Disconnect switches

Phase opposition can occur within the GIS when two breaker terminals are out of phase and potential transfer takes place through circuit breaker grading capacitors.

The Itaipu disconnect switches are not designed to operate under phase opposition, therefore the operating procedures at Itaipu are modified accordingly. During the supply contract spring loaded follow up contacts were added to all disconnect switches. This modification, which was verified by tests, gave the following advantages:

- The range of spread in the sparking distances was reduced.
- The arc was centered in the middle of the contacts.
- Arcing time was reduced.
- There were no flashovers to the grounded enclosure, even with overvoltage of 1.6 p.u.

See Fig. 12.91 for a cross-section of the disconnect switch and Fig. 12.92 for a cross-section of a typical circuit breaker.

Insulation between the supporting structure and the GIS enclosures

In the original design of the GIS insulation (2 kV) between the GIS enclosures and the supporting steel structures was provided. Later, this insulation was deleted because it eliminated the possible arcing between the enclosures and structures, which could occur during voltage transients. The disadvantage due to elimination of insulation was that it became impossible to estimate the flow of ground currents during faults and to calculate touch potentials.

Factory tests

At the factory, the components of the GIS were assembled into shipping sections and tested before dispatching. The tests performed were: gas leakage, voltage drop, mechanical switching and HV tests. The HV tests were particularly important to ascertain the required dielectric strength of the assemblies.

The average equipment failure rate, after somewhat high initial values, decreased with the increased number of tested shipping sections tested to an approximate value of 0.5%. The calculation was based on the number of conical spacers within the tested sections.

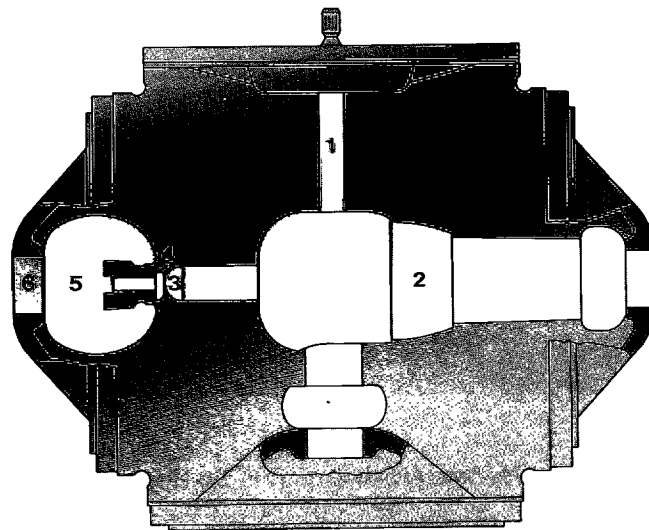


Fig. 12.91 GIS disconnect switch cross-section

- | | |
|------------------|---------------------|
| 1 Operating rod | 4 Follow-up contact |
| 2 Shield | 5 Fixed contact |
| 3 Moving contact | 6 Insulator |

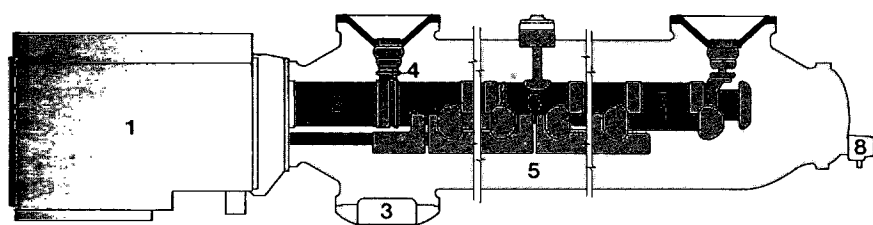


Fig. 12.92 Typical SF₆ GIS circuit breaker cross-section

- 1 Driving mechanism
- 2 Insulator
- 3 Moisture absorbent
- 4 Bus connection
- 5 Enclosure
- 6 Interrupter units
- 7 Grading capacitors
- 8 Gas density relay

Installation

SF₆ equipment is very sensitive to contamination due to dirt or dust particles which are normally present in a powerhouse, especially during construction. Therefore, clean conditions were essential during all phases of unpacking, installation and testing and also during operation and maintenance. To ascertain cleanliness temporary bulkheads were installed in the SF₆ gallery. The bulkheads isolated the area where the equipment was being installed from the rest of the station under construction. Doors were provided at all access points to the installation area and guards ensured that only authorized personnel entered the area, and that they did not bring in dirt. Ventilation fans complete with coarse mesh filters were mounted in the bulkheads to provide a regulated supply of air to the installation area. The SF₆ switchgear was unpacked and cleaned in a separate air conditioned area within the gallery.

Due to the initial problems experienced during the operation, which were the result of contaminations, it is now thought that additional precautions to improve the cleanliness of the area should have been taken. In particular it would have helped considerably if the powerhouse ventilation system had been operative at the time of installation of GIS, as this system has fine filters as a result of the evaporative cooling, see Chapter 13.

TESTING AND COMMISSIONING

When GIS was specified for Itaipu, it was recognized that the technology was somewhat new and that problems might be encountered during the execution of the project. These potential problems were accepted because of the overwhelming technical advantages of the GIS alternative over the other alternatives, see Chapter 2. The problems described below were within the limits of this general philosophy and were considered incidental

compared to the otherwise successful operation of the GIS equipment.

Problems provoked by transport

A number of GIS components arrived at the site with traces of external damage apparently due to transport by trucks and rough handling during loading.

Two metal oxide surge arresters were subjected to accelerations of more than 2 G, which caused misalignment of some discs and the units were rejected.

Some spacer insulators had a separation between the central part of the spacer body and the hub. These defects were found only after energization by detection of partial discharges which were in the range of 6000 pC to 10 000 pC.

The main problem, however, was the presence of conducting particles, which became free or were generated by excessive acceleration and shocks during transportation. This was especially true in case of cast corona shields.

Particles were also generated by the transport cover plates, some of which were improperly manufactured.

GIS experience at Itaipu project confirmed that long distance transportation and handling may jeopardize the dielectric integrity of the equipment which was achieved at the factory.

Tests at site

High voltage site testing was performed by using two types of dielectric test equipment: series resonance test having with 600 kV/6000 kVA rating, and an oscillating switching surge generator rated ± 940 kV/35 kJ. Since a switching surge test is considered to be superior in detecting damages caused by shipping or erection, this test was performed first and was followed by the applied voltage test. During the testing, it became apparent that the main problem with the GIS equipment was particle contamination, which is better detected by the applied power frequency voltage test. Therefore later it was agreed to interchange the order of the tests.

The tests equipment was connected at the terminals of the line bushings. The test sections were extended step by step by closing the disconnect switches and circuit breakers. The tests were made phase to ground and across the gaps of circuit breakers and disconnect switches. Therefore it was unavoidable that some sections of GIS were repeatedly stressed by the test voltage, up to 400 times. Because very large sections were tested at a time having large capacitance, when a flashover over the conical spacer occurred, the damage to the insulator was great and in all cases required the replacement of the conical insulator.

Failures during site testing

The dielectric failures which occurred during testing at site of the first portion of GIS installed were as follows:

Group A : number of failures due to shipping and erection reasons

Metallic particles	6
Discharge through gas	3
Defective spacer insulator	2
Damaged shields (erection error)	2
Total	13

Group B : number of failures due to other reasons

Spacer insulator failures	2
Potential transformer spacer failures	1
Accidental gas drainage	1
Circuit breaker drive rod failures (design inadequate, later replaced)	4
Disconnect switch failures	2
Total	10

It was observed that even after successful tests with oscillating switching surges, the same GIS component in some cases failed later during the applied voltage tests.

High voltage site tests were performed to detect shipping damages and deficiencies due to improper assembly. Consequently, only group A failures were used in the calculation of site testing failure rate:

Total group A failures	13
Number of spacer insulators	690

The corresponding failure rate of 1.88% of the spacers and the associated gas compartments was accepted as reasonable, considering the long overseas transport, difficult site conditions and the fact that these figures represented failures in the first equipment group.

OPERATING EXPERIENCE

Failures during initial operation

The GIS was put in service in April 1984. The failures listed below occurred during the first months of operation:

Circuit breaker drive rods	4
Circuit breaker support rod	1
Discharge through gas	1
Disconnect switch	2

Solutions

Disconnect switch. The first failure of the disconnect switch was attributed to an abnormal temporary operation when the switch was opened under phase opposition. The second failure occurred during opening of the switch under normal synchronous conditions and it was assumed to be caused by prestressed shieldings which was caused by incorrect manual operation.

Cracks in the operating mechanism housings of grounding switches appeared to be a result of impacts produced by the operation of circuit breakers. The problem was solved by arranging a simple support link which helped to avoid resonant vibration of the free end of the grounding switch. Although these housings were not filled with gas, all of them were replaced.

Circuit breakers. The combined influence of the following factors was responsible for the drive rod failures:

- Entrance of conducting particles into the inside of rod tube during fabrication.
- Particularly high dielectric stresses in the rod region.

Circuit breakers to the same general design had been successfully used at other installations. However, those circuit breakers were equipped with pre-insertion resistors, their tank diameter was larger and the electric field stresses were considerably lower. Hence the equipment was less sensitive to the presence of conductive particles.

The corrective measures taken were as follows:

- Plugs were installed at the ends of the circuit breaker drive rods to prevent particle entrance inside the rod.
- During the final design the shape of the end plug was modified to semi-spherical which provided a better electric field distribution.
- Another difficulty with the drive rod fabrication was metal-to-dielectric threads which were fabricated with sharp edges. In the presence of humidity, corona could form surface films, resulting in field distortions, which could initiate a flashover. In the revised rod design, the thread design was improved by a cover of special varnish.

As a result of all these modifications, the electric field stresses along the driving rod were reduced to about 60% of the stresses experienced with the original rod design.

Failures in the circuit breaker driving rods were due to inadvertent design changes, which turned out to be inadequate. Some failures of the circuit breaker support rod could not be explained, because of heavy damage during the fault. After the implementation of improved design of the circuit breaker drive rod, no electrical failures occurred.

Failures during operation

There were several further dielectric failures of the GIS equipment during operation. An extensive investigation was conducted involving the supplier, special consultant design and ITAIPU personnel. The investigation results indicated contamination as the problem source. The contamination was caused by inadequate field erection procedures and airborne dust particles present during the erection and maintenance. The problem was finally resolved by improved erection procedures and better ambient conditions as the powerhouse ventilation system came into full operation and the powerhouse civil works were completed.

ORGANIZATION OF CONTRACTS FOR PERMANENT EQUIPMENT

Specification packages for competitive bidding for the permanent electrical and mechanical equipment were determined by:

- Type of equipment.
- Convenience of interfacing with powerhouse structure and other suppliers.
- Expected source of supply, especially whether from Brazil or Paraguay or from overseas.
- Most economical package with respect to supply, engineering and erection.
- Possibility of consortiums of several companies bidding together.

For the main generating equipment these considerations resulted in three main contracts:

1. Turbines, governors, generators, unit control and bus ducts.
2. Main step-up transformers.
3. GIS equipment.

Contracts were for design, manufacture and supervision of erection; transport and erection being by others under contract with ITAIPU.

Commissioning was performed by ITAIPU in the presence of the manufacturer's representative.

Specifications were performance type, with detailed design requirements defined as necessary. Where appropriate, Brazilian and Paraguayan standards were specified; where not, international standards were used. For some features, i.e., painting, wiring, quality control, etc., ITAIPU produced separate standards which formed an integral part of the specification.

Contractors were required to submit a list of the contractual information they were to submit for approval, together with an expected chronogram of submittals. The purpose of this was to ensure that the necessary information would be submitted and that it would be sent to ITAIPU in an orderly manner.

Subcontracts had to be identified at the proposal stage and supporting data showing the extent of sub-contracted work and capacity of the sub-contractor to execute it was required.

Detailed erection manuals were submitted to ITAIPU for approval to orientate and guide ITAIPU's work force acting under the instructions of the manufacturer's erection supervisor.

Commissioning instructions were prepared jointly by the manufacturer and ITAIPU's engineering and commissioning departments, which chronologically listed all tests to be made and results expected.

QUALITY CONTROL OF MANUFACTURE

Quality control of the manufacture of the electrical and mechanical permanent equipment for Itaipu was complicated by the size and importance of this equipment, and that it was being manufactured within a short time span at many different locations. It was imperative that uniform standards and procedures should be used, which could only be achieved by ensuring that all parties worked within a common set of guidelines administered by a central authority. To this end, ITAIPU in 1980 contracted IECO-ELC to establish the "Quality Control Group" (GCQ), under whose direction all quality control documentation and subsequent shop floor inspection would be made. As a reference, the Canadian Standard (CSA) Z299.2, "Quality Control Program Requirements", was chosen which in turn was made an integral part of the procedure manual, which was produced by GCQ to interpret the requirements of the standard for the particular conditions of Itaipu project.

Normally for CSA Z299.2 the hierarchy is two-tiered: the manufacturers and the client. For Itaipu, however, the relationship was more complicated because of the existence of the separate GCQ organization and various inspection agencies working directly under contract with ITAIPU. This was further complicated in that the ITAIPU engineering department, which would have to be consulted in the event of non-conformities, was a distinctly separate organization from that of GCQ. The main objective of the procedure manual was therefore to systemize the role to be played by all these entities and to ensure a regular flow of correspondence and decision making. Standard CSA Z299.2 in effect specifies and controls the manufacturer's quality control organization and inspection. It determines the type of documentation to be produced by the manufacturer, the way the manufacturer's quality control personnel and client's representative should interact, and how manufacturing non-conformities should be dealt with. As such it does not specify the methodology nor extent of inspection. These remain under the control of the equipment specifications and client-approved contractual documentation (drawings, calculations etc.). Standard CSA Z299.2 is one of a series of four with CSA Z299.1 as the most rigid, leading to CSA Z299.4 as the least.

The following factors were considered in choosing CSA Z299.2 for the Itaipu main equipment:

- Design process complexity.
- Design maturity, i.e., whether a new design or an evolution of an existing design.
- Manufacturing process complexity.

- Service characteristics, i.e., complexity of service, number of interactive parts etc.
- Probability and consequence of failure.
- Economic penalties paid to impose the quality control system on the manufacturer.

Obviously the criteria and factors used were somewhat subjective but the following principal conclusions could be formed:

- Where possible, well tried designs were specified and adopted. However, for these designs to be used for Itaipu an extrapolation with unknown risk was unavoidable. Also, of necessity, some innovative designs were required.
- In addition to other factors, manufacturers were chosen for their high content of Brazilian and Paraguayan manufacture (in the case of the turbine/generator units, 85%). In some cases this involved a substantial extension of the manufacturer's previous experience, especially in respect of component size and complexity.
- The manufacturing period was concentrated with the involvement of most major factories in Brazil and Paraguay. In many cases components would travel from their place of manufacture to site for final assembly. The program could not tolerate extensive remedial measures at site, or worse, return of items to the factory.
- Failure of component parts in service could range in their seriousness from inconvenient to catastrophic, depending on the scenario considered. Workmanship therefore had to be of the highest quality.

The highest control program (CSA Z299.1) could not be justified, but adoption of the second (CSA Z299.2) was both prudent and necessary.

MANUFACTURER'S QUALITY CONTROL ORGANIZATION

A prime requisite of CSA Z299.2 is that the manufacturer should have a well structured quality control organization independent of, and separate from the production departments. The structure of the organization should be well documented in a quality control manual, which is subject to revision as personnel and facilities change. Therefore, as an integral part of pre-qualification for the acceptance of any manufacturer, ITAIPU conducted a survey of manufacturer's quality control department and if necessary recommending changes to ensure its compliance with the standard. Of course the requirements depended somewhat on the equipment to be made, the main generating equipment (turbines, generators, GIS transformers etc.) demanding the highest compliance with the standard.

At the time of the survey names of the manufacturer's personnel who were to coordinate the various activities of quality control, such as document preparation, inspection programming and equipment release, were established and the requirements of the procedure manual discussed and finalized.

QUALITY CONTROL DOCUMENTATION

All documentation relating to quality control of specific items was produced by the manufacturer to a standard format specified in the procedure manual. The major required documentation was as follows:

Quality control manual

As explained previously, this described the manufacturer's quality control organization and was subject to review by ITAIPU at the pre-qualification stage.

Inspection and test plan

The inspection and test plan (PIT) was the master document for quality control and assurance. There was a PIT for each major item i.e., turbine runner, generator rotor, upper generator shaft etc., the general form of the document being:

- Reference documents. A list of applicable technical specifications, approved drawings and special procedures (weld procedures, test procedures etc.).
- Inspection and control schedule. This was in the form of a table, a typical example being shown in Table 12.15. The major steps of the inspection were given, and in particular requirements for presentation of test documentation and presence of ITAIPU's representatives were defined. Of particular importance was the concept of a "hold point" which specified a stage in manufacture which could not be passed without the successful completion of all specified inspection in the presence of ITAIPU's representative. For inspections other than "hold points", the presence of ITAIPU's representative was preferred but not mandatory. To facilitate such attendance, a 3 week program was evolved with the manufacturer giving probable dates of inspection should ITAIPU's representative wish to attend.
- Explanatory notes. These elaborated the information given in the table giving any special requirements or explanations. Special explanatory documents were attached as required.

Non-conformity report

Every non-conformity discovered during inspection was covered by a formal report. Non-conformities fell into three main groups:

1. To be corrected
2. To be substituted
3. Could be accepted as it is.

In the first category were problems such as material defects to be repaired by welding, wiring defects and pieces requiring further machining or finishing.

In the second category were minor failures and items such as relays and electrical equipment which were either below standard or damaged in some manner. In both cases, the non-conformity was eliminated after correction.

The third category was more problematic because it involved the acceptance of equipment which did not conform to specification, the alternative being rejection of the piece, possibly resulting in considerable delay in the construction program. Naturally, only a small number of these non-conformities which were not to be corrected required extensive critical consideration for them to be accepted. The majority took the form of small dimensional deviations, material properties slightly different than specified, or minor defects where repair would have been more problematic than the acceptance. Here the normal safety factors and tolerances inherent to design and erection could easily accommodate the deviation. However, in all cases the non-conformity was reviewed by the manufacturer's design department and approved by ITAIPU's designers before acceptance and a permanent record was included in the data book for future reference. In the few cases where non-compliances outside these criteria were accepted, they were subjected to the most exacting test program, normally by the manufacturer under the auspices of ITAIPU's design department but in some instances by third party consultants.

The amount of effort in properly dealing with manufacturing non-compliances in a project of the size of ITAIPU should never be underestimated as it is indicated in Fig. 12.93.

Data book

All documents relating to the quality control and inspection for each PIT item were compiled into a single data book which accompanied the equipment to site and remained in ITAIPU's files. Because of the size of the data book and the extent of the information contained therein, a separate resume was made, which provided easy reference to the main document. Again the amount of work in handling this documentation should not be underestimated, as shown in Fig. 12.94. No item could be shipped to site unless the data book was complete and all inspection documentation approved.

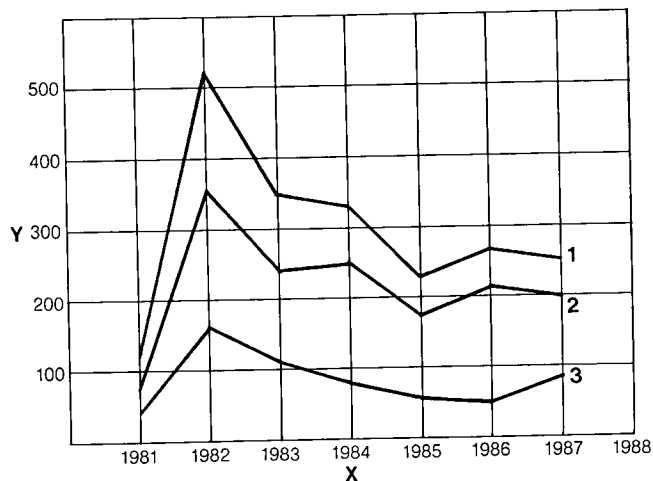


Fig. 12.93 Manufacturing divergencies

Y Amount of divergencies
X Years

1 Total divergencies
2 Divergencies not corrected
3 Divergencies corrected

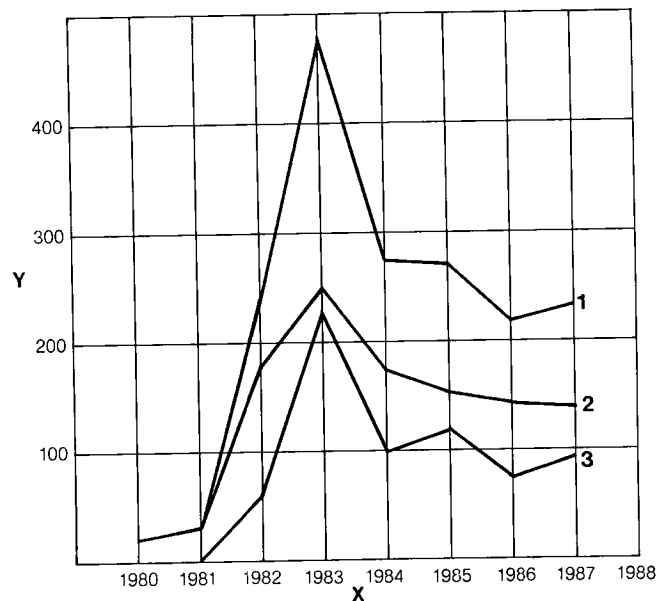


Fig. 12.94 Amount of documentation by type of equipment

Y Amount of documentation
X Years

1 Total
2 Mechanical
3 Electrical

Table 12.15 Inspection and controls foreseen

Item	Inspections to be executed	Items subject to inspection								
		1	2	3	4	5	6	7	8	9
A	Purchase specification			DA	DA					DA
	Standards									DA
	Chemical analysis certificate			DA	DA					DA
	Mechanical properties certificate			DA	DA					DA
	Metallurgy certificate									
	Certificate for hardness test					DA		DA	DA	DA
	Dimensional check sheet	DA				DA				
	Indication and localization of material									
	Ultrasonic test certificate		DA	DA	DA					
	Dye-check test certificate	DA	DA			DA		DA		
	Magnetic particle test certificate									
	X-Ray test certificate									
	Certificate for heat treatment		DA							DA
	Certificate of welder qualification		DA			DA				DA
	Weld process certificate		DA			DA				DA
	Test plate identification									
	Pressure test certificate (piping)		DA							
	Functional test certificate									
	Deviation from drawing report									
	Final release certificate	DA					DA	DA		
	Shipping document	DA					DA	DA		

Table 12.15 Continued

Item	Inspections to be executed	Items subject to inspection								
		1	2	3	4	5	6	7	8	9
B	Chemical analysis			CS	CS					CS
	Tension test			CC	CI					CC
	Impact test			CC	CI					CC
	Macrograph									
	Hardness test							CI		CC
	Visual analysis			CI	CI					CI
	Dimensional check			CI	CI					CI
	Ultrasonic test			CC	CI					
	Dye-check									
	Magnetic particle check									
	X-Ray									
	Heat treatment									
	Other test									
C	Set up before welding		CI						CI	
	Visual control		CI			CI			CI	
	Dimensional check		CI			CI			CI	
	Ultrasonic test		HP							
	Dye-check	CI	HP			CI			CI	
	Magnetic particle check									
	X-Ray check									
	Heat treatment		CI						CI	
	Test components									
	Other tests		CI							
D	Visual control	HP					CI	CC		
	Dimensional check	HP					CI	CC		
	Ultrasonic test									
	Dye-check	HP						CC		
	Magnetic particle check									
	X-Ray									
	Pressure test									
	Factory pre-erection	HP								
	Functional check									
	Hardness check					CI				
	Painting	CI								
	Packing	CI								

A Documents to be submitted**B** Control of materials**C** Control of welds**D** Final controls**DA** Document approved and available for ITAIPU inspector**CS** Control by subcontracts**CC** Control by subcontracts as a procedure of contractor**CI** In-progress control by ITAIPU inspector**HP** "Hold point" inspection by ITAIPU**1** Bottom ring machined and finished**2** Bottom ring welded**3** Bottom ring welded steel plate**4** Bottom ring steel castings (bearing holders)**5** Welding overlays**6** Self lubricating bearing bush**7** Wearing ring machined and finished**8** Wearing ring welded**9** Wearing ring stainless steel plate

POWERHOUSE AUXILIARY EQUIPMENT AND SYSTEMS

POWERHOUSE SERVICE SYSTEMS	13.3
Cooling Water	13.3
Compressed Air	13.6
Pumped Drainage Systems	13.8
Turbine Filling System	13.12
Transformer and Lubricating Oil	13.12
Treated Water	13.17
Sewage	13.18
Fire Protection	13.18
Ventilation	13.20
Air Conditioning	13.27
 DRAFT TUBE STOPLOGS	 13.29
 POWERHOUSE CRANES AND ELEVATORS	 13.32
Cranes	13.32
Elevators	13.47
 ELECTRICAL POWER SYSTEMS	 13.53
Alternating Current Systems	13.53
Sources of Auxiliary Power Supply	13.54
Reliability of Various Power Sources	13.55
Supplies to Auxiliaries of the Generating Units	13.55
Load Classification	13.56
13.8 kV Systems	13.57
460 V ac General Systems	13.59
Direct Current Systems	13.59
Emergency Diesel Generators	13.61

OPERATIONAL EXPERIENCE

13.62

ELECTRICAL GENERAL SERVICES

13.62

Lighting System

13.62

Grounding System

13.62

Wiring Systems

13.63

Cabling

13.63

Communications

13.63

Fire Surveillance

13.67

POWERHOUSE AUXILIARY EQUIPMENT AND SYSTEMS

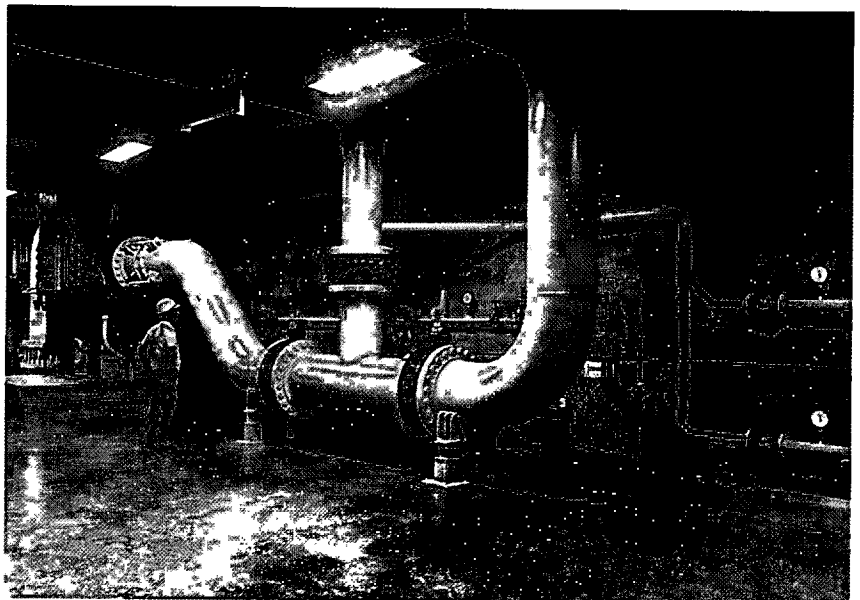
The powerhouse auxiliary systems serve the main generating units and their auxiliaries, and the various general operating facilities in the powerhouse.

POWERHOUSE SERVICE SYSTEMS

COOLING WATER

Cooling water is taken from a connection on the turbine spiral case and, after coarse straining, is distributed to the various equipment in the station. The alternative to this source of supply would have been to pump the water from the tailrace. However, this was discarded as a possibility for economic and technical reasons, because:

- The large amount of water required would necessitate considerable pumping capacity.
- Reserve pumps and alternative electrical supplies would be required to give the system the same degree of reliability as a system supplied from the spiral case.
- Pumping from the tailrace would greatly complicate the unit start/stop sequence.



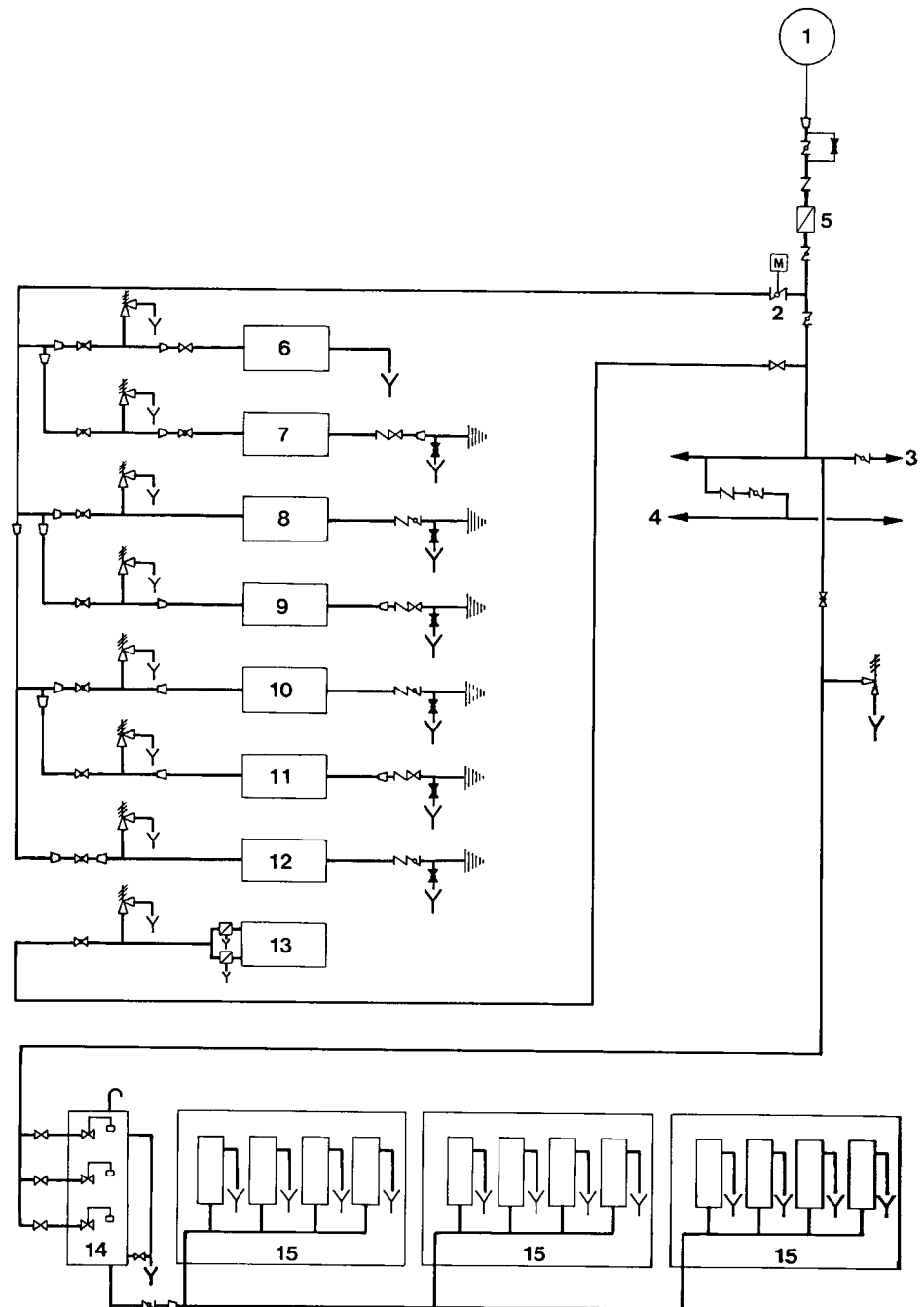
*Mechanical service
gallery – El. 92.4*

The only objection to taking the cooling water from the spiral case was that the pressure at approximately 110 m was traditionally high for this service, 70 m being more usual. As a compromise, equipment supplied by the system was specified for a normal working pressure of 105 m (test pressure 158 m), and safety valves were provided in the system to accommodate the 30% overpressure at turbine load rejection, see Chapter 12.

The only exception to this is the supply to the powerhouse station and generating unit air compressors which is regulated to 50 N/cm² (51 m) with pressure reducing valves. A simplified schematic diagram is shown in Fig.13.1. From the spiral case connection, the water passes through a strainer with automatic cleaning to a 600 mm header, which runs the length of the powerhouse in the downstream gallery at El. 92.4. The supply to each

Fig. 13.1 Cooling water system-schematic

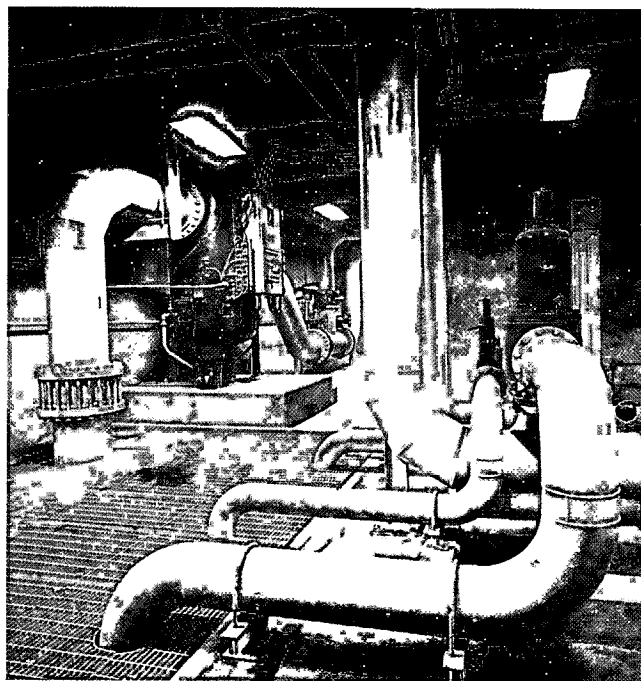
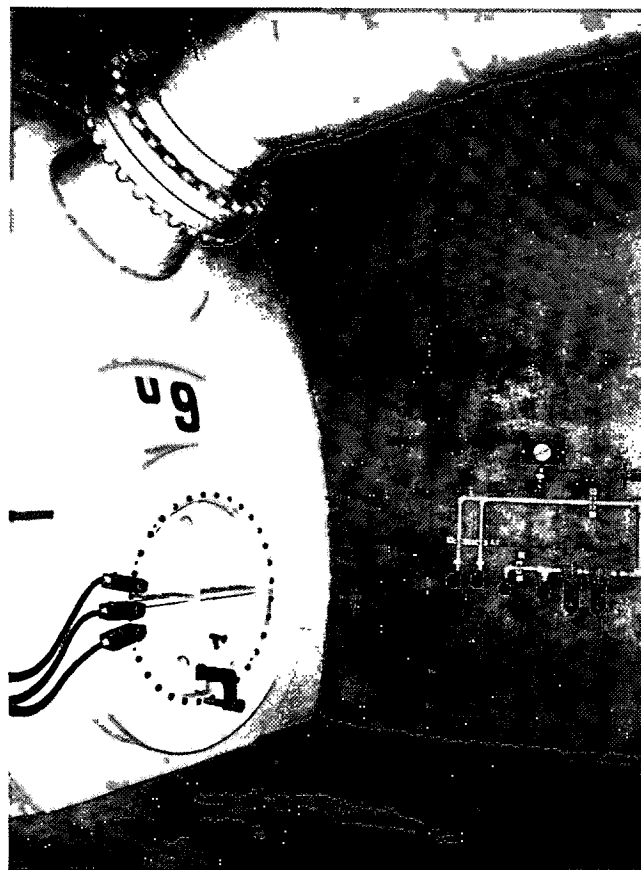
- 1 Spiral case
- 2 Motorized valve to unit coolers
- 3 To main header
- 4 Fire water
- 5 Strainer
- 6 Generator excitation coolers
- 7 Governor oil coolers
- 8 Generator deionized water coolers
- 9 Turbine guide bearing coolers
- 10 Generator combined bearing coolers
- 11 Generator upper bearing coolers
- 12 Generator air coolers
- 13 Turbine shaft seal
- 14 Main transformer cooling water break tank
- 15 Main transformer coolers
- M Electric motor
- ⋈ Gate valve open
- ⋈ Globe valve open
- ⋈ Globe valve closed



generating unit is taken from the header via a motorized butterfly valve, which is opened and closed as part of the unit start/stop sequence. The supply circuit from spiral case to header is sized for the flow requirements of two units, thus making the general system extremely flexible and reliable, in that any unit can supply any other unit and, if necessary, one unit can supply two. The common services supplies (air conditioning, compressors, diesels, etc) and supply to the main step-up transformers cooling water break tank at El. 118.3, upstream of the powerhouse line A wall are also taken from the header. Flow to the break tank is automatically regulated by float valves and supply to the cooler of the three single phase transformers of each unit is on demand from valves in the transformer cooling circuits.

The Cuno-Flow strainer with nominal capacity of 4200 m³/h, see Fig. 13.2, strains particles to a minimum of 1 mm; backwashing of the strained elements occurs automatically when the differential pressure across the strainers reaches 5 m. There are eighteen strainer elements, each with a pneumatically controlled valve, which opens to drain. The valves open sequentially, hence the head and flow fluctuations during backwashing are minimal. Air supply is from the powerhouse compressed air system. There is a 138 l air tank at the strainer which is sufficient for three backwashes and thus eliminates dependency of the operation of the strainer on the powerhouse compressed air supply, which is not regarded as an essential service. The body of the strainer was pressure tested at 260 N/cm². Stainless steel was used extensively for the internal working parts.

The majority of cooling water is discharged from the equipment to the tailrace at El.125. Non-return and isolating valves at the discharge protect the powerhouse from ingress of water in the unlikely event that a pipe should break when the tailrace water level is higher than the discharge pipe. Water from the coolers of main step-up transformers drains into the anti-flooding gallery, to be pumped from there to discharge into the tailrace at El.125. This system permits the transformer cooling water to be at a lower pressure than the oil, thus avoiding any possibility of the water entering the oil, and gives the anti-flooding pumps a regular usage cycle, ensuring that they are ready for any emergency. Compressor cooling water is discharged to the powerhouse drainage system. The discharge from the turbine seal is piped through the dividing vane of the turbine stay ring, to drain to the powerhouse drainage system.



Cooling water takeoff from spiral

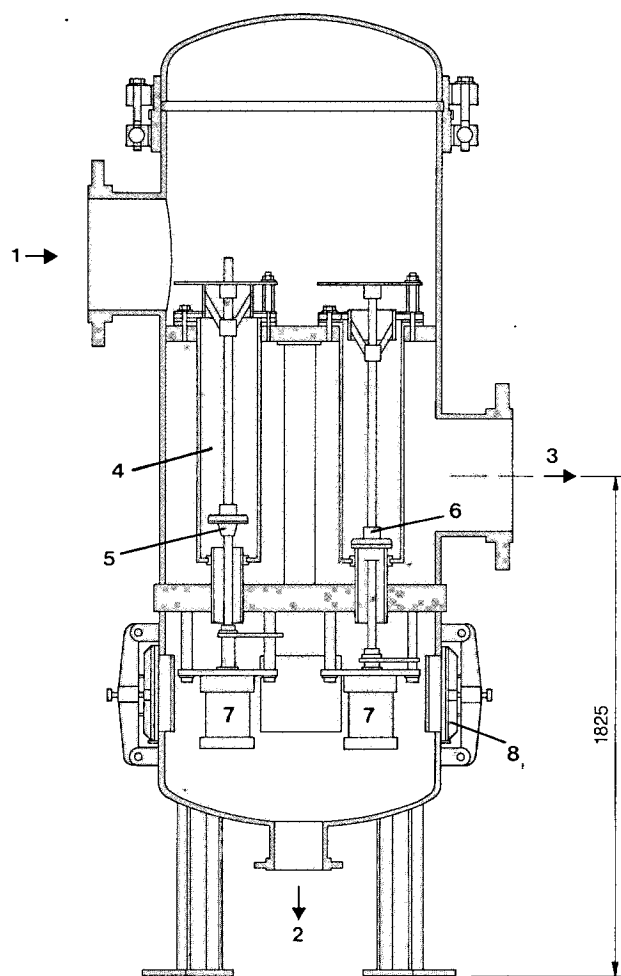


Fig. 13.2 Cooling water strainer

- | | |
|------------------|----------------------|
| 1 Raw water | 5 Valve open |
| 2 Debris | 6 Valve closed |
| 3 Strained water | 7 Pneumatic actuator |
| 4 Strain element | 8 Inspection door |

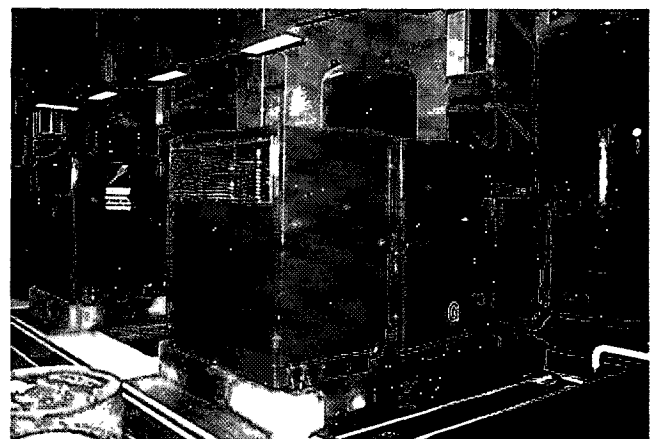
COMPRESSED AIR

A schematic diagram of the compressed air system is shown in Fig. 13.3. Compressed air for the system is supplied by two groups of four compressors. Each group is in a room at El. 98.5 between lines C and D, one room being in the right assembly area and the other in the central assembly area. Only three compressors of each group supply the system, the fourth compressor is in reserve should any one of the other three fail. Also in each room are the 5 m³ compressed air receivers (one for each compressor) and the electrical control cubicle.

From the receivers the air feeds into a 150 mm diameter header, running the length of the powerhouse at El. 98.5, from which it is distributed to the various points of demand. Operation of the system is automatic, the compressors starting and stopping in response to pressure switches connected in a joint circuit to all four pressure receivers. A compressor can also be started manually to charge the receiver after being out of service for maintenance. Maximum and minimum receiver pressure, as maintained by the pressure switches, are respectively 88 N/cm² and 70 N/cm². The system is sized to give a minimum pressure of 61 N/cm² at all demand points other than the generator brakes, at which a minimum of 66 N/cm² is maintained.

The chosen arrangement gives the system great flexibility and reliability; however, in view of unpredictability of the demand (i.e. pneumatic tools, drying of ventilation filters etc.), the compressed air system like the others regarded as essential to power generation, is designed to operate with the rest of the system inoperative for a limited period. Thus items such as the generator air brakes and cooling water strainers all have supplementary air receivers which guarantee continued operation in the event of failure or exhaustion of the compressed air system.

Selected for quietness of operation, the compressors are the screw oil type, see Fig. 13.4. Table 13.1 gives the principal characteristics of the compressors and their aftercooler, for the 50 Hz and 60 Hz sectors. Receivers are equipped with safety valves, pressure gauge and automatic condensate drain valves. Compressors are automatically switched off in the event of high air exit temperature and high air pressure in the receivers. Blocked filters, blocked oil separators and loss of cooling water give alarms.



Powerhouse compressed air room

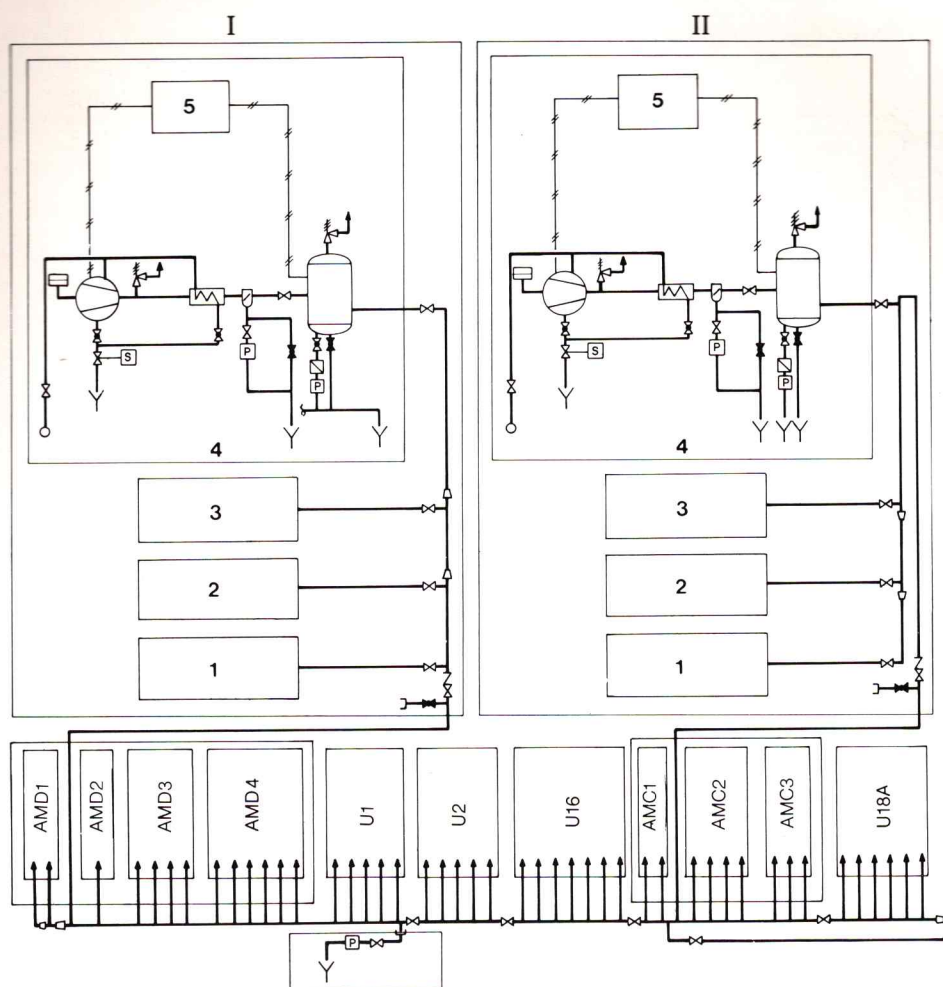


Fig. 13.3 Station compressed air system schematic

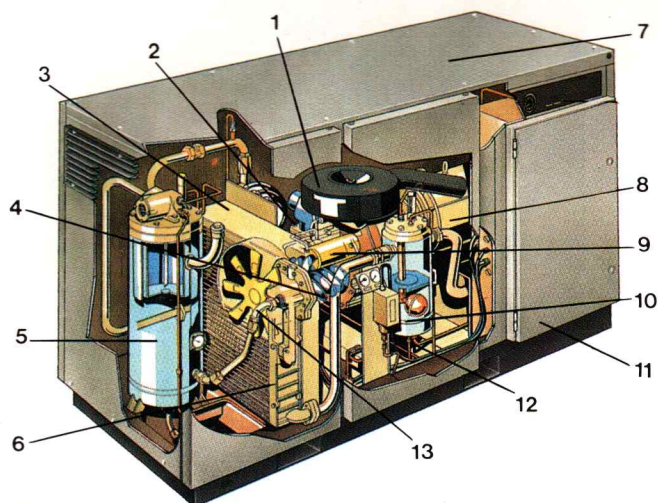


Fig. 13.4 Powerhouse air compressor

- 1 Admission air filter
- 2 Admission air valve
- 3 Differential pressure switch
- 4 Screw type compressor
- 5 Reservoir with oil separator
- 6 Oil and air refrigerator
- 7 Acoustic isolated case
- 8 Electric motor
- 9 Oil filter
- 10 Control pressure switch
- 11 Automatic start
- 12 Condenser separator
- 13 Cooling fan

Table 13.1 Service air compressors – principal technical data

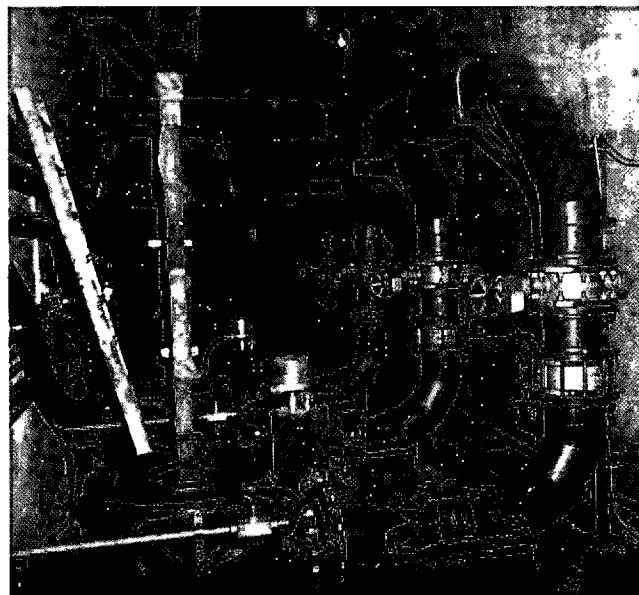
	60 Hz	50 Hz
Manufacturer	Atlas-Copco	
Type	Stationary, helicoidal, screw-rotors, injection oil lubricated, single stage, with oil cooler and aftercooler (water cooled), both shell and tube type	
Model	GA 810 W pack	
Operating maximum pressure (manometric)	1000 kN/m ²	
Discharge maximum pressure (manometric)	860 kN/m ²	
Discharge rated pressure (manometric)	690 kN/m ²	
Effective free air discharge at full load and 860 kN/m ² (manometric) in accordance with ISO 1217	13 m ³ /min	10.8 m ³ /min
Required BHP at full load and 860 kN/m ² (manometric)	88.3 kW	73.6 kW
No load power	18.1 kW	15.1 kW
Electric motor power	110 kW	92 kW
Air temperature at 690 kN/m ² (manometric) at discharge flange of compressor	~10°C above temperature of cooling water	
Main dimensions		
Length	3230 mm	
Width	1636 mm	
Height	1750 mm	
Net weight	22.36 kN	

PUMPED DRAINAGE SYSTEMS

There are separate, independent, pumped drainage systems in the powerhouse, all of which discharge to the tailrace at El.125. This elevation was chosen as a compromise between pumping head, and hence cost of equipment and operation, and the risk of ingress of water from the tailrace should a pipe break on the tailrace side of the non-return valve. The chosen discharge elevation (125 m) is reached only in exceptional Iguaçu river discharge conditions which, together with the extreme odds against a concurrent pipe break, signified negligible risk to the powerhouse.

A general schematic of the systems, together with a table of data is shown in Fig. 13.5.

Pump sumps, to which the water is piped are located between lines C and D downstream between selected turbine generator units. Pumps are vertical, multistage turbine, oil lubricated type with semi-enclosed impellers. Their motors and control



Powerhouse drainage pumps

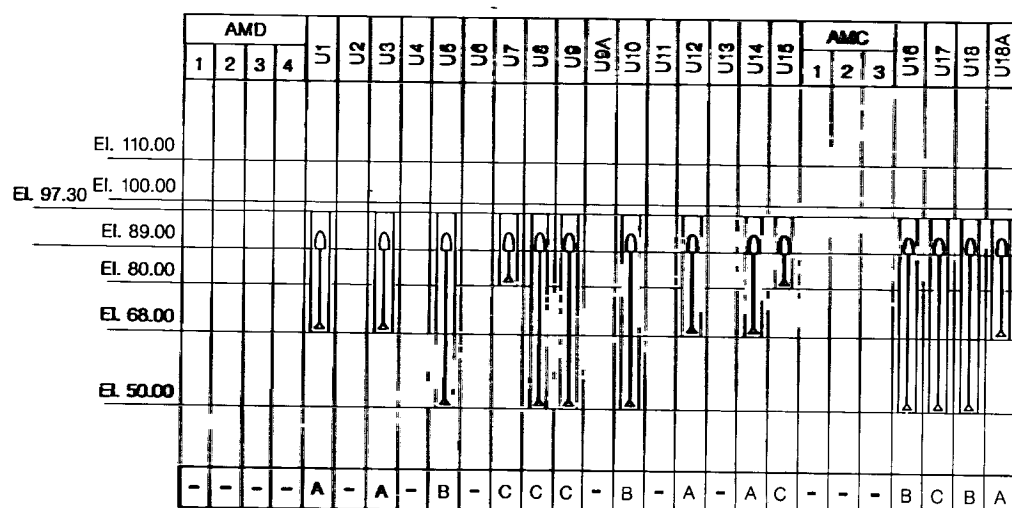


Fig. 13.5 Powerhouse pumped drainage system schematic

A Anti-flooding system
B Turbine and penstock dewatering system
C Drainage system

System		Volume (m ³)	No of pumps				Characteristics		
			Normal	Reserve	Future	Total	Flow (m ³ /h)	Head (m)	Power (kW)
U 1	Anti-flooding system	942	4	1		5	545	68.7	150
U 3	Anti-flooding system	942	4	1		5	545	68.7	150
U 5	Turbine and penstock dewatering system	1761	3	1		4	800	72.5	250
U 7	Drainage system	350	2	1		3	406	50.4	90
U 8	Drainage system	2105	2	1	1	4	300	80.7	110
U 9	Drainage system	2105	2	1	1	4	300	80.7	110
U 10	Turbine and penstock dewatering system	1761	3	1		4	600	72.5	250
U 12	Anti-flooding system	942	4	1		5	545	68.8	150
U 14	Anti-flooding system	942	4	1		5	545	68.8	150
U 15	Drainage system	350	2	1		3	406	50.4	90
U 16	Turbine and penstock dewatering system	1761	3	1		4	800	72.5	250
U 17	Drainage system	2105	2	1	1	4	143	83.2	55
U 18	Turbine and penstock dewatering system + Drainage system	1761	3	1		4	800	72.5	250
U 18A	Anti-flooding system	942	4	1		5	545	68.8	150

cubicles are located in a dry pit at El. 89, accessible by vertical ladder from the gallery at El. 92.4. Motorized monorail cranes above the dry pit are used to handle pumps, motors and associated valves.

Vertical turbine pumps were chosen for this service because of the following:

- Ease of maintenance of motors and pumps from a relatively high floor elevation (El. 92.4), compared with the alternative of a horizontal centrifugal pump in a deep dry well.
- Convenience of accommodating the multistages, necessary for the relatively high head, within the pumping sump.

Between El. 57.25 and El. 78, surface drains discharge into sumps at El. 50 at U8, U9, U17 and U18.

Turbine and penstock dewatering system

Water passages of the units are drained from two outlets on either side of the draft tubes, see Fig. 12.19, Chapter 12. From there the water is conveyed in a 500 mm header to pump sumps at El. 50 as follows:

- For U1 to U5 and U10.
- For U16 to U18 at U16 and U18 (U18 doubling also as a drainage sump).

Pump sumps U5 and U10 are connected as are U16 and U18. However, there is no interconnection between the two sets of sumps.

A schematic diagram of the system is shown in Fig. 13.6. Isolating valves are provided in the pipes leading from the header to the pump sumps such

- Adequate room in the vertical multistage arrangement to accommodate the semi-enclosed impellers required to accept the possibility of a high silt or dirt content in the flow.

Pump sumps are accessed from manholes at El. 92.4, with caged vertical ladders leading to the bottom of the sumps.

The systems are as follows:

Powerhouse drainage systems

Surface water above El. 144 is conveyed by gravity drains direct to the tailrace.

Surface drains in the powerhouse between El. 98.5 and El. 133.2 lead to one of two pump sumps at U7 and U15. The sumps are located between El. 80 and 89. The sump at U7 normally collects water from the right assembly area and U1 to U9A, and the sump at U15 collects water from the central assembly area and U10 to U18A.

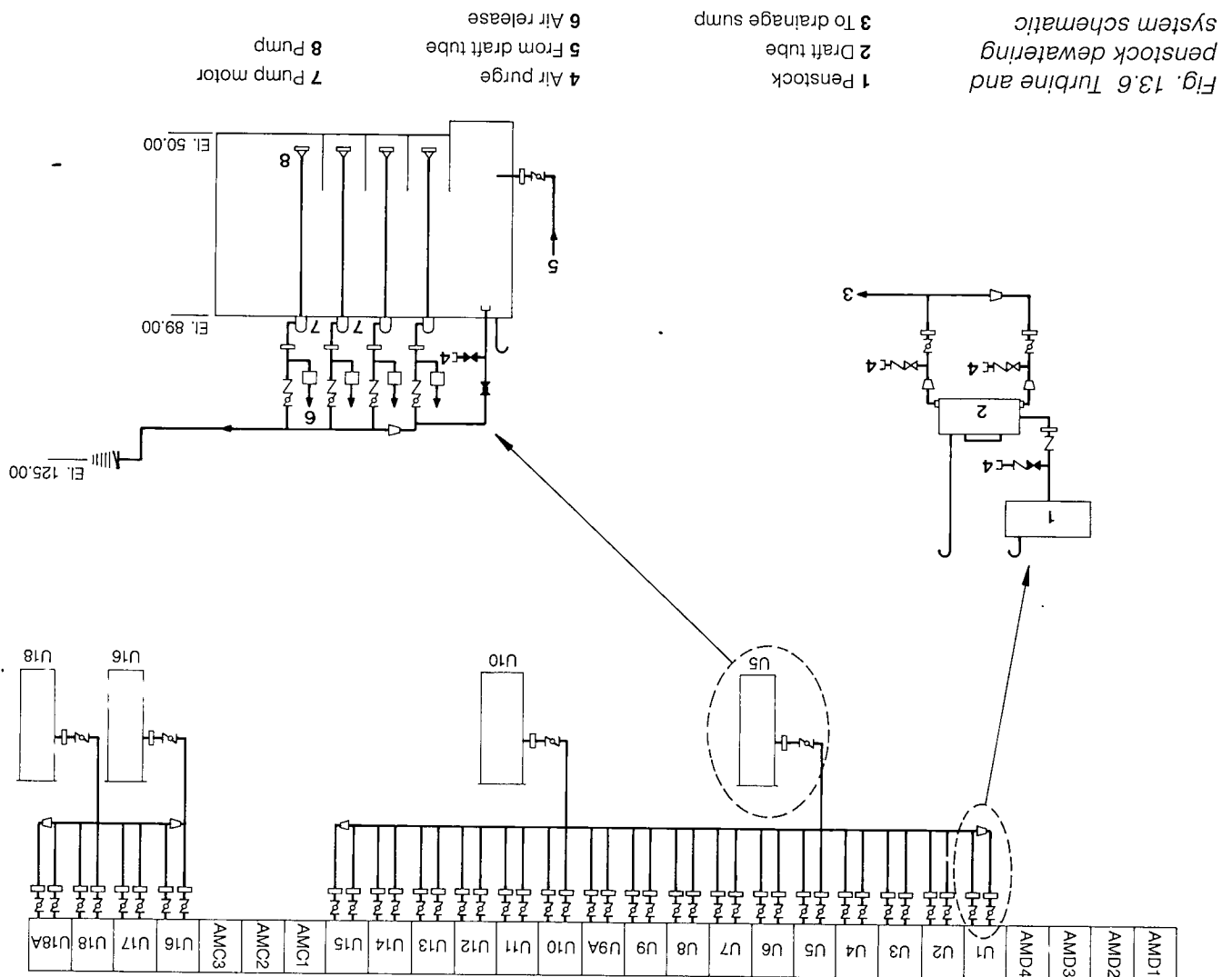


Fig. 13.6 Turbine and penstock dewatering system schematic

that either sump can be isolated for maintenance while the other continues in service. To this end the 500 mm diameter pump delivery header from each sump discharges separately to the tailrace at El. 125.

The penstock and spiral case are drained to the draft tube through a 600 mm pipe normally isolated by a 400 mm diameter butterfly valve.

Design of the system is such that only one unit is dewatered at a time; dewatering takes five hours to complete at an average flow of $60 \text{ m}^3/\text{min}$.

The pump sumps are designed to be pressurized to maximum tailwater level, should the incoming flow exceed the pump capacity.

Powerhouse anti-flooding system

The powerhouse anti-flooding system consists of a gallery at El. 77.3, on the downstream side of the powerhouse between lines C and D, and five sumps at U1, U3, U12, U14 and U17. Storage volume in the gallery and pump capacity are such as to give the operating staff sufficient time to lower intake gates or deploy draft tube stoplogs in the event of an emergency ingress of water into the powerhouse. Emergency conditions considered were:

- Rupture of the 600 mm diameter cooling water header at El. 92.4; water flowing under reservoir

head. The time available before the anti-flooding gallery is full under this condition is 30 minutes, which is more than adequate to lower the intake gates or isolate the rupture.

- A 1.5 cm x 10 m crack in a turbine head cover; water flowing under maximum tailrace head. Under this condition the anti-flooding system takes five hours to fill, which is an adequate time for the draft tube stoplogs to be deployed. A schematic of the system is given in Fig. 13.7, together with pumping capacities and relevant data.

To give the anti-flooding system pumps constant use and hence guarantee their operation should an emergency occur, the cooling water from the unit main step-up transformers and the discharge from the cooling water relief valves is drained to the system.

Contaminated water drainage

In the event of a fire or explosion in the transformer bays, oil storage and treatment areas and diesel fuel areas, the fire water spray system is activated. The resulting water oil mixture passes through a chilling drain before being channelled to sumps at El. 90 upstream of units 1, 3, 7, 10, 14, 15 and 18 from where it is pumped to a mobile bowser at El. 144 for disposal.

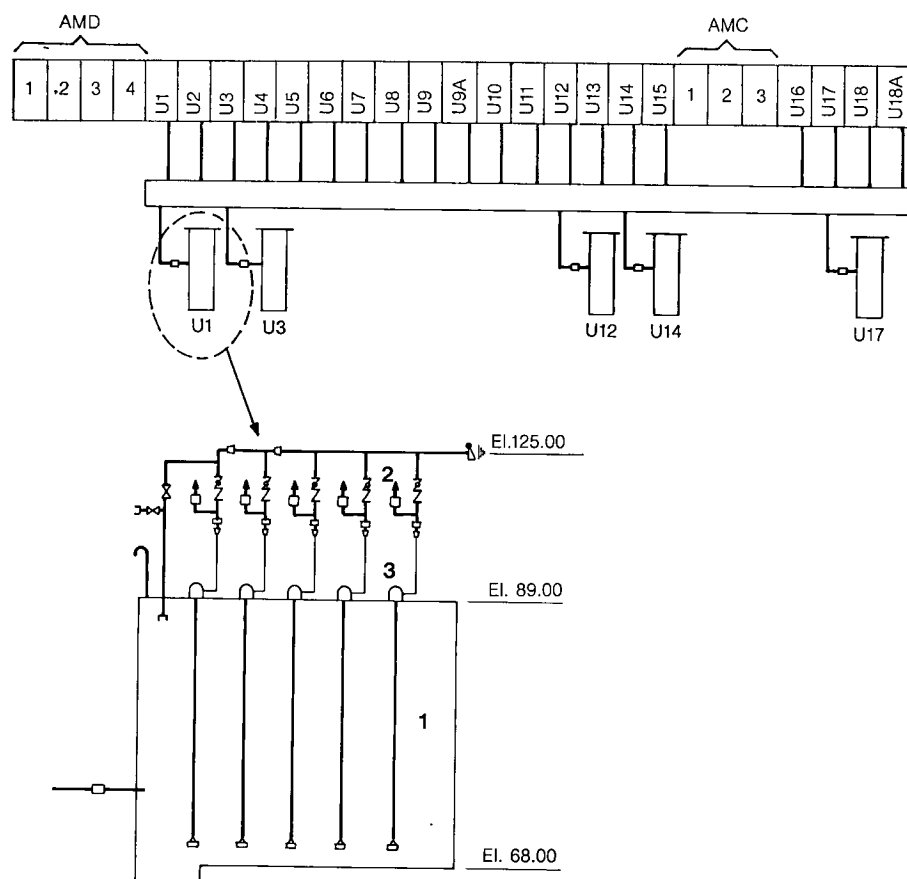


Fig. 13.7 Powerhouse anti-flooding system schematic

- 1 Pump
- 2 Vent
- 3 Motor

TURBINE FILLING SYSTEM

The turbine draft tube, spiral case and lower reducing bend are filled with water from the tailrace through a 500 mm diameter connection to the tailrace at El. 90, see Fig. 13.8. When the level in the lower reducing bend reaches tailrace level (the water passing through the 600 mm diameter connection from the draft tube), the penstock is then filled with the intake gate by-pass system, see Chapter 10. During filling, air is automatically discharged from the draft tube through the 400 mm diameter pipe which extends above maximum tailwater level. Draft tube stoplogs must be removed before the penstock is finally filled. Maximum time to fill the draft tube under unfavorable conditions is approximately four hours.

To reduce cavitation at the valve during filling, station compressed air is injected upstream of the valve. The same compressed air is used to clear the inlet grill of debris.

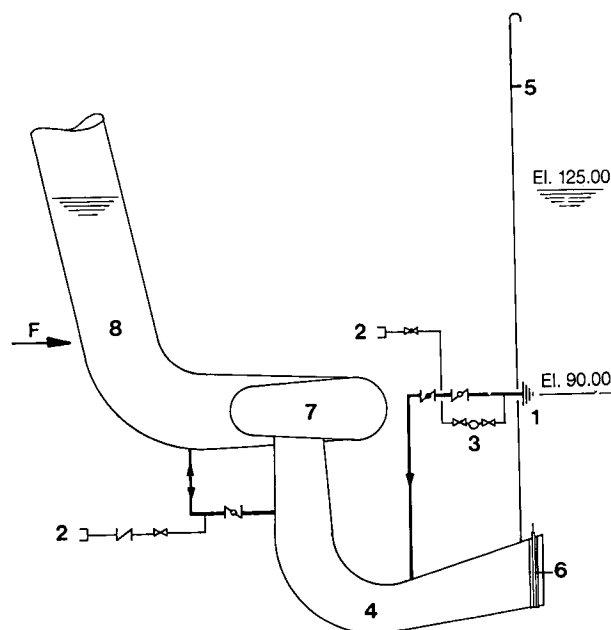


Fig. 13.8 Turbine draft tube filling system schematic

- | | |
|-----------------------------|------------------|
| 1 Tailrace | 6 Stoplog |
| 2 Compressed air connection | 7 Turbine |
| 3 Flow switch | 8 Penstock |
| 4 Turbine draft tube | F Flow direction |
| 5 Draft tube vent | |

TRANSFORMER AND LUBRICATING OIL

Because of the size of the Itaipu powerhouse and number of generating units installed, it was considered impractical, in the long term, to transport oil in barrels or containers for replacement and cleaning during maintenance of the equipment. Although first filling could be effected by this method, centralized systems were installed for subsequent maintenance operations.

Transformer oil system

The transformer oil system serves all the transformers in the powerhouse and is used for drainage and filling of the transformer, for purification of the transformer oil, either at the transformer or at purification, and as a storage center.

The total oil volume of the transformers which can be connected to the system is 3029 m³, comprising the following equipment:

Equipment	Unit volume (m ³)	Total volume (m ³)
28 + 3 (future) main step up transformers 50 Hz – 275 MVA	49	1519
28 + 3 (future) main step up transformers 60 Hz – 256 MVA	40	1240
4 auxiliary transformers 50 Hz – 15 MVA	23	92
4 auxiliary transformers 60 Hz – 15 MVA	22	88
1 auxiliary transformer 50 Hz – 45 MVA	19	19
1 auxiliary transformer 60 Hz – 41.6 MVA	19	19
2 regulating transformers 50 Hz – 25 MVA	13	26
2 regulating transformers 60 Hz – 25 MVA	13	26
Total		3029

Oil specification is given in Table 13.2.

The system comprises two storage and purification centers, respectively, in the right and central assembly areas at El. 98.50, together with associated piping to the equipment served by the system and the necessary valved connections for local use of the mobile purifiers.

A schematic diagram of the system is shown in Fig. 13.9.

Each center contains the following equipment:

- A tank for the storage of contaminated oil; the tank has a volume of 85 m³, is cylindrical, vertically mounted on a concrete base and is complete with level indicator, drain, manhole at the base, silica gel filled air breather and a vertical caged ladder leading to another manhole in the tank cover.

The tank was welded in situ from rolled steel plate and was designed to petroleum standards.

The concrete bases are supported on 2.3 m high pillars and the space filled to floor elevation with coarse gravel, which acts as a chilling drain in the event of spillage coupled with fire. A water spray fire protection system circumscribes the top of each tank.

Table 13.2 Transformer oil specification

Characteristics	Units	Specifications		Methods
		Minimum	Maximum	
Aspect		The oil should be clear, limpid, free of stuff in suspension or dregs.		Visual
Density (20/4°C)		0.861	0.9	NBR 7148
Viscosity 20°C	cSt		25	
40°C	cSt		11	ABNT-MB-293
100°C	cSt		3	
Flash point	°C	140		ABNT-MG-50
Pour point	°C		- 39	ABNT-MB-820
Neutralization index, JAT	mg KOH/g		0.03	ABNT-MB-101
Interfacial tension (25°C)	mN/m	40		NBR 6234
Color			1	ABNT-MB-351
Water	ppm		35	NBR-5775
Chlorides		Absent		NBR-5779
Sulphates		Absent		NBR-5779
Corrosive sulphur		Not corrosive		ABNT-IMB-899
Aniline point	°C	63	84	ABNT-MB-899
Refractive index (20°C)		1.485	1.5	NBR-5778
Dielectric strength	kV	30		NBR-6869
Power factor (25°C)	%		0.05	ASTM-D-924
Power factor (100°C)	%		0.5	ASTM-D-924
Dissipation factor tgδ (90°C)	%		0.4	IEC-247
Stability at oxidation				
Neutralization index (IAT)	mg KOH/g		0.4	IEC-74
Sludge	% mass		0.1	
Dissipation factor (90°C)	%		20	
Oxidation inhibitor (DBPC/EBP)	% mass		0.08	ASTM-D-2668

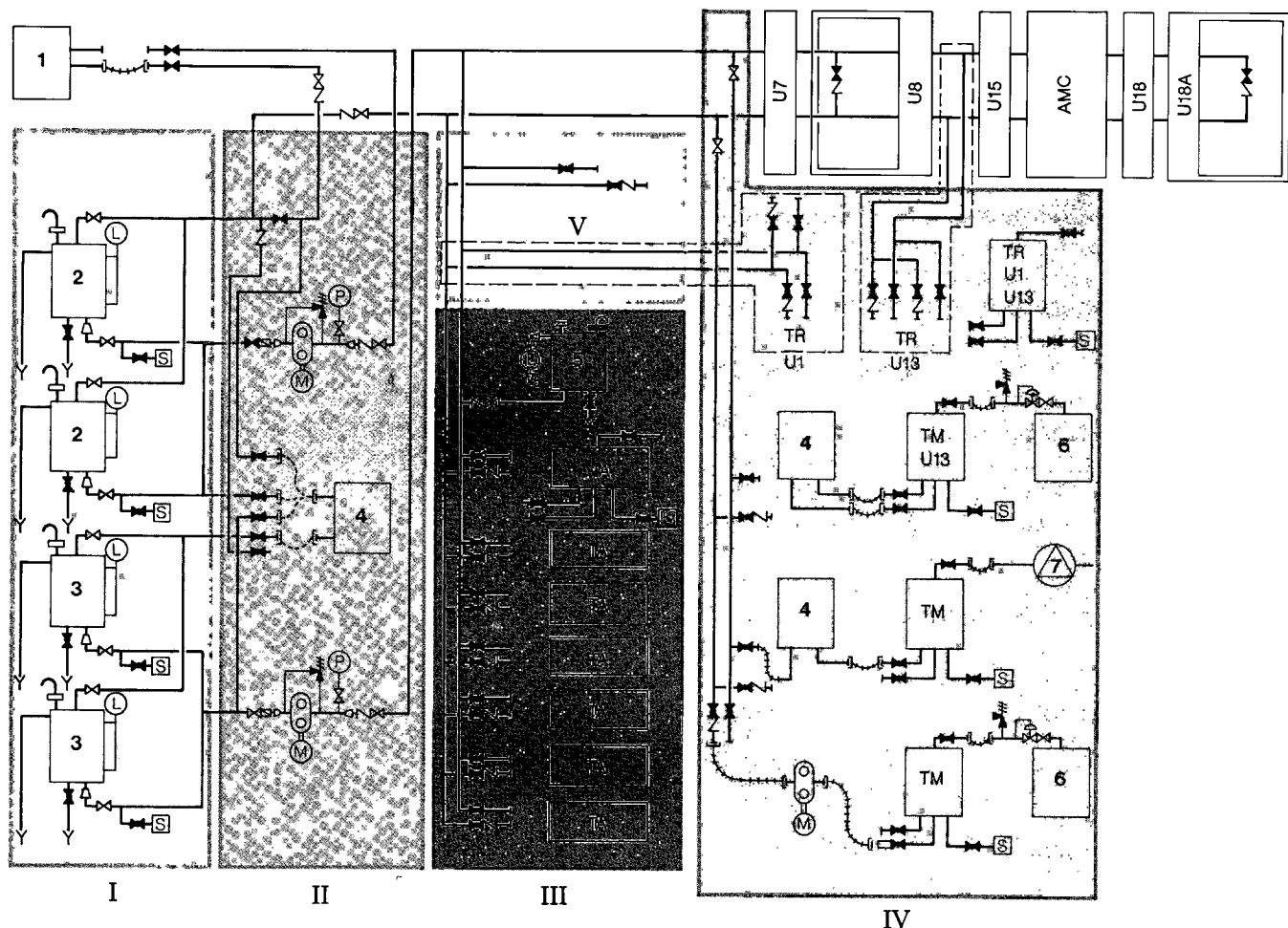


Fig. 13.9 Transformer oil system-schematic

- I Oil storage room
 II Oil treatment room
 III Auxiliary transformer area
 IV Typical unit
 V Transformer maintenance area
 1 Bowser (truck)
 2 Contaminated oil storage tank

- 3 Clean oil storage tank
 4 Mobile oil purifier
 5 Compensation tank
 6 Inert gas tank
 7 Vacuum pump
 L Level gage
 M Electric motor

- S Sample point
 TA Auxiliary transformer
 TM Main step-up transformer
 TR Regulating transformer
 Gate valve open
 Gate valve closed
 Globe valve closed

- A tank for storage of treated oil, the tank being as described above and located in the same room as the tank containing contaminated oil.
- Two electric motor driven Imo type (helical screw) pumps each with a capacity of $4.5 \text{ m}^3/\text{h}$ at 70 N/cm^2 head. The motors of the pumps in the right assembly area operate at 50 Hz and rotate at 920 rpm, whereas those in the central assembly area operate at 60 Hz and 1150 rpm. One pump is used to deliver contaminated oil to a bowser at El. 144. Oil make up for treatment can also be gravity fed from the bowser to the storage tank for contaminated oil. The second pump is used to supply treated oil to the transformers.
- One mobile oil purifier, see Fig. 13.10, capable of purifying $6 \text{ m}^3/\text{h}$ of oil to a residual water content

< 3 ppm and a residual gas content 0.1% by volume. The purifier is wheel mounted, complete with dehumidification and degassing chambers, three 50 kW electric heaters, two vacuum pumps to pull a vacuum of 26 N/m^2 , circulating pumps, filters and connection for cooling water. In addition to treating stored oil in the treatment center, the same purifier can be moved to any transformer to treat its oil locally or to act as a final filter when filling a transformer.

- Electrical control panels. The arrangement of this equipment in the right assembly area and that of the central assembly area is similar, but not identical, because of structural differences in the two areas.

Stainless steel pipework was used exclusively in the interconnected system. Main headers are 50 mm diameter and the pipework is arranged such that the untreated and treated circuits are completely independent. A 200 l compensating tank at El. 144 ensures that the piping system is always full of oil. The tank is open to atmosphere via a silica gel filled air breather. Quick acting couplings and flexible hoses connect the transformers to the purifier or a mobile transfer pump (having the same specification as the pumps at the treatment center), depending on the operation to be performed.

Functioning of the system is as follows:

- Receiving external oil. Gravity fed from a bowser to the contaminated oil tank.
- Discharging to the exterior. Pumped to a bowser from the contaminated oil tank.
- Purification of oil in the contaminated oil tank. Oil is transferred from the contaminated oil tank to the treated oil tank via the mobile purifier.
- Filling a transformer. Oil is pumped from the treated oil tank to the transformer to be filled, the mobile purifier having been moved to the transformer and connected between the transformer and the treated oil supply pipe. During this operation negative pressure is maintained in the transformer with a vacuum pump, oil being admitted via a connection at the base of the transformer.
- Draining a transformer. Oil is piped from the transformer to the mobile oil pump which delivers it to the contaminated oil tank for purification. At the

same time inert gas or dry air is admitted to the top of the transformer.

- Local purification of transformer oil. The mobile purifier is connected to receive oil from the transformer and return it after purification. A dry air or inert gas supply is connected to the top of the transformer during this operation.

Lubricating oil system

The lubricating oil system is used for storage and treatment of the oil of the generating units. External connections are provided to supply the system with clean oil from, and to pump contaminated oil to a bowser. Equipment in each generating unit served by the system is as follows:

Equipment	Volume (m ³)
Upper generator guide bearing	5
Thrust and guide bearing	32
Turbine guide bearing	5
Governor	18
Generator jack / brakes	2
Total	62

Oil specification

Type	Marbrax TR-50
Density 20/40° C	0.8686
Viscosity at 50° C (cSt)	33.7 to 35.7

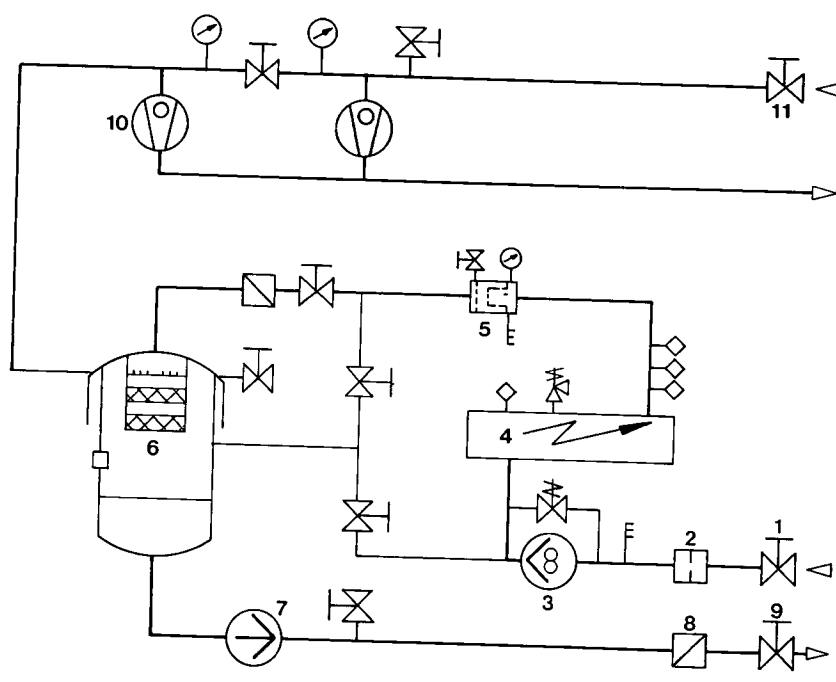


Fig. 13.10 Mobile transformer oil purifier schematic

- Oil inlet valve
- Coarse filter
- Oil inlet pump
- Oil heater
- Micro filter
- Degassing tank
- Oil outlet pump
- No return valve
- Oil outlet valve
- Vacuum pump
- Vacuum valve

The system comprises two storage and purification centers in respectively, the right and central assembly areas at El. 98.50, between powerhouse lines C and D, together with associated piping to the generating units.

A schematic diagram of the system is shown in Fig. 13.11.

Each center contains the following equipment:

- A tank for storing contaminated oil. The tank has a volume of 90 m^3 , which was based on the need to store the oil volume of one generating unit (62 m^3) plus 20% reserve (13 m^3), plus the oil volume in the transfer piping. The tank is cylindrical, vertical and mounted on a concrete slab supported on pillars, to provide a 2.3 m deep gravel chilling drain. Two mandors are provided, one at the base of the tank at the side and the other on the roof. The manhole on the roof is accessed by a caged step ladder which also gives access to the level indicator and air vent.

The tank was welded in situ from rolled mild steel plate and was designed to petroleum standards.

- A tank for storing treated oil. This is identical to the tank for contaminated oil.
- Two electric motor driven Imo type (helical screw) pumps, one to return treated oil to the units and the other to supply contaminated oil to a bowser. The motors of the pumps in the right assembly area operate at 50 Hz and those in the central assembly area at 60 Hz.

Characteristics of the pumps are:

Service	Flow (m^3/h)	Pressure (N/cm^2)	Speed rpm	
			50 Hz	60 Hz
Treated oil	30	80	1450	1150
Contaminated oil	10	70	920	1150

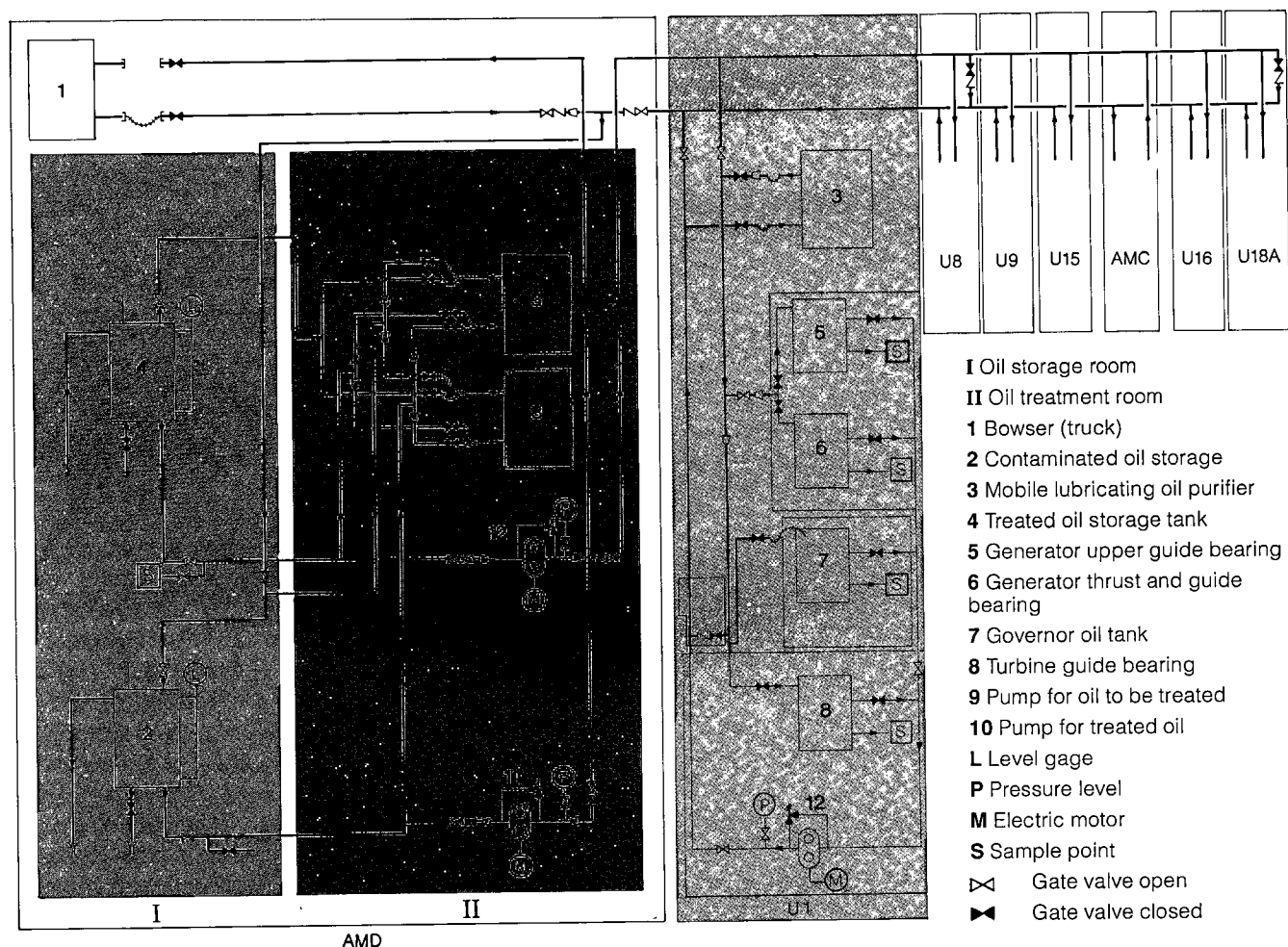


Fig. 13.11 Lubricating oil-system schematic

- Two mobile centrifugal oil purifiers, see Fig. 13.12, each with a capacity of $7 \text{ m}^3/\text{h}$. The oil purifiers are wheel mounted complete with oil heaters, pumps, strainers and water tank for seal water.
- Electrical control panels.

The arrangement of the equipment in the right assembly area and that of the central assembly area is virtually identical.

Pipework in the interconnected system is made of copper and the system is arranged so that the treated and untreated oil networks are separated. Untreated oil is delivered from the generating unit by the pump installed in the turbine head cover, see Chapter 12.

Operation of the system is as follows:

- Receiving external oil. Gravity fed from a bowser to the contaminated oil tank.
- Discharging to the exterior. Pumped to a bowser from the contaminated oil tank.
- Purification of oil in the contaminated oil tank. Oil is transferred from the contaminated oil tank to the treated oil tank via the mobile purifiers.
- Filling all or some of the oil receptacles of a generating unit. Treated oil is pumped from the treated oil tank to the receptacle, valves as necessary at the receptacle being open.
- Draining all or some of the oil receptacles of a generating unit. Contaminated oil is drained from the receptacle to the oil pump in the turbine head cover which delivers it to the contaminated oil tank.
- Treatment of oil at the generator. A mobile purifier is connected to the drain and fill valves of the receptacle and the oil circulated through the purifier.

TREATED WATER

Treated water is piped from the storage tanks in the main dam into three separate systems in the powerhouse. The potable water tanks in the main dam are supplied by the two treatment plants, ETA1 in main dam block E3/4 and ETA2 in block F33/34, see Chapter 10. Two additional water treatment plants are located close to ETA1 and ETA2, providing clarified water. The systems in the powerhouse are:

- Potable water. Used in toilets, drinking facilities, and as make up water for the air conditioning systems.
- Dechlorinated water. Used only for make up to the demineralized cooling water system of the generator stator winding, see Chapter 12.
- Clarified water. Used only for make up to the evaporative coolers of the upstream ventilation system.

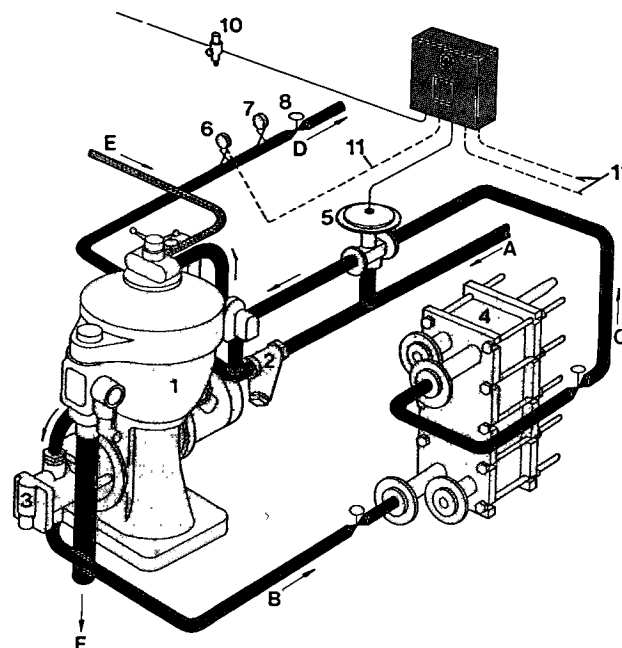


Fig. 13.12 Mobile lubricating oil purifier-schematic

- 1 Separator
- 2 Oil strainer
- 3 Integral feed pump
- 4 Plate heat exchanger
- 5 Three-way pneumatic valve
- 6 Pressostat
- 7 Pressure gauge
- 8 Regulating valve
- 9 Liquid-seal alarm cabinet
- 10 Air reducing valve
- 11 Electric connection
- A Dirty oil to feed pump inlet
- B Dirty oil to heater
- C Heated dirty oil to separator bowl
- D Clean oil outlet
- E Liquid seal water supply
- F Sludge outlet

All pipework used to convey cold treated water in the powerhouse is galvanized and the systems were designed in general to comply with Brazilian potable water standards.

SEWAGE

The sewage handling and treatment system is designed to serve 1350 people comprising 850 operation and maintenance employees and 500 visitors. Estimated flows of raw sewage is 0.15 m³/ person/day for employees and 0.02 m³/ person/day for visitors, considering that visitors are expected to spend a much shorter time at the site than employees. The system was designed to Brazilian sewage treatment codes and handles all sewage from the various toilets in the powerhouse and in the main dam, see Chapter 10.

Sewage is gravity fed from the toilets in the powerhouse and operation and maintenance building to one of three tanks, at U2, U12 and U17 in the downstream gallery between lines C and D at El. 92.4. Also collected in the three tanks is sewage pumped from the main dam. The tanks are built from reinforced concrete and have two separate compartments 0.45 m³ volume each so that one can be cleaned, whilst the other remains in use. Each compartment has an electric motor driven agitator/mixer, a vent to atmosphere at El. 148.2 and an outlet pipe to a pump. The outlet lines are interconnected and valved between compartments so that either pump can be used with either compartment. Helicoidal screw pumps, 10 m³/h capacity at 70 m head deliver the sewage to septic tanks on the downstream side of the right and central assembly building. Effluent from the tanks is chlorinated before being discharged into the tailrace.

FIRE PROTECTION

Depending on the area and type of equipment to be protected against fire, four types of systems are used:

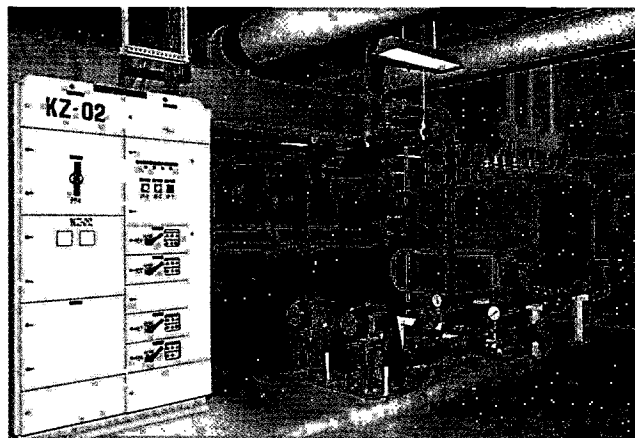
Water

Water for fire fighting is taken from the 600 mm cooling water header, which is supplied from the connection to each turbine spiral casing. There is a 300 mm diameter take-off for fire fighting water at each unit, which in turn feeds into a 300 mm diameter header which extends along the complete length of the powerhouse. Connections to this header supply the following:

At Each Unit.

These connections cover the main step-up transformer and the hydrant network as follows:

- Main step-up transformer fire protection system. The main step-up transformers are protected by two systems:



Sewage tank and pumps - El. 92.4

1. An automatic water spray system which is activated when quartz bulb sensors at pneumatic lines around the transformer break at 68 to 79°C, releasing air pressure by opening a deluge valve which admits water to the spray line.

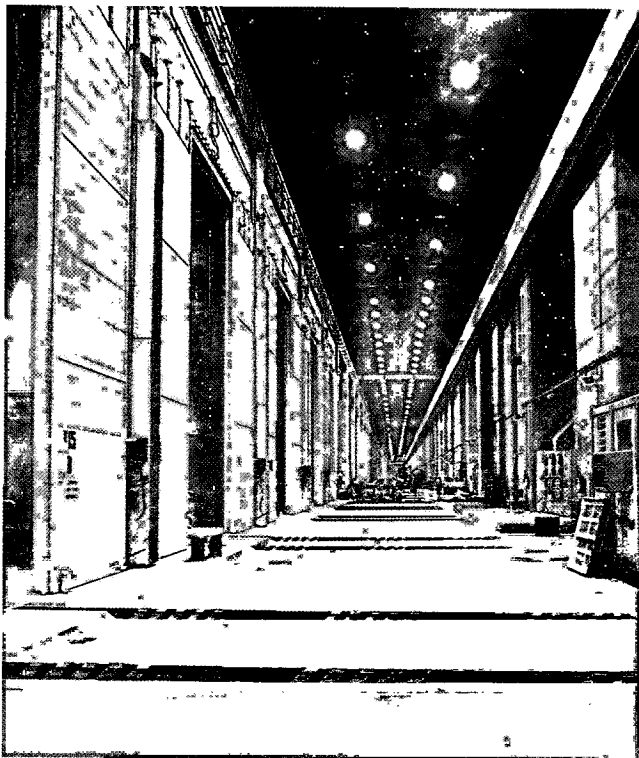
2. A manually operated system above the transformer, comprising a hand operated valve at El. 124, which, when open, admits water to sprinklers located on the ceiling of transformer bays.

- Hydrant network. Hydrants with quick release couplings for fire hoses are located inside the powerhouse, near equipment or places subject to fire, such as:

Location	El.
Oil storage areas (outside)	144.00
Cable gallery	128.20
Electrical equipment gallery	115.00
Main step-up transformer gallery and maintenance transformer areas	108.00
Equipment galleries	98.50
Operating floor	108.00

Auxiliary and Assembly Areas. These connections cover the transformers outside the powerhouse, the lubricating and transformer oil storage treatment and pump rooms, fuel (diesel) oil storage, treatment and pump rooms and operation and maintenance building and visitors facilities.

- Transformers' fire protection systems at El. 144, outside the powerhouse. These are protected by automatic water spray systems similar to the main step-up transformers and have concrete fire walls between transformers and attached structures.



- Lubricating and transformer oil storage treatment and pump rooms, at El. 98.5. Fire protection system as described above, with fire doors.
- Fuel (diesel) oil storage, treatment and pump rooms, El. 135.5 m. These use the same system already described, with fire doors.
- Operation and maintenance building fire protection and visitors facilities. These have the sprinklers and hydrants with water supply piped from the powerhouse firewater header. They also have extinguishers distributed inside the building.

The pneumatic detection systems of automatic water spray systems, besides automatically opening deluge valves, give an alarm at local fire control panel and in the central control room which is registered on SCADA; automatically close relevant fire doors, activate compressed air actuated dampers on ventilation inlet and exhaust grills and close fire doors.

Mobile fire extinguishers (CO₂ or chemical powder)

Manually operated, they are permanently stationed along the main galleries and access areas inside the powerhouse and at the following locations:

Location	El.
Local control room	108.00
GIS equipment room	128.20
Central control room	135.80
Communication room	135.80
Terminal and auxiliary devices cubicle	131.50
Technicians' room	139.00
Visitor area	139.50
Auditorium	145.42
Load dispatch room	145.72

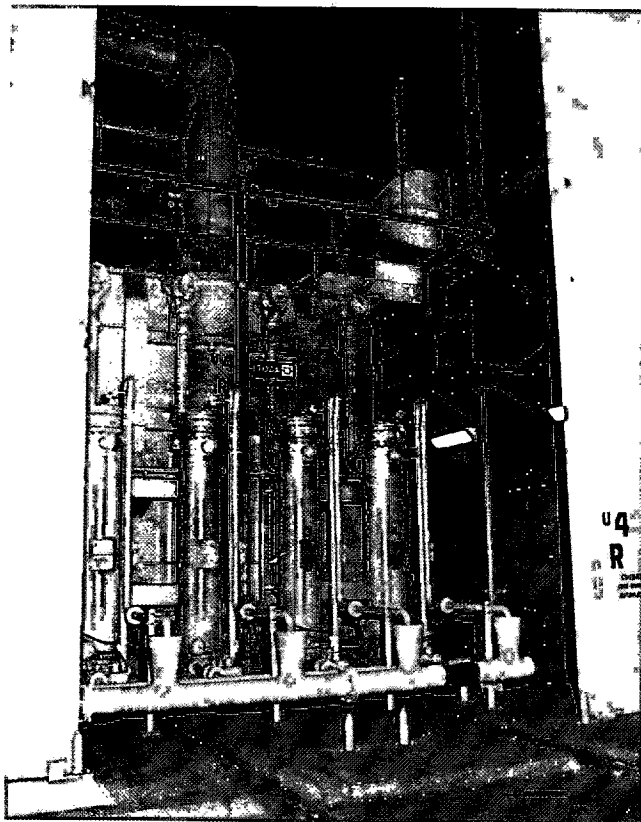
At each location there are break glass emergency buttons which, when pressed, actuate an alarm in the central control room.

Computer room CO₂ fire protection system

An automatic CO₂ system is installed in the computer room and associated programming and computer training rooms at El. 135.8. The system comprises bottles of CO₂ under pressure connected to a piped distribution network in the room. It is activated in response to a signal from the fire surveillance sensors (smoke and ion).

Generator CO₂ fire protection system

The generator is protected by a CO₂ inundation system, see Chapter 12.



Step-up transformer fire protections doors

Besides these water and CO₂ protection systems, automatic closing fire doors are used to contain fires in critical areas and through stairs and galleries to prevent the spread of smoke through the powerhouse. The following areas are equipped with fire doors:

- Transformer and lubricating oil rooms
- Diesel fuel oil storage rooms
- Individual main step-up transformer bays
- Some galleries at stairs access.

Of particular interest are the fire doors of the transformer bays, which are 10 m high and 10.4 m wide.

VENTILATION

The ventilation system supplies and/or extracts air in selected locations in order to:

- Regulate temperature and air quality in those areas in which equipment is a major heat source and/or clean air conditions are required. Areas in this category are the galleries on the upstream of the powerhouse which contain the main step-up transformers, SF₆ equipment and electrical equipment of the generating units. Air directed to these galleries is cooled with an evaporative cooling system which also serves as a scrubbing filter.
- Regulate humidity in areas in contact with water. Examples of this category are the lower galleries of the powerhouse which carry drainage water, and the downstream gallery at El. 92.4 which has floor gratings open to the antiflooding gallery which always has drainage water from the main step-up transformer cooling system.
- Remove and dilute dangerous or objectionable fumes or odors from certain areas. Toilets fall into this category, as do the transformer and lubricating oil rooms, fuel oil rooms for the diesel generators and exhaust of CO₂ from the generator enclosure, in the event of fire.
- Provide fresh air for operator comfort and longevity of equipment. All other locations where ventilation is employed fall into this last category.

Dimensioning of the ventilation systems, depending on the end objective of ventilating the area, took into consideration the heat load in the area and recommended air changes per hour.

The powerhouse design and arrangement of equipment enabled the various objectives of ventilation to be accommodated within three separate systems (cooled air, uncooled air and exhaust) see Fig. 13.13 for a typical turbine/generator unit schematic

Delivery of cooled air

This system is restricted to the upstream galleries of the powerhouse. Ambient air is drawn through intakes upstream of the powerhouse at El. 132 by banks of vane-axial fans. Before passing through the fans the air is cooled in evaporative cooling units which use the evaporation of water to reduce the dry bulb temperature of the air. There is one evaporative cooling unit, and one bank of four fans per generating unit, which deliver air to a plenum chamber from where it is distributed to individual ducts, which convey it to the galleries served by the system.

Fig. 13.14 shows the general arrangement of the evaporative cooling, fan and plenum combination.

Areas served by the upstream ventilation system are:

- Powerhouse galleries between lines A and B
- Electrical equipment at El. 98.5
- Main step-up transformer gallery at El.108
- SF₆ gallery at El.128.2
- Turbine pit at El. 905.
- Drainage galleries at El. 78.5 and El.57.25.

In the design it was estimated that operation of the evaporative cooling plants for cooling air would be required for only four summer months, November to March; however, the operation period could be extended if thought necessary to reduce ingress of dust and airborne particles to the galleries (especially the galleries containing SF₆ equipment). Maximum external ambient temperature and humidity was assumed to be 35°C and 50% respectively, and the evaporative cooling plant was sized to reduce the dry bulb temperature of the air to 27°C before it entered the galleries, see Fig. 13.15. There the pick up of thermal load increases the dry bulb air temperature to 38°C, considered to be the maximum allowable in these galleries.

The external ambient air temperature assumption of 35°C hardly happens. In fact, the air at intake has the temperature lowered by the cool massive concrete dam structure and increasing cooling ventilation system efficiency.

The basic design principle of the evaporative coolers was to expose the greatest water area possible to the incoming air. This was achieved in two manners, by:

- Passing the air through a bank of fine water sprays producing a fog of droplets easy to evaporate. This action also acts as a very effective dust scrubber for the air.

- Allowing the water to cascade in thin sheets over a polystyrene / fiberglass venetian blind configuration and passing the air at relatively low velocity through the cascade.

On exit from the water cascade system, the air passes a second polystyrene/fiberglass venetian blind array which removes water droplets carried by the air before it contacts the fans.

From the sprays and cascades the water falls into a concrete tank, from which it passes to two 66.5 m³/h, 25 m head pumps which supply the cascade system and two 33.2 m³/h, 25 m head pumps for the spray system. In both cases only one pump is operated, the other acting as reserve. Pumps are electric motor driven, 1750 rpm in the 60 Hz sector of the powerhouse and 1460 rpm in the

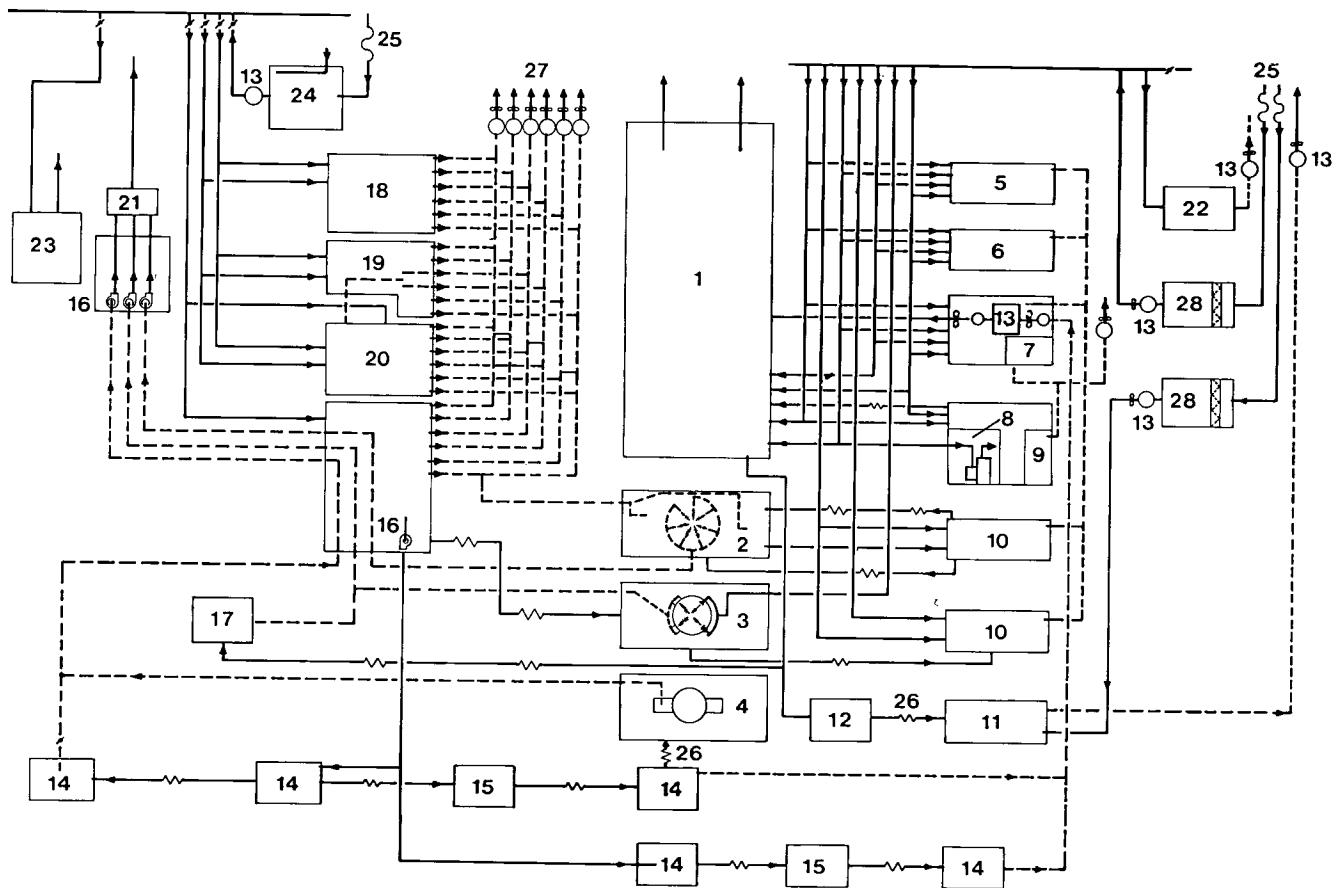


Fig. 13.13 Ventilation equipment for a typical unit-schematic

- | | |
|--|---|
| 1 Generator hall, El. 108 | 15 Interconnection galleries |
| 2 Generator pit, El. 98.5 | 16 Booster centrifugal fan |
| 3 Turbine tube, El. 90.5 | 17 Spiral case, El. 86.5 |
| 4 Draft tube access gallery, El. 80.88 | 18 SF ₆ gallery, El. 128.2 |
| 5 Electrical equipment galleries | 19 Access gallery, El. 124 |
| 6 Ventilation equipment gallery, El. 122 | 20 Main step-up transformer gallery, El. 108 |
| 7 Battery room, El. 115 | 21 Exhaust air collector |
| 8 Local control room, El. 108 | 22 Central refrigeration plants, El. 122 |
| 9 Toilets | 23 Maintenance area for penstock joint, El. 111 |
| 10 Mechanical equipment galleries | 24 Evaporative cooling units |
| 11 Pump sumps, El. 89 | 25 Outside air intake |
| 12 Pump sumps vertical access, El. 89 | 26 Air flow between galleries |
| 13 Motor driven vane-axial fans | 27 Discharge air to atmosphere |
| 14 Drainage galleries | 28 Ventilation units (uncooled air) |

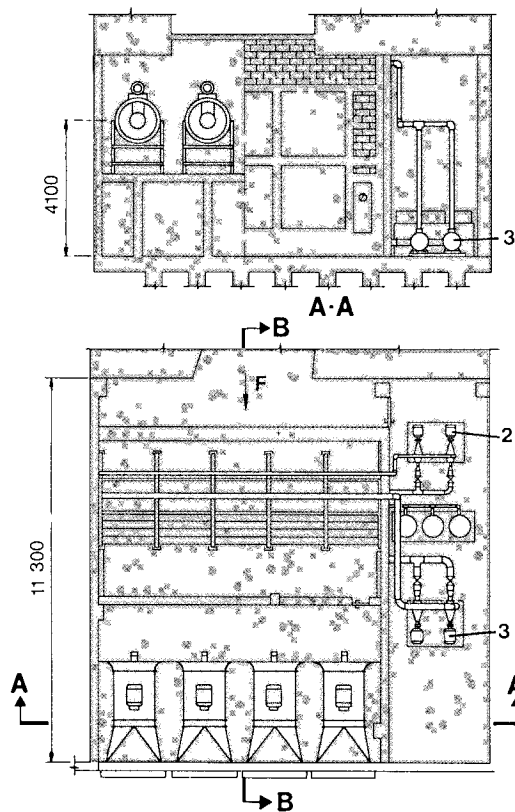
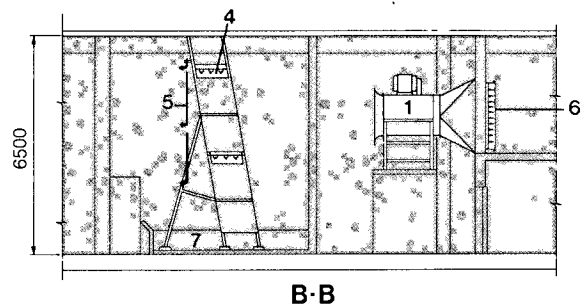


Fig. 13.14 Evaporative cooler plant arrangement

- 1 Axial fans
- 2 Pumps for spray system
- 3 Pumps for cascade system
- 4 Cascade
- 5 Spray
- 6 Filter
- 7 Water tank
- F Air flow direction



Venetian blind array of evaporative cooler and water spray system

50 Hz. Make up water to the tank is supplied from the clarified water system and water quality in the tank is checked periodically and chemicals added manually to control pH and bacteriological content as necessary.

The main structure of the evaporating cooler is galvanized mild steel secured by stainless steel fittings.

A connection from the powerhouse cooling water system is provided near the tank for hosing down the equipment during maintenance.

Each of the vane-axial fans in the central plant can deliver $25.75 \text{ m}^3/\text{s}$ air at 635 N/m^2 , three fans only being required, the fourth acting as a reserve.

A booster centrifugal fan in the gallery at El. 98.5 directs air to the lower drainage galleries.

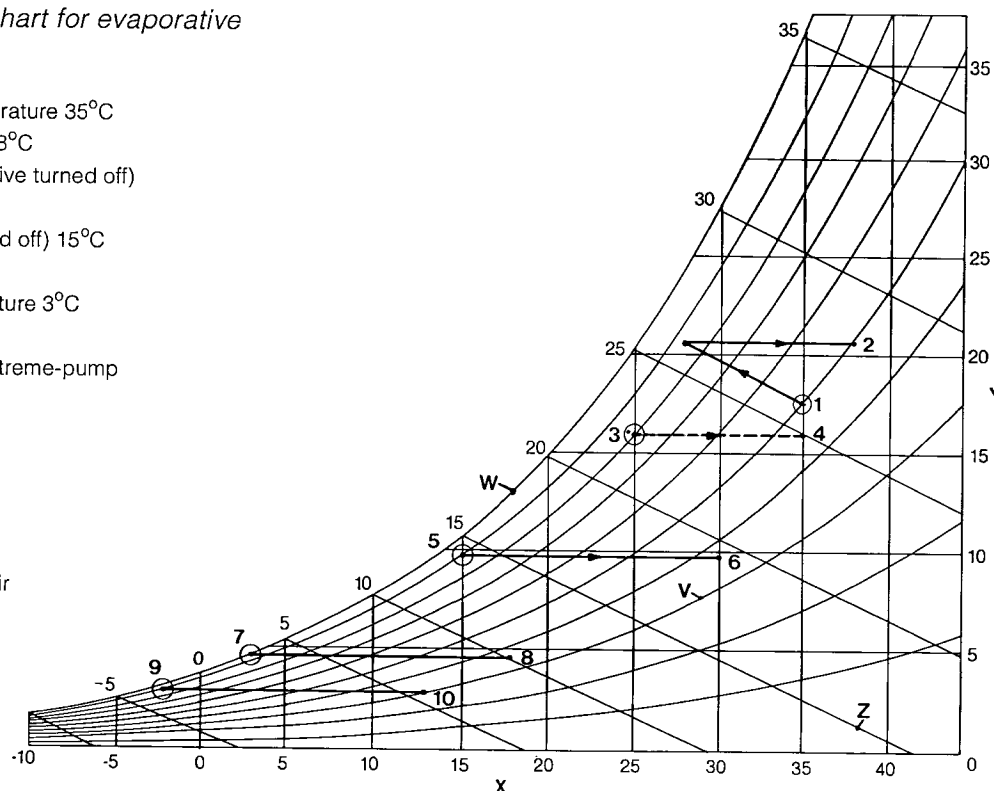
Delivery of uncooled air

The heat load of equipment on the downstream side of the powerhouse is much less than that of the upstream and the maximum temperature can be maintained without cooling the incoming air. A central ventilation plant at each unit comprises the following:

- A bank of four vane-axial fans (three normal, one reserve) each $20.44 \text{ m}^3/\text{s}$ at 635 N/m^2 serving:
 1. Main powerhouse between lines B and C. Gallery El.108.

Fig. 13.15 Psychrometric chart for evaporative cooling

- 1 Design external summer temperature 35°C
 - 2 Internal summer temperature 38°C
 - 3 External temperature (evaporative turned off)
 - 4 Internal temperature 35°C
 - 5 External temperature (fan turned off) 15°C
 - 6 Internal temperature 30°C
 - 7 Design external winter temperature 3°C
 - 8 Internal temperature 18°C
 - 9 External winter temperature (extreme-pump filter turned off) 2°C
 - 10 Internal temperature 13°C
- W Wet bulb temperature (°C)
 X Dry bulb temperature (°C)
 Y Vapor weight (g/kg of dry air)
 V Relative humidity (%)
 Z Specific volume (m^3/kg of dry air)



2. Main powerhouse between lines C and D. Galleries at Els. 92.4, 98.5, 115, 127.6, 122 and 133.2.

- A bank of two vane-axial fans (one normal, one reserve) each $5.15 \text{ m}^3/\text{min}$, 380 N/m^2 , serving the station drainage pump area at El. 89.

At each generating unit, ambient air for the plant is drawn from El. 144 and, after passing through an oil impregnated filter, is conveyed in a 30 m^2 concrete duct to a sealed plenum chamber at El. 122. Vane-axial fans take air from the chamber and deliver it through ducts to the galleries, see Fig. 13.13.

Similar ventilation plants are located in the right and central assembly areas, see Figs. 13.16 and 13.17, but these are without the two fans which direct air to the pump sumps. There are two plants in the right assembly area and one in the central. Air from these plants is ducted to galleries at Els. 98.5, 108, 115, 122 and 127.6 as well as to some toilets.

The diesel room and the diesel oil storage and transfer areas have separate systems, each with individual inlet air fans and oil impregnated filters, drawing ambient air from El. 144.

Exhaust system

As a general principle exhausts are separated by function, for better control and to avoid mixing of gases and fumes with air. Hence the exhaust

systems for toilets and battery rooms are separate from those of the general galleries, and always discharge to atmosphere. Main discharge from the downstream galleries is into the powerhouse generators hall, to eventually exit by natural convection through roof slots, whereas that from the upstream galleries is direct to atmosphere at El. 144.

Because of fire risk, diesel and diesel oil rooms have separate exhaust systems, discharging to ambient at El. 144. Exhaust systems are shown in Figs. 13.13, 13.16, and 13.17.

Filter cleaning facilities

Oil filter cleaning machines and associated equipment are located in rooms between lines C and D of the powerhouse at El. 122 at blocks U4 and U15. The machines comprise a conveyor belt which transfers the filters through a high pressure water spray containing detergent, for washing the filters, and a bank of compressed air nozzles for drying them.

In the rooms, with the cleaning machines, are:

- A machine for immersing the filters in an oil bath with a centrifuge for removing excess oil.
- Racks for storing cleaned and newly oil impregnated filters.
- Equipment to handle the filters

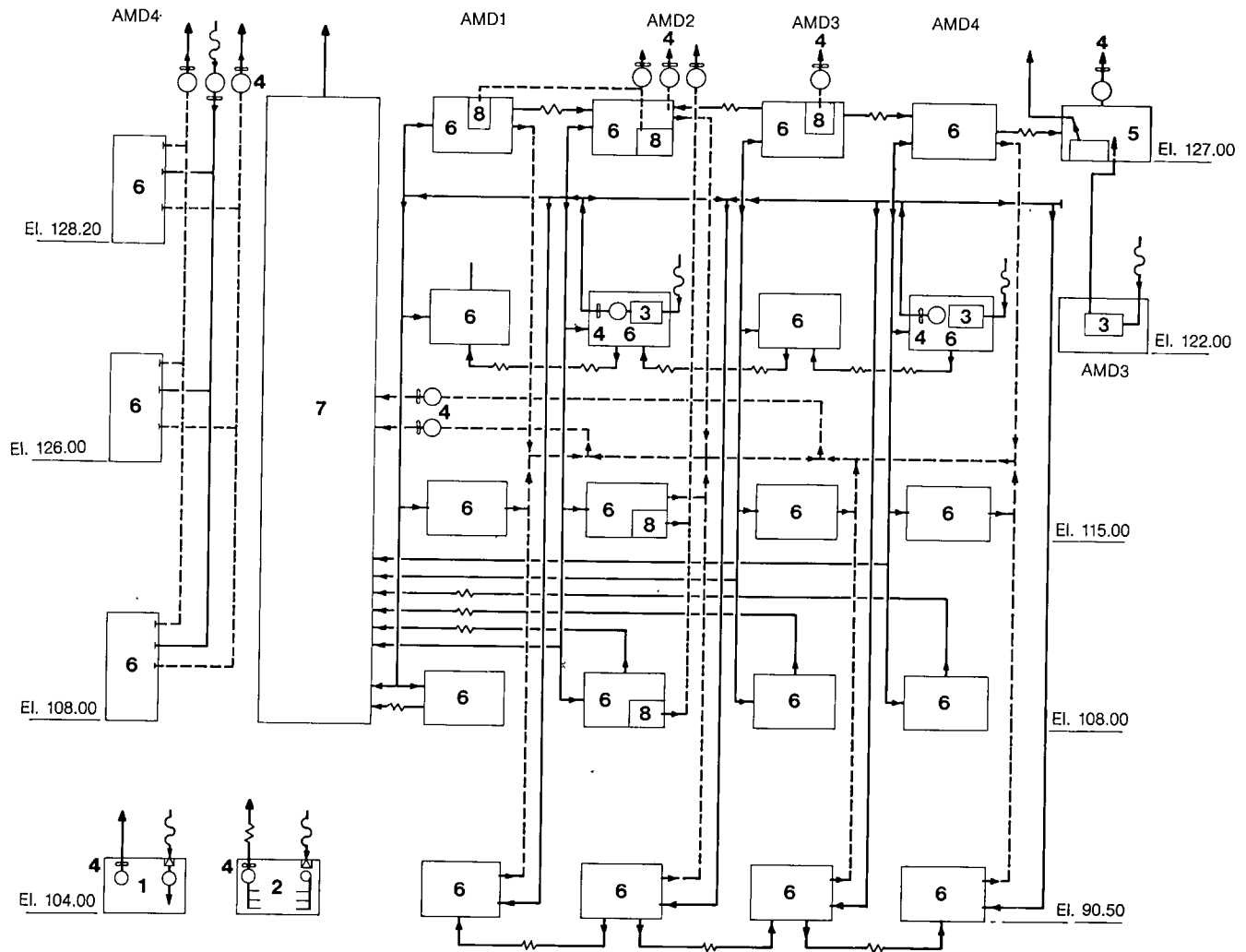


Fig. 13.16 Ventilation of right assembly area-schematic

- | | |
|--------------------------------|---------------|
| 1 Oil transfer room | 6 Galleries |
| 2 Oil storage room | 7 Powerhouse |
| 3 Filters | 8 Toilets |
| 4 Motor driven vane-axial fans | — Air in |
| 5 Diesel room | - - - Air out |

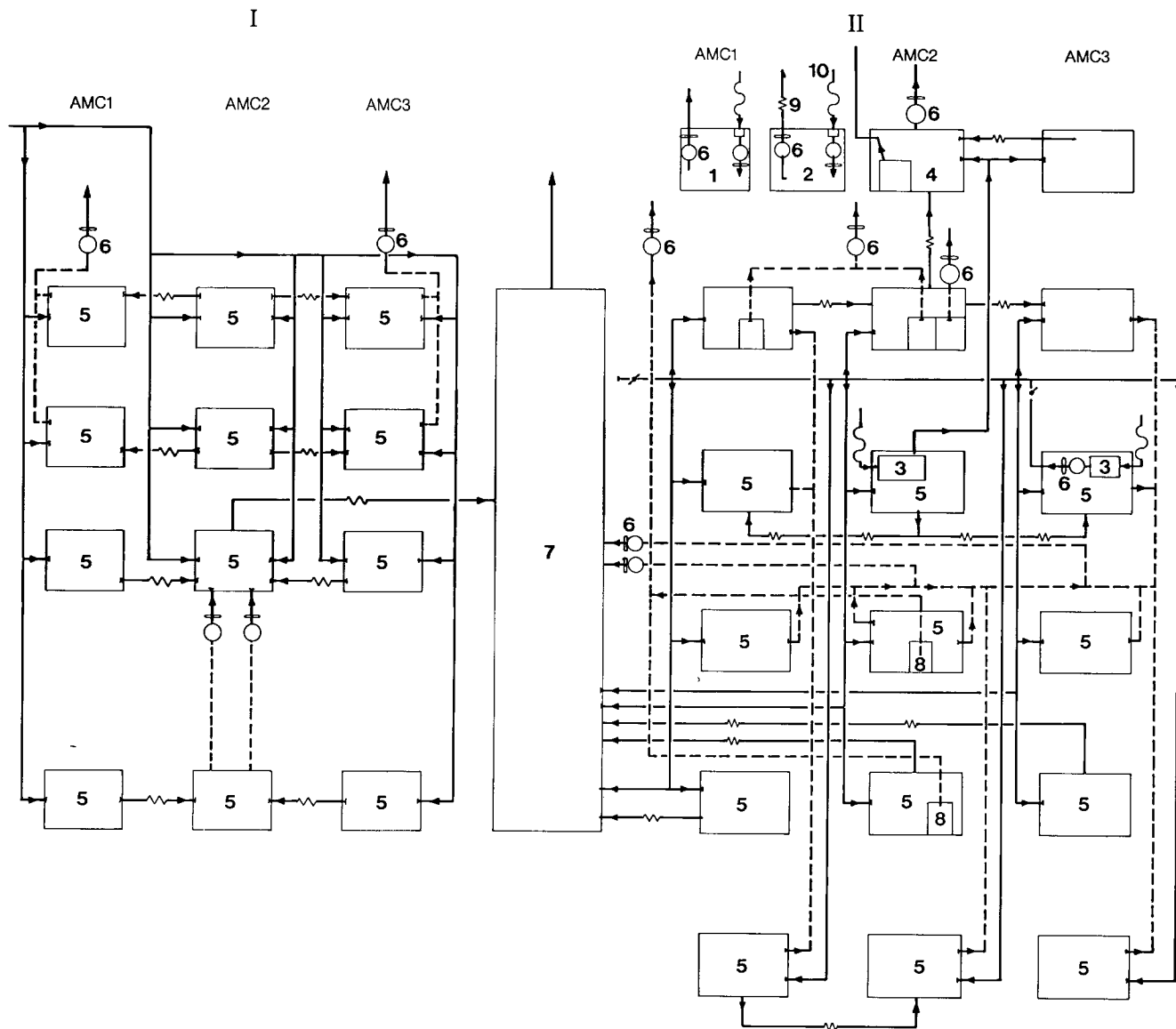


Fig. 13.17 Ventilation of central assembly area-schematic

- | | |
|---------------------|--------------------------------|
| I Upstream | 6 Motor driven vane-axial fans |
| II Downstream | 7 Powerhouse (assembly area) |
| 1 Oil transfer room | 8 Toilets |
| 2 Oil storage room | 9 Outlet |
| 3 Filter | 10 Outside air intake |
| 4 Diesel room | — Air supply |
| 5 Galleries | - - - Air exhaust |

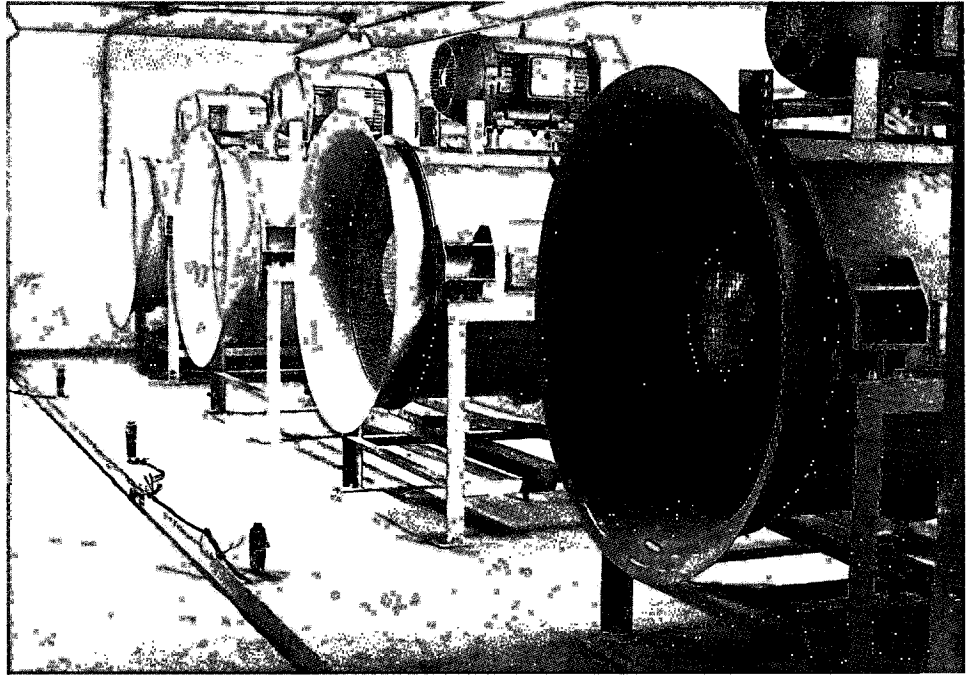
Dampers

Gravity dampers for ventilation fans. Fans which operate as a group are equipped with gravity dampers which close when the fan is not in use and open with flow when the fan is operating.

Fire dampers for critical areas. Automatic fire dampers are installed at inlet and exhaust air grills in areas which are potentially fire prone. These are the

transformer, lubricating and diesel oil rooms and transformer bays. Closure of the dampers prevent combustion air reaching the fire and stops the spread of smoke to other areas. The dampers are air actuated by compressed air servomotors which respond to a thermostat in the equipment room, calibrated for 100°C. They also close in response to signals from the powerhouse fire detection system, also mounted in the room.

Ventilation fans for downstream galleries



Galleries' ventilation ducts - downstream gallery



AIR CONDITIONING

Powerhouse

The powerhouse air conditioning system regulates the temperature and, in critical areas, the humidity of the air in rooms used by operating staff. Also rooms containing sensitive instruments or equipment are air conditioned. However, as a general philosophy, equipment was specified as capable of operating at the extremes of the site ambient temperature and humidity, their use thus not being dependent on the operation of the air conditioning system.

Main areas served by the powerhouse air conditioning system are as follows:

Main powerhouse

- Local control rooms at El. 108 for U1/2, U3/4, U5/6, U7/8, U9/9A, U10/11, U12/13, U14/15, U16/17 and U18/18A, one room for two unit blocks.
- Central control room, technicians' rooms and computer rooms at El. 135.8 for U9A/10.
- Visitors' area and load dispatch center for U9A/10.
- Technicians' rooms at El. 139, U8/9 and U11/12.

Right and central assembly areas

- Technicians' rooms at El. 135.8.
- Medicals' rooms at El. 127.6.
- Instrument rooms at El. 108.
- Visitors' area (right assembly area only)

Water chilled to 6°C by a central refrigeration plant is delivered, in insulated pipes, to fan coil units in or near the areas to be air conditioned. Fan coil units consist of a coil (radiator) through which the chilled water passes, and a fan which draws air through the coil. Cool air thus produced is distributed in insulated ducts to air terminals in the various rooms. After circulating in the room, it passes through return grills to ducts which convey it back to the fan coil units. Approximately 10% exterior air is admitted at the fan coil units to maintain air quality.

Central refrigeration plants

There are two central refrigeration plants housed in rooms between lines C and D of the powerhouse at El. 122, one plant in U9 block and the other in U11. Both plants house the same equipment, but arrangement of the equipment in the two rooms is slightly different because of differences in the civil structure. The equipment of the plant in U9 is as follows:

- Two main refrigeration units 698 kW (200 TR) capacity with a Freon R12 refrigeration circuit comprising centrifugal compressor, expansion valves, refrigerant/chilled water heat exchangers, and refrigerant/cooling water condensers with the following characteristics:

Exit temperature chilled water	6° C
Entering temperature chilled water	12° C
Maximum inlet temperature cooling water	30° C

Centrifugal compressors were chosen for their silent operation and because of the size of the refrigeration unit.

- One emergency refrigeration unit 208 kW (60TR) capacity with a Freon R12 refrigeration circuit with four semi-hermetic compressors, all other details and factors being the same as the main refrigeration units.
- Three chilled water pumps each 0.03 m³/s capacity, 75 m head; one pump for each main refrigeration unit and one in reserve.
- Two chilled water pumps, each 0.0083 m³/s capacity 40 m head, for the emergency refrigeration unit, one pump being a reserve.
- Panel for electric motors and control.

System

A simplified schematic of the powerhouse air conditioning system is shown in Fig. 13.18. Control of the refrigeration plant is effected via chilled water return temperature; the second main refrigeration unit is switched on and off as necessary, together with the chilled water pump operating with the unit at that time. To facilitate control, pump flow is maintained constant with a constant flow valve on the discharge side. In the event of limited electrical power (standby diesel or frequency converter in operation) the main refrigeration unit stops and the emergency unit is used to supply chilled water only to the fan coils of the central control room, computer room, load dispatch center and telex rooms. If for any reason powerhouse cooling water supply is also interrupted then water is supplied to the emergency unit by two pumps (one in reserve) which take water from the tailrace.

A 1000 l expansion tank at El. 155.8 in the operation and maintenance building maintains general pressure in the chilled water system.

Fan coils

A view of a typical fan coil unit is shown in Fig. 13.19. Chilled water flow to the unit is controlled in response to return air temperature by a three-way or a two-way valve which by-passes or restricts flow respectively. The majority of the fan coils are controlled by three-way valves, two-way valves being used only for fan coils in which the by-pass system could deprive other units of water.

All fan coils are provided with electrical heaters for winter use; those which serve the local control rooms, central control room and computer room also

have humidity control. To lower humidity a combination of air cooling and subsequent heating is used and, to increase humidity, water vapor is added.

Ducting and distribution

The air conditioning ducts are made from galvanized steel and are insulated with aluminum covered fiberglass. In the local control room, air enters and leaves through the light fittings, in other areas (notably the central control room, dispatch center and visitors' area), wall or ceiling grills are used.

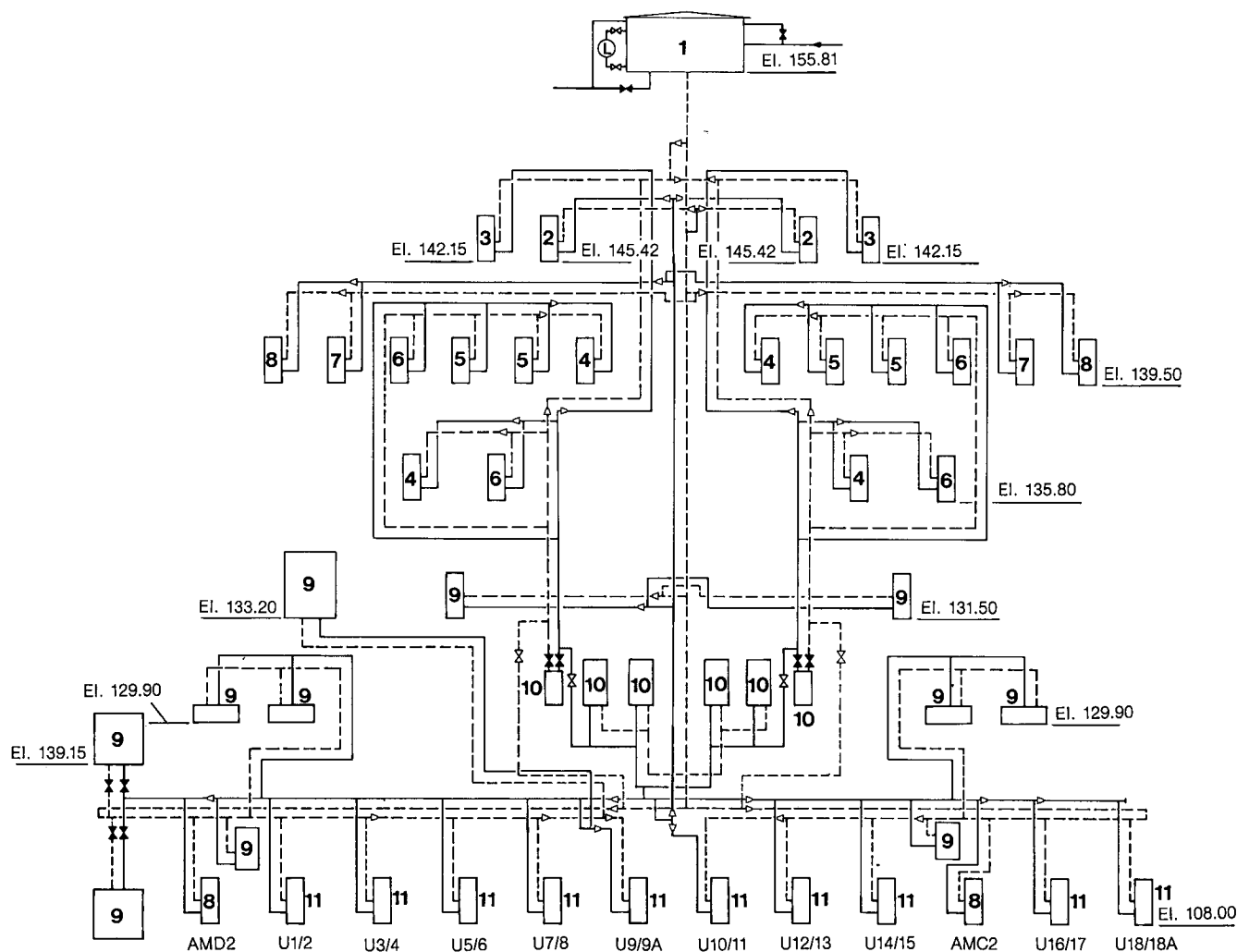


Fig. 13.18 Air conditioning system chilled water distribution-schematic

- 1 Expansion tank
- 2 Entrance hall
- 3 Load dispatch center
- 4 Central control room
- 5 Computer room
- 6 Communication room
- 7 Visitors' hall
- 8 Instrument room

- 9 Administration room (technicians' offices, medical centers, etc)
- 10 Central refrigeration units (main and emergency units)
- 11 Local control rooms (unit block numbers)
- L Level gage
- Chilled water delivery
- - - Chilled water return
- Gate valve open
- Gate valve closed

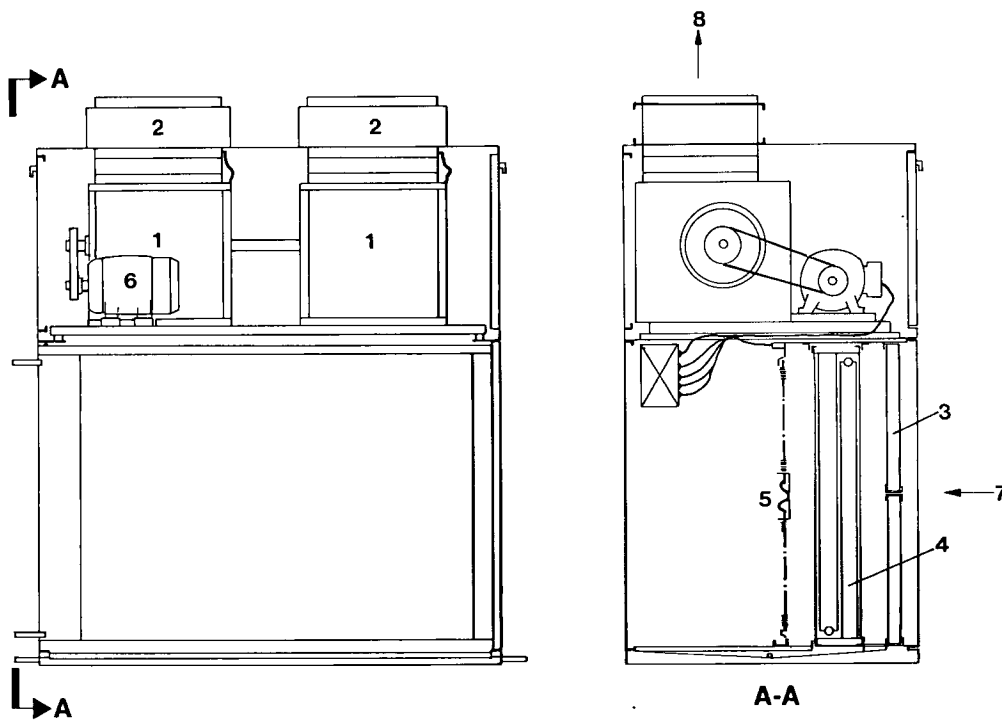


Fig. 13.19 Typical fan coil unit cross-section

- | | | |
|-------------------|--------------------------|----------------|
| 1 Centrifugal fan | 4 Coil (radiator) | 7 Air flow in |
| 2 Air duct outlet | 5 Heater | 8 Air flow out |
| 3 Filter panel | 6 Electric motor, 4 42 W | |

DRAFT TUBE STOPLOGS

There are ten draft tube stoplogs which can isolate five turbines from the tailrace for purposes of maintenance and inspection, two draft tube stoplogs being required for each turbine unit. The number of stoplogs was based on the load factor of the station, coupled with estimated maintenance peaks during periods of low water flow.

Embedded parts were installed in the draft tubes of all blocks, including U9A and U18A. Stoplogs are handled by the draft tube gantry crane and, when not in use, are stored in pits at U1, U2, U12, U14, central assembly area and V1 (left-end block), downstream of the draft tube stoplog slots. Two cranes are used to serve the stoplogs of U1 to U15 and one to serve those of U16 to U18A. Normally attached to a draft tube gantry crane, three lifting beams are used to deploy the stoplogs. Stoplogs are deployed in balanced water conditions only, a differential head indicator being used to determine

when the water level in the draft tube reaches tailwater level during refilling.

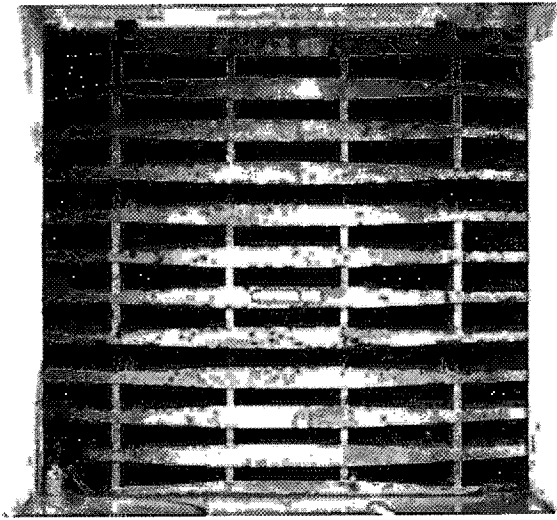
Design criteria were:

Normal maximum tailwater level	El. 107.1
Exceptional tailwater level	El. 143.5
Minimum tailwater level	El. 92
Width of draft tube	10 m
Height of draft tube	9.9 m
Elevation of bottom sealplate in draft tube	El. 66.01

All design water levels included an allowance of 1 m for waves in the tailrace, and the maximum exceptional tailrace level of El. 142.5 (without waves) combined the effects of future projects to be built downstream of Itaipu, together with maximum flood conditions.

Although painted with a zinc rich and coal tar epoxy system, the specifications required in addition 2 mm corrosion allowance on all plates. Minimum plate thickness was specified as 9.5 mm.

A general view of the draft tube stoplog together with salient features is shown in Fig. 13.20. A stoplog consists of three separate panels bolted and seal welded at site, the complete assembly (for handling



Draft tube stoplogs in position

by the gantry crane) weighing 1.06 MN. Each panel comprises a 31.5 mm skin plate welded to four horizontal beams, stiffened at intervals by cross members. Between the beams, the skin is reinforced by two horizontal T section stiffeners. The music note type side and lintel seals are attached with stainless steel bolts, as is the rectangular bottom seal, see Fig. 13.21. U sections at the side guide the stoplog in the slot. Precompression of the seal, to assist in sealing before dewatering of draft tube, is maintained by a leaf spring bearing on the downstream of the embedded parts, see Fig. 13.22. Embedded seal plates are stainless steel and alignment of the embedded parts was facilitated by mild steel plates embedded in blockouts in the first stage concrete, to which the adjusting screws of the embedded parts were welded. For storage, the stoplog is supported on an extended side beam, thus keeping the bottom seal free, see Fig.13.22. The wheeled lifting beam weighing 58.9 kN, engages lugs at the top of the stoplog. To automatically release the stoplog when in position in the slot, the counterweight is placed in the disengage position.

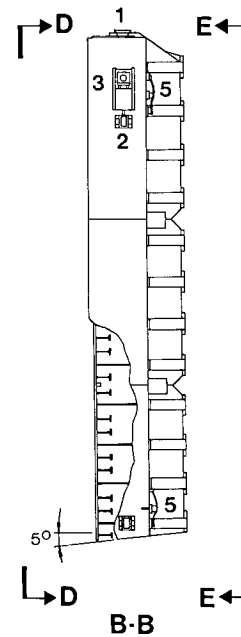
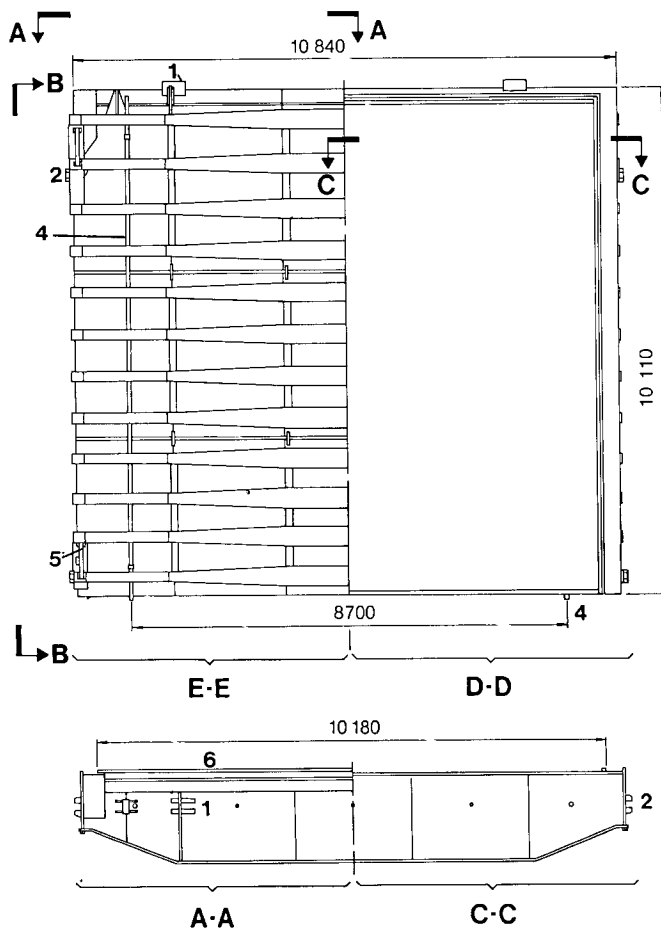
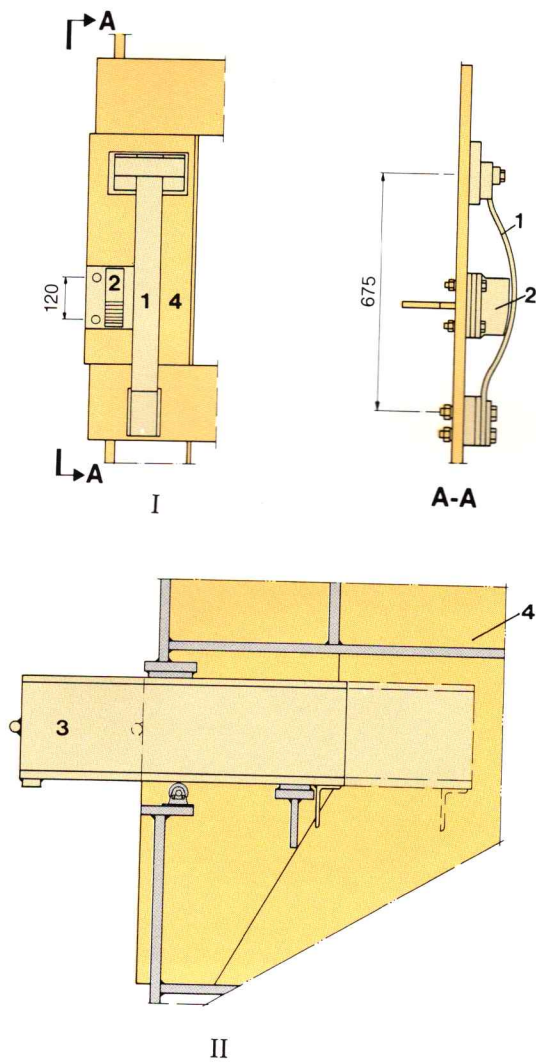
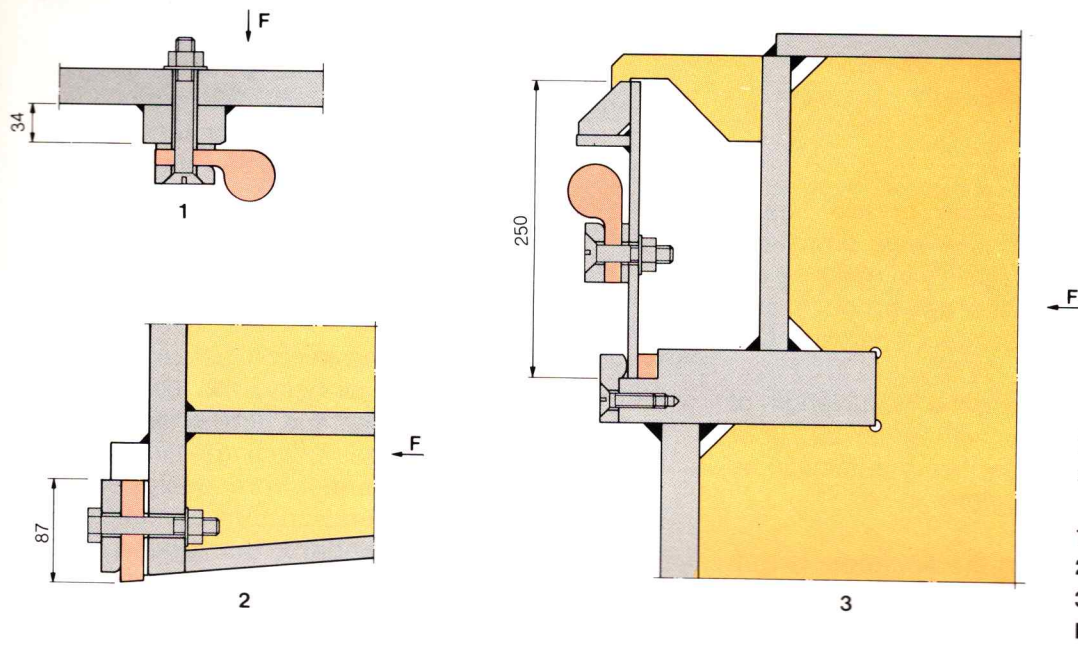


Fig. 13.20 General arrangement of stoplogs

- | | |
|-----------------------|---|
| 1 Lifting lug | 4 Activating rod for lifting beam safety device |
| 2 Side guide | 5 Spring |
| 3 Support for storage | 6 Seals |



POWERHOUSE CRANES AND ELEVATORS

CRANES

The cranes for transportation of the heavy equipment within the powerhouse were sized and designed to give maximum flexibility in handling the equipment on delivery to the powerhouse and during its erection and subsequent operation and maintenance.

All cranes which travel along the whole length of the powerhouse can operate with either 50 Hz or 60 Hz supply, the change-over being automatic as they pass between the two regions.

Cranes which operate along the complete length of the powerhouse

Four 10 MN bridge cranes with rails at El. 128, two of which can be coupled and, with the use of a lifting beam, can handle a 20 MN load, e.g. the generator rotor (the heaviest single load).

Two 2.5 MN bridge cranes with rails at El. 128 which can also be coupled and therefore handle a 5 MN load.

Two 1 MN bridge cranes, with rail at El. 136.5.

Cranes operating in equipment galleries

Two 2.5 MN bridge cranes operating along the complete length of the transformer gallery.

Two 100 kN bridge cranes operating along the length of the SF₆ gallery.

Cranes operating outside the powerhouse

Three 1.4 MN draft tube stoplog gantry cranes operating at El. 144 on the downstream side of the powerhouse. Two gantry cranes operate between blocks U1 to U15 and one between blocks U16 to U18A. These cranes cannot cross the central assembly area.

Cranes operating in the assembly areas, with rails at El. 160

- Two 2.5 MN bridge cranes which can be coupled, operating in the right assembly area.
- Two 2.5 MN bridge cranes which can be coupled, operating in the central assembly area.

There are other small cranes, monorails and handling devices in the powerhouse which are used to lift and transport specific items of equipment, for example in the turbine pit, over the drainage pumps and in the workshops. These devices are described

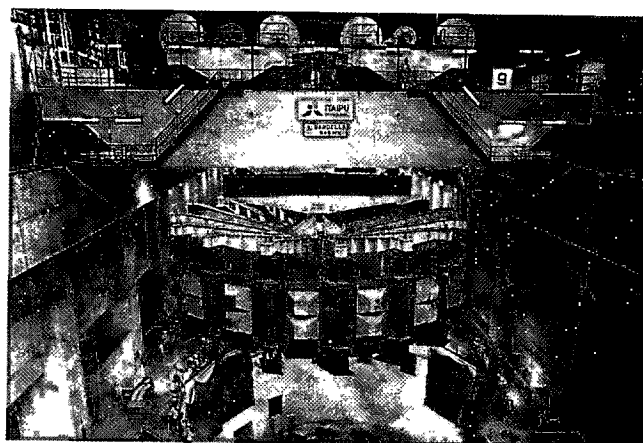
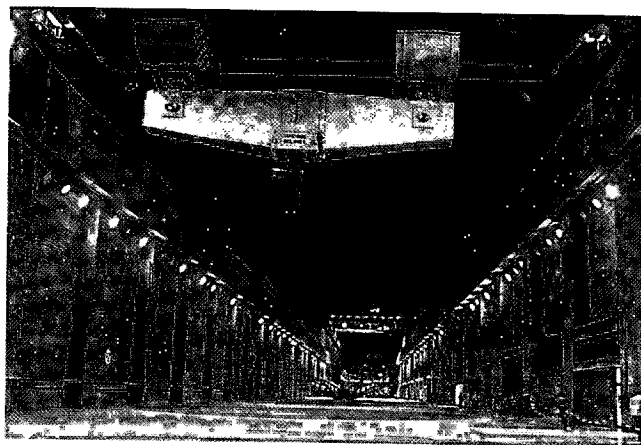
where necessary in the relevant chapters dealing with that equipment.

During construction of the powerhouse, the configuration of the powerhouse cranes was changed in order to accommodate the requirements of the particular stage of construction and changing necessities of equipment erection. Main differences were as follows:

- The two 2.5 MN cranes in the central assembly area operated in the powerhouse at El. 125, between 1982 and 1985.
- In the initial stages of construction, before the 10 MN cranes were available, all heavy lifts up to 5 MN (including turbine stay ring and turbine runner) were made with these two cranes operating in tandem.

All powerhouse cranes were designed and manufactured to Fédération Européenne de la Manutention (FEM) standard; the groups of the standard used for the various cranes together with details of performance are given in Table 13.3.

Fig. 13.23 shows a schematic of the location of the cranes operating inside the powerhouse.



Powerhouse cranes

Table 13.3 Powerhouse cranes

	Main (power- house)	Auxiliary (power- house)	Auxiliary (power- house)	Right assembly area	Central assembly area	Main step-up transformers gallery	SF ₆ gallery	Draft tube stoplog
Type	Bridge	Bridge	Bridge	Bridge	Bridge	Bridge	Bridge	Gantry
Number	4	2	2	2	2	2	2	2
Manufacturer	Pohlig- Heckel (2) Bardella (2)	Mecânica Pesada	Sermec	ISHIBRÁS	Mecânica Pesada	Villares	Pohlig Heckel	Villares
Capacity of main hook	5 MN	2.5 MN	1 MN	2.5 MN	2.5 MN	2.5 MN	100 kN	1.4 MN
Capacity of one crane, two cars coupled	10 MN							
Capacity of two cranes coupled	20 MN	5 MN		5 MN	5 MN			
Crane travel speed without load (m/min)	20.0		120			100 (50 Hz) 120 (60 Hz)		
Crane travel speed with load (m/min)	5.0	21.0 (50 Hz) 26.0 (60 Hz)	50	13.5	26.0 (60 Hz)	12.5 (50 Hz) 15.0 (60 Hz)	66.60 (50 Hz) 80.00 (60 Hz)	30.0 (50 Hz) 36.0 (60 Hz)
Crane travel speed inching (m/min)	0.1		0.60				6.6 (50 Hz) 8.0 (60 Hz)	
Car travel speed without load (m/min)	5.0							
Car travel speed with load (m/min)	2.0	11.0 (50 Hz) 13.5 (60 Hz)	15.0	13.5	13.5 (60 Hz)	12.5 (50 Hz) 15.0 (60 Hz)	10 (50 Hz) 12 (60 Hz)	
Car travel speed inching (m/min)	0.1		0.60				1.25 (50 Hz) 1.50 (60 Hz)	
Main hook lifting speed without load (m/min)	2.0	15.8	15.0	15.8	15.8			12.5 (50 Hz) 15.0 (60 Hz)
Main hook lifting speed with load (m/min)	0.8	1.7	3.0	1.7	1.7	0.83 (50 Hz) 1.0 (60 Hz)	4.16 (50 Hz) 5.0 (60 Hz)	2.0 (50 Hz) 2.4 (60 Hz)
Main hook lifting speed inching (m/min)	0.1		0.60			0.17 (50 Hz) 0.2 (60 Hz)	0.41 (50 Hz) 0.50 (60 Hz)	
Main hook maximum travel	38.0 m	31.0 m	74.0 m	51.0 m	31.0 m	47.0 m (low.) 19.8 m (displ.)	14.0 m	82.0 m
Auxiliary hook capacity		200 kN	200 kN	200 kN	200 kN	150 kN		147 kN
Auxiliary hook lifting speed (m/min)		9.0 (50 Hz) 11.0 (60 Hz)	15.0 0.60	11.2 (50 Hz)	11.0 (60 Hz)	3.3 (50 Hz) 4.0 (60 Hz)		2.9 (50 Hz) 4.5 (60 Hz)
Auxiliary hook inching (m/min)			0.60			0.83 (50 Hz) 1.0 (60 Hz)		

Table 13.3 continued

	Main (power- house)	Auxiliary (power- house)	Auxiliary (power- house)	Right assembly area	Central assembly area	Main step-up transformers gallery	SF ₆ gallery	Draft tube stoplogs
Auxiliary hook maximum travel		51.0 m	74.0 m	51.0 m	51.0 m	20.0 m		22.27 m
Span of bridge or gantry	29.0 m	28.0 m	29.0 m	28.0 m	28.0 m	10.0 m	20.65 m	7.0 m
FEM structure								
Class of utilization	D	D	D	D	D	B	B	B
State of loading	3	3	3	3	3	3	2	3
Group	6	6	6	6	6	5	4	5
FEM mechanism								
Hoisting motion (class, state,group)	V5-3-5 m	V5-3-5 m	V5-3-5 m	V5-3-5 m	V5-3-5 m	V2-3-3 m	V3-2-3 m	V2-3-3 m
Crane travelling motion (class,state, group)	V2-3-5 m	V4-3-5 m	V4-3-5 m	V4-3-5 m	V4-3-5 m	V2-3-3 m	V4-2-4 m	V2-3-3 m
Car travelling motion (class, state, group)	V5-3-5 m	V5-3-5 m	V5-3-5 m	V5-3-5 m	V5-3-5 m		V3-2-3 m	V05-3-1A m

Access to the control cabins of the cranes operating at El. 125 and El. 136.5 is via caged step ladders in the right and central assembly areas and from doors in the powerhouse stair wells at U4, U8, U11 and U15. Access to the control cabins of the cranes operating in the right and central assembly areas is by caged step ladders from El. 144.

10 MN powerhouse cranes

The 10 MN bridge cranes serve to lift and transport the heavy items of equipment of the eighteen turbine generator units. Because of their lifting capacity these cranes are slow, but it was necessary that they be placed at the lower elevation (below the faster running auxiliary cranes) to:

- Reduce the sheeting length of cable and hence increase the accuracy of positioning.
- Keep crane drum size to a minimum.
- Allow the passage of the faster cranes (without load) when the 10 MN cranes were operating above a unit) it being envisaged that the heavy lifts for which the 10 MN would be used would be of long duration (for example the installation of a generator rotor).

It was recognized that the 10 MN cranes when parked and out of use (which happens for a good

percentage of the time), would interfere with the operation of the faster cranes operating above them. To minimize this, recessed parking areas were provided for a crane in the right assembly area and left end block V1 and there is space for the other two cranes to be parked at blocks U9A and U18A, respectively.

Because of the size of these cranes and the demands of the delivery schedule they were purchased from two separate suppliers, two from Pohlig-Heckel do Brasil S.A. and two from Bardella S.A., Indústria Mecânica. Cranes from the different suppliers were made to the same specification and in general their design is identical; however, because of differences in detail, only cranes of the same manufacturer can be coupled.

The rails were placed at El. 125 to allow the passage of one generator rotor above another being erected at El. 108. The height of the crane, which in effect limited its drum diameter, was determined by freedom of passage under the cranes at El. 136.5.

A general view of the 10 MN Pohlig-Heckel crane is given in Fig. 13.24.

To increase flexibility and assist design, each 10 MN crane comprises two 5 MN lifting capacity, **wheeled**,

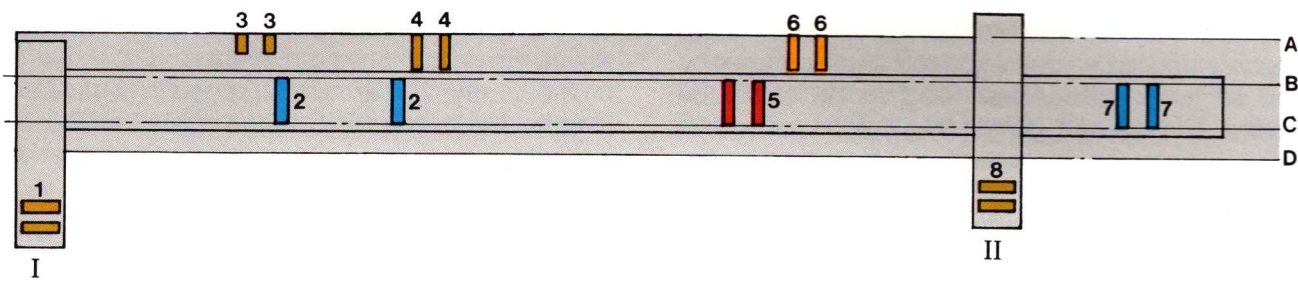


Fig. 13.23 Schematic of location of bridge cranes inside the powerhouse

I Right assembly area

II Central assembly area

A, B, C, D Powerhouse reference lines

1 2.5 MN crane along right assembly area, rails at El. 160 (ISHIBRÁS)

2 10 MN main crane, rails at El. 128 (Bardella)

3 2.5 MN crane along transformer gallery, rails at El. 108 (Villares)

10 MN crane

2.5 MN crane

1 MN crane

100 kN crane

4 2.5 MN auxiliary crane, rails at El. 128 (Mecânica Pesada)

5 1 MN auxiliary crane, rails at El. 136,5 (Sermeç)

6 100 kN crane along SF₆ gallery, rails at El. 139 (Pohlig - Heckel)

7 10 MN main crane, rails at El. 128 (Pohlig-Heckel)

8 2.5 MN crane along central assembly area, rails at El. 128 (Mecânica Pesada)

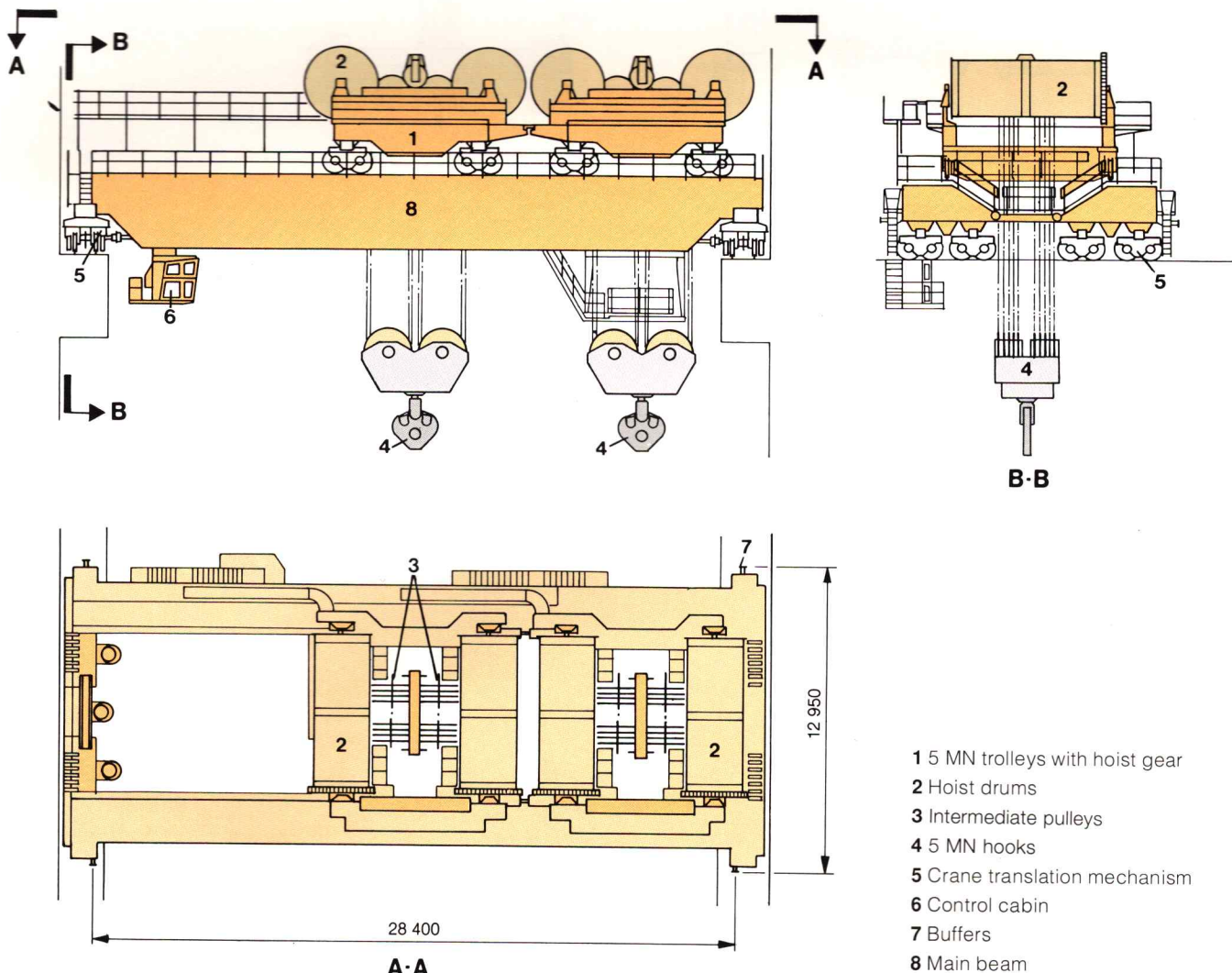


Fig. 13.24 General view of Pohlig-Heckel 10 MN crane

- 1 5 MN trolleys with hoist gear
- 2 Hoist drums
- 3 Intermediate pulleys
- 4 5 MN hooks
- 5 Crane translation mechanism
- 6 Control cabin
- 7 Buffers
- 8 Main beam

motorized trolleys on a common bridge structure. Hence with various lifting beams the hooks of each trolley can be used singly or together depending on the load to be handled. Examples of lifting configurations for various turbine/generator loads are shown in Fig. 13.25.

The crane runs on four rails, two upstream and two downstream mounted on concrete plinths at El. 125.

Beneath each rail is a continuous steel plate for fixing the rail and distribution of the load to the concrete. At each end of the powerhouse there is a buffer stop which encounters the hydraulic buffers on the crane in the event of overrun.

Electrical supply to the crane is through four copper 13.8 kV conductor bars (three-phase

system with neutral) mounted on the downstream wall of the powerhouse at El. 133.6.

The conductor bars are arranged in two separate lengths, the length between the right assembly area and U9A receiving supply at 50 Hz and that between U9A and block V1 at 60 Hz.

The 13.8 kV/460 V transformers are located in the main beams of the crane, as is the dc conversion equipment. Motors for crane travel, trolley travel and lifting, are dc variable speed and are equipped with electro/hydraulic brakes. In addition, the motors of the lifting gear have an additional hydraulic, and the crane travel motor has an additional hydraulic brake, pedal actuated from the control cabin.

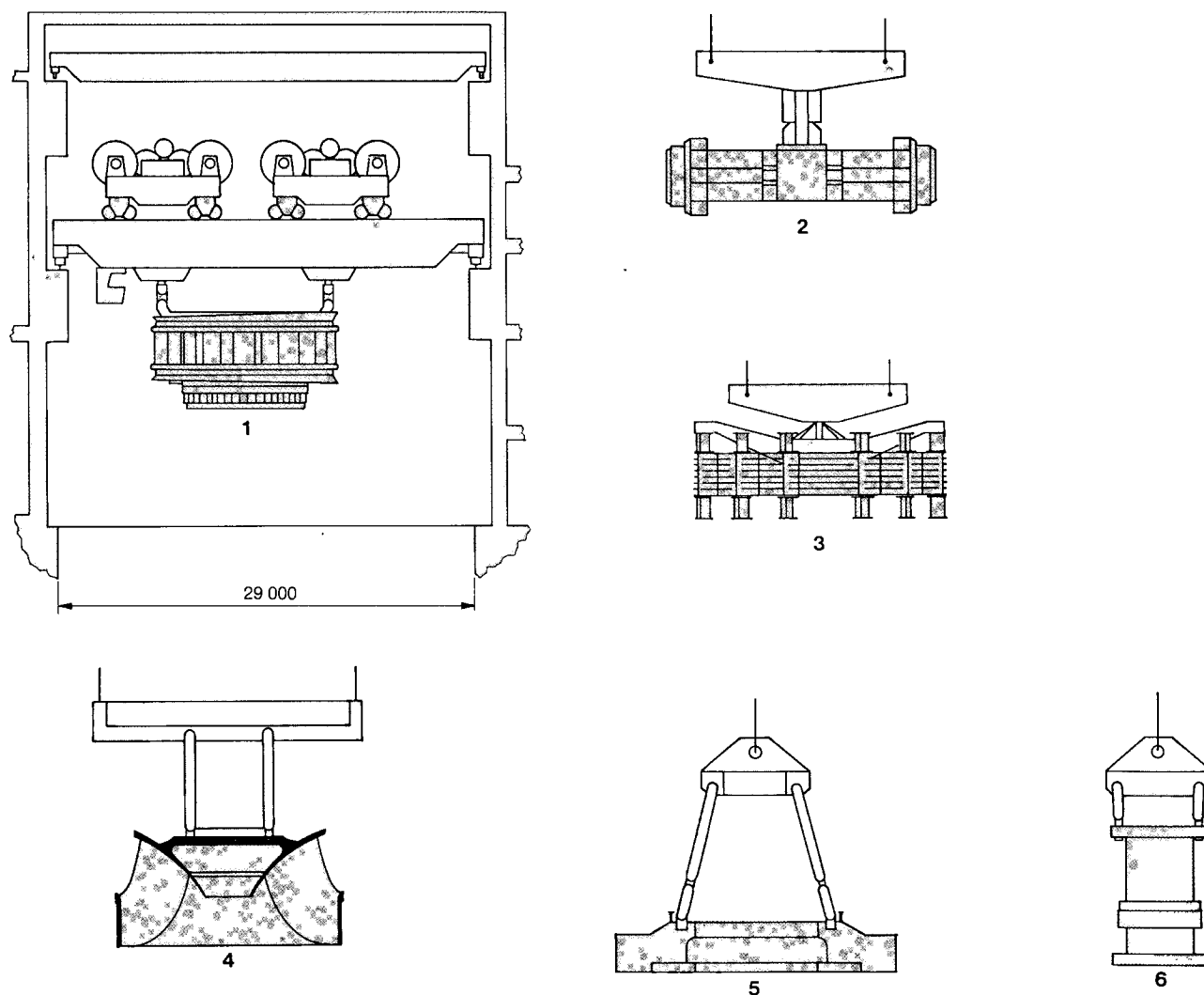


Fig. 13.25 Lifting arrangements of the main powerhouse cranes

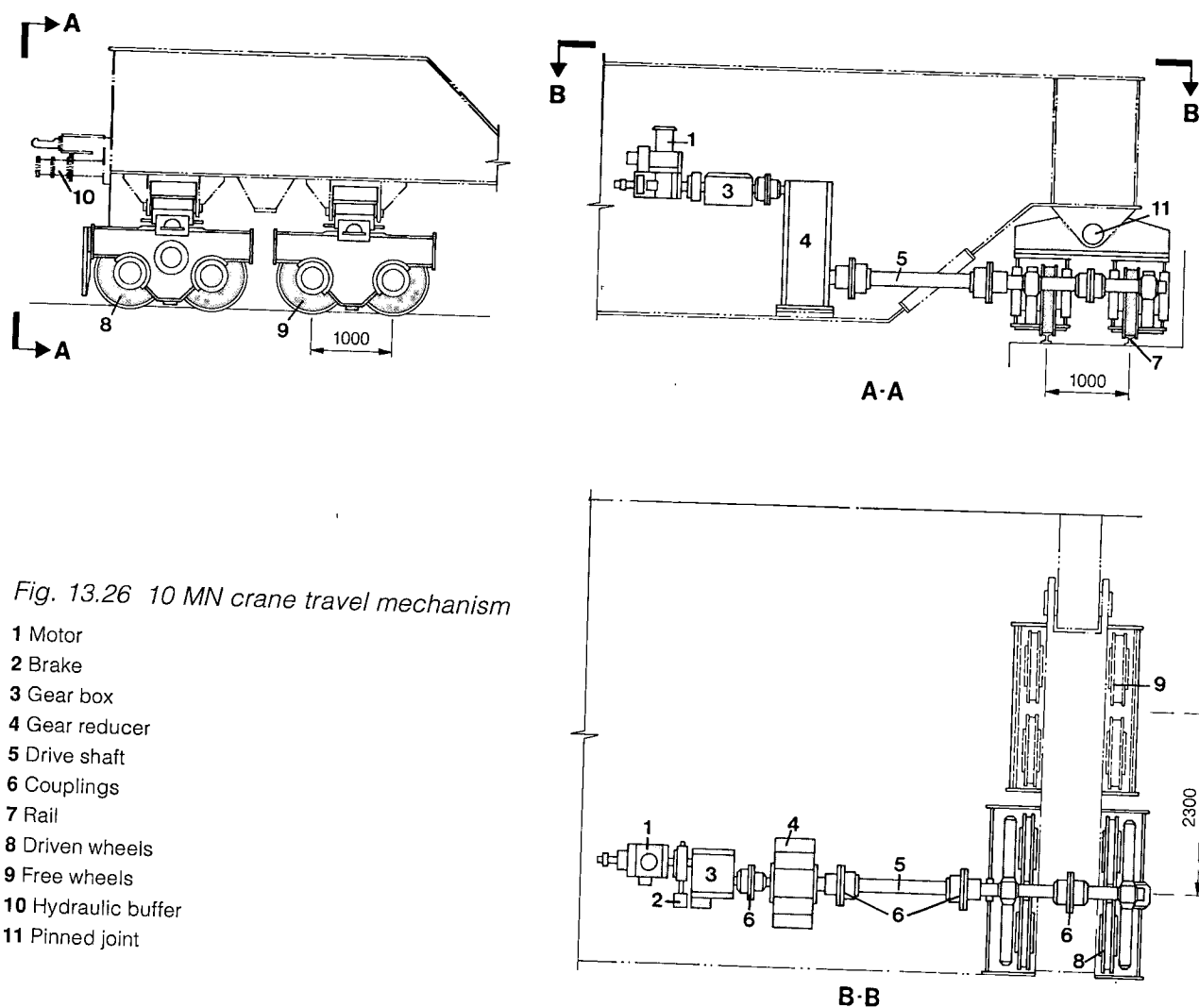
- | | |
|------------------------------------|---------------------|
| 1 Turbine stay ring | 4 Turbine runner |
| 2 Generator rotor | 5 Turbine top cover |
| 3 Generator frame with stator core | 6 Turbine shaft |

Two plate steel welded box section beams, connected with end beams, comprise the bridge of the crane, which is mounted on eight trolleys (four on either side), each with four forged steel wheels, which run on the crane rails.

One trolley upstream and one downstream are driven from a dc electric motor through a gear reducer, see Fig. 13.26. The two trolleys, carrying the 5 MN hoist gear, have eight wheels, two at each corner, which run on rails mounted on the bridge of the crane. Travel of the trolley is by a dc motor through a gear reducer to two shafts, which, via gears, drive the end two wheels on each side, see Fig. 13.27.

Hoist drums are rotated by a dc motor driving through a shared gear reducer. The lifting cables are attached to a drum and pass through three fixed pulleys, four pulleys at the hook and a compensating pulley before going through a similar pulley arrangement to the other drum, see Fig. 13.28. Overload, loose cable devices etc. are attached to the compensating pulley.

Trolleys are coupled when used together to lift loads up to 10 MN and controls are shared when two 10 MN cranes are used together. When cranes are coupled for use, the trolleys of each crane must also be coupled together.



2.5 MN central assembly area and powerhouse cranes

The 2.5 MN cranes which operate in the powerhouse and the central assembly area were made by Mecânica Pesada S.A and are identical. A general arrangement of the crane is shown in Fig. 13.29. Crane travel, trolley travel and the lifting gear of the auxiliary hook are driven by ac motors, the speed of which is controlled by thyristors acting on the stator supply, coupled with stepped rotor resistances. The main hoist variable speed dc motor is supplied from a thyristor converter.

Travel of the auxiliary hook trolley is from a fixed speed ac motor. In the powerhouse, electrical

supply at 13.8 kV is from the same two sets of copper conductor bars which supply the 10 MN cranes; however, the crane has two separate sets of shoes for the different frequencies, switching between the two being automatic as the crane passes. To operate in the central assembly area the shoe structure was modified to pick up from a set of four horizontal conductor bars at El.167.5. All electrical equipment, transformers, panels, etc., are mounted in the crane beam. The 2.5 MN cranes in the main hall of the powerhouse use the inside set of rails of the 10 MN cranes.

Crane travel mechanism consists of a cluster of four wheels mounted in two pairs at each corner of

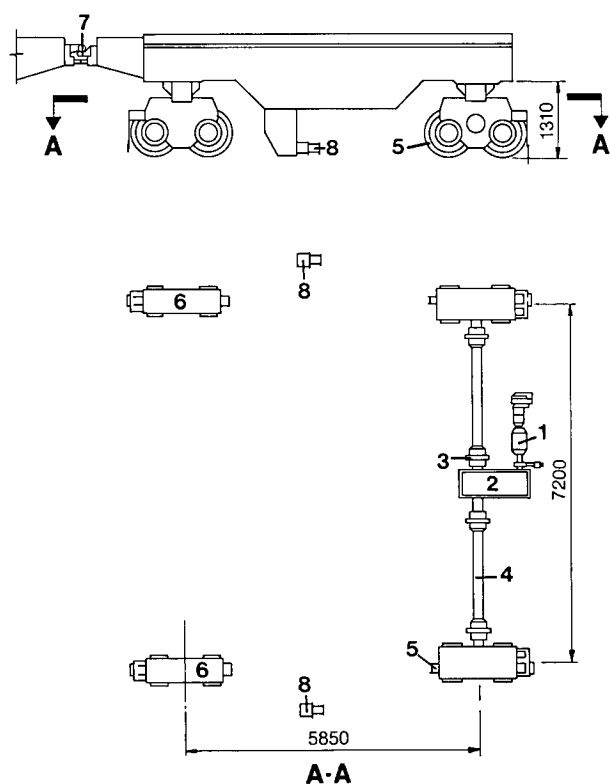
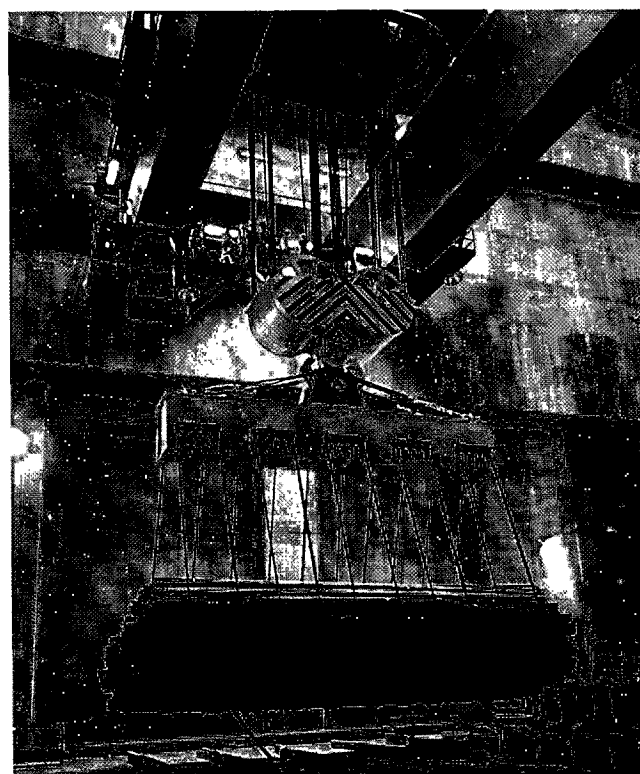


Fig. 13.27 10 MN crane travel mechanism for 5 MN trolley

- 1 Direct - current motor
- 2 Gear reducer
- 3 Couplings
- 4 Shaft
- 5 Driven wheels
- 6 Free wheels
- 7 Coupling to other 5 MN trolley
- 8 Hydraulic buffer



Testing of 2.5 MN powerhouse crane

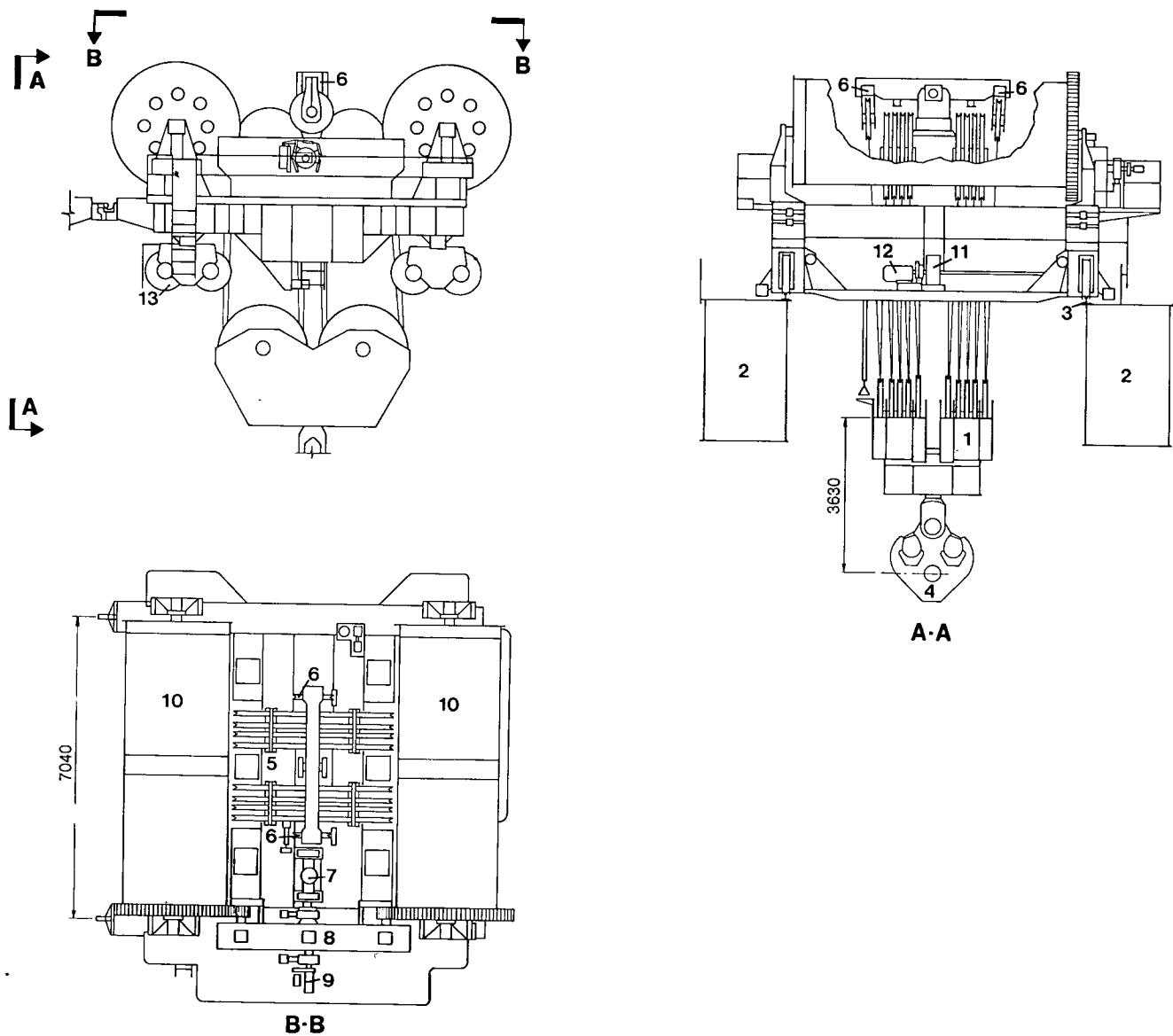


Fig. 13.28 10 MN crane-main lifting hoist mechanism (5 MN)

- | | |
|------------------------|-------------------------|
| 1 Pulley block | 8 Gear reducer |
| 2 Crane beams | 9 Brakes |
| 3 Rails | 10 Main hoist drums |
| 4 Hook | 11 Gear reducer |
| 5 Overload device | 12 Trolley travel motor |
| 6 Compensating pulley | 13 Driven wheels |
| 7 Direct-current motor | |

the bridge. The corner wheel pairs at one end are motorized, see Fig. 13.30, all other pairs being free-wheeling. Acting on the driving motor is an electromagnetic automatically actuated disk brake and a hydraulic brake pedal being applied from the control cabin.

The trolley carrying the main 2.5 MN hoist runs on rails mounted on the top of the bridge, and the auxiliary trolley carrying the 200 kN hoist travels on a second set of rails 1.4 m below. A set of two wheels at each corner support the main hoist trolley, two sets of which are shaft driven from a single electric motor through a shared gear reducer, and gear train, see Fig. 13.31. A similar arrangement is used to drive the trolley of the auxiliary hoist. The main hoist comprises a single winch drum rotated by a dc

electric motor through a gear reducer and gear train. There are two crane cables, each of which is attached to one end of the drum and passes through a train of three fixed pulleys and four pulleys on the crane before terminating at an equalizing balance beam. This is attached to a pivoted beam which actuates the overload device. The hoist motor has two disc brakes which, in normal use, are automatically applied at a 0.5 second interval, when zero velocity is detected. In the case of emergency, both brakes are applied simultaneously.

2.5 MN cranes right assembly area

Although made by another manufacturer, Ishikawajima do Brasil Estaleiros S.A. - ISHIBRÁS, the 2.5 MN cranes in the right assembly area are very

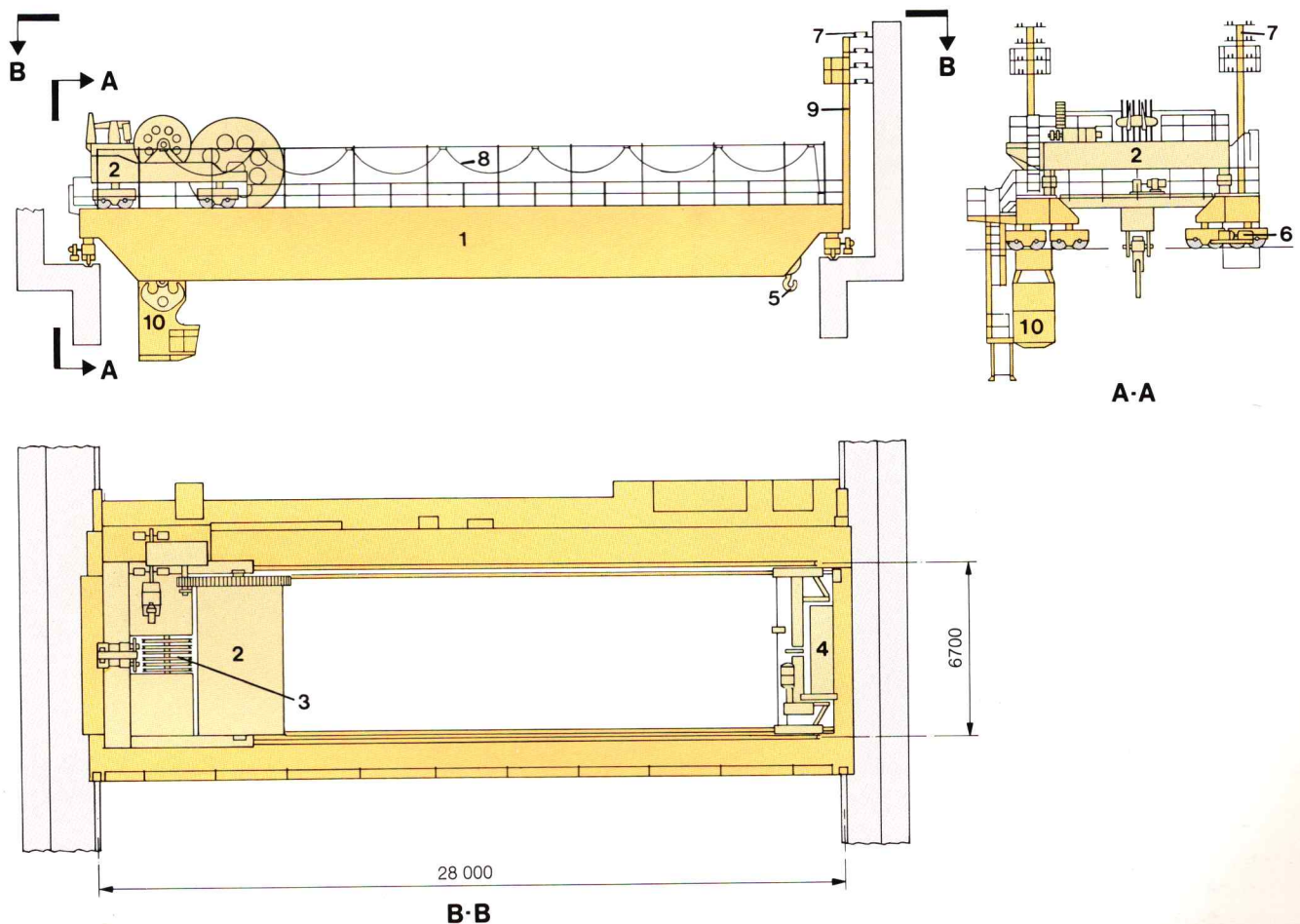


Fig. 13.29 *Mecânica Pesada* 2.5 MN crane general arrangement

- 1 Crane bridge
- 2 Main hoist drum
- 3 Intermediate pulleys
- 4 Auxiliary hoist

- 5 Main hook
- 6 Crane travel mechanism
- 7 Electrical supply
- 8 Main hoist supply cable

- 9 Extension arm for use of crane in powerhouse
- 10 Control cabin

similar to that of the central assembly area. Main differences are:

- The main hoist variable speed motor for use with load is ac, speed control being with thyristor modulation of the stator supply and variable resistors connected to the rotor winding through slip rings.
- Hoisting without load is made with a second ac motor, acting through the same gear box. This motor is speed controlled with variable rotor resistances.
- The main hoist cable is continuous, see Fig. 13.32. It is attached to each end of the drum and passes through six fixed pulleys and eight pulleys on the hook with a compensating pulley between. Overload and loose cable devices are attached to the compensating pulley.

1 MN powerhouse cranes

The 1 MN powerhouse cranes are powered from four 13.8 kV copper conductor bars which extend from the right assembly area to U9A and from U9A to block V1 (60 Hz sector) below the crane on the downstream wall, at El. 135.90. Both cranes can operate with either frequency, change-over being automatic as the crane passes between the two regions. Transformers (13.8 kV/460 V) are mounted on the bridge of the crane. All electrical motors are direct current driven obtained from the 460 V supply with a thyristor conversion, the crane and trolley travel motor having one electromagnetic brake and the hoist motors two. The crane travels on twelve wheels, three at each corner. The two extreme wheels on each rail are driven by a single variable speed dc motor through a gear reducer and shafts, see Fig. 13.33.

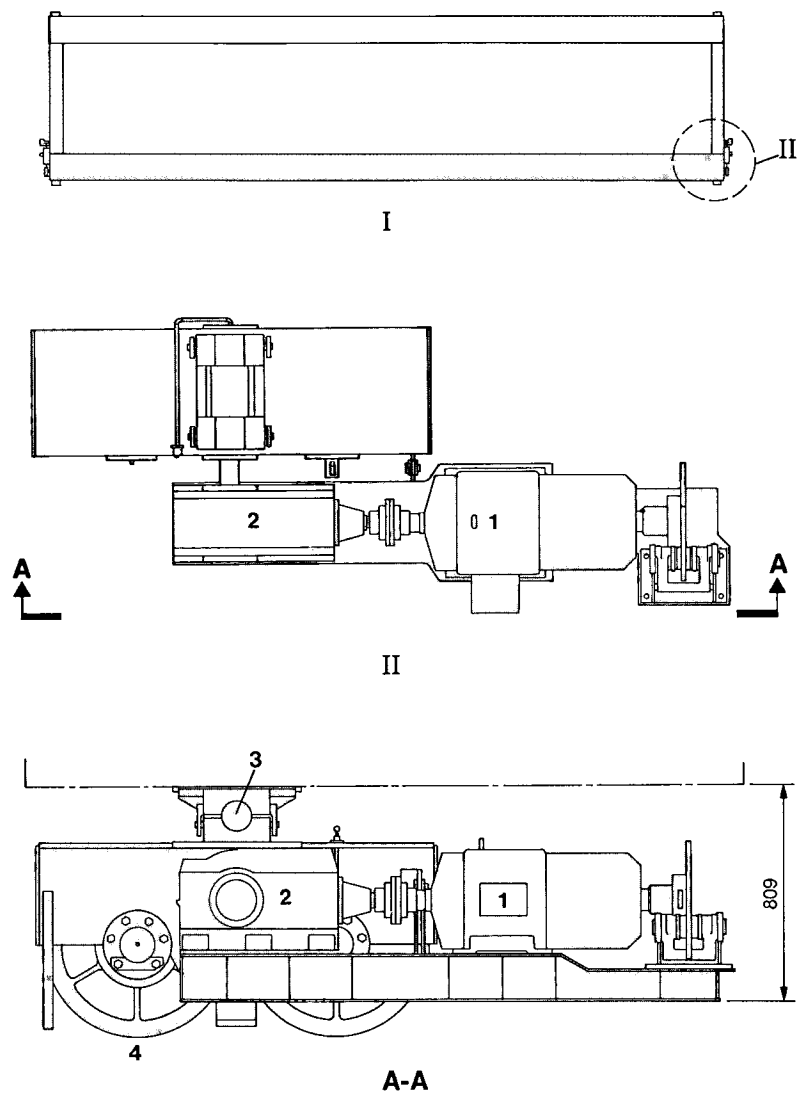


Fig. 13.30 MEP 2.5 MN crane travel mechanism

I Plan view

II Detail

1 ac motor

2 Gear reducer

3 Pinned connection to bridge

4 Driven wheels

5 Plan view of crane bridge

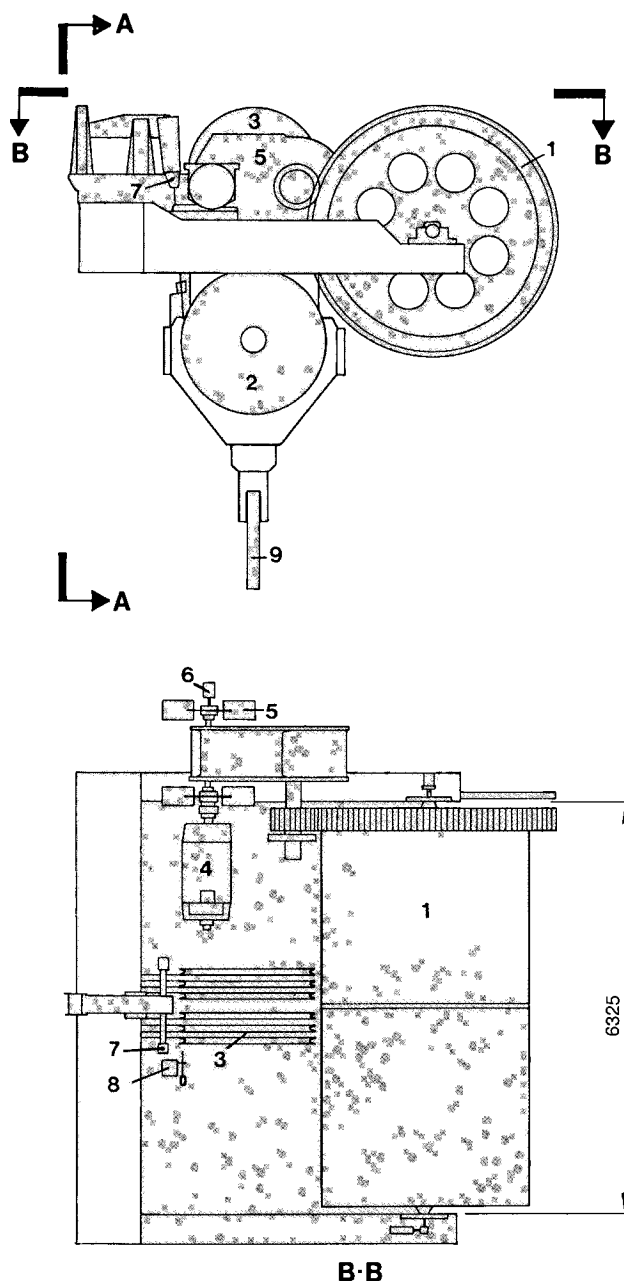


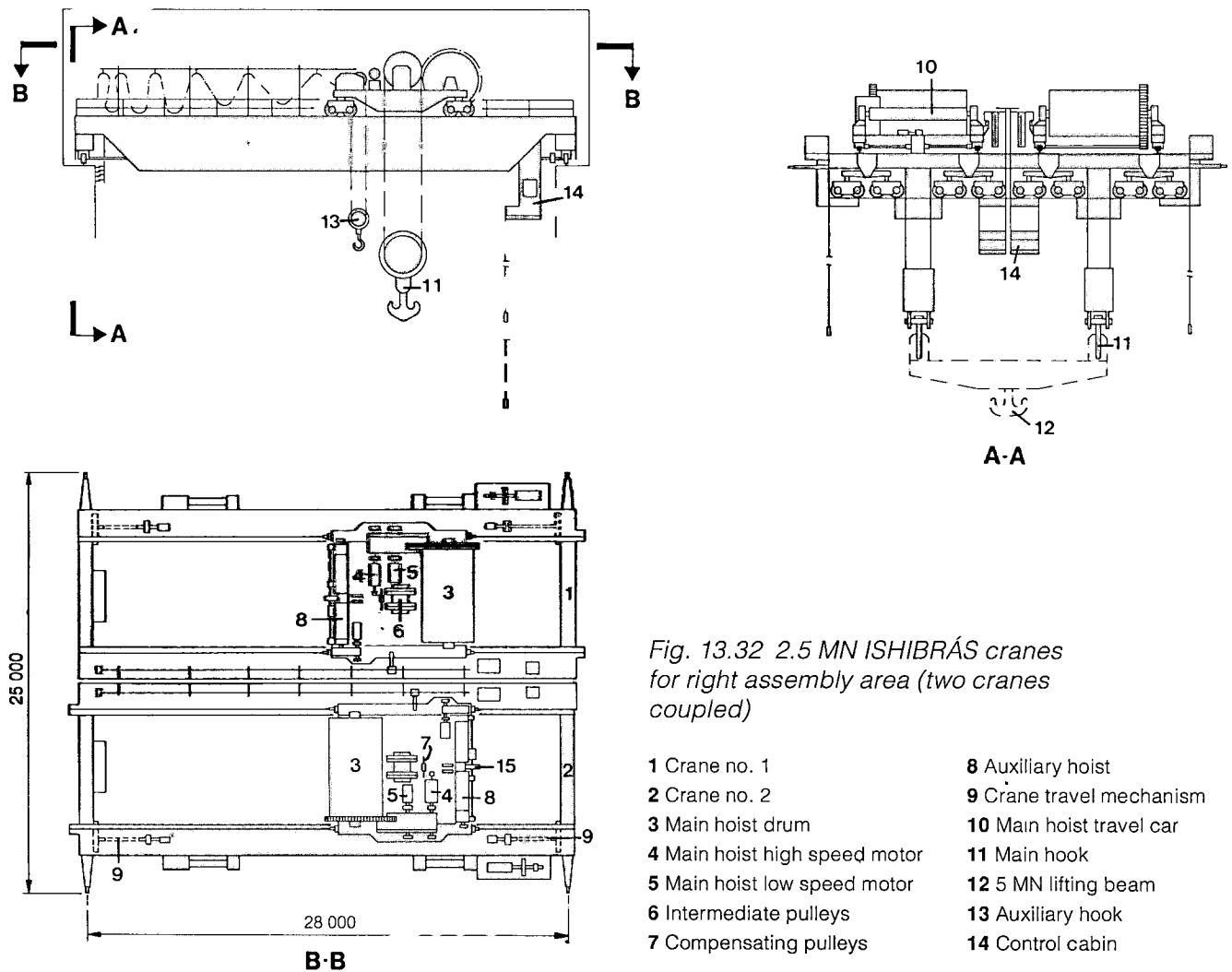
Fig. 13.31 Mecânica
Pesada 2.5 MN crane-main
lifting hoist

- 1 Hoist drum
- 2 Pulley block
- 3 Intermediate pulleys
- 4 Direct current motor
- 5 Gear reducer
- 6 Brake
- 7 Fixed point beam
- 8 Loose cable device
- 9 Main hook

Main and auxiliary hoists are contained in a single trolley mounted on eight wheels (two at each corner) running on rails attached to the beams of the crane. Travel of the trolley is from a single dc motor driving (through a gear reducer and split shafts) two wheels on each rail. Both hoists have single winch drums driven by variable speed dc motors through gear reducers and gear trains, see Fig. 13.34. The main hoist has six fixed pulleys and eight pulleys on the hook with a compensating pulley on which are mounted the overload and loose cable devices. These cranes were made by Sermec S.A., Indústrias Mecânicas.

2.5 MN transformer gallery crane

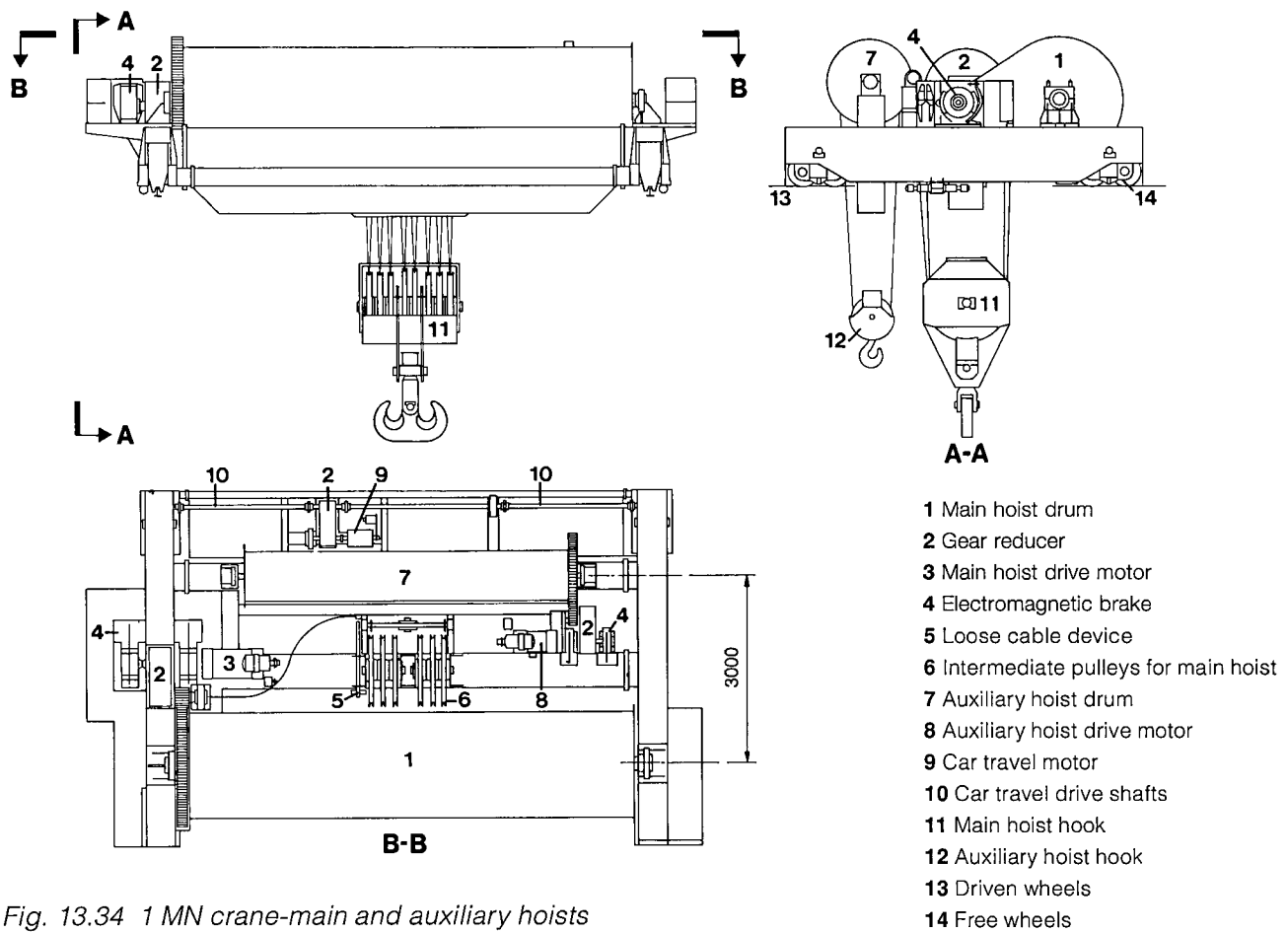
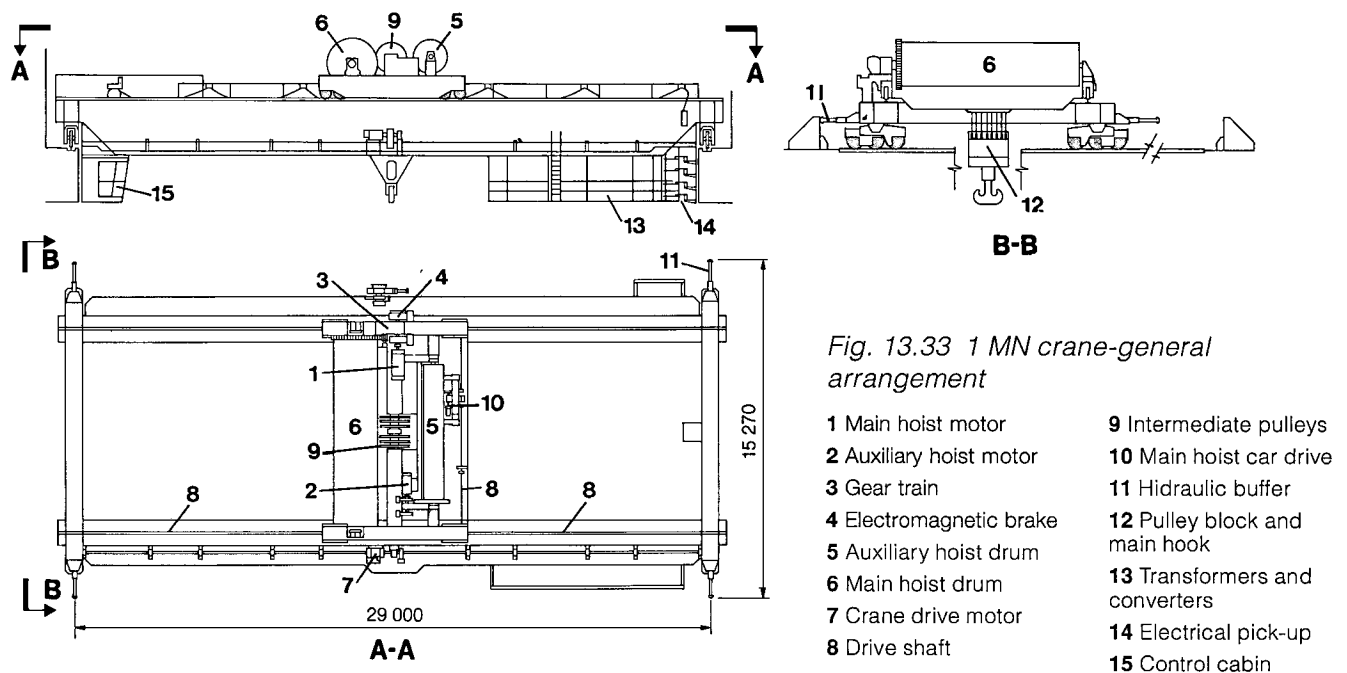
The two 2.5 MN cranes, made by Equipamentos Villares S.A., are used to move the main step-up transformers along their gallery, on the upstream side of the powerhouse at El. 108. Transformers are brought into the powerhouse by the right or central assembly area cranes and, in the case of the right assembly area, transported to the access doors leading to the transformer gallery by the main powerhouse cranes and moved on rails into the gallery. At the central assembly area the transformers are lowered directly by the assembly area cranes into the gallery through a hatch



between lines A and B at El. 144. From the end of the gallery the transformer cranes convey the transformers to the rails of the required transformer bay, where they are moved into the bay. Hence the cranes are actually special handling hoists and are without a trolley for transverse movement. The cranes run on rails at El.120.3 and, because of height limitations within the gallery they are of low profile design. They receive electrical supply at 460 V from copper conductor bars at El. 119.35. The general arrangement of the crane is shown in Fig. 13.35. Crane travel is on eight wheels (two at each corner of the crane), the end two wheels on each rail being driven by a variable speed ac motor through a gear reducer and split shaft. Motor speed control is by electronic regulation of the rotor current

through slip rings. The main hoist mounted on the crane bridge comprises a single drum driven by an ac variable speed motor through a gear reducer and gear train. Speed control of the motor is effected with electronic regulation of the rotor current via slip rings together with a dynamic brake, also with similar regulation. The hoist mechanism is equipped with two electromagnetic brakes. Two lifting cables are attached to each end of the drum and, after passing three fixed pulleys and four pulleys on the crane hook, each are attached to a balancing beam on which is mounted the overload device, etc.

A 150 kN electrically driven hoist used for transformer maintenance runs on the lower beam of the crane.



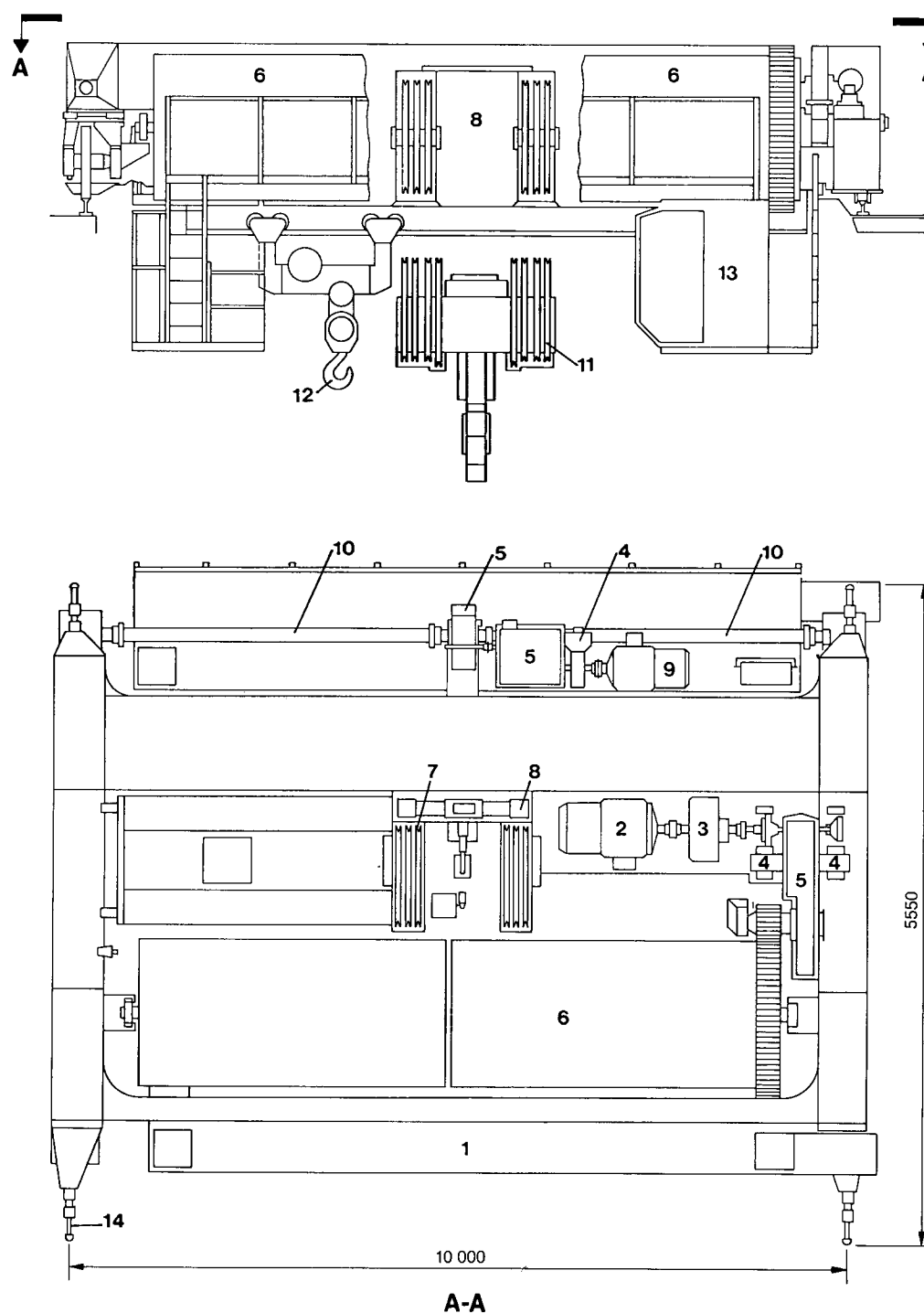


Fig. 13.35 Main step-up transformer gallery crane - general arrangement

- | | | |
|-------------------------|-------------------------|-------------------------------|
| 1 Bridge structure | 6 Main hoist cable drum | 11 Pulley block and main hook |
| 2 Main hoist motor | 7 Intermediate pulleys | 12 Auxiliary hoist |
| 3 Dynamic brake | 8 Fixed point beam | 13 Control cabin |
| 4 Electromagnetic brake | 9 Crane travel motor | 14 Hydraulic buffer |
| 5 Gear reducer | 10 Drive shaft | |

SF₆ gallery crane

The two cranes which operate along the length of the SF₆ gallery were made by Pohlig-Heckel and are used for general maintenance of the SF₆ equipment. Crane rails are at El. 139, and conductor bars below the crane on the upstream wall of the gallery supply power at 460 V, 50 Hz up to U9A and 60 Hz from U9A to block V1. Both cranes can operate at either frequency, there being automatic switching of circuits as the cranes pass between the two sectors.

Fig. 13.36 shows the general arrangement of the cranes. The crane bridge is mounted on four wheels (one at each corner); one wheel on each rail is driven by a variable speed ac motor through a gear reducer. A four wheeled trolley carries the hoisting gear on rails mounted on the bridge of the crane, one set of wheels being driven by an ac motor acting

through a gear reducer and split shaft. The single drum of the main hoist is driven by a variable speed ac motor through a gear reducer.

Both the crane travel and the hoist motors are coupled to dynamic brakes. The hoist mechanism also has two electrohydraulic brakes and the travel mechanism one. Velocity control is by variable rotor resistance coupled with the action of the dynamic brakes.

Attached to each end of the drum, the main hoist cable passes through a pulley at each side of the hook and over the compensating pulley.

1.4 MN gantry cranes

Operating outside the powerhouse downstream at El. 144, the 1.4 MN gantry cranes are used to handle the draft tube stoplogs. Although of different

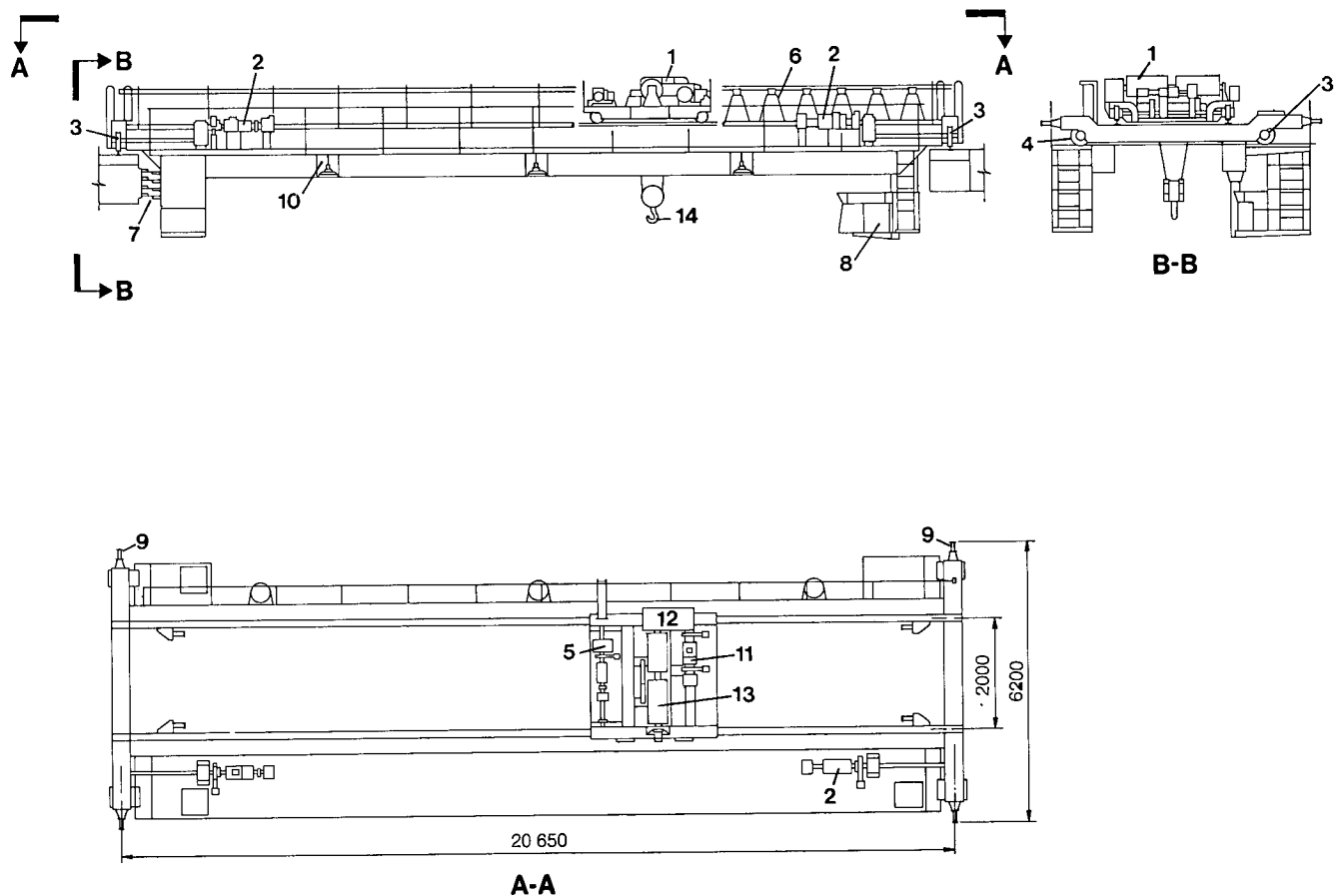


Fig. 13.36 SF₆ gallery crane general arrangement

- | | | | |
|--------------------------|------------------------|----------------------------|---------------|
| 1 Main hoist and trolley | 5 Car travel mechanism | 9 Buffers | 13 Hoist drum |
| 2 Crane travel mechanism | 6 Trailing cable | 10 Lights | 14 Hook |
| 3 Driven wheels | 7 Electrical supply | 11 Trolley travel ac motor | |
| 4 Free wheels | 8 Control cabin | 12 Gear reducer | |

capacity and height, the basic design is very similar to that of the spillway gantry crane described in Chapter 8. Both cranes were supplied by the same manufacturer, Equipamentos Villares S.A. As can be seen from the general arrangement shown in Fig. 13.37, the differences in design arrangement are as follows:

- The 1.4 MN gantry crane runs on four sets of two wheels on each rail. Each set is similar to those of the spillway crane, as is the drive train.
- The hoist mechanism is carried on a trolley permitting transverse movement of the stoplogs between storage and draft tube slots. The trolley runs on four wheels, two of which are driven from an ac variable speed motor through a gear reducer and split shaft.
- Motors of the hoist mechanism are equipped with dynamic brakes, see Fig. 13.38.
- Drums have a single cable each, one end of which is attached to the drum. After passing six pulleys on the hook and five fixed pulleys the cable is attached to a fixed point beam which incorporates the overload and loose cable devices.

ELEVATORS

Passenger Elevators

The arrangement of elevators in the powerhouse and the main dam is shown in Fig. 13.39. Details of the elevators are given in Table 13.4. All elevators, other than the two cargo elevators located in the assembly areas, are of the typical passenger type and are used to convey personnel and light equipment. Salient features of the passenger elevators are:

- Design and construction to Brazilian standard ABNT-P-NB-30/1977 - Construção e Instalação de Elevadores - Procedimentos.
- Elevator cables. Seale type 8 x 19 fiber cored.
- Motor/generator Ward Leonard drive. 440 V, three - phase, on line starting.
- Electro-mechanical brakes.
- Doors with viewing windows.
- Electro- mechanical brakes.
- Doors with viewing windows.
- Elevators internally lined with stainless steel sheeting.
- Emergency exit doors at selected levels, each 2 0.8 m.

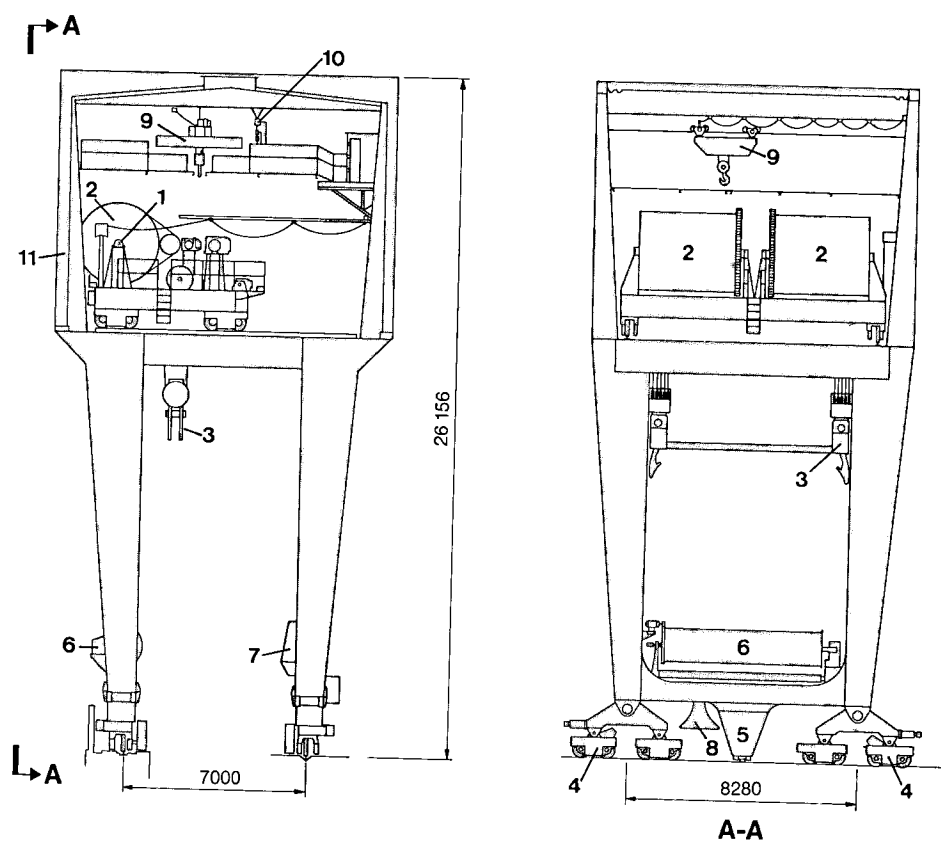


Fig. 13.37 1.4 MN gantry crane - general arrangement

- 1 Main hoist
- 2 Main hoist cable drum
- 3 Lifting beam
- 4 Crane travel mechanism
- 5 Crane travel lock
- 6 Electrical cable drum
- 7 Control cabin
- 8 Electrical norm
- 9 Maintenance crane
- 10 Maintenance hoist
- 11 Enclosure

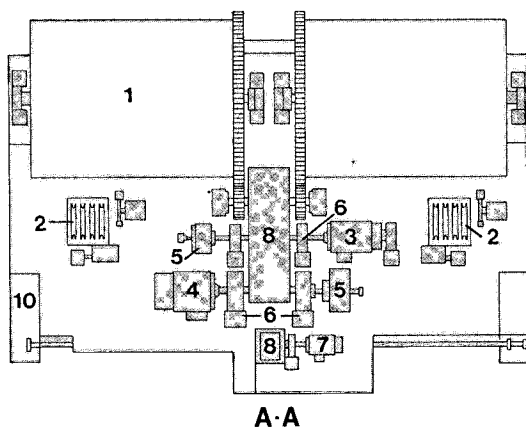
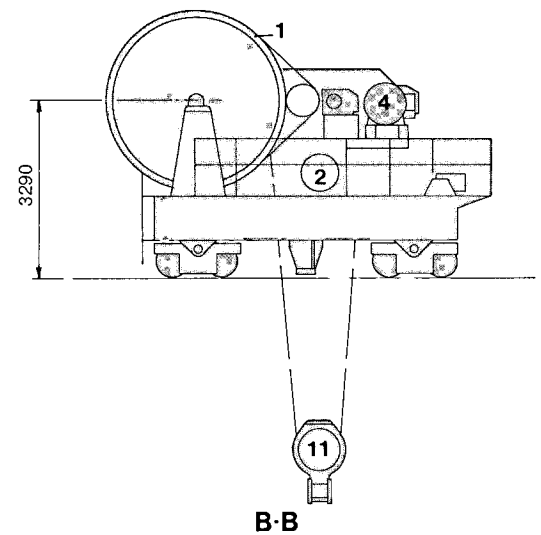
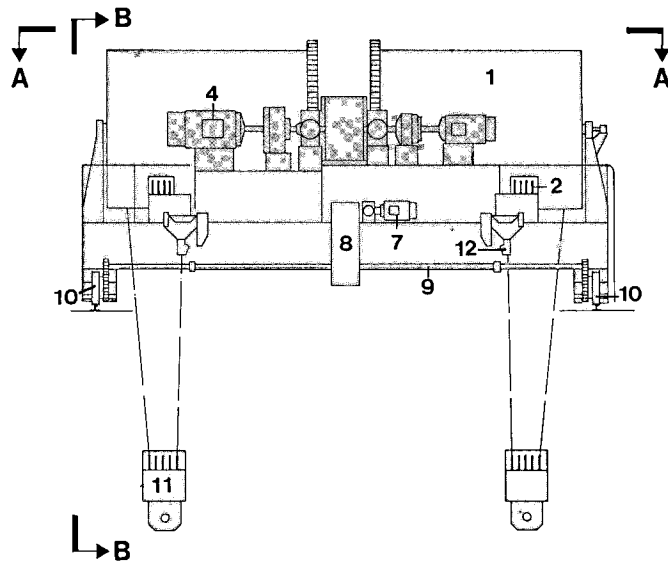


Fig. 13.38 1.4 MN gantry crane
- main hoist and car

- 1 Main hoist drum
- 2 Intermediate pulleys
- 3 High speed motor
- 4 Low speed motor
- 5 Dynamic brake
- 6 Electromagnetic brake
- 7 Car travel motor
- 8 Gear reducer
- 9 Drive shaft
- 10 Driven wheels
- 11 Pulley block
- 12 Fixed point

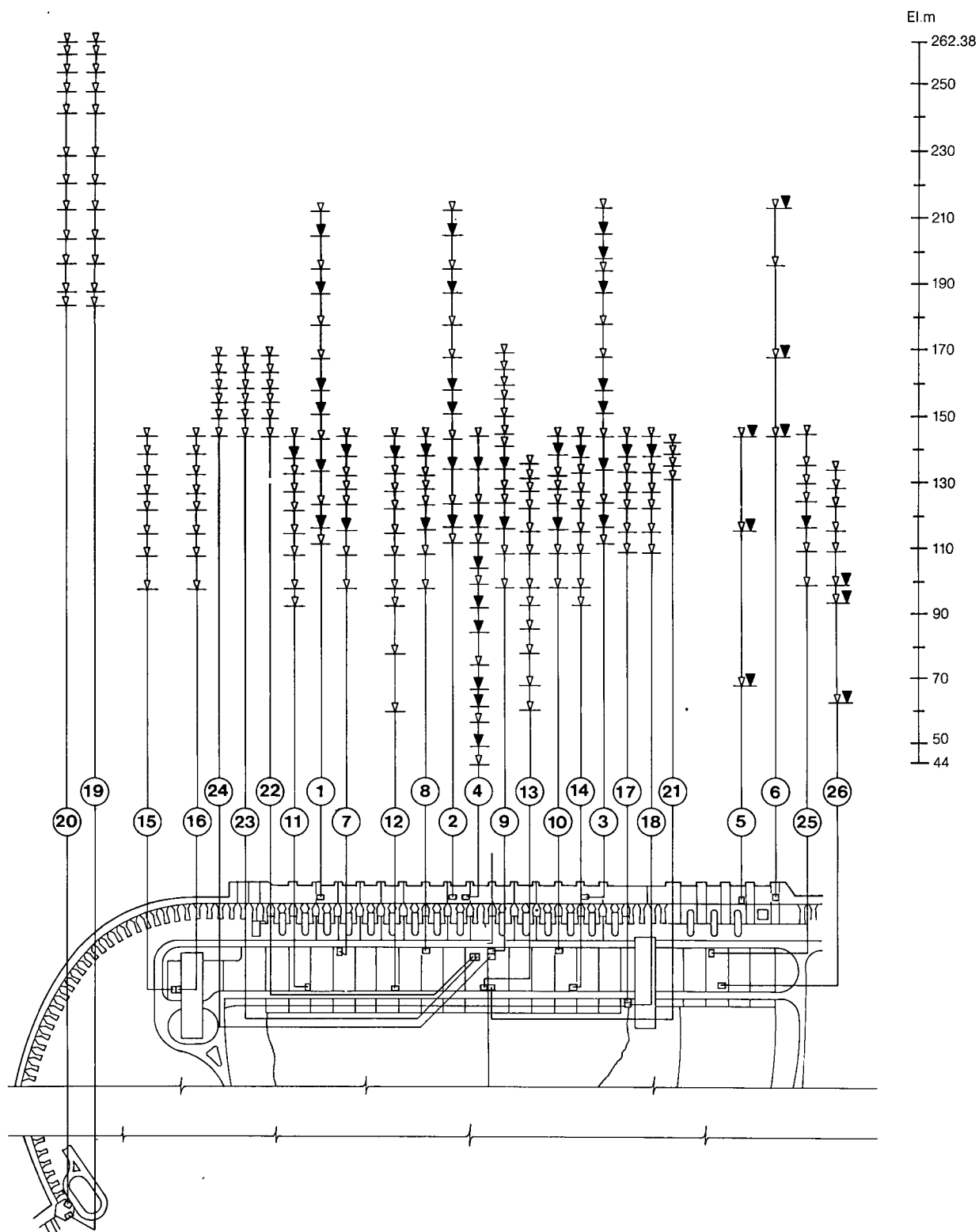


Fig. 13.39 Arrangement of elevators in the powerhouse and main dam

- ① ... Identification number of elevator
- ▼ Emergency doors
- ▽ Stops

Table 13.4 *Passengers elevators*

Elevator number	Location	Nominal capacity	Velocity (m/min)
E1	Main dam F5/6	20 passengers or 14 000 N	105
E2	Main dam F17/18	20 passengers or 14 000 N	105
E3	Main dam F29/30	20 passengers or 14 000 N	105
E4	Main dam F17/18	20 passengers or 14 000 N	105
E5	Main dam H9/10	14 passengers or 9800 N	105
E6	Main dam H14	17 passengers or 11 900 N	105
E7	Powerhouse U4	17 passengers or 11 900 N	105
E8	Powerhouse U8	17 passengers or 11 900 N	105
E10	Powerhouse U13	17 passengers or 11 900 N	105
E9	Powerhouse U9A	14 passengers or 9800 N	105
E11	Powerhouse U2	14 passengers or 9800 N	105
E14	Powerhouse U13	14 passengers or 9800 N	105
E12	Powerhouse U6	14 passengers or 9800 N	105
E13	Powerhouse U9A	14 passengers or 9800 N	105
E15	Powerhouse AMD1	42 passengers or 29 400 N	105
E16	Powerhouse AMD1	42 passengers or 29 400 N	105
E17	Powerhouse AMC1	42 passengers or 29 400 N	105
E18	Powerhouse AMC1	42 passengers or 29 400 N	105
E19	Spillway observation tower	25 passengers or 17 500 N	105
E20	Spillway observation tower	25 passengers or 17 500 N	105
E21	Powerhouse U10	8 passengers or 5600 N	60
E22	Powerhouse U9A Operations building	14 passengers or 9800 N	105
E23	Powerhouse U9A Operations building	14 passengers or 9800 N	105
E24	Powerhouse U10 Operations building	17 passengers or 11 900 N	105
E25	Powerhouse U17	17 passengers or 11 900 N	105
E26	Powerhouse U17	17 passengers or 11 900 N	105

Cabin equipped with ventilation fan, fluorescent lights, position indicators, and telephone.

Devices for manual movement of elevator at the hoist gear, in the event of an emergency.

Shock absorbers at the bottom of the elevator shaft for both the cabin and the counterweight

All passenger elevators were supplied by Indústrias Villares S.A., Brazil.

Cargo elevators

The cargo elevators in the assembly areas are used to transport heavy equipment, including fully loaded

trucks, to the downstream galleries at Els. 98.5, 108, 115, 122, 127.6 and 133.2.

Entrance to the elevators is from the roadway at El. 144.

Design of the cargo elevator was to:

ABNT-P-NB-283 – Aparelhos de levantamento – Norma para cálculo (1976).

• FEM – Fédération Européenne de la Manutention – Section Règles pour le calcul des appareils de levage (1970).

• ABNT-P-NB-30/1974 – Construção e Instalação de Elevadores – Procedimentos.

Details, structures and mechanisms were specified to ABNT-P-NB-283:

- Structures. Utilization class B, state 2, group 4.
- Hoist gear – Class of functioning VI, state 2, group 4m.
- Coefficient of safety for cable: 12.
- Door operating mechanism – Class of functioning VI, state 3, group 2 m.

Basic characteristics of the cargo elevators are:

Nominal capacity	300 kN
Number	2
Location	
Right assembly area	1
Central assembly area	1
Internal dimensions of car	
Length	4 m
Width	12.75 m
Height	4.5 m
Lift height	46.1 m
Maximum and minimum elevations served	144.6 m/98.5 m
Number of stages	6
Maximum velocity	0.12 m/min.
Minimum velocity	3 m/min.

General arrangement of the cargo elevator of the central assembly area is given in Fig. 13.40. Access to the elevator from El. 144 is through the 4 m wide, 4.5 m high side door. Exit at the chosen elevation into the powerhouse is through a similar door on the other side, thus facilitating drive on/drive off for trucks. There are double doors at El. 144, which close off the total 4.5 m opening and thus protect the entrance to the powerhouse. At floors in the powerhouse there are single doors which protect only the lower 2 m of the opening. Doors are manufactured from welded mild steel angle and covered in steel mesh. At each elevation, the doors are automatically opened and closed by cables actuated by pulleys driven from an electric motor through a gear reducer and split shafts, mounted above the doors.

The platform of the elevator is made from welded mild steel lattice supports, with a checker plate base and 2 m high mild steel sheeting side protection. At the top of the structure are four sets of two pulleys through which run the suspension cables from the main hoist. Each set of two pulleys is attached to a central pivoted beam (one each side) and any difference in cable tension between the two pulleys rocks the beam and, via limit switches, stops the elevator.

Four hydraulic servomotors, in each corner of the platform, operate horizontal cylindrical pins which engage steel support lugs embedded in the concrete, at all elevations served by the elevator. These steady the elevator during loading and are operated automatically when the elevator stops and starts. Pressure oil for the servomotors is supplied from a pumping set mounted on the platform.

The platform is guided by grease lubricated wheels running on rails attached to the side walls of the elevator shaft. Two of the guides have single wheels bearing on a flat plate and restrain the elevator in one direction, whereas the other two have three wheels each running on one side of a protruding rail and hence restrain the elevator in both directions (laterally and transversely).

Six spring loaded shock absorbers mounted at the bottom of the shaft at El. 95.3 protect the elevator platform in the event of an overrun.

The main hoist mechanism is located in a room above the elevator at El. 152.5, see Fig. 13.41.

Above the main hoist mechanism there is a 50 kN bridge crane for erection and maintenance. The bridge crane has an electric motor driven hoist (440 V, 50 Hz right assembly area, 60 Hz central assembly area) and manual travel of the bridge and trolley.

Two electric motors are used to drive the main hoist, one for rapid travel and the other for inching movements (automatically engaged when the platform approaches the chosen elevation). Velocity of both motors is controlled by rotor resistances (for starting and stopping) and each is equipped with two electromagnetic brakes. Through a shared gear reducer, the motors drive a split shaft which rotates the four drums of the hoisting mechanism, via a gear train. Each drum carries two cables, their ends attached by a bolted plate to the drum. The cables are wound around the drum and then pass through one of the pulleys on the upper structure of the platform before terminating in a fixed point mounted on the floor of the hoist room. A load cell in the mounting indicates overload and blocks operation of the elevator.

The cargo elevators were manufactured by Pohlig-Heckel do Brasil, S.A.

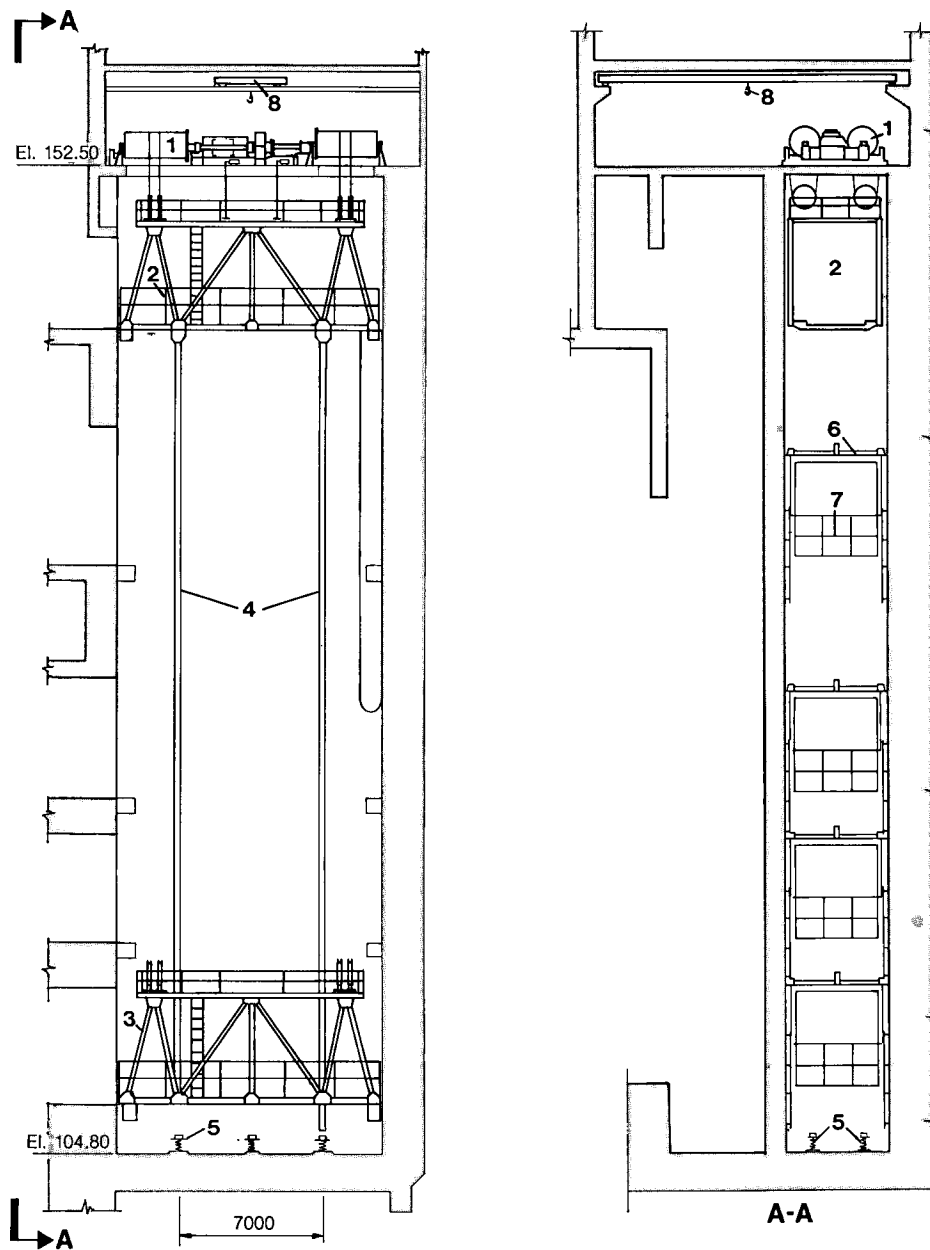


Fig. 13.40 General arrangement of cargo elevator - central assembly area

- 1 Hoisting mechanism
- 2 Cargo elevator in upper position
- 3 Cargo elevator in lower position
- 4 Guide rails
- 5 Shock absorbers
- 6 Mechanism for lifting the safety gate
- 7 Safety gate
- 8 Maintenance crane

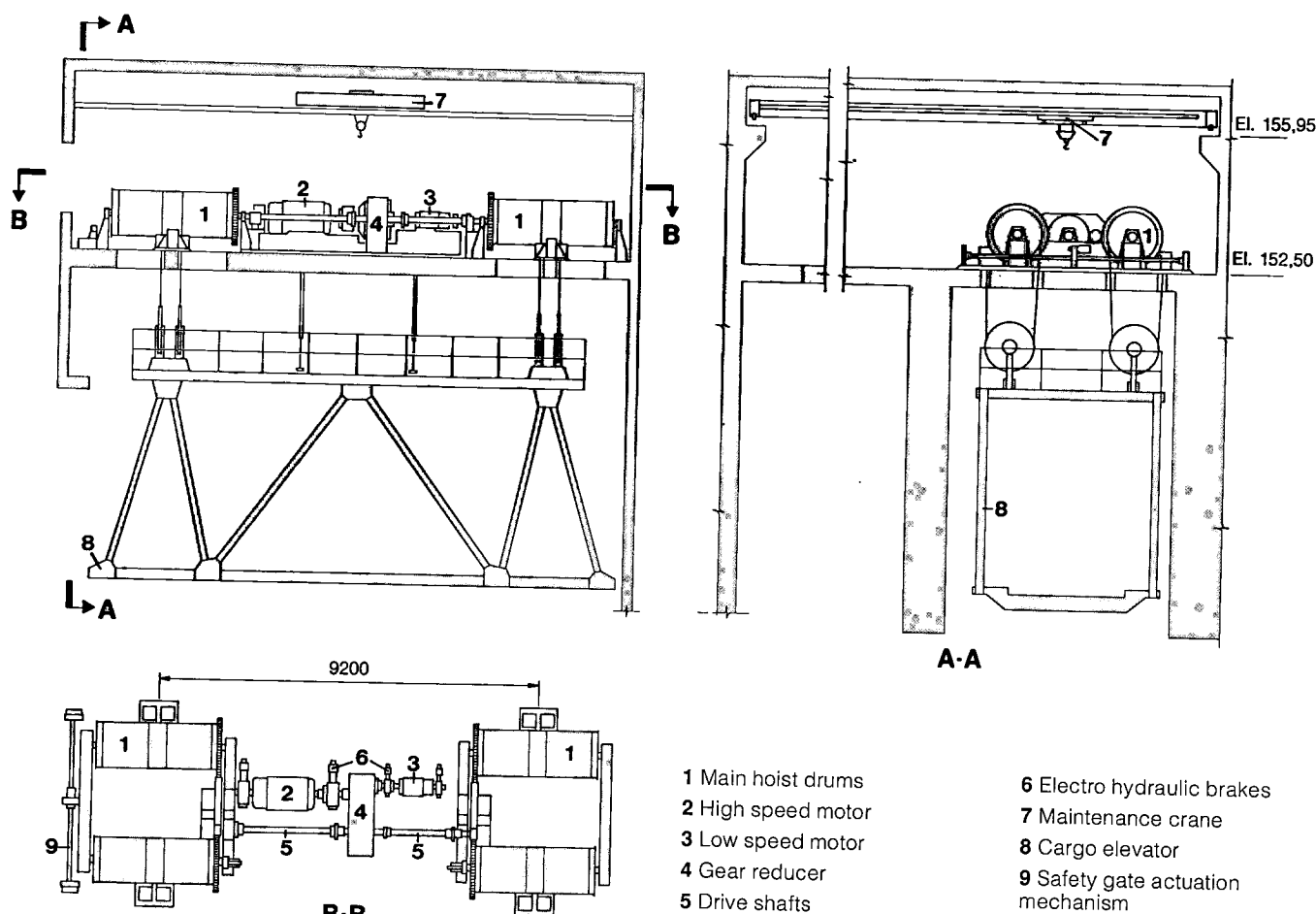


Fig. 13.41 Cargo elevator - main hoist mechanism

ELECTRICAL POWER SYSTEMS

ALTERNATING CURRENT SYSTEMS

The basic sources of electrical power for various auxiliary systems of the project including the powerhouse, intake, spillway and dam areas are centered in the powerhouse, the exception being the right bank substation, which derives its basic

and emergency power from the equipment within the substation.

Two separate systems are provided, one for 50 Hz project loads and another for 60 Hz. Fig. 13.42 shows in simplified form the single line diagram of the auxiliary electrical systems.

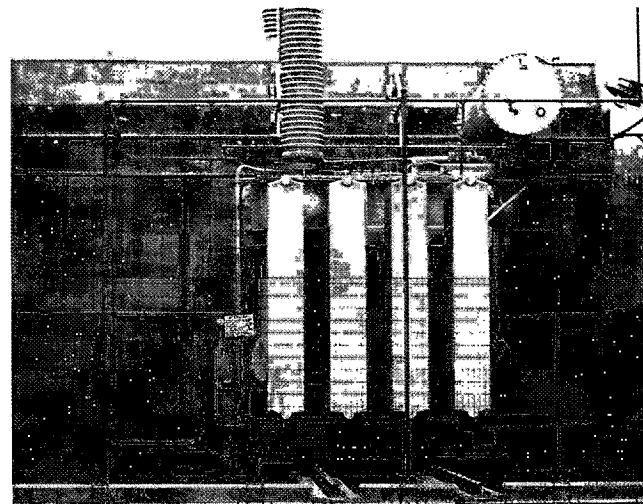
The auxiliary electrical systems are designed to be self-sufficient, i.e. independent from the external electrical networks. Some limited interconnections are provided, but they are redundant and not essential to the proper and reliable functioning of the auxiliary systems.

SOURCES OF AUXILIARY POWER SUPPLY

Principal sources

The principal sources of the auxiliary power supply are the generating units themselves. The power is generated at 18 kV, stepped up to 525 kV, fed into the SF₆ gas insulated switchgear (GIS) double bus scheme, and then stepped down to 13.8 kV by the 45 MVA transformer bank consisting of three single-phase units and one "jumper" connected spare unit. Two such banks are provided, one for the 50 Hz sector (TA-01) and one for the 60 Hz (TA-02); as a result, any of the nine generating units in each sector can supply power to the auxiliary transformer bank.

The 45 MVA rating is sufficient to supply all the loads of one frequency sector including the auxiliaries of the generating units; however, for



Auxiliary service transformer

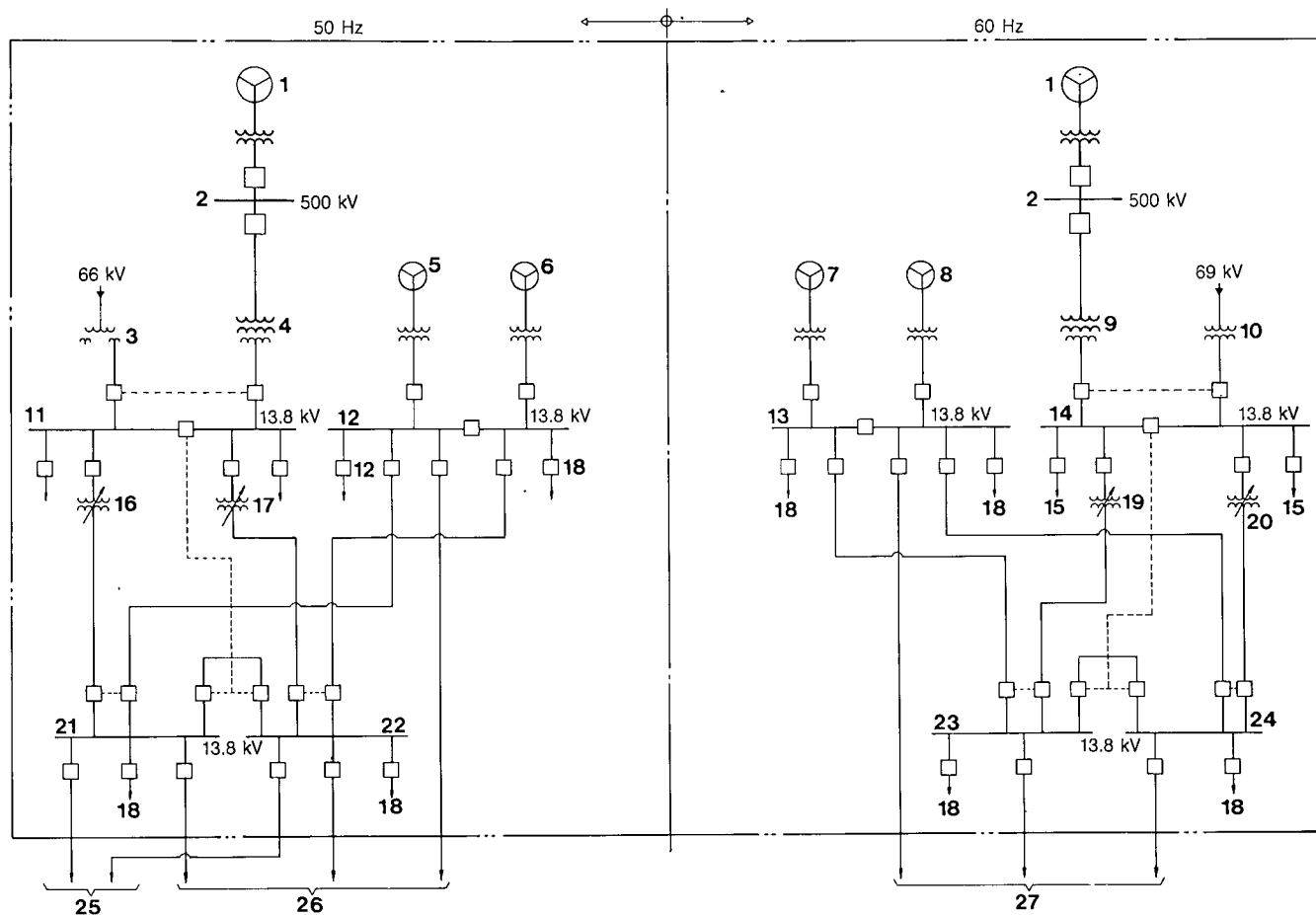


Fig. 13.42 Auxiliary electrical power systems

- | | | | | |
|------------------------------|------------------|------------------------|----------|--------------------------------------|
| 1 Generator (typical) | 7 GD-03 (diesel) | 13 CS-02 | 19 TD-03 | 25 To spillway 50 Hz auxiliary power |
| 2 SF ₆ substation | 8 GD-04 (diesel) | 14 QA-02 | 20 TD-04 | 26 To dam 50 Hz auxiliary power |
| 3 TB-01 | 9 TA-02 | 15 Spare | 21 QP-01 | 27 To dam 60 Hz auxiliary power |
| 4 TA-01 | 10 TB-02 | 16 TD-01 | 22 QP-02 | |
| 5 GD-01 (diesel) | 11 QA-01 | 17 TD-02 | 23 QP-03 | |
| 6 GD-02 (diesel) | 12 CS-01 | 18 To powerhouse loads | 24 QP-04 | |

reasons of reliability the normal operation is that each generating unit supplies its own auxiliaries via 18 kV - 460 V transformation (TAU-1 to 9 and TAU-10 to 18) subsequent to its starting.

In the 50 Hz sector the 525 kV transformer bank (TA-01) cannot be energized from the external system interconnections because the HVDC system is unidirectional, with power flowing away from Itaipu only. Energization from the ANDE system, through 220/525 RV transformation, is not feasible because of excessive capacitance of the 500 kV circuits and the possible danger of ferroresonance, together with the relatively small rating of ANDE's generators at Acaray station.

In the 60 Hz sector the 525 kV transformer bank (TA-02) can be energized from the 500 kV system providing that the first intermediate substation, Ivaiporã, on FURNAS 765 kV transmission system has connected loads and infeed of generation.

Standby (external) sources

In the 50 Hz sector an external source of power originates from the 220 kV buses of the ANDE Acaray station. In the right bank substation there is 220/66 kV transformation and interconnection with the Itaipu powerhouse via 66 kV buried cables. At Itaipu powerhouse there is a 66-13.8 kV, 45 MVA three-phase transformer (TB-01). Although basically the 66 kV interconnection serves as a standby supply to Itaipu powerhouse, it may be used to transmit limited power in the opposite direction to the right bank substation and from there across the river to the Foz do Iguaçu converter station as standby auxiliary power for the converters. In the 60 Hz sector the equivalent external supply is derived from the COPEL substation located on the left river bank, via a 69 kV transmission circuit and a 69-13.8 kV, 41.6 MVA, three-phase step-down transformer TB-02 at the powerhouse.

Emergency diesel supplies

The emergency sources comprise four diesel generators each rated 5.25 MVA, two for each frequency sector (GD-01/02 for 50 Hz and GD-03/04 for 60 Hz sector). The diesel generator terminal voltage 6.9 kV is stepped up to 13.8 kV by an auxiliary delta-wye grounded transformer. The diesel generators are located at El. 127 downstream of the powerhouse, at the right and central assembly areas. Normally the diesel generators are not paralleled, but there is a provision for this should it become necessary.

Details of the diesel sets and load classification criteria are given later in this chapter.

RELIABILITY OF VARIOUS POWER SOURCES

Reliability of the principal source is a function of number of the generating units available for operation and energization of the 500 kV buses. With nine generating units in operation the availability of this source approaches 100%. The supply to the 13.8 kV systems, however, may still be lost through failures:

- In the SF₆ kV feeder to the auxiliary transformer (TA-01/02).
- Of both 500 kV SF₆ buses.
- Within the auxiliary transformer bank.
- Of the 13.8 kV interconnection between TA and the respective switchgear (QA-01/02).

The transformer banks (TA-01 and TA-02) have "jumper" connected spare units which allows for replacement, in case of a failure, of any one of the single-phase units by the spare without the necessity of removing the faulty unit. The estimated time for reconnection is about three hours.

Hence because of redundancies incorporated, and the types of the equipment selected, the overall availability of this source at the 13.8 kV bus is estimated to be in the order of 99%.

Reliability of 66 kV supply from the right bank substation is much lower, as repairs to the 66 kV cable or 45 MVA three-phase transformer bank take considerable time. This is somewhat alleviated by a spare single-phase cable, complete with potheads in the same cable trench as the three others. Thus a single cable failure substitution, and hence outage time, is reduced.

The reliability of the external source in the 60 Hz sector is similar to that of the 50 Hz sector.

Emergency supply by the two 5.25 MVA diesel generators for each frequency sector makes the reliability of the auxiliary power supply 100%. Each diesel generator, in its frequency sector, has the capability to feed alone all powerhouse and dam critical loads and start any of the generating units.

SUPPLIES TO AUXILIARIES OF THE GENERATING UNITS

Unit motor control centers

Each generating unit is provided with a 460 V motor control center (UMCC), which supplies all unit auxiliaries.

With the generator inoperative, the UMCC may be energized by the normal or emergency power sources associated with the 13.8 kV auxiliary system. When the UMCC is supplied from one of the

normal regulated sources, a 1500 kVA transformer is fed through the 13.8 kV switchgear (QP-01/02 or QP-03/04). When supplied from the diesel generators, the UMCC is fed through a 1000 kVA transformer.

With the generator running, a source is derived from the generator terminals at 18 kV. This is stepped down to 460 V by a 1500 kVA transformer bank of three single-phase units (TAU 1 to 18).

The supply from the generator is the preferred source because failure of the shared auxiliary system affects more than one unit. This source, however, is not available until the generating unit is at rated speed and voltage.

Therefore the unit must always be started and stopped with UMCC supplied by one of the other sources and then automatically transferred, depending on generator voltage, to or from the generator source. This transfer can be made manually with the selector switches in the local and central control rooms.

During load rejection of a generating unit an overspeed and (because in some cases the generator excitation remains connected) an overfrequency up to 45% occurs at equipment supplied by the UMCC. The motors and associated systems are designed to accommodate the maximum overspeed, without any damage or unnecessary trips by the overload protection, and are thus not disconnected. The only exception to this are the motors of the generator deionized water cooling pumps. Because there is a possibility of dangerously high water pressures developing, the pump which is running at the time of overspeed is automatically disconnected at 110% of the rated speed and, after a few seconds, when the generator speed is near normal, it is automatically reconnected.

Essential services

Essential services require not only alternative power supplies but also a duplication of equipment, and are:

- Turbine headcover drainage pumps.
- Governor oil pumps.
- Generator thrust bearing high pressure oil lift pumps (for unit starting).
- Stator winding deionized water cooling pumps (for unit starting).

These loads have one motor supplied by UMCC and the second from another source of the auxiliary system via a motor starter installed directly at the equipment. As failure of the generator high pressure oil system prevents starting of the turbine generator

unit, the second pump is supplied by a feeder from the other frequency sector.

Illumination of the central control room is supplied (by sector) with both frequencies.

LOAD CLASSIFICATION

Classification of the loads is:

Class I

Loads which are essential to the integrity of the powerhouse and safety of personnel and equipment, both during and after emergencies. These are supplied by fast transfer from normal standby and emergency source. Included are drainage and anti-flooding systems, battery chargers, telecommunications, critical air conditioning and ventilation of the diesel/generator halls, and critical lighting.

Totals of the installed capacities are:

Sector	kW
50 Hz	5000
60 Hz	4000

Class II

Loads which are necessary for the generation of power. These include unit motor control centers supplying the turbine governor oil pumps, turbine headcover drainage pumps, thrust bearing oil lift pumps, excitation cooling, generator stator winding deionized water circulation, main transformer oil cooling pumps, powerhouse elevators, normal lighting, 500 kV SF₆ auxiliary services, generator field flashing and selected ventilation and air conditioning.

Totals of the installed capacities are:

Sector	kW
50 Hz	21 000
60 Hz	20 000

Class III

Loads which assure continuous maintenance of the units and their accessories, and which are also important for comfort of personnel. They are supplied only by non-emergency sources and they are automatically disconnected when these are lost and the supply is switched to emergency sources.

Totals of the installed capacities are:

Sector	kW
50 Hz	12 000
60 Hz	14 000

13.8 kV SYSTEMS

13.8 kV voltage was chosen for primary distribution of the auxiliary systems because of the rating of the connected loads and the distances involved. Fig. 13.43 shows a simplified diagram of the 50 Hz auxiliary system, the 60 Hz system being similar.

There are six 13.8 kV switchgear assemblies for each sector, all 13.8 kV switchgear assemblies being metal-clad type.

Different 13.8 kV power sources should never be paralleled at the switchgear. There are safety interlocks, which permit only alternate connections of supplies and result in simplified and reliable

switching operations, since no synchronization is required, leading to the minimization of the short circuit currents in the switchgear and cabling. The only exception is that the two emergency diesel generators of the same sector can supply the system under manual control.

There is considerable redundancy in that the loss of one, or even more, component of the system, such as a cable, circuit breaker, or a section of switchgear, will not jeopardize supply to essential station loads.

In the 50 Hz area, the 13.8 kV main supply switchgear (QA-01) located at El. 144.6 has two main bus sections with a tie circuit breaker between them. One of the bus sections is supplied from the

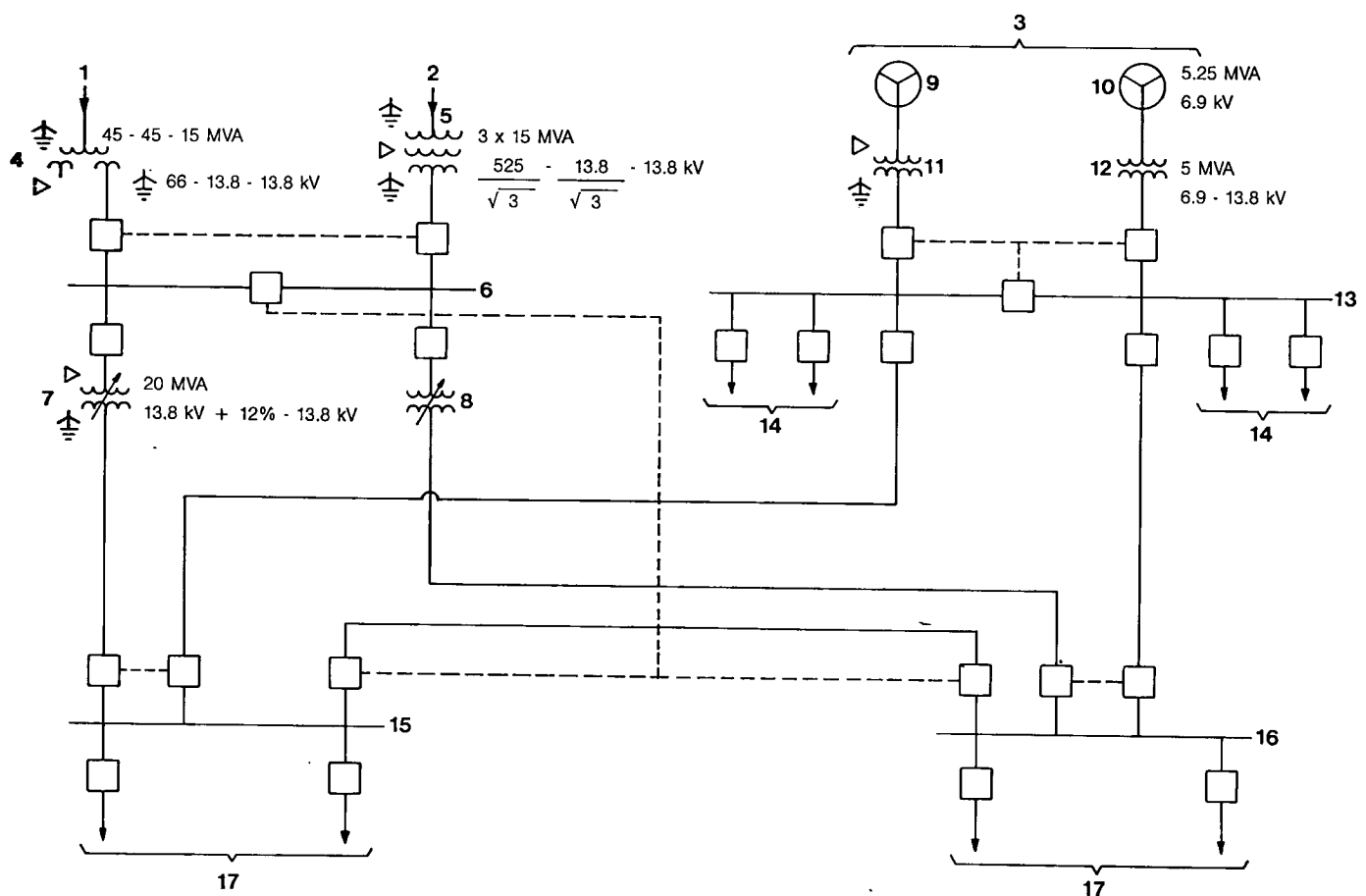


Fig. 13.43 13.8 kV auxiliary system (50 Hz)

- 1 Standby source (from external source, 66 kV)
- 2 Principal source (from SF₆ substation, 500 kV)
- 3 Diesel sets
- 4 TB-01
- 5 TA-01
- 6 Switchgear QA-01

- 7 TD-01
- 8 TD-02
- 9 GD-01
- 10 GD-02
- 11 TS-01
- 12 TS-02

- 13 Switchgear CS-01
- 14 To class I unit substations
- 15 Switchgear QP-01
- 16 Switchgear QP-02
- 17 To unit substations (38 circuits)

525-13.8 kV transformer bank (TA), which has a rating of 45 MVA, and the other from the three - phase 66-13.8 kV transformer (TB) standby source, with the same rating. The 60 Hz area is similar except that the standby source from the 69 kV system has a rating of 41.6 MVA.

As the two sources are not paralleled, the normal operating mode is with the tie breaker closed and both bus sections supplied from the 500 kV SF₆ through one incoming 13.8 kV breaker. If this source is lost the incoming breaker is automatically tripped and transfer to the 66 kV (or 69 kV) is made by closing automatically the incoming breaker from that source.

The return transfer to the main source, when it is re-established, can also be made automatically. The source circuit breakers are electrically interlocked and under automatic operation, and are controlled by undervoltage relays. Except for the bus-tie breaker, all circuit breakers of this assembly can be controlled manually, locally at the switchgear, remotely from the central control room (panelboard ASP), from the local control rooms of units 1 and 2, or 14 and 15 (panelboard ASLP) and from SCADA. There are control mode selector switches at the switchgear.

The automatic source transfer ensures that one of the full capacity sources is always available. For an internal switchgear fault the bus-tie circuit breaker isolates the fault, and the healthy section continues to supply station auxiliary loads without interruption.

The loads supplied by the switchgear QA-01/02 are:

- Switchgears QP-01/02 for 50 Hz
- Switchgears QP-03/04 for 60 Hz

The supply sources to the switchgear assemblies (QA) are not voltage regulated. Thus the feeders to the 13.8 kV main load switchgear (QP), located at El.133.2, are equipped with voltage regulators.

The two regulating transformers in each sector (TD-01 and TD-02 for the 50 Hz sector and TD-03 and TD-04 for the 60 Hz sector) are at El.144.6. These maintain the voltages at the QP switchgear and compensate for variations in the source voltages. They also reduce the magnitude of the short circuit currents on the 13.8 kV and 460 V systems by introducing additional reactance.

The regulating transformers have a thirty-two step automatic underload tap changing mechanism in the primary (delta) winding. This gives a range of 15.46 kV (12 taps at 1%) to 11.04 kV (20 taps at 1%) above and below the nominal 13.8 kV rating. Tap changeover can be automatic or manually

controlled locally, or remotely from units 1 and 2 and units 14 and 15 local control rooms, or from the central control room. The transformers are rated 20/25 MVA and are forced-air cooled. Cooling fans can be controlled automatically by a thermal replica device or manually. They have oil temperature, gas accumulation and gas pressure relays.

The 13.8 kV main load switchgear (QP) comprises two separate switchgears, (QP-01/QP-02) for the 50 Hz and (QP-03/QP-04) for the 60 Hz, each having its own main bus, with two circuit breakers in series to form the bus-tie and thirty-two feeder circuit breakers. Single bus-tie circuit breakers were not used because of the distance between the two assemblies. Each section of the switchgear is supplied from one of the regulated sources and can also be supplied from the emergency diesels. The two main sources are not paralleled and the normal operating mode is with tie breakers open and each section supplied separately. If there is a loss of one source its circuit breaker can be opened manually or automatically. In the automatic mode the transfer is to the adjacent section. If the normal sources are lost, the switchgear is manually connected to the emergency diesels.

The 13.8 kV emergency switchgear (CS) located at El.133.2 has two main bus sections with a tie breaker between them. Each section is supplied from one of two 5.25 MVA diesels (GD) through a 6.9-13.8 kV transformer (TS) also rated at 5.25 MVA. If the second diesel is available, it can be used to supply additional loads either separately or after being manually synchronized to the first unit.

Switchgear (CS-01/02) directs emergency power to the critical essential loads. Other loads on a selective basis can also be supplied via switchgear assembly QP.

Diesel-generator capacity is sufficient to supply class I loads. Loads of class II and III are shed, although the operator could connect some class II loads to diesel sets, see note of Fig. 13.44.

Shedding is normally automatic, but it can be manual on a selective basis.

All 13.8 kV switchgear assemblies are metal-clad and have metal-clad draw-out type circuit breakers. The switchgear cubicles have internal lighting, heaters and plug receptacles. Their auxiliaries are supplied by an external circuit at 220 V ac. The 125 V dc control circuits are supplied by two dc feeders, one is "normal supply" and the other is "standby". Motors of the circuit breakers are supplied by external 230 V, three-phase feeders originating at the panelboard (KN-01/02).

The protection of outgoing feeders and supply circuits for phase-to-phase and phase-to-ground faults is by overcurrent relays with instantaneous trip attachment. The protective scheme throughout the 13.8 kV system is fully selective. The instrumentation includes ammeters, voltmeters for source and bus voltage indications and transducers for interfacing with SCADA.

All the circuit breakers can be controlled manually at the switchgear. The incoming source circuit breakers are electrically interlocked to prevent paralleling and can also be operated remotely, from the unit 1 and 2 local control room for the 50 Hz, unit 14 and 15 local control room for the 60 Hz, from the central control room and from SCADA. The feeder circuit breakers supplying class III loads are controlled by the automatic load shedding system.

460 V ac GENERAL SYSTEMS

The project auxiliary equipment and systems are supplied by the 460 V, three-phase systems which in turn come from the 13.8 kV systems via dry type transformers. In general there are no restrictions on the loads which can be handled except for connection to the frequency converters or diesel generators.

The detailed arrangements of the switchgear vary to suit the specific substation but, in general, the substations are standardized and have the following compartments:

High voltage (13.8 kV) for circuit breaker and/or disconnect switch. The circuit breaker is the draw-out type rated 800 A, 500 MVA, 13.8 kV.

Transformer for 500 to 2 000 kVA, three-phase, 13.8 kV-460 V, self-cooled, dry type.

Low voltage (460 V) for secondary and bus-tie circuit breaker. The circuit breaker is the draw-out type rated 3200 A (to 1200 A), 50 kA, closing motor operated.

Low voltage (460 V) for feeder circuit breakers. The circuit breakers are the molded case type, 480 V, manually operated.

Types of 460 V panels

There are several configurations of 460 V panelboards, dictated by the class of load. The bus is normally split into two or three sections interconnected by bus-tie circuit breakers to facilitate load shedding when necessary.

Connections of the bus sections for the various load classes are:

- Class I. One normal source through switchgear (QP) and one emergency source through switchgear (CS).

- Class II. One normal source (QP).

- Class III. To adjacent class I or class II buses. Connections to all sources are made through a 13.8 kV - 460 V dry type transformer via circuit breakers.

Automatic load shedding

When both principal and standby sources of auxiliary power are lost, automatic load shedding occurs to the extent necessary for the emergency source.

When a diesel-generator is to supply the loads, all class III and class II loads are to be disconnected. This is done within the 460 V switchgear and it is actuated by the closure of the switchgear CS circuit breakers. Fig. 13.44 illustrates several cases of the automatic load shedding.

Overfrequency

When supply is from the generators, a remote load rejection of the high voltage transmission system could result in a frequency increase up to 45%. Most motors and associated systems are designed to accommodate the maximum overspeed.

DIRECT CURRENT SYSTEMS

Direct current systems are normally used to perform especially critical control and protective functions, their basic characteristic being complete independence, for a limited time, from external power supplies. Storage batteries are used to achieve this and under normal conditions are "floating" on the system, meaning that the battery is kept fully charged and the connected loads are supplied by a battery charger. When the ac supply fails or the load increases beyond the charger capacity, the battery assumes the supply of the whole or a portion of the connected load.

In the powerhouse there are a total of twelve groups of batteries with their chargers, each group consisting of two batteries and two chargers. Five of these groups are for generating unit loads, one group for each four generating units. The other seven groups are for powerhouse emergency lighting-one group for each four units, one for the right assembly area and the last one for the central assembly area. There are separate dc systems serving the central control room and the communication system.

Principal equipment characteristics:

Batteries

Type	Alkaline
Number of cells	94
Nominal voltage	112.8 V
Nominal system voltage	125 V
Equalizing charge voltage	32 V
Capacity	
Other than assembly areas	700 Ah
Assembly areas	400 Ah

Battery chargers

Type	Static
Nominal supply voltage	460 V ac three-phase (50 or 60 Hz)
Nominal output voltage	125 V dc
Nominal output current	300 A dc (generating unit loads) 200 A dc (emergency lighting) 100 A dc (emergency lighting assembly areas)

EMERGENCY DIESEL GENERATORS

Standby diesel generator facilities are located at El. 127 downstream of powerhouse line D at the right and central assembly areas, and comprise the following equipment at each facility:

- Two diesel generators with the following characteristics:

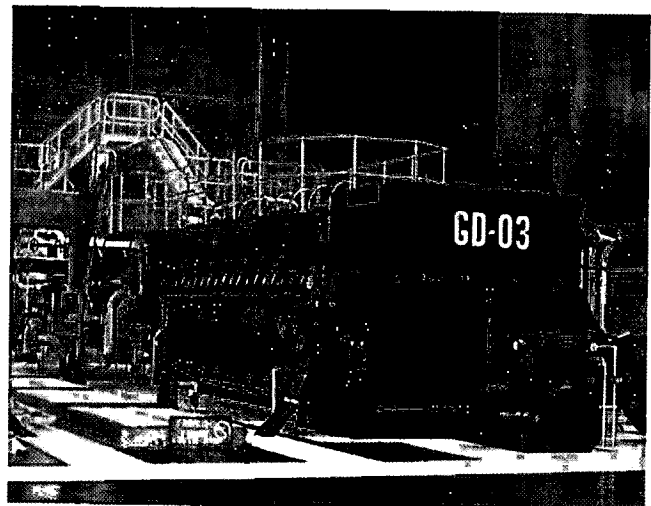
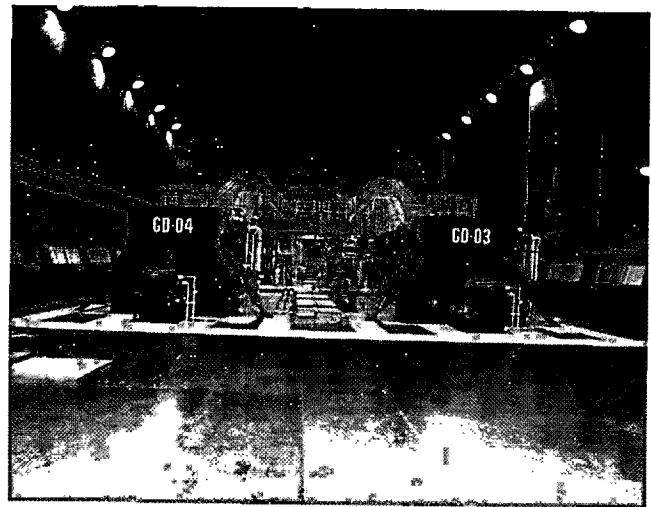
Rated output	5.25 MVA
Power factor	0.8
Frequency	50 Hz (right assembly area) 60 Hz (central assembly area)
Voltage	6.9 kV

- Two power transformers three-phase 6.9-13.8 kV, delta-wye, to step up the generator voltage (6.9 kV) to the auxiliary system voltage (13.8 kV).
- One 13.8 kV switchgear (CS) with a split main bus and tie-breaker for the distribution of emergency power.
- Fuel storage area with two tanks for storage of filtered diesel oil, one tank for filtered diesel oil, filtering and pumping equipment.

- Bridge crane for handling diesel and generator parts.
- Distribution cubicles.
- Control room.
- Compressed air starting equipment.
- Diesel exhaust piping and silencer.
- Closed loop water cooling system with water/powerhouse cooling water heat exchangers.

Raw cooling water is normally taken from the powerhouse cooling water supply. If this is not available then the supply is from two emergency pumps taking water from the tailrace at El. 92.4.

- Lubricating oil circuit, complete with holding tanks.

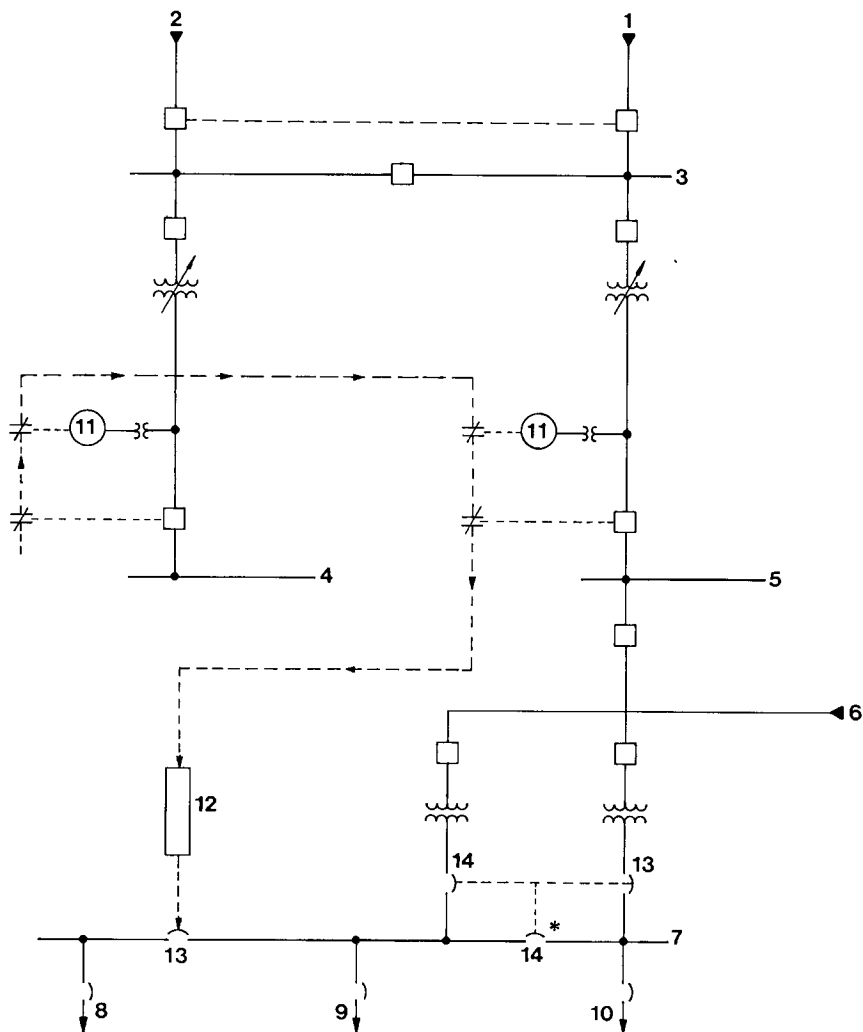


Standby diesel generators

Fig. 13.44 Automatic load shedding diagram

- 1 From standby shedding
- 2 From principal source
- 3 Switchgear QA-01
- 4 Switchgear QP-01
- 5 Switchgear QP-02
- 6 From diesel sets
- 7 Unit substation 13.8 kV - 460 V (typical)
- 8 Class III loads
- 9 Class I loads
- 10 Class II loads
- 11 Undervoltage relay
- 12 Trip
- 13 Normally closed
- 14 Normally open

* Note: During load shedding, the breaker indicated with * remains open. However, if required, the operator can close it manually and therefore connect some class II loads to the diesel sets



The dc systems are two-wire ungrounded which contribute to their reliability, since occurrence of the first ground does not require immediate disconnection but nevertheless is detected. The batteries are of alkaline type with a nominal voltage of 125 V and are installed on metal racks in the various battery rooms.

The battery chargers are of a static type supplied from either the 50 Hz or 60 Hz 460 V - three-phase system via a transfer switch.

Selection of the required operating mode of floating charge or equalizing charge (automatic or manual) is made at the charger control panel. When in automatic operation, a battery is automatically returned to the floating mode after it is fully charged and equalized. Manual charging and equalizing has to be continuously supervised until completed. Because of the high voltages involved, during

equalizing a charger supplies only its own battery with the loads disconnected.

Chargers have internal heaters, lighting and plug receptacles which are supplied from external 220 V auxiliary power sources.

Battery charger panelboards are divided into three sections:

Full wave rectifier groups.

- Circuit breakers for supply of the various distribution panelboards.
- Circuit breakers for interconnection with the other battery charger.

There are interlocks to prevent paralleling of two chargers when in the equalizing charge mode or if the load or the interconnection circuit breakers are closed. The circuit breakers are equipped with devices which prevent their removal under load.

Principal equipment characteristics:

Batteries

Type	Alkaline
Number of cells	94
Nominal voltage	112.8 V
Nominal system voltage	125 V
Equalizing charge voltage	32 V
Capacity	
Other than assembly areas	700 Ah
Assembly areas	400 Ah

Battery chargers

Type	Static
Nominal supply voltage	460 V ac three-phase (50 or 60 Hz)
Nominal output voltage	125 V dc
Nominal output current	300 A dc (generating unit loads) 200 A dc (emergency lighting) 100 A dc (emergency lighting assembly areas)

EMERGENCY DIESEL GENERATORS

Standby diesel generator facilities are located at El. 127 downstream of powerhouse line D at the right and central assembly areas, and comprise the following equipment at each facility:

- Two diesel generators with the following characteristics:

Rated output	5.25 MVA
Power factor	0.8
Frequency	50 Hz (right assembly area) 60 Hz (central assembly area)
Voltage	6.9 kV

- Two power transformers three-phase 6.9-13.8 kV, delta-wye, to step up the generator voltage (6.9 kV) to the auxiliary system voltage (13.8 kV).

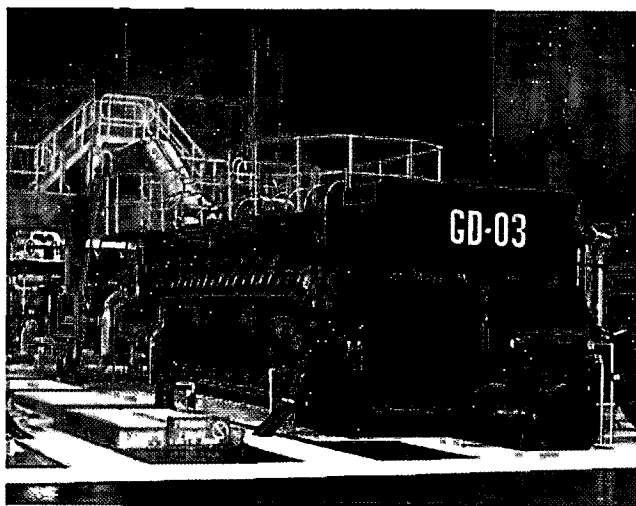
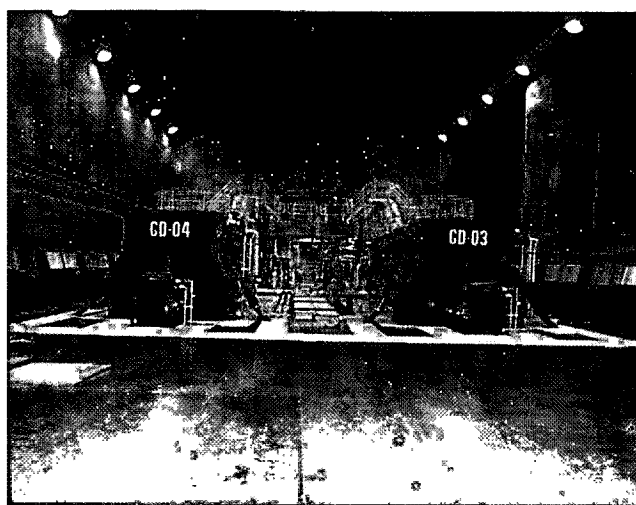
- One 13.8 kV switchgear (CS) with a split main bus and tie-breaker for the distribution of emergency power.

- Fuel storage area with two tanks for storage of filtered diesel oil, one tank for filtered diesel oil, filtering and pumping equipment.

- Bridge crane for handling diesel and generator parts.
- Distribution cubicles.
- Control room.
- Compressed air starting equipment.
- Diesel exhaust piping and silencer.
- Closed loop water cooling system with water/powerhouse cooling water heat exchangers.

Raw cooling water is normally taken from the powerhouse cooling water supply. If this is not available then the supply is from two emergency pumps taking water from the tailrace at El. 92.4.

- Lubricating oil circuit, complete with holding tanks.



Standby diesel generators

OPERATIONAL EXPERIENCE

Dry type transformer used in the 460 ac general systems are class F epoxi insulated, numbering eighty units. During operation, many units failed. Extensive studies and investigations showed many manufacturing defects in insulation. Considering the equipment not reliable, ITAIPU decided to buy six spare units from another supplier.

ELECTRICAL GENERAL SERVICES

LIGHTING SYSTEM

In the powerhouse the system consists of six principal unit substations (QI), and a number of auxiliary panels (CLF). The substations (QI) receive power from the main 13.8 kV switchgear assemblies (QP-01/02 or QP-03/04) and from the emergency switchgear CS-01/02. Each unit substation has three-phase, 13.8 kV-460/266 V, 1500 kVA (500 kVA emergency), delta-wye grounded connected dry type transformers, three bus supply 460 V circuit breakers and a number of outgoing feeder circuit breakers supplying the CLF panels. Between the bus sections are circuit breakers for shedding of class II and III loads.

The auxiliary panels (CLF) are equipped with three-phase, 460-230 V, 300 kVA dry type transformers with incoming and secondary circuit breakers. The panel feeders supply the local lighting panels (QL).

Emergency dc lighting is used in strategic locations to assure safe circulation of the operating personnel.

Illumination levels

Illumination levels in lux, are as follows:

Local control room	500
Rooms containing distribution substations, motor control centers, panelboards and various electromechanical equipment	200

Drainage and inspection galleries

General	20
Instrument areas	200
Pipes and inspection galleries	100
Inspection pits and their accesses	10
Galleries and passages in the main dam	20

Dam crest

General	10
Vehicle access areas	20
Areas external to the powerhouse	10
Emergency lighting (dc)	5

Types of lighting

The following types of illumination are used:

- Incandescent lighting in closed areas, such as galleries, recesses and also for emergency lighting.
- Fluorescent lighting in the areas where high lighting levels are needed to facilitate supervision and operation of equipment, or in some specific areas, such as the generator pit walls, where incandescent lamps are damaged by vibrations in the structure.
- Mercury vapor lighting where lighting fixtures had to be installed at the height of 6 m or more and where high lighting levels are required.

GROUNDING SYSTEM

The grounding system encompasses the powerhouse main dam and diversion structure, right bank lateral dam and the spillway. The use of low voltage cabling between the various areas meant that the grounding systems had to be solidly interconnected to control ground potentials and to avoid insulation failures and incorrect operation of protective relays due to transient potential differences.

The general philosophy applied to the design of the grounding system was that every metal part irrespective of its location must be connected to the grounding system.

Overall grounding system resistance was calculated to be 0.254 Ω , which was confirmed by measurements. This value is satisfactory for the proper functioning of various protections and the control of overvoltages. There is no direct interconnection between the powerhouse grounding mat and grounding mats of the right or left bank substations, although the transmission line ground wires are continuous. Control and protective functions associated with substations are performed through microwave channels and powerline carrier.

The grounding mat placed under the powerhouse is made of 1000 kcmil copper cables with vertical risers of 1000 kcmil provided in each powerhouse structural block. Embedded grounding plates are

located at various locations and elevations so that grounding connections to the equipment can easily be made. Interconnection between the powerhouse and the main dam renders them one common system. Interconnection between the grounding systems of the spillway and the powerhouse is made by two 1000 kcmil stranded copper cables, a grounding mat under the area being unnecessary. To ensure reliable low impedance grounding, one cable is run at the crest of the right bank lateral dam in trenches together with the control cables, and the other over foundation rock. These two cables have multiple vertical interconnections spaced approximately 15 m apart along the length. The cable which runs along the dam crest also serves to ground all the metal structures such as piping, railings and lighting posts. Reinforcing bars of each dam block are separated and their grounding depends on connections to the metal structures and the grounding cable.

Insulation coordination studies showed that the fast front voltages, which could be produced by transmission line circuit shielding failure or by flash-over across line insulators, should not encounter at the lightning arresters a ground impedance in excess of 5 Ω . This requirement could not be assured with conventional grounding mats and it was decided to construct supplementary grounding mats from prefabricated iron grids (with spacing of 15 cm) and to interconnect it vertically with a copper grounding grid at various points. In the powerhouse such mats are installed along the SF₆ and the transformer galleries, and at El.144 at the outgoing 500 kV lines. A similar solution was adopted at the intake portion of the dam, where lightning arresters are mounted on platforms at El.195. Here transient grounding mats are provided and also connected to the respective trash rack and gate-guides.

Additional grounding was also placed at the footings of nearby transmission towers by increasing the area of the grounding grid at the tower footing. The grids were constructed from no. 2 AWG copper cables with 2 m x 2 m spacing and with the areas between 20 m x 20 m to 50 m x 50 m and corresponding impedances from 9.5 Ω to 5.2 Ω .

WIRING SYSTEMS

Control and power cables are run in cable trays, steel conduits and cable trenches. Cable trays are the preferred method and are used wherever

feasible. Cable trenches are avoided generally, but are utilized in the galleries containing the SF₆ equipment, in the transformer gallery and at locations where other solutions would be difficult or costly. During construction some of the trenches were accidentally filled with water when concrete floors were washed and hence later design of the cable trenches included drainage connections.

The cable trays are of ladder type and are manufactured from hot dipped galvanized steel. Widths of the trays vary from 200 mm to 600 mm with intermediate sizes of 400 and 500 mm.

CABLING

Cables were used for control, lighting systems and auxiliary power of different voltage classes.

- Control cables, insulation class 600 V. These cables are predominantly multiconductors. The conductors are made of tinned, soft twisted copper wires. Cables larger than no. 14 AWG have nineteen individual strands. Insulation of the conductors is PVC for normal operation at 70°C. The cables are equipped with an outer protective jacket of flame resistant PVC. Where necessary external shielding consists either of two copper tapes or copper braid.
- Cables for low level signals such as transducers, resistance temperature detectors etc. These cables are insulation class 300 V and are made of twisted pairs or three wires and have an overall shield.
- Cables for lighting systems, insulation class 600 V. These are single conductor, without external protective jacket. The materials used in their fabrication are the same as for control cables, except they are for normal operation up to 75°C.
- Power cables. This group includes cables of 600 V class and also cables of 15 kV class. Their insulation is thermosetting for normal operation at temperatures up to 90°C. These cables are single conductor, equipped with an external PVC protective sheath. The 15 kV class cables are also provided with a metallic armor.

COMMUNICATIONS

The communication systems were designed to give reliable performance for voice communication to operation and administration purposes, transmission line teleprotection, control and data transmission, teletype and facsimile transmission and personnel paging systems within the power plant.



Cable trays

Telephone systems

The basic automatic telephone system provides voice communications in the project area. Included are a central PABX exchange in each of the 50 Hz and 60 Hz areas of the powerhouse, a secondary PABX in each of the right and left bank areas, and a PAX exchange in the right bank substation, the right bank staff housing (Area 1), and the left bank staff housing (Vila B). It also interconnects with the public systems of Paraguay (ANTELCO) and Brazil (TELEPAR), see Fig. 13.45.

The central PABX exchanges can each accommodate 450 extensions and are interconnected by forty tie-lines. The PABX in the 50 Hz sector is equipped with fifty-four trunk lines to the ANTELCO system in Paraguay while the 60 Hz has the same to TELEPAR in Brazil. Some of the interconnections utilize voice channels of the microwave and UHF radio systems.

It is foreseen the installation of a telecommunication integrated network including a digital telephone station in the powerhouse as well as the substitution of the previously installed PABX systems with the new interconnected digital telephone centers in right bank and Foz do Iguaçu substations. This network will provide data and voice transmission in one integrated system and will allow interconnection with normal phone systems in Brazil and Paraguay.

The selective switching telephone system provides voice communications in the powerhouse and spillway sectors. It is a hardwired system between the locations of operating priorities of load dispatch, central control, unit control, and spillway.

Powerline carrier

Powerline carrier systems are used for transmission line primary protection and voice communications on the 500 kV and 220 kV systems. Each 500 kV transmission line utilizes two channels for protection (in each direction) giving a total of sixteen channels for the eight 500 kV lines at the powerhouse. In addition, two channels are used for communications to each of the right bank and Foz do Iguaçu substations. The 500 kV transmission line interconnections between the right bank and Foz do Iguaçu substations are similar. The 220 kV transmission lines from the right bank substation to Acaray and Limpio substations utilize four channels for protection (in each direction) and two channels for voice communications, see Fig. 13.46.

Microwave system

The microwave system is used for transmission line protection on the 500 kV systems. In addition, it is used for data transmission from the right bank and Foz do Iguaçu substations to the powerhouse and for control of the right bank substation from the

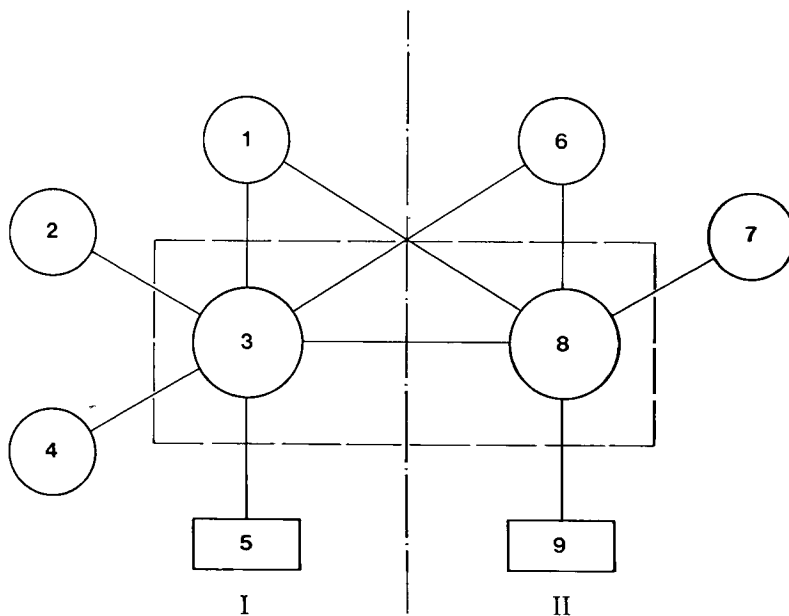


Fig. 13.45 Telephone system

- I Right bank
- II Left bank
- 1 PAX area 1
- 2 PABX right bank work area
- 3 PABX-1 50 Hz sector
- 4 PAX right bank substation
- 5 Public office ANTELCO
- 6 PAX vila B
- 7 PABX left bank work area
- 8 PABX-2 60 Hz sector
- 9 Public office TELEPAR

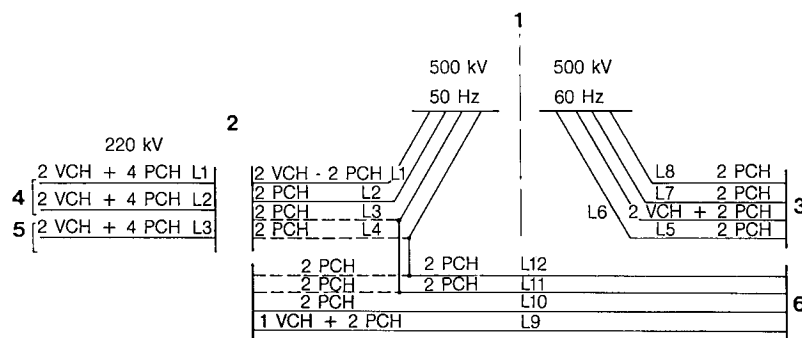


Fig. 13.46 Powerline carrier system

- 1 Powerhouse
- 2 Right bank substation
- 3 Foz do Iguaçu substation
- 4 Acaray substation
- 5 Limpio substation
- 6 Converter substation
- VCH Voice channel
- PCH Protection channel
- Future

powerhouse. The microwave system is basically an extension of the FURNAS system and connects with Brasília, Campinas, Rio de Janeiro and Curitiba. The frequency band utilized is 6 GHz, see Fig. 13.47.

Fiber optic cable

The fiber optic cable system is used for 500 kV line protection between the powerhouse and the Foz do Iguaçu substation. The system consists of two separate, redundant, cable circuits using multifiber cables. One circuit is installed in underground ducts and the other on an overhead messenger wire.

UHF radio

The UHF radio is used primarily for voice communications in and beyond the project area and consists of three links. The powerhouse has separate links to TELEPAR and ANTELCO. The third

link is between the right bank substation and Acaray. The frequency band for the links to TELEPAR and ANTELCO is 1500 MHz and to Acaray is 370 MHz, see Fig. 13.48.

VHF radio

The VHF radio is used only for voice communications in the project area and consists of a base station at the powerhouse with twenty mobile (vehicle) transceivers and twenty walkie-talkies. There are four channels available in the frequency band of 160 MHz. The system can be interconnected with the PABX exchanges in the powerhouse, see Fig. 13.49.

Paging systems

The basic paging systems are of a public address type, with one system for the 50 Hz and one for the 60 Hz sectors. These can be interconnected for

Fig. 13.47 Microwave system

- I Right bank substation
 II Itaipu power plant
 III Foz do Iguaçu substation
 1 Multiplex
 2 Radio
 3 Hybrid
 CH Channel
 V Voice channel
 TP Teleprotection channel
 RC Remote control channel
 DT Data transmission channel
 TLX Telex channel

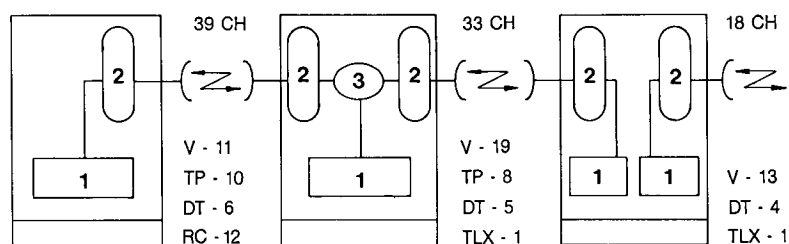
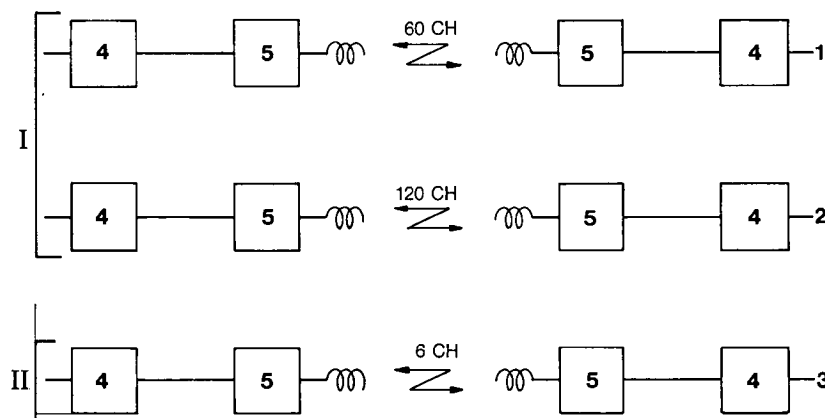


Fig. 13.48 UHF Radio

- I Powerplant
 II Right bank substation
 1 Telepar
 2 Antelco
 3 Acaray substation
 4 MUX
 5 Radio
 CH Channel



common operation. Each system has a main intercommunication unit (UIP), several secondary units (UIS), and an extensive system of area (AF) and room (CAC) type speakers. These total 360 (UIS), 1030 (AF) and 100 (CAC), see Fig. 13.50.

For areas beyond the fixed speakers of the basic system, including the residential areas, a beeper system (BIP) is used. In the powerhouse there is a master station consisting of a radio system, command console, codifying unit and two interfaces for the PABX exchanges. Repeater transmitters are used to cover zones remote from the powerhouse. The system utilizes seventy pocket type beepers with code number displays for messages, see Fig. 13.51.

Direct current power supplies

The communication systems have their own dc power supplies. These consist of storage batteries, chargers, distribution switchboards, and in some cases, 125/48 V dc converters as shown in Table 13.5.

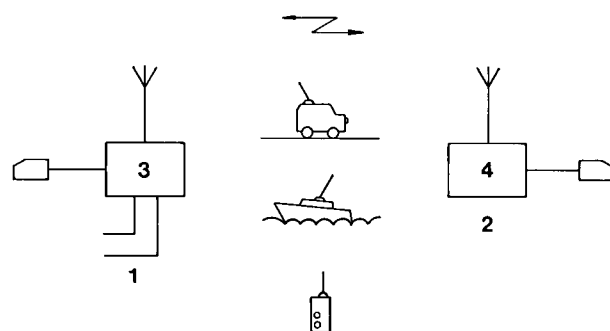


Fig. 13.49 VHF Radio

- 1 Powerhouse
 2 Right bank substation
 3 Base station
 4 Fixed station

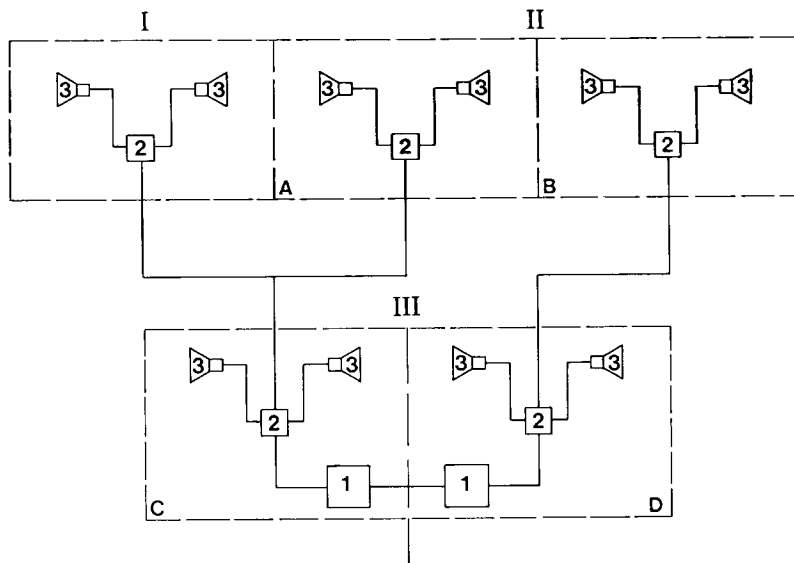


Fig. 13.50 Paging system

- I** Spillway
II Main dam
III Powerhouse
A Blocks F1/F24
B Blocks F25/F36, H1/H14, I1/I21
C AMD1/U9A
D U10/U18A
1 Primary intercommunication
2 Secondary intercommunication
3 Loudspeaker

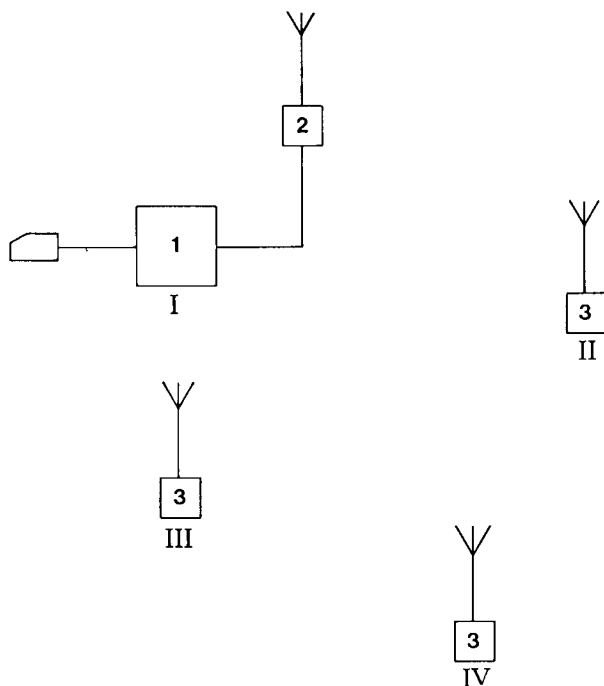


Fig. 13.51 Display for pocket beeper messages

- I** Itaipu project area
II Left bank residential area
III Right bank residential area and Ciudad del Este
IV Foz do Iguaçu
1 Central unit
2 Master station
3 Repeater station

FIRE SURVEILLANCE

Effective fire fighting requires early detection of fire and an accurate indication of its location. To accomplish this the project has been subdivided into areas, or zones, each equipped with an extensive network of detectors connected to automatic alarm units. In addition to giving an alarm the system, in some areas, carries out operating functions such as shutting off ventilation equipment and closing fire doors.

The system was developed in two stages, and although the equipment and functions are similar, the designs are somewhat different. The earlier stage used a four wire system with a mixture of electronic and electromechanical relays. The later stage used a two wire system and is totally electronic. Both systems include extensive self-monitoring and test facilities to confirm the readiness of the equipment to function.

The system uses a variety of fire and combustion product detectors depending on the location and the expected type of fire. The main units are:

- Ionization detectors. In which the combustion products, visible or not, that penetrate the detector cause the loss of equilibrium between two ionization chambers.
- Optical detectors. In which the combustion products, mainly visible (smoke), that penetrate the detector cause the loss of equilibrium between two light chambers.

Table 13.5 Communication system – dc power supply

Area	Equipment			
	Charger	Distribution panel	Batteries	Converter
Powerhouse (50 Hz sector)	48 V/150 A	48 V/400 A	48 V/700 Ah	
Powerhouse (60 Hz sector)	48 V/150 A	48 V/400 A	48 V/700 Ah	
Powerhouse (U9 / El. 124)	48 V/75 A	48 V/200 A	48 V/330 Ah	
Main dam				125/48 V/40 A
Right bank substation	48 V/50 A	48 V/200 A	48 V/235 Ah	

- Heat detectors. In which the rate of temperature rise or a fixed temperature limit is exceeded. (Mainly for areas where combustion products can be present in normal operations).

- Manual stations. In which the fire is detected visually and a break-glass station is used.

The application of the type of detectors was made on an assessment of the type of fire that might occur and the area involved. In general, the ionization and optical detectors were used to cover an area of 81 m² and mounted at maximum height of 8 m, while the heat detectors were used to cover 36 m² at a height of 7 m.

The powerhouse fire detection system which formed the first four-wire-stage consists of twenty-two local control units (LCU's) 276 ionic, 168 optic, twenty rate-of-rise temperature, and sixty-eight manual stations or detectors. The areas covered are:

- Excitation equipment gallery (El. 98.5), with ten LCU's and twenty circuits (one for each generator area).
- Cable gallery (El. 127.6), with four LCU's and twenty-two circuits.
- Cable gallery (El. 108 above local control rooms), with four LCU's and twenty-two circuits.
- Emergency diesel generator rooms, with one LCU and one circuit in each of the two rooms.
- Standby frequency converter rooms, with one LCU and one circuit in each of the two rooms.

The system alarms locally at the associated LCU and remotely at the local control room (panels ASLP01 and ASLP02) and at the SCADA system. No secondary operating actions, such as ventilation

control, are undertaken. The local display shows not only the circuit, detector or manual station initiating the alarm but several possible types of circuit failures and allows circuit testing.

The powerhouse fire detection system which formed the two wire stage covered:

- Communication rooms (central control area), with one LCU having two circuits and one spare in each of the two rooms.
- Load dispatch area, with one LCU and fifteen circuits in the dispatch room and visitors area.
- Local control rooms (El. 108), with one LCU having two circuits and three spares in each of the ten rooms.
- Central control room, with one LCU having two circuits in the control room and four circuits in the auxiliary services room.

The system alarms locally at the associated LCU and remotely at the central control room (panel ASP) and at the SCADA system. Audible and visual signals are given in some locations. The local display shows not only the circuit, detector or manual, indicating the alarm but allows resetting and functional testing.

The right bank substation which formed part of the second two-wire-stage covered:

- Relay house, with one LCU having eight circuits on the first floor and nine circuits on the second floor.

In addition to visual and audible signals, on both floors, the system gives an outside audible alarm, remote signals to the powerhouse central control room and SCADA, and shuts down the ventilation and air conditioning systems.

CONTROL, SUPERVISION AND

PROTECTION

INTRODUCTION	14.3
CONTROL	14.3
General Description	14.3
Control of the Generating Units	14.5
Local Control Rooms	14.8
Facilities External to Local Control Rooms	14.11
Central Control Room	14.13
Load Dispatch Center	14.18
SUPERVISION	14.19
Generating Units	14.20
Step-up Transformers	14.21
Gas Insulated Switchgear (GIS)	14.21
Revenue Metering	14.21
TADMIC Supervisory System	14.22
SCADA SYSTEM	14.23
General Description	14.23
System Functions	14.23
System Configuration	14.23
Design and Performance Features	14.25
PROTECTION	14.25
Generating Units	14.25
Step-up Transformers	14.27
Unit Auxiliary Transformers	14.27
Special Current Transformers	14.27
500 kV GIS BUS	14.28
500 kV Transmission Lines (50 Hz)	14.29
500 kV Transmission Lines (60 Hz)	14.29
HVDC Converter Station Interface	14.29
Forced Isolation Scheme	14.29
Protection Panels	14.30

CONTROL, SUPERVISION AND PROTECTION

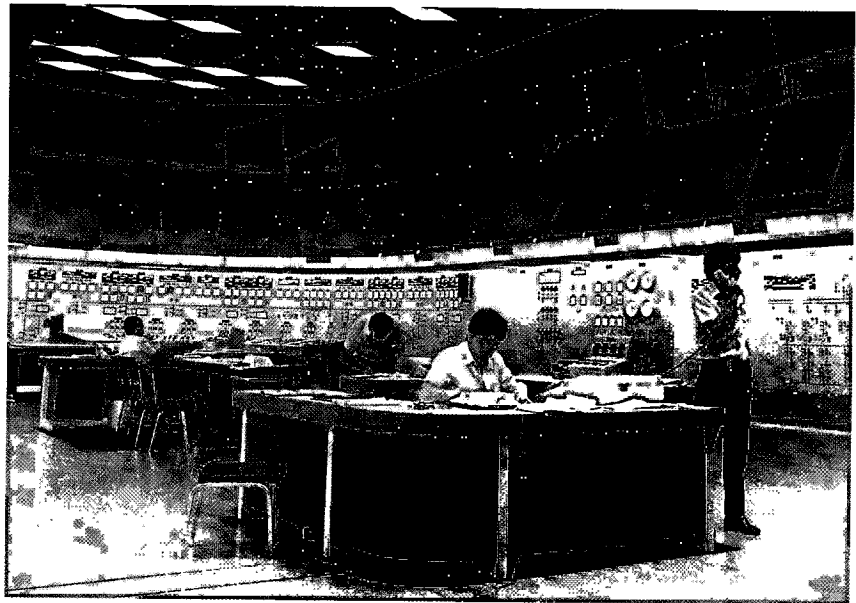
INTRODUCTION

The Itaipu powerplant control, operations, supervision and equipment protection features cover all parts of the project and involve generation, power transformation, transmission lines, substations, plant auxiliary systems, water use management, operation and maintenance scheduling, training and the security of the project facilities. These systems are described in this Chapter. Excluded are systems and equipment used for powerplant operation and maintenance such as cranes, ventilation, potable water and other similar non-essential plant equipment.

CONTROL

GENERAL DESCRIPTION

The basic control of the powerplant generating units and ancillary equipment can be performed from two different locations: the unit local control rooms and the powerplant central control room. The initial control system installation uses hardwired circuitry to perform powerplant control functions. In the future the present analog hardwired control system will be supplemented by a digital



*Central control
room*

supervisory control and data acquisition (SCADA) system which will include controls and additional detailed information for better powerplant monitoring and will have approximately 25 000 data and 1000 control points. When the new digital SCADA system is in operation the present analog system will serve as a backup. The block diagram for the future powerplant control scheme is shown in Fig. 14.1.

The main features of the powerplant control system are:

- Central control room (CCR) which is located in the powerhouse main structure, downstream part of blocks 9A and 10, and has facilities for control and supervision of the powerplant and the right bank substation.
- Local control rooms (LCR) . There are ten local control rooms. Each pair of generating units has one

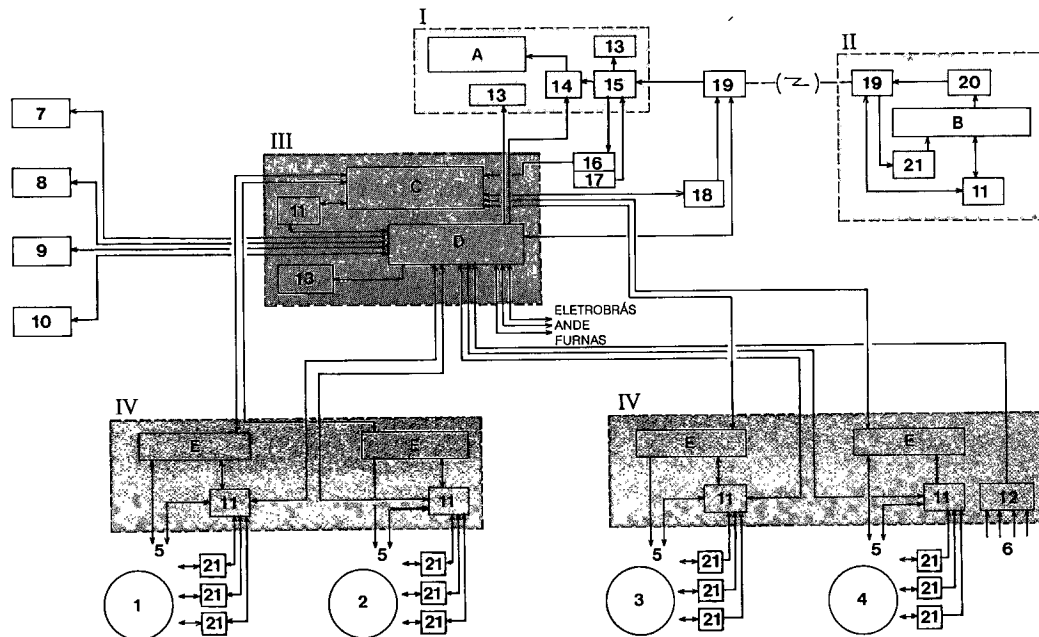


Fig. 14.1 Plant control - general block diagram

- I Load dispatch room
- II Right bank substation
- III Central control room (CCR)
- IV Local control room (LCR)

- A Mimic board and registers
- B Control switchboards 500 kV, 220 kV, 66 kV and auxiliary services
- C Control switchboards (hardwired system)
- D SCADA master station
- E Unit control switchboard (hardwired)
- 1, 2, 3, 4 Generator
- 5 To unit devices
- 6 From monitor devices
- 7 Spillway RTU

- 8 Dam RTU/MOD, typical (4)
- 9 Auxiliary services RTU/MOD, typical (10)
- 10 500 kV SF₆ RTU/MOD, typical (6)
- 11 RTU - Remote terminal unit, typical (2)
- 12 RC - Equipment cabinet (MONDIG)
- 13 CRT's and printers
- 14 CPMR - Mimic board and registrar controller (TADMIC)
- 15 TDC - Load dispatch terminal (TADMIC)
- 16 CRMP - Right bank substation panel controller (TADMIC)
- 17 TCC - Central control terminal (TADMIC)
- 18 PTC - Telecontrol panel

- 19 MCW - Microwave
- 20 TMD - Right bank terminal (TADMIC)
- 21 Modem
- SCADA - Supervisory control and data acquisition
- TADMIC - Digital data acquisition system (right bank substation)
- MONDIG - Monitoring and diagnostic subsystem
- MOD - Data acquisition and control module
- Control cable
- Fiber optic cable
- Note: Numbers in parenthesis indicate quantities

common local control room. At each LCR two generating units can be controlled and monitored including the corresponding transmission line to the substation.

- Right bank substation control room is located at the right bank substation. It has facilities for controlling 500 kV and 220 kV transmission lines which deliver 50 Hz power to Paraguay and to the Foz do Iguaçu HVDC converter station in Brazil.
- Foz do Iguaçu substation control room is located at the substation and has controls for transmission of the 60 Hz and HVDC power to Brazil.
- Spillway control room is located at the left side of the spillway structure and has controls for opening and closing of the fourteen spillway gates.

In general local controls are also available at specific equipment locations. These controls are not used during the normal mode of operation but are there only for testing and maintenance. Where dual equipment exists, for example like pumps or coolers, a pre-selection of a "lead" device is made at this location.

Central control is the normal operating mode for the powerplant. Control from the unit local control rooms is primarily used during commissioning, testing, initial operation and in case of emergency when the central control room is not available. Because of a large number of generating units, and the possibility of having a limited number of operators during an emergency, a considerable amount of control automation is incorporated in the unit local control rooms.

Local controls are effective only when the corresponding "local-central" control selector switch located in the CCR is in the "local" position.

In general all control levels are mutually exclusive, each device is either under "central" or "local" control, but never simultaneously under both. There are exceptions to this rule where equipment functions independently of the chosen control level, for example:

- Protective features, such as circuit breaker trips.
- Unit emergency shut-downs.
- Lowering of intake gates.
- Release of CO₂ generator fire protection.
- Safety interlocks.
- Instrumentation.
- Alarm annunciation.

Local alarm annunciator windows are combined in groups before information is transmitted to the CCR to minimize the number of the annunciator windows at CCR.

The local control facilities at the spillway and substations are described in the respective sections dealing with these areas. Following is the description of the powerhouse controls.

CONTROL OF THE GENERATING UNITS

Starting sequence

The unit starting sequence is divided into three distinct steps:

- Preparation to start.
- Start.
- Synchronize.

The first two steps can be accomplished automatically or manually at the unit local control room, however synchronizing can be done only manually.

Unit manual control is possible only at the local control room and is foreseen to be used only during unusual operating conditions such as unit testing, failure of the automatic control system or for training of the operator.

Preparation to start - Automatic mode

Pressing the "preparation to start" push-button will automatically bring all generating unit auxiliary equipment and devices to their required ready to start position. As they progress all sequential operations are shown on the order indicators and when all sequential operations are completed, the indication "preparation to start completed" is given. The total time of this process is supervised and if the time is greater than the preset limit the timing relay will interrupt the starting sequence and sound an alarm. Devices which were already actuated will remain so, and by observing the order indicator, the faulted event in the starting sequence can be identified. To return the unit to the initial condition, after a "preparation to start" sequence is completed or interrupted, the "stop" command must be given.

Preparation to start - Manual mode

To perform "preparation to start" manually the following action must be taken by the operator:

- Place the selector switch to manual control position.
- Open the unit cooling water valve.
- Start excitation cooling.
- Start unit step-up transformer cooling.
- Start governor oil pumps.
- Apply generator brakes.
- Check position of the field circuit breakers (normally closed).
- Set turbine wicket gate limiter to 100%.
- Set load-frequency control at nominal "speed-no-load" position.
- Adjust excitation controls for starting. The voltage regulator must be adjusted to nominal no-load voltage.

Automatic start

In this mode a generating unit can be started only if the "preparation to start" sequence is completed and all required pre-conditions are met for water intake, turbine and governor. The generator brakes must be released, lock-out relays reset, motor control center (MCC) energized, dionized cooling water system in operation, field flashing circuit breaker closed and other necessary pre-starting conditions met.

When the starting command is given, it is registered on the order indicator as "unit starting". This indication remains until the starting sequence is completed and then the indicator changes to "ready to synchronize".

The unit starting is supervised by a timer, which will give alarm and return the unit to the "preparation to start" condition if the preset time expires before the completion of unit starting sequence, so that after localizing and correcting the defect a new automatic start can be attempted.

Manual start

To perform a manual start the following action must be taken by the operator:

- Place the selector switch to manual control position.
- Start the high pressure thrust bearing oil lift pump.
- Release generator brakes.
- Open governor oil pressure tank valve.
- Release the turbine servomotor locks.
- Set the shut-down solenoids to the "start position" (turbine governor assumes control of unit acceleration).
- Apply excitation (at this step the stator dionized water cooling system would be operating).

When machine reaches 90% of the nominal speed and voltage the unit start is completed and the machine is ready to be synchronized.

Synchronizing

At the unit local control room only manual synchronization is possible. In the future, when SCADA system is operational, manual synchronization from the central control room will also be possible. The operator using a synchroscope, double scale voltmeter and double scale frequency meter, initiates the closure of the circuit breaker when conditions are appropriate.

Normally, synchronization is made across the unit circuit breaker (152U), to the adjacent section of the main 500 kV bus. However, it is also possible to synchronize the unit across the 500 kV center circuit breaker (152T) to the adjacent generator and the

alternate 500 kV main bus. **Two synchronizing selector switches (with removable handles) assure that the correct bus potential is used.** The bus voltage, taken from potential transformers, is designated as "running" and the generator voltage taken from the capacitive potential device of the unit transformer high voltage bushing as "incoming".

The closure of the circuit breaker is supervised by a synchronism check relay, which requires that:

- Voltage difference be less than 3%
- Angle difference be less than 30°
- Slip frequency be less than 0.02 Hz.

Normal unit stop

Once normal unit stop command is initiated it will be completed without further action by the operator and is independent of the selected operating mode. The unit load is automatically reduced by the turbine governor and, when the turbine wicket gates are in the "speed-no-load" position, the unit is disconnected from the system. The turbine wicket gates are closed, excitation removed and subsequent steps are taken automatically until the unit is stopped and the auxiliary systems disconnected. The operation of dionized water cooling system for the stator winding is maintained to keep the winding temperature above the condensation point. Heaters are switched on if the unit is stopped for a long period of time.

All principal steps in this sequence are supervised by timers which actuate alarms and implement further measures if required. The unit can be restarted prior to the completion of the sequence, but only after the unit has stopped. To restart the unit again the "preparation to start" push-button must be depressed and followed by the "start" command.

Unit shutdown

Unit shutdowns are necessary for the safety of the unit and to minimize possible damage to the equipment due to a fault, and which also typically result in a load rejection and thus in a unit overspeed. In cases like high bearing temperature condition, unit overspeed could subject the bearings to further damage, therefore shutdown sequence initiated by a bearing high temperature detection does not permit unit overspeed. Some protective relays are associated with types of faults which require unit inspection prior to restarting, hence these protective schemes employ lockout relays which can be reset only manually.

Other protection operation such as those associated with the transmission system

disturbances and equipment overload normally do not cause equipment damage and therefore are of the non-lockout type and do not require manual resetting of the lockout relays. For certain faults it is not necessary to stop the unit and it is sufficient to disconnect the unit from the system and continue to operate the unit at speed-no-load. This mode permits a faster return of the unit to operation, after the extent of the fault condition is verified and the unit safety is assured.

All combinations of unit shutdown are as follows:

	D	E	F	G
A		05	86M	05A
B	86N			05B
C	86E			

- A With overspeed but without trip of excitation
- B Without overspeed
- C With overspeed and with trip of excitation
- D With lockout
- E Without lockout
- F With lockout and intake gate closure
- G Without lockout and unit going to speed no load

Following are the detailed descriptions of function of individual relays used:

Lockout relays 86E and 86TR. The protective relays which actuate these lockout relays are those which detect internal faults in the generator, excitation system, unit auxiliary transformers, isolated phase bus and the unit step-up transformers. These types of faults require the fastest possible unit disconnection from the system, quick generator de-excitation and the complete closure of the turbine wicket gates. Under these conditions the unit is subjected to overspeed.

Lockout relay 86M. This lockout relay is actuated by the mechanical overspeed switch and initiates complete unit shutdown with emergency closure of the intake gates. If necessary, the operator can operate the 86M relay by concurrently operating two emergency stop pushbuttons either at the panel ULP in the local control room or at the CCR control desk.

Lockout relay 86N. This lockout relay will operate when the protective relays and monitoring devices require a complete unit shutdown, so as to permit corrective action, but the nature of the fault is such that during the shutdown the unit has to be unloaded and there is no unit overspeed.

Complete shutdown relay 05 (non-lockout). The protective relay 05 detects unsatisfactory operating conditions within the unit and initiates a complete unit stop, but because of the transient and self-clearing nature of these faults, typically the unit can be re-started immediately.

Partial shut-down relay 05A (non-lockout). This partial shut-down relay is used in conjunction with the protective relays and devices that detect unsatisfactory operating conditions external to the unit and require the unit to be rapidly separated from the power system. Because the fault is external to the unit a complete shutdown is not required and the relay trips only the unit circuit breakers and actuates a partial shutdown so as to bring the unit to the "speed-no-load". The tripping action is immediate and the unit is subjected to overspeed.

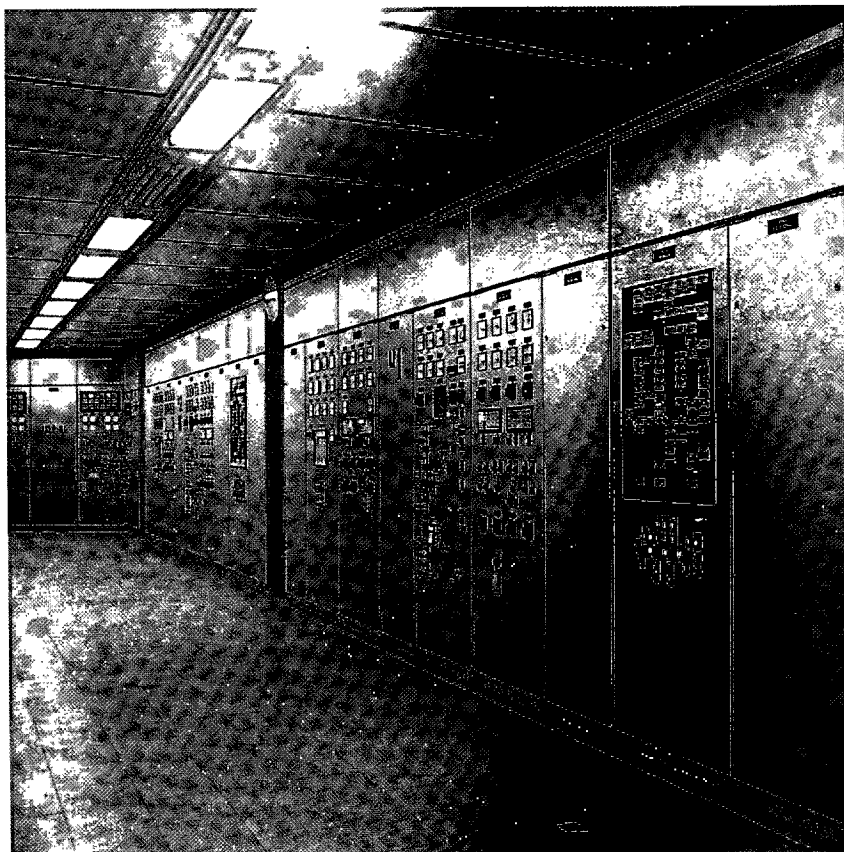
Partial shutdown relay 05B. The protective relays and devices that respond to unsatisfactory operating conditions of a possible temporary nature within the unit bring the unit to "speed-no-load" without overspeed. Alarms such as unit bearing high temperature (first stage of temperature relays), excessive unit vibrations, excessive shaft deflection and operation of some devices that monitor the dionized water stator winding cooling system require that the unit remains running, so that behavior of the unit's malfunctioning may be verified and the necessary corrective action taken.

Protective device alarms

Some protective devices associated with unit operation do not initiate a shutdown but only actuate an alarm. It is the operator's responsibility to take the necessary corrective action and if the action is not successful within a preset time or if the faulty condition reaches an undesirable level, the unit goes into a complete shutdown.

Routine testing of tripping circuits

Test facilities are provided to permit actuation of a special test lockout relay for testing the integrity of any of the input circuits to the tripping relays. Prior to such testing, the actual shutdown relay is blocked for operation.



Local control room panelboards

LOCAL CONTROL ROOMS

There are ten local control rooms (LCR) one for each two generating units, including future units nos. 9A and 18A. Local control rooms also have controls for the corresponding outgoing 500 kV overhead transmission lines.

Local control rooms are located at El. 108 at the downstream side of the generating units. All local control rooms are 32 m x 12 m in size, they are air conditioned and have vibration damped floors. A typical local control room layout is shown in Fig. 14.2 and the local unit control panelboard (UPL) arrangement is shown in Fig. 14.3. The UPL panelboard is made up of sections which include the devices as described below:

Panel ULP/01, 04, 07 and 09

- Terminal blocks.

Panel ULP/02

- Indicating instruments for the unit thrust and guide bearing temperatures (Dev. 38).
- Indicating instruments for the unit bearing oil levels (Dev. 71).

- Temperature recorder for selected unit temperature detectors (**twelve point**).
- Indicating instrument for selected unit temperature detectors.
- Receptacle for a **portable** temperature recorder.

Panel ULP/03

- Indicating instruments for turbine spiral case and the draft tube **water pressures**.
- Indicating instruments for cooling water temperatures.
- Indicating instrument for the turbine water flow.
- Indicating instruments for stator winding direct cooling **system water conductivity** (dionized water).
- **Two order indicators**, 20 points each.
- **Controls** for the governor oil pumps, main cooling water valve, stator winding pure water system, excitation system cooling ventilators and the heat exchangers of unit step-up transformers.

Panel ULP/05

- Meters for the generator output current, terminal voltage, active and reactive power
- Load-frequency setting indicators.

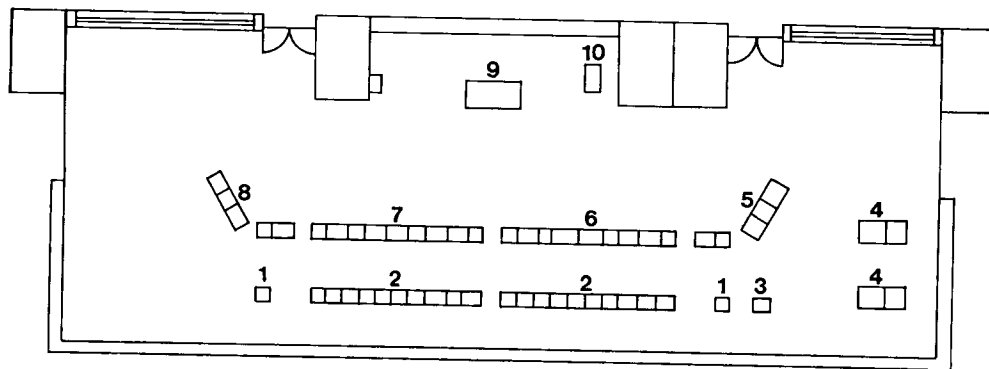


Fig. 14.2 Local control room arrangement

- | | | |
|------------------------------|--|---|
| 1 Turbine panels | 5 500 kV line control panel | 9 Operator's desk |
| 2 Protection and auxiliaries | 6 Generator no. 2 control panel | 10 Fire protection control panel (CO ₂) |
| 3 Line synchronizing | 7 Generator no. 1 control panel | |
| 4 SCADA's RTU | 8 Main auxiliary transformer control panel | |

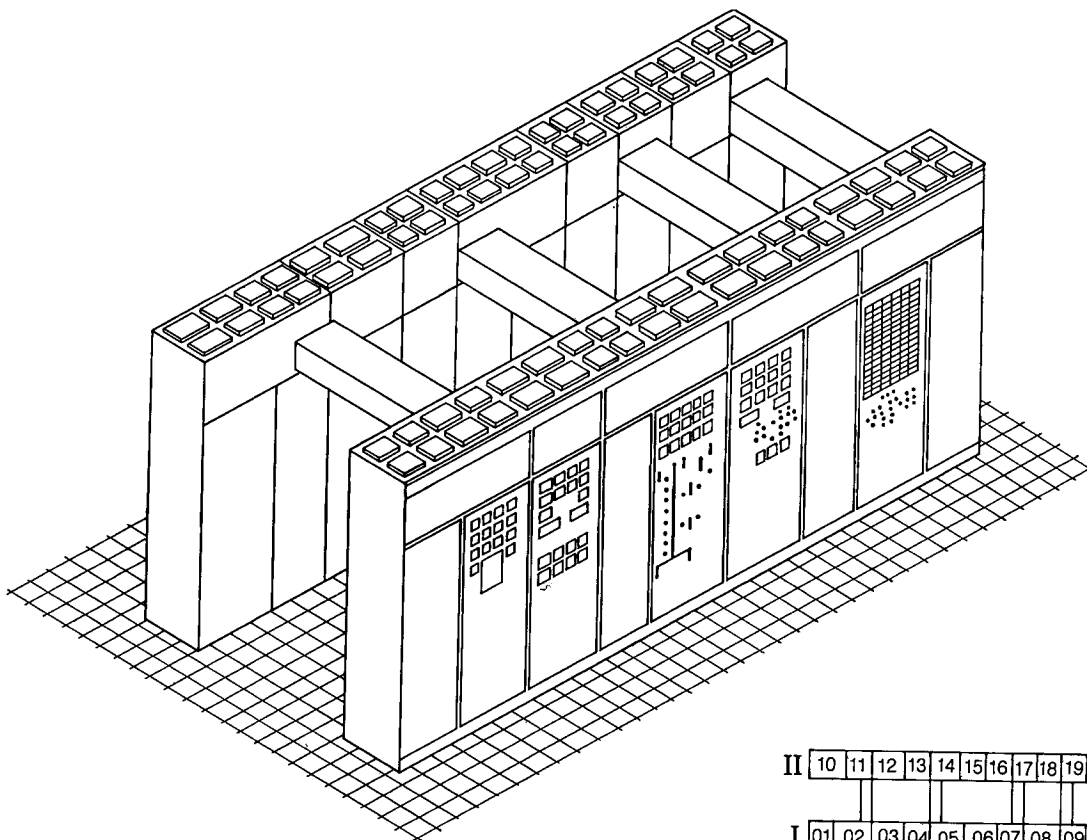


Fig. 14.3 Local control room panelboard layout

- | | |
|----------------------------------|------------------------------------|
| I Front panels (controls) | II Rear panels (protection) |
| 02/03 Indicating instruments | 10/12 Unit protection |
| 05/06 Control and indication | 13 dc distribution |
| 08 Annunciators | 11/14 Terminal block panels |
| 01/04 Terminal block panels | 15/16 Auxiliary relays |
| 07/09 Terminal block panels | 17/18 Terminal block panels |
| | 19 Indication and alarms |

- Synchronoscope with two volt and two frequency meter.
- Switches for the associated circuit breaker and disconnectors and position indicators for the grounding switches, all incorporated into mimic diagram of the panelboard. For the second generator of the same breaker-and-one-half bay, only semaphore type indicators are provided and the controls are on the other ULP assembly.
- Circuit breaker 52T controls (center breaker in the breaker-and-one-half scheme) which are duplicated on both unit ULP assemblies. Two synchronizing selector switches permit connection of the synchronizing equipment across the generator circuit breaker (52U) or the tie circuit breaker (52T).

Panel ULP/06

- Generator excitation system controls for manual and automatic voltage regulation.
- Indicating instruments for the unit speed, voltage regulator balancing, turbine gate limiter setting, and turbine gate limit position.
- Controls for reference voltage setting of the automatic voltage regulator, selector switches for

manual or automatic **voltage regulation**, manual excitation and turbine **gate opening**.

- Two order indicators, 20 points each.
- Partial unit shut-down and unit emergency shut-down solenoids.
- Switches to open or close the isolating valve of the governor oil pressure tank.
- Controls for manual application of the generator brakes, and removal or application of the servomotor locks.
- Controls for setting the shut-down solenoid in the start or stop position and for preparation of unit start.
- Controls for setting the turbine governor and voltage regulator to unit start positions, connection of the excitation and resetting of the unit creep detector.
- Controls for emergency closure of the intake gates.
- Selector switches for power system stabilizer manual or automatic control and unit start and stop controls.

Panel ULP/08

- Alarm annunciator (24 x 8 points) placed in one common enclosure with the associated control push-buttons.
- Indicating lamps to supervise the trip coil circuit continuity for the five shut-down relays (86E, 86N, 86M, 05A, 05B).

Rear Panels

Located behind the ULP control panelboard, there is a row of rear panels containing the generator protective relays, protection system accessories and the associated terminal blocks. The panels are:

ULP 10 and 12	Unit protection
ULP 13	DC distribution
ULP 15 and 16	Auxiliary relays
ULP 19	Annunciator relays
ULP 11, 14, 17 and 18	Terminal blocks

500 kV line local control panel (LLP) (Fig. 14.4)

- Mimic diagram and control switches for the two 500 kV breakers.
- Controls for lines L3 and L6 500 kV breakers.
- Controls for 500 kV bus sectionalizing circuit breakers.
- Position indicators for grounding switches.
- Line instrumentation (ammeter, voltmeter, wattmeter and varmeter).
- Alarms
- Annunciator, 40 points.

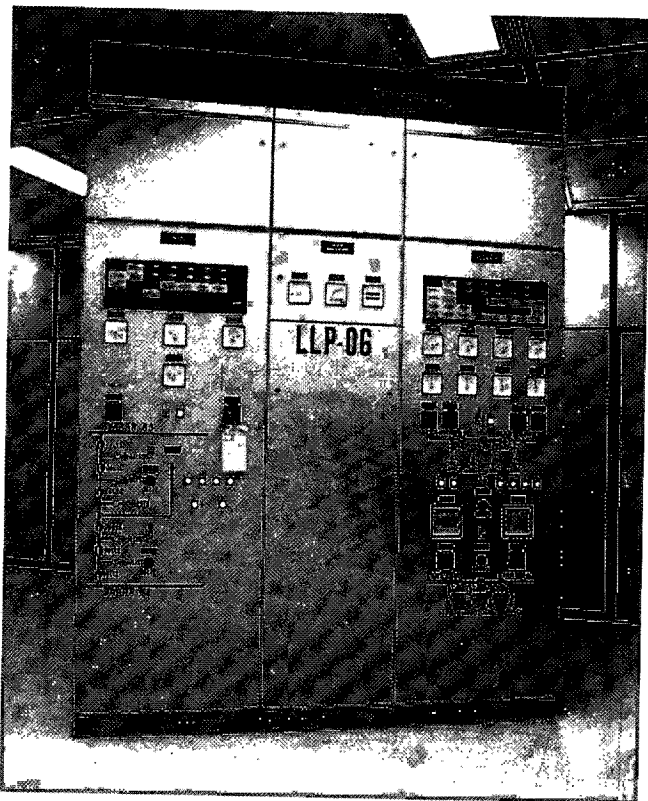


Fig. 14.4 Transmission line local control panel

Auxiliary services local control panel (ASLP)

- Control of frequency converter.
- Controls for emergency diesel generators.
- Controls for regulating transformers.
- Annunciators for auxiliary services.
- Auxiliary system mimic display.

Generator fire protection control panel (GFP)

Stand alone control panel for generator fire protection CO₂ system, one panel for each two generators.

Control panel description

The following panelboard components are identical, or very similar:

- Annunciators. Each window has four lamps which operate on 24 V dc. One window is used for supervision of the dc and it is actuated by a 120 V ac to 24 V dc converter. Failure of the dc also actuates a 120 V ac alarm horn. Each annunciator has a set of push-buttons for the following functions: event acknowledgement, function test, lamp reset, lamp test and "horn-off". An alarm event is indicated by a flashing light in the respective window and the sounding of the horn. Operation of acknowledge button silences the horn and changes the flashing light to steady light. The annunciator lamp remains lit until the alarm initiating event is eliminated and the lamp reset push-button depressed. The "horn off" push-button permits the disconnection of the alarm horn when it is not required, as in the LCR room where there are several annunciator assemblies and several horns inside the same room.
- Mimic buses and symbols. All 500 kV circuits are green, with square symbols for circuit breakers and round symbols for disconnecting switches.
- Control switches. All 500 kV circuit breaker and disconnect control switches are discrepancy type. When there is a change in the device position due to an external event, the light on the switch handle flashes until the operator manually resets the switch to the correct position. Grounding switches are not operated remotely, but the control room operator knows their position from semaphore type indicators which are 45° out of alignment with the mimic bus, when the grounding switch is open.
- All indicating instruments are 96 mm x 96 mm size.
- Auxiliary relays are installed inside the ULP assembly for contact multiplication and when the generating units are under central control, auxiliary interposing relays provide separation of the CCR and the local control room dc power supply.
- The unit control and metering panel (ULP/05) indicating instruments related to the generator and

the step-up transformer, are connected to the secondaries of the instrument transformers. Other instruments receive their input via transducers having various characteristics, but mostly 4-20 mA.

FACILITIES EXTERNAL TO LOCAL CONTROL ROOMS**Generating unit**

Outside the local control room each generating unit has four auxiliary panelboards for unit supervision. The panelboards are:

- Local instrumentation panel (LIP) located at the El. 92.4 which is recessed in the wall of the turbine pit access gallery.
- Generator gage board (GGB) located in the powerhouse downstream gallery at El. 98.5.
- Local panel (CLD) containing turbine auxiliary motor starters.
- Turbine and generator auxiliary (TGA) panelboards located at El. 98.5. Panel arrangement is shown in Fig. 14.5.

Panels LIP and GGB serve very similar purposes. LIP accommodates auxiliary devices associated with the sensors pertaining to supervision of the turbine accessories such as turbine bearings, shaft seal, wicket gates, servomotors, etc. GGB contains similar devices for the generator thrust and guide bearings, generator shaft vibration and deflection

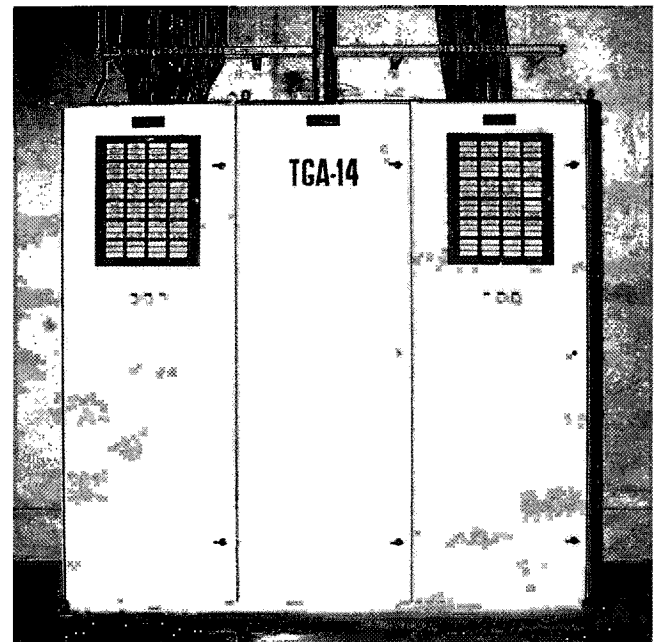


Fig. 14.5 Turbine - generator auxiliary panel

monitoring, air gap supervision, water in bearing oil detection and humidity sensors.

The auxiliary relays within the LIP and GGB panelboards are for contact multiplication which are required for annunciation alarm tripping action and for inputs to SCADA system. Some instruments for indicating temperatures, pressures and flows are also located in these panels. Other instruments are mounted directly on the connection piping or, in the case of level gages, on the containers.

CLD panel contains starters for the turbine headcover drainage pump motors and the lubricating oil pump motor.

TGA panelboards, have detailed annunciator information on alarms in the area of the generating units. Alarms are arranged in functional groups and a common alarm representing each group is transmitted to the annunciator located in the local control room. On the front panels on the left and right cubicles there are 72 point annunciators to monitor the turbine-governor and generator auxiliary systems respectively. Inside the panel there are auxiliary relays and terminals. The center cubicle contains terminals for the TGA interconnection with the external devices.

Step-up transformers

The local control and supervision of the step-up transformer bank is concentrated in the cubicle assembly KT, located in the transformer gallery at El. 108.

The KT cubicle assembly consists of four metal enclosed cubicles, one cubicle for each single phase transformer and a common cubicle for the three-phase transformer bank. The supervisory and control functions for the step-up transformers are:

- Alarm annunciation of defects in the transformer components and auxiliary systems.
- Selection of oil-to-water heat exchangers and manual or automatic operating mode.
- Monitoring of the cooling water system including oil and water flows and water level in the supply tank.
- Setting of the taps on the transformer windings and tap position verification.
- Transmission of selected alarms and indications to the local control room.

A local control panel (ATLP) for auxiliary service transformers GA and TB is shown in Fig. 14.6.

GIS gallery

The local controls and supervision devices for the 500 kV GIS switchgear are located on the following panels located in the GIS gallery at El. 128.2:

- A supervisory and control equipment for GIS (Fig. 14.7).
- XC transducer cubicles for the 500 kV transmission lines and station auxiliary power transformer banks.
- CSF supervisory panel for the 500 kV circuit breaker trip coil circuits.
- BBP for primary differential protection for the 500 kV bus.
- BAP for alternate differential protection for the 500 kV bus.
- OP for oscillograph for fault event monitoring of the 500 kV buses and transmission lines.
- Oscillographs associated with the generator monitoring.
- CSP panel containing revenue metering and bus overvoltage protection.
- LPP panel for line primary protection for the 500 kV line.
- LAP panel for line alternate protection for the 500 kV line.
- PLC power line carrier equipment cubicles.
- Remote terminal unit (RTU) for SCADA system.
- Forced isolation panel FIP (includes control equipment interface between Itaipu generating plant, HVDC converter station and Paraguayan power system).

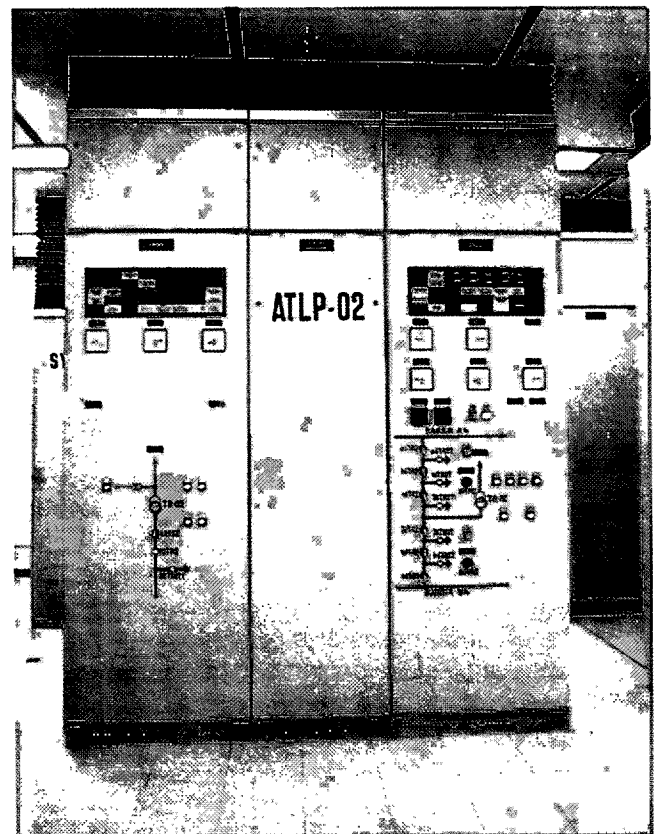


Fig. 14.6 Auxiliary service transformer local control (ATLP)

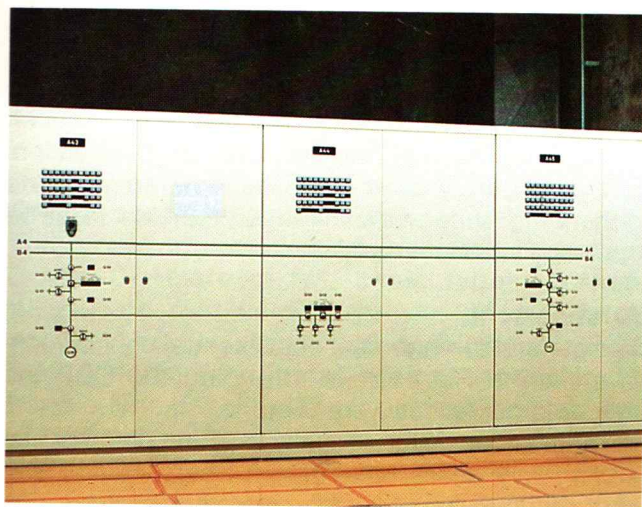


Fig. 14.7 500 kV GIS local control panel

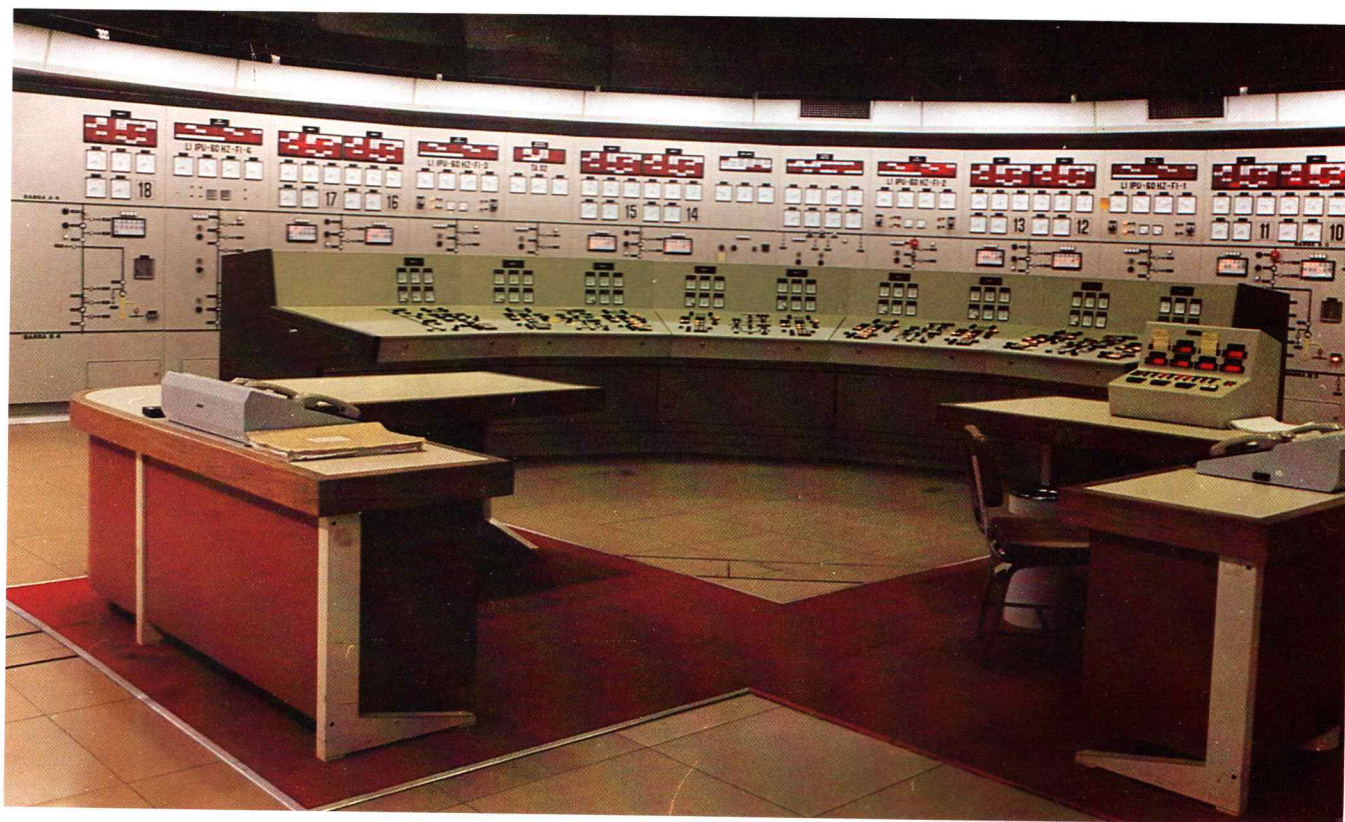
- CIC (A, B and C) for interface between Itaipu generating plant and HVDC converter station.

Ground switch interlocks

This interlock system assures that the GIS grounding switches cannot be closed when the associated section of 500 kV circuit is energized. Three single-phase undervoltage relays are connected to the corresponding equipment potentials and, when energized, the closing of the grounding switch is blocked by a 125 V dc solenoid.

CENTRAL CONTROL ROOM

The central control room (CCR) is located at El. 135.8 at the downstream side of unit blocks 9A and 10. Adjacent to the CCR are computer room, communication equipment rooms, small instrument repair shop, file room and rooms for training operators. Immediately below the CCR, at El. 131.5, there is a large cable spreading room where all cable termination cubicles (TAC's) and accessory equipment are located.



Central control room 50 Hz panel boards and control bench

The CCR has an area of 520 m² and has a vibration resistant floor. Above the CCR there is an observation gallery for visitors with slanting windows looking down into the central control room.

Two separate independent control and supervision systems are installed in the central control room: the hardwired control and supervision system and digital SCADA system.

When the installation of SCADA system is completed, the SCADA system will be the primary control and monitoring system and the hardwired system will serve as a backup.

The hardwired central control system functions by operating control switches and pushbuttons in the CCR which energize interposing relays in the unit local control room panelboards. For reliability reasons the interposing relays are not used for emergency operation functions.

The choice of the operating mode is made by the use of the local-central control selector switches installed at CCR control desks. These switches in turn operate bi-stable change-over relays housed at the various local assemblies. The coils of the interposing relays are energized from a separate 125 V dc source. There is a complete separation of the CCR dc system from the local control dc systems. This improves the reliability of the local

control system and makes the system independent of the CCR system. The dc circuits for the remote control of the spillway equipment are fed via dc/dc converters, which provide a similar separation.

Controls initiated by pushbuttons (such as raise-lower, joint-individual unit control mode selection or operation of the spillway gates) require simultaneous depression of the control pushbutton and the common permissive auxiliary pushbutton. For emergency operations associated with the generating units two control pushbuttons must be operated simultaneously.

Arrangement

The general arrangement of the central control room is shown in Fig.14.8. In arranging the CCR the following guidelines were used:

- The plant operator normally is at one of the digital supervisory desks (DSD), from where control and status verification of all equipment and systems can be performed and monitored via SCADA.
- From the same position the operator can easily observe the vertical panels of the hardwired system.
- The hardwired controls are arranged for convenient use at control desk.
- Normally the units are under joint controls and operated from the joint control console (JCC).

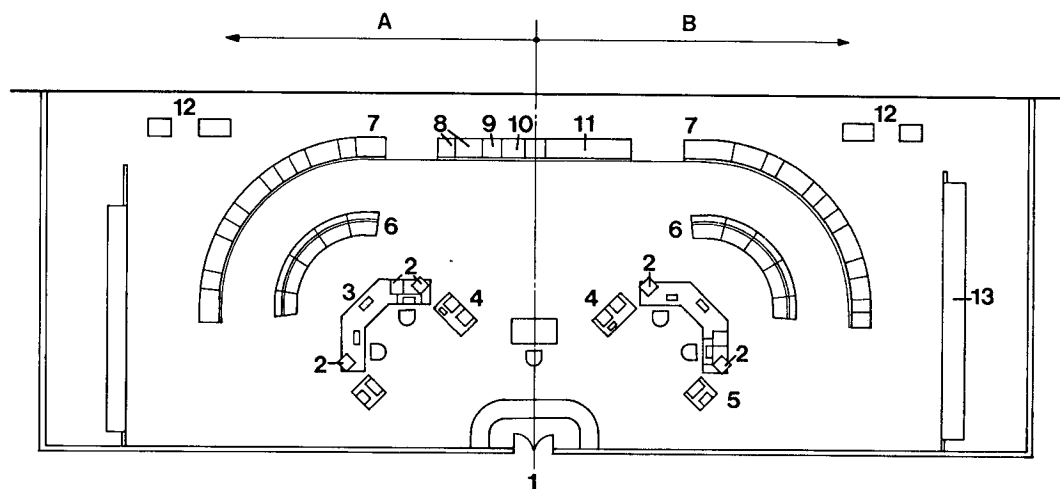


Fig. 14.8 Central control room arrangement

- | | |
|--------------------------|---|
| A Unit block no. 10 | 7 Control, instrument and indicating panels |
| B Unit block no. 9A | 8 Spillway control |
| 1 Entrance | 9 Hydraulic control |
| 2 CRT | 10 Totalizing meters |
| 3 Digital desk | 11 Right bank substation control |
| 4 TV console | 12 Joint control equipment |
| 5 Printer | 13 Auxiliary service panels |
| 6 Generator control desk | |

- When the hardwired control mode is used, operations such as unit starting, stopping, reference settings, status checks, synchronizing, emergency shutdown etc. are done from the control desks (CD).
- Other, less frequent operations, such as transmission line and bus switching, operation of the spillway gates etc. are done at the vertical control panels.

Central control room panels

The hardwired control and supervisory assemblies in the CCR are of two basic types: vertical panelboards and the desk type control assemblies, see Fig. 14.9. The vertical type panelboards include conventional type metal enclosed panels and mosaic type panels with miniaturized controls and instruments.

Principal control and supervisory panelboard assemblies located in the CCR and their abbreviations are as follows:

Unit vertical panel

(one complete assembly for 50 Hz and 60 Hz sector).

Section	Quantity (per sector)	Description
GUS	5	Generating unit control and supervision
L	4	500 kV transmission line
AUX	1	Auxiliary service control
JC	1	Joint controls
BUS	1	500 kV bus sectionalizing
SYB	2	Synchronizing panels

Generating unit supervision (GUS). These panels have annunciation, instrumentation and mimic representation required for operator's supervision of two adjacent generating units. The vertical panel contains only a few control devices which are required for infrequent operations. Control devices for normal operations are located on the corresponding section of the control desk (CD).

Alarm annunciators are located at the top of GUS panels. The indicating instruments for currents, voltages, active and reactive power are in the upper portion of the GUS panel.

The lower portion of the GUS panel has mimic diagram, position indicators for the GIS unit bay

circuit breakers, grounding switches, control switches for isolators, unit starting sequence order indicators and space for trend recorders.

500 kV Transmission line (L). This section contains instruments for the 500 kV transmission line and also the controls for the associated circuit breakers and isolators. The section is equipped with two synchronizing selector switches to permit line synchronization with either one of the other 500 kV main buses to the transmission line.

Switching of the transmission line is considered an infrequent operation, normally not requiring synchronization. Thus line controls are on the vertical panels rather than on the control desk. The synchronizing mode is manual only.

This panel section also has instruments, indicating lamps and test switches for testing the power line carrier and microwave communication channels required for the line relaying protection.

Auxiliary service transformer (AUX). Contains controls and instrumentation for 500 - 13.8 kV main auxiliary transformers (TA-01/02). A "central-local"

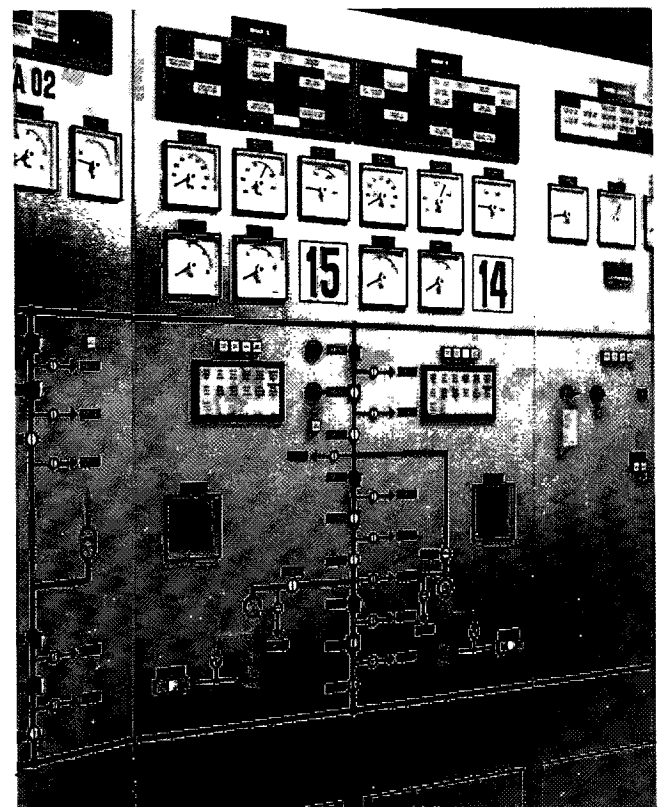


Fig. 14.9 Central control room panel details

selector switch, and two synchronizing selector switches, permit synchronization between two main 500 kV buses.

Joint control (JC). Accommodates the indicating instruments for the nine generating units of each frequency. The instruments located on this panel are: MV, MVAR and the speed droop setting indicator for units under joint control which functions in conjunction with the joint control console (JCC). Joint control panel sections for 60 Hz and for 50 Hz are identical, except that the 50 Hz section has a set of nine pushbuttons for selection of one specific turbine to operate with zero speed droop.

Bus sectionalizing section (BUS). This panel section contains instruments control devices and annunciator for the 500 kV GIS bus sections A1, A2, B1 and B2 for the 50 Hz sector and A3, A4, B3 and B4 for the 60 Hz sector.

As there are four bus sections for each frequency sector, four voltmeters and four frequency meters are installed. Two synchronizing selector switches allow the same synchronizing equipment to be used for reading voltages and frequencies of either one of the pairs of bus sections.

The synchronizing mode is manual only. The panel section also has space for two trend recorders for the SCADA system, local-central control selector switch and two ammeters. The ammeters show currents in the 500 kV buses, which depend on the relative configurations of bus sections, generating units and the transmission lines.

Synchronizing brackets (SYB). They are used to assist the operator to synchronize the generating units, transmission lines and the bus sections manually. Each bracket contains one synchronoscope, one double scale voltmeter and one double scale frequency meter.

Common vertical panels (for both frequencies)

Section	Description
HYP	Hydraulic status indication
SWP	Spillway control and supervision
TOP	Totalizing outputs
CLP	Station clocks

Hydraulic section (HYP). Accommodates alarm annunciators, indicating recorders and instruments

for water levels at the reservoir intake and powerplant tailrace and their difference. Inputs are from bubble type level gauges: two in the main dam (Blocks E5/6, F35/36) and two in the powerhouse (U7, U18). This panel section also houses two indicating recorders the first totalizing water discharge through the 50 Hz turbines and the second totalizing water discharge through the 60 Hz turbines, and two total water flow integrators.

Spillway gate control section (SWP). Contains position indication, controls and alarm annunciation for the spillway gates and their auxiliaries. The position of each gate is indicated. The gate operation can be either individual or simultaneous for all gates in one spillway chute.

Totalizing panel (TOP). Has three sets of indicating meters for MW and MVAR. One set is for the 50 Hz generation, the second set for the 60 Hz and the third set for the total. It also has four double scale indicating recorders for voltages and frequencies, two sets for 50 Hz and two sets for 60 Hz GIS buses and selector switches to select the desired bus section for measurement.

Clock system panel (CLP). Contains two system clocks, one for the 50 Hz system and one for the 60 Hz system, and two reference secondary clocks with time setting switches. The clocks have 24 hour dials. The final reference standard is an electronic quartz clock, having two master control units. One unit operates as a main unit transmitting pulses to twenty-five secondary clocks located in the local unit control rooms, generator areas, erection bays etc. The second unit is a hot standby.

Vertical panels of mosaic type

Section	Description
RMP	Right bank substation (one assembly)
ASP	Auxiliary services (one assembly for each sector)

Right bank substation (RMP). Accommodates alarm annunciators, instruments and control devices for the control of the right bank substation, including the 500 kV, 220 kV and 66 kV sectors.

The controls include switching of the circuit breakers for all three voltage levels, switching of the associated isolators, selection of manual or automatic operating mode for the 220 kV voltage regulators and manual controls for the voltage regulators.

Auxiliary services panelboards (ASP). Contains alarm annunciators, instruments and control devices for centralized control of principal elements of the 50 Hz and the 60 Hz auxiliary systems. The two panelboards are practically identical, except for minor differences in the nomenclature. Panelboards have controls for:

- Selection of the supply source for station auxiliaries, switching of interconnections between switchgear assemblies QA and QP, etc.
- Controls for the tap changing mechanisms of voltage regulating transformers (TD-01/02 and TD-03/04).
- Start and stop control for the emergency diesel generators (GD-01/02 and GD-03/04).
- Emergency switchgear CS for starting and operating frequency converters (HF 01/02 and HF 03/01). One portion of each panelboard contains alarm annunciators for auxiliary system components.

Desk type assemblies

(two assemblies, one for 50 Hz and one for 60 Hz).

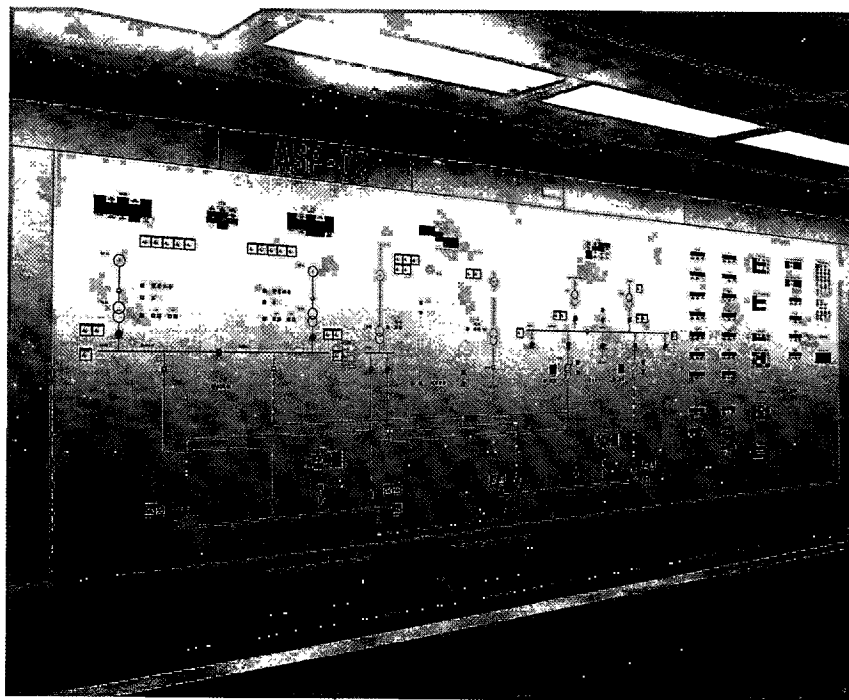
Section	Description
CD	Generating unit control desk
JDC	Joint control console

Generating unit control desk (CD). Accommodates controls for the unit starting, synchronizing, operating, selection of operating modes, normal and emergency shut-downs. The desk consists of five sections. Each section has controls and instruments for two adjacent units. The upper vertical section of the CD contains two identical groups of six instruments for indication of the quantities associated with the unit starting, excitation and loading.

Sets of pushbuttons permit setting of the reference values, unit start-stop control, selection of the operating mode, UMCC supply source selection, and status check. There are switches for selection of either manual or automatic synchronizing. The mimic diagram incorporates circuit breaker and the unit transformer isolator control switches.

During unit operation, the specific section of CD is associated with the corresponding section of GUS, where large indicating instruments provide the necessary displays for unit supervision.

Joint control console (JCC). One JCC console is provided for each frequency sector. Each console functions in conjunction with the corresponding JC section of the vertical panels (GUP). The JCC console contains digital type indicating meters for Hz, MW and MVAR, total for each sector and the total for units placed under joint control. Digital meters are also provided for 500 kV bus voltage and the corresponding voltage reference setting.



Central control room auxiliary service mimic panel

Four sets of twin pushbuttons are used for making adjustments. Nine sets of three-lamp order indicators show the status of each generating unit i.e. under joint MW control, joint MVar control or under joint control by SCADA. There is also an indicating lamp indicating control from the power system dispatch center (FURNAS). Two momentary type pushbuttons are used to raise or lower powerplant total MW.

Digital supervisory desk (DSD)

There are two identical supervisory desks, each desk with two digital control keyboards and one communication panel. Each keyboard also controls two video display units (VDU) located in front of the respective desk. The cabinets for peripheral equipment are in the same area, but near the front wall of the CCR.

Terminal and auxiliary device cubicles (TAC's)

These are located on the floor below the central control room. They contain terminal blocks for interconnecting wiring to various switchboards in the CCR and for wiring to all unit local control panelboards. They also contain certain auxiliary devices, such as dc circuit breakers, auxiliary relay for galvanic uncoupling of the annunciators, dc/ac converters, annunciator logic, etc. The interconnection from various local panelboard to TAC's is made by multicore shielded control cables. The connection from TAC's to the corresponding panels in the CCR are made by shielded wires with plug-in type connectors in installed metal wiring troughs.

TAC's room arrangement permitted convenient cable termination, allowed circuit testing in both directions, minimized interference between units already in operation and permitted convenient testing of the circuitry of the units being added.

Specific design features

Metal enclosed conventional type vertical panel assemblies (GUS, L, HYP, SWD, AUX, etc.) employ components and details very similar to those used at unit local panelboards. Certain features, however, are different:

- The indicating instruments are 144 mm x 144 mm size.
- Transducer inputs are used to all instruments.
- All panels containing instruments have plug type test facilities suitable for low transducer current.
- The panels are normally dark with all indicating lamps extinguished. The indicating lights are illuminated only when there is a change in status, or when a status check is requested by the operator.

The panelboard mimic buses are color coded to represent voltages as follows:

500 kV	Green
230 kV	Red
66 kV	Black
18 to 25 kV	Yellow
4 to 16 kV	Orange
460 V	Brown

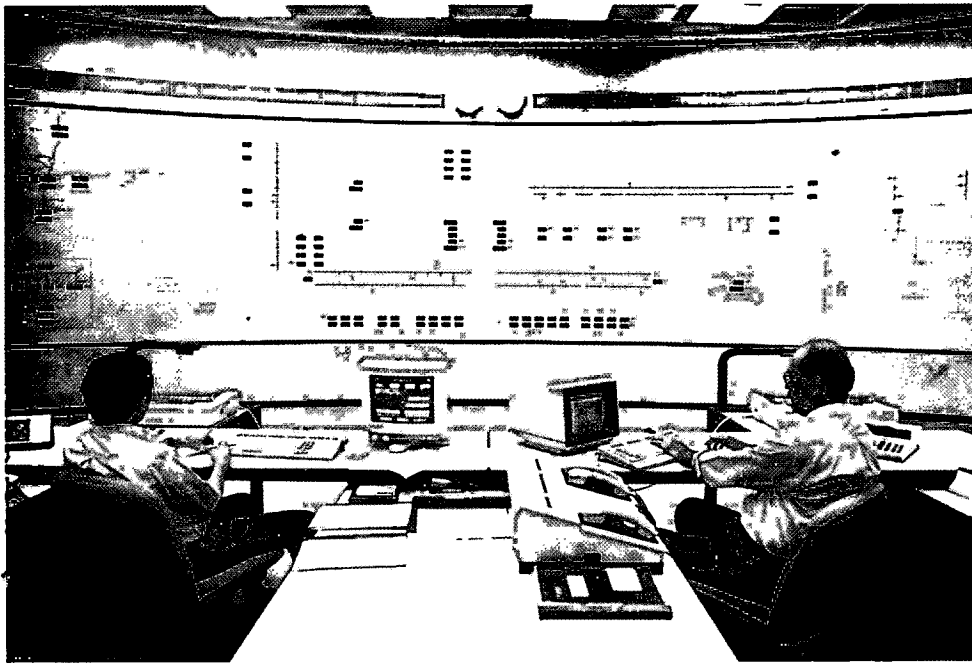
Mosaic type panelboards (RMP, ASP-1 and ASP-2) have a sheet steel structure and a front panel composed of the mosaic tiles 25 mm x 25 mm, which make up the modular elements. The instruments have transducer inputs and are miniature type (25 mm x 25 mm). Control devices, indicating instruments, and annunciators are also miniature type and are dimensioned to fit into an integral number of tiles.

LOAD DISPATCH CENTER

Because of the project importance and the role that ITAIPU generation plays in the operation of Brazilian and Paraguayan power systems, the complexity of hydrological conditions and numerous electrical transmission interconnections with the power utilities, the powerplant has a load dispatch center. The principal functions of the load dispatch center are to forecast availability of ITAIPU generation and to correlate it with the needs of the two power systems. Hydrological conditions, unit maintenance schedule and estimated down time due to possible forced outages are taken into account.

The load dispatch center room is located above the powerhouse main structure inside the administration building at El. 145.65. The general arrangement of the room is shown on Fig. 14.10. The room has a large dynamic mimic board with status displays and recording meters. Communication equipment and dispatch console, which includes four CRT's for data access which is required for effective powerplant dispatch, are installed there. The load dispatch center equipment is interfaced with the equipment located in the central control room, TADMIC system and will be interfaced with the future SCADA systems.

All control wiring for load dispatch center is collected in the terminal cabinet TCC which is located adjacent to TAC's. The interconnections between TAC's and TCC are by control cables and



*Load dispatch room
mimic board*

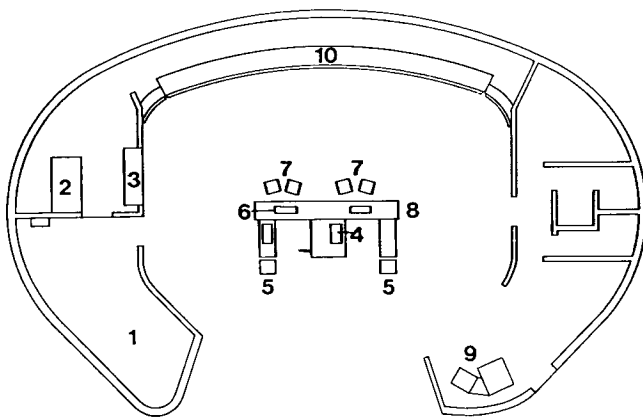


Fig. 14.10 Load dispatch room arrangement

- 1 Communication equipment room
- 2 RTU
- 3 Recording instrument
- 4 Communication equipment
- 5 Printers
- 6 Keyboard
- 7 CRT's
- 8 Dispatcher's console
- 9 Training console
- 10 Mimic board

from TCC to the station dispatch displays by fiber optic cable. At the present time the right bank substation dynamic board displays are driven by TADMIC system but in the future the displays will get their signals through the new SCADA system.

SUPERVISION

Most of the powerplant supervision, same as controls, is performed at two locations: the unit local control rooms and the central control room. The initially installed hardwired control and supervision system is being supplemented by a new digital SCADA system which will have approximately 25 000 data points available to the operators at the central control room.

Depending on the nature of the supervised parameters, the data point may serve only for observation, give a warning alarms or actuate unit shutdown. The alarm and shutdown facilities are part of the general protection scheme which is described in the section on protection.

GENERATING UNIT

The following critical components of each generating unit are supervised:

General

- Generating unit bearing oil and pad temperatures, oil levels, presence of water in oil, cooling water flow, and cooling water outlet temperatures.
- Generator thrust bearing high pressure oil lift system.
- Shaft seal.
- Generator cooling water system.
- Turbine head cover drainage pumps.
- Unit overspeed.
- Unit creep detection.
- All bearing supports are equipped with vibration detection devices and the shaft deflections are monitored at the turbine guide bearing location.

Generator

Stator winding temperatures are monitored continuously by means of RTD's in the stator slots. Stator winding bar ionized cooling water temperature is monitored at the inlet and the outlet water headers. Supervision of the generator raw water-to-air heat exchangers includes monitoring of the cooling water flow and inlet and outlet water temperatures. The temperature of cooling air at each heat exchanger is monitored by RTD's. Level switches and water in oil switches are of the capacitive probe type where the vessel and the probe act as electrodes and the liquid is the electrolyte.

Shaft position deflection and oscillations are mostly monitored by contactless pickup devices with transmitters where the probe is attached to the moving part.

Resistance temperature detectors (RTD's) are used for continuous supervision and in combination with temperature indicators and recorders. RTD's are platinum 100 ohm, three-wire type. Thermocouples are also used for hot spot measurements, calibration and for periodic checks.

All current, voltage and other measurements are converted by transducers to 4-20 mA dc signals which are carried by a twisted pair shielded cables to the respective indicating devices.

Generator slip-ring assembly enclosure air temperature is also monitored.

Air gap monitoring

The generator air gap monitoring system checks the uniformity of the air gap and is capable of detecting a 0.5 mm offset between stator and rotor vertical

axis. The offset appears on the instruments as a constant deflection of the pointer. Excentricities or rotor bulges appear as an oscillating deflection of the pointer.

The system sensors are semiconductors whose resistance increases proportionally to the strength of the surrounding magnetic field. Four sensor groups are installed, each group consisting of ten magneto resistors connected in series.

The system does not give precision measurements and its indications are affected by generator output, stator voltage and temperature. Detection error is in the order of 10 %. The system functions only with the machine excited and has poor sensitivity to unilateral bulges on the rotor or stator.

Considering the importance of air gap uniformity the present system will be supplemented with a fiber optic monitoring system which will provide a more accurate measurement of air gap variations and will show rotor and stator distortions including unit axis offset.

Ozone detection

The presence of ozone in the ambient air within the generator housing is an indication of electrical partial discharges which are detrimental to the life of the stator winding bar insulation. An ozone detector (Dev.45) is used to monitor the presence of ozone inside the generator housing. The detector analyzes the gas content to a high degree of accuracy by using continuously operating photometers. Ambient air within the generator housing is sampled at four points and is passed through filters to the detector. The detector output is a 4-20 mA signal which actuates an indicating instrument having a range of 0-10 mg/m³.

System disturbance monitoring

System faults and disturbances which influence the behaviour of the generator and the excitation system are registered by oscillograph. Each generator has a high speed event oscillograph with sixteen analogical inputs and thirty-two digital inputs, test facilities, power supply and a data modem. The collected information is transmitted in digital form to the central processor unit (CPU). The oscillographs are located in the upstream gallery at El.98.5 close to the generator excitation equipment. The CPU and its peripheral equipment (printer, VDU and keyboard) are located in the central control room. The CPU memory consists of both flexible and rigid disks. The following variables are monitored: Generator stator currents (each phase), step-up transformer neutral current, real power, frequency, field current, negative thyristor bridge field current,

positive bridge control signal, negative bridge control signal, voltages on the ac side of the supply to the negative bridge (three phases) and the positive and negative bridge dc voltages.

Partial discharges

Partial discharges in the stator winding are detected by capacitive couplers type detectors which are connected to the stator winding neutral end terminations, one capacitor coupler for each of the six parallel circuits or a total of eighteen couplers per unit.

Vibrations

In addition to the normal protective sensors installed on the unit the following additional devices are used:

- Shaft radial vibration sensors for each of the guide bearings, two probes placed in quadrature .
- Guide bearing radial vibration sensors installed in quadrature.
- Two axial vibration sensors for thrust bearing.
- Four tangential sensors for stator frame support plates.

The outputs of these sensors will be interfaced with the new SCADA system where they will be compared with the previous readings, thus indicating changes in vibration patterns due to mechanical, magnetic and thermal unbalance, or abnormal hydraulic excitation. The stator frame sensors detect low frequency oscillations attributed to interfaces with the transmission system and with the operation of HVDC converter station in the case of the 50 Hz machines.

STEP-UP TRANSFORMERS

Each transformer has sensors for monitoring oil and winding temperatures, oil levels, oil circulation, cooling water flow, sudden gas pressure increase and pressure relief valves. High voltage and neutral bushings have current transformers for protective relays and for inputs to the replica type temperature measuring and monitoring device. The phase "B" unit transformer high voltage bushing has a bushing type potential device which provides voltage for unit synchronization.

GAS INSULATED SWITCHGEAR (GIS)

There are two oscillographs, one for the 50 Hz and one for the 60 Hz sector, each consisting of thirty-two channels and sixteen starting sensors. The channels are utilized as follows:

- Sixteen analog channels are used for bus voltage supervision (phase A, B, C and the residual of each bus section).
- Twelve analog channels are used for line current supervision (phase A, B, and the residual of each line).
- One analog channel (spare).
- Two event marker channels are used to supervise sixteen events (trip coil energization of each circuit breaker).
- One for time marking channel.

The sixteen starting sensors are connected as follows:

- Four single-phase overcurrent sensors are connected in the residual circuits of the alternate protection CT's (one for each 500 kV line).
- Four three-phase negative sequence overvoltage sensors are connected at bus PT's (one for each 500 kV bus section).
- Four three-phase overvoltage sensors (connected as above).
- Four three-phase undervoltage sensors with operation limiter (connected as above).

The oscillograph panels OP-01 and OP-02 are located in the GIS gallery.

The GIS has a two-stage low gas density alarm system. Both stages of low gas density indication give only alarms and do not initiate circuit breaker tripping.

REVENUE METERING

There are two separate systems for the revenue metering, one for the 50 Hz and the other for the 60 Hz sector.

The energy for the 50 Hz sector is measured at the following locations:

- At the powerhouse for the two outgoing 500 kV transmission lines L3 and L4 which transmit power directly to Foz do Iguaçu HVDC converter station.
- At the right bank substation for the two 500 kV transmission lines (L9 and L10) which transmit power to Foz do Iguaçu HVDC converter station, for the four 220 kV transmission lines (L1, L2, L3 and L4) interconnected with ANDE power system and for the 66 kV line to Foz do Iguaçu substation.

The energy measured at the right bank substation, the outgoing 500 kV and 220 kV lines, is locally processed by a telecounting programmable instrument (TPI) and printed locally and remotely (at the powerhouse load dispatch center room).

The energy measured at the powerhouse (500 kV lines L3 and L4) is processed by a TPI and printed at the load dispatch center room.

The energy for the 60 Hz sector (500 kV lines L5, L6, L7 and L8) is measured at the powerhouse, then processed by a TPI and printed at the powerhouse load dispatch center room.

The printed values in all cases are kWh and kVarh and include hourly, daily and monthly totals and maximums.

TADMIC SUPERVISORY SYSTEM

This system is used for collection and multiplexing of supervisory data at the right bank substation so as to minimize the number of microwave channels required for transmission of this information to the powerhouse load dispatch

center displays. TADMIC system has a capacity of 1000 digital points and 300 analog signals and includes provisions for future expansion. System architecture consists of a local network of microcomputers, which are compatible with the IBM personal computer. The system consists of a master unit, remote terminal units for data collection and interfaces for actuation of mimic displays and VDU's.

The TADMIC system is a flexible supervisory system which supplies information on performance of electrical and mechanical subsystems and measures electrical quantities in real time. The principal components and the functional arrangement of the TADMIC systems are depicted in Fig. 14.11.

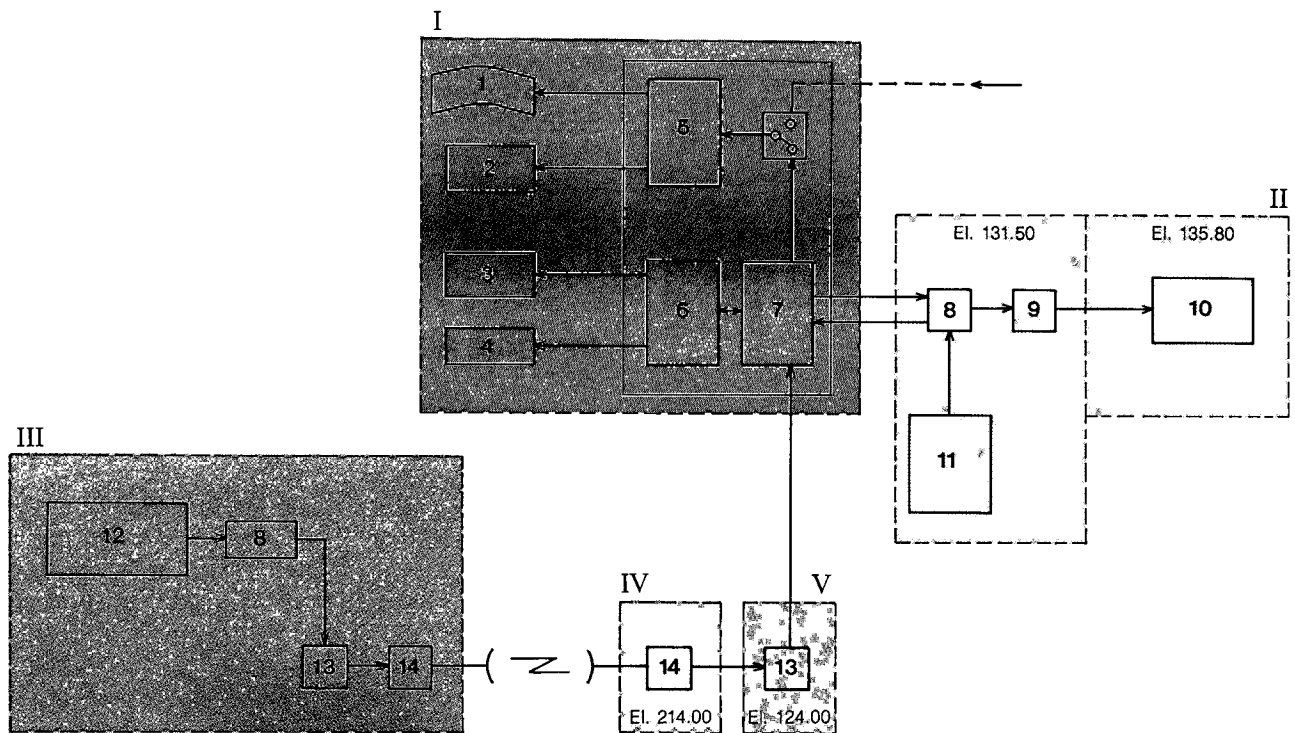


Fig. 14.11 TADMIC system block diagram

- I Dispatch room
- II Central control room
- III Right bank substation
- IV Main dam
- V Unit block no. 9

- 1 Mimic board
- 2 Recording instrument
- 3 CRT
- 4 Printers
- 5 Controller no. 1
- 6 Controller no. 2
- 7 Central processor

- 8 RTU
- 9 TAC's 561-566
- 10 Right bank substation control panel
- 11 TAC's 532-535/541-545/632-634/641-646
- 12 Control switchboards
- 13 Microwave multiplex
- 14 Microwave transmitter/receiver

SCADA SYSTEM

GENERAL DESCRIPTION

The general objective of the new SCADA system is to provide a modern and highly flexible system not only for control and supervision of the complete powerplant but also for energy management, monitoring and diagnostic functions of the generating units.

The SCADA system consists of powerplant digital control subsystem (SCD) and generating unit monitoring and diagnostic subsystem (MONDIG).

The SCD subsystem provides the plant operators and load dispatchers with real-time information on the existing operating conditions of the equipment and also provides facilities to perform supervisory control through video display units and keyboards. The SCD subsystem will also provide on-line interfaces with ELETROBRÁS, ANDE and FURNAS power system operators and will use a variety of software application programs for optimizing ITAIPU generation.

The MONDIG subsystem will monitor the generating unit performance by detecting abnormalities and providing warning as to possible deterioration of operating conditions in order to avoid unnecessary inspection of the generating units and to minimize the duration and number of such inspections. The key parameters of diagnosis of the unit conditions are: vibration, air gap variation, partial discharges and temperatures. The results of the monitoring and diagnostic procedures are presented to the plant operators via the SCD subsystem.

The SCADA system is also interconnected with other powerplant internal stand alone digital systems such as: SOM (operation and maintenance system), SCH (hydrometeorological control system), TADMIC (mimic board) and SIS (integrated security system).

SYSTEM FUNCTIONS

The SCADA system functions are grouped as described below:

- General functions like acquisition, processing and storage of data, visual displays, recording of data, supervisory control and exchange of information with internal and external systems.
- Plant operation scheduling functions such as hydrological forecasting, generation and maintenance scheduling and provision of electrical and hydraulic system operation guidelines.

- Supervision and control functions such as monitoring of electrical and hydraulic systems; automatic generation and voltage control; state estimation; generation unit monitoring and diagnostics; disturbance analysis, power system restoration procedures and collection of historical data.
- Post operation reports like elaboration of statistical data, operational reports and power interchange accounting.
- Other miscellaneous functions such as software, data base, display development and maintenance, dispatcher/operator training, system engineering studies, hardware preventive and corrective maintenance and storage and revision of operating instructions and rules.

SYSTEM CONFIGURATION

The SCADA system will consist of a master station, thirty-eight remote terminal units (RTU), fifty-nine data acquisition modules (MOD) and ten MONDIG subsystem equipment cabinets (five for generating unit vibration monitoring and five for generator air gap monitoring).

The SCADA system will be functionally divided in the following parts: computers, data acquisition and control, man-machine interface and development and training subsystem. The basic configuration of the system is shown in Fig. 14.12.

Computers

Three identical computers are responsible for the performance of all the above described functions and for managing the entire system configuration. An ETHERNET standard double local area network (LAN) will be used to connect all system components, with the exception of the support terminals like PC's for software development, programming and maintenance, which will communicate with the computers via two separate office LAN systems.

When all three computers are available, the first computer will operate in the primary mode, the second computer in an immediately available stand-by mode, and the third computer will be used for training and development of the software. In the event that only two computers are available, the first will operate in the primary mode and the second will perform the two remaining functions. If only one computer is available, only the primary mode functions will be attended.

Data acquisition and control

This subsystem will be composed of telecontrol interfaces (TCI's), RTU's, MOD's and gateways and will serve both the external ELETROBRÁS, ANDE and FURNAS systems and the internal powerplant system.

The TCI's will interface computers with approximately 25 000 data points collected at the RTU's and MOD's as well as at the equipment cabinets of MONDIG. Besides performing basic communication functions, the TCI's will also perform pre-processing functions such as validity checking,

engineering unit conversion and automatic channel fail-over switching.

The RTU will be linked point-to-point to the master station by fiber optic network. They will employ MOD's which will be located near the actual physical process, assuring a greater reliability and a better response. The MOD's are connected to the RTU's via local area network which will use fiber optic links.

The gateways and servers will connect the external and internal systems as well as the printers to the double process LAN. This equipment will consist of industrial PC compatible microcomputers.

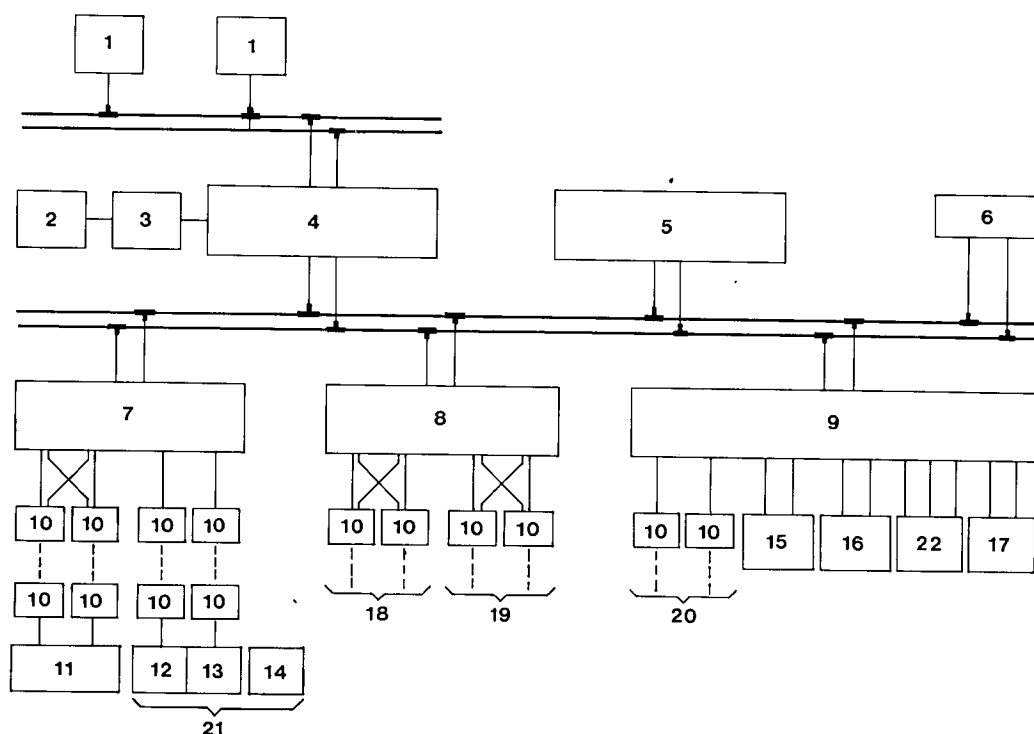


Fig. 14.12 SCADA system configuration

- 1 PC's and printers (9)
- 2 Printers (3)
- 3 System terminals (3)
- 4 Host computers, each with two disks and one tape (3)
- 5 Workstations, each with two monitors and four video copiers (8)
- 6 Workstation and video projector (1)
- 7 Telecontrol interfaces A and B (4)
- 8 Gateways A and B (4)
- 9 Servers A, B, and C (3)
- 10 Modems (38)
- 11 RTU's (38) and data MOD's (59)

- 12 Equipment cabinet for vibration monitoring (5)
- 13 Equipment cabinet for air gap monitoring (5)
- 14 PC's (2)
- 15 Time and frequency system
- 16 Audible alarm units
- 17 Line printers (2)
- 18 External systems (ELETROBRÁS, ANDE and FURNAS)
- 19 Internal systems (SOM, SIS)
- 20 Internal systems (TADMIC, SCH)
- 21 MONDIG
- 22 Printers (11)

Note: numbers in parenthesis indicate quantities

Man-machine interface

This subsystem is made up of four operator consoles, two dispatcher consoles, one demonstration console with video projector and subsystem support terminals. The consoles are full-graphics type workstations with panning, zooming, decluttering and windowing features for better information access and presentation.

The support terminals will be PC type microcomputers. Video projector will be connected to a dedicated workstation without affecting the real-time system operation.

Development and Training

This subsystem will allow simulation of real operating conditions for operator and dispatcher training as well as will have means for developing and maintaining software. It consists of two consoles, associated terminals and other peripheral devices. The consoles will be identical to the man-machine interface consoles.

DESIGN AND PERFORMANCE FEATURES

The design approach used for SCADA system will take into consideration all functional requirements of the powerplant operation and will adopt state-of-the-art technology, such as the following innovative features:

- A fully open architecture system configuration with all functional hardware elements interconnected via local area networks.
- Three main computers, each capable of performing the entire set of critical operating functions, offering benefits unrealizable in the traditional dual-computer configuration.
- RISC (reduced instruction set computer) graphic workstations for the man-machine interface consoles.
- Personal computers instead of the traditional video programmer terminals.
- An open architecture RTU design with distributed input/output modules.

PROTECTION

GENERATING UNITS

The generating units are protected by conventional groups of the static type relays. The unit protection device list is as follows:

Device no.	Function
87V	Differential relay for protection of the 500 kV section (SF ₆) between step-up transformer bushing and unit circuit breakers
21	Back-up impedance relay
40	Loss of field and under excitation relay
46	Generator load unbalance relay (negative sequence current)
51/50A	Unit service power supply overcurrent relay
51N	Step-up transformer ground overcurrent relay
51NA	Unit service transformer ground overcurrent relay
59	Generator instantaneous overvoltage relay, frequency compensated.
59T	Generator time delay overvoltage relay, frequency compensated.
60	Voltage balance relay: Blocks 64SA and 21 relays
64SA	Generator stator ground detector relay (90 %)
64SB	Generator stator ground detector relay (100 %)
87G	Generator differential relay
87SP	Generator split phase differential relay
87TA	Unit service transformer differential relay
87U	Unit bay differential relay
87TR	Step-up transformer differential relay
87TRG	Step-up transformer ground differential relay
95-1/2/3	Volt/Hertz overfluxing protection relay

The protective relays used and their functions are described below:

Loss of excitation and underexcitation protection (Dev. 40)

Protects the generator against failure of excitation or against excessive reduction in the field current which could result in the asynchronous operation of the generator and unit overheating. Approximately 0.1 second time delay allows the automatic voltage regulator to take corrective action before a shutdown is initiated via lockout relay Dev. 86N and 05A.

Back-up protection (Dev. 21/50V)

This protection consists of a two-stage distance type relay whose operation is initiated by a voltage drop

and increase in current. The first stage has "mho" type characteristics and it reaches 30% into transformer winding and operates with a small time delay. The second stage reaches into the transmission system and has a longer time delay to permit other protective devices to isolate the fault prior to operation of this relay.

The first stage of this protection operates the shutdown lockout relay 86E and the second stage operates relay 05A.

Generator differential protection (Dev. 87G)

The protective zone of this relay for the stator phase-to-phase winding fault detection extends from the generator phase winding neutral end to the generator terminal bushings. It compares the current entering a phase winding with that exiting and produces a rectified output proportional to the difference which operates shutdown lockout relay 86E if the minimum setting is exceeded. There is a stabilizing winding to render this relay inoperative in case of high magnitude through fault currents.

The protection is effective for the detection of the generator stator winding phase-to-phase faults but, because of high resistance neutral grounding, in case of a ground fault, the current is limited to a low value (approximately 20 A) such that the differential protection remains inoperative.

Generator split-phase differential protection (Dev. 87SP)

This relay detects shorted bars or groups of bars within each phase winding of the stator. Each of the phase conductors beyond the neutral end of the stator winding are split into two parallel conductors, the currents in which are measured by the current transformers and compared by the relay. Under normal conditions the currents are equal. However, if some portion of winding is shorted, a circulating current results which is sensed by this protection, which in turn initiates a shut-down through a lockout relay 86E.

Generator and transformer overall differential protection (Dev. 87U)

This protection is similar to the other differential protections. The protected zone includes generator stator winding both windings of the unit step-up transformer and a section of the 500 kV SF₆ GIS bus up to the circuit breakers. It serves as a back-up for relays 87G, 87TR and 87V. The relay 87U operates for all phase-to-phase faults within the protected zone and also for ground faults in the transformer high voltage winding. It does not operate for ground faults in the generator stator winding or in the low

voltage transformer winding. This protection operates the shut-down lockout relay 86E.

Generator unbalanced load protection (Dev. 46)

This relay protects the generator rotor against prolonged contribution of the unit to an external unbalanced load condition, such as that caused by a broken phase conductor, not properly closed circuit breaker contacts, etc. The negative sequence currents that flow during the unbalanced load conditions induce twice-rated frequency rotor currents which can overheat the rotor structure.

The solid state protective relay is a thermal replica type negative sequence relay, the first stage of which gives an alarm and the second stage operates the partial shut-down relay 05A.

Voltage balance protection (Dev. 60)

This protection monitors the supply voltage to excitation equipment (no primary fuses) and the voltage supply to the protective relays (with primary fuses) and blocks the operation of 21 and 64SA when the two voltages are different.

Generator stator winding ground fault 90% protection (Dev. 64SA)

The protective zone of this relay, for stator phase-to-ground winding faults, extends from the generator line terminals to approximately 10% from the neutral. Ground faults occur when there is a breakdown of the insulation between the bar conductor and the stator slot iron. The resulting displacement voltage is detected by the generator potential transformers with a broken delta secondary winding output applied to the relay which operates the shutdown lockout relay 86E.

Generator stator winding ground fault 100% protection (Dev. 64SB)

The function of this relay is similar to 64SA except that the protective zone is 100% of the stator winding including neutral. A 20 Hz signal fed by the wye connected generator potential transformers is superimposed across the generator neutral grounding transformer secondary circuit, causing a low 20 Hz current to flow through the generator resistance and capacitance to ground. In the relay this current is compensated by a second 20 Hz current in the relay measuring circuit, so that when the internal fault occurs and the operating current increases because of a decrease in the impedance to ground, the relay responds to the unbalance between the two currents and operates the shut-down relay 86N.

The 90% and 100% fault protections have an important conceptual difference. With the 90% protection, the sensibility at fault detection is maximum near generator terminals and decreases toward neutral point, while with the 100% detection the maximum sensitivity is at the neutral end and decreases toward winding terminals.

Overvoltage protection (Dev. 59/59T)

This protective relay prevents sustained over-voltages caused by the faulty operation of the automatic voltage regulator or a full load rejection when the excitation system is in manual control. It is set for voltage and time in such a way that during a full load rejection and properly operating voltage regulator, it does not operate. The protection operates the shutdown relay Dev.05 (59T and 05A) and has two stages. A large overvoltage results in a shut down after a short time delay and a small overvoltage initiates a shutdown after a longer time delay.

STEP-UP TRANSFORMERS

Transformer-restricted ground fault protection (Dev. 87TRG)

The protective zone of this relay for transformer winding ground faults is 90% of the winding starting from the HV bushing. The relay operates the shutdown lockout relay 86E.

Transformer differential protection (Dev. 87TR)

This relay protects the step-up transformers from the HV bushings to the LV bushings and for stabilization utilizes the second harmonic of the inrush current when the circuit breaker closes. This protection operates the shutdown lockout relay 86E and the local lockout relay 86TR.

Transformer volts/hertz protection (Dev. 95)

This relay protects the transformer core from overfluxing by measuring the ratio of voltage and frequency. An increase in this ratio indicates an increase in the magnetic flux density which in turn results in a saturation of the iron core and excessive eddy currents in the transformer iron parts and the adjacent structures. The protection has a time delay and operates the shutdown relay Dev. 86E.

Transformer ground overcurrent protection (Dev. 51N)

The protective zone of this relay for transformer winding ground faults is not limited and it will operate

for the faults within GIS and the transmission lines. It performs the same function as the restricted ground fault protection Dev. 87TRG and is coordinated with other protection by a time delay. The relay operates Dev. 05A.

500 kV stub bus-differential protection (Dev. 87V)

The protective zone of this relay, for the 500 kV GIS stub bus, which extends from the transformer high voltage bushing to the 500 kV GIS and includes the two 500 kV circuit breakers (52U and 52T). The relay operates the shut-down lockout relay Dev. 86E and the auxiliary lockout relay Dev. 86SF.

UNIT AUXILIARY TRANSFORMERS

Transformer overcurrent protection (Dev. 51/50A)

On the 18 kV side, the transformer is protected by three inverse time overcurrent relays (Dev. 51) which have instantaneous trip attachments (Dev. 50). The protection operates for faults and overloads on the 460 V side and activates the shutdown Dev. 86E. The ground faults on the 18 kV side are sensed by the generator stator ground fault protection. (Dev. 64SA and 64SB).

Transformer differential protection (Dev. 87TA)

This protection is effective for internal phase-to-phase faults but does not operate for line-to-ground faults. The relay operates Dev. 86E.

Transformer ground overcurrent protection (Dev. 51N)

The relay is installed in the ground connection of the secondary zig-zag, 460 V winding and operates Dev. 86E.

SPECIAL CURRENT TRANSFORMERS

The protective relays 87G, 87U, 87TR, 87SP operate on principle of comparison of currents in two or more circuits to detect faults. For a normal operating state these currents are practically equal and in the same vectorial position so that they basically cancel each other out and only a small residual current flows into the relay.

When an external fault occurs, outside of the protected zone, the transient through current can cause CT saturation, which in turn results in unbalanced CT outputs and a danger of a false relay operation. For this reason, special linear type CT's of the gapped-core type were used at Itaipu.

500 kV GIS BUS

Very rapid isolation of a faulted GIS bus is necessary to prevent a burn-through in the aluminum enclosure which could result in the release of toxic gases. To minimize this possibility two very fast acting bus differential protection schemes are used. To avoid common mode failure, the two protection schemes are independent and utilize different operating principles. The two protection schemes are:

- Primary bus differential protection (87P)
- Alternative bus differential protection (87A).

The protection schemes are identical for the 50 Hz and 60 Hz sectors. The action of both differential protection schemes are similar and perform the following functions:

- Energize both trip coils of the circuit breakers.
- Energize lockout relays to block any attempt to close the circuit breakers into faulted bus section.
- Initiate "breaker failure" protection.
- Provide alarm signal in the local control room.

Primary bus differential protection (87P)

Each protective system (50 Hz and 60 Hz sectors) consists of four differential zones to accommodate two 500 kV buses, each bus being longitudinally sectionalized into two parts. The four sets of protection cubicle assemblies are installed in the GIS gallery, each assembly containing two differential protections (BBC type IZX1) one for the section of bus A and another for bus B. Additionally there are two test sets, blocking relays and indicating lamps, high speed tripping relays, miniature circuit breaker for the protection of the auxiliary circuits, filters for transient harmonics, dc-dc converters and modules for supervision and annunciation. The assembly has internal lighting, heating and plug receptacles.

This protection is of the high impedance type. In normal service, the difference between the incoming and outgoing feeder currents is zero. During a busbar fault there is a differential current which passes through a high impedance inside a IZX1 relay and produces a voltage drop higher than the relay setting and therefore, the protective relay operates.

In operation, this protection automatically supervises the differential circuits and the internal circuits of the relay and defects are indicated through audible alarm and visual signal.

Alternate bus differential protection (87A)

This protection covers the same bus sections as the primary protection described above. Located in the same cubicles are relays associated with the "breaker failure" protection for the bus sections.

Each assembly consists of two cubicles. The protection is BBC type INX2 which uses the directional comparison principle and trips if the following occur simultaneously:

- All feeder currents are flowing into the busbar.
- The differential current exceeds the preset value.

There is an automatic test unit which checks regularly if the protection is "ready to operate". This check is accomplished by a continuous supervision and by an automatic test sequence. The continuous supervision supervises the main internal circuits and the auxiliary supply voltages. The automatic test sequence supervises the most important protection functions and is initiated periodically through the internal timer or manually at any time. Defects are indicated through audible alarm and visual signal.

Circuit breaker failure protection (50/62BF)

Each 500 kV GIS circuit breaker is equipped with a circuit breaker failure protection. When a failure in the protected equipment occurs, it must be detected and cleared at the same terminal in accordance with the philosophy of "local backup".

Whenever any protective trip of a circuit breaker is initiated, the breaker failure scheme is also initiated. If the circuit breaker trips and interrupts within the prescribed time, the breaker failure protection resets. If, however, the breaker fails to trip or to interrupt the fault current, the breaker failure protection completes its cycle and trips all the adjacent circuit breakers.

The breaker failure scheme consists of three current sensing relays (50BF), one timer relay (62BF) and one lockout relay (86BF). For faults that do not involve currents high enough to operate current relays (50BF), the protection can also be actuated by the auxiliary contacts of the circuit breaker.

Trip coil supervision CSF system

This system which is continuous and automatic, is effective when the circuit breaker is closed. It uses an auxiliary low-current relay in series with an adjustable resistor and the trip coil. On interruption of the trip circuit, the current relay drops out and actuates, within a time delay, an auxiliary relay with auxiliary contacts for alarm. There are six sets of equipment per circuit breaker, one for each trip coil.

The relay through current is limited by the resistor to such a low value that tripping cannot occur. The relay is continuously energized, but should any of six trip coil circuits open, the relay drops out, and after a time delay actuates the local and remote alarms.

Each CSF cubicle has internal lighting, thermostatically controlled heaters, and miniature circuit breakers.

500 kV TRANSMISSION LINES (50 Hz)

The transmission line protection scheme can detect three-phase, single-phase, phase-to-phase and double phase-to-ground faults. Two basically identical, independent systems provide a primary (LPP) and alternative (LAP) protection for the lines. Each consists of a distance relay (21) and an overcurrent directional ground relay (67N) associated with power line carrier and microwave communication channels to form a permissive overreaching unblocking transfer tripping scheme. The distance relay also actuates a timer to cover the possible loss of teleprotection communication channels during a line fault. Furthermore, whenever any line protection decides to trip the circuit breakers, the remote terminal is also tripped through a transfer trip channels.

Both systems actuate trip coils of the line circuit breakers within a maximum time of 2.5 cycles after

the occurrence of fault. Breaker failure relaying is also supplied. The protective relays for both schemes are of the static type.

The line protection cubicles are located in the GIS gallery close to the line circuit breakers, see Fig. 14.13.

500 kV TRANSMISSION LINES (60 HZ)

The protection scheme can detect the same faults as that for the 50 Hz sector but here the primary protection system is different from the alternative one.

The primary system consists of a line differential protection scheme using the fiber optics communication channel and is supplemented by a ground overcurrent directional relay associated with microwave channels to form a permissive overreaching unblocking transfer tripping scheme (87LP/67NP).

The fiber optic link for the differential (87P) is redundant and has two routes, one aerial and the other underground. In case of a fault on the line, the primary protection trips both line terminals through a direct transfer trip signal through the fiber optic communication link. The fiber optic signal is continuously monitored, and an alarm occurs if the signal is lost or drops below acceptable level.

The alternate protection system is a permissive overreaching unblocking transfer trip scheme actuated by a distance relay (21A), which uses the power line carrier communication link as the teleprotection channel.



Fig. 14.13 500 kV Transmission lines (50 Hz) primary and alternate protection panels

HVDC CONVERTER STATION INTERFACE

The number of generators in service at the Itaipu 50 Hz powerhouse must be adequate to supplement the reactive power requirements at Foz do Iguaçu HVDC converter station. Foz do Iguaçu substation computer continuously receives information on the operating status of the 50 Hz generators at the powerhouse and, depending on various possible filter and HVDC converters configurations, initiates the necessary signals for corrective action.

FORCED ISOLATION SCHEME

Capacity of the ANDE Acaray hydroelectric power station in Paraguay is not sufficient to supply reactive power needs of the Foz do Iguaçu HVDC

converter station without contribution of Itaipu generators. If Itaipu reactive power contribution is lost, the ANDE system must be immediately isolated. The forced isolation protective scheme (FIP) which implements this action consists of two installations, FIP 1 panel located in the GIS equipment gallery at the powerhouse and FIP 2 panel is located in the control building of the right bank substation.

Protective devices in FIP 1 panel detect the loss of the last 500 kV line interconnection or the loss of the last generating unit at the powerhouse and sends a transfer trip signal to open all 220 kV line circuit breakers at the right bank substation, thus isolating ANDE power system from Itaipu system.

Panel FIP 2 equipment detects various system disturbances like overvoltage, underfrequency, power flow reversal, etc. which indicate the loss of Itaipu powerplant generation contribution and trips all 220 kV line circuit breakers as described above.

PROTECTION PANELS

The construction of protection panels is similar to the control panels, except that the front and rear access is through swing-out doors. Access to the terminal cubicles and to the overhead wiring troughs is by removable steel plates. Protective relays are of the static type and have the following features:

- Short tripping times, which facilitate relay coordination and tend to reduce damage to the protected equipment.
- Low power consumption, reducing burden on the instrument transformers.
- Standardized modules, assuring well tried components.
- Reduced vulnerability to vibrations.
- Low voltage and current tripping signals programmed in tripping matrix.
- Incorporated test sets, for rapid verification of readiness of each protective relay.
- Plug-in type connections.

Secondary wiring of the generating unit potential and current transformer is connected by plug type connectors to the front of the associated sub-racks. The internal electronic signals are run on the sub-racks thus providing a physical separation between the two different classes of wiring.

THE INTERCONNECTED ELECTRICAL SYSTEM

GENERAL	15.3
50 Hz SYSTEM	15.6
Right Bank Substation	15.6
500 kV Transmission Lines	15.13
HVDC Transmission System	15.14
Control and Operation	15.22
HVDC Transmission Lines	15.27
60 Hz SYSTEM	15.29
Description and Principal Characteristics	15.29
Foz do Iguaçu Substation	15.29
Transmission Lines	15.35

THE INTERCONNECTED ELECTRICAL SYSTEM

GENERAL

The Brazilian and Paraguayan sectors of Itaipu hydroelectric plant generate power respectively at 60 and 50 Hz according to the frequencies existing in the respective countries. The power generated at 18 kV is transformed at the powerhouse to 500 kV for transmission to the Brazil and Paraguay systems.

The 60 Hz powerhouse sector is connected by four Itaipu 500 kV lines to the Foz do Iguaçu substation, located on the left bank of the river and operated by FURNAS. There the voltage is stepped-up to 765 kV (during the feasibility stage of the project the voltage corresponded to 750 kV). From the Foz do Iguaçu substation the power is transmitted by three 765 kV lines to Tijuco Preto substation in São Paulo area. There are also two intermediate substations at Ivaiporã and Itaberá.

The 50 Hz sector was designed to accommodate future system changes. Initial requirements were for a reliable, but relatively small, load supply to Paraguay at 220 kV and the transmission of the remaining power to Brazil. Gradually this will change with more power being used at 50 Hz, first in the 220 kV and then in the future 500 kV Paraguayan network.



*Aerial view of Foz do Iguaçu
substation*

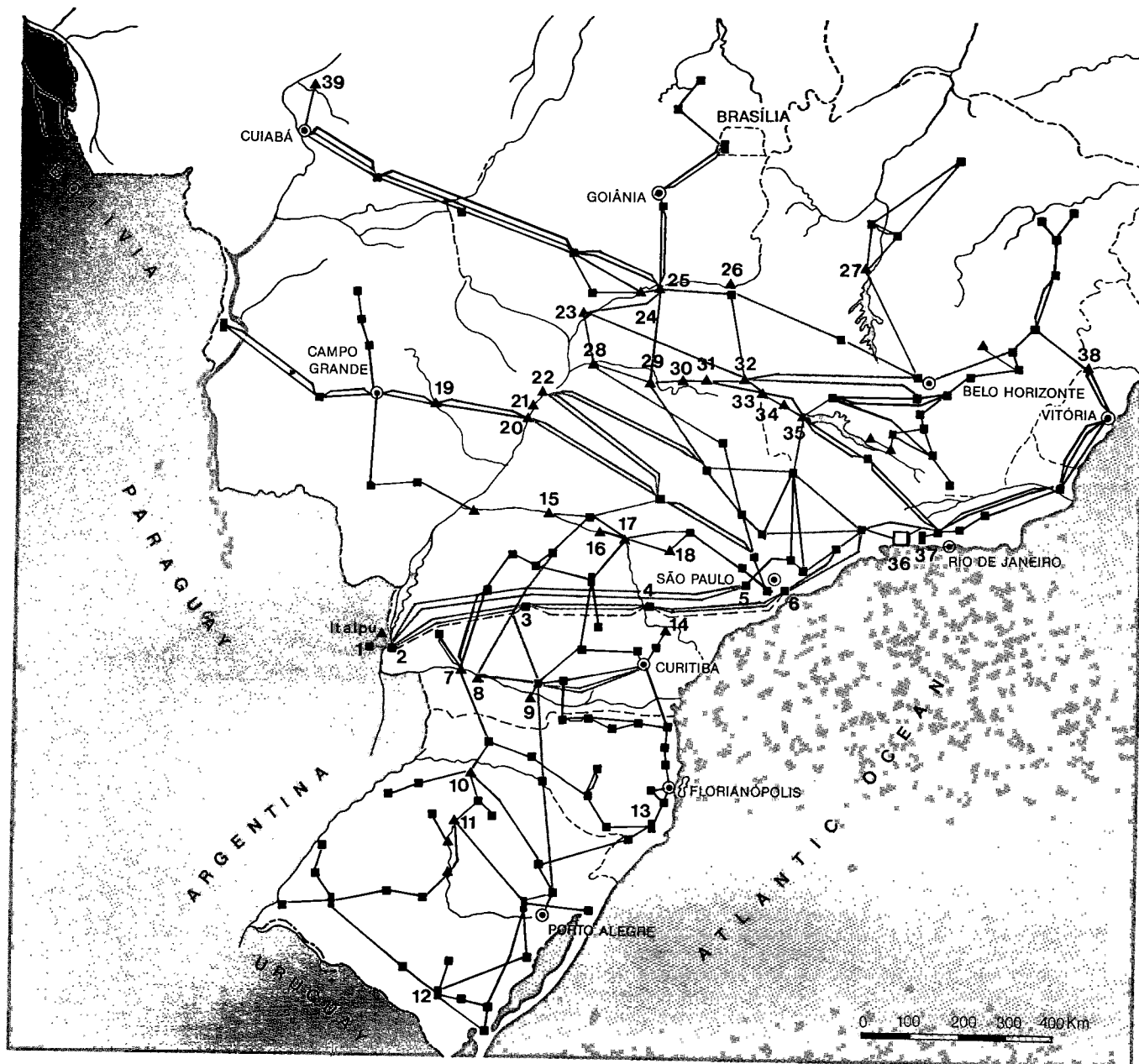


Fig. 15.2 Electrical system of Southern Brazil – 1991

- | | | | |
|-------------------------|--------------------------|-------------------|----------------------------|
| 1 Right bank substation | 14 Gov. Parigot de Souza | 27 Três Marias | ▲ Hydroelectric powerplant |
| 2 Foz do Iguaçu | 15 Capivara | 28 Água Vermelha | □ Nuclear powerplant |
| 3 Ivaiporã | 16 Salto Grande | 29 Marimbondo | ■ Thermal powerplant |
| 4 Itaberá | 17 Xavantes | 30 Porto Colombia | ■ Substations |
| 5 Ibiúna | 18 Jurumirim | 31 Volta Grande | — 765 kV lines |
| 6 Tijuco Preto | 19 Mimoso | 32 Jaguará | - - - Future 765 kV line |
| 7 Salto Osório | 20 Jupia | 33 L.C. Barreto | — ± 600 kV dc lines |
| 8 Salto Santiago | 21 Três Irmãos | 34 M. Moraes | — 500 kV lines |
| 9 G. B. Munhoz | 22 Ilha Solteira | 35 Furnas | — 440 kV lines |
| 10 Passo Fundo | 23 São Simão | 36 Angra dos Reis | — 345 kV lines |
| 11 Passo Real | 24 Cachoeira Dourada | 37 Santa Cruz | — 230 kV lines |
| 12 P. Medici | 25 Itumbiara | 38 Mascarenha | — 138 kV lines |
| 13 J. Lacerda | 26 Emborcação | 39 Casca III | |

Fig. 15.3 Electrical system of Paraguay - 1991

- 1 Right bank substation
- 2 Acaray
- 3 Itaquyry
- 4 Catuete
- 5 Limpio
- 6 Lambare
- 7 San Lorenzo
- 8 Itauguá
- 9 Alberdi
- 10 Quindy
- 11 Pilar
- 12 Villabin
- 13 Ayolas
- 14 Yacyreta
- 15 San Pedro del Paraná
- 16 Encarnación
- 17 Natalio
- 18 Paranambu
- 19 Cruce Bella Vista
- 20 Horqueta
- 21 San Estanislao
- 22 Rosário
- 23 Caruguaty

▲ Hydroelectric powerplant

△ Hydroelectric powerplant (in construction)

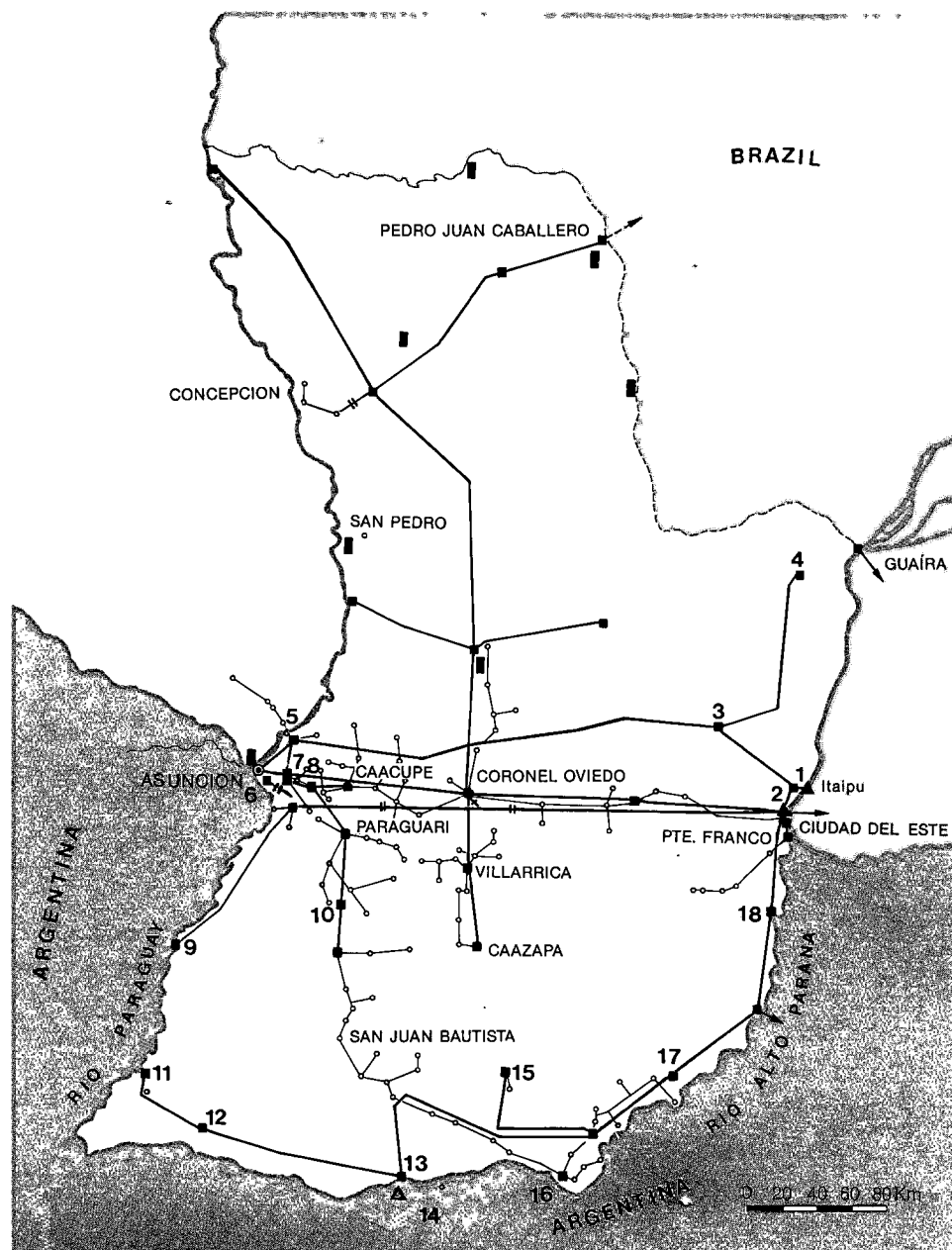
■ Thermal powerplant

■ Substations

— 220 kV lines

— 66 kV lines

— 23 kV lines



50 HZ SYSTEM

RIGHT BANK SUBSTATION

The right bank substation carries the power of the Itaipu 50 Hz powerhouse sector to the Paraguayan network. This power is the main energy source for Paraguay, therefore the greatest concern in the substation design was to obtain a high reliability

together with the required expandability and flexibility of operation.

The initial configuration of the substation includes two 500 kV lines from Itaipu powerhouse, two 500 kV lines to Foz do Iguaçu HVDC converter station, two 220 kV lines to Acaray hydroelectric plant, three three-phase 525/241.5 kV 375 MVA autotransformers with separate voltage regulator transformers, two 8.3 MVA three windings 200/66/13.8 kV auxiliary service transformers, one 66 kV line to Foz do Iguaçu converter station and one 66 kV oil-filled cable to Itaipu powerhouse.

The substation can be expanded to include, in the ultimate configuration a total of four 500 kV and seven 220 kV line bays and five 375 MVA transformers.

The breaker-and-one-half scheme was adopted for the 500 and 220 kV switchyards. Initial and ultimate stages of substation are shown in the single line diagram of Fig. 15.4.

The substation main buses are combinations of strain conductor and rigid aluminum tube. Structures supporting strain conductors are of the lattice steel type. Equipment support structures are of reinforced concrete. Disconnecting switches are of the vertical opening type.

Structures and rigid buses are designed for wind loadings resulting from 3 gusts at 167 km/h, (corresponding to a recurrence interval of 50 years), with rigid buses additionally designed for

short-circuit stresses coinciding with 15 gusts at 140 km/h.

Protection against direct lightning is provided by shielding wires over the substation designed for 99.9% strike interception and iskeraunic level of 100 (20 strikes per km²/year).

Wiring systems are installed in concrete cable trenches and pullboxes. Multicore cables are used for control and protection and single conductor cables for 460 V auxiliary power.

The substation is functionally divided into sectors as follows:

500 kV switchyard

The four 500 kV overhead lines from the powerhouse are matched by the four lines to the converter station, in the same breaker-and-one-half

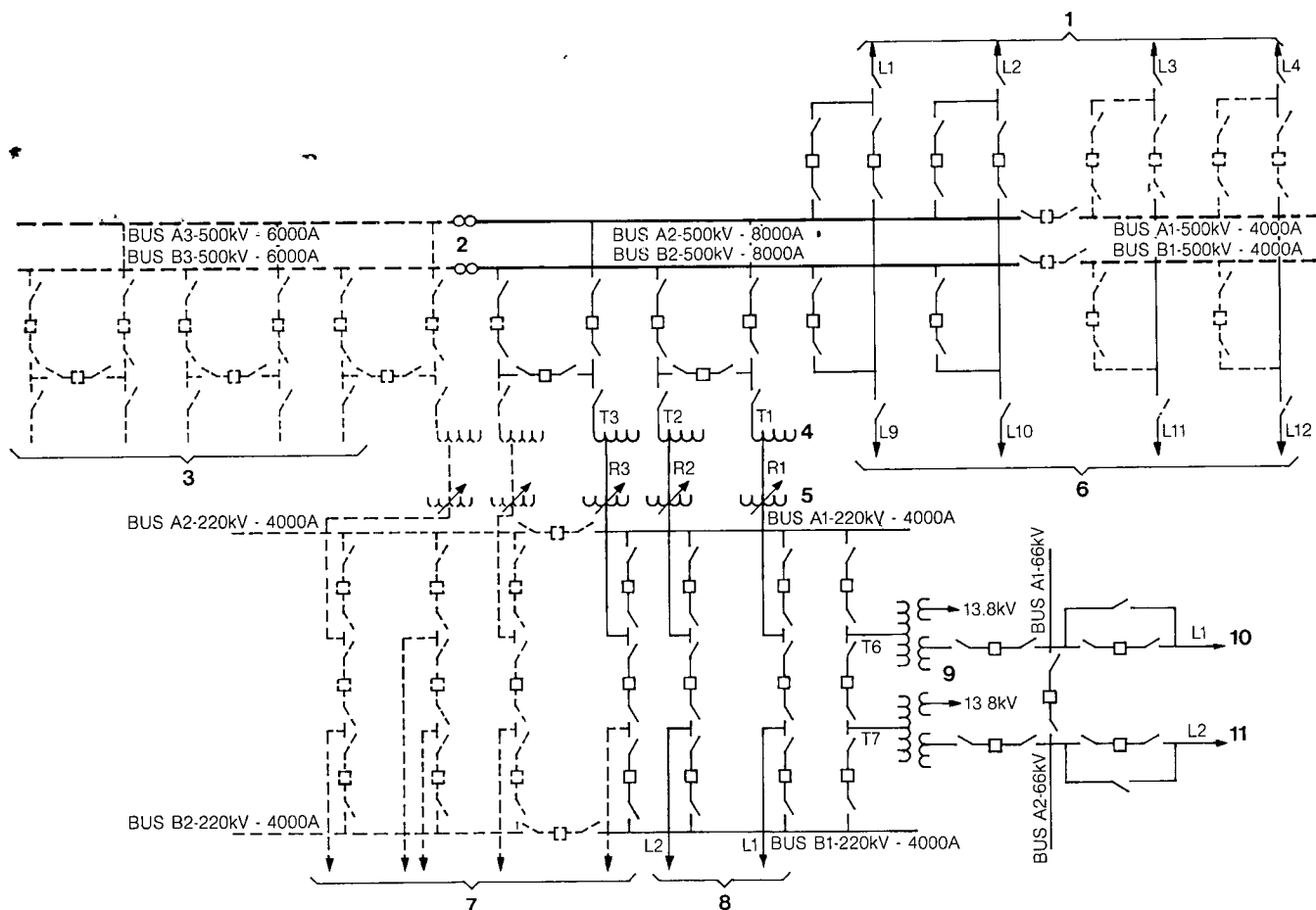


Fig. 15.4 Right bank substation - single line diagram

- 1 500 kV lines from Itaipu powerhouse
- 2 Removable link
- 3 500 kV line (future)
- 4 Autotransformer 3 ϕ - 375 MVA (typical)

- 5 Voltage regulator 3 ϕ - 375 MVA (typical)
- 6 500 kV line to Foz do Iguaçu substation
- 7 220 kV line (future)
- 8 Acaray hydroplant

- 9 Transformer 3 ϕ - 25 MVA
- 10 Itaipu powerhouse
- 11 Foz do Iguaçu substation



Aerial view of right bank substation

bay. This allows the direct through connection of the lines if necessary. In fact, in the initial arrangement two of the lines by-passed the substation altogether. The breaker-and-one-half scheme is arranged with an inverted bus, that is, with the main bus located centrally to the line and transformer take-off structures. This arrangement avoids three conductor levels but requires a considerable increase in bay width making it more expensive. Nevertheless it was chosen because of the foreseen future changes in the number of the incoming and outgoing 500 kV circuits. The adopted arrangement, placing the heavy main buses at the lowest level and reducing the overall height, had the additional benefit of improving the aesthetics and reliability.

As the lines from the powerhouse and converter station approach the main buses from opposite sides, the "C" arrangement with circuit breakers on both sides of the main buses was used. For the auto-transformers and the other 500 kV lines, which are located on one side of the main buses only, the "U" arrangement with breakers on one side only was adopted.

With the four lines from the powerhouse connected at one end of the main buses and, ultimately, the five lines to the 50 Hz system at the other, the central portion of the main buses will carry the total 50 Hz output of the powerhouse. Thus that portion of the bus is 254 mm diameter aluminum tube, rated 6000 A for normal (70°C) and 8000 A for emergency (90°C) service. For the rest of the main and auxiliary buses, 127 mm diameter aluminum tube or, where greater flexibility is required for connection to equipment, two 4000 ASC conductor bundles are used, rated 3000 A for normal and 4000 A for emergency service.

Because of the extended construction period and high probability of dust contamination the equipment bushings and all insulators have a basis impulse level (BIL) of 1800 kV.

Surge arresters are metal oxide, 420 kV having a maximum continuous voltage of 340 kV L-N. The air blast type circuit breakers have a continuous rating of 4000 A, interrupting capability of 50 kA and a BIL of 1800 kV. The SF₆ circuit breakers have a continuous rating of 2000 A and otherwise are rated identically as the air blast circuit breakers.

Clearances adopted for the 500 kV switchyard are:

	Nominal (m)	Minimum (m)
Phase to ground (metal to metal)	4.5	4.1
Phase to phase (metal to metal)	6	5.3
Phase to phase (centerlines)	9	
Vertical distances:		
Main busbar	11	
Auxiliary busbar	10	
Strain conductors	22	
Busbar – heavy vehicle road	16.5	
Shield cable	27	

Step-down transformers and voltage regulators.

In the initial arrangement three 525/241.5 kV autotransformers are used each rated 375 MVA. In the final arrangement, four of the five autotransformers, supplying the 220 kV switchyard, are paired on breaker-and-one-half bays while the fifth is paired with one of the 500 kV lines.

To assure complete independence of voltages required by the ANDE power system under different operating conditions and the voltage on the 500 kV buses, the step-down autotransformers are connected to separate booster-transformer units for voltage regulation.

The main step-down transformer characteristics are:

Autotransformers

Voltage (kV)	525/241.5/13.8
Connection	wye/wye/delta
Rating (MVA)	375/375/12.5
Cooling	OA/FOA/FOA
BIL winding (kV) (crest)	1550/950/110
BIL bushing (kV) (crest)	1800/1050/150

Booster voltage regulator transformers

Voltage (kV)	241.5 ± 10%
Rating (MVA)	375
Cooling	OA/FOA/FOA
BIL (kV) (crest)	950

220 kV switchyard

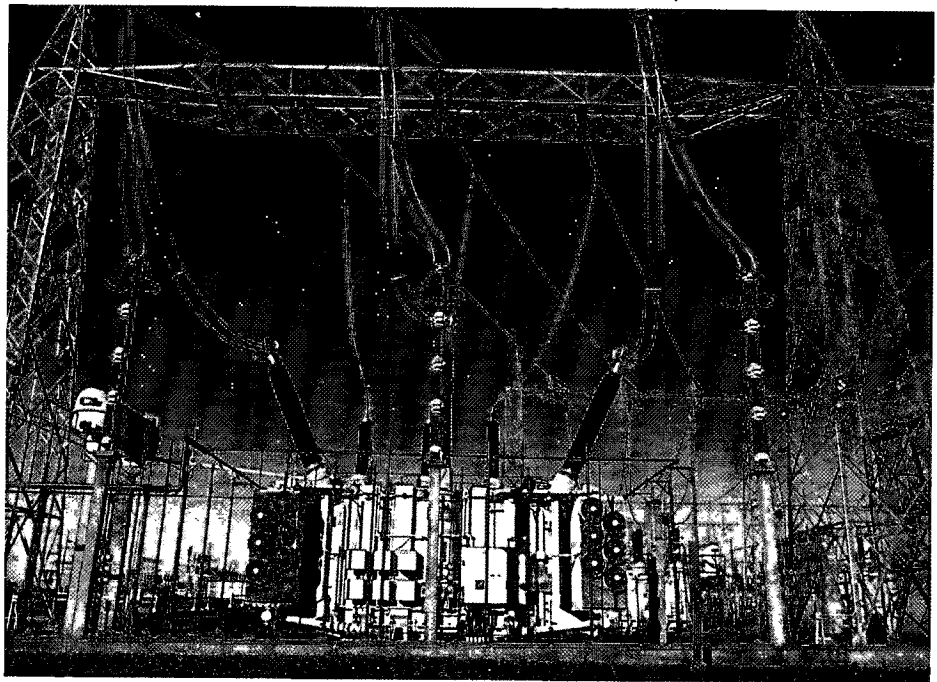
The 220 kV switchyard is also arranged in the breaker-and-one-half scheme conventionally with the three circuit breakers in-line, three levels of conductors, and the main buses outside the



Partial view of 500 kV switchyard



500 kV circuit breaker



500/200 kV step-down transformer

switchgear. This arrangement was chosen because of the number of incoming and outgoing circuits to and from the buses and hence the loadings were nearly equal.

The five overhead strain buses from the autotransformer/voltage regulator areas are paired with 220 kV transmission lines. The two 25 MVA transformers supplying the 66 kV and 13.8 kV systems are paired and supplied from an end bay and the remaining two 220 kV lines are paired towards the opposite end of the switchyard.

As the 220 kV transmission lines have a load capacity of 2000 A each it is possible, although very unlikely, that the main buses may carry the output of four autotransformers, 1500 MVA (4000 A). Thus they are 127 mm diameter aluminum tube or two bundle 4000 kcmil ASC cable rated 2000 A for normal (70°C) and 4000 A for emergency (85°C) service.

The equipment bushings and insulators have a BIL of 1050 kV.

Surge arresters are metal oxide, 240 kV, having a maximum continuous capacity 171 kVL-N. The SF₆ circuit breakers have a continuous rating of 2000 A, interrupting capability of 31.5 kA and a BIL of 1050 kV.

Clearances adopted for the 220 kV substation are:

	Nominal (m)	Minimum (m)
Phase to ground (metal to metal)		2.1
Phase to phase (metal to metal)		2.7
Phase to phase (centerlines)		
Rigid	4.5	
Flexible	5	
Vertical distances:		
Main busbar height	8	
Strain conductors	17	
Busbar – light vehicle road	8.5	
Shield cable	22	

66 kV switchyard

The 66 kV substation has a single sectionalized main bus and radial feeder circuit breakers. Each of the two 220/66/13.8 kV transformers are paired with an outgoing circuit on a main bus section. One oil cable circuit provides stand-by auxiliary power to the 50 Hz sector of the powerhouse. The other circuit supplies 50 Hz power to the Foz do Iguaçu substation. The transformers are rated

220/66/13.8 kV (wye grd./wye grd./delta), 25/25/8.33 MVA (ONAN/OFAN/OFAN) and they have BIL ratings of 950/350/150 kV. Circuit breakers have an interrupting capability of 31.5 kA symmetrical, a BIL of 350 kV and a continuous current rating of 1000 A. The surge arresters have a rating of 72 kV.

Substation auxiliary services

The primary distribution voltage for the auxiliary services is 13.8 kV and is taken from the 13.8 kV delta tertiary windings of the two 220/66/13.8 kV step-down transformers. Each tertiary winding is connected by an underground cable to a 3000 kVA auxiliary stabilizing transformer connected in delta/wye grd./wye grd. with respectively voltages 13.8/13.8/1.34 kV (the last winding has no external connection).

Grounded wye connected secondary windings of the stabilizing transformers feed, through underground cables, two 13.8 kV metal-enclosed outdoor type switchgear assemblies.

Final substation auxiliary voltage is 460 V taken from two 1000 kVA 13.8 kV – 460 V transformers fed from the 13.8 kV switchgear. The 460 V buses, which are fed by underground cable from the transformers, are located in the relay house and consist of three sections, interconnected by circuit breakers. The middle section supplies essential loads and can be energized from either of the outside sections or from the 75 kVA emergency diesel generator.

Control facilities

The right bank substation was designed either for remote unattended operation or for local operation from the local control room which is located in the relay house.

Remote control is performed from the powerhouse central control room (CCR) panelboard RMP and is considered the normal operating mode. The selection of "remote" or "local" control mode is made by the selector switch located on RMP.

All controls within the substation are hardwired. Remote control of essential apparatus such as circuit breaker disconnecting switches and tap changing mechanisms of the voltage regulators is through microwave system. Hardwired cable connections between the powerhouse and the right bank substation were not considered because of possible high transient potential differences. The large amount of information such as alarms, instrumentation and status indication, which is transmitted from the substation to the powerhouse, necessitated an auxiliary digital data acquisition system (TADMIC) which reduced the required number of microwave channels.

Relay house. The relay house is a two-story air conditioned building. Each floor of the building has an approximate area of 500 m². The first floor has cable trays and cable terminal cubicles which are used for transition of the external multi-conductor cables to internal bundled wire connections. It also accommodates storage batteries and battery charges, air conditioning equipment, central telephone central (PAX), and cubicles containing TADMIC and SCADA terminals.

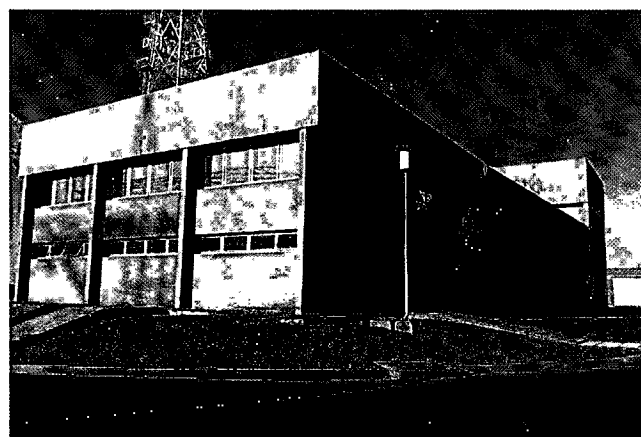
The second floor houses the main control room with control panels, protective relaying equipment, auxiliary service equipment, switchgear assemblies, separate rooms for power line carrier and microwave equipment and test and repair facilities for the protective relays and communication equipment.

Protective relays

500 kV transmission lines. The protective scheme for all 50 Hz, 500 kV transmission lines (L1 to L4 and L9 to L12) is the same as for line terminations at the powerhouse, see Chapter 14.

500 kV busbar. There are two independent busbar protection schemes; primary 87P and alternate 87A. Each protection scheme includes two relaying groups one for bus A and another for bus B.

525/241.5 kV autotransformers. All step-down autotransformers are protected by the primary differential protections 87TP. In addition, the transformer-regulators are protected by an alternate differential protection 87TP. The transformer back-up protection consists of an overcurrent relay 51 OL with instantaneous trip attachment 50. Protection against ground faults is provided by the ground overcurrent relay 51NT.



Relay house



Control room of right bank substation

Voltage regulators. The voltage regulators are protected by the differential protections 87VR. Protection against ground faults is provided by relay 51NVR.

220 kV busbar.

- | | |
|-------------------------------|----------|
| • Bus differential protection | 87A, 87B |
| • Overvoltage protection | 59A, 59B |

220 kV transmission line.

- | | |
|--|----------|
| • Line distance protection (Primary and secondary) | 21P, 21A |
| • Power oscillation trip blocking relay | 68B |
| • Power oscillation tripping relay | 68T |
| • Undervoltage protection | 27L |

220 - 66 kV transformer.

- | | |
|---------------------------|--|
| • Differential protection | 87T |
| • Overcurrent protection | 51 |
| • Neutral overcurrent | 51NT (wye connected secondary winding) |
| • Ground fault sensor | 64T (on delta secondary winding) |

66 kV transmission circuits.

- | | |
|-----------------------------------|---------|
| • Overcurrent protection | 50, 51 |
| • Overcurrent residual protection | 50, 51N |

Breaker failure. All 500 kV and 220 kV circuit breakers are equipped with the breaker failure protection 50BF.

Forced isolation protection (FIP)

This group of protective devices detect disturbances, which are dangerous or undesirable to the 220 kV ANDE power system.

System disturbances may be caused by load rejection on the dc transmission systems, thyristor blocking, loss of Itaipu generation or loss of interconnections between the right bank substation and the Foz do Iguaçu converter station. This protection scheme trips all 220 kV line circuit breakers.

System disturbances are measured by the coupling capacitor potential devices connected to the 500 kV main buses and includes the following protective relays:

Overfrequency	81
Overvoltage	59
Undervoltage	27
Directional overcurrent	67

Synchronization

Only manual synchronization is possible at the relay house control room. One set of instruments can be switched to either the 220 kV line or autotransformer 220 kV circuit breakers. There is no generating unit speed adjustment at the relay house control room. When required, it is done at the Acaray or the Itaipu powerhouses.

Fire protection and oil containment

All large transformer units (three autotransformers, three voltage regulators and two auxiliary service transformers in the initial stage) are protected against fire by a water deluge system.

Fire resistant walls separate autotransformers and voltage regulators to prevent spread of fire to adjacent units.

Following a fire, oil and water from the fire protection system is collected in containment reservoirs filled with crushed stone. The volume of the reservoirs is one and half times the oil volume of the respective equipment, thus the reservoir has the capacity for rain and fire protection water.

Ambient temperature ($^{\circ}\text{C}$)

Maximum 40

Minimum - 5

Maximum conductor stress at 15°C and wind velocity of 168 km/h 45% of tensile strength

Normal conductor of stress at 20°C no wind 18% tensile strength

Isokeraunic level 80

Dampers: approx. spacing (m) 75

Right-of-way width per line (m) 70

500 kV TRANSMISSION LINES

The principal physical and electrical characteristics of the 500 kV transmission lines are:

Physical characteristics

Line length (km)

Powerhouse to right bank substation 2.1

Right bank substation to Foz do Iguaçu converter station 8.9

Span (m)

Average length 400

Maximum length 650

Minimum clearance at mid span (m) 12.5

Phase arrangement Horizontal

Clearance between phases (m) 11.5

Conductor arrangement in the bundle Square

Distance between conductors in the bundle (m) 0.457

Tower type (%)

Suspension 66

Dead end 32

Special 2

Electrical characteristics

Nominal voltage (kV) 500

Maximum operating voltage (kV) 550

Normal rating (MVA) 2470

Conductor ACSR "RAIL" 954 kcmil stranding 45 x 7

Number of conductors per bundle 4

BIL (kV) 1800

Suspension insulators 28 per string
Standard disc type
254 mm x 146 mm
strength 120 kN
Fog disc type
280 mm x 146 mm
strength 120 kN

Shield wires ACSR "PARTRIDGE"
266.8 kcmil
Stranding 26/7
2 wires normal
protection and
4 wires for the first
three spans from
powerhouse

Counterpoise Radial, bare
copper, 2 AWG
(34 mm²) or
galvanized steel
wire 4 BWG
(28.75 mm²)

Design conditions

Maximum wind velocity (km/h) 168

A drawing of a typical 500 kV self-supporting tower is shown in Fig. 15.5.

500 kV transmission line tower (on top of the right wing buttress dam)

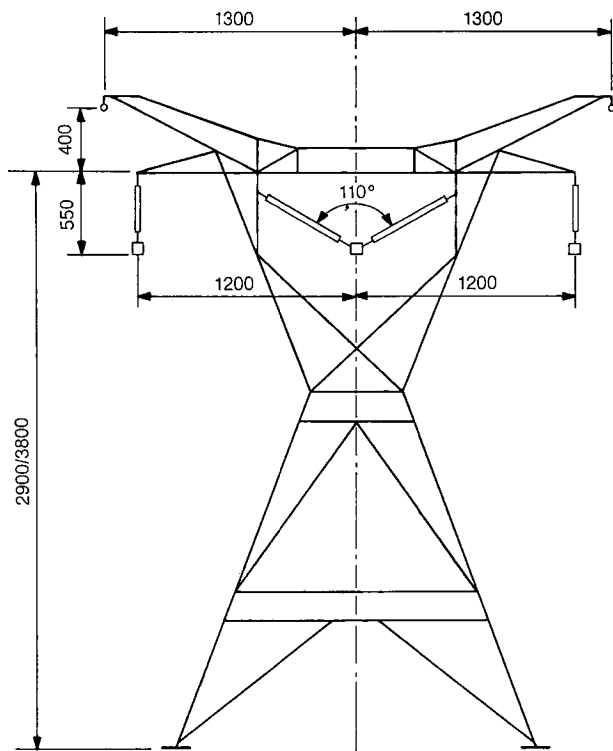


Fig. 15.5 500 kV ac line - typical self-supporting tower

THE HVDC TRANSMISSION SYSTEM

General

At present a large part of Itaipu 50 Hz powerplant output is converted from 50 Hz to HVDC and then transmitted to São Paulo area in Brazil by two bipolar ± 600 kV dc transmission lines.

The Foz do Iguaçu converter station, located near the Itaipu powerhouse, operates as a rectifier with two bipolar converters supplying power to two bipolar transmission lines. The Ibiúna station, near São Paulo, operates as an inverter with two bipolar converters receiving the transmitted dc power. Normal direction of power flow is from Foz do Iguaçu to Ibiúna but the reverse is possible if ever required. A simplified single line diagram of the overall system is shown in Fig. 15.6.

Converter station buses at Foz do Iguaçu are 500 kV ac and at Ibiúna 345 kV ac. Ultimately the Ibiúna converter station will be connected to the receiving power system via six 345 kV transmission lines as well as via 345/500 kV interconnecting autotransformers.

Both stations have the following general features:

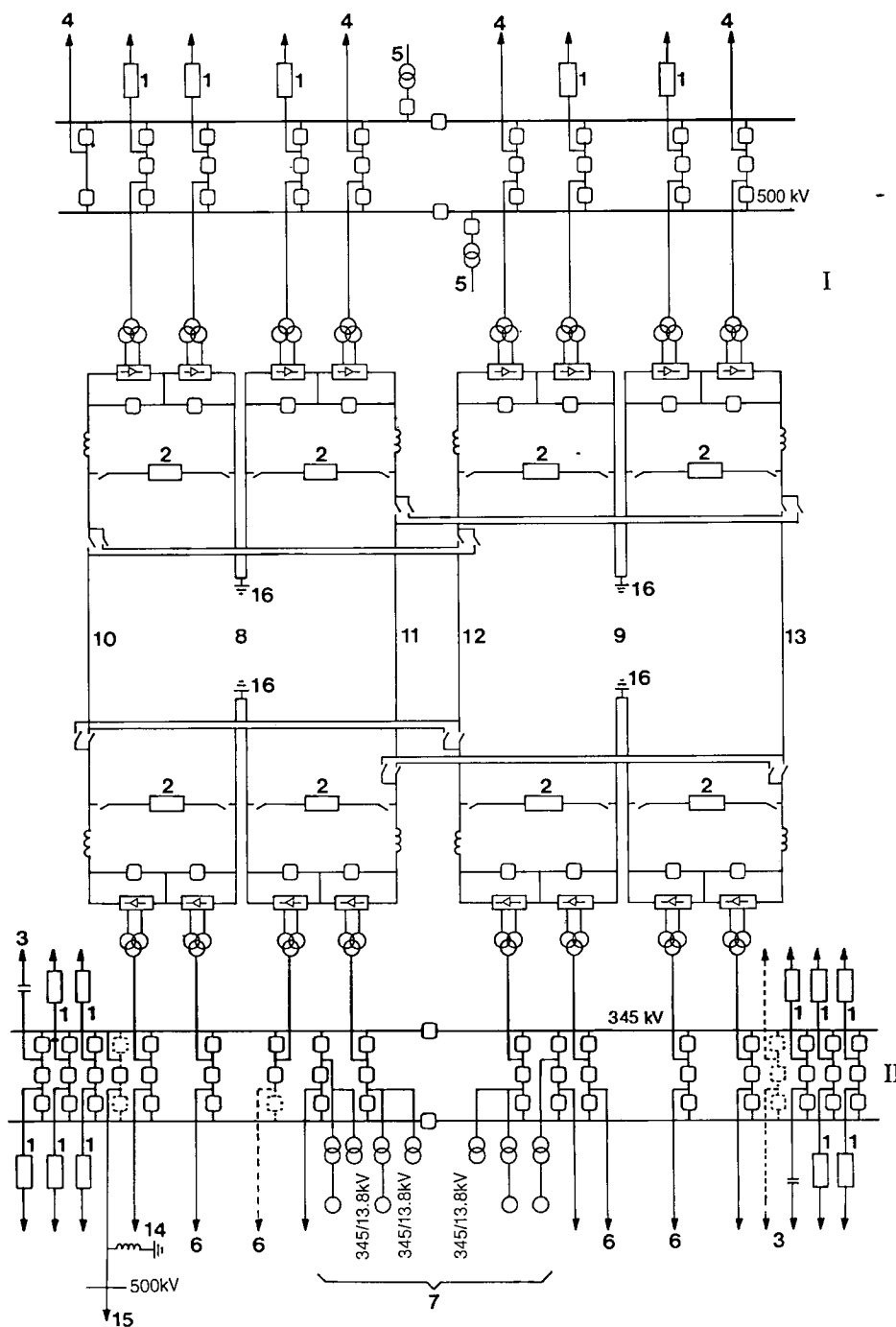


Fig. 15.6 Simplified single line diagram of Itaipu HVDC transmission system

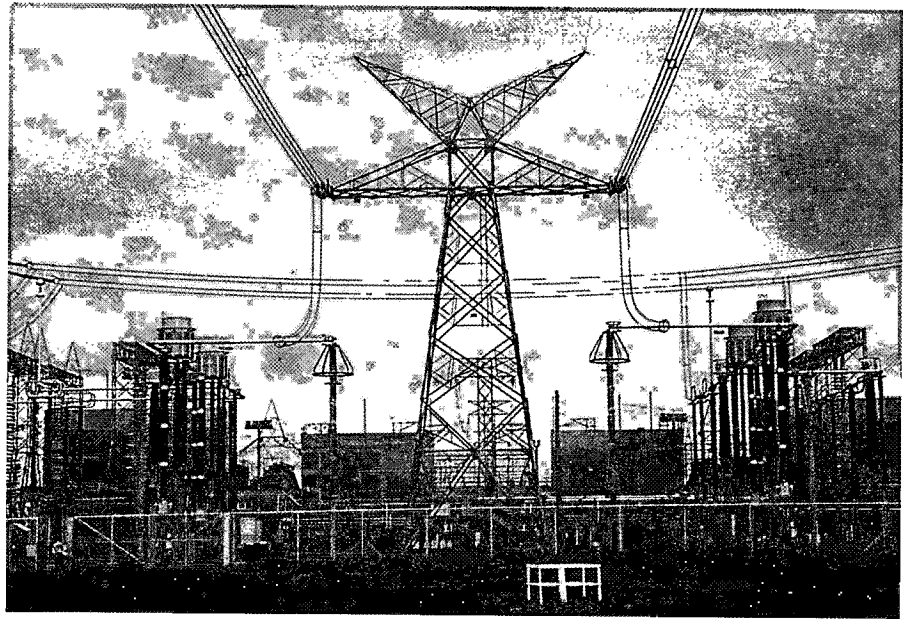
- I Foz do Iguaçu
- II Ibiúna
- 1 ac filter
- 2 dc filter
- 3 Shunt capacitor
- 4 Line to Itaipu powerhouse
- 5 Auxiliary service transformer
- 6 345 kV lines
- 7 Synchronous converters
- 8 Bipole 1
- 9 Bipole 2
- 10 Pole 1
- 11 Pole 2
- 12 Pole 3
- 13 Pole 4
- 14 500/345 kV interconnection
- 15 Line to Campinas
- 16 Electrode lines and ground electrodes

The HVDC Converter Stations

The general structure of both stations can be divided in the following parts:

- Station control house.
- ac switchyard, including the switchgear and buses for interconnection of the ac transmission lines, converters, ac filters, shunt capacitor banks, synchronous compensators (Ibiúna only) and the main auxiliary power transformers.

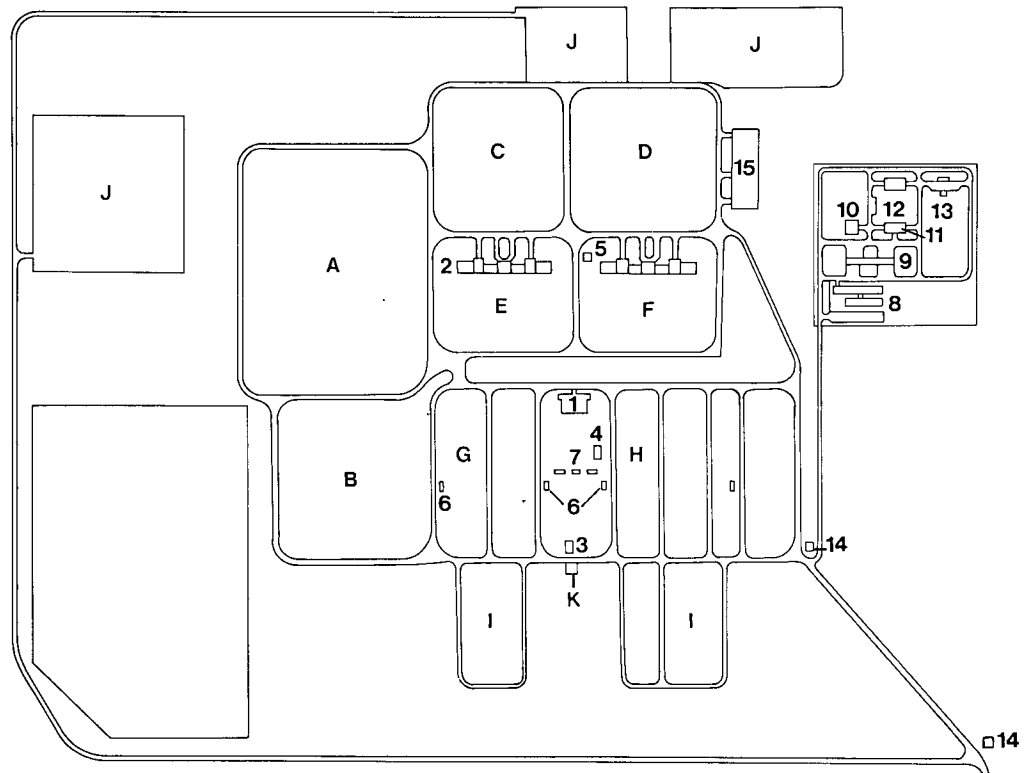
- Converter area, including the converter transformers and thyristor valves housed inside the valve buildings.
 - dc switchyard, including the dc transmission line termination, smoothing reactors, filters, line paralleling equipment, converter by-pass and isolation equipment, and the neutral bus equipment.
- The general layouts of the Foz do Iguaçu and Ibiúna converter stations are shown in Figs. 15.7 and 15.8.



General view of converter stations

Fig. 15.7 Foz do Iguaçu converter station – general layout

- A** 765 kV - 60 Hz switchyard
- B** 500 kV - 60 Hz switchyard
- C** 600 kV dc switchyard bipole 2
- D** 600 kV dc switchyard
- E** Converter transformers bipole 2
- F** Converter transformers bipole 1
- G** 500 kV-50 Hz switchyard
- H** 500 kV-50 Hz switchyard bipole 1
- I** ac filter
- J** Temporary construction facilities
- K** 66/13.8 kV substation
- 1** Station control house
- 2** Converter buildings
- 3** Relay house
- 4** Emergency diesel generator house
- 5** Service air compressor house



- 6** Central compressed air station for 500 kV power circuit breaker
- 7** 13.8 kV metal-clad switchgear
- 8** Administration building

- 10** Electromechanical workshop
- 11** Main warehouse
- 12** Warehouse for insulators and drums

- 13** Warehouse for combustible material
- 14** Guard house
- 15** Water treatment plant

The basic ratings of a bipole at each station are:

	Foz do Iguaçu	Ibiúna
Maximum ambient temperature		
Rated continuous input power (MW/bipole)	3150	3010
Rated continuous current (A)	2610	2610
Rated dc voltage (kV)	± 600	± 576.6
Maximum continuous voltage (kV)	± 613.6	± 613.6
Minimum direct current (A)	260	260
Low ambient temperature (24° C)		
Maximum continuous power (MW/bipole)	3392	Not defined
Maximum continuous current (A)	2840	2840

Short term overload capabilities of each bipole, based on the respective maximum ambient or low ambient ratings, are 3310 A or 3590 A during 5 seconds followed by an overload of 3030 A or 3290 A during an additional 20 seconds.

The two 3150 MW HVDC bipoles are designed to operate independently such that no single contingency in the converter station should shutdown a complete bipole. Temporary operation in the monopolar mode with ground return is possible when one pole is inoperative.

Conversion of power from ac to dc and vice versa requires both a source of reactive power and extensive harmonic filters. As these requirements vary with the loading conditions and the associated ac systems, there are significant differences between the two stations especially in the ac portions.

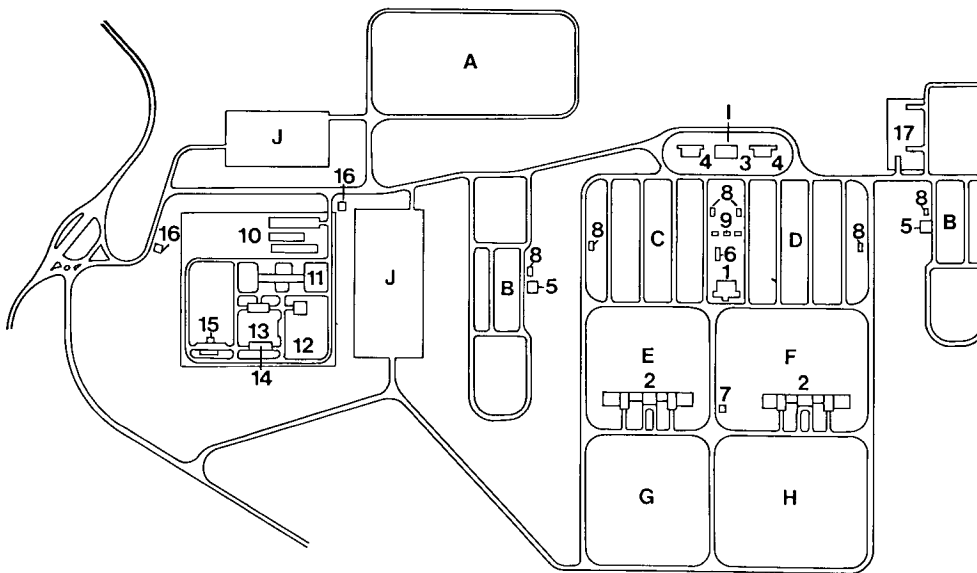


Fig. 15.8 Ibiúna converter station - general layout

- | | | |
|--|---|--|
| A 500 kV ac switchyard | 1 Station control house | 9 13.8 kV metal-clad switchgear |
| B ac filter bays | 2 Converter buildings | 10 Administration building |
| C 345 kV ac switchyard bipole 2 | 3 Synchronous compensators control building | 11 Garage |
| D 345 kV ac switchyard bipole 1 | 4 Synchronous compensators building | 12 Electromechanical workshop |
| E Converter transformers bipole 2 | 5 Relay houses | 13 Main warehouse |
| F Converter transformers bipole 1 | 6 Emergency diesel generator house | 14 Warehouse for insulators and drums |
| G 600 kV dc switchyard bipole 2 | 7 Service air compressor house | 15 Warehouse for combustible material |
| H 600 kV dc switchyard bipole 1 | 8 Central compressed air station for 345 kV power circuit breakers | 16 Guard house |
| I Synchronous compensators | | |
| J Temporary construction facilities | | |

ac switchyards

The 345 kV ac switchyard at Ibiúna and the 500 kV ac switchyard at Foz do Iguaçu are arranged in the conventional breaker-and-one-half scheme. Ibiúna station has synchronous compensators and capacitor banks in addition to the converters, and dc and ac filters.

Main buses are of the strain type and use ACSR conductors. A bundle of four subconductors 1431 kcmil was chosen because of corona effects. Based upon thermal capacity, the grounding buses have three subconductors. For enhanced reliability the main buses have sectionalizing circuit breakers.

Lower level equipment interconnections are made with 152 mm diameter aluminum tubes. All supporting structures are lattice steel type.

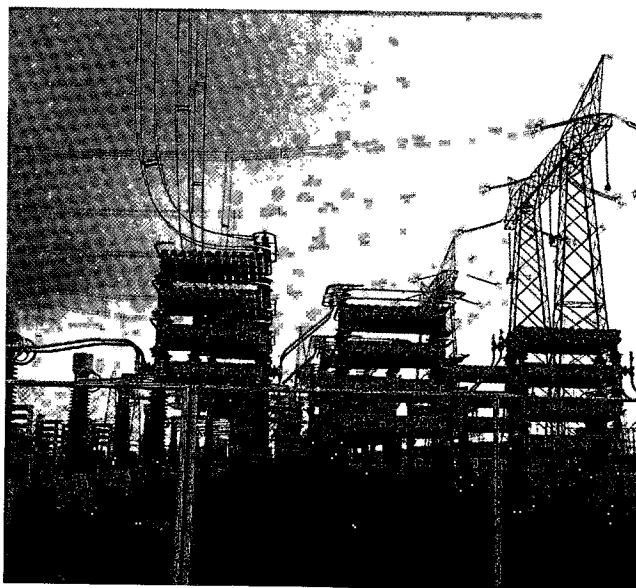
Air-blast circuit breakers are used throughout. The transient recovery voltage studies showed that the peak recovery voltage for the 550 kV circuit breakers at Foz do Iguaçu may be higher than the standard IEC values, thus uprated breakers were used. All breakers, are equipped with closing resistors. All surge arresters are of metal oxide type rated 420 kV.

Converter area

ac filters and VAR balance. To reduce harmonic voltages to an acceptable level, ac harmonic filters are installed at both converter stations. Filters are RLC circuits connected phase-to-ground. They are either tuned to a specific harmonic frequency, for which the filter branch has a low impedance, or operate as high-pass filters with a low impedance over a wide frequency range. The ac filters also serve as reactive power sources to compensate for reactive power absorbed by the converters.

Design of the ac filters and study of the reactive power balance progressed concurrently to ensure an optimum filter performance considering the imposed reactive power balance and switching constraints. As a result, considerably different ac filters were adopted at the two stations.

At Foz do Iguaçu, a large portion of the reactive power consumed by the converter station is supplied by the 50 Hz generators, which have a power factor of 0.85. This allowed a reduction in the size of the filter capacitor banks and minimized the risk of self-excitation of the generators in the event of an unforeseen loss of some connected generators. Thus the 11th and 13th and the 3rd and 5th harmonic filters act as double tuned filter branches to produce minimum reactive power and still fulfill the



Partial view of ac switchyard showing filters

necessary filtering. Different types of high pass filters are used to optimize performance with respect to telephone interference factor (TIF).

For the Ibiúna converter station the requirements of reactive power compensation have to be met with a minimum MVA exchange with the receiving ac network. Therefore the largest part of the reactive power is supplied by the capacitor banks. Four 300 MVA synchronous compensators and two 294 MVA shunt capacitor banks are also provided. Consequently the 11th and 13th harmonics are filtered by individual single-tuned filter branches; different types of high-pass filter branches are used to avoid too high a voltage variation when filter switching. Small double tuned 3rd and 5th harmonic filters were used as their reactive power generation is not important for reactive power balance.

Converters. Each of the 600 kV dc poles consists of two series-connected 300 kV, twelve-pulse converters; making a total of eight converters per station. A simplified single-line diagram of one converter pole is shown in Fig. 15.9.

There are two outdoor transformer yards, each yard having two banks of three single-phase transformers.

Each transformer bank supplies three quadruple thyristor valves located in the valve halls. On the

primary side the transformer banks are connected in wye grounded. Each transformer has two secondary windings one connected as wye and the other as delta. This arrangement reduces the harmonics on the ac side of the converter. On-load tap changers, located in the neutral of the ac-side windings have a range of $+ 20 \times 1.25\%$; $- 6 \times 1.25\%$, and allow operation of the HVDC transmission at the rated dc voltage within the entire load range and under different ac network conditions.

Thyristor valves of the converter are arranged in quadruple assemblies in which four valves are placed vertically in one assembly. Each valve consists of eight modules, each module containing twelve thyristors connected in series. Therefore each valve has ninety-six thyristors and one quadri-valve has 384 thyristors.

In the bipole system one converter (high voltage) is connected to the dc transmission line and the other (low voltage) to the ground electrode. The basic rating of the converters valves are:

	Foz do Iguaçu	Ibiúna
Continuous current (A)	2610	2610
Overload current 20 s (A)	3030	3030
Minimum current (A)	260	260
Nominal voltage (kV)	150	144.2
No-load voltage (kV)	172	164.7

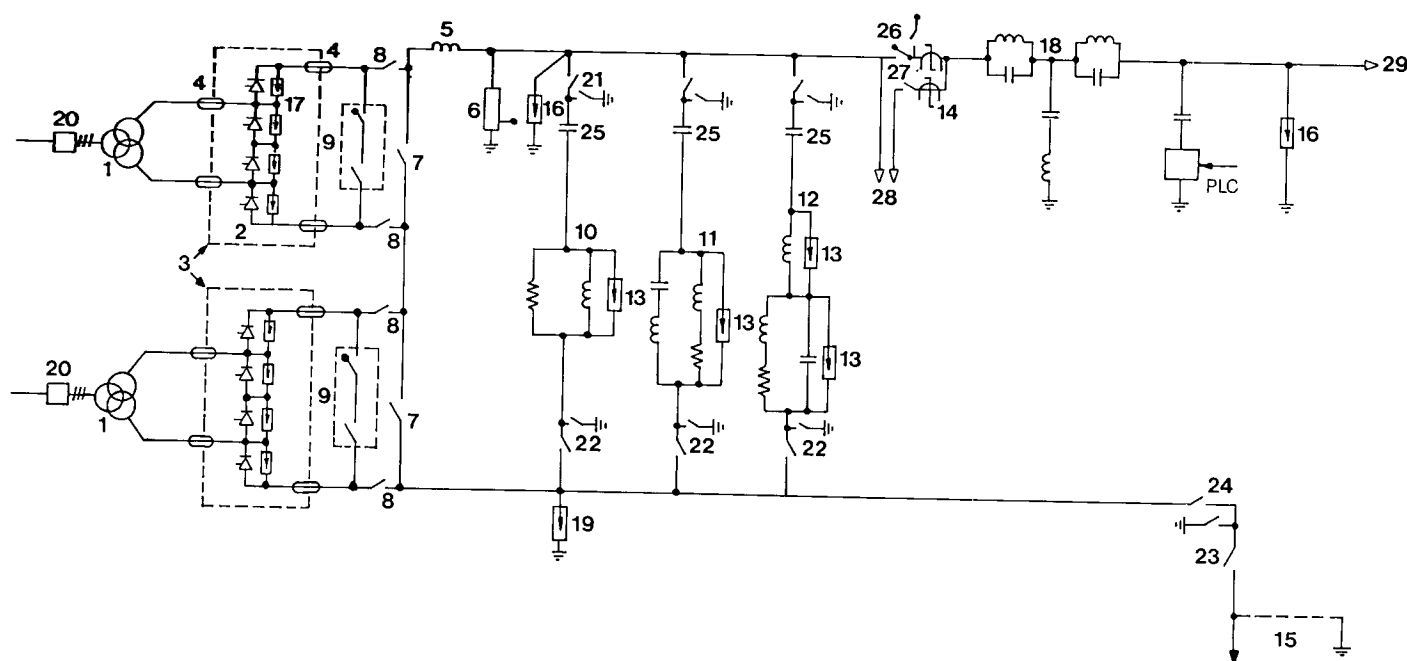
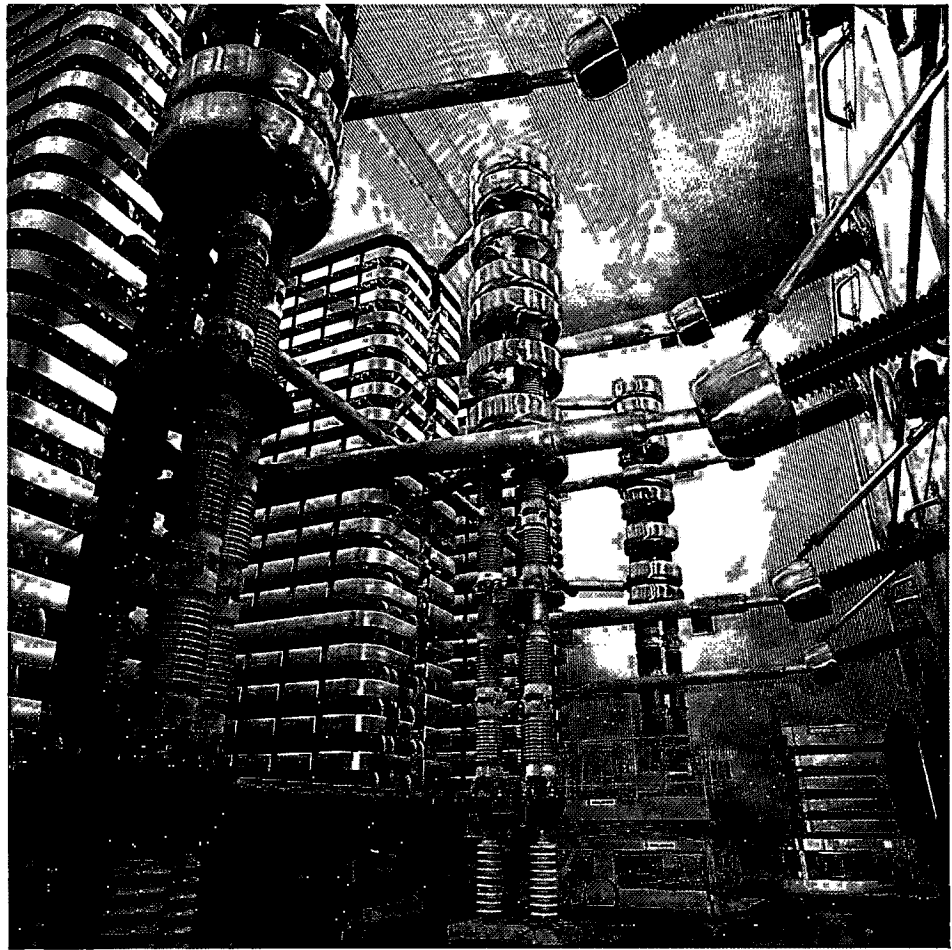


Fig. 15.9 Simplified diagram single-line of one converter station pole

- | | | |
|------------------------------|---|---|
| 1 Converter transformer | 11 12 th dc filter | 21 Upper dc filter disconnectors with ground blade |
| 2 Thyristor valve | 12 2 nd /6 th dc filter | 22 Downer dc filter disconnectors with ground blade |
| 3 Valve hall | 13 Filter arrester | 23 Neutral disconnector |
| 4 Wall bushing | 14 dc current measuring | 24 Neutral bus load breaker switch |
| 5 Smoothing reactor | 15 Electrode line and ground electrode | 25 dc filter main capacitors |
| 6 Voltage divider | 16 dc line arresters | 26 dc line disconnector with ground blade |
| 7 Bypass disconnector | 17 Valve arresters | 27 dc paralleling disconnector |
| 8 Converter isolating switch | 18 PLC filter | 28 Paralleling to bipole 2 |
| 9 Bypass breaker | 19 Neutral bus arresters | 29 ± 600 kV dc line |



Thyristor converter valve

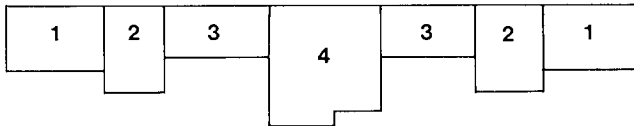


Fig. 15.10 Layout of HVDC converter building

- 1 High voltage valve section
- 2 Service
- 3 Low voltage valve section
- 4 Control section

Thyristor valves are cooled with demineralized, deionized water. The cooling system consists of a closed loop purified water system, heat exchangers and a secondary cooling water circuit using cooling towers located on the top of the valve buildings. The system is arranged such that a component member of the valve can be removed and substituted without opening the water circuit.

Valves of each bipole are located in a separate building each comprising seven sections; see Fig.15.10. Section 1 and 3 of the building, in addition to the valves, also contain wall bushings, surge arresters and grounding switches. Shielding meshes are installed in wall, ceiling and floor to minimize the propagation of electromagnetic fields. The building is air conditioned to ensure clean dry air conditions.

Any converter can be taken out of service and disconnected for maintenance, without interfering with the operation of the rest of the station.

dc switchyard

dc filters. The dc filters connected between each 600 kV station bus and the neutral bus reduce the harmonic currents in the dc transmission line in either bipolar or monopolar operation. Filters at both stations are to the same design with three dc filter branches per pole one double-tuned to the 2nd and the 6th harmonics, one single-tuned to the 12th harmonic and one high-pass filter branch.

Each dc filter branch has motor-operated disconnecting switches complete with grounding switch on both the 600 kV dc side and the neutral bus side of the station pole. Thus any of the dc filter branches in the stations can be connected and/or isolated in a fully automatic sequence.

For increased reliability, capacitor units of the dc filters have internal fuse and internal resistors for dc voltage grading, all located inside weather proof enclosures. The main capacitors are suspended from gantry type steel structures. The dc filter reactors are of the air insulated type. Metal oxide surge arresters are used for overvoltage protection of the low voltage reactor/resistor branches.

Smoothing reactor. The dc smoothing reactor reduces the harmonic currents generated by the converter and limits the dc current surges in the event of a ground fault on the dc line. There is one oil-insulated reactor per pole inserted between the 600 kV station bus and the dc transmission line.

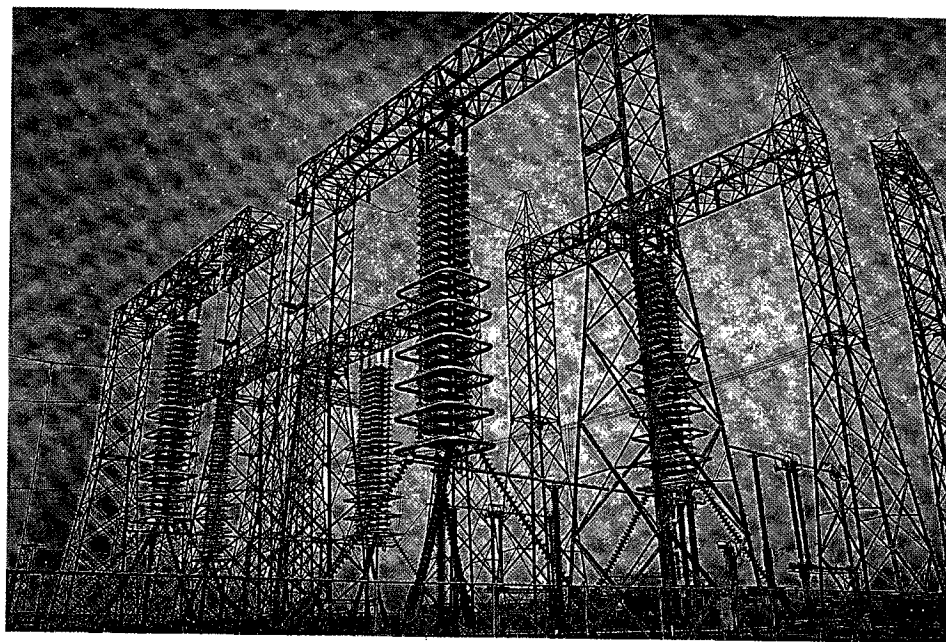
Converter by-pass and disconnecting equipment.

Each converter is equipped with by-pass and disconnecting equipment, located in the dc switchyard outside the valve halls. The equipment consists of one by-pass disconnector, two isolating disconnectors and one by-pass breaker.

These are essentially slow-acting motor-operated dc disconnect switches without any current interrupting capability.

The by-pass breaker is used for rapid by-pass or release of converters, without power interruption to any other converter in service in the bipole, and has interrupting and recovery voltage capability. Each by-pass breaker consists of one breaking unit which interrupts the ripple current at start of a converter and one isolating unit for normal operation with the by-pass path open. By-pass breaker operation is either manual or in response to a protective relay.

Neutral bus load-break switch. Each converter pole neutral bus is equipped with a dc neutral load break switch between the neutral bus and the electrode line. Normally this load break switch operates under zero current conditions. For a ground fault within the station, which leads to a permanent monopolar operation, the neutral bus load-break switch must commutate dc current of the other pole to the ground electrode line.



dc switchyard - details of filters

Paralleling equipment. In the event of a prolonged outage of a dc transmission line bipole or pole, the affected pole(s) of the converter station can be connected to operate in parallel with the corresponding pole(s) of the other bipole using the remaining dc transmission line. The equipment for paralleling includes motor operated dc paralleling switches, paralleling bus and current-measuring equipment.

The paralleling and de-paralleling sequences are operator initiated and are automatically completed. Only paralleling of the same polarity poles having the capacity to operate at full voltages is possible. The paralleling operation is performed on a per pole basis, i.e., paralleling of pole no. 1 implies connection of the converters of pole no. 1 to the dc transmission line of pole no. 3 and subsequent start-up of pole no. 1.

Overvoltage protection. The interface for the overvoltage protection scheme of the HVDC converter station is the converter transformers, as this equipment may be stressed by either the ac or dc side transients. The overvoltage protection is provided by metal oxide type surge arresters.

For the ac portion each major component connected to an ac bus, such as converter transformer, ac transmission line, synchronous compensators (at Ibiúna) step-up transformer and auxiliary power transformer are individually protected with one surge arrester per phase. The exceptions to this are the main ac filter capacitor banks and shunt capacitor banks (at Ibiúna) which are protected against switching surges only by the other surge arresters connected to the ac buses, as they are not exposed to lightning. The low voltage branches of the ac filter reactors and resistors are individually protected.

For the dc portion, the required energy duty for most dc side surge arresters is higher than the energy capability of only one column of surge arresters. Thus the required energy duty is obtained by connecting a sufficient number of disk columns in parallel. For arresters with two or more columns in parallel the current in any column does not deviate by more than $\pm 10\%$ of the average value per column, in the range of 100 to 50 % of the maximum design current.

Ground electrode system

The ground electrode system for temporary monopolar operation consists of four ground electrodes (one per station for each bipole), located at remote locations to minimize the adverse effects

of the ground currents. Electrode sites are approximately 65 km from the Ibiúna converter station and 15 km from the Foz do Iguaçu converter station. The connection between the converter stations and electrodes is made by dedicated overhead lines; one for each bipole. There is no paralleling of either the lines or the ground electrodes of the two bipoles.

All four ground electrodes are of a shallow-type design, and are approximately circular 740 m diameter for Ibiúna and 870 m diameter for Foz do Iguaçu. The electrodes consist of many 5 cm diameter silicon-iron rods embedded in a 50 cm x 50 cm layer of granular coke at a 3 m depth and are designed to carry:

- 2.5% of the bipole's nominal current continually.
- The bipole's nominal current 2.5% of total time.
- The bipole's nominal current continuously for 30 days once in the lifetime of the system. In this case the design maximum temperature rise is 50°C over an initial soil temperature of 25°C.

CONTROL AND OPERATION

HVDC control

The structure of the HVDC control system is shown in Fig. 15.11. For high availability of transmission all controls are at the lowest possible level of the hierarchy, giving maximum independence of operation of the power blocks.

Each bipole is controlled by the operator using any one of four similar control desks in the station and bipole control rooms of each station. At any time only one bipole control desk can be active in each station, and one of the stations must be selected as master. The bipole control rooms are used mainly during testing and commissioning and later as a back-up. For normal operation all control commands are from the Ibiúna station inverter control room.

Remote control of some commands and settings is possible from the FURNAS system operation centers in Rio de Janeiro and Campinas. Communications between the FURNAS system SCADA and the HVDC controls are made through a SINDAC computer which is also used for the station main alarm and status monitoring system. Each control desk consists of the following:

Station control. Deals with those aspects of the HVDC terminal which require coordinated action and which cannot be implemented at a lower hierarchy level. As the two bipoles operate independently as much as possible, only the ac side

harmonic filters and other reactive power sources are common to both bipoles. Station control therefore supervises the connection and disconnection of the ac filters and shunt capacitor banks in response to a fast continuous analysis of the harmonic filtering requirements and reactive power balance at the terminal.

At both converter stations, station control determines the minimum number and type of filters to be connected by monitoring the level of dc power transmission and the number of converters in operation. These are directly related to the level of harmonic current generation and ac filter requirements. The ac filters and shunt capacitor banks are usually connected in accordance with a pre-determined order, which ensures sufficient filtering of all harmonics for all operating conditions.

At Ibiúna, in addition to meeting the filtering requirements, station control also ensures that the connected static reactive power sources maintains an adequate reactive balance in addition to maintaining contact, through the FURNAS system SCADA with the system operating centers.

Microwave and PLC communication channels are used for integrated control between Foz do Iguaçu converter station control and Itaipu powerhouse central controls.

Bipole control. Communicates with higher and lower control levels, and compensates for the loss of power transmission in one bipole by sending an additional power order to the other. It handles additional power order inputs at bipole level, supervises the electrode current, and executes

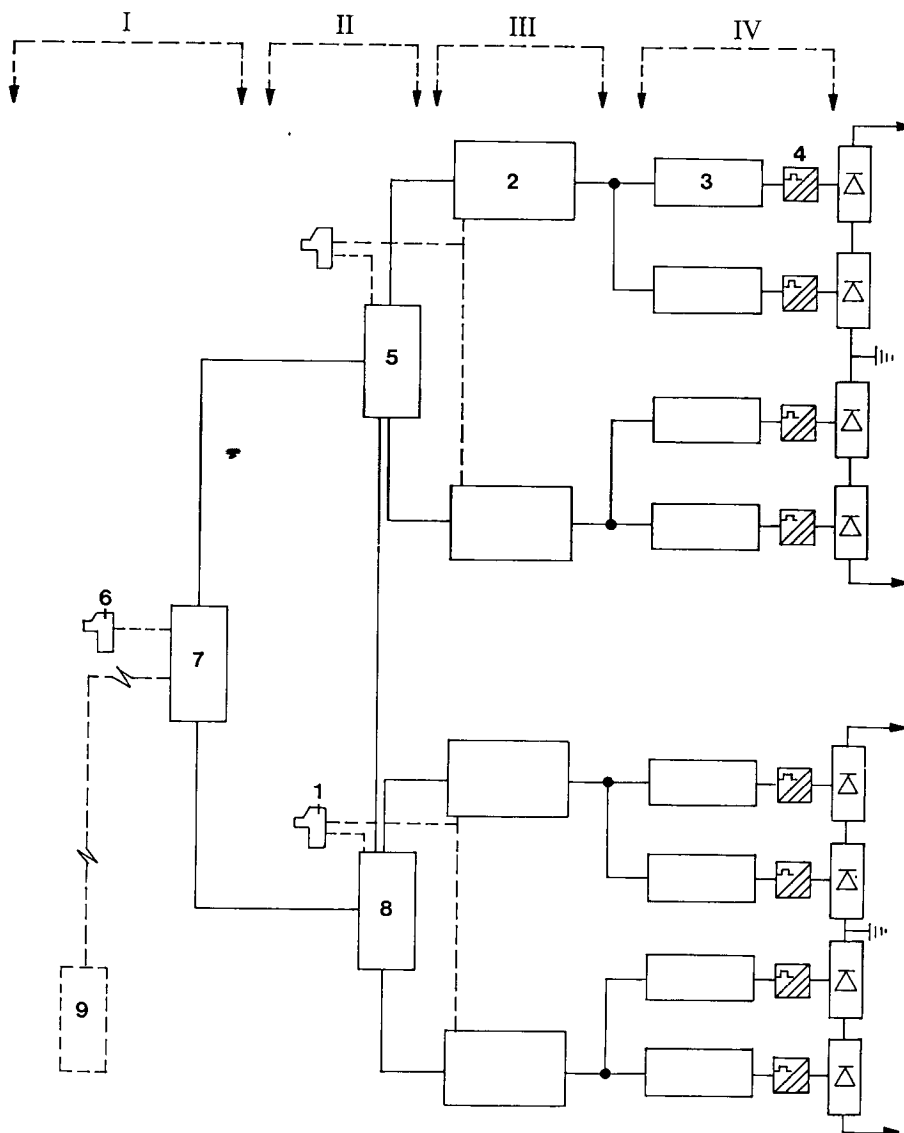
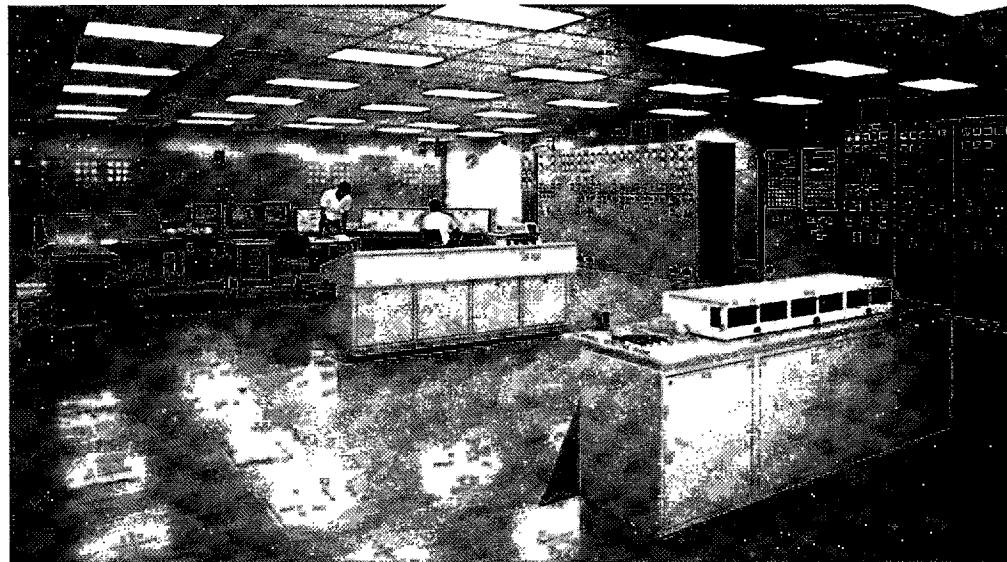


Fig. 15.11 Control hierarchy

- I Station level
- II Bipole level
- III Pole level
- IV Converter level
- 1 Bipole control desk
- 2 Pole control
- 3 Converter control
- 4 Valve control
- 5 Bipole 2 control
- 6 Station control desk
- 7 Station control
- 8 Bipole 1 control
- 9 ac system control



HVDC control room

bipole sequences, which include control location and power direction.

Pole control. May execute power/current orders and limits, operation mode changes and start/stop orders. The pole power control receives the power order and calculates the current to be delivered, applying specific control functions and limits. The pole current control which accepts the current order compares it with the actual measured current and passes the error signal to the converter firing control. Also there is the pole sequence control, which manages the control mode changes, automatic start/stop and connect/isolate sequences and the tap changer control at pole level.

Converter control. Executes the firing control, which controls the delay angle and delivers the control pulses to the valve control. It also handles the converter sequences, protection and tap changer control (which extend the related pole level functions), and the valve control, which supervises and distributes the pulses to the valves through fiber optics system.

Special controls. In addition to the various control functions described above, there are others which are not specifically linked to any particular operation mode. These are:

- ac voltage limitation at Foz do Iguaçu. This control feature was introduced to increase the consumption of reactive power and thereby controls the ac voltage.

- Modulation of commutation angle. Modulation of the commutation angle of the invertors improves the transient damping of the system. The regulator for this damping is placed on the converter control and, in effect, the converters are used as controllable static reactive devices.

- Reduced dc voltage operation. To enable continued operation on a dc line, which has insulation withstand lower than rated, (broken insulator, excessive pollution and moisture) any pole can be operated at between 75 and 100 % of rated voltage.

Normal operation

dc portion. Operation of dc portion of the system requires considerable coordination between the terminal converter stations, Itaipu powerhouse and the FURNAS operations center. Although the two bipolar systems are basically independent, their operation too must be coordinated for various operating conditions, especially when communication system and/or converter elements are out of service.

The normal operation mode is synchronous constant power control, which has the advantage of minimizing the effect on the sending and receiving ac systems of loss of converters, poles or dc lines. Additionally, it facilitates dispatch coordination between the HVDC transmission system and the Itaipu powerhouse.

Within the control system hierarchy, power control is made at the pole level. It is assumed that full telecommunication between stations is operative and that the current order is automatically synchronized at the rectifier and inverter.

The power order set by the operator on the active control desk at the system operation center always refers to the power required per bipole. Using an adjacent control the operator can also adjust the rate of change of the power order and maximum limit for the bipole power. This, added to the power order limit of the other pole, must not exceed the available generation capacity at the Itaipu powerhouse.

Independent of the control location used, the set bipole power order is transmitted to each pole power control (PPC) equipment in the lead station (normally Foz do Iguaçu) where the power control functions are executed. After receiving the power order and the required rate of change, which may be between 0.1 and 10 MW/s per bipole, the PPC increases the power order in 5 MW steps at intervals determined by the required power ramp. While the process of establishing a new power order is in progress, the power setting control on the control desk remains illuminated.

To increase the flexibility and availability of the dc control, three other control modes are possible. These modes are normally used only if the telecommunication between stations is lost or during maintenance of the pole power control and are:

- Asynchronous constant power
- Constant current
- Automatic current margin control (AMC)

Change from one mode of operation to another does not result in sharp changes in the power transmitted. If there is a fault in the telecommunication or pole power control, the mode of operation changes automatically to the asynchronous power or current control mode respectively, keeping the current order frozen until a new order comes from the operator. During this process all the conditions are analyzed by the sequence control which, if necessary, blocks the mode change until the operator has taken the necessary action or system conditions are suitable.

When a fault occurs in only one pole of the bipole, it is possible to maintain synchronous power control of the complete bipole. If, however, the bipole power order is altered either by the operator or because of a change in the additional power order signals in the healthy pole, then current will flow in the neutral connection.

Constant current mode is necessary when the pole power controller is out of operation and the power transmitted by the pole is to be changed. The operators act directly on the current order of the

pole, maintaining telephone contact to coordinate their actions.

When contact between the two stations is completely lost, the power or current of a pole can only be changed in the automatic margin control (AMC). The use of AMC is conditional on the loss of telecommunication between pole power controllers and the change must be initiated at the rectifier station. In the event of simultaneous loss of telecommunication between both pole power controllers and pole sequence controllers in the two poles of one bipole, the operation changes to AMC.

Abnormal operation

In the initial years of operation, the combination of the relatively small directly connected 50 Hz ANDE system load, the large converter load of the HVDC system and the large generators at Itaipu powerhouse can lead, during abnormal system operation, to unacceptable over or under frequencies and voltages, high harmonic levels, and possible autoexcitation of generators as follows:

Overfrequency transients. On sudden loss of load, the Itaipu generators are subjected to a transient overspeed whose magnitude depends on the load rejected. The inertia of the ANDE system remaining connected to Itaipu generators has negligible effect on the overspeed. The acceptable limit for the overfrequency transients is 10%, which corresponds to the loss of approximately 40% of the load of the 50 Hz Itaipu units.

In case of loss of one or more poles of the HVDC converter, the remaining poles can be temporarily overloaded to minimize the change of power of the Itaipu units. Another possibility is to disconnect one of the Itaipu generators but this can be done only when six or more Itaipu units are connected to the HVDC converter filters which keeps enough margin against the risk of self-excitation. ANDE could be supplied with one separate Itaipu unit but even then a protection scheme is needed to isolate ANDE system from Itaipu powerplant when the established overfrequency limits are exceeded.

Underfrequency. Loss of generation at Itaipu powerplant results in underfrequency in the ANDE system and a special stabilizing device is used in the HVDC master control to limit this. This controller reduces the power order to the HVDC converter, thus reestablishing the equilibrium of the active power and avoiding the collapse of the frequency. The gain

of the "50 Hz stabilizer" is adjusted to maintain the frequency above 49.5 Hz for a loss of up to 50% of the Itaipu generation. Dynamic response is a compromise between the limit of the underfrequency transient in the 50 Hz system and the load transient in the 60 Hz system. In addition to the "50 Hz stabilizer" a protection scheme isolates the ANDE system from Itaipu for severe underfrequency transients (48 Hz).

Self-excitation of Itaipu and Acaray generators. The ac filters at the Foz do Iguaçu station give capacitive reactive power which in normal operation compensates for most of the inductive reactive power absorbed by the converter. When the converters are blocked, a sudden capacitive load is applied to the Itaipu generators resulting in an overvoltage transient. Underexcited reactive power limit of one Itaipu generator at full load rejection can compensate the reactive absorption of one filter and maintain correct voltage regulation.

Outside one filter per generator, voltage regulation is no longer possible and, when the unbalance filters/generators is larger than two filters per generator, a quick and severe overvoltage with self-excitation immediately occurs. Voltage rise is limited by the saturation of the machines and transformers and eventually by the metal oxide arresters at 2 p.u.

Unbalance of the filter/generator capacity is more critical for the Acaray generators which remain connected to the HVDC filters without the Itaipu generators and with the converter blocked. This occurs when there is complete loss of Itaipu generation or loss of the lines connecting Itaipu powerhouse to the right bank substation with simultaneous blocking of the converter, but the probability of this to happen is very low.

With one filter remaining connected to the four Acaray generators the transient is a very fast overvoltage limited only by the surge arresters. For two or more filters connected to four Acaray generators this transient results in currents and torques exceeding the design values and the breakers. Thus the only solution is to ensure that these conditions do not occur.

During the early stages of project operation the GIS switchgear at the Itaipu powerhouse was used with separate lines, leaving the two bus bars in the right bank substation open. With this scheme, no fault would have left ANDE and FURNAS connected without the Itaipu generators.

For the later stages of project operation a coordinated protection scheme "Forced Isolation

Protection" (FIP) was used. The main purposes of FIP protection scheme are:

- Automatically ensures that there are more generators than filters connected. The information on the number of Itaipu generators connected to the system is transmitted via PLC to the converter station control room where in the event of loss of generation at Itaipu automatically trips out the excess filters.
- Overvoltage protection. Through the control system of the converter, for overvoltages above 1.2 p.u there is a sequential disconnection of the filters, and, for overvoltages above 1.5 p.u., the 500 kV lines feeding the Foz do Iguaçu substation are opened.
- Delta current order overvoltage limiter. This controls the voltage through the reactive power absorbed by the converter. For a voltage above 1.25 p.u. it regulates the power control and the frequency stabilizer.
- Delta frequency stabilizer. This creates stable power/frequency characteristics for the HVDC load similar to the natural autoregulation characteristics of an ac load. It also limits the power transmitted in the HVDC link in case of loss of generation at Itaipu.
- Loss of the last generator protection. For the last generator or the loss of the last line, the ANDE system is isolated.
- Power reversal protection. This is sensitive to the reversal of the power flow between Itaipu and ANDE system and isolates the ANDE system in the event of loss of Itaipu generation. This protection is faster than the underfrequency protection.
- Underfrequency protection. When the frequency drops in the 50 Hz system as a consequence of a loss in Itaipu generation the protection isolates the ANDE system. This protection is redundant to the power reversal protection.
- Undervoltage protection. When the voltage in this 500 kV system remains lower than 0.5 p.u. for more than 380 ms, the protection isolates the ANDE system.

Transient overvoltages. When a fault occurs in the 500 kV system the voltage of the phases affected by the fault falls to zero and when the fault is cleared the full voltage is suddenly reapplied. This can result, especially in the cases of two and three-phase faults, in heavy inrush currents with overvoltages having a relatively high content of low-order harmonics.

The resulting overvoltages are within the limits acceptable by the Itaipu system but the low-order harmonic current injected in the ANDE system results in unacceptable overvoltages in some parts of the network, especially on the long radial low-loaded lines. Remedial actions studied were:

- To install series filters at the entrance of the 220 kV lines at the right bank substation and resonant dampers at some points of the ANDE system.
- Metal-oxide surge arresters with a heavy thermal overload capability.
- Switchable reactors and overvoltage relay at the critical points of the ANDE system to disconnect the ANDE system.

As the probability of two or three-phase faults in the 500 kV system, with its very short lines, is very small, disconnection of the ANDE system by overvoltage relays can be adopted.

Voltage and current harmonics. Even if the voltage and current harmonics produced by the HVDC converter are within the specified limits, their effect in the Paraguayan system, with its relatively long low-load lines, can exceed the limits allowed by ANDE, see Table 15.1. Parallel resonant filters at the right bank substation and at San Lorenzo substation can solve this problem. The filters will absorb the harmonic generated at HVDC converter station but not the harmonics present in the Paraguayan system which occur without the HVDC converter station. This can be corrected by measures taken within the ANDE network, including elimination of possible resonant conditions at some substation buses.

Table 15.1 Harmonic distortion: maximum allowable limits for ANDE system

	220 and 66 kV buses		23 kV buses	
	even order	odd order	even order	odd order
Individual harmonic distortion (%)	0.5	1	1	2
Total harmonic voltage distortion (%)		1.5		3
Telephone interference factor (TIF)		25		50

HVDC TRANSMISSION LINES

Studies of availability and reliability, together with wind velocities and topographic characteristics of the route indicated two transmission lines with a minimum of 10 km separation. The principal characteristics of the two ± 600 kV dc transmission lines are:

Physical characteristics

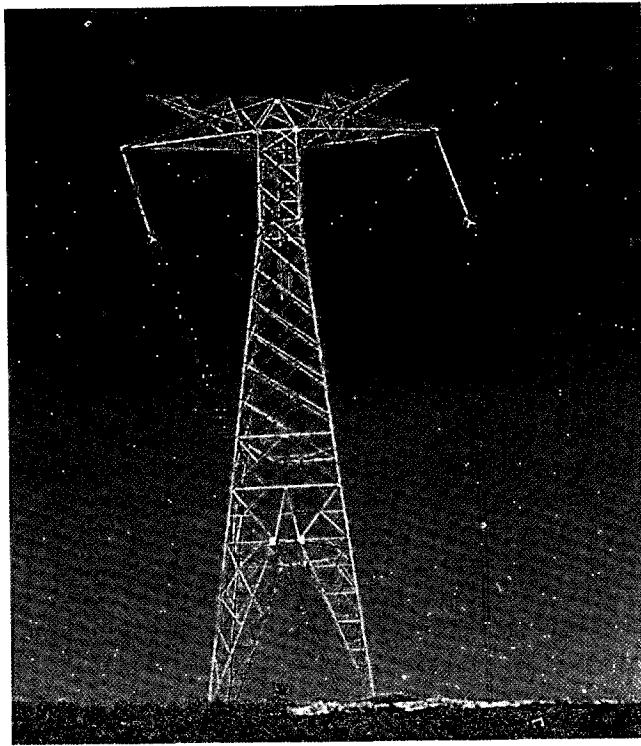
Length of the lines (km)	
Itaipu – Ibiúna, south route	792
Itaipu – Ibiúna, north route	816
Line routes	
Right-of-way width for one line(m)	72
Separation between two lines: minimum (km)	10
Tower type (%)	
Guyed	79
Self-supporting	21
Maximum height (m) (crossarm – ground)	
Guyed	43.5
Self-supporting	58.5
Average span length (m)	467
Minimum pole spacing (m)	15.4
Minimum clearance, pole– ground (m)	13

Design conditions

Maximum wind velocity (km/h)	150
Ambient temperature (°C)	
Maximum	40
Minimum	5
Isokeraunic level	70
Altitude (m)	
Medium	800
Maximum	1100

Electrical characteristics

Conductor type	4 x BITTERN ACSR-1272 kcmil 45/7, Ø=34.12 mm
Insulators	Single "I" strings with 32 insulators, strength 160 kN 530 mm creepage, special dc design
Ground wires	Galvanized steel cable EHS, 7 strands, Ø = 9.525 mm
Counterpoise	no.6 m AWG copperweld



The predicted outages due to lightning strikes is 1.2-1.7/100 km/year, based on the assumed isokeraunic level of 70. The flashover probability for switching surge overvoltages in the range of 1.7-2.0 p.u. is between 3×10^{-4} and 2×10^{-7} . The highest theoretical value of the switching surge overvoltage is 1.8 p.u., occurring on one of the pole conductors in the event of a ground fault on the other pole conductor.

Conductor selection was based on the cost of losses, corona phenomena, electrostatic field strength, as well as maximum temperature during the parallel operation.

Simplified drawings of the self-supporting and guyed towers are shown in Figs. 15.12 and 15.13.

600 kV dc transmission tower

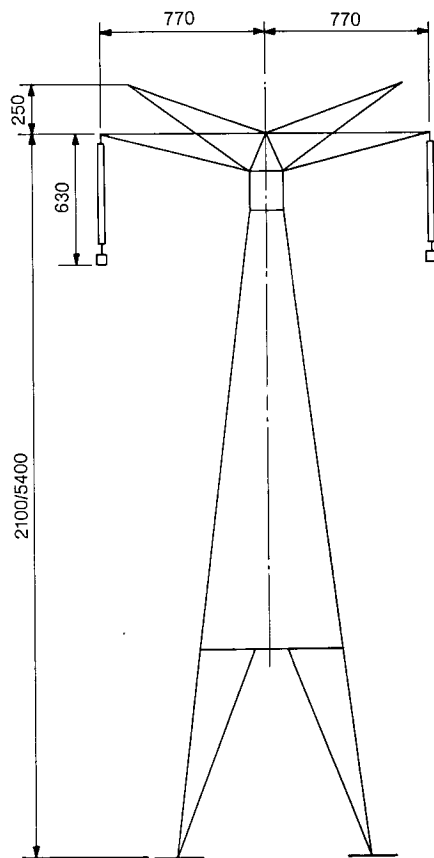


Fig. 15.12 600 kV dc line - typical self-supporting tower

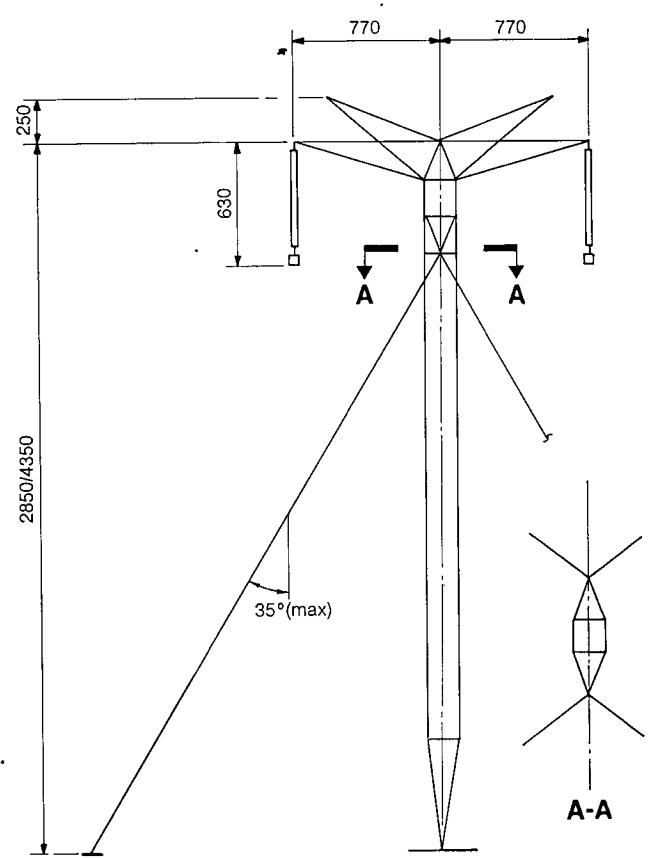


Fig. 15.13 600 kV dc lines - typical guyed tower

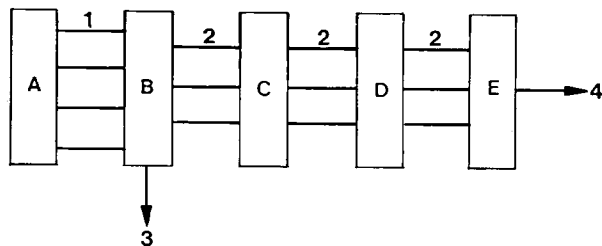
60 HZ SYSTEM

DESCRIPTION AND PRINCIPAL CHARACTERISTICS

The 60 Hz transmission system receives power from the nine 60 Hz Itaipu generators and transmits it at 765 kV to São Paulo area and provides additional intermediate interconnection with the ELETROSUL system. The generated power is stepped up to 500 kV at the powerhouse and then transmitted by four overhead lines to the nearby Foz do Iguaçu substation.

At Foz do Iguaçu substation the power is stepped up to 765 kV and then transmitted by three overhead lines to São Paulo area. All three lines are sectionalized at Ivaiporã substation (interconnecting point with the Brazilian south transmission system), Itaberá substation and then terminated at Tijuco Preto substation in São Paulo area for interconnection with the Brazilian southeast transmission system, see Fig. 15.14. The main electrical characteristics of the 60 Hz system are:

	765 kV	500 kV
Voltage (kV)		
Nominal	765	500
Maximum	800	550
Symmetrical fault current (kA)	40	40
BIL (kV)	2100	1800



- | | |
|------------------------------------|--|
| A Itaipu powerhouse (60 Hz) | 1 Four 500 kV lines |
| B Foz do Iguaçu substation | 2 Three 765 kV lines |
| C Ivaiporã substation | 3 Interconnection with south transmission system |
| D Itaberá substation | 4 Interconnection with south-east transmission system |
| E Tijuco Preto substation | |

Fig. 15.14 60 Hz transmission system

THE FOZ DO IGUAÇU SUBSTATION

The 60 Hz sector of the Foz do Iguaçu substation is the interconnecting point of Itaipu 500 kV system and the 765 kV FURNAS transmission system. It is connected to Itaipu power station by four 500 kV short transmission lines (approximately 8 km), it has four 1650 MVA - 765/525/69 kV autotransformers and three 765 kV transmission line bays. Figure 15.15 shows the substation single line diagram. The substation is divided into sectors as follows:

765 kV switchyard

The 765 kV switchyard is arranged in the breaker-and-one-half concept in the conventional three circuit breaker in-line arrangement with the main buses to the outside of the switchyard. Although this requires the use of a third bus level for the external interconnections to reach the position between circuit breakers, these are made in relatively short spans to a separate structure for high reliability.

Three of the four overhead lines from the autotransformer area are paired with 765 kV transmission lines on a breaker-and-one-half bay. The fourth line is connected in a double breaker mode in a fourth bay which can be converted if another line position is required.

The bay width is 45 m with a 39 m separation between the second and third bays for an access road, relay building and stand-by emergency generator building.



Partial view of 765 kV switchyard

On the transmission line side of the station the 765 kV shunt reactors are installed, including a spare unit with a cross-bus for interconnection. Line terminal equipment, surge arresters for the reactors and line terminations are installed there. There are

also the coupling capacitive potential devices, current transformers and wave traps for each line phase.

The lowest bus at 12 m above grade is a 152.4 mm diameter aluminum tube bus used to connect the

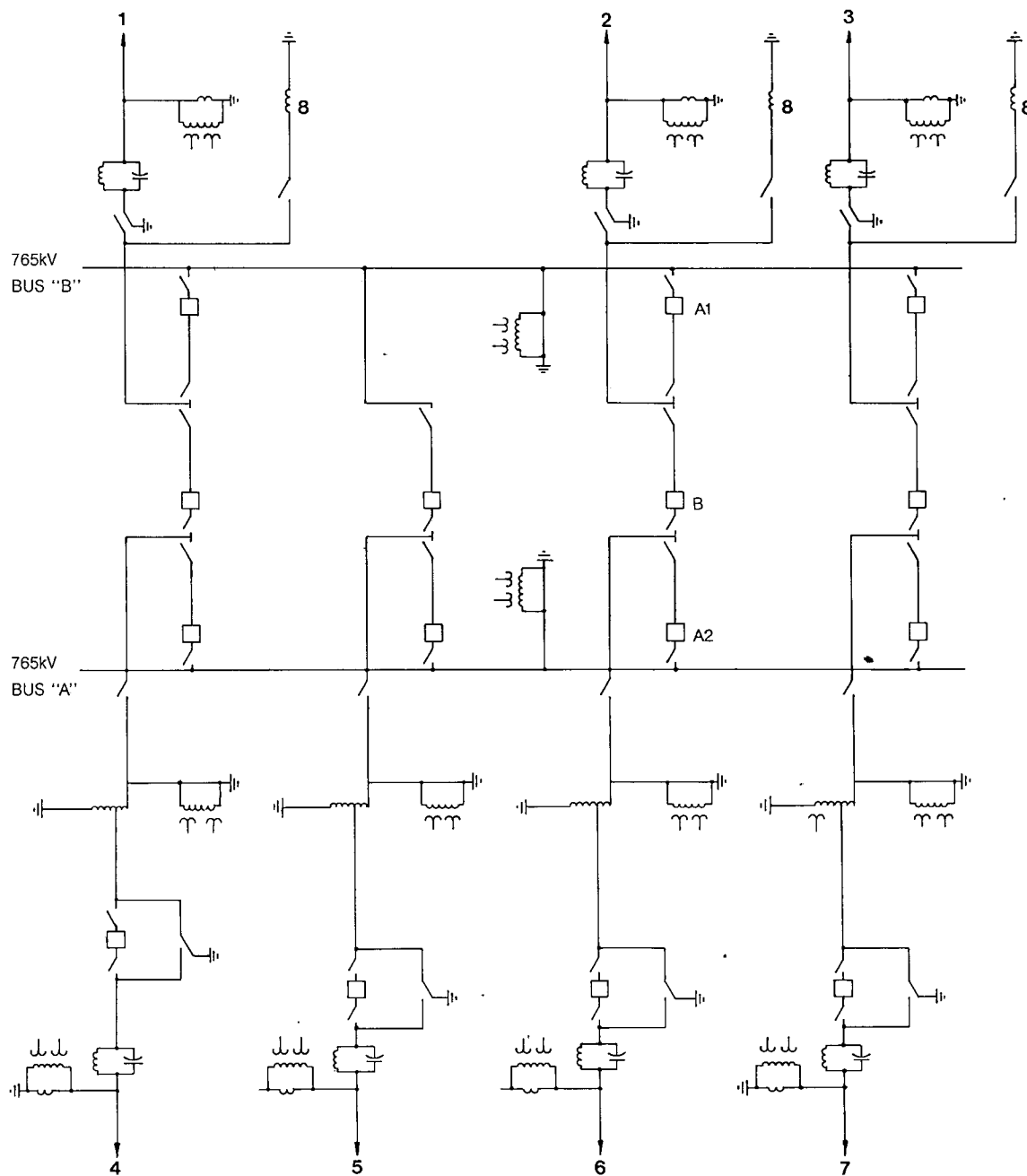


Fig. 15.15 Foz do Iguaçu 765/500 kV substation - single line diagram

- 1 Ivaporã 3 (765 kV line)
- 2 Ivaporã 2 (765 kV line)
- 3 Ivaporã 1 (765 kV line)
- 4 Itaipu 4 (500 kV line)

- 5 Itaipu 3 (500 kV line)
- 6 Itaipu 1 (500 kV line)
- 7 Itaipu 2 (500 kV line)
- 8 Three $800/\sqrt{3}$ kV 110 MVar reactors

A1, A2, B1 Breakers

circuit breaker, current transformer and disconnecting switches. The highest bus, 40 m above grade, is a four conductor bundle of 1590 kcmil ACSR (FALCON) cables as are the strain jumpers and bus drops. The intermediate main bus, at 23 m above grade, consists of 203.2 mm diameter aluminum tube.

The overhead shield wire, 50 m above grade, is 9.525 mm diameter EHS cable.

765 kV sector

The main characteristics of the key equipment are:

Circuit breakers

Type	SF ₆ and air blast
Continuous current (A)	3150
Interrupting capability (kA)	40
BIL (kV)	2100

Current transformers

Continuous current (A)	3000
Ratio 4	600/500/400/320/300 : 1
Ratio 2	400/200 : 1
Accuracy 4	C800
Accuracy 2	0.3 B2

Disconnect switches

Type	Vertical break
Continuous current (A)	3150
Momentary current (kA)	40
BIL (kV)	2100

Shunt reactors single phase

Voltage (kV)	$800/\sqrt{3}$
Rating (MVar)	120
BIL (kV)	1800 and 1950

Surge arresters (kV)	588
-----------------------------	-----

Capacitive voltage dividers (kV)

$765/\sqrt{3}$

Bus insulator BIL (kV)	2100
-------------------------------	------

Nominal electrical clearances in meters are:

Phase to ground (metal to metal)	5
Phase to phase (metal to metal)	10
Main bus height above ground	23
Auxiliary bus height above ground	12
Strain bus height above ground	40
Bus height – vehicle road clearance	23
Shield cable height above ground	50
Bay width (centerlines)	45

500 kV switchyard

The 500 kV substation does not have main buses, see Fig. 15.15. Each incoming 500 kV line is fed directly through a circuit breaker and associated disconnect switch into 525/765 kV auto-transformer bank, one bank per line. Therefore there is a reduction in load transfer capacity in the event of a permanent line outage. As the 500 kV transmission lines are conservatively designed and very short, the risk involved was considered to be acceptable. A similar reduction could result from an autotransformer major failure, but a spare unit (complete with a reconnectable buswork) is available, therefore the outage would be of short duration. For temporary line outage, the available short-time overload capability of the remaining lines and transformers can be used to replace the lost capacity. During the maintenance of a line/transformer 500 kV power circuit breaker, the line and/or transformer protection actuates the 765 kV transformer breakers and starts the transmission of a transfer trip signal to open the 500 kV transmission line breakers at Itaipu power station.

As described above, the 500 kV switchgear sector has no mainbus. The equipment interconnections and line entrances are arranged at two bus levels. The lowest one, 10 m above the grade and 9 m phase-to-phase spacing, is a 154.4 mm diameter aluminum tube bus supported by porcelain pedestal insulators and is used to interconnect the main equipment. The highest bus level, at 28.5 m above grade, is a bundle of four 954 kcmil-ACSR conductors, spaced at 45.7 cm and anchored to self-supported steel lattice structures. The physical arrangement of the substation was designed with provision for addition of a third level, at 16.5 m above grade. This level would be used as main bus in case it is decided to change the present switching scheme to a breaker-and-one-half scheme.

The substation protection against direct lightning strikes is provided by extra high strength steel 9.525 mm diameter shielding wires, installed over the substation at 33.5 m above grade.

500 kV sector

The main characteristics of the key equipment are:

Circuit breakers

Type	SF ₆ and air blast
Interrupting capability (kA)	40 and 31.5
Continuous current (A)	3150
BIL (kV)	1550

Current transformers

Continuous current (A)	3000
Ratio 4	600/400/300 /200 /100 : 1
Ratio 2	400/200 : 1
Accuracy 4	C800
Accuracy 2	0.3 B2

Disconnect switches

Type	vertical break and vertical reach
Continuous current (A)	3150
Momentary current (kA)	40
BIL (kV)	1550
Surge arrester – metal oxide (kV)	420
Capacitive voltage transformer (kV)	525
Wave filters (mH)	0.1
Bus insulator BIL (kV)	1800

Nominal electrical clearances in meters are:

Phase to ground (metal-to-metal)	4.1
Phase to phase (metal-to-metal)	5.3
Phase to phase (centerlines)	9
Main busbar height above ground (future)	16.5
Auxiliary busbar height above ground	10
Strain bus height above ground	28.5
Bus height – vehicle road clearance	28.5
Shield cable height above ground	33.5
Bay width (centerlines)	32

765/525 kV autotransformers sector

There are four banks of autotransformers located in the area between the 500 kV and 765 kV switchyards. The single-phase units are on 15 m centerlines with a fire wall between them. The 45 m bay matches the width used for the 765 kV switchgear bay. A 39 m separation between the second and third banks is for the spare transformer.

The strain bus, 40 m above grade, over the transformer connects this sector with the 765 kV switchyard. A single-phase rigid cross bus facilitates connection of the spare transformer to the strain bus.

The strain conductors from the 500 kV switchyard dead end on the other side of the structure, and the connection to the transformer is through a bus-drop to a rigid bus at a lower level. It is possible to connect it, through a single phase cross bus to the spare transformer from this lower level bus.

The bank rating, formed by single-phase autotransformers, is 765/525/69 kV (star/star/delta), 1650/1650/15 MVA, ONAN/ONAF/ONAF and the winding BIL's are 1950/1550/350 kV or 1950/1425/350 kV. The 69 kV delta winding of the autotransformer is used as a source of auxiliary service power. Metal oxide surge arresters which are mounted close to the transformers are rated 588 kV and 420 kV for the 765 kV and 500 kV systems respectively. The delta winding of the transformer, when used for auxiliary service power, is interconnected by a rigid, 76.2 mm diameter tubular bus system. A separate two conductor, single-phase system extends the delta winding of the spare transformer to allow its interconnection, if required.

Control facilities

The Foz do Iguaçu 765/500 kV substation was designed for attended operation from the substation control room. All control equipment is located in this room, while all protection, annunciation and metering equipment is located in a separate relay house or in the relay room located in the control house.

The relay house shall be unattended. Equipment and lines, which have their protective equipment installed in the relay house shall have their control function performed at the control room through interposing sealed type relays interconnected with the controls located in the control room by control cables.

For all lockout functions required at the relay house, manually/electrically reset lockout relays shall be provided. Remote resetting of these relays shall be from switches located in the control room. Trip and

lockout function required in the relay room shall be performed through the use of hand reset lockout relays, which are located on the control panels in the control room.

The indication of the status of equipment will be given by indicating lamps mounted on the control panels located in the control room.

A supervisory system is provided consisting of a sequential printing of events performed by SCADA system RTU and supplemented by visual annunciation on panels located in the control room of the control house and at the relay house and/or relay room of the control house. The sequential printing of events provides the operator in the control room a readily usable indication and recording of every individual trouble alarm and event and status record of all relay target located in the relay house. In case SCADA system is out of service, the visual annunciators located in the relay house together with protective relay targets, form a back-up system to indicate locally in the relay house any alarm and event independently of SCADA system indication. A visual annunciator located in the control room provides a general indication of troubles in any line or equipment such as "line to in abnormal conditions" or "transformer in abnormal conditions". An input scanning device is located in the relay house so that it is not necessary to extend wiring for every initiating device from the relay house to the control house.

Relay house. The relay house is an air conditioned building located in the 765 kV switchyard, remote from the attended control house. It is intended that the relay house serve as a central point to make connections as well as a location for installation of protective and energy metering equipment for all 500 and 765 kV switchyard equipment which is located remote from the control house. However, all switchyard equipment located in the vicinity of the control house will have their connections made directly to the control house where rooms are provided for control equipment (control room) as well as for protective and energy meter equipment (relay room). All control panel devices are located in the control room while all protective relaying equipment and metering equipment, including the reclosing relays, are located either in the relay house or part in the relay house and part in the relay room of the control house.

System protection

765 kV transmission line protection. The 765 kV series compensated lines of the Itaipu transmission system are protected by two equal and independent

sets of protective relays (primary and alternate protection schemes). Each protective scheme shall operate over independent communication channel. Each of these protective relay sets shall provide high speed primary protection with correct operation independent of series capacitor gap flashing and contain all elements of the back-up protective scheme (without taking into account the operation of the communication channels). The primary protective relaying communication channel will operate over power line carrier channels, and the alternate protection will operate over microwave channels. The first two lines, which are already in operation, use two different types of protection complying with the criteria described above. The first scheme is an unblocking directional comparison (wave type), with a supplementary directional overcurrent protection using a communication channel, and a scheme of out-of-step blocking and out-of-step tripping. The second scheme is a conventional blocking directional comparison system using negative current for unbalanced faults, with out-of-step tripping and blocking.

The line protective scheme is provided with high speed automatic reclosure with an adjustable time delay having a range from 0.5 to 2 seconds. Only one of the line circuit breakers, at each end, will automatically reclose. The other breakers will be manually closed after the line is re-energized. A selector switch is provided to enable the operator to determine when a line is to be automatically reclosed and which breaker will reclose automatically. The automatic reclosing shall be initiated after faults of any kind cleared by the high speed line protection operation, but only when at least one of the two transfer trip channels is in operation. It will be blocked after faults cleared by time delayed protection and other breaker trip initiated by breaker failure, reactor, transformer, overvoltage, out-of-step and bus differential protections. The reclosure will only be permitted when at least one parallel line is in operation. A synchro-check relay is used to verify this operational condition.

A loss of voltage protection is also installed for all 765 kV lines, except the first one, to avoid misoperation of the line protective schemes under some particular operational conditions, such as loss of polarizing voltage due to tripping of the secondary feeder circuit breaker or due to a fault in the secondary feeder to the relays.

765/525 kV autotransformer protection. The autotransformers protective scheme consists mainly of two independent protection schemes (primary and

alternate) connected to operate separate lock-out relays which will trip and block closing and reclosing of all transformer breakers. The primary protection includes a set of percentage differential relays, with harmonic restraint and a sudden pressure rise protection consisting of a Buchholz relay and an instantaneous pressure relay. The alternate protection consists of a second set of percentage differential relay with harmonic restraint, to provide protection for the transformer and associated bay connections and a transformer overpressure protection provided through a pressure relief valve with trip and alarm contacts.

In addition to the two main protective schemes, the transformers have the following additional protection, which trips the associated circuit breakers through a high speed tripping relay without actuating the auxiliary lockout relay of the main protective schemes:

- Overload protection. Set (one per phase) of non-directional relays with instantaneous and time delay units.
- Overcurrent protections. A non-directional, inverse time overcurrent relay connected in the residual current circuit on the low voltage side of the transformer.
- Temperature protection. Winding hot spot protection through the use of a thermal image relay to start a timing relay and a high oil temperature protection through a relay, associated with the oil temperature detectors, to start a timing relay. After a time delay of 20 minutes these protections will trip the transformer breakers and activate an alarm.

765 kV reactor protection. The primary protection for reactors is provided by high speed differential relays, similar to the ones used to protect an ac generator. The alternate protection is provided by a sudden pressure rise protection, a pressure relief valve with trip and alarm contacts, a thermal image relay for overtemperature, protection and a non-directional, inverse time, overcurrent relay, connected in the residual current circuit of the reactor high voltage side current transformers. The two protection schemes will actuate two independent auxiliary lockout relays which will trip and block the reclosing of all circuit breakers associated with the reactors, initiate a transfer trip signal and also initiate the blocking of the reclosing of the associated breakers at the other line terminal.

765 kV bus bar protection. The buses of the 765 kV substation are protected by a high speed conventional current differential protection scheme.

The protection operates an auxiliary relay to trip and lockout the breakers.

500 kV transmission line protection. The protection scheme for the 500 kV transmission lines consists of three independent protection systems as follows:

- Primary protection. Percentage current differential segregated phase system using four frequency modulated fiber optical channels, two for each direction.
- Alternate protection. Two zone permissive overreach transfer trip scheme over four power line carrier channels, two for each direction.
- Supplementary protection. For ground faults, using zero sequence directional overcurrent relay in a permissive overreach transfer trip scheme over four microwave channels, two for each direction.

No reclosing is used in the protective scheme. During the maintenance of the 500 kV power circuit breaker, the transformer and the 500 kV line protections will actuate the 765 kV transformer power circuit breaker and will send a transfer trip signal to open the 500 kV line power circuit breaker at Itaipu power station.

Breaker failure protection. The breaker failure scheme is composed of a circuit breaker position indicating relay, a timing relay and a lockout relay for each circuit breaker and for each 765 kV bus. When the timer times-out it actuates the lockout relay and performs the following functions:

- Trip and block closing and reclosing of all adjacent circuit breakers;
- Trip and block closing and reclosing of one circuit breaker of the adjacent lines at the remote terminal.

Load rejection protection. The load rejection protective scheme for the 765 kV substation sector consists of the following relays: overfrequency, underfrequency, overvoltage, undervoltage, and high speed auxiliary (maximum 8 ms) and lockout (maximum 15 ms) relays.

Dead zone protection. The bus section between any current transformer and its circuit breaker (dead zone) is protected by a time delayed protection scheme of the remote terminal of the line or by the overload protection of the transformer, in whose protection zone such dead zone lies.

Synchronization

Only manual synchronization is possible at the 765/500 kV Foz do Iguaçu substation. Voltage sources for synchronization for all 765 kV lines and

transformers exits are available. To permit synchronism check in any of the possible operating conditions, a synchronizing switch with two positions is used when this switch is associated to the bus side breakers A1 and A2, see Fig. 15.15, and a switch with four positions when the switch is associated with the breaker B, see Fig. 15.15.

Fire protection and oil containment

Fire protection is provided for equipment which is critical to station operation and for equipment having a significant fire hazard because of its construction or content, i.e. oil filled or cooled equipment. The following specific equipment and areas are included: transformers, reactors, insulating oil storage and handling equipment, and all buildings. The main fire protection system consists of a fire water system serving the main station. A fire alarm system is provided, which initiates an alarm on the station fire alarm control panel installed in the control room. Single-phase transformers and other adjacent transformers are separated by fire resistant walls to protect each other from the effects of fire in another unit. The walls are designed and constructed with a 3 hour fire rating and

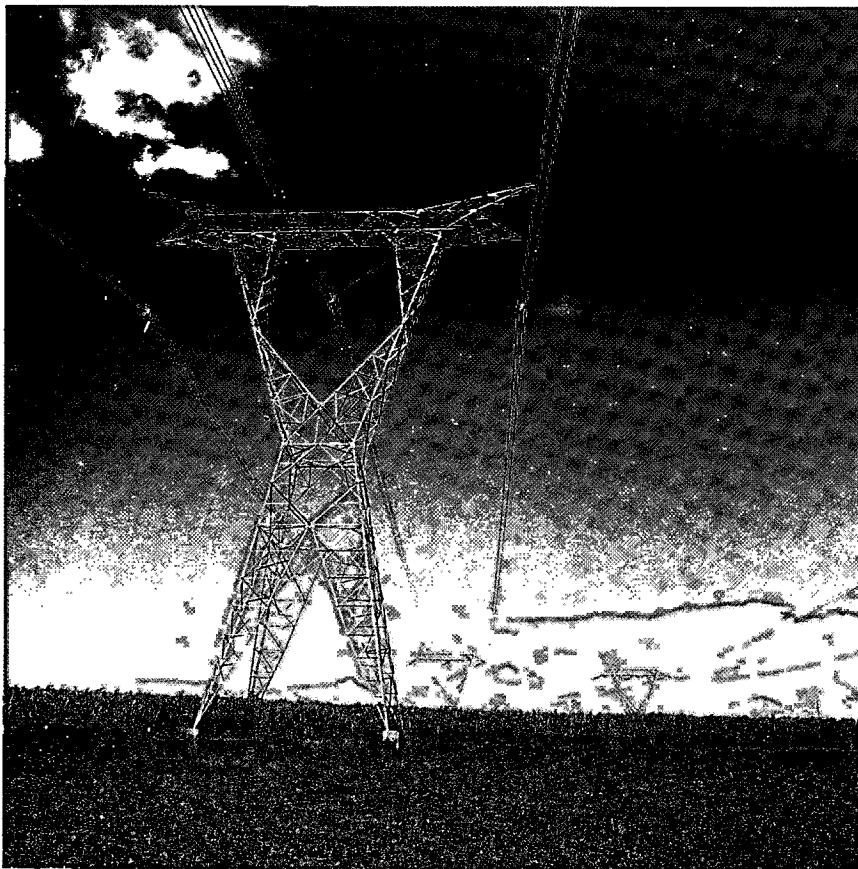
to protect against the effects of radiant heat and flying debris from an adjacent fire. Each transformer and reactor is equipped with an automatic water deluge type of fire extinguishing system.

Following a fire, oil and water from the fire protection system are collected in containment vessel below the transformers and reactors which are filled with crushed stones. The volume of each containment vessel is 80 % of the volume of the equipment oil. The oil containment vessels are capable of being drained of collected oil, rain water or deluge system water to avoid the risk of a fire spreading due to oil overflowing.

TRANSMISSION LINES

765 kV ac transmission lines

The three 765 kV transmission lines are relatively long lines, between the Foz do Iguaçu substation and Tijuco Preto substation near São Paulo. Studies of availability and reliability, together with wind velocities and topographic characteristics dictated that two lines share a common right-of-way but the third line be separated by a minimum of 10 km. The 765 kV lines are also at 10 km minimum distance from the 600 kV dc lines.



765 kV ac lines

Simplified drawings of the self-supporting and guyed towers for 765 kV lines are shown in Figs. 15.16 and 15.17.

The main physical and electrical characteristics of the 765 kV transmission lines are:

Physical characteristics

Line length (km)	
Foz substation to Ivaiporã	320
Ivaiporã to Itaberá	265
Itaberá to Tijuco Preto	304
Span (m)	
Average length	430
Maximum length	930

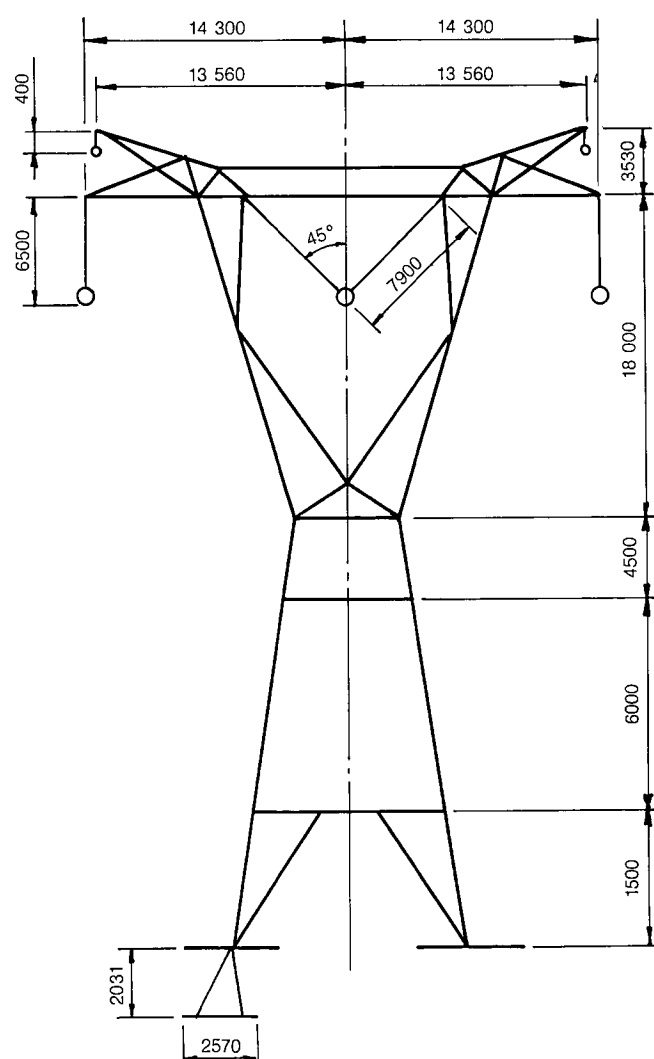


Fig. 15.16 765 kV ac lines typical self-supporting tower

Minimum clearance to ground at mid span (m)	15
Phase arrangement	Horizontal
Clearance between phases (m)	14.4 (Rigid tower) 15.5 (Guyed tower)
Conductors' arrangement in the bundle	Square
Distance between conductors in the bundle (cm)	45.7
Tower type (%)	
Suspension guyed	82
Suspension self-supporting	16
Dead end	2
Right-of-way (m)	
Single line	94.5
Two lines	175

Design conditions

Maximum load (kN)	44
Stress at 15° C and wind speed 150 km/h	33% ultimate tensile strength
Normal load (kN)	24
Stress at 20° C and no wind	18% ultimate tensile strength

Electrical characteristics

Nominal voltage (kV)	765
Max. operating voltage (kV)	800
Max. operating current (A)	2000
Normal rating (MVA) (60° C and 40° C amb.)	2780
Conductor	1113 kcmil 45/7 ACSR "BLUEJAY"
no. of conductors per bundle	4
BIL (kV)	2800
Insulators	arrangement IVI disk type, 254 mm x 146 mm strength 120 kN 35 insulators per string
Shield wires – 2 per line	176.9 kcmil ACSR "DOTTEREL" 110.8 kcmil ACSR "MINORCA"
Counterpoise	Galv. steel 4 BWG and 9.525 mm SM galvanized steel cable (near the substations)

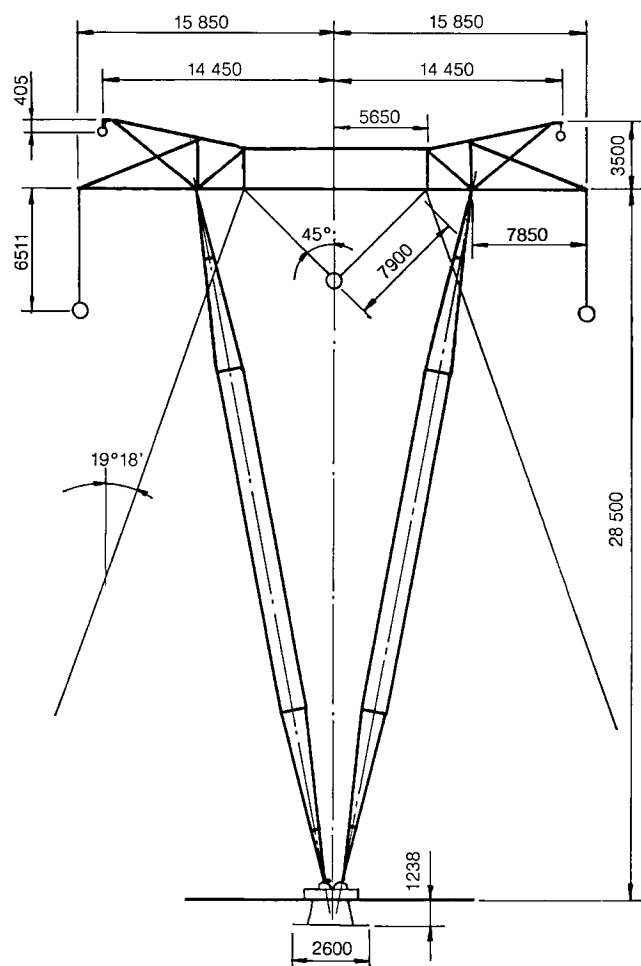


Fig. 15.17 765 kV ac lines typical guyed tower

500 kV ac transmission lines

The 60 Hz 500 kV transmission lines are relatively short lines, 8.1 km long, between the powerhouse and the Foz do Iguaçu substation. The main physical and electrical characteristics are the same as those for the 50 Hz lines.

ENVIRONMENTAL AND ECOLOGICAL ASPECTS

BASIC CONSIDERATIONS	16.3
Background	16.3
BASIC PLAN FOR CONSERVATION OF THE ENVIRONMENT	16.4
ENVIRONMENTAL SURVEYS	16.5
Physical Environment	16.5
Biological Environment	16.6
Social Environment	16.7
PROVISIONS TAKEN TO PROTECT AND ENHANCE THE ENVIRONMENT	16.9
Protection of Existing Forests and Reforestation	16.9
Biological Reserves and Refuges	16.11
Animal Rescue	16.12
Aquaculture	16.12
Recuperation and Landscaping of the Construction Site	16.14
MASTER PLAN FOR UTILIZATION OF THE RESERVOIR AREA	16.15
RELOCATION OF POPULATION	16.15
ENVIRONMENTAL EDUCATION	16.16
TOURISM	16.17
REGIONAL DEVELOPMENT	16.18

ENVIRONMENTAL

AND ECOLOGICAL ASPECTS

BASIC CONSIDERATIONS

BACKGROUND

Construction of the Itaipu hydroelectric project has created an artificial lake 170 km long, with a maximum depth of 170 m and storing 29 billion m³ of water. The lake has a surface area of 1350 km², of which 780 km² are in Brazil and 570 km² in Paraguay, see Fig. 16.1. Obviously this has resulted in considerable environmental changes in the Paraná river system, which is the seventh largest in the world, and which extends over an area of 30 000 km².

Anticipating that the implementation of the project would have a major environmental impact over a significant area, studies to evaluate such changes and mitigate their effects were conducted during the feasibility study stage, as well as during the execution and the first 5 years of operation of the project.

The first evaluation of the environmental impact of the project was conducted in 1973 by the IECO-ELC consortium. As a result of these studies a report entitled "Reconnaissance of the Ecological Impact of the Project" was prepared for the Brazilian - Paraguayan Joint Technical Commission.



View of Itaipu Lake

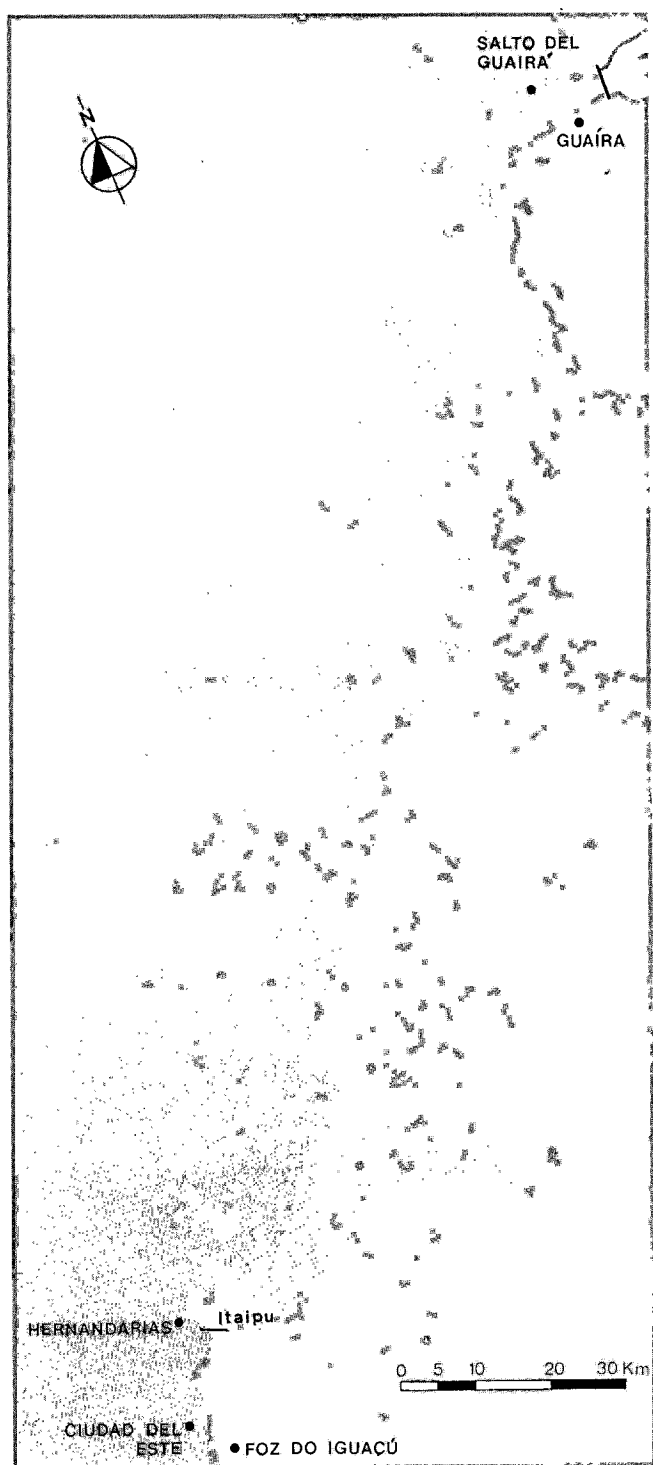


Fig. 16.1 Itaipu Lake

The objective of the study was to provide, at a preliminary level, factual information on the probable physical, biological and social effects of the project and to provide guidelines for the enhancement and protection of the environment in the project area and the affected regions.

Unavoidable significant environmental changes were:

- Elimination of a 170 km long stretch of free flowing river.
- Submersion of the Sete Quedas Falls or Saltos del Guairá.
- Reduction of wildlife habitat.
- Elimination of 700 km² of virgin forest.
- Flooding of 600 km² of agricultural land.
- Submersion of possible unknown mineral deposits.
- Submersion of possible unknown historic sites.

Considering the enormous amount of power to be generated and its associated social and economic benefits, the unavoidable adverse environmental impact resulting from the project was considered acceptable, especially if kept to a minimum by suitable countermeasures.

BASIC PLAN FOR CONSERVATION OF THE ENVIRONMENT

The studies conducted in 1973, as well as other studies previously carried out by Brazilian and Paraguayan electric utilities, served as the basis for a 1975 program entitled "Basic Plan for Conservation of the Environment" which defined ITAIPU's environmental conservation policy, see Fig 16.2.

The purpose of the plan was to set up guidelines for the control of the quality of the environment in the area in question and to define necessary measures for the protection of the environment and of areas for further study.

The main activities defined in the plan were as follows:

- Elaboration of an environmental survey of the project area.
- Elaboration of a master plan for the utilization of the reservoir area.
- Implementation of environmental protection measures.

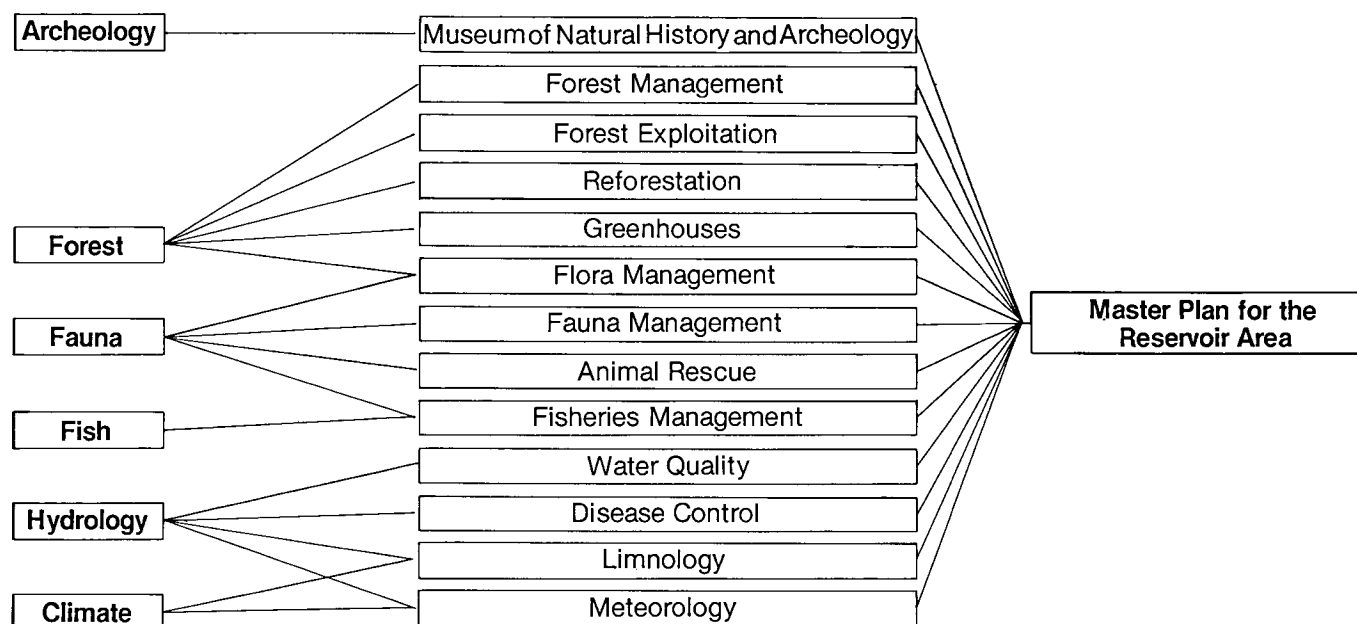


Fig. 16.2 Summary of studies conducted for the master plan for conservation

ENVIRONMENTAL SURVEYS

To assess and quantify the ecological and social effects of the project, an environmental survey of the area was conducted and organized as follows:

- Physical environment.
- Biological environment.
- Social environment.

PHYSICAL ENVIRONMENT

The major activities involved in the survey were:

WATER QUALITY. The quality of water upstream and downstream from the dam was monitored both before and after the creation of the reservoir. About forty parameters (physical, physical-chemical, chemical, biological and bacteriological) were covered, with more than 40 000 data points being collected before the filling of the reservoir, to determine the limnological characteristics of the river system and the future lake. During the 5 years after the filling of the lake, this monitoring was continued over a twenty-two station network collecting about 30 000 data points per year.

The principal limnological characteristics of the newly formed reservoir indicated that no eutrophication process was underway; nevertheless, careful control should be exercised over the nutrient load input from the tributaries. The reservoir was classified as mesotrophic (intermediate level of primary production) with no thermal nor chemical stratification.

Concentration of dissolved oxygen was relatively high throughout the year, being 80% to 100% saturated. Phosphorus seemed to be the limiting factor for primary productivity.

The residence time of the reservoir volume varied from 3 to 15 days depending on storage and flow conditions.

The principal limnological and chemical characteristics in the reservoir water were as follows:

Temperature	19 – 30	°C
Dissolved oxygen	6.82 – 8.18	mg/l
Turbidity	4.5 – 30	NTU
pH value	6.9 – 7.9	
Conductivity	43 – 50	µmhos/cm
Total alkalinity	18 – 22	mg/l
Total nitrogen	0.15 – 0.36	mg/l
Total phosphorus	0.005 – 0.022	mg/l
Phytoplanktons	65%	Nostocoficeae
	20%	Cloroficeae
Zooplanktons	55%	Rotifiers
	30%	Cladocerae
Chlorofila a	2.6 – 7.3	mg/m ³
Fecal coliform	5 – 20	MPN/100 ml
Pesticides (in sediments):		
BHC	2.27	mg/ kg
Lindane	1.53	µg/kg
TDE	28.85	mg/kg
DDT	16.07	µg/kg

It was concluded that the Itaipu reservoir did not degrade the quality of the Paraná river water; it being suitable for raw water supply to municipal systems as well as for recreation, commercial fishery and irrigation purposes.

RESERVOIR SITE CLEARANCE. After an in-depth evaluation of the resulting consequences, ITAIPU had decided not to remove the vegetation in the area to be flooded, as subsequent decomposition of the vegetation would be slow and have very little effect on the long term quality of the water. However, as a safety measure, vegetation was removed from a restricted area, about 100 km² between El. 200 and 220, comprising mainly high forests. The volume extracted was small, about 10%, in relation to the total forest biomass of the flooded area, estimated to be about 2 million t.

CLIMATIC EFFECTS. The climate of the area is classified as humid sub-tropical with an average temperature of 22°C, a maximum of 40°C in December/January and a minimum of - 5°C in July/August. The annual average relative humidity is 80%. A monitoring program was established to determine the possible microclimatic modifications which the reservoir could provoke in the region adjacent to the project. For this purpose six agroclimatologic stations were established and integrated with the Brazilian meteorological network. The data collected over 8 years showed an absence of any tendency for climatic variation in the region, as a result of the creation of the reservoir.

SEDIMENT TRANSPORT. The sediment transport characteristics of the river basin were studied together with the corresponding load input into the reservoir. The average annual sediment load is estimated to be 5 million t, indicating a minimum of 350 years as the useful life of the reservoir.

BIOLOGICAL ENVIRONMENT

These survey activities were as follows:

FORESTRY SURVEY. The main activities included identification of forest structure and composition, forest ecology and fauna relationships, identification of botanical species, elaboration of forest management projects, installation of greenhouses to accommodate collected species and elaboration of reforestation projects for the protection of the area adjacent to the reservoir.

As a result, 3860 km² were surveyed in 1975 and the following land use pattern was identified for both sides of the project area:

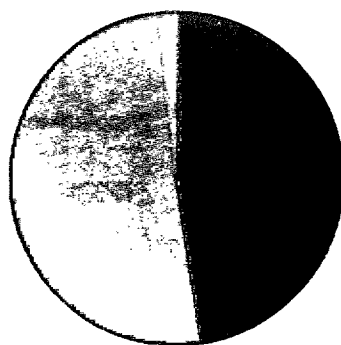
Land use	Brazil %	Paraguay %
Forest	47.6	82.4
Agriculture	50.5	15.7
Wetlands	0.7	0.9
Water bodies	0.7	0.9
Urban	0.5	0.1

As shown above, land use patterns varied considerably for the two sides of the river, but in both cases it was predominantly composed of virgin forest and agricultural lands, see Fig 16.3.

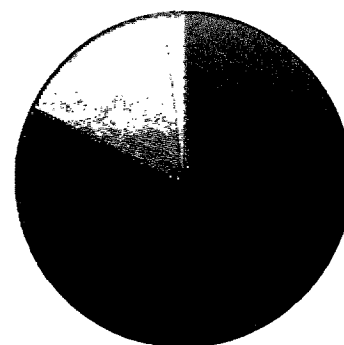
The natural forest of the area was classified as a sub-tropical rainforest. From the survey, 110 tree species of commercial value were identified, and the area had an average commercial forest volume of 191 500 m³/km². The species with the greatest commercial value were: cedar, ipê, pau-marfim, peroba and cinnamon. Also identified were 103 families and 463 botanical species, with 2 rare species, *Miconia Jucunda* and *Marsdenia* SP.

Fig. 16.3 Reservoir area land use pattern in 1975

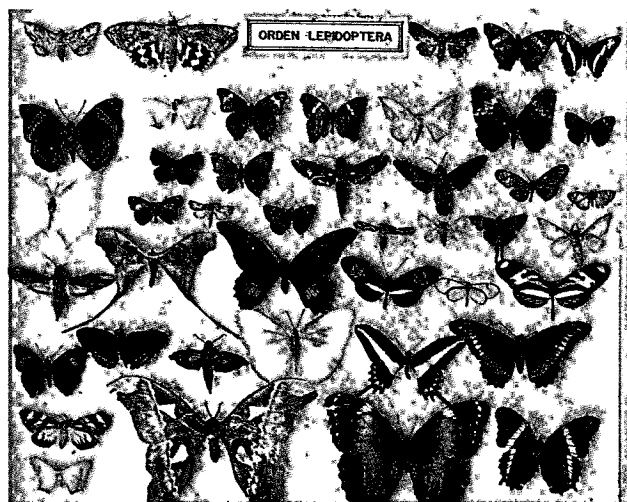
I Brazil
II Paraguay
Forest
Agriculture
Other



I



II



Fauna of the area

FAUNA SURVEY. Endemic and rare species of the area were identified and collected and their food, habitat, migration and reproductive cycles studied. Other studies covered wildlife management projects for the future relocation of the wildlife population from the flooded area and the elaboration of an animal rescue project to be executed during reservoir filling. The collection of species is also part of the creation of a Natural History Museum to accommodate samples of the fauna of the region. Considering that the majority of the virgin forests were located on the Paraguayan side, most of the activities of this program were concentrated in that area. The following fauna were identified and classified:

- Mammals: 61 species belonging to 24 families and 9 orders.
- Birds: 323 species belonging to 58 families and 20 orders.
- Reptiles: 28 species belonging to 12 families and 3 orders.
- Insects: 116 families and 20 orders.

FISHERY SURVEY. Surveys were conducted with the objective of obtaining a general description of the aquatic biological environment, identifying and describing the species which could be affected by the changes in the river system from fast running to impounded conditions. A taxonomic identification of species was developed, including composition and interrelations. The fish population was investigated on a seasonal basis, and habitat requirements such as food, spawning areas and water quality were evaluated. Other considerations included food webs, reproduction and life cycles and migration routes. The relationship between fish population dynamics, water quality conditions and the growth of aquatic plants was evaluated, with special emphasis being placed on the possible development of vectors of tropical diseases such as malaria, schistosomiasis and filariases. Other studies involved projects of aquaculture stations and replenishment of fish stocks.

Before the creation of the reservoir, 129 species belonging to 25 families were identified. After the creation of the reservoir 82 species were identified, including 15 not found before.

SOCIAL ENVIRONMENT

The two aspects covered by this survey were sanitation and health conditions in the project area, and the archeological investigations of the ceramic and historic sites found in the region.

SANITARY AND HEALTH PROGRAMS. Basic sanitary requirements of the infrastructure necessary for the



Fish collecting



View of a Jesuit Mission site.

execution of the project were defined together with a study of the effects of the project on the health of the population. The survey identified the pre-project conditions and established a health program to assure the well-being not only of the work force at the project, but also of the population of the region. Special attention was given to the possible spread of tropical diseases resulting from the creation of the lake.

ARCHEOLOGICAL INVESTIGATIONS. As a result of the favorable natural conditions of the Paraná river valley, the area was densely populated by native Indians of the Tupi-Guarani tribe during the XVI and XVII centuries, and already featured in the

early Spanish and Portuguese exploration of the southern part of South America; for example, the expeditions by Aleixo Garcia in 1522 and Alvar Nuñez Cabeza de Vaca in 1594. Because of the Treaty of Tordesillas (1494), the area was mainly explored by the Spanish and early colonization of Asunción occurred in the XVI century. The region was also the setting for the Indian villages founded by the Jesuits in the XVII century, known as the Jesuit Reductions or Missions.

Occupation of the area during the late XIX century was encouraged by English and Argentinian timber and mate (herbal tea) enterprises centered around small ports on the Paraná river at that time.

*Ceramic collection*

Pre-ceramic artifacts found in the region indicate possible branches of the Preambiru trail, which was a transcontinental connection between the Indians of the Atlantic coast and the Incas of Peru. The artifacts collected in the region are divided into two categories, namely, those existing before the arrival of the Europeans and those created afterwards. A total of 237 sites were investigated and 171 500 specimens were collected and analyzed, giving a general picture of the human occupancy and history of the area from 6000 B.C. to 1920 A.D.

The archeological investigations in the Itaipu project area are of great significance for the understanding of the ethnology of the region. Its findings are collected in the Natural History Museum and the Ecomuseum located near to the project site.

MEASURES TAKEN TO PROTECT AND ENHANCE THE ENVIRONMENT

As part of the ITAIPU conservation plan, the following measures were taken with the objective of maintaining the environmental quality of the project area:

PROTECTION OF EXISTING FORESTS AND REFORESTATION

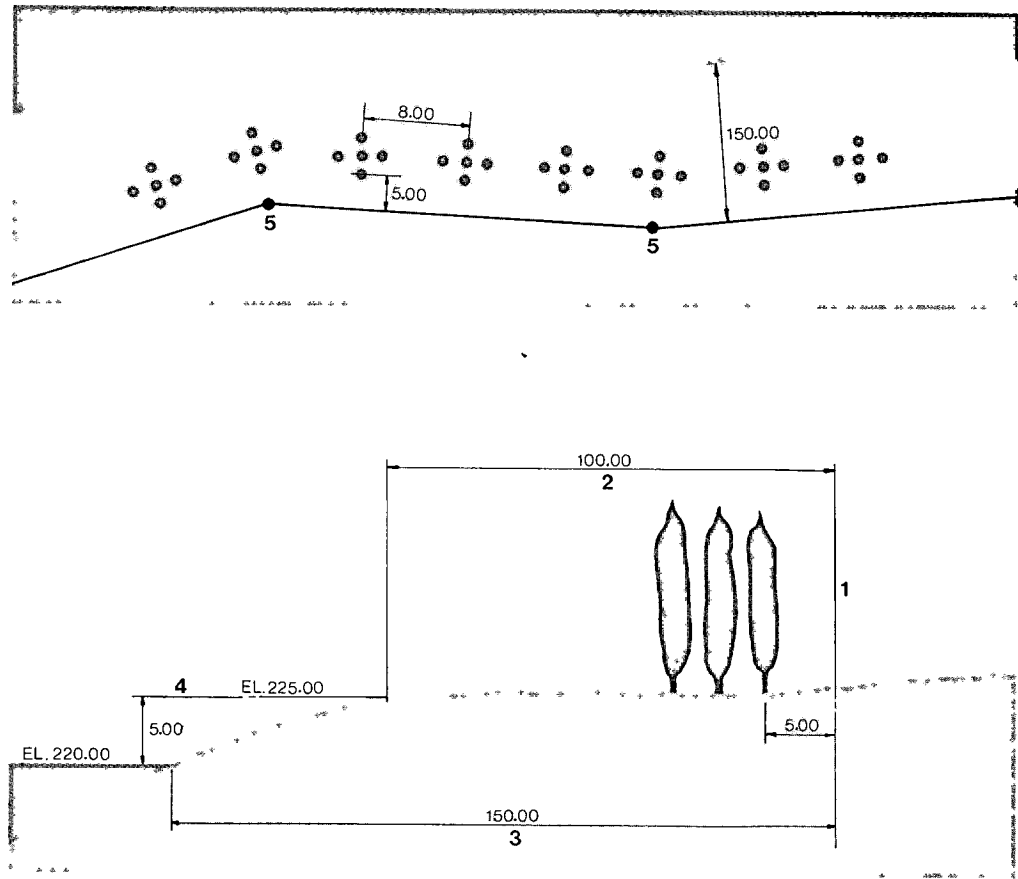
To protect the reservoir area, a security or protected zone was established; see Fig. 16.4; it being an area extending along the reservoir rim at El. 225 m and

having a width varying from 100 to 500 m on the Brazilian side and 100 to 3000 m on the Paraguayan side. The respective areas being 280 km² in Brazil and 354 km² in Paraguay. The boundary line which encloses this zone is defined as the perimetrical polygon and is 1395 km long.

Whereas about 90% of the reservoir area along the Paraguayan side was covered by virgin forest, the situation was quite different on the Brazilian side, where only 8% of the area was still covered by virgin forest because of the intense use of the land for agricultural purposes. Thus the "Gralha Azul" project, named after a bird (*Cyanocora Caeruleus*) known for the spreading of forest tree seeds, was implemented with the objective of restoring the forest cover in the protected zone on the Brazilian side. To reforest the entire area 22 million trees would have been required, but because of the natural regeneration capability of the existing forest, only 15 million trees were necessary. The reforestation program started in 1983 and continued until the entire forest cover was planted. The protected zone served several purposes, such as:

- Reduction of erosion of the reservoir shoreline.
- Prevention of contamination of the reservoir from agricultural and associated pollutants.
- Acting as windbreaks and mist barriers.
- Preventing establishment of human settlements in areas subject to flooding.
- Providing a natural habitat for wildlife.
- Enhancing the scenic environment.

Complementary to the reforestation program in the protected zone, ITAIPU also created a permanent green belt along the perimetrical polygon to mark the reservoir area boundary line previously established.



Greenhouses



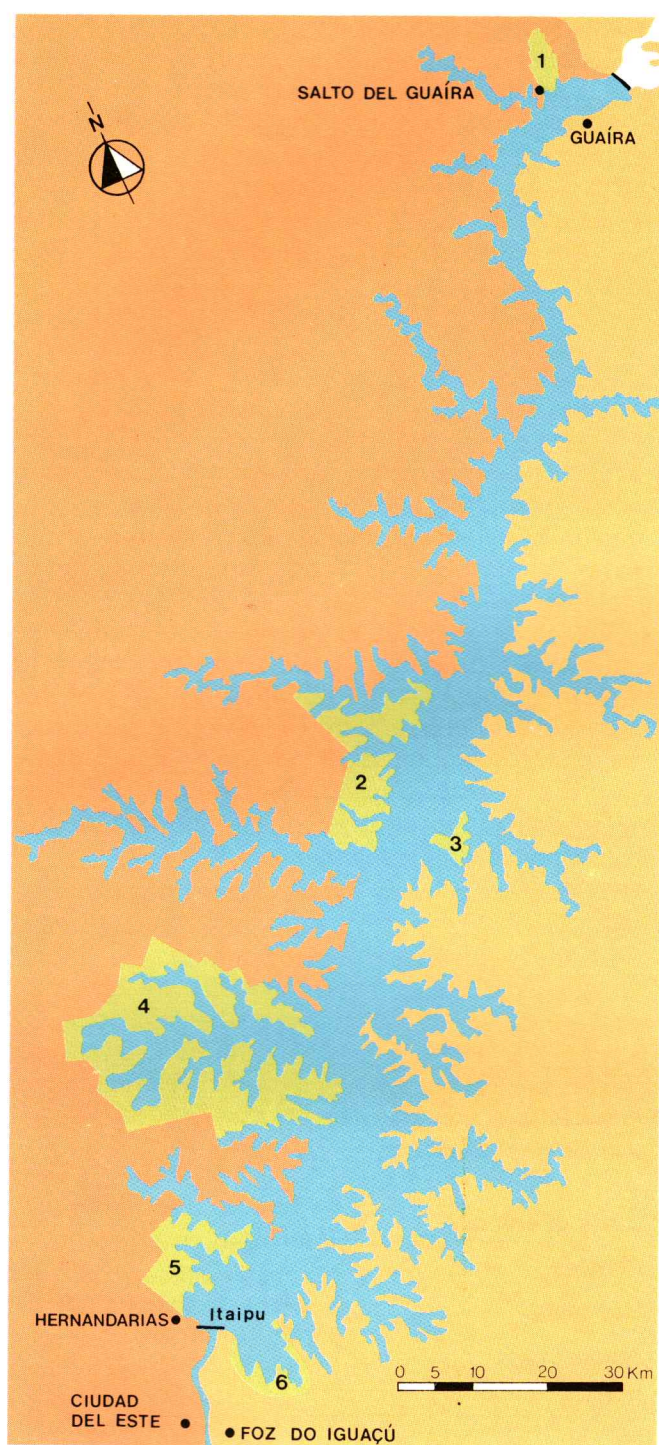


Fig. 16.5 Location of biological reserves

- | | |
|----------------|--------------|
| 1 Maracaju | 4 Itabó |
| 2 Limoy | 5 Tati-Yupi |
| 3 Santa Helena | 6 Bela Vista |



Itabó biological reserve entrance

One million trees of 50 different native species were planted in the green belt in 1981–82.

To support the reforestation program, greenhouses were established to provide seedlings of native plants collected from the area. In eleven years, the greenhouses produced about twenty million seedlings which were used in the reforestation program and also in the landscaping of the residential areas of ITAIPU.

BIOLOGICAL RESERVES AND SANCTUARIES

Another measure taken to guarantee the survival of many animal and plant species was the establishment of specific protected areas where special conservation activities such as protection and recuperation of existing forests, animal resettlement, ecological research, wildlife management and environmental education are undertaken, see Fig. 16.5.

The following areas were established:

Location	Name	Area km ²
Paraguay	Limoy	148
	Itabó	83
	Tati-Yupi	24
Brazil	Bela Vista	17
	Santa Helena	15
Brazil / Paraguay border	Maracaju	14

The following factors were considered in the selection of the areas:

- Amount of dry surface area.
- Amount of natural forest area.
- Wildlife population densities and habitats.
- Demographic pressures.
- Tourism and cultural potential.

The areas of Limoy and Itabó are classified as reserves because of their size and natural conditions, whereas the others are classified as refuges, since they are smaller and already subject to some human development.

Also an area of 240 000 m², known as the Flora and Fauna Unit, was established for a research center, plant nursery, Natural Science Museum, regional zoo, animal hospital and a logistic center for the reservoir area forest guards. This unit is located on the Paraguayan side and is very close to Ciudad del Este, thus providing a tourist attraction and a point of interest for the local population.

A direct result of the creation of these protected areas was the increase in the number of waterfowl species on the reservoir, which cannot be found in the nearby regions.

ANIMAL RESCUE

In an effort to mitigate the effects of flooding of the area during the reservoir filling, an animal rescue project named Mymba Kuera (meaning animal catching in guarani), was undertaken.

This project was planned from the very start of the ITAIPU environmental program, with the following objectives:

- Collect data on existing animal species, and corresponding population densities.
- Establish a program for animal rescue before, during and after reservoir filling.
- Establish the resettlement of the rescued animals in special protected areas, such as biological reserves and refuges.
- Follow-up on the adjustment of the ecosystem of the reservoir area.

To gather experience in animal rescue operations, ITAIPU personnel participated in similar operations undertaken by other hydroelectric projects such as Agua Vermelha, Salto Santiago and Foz do Areia. Special training was also provided by Instituto Butantan of São Paulo and the São Paulo and Curitiba Zoos.

The Mymba Kuera project was conducted in three stages as follows:

STAGE I. The rescue personnel were put on alert in case of exceptional rising of the water level to El. 142 during opening of the diversion channel in 1978. There was no need to activate this stage.

STAGE II. This comprised the following activities, starting at the end of 1978:

- Identification of temporary islands which were to eventually disappear and would, therefore, serve as oases for many animals.

- Identification of areas where concentration of animals was to be expected.
- Relocation of animals which otherwise would have little chance to survive during the flooding.
- Establishment of temporary reserve areas which would receive the relocated animals during this period.
- Biological research and studies to support the rescue and resettlement operation.
- Personnel training.

During this stage about 2000 animals were collected and relocated.

STAGE III. Activated 8 months before the scheduled reservoir filling, this stage consisted of:

- Setting up the infrastructure necessary for the rescue operation during reservoir filling, including purchase of equipment, veterinary assistance, medical assistance to rescue personnel, ground and water transportation, communications, living accommodations, etc.
- Rescue of animals during reservoir filling. This activity was divided into two stages: October 13 through October 31, 1982, when the rescue was more intensive in view of the rapidly rising water level and from November, 1982 through February, 1983, when the reservoir was already formed.
- Resettlement of the rescued animals in the existing biological reserves and refuges.

Rare animals were sent to biological research institutes. Most of the snakes captured were forwarded to Instituto Butantan in São Paulo.

During this stage, more than 200 persons were involved and about 9000 animals were rescued on the Brazilian side and about 20 000 on the Paraguayan side, the difference being due to the greater virgin forest area on the Paraguayan side. The percentage of the rescued animals was as follows:

Class of animals	%
Reptiles	45
Mammals	27
Arachnids	21
Birds	7

AQUACULTURE

The activities in this area dealt not only with providing an equilibrium for the new aquatic environment and restoring natural conditions, but also with the evaluation of production and maximum sustainable yield of the fish population.



Animal rescue

The techniques used were:

- Population management
- Selective fishery
- Replenishment of stocks
- Establishment of fish farms
- Habitat management
- Control of macrophytes
- Control of water level
- Artificial spawning areas
- Fishery regulation
- Management and control of commercial and sport fisheries
- Protection of young fish
- Restrictions on fishing in certain areas and periods.

In 1988, the average monthly production of fish in the Itaipu lake was 116 t. About 840 professional fishermen worked in the reservoir area, 57% of them having started their activities after filling of the reservoir. The most common commercial species of fish are Curimba (*P. scrofa*) Curvina (*P. Squamosissimus*), Mapará (*H. edentatus*) and Armado (*P. Granulosus*). Inventories show that the species Curimba has decreased after lake impoundment, while Mapará has increased considerably. After impoundment of the reservoir, there was an increase in the plankton, insect and fish eating species and a reduction in the herbivorous and omnivorous ones.

Reproduction appeared to be taking place in areas outside still water conditions and the reproduction peak occurred between October and February.

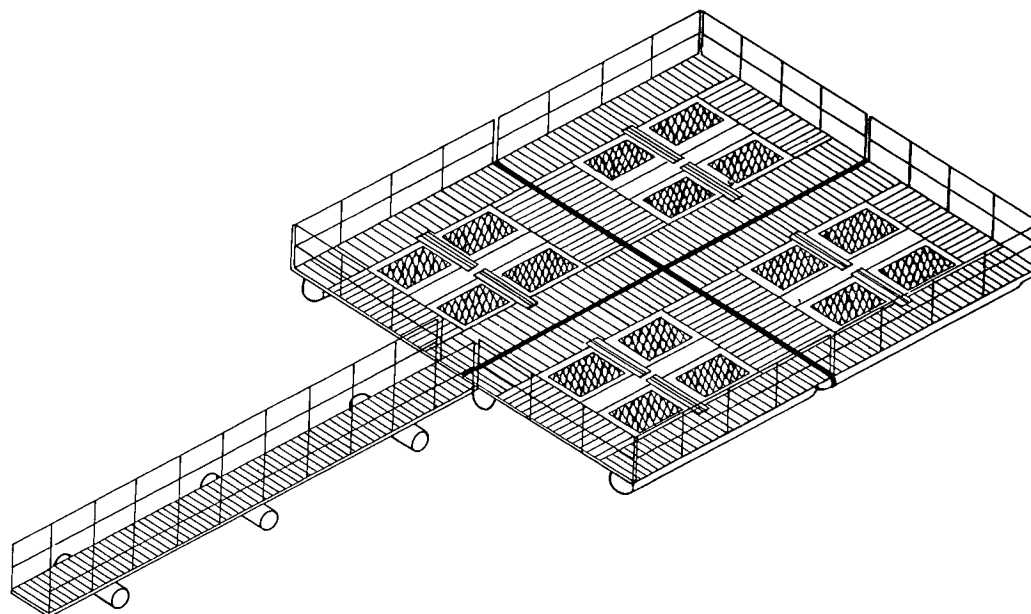


Fig. 16.6 Experimental fish tanks

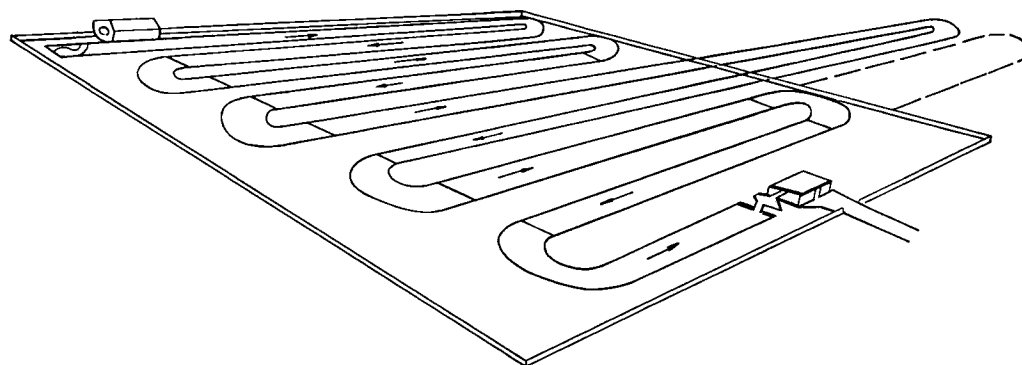


Fig. 16.7 Spawning channel

Floating tanks served as fish farms and as experimental stations for the development of an aquaculture technology for the reproduction and stocking of native fishes of the Paraná river, see Fig. 16.6.

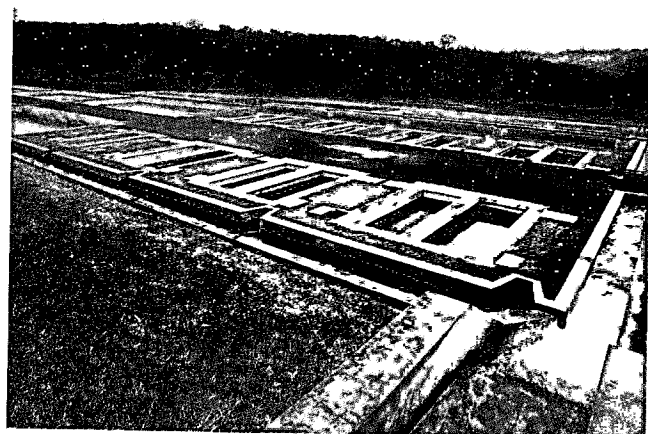
Because it constitutes a fish spawning area, it was important to preserve the fish population in the region just downstream from the powerhouse. It is of interest that, on the average, 2 t/month of fish are rescued during turbine maintenance periods and returned to the downstream portion of the river. For this purpose, a spawning channel, located 5 km downstream of the dam, 2 km in length, 2 m wide and 1 m deep will be constructed to provide natural spawning conditions, see Fig. 16.7.

RECUPERATION AND LANDSCAPING OF THE CONSTRUCTION SITE AREA

The project construction area and adjacent region comprises an area of about 50 km² which was rehabilitated after construction by returning non-operational areas to the natural landscape. Also an environmental treatment was given to the project facilities, such as roads, parking lots, substations and transmission lines.

First, a general survey of the area was conducted including topography, surface drainage, soils, and vegetation, which formed the basis for a recuperation plan.

For planning purposes the area was divided into 19 sectors, and specific areas such as biological reserves,



Aquaculture facilities

parks, transmission lines, substations, special structures and residential areas were identified in order to determine the specific type of treatment to be applied. Then, for each area a landscaping scheme with appropriate vegetation was devised.

Special attention was given to the integration of the roads with the natural landscape according to their function and circulation of vehicles.

Lookout points were provided at various locations of scenic beauty and also inside the powerhouse, thus giving visitors general views of the project and the power generating facilities.

MASTER PLAN FOR UTILIZATION OF THE RESERVOIR AREA

In view of the potentially conflicting multiple uses, ITAIPU developed a Master Plan to regulate the use of and to protect the reservoir area. The plan considered the following multiple uses: navigation, fisheries, water supply for domestic consumption and irrigation, tourism and recreation. The plan also defined zones into which the reservoir area was divided and determined the specific activities and programs to be developed within those zones.

RESERVOIR ZONE. Comprises the water surface of the reservoir along El. 220 up to the Itaipu dam.

LITTORAL ZONE. Comprises all land adjacent to the reservoir purchased by ITAIPU. Within this zone is the reservoir protection area.

Within the zones, several sectors are defined for specific uses, such as:

- Special sectors. Biological reserves, wildlife management and environmental conservation and recuperation.
- Multiple use sectors. Fisheries, navigation and water supply.
- Recreational sectors. Tourism and cultural activities.
- Urban integrating sectors. Activities concerned with development of road systems, health programs, communications and energy supply.

Finally, the plan defines the administrative procedures for management of the multiple uses of the reservoir area and its coordination with local government authorities.

To assure compliance with the objectives defined in the Master Plan, ITAIPU established a management structure responsible for its implementation and administration. Any activity to be developed in the reservoir area is subject to ITAIPU's approval. ITAIPU supervises the implementation and operation of the activities according to the guidelines and objectives defined in the Plan.

RELOCATION OF POPULATION

Formation of the Itaipu reservoir flooded an area of 1460 km². On the Brazilian side, most of the area was agricultural and required the purchase of 1000 km², including 8500 properties, of which 6900 were rural and 1600 urban. A complex ownership situation was the frontier nature of the area, most of which had only been settled in the last 20 years. This called for an

integrated effort between ITAIPU officials and government agencies to effect solutions acceptable to all parties. About 40 000 persons had to be relocated to other areas. More than 4000 ownership titles were issued by the government to assure indemnity to a large number of squatters.

The land acquisition program was carried out from 1978 to September 1982. During 1974 to 1976 the purchases were confined to the immediate vicinity of the project and the areas set aside for the workers' townships. To obtain cooperation from the affected persons, ITAIPU held periodic meetings which were accompanied by a large scale public relations campaign that included the press, radio and television and visits to the site to show the necessity and effects of the project.

Because of the steep canyon walls of the Rio Paraná, only a very small number of human settlements were located along the river. On the Brazilian side, five settlements comprising 1145 houses were submerged. On the Paraguayan side, which was a far less populated area, about 350 houses were inundated and about 25 000 persons had to be relocated.

A total of 577 km of roads were flooded and 390 km were re-routed. The average rural density was 35 persons/km² and the area of the average property was 100 000 m².

The crop area lost as a result of the Itaipu project occurred mainly on the Brazilian side and amounted to about 1000 km².

About 87% of the displaced population remained in the vicinity of the project region. The new land purchased by them with the compensation received from ITAIPU, was on the average 50% larger in area than the land which they had sold to the project.

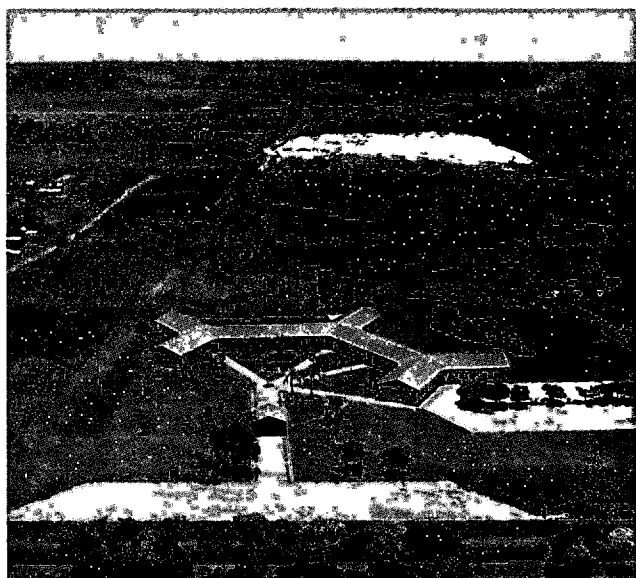
Total compensation paid by ITAIPU for land acquisition was the equivalent of US\$ 190 million.

In Brazil, as part of a federal government program, several displaced families were settled in special resettlement project areas in the states of Bahia (399 persons), Acre (1193 persons) and Paraná (2390 persons). Each relocated family received a house and a plot of land, from 200 000 m² to 400 000 m² in area. A ten year financing plan at an interest rate of 6% per annum was provided.

ENVIRONMENTAL EDUCATION

ITAIPU established an education program for the general public and in particular for the local community, including facilities which provide information on the environment. Also, a line of communication was established between the project, the environmentalists and the general public. The focal points of this program are two museums, which have since had their activities extended to include the biological reserves and refuges for educational purposes.

Museum facilities



The Ecomuseum is located on the Brazilian side near the entrance to the project site and has an area of 1200 m², housing the following:

- A greenhouse with an area of 52 m² containing 130 different plant species collected from the project area, especially from the Sete Quedas region.
- A herbarium containing samples of 820 plants also collected from the project area.
- Twelve aquariums containing samples of twelve different aquatic ecosystems of the area with respective native species.
- Exhibition halls containing:

Samples of the fauna of the region.

Samples of the pottery and ceramics collected from the excavated archeological sites.

A collection of historical items pertaining to the area.

- Research laboratories.
- Libraries.
- Conference rooms.
- Workshops.

The Museum of Natural Sciences is located on the Paraguayan side near the entrance to the project area. It has an area of about 2000 m² and houses the following facilities:

- Exhibition halls containing samples of fauna, flora and ceramics found on the Paraguayan side.
- Research laboratories.

The museums serve as the central units of the environmental education programs through the promotion of activities which stimulate study and discussion and direct involvement of the public.

These activities include:

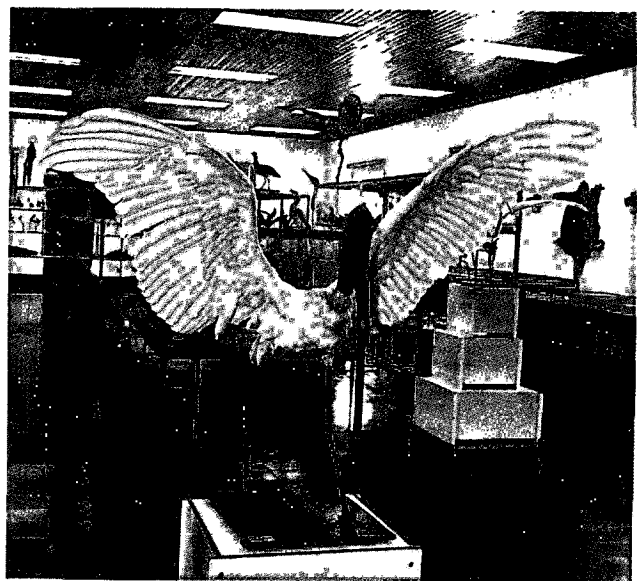
- Exhibitions.
- Lectures.
- Workshops.
- Theater.
- Programmed visits for school children.
- Ecological visits to the biological reserves.

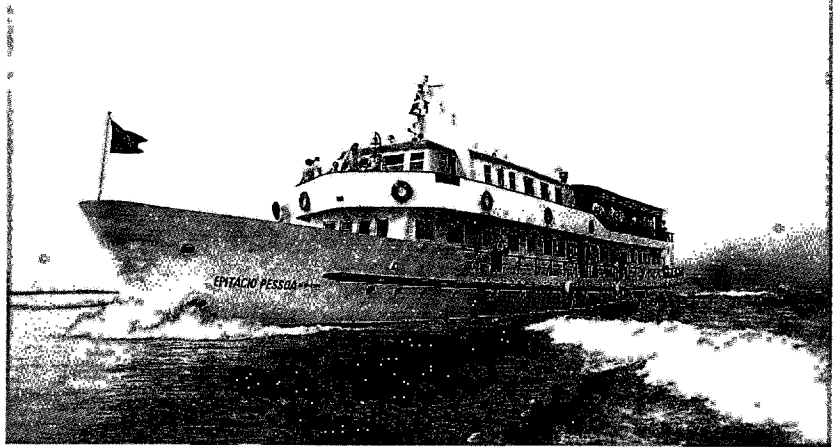
Other activities developed in the museums include cultural and scientific research in the following areas:

- Archeology.
- Ethnology.
- Paleontology.
- Anthropology.
- Zoology.
- Botany.
- Aquatic biology.

TOURISM

The project facilities have proven to be a major tourist attraction, receiving an average of 600 000 visitors per year. As the level of the reservoir is essentially constant, it has been possible to develop the shoreline in the manner of a lake resort with swimming beaches and lakeside marinas. The program also foresees the establishment of resort hotels, camping sites, sports and country clubs, as well as other facilities for leisure activities such as sailing,





Tourist facilities

water skiing and fishing. The close proximity of the project to the cities of Foz do Iguaçu and Ciudad del Este makes it easily accessible to visitors and the local communities alike, and together with the Iguaçu Falls creates an integrated popular international touristic region.

REGIONAL DEVELOPMENT

Construction of the project has led to far reaching changes in the social and economic development of the affected region. The changes can be evaluated in terms of the increase in population and the improvements and expansion of infrastructure and municipal facilities.

At the peak of construction about 30 000 persons were employed on the project. About 10 000 housing units were constructed in several residential areas on both sides, with paved roads, electricity, water supply and sewerage systems. The impact of the purchasing power on the nearby cities of Foz do Iguaçu and Ciudad del Este was considerable, and their skills and involvement in local society improved the living standards of the nearby urban areas. Since then, the influx of tourists has continued the process.

As previously indicated, in 1975 the Paraguayan area influenced by the project was less developed than the Brazilian side. This area, known as eastern Paraguay, had its initial economic development in the late XIX century when European settlers explored timber and mate herb resources of the area. However, this development did not provide sufficient stimuli for an extensive social and economic expansion of the area.

As part of a Paraguayan government policy, whose objective was to provide an access to the Atlantic coast for further trade and development, the city of Puerto Presidente Stroessner (now named Ciudad del Este) was founded in 1957. Afterwards, some agricultural development of the area took place, specially influenced by Brazilian settlers, but still it was not sufficient to promote economic growth and development. The agricultural development was mainly limited to the small scale harvests of corn and soybean crops. In 1973, the population of the region was 64 100 and the urban infrastructure services such as housing, public utilities, schools, health and recreational facilities and transportation were rather parochial. The economic development of the area still depended mainly on timber exploitation and border commerce between Brazil and Paraguay. There were only four commercial banks in the region. With the advent of the construction of Itaipu project, the socioeconomic and demographic character of the region changed enormously. About 10 000 persons were directly engaged in construction at the project site, and another 40 000 were involved at a regional level. By 1988, the regional population had increased to 267 900, of which 61% was urban. This represents an average annual increase of about 11% since 1973. The land use pattern also changed dramatically, as shown below:

Land use	1974 %	1988 %
Forests and natural	91.4	53.0
Agricultural	7.5	41.0
Water bodies	0.6	4.5
Urban	0.5	1.5

The agricultural land use expanded from 1150 km² in 1974 to 6000 km² in 1987, the crops having been diversified from soybean and corn to include wheat, cotton, manioc, sugar cane and rice. Other agroindustrial development included beef cattle, poultry and milk production (17 000 l/day).

No major manufacturing industry has been established to date on the Paraguayan side. However, with the availability of energy produced by the project and the increased availability of skilled labor, this situation is likely to change in the future. Construction activity in the region has substantially increased to serve the needs of the increasing population. In 1988 three facilities were supplying construction materials, including cement and concrete products. Major emphasis is also being given to the agroindustry through the establishment

of storage silos and mills. The commercial sector also increased, with 1,800 stores operating with about 16 000 employees. Also, sixteen commercial banks were serving the community. In 1988, the occupational structure of the employed population of the region was as follows:

Sector	Persons	%
Agroindustry	29 700	31
Commercial	18 300	19
Construction and mining	14 700	15
Miscellaneous	12 500	13
Basic services	11 200	12
Industrial	6800	7
Forestry, fishery and game	3400	3
Total	96 600	100

On the Brazilian side of the project area, considerable development had occurred before the construction of Itaipu. This development was mainly supported by agricultural activities and by the tourism generated by the Iguazu Falls. However, the project caused a moderate increase in the previous growth rate. While with the continuing increase in tourism such development would have eventually occurred anyway, Itaipu served as the catalyst providing the necessary growth stimulus. In 1975, the population of the city of Foz do Iguazu was 40 000; by 1988 it reached 230 000, corresponding to an average annual increase of 14%.

Although before Itaipu project the city of Foz do Iguazu had an adequate infrastructure, it was substantially improved and expanded during the construction of the project. More than 350 000 m² of leisure areas were created. About 400 000 m² of roads and access roads were paved, and 150 km of railways, 120 km of bridges and 1300 km of highways were laid out. Educational, tourist and health centers were created, upgraded and expanded. Modernization of the Foz do Iguazu airport was implemented. A sewer system comprising 120 km of pipe and a 170 km water distribution network were constructed.

PROJECT SITE

INFRASTRUCTURE

BACKGROUND	17.3
FACILITIES	17.4
Housing	17.4
Social Infrastructure	17.6
Utilities Services	17.8
Access Roads	17.9
Tourist Facilities	17.9

PROJECT SITE

INFRASTRUCTURE

BACKGROUND

Although the Itaipu project is close to the urban areas of Foz do Iguaçu and Ciudad del Este, see Chapter 3, at the beginning of construction there was an inadequate physical and social infrastructure in the vicinity to support the needs of the project. It was therefore, necessary to provide adequate living conditions for the workers and their families, as well as access roads to the site in order to assure proper transportation of material, heavy equipment and personnel.

The planning criteria used for establishing the infrastructure for the project were as follows:

- Definition of the needs of the project.
- Verification of suitability of additional infrastructure in the area.
- Utilization, whenever possible, of existing infrastructure from nearby cities; improving and expanding it, as and when necessary.
- Execution and coordination, with government agencies, of the construction of unavailable and necessary infrastructure.
- Maintenance and operation of the newly established services.
- Eventual transfer of services to local governments on completion of the project.



*View of Itaipu
residential area*

The additional infrastructure created for the project comprised the following:

- Construction of housing facilities in the vicinity of the project, including services such as water treatment and supply, sewage and waste disposal, electric supply and telecommunications.
- Establishment of a social infrastructure including schools, hospitals, commercial, cultural, religious and recreational centers.
- Transportation facilities.

To assure an adequate integrated infrastructure between the project and the neighboring cities, a plan of urban development for the cities of Foz do Iguaçu and Ciudad del Este was compiled.

The plan served as a guideline for the establishment of housing, utilities and transportation facilities for the project, in keeping with the orderly and integrated growth of the region. The plan was developed by the Universidade Federal do Paraná

for the city of Foz do Iguaçu and by the Instituto de Administração Municipal do Rio de Janeiro for the city of Ciudad del Este.

FACILITIES

HOUSING

Preliminary studies were conducted in 1974 to determine the location of the residential areas of the project in accordance with the following criteria:

- Availability of land close to the project.
- Capacity to build relatively large villages rapidly and continuously.

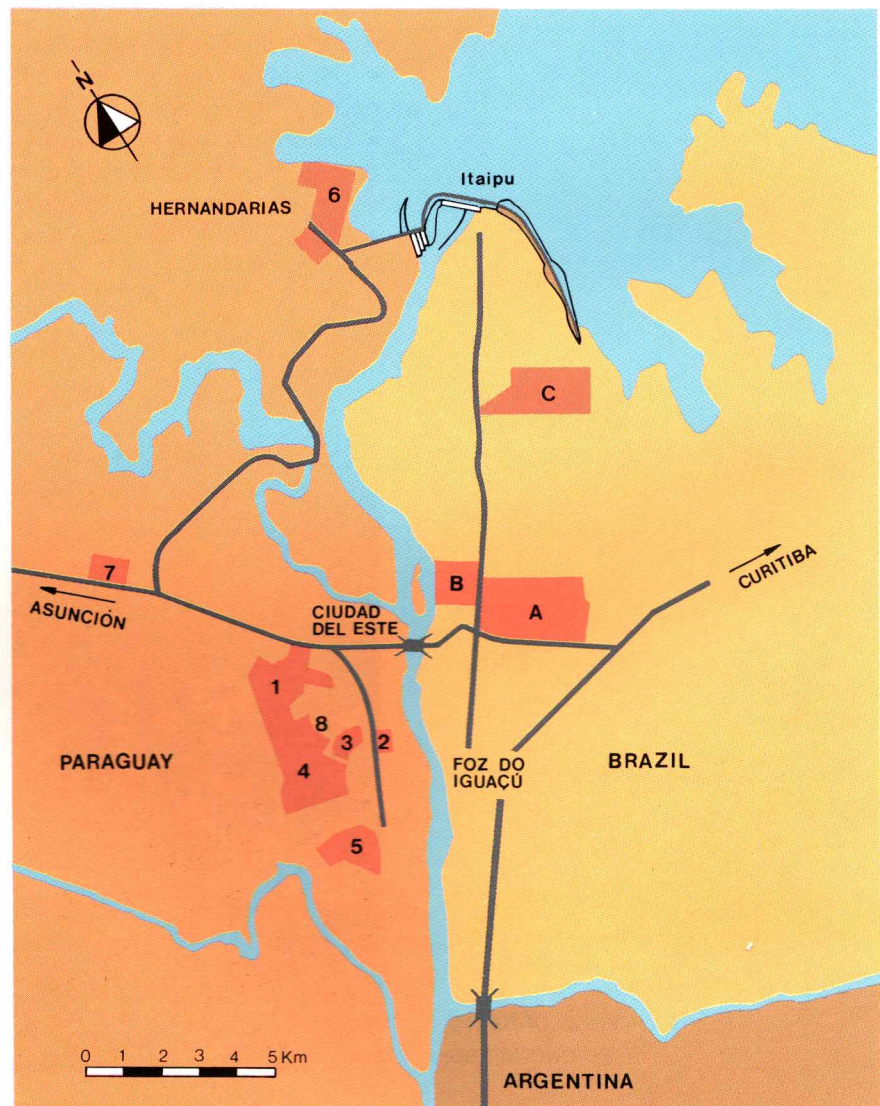


Fig. 17.1 Location of Itaipu residential areas

A, B, C Brazilian residential villages

1, 2 ... 8 Paraguayan residential villages

- Urban integration of the residential villages with the cities of Foz do Iguaçu and Ciudad del Este.
- Consideration of the location of the international highway that links the cities of Ciudad del Este, Foz do Iguaçu and Curitiba and its interference with the villages. Fig. 17.1 shows where the areas for housing were located.
- Eventual transfer of the housing facilities to the public through the local real estate market.

Three types of permanent houses, with some variations in design and size, were established as follows:

Type	Level	Personnel
Superior	1,2,3	Supervisory and engineering
Average	4,5,6	Technicians
Low	7,8,9	Construction

The houses were grouped in villages. On the Brazilian side there are three separate villages, namely A and B (close to the city of Foz do Iguaçu) and C which is located at the entrance to the project site.

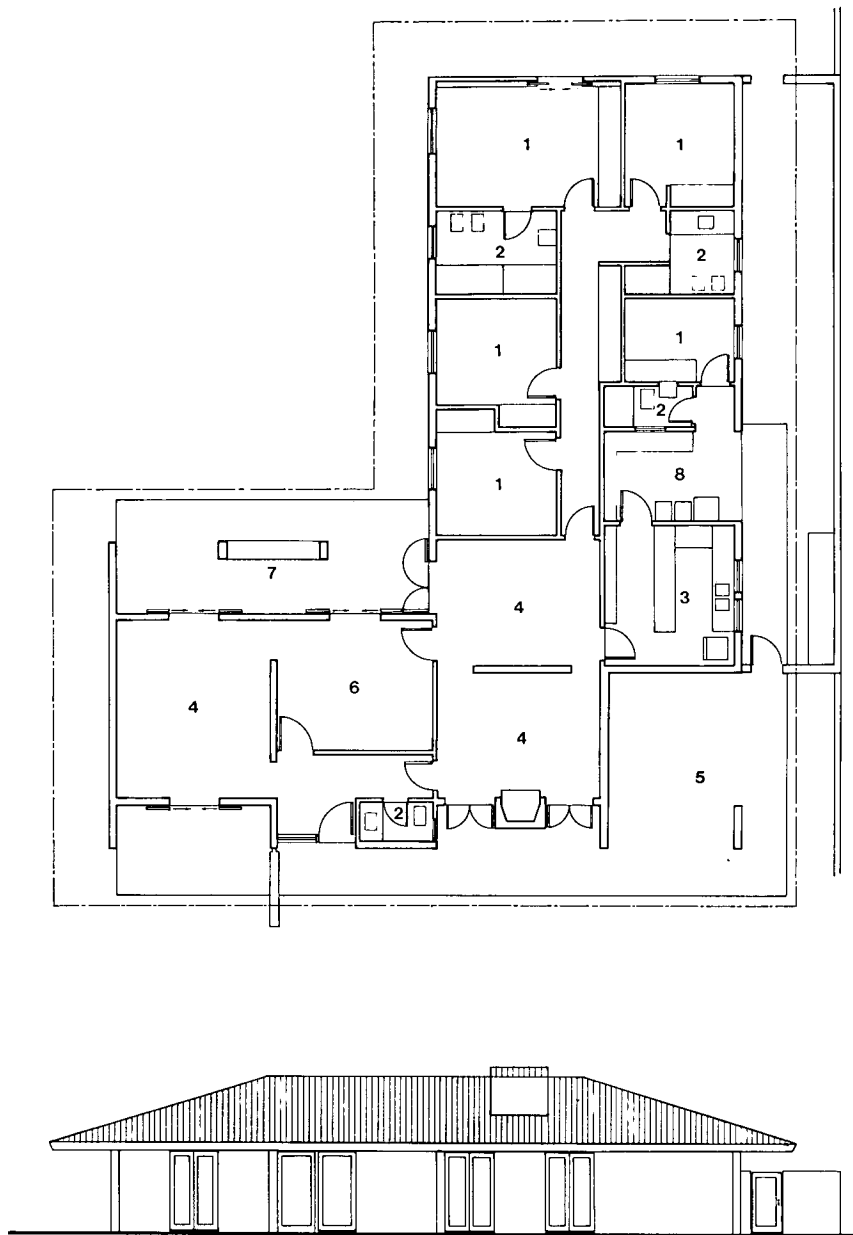
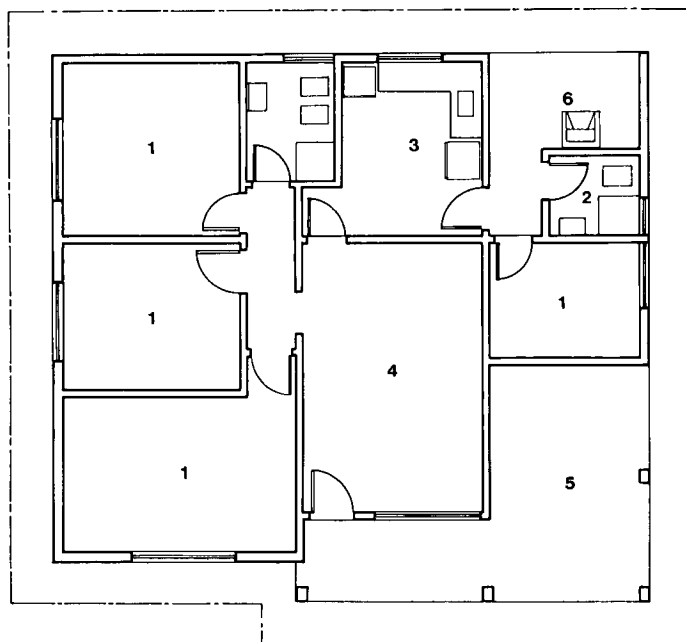


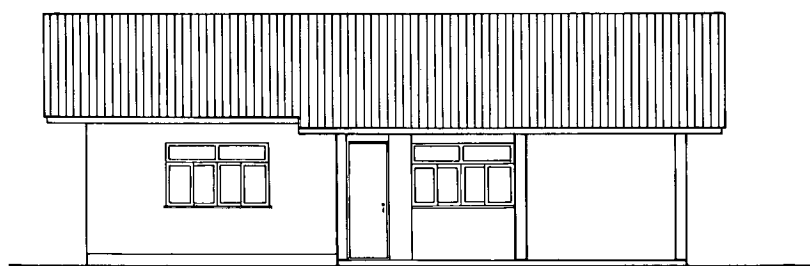
Fig. 17.2 Typical level
1 house

- 1 Bedroom
- 2 Bathroom
- 3 Kitchen
- 4 Living room
- 5 Garage
- 6 Dining room
- 7 Veranda
- 8 Service area



*Fig. 17.3 Typical level
4 house*

- 1 Bedroom
- 2 Bathroom
- 3 Kitchen
- 4 Living room
- 5 Garage
- 6 Service area



On the Paraguayan side there are eight villages five (no. 1 to 4 and no. 8) of which are located in the neighborhood of Ciudad del Este, one (no. 5) close to Puerto Presidente Franco, another (no. 7) near Acaray and one (no. 6) at the right bank entrance to the site.

Figures 17.2, 17.3 and 17.4 show the design of some typical houses. A temporary type of multifamily house was also built to accommodate the main force of the construction workers, which consisted of four adjacent houses, two with two bedrooms and two with three bedrooms, see Fig. 17.5. These houses are located in area C on the Brazilian side, and in area no. 6 on the Paraguayan side.

In early 1975 the first houses were built according to the needs of the labor force for the project. These houses were prefabricated and of the average type.

Before continuing with the housing construction program, studies of the real estate market of the cities of Foz do Iguaçu and Ciudad del Este were conducted to determine the

amount and type of houses that the local market could absorb after project completion. The studies indicated that 4000 units should be built on each side of the river. Because of project needs, the actual number of houses built was 9515, comprising a total area of 816 000 m².

Table 17.1 indicates the number of houses built on each side of the river.

SOCIAL INFRASTRUCTURE

In addition to the housing facilities, a social infrastructure, which included educational, health, recreational and commercial centers was provided. ITAIPU was responsible for the construction of the facilities and for implementing the necessary administrative measures for their operation, but the actual services were provided by specialized companies under contract to ITAIPU.

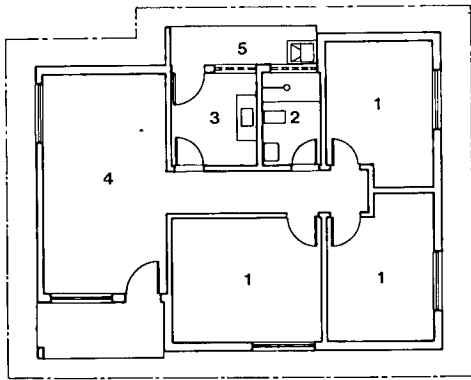
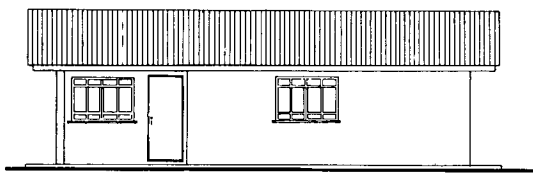


Fig. 17.4 Typical level 8 house



- 1 Bedroom
- 2 Bathroom
- 3 Kitchen
- 4 Living room
- 5 Service area

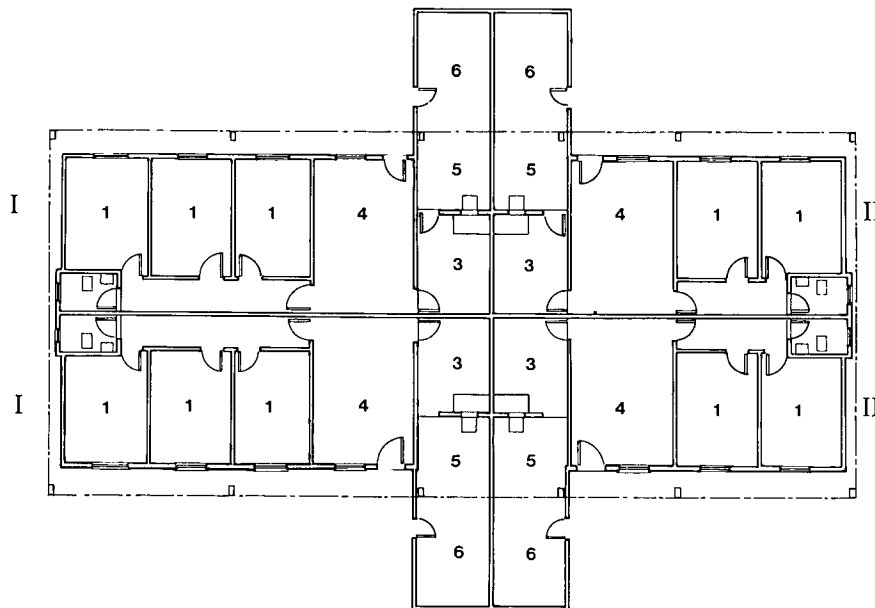
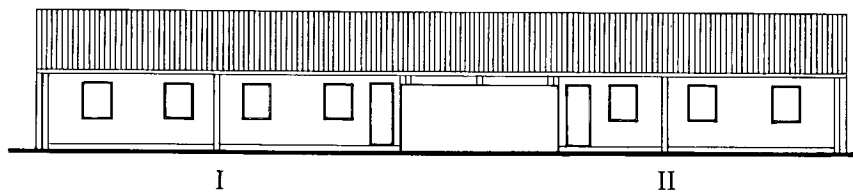
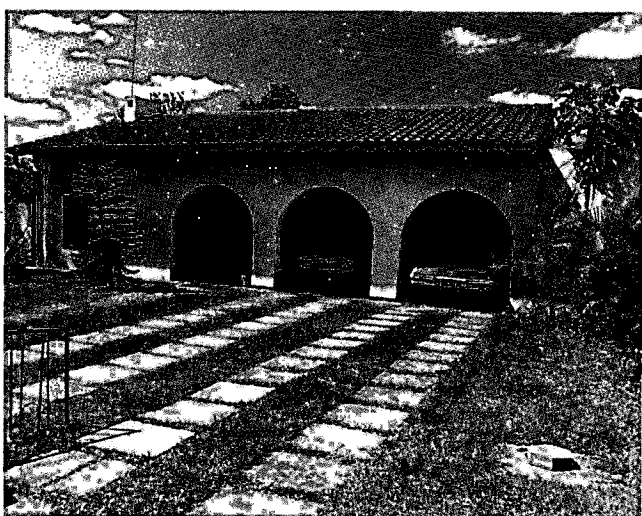


Fig. 17.5 Typical multifamily house (level 9)



- I Three bedroom house
- II Two bedroom house
- 1 Bedroom
- 2 Bathroom
- 3 Kitchen
- 4 Living room
- 5 Service area
- 6 Backyard



Views of typical Itaipu houses

Table 17.1 Quantity of houses built by ITAIPU

	Village	Quantity
Brazil	A	2105
	B	221
	C	2500
Subtotal		5226
Paraguay	1	276
	2	249
	3	378
	4	837
	5	652
	6	1680
	7	53
	8	164
Subtotal		4289
Total		9515

Table 17.2 indicates the facilities existing in 1988, their characteristics and capacities.

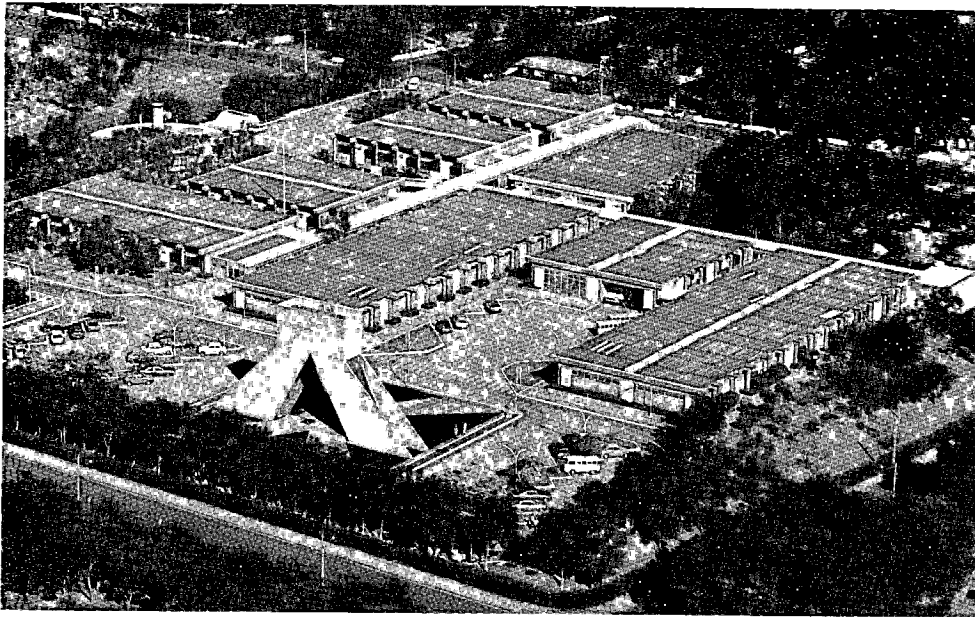
Table 17.2 Social infrastructure

Activity	Facility	Quantity
Education	Classrooms	245
	Students	20 000
Health	Medical Center	8 (50 beds)
	Maternities	2
	Hospitals	2 (300 beds)
Social	Community Centers	3
	Commercial Centers	5
Leisure	Recreational Centers	4 (8000 m ²)

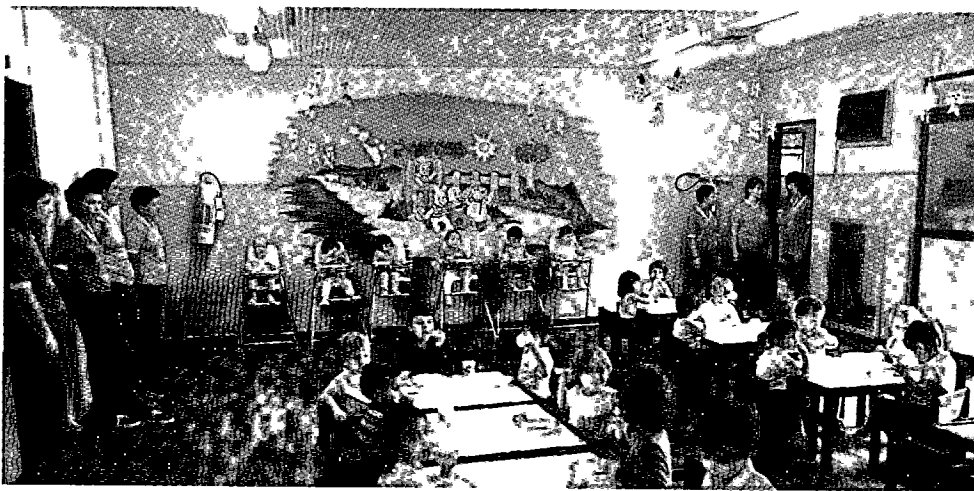
UTILITIES SERVICES

Electricity, water and sewage services were provided for the villages on both sides of the river. From the start, the services for villages A and B on the Brazilian side and no. 1 to 5 and no. 7 to 8 on the Paraguayan side were integrated with the cities of Foz do Iguaçu and Ciudad del Este, respectively.

Utilities for villages C and no. 6 were provided from the project site. A compact conventional water treatment



View of ITAIPU hospital



View of school facilities

plant with capacity of $250 \text{ m}^3/\text{h}$ was installed and serves the villages located at the project entrance as well to other facilities such as the public relations building and the museums. Telecommunication services were provided by the government phone companies of Brazil (TELEPAR – Companhia de Telecomunicações do Paraná) and Paraguay (ANTELCO – Administración Nacional de Telecomunicaciones).

ACCESS ROADS

Permanent paved access roads to the project were built by ITAIPU in order to guarantee adequate transportation of materials, equipment and

personnel. Also, the existing road network was improved and expanded in order to achieve integration of the project facilities with the cities of the area as foreseen in the plan of urban development.

Fig. 17.6 shows the established road network.

TOURIST FACILITIES

Itaipu, because of its size, importance and convenient location, has become a major tourist attraction, complementing in the region the already well established attraction of Iguazu Falls. In addition to regular tourists, the site hosts conferences and group visits of professionals and dignitaries.

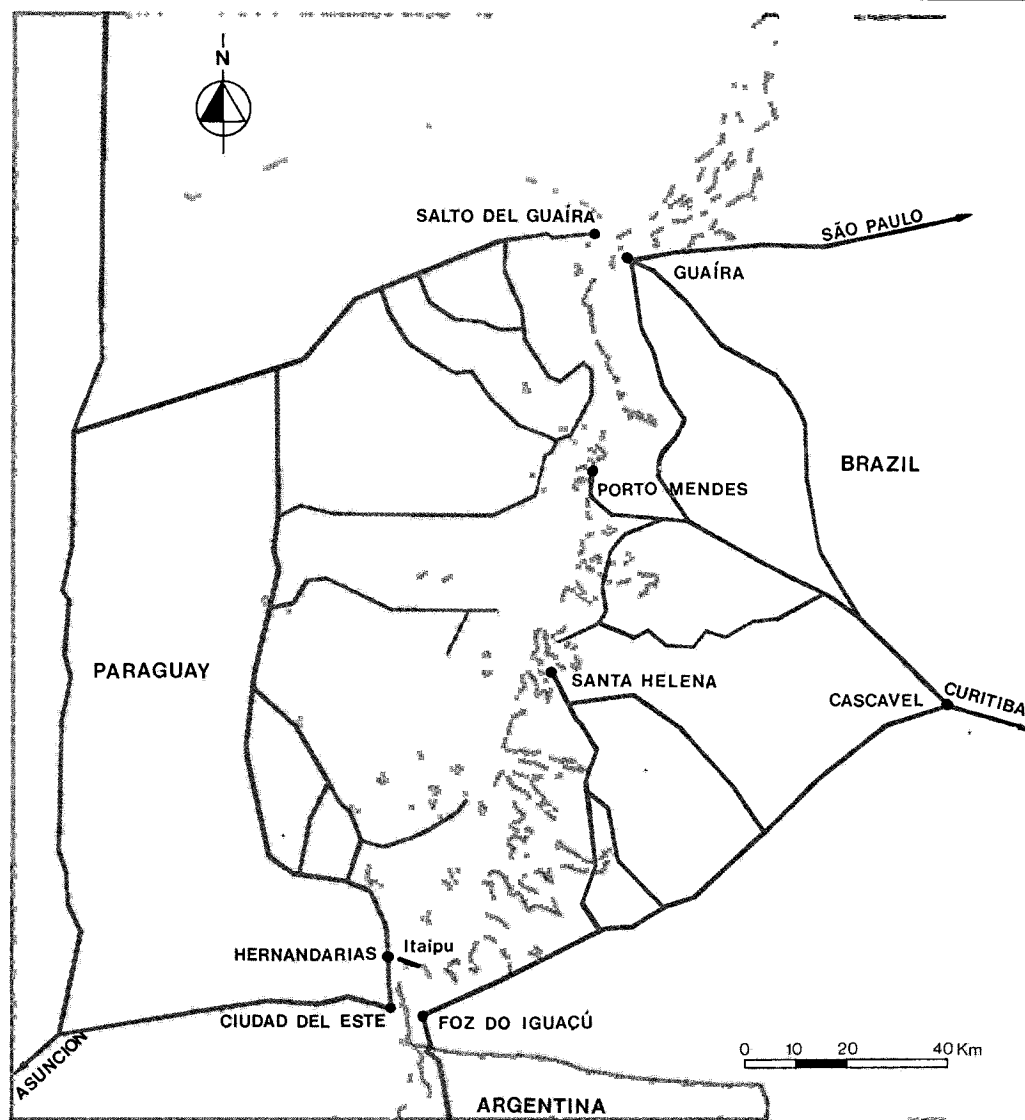
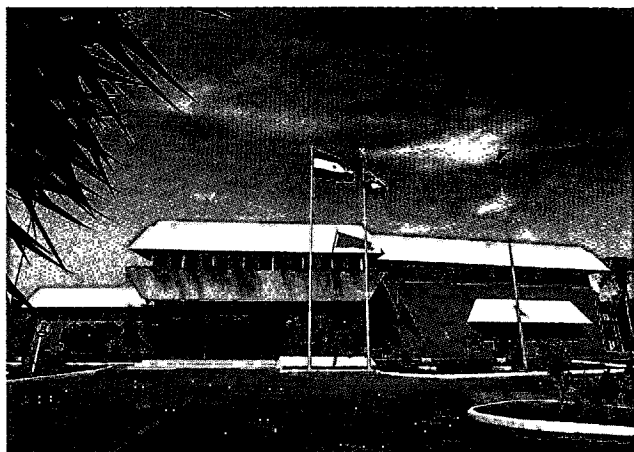


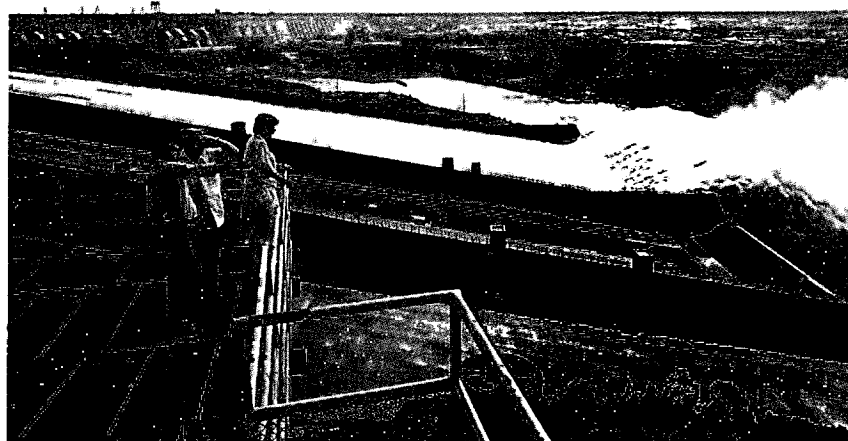
Fig. 17.6 Road network around Itaipu lake



Right bank entrance reception center



Left bank entrance reception center



Right bank look-out area

Table 17.3 shows the number of persons who visited the project in 1988.

Table 17.3 Monthly movement of visitors in 1988

Month	Quantity
January	89 845
February	60 809
March	49 174
April	52 749
May	35 630
June	41 526
July	108 969
August	56 904
September	57 911
October	60 471
November	44 699
December	56 925
Yearly total	715 612

Look-outs on left and right banks. On the left bank between the reception and the powerhouse there is a prepared area for visitors, which overlooks the complete project. There is a similar area on the right bank, just downstream of the spillway. These areas were used for ceremonies marking important milestones such as the first operation of the spillway and closure of the diversion gates.

Visitor areas in the powerhouse. Areas in the right assembly building and operation and administration building overlook El.108 of the powerhouse. The area in the operation and administration building accesses an observation gallery above the central control rooms.

Observation tower to the left of the spillway. There are plans to build an observation tower on the left of the spillway which will be accessible by cable cars from the right and the left banks.

Reception areas for visitors are as follows:

Project entrances at left and right banks . On each bank there is a reception building containing an auditorium, a hall housing permanent exhibits and display rooms for special functions.

REFERENCES AND

FURTHER READINGS

GENERAL	18.3
CIVIL	18.5
ELECTRICAL	18.10
MECHANICAL	18.22
ENVIRONMENT	18.22

REFERENCES AND FURTHER READINGS

GENERAL

- AMERICANO DA COSTA, J. & HABLITSCHKE, W. W. Estimativa de custos do projeto Itaipu. In: VII SEMINÁRIO NACIONAL DE PRODUÇÃO E TRANSMISSÃO DE ENERGIA ELÉTRICA, Brasília, dez. 2-6, 1984. Trabalhos ... Brasília, 1984. BSB/GTA/16. 11 p.
- ARCE, O. B. Itaipu e o desenvolvimento da cooperação econômica entre Brasil e Paraguai. *Informativo da Fundação Getúlio Vargas*, Rio de Janeiro, (6) : 84-8, jun. 1974.
- ASSESSORIA DE RELAÇÕES PÚBLICAS DA ELETROBRÁS. As grandes usinas hidrelétricas do Paraná. *Referência em Planejamento*, (10), 1979, p. 34-37.
- _____. A Itaipu Binacional. Panorama do Setor de Energia Elétrica no Brasil. *Memória da Eletricidade*. Rio de Janeiro, 1988. : 253-6.
- ATLAS COPCO BRASILEIRA S.A. Itaipu: o maior complexo hidrelétrico do mundo. *Ar Comprimido*, São Paulo, 3(27) : 14-20, set. 1976.
- _____. O projeto Itaipu. *Edição Especial*, p.15-19. s.d.
- BETIOL, L. Itaipu: modelo avançado de cooperação internacional na Bacia da Prata. 1. ed. Rio de Janeiro, Editora da Fundação Getúlio Vargas, 1983. 322 p.
- BIBLIOTECA DO EXÉRCITO EDITORA. Itaipu e outros projetos internacionais. *A Energia Elétrica no Brasil*, Rio de Janeiro, : 197-202, 1979.
- BLOCH EDITORES. Itaipu - crescimento de um gigante, *Revista Geográfica Universal*, 97, : 43-57, dez. 1982.
- CAVALCANTI, J. C. A Itaipu Binacional. Um exemplo de cooperação internacional na América Latina. *Revista de Adm. Pública*, Rio de Janeiro, 10(1) : 19-68, jan./mar. 1976.
- CIER. Resumen sobre el proyecto Itaipu. *Boletín de la CIER*, s.l., (88), : 1-10, feb./mar. 1976.
- CÍRCULO DE ENGENHARIA MILITAR. Itaipu - A força do homem. *Círculo de Engenharia Militar*, 86, 1983, p. 9-40.
- COMISSÃO MISTA TÉCNICA BRASILEIRO-PARAGUAIA. Rio Paraná study - Itaipu project. Final report - Project feasibility, Jul. 1974 (Portuguese/Spanish/English).
- _____. Relatório. Resumo do Projeto Itaipu. 37 p. s.d.
- COMITÊ BRASILEIRO DE GRANDES BARRAGENS. Itaipu. *Barragens do Brasil/Dams in Brazil*, Rio de Janeiro, : 104-7, 1982.
- COMPANHIA EDITORA AMERICANA. Itaipu. A 1a. do mundo em futuro próximo. *Revista do Clube de Engenharia*, (405), : 4-11, 1976.
- _____. Os grandes projetos: Itaipu. Uma vitória sobre o tempo. *Revista do Clube de Engenharia*, (420), : 8-13, dez. 1979.
- COOPERATIVA MILITAR EDITORA E DE CULTURA INTELECTUAL. A Central hidrelétrica de Itaipu. *A Defesa Nacional*, s.l., (696) : 5-20, jul./ago. 1981.
- _____. As implicações geopolíticas de Itaipu. *A Defesa Nacional*, s.l., (683) : 5-16, 1979.
- CORDOVA, E. Regimen laboral de obras fronterizas: el caso de Itaipu, *Revista Internacional del Trabajo*, 93 (3), : 335-349, may./jun. 1976.
- CORREA, A.V. Itaipu - una usina contemporánea del futuro. *Revista Siderurgia Latino americana* (277), : 42-48, mayo 1983.
- COTRIM, J. R. The Itaipu Hydroelectric plant - An example of cooperation between two neighboring countries in the development of their energy resources. In: XIII CONGRESS OF THE WORLD ENERGY CONFERENCE, Cannes, Oct. 1986. 22p.
- COTRIM, J.R.; KRAUCH, H.W.; GELÁZIO DA ROCHA, J.; GALLICO, A.; SARKARIA, G.S. The bi-national Itaipu hydropower project. *International Water Power & Dam Construction*, Sutton, 29(10, pt 1) : 40-7, oct. 1977. 29(11, pt 2) : 44-52, nov. 1977.

CORENA ED. ESPECIALIZADA DE CONSTRUÇÃO E RECURSOS NATURAIS LTDA. Itaipu sobe o rio, morre o salto, nasce o lago: a maior UH do mundo está pronta. *Construção Hoje*, 8 (11), : 15-25, 1982.

DA MATTA, C. J. O lago de Itaipu e sua importância para o transporte fluvial na bacia hidrográfica do Rio Paraná. *Revista Marítima Brasileira*, s.l., (2º trim.) : 111-29, 1985.

DONADON, J.M. Algumas considerações comparativas entre as grandes hidrelétricas do Brasil e do Mundo. *RBE*, v. 3(1), 1988, n.p.

EDITORIA PINI LTDA. Hoje Itaipu está a 153 dias da data-marco do desvio. *Construção São Paulo*, 31 (1579), : 8-13, maio 1978.

EDITORIA VISÃO LTDA. Itaipu: o momento e o futuro. *Dirigente Construtor*, Rio de Janeiro, 14 (10) : 19-28, out. 1978.

EDITORIA TÉCNICA GRUENWALD LTDA. Sete Quedas, a Paulo Afonso da Região Sul do Brasil. *Mundo Elétrico*, (42), : 186-7, mar. 1963.

_____. Itaipu já é a maior hidrelétrica do mundo. *Mundo Elétrico*, 30 (360), : 89-93, out. 1989.

_____. Itaipu, hoje, uma realidade. *Mundo Elétrico*, 18 (217), : 20-25, out. 1977.

_____. A maior usina do mundo. *Mundo Elétrico*, 20 (248), : 114-117, set. 1979.

_____. Itaipu. Inaugurada a maior hidrelétrica do mundo, *Mundo Elétrico*, 24 (278), : 36-39, nov. 1982.

_____. Itaipu já está gerando energia. *Mundo Elétrico*, 26 (300), : 126-7, set. 1984.

_____. Itaipu desperta. *Dirigente Construtor*, Rio de Janeiro, 20 (11), nov. 1984. 1 p.

ENGETEC. Usina hidrelétrica de Itaipu. *Engenharia Civil*, Rio de Janeiro, 6 (56) : 4-12, 1980.

FERRAZ, O.M. Aproveitamento do potencial do Salto de Sete Quedas (Rio Paraná). In: CONFERÊNCIA SOBRE POTENCIAL HIDRELÉTRICO DE SETE QUEDAS, São Paulo, 1963, 27 p.

FERRAZ, O.M. ESCRITÓRIO TÉCNICO OMF LTDA. Relatório preliminar sobre o aproveitamento do Salto de Sete Quedas. *Ministério das Minas e Energia*, dez. 1962, 22 p.

GABLE, H. Itaipu Wasser Kraftwerk der Superlative (Itaipu - The gigantic hydropower station). *Elektrotech, ZETZ*, 103 (10), : 522-8, may 1982.

GRAMOW, A. Itaipu - um desafio a caminho da consolidação. *Deutsche - Brasilianische Hefte/ Cadernos Germano-Brasileiros*, 2, : 94-101, 1983.

GROSZ, H. Itaipu como catalisador no desenvolvimento industrial. *Energia Elétrica*, 6 (65) : 20-22, set. 1983.

GRUPO BORDIN. Itaipu Binacional. Complexo industrial, equipamentos e turbinas. *Informativo do Grupo BORDIN*, : 16-18, s.d.

HECKER, M. Itaipu Binacional. *Mercedes Benz*, s.l., (179) : 5-13, 1982.

INSTITUTO DE ENGENHARIA. Usina hidrelétrica de Itaipu. *Engenharia São Paulo*, (423) : 10-4, 1980.

ITAIPU BINACIONAL. La hidroeléctrica de Itaipu. Prospecto. (11), 1976, 4 p.

_____. Itaipu hydroelectric powerplant 12.600 MW. Paraná River. Brazil-Paraguay. 1977, 18 p.

_____. Mapa. Projeto. 1979, 4 p.

_____. Summary of Itaipu project (portuguese/spanish/english), dec. 1980, 41 p.

_____. Projeto Itaipu, out. 1982, 47 p.

_____. Aspectos técnicos do empreendimento Itaipu, Rio de Janeiro, 1989, 111 p.

_____. A Usina hidrelétrica de Itaipu (portuguese/spanish/english), Rio de Janeiro, set. 1990, 54 p.

_____. Itaipu hydroelectric development. The project of the century,. *Itaipu Binacional*, Asuncion, may 1991. 87 p.

_____. Relatório Anual. 1974, 1975. n.p.

_____. Relatório Anual. 1975, 1976. n.p.

_____. Relatório Anual. 1976, 1977. 56 p.

_____. Relatório Anual. 1977, 1978. n.p.

_____. Relatório Anual. 1978, 1979. 95 p.

_____. Relatório Anual. 1979, 1980. 100 p.

_____. Relatório Anual. 1980, 1981. 105 p.

- _____. Relatório Anual. 1981, 1982. 130 p.
- _____. Relatório Anual. 1982, 1983. 135 p.
- _____. Relatório Anual. 1983, 1984. 53 p.
- _____. Relatório Anual. 1984, 1985. 75 p.
- _____. Relatório Anual. 1985, 1986. 80 p.
- _____. Relatório Anual. 1986, 1987. 78 p.
- _____. Relatório Anual. 1988, 1989. 70 p.
- _____. Relatório Anual. 1989, 1990. 72 p.

KRAUCH, H. W.; FACETTI, C. A.; TARDIVO, F. J.; POPOW, M. An example of an integrated binational development with an energy project as base. In: XII CONGRESS OF THE WORLD ENERGY CONFERENCE, New Delhi, sept. 1983. Paper.

LEÃO, M. L. O aproveitamento dos Saltos das Sete Quedas. *Revista Brasileira de Energia Elétrica*, Rio de Janeiro, (4) : 28-31, jan./fev., 1964.

McGRAW-Hill INC. Taming South America's Parana for 12.600 MW. *Engineering News-Record*, New York, 202 (16) : 24-31, apr. 1979.

_____. Itaipu dam readied for filling. *Engineering News-Record*, New York, 209 (7) : 29-31, aug. 1982.

_____. Construction begins on huge hydro plant. *Electrical World*, New York, 179 : 46-49, July 1, 1977.

MERMEL, T. W. Major dams of the world. *International Water Power & Dam Construction*, Sutton, 30(8):43-53, aug. 1978.

MM ED. LTDA. A balança das decisões. *Elettricidade Moderna*, São Paulo, 1 (8) : 36-8, jun. 1973.

_____. Destino: Itaipu. *Elettricidade Moderna*, São Paulo, 1 (8) : 46-49, jun. 1973.

MORRISON KNUDSEN CORP. Itaipu: biggest hydropower project under way with "IECO" in coordinator role. *The McKay Magazine*, Idaho, 36(5): 10-3, June 1977.

NOVO GRUPO EDITORA TÉCNICA LTDA. O tratado de Itaipu. In: ANUÁRIO BRASILEIRO DE HIDRELÉTRICAS, s.l., : 38-52, 1974.

_____. Itaipu. A obra, o homem. *Construção Pesada*, São Paulo, 9(98) : 3-106, mar. 1979.

_____. O que pensam as companhias seguradoras a respeito dos riscos de engenharia. Como foram feitos

os seguros de Itaipu e Tucuruí. *Construção Pesada*, São Paulo, 12(140) : 114-28, set. 1982.

_____. Itaipu, o desafio. *Energia Elétrica*, São Paulo, 2 (18) : 16-50, set. 1979.

_____. Entrevista com o Gen. Costa Cavalcanti. *Construção Pesada*, São Paulo, 12(135) : 20-2, abr. 1982.

_____. O tratado de Itaipu. *Energia Elétrica*, São Paulo, 50(24) : 46-57, 1973.

_____. Os principais dados sobre a maior hidrelétrica: Itaipu. *Construção Pesada*, São Paulo, 6(61) : 68-73, fev. 1976.

SM2 EMPRESA JORNALÍSTICA LTDA. Itaipu: um monumento da engenharia nacional. *Engenharia Civil*, São Paulo, (3), jun. 1983, 29 p.

SOUZA, S. Guaíra: 25 milhões. In: CONGREGAÇÃO DOS PRESIDENTES DE ÓRGÃOS DE CLASSES DE ENGENHEIROS E ARQUITETOS DO PARANÁ, CR-1961, 15 p.

THOMAS TELFORD LTD. All eyes on Itaipu. *World Water*, Liverpool, 5 (10) : 44-5, oct. 1982.

_____. Power on the Paraná boosts Brazil's potential. *World Water*, Liverpool, 6 (10), oct. 1983.

WAPLER, H. Itaipu Binacional the superdam. *Indiaqua*, s.l., (26) : 73-5, mar. 1980.

ZADJ, L. Sete Quedas-Eletróbás estuda seu aproveitamento energético. Separata da Revista Brasileira de Energia Elétrica, (2), set./out. 1963, 19 p.

ZUPPKE, B. Die Wasserkraftanlage Itaipu in Brasilien. *Wasser Und Boden* (2) : 52-59, 1983.

CIVIL

ABRAHÃO, R.A. Seepage analysis for Itaipu dam through electrical analogy. In: SYMPOSIUM ON ROCK MECHANICS RELATED TO DAM FOUNDATION, Rio de Janeiro, sept. 1978, p. 129-43.

AMORIM, R. Aproveitamento hidrelétrico de Itaipu. Limpeza de fundação submersa das enseadeiras principais. In: XIII CBGB. SEMINÁRIO NACIONAL DE GRANDES BARRAGENS, Rio de Janeiro, 1980. Anais... Rio de Janeiro, abr. 1980, v.1. t. 3., p. 545-70.

- ANDRIOLO, F.R. Controle de qualidade do concreto em construções de barragens. In: CBGB. XIII SEMINÁRIO NACIONAL DE GRANDES BARRAGENS, Rio de Janeiro, 1980. Anais ..., Rio de Janeiro, abr. 1980, v.2, p. 379-406.
- AYALA, A.C.C.; HAYASHIDA, T.; BETIOLI, I.; SQUEFF, L.F.A. Utilização de formas deslizantes na construção da obra de Itaipu. In: CBGB. XIII SEMINÁRIO NACIONAL DE GRANDES BARRAGENS, Rio de Janeiro, 1980. Anais..., Rio de Janeiro, abr. 1980, v.1, t.2, p. 345-76.
- BARBI, A. L. & BARROS, F.P. de. Análise do comportamento das fundações das estruturas de concreto de Itaipu. In: CBGB. XV SEMINÁRIO NACIONAL DE GRANDES BARRAGENS, Rio de Janeiro, 1983. Anais ... , Rio de Janeiro, nov.20-23, 1983, v.1. t. 3 p. 287-310,
- BARBI, A. L. & PORTO, E. C. Aproveitamento hidrelétrico de Itaipu. Instrumentação das ensecadeiras principais. In: CBGB. XVII SEMINÁRIO NACIONAL DE GRANDES BARRAGENS, Rio de Janeiro, 1980. Anais... Rio de Janeiro, abr. 1980, v. 1. t. 3, p. 597-619,
- BARBI, A. L.; GOMBOSSY, Z. M.; SIQUEIRA, G. H. Controle de qualidade de calda de cimento para injeção. Utilização de traço variável. In: CBGB. XIV SEMINÁRIO NACIONAL DE GRANDES BARRAGENS, Recife, 1981. Anais... Recife, ago./set. 1981. v. 1. t. 2. p. 207-23.
- _____. Injeções de cimento na fundação da barragem principal de Itaipu. In: CBGB. XIV SEMINÁRIO NACIONAL DE GRANDES BARRAGENS, Recife, 1981. Anais ... Recife, ago/set. 1981, v. 1. t. 2, p. 225-45.
- BARROS, F. P. DE; MULLER, M.; MEYER, L. F.; SHAYANI, S. Monitoring system for seismic activity before and after filling binational Itaipu reservoir. In: CIBG. XIII CONGRESS ON LARGE DAMS, New Delhi, oct. 1979. v.II Transactions ... Paris, oct./nov., 1979. R5, p. 855-70.
- BARROS, F. P. DE & GUIDICINI, G. Um processo natural de alívio de tensões e o projeto de drenagem das fundações da barragem de Itaipu. In: CBGB. XIV SEMINÁRIO NACIONAL DE GRANDES BARRAGENS, Recife, 1981. Anais... Recife, ago./set. 1981. v. 1. t. 2. p. 519-39.
- BARROS, F. P. DE; PANKOW, R. H.; BARBI, A. L. General behaviour of Itaipu dam foundations. In: XV CONGRESS ON LARGE DAMS, Lausanne, june, 1985. Transactions ... Paris, 1985, R.61. p. 1153-68.
- BARROS, F. P. DE; CARVALHO, J. C.; MARTINEZ, L.; MARTINELLI, D. A.O.; FERREIRA, J. C. Itaipu project. Geomechanical model safety assessment. In: CIBG. XIV CONGRESS ON LARGE DAMS, Rio de Janeiro, may, 1982. Transactions ... Paris, 1982. R72. p. 1219-44.
- BARROS, F. P. DE; SILVEIRA, J. F. A.; ABRAHÃO, R. A. Fundações da barragem principal de Itaipu, projeto e desempenho durante a construção e enchimento parcial. *Construção Pesada*, São Paulo, 12 (140) : 64-86, set. 1982.
- BARROS, F. P. DE; ABRAHÃO, R. A.; SILVEIRA, J. F. A. Itaipu main dam foundations. Design and performance during construction and preliminary filling of reservoir. In: V INTERNATIONAL CONGRESS ON ROCK MECHANICS, Melbourne, apr. 1983, p. 191-7.
- BARROS, F. P. DE; COLMAN, J. L.; GALLICO, A.; MARTINELLI, D.A.O.; FERREIRA, J. C. Itaipu project: the structural safety assessment through physical models. In: CIBG. XIV CONGRESS ON LARGE DAMS, Rio de Janeiro, may, 1982. Transactions ... Paris, 1982. R7. p. 117-42.
- BETIOLI, I.; SCANDIUZZI, L., ANDRIOLO, F. R. Concreto adensado com rolo vibratório. In: CBGB. XIII SEMINÁRIO NACIONAL DE GRANDES BARRAGENS. Rio de Janeiro. Anais ... Rio de Janeiro, abr. 1980. v. 1. t. 2. p. 377-412.
- BETIOLI, I.; SCANDIUZZI, L.; SONODA, A. Método de concretagem das chavetas da fundação da barragem principal de Itaipu. In: CGBG. XIV SEMINÁRIO NACIONAL DE GRANDES BARRAGENS. Recife, 1981. Anais ... Recife, ago./set. 1981. v. 2. t. 2. p. 87-109.
- BRAGA, J.A. & SCANDIUZZI, L. Produção industrial de peças pré-moldadas curadas a vapor. In: CGBG. XIII SEMINÁRIO NACIONAL DE GRANDES BARRAGENS, Rio de Janeiro, 1980. Anais ... Rio de Janeiro, abr. 1980, v. 2. p. 407-35.
- BRAGA, J. A. & SONODA, A. Auxílio do foto-cordinômetro digital no controle das estruturas de concreto de Itaipu. In: CBGB. XV SEMINÁRIO NACIONAL DE GRANDES BARRAGENS. Rio de Janeiro, 1983. Anais ... Rio de Janeiro, nov. 1983. v. 1. t. 3. p. 493-511.
- CARIC, D. M.; EIGENHEER, L. P.; URIARTE, J.; SZPILMAN, A. The Itaipu hollow gravity dam. *International Water Power & Dam Construction*, Sutton, 34, (5) : 30-44, may 1982.

CARIC, D. M.; NIMIR, W. A.; EIGENHEER, L. P.; CARDOZO, F.S. Comparison of the recorded behaviour of the Itaipu hollow-gravity dam with values obtained by mathematical and physical models. In: CIGB. XV CONGRESS ON LARGE DAMS, Lausanne, June, 1985. Transactions ... Paris, 1985. R11. p. 249-68.

CASANOVA, E. Concrete cooling on dam construction for world's largest hydroelectric power station. *Sulzer Technical Review*, 61 (1) : 3-19, 1979.

CESP. Abrem-se as comportas de Itaipu. *Cespaquista*, São Paulo, (39) : 19-21, 1983.

CHANTIERS MAGAZINE. La construction du complexe hydro-électrique d'Itaipu (Brésil). *Chantiers Magazine*, s.l., (94) : 57-62, août./sept., 1978.

CIER. Enchimento do reservatório de Itaipu. *Boletim do CIER*, Montevideo, (150), feb./mar., 1983. 11 p.

CORENA EDITORA ESPECIALIZADA DE CONSTRUÇÃO E RECURSOS NATURAIS LTDA. Forma de grande área acelera concretagem em Itaipu. *Construção Hoje*, São Paulo, 5, (8) : 16-18, ago. 1979.

_____. Itaipu sobe o rio, morre o salto, nasce o lago: a maior UH do mundo esta pronta. *Construção Hoje*, 8 (11) , : 15-25, 1982.

COTRIM, J.R.; KRAUCH, H. W.; SZPILMAN, A.; MEDAGLIA, L. Instrumentation for evaluating the performance of Itaipu structures and foundations. In: CIGB. XIV CONGRESS ON LARGE DAMS, Rio de Janeiro, May 1982. Transactions ... Paris, 1982. R71. p. 1195-217.

COTRIM, J.R.; MEDAGLIA, L.; SARKARIA, G.S. Design and construction techniques for Itaipu. In: CIGB. XIII CONGRESS ON LARGE DAMS, New Delhi, oct./nov., 1979. Transactions ... Paris, 1979. C6. p. 101-25.

DI VICENZO, E. & SILVEIRA, J. F. A. Análise comparativa entre subpressões medidas e calculadas para as fundações das barragens de Água Vermelha e Itaipu. In: CBGB. XVII SEMINÁRIO NACIONAL DE GRANDES BARRAGENS, Brasília, 1987. Anais ... Brasília, ago. 1987. v.1. t.1, p. 177-90.

DUARTE, J.D.C.; MARTINS, M.J.; BETIOLI, I. Orientações para concretagens com a utilização de equipamentos não convencionais. In: CBGB. XIII SEMINÁRIO NACIONAL DE GRANDES BARRAGENS, Rio de Janeiro, 1980. Anais ... Rio de Janeiro, 1980. v.1. t.2. p. 315-43.

EDITORA VISÃO LTDA. Itaipu: cinco anos de obras. *Dirigente Construtor*, Rio de Janeiro, 15 (8) : 5-25, set. 1979.

EMEP EDITORIAL LTDA. Itaipu: Projeto de engenharia define opções. *O Empreiteiro*, 8 (98), : 3-227, nov. 1977.

_____. Equipamentos inéditos e técnicas avançadas lançamento concreto em Itaipu. *O Empreiteiro*, São Paulo, 10 (131), : 30-40, dez. 1978.

DONADON, J.M. A compressão dos prazos de construção da casa de força do canal de desvio de Itaipu. *RBE*. 3 (1), p. 15-34, 1988, UNICON.

_____. A concepção do Projeto de Itaipu e seus principais aspectos construtivos. In: CBGB. XVIII SEMINÁRIO NACIONAL DE GRANDES BARRAGENS. Foz do Iguaçu, 1989. Anais ... Foz do Iguaçu, abr. 1989, t.4. p. 1243-69.

_____. Estratégias de Planejamento adotadas na construção de Itaipu. In: CBGB. XIX SEMINÁRIO NACIONAL DE GRANDES BARRAGENS, p. 417-21. s.d.

FERRAZ, H. Itaipu, 14 anos depois ouro em pó. *Construção São Paulo*, (2170), : 13-15, set. 1989.

FERREIRA, C.; BARRETO, L. A. L.; AMARO DA SILVA, L. F. C.; DANTAS, H. M. G.; DIB, K. R. Estudos hidráulicos e energéticos para o enchimento do reservatório de Itaipu. In: VII SEMINÁRIO NACIONAL DE PRODUÇÃO E TRANSMISSÃO DE ENERGIA ELÉTRICA, Brasília, dez., 1984. Trabalhos ... BSB/GOP/08.

FUKUROZAKI, Y.; BETIOLI, I.; SILVA, R. R. da; SONODA, A. Utilização de formas deslizantes na execução da casa de força da hidrelétrica de Itaipu. In: CBGB. XIV SEMINÁRIO NACIONAL DE GRANDES BARRAGENS, Recife, 1981. Anais ... Recife, ago./set., 1981. v. 2. T. 3. p. 241-64.

HOLTZ, A.C.T. The future of hydropower in Brazil. *Water Power and Dam Construction*, : 16-19, jan. 1985.

INSTITUTION OF CIVIL ENGINEERS. Dams. Clears the way for Itaipu. *New Civil Engineer International*, (5) : 34-6, feb. 1979.

ISMES. Itaipu. The largest dam in the world. *ISMES News*, Bergamo, mar. 1979. 2 p.

ITAIPU BINACIONAL. Construção da Casa de Força no Canal de Desvio - 1986/1990. *Itaipu Binacional*, 1989, 183 p.

_____. The Itaipu hydroelectric project. 12.600 MW. Design and construction features. *Itaipu Binacional*, dec. 1981. 47 p.

KOHNE, R.E. Itaipu project. Stretching construction and equipment limits. In: ENGINEERING FOUNDATION CONFERENCE, Pacific Grove, apr./may, 1978. 12 p.

KRAUCH, H. W. & SARKARIA, G. S. Interface scheduling construction planning and progress at Itaipu project. In: CIGB. XIII CONGRESS ON LARGE DAMS, oct./nov., 1979. Transactions ... Paris, 1979. R42. Discussion of Q48. 13 p.

LEWIS, A. A world-beating power project that distracts even honeymooners. *Construction News*, : 20-25, sept. 1980.

_____. Itaipu progress a tribute to plant transport control. *Construction News*, : 17-22, sept. 1980.

LYRA, F. H. Planning and construction sequence at Itaipu. *International Water Power & Dam Construction*, Sutton, 34 (5) : 27-30, may 1982.

MARTINEZ, L. A.; BARROS, F. P. de; OLIVEIRA, H. B. de. Vertedero de Itaipu: protección del talud de aguas abajo del Salto Esqui. In: I SEMINÁRIO INTERAMERICANO DE MECÂNICA DE ROCAS, Bogotá, nov. 1982, 6 p.

MILLER FREEMAN PUB. Itaipu enters main construction phase. *Energy International*, San Francisco, 16 (7) : 31-34, july 1979.

MONTEIRO, J.R. & PEYFUSS, K.F. Demolishing Itaipu's arch cofferdams. *International Water Power & Dam Construction*, Sutton, 31 (11) : 91-4, nov. 1979.

MORAES, J. de; VILLALBA, J.R.; MELLO, W.F. de; POTY, L.C.; BERNY, O.; ACOSTA, A.G.; SARKARIA, G.S. Selection of basic design of Itaipu spillway. In: CIGB. XIII CONGRESS ON LARGE DAMS, New Delhi, oct./nov. 1979. Transactions ... Paris, 1979. R14. p.249-72.

MORAES, J. de; VILLALBA, J. R.; BARBI, A. L.; PIASENTIN, C. Subsurface treatment of seams and fractures in foundation of Itaipu dam. In: CIGB. XIV CONGRESS ON LARGE DAMS, Rio de Janeiro, may, 1982. Transactions ... Paris, 1982. R10. p. 179-98.

MORAES, J. de; VILLALBA, J. R.; SARKARIA, G. S. Itaipu project implementation of design concepts in construction. *Construction News Magazine*, s.l., (Part 1) : 18-23, mar. 1982, (Part 2) : 24-7, apr. 1982.

McGRAW-HILL INC. Paraná diversion drama starts at Itaipu. *Engineering News-Record*, New York, 201 (18) : 15-6, nov. 1978.

NOVO GRUPO ED. TÉCN. LTDA. Itaipu: planejamento geral da obra. Instalação do canteiro de obra. Progresso e acompanhamento dos serviços. *Construção Pesada*, São Paulo, 7 (82) : 3-227, nov. 1977.

_____. Itaipu. Resultados do pré-enchimento asseguram confiabilidade na etapa do enchimento do reservatório. *Construção Pesada*, São Paulo, 12 (140) : 31-8, set. 1982.

_____. Itaipu. No término das obras de concreto Itaipu desmobiliza equipamentos. *Construção Pesada*, São Paulo, 12 (140) : 40-46, set. 1982.

_____. Itaipu. A obra atinge pico de concretagem de 15.000 m³ diários. *Construção Pesada*, São Paulo, 9 (110) : 56-64, mar. 1980.

_____. Planejamento da operação hidráulica do enchimento do reservatório de Itaipu. *Construção Pesada*, São Paulo, 12 (142) : 129-35, nov. 1982.

_____. Itaipu se equipa para concretar no prazo a estrutura do desvio. *Construção Pesada*, São Paulo, 6 (66) : 8-22, jul. 1976.

_____. Projeto Itaipu. Geral. *Construção Pesada*, São Paulo, 10 (122) : 4-170, mar. 1981.

PATERNIO, N. T.; PIMENTA, M. A.; SCANDIUZZI L. Itaipu. Limitações de temperatura para estruturas metálicas de caixas espirais. In: CBGB. SEMINÁRIO NACIONAL DE GRANDES BARRAGENS, 15, Rio de Janeiro, nov., 1983. Rio de Janeiro, 1983. Anais ... Rio de Janeiro, 1983. v. 1. t. 3. p. 229-48.

_____. Estudo térmico do contraforte de jusante da casa de força de Itaipu. In: CBGB. XV SEMINÁRIO NACIONAL DE GRANDES BARRAGENS, Rio de Janeiro, nov. 1983. Rio de Janeiro, 1983. Anais ... Rio de Janeiro, 1983. v. 1. t. 3. p. 211-27.

PROMON ENGENHARIA S.A. Itaipu, a realização de um sonho. *Promon Engenharia S.A.* maio, 1982. 9 p.

_____. Itaipu. Agora, é esperar que se esgote a enxada. *O Empreiteiro*, São Paulo, 10 (131) : 41-6, dez. 1978.

SAMPAIO, A. J. M. Síntese da evolução das principais técnicas empregadas no tratamento das fundações de vertedouros em barragens do tipo gravidade. In: SIMPÓSIO SOBRE GEOTECNIA DA BACIA DO ALTO PARANÁ, São Paulo, set. 1983, p. 289-313.

- SANIER, E. & NEIDERT, S. H. Aprovechamiento Hidroeléctrico de Itaipu. Acciones erosivas aguas abajo del vertedero. In: IAHR. X CONGRESO LATINOAMERICANO DE HIDRÁULICA, Belo Horizonte, 1987, p. 430-40.
- SANTOS, O. G. dos; BARBI, A. L.; SOERENSEN, A. J. A.; SONODA, A. Quality control and instrumentation of clay core placed in deep water for Itaipu cofferdams. In: CIGB. XIV CONGRESS ON LARGE DAMS, Rio de Janeiro, may 03-07, 1982. Transactions ... Paris, 1982. R50. p. 841-71.
- SANTOS, O. G. dos & AMORIM, R. Aproveitamento hidrelétrico de Itaipu. Execução dos diques de enrocamento, transições e argila submersa das ensecadeiras principais. In: CBGB. XIII SEMINÁRIO NACIONAL DE GRANDES BARRAGENS, Rio de Janeiro, 1980. Anais ... Rio de Janeiro, abr. 1980, v. 1. t. 3. p. 571-45.
- SANTOS, O.G. dos & QUEIRÓZ, R.R.F. Aproveitamento hidrelétrico de Itaipu. Controle de qualidade do núcleo submerso das ensecadeiras principais. In: CBGB. XIII SEMINÁRIO NACIONAL DE GRANDES BARRAGENS, Rio de Janeiro, 1980. Anais ... Rio de Janeiro, abr. 1980. v. 1. t. 3. p. 571-96.
- SARKARIA, G.S. Critical design decisions for Itaipu power project. In: WESTERN CONFERENCE ON WATER AND ENERGY, Ft. Collins, june 1982. 6 p.
- SCHULMAN R.L; KRAUCH, H.W.; ZALESKI J.M.; SZPILMAN, A.; EMERSON, W.M.; PIASENTIN, C. Itaipu Project Spillway, behavior during the maximum recorded flood. In: COMMISSION INTERNATIONALE DES GRANDS BARRAGES, Q.63, R.74, San Francisco, 1988, p. 1239-60.
- SEIFART, S.L.A.; SZPILMAN, A.; PIASENTIN, C. Itaipu structures. Evaluation of their performance. In: CBGB. XV CONGRESS ON LARGE DAMS, Lausanne, june 04-25, 1985. Transactions ... Paris, 1985. R15. p. 287-317.
- SILVA, R.F. da & SCANDIUZZI, L. Concreto com fibras de aço para combate aos efeitos de alta velocidade d'água. In: CBGB. XIII SEMINÁRIO NACIONAL DE GRANDES BARRAGENS, Rio de Janeiro, 1980. Anais ... Rio de Janeiro, abr. 1980. v.1. t. 1. p. 153-82.
- SIQUEIRA, G. H.; BARBI, A. L.; GOMBOSSY, Z. M. Injeções profundas nas fundações da usina de Itaipu. Equipamentos e produção. In: CBGB. XIV SEMINÁRIO NACIONAL DE GRANDES BARRAGENS, Recife, ago. 1981, v. 1. t. 2., p. 187-205.
- SODETEC. Une concentration exceptionnelle d'équipements de forage, d'abattage et de sautage pour le creusement (22.000.000 m³) du canal de derivation de la centrale d'Itaipu. *Équipement Mécanique, Carriers et Matériaux*, Paris: 27-31, s.d.
- SONODA, A. & BETIOLI, I. Métodos e processos de concretagem utilizados na construção da Hidrelétrica de Itaipu. *Revista Engenharia Mackenzie*, São Paulo : 6-69, abr./jun., 1983.
- SOUZA LIMA, V. M. & ABRAHÃO, R. A. Two practical examples of numerical approaches for solving discontinuity problems in dam design. In: SYMPOSIUM ON IMPLEMENTATION OF COMPUTER & STRESS, Chicago, aug. 03-06, 1981. 17 p.
- SOUZA LIMA, V. M.; ABRAHÃO, R. A.; PINHEIRO, R.; DEGASPARE, J. C. Rock foundations with marked discontinuities criteria and assumptions for stability analysis. In: CIGB. XIV CONGRESS ON LARGE DAMS, Rio de Janeiro, may 27-30, 1982. Transactions ... Paris, 1982. R69. p. 1155-82.
- SOUZA LIMA, V. M.; SILVEIRA, J. F. A.; DEGASPARE, J. C. Nota sobre os deslocamentos horizontais na barragem principal de Itaipu. In: CBGB. XV SEMINÁRIO NACIONAL DE GRANDES BARRAGENS, Rio de Janeiro, nov. 20-23, 1983. Rio de Janeiro, 1983. Anais ... Rio de Janeiro, 1983. v. 1. t. 3. p. 155-67.
- _____ Horizontal and vertical displacements of the Itaipu main dam. A study on field measurements and theoretical predictions. In: CIGB. XV CONGRESS ON LARGE DAMS, Lausanne, june 04-25, 1985. Transactions ... Paris, 1985. R10. p. 229-46.
- SZPILMAN, A.; AZEVEDO JUNIOR, N. L.; TAGLIATELLA, E. P.; HAHNER, I. Itaipu. Análise estrutural do concreto envolvente da caixa espiral. *Construção Pesada*, São Paulo, 12(140): 88-113, set. 1982.
- SZPILMAN, A.; MEDAGLIA, L.; MORI, R. T.; MEYER, L. F. Barrag. de terra e de enroc. de Itaipu. Transições entre seções homogêneas de terra e seções de enrocamento com núcleo e correspondentes abraços com estruturas de concreto. In: CBGB. XIV SEMINÁRIO NACIONAL DE GRANDES BARRAGENS. Recife, 1981. Anais... Recife, ago./set. 30-2, 1981, v. 1. t. 1. p. 71-103.
- SZPILMAN, A.; MEDAGLIA, L.; NEIDERT, S. H. Vertedouro de Itaipu. Dissipação de energia e outros aspectos. In: CBGB. XIII SEMINÁRIO NACIONAL DE GRANDES BARRAGENS. Rio de Janeiro, 1980. Anais ..., Rio de Janeiro, abr. 1980, v. 1. t. 1. p. 183-206.

SZPILMAN, A.; ROSSO, J. A.; PIASENTIN, C.; FIORINI, A. S. Estabelecimento dos níveis das cristas das ensecadeiras do projeto Itaipu. Critérios de segurança hidrológicos adotados. In: CBGB. XVI SEMINÁRIO NACIONAL DE GRANDES BARRAGENS. Belo Horizonte, 1985. Anais ... Belo Horizonte, nov. 24-27, 1985, v. 1. t. 3. p. 667-96.

_____. Barragem de Itaipu. Subpressão no contato concreto-rocha. In: CBGB. XVII SEMINÁRIO NACIONAL DE GRANDES BARRAGENS, Brasília, 1987. Anais ... Brasília, ago. 03-5, 1987, v. 1. t. 1. p. 93-116.

_____. A.S. Vertedouro de Itaipu e região a jusante do trampolim - comportamento hidráulico e estrutural após 8 anos de operação. In: XIX SEMINÁRIO NACIONAL DE GRANDES BARRAGENS, s.d. p. 239-254.

SZPILMAN, A.; ROSSO, J. A.; PIASENTIN, C. Auscultação e inspeção durante o enchimento parcial e total do reservatório de Itaipu. In: CBGB. XV SEMINÁRIO NACIONAL DE GRANDES BARRAGENS. Rio de Janeiro, 1983. Anais ... Rio de Janeiro, nov. 20-23, 1983, v. 1. t. 3. p. 311-37.

SZPILMAN, A.; PIASENTIN, C. A concepção da barragem principal de Itaipu e seleção do tipo de barragem. In: XVIII SEMINÁRIO NACIONAL DE GRANDES BARRAGENS. Foz do Iguaçu, 1989. Anais ... Foz do Iguaçu, abr. 1989, t.4, p. 1205-27.

TARRICONE, N.L.; NEIDERT, S.; BEJARANO, C.; FONSECA, C.L. Hydraulic model studies for Itaipu spillway. In: CIGB. XIII CONGRESS ON LARGE DAMS, New Delhi, oct./nov., 29-2, 1979. Transactions ... Paris, 1979. R43. p. 749-66.

TENENGE. Itaipu: O desvio do Rio Paraná. *Jornal da Tenenge*, s.l., (25), out./nov., 1978. 1 p.

THOMAS TELFORD LTD. Itaipu contractors win diversion race. *World Water*, Liverpool, 2 (1) : 18-24, jan. 1979.

_____. Successful outcome to Itaipu dam. *World Water*, Liverpool, 5 (11), nov. 1982. p.9.

URIARTE, J. A.; CARIC, D. M.; NIMIR, W. A.; EIGENHEER, L. P.; NITTA, T. Itaipu main dam. Geological and geotechnical features affecting the design. In: CIGB. XIV CONGRESS ON LARGE DAMS, Rio de Janeiro, may 03-07, 1982. Transactions ... Paris, 1982. R12. p. 219-40.

VASCONCELOS, G.R.L. de; SCANDIUZZI, L. Avaliação de compressões instaladas em estruturas de concreto, através de tensômetros elétricos. In: CBGB. XIII

SEMINÁRIO NACIONAL DE GRANDES BARRAGENS, Rio de Janeiro, abr. 1980. Rio de Janeiro, 1980. Anais ... Rio de Janeiro, 1980. v. 2. p. 435-63.

VIANNA DE ANDRADE, R.; BOJANOVICH, F.L.; AMORIM, R. Construction and rockfill dikes transition zones and clay core placed in deep water for Itaipu cofferdams. In: CIGB. XIV CONGRESS ON LARGE DAMS, Rio de Janeiro, may 03-07, 1982. Transactions ... Paris, 1982. R4. p. 47-69.

VIANNA DE ANDRADE, R.; BOJANOVICH, F.L.; JUNQUEIRA NETO, J.A. Construction planning and interface scheduling for dams & others features of Itaipu project. In: CIGB. XIII CONGRESS ON LARGE DAMS, New Delhi, oct./nov., 29-2, 1979. Transactions ... Paris, 1979. R42. p. 749-78.

VIANNA DE ANDRADE, R.; SEIFART, L.; SZPILMAN, A.; MEDAGLIA, L. L'impianto idroelettrico di Itaipu sul Rio Paraná al confine tra Brasile e Paraguay. *Revista L'Industria Italiana del Cemento*, Roma, (11) : 668-91, nov. 1984.

VILLALBA, J. R.; SZPILMAN, A.; ROSSO, J. A.; SOERENSEN, A.; SILVEIRA, J.F.; PIASENTIN, C. Observação do comportamento dos drenos moldados no concreto dos blocos da barragem de Itaipu. In: CONFERÊNCIA IBERO-AMERICANA SOBRE APROVEITAMENTO HIDRÁULICO, Lisboa, 1987, n.p.

VILLALBA, J.R.; SEIFART S.L.A.; SZPILMAN, A.; ROSSO, J.A.; PIASENTIN, C.; FIORINI, A.S. Safety criteria adopted for construction of the Itaipu cofferdams. In: COMMISSION INTERNATIONALE DES GRANDS BARRAGES, San Francisco, 1988, p. 107-127.

WILKE, G. Cable cranes at Itaipu. *International Water Power & Dam Construction*, Sutton, 34 (2) : 13-27, feb. 1982.

ZALESKI J.M.; SEIFART L.A.; BRAGA J.A.; ROSARIO, L.C. Concreto adensado com rolo vibratório - dados sobre uso na Itaipu Binacional com aproximadamente 10 anos de idade. In: CBGB. XVIII SEMINÁRIO NACIONAL DE GRANDES BARRAGENS, Foz do Iguaçu, abr. 1989, t.1. p. 363-84.

ELECTRICAL

ABREU, M. A.; VILLALBA, J. R.; ANDRADE FILHO, G. D.; SALTARA, M.; REGGIANI, F. Limites de funcionamento dos geradores de Itaipu. In: IX

SEMINÁRIO NACIONAL DE PRODUÇÃO E TRANSMISSÃO DE ENERGIA ELÉTRICA, Belo Horizonte, out. 25-29, 1987. Trabalhos ... Belo Horizonte, 1987. BHZ/SGM/13. 7 p.

ANDRADE FILHO, G. D.; CURVELO, W. L. F.; SANTANA, J. L.; FERNANDES FILHO, A. M.; DEMIANUK, J.S.; LOPES, A.A.V.; ABREU, M.A. Comissionamento de Itaipu. Planejamento, execução e resultados globais. In: IX SEMINÁRIO NACIONAL DE PRODUÇÃO E TRANSMISSÃO DE ENERGIA ELÉTRICA, Belo Horizonte, out. 1987. Trabalhos ... Belo Horizonte, 1987. BHZ/GTA/05-8 p.

ANDREOLI, A. A Copel e Itaipu. *Revista Paranaense de Desenvolvimento* (37), : 7-35, abr. 1973.

ARAÚJO, K. S.; BRESSANE, J. M.; PINTO, L. J.; BRUZZI, R. L.; LOBLEY, D. J. Projeto eletromecânico dos barramentos 800 kV das subestações do sistema de Itaipu. In: IV SEMINÁRIO NACIONAL DE PRODUÇÃO E TRANSMISSÃO DE ENERGIA ELÉTRICA, Rio de Janeiro, set. 18-23, 1977. Trabalhos ... Rio de Janeiro, 1977. RJ/GSE/16. 25 p.

BARAN, I. S.; SANTIAGO, N. H. C.; BRASIL, D. O. C.; TAHAN, C. M. V.; VIAN, A. Escolha de cabos pára-raios para o sistema de transmissão de Itaipu. In: IV SEMINÁRIO NACIONAL DE PRODUÇÃO E TRANSMISSÃO DE ENERGIA ELÉTRICA, Rio de Janeiro, set. 18-23, 1977. Trabalhos ... Rio de Janeiro, 1977. RJ/GLT/21. 13 p.

BARAN, I. S.; TAAM, M. Z.; JUSTO, F. P. Efeitos da transmissão em CCAT sobre as proteções de linha CA. In: IX SEMINÁRIO NACIONAL DE PRODUÇÃO E TRANSMISSÃO DE ENERGIA ELÉTRICA, Belo Horizonte, out. 25-29, 1987. Trabalhos ... Belo Horizonte, 1987. BHZ/GPC/06. 6 p.

BARROSO, A.E.V.; OURIQUE, M. A. L.; SHAF, M.; FERNANDEZ, M.; CACERES, C. R. B.; BRASA, R. Sistemas de serviços auxiliares da central de Itaipu: projeto, equipamentos, comissionamento, operação e manutenção. In: IX SEMINÁRIO NACIONAL DE PRODUÇÃO E TRANSMISSÃO DE ENERGIA ELÉTRICA, Belo Horizonte, out. 25-29, 1987. Trabalhos ... Belo Horizonte, 1987. BHZ/GPH/14. 4 p.

BRASIL, D. O. C.; RESENDE, F.; JARDINI, J. A.; VIAN, A. Comportamento a descargas atmosféricas das linhas 800 kV de Itaipu. In: IV SEMINÁRIO NACIONAL DE PRODUÇÃO E TRANSMISSÃO DE ENERGIA ELÉTRICA, Rio de Janeiro, set. 18-23, 1977. Trabalhos ... Rio de Janeiro, 1977. RJ/GLT/35. 21 p.

BRASIL, D.O.C.; JARDINI, J. A.; VIAN, A. Investigações sobre os efeitos eletrostáticos nas linhas 800 kV de Itaipu. In: IV SEMINÁRIO NACIONAL DE PRODUÇÃO E TRANSMISSÃO DE ENERGIA ELÉTRICA, Rio de Janeiro, set. 18-23, 1977. Trabalhos ... Rio de Janeiro, 1977. RJ/GLT/37. 23 p.

BRITO JUNIOR, G.C.; ROMERO, A.V.M.; GONZALES, A.B.F., TEIXEIRA, P.H. Comparação dos métodos de medição de oscilação do eixo e de medição de vibração nos mancais, para fins de balanceamento, nos geradores de Itaipu. In: X SEMINÁRIO NACIONAL DE PRODUÇÃO E TRANSMISSÃO DE ENERGIA ELÉTRICA, Curitiba, 1989, Grupo V SGM-21. 5 p.

CAROLI, C. E.; SANTOS, N.; NAGOYA, J. T.; PEREIRA, J.C.C.; KOVARSKY, D.; MARQUES, M. A. M.; PINTO, L. J. Medição de potencial de toque em cercas e tubulações nas áreas de influência dos eletrodos do sistema CCAT de Itaipu. In: IX SEMINÁRIO NACIONAL DE PRODUÇÃO E TRANSMISSÃO DE ENERGIA ELÉTRICA, Belo Horizonte, out. 25-29, 1987. Trabalhos ... Belo Horizonte, 1987. BH/GSE/03. 6 p.

CAROLI, C.E.; SANTOS, N.; KOVARSKY, D.; FREIRE, P.E.F.; PINTO, L.J. Curvas de potencial dos eletrodos de aterramento do sistema CCAT de Itaipu: resultados das medições durante o comissionamento do Bipolo II. X SEMINÁRIO NACIONAL DE PRODUÇÃO E TRANSMISSÃO DE ENERGIA ELÉTRICA, Curitiba 1989, Grupo VIII, GSE-11. 9 p.

CAROLI, C.E.; SANTOS, N.; KOVARSKY, D.; MARQUES, M.A.; PINTO, L.J. Potenciais de toque medidos em tubulações metálicas durante o comissionamento do Bipolo II do sistema CCAT de Itaipu. *Grupo IV, GSP*, Curitiba 1989, GSP/37. 5 p.

CAROLI, C.; SANTOS, N. dos; PEREIRA, J. C. C.; KOVARSKY, D.; MARTINI, C.R.; PINTO, L. J. Medição dos potenciais na superfície do solo devido à operação monopolar do sistema CCAT de Itaipu. In: VIII SEMINÁRIO NACIONAL DE PRODUÇÃO E TRANSMISSÃO DE ENERGIA ELÉTRICA, São Paulo, maio 4-8, 1986. Trabalhos ... São Paulo, 1986. SP/GSP/35. 10 p.

CARUSO, J. M.; RINGLEE, R. J.; REPPEN, N. D. Critérios de confiabilidade nos estudos do sistema de transmissão de Itaipu. In: IV SEMINÁRIO NACIONAL DE PRODUÇÃO E TRANSMISSÃO DE ENERGIA ELÉTRICA, Rio de Janeiro, set. 18-23, 1977. Trabalhos ... Rio de Janeiro, 1977. RJ/GPO/33. 28 p.

CARVALHO, F. M. S.; VAISMAN, R.; FONSECA, C.S. Reavaliação dos níveis de isolamento a impulso atmosférico dos transformadores das subestações de 500 kV do tronco de Itaipu. In: IX SEMINÁRIO NACIONAL DE PRODUÇÃO E TRANSMISSÃO DE ENERGIA ELÉTRICA, Belo Horizonte, out. 25-29, 1987. Trabalhos ... Belo Horizonte, 1987. BHZ/GSP/08. 6 p.

CASTELO BRANCO, A.; TAAM FILHO, M.Z.; PRACA, A.; BARAN, I.; SHORE, N.L.; RAMOS, A.; FIGUEIREDO, A.; BITTENCOURT A.S. Testes de sistema durante o comissionamento do estágio inicial do sistema CCAT de Itaipu. In: VIII SEMINÁRIO NACIONAL DE PRODUÇÃO E TRANSMISSÃO DE ENERGIA ELÉTRICA, São Paulo, maio 4-8, 1986. Trabalhos ... São Paulo, 1986. SP/GSP/42. 11 p.

COHEN, A.; KEMPER, E.; CREMA, L.; SERTICH, A.; MEISEL, J. Critérios para especificação de interface homem-máquina para sistemas SCADA/EMS. In: CIGRE - III ENCONTRO REGIONAL LATINO AMERICANO, Foz do Iguaçu, abr./maio 1989, 6 p.

COHEN, A.; KEMPER, F.; CACERES, D.; CREMA, L.A.; SERTICH, A. Sistema de supervisão e controle digital e gestão de energia (SCADA/EMS) para a Central Hidrelétrica de Itaipu. In: VII CONGRESSO BRASILEIRO DE INFORMÁTICA ITA, São José dos Campos, 1988, p. 957-62.

COHEN, A.; KEMPER, F.; MARTINS, L.F.; SERTICH, A. Software de aplicación del sistema SCADA/EMS de Itaipu Estructura y organización. LATINICON 1988. In: CONFERÊNCIA LATINO AMERICANA IEEE, feb. 1988, 26 p.

COHEN, A.; KEMPER, F.; BACHMANN, E.; HANDEL, R.; COSTA FILHO, A.M. Sistema de monitoração e diagnóstico dos hidrogeradores da Usina de Itaipu. In: X SEMINÁRIO DE PRODUÇÃO E TRANSMISSÃO DE ENERGIA ELÉTRICA, Curitiba 1989, Subgrupo I/II-01, SGM, 22. 7 p.

COHEN, A.; KEMPER, F.; CACERES, D.; ROSA E SILVA, F. Sistema de supervisão/control digital (SCADA/EMS) para la Central Hidroeléctrica de Itaipu. LATINICON 1988. In: CONFERÊNCIA LATINO AMERICANA IEEE, feb. 1988, 13 p.

COSTA FILHO, A. M.; SIMAO, J.; FLEMING, A. M.; GROSZ, H. Medição de resistência de isolamento em hidrogeradores resfriados por água pura. In: IX SEMINÁRIO NACIONAL DE PRODUÇÃO E TRANSMISSÃO DE ENERGIA ELÉTRICA, Belo Horizonte, out. 25-29, 1987. Trabalhos ... Belo Horizonte, 1987. BHZ/SGM/02. 6 p.

CRUSIUS, R. L.; ASSUNÇÃO, L.A. R.; NIGRI, A. I. Desempenho dos isoladores da linha de transmissão de corrente contínua ± 600 kV (Foz do Iguaçu - São Roque). In: IX SEMINÁRIO NACIONAL DE PRODUÇÃO E TRANSMISSÃO DE ENERGIA ELÉTRICA, Belo Horizonte, out. 25-29, 1987. Trabalhos ... Belo Horizonte, 1987. BHZ/GLT/03. 4 p.

DERZHKO, M.Z., KAMINSKII, P.V., KOZHAN, S.M. Features of the electrical portion of contemporary foreign bright power hydroelectric power generating installations. IZV. VUZ ENERG. (USSR) (4), Apr. 1983. p. 117-20.

DIAS, P.P.T.R.; VALVERDE, A.R.; LOURENCO A.A.; BROCHADO, A.C.; FERRAZ, A.V., SOUZA, H.S. Modelagem do sistema de regulação de tensão das máquinas 60 Hz de Itaipu no programa EMTP utilizando a rotina Tacs-Transient Analysis of Control Systems. In: X SEMINÁRIO NACIONAL DE PRODUÇÃO E TRANSMISSÃO DE ENERGIA ELÉTRICA, Curitiba 1989, Grupo X, GOP-21, 8 p.

EDITORA TÉCNICA GRUENWALD LTDA. Itaipu já é a maior hidrelétrica do mundo. *Mundo Elétrico*, 30(360), : 89-93, out. 1989.

ERIKSON, K.; MENZIES, D.; TAAM FILHO, M.Z.; FRAGA, R.M.; FRONTIN, S.O.; PORONGABA, H. D.; TOLEDO, P.F. de; XIMENES, M. J. Desempenho dinâmico do sistema de transmissão CCAT de Itaipu. In: VIII SEMINÁRIO NACIONAL DE PRODUÇÃO E TRANSMISSÃO DE ENERGIA ELÉTRICA, São Paulo, maio 4-8, 1986. Trabalhos ... São Paulo, 1986. SP/GSP/36. 7 p.

ESMERALDO, P. C. V.; DIAS, L. E. N.; FONSECA, J. R. Calculation of minimum safety distances for live-line maintenance. A statistical method applied to 765 kV AC Itaipu lines. *IEEE Transactions on Power Apparatus and Systems*, 1 (2) : 264-71, apr. 1986.

ESMERALDO, P. C. V.; FONSECA, C. S.; RAJA GABAGLIA, C. P.; PEREIRA, M.P.; DIAS, L. E. N. Uma proposta alternativa para as linhas de transmissão de Itaipu em 765 kV CA: a torre de trapézio. In: VIII SEMINÁRIO NACIONAL DE PRODUÇÃO E TRANSMISSÃO DE ENERGIA ELÉTRICA, São Paulo, maio 4-8, 1986. Trabalhos ... São Paulo, 1986. SP/GLT/15. 20 p.

ESPINOZA, H.; ELLIOT, R. A.; SOBRAL, S. T.; MUKHEDKAR, D.; FLEURY, V. G. P.; VILLALBA, J. R.; PEREIRA, F. A. Utilização de contrapesos contínuos nas imediações de subestações devido a problemas de ampacidade dos cabos pára-raios. In: IX SEMINÁRIO NACIONAL DE PRODUÇÃO E TRANSMISSÃO DE ENERGIA ELÉTRICA, Belo Horizonte, out. 25-9, 1987. Trabalhos ... Belo Horizonte, 1987. BHZ/GLT/12. 9 p.

- FADINI, H. A. M.; MELLO, F.P.; MOUNTFORD, J. D. Estudo de fluxo de potência e estabilidade para a comparação das altern. do sist. de transmissão de Itaipu. Compensação-série versus suporte de tensão. In: IV SEMINÁRIO NACIONAL DE PRODUÇÃO E TRANSMISSÃO DE ENERGIA ELÉTRICA, Rio de Janeiro, set. 18-23, 1977. Trabalhos ... Rio de Janeiro, 1977. RJ/GPO/32. 28 p.
- FARIA, F.M.M.; PEDRASSANI, E.L.; MARTINEZ, M.S. Subestação isolada a gás SF₆ de 500 kV de Itaipu - Comissionamento e experiência operacional relativa a todas as etapas (50/60 Hz). In: X SEMINÁRIO NACIONAL DE PRODUÇÃO E TRANSMISSÃO DE ENERGIA ELÉTRICA, Curitiba 1989, Grupo VIII, GSE-17, 5 p.
- FERNANDES, C.; ARAUJO, K. S.; BRESSANE, J. M.; LOBLEY, D.J.; RODRIGUES, A. F. Arranjo físico e considerações sobre os efeitos eletrostáticos nas subestações 800 kV do sistema de Itaipu. In: IV SEMINÁRIO NACIONAL DE PRODUÇÃO E TRANSMISSÃO DE ENERGIA ELÉTRICA, Rio de Janeiro, set. 18-23, 1977. Trabalhos ... Rio de Janeiro, 1977. RJ/GSE/15. 20 p.
- FERNANDES, C.; SATO, W.; JARDINI, J. A.; VIAN, A. Linhas 800 kV de Itaipu - Interferência em sinais de rádio e TV, ruído audível e efeito coroa visível. In: IV SEMINÁRIO NACIONAL DE PRODUÇÃO E TRANSMISSÃO DE ENERGIA ELÉTRICA, Rio de Janeiro, set. 18-23, 1977. Trabalhos ... Rio de Janeiro, 1977. RJ/GLT/36. 37 p.
- FERNANDES, D.; GUIMARÃES, E. B.; RODRIGUES, A. B.; GALIANO, D. B. Considerações sobre parâmetros meteorológicos para o projeto das linhas 800 kV do sistema de Itaipu. In: IV SEMINÁRIO NACIONAL DE PRODUÇÃO E TRANSMISSÃO DE ENERGIA ELÉTRICA, Rio de Janeiro, set. 18-23, 1977. Trabalhos ... Rio de Janeiro, 1977. RJ/GLT/32. 14 p.
- FERNANDES, D.; LOBLEY, D. J.; PINTO, L. J.; MARQUES, O. Considerações sobre o comportamento das cadeias de isoladores das linhas 800 kV de Itaipu quanto aos arcos de potência. In: IV SEMINÁRIO NACIONAL DE PRODUÇÃO E TRANSMISSÃO DE ENERGIA ELÉTRICA, Rio de Janeiro, set. 18-23, 1977. Trabalhos ... Rio de Janeiro, 1977. RJ/GLT/34. 19 p.
- FERNANDES, D.; OLIVEIRA, J. D.; ALBUQUERQUE, D.; PALADINO, L.; REINART, I. Considerações sobre o estudo dos solos e escolha dos tipos de fundações para as torres das linhas 800 kV de Itaipu. In: IV SEMINÁRIO NACIONAL DE PRODUÇÃO E TRANSMISSÃO DE ENERGIA ELÉTRICA, Rio de Janeiro, set. 18-23, 1977. Trabalhos ... Rio de Janeiro, 1977. RJ/GLT/33. 30 p.
- FERNANDES, P. C. A.; BRASIL, D. O. C.; VEIGA, J. B.; FERREIRA, L. E. B. Programa digital para cálculo das condições em regime permanente do elo de corrente contínua de Itaipu. In: VI SEMINÁRIO NACIONAL DE PRODUÇÃO E TRANSMISSÃO DE ENERGIA ELÉTRICA, Camboriú, out. 18-22, 1981. Trabalhos ... Camboriú, 1981. BC/GSP/22. 20 p.
- FIGUEIREDO, A. G.; SHORE, N. L.; BJORKLUND, H.; PRACA, A. A. S.; FRAGA, R. Master control CCAT para as estações conversoras do sistema de transmissão de Itaipu. In: IV SEMINÁRIO NACIONAL DE PRODUÇÃO E TRANSMISSÃO DE ENERGIA ELÉTRICA, Camboriú, out. 18-22, 1981. Trabalhos ... Camboriú, 1981. BC/GSP/36. 18 p.
- FRANCO, N. The Superelectrification of Brazil. *IEEE Spectrum*, 19 (5), may 1982, p. 57-62.
- _____. La superelettificazione del Brasile. *L'Elettrotecnica*, LXX (5), : 397-402, Magg. 1983
- FRANCO, N.; NEVILLE, J. E.; RENE, J. G. Estudo de viabilidade de transmissão de Itaipu. In: III SEMINÁRIO NACIONAL DE PRODUÇÃO E TRANSMISSÃO DE ENERGIA ELÉTRICA, Curitiba, out. 12-18, 1975. Trabalhos ... Curitiba, 1975. CTBA/GPO/10, p. 183-219.
- FRONTIN, S. O.; KASTRUP FILHO, O.; MARCUZZI, E.; FAINGUELERNT, A. Interruption of induced currents by grounding switches at the HVAC lines of the Itaipu HVDC transmission system converter stations. In: CIGRE. INTERNATIONAL CONFERENCE ON LARGE HIGH VOLTAGE ELECTRIC SYSTEMS, Paris, 1984. 15 p.
- FURNAS CENTRAIS ELÉTRICAS S.A. Itaipu System, Rio de Janeiro, 005/2, mar. 1983, 23 p.
- _____. Sistema de Transmissão de Itaipu. Rio de Janeiro, 028/2, out. 1987, 19 p.
- GALVÃO, A.; OLIVEIRA FILHO, A.; PEREIRA, F. P.; MEDEIROS, J. R.; CORREA, R. L. D.; SOTO, A. R. S.; PORTELA, C. M. Método de medição do componente de sequência negativa da tensão, aplicáveis às tensões das SE's conversoras de Itaipu. In: VIII SEMINÁRIO NACIONAL DE PRODUÇÃO E TRANSMISSÃO DE ENERGIA ELÉTRICA, São Paulo, maio 4-8, 1986. Trabalhos ... São Paulo, 1986. SP/GSP/34. 9 p.
- GARCIA, R. W. S.; FONSECA, J. R.; ASSUNÇÃO, L. A. R. Investigações sobre aspectos de segurança em manutenção de linhas de corrente contínua ± 600 kV. In: IX SEMINÁRIO NACIONAL DE PRODUÇÃO E TRANSMISSÃO DE ENERGIA ELÉTRICA, Belo Horizonte, out. 25-29, 1987. Trabalhos ... Belo Horizonte, 1987. BHZ/GLT/16. 8 p.

GELÁZIO DA ROCHA, J.; VILLALBA, J. R.; SALATKO, V. F. Seleção das características do projeto para os hidrogeradores de 737 MVA de Itaipu. In: IV SEMINÁRIO NACIONAL DE PRODUÇÃO E TRANSMISSÃO DE ENERGIA ELÉTRICA, Rio de Janeiro, set. 18-23, 1977. Trabalhos ... Rio de Janeiro, 1977. RJ/GPH/10. 25 p.

GRAMOW, A. A Siemens e sua participação no aproveitamento hidrelétrico de Itaipu. *Revista Siemens*, s.l., 3 (1) : 15-7, jan./mar. 1983.

_____. ITAIPU. Refrigeração direta por água das barras estatóricas. *Energia Elétrica*, 5 (52), : 16-25, jul. 1982.

_____. O controle das unidades geradoras de Itaipu. *Revista Engenharia Mackenzie*, São Paulo:24-8, abr./jun. 1983.

GROSZ, H. W. Considerações sobre a importância da análise da combinação de materiais quando da avaliação dos critérios de inflamabilidade. In: IX SEMINÁRIO NACIONAL DE PRODUÇÃO E TRANSMISSÃO DE ENERGIA ELÉTRICA, Belo Horizonte, out. 25-29, 1987. Trabalhos ... Belo Horizonte, 1987. BHZ/SGM/03. 2 p.

GUIMARÃES, E. B.; JARDINI, J. A.; WEY FILHO, A.; PAAJARVI, B.; EKSTROM, A. Insulation coordination and arrester protections of the Itaipu HVDC stations. Part I - Insulation coordination. In: CIGRE. INTERNATIONAL CONFERENCE ON LARGE HIGH VOLTAGE ELECTRIC SYSTEMS, Rio de Janeiro, 1981. 29 p.

GUIMARÃES, E. B.; KASTRUP FILHO, O.; OLIVEIRA, G. S. G.; DRUMMOND, M.; WEY FILHO, A.; ERIKSSON, K. Sistema de transmissão de Itaipu em corrente contínua. Estudos de dimensionamento dos pára-raios dos filtros de corrente alternada a sobretensões temporárias. In: VII SEMINÁRIO NACIONAL DE PRODUÇÃO E TRANSMISSÃO DE ENERGIA ELÉTRICA, Brasília, dez. 2-6, 1984. Trabalhos ... Brasília, 1984. BSB/GSP/27. 13 p.

GUIMARÃES, E. B.; LESER, E.; SHEMIE, R.; EKLUND, L. Sistema de transmissão de Itaipu em corrente contínua - Ensaio de válvulas a tiristores das conversoras CCAT. In: VII SEMINÁRIO NACIONAL DE PRODUÇÃO E TRANSMISSÃO DE ENERGIA ELÉTRICA, Brasília, dez. 2-6, 1984. Trabalhos ... Brasília, 1984. BSB/GSP/14. 20 p.

GUIMARÃES, E. B.; PEREIRA, M. P.; KASTRUP FILHO, O. Coordenação de isolamento e proteção por pára-raios de óxido de zinco das estações conversoras de corrente contínua de Itaipu. In: COMISIÓN DE INTEGRACIÓN ELÉCTRICA REGIONAL. CIER, Lima, 1983. 14 p.

GUIMARÃES, E. B.; PEREIRA, M. P.; VAISMAN, R.; DRUMOND, M.; MOASSAB, P. J.; OLIVEIRA, G. S. G.; PAAJARVI, B.; EKSTROM, A. Itaipu HVDC converter stations. Overvoltages studies. In: CIGRE. INTERNATIONAL CONFERENCE ON LARGE HIGH VOLTAGE ELECTRIC SYSTEMS, Rio de Janeiro, aug. 1981. 16 p.

_____. Sistema de Itaipu em corrente contínua - Estudos de sobretensão e coordenação de isolamento das estações conversoras. In: VI SEMINÁRIO NACIONAL DE PRODUÇÃO E TRANSMISSÃO DE ENERGIA ELÉTRICA, Camboriú, out. 18-22, 1981. Trabalhos ... Camboriú, 1981. BC/GSP/26. 19 p.

HACKER, P. Itaipu hydroelectric giant makes tough demands on transformers. *Electrical Review*, Sussex, 212 (21): 31-3, June 1983.

JARDINI, J. A.; VIAN, A.; HEDMAN, D. E.; PEIXOTO, C. A. O.; FRONTIN, S. O. 800 kV Itaipu transmission system surge arrester and circuit-breaker special duties. In: CIGRE. INTERNATIONAL CONFERENCE ON LARGE HIGH VOLTAGE ELECTRIC SYSTEMS, Paris, aug. 1980. 14 p.

JARDINI, J. A.; ZANETTA, L. C.; SATO, W.; VIAN, A. Determinação das sobretensões de manobra no sistema de transmissão de Itaipu. In: IV SEMINÁRIO NACIONAL DE PRODUÇÃO E TRANSMISSÃO DE ENERGIA ELÉTRICA, Rio de Janeiro, set. 18-23, 1977. Trabalhos ... Rio de Janeiro, 1977. RJ/GSP/34. 16 p.

KASTRUP FILHO, O.; SATO, W.; MASUDA, M.; JARDINI, J. A.; VIAN, A. Coordenação de isolamento das linhas do sistema de transmissão de Itaipu. In: IV SEMINÁRIO NACIONAL DE PRODUÇÃO E TRANSMISSÃO DE ENERGIA ELÉTRICA, Rio de Janeiro, set. 18-23, 1977. Trabalhos ... Rio de Janeiro, 1977. RJ/GLT/38. 26 p.

KASTRUP FILHO, O.; ZANETTA, L. C.; BRASIL, D. O. C.; JARDINI, J. A.; VIAN, A. Coordenação de isolamento das subestações do sistema de transmissão de Itaipu. In: IV SEMINÁRIO NACIONAL DE PRODUÇÃO E TRANSMISSÃO DE ENERGIA ELÉTRICA, Rio de Janeiro, set. 18-23, 1977. Trabalhos ... Rio de Janeiro, 1977. RJ/GSE/13. 31 p.

KULICKE, B. & SCHRAMM, H. H. Clearance of short-circuits with delayed current zeros in the Itaipu 550 kV-substation. *IEEE Transactions on Power Apparatus and Systems*, 99 (4) : 1406-14, July/aug. 1980.

LEFEVRE, M. A. P.; ESCOBAR, O. B. V.; TRIGONA, G.; BANDAU, J. K.; ABREU, M. A.; VILLALBA, J. R. Interligação Itaipu/ANDE/FURNAS, 50 Hz. Experiência operativa. In: IX SEMINÁRIO NACIONAL DE PRODUÇÃO E TRANSMISSÃO DE ENERGIA ELÉTRICA, Belo Horizonte, out. 25-29, 1987. Trabalhos ... Belo Horizonte, 1987. BHZ/GOP/14. 6 p.

LIMA JUNIOR, M. P.; UNDRILL, J. M.; HANNETT, J. N.; JOHNSON, B. K. Novo método para análise de ressonância subsíncrona e sua aplicação no sistema de transmissão de Itaipu. In: IV SEMINÁRIO NACIONAL DE PRODUÇÃO E TRANSMISSÃO DE ENERGIA ELÉTRICA, Rio de Janeiro, set. 18-23, 1977. Trabalhos ... Rio de Janeiro, 1977. RJ/GSP/33. 24 p.

LIMA JUNIOR, M. P.; VIAN, A.; GRAHAM, J. F.; PINTO, E. M. Apresentação e análise dos estudos de ressonância subsíncrona no sistema de transmissão de Itaipu. In: IV SEMINÁRIO NACIONAL DE PRODUÇÃO E TRANSMISSÃO DE ENERGIA ELÉTRICA, Rio de Janeiro, set. 18-23, 1977. Trabalhos ... Rio de Janeiro, 1977. RJ/GSP/25. 14 p.

MACHADO, G. U. A.; ANDRADE FILHO, G. D.; TAVARES, L. A.; VILLALBA, J. R.; SZWATO, J.; VILLASSANTI, A. Treinamento de pessoal técnico para a operação e manutenção da Central Hidrelétrica de Itaipu. In: VIII SEMINÁRIO NACIONAL DE PRODUÇÃO E TRANSMISSÃO DE ENERGIA ELÉTRICA, São Paulo, maio 4-8, 1986. Trabalhos ... São Paulo, 1986. SP/GTA/17. 20 p.

MEDEIROS, J. R.; MORAIS, S. A.; SOTO, A. R. S.; CLARKE, C. D.; BRESSANE, J. M. Sistema de transmissão de Itaipu CC/CA. Determinação dos requisitos dos filtros nas estações terminais CA. In: VI SEMINÁRIO NACIONAL DE PRODUÇÃO E TRANSMISSÃO DE ENERGIA ELÉTRICA, Camboriú, out. 18-22, 1981. Trabalhos... Camboriú, 1981. BC/GSP/30.21 p.

MEDEIROS, W. B.; DANZIGER, F. A. B.; PINTO, C. P. Análise do comportamento de fundações para estais a partir dos testes de carga do sistema de transmissão de Itaipu. VII SEMINÁRIO NACIONAL DE PRODUÇÃO E TRANSMISSÃO DE ENERGIA ELÉTRICA, Brasília, dez. 2-6, 1984. Trabalhos ... Brasília, 1984. BSB/GLT/20. 20 p.

MELLO, F. P.; MOUNTFORD, J. D.; VIAN, A.; JARDINI, J. A.; GRAHAM, J. F. Estudos preliminares para aplicação de compensação estática em alternativa com suporte de tensão para o sistema de transmissão de Itaipu. In: IV SEMINÁRIO NACIONAL DE PRODUÇÃO E TRANSMISSÃO DE ENERGIA ELÉTRICA, Rio de Janeiro, set. 18-23, 1977. Trabalhos ... Rio de Janeiro, 1977. RJ/GSP/24. 11 p.

MENDEZ, J. C. V.B.; LOBO, S. E.; GIACOMET, L. F.; FERNANDEZ, L. F.; GUILLEN, M. A.; TEME, P.P.; BRASA, R.; FLEMING, A. M. Problemas nos enrolamentos do estator do gerador 1 da central hidroelétrica de Itaipu. In: VIII SEMINÁRIO NACIONAL DE PRODUÇÃO E TRANSMISSÃO DE ENERGIA ELÉTRICA, São Paulo, maio 4-8, 1986. Trabalhos ... São Paulo, 1986. SP/SGM/15. 15 p.

MENDONÇA, W. C.; OLIVEIRA, J. C. C.; WEY FILHO, A.; ADIELSSON, T. Sistema de transmissão de Itaipu em corrente contínua. Análise das diversas condições de operação em regime permanente. In: VI SEMINÁRIO NACIONAL DE PRODUÇÃO E TRANSMISSÃO DE ENERGIA ELÉTRICA, Camboriú, out. 18-22, 1981. Trabalhos ... Camboriú, 1981. BC/GSP/24. 11 p.

MESSEGUER, F. L.; BARATA, G. O. Localizador de falhas a terra em sistemas alimentados em corrente contínua. In: IX SEMINÁRIO NACIONAL DE PRODUÇÃO E TRANSMISSÃO DE ENERGIA ELÉTRICA, Belo Horizonte, out. 25-29, 1987. Trabalhos ... Belo Horizonte, 1987. BHZ/GPC/12. 16 p.

MICKEVICIUS, A.; KAWAHATA, K. World's Largest SF₆ gas-insulated substation. In: ENVIRONMENTAL ENGINEERING PROCEEDINGS OF SPECIALTY CONFERENCE, 1986. EE Div. ASCE, CINCINNATI, OH, July 8-10. p. 746-55.

MM ED. LTDA. A dança dos bilhões. *Eleticidade Moderna*, São Paulo, 1 (8) : 28-31, jun. 1973.

_____. Itaipu. Fiel aos prazos, apesar das pendências. *Eleticidade Moderna*, São Paulo, 6 (65) : 14-37, out. 1978.

_____. Nasce uma usina. *Eleticidade Moderna*, São Paulo, 1 (8) : 32-5, jun. 1983.

MORAES E SILVA, J.M.; NORONHA, R.F.; PEDRASSANI, E.L.; CABOCLO, R.L.F.; ESTIGARRIBIA, E.A.; GIMENEZ, A.A.; RILINI, M.A.A.; SANABRIA F.R. Subestação isolada a gás SF₆ de 500 kV da Usina Hidrelétrica de Itaipu. Comissionamento e experiência operacional relativa à 1a. etapa de 50 Hz. In: VIII SEMINÁRIO NACIONAL DE PRODUÇÃO E TRANSMISSÃO DE ENERGIA ELÉTRICA, São Paulo, maio 4-8, 1986. Trabalhos... São Paulo, 1986. SP/GSE/19. 6 p.

MORAES J. de; VILLALBA, J.R.; SALATKO, V.F. Selection of design features for 737 and 823 MVA hydrogenerators for Itaipu project. *IEEE Trans. on Power Apparatus and Systems*, s.l., 98 (6) : 2329-37, nov./dec. 1979.

MORAES, J. J. R.; LISBOA, T. A.; PINHEIRO, J. T. Escolha das rotas e implantação do traçado das linhas de transmissão 800 kV de Itaipu. In: IV SEMINÁRIO NACIONAL DE PRODUÇÃO E TRANSMISSÃO DE ENERGIA ELÉTRICA, Rio de Janeiro, set. 18-23, 1977. Trabalhos ... Rio de Janeiro, 1977. RJ/GLT/27. 18 p.

MORAES, J. de & SALATKO, V. F. Coming: 12.600 megawatts at Itaipu Island. IEEE Spectrum, New York, 20 (8) : 46-52, aug. 1983.

MORAES, J. de; VILLALBA, J.R.; SALATKO, V.F. Electrical and related design aspects of Itaipu hydroelectric project. IEEE Transactions on Power Apparatus and Systems, s.l., 101 (5) : 1012-20, may 1982.

MORAIS, S. A.; MEDEIROS, J. R.; TOLEDO, P. F.; BERGDAHL, B. L.; ERIKSSON, K.; LAZARS, T. Harmonic current calculations for Itaipu HVDC transmission system. In: INTERNATIONAL CONFERENCE ON HARMONIC IN POWER SYSTEMS. UMIST, Manchester, 1981, n.p.

MORAIS, S. A.; MENDES, R.; RUOSS, E.; WAADDLETON, M. P. Interrupção de correntes de falta com zeros atrasados pelos disjuntores de 550 kV de Foz do Iguaçu. In: VII SEMINÁRIO NACIONAL DE PRODUÇÃO E TRANSMISSÃO DE ENERGIA ELÉTRICA, Brasília, dez. 2-6, 1984. Trabalhos ... Brasília, 1984. BSB/SGE/15. 20 p.

MORAIS, S. A.; MORAND, S. R.; ERIKSSON, K.; BERGDAHL, B. Sistema de transmissão CCAT de Itaipu. Impacto da indutância de barramentos no desempenho e sintonia dos filtros CA. In: IX SEMINÁRIO NACIONAL DE PRODUÇÃO E TRANSMISSÃO DE ENERGIA ELÉTRICA, Belo Horizonte, out. 25-29, 1987. Trabalhos ... Belo Horizonte, 1987. BHZ/GSP/10. 5 p.

MUSIL, R. V. & VOEGELE, H. Special design problems with large low-speed hydrogenerators. In: CIGRE. INTERNATIONAL CONFERENCE ON LARGE HIGH VOLTAGE ELECTRIC SYSTEMS, Rio de Janeiro, Nov. 1983. 16 p.

NASCENTES, J. C. M.; MARCHI, R. D.; VALDES, O. B.; TRIGONA, G.; WEINER, A. Aspectos da coordenação da operação de Itaipu. In: VIII SEMINÁRIO NACIONAL DE PRODUÇÃO E TRANSMISSÃO DE ENERGIA ELÉTRICA, São Paulo, maio 4-8, 1986. Trabalhos ... São Paulo, 1986. SP/GTA/04. 16 p.

NILSSON, A. & CUNHA, W. J. L. Transferência de tecnologia nos estudos e projeto das estações conversoras de CC/CA de Itaipu - Organização e estágios iniciais. In: VI SEMINÁRIO NACIONAL DE PRODUÇÃO E TRANSMISSÃO DE ENERGIA ELÉTRICA, Camboriú, out. 18-22, 1981. Trabalhos ... Camboriú, 1981. BC/GTA/12. 18 p.

NOGUEIRA, L.; DE CONTI, R.; ARANTES, J.; MOTTA A.; SIVIERO, J.C.; STEFFEN, F.; BOVEDA, J.; RAMIREZ, H.; GARCIA, E.; FRIEDMAN, A. Aspectos relevantes da fase inicial de operação das três primeiras unidades da central hidrelétrica de Itaipu. In: VIII SEMINÁRIO NACIONAL DE PRODUÇÃO E TRANSMISSÃO DE ENERGIA ELÉTRICA, São Paulo, maio 4-8, 1986. Trabalhos ... São Paulo, 1986. SP/GPH/07. 15 p.

NOVO GRUPO EDITORA TÉCNICA LTDA. Itaipu. O desafio está sendo vencido. Energia Elétrica, São Paulo, 5 (45) : 14-45, dez. 1981.

_____. Itaipu. Sucesso na montagem nasceu da união de oito montadoras. Energia Elétrica, 5 (52), : 44-50, jul. 1982.

_____. CIEM. Cumprindo os objetivos com alta tecnologia. Energia Elétrica, : 37-42, jul. 1982.

_____. Itaipu. Sucesso na montagem nasceu da união de oito montadoras. Energia Elétrica, São Paulo 5 (52): 44-50, jul. 1982.

_____. Itaipu. Ciem implanta minucioso trabalho de supervisão no canteiro de obras. Construção Pesada, São Paulo, 12 (140) : 54-6, set. 1982.

_____. As linhas de Itaipu: uma das maiores tensões do mundo. Energia Elétrica, São Paulo, 1 (2) : 16-22, nov. 1977. Suplem. Bim. da Rev. Construção Pesada.

_____. Itaipu. Consórcio de montagem já executou 18% do total dos serviços contratados. Construção Pesada, São Paulo, 12 (140) : 48-52, set. 1982.

_____. Potencial hidrelétrico do Brasil. Energia Elétrica, São Paulo, 2 (20) : 64-75, nov. 1979.

_____. Montagem eletromecânica de Itaipu avança lentamente. Energia Elétrica, São Paulo, 6 (65) : 14-8, set. 1983.

OLIVEIRA, F. E.; PEDROSO, A.; OLIVEIRA, S. E. M. Estudos da fase de antecipação do sistema de transmissão de Itaipu. In: IV SEMINÁRIO NACIONAL DE PRODUÇÃO E TRANSMISSÃO DE ENERGIA ELÉTRICA, Rio de Janeiro, set. 18-23, 1977. Trabalhos ... Rio de Janeiro, 1977. RJ/GPO/37. 19 p.

ORDACGI, J.M.; LOPEZ, L.A.Z.; MORAES, L.C. A primeira proteção diferencial de linha com comunicação via fibra ótica do Brasil. Caderno de Engenharia Elétrica - RBE. 6 (1), 1980. 205 p.

OURA, J.M.; CABRAL, F.L.M. Uso de micro-processadores no registro da perturbação e ensaios da proteção. In: X SEMINÁRIO NACIONAL DE

PRODUÇÃO E TRANSMISSÃO DE ENERGIA ELÉTRICA, Curitiba 89, Grupo V, GPC-17, 3 p.

OZELAME, M.L.; FURMANN, J.C.; COLOMBO, C. VELASQUEZ, M. Sistema de resfriamento a água pura dos geradores da Central Hidrelétrica de Itaipu. VIII SEMINÁRIO NACIONAL DE PRODUÇÃO E TRANSMISSÃO DE ENERGIA ELÉTRICA, São Paulo, maio 4-8, 1986. Trabalhos...São Paulo, 1986. SP/SGM/13. 15 p.

OZELAME, M.L.; CUEVAS, C.C.; SILVA, M.D.; MAIMONE, E. C. C. Ensaio especiais em mancais de hidrogeradores de grande porte, para avaliação do desempenho dos mesmos e aferição do projeto. In: IX SEMINÁRIO NACIONAL DE PRODUÇÃO E TRANSMISSÃO DE ENERGIA ELÉTRICA, Belo Horizonte, out. 25-29, 1987. Trabalhos ... Belo Horizonte, 1987. BHZ/SGM/12. 6 p.

PEER, F. & LUBASCH, R. Static excitation equipment for Itaipu. *International Water Power & Dam Construction*, Sutton, 34 (9) : 25-6, sept. 1982.

_____. Unitrol static excitation equipment for the generators of the world's largest hydro power plant Itaipu. *Brown Boveri Review*, Baden, 69(3) : 65-8, 1982.

PEGADO, P. A. S.; FRONTIN, S.O.; ERIKSSON, K.; MADZAREVIC, V. Estudos de engenharia para o projeto das estações conversoras do sistema de corrente contínua de Itaipu. In: VII SEMINÁRIO NACIONAL DE PRODUÇÃO E TRANSMISSÃO DE ENERGIA ELÉTRICA, Brasília, dez. 2-6, 1984. Trabalhos ... Brasília, 1984. BSB/GSP/28. 25 p.

PEGADO, P. A. S.; GUIMARÃES, E. B.; MADZAREVIC, V.; WEY FILHO, A.; ERIKSSON, K. Sistema de transmissão de Itaipu em corrente contínua - Estudos de sistemas para o projeto das estações conversoras. In: VI SEMINÁRIO NACIONAL DE PRODUÇÃO E TRANSMISSÃO DE ENERGIA ELÉTRICA, Camboriú, out. 18-22, 1981. Trabalhos ... Camboriú, 1981. BC/GSP/23. 11 p.

PEIXOTO, C. A. O. Itaipu 6300 MW HVDC transmission system. Feasibility and planning aspects. In: INCORPORATION HVDC POWER TRANSMISSION INTO SYSTEM PLANNING SEMINAR, Arizona, 1980, 32 p.

PEIXOTO, C. A. O.; CAROLI, C. E.; LOBLEY, D. J.; ARAUJO, K. S.; BRESSANE, J. M. Critérios de projeto das subestações 750/550/345 kV CA do sistema de transmissão de Itaipu. In: VI SEMINÁRIO NACIONAL DE PRODUÇÃO E TRANSMISSÃO DE ENERGIA ELÉTRICA, Camboriú, out. 18-22, 1981. Trabalhos ... Camboriú, 1981. BC/GSE/07. 23 p.

PEIXOTO, C. A. O.; CLARKE, C. D.; JARDINI, J. A.; MOUNTFORD, J. D. Simulator and digital studies on VAR compensation for the Itaipu HVDC. In: Institute of Electrical and Electronics Engineers - Winnipeg, Canada, 1980, 30 p.

PEIXOTO, C. A. O.; ESMERALDO, P. C. V.; FONSECA, C. S.; BRESSANE, J.M.; MOUNTFORD, J. D. Sistema de transmissão de Itaipu CA/CC. Sobretensões dinâmicas e transitórias e suas influências nas características dos equipamentos. In: VI SEMINÁRIO NACIONAL DE PRODUÇÃO E TRANSMISSÃO DE ENERGIA ELÉTRICA, Camboriú, out. 18-22, 1981. Trabalhos ... Camboriú, 1981. BC/GSP/33. 20 p.

PEIXOTO, C. A. O.; FERNANDES, D.; DART, F. C.; RODRIGUES, A. F. Desempenho da malha de aterramento da estação conversora de Foz do Iguaçu do sistema CCAT de Itaipu. In: VIII SEMINÁRIO NACIONAL DE PRODUÇÃO E TRANSMISSÃO DE ENERGIA ELÉTRICA, São Paulo, maio 4-8, 1986. Trabalhos ... São Paulo, 1986. SP/GSE/19. 16 p.

PEIXOTO, C. A. O.; FIGUEIREDO, E. P.; FRONTIN, S. O.; TAAM, M. Z.; PORONGABA, H. D.; SVENSSON, S. Itaipu HVDC transmission system stability studies. In: CIGRÉ. INTERNATIONAL CONFERENCE ON LARGE HIGH VOLTAGE ELECTRIC SYSTEMS, Rio de Janeiro, 1981. 22 p.

PEIXOTO, C. A. O.; FRONTIN, S. O.; JARDINI, J. A. Engineering studies for Itaipu converter station design. In: INTERNATIONAL CONFERENCE ON THYRISTOR AND VARIABLE STATIC EQUIPMENT FOR AC AND DC TRANSMISSION. IEEE. London, 1981, n.p.

PEIXOTO, C. A. O.; GABAGLIA, C. P. R.; JARDINI, J. A.; BRESSANE, J.M.; PORTELA, C.M. Sistema de transmissão de Itaipu CA/CC. Estudos elétricos das linhas CC e das linhas dos eletrodos. In: VI SEMINÁRIO NACIONAL DE PRODUÇÃO E TRANSMISSÃO DE ENERGIA ELÉTRICA, Camboriú, out. 18-22, 1981. Trabalhos ... Camboriú, 1981. BC/GLT/22. 22 p.

PEIXOTO, C. A. O.; MELLO, F. P.; VIAN, A. Estudos para a seleção final do sistema de transmissão 800 kV de Itaipu. In: IV SEMINÁRIO NACIONAL DE PRODUÇÃO E TRANSMISSÃO DE ENERGIA ELÉTRICA, Rio de Janeiro, set. 18-23, 1977. Trabalhos ... Rio de Janeiro, 1977. RJ/GPO/24. 21 p.

PEIXOTO, C. A. O.; MELLO, J. C. P.; SHEMIE, R. K.; JARDINI, J. A.; SANTOS SILVA, J. B. Análise da viabilidade da interligação dos barramentos 60 Hz e 50 Hz da Usina de Itaipu, utilizando-se estação conversora "back-to-back". In: VII SEMINÁRIO NACIONAL DE PRODUÇÃO E TRANSMISSÃO DE ENERGIA ELÉTRICA, Brasília, dez. 2-6, 1984. Trabalhos ... Brasília, 1984. BSB/GSP/39. 12 p.

PEIXOTO, C. A. O.; MELLO, J. C. P.; SANTIAGO, R. C.; JARDINI, J. A. Isolamento das linhas de transmissão ± 600 kV CC de Itaipu, com destaque para as características dos isoladores especiais dessas linhas. In: VII SEMINÁRIO NACIONAL DE PRODUÇÃO E TRANSMISSÃO DE ENERGIA ELÉTRICA, Brasília, dez. 2-6, 1984. Trabalhos ... Brasília, 1984. BSB/GLT/22. 17 p.

PEIXOTO, C. A. O.; MOUNTFORD, J. D.; SHEMIE, R. K.; VIAN, A.; MELLO, J. C. P. de. Sistema de transmissão de Itaipu CA/CC - Definição da configuração básica do sistema. In: VI SEMINÁRIO NACIONAL DE PRODUÇÃO E TRANSMISSÃO DE ENERGIA ELÉTRICA, Camboriú, out. 18-22, 1981. Trabalhos ... Camboriú, 1981. BC/GPL/21. 21 p.

PEIXOTO, C. A. O.; OLIVEIRA, J. D. C.; SANTIAGO, R. C. Sistema de transmissão de Itaipu CA/CC. Projeto das linhas de transmissão CC e das linhas dos eletrodos. In: VI SEMINÁRIO NACIONAL DE PRODUÇÃO E TRANSMISSÃO DE ENERGIA ELÉTRICA, Camboriú, out. 18-22, 1981. Trabalhos ... Camboriú, 1981. BC/GLT/23. 21 p.

PEIXOTO, C. A. O.; SANTIAGO, R. C.; LOBLEY, D. J.; MELLO, J. C. P. Estudos de otimização das linhas 800 kV de Itaipu. In: IV SEMINÁRIO NACIONAL DE PRODUÇÃO E TRANSMISSÃO DE ENERGIA ELÉTRICA, Rio de Janeiro, set. 18-23, 1977. Trabalhos ... Rio de Janeiro, 1977. RJ/GLT/19. 28 p.

PEIXOTO, C. A. O.; SANTOS, N. dos; KOVARSKY, D.; SHEMIE, R. K.; PORTELA, C. M. Sistema de transmissão de Itaipu CA/CC. Eletrodos de terra e o impacto em seu meio ambiente. In: VI SEMINÁRIO NACIONAL DE PRODUÇÃO E TRANSMISSÃO DE ENERGIA ELÉTRICA, Camboriú, out. 18-22, 1981. Trabalhos ... Camboriú, 1981. BC/GSE/09. 28 p.

PEIXOTO, C. A. O.; SHEMIE, R. K.; MELLO, J. C. P.; VIAN, A. Sistema de transmissão de Itaipu CA/CC. Diretrizes para especificação de projetos "Turn-key". In: VI SEMINÁRIO NACIONAL DE PRODUÇÃO E TRANSMISSÃO DE ENERGIA ELÉTRICA, Camboriú, out. 18-22, 1981. Trabalhos ... Camboriú, 1981. BC/GTA/10. 10 p.

PEIXOTO, C. A. O.; SOUZA, J. T. P.; MEDEIROS, J. R.; PATTERSON, N. A.; SOTO, A. R. S.; CLARKE, C. D. Sistema de transmissão de Itaipu CA/CC. Coordenação indutiva do sistema de corrente contínua. In: VI SEMINÁRIO NACIONAL DE PRODUÇÃO E TRANSMISSÃO DE ENERGIA ELÉTRICA, Camboriú, out. 18-22, 1981. Trabalhos ... Camboriú, 1981. BC/GSP/33. 33 p.

PEIXOTO, C. A. O.; BRASIL, D. O. C.; CLARKE, C. D.; BROCHADO, A. C. Sistema de transmissão de Itaipu CA/CC. Utilização do simulador para avaliação do desempenho dos conversores de Itaipu e seus controles. In: VI SEMINÁRIO NACIONAL DE PRODUÇÃO E TRANSMISSÃO DE ENERGIA ELÉTRICA, Camboriú, out. 18-22, 1981. Trabalhos ... Camboriú, 1981. BC/GSP/31. 22 p.

PEIXOTO, C. A. O.; FERREIRA, L. E. B.; PACHECO J. G.; VILLALBA, J. R.; KRONANDER, H.; ALVARENGA, L.; PORONGABA, H. D.; TOLEDO, P. F. de. Desempenho das proteções de C.A. da usina de Itaipu e subestações da margem direita diante da operação das estações conversoras CCAT do sistema de transmissão de Itaipu. In: VII SEMINÁRIO NACIONAL DE PRODUÇÃO E TRANSMISSÃO DE ENERGIA ELÉTRICA, São Paulo, maio 4-8, 1986. Trabalhos ... São Paulo, 1986. SP/GSP/44. 16 p.

PELOSI JUNIOR, A.; SOUSA, J. T. P.; FURLONI, W.; ALM, S.; BACON, J. Estudos de interferência para o sistema de ondas portadoras das linhas de CCAT de Itaipu. In: VII SEMINÁRIO NACIONAL DE PRODUÇÃO E TRANSMISSÃO DE ENERGIA ELÉTRICA, Brasília, dez. 2-6, 1984. Trabalhos ... Brasília, 1984. BSB/GLT/10. 8 p.

PENEFER, F.; PEER, F.; SCHWEICKARDT, H. E. Static excitation system for the Itaipu generators. In: CIGRE. INTERNATIONAL CONFERENCE ON LARGE HIGH VOLTAGE ELECTRIC SYSTEMS, Rio de Janeiro, Nov. 1983, p. 10-16.

PEREIRA, F. P.; MEDEIROS, J. R.; SOTO, A. R. S.; BRASIL, D. O. C. Itaipu HVDC transmission line - Aspects of inductive coordination. In: CIGRE. INTERNATIONAL CONFERENCE ON LARGE HIGH VOLTAGE ELECTRIC SYSTEMS, Tchechoslovaquia, 1981. 17 p.

PEREIRA, M. P.; JUSTO, C. P.; BRESSANE, J. M.; RODRIGUES, A. F. Blindagem contra descargas atmosféricas das subestações 800 kV do sistema de Itaipu. In: IV SEMINÁRIO NACIONAL DE PRODUÇÃO E TRANSMISSÃO DE ENERGIA ELÉTRICA, Rio de Janeiro, set. 18-23, 1977. Trabalhos ... Rio de Janeiro, 1977. RJ/GSE/09. 13 p.

PERES, L. A. P.; PORONGABA, H. D.; LUZ, G. S.; ROSENQVIST, R. Análise das interações subsíncronas entre a estação conversora CCAT de São Roque e turbogeradores do sistema receptor. In: VIII SEMINÁRIO NACIONAL DE PRODUÇÃO E TRANSMISSÃO DE ENERGIA ELÉTRICA, São Paulo, maio 4-8, 1986. Trabalhos ... São Paulo, 1986. SP/GSP/33. 18 p.

PIERANTI FILHO, O.; MENEGALE, D.; ERIKSSON, K. Estudos e critérios de projeto para as estações de corrente contínua do sistema de transmissão de Itaipu. In: VI SEMINÁRIO NACIONAL DE PRODUÇÃO E TRANSMISSÃO DE ENERGIA ELÉTRICA, Camboriú, out. 18-22, 1981. Trabalhos ... Camboriú, 1981. BC/GSE/15. 17 p.

PINHEIRO, J. L. P.; CHAGAS, H. P.; WILHELMSSON, L. Critérios básicos para o projeto do sistema de serviços auxiliares para estações conversoras do sistema de transmissão em CCAT de Itaipu. In: VI SEMINÁRIO NACIONAL DE PRODUÇÃO E TRANSMISSÃO DE ENERGIA ELÉTRICA, Camboriú, out. 18-22, 1981. Trabalhos ... Camboriú, 1981. BC/GSE/14. 13 p.

PORTELA, C.; ESMERALDO, P. C. V.; MEDEIROS, J. R. Harmônicas provocadas pelo sistema de transmissão de Itaipu nas redes sudeste e sul. In: VIII SEMINÁRIO NACIONAL DE PRODUÇÃO E TRANSMISSÃO DE ENERGIA ELÉTRICA, São Paulo, maio 4-8, 1986. Trabalhos ... São Paulo, 1986. SP/GSP/06. 19 p.

PULHEZ, N. V.; ERIKSSON, K.; SANTOS, N. dos. Aspectos do projeto do pátio de manobra para equipamentos de corrente contínua das estações conversoras do sistema de transmissão de Itaipu. In: VI SEMINÁRIO NACIONAL DE PRODUÇÃO E TRANSMISSÃO DE ENERGIA ELÉTRICA, Camboriú, out. 18-22, 1981. Trabalhos ... Camboriú, 1981. BC/GSE/11. 21 p.

RAJA GABAGLIA, C. P.; DART, F. C.; FERNANDES, C. Environmental effects of Itaipu 750 kV transmission lines. In: CIGRE. HV AND UHV TRANSMISSION LINES. OPEN CONFERENCE, *Rio de Janeiro*, 1983. 12 p.

REIS, L. B.; FRONTIN, S. O.; ERICKSSON, K. Operação do sistema de transmissão CCAT de Itaipu em carga leve. In: IX SEMINÁRIO NACIONAL DE PRODUÇÃO E TRANSMISSÃO DE ENERGIA ELÉTRICA, Belo Horizonte, out. 25-29, 1987. Trabalhos ... Belo Horizonte, 1987. BHZ/GSP/34. 5 p.

REIS, L. B.; SILVA, N. F. da; ROSEMBRACH, R.; KLINTERBACK, T.; CHAGAS, H.P., DUNA, R. Impacto da sobrefrequência no comportamento dos motores de indução da subestação conversora CCAT de Itaipu. In: VIII SEMINÁRIO NACIONAL DE PRODUÇÃO E TRANSMISSÃO DE ENERGIA ELÉTRICA, São Paulo, maio 4-8, 1986. Trabalhos ... São Paulo, 1986. SP/SGE/18. 8 p.

RESENDE, F. M. Capacitores série do sistema de Itaipu. Características elétricas básicas. In: IX SEMINÁRIO NACIONAL DE PRODUÇÃO E TRANSMISSÃO DE ENERGIA ELÉTRICA, Belo Horizonte, out. 25-29, 1987. Trabalhos ... Belo Horizonte, 1987. BHZ/GSP/12. 5 p.

RESENDE, F. M.; ROSS, R. P.D.; BRESSANE, J. M.; PEREIRA, S. T. Sistema de transmissão de Itaipu CA/CC Aplicação de capacitores série no tronco 750 kV de Itaipu. In: VI SEMINÁRIO NACIONAL DE PRODUÇÃO E TRANSMISSÃO DE ENERGIA ELÉTRICA, Camboriú, out. 18-22, 1981. Trabalhos ... Camboriú, 1981. BC/GSP/32. 20 p.

ROBINSON, P. J.; EDLINGER, A.; SCHLICHT, D. W.; D'AVILA MELO, E. S.; SALATKO, V. F. Lightning overvoltage protection of the 550 kV Itaipu SF₆ gas insulated substation. In: CIGRE. INTERNATIONAL CONFERENCE ON LARGE HIGH VOLTAGE ELECTRIC SYSTEMS, Paris, Sept. 1982. 7 p.

RUOSS, E. M.; MOASSAB, P. J.; FRONTIN, S.O.; AMON FILHO, J. Estudos de TTR para os disjuntores de 362 kV e de 500 kV das estações conversoras CC/CA de Itaipu. In: VII SEMINÁRIO NACIONAL DE PRODUÇÃO E TRANSMISSÃO DE ENERGIA ELÉTRICA, Brasília, dez. 2-6, 1984. Trabalhos ... Brasília, 1984. BSB/GSP/26. 19 p.

SALATKO, V. F.; VILLALBA, J. R.; FIESENIG, K. Mechanical design aspects of 737 and 823 MVA hydro generators at Itaipu power station. In: CIGRE. INTERNATIONAL CONFERENCE ON LARGE HIGH VOLTAGE ELECTRIC SYSTEMS, Rio de Janeiro, Nov. 1983. 6 p.

SALATKO, V.F. & GROSZ, H. W. Aspects of quality and reliability of hydrogenerators. In: CIGRE. INTERNATIONAL CONFERENCE ON LARGE HIGH VOLTAGE ELECTRIC SYSTEMS, Rio de Janeiro, nov. 1983. 4 p.

SALMEN, F. A.; FLETCHER, D. E.; MELLO, J. C. P. Aplicação de capacitores série no sistema 800 kV de Itaipu. In: IV SEMINÁRIO NACIONAL DE PRODUÇÃO E TRANSMISSÃO DE ENERGIA ELÉTRICA, Rio de Janeiro, set. 18-23, 1977. Trabalhos ... Rio de Janeiro, 1977. RJ/GSP/15. 19 p.

- SALTARA, M. A concepção do estator dos geradores para Itaipu. *Energia Elétrica*, São Paulo, 5(52) : 13-14, jul. 1982.
- SCHEIBENGRAF, H. & HERZOG, H. Interaction of the various limit controllers of a static excitation system with reference to the equipment for the Itaipu power plant. *Brown Boveri Review*, Baden, 69 (3) : 69-72, 1982.
- SIEMENS. Itaipu: está nascendo um gigante. *Revista Siemens*, s.l., 3 (1) : 18-23, jan./mar. 1983.
- SILVEIRA, J. R.; SANCHES, T. J.; FARIA, F. M. M.; CARVALHO, F. M.S.; SILVA, J. M. M. Avaliação dos surtos de manobra produzidos por seccionadoras, no setor de 60 Hz da GIS de Itaipu, usando o programa EMPT. In: IX SEMINÁRIO NACIONAL DE PRODUÇÃO E TRANSMISSÃO DE ENERGIA ELÉTRICA, Belo Horizonte, out. 25-29, 1987. Trabalhos ... Belo Horizonte, 1987. BHZ/GSP/01. 6 p.
- SIMÃO, J.; LATINI, M. F.; MENDEZ, J. C. V. B.; TORALES, R. D. G.; GONZALES, A. F.; GUILLEN, M. A. Ensaio de alta tensão e de resistência de isolamento nos geradores da central hidroelétrica de Itaipu. In: VIII SEMINÁRIO NACIONAL DE PRODUÇÃO E TRANSMISSÃO DE ENERGIA ELÉTRICA, São Paulo, maio 4-8, 1986. Trabalhos ... São Paulo, 1986. SP/SGM/14. 7 p.
- SOARES NETO, J. B. G.; MIRANDA, L. F. S. A.; AZEVEDO FILHO, L.P. de; MOASSAB, P. J.; BIRON, B.; ALM, S. Estudo da confiabilidade das estações conversoras de Itaipu. In: VII SEMINÁRIO NACIONAL DE PRODUÇÃO E TRANSMISSÃO DE ENERGIA ELÉTRICA, Brasília, dez. 2-6, 1984. Trabalhos ... Brasília, 1984. BSB/GPL/17. 13 p.
- SOBRAL, S. T.; FLEURY, V. G. P.; SALATKO, V. F.; COELHO, A.S.R.; MUKHEDKAR, D. Distribuição da corrente de defeito nas SE'S do complexo gerador de Itaipu. In: VIII SEMINÁRIO NACIONAL DE PRODUÇÃO E TRANSMISSÃO DE ENERGIA ELÉTRICA, São Paulo, maio 4-8, 1986. Trabalhos ... São Paulo, 1986. SP/GSE/09. 24 p.
- SOBRAL, S.T.; FLEURY, V. G. P.; VILLALBA, J.R.; MUKHEDKAR, D. "Decoupled method" for studying large interconnected grounding systems using microcomputers. Part I. Fundamentals. *IEEE Power Engineering Society*, Summer Meeting, Mexico City, July 20-25, 1986. Paper n.86 SM 456-8. 9 p.
- _____. "Decoupled method" for studying large interconnected grounding systems using microcomputers. Part II. Utilization on Itaipu ground system and complementary aspects. *IEEE Power Engineering Society*, Summer Meeting, Mexico City, July 20-25, 1986. Paper n.86 SM 455-0. 8 p.
- SOBRAL, S. T.; PEIXOTO, C. A. O.; FERNANDES D.; MUKHEDKAR, D. Grounding measurements at the Itaipu generating complex using the "extended elect method". *IEEE Power Engineering Society*, Summer Meeting, Mexico City, July 20-25, 1986. Paper n.86 SM 457-6. 10 p.
- SOBRAL, S. T.; PEIXOTO, C. A. O.; FERNANDES D.; SALATKO, V.F.; MUKHEDKAR, D.; Medições no sistema de aterramento das principais subestações do complexo gerador de Itaipu. In: VIII SEMINÁRIO NACIONAL DE PRODUÇÃO E TRANSMISSÃO DE ENERGIA ELÉTRICA, São Paulo, maio 4-8, 1986. Trabalhos ... São Paulo, 1986. SP/GSE/08. 13 p.
- SOBRAL, S. T.; PEIXOTO, C. A. O.; MUKHEDKAR, D. Ground potential distribution in the neighbourhood of the Itaipu generation complex. *IEEE Trans. on Power Delivery*, New York, 1 (1) : 85-90, Jan. 1986. paper 85.
- SOTO, A. R. S.; JARDINI, J. A.; PEREIRA, F. P.; MEDEIROS, J. R.; MORAIS, S. A.; FRONTIN, S. O. Limitation of AC-SIDE telephone interference for Itaipu HVDC project with consideration of series filters. In: CIGRE. INTERNATIONAL CONFERENCE ON LARGE HIGH VOLTAGE ELECTRIC SYSTEMS, Rio de Janeiro, 1981. 25 p.
- SOUZA, A. R. M.; HILDEN, V.; MAARTENSSON, H.; MONTEIRO, L. A. P.; DAVID, P. Descrição dos sistemas de alarme, monitoração e aquisição de dados das subestações conversoras de Foz do Iguaçu e São Roque. In: VII SEMINÁRIO NACIONAL DE PRODUÇÃO E TRANSMISSÃO DE ENERGIA ELÉTRICA, Brasília, dez. 2-6, 1984. Trabalhos ... Brasília, 1984. BSB/GTC/19. 20 p.
- SPINELLI, J. S.; NORONHA, R. F.; VILLALBA, J. R. Subestação isolada a gás SF₆ de 500 kV da Usina Hidrelétrica de Itaipu - Aterramento e blindagens adicionais para condições transitórias. In: IX SEMINÁRIO NACIONAL DE PRODUÇÃO E TRANSMISSÃO DE ENERGIA ELÉTRICA, Belo Horizonte, out. 25-29, 1987. Trabalhos ... Belo Horizonte, 1987. BH/GSE/08. 6 p.
- SUTTER, C. R.; BIRON, B. A.; ERIKSSON, K.; MENEGALE, D. Aspectos do projeto do pátio de manobra para transformadores conversores das estações conversoras do sistema de transmissão de Itaipu. In: VI SEMINÁRIO NACIONAL DE PRODUÇÃO E TRANSMISSÃO DE ENERGIA ELÉTRICA, Camboriú, out. 18-22, 1981. Trabalhos ... Camboriú, 1981. BC/GSE/13. 21 p.

SUTTER, C. R.; SANTOS, L. I. F.; ERIKSSON, K.; SANTOS, N. dos. Aspectos do projeto dos edifícios para válvulas a tiristores do sistema de transmissão de Itaipu em corrente contínua. In: VI SEMINÁRIO NACIONAL DE PRODUÇÃO E TRANSMISSÃO DE ENERGIA ELÉTRICA, Camboriú, out. 18-22, 1981. Trabalhos ... Camboriú, 1981. BC/GSE/12. 19 p.

SZENTE-VARGA, H. P. 550 kv SF₆ gas-insulated switchgear for the Itaipu hydro-power station. *Brown Boveri Review*, Baden, 68 (3/4) : 157-9, 1981.

TAAM FILHO, M. Z.; FRONTIN, S. O.; JUHLIN, L. E.; PORONGABA, H. D. Análise do fenômeno de auto-excitação dos compensadores síncronos da subestação conversora de São Roque - Aplicação da chave de amortecimento. In: VII SEMINÁRIO NACIONAL DE PRODUÇÃO E TRANSMISSÃO DE ENERGIA ELÉTRICA, Brasília, dez. 2-6, 1984. Trabalhos ... Brasília, 1984. BSB/GSP/29. 8 p.

TAAM FILHO, M. Z.; GRIBEL, J. B. S. N.; MARTIN, P.; REIS, L. B.; PETERSON, T. Sistema de transmissão de Itaipu em corrente contínua - Compensação reativa das estações conversoras. In: VI SEMINÁRIO NACIONAL DE PRODUÇÃO E TRANSMISSÃO DE ENERGIA ELÉTRICA, Camboriú, out. 18-22, 1981. Trabalhos ... Camboriú, 1981. BC/GSP/25. 21 p.

TAAM FILHO, M. Z.; OGALE, A.; LOPES, J. C. Sistema de transmissão de Itaipu em corrente contínua. Aspectos sobre a operação em paralelo das estações conversoras. In: VI SEMINÁRIO NACIONAL DE PRODUÇÃO E TRANSMISSÃO DE ENERGIA ELÉTRICA, Camboriú, out. 18-22, 1981. Trabalhos ... Camboriú, 1981. BC/GSP/21. 16 p.

TAAM FILHO, M. Z.; PRAÇA, A. A. S.; PORONGABA, H. D.; TOLEDO, P. F.; MENZIES, D. Sistema de transmissão de Itaipu - Principais aspectos da interação CA/CC. In: IX SEMINÁRIO NACIONAL DE PRODUÇÃO E TRANSMISSÃO DE ENERGIA ELÉTRICA, Belo Horizonte, out. 25-29, 1987. Trabalhos ... Belo Horizonte, 1987. BHZ/GSP/11. n.p.

TAAM, M.Z.; FRAGA, R.; DAVID, P.A.M.S.; OLIVEIRA, C. H.V.D.R.; MENZIES, D.F. Sistema de transmissão de Itaipu em corrente contínua. Desempenho dinâmico da operação paralela das conversoras. In: X SEMINÁRIO NACIONAL DE PRODUÇÃO E TRANSMISSÃO DE ENERGIA ELÉTRICA, Curitiba, 89, Grupo X, GOP-17, 6 p.

THANASSOULIS, P.; FRANCO, N.; CLERICI, A.; CAZZANI, M. Overvoltages on a series-compensated 750 kV system for the 10000 MW Itaipu project. In: IEEE

TRANS. ON POWER APPARATUS AND SYSTEMS, 94 (2) : 622-31, mar./apr. 1975.

TOLEDO, P. F.de; TAAM, M. Z.; ANDERSSON, G. Sharing the Brazilian experience. Reactive power balance and AC filter switching schemes of the Itaipu converter stations. In: INTERNATIONAL SYMPOSIUM ON HVDC TECHNOLOGY, Rio de Janeiro, mar. 20-25, 1983. 16 p.

UNITED TRADE PRESS LIMITED. ITAIPU transformers and SF₆ switchgear break new ground. *Modern Power Systems*, London, 2 (2) : 56-7, june 1982.

UTECHT, M. Vibration analysis for the Itaipu generator turbine units. In: CIGRE. INTERNATIONAL CONGRESS ON LARGE HIGH VOLTAGE ELECTRIC SYSTEMS, Rio de Janeiro, nov. 1983. 6 p.

VARGA, H.P.; SCHMIDT, K.D. 550 kV SF₆ gas-insulated switchgear for the Itaipu Power Plant. *Brown Boveri Review*, out. 1986, p. 488-497.

VARGA, H. P. S. & SCHMIDT, K. D. Brasil. Paraguay. Compact switchgear fits in plant, eliminates long overhead lines. *International Power Systems*, 86 :15-17, 1986.

VIAN, A.; GRAHAM, J. F.; COSTA, L. S.; SATO, W. Investigação dos níveis de sinais de rádio na rota das linhas 800 kV do sistema de transmissão de Itaipu. In: IV SEMINÁRIO NACIONAL DE PRODUÇÃO E TRANSMISSÃO DE ENERGIA ELÉTRICA, Rio de Janeiro, set. 18-23, 1977. Trabalhos ... Rio de Janeiro, 1977. RJ/GTC/15. 5 p.

VIEIRA FILHO, X.; CHIPP, H. J.; SARDINHA, S. L. A.; PRACA, A. A. S.; CALDAS, G. P.; POPOV, M.; XAVIER, E. M.; ROMEI, O. P. Estudo de regulação de frequência do sistema interligado de 50 Hz considerando o elo de transmissão em corrente contínua. In: VIII SEMINÁRIO NACIONAL DE PRODUÇÃO E TRANSMISSÃO DE ENERGIA ELÉTRICA, São Paulo, maio 4-8, 1986. Trabalhos ... São Paulo, 1986. SP/GOP/23. 17 p.

WEY FILHO, A.; GUIMARÃES, E. B.; PAAJARVI, B. Sistema de transmissão de Itaipu em corrente contínua - Esforços de corrente nas válvulas e no reator de alisamento. In: VII SEMINÁRIO NACIONAL DE PRODUÇÃO E TRANSMISSÃO DE ENERGIA ELÉTRICA, Brasília, dez. 2-6, 1984. Trabalhos ... Brasília, 1984. BSB/GSP/40. 11 p.

MECHANICAL

DEL BRENNNA, F.; JIMENEZ, M. L.; KLEINMAN, M. O sistema de garantia de qualidade adotado para as unidades geradoras de Itaipu. In: IX SEMINÁRIO NACIONAL DE PRODUÇÃO E TRANSMISSÃO DE ENERGIA ELÉTRICA, Belo Horizonte, out. 25-29, 1987. Trabalhos ... Belo Horizonte, 1987. BHZ/SGM/17. 9 p.

EDITORA VISÃO LTDA. Itaipu. Já em montagem. *Dirigente Construtor*, Rio de Janeiro, 27 (11) : 12-20, dez. 1981.

FAGENBAUM, L. Brazil's Itaipu Dam. *Mechanical Engineering*, : 20-29, nov. 1982.

HARDT, E. Manufacture of a spiral case and runner for a Francis turbine. Voith Research and Construction, 32e Paper 4, 1986. 6 p.

INDÚSTRIA DE BASE. Pontes Rolantes para Itaipu. *Indústria de Base*, s.l., jul. 1979. 1 p.

LACHER, W. G. Peculiaridades do projeto das turbinas de Itaipu. *Energia Elétrica*, São Paulo, 5 (52) : 26-34, jul. 1982.

MORAES, J. DE; RODRIGUEZ, J.; GUMMER, J. H.; DEL BRENNNA, F. Turbines for Itaipu. *International Water Power & Dam Construction*, Sutton, 33 (12), : 36-41 (Part 1), dec. 1981, 34 : 28-33, (Part 2), jan. 1982.

NOVO GRUPO ED. TÉCN. LTDA. Itaipu. Joint-Venture: equipamentos hidromecânicos. *Energia Elétrica*, São Paulo, 5 (52) : 52-4, jul. 1982.

_____. Itaipu. O ritmo crescente da solda. *Soldas e Eletrodos*, São Paulo, (6) : 14-16, abr./maio 1978.

TEIXEIRA, A.; WEGNER, M.; SAURON, A.; DIANA, J.C. Itaipu. Exemple de résolution de problèmes posés par la conception et la réalisation des turbo-machines de grande dimension. *Revue Technique, Paris* (3): 39-62, 1984.

VILLALBA, J. R.; MONTEIRO, R. C.; RAIUNEC, A. E.; GUMMER, J. H.; BAROUX, J. P. Use and re-use of Itaipu's diversion gates. *International Water Power & Dam Construction*, Sutton, 36 (5, Part I): 24-8, may 1984. 36 (7, Part II) : 44-9, jul. 1984.

VOITH. Brazil/Paraguay. Itaipu - Commissioning of the first 60 - Hz turbines. *VOITH Information*, (1), 1987. n.p.

_____. Itaipu hydroelectric power station. *VOITH Publication*, t 2658 e, s.d. 19 p.

WERNICKE, G. Protection of gate operating mechanism of large Francis turbines. In: IAHR. XI INTERNATIONAL ASSOCIATION FOR HYDRAULIC RESEARCH SYMPOSIUM, Amsterdam, sept. 13-17, 1982. Proceedings ... v. 2. 10 p.

ENVIRONMENT

AGOSTINHO, A.A.; BORGHETTI, J.R.; DOMANICZKY, C.M.; NOGUEIRA, S.V.G.; OKADA, E.K. Produção Pesqueira e Situação da Pesca no Reservatório de Itaipu. In: CGBG. XVIII SEMINÁRIO NACIONAL DE GRANDES BARRAGENS. Foz do Iguaçu, 1989. Anais ... Foz do Iguaçu, abr. 1989, t.3. p. 1059-75.

ASSESSORIA DE RELAÇÕES PÚBLICAS DA ELETROBRÁS. Ecomuseu de Itaipu, único no gênero na America Latina. *Memória da Eletricidade*, (1), out. 1986. 11 p.

CARVALHO E SILVA, J. Itaipu. Duas idéias, uma obra. *Deutsche-Brasilianische Hefte/Cadernos Germano-Brasileiros*, Bonn, 2,: 1-23, 1983.

CHMYZ, I. Estado atual das pesquisas arqueológicas na margem esquerda do Rio Paraná (Projeto Arqueológico Itaipu. *Estudos Brasileiros*, Curitiba, 8 (13) :5-39, jul. 1982. 35 p.

COMISSÃO MISTA TÉCNICA BRASILEIRO-PARAGUAIA. Reconnaissance of the ecological impact of the project, apr. 1973.

COUTINHO, A. A proteção do ambiente na hidrelétrica de Itaipu. *Engenharia Sanitária*, Rio de Janeiro, 19 (3) : 248-52, jul./set., 1980.

COUTINHO, A.; CERVERA, E. C.; MULLER, A. Hidrelétrica de Itaipu. Plano básico para conservação. *Engenharia*, São Paulo (415), : 2-7, abr. 1979,

COUTINHO, A.S. & CERVERA, E.C. Relatório de viagem: conservação ambiental (viagem de estudos). *Revista DAE da SABESP*, 39 (120) : 25-35, 1979.

FACETTI, C. A. Ações da Itaipu no meio ambiente. In: IX SEMINÁRIO NACIONAL DE PRODUÇÃO E TRANSMISSÃO DE ENERGIA ELÉTRICA, Belo Horizonte, out. 25-29, 1987. Trabalhos ... Belo Horizonte, 1987. BHZ/SGA/05. 5 p.

INSTITUTO PARANAENSE DE DESENVOLVIMENTO ECONÔMICO E SOCIAL. Alterações ecológicas decorrentes de Itaipu. *Fundação IPARDES*, Curitiba, jun. 1977. 113 p.

_____. Impacto ambiental de Itaipu. *Fundação IPARDES*, Curitiba, nov. 1981. v. 2. 218 p.

_____. Impacto ambiental de Itaipu. *Fundação IPARDES*, Curitiba, nov. 1981. v. 2, p. 36-40.

ITAIPU BINACIONAL. In: I SEMINÁRIO DE LA ITAIPU BINACIONAL SOBRE MEDIO AMBIENTE, Asunción, abr. 1979. 1 v. 347 p.

_____. Ecomuseu de Itaipu, out. 1987. 46 p.

_____. In: II SEMINÁRIO DA ITAIPU BINACIONAL SOBRE MEIO AMBIENTE, Foz do Iguaçu, ago. 1987. v.1. 249 p.

KOHLHEPP, G. Itaipu. Socio-economic and ecological consequences of the Itaipu dam and reservoir on the Rio Parana (Brazil/Paraguay). Deutsches Zentrum für Entwicklungstechnologien-GATE. . . Deutsche Gesellschaft für Tech. Zusamm. (GTZ) GmbH. Braunschweig, Friedr. Vieweg & Sohn, 1987. 100 p.

MINISTÉRIO DO INTERIOR. "MYMBA Kuera" resgata animais na área inundada pela represa de Itaipu. *Interior*, s.l., (46) : 12-3, set./out., 1982.

NOVO GRUPO ED. TÉCN. LTDA. Itaipu deixa espaço para implantar projeto ecológico. *Construção Pesada*, São Paulo, 12(140) : 60-2, set. 1982.

SZPILMAN, A.; COSTA, A. S.; GULINO, S. O.; CERVERA, E. C.; CHACEL, F. M. Projeto Itaipu. Metodologia e critérios adotados no tratamento dos impactos ambientais ocorridos na área de implantação das estruturas da usina. In: IX SEMINÁRIO NACIONAL DE PRODUÇÃO E TRANSMISSÃO DE ENERGIA ELÉTRICA, Belo Horizonte, out. 25-29, 1987. Trabalhos ... Belo Horizonte, 1987. BHZ/SGA/04. 5 p.

APPENDIX

INTRODUCTION	19.3
ENGINEERING DESIGN	19.3
SPECIAL CONSULTANTS	19.4
LABORATORY TESTING	19.4
CONSTRUCTION	19.4
PERMANENT ELECTROMECHANICAL EQUIPMENT	19.5

APPENDIX

INTRODUCTION

A very large number of firms and individuals of different specialties in engineering, planning, construction and supplies, were involved in one way or another in the execution of the project.

However, a complete list of such participants would be rather out of place in a book of this nature that concentrates mainly on the engineering aspects of the project.

Therefore only the firms and special consultants involved in the executive engineering design and construction of the project as well as in the manufacturing of the main permanent electro-mechanical equipment, are listed in this Appendix.

ENGINEERING DESIGN

Final design and specifications for the spillway and the right wing buttress dam, including spillway gates and associated equipment.

Consortium ENGEVIX-GCAP formed by Engevix Engenharia S.A. and Grupo Consultor Alto Paraná.

Final design and specifications for the main hollow gravity dam, including power intake equipment and penstocks.

Consortium PROMON-GCAP formed by Promon Engenharia Ltda. and Grupo Consultor Alto Paraná.

Final design and specifications for the powerhouse and the equipment assembly areas, including powerhouse auxiliary equipment.

Consortium THEMAG-GCAP formed by Themag Engenharia Ltda. and Grupo Consultor Alto Paraná.

Final design and specifications for the earthfill dams and the future navigation facilities.

Consortium HIDROSERVICE-GCAP formed by Hidroservice Engenharia Ltda. and Grupo Consultor Alto Paraná.

Engineering coordination.

Consortium IECO-ELC formed by IECO International Engineering Company Inc. and ELC-Electroconsult Spa with the support of the Brazilian consortium IESA-ENERCONSULT formed by IESA - Internacional de Engenharia S.A. and Enerconsult Engenharia Ltda., and the Paraguayan consortium PARELC-CII formed by ELC-Electroconsult del Paraguay S.A., and CII Compania Internacional de Ingeniería).

Designs and specifications for the diversion works and the rockfill dam.

Consortia IECO-ELC, IESA-ENERCONSULT and PARELC-CII.

Specifications and contract administration for the turbines, generators, main transformers and gas insulated switchgear (GIS).

Consortia IECO-ELC, IESA-ENERCONSULT and PARELC-CII.

500, 220 and 60 kV aerial interconnections between the powerhouse and substations.

Consortia IECO-ELC, IESA-ENERCONSULT and PARELC-CII.

Right bank substation.

Consortia GCAP-ELECTROPAR, IECO-ELC, IESA-ENERCONSULT and PARELC-CII.

Expansion of the right bank substation.

Consortium PARELC-GCAP with the coordination of Consortia IECO-ELC and IESA-ENERCONSULT.

Foz do Iguaçu substation cc system.

Consortium ASEA-PROMON formed by Asea Brown Boveri AB, Asea Brown Boveri and Promon Engenharia Ltda. under a turn-key contract to FURNAS.

Foz do Iguaçu substation ac system.

Consortium ELECTRA-PTel formed by Electra - Eletrotécnica Consultoria e Projetos S.A. and Ptel - Projetos e Estudos de Engenharia Ltda.

SPECIAL CONSULTANTS

ITAIPU retained a permanent panel of international consultants, which met on a regular basis to review special aspects of the design and construction of the civil works:

Consultant	Country	Field of specialization
F.H. Lyra	Brazil	Chairman of the Panel
C. Blanchet	France	Hydraulics
R.W. Carlson	USA	Concrete Technology
A. Casagrande	USA	Soil Mechanics
D.U. Deere	USA	Geology and Rock Mechanics
K.W. John	West Germany	Geology and Rock Mechanics
L.D. Wilbur	USA	Project Layout and Construction Aspects

For problems related to the design and manufacture of the generating units, the following consultants were used:

Consultant	Country	Field of specialization
J. Parmakian	USA	Turbines
M. Braikevitch	Great Britain	Turbines
G. Wernicke	Germany	Turbines
E.T. Metcalf	Great Britain	Generators
E.C. Whitney	USA	Generators

LABORATORY TESTING AND SPECIAL STUDIES

To define special aspects of the project, studies and model testing were performed as follows:

Optimization of layout and shape of hydraulic structures (diversion structure, cofferdams, and spillway).

Centro de Estudos Hidráulicos Prof. Parigot de Souza (CEHPAR), Curitiba, Brazil.

Geomechanical and structural model of main dam and diversion structure.

Istituto Sperimentale Modelli e Strutture (ISMES), Bergamo, Italy and Instituto de Pesquisas Tecnológicas (IPT), São Paulo, Brazil.

Hydromechanical equipment.

Société Grenobloise d'Études Hydrauliques (SOGREAH), Grenoble, France.

Turbine characteristics.

Hydraulic Machine Institute of the Federal Institute of Technology of Lausanne (IMH), Lausanne, Switzerland.

Seismography.

Laboratório da Universidade de Brasília, Brasília, Brazil.

Interconnection of ITAIPU, FURNAS and ANDE electrical systems.

Consortium ELECTROPAR-PTEL formed by Electropar S.R.L. from Paraguay and Ptel-Projetos e Estudos de Engenharia S.A. from Brazil.

Studies on harmonic penetration in the interconnected system of ITAIPU, FURNAS and ANDE.

Centro Sperimentale Eletrotecnico Italiano (CESI), Milano, Italy.

CONSTRUCTION

CONSTRUCTION PLANNING

Consortium ENGE-RIO-LOGOS/GCAP formed by Enge-Rio, Engenharia e Consultoria S.A. and Logos Engenharia S.A. and the Grupo Consultor Alto Paraná.

CONSTRUCTION OF CIVIL WORKS

The civil works were contracted to the consortium UNICON-CONEMPA, which consisted of five large Brazilian contractors in joint-venture (UNICON): Cetenco Engenharia S.A., Companhia Brasileira de Projetos e Obras-CBPO, Camargo Correa S.A., Andrade Gutierrez S.A., and Mendes Junior S.A., and six Paraguayan contractors also in joint-venture (CONEMPA): Barrail Hermanos S.A. de Construcciones, Cia. General de Construcciones

S.R.L., Ing. Civil Hermann Baumann - Empresario de Obras, Ing. Juan Carlos Wasmosy y Asociados, and Jimenez Gaona y Lima Ingenieros Civiles - Empresa de Construcciones.

SITE LANDSCAPE RECUPERATION

The project site and adjacent area was rehabilitated after construction by returning non-operational areas to the natural landscape. The landscaping services were performed by the Brazilian firm Arquitetura Ambiental S.C. Ltda., and the Paraguayan Consortium PARELC-GCAP.

PERMANENT ELECTROMECHANICAL EQUIPMENT

Generating units, including turbines and lower bend of penstocks, generators, isolated bus-bars, local control panels and motor control centers.

Consortium CIEM, which consisted of six firms from Brazil: Bardella S.A. Indústrias Mecânicas, BSI - Indústrias Mecânicas S.A., Mecânica Pesada S.A., Siemens S.A., Voith S.A. Máquinas e Equipamentos; one firm from Paraguay: Consórcio de Ingeniería Electromecánica S.A. - CIE; formed by the following Paraguayan firms: Saguan S.R.L., 14 de Julio S.R.L., Oti, Electromec S.A., Cotepa S.R.L. and Ing. Dorino da Re and seven firms from Europe: AG Brown Boveri & Cie. from Switzerland, Alsthom Atlantique, Creusot Loire and Neyrpic from France and Brown Boveri & Cie. AG, Siemens Aktiengesellschaft and J.M. Voith GmbH from Germany.

Generator step-up transformers.

Consortium Citram formed by Indústria Elétrica Brown Boveri S.A. and TUSA - Transformadores União Ltda.; and by Coemsa - Construções Eletromecânicas S.A.

SF₆ gas-insulated 500 kV switchgear and switching equipment.

AG Brown Boveri & Cie.

Centralized control system.

Brown Boveri & Cie AG and Cie-Siemens AG

Diversion and water-intake gates.

Mecânica Pesada S.A., Bardella S.A. - Indústrias Mecânicas, BSI - Indústrias Mecânicas S.A. and BVS - Bouchayer Viallet Schneider.

Spillway gates.

Badoni ATB Indústria Metal-Mecânica S.A., Coemsa - Construções Eletromecânicas S.A. and Ishikawagima do Brasil Estaleiros S.A. - Ishibrás.

Penstocks (excluding lower bend).

Badoni ATP - Indústria Metal-Mecânica S.A.

Auxiliary services transformers.

Coemsa - Construções Eletromecânicas S.A.

Right bank substation transformers.

Consortium Citram: Indústria Elétrica Brown Boveri S.A. and TUSA - Transformadores União Ltda.

Right bank substation 500 kV and 220 kV main switchgear equipment.

AG Brown Boveri & Cie.

Right bank substation 500 kV tripolar switch disconnectors.
Lorenzetti S.A. Indústria Eletro-Metalúrgica.

Right bank substation 500 kV tripolar switch disconnectors.
Lorenzetti S.A. Indústria Eletro- Metalúrgica

Right Bank substation 500 kV tripolar breakers.
Camargo Corrêa Brown Boveri S.A.

Foz de Iguaçu converter substation 550 kV converter transformers.
ASEA

Foz do Iguaçu converter substation 550 kV ac breakers.
Camargo Corrêa Brown Boveri S.A.

Foz do Iguaçu converter substation 550 kV ac switch disconnectors.
Lorenzetti S.A. Indústria Eletro- Metalúrgica

Foz do Iguaçu converter substation 614 kV cc breakers.
ASEA

Foz do Iguaçu converter substation 614 kV cc switch disconnectors.
ASEA

Foz do Iguaçu converter substation 614 kV cc filters.
ASEA

Foz do Iguaçu step-up substation 800/550 kV transformers.
Brown Boveri and Toshiba

Foz do Iguaçu step-up substation 800/550 kV ac breakers.

Lorenzetti, Inebras and Brown Boveri

Foz do Iguaçu step-up substation 800/550 kV ac switches

Lorenzetti, Iafa and Alcace

cc equipment for the spillway, main dam, diversion structure and auxiliary services of the powerhouse.

NIFE Brasil Sistemas Elétricos Ltda.

ac equipment for the spillway, main dam and diversion structure.

Sigla - Equipamentos Elétricos Ltda.

ac equipment for the auxiliary services of the powerhouse.

Siemens S.A., Inepar S.A. Indústria e Construção and TUSA - Transformadores União Ltda.

Diesel generators for the powerhouse.

Consortium FINCANTIERI formed by: Grandi Motori Trieste, Fiat, Ansaldo Spa. and C.R.D.A. Spa.

Control and protection panels for SF₆ and right bank substation.

AG Brown Boveri & Cie.

Ventilation system for the powerhouse and assembly areas.

Gema S.A. Equipamentos Industriais, Trox do Brasil - Difusão de Ar, Acústica, Filtragem, Ventilação Ltda., Telemecanique S.A., Fonseca e Almeida - Comércio e Indústria S.A., Termocontrol S.A., Tecmont S.R.L. and Técnica Eletromecânica S.A.

Air conditioning system for the powerhouse and assembly areas.

Sulzer do Brasil S.A. Indústria e Comércio, Inepar S.A. Indústria e Construção, Termocontrol S.A. and Tecmont S.R.L.

Trashracks for water-intake.

Ishikawagima do Brasil, Estaleiros S.A. - Ishibrás, Coemsa - Construções Eletromecânicas S.A. and Badoni ATB Indústria Metal-Mecânica S.A.

Trashrack cleaning machines.

Bardella S.A. - Indústrias Mecânicas.

Draft tube gates.

BSI - Indústrias Mecânicas S.A. and Mecânica Pesada S.A.

Powerhouse main bridge cranes.

Pohlig-Heckel do Brasil S.A. and Bardella S.A. - Indústrias Mecânicas.

Powerhouse auxiliary bridge cranes.

Mecânica Pesada S.A. and Sermec S.A. - Indústrias Mecânicas.

Assembly area bridge cranes.

Ishikawagima do Brasil Estaleiros S.A. - Ishibrás and Mecânica Pesada S.A.

Step-up transformer bridge cranes.

Equipamentos Villares S.A.

SF₆ equipment bridge cranes.

Pohlig-Heckel do Brasil S.A.

Draft tube gates gantry crane.

Equipamentos Villares S.A.

Spillway gantry crane.

Equipamentos Villares S.A.

Diversion structure and water intake gantry crane.

Mecânica Pesada S.A., Bardella S.A. - Indústrias Mecânicas, BSI - Indústrias Mecânicas S.A. and BVS - Bouchayer Viallet Schneider.

Anti-flooding system for the powerhouse.

KSB Bombas Hidráulicas S.A.

Pumping stations and drainage system for the diversion structure and powerhouse.

KSB Bombas Hidráulicas S.A.

Pumping stations and drainage system for the main and right wing dam.

Bombas Esco S.A.

Pumping station and dewatering system for penstocks and draft tubes.

Sulzer-Weise S.A.

Cooling water strainer for the generating units and auxiliaries.

AMF do Brasil S.A.

